32nd Annual Conference of the European Society for Biomaterials

Book of Abstracts – Posters

September 4 – 8 2022

Bordeaux, France

European Society for Biomaterials

www.ESBbordeaux2022.org

POSTERS |

Innovative luminescent porous 3D-printed scaffolds based on 13-93B20 bioactive glass and persistent luminescent particles for bone bioengineering.

Amel Houaoui[1*], Agata Szczodra[1], Susanna Miettinen[1], Laeticia Petit[2], Jonathan Massera[1]
[1]Faculty of Medicine and Health Technology, Tampere University, Tampere, Finland
[2]Faculty of Engineering and Natural Science, Tampere University, Tampere, Finland
[*]amel.houaoui@tuni.fi

INTRODUCTION

Complex and critical-size bone defects require innovative devices presenting osteoproperties: from osteocompatibility to osteogenesis. Due to its ability to release ions in solution and trigger signaling pathways leading to "osteocompetent responses", bioactive glass (BAG) appears as a pertinent solution to face the needs in bone engineering[1]. However, imaging BAG *in-vivo* remains a difficulty as they are typically radio-transparent and therefore cannot be detected easily and unambiguously radiographically[2]. But it is crucial to track glass behavior in bone implants in order to allow an easy follow-up of the dissolution, mineralization and resorption of the scaffold after implantation[3]. The proposed alternative is to use persistent luminescence (PeL) microparticles (MPs) which would allow one to track *in-situ* glass behavior while improving cells proliferation and osteogenic differentiation by using low light therapy[4].
In this study, porous 3D scaffolds based on 13-93B20 BAG and different PeL MPs were developed. The effect of these PeL MPs on the scaffolds' bioactivity and their cytocompatibility using human fat stem cells (HFSCs) were investigated.

EXPERIMENTAL METHODS

The porous scaffolds combining 13-93B20 BAG and MPs with blue, green, turquoise, and red PeL were obtained by robocasting with a ratio of 90/10 (weight %) respectively.
The bioactivity *in-vitro* of the scaffolds was studied in Simulated Body Fluid (SBF) for up to two weeks. The ion release was quantified using ICP-OES, and the materials were observed and analyzed by SEM-EDX.
The cytocompatibility of the scaffolds with the different PeL MPs was investigated using HFSCs. The scaffolds were excited under white light for 15min every hour for the duration of the test.

RESULTS AND DISCUSSION

The scaffolds were obtained by 3D-printing and exhibit PeL after being charged with white light indicating that the fabrication method used to prepare the scaffolds does not affect the spectroscopic properties of the PeL MPs (Figure 1).
The *in-vitro* bioactivity test of all the investigated scaffolds, in SBF, showed a decrease of [P] and [Ca] concentrations overtime, suggesting a precipitation of an apatite like-layer which was confirmed by SEM (Figure 2A) and EDX.
The HFSCs viability experiments, in direct contact with the PeL scaffolds and under subsequent excitation and

Figure 1: 3D-printed scaffolds before (top) and after (bottom) excitation under white light (Scale bar 10mm).

emission, showed that the cells are alive and numerous after 24h of incubation except for the scaffolds with red PeL MPs where a much lower density of cells is seen (Figure 2B). It must be investigated if this is due to a toxicity of red PeL MPs or due to the red-light emission which the cells cannot bear. After selecting the most appropriate PeL MPs for the targeted applications, the osteoinduction capacity of these materials and their mineralization will be studied *in-vitro* and *in-vivo*.

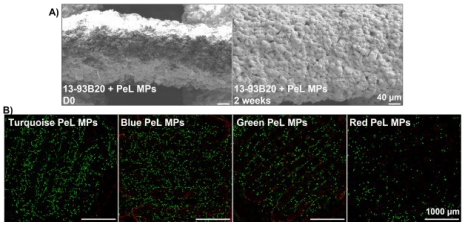

Figure 2: A) SEM images of the scaffolds with PeL MPs before and after 14 days of immersion in SBF. B) Live-Dead images of the scaffolds with PeL MPs after 24h with HFSCs.

CONCLUSION

Our results demonstrate that the PeL MPs do not inhibit the bioactivity of our scaffolds. Cellular experiments reveal promising behavior toward the potential use of these scaffolds in hard tissue regeneration and mineralization. This work not only opens the path to bioimaging but also to the photo-release of molecules of therapeutic interest.

REFERENCES

1. Hench L.L. *et al*., New J. Glass and Ceram. 3:67-73, 2013
2. Pekkan G. *et al*., J. Caranio-Maxillofac. Surg. 40:e1–e4, 2012
3. Petit L. *et al*., J. Eur. Ceram. Soc. 38(1):287-295, 2018
4. Peng F. *et al.*, Lasers Med. Sci. 27:645-653, 2012

ACKNOWLEDGMENTS

The authors would like to thank Academy of Finland and Jane and Aatos Erkko foundation for providing financial support to this project.

Deposition of a polymer-based honeycomb-like membrane on 3D printed bioactive glass scaffold and decellularized bone matrix as scaffolds for bone tissue engineering

Audrey Deraine Coquen[1,2*], Emmanuel Pauthe[1], Minna Kellomäki[2], Michel Boissière[1], and Jonathan Massera[2]

[1] CY Cergy Paris Université, BioSan Group, Laboratory ERRMECe, Department of Biology, Neuville sur Oise, France

[2] Laboratory of Biomaterials and Tissue Engineering, Faculty of Medicine and Health Technology, Tampere University, Tampere, Finland

[*] audrey.deraine@cyu.fr

INTRODUCTION

Materials used to regenerate bone tissue must present several essential properties *i.e.* biocompatibility, osteoconductivity/osteoinductivity, while promoting angiogenesis[1]. One major challenge often encountered when using these materials (naturel or synthetic) is the invasion of the implantation site by fibrous tissue before complete bone regeneration. The implant site invasion is due to the faster proliferation rate of the cells involved in the wound healing process (*e.g.,* fibroblasts) compared to bone cells proliferation rate[2] leading to incomplete bone regeneration[3]. To prevent this fibrous tissue invasion, barrier membranes have been used to cover the defects and avoid this adverse effect. However, with the currently available products, membranes degrades faster than the bone regeneration occurs which does not solve the problem of fibrous tissue ingrowth[4]. To overcome this second challenge, researchers have turned their eyes on the bone regeneration itself, with the aim to make it faster to close the gap between the membrane degradation and the bone regeneration rate. One strategy to accelerate bone regeneration is the use of bone graft in combination with the barrier membrane[5]. In such cases, the barrier membrane and the graft are two distinct materials that are not in direct contact which requires a two-step procedure that can be challenging for surgeons. In this study, combining bioactive glass (BaG) and/or cortical bone (CB) with a polymer-based honeycomb membrane, a new type of biphasic scaffold is proposed to avoid the two-step procedure.

EXPERIMENTAL METHODS

The two phases affixed are 1) the organic phase formed of poly-L-co-D, L-lactic acid (PLDLA), known to be biodegradable and biocompatible, shaped with a honeycomb-like structure through the Breath Figure Method (BFM), and 2) an inorganic phase. The inorganic substrates used are a) the 13-93B20, an experimental BaG composition containing boron, already reported in our previous work[6] and b) a decellularized xenogenic CB matrix provided by BIOBank©. The BaG used here has been specially designed and 3D printed to allow the deposition of the membrane through the BFM. Our BaGs were used pre-immersed (conditioned) in TRIS buffer or bare prior to membrane deposition.

RESULTS AND DISCUSSION

Our study demonstrated that PLDLA honeycomb-like membrane was successfully deposited onto CB and 3D printed BaG scaffold through BFM. Materials were incubated in TRIS to study their degradation and bioactivity. After 28 days of immersion in TRIS, no membrane detached from their substrate regardless of their nature, exhibiting the strong link of the membrane/substrate assembly. Furthermore, on the BaG based scaffolds, Ca/P precipitation was evidenced by SEM (Figure 1). However, such finding was not visible on the materials prepared from CB. ICP EOS analysis evidenced the important SiO_2, Ca^{2+} and PO_4^{2-} release from BaG based scaffolds compared to bone. This explains that bone scaffolds do not precipitate an apatite layer compared to BaG scaffolds. Indeed, BaGs degrade upon immersion, releasing biologically interesting ions, resulting in apatite precipitation.

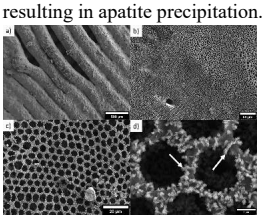

Figure 1. SEM images of a) BaG scaffold 3D printed without treatment (scale bar 500 µm), b) BaG scaffold untreated after membrane deposition (scale bar 50 µm), c) and d) BaG scaffold untreated after membrane deposition and immersion in TRIS for 28 days (scale bar 20 µm and 2µm respectively), white arrows show Ca/P precipitates.

CONCLUSION

The next step of this study will focus on the membrane/substrate assembly-cell interactions using osteogenic progenitor cells, MC3T3 and HGF to elucidate the effect of such assembly on cells involved in bone regeneration processes.

Our hope is to prove a surface dependent cell proliferation and growth showing that osteogenic progenitor cells develop mostly on the BaG/bone surfaces while fibroblastic cells grow better on the PLDLA membrane. This would support the fact that having a biphasic material allowing a one-step procedure and a separation of the underlying bone (or graft) from the outside (or fibrotic tissue) would be beneficial for a proper bone regeneration and an easier procedure for surgeons.

REFERENCES

1. W. Wang and K. W. K. Yeung, Bioactive Materials 2 (2017) 224–247.
2. N. S. Fedarko *et al.*, J Bone Miner Res 10 (2009) 1705–1712.
3. B. Ogiso, F. J. Hughes, A. H. Melcher, and C. A. G. McCulloch, J. Cell. Physiol. 146 (1991) 442–450.
4. R. P. Meinig, Orthopedic Clinics of North America 41 (2010) 39–47.
5. R. Dimitriou, G. I. Mataliotakis, G. M. Calori, and P. V. Giannoudis, BMC Med 10 (2012) 81.
6. A. Deraine *et al.*, ACS Appl. Mater. Interfaces (2021) acsami.1c03759.

ACKNOWLEDGMENTS

The authors would like to thank the Chair RETIS and Jane and Aatos Eerko Foundation for providing financial support to this project.

Synthesis and Characterization of Strontium and/or Copper Doped Nanoparticles in the Composition of Akermanite

Georgia K. Pouroutzidou[1,2*], Ioannis Tsamesidis[2], Chrysanthi Papoulia[1], and Eleana Kontonasaki[2]

[1]School of Physics, Faculty of Sciences, Aristotle University of Thessaloniki, 54124 Thessaloniki, Greece
[2]School of Dentistry, Faculty of Health Sciences, Aristotle University of Thessaloniki, 54124 Thessaloniki, Greece
[*] gpourout@physics.auth.gr

INTRODUCTION

Bone tissue engineering targets the development of functional substitutes for bone defects. Designing a graft that mimics all tissue properties still remains a challenge in bone regeneration. Nanotechnology can provide nanostructures that mimic natural bone structure[1]. Previous studies have reported that Silicon, Calcium, and Magnesium-containing ceramics, such as akermanite, merwinite, and diopside, are highly bioactive, biodegradable, support osteoblast adhesion and proliferation, and could be used as a biomedical materials[2]. Moreover, Strontium (Sr) and Copper (Cu) constitute key elements of bone biology and metabolism and can promote synergetic osteostimulating effects and angiogenesis respectively[3,4].

The aim of this study was the synthesis and characterization of Cu and/or Sr doped nanoparticles (NPs) as fillers for tissue engineering applications. Doping was performed by modification of the composition of Akermanite $Ca_2MgSi_2O_7$.

EXPERIMENTAL METHODS

Sol-gel derived bioactive glasses were produced by the hydrolysis of TEOS in a mixture of double-distilled H_2O, ethanol, and HNO_3. Afterwards Ca, Mg, Cu and Sr were added as nitrate salts while ammonia solution was inserted dropwise under stirring in an ultrasonic bath[4].

The composition in %mol of each sample is presented in Table 1.

The apatite forming ability was conducted in c-SBF, with a ratio of 1.5 mg/mL for 1, 3, and 5 days under renewal conditions[5]. FTIR, XRD, and SEM/EDS were used for the characterization of the NPs. The hemocompatibility of NPs in contact with human erythrocytes was also evaluated.

Table 1: Composition of the synthesized nanoparticles in %mol.

	SiO_2	CaO	MgO	CuO	SrO
nAk	40	40	20		
nAkCu	40	40	15	5	
nAkSr	40	40	15		5
nAkCuSr	40	40	15	2.5	2.5

RESULTS AND DISCUSSION

The FTIR spectra of all MSNs presented the characteristic bands of amorphous silicate glasses, while the XRD patterns revealed a high presence (up to 49%) of an amorphous phase. Moreover, SEM micrographs revealed the presence of aggregated NPs with particle size in the range of 82-185 nm. The apatite forming ability evaluation indicated the formation of apatite after 24 h for nAk and after 3 days for the rest of the samples. Moreover, the investigation of hemolytic activity in contact with human red blood cells (RBCs) at various concentrations revealed the hemocompatibility of all NPs under 50 μg/ml. The samples doped with Sr (nAkSr) and Sr and Cu (nAkCuSr) presented the most hemocompatible profile presented hemolysis only for 125μg/ml.

CONCLUSION

In this study, four different bioactive nanomaterials were successfully synthesized through the sol–gel method. The optimum NPs were observed in the Sr and Sr and Cu doped Akermanite NPs. Due to their enhanced apatite-forming ability and their hemocompatibility, these sol-gel synthesized NPs, can be suggested in various tissue engineering processes.

REFERENCES

1. Vieira S, et.al. Biotechnol Prog, 33(3):590-611, 2017
2. Wu C, et.al., J Biomed Mater Res Part B Appl Biomater, 78B(1):47-55, 2006
3. Pouroutzidou GK, et.al., Int J Mol Sci, 22(2):577, 2021
4. Pouroutzidou GK, et.al., J Mater Sci Mater Med, 30(9):98, 2019
5. Kokubo T, et.al., J Biomed Mater Res, 24(6):721-734, 1990

ACKNOWLEDGMENTS

This research is co-financed by Greece and the European Union (European Social Fund- ESF) through the Operational Programme «Human Resources Development, Education and Lifelong Learning» in the context of the project “Strengthening Human Resources Research Potential via Doctorate Research” (MIS-5000432), implemented by the State Scholarships Foundation (IKY).

Synthesis and Characterization of Akermanite Scaffolds Towards Bone Tissue Regeneration

Georgia K. Pouroutzidou[1,2*], Maria Lazaridou[3], Lambrini Papadopoulou[4], Konstantinos Chrissafis[1], George Vourlias[1], Dimitrios Bikiaris[3] and Eleana Kontonasaki[2]

[1]School of Physics, Faculty of Sciences, Aristotle University of Thessaloniki, 54124 Thessaloniki, Greece
[2]School of Dentistry, Faculty of Health Sciences, Aristotle University of Thessaloniki, 54124 Thessaloniki, Greece
[3] School of Chemistry, Faculty of Sciences, Aristotle University of Thessaloniki, 54124 Thessaloniki, Greece
[4] School of Geology, Faculty of Sciences, Aristotle University of Thessaloniki, 54124 Thessaloniki, Greece
[*] gpourout@physics.auth.gr

INTRODUCTION

Si-based ceramics doped with Ca and Mg have been proposed as suitable materials for scaffolds fabrication. Akermanite ($Ca_2MgSi_2O_7$) has attracted interest for bone regeneration due to its controllable biodegradation rate, improved mechanical properties, and high apatite forming ability[1,2]. Despite the profound advantages, ceramic scaffolds provide weak fracture resistance. The use of synthetic biopolymers, such as poly(lactic-co-glycolic acid) (PLGA), as coating materials, improve the mechanical performance of ceramic scaffolds and tailor their degradation rate. Moxifloxacin (MOX) is one of the fourth generation of fluoroquinolone antibiotics with antimicrobial activity against numerous aerobic and anaerobic bacteria. The aim of this study was to produce Akermanite and composite Akermanite/PLGA MOX-loaded scaffolds through the Foam Replica Technique combined with the Sol-Gel method to improve the overall effectiveness towards potential hard tissue regeneration.

EXPERIMENTAL METHODS

The methodology followed was similar to the one proposed in the literature[1]. Briefly, tetraethyl orthosilicate (TEOS), d.d.H_2O, and HNO_3 were mixed for 30min. Then, Mg and Ca were added to the solution as nitrate salts and stirred for 5h. The solution was aged and dried to produce a xerogel, sieved, and heated up to 700°C. The powder was thermally characterized before the fabrication of scaffolds with TGA/DSC. The Akermanite scaffolds (Ak) were produced by the immersion of PU foams into Sol-Gel solution several times, then dried, heated up to 700°C, and sintered at 1300°C. The scaffolds were loaded with Moxifloxacin and then coated with 10% w/v PLGA solution, using acetone as solvent (AkP). The characterization was performed by XRD and SEM/EDS. The bioactivity, degradability, and mechanical properties were also investigated. Drug loading/release profiles were assessed with HPLC.

RESULTS AND DISCUSSION

The fabricated highly porous scaffolds consisted of 93% Akermanite (XRD Rietveld Analysis) and presented a high drug loading capacity (84%) and controlled release rate, while the composite scaffolds presented a more prolonged release rate. Composite Akermanite/PLGA scaffolds presented higher compressive strength confirming the improvement of the mechanical strength after the polymeric coating. Moreover, the *in-vitro* bioactivity evaluation indicated the formation of a Ca-P layer on the surface of the samples after 14 days of immersion. Akermanite scaffolds (Ak) and PLGA coated akermanite scaffolds (AkP) showed high solubility, presenting an average mass loss of 5.4 and 6.5% after 4 weeks of incubation respectively.

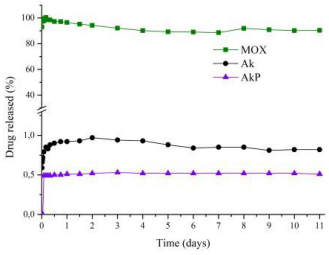

Fig. 1: In vitro release rate of moxifloxacin from Akermanite (Ak) and composite Akermanite/ PLGA scaffolds (AkP) at pH 7.4.

CONCLUSION

In this study, Akermanite and composite Akermanite/PLGA 3D scaffolds were successfully synthesized. The polymeric coating improved the *in-vitro* release rate of MOX and enhanced compressive strength keeping a highly porous structure. Such scaffolds are promising candidates for tissue regeneration applications.

REFERENCES

1. Goudouri O.M. *et al*, Mater Res Bull. 49:399-404, 2004
2. Wu C *et al*, J Biomed Mater Res Part B Appl Biomater. 78B(1):47-55, 2006

ACKNOWLEDGMENTS

This research is co-financed by Greece and the European Union (European Social Fund- ESF) through the Operational Programme «Human Resources Development, Education and Lifelong Learning» in the context of the project "Strengthening Human Resources Research Potential via Doctorate Research" (MIS-5000432), implemented by the State Scholarships Foundation (IKY).

Synthesis and Characterization of Mesoporous Silica Nanoparticles Doped with Cerium for Biomedical Applications

Chrysanthi Papamarinou[1], Georgia K. Pouroutzidou[1,2], Eleana Kontonasaki[2*]

[1]School of Physics, Faculty of Sciences, Aristotle University of Thessaloniki, 54124 Thessaloniki, Greece
[2]School of Dentistry, Faculty of Health Sciences, Aristotle University of Thessaloniki, 54124 Thessaloniki, Greece
[*] kont@dent.auth.gr

INTRODUCTION

Mesoporous silica-based nanoparticles (MSNs) are studied for their potential applications as drug delivery systems, due to their ordered pore structure, their extremely high surface area, and narrow pore size distributions. Modifying the reaction conditions such as pH or reactant stoichiometry, structure, pore size, and other functional properties of these materials can be enhanced. The aim of this study was the synthesis and characterization of Si-based MSNs and Ce-doped MSNs[1]. Cerium was selected as doping ion due to its unique antioxidant and antibacterial actions which are fundamental in biomedical applications.

EXPERIMENTAL METHODS

Mesoporous silica (Si-NPs) and cerium doped silicate nanoparticles (SiCe-NPs) were synthesized via modified sol-gel method in basic environment (aqueous solutions with pH 12 & 12,59)[2,3]. Cetyltrimethylammonium bromide (CTAB) was used as a surfactant to make the mesoporous structure by creating micelles. The source of silica was the tetraethyl orthosilicate (TEOS). Ce-doped MSNs were synthesized with cerium nitrate hexahydrate added in the percentage of 10% mol. The synthesized samples underwent calcination at 600ºC for 5 hours after drying at 60ºC overnight. MSNs were characterized using Fourier Transform Infrared Spectroscopy (FTIR), X-Ray Diffraction (XRD), Scanning Electron Microscopy (SEM) with Energy Dispersive X-ray Analysis (EDS), Brunauer-Emmett-Teller (BET) & Brunauer-Jayner-Halenda (BJH) and ζ-potential measurements.

RESULTS AND DISCUSSION

The FTIR spectra of all the synthesized MSNs showed the characteristic bands of amorphous glasses. By studying the XRD patterns some of the samples were rejected due to the presence of undesired crystalline phases. The optimum MSNs were observed with SEM. Micrographs presented nanoparticles with particle size ~200nm and round shape. From ζ-potential measurements, it was found that all MSNs were negatively charged. The optimum formulation of MSNs was selected for doping with cerium ions. The results of Ce-doped MSNs showed small round-shaped nanoparticles, also negatively charged. From EDS analysis, cerium peaks were observed which suggests successful incorporation.

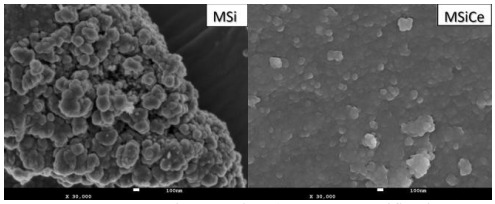

Figure 1: SEM micrographs (30.000×magnification, scale bar 100 nm)

CONCLUSION

In this study, silica mesoporous nanoparticles and Ce-doped silicate mesoporous nanoparticles were successfully synthesized by the sol-gel technique. High surface area and large pore volume were significant properties for drug carriers. Cerium ions were incorporated successfully. These NPs can be used as a drug delivery systems and antibacterial agents, therefore studies on their antioxidant and antimicrobial activity will be performed.

REFERENCES

1. Alothman Z. A., Materials, 5(12), 2874–2902, 2012
2. Pouroutzidou GK, *et.al*, Int J Mol Sci., Jan 8;22(2):577, 2021
3. Liverani, L, et al., Polymers, 9, 487, 2017

ACKNOWLEDGMENTS

This work is supported by European Union's Horizon 2020 research and innovation programme under grant agreement No 953128, project: Smart, Multifunctional Dental Implants: A solution for peri-implantitis and bone loss.

The Effect of pH Value on the Properties of MCM-41 Calcium and Cerium Doped Silica-Based Mesoporous Nanoparticles

Georgia K. Pouroutzidou[1,2*], Evangelia Deli[1], Chrysanthi Papoulia[1], Antigoni Margellou[3], Dimitrios Gkiliopoulos[3], George Vourlias[1], Konstantinos Chrissafis[1], Konstantinos S. Triantafyllidis[3], Dimitrios Bikiaris[3] and Eleana Kontonasaki[2]

[1] School of Physics, Faculty of Sciences, Aristotle University of Thessaloniki, Thessaloniki, Greece
[2] School of Dentistry, Faculty of Health Sciences, Aristotle University of Thessaloniki, Thessaloniki, Greece;
[3] School of Chemistry, Faculty of Sciences, Aristotle University of Thessaloniki, Thessaloniki, Greece;
[*] gpourout@physics.auth.gr

INTRODUCTION

Mesoporous silica nanoparticles (MSNs) are considered promising drug carriers due to their ordered pore structure that allows high drug loading and release capacity. Si and Ca represent important components of bone biology and bone metabolism. The dissolution of such ions from MSNs can lead to osteogenic differentiation of stem cells in the direction of extracellular matrix calcification[1]. Moreover, Ce ions have received a lot of attention due to their desirable properties, such as antioxidant, anti-inflammatory, and antibacterial, which are considered to be prerequisites for tissue regeneration[2]. The aim of this work was to study the effect of different pH values on the physicochemical properties of sol-gel derived MSNs.

EXPERIMENTAL METHODS

The synthesis of Ca/Ce-doped MSNs of MCM-41 type was performed via the CTAB-assisted Sol-Gel method[1,3]. The synthesis of the MSNs was conducted via the Sol-Gel method using tetraethyl orthosilicate (TEOS) as the silica source and Cetyltrimethylammonium bromide (CTAB) as the pore directing agent in an alkaline environment (for pH values=11, 12 and 13, MS11, MS12, and MS13 respectively). For the synthesis of Ca/Ce-doped MSNs, the ions were added to the solution as nitrate salts. The physicochemical properties of MSNs were investigated by X-ray photoelectron spectroscopy (XPS), Scanning Electron Microscopy/Energy Dispersive Spectroscopy (SEM/EDS), X-ray Diffraction (XRD), ζ-potential, and N_2 porosimetry.

RESULTS AND DISCUSSION

Different pH values affected the particle size and the mesoporous structure. More specifically, XRD patterns revealed that the higher pH value (MS13) leads to the formation of undesirable crystalline phases, while the XPS measurements revealed the weakness of the sample with the lowest pH value (MS11) to incorporate the cerium ions into the mesoporous structure. Thus, the sample MS2 synthesized at 12 pH value retained its nanosize (Fig.1) and its textural characteristics, presenting high surface area (681 m^2/g), small particle size (70nm) and negative surface charge (-19,5 mV).

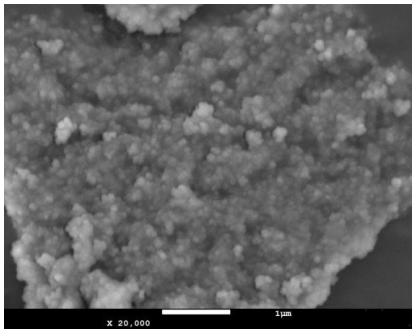

Fig.1: SEM micrographs (20.000× magnification, scale bar 1 μm) of the MS12 sample.

CONCLUSION

In this study, the effect of pH value on the synthesis of silica-based MSNs doped with Ca and Ce was investigated. The pH value played a key role in the synthesis of MSNs, with the optimum pH value approaching 12. The textural properties of such samples make them excellent candidates for hard tissue regeneration applications as nanocarriers for drug delivery systems.

REFERENCES

1. Pouroutzidou G.K. et al., Int J Mol Sci. 22(2):577, 2021
2. Tsamesidis I. et al., Nanomaterials. 11(9):2189, 2021
3. Liverani, L, et al., Polymers, 9, 487, 2017

ACKNOWLEDGMENTS

This work is supported by European Union's Horizon 2020 research and innovation programme under grant agreement No 953128, project: Smart, Multifunctional Dental Implants: A solution for peri-implantitis and bone loss.

Bone Repair monitoring using K-edge Spectral Imaging

Maxence Limelette[1*] , Bruno Bujoli[1] , Frédéric Lerouge[2] , Szilvia Karpati[2] , Stéphane Parola[2] , Olivier Gauthier[3] , Phillipe Douek[4]

[1] Chimie et Interdisciplinarité : Analyse, Synthèse et Modélisation – CNRS : UMR 6230, Université de Nantes – France
[2] Université de Lyon, UMR 5182 UCBL-CNRS-ENS, Laboratoire de chimie, ENS Lyon - France
[3] Ecole Nationale Vétérinaire de l'Alimentation et de l'Agroalimentation, Nantes Atlantique, route de Gachet – France
[4] Hospices Civils de Lyon (Radiology Department) – 69677 Bron – France
* maxence.limelette@univ-nantes.fr

INTRODUCTION

Injectable calcium phosphate cements (CPCs) have been successfully used in clinics as bone substitutes for several decades.[1] However, the use of X-rays to monitor the evolution of the implanted area remains very limited because a large part of commercial injectable CPCs has the same attenuation coefficient (HU) as natural bone. We have therefore studied the potential of a brand-new generation of scanner detector (SPCCT for spectral scanner with photon counting) to monitor the *in vivo* degradation of CPC and its replacement by natural bone. This new scanner technology allows to select an X-ray energy window, and selectively detect and quantify heavy elements using their K-Edge energy level.

The objective of our work was to combine CPCs with SPCCT contrast agents based on rare earth trifluoride (REF_3) nanoparticles (NPs),[2,3] and to study: (i) the stability of the contrast agent in the cement matrix; (ii) the minimum concentration of contrast agent to be added to the CPC to allow its good visualisation by SPCCT, and (iii) whether SPCCT can help to monitor the *in vivo* behaviour of this implant.

EXPERIMENTAL METHODS

In a typical synthesis, REF_3 NPs were prepared by addition of hydrofluoric acid solution (HF) in N'N-dimethylformamide (DMF) to a $RECl_3.6H_2O$ solution in methanol. A stable colloidal suspension was obtained, and the resulting NPs were isolated and purified by dialysis. Coating of NPs was performed using two types of functionalized poly(methyl methacrylate) [i.e., respectively, poly(poly(ethylene oxide) methacrylate -co- dimethyl(methacryloyloxy)methyl phosphonic acid or poly(poly(ethylene oxide) methacrylate -co-methacrylic acid)].

The coated REF_3 NPs were found to be stable in a 0.5wt.% Na_2HPO_4 solution for several weeks. This was confirmed by FT-IR, MAS NMR, XRD, TEM and DLS studies of NPs after phosphate treatment.

In vivo experiments were carried out with all relevant licenses and ethics approval. For this study, adult New-Zealand rabbits (4 males) were anaesthetised and a 6x12mm critical bone defect was drilled in each distal tibia. Each hole was then filled with CPC+REF_3 NPs and a SPCCT monitoring was performed until 8 weeks.

RESULTS AND DISCUSSION

We have shown that polymer coated REF_3 NPs were stable in the cement matrix and did not aggregate despite the high concentration of phosphate ions in the cement paste. Indeed, when coated with a polymer bearing multiple binding groups (i.e., CO_2H or PO_3H_2), the NPs stability in water and phosphate buffer was sufficient to be dispersed in a CPC.

In vitro implantations – in cadaver cow bone – showed that a minimal amount of 9 mg of rare earth per mL of cement paste was necessary to allow a good visualization of the implant by SPCCT. Using this technique, quantification of the rare earth was also possible and measured values were in accordance with the amount of contrast agent introduced in the sample.

Finally, the *in vivo* implantation of a CPC combined with GdF_3 NPs has demonstrated that it was possible to easily visualize the implanted area by selecting the K-edge energy threshold of gadolinium, thus providing very complementary data to those obtained by conventional scanner (Figure 1). This suggests that the *in vivo* monitoring of the implant evolution with time might be possible using this strategy.

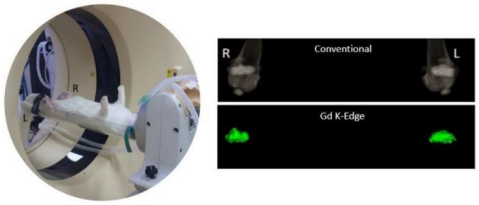

Figure 1. In vivo visualization of implanted area (rabbit femoral heads) using an injectable calcium phosphate cement loaded with GdF_3 NPs. Right :(top) conventional image, (bottom) SPCCT image by selecting the K-edge energy threshold of gadolinium.

CONCLUSION

We have successfully designed a calcium phosphate cement formulation incorporating functionalized REF_3 NPs. The nanoparticles stability in the CPC was good when coating the NPs with a polymer bearing multiple binding groups. Additionally, we have shown that the CPC containing the SPCCT contrast agent can be easily visualized under *in vivo* conditions.

REFERENCES

1. Dorozhkin S. V. *et al.*, J. Mater Sci. 43, 2008.
2. Pan *et al.*, ACS Nano, 6:3364, 2012.
3. Halttunen *et al.*, Scientific reports, 9:12090, 2019.

Injectable Bone Cement Containing CMC Microparticles for Silver Delivery Able to Reduce Implant-Associated Infection Risk

Sylvaine Jacquart[a], Sophie Girod-Fullana[b], Fabien Brouillet[b], Christel Pigasse[c], Robin Siadous[d], Mohamed Fatnassi[a], Julien Grimoud[c], Christian Rey[a], Christine Roques[c,e], Christèle Combes[a]

[a]CIRIMAT, Université de Toulouse, CNRS, Toulouse INP - ENSIACET, Toulouse, France
[b]CIRIMAT, Université de Toulouse, CNRS, Université Toulouse 3 - Paul Sabatier, Toulouse, France
[c]Laboratoire de Génie Chimique, Université de Toulouse, CNRS, INPT, Université Toulouse 3 - Paul Sabatier, Toulouse, France
[d]Université de Bordeaux, Inserm U1026 Bioingénierie Tissulaire (BioTis), Bordeaux, France
[e]CHU Toulouse, Hôpital Purpan, Service de Bactériologie-Hygiène, Toulouse, France

INTRODUCTION

The burden of implant-associated infections (IAIs) in surgery has grown together with the number of implanted medical devices. In the challenging quest for reducing the risk of IAIs in bone surgery, the use of silver ions is promising regarding its broad spectrum on planktonic as well as multiresistant bacteria [1-3]. In view of controlling its early delivery *in situ* at the desired dose, we investigated its encapsulation in carboxymethyl cellulose (CMC) microparticles (µ-CMC-Ag) by spray-drying and included them in an apatitic bone cement whose Ag^+ load/release could be adapted to reduce the risk of infections by the main pathogens introduced during the surgery [4-5]. The µ-CMC-Ag microspheres must combine: 1) A high silver encapsulation efficiency; 2) Controlled release properties, especially regarding "race to the surface", of efficient Ag^+ quantities for the early control of adhesion and biofilm formation; 3) Size distribution permitting to improve cement paste injectability and self-setting ability. We implemented a step-by-step methodology starting from the *in vitro* study of the antibacterial properties and cytotoxicity of $AgNO_3$ and Ag_3PO_4 salts presenting different solubilities. Then we were able to design cements containing efficient concentrations in silver regarding biofilm formation inhibition.

EXPERIMENTAL METHODS

The *in vitro* cytotoxicity test on silver salts and cements was performed on human bone marrow stroma cells (HBMSCs) by the neutral red and MTT assay methods according to the ISO 10993-12 standard. The *in vitro* antibacterial activity (Minimal inhibitory (MIC) and bactericidal (MBC) concentrations) of $AgNO_3$ and Ag_3PO_4 salts was assessed on *S. aureus* CIP 4.83, *S. epidermidis* CIP 6821T, *S. aureus* CRBIP 21.18 (MRSA and multiresistant) (Institut Pasteur Collection, Paris, France) and *S. aureus* ATCC 33591 (MRSA) (American Type Culture Collection) strains. The two first strains were selected for assays on biofilm formation on silver salts and cements. We thoroughly investigated CMC microspheres preparation using spray-drying: the processing conditions were optimized from CMC-$AgNO_3$ solution. Composite cements (C-µAg-CMC) were prepared by mixing a solid phase including a mixture of vaterite-$CaCO_3$, dicalcium phosphate dihydrate and 2 or 10% (w/w) of Ag-loaded CMC microspheres with a liquid phase (deionized water). The influence of µ-CMC-Ag microspheres on the setting, injectability and drug release properties of the composite cement was studied.

RESULTS AND DISCUSSION

We showed that the silver release (37°C, in Tris buffer) occurred over two weeks without burst effect and at a dose range conferring anti-biofilm efficiency without cytotoxicity from 3 hours of release. Modelization of the silver release data supported a higher release rate of C-µAg-CMC attributed to lower silver/cement interactions and to the presence of hydrophilic reservoir zones, leading more rapidly to silver active doses. In addition, the presence of µCMC-Ag in the cement formulation led to a fully injectable and highly porous (77%) cement, showing a compressive strength analogous to cancellous bone. Our results demonstrated that the introduction of 2 or 10% silver-CMC microspheres in the cement led to a fully injectable self-setting paste, suppressing the filter-pressing phenomenon during its extrusion.

CONCLUSION

The developed C-µCMC-Ag biomimetic cement formulation including 10% (w/w) of µCMC-Ag and 0.375% (w/w) of Ag appears promising as an antibacterial and injectable bone filling material able to reduce the risks of infection at the implantation site. This injectable composite cement constitutes a versatile bone substitute with tunable drug delivery properties, able to fight against bone IAIs. The development of such injectable paste which can be implanted using mini-invasive surgery technique contributes also to the decrease in bone IAIs risk.

ACKNOWLEDGMENT: The authors thank the Agence Nationale de la Recherche for supporting this research work (BIOSINJECT project, grant n° ANR-09-TECS-004).

REFERENCES

1. Tande A.J. *et al*., Clin. Microbiol. Rev. 27:302–345, 2014
2. Gordienko M.G. *et al*., J. Hazard Mater. 378:120754, 2019
3. Feng Q.L. *et al*., J. Biomed. Mater. Res. 52:662–668, 2000
4. Jacquart S. *et al*., J. Mater. Sci.:Mater.Med.24:2665-75, 2013
5. Rau J.V. *et al*., J. Funct. Biomater. 7: 10, 2016

Bioactive Glasses From The SiO_2-Cao-Na_2O System With Angiogenic Properties For Bone Regeneration Application

Martyna Nikody[1,2*], Matthias Schumacher[1], Lilian Kessels[4], Tim Wolfs[4], Lizette Morejón[3], José A. Delgado[3], Lorenzo Moroni[2], Pamela Habibovic[1], Elizabeth R. Balmayor[1]

[1]Department of Instructive Biomaterials Engineering, MERLN Institute for Technology-Inspired Regenerative Medicine, Maastricht University, Maastricht, the Netherlands
[2]Department of Complex Tissue Regeneration, MERLN Institute for Technology-Inspired Regenerative Medicine, Maastricht University, Maastricht, the Netherlands
[3]Department of Ceramics and Composite Materials, BIOMAT Center for Biomaterials, University of Havana, Havana, Cuba
[4]Department of Paediatrics, Maastricht University, Maastricht, the Netherlands
* m.nikody@maastrichtuniversity.nl

INTRODUCTION

Supporting neo-vascularization upon biomaterial implantation into a critical-sized bone defect remains a major clinical challenge. Lack of vascular network leads to insufficient nutrient and oxygen supply with subsequent graft failure. This often results in compromised implant survival and functionality. Bioactive glasses are being widely used for vascularized bone regeneration applications due to their excellent biocompatibility demonstrated through the ability to form strong bonds to bone mediated by the formation of a hydroxyapatite layer[1].

This study investigates a novel type of bioactive glasses from the SiO_2-CaO-Na_2O system produced using natural silica and calcite raw materials. These glasses lack P_2O_5 groups, which may be responsible for some of the observed features. Preliminary in vivo tests using a zebrafish model suggest that some of these glasses possess angiogenic properties.

EXPERIMENTAL METHODS

To investigate these properties further, human mesenchymal stromal cells (hMSCs) and human umbilical vein endothelial cells (HUVECs) were exposed to the materials both directly and indirectly. Five different bioactive glasses were tested at concentrations of 100, 200, 300, 400 and 1000 µg/mL. Fourier transform infrared spectroscopy (FTIR) and X-ray diffraction spectroscopy (XRD) was performed to characterize atomic and molecular structure of the materials. Furthermore, cell viability, tubule-like structure formation, cell migration and proliferation as well as ALP production were investigated. After a selection of the best performing formulations, their angiogenic properties were further assessed in a chick chorioallantoic membrane (CAM) model.

RESULTS

The XRD results confirmed the amorphous character of the tested bioactive glasses. Together with results obtained using FTIR, the obtained diffractograms suggested the presence of different nanocrystalline domains indicating that differences in the material (macro) properties can be expected. Initial in vitro experiments showed an overall increase of hMSCs proliferation over the period of 14 days. Furthermore, a steady ALP production was observed during the early time points (day 3 and 7) in case of the highest tested concentration and an increase at day 14 in case of lower concentrations (100 and 200 µg/mL). Culture of HUVECs with bioactive glass conditioned medium showed altered cell arrangements in comparison to the untreated control demonstrating tubule-like structures formation. Furthermore, bioactive glasses tested in a CAM model influenced the number, distribution and diameter of the blood vessels.

CONCLUSION

These investigations show different material properties of the glasses when compared among themselves and to traditional bioglasses formulations. Furthermore, a dose-dependent osteogenic and angiogenic stimulation was exerted by the bioglasses. In addition, the three best performing formulations of bioglasses were shown to alter vascular distribution, number of connections as well as vessel diameter. Future work will focus on in-depth investigation of the osteogenic and angiogenic properties of the bioactive glasses.

REFERENCES

1. Kargozar S. *et al*., Drug Discov. 23:1700-1704, 2018

Investigating ionic therapy to restore bone regeneration following bisphosphonate related osteonecrosis of the jaw (BRONJ)

Weijia Huang[1*], Azadeh Rezaei[1], Yutong Li[1], Sahar Aloraibi[1], Kaveh Shakib[1], Gavin Jell[1]
[1]Division of Surgery, University College London, London, UK.
[*] weijia.huang.18@ucl.ac.uk

INTRODUCTION

The mechanisms of how bisphosphonates (BPs) cause osteonecrosis of the jaw (BRONJ) remain unclear, and effective therapeutic approaches are limited. The reduction of bone regeneration is one of the potential etiologic theories for BRONJ [1]. Si-based bioactive glasses (Si-BGs) have been reported to induce bone formation and enhance osseointegration through ion release causing apatite formation [2]. The glass network of Si-BGs also allows the incorporation of other ions, with known biological properties (e.g., Co, Mg), for their controlled release. Recently, work within our research group has shown that Si ion may reduce reactive oxygen species (ROS) production via the inhibition of the Fenton reaction, while cobalt ion as an HIF-1α mimetic may increase osteclast formation [3]. Considering that BPs have been reported to increase ROS in vitro [4], ROS scavenging and HIF-1α mimetics may be potential therapeutic targets to treat BRONJ. Therefore, Si ion and the HIF-1α mimetic Co released from BG may decrease ROS production caused by BPs and restore healthy bone remodelling. Here we quantify the effect of Si, on osteoblast bone nodule formation in vitro, and the effect of Cobalt on osteoclast formation, to investigate if these ions can help restore osteoblast and osteoclast function following treatment of BPs.

EXPERIMENTAL METHODS

An osteoclastic subclone of RAW264.7 cells were treated with 2μM desferoxamine (DFO) and 25μM Cobalt, with and without two types of bisphosphonates, ZA and AL for 5 days. Cells were cultured in DMEM GlutaMAX medium, supplemented with 10% FBS and 100 U/ml penicillin, 100 μg/ml streptomycin and 3ng/ml RANKL (R&D Systems, UK). Metabolic activity, proliferation, TRAP staining, TRAP-5b assay and ROS production assays were performed to measure the osteoclast formation and function.

Calvarial osteoblasts were isolated from neonatal rats and seeded in α-MEM with 2mM β-glycerophosphate, 10nM dexamethasone, and 50μg/ml ascorbate. Cells were treated with Si (0.5mM) with and without two types of bisphosphonates, zoledronate (ZA) and alendronate (AL) for 21 days. Ion release profiles, metabolic activity, proliferation, ROS production, VEGF expression and ALP activity of the cells were measured. Alizarin red staining and interferometry characterisation were performed to measure the size of the nodules.

RESULTS AND DISCUSSION

The HIF mimetics (DFO and Cobalt) partially restored BP (ZA and AL) inhibited osteoclastogenesis as determined by TRAP5b expression ($P<0.001$). For osteoblast, treatment with ZA inhibited bone nodule formation. Microscopic images showed Si ions (0.5mM) reversed the inhibition of early collagen formation induced by ZA and decreased BP induced ROS production. The reversing effect of Si, DFO and Cobalt on BP treated osteoblast and osteoclast revealed a possibility of ionic therapy for BRONJ (Figure 1). Furthermore we suggest a possible mechanism for OB restored functionality via the ROS pathway.

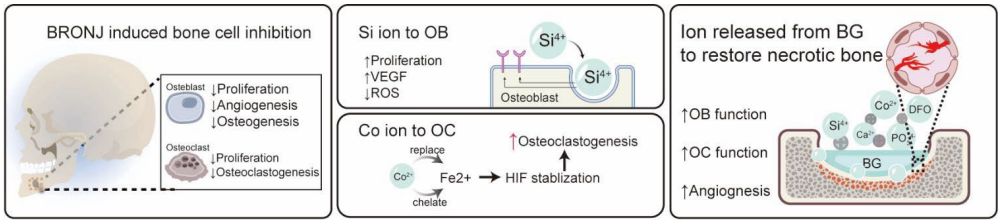

Figure 1. Hypothesis of ionic therapy for restoring bone regeneration follow BRONJ. Ions (Si4+, Co2+, Ca2+ and other ions) released from bioactive glass restore osteoclast and osteoblast cell function.

CONCLUSION

Here we demonstrated that BP induced changes in OB and OCs could be partially reversed by ions released from Si-BGs. This could allow the design of Si-BGs with specific ion release profiles for restoring bone regeneration following BRONJ.

REFERENCES

1. Rollason V. *et al.*, Interventions for treating BP-related osteonecrosis of the jaw (BRONJ). Cochrane Database of Systematic Reviews 2016, 2

2. Hench, L. *et al.*, Bioactive Glasses: Frontiers and Challenges. Front Bioeng Biotechnol 3: 194. 2015

3. Yutong L. *et al.*, Silicate mediated inhibition of osteoclastogenesis and the modulating role of Fe. Submitted. 2022

4. Taniguchi, N. *et al.*,. Bisphosphonate-induced reactive oxygen species inhibit proliferation .. J. Periodontology 91(7): 947-955. 2020

Nanometric-sized Zirconias for dental applications: improving further the compromise between translucency, mechanical properties and aging resistance

Erica Roitero[1*], Helen Reveron[1], Laurent Gremillard[1], Vincent Garnier[1], Christian Ritzberger[2], Jérôme Chevalier[1]

[1]*Univ Lyon, INSA Lyon, UCBL, CNRS, MATEIS, UMR5510, 69621 Villeurbanne , France.*
[2]*Ivoclar Vivadent AG, Benderstrasse 2, Li-9494 Schaan, Principality of Liechtenstein.*
[*] erica.roitero@insa-lyon.fr

INTRODUCTION

During the last years, the market of dental Yttria-Stabilized Zirconia (YSZ) has shown a growing interest in the development of grades with higher translucency in order to meet the aesthetic appearance of natural teeth, without compromising mechanical properties and Low Temperature Degradation (LTD) resistance. The limited transparency of this family of ceramics is caused by scattering, both on porosity and grain boundaries due to the birefringence inherent to tetragonal structure[1]. To reduce the negative effect of birefringence on the optical properties, it is possible to decrease the grain size down to 100nm to limit the scattering cross section of the nano-grains[2].

EXPERIMENTAL METHODS

In this study, nanometric-sized YSZ doped with 1.5 and 3 mol.% of Y_2O_3 (referred to as nano-1.5YSZ and nano-3YSZ, respectively) provided by Ivoclar Vivadent was characterized in terms of microstructure, mechanical properties, low temperature degradation (LTD) resistance and optical properties. Their performances were compared to those of the submicronic benchmark 3 mol.% Yttria Tetragonal Polycrystals (3YTZP). Microstructural characterization consists of grain and porosity size-distributions measured by SEM and phase composition and Yttria content measured by XRD. Mechanical resistance is characterized by biaxial flexural tests with Weibull statistical analysis and toughness single edge V-notch beam-SEVNB- method (the sharp notch was made by ultrashort pulsed laser ablation). LTD resistance is quantified by measuring the flexural resistance after 10 hours in an autoclave with saturated vapor at 134°C and 2bars and its kinetics is studied thanks to accelerated tests in autoclave with saturated vapor at 134°C and 2bars by quantifying the transformed monoclinic phase as a function of test time by XRD. Finally, the optical properties are characterized with UV-vis spectrophotometry and the Real In-line Transmission, Total Forward Transmission, Total Reflectivity, Contrast Ratio and Opalescence are evaluated.

RESULTS AND DISCUSSION

Results show that, for nano-3YSZ decreasing the grain size below 100nm improves the translucency and opalescence, together with the flexural resistance and LTD resistance. Only toughness is slightly reduced, if compared to benchmark 3YTZP. The material is entirely composed of tetragonal phase, which is stable thanks to the reduced grain size of 113.6±45 nm, preventing aging but also the activation of transformation toughening mechanisms. On the other hand, nano-1.5YSZ exhibits very high toughness, strength, resistance to contact damage and LTD resistance, superior to both benchmark 3YTZP and nano-3YSZ. Thanks to the combination of very small grain size (128±48 nm) and the low content of Yttria (1.5 mol.%) the material is composed of highly transformable tetragonal phase, plus a small amount of monoclinic phase (volumetric fraction of 5%). Surprisingly, this tetragonal phase easily undergoes stress-induced phase-transformation when the sample is subjected to mechanical tests but it is resistant to aging, i.e. the transformation triggered by the presence of water vapor. The transparency of nano-1.5YSZ is higher than 3YTZP's and the material is opalescent, but it does not achieve the RIT of n3YSZ. This is related both to the scattering on the residual nano-porosity, which is higher than in the other ceramics, and to the larger scattering cross section of its tetragonal grains with 1.5 mol.% Yttria, which have a higher tetragonality and, therefore, a larger birefringence.

CONCLUSION

Both these nano-zirconias show a superior compromise between mechanical properties-LTD resistance-translucency than the zirconias currently used in the dentistry field. They overcome the limitations of other sub-micrometric Yttria-richer grades, which show a high transparency and LTD resistance at the expense of toughness and mechanical strength because of their high content in cubic-phase. The strategy of grain-size reduction is, therefore, extremely promising.

REFERENCES

1. Apetz R. *et al.*, J. Am. Ceram. Soc. **86**, (2003).
2. Klimke J. *et al.*, J. Am. Ceram. Soc. **94** (2011).

Understanding soluble silicate species (Si) interactions with bone cells

Joel Turner[1*], Azadeh Rezaei, Julian Jones[2], Gavin Jell[1]
[1]Division of Surgery and interventional sciences, UCL, London, UK
[2]Department of materials, Imperial college London, UK
[*]joel.turner.17@ucl.ac.uk

INTRODUCTION

Despite 50 years of silicate bioactive glasses (SBG) research[1,2] (with over 100 different SBGs formulations and in excess of 500 papers) there remains a lack of understanding of how soluble silica species (Si) released from the SBGs influences cellular responses. This includes how Si is internalised (and possibly excreted), the intracellular concentration and location of these ions. With an aim to optimise of SBG ion release rates for more precise control of cell behaviour, this study attempts to investigate silicate ion uptake dynamics in osteoblasts whilst examining some the roles these ions may play in bone regeneration.

EXPERIMENTAL METHODS

Si uptake and secretion:

Osteoblast-like (SaOS-2) cells were cultured in McCoy's Glutamax 5A medium containing 2mM [Si] (preconditioned by sodium silicate hydrate, Fluorochem, UK). At regular time intervals, cells were lysed in 1M Nitric acid at 85°C. The resulting solutions were filtered, and intracellular Si content quantified by ICP-OES. Si secretion via exocytosis was evaluated by isolation of exosomes contained in cell supernatants and [Si] quantified. Uptake of different Si species (ortho, di, trisilicates) were also compared to 4S55 bioactive glass dissolution products. Significance was determined by a Kruskall-wallace test following verification of normality

Si species Identification in 45S5 bioactive glasses

45S5 bioactive glasses containing Si-29 silica was synthesised by a melt-derivation at 1400ºC. Glasses were then dissolved in de-ionised water. Dissolution products were then filtered, and the species of Si determined by Si-29 NMR.

Si intracellular localisation

Medium containing Lysosensor yellow/blue DND160 containing PDMPO (Thermofisher, UK) was added to SaOS-2 cells following a 4 day culture in 2mM Si media to qualitatively assess changes in local pH. Endosomes inside cells were additionally stained with lysoRed (Abcam, UK). Fluorescence of cells viewed by a Leica SP8 fluorescence microscopy (Ex 405nm Em: 550&670)

RESULTS AND DISCUSSION

A total increase in intracellular Si uptake was observed up to 96h (whilst the amount of uptake rate per hour decreased over time) (fig. 1A). Upon replacement of Si containing serum with a control (no Si containing media), the concentration of Si decreased ($p<0.05$), along with Si found in cell supernatants. An increase in [Si] was observed over time (1-4 days) in isolated exosomes (Fig. 1b). Intracellular [Si] was found to decrease with Di and trisilicates compared to orthosilicates (Fig. 1c). Culture with 45S5 was observed to produce intracellular Si concentrations similar to trisilicates, suggesting that other ions may influence Si uptake. Si-NMR, however, showed that at 2mM Si, bioactive glasses to produce only ortho and disilicates (Fig. 1d). An increase in Si concentration from bioactive glasses was found to increase the concentration of di and trisilicate species. Si at 2mM was found to be localised within lysosomal vesicles suggesting that both ion and particles may be uptaken.

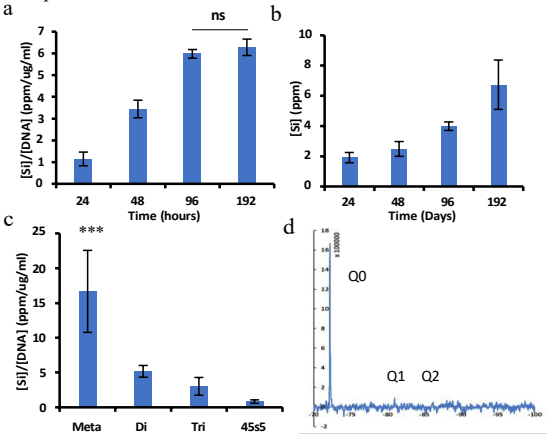

*Figure 2 – a) Intracellular Si concentration over time, b) Si secretion via exocytosis c) Uptake of different Si species from meta,di and tri silicates and 45S5 bioactive glass. d) Si species released from 45S5 bioactive glasses at 2mM [Si] determined by Si-29 NMR. ***=p<0.01 +/- SD*

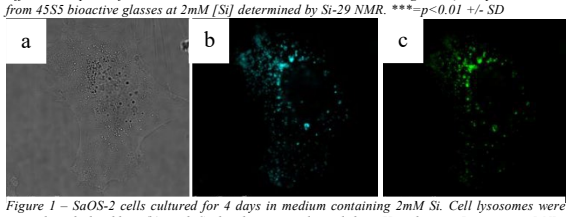

Figure 1 – SaOS-2 cells cultured for 4 days in medium containing 2mM Si. Cell lysosomes were stained with lysoblue (b) and Si localisation indicated by pH indicator Lysosensor DND-160(PDMPO) (c). A bright field image is shown in (a)

CONCLUSION

Our study suggested that Osteoblast-like cells may reach a maximum uptake of Si ions over time. Additionally, cells may begin excreting particles and ions at specific stages during their proliferation. For the first time Si has been visualised in bone cells using fluorescence microscopy. As such, new BG materials should be tailored to release silicate and other ions to target specific cell types dependent on their uptake rates and mechanisms.

REFERENCES

[1] Logroscino G. Journal of Materials Science: 2014;25(10):2445-2461.

[2] Hench L. Journal of Materials Science: 2006;17(11):967-978.

Formation of β-TCP in α-TCP by intrinsic stress

Antonio Jesús Salinas[1*], Christoph Stähli[2], Nicola Döbelin[2], Marc Bohner[2]

[1]Departamento de Química en Ciencias Farmacéuticas, Universidad Complutense, Madrid, Spain
[2]RMS Foundation, Bettlach, Switzerland
[*] salinas@ucm.es

INTRODUCTION

α-tricalcium phosphate (α-TCP) is commonly used in self-setting bone cements and as bone graft substitutes in the form of granules and blocks. Since α-TCP is much more reactive than β-TCP, the control of the phase composition is critical in the production of TCP-based bioceramics. Dense α-TCP samples are of interest for investigations of materials properties, for example as a reference to distinguish chemical from microstructural effects, to examine the effect of grain size on phase transformations, or to study the interactions between α-TCP and bone cells. However, α-TCP production is challenging because (i) the β- to α-TCP phase transition occurs at a temperature ideal for sintering (1125°C), (ii) minute amounts of Mg – a common impurity in calcium phosphates – affect the α- / β-TCP phase composition and (iii) the β- to α-TCP phase transformation is accompanied by a 9% volume expansion [1]. Here, we investigated the potential of a nano-crystalline α-TCP powder to produce pure and dense bulk materials.

EXPERIMENTAL METHODS

Nano-crystalline α-TCP (particle size < 100 nm, < 2% foreign phases, ~250 mg/kg Sr, < 20 mg/kg Mg) was produced through wet chemical synthesis of amorphous calcium phosphate and subsequent thermal conversion for a short period of time at 775°C (Ostwald's step rule) [2]. Bulk samples were produced by slip casting and sintered by heating them at a rate of 20°C/min until the target temperature of 1200°C was reached (sintering time '0 h') and subsequently keeping them at that temperature for different durations. The porosity fraction was determined by comparing cylinder dimensions and weights to the theoretical densities of the crystalline phases. The microstructure was analysed by scanning electron microscopy (SEM) after resin embedding and polishing of a cross section, and the phase composition was measured by x-ray diffraction (XRD).

RESULTS AND DISCUSSION

Sintering of slip-cast nano-crystalline α-TCP (Fig. 1a) resulted in an irregular pore microstructure (Fig. 1b). The pores were partly closed as inferred from Archimedes method experiments (not shown). A porosity fraction of 25, 23 and 20% was determined (from cylinder dimensions) after 0, 2 and 8 h of sintering, respectively. Interestingly, the sintered samples contained up to 7 wt-% β-TCP with an increasing trend over the first 8 h of sintering (Fig. 2). The phase composition was well reproducible between operators but was sensitive to starting material batches. β-Ca-pyrophosphate and hydroxyapatite contents were always lower than 2 wt-%. The presence of β-TCP is surprising considering the β- to α-TCP phase transition temperature of 1125°C and may be attributable to a hypothetical pressure build-up in the microstructure during sintering, which would favour the crystallographically denser β-TCP phase. Contents of elements favouring the β-TCP phase, such as Sr and Mg, are too low to explain the presence of β-TCP after sintering [3]. Recent data (not shown) indicate that a faster heating rate by introducing the samples into a pre-heated furnace leads to a much higher density (>95%) while still producing similar amounts of β-TCP at 1200°C.

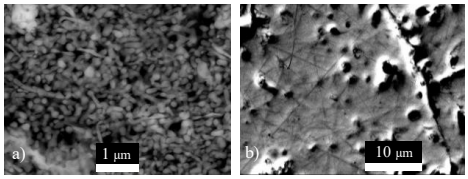

Fig. 1: SEM micrographs of slip-cast nano-αTCP before (a) and after 2 h of sintering at 1200°C (b).

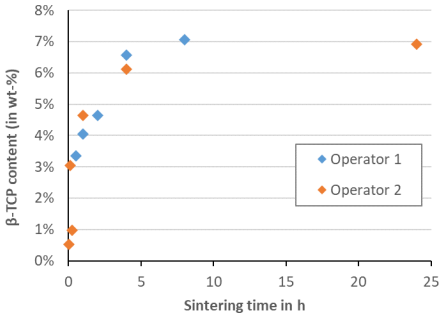

Fig. 2: Evolution of the β-TCP content of α-TCP bulk samples sintered at 1200°C.

CONCLUSION

Sintering of nano-crystalline α-TCP resulted in a thus far unexplained presence of β-TCP and a porosity fraction in the order of 20%. Ongoing work is focussing on the effect of green body density as well as sintering time and temperature on the phase composition and density.

REFERENCES

1. Carrodeguas *et al.*, Acta Biomater. 7:3536-46, 2011
2. Vecbiskena *et al.*, Biomed. Mater. 10:025009, 2015
3. Sarver *et al.*, J. Electrochem. Soc. 108:1103-10, 1961

ACKNOWLEDGMENTS

This project is internally funded by RMS Foundation. A.J Salinas is funded by Instituto de Salud Carlos III through PI20/01384 project.

Laser spinning of bioactive glass nanofibers for wound healing applications

A. Riveiro[1,3*], M. Fernández-Arias[1,4], J. del Val[1], R. Comesaña[1,3], F. Quintero[1,2], F. Lusquiños[1,2], J. R. Jones[4], J. Pou[1,2]
[1] LaserOn research group, CINTECX, Univ. of Vigo, Lagoas-Marcosende 36310 Vigo, Spain
[2] Applied Physics Dept., E.E.I., Univ. of Vigo, Lagoas-Marcosende 36310 Vigo, Spain
[3] Materials Eng., Applied Mechs. and Construction Dept., E.E.I., Univ. of Vigo, Lagoas-Marcosende 36310 Vigo, Spain
[4] Department of Materials, Imperial College London, South Kensington Campus, London, SW7 2AZ, UK
[*]ariveiro@uvigo.es

INTRODUCTION

Chronic wounds are typically colonized with aerobic and anaerobic microorganisms. This microbial colonization of wounds and proliferation can cause infection and sepsis, which inhibits the natural healing process. The treatment in these cases involves the use of different types of wound dressings that try to avoid the colonization of bacteria and control the environment of the wound. Conventional dressings are not suitable to treat acute or chronic wounds; then, as pointed out by Cooper et al. [1] new approaches taking into account multiple levels (cellular and even molecular levels) are necessary to improve the treatment of wounds. Among them, bioactive glasses were demonstrated as an effective, simpler and lower cost alternative for the manufacture of mats suitable to treat chronic wounds [2]. Despite the potential and possible applications of bioactive glasses to produce suitable bioactive wound dressings, the main problem consists in the production of the micro- and nanofiber meshes suitable for the manufacture of fibrous dressings. In this project, we propose an alternative approach, the use of the laser spinning technique to produce bioactive wound dressings based on bioactive glass nanofibers.

EXPERIMENTAL METHODS

Bioactive glass plates in the system SiO_2-Na_2O-CaO-P_2O_5 were prepared using a melt–quench route. Mats of micro- and nanofibres were produced using the laser spinning technique [3]. In short, this technique uses a high-power CO_2 laser (Rofin Sinar DC035) emitting infrared laser radiation (λ = 10.6 μm) in continuous-wave (CW) mode to locally melt the glass plates (irradiance ~ 8×10^5 W/cm^2, scanning speed=10 mm/s. Simultaneously, a supersonic gas jet (compressed air) is used to produce the fast elongation and cooling of a small volume of molten material in order to produce a large quantity of micro- and nanofibres.

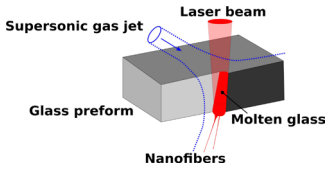

Fig. 1. *Scheme of laser spinning process*

RESULTS AND DISCUSSION

Mats of micro- and nanofibres, with a cotton-wool like appearance (Fig. 2), were produced using the laser spinning technique. They form a disordered mesh of intertwined fibres with diameters ranging from tens of nanometers to micrometers, and with lengths of several millimeters (even in the centimeter range in some cases). The cotton-wool like appearance makes fibers produced by this technique an excellent candidate to be used as wound dressing (as they can be easily combined with conventional wound dressings).

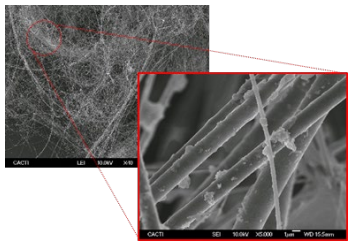

Fig. 2. *BG nanofibers of 45s5 glass*

The composition and structure of these bioactive glass fibers have been determined by XRD and ICP. The fibers remain amorphous (crystallization is not produced) and have a composition similar to that of the bulk material. Moreover, the dissolution profile of the fibers has been determined by immersion tests in TRIS buffer solution. The release of Ca ions can act as a crucial coagulation factor during hemostasis, but also triggers other cellular functions during wound healing. Moreover, I-ions incorporated into the glass composition can act as a fundamental factor to control bacterial infection. The antibacterial properties of these bioactive glass nanofibers are currently being determined by means of antimicrobial testing methods.

CONCLUSIONS

Bioactive glass nanofibers with amorphous structure were successfully produced from glass plates. These fibers show potential application in wound healing.

REFERENCES

1. Cooper DM. Nurse Pract. Forum 1999;10:74–86.
2. Yang Q, *et al.* Mater. Sci. Eng. C 2015;55:105–17.
3. Quintero F, *et al.* Adv. Funct. Mater. 2009; 19.19:3084-3090.

ACKNOWLEDGMENTS

Authors wish to thank the technical staff from CACTI (University of Vigo). This work was supported by the Government of Spain (PID2020-117900RB-I00 (MCIU/AEI/FEDER, UE)).

Identification of signatures characterizing the physiological state of bone cells at the surface of hydroxyapatite bioceramics

Alice Abélanet[1*], Éric Champion[1], Amandine Magnaudeix[1]

[1]Univ. Limoges, CNRS, Institut de Recherche sur Les Céramiques, UMR 7315, F-87000, Limoges, France

[*]amandine.magnaudeix@unilim.fr

INTRODUCTION

Calcium phosphate hydroxyapatite (HA) is a bioceramic material commonly used in bone regeneration applications because it exhibits an excellent biocompatibility, osteoconductivity, and bioactive characteristics[1]. But, monitoring the evolution of the biomaterial-tissue interface during tissue reparation after HA grafting in patients remains nearly impossible in a non-invasive way. Moreover, *in vitro*, the characterization of the biological properties of bioceramics are time and sample-consuming using conventional methods of cell and molecular biology.

In this context, the aim of this work was to identify robust and reproducible signatures characterizing the different steps of bone cell differentiation, from mesenchymal stromal precursors to mature bone cells. For this purpose, the features identified must be detectable using any label-free imaging method. For this reason, we focused on cell structure and morphology. This study was performed on bone precursor cells grown on hydroxyapatite ceramics in comparison with cells grown on non-bioceramic supports such as borosilicate glass or culture plastic either in growth medium unable to induce cell differentiation by itself or in osteogenic medium. Computer-assisted image analysis was used to determine which parameter is relevant for the building of signatures. Conventional cell biology methods were used as a comparison to validate this new approach.

EXPERIMENTAL METHODS

Human mesenchymal stromal cells (hMSCs) isolated from adipose tissue and characterized according to international standards[2] were cultured on glass coverslips or ceramic surfaces in a complete growth medium (GM) or osteogenic differentiation medium (ODM). After 48h and 7 days of culture, cells were fixed and stained for actin cytoskeleton (phalloidin-DyLight 488) for studying cell morphology. Nuclei staining by Hoescht 33342 was used to identify cells and compare the nucleus morphology. Focal adhesions were identified by immunofluorescence staining targeting vinculin. cell ability to produce an extracellular matrix was evaluated by type I collagen (Col.I) detection. The images were analyzed using ImageJ. Statistical analysis was performed using Prism 9 and Past.

RESULTS AND DISCUSSION

The first changes are visible as soon as 48h of culture. After 48h, a decrease in cellular density along with significantly larger nuclei for cells cultured in ODM compared to GM was observed whatever the culture support, glass or bioceramics. Differentiating cells also demonstrated obvious morphological modifications. Cells were bigger with oriented stress fibers and a reinforcement of focal adhesions. Col.I staining appeared more intense in OGM as a common marker of osteogenic differentiation. After 7 days, we noted an accentuation of the phenotypes observed at 48h of culture. Interestingly, the formation of collagen fibers was enhanced for cells cultured on bioceramics in comparison for those that have grown on glass.

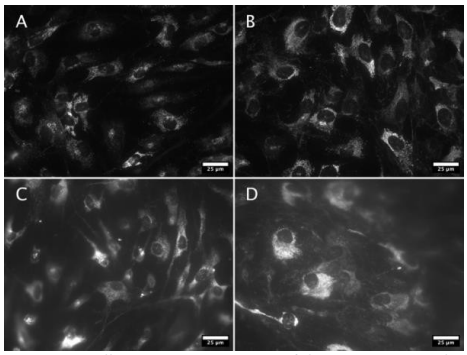

Figure 1: Collagen I *immunostaining of hMSC grown on glass coverslips (A, B) or* hydroxyapatite *(C, D) in GM* (A, *C) or OGM (B, D). Scale bar: 25 µm*. Note the bigger size of cells in OGM in comparison with GM and extracellular presence of Col.I for HA conditions.

CONCLUSION

Some early morphological changes of hMSC during osteogenic differentiation were identified and put in relation with the expression of recognized biomolecular markers. Used in combination they should allow to characterize the differentiation state of bone precursor cell at the surface of biomaterials reducing the number of needed samples to do so. Efforts are made now to reinforce time points and to validate this approach using machine learning and unlabeled data sets.

REFERENCES

1. Jarcho M, Clin Orthop Relat Res. 1981:259-278
2. Dominici et al., Cytotherapy, 2006, 315–317, 8(4).

ACKNOWLEDGMENTS

This work was funded within the scope of the INTENSIVE project funded by FEDER and by institutional grants from the French Research National Agency, project CharaBioC (ANR-19-CE08-0003-01).

Magnetic bioactive glass-based 3D systems for bone cancer therapy and regeneration

Ricardo J.R. Matos[1], Jorge Carvalho Silva[2], Paula I.P. Soares[1], João Paulo Borges[1*]
[1]Departamento de Ciência dos Materiais - CENIMAT/i3N, FCT-NOVA, Caparica, Portugal
[2]Departamento de Física - CENIMAT/i3N, FCT-NOVA, Caparica, Portugal
[*]jpb@fct.unl.pt

INTRODUCTION

Several diseases, such as osteoporosis and bone cancer, are causing an increasing need for advanced bone repair materials suitable for skeletal reconstruction [1]. Malignant bone tumors are one of the main non-trauma factors resulting in critical size bone loss/defects. The treatment of such bone defects is still a considerable challenge, and it is currently recognized that the increasing request for bone substitute materials cannot be tackled solely by autogenous or allogenic bone grafts [2]. On the other hand, surgical resection often fails to completely remove the tumor, which is the main cause of postoperative recurrence and metastasis. Therefore, a polymeric scaffold for bone regeneration that simultaneously kills residual tumor cells is of much benefit. Magnetic hyperthermia using superparamagnetic iron oxide nanoparticles (SPIONs) has emerged as a potential cancer treatment option since it is considered an effective treatment without adverse side effects [3]. These SPIONs will generate clinically relevant heat (41º-45ºC) under the application of an alternating magnetic field to kill or sensitize tumor cells. On the other hand, mesoporous bioactive glasses (MBGs) dissolution products have demonstrated their effect on osteoblast cell gene expression and the potential effect on angiogenesis and neovascularization, which in turn promotes bone healing. We therefore propose a new concept for the treatment of bone cancer and subsequent regeneration of bone defects: a polymeric scaffold produced by electrospinning containing MBG to stimulate bone regeneration, and simultaneously combining magnetic hyperthermia therapy through the incorporation of the SPIONs into the scaffold and local drug delivery [4].

EXPERIMENTAL METHODS

This section is divided into 3 parts: 1) production and characterization of SPIONs (chemical precipitation) and MBG (SOL-GEL route); 2) Incorporation of these individual materials into a polyvinylpyrrolidone (PVP) matrix produced by electrospinning; 3) Characterization and selection of such composites based on its bioactivity, biodegradability, biocompatibility, heating ability, drug encapsulation and releasing profile (still be under characterization) to select the membranes with the most desirable properties. To assess whether the materials keep their individual properties after the final blending, the composites were produced and characterized in different stages: PVP/SPIONs; PVP/MBG; PVP/SPIONs/MBG.

RESULTS AND DISCUSSION

Both SPIONs and MBG were successfully synthesized and incorporated into PVP matrices. The composites revealed their biocompatibility and heating ability. The research team have already produced the final PVP/SPIONs/MBG. However, composites still be under optimization in terms of degradation ratio, which is directly related with anticancer drug releasing profile and composite's bioactivity. It's a consequence of having both anticancer drug and MBG located into the PVP fibers. However, the swelling assay revealed the PVP capability to be used as an anticancer drug carrier.

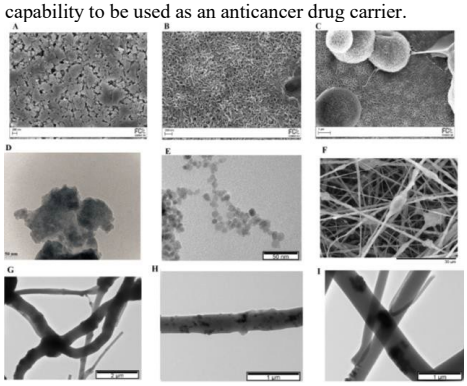

Fig. 1 -SEM image of MBG before soaking in SBF solution (A), 1 day (B) and 5 days (C) after soaking in SBF solution; TEM images of MBG (D) and SPIONs (E); SEM image (F) and TEM image (G) of PVP/MBG composite; TEM image of PVP/SPIONs (H, I).

CONCLUSION

So far, the composites revealed their ability to perform magnetic hyperthermia. The bioactivity assay of the MBG has shown the high potential of this individual material to be used as a bone regeneration promoter. The degradation ratio optimization intends to achieve a quick exposure of the MBG particles, to keep the fast HCA layer formation, and simultaneously maintain the composite's mechanical stability and a suitable drug releasing profile.

REFERENCES

1. M. Erol-Taygun, et al., Adv. Eng. Mater., vol. 21, no. 8, pp. 1–24, 2019.
2. C. Wu et al., Acta Biomater., vol. 7, no. 10, pp. 3563–3572, 2011.
3. Rajendra. K. Singh, et al., Materials Science: Materials in Medicine, pp. 147–151, 2009.
4. Montazerian M., et al., J Biomed Mater Res Part A, 104, pp.1231-1249, 2016

ACKNOWLEDGMENTS

This work is co-financed by FEDER, European funds, through the COMPETE 2020 POCI and PORL, National Funds through FCT—Portuguese Foundation for Science and Technology and POR Lisboa2020, under the project POCI-01-0145-FEDER- 007688, reference UIDB/50025/2020-2023, and project DREaMM, reference PTDC/CTM-CTM/30623/2017. Ricardo Matos also acknowledges FCT for the PhD grant with reference SFRH/BD/140090/2018.

Evaluation of the Bioactivity and Antioxidant Properties of Gentamicin and Polyphenols loaded Ce-MBGs

Francesca Fraulini, Alfonso Zambon, Gigliola Lusvardi*

Department of Chemical and Geological Sciences, University of Modena and Reggio Emilia, Modena, Italy
*gigliola.lusvardi@unimore.it

INTRODUCTION

Bioceramics, and in particular bioactive glasses (BGs), are biomaterials used in the biomedical field for hard tissue regeneration. BGs present the characteristic ability to form an apatitic phase, chemically and structurally similar to hydroxyapatite (HA, $Ca_{10}(PO_4)_6(OH)_2$), the main inorganic component of bones, which is responsible for a lasting material-bone bond. Present-day research focuses on improving the BGs' performance, conferring them desirable properties and inducing specific effects in the biological environment; this has led to develop new synthetic methods to achieve different morphologies and to include biologically useful elements, such as therapeutic inorganic ions (TIIs).[1] Among these, cerium and its compounds have attracted attention for their therapeutic applications as antioxidant, bacteriostatic, antiemetic and anticancer agents.[2]

The aim of this work is the evaluation of some properties of a mixture of Ce-doped mesoporous bioactive glasses (Ce-MBGs) loaded with gentamicin, a broad-spectrum antibiotic, and natural polyphenols from chestnut flour, respectively. In our preliminary studies, we obtained loading values of 6% for gentamicin and 1.5% expressed as C content in the final material for polyphenols, independently from Ce-doping. We posit that the combined action of these two biomolecules would add antibacterial properties, useful in the case of bacterial infection in real-life implants, and enhance antioxidant properties to decrease the oxidative stress correlated to tissue inflammation.[3]

EXPERIMENTAL METHODS

MBGs synthesis and drug loading - The SiO_2-CaO-P_2O_5-CeO_2 systems were synthesized by sol-gel EISA modified method with 0-5.3 mol% CeO_2. The MBGs were grafted separately upon contact with a gentamicin sulphate or polyphenols solution, and the dried materials were mixed in a 1:1 ratio. The loading content was calculated using TGA and elemental analysis (EA).

Bioactivity evaluation (HA formation)- The retention of bioactivity was monitored through FT-IR, XRD and SEM-EDS analyses after soaking in a Simulated Body Fluid (SBF) solution for 3 and 7 days.

Antioxidant properties evaluation - The catalase (CAT)-like activity was measured by the Fluorometric Hydrogen Peroxide Assay Kit and the superoxide dismutase (SOD)-like activity was tested using the SOD Determination Kit.

RESULTS AND DISCUSSION

FT-IR and SEM-EDS analysis show that the materials have adequate bioactivity, with the presence of HA already after 3 days of soaking in SBF, and after 7 days HA characteristic peaks are highlighted by XRD measurements. We previously observed that MBGs bioactivity is not influenced by gentamicin loading, while it is slowed by polyphenols.

The ability to dismutate H_2O_2 (CAT-like activity) of the MBGs mixture is found to be strongly dependent on cerium doping and not on the drugs loading. After 2 hours of contact, the CAT efficiency of Ce-doped MBGs is 100%. Regarding the SOD-like activity, the Ce-doped MBGs mixture is able to dismutate 98% of superoxide anions after 20 minutes.

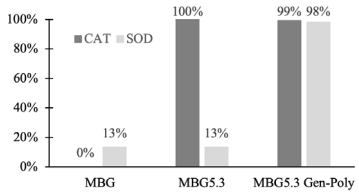

Antioxidant properties results.

CONCLUSION

We have shown that a mixture of Ce-doped MBGs loaded with gentamicin and polyphenols is a promising system to maximize each substance benefits. The system bioactivity is accelerated with respect to the polyphenols loading only, and the antioxidant properties conferred by Ce-doping and loading of polyphenols proved to be complementary, the former being essential for CAT activity and the latter for SOD activity. Future effort should be concentrated on testing the antibacterial properties of this system.

REFERENCES

1. Baino F. *et al.*, J. Funct. Biomater. 9:1-25, 2018
2. Zambon A. *et al.*, ACS Biomater. Sci. Eng. 7:4388-4401, 2021
3. Zhu, H. *et al.*, Acta Biomater. 129:1-17, 2021

ACKNOWLEDGMENTS

The authors would like to thank Dr. Chiara Cavazzoli for the helpful assistance in carrying out the analyses and enzymatic tests.

Composite (Bio)inks with Mesoporous Bioactive Glasses – Advantages and Challenges

Vera Guduric*, Anne Bernhardt, Anja Lode, Michael Gelinsky

Centre for Translational Bone, Joint and Soft Tissue Research, Faculty of Medicine Carl Gustav Carus, TU Dresden, Germany
* vera.guduric@tu-dresden.de

INTRODUCTION

Bioactive glasses (BG) are clinically established and commonly used for dental and orthopedic applications, thanks to their excellent osteoconductivity and bioactivity. BG can be modified with various bioactive metal ions assessing desired therapeutic effects. Mesoporous bioactive glasses (MBG) are special type of BG, specific for highly ordered mesoporous channel structure, which can be loaded with drugs and growth factors, giving the potential to use MBG as delivery system. As particulate material, MBG is not extrudable. To overcome this limitation and broaden its applicability, MBG can be combined with pasty materials, such as established (bio)inks. Depending on the (bio)ink composition and modifying ion in the MBG, an effect on different properties of composite inks is to be expected. In our previously published work, we evaluated these effects on rheological properties of composite bioinks consisting of 7 wt% MBG in alginate-methylcellulose (algMC) blends, shape fidelity of 3D printed scaffolds and direct and indirect effects on human cells[1]. However, common cell analyses can be affected by the presence of MBG in composite materials, resulting in misleading interpretation of obtained data. The aim of this work was to investigate the effect of the MBG in composite bioinks on investigation of cell viability, DNA quantification and alkaline phosphatase (ALP) activity in bioprinted constructs. Furthermore, we suggest possible solutions to overcome limitations Live/Dead staining as well as enzyme-activity assay in the presence of MBG particles.

EXPERIMENTAL METHODS

Different MBG were synthesized by protocol of Zhu *et al.*[2] with modifications by full substitution of Ca (15 mol%) with Zn and Mg. AlgMC-MBG composite scaffolds were produced using extrusion-based (bio)printing. To identify whether the channel structure of the MBG is responsible for specific effects, BG with the same composition as the starting glass (15 mol% Ca) was used as additional control, besides the one without glass addition.

The effect of MBG on the evaluation of cell viability by fluorescence imaging was performed by investigating the autofluorescence of the MBG and its binding of calcein-AM, commonly used to stain metabolically active cells in Live/Dead assay. To observe the total number of human mesenchymal stem cells in bioprinted composite constructs, they were labelled with Vybrant DiD prior to bioprinting. The effect on the evaluation of cell differentiation and viability was investigated by placing MBG particles in the lysis buffer during cell lysis, following with measuring of ALP and cytosolic lactate dehydrogenase (LDH) activity. In order to determine whether release products of MBG are responsible for certain effect and not the presence of mesoporous particles themselves, in additional experiment MBG powder was incubated with the lysis buffer one hour before starting the lysis of cells.

RESULTS AND DISCUSSION

Autofluorescence of the MBG particles and their affinity to calcein-AM revealed green signal for both, MBG particles and metabolically active cells, while prelabeled cells were showing red signal. Metabolically active cells could be successfully identified by expressing signals in both channels. DNA quantification in bioprinted scaffolds was not affected by the presence of MBG particles or MBG-release products. However, measuring of LDH and ALP activity was strongly affected (Figure 1). When MBG was present during the cell lysis, measured LDH activity was decreased in the presence of CaMBG and ZnMBG for approximately 50%, probably due to binding of released LDH to the MBG. It was confirmed that released products were not responsible for this effect. On the other side, release products of the MgMBG highly affected measuring of the ALP activity, showing approximately 50% increased signal, probably due to Mg reacting as a co-factor of the enzyme.

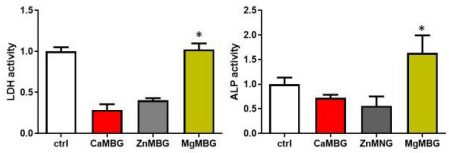

Figure 2. Effect of MBG-release products on cell assays based on LDH and ALP activity measurement

CONCLUSION

Our findings showed that interfering of MBG in the fluorescence imaging of metabolically active cells can be overcome by prelabelling the cells prior to bioprinting. Misleading results when measuring LDH and/or ALP activity in scaffolds containing MBG particles can be avoided by investigating whether and how each ion-modified MBG affects mentioned assays through its mesoporous channel structure and/or release products.

REFERENCES

1. Guduric V. *et al.*, Materials, 14, 1225, 2021
2. Zhu J. *et al*., Micropor Mesopor Mater, 112, 2008

ACKNOWLEDGMENTS

The authors thank the German Research Foundation (Grant no: GE 1133/24-1) for financial support.

Injectable Bone Substitutes with Enhanced Therapeutic Properties

Maria Grazia Raucci[1*], Xiao Yang[2], Ines Fasolino[1], Alessandra Soriente[1], Matteo Santin[3], Henri S. Schrekker[4], Xingdong Zhang[2], Luigi Ambrosio[1]

[1]Institute of Polymers, Composites and Biomaterials – National Research Council (IPCB-CNR), Naples, Italy.
[2]National Engineering Research Center for Biomaterials, Sichuan University, Chengdu, China
[3]School of Pharmacy & Biomolecular Sciences, University of Brighton, Brighton, UK
[4]Laboratory of Technological Processes and Catalysis, Institute of Chemistry, Universidade Federal do Rio Grande do Sul-UFRGS, Porto Alegre – Brazil.
[*]mariagrazia.raucci@cnr.it

INTRODUCTION

Injectable therapies are preferred for their minimally invasive nature, ease of use, and ability to fill complex 3D regions of low bone mass. Recently, efforts have been paid to optimize injectable calcium phosphate cements which have been recognized as excellent alloplastic material for osseous augmentation because of their unique combination of osteoconductivity, biocompatibility and mouldability. The sol-gel synthesis approach appears to be a suitable route towards performing injectable calcium phosphates with the possibility to load bioactive and therapeutic compounds. Here, an overview of different strategies used to prepare bioactive and osteoinductive injectable calcium phosphates (CaP) is reported[1]. The first system concerns the loading of an osteoinductive hyperbranced nanostructures as phosphoserine-tethered poly(ε-lysine) dendrons (G3-K PS) in CaP gels with and without strontium (Sr) element used to reduce the bone resorption (G3KPS-CaP, G3KPS-SrCaP). The second one is based on the use of antimicrobial injectable materials (IL-CaP). It has been demonstrated that some imidazolium ionic liquids (ILs) have antimicrobial activity against some different clinically significant bacterial and fungal pathogens.

EXPERIMENTAL METHODS

For both systems, CaP materials were synthesized by sol-gel approach at room temperature by using distilled water as solvent. The first system was obtained by loading freeze-dried G3-K PS semi-dendrimers, in ethanol solution (5 mg mL^{-1}) at 1% (w/w), to CaP and Sr-CaP under 200 rpm and 37 °C stirring until gelation occurred. In the second system, ILs at different alkyl chain length [C_nMIm]Cl (and C_n= $C_nH(2n+1)$; n= 4, 10, 16), at 1.0 and 2.0 wt%, were loaded in the gelling CaP. For both systems, morphological analysis (TEM FEI Tecnai G12 Spirit Twin model) and X-Ray diffraction were performed. The handling properties of the pastes were analyzed on the basis of their injectability and moulding. Furthermore, *in vitro* biological investigations to evaluate the effect of therapeutic compounds on bioactive and osteogenic properties were investigated by *in vitro* cell culture models using Elisa assay and RT-PCR analyses. Furthermore, the first system was validated by *in vivo* osteoporotic model using ovariectomized female Sprague Dawley rats. Immunohistochemistry analysis, SEM and micro-CT were performed to evaluate the new bone tissue formation and osteointegration. Meanwhile, for the second system, the effect to prevent the biofilm formation by using fungi (C. albicans, C. tropicalis) and bacteria (E. Coli, S. Aureus) was also analyzed.

RESULTS AND DISCUSSION

In this study, injectable bone substitute materials integrating G3-K PS or ILs were successfully synthesized by sol-gel approach. For G3KPS-CaP, both *in vitro* and *in vivo* findings showed that the integration of hyperbranched nanostructures would downregulate Cxcl9 gene and protein expressions to achieve an enhanced bone regeneration effect, with respect to a higher BMD and BV/TV. Immunohistological staining of Cxcl9, Runx2 and RANKL proteins were also conducted. The positive expression of Cxcl9 seemed to be less in G3KPS-CaP and G3KPS-SrCaP groups. Runx2 and RANKL positive expressions were more in G3KPS-CaP group than others. The result was in accordance with *in vitro* gene and protein expression and *in vivo* serum biomarker analysis. However, no additional benefit to osteoporotic bone regenerating ability of G3KPS-CaP material was found with Sr incorporation. For IL-CaP system, the materials induced a pre-osteoblast differentiation at short time (ALP, 3 days) in basal conditions, and stimulated osteocalcin expression after 14 days of cell culture. The expression of osteogenic markers increased with an increasing IL N-alkyl chain-length. The antimicrobial studies demonstrated that IL-CaP at long alkyl chain, at 48hrs of incubation time, showed antimicrobial and antifungal activity without biofilm production.

CONCLUSION

The results indicated that sol-gel technology allows to synthesize therapeutic and multifunctional injectable CaP materials which can become high-performance bone substitutes for the treatment of bone defects.

REFERENCES

1. Raucci M.G., *et al*., Adv. Healthc. Mater., 9: 2000349, 2020.

ACKNOWLEDGMENTS

The authors would like to thank the Progetto Premiale di AREA SCIENCE PARK "OPEN LAB - A System of Open Research Facilities" and *H2020-MSCA-RISE-2016*, SECOND.R.I., Grant Agreement No 734391 for financial support.

Tailoring hydroxyapatite bio-ceramic feedstock properties for masked stereolithography 3D printing

Pedro Navarrete-Segado[1,2*], David Grossin[1], Mallorie Tourbin[2], Christine Frances[2]

[1] CIRIMAT, Université de Toulouse, CNRS, 4 Allée Émile Monso, 31030, Toulouse Cedex 4, France
[2] Laboratoire de Génie Chimique, Université de Toulouse, CNRS, 4 Allée Émile Monso, 31432, Toulouse Cedex 4, France
[*] pedro.navarrete@imdea.org

INTRODUCTION

Hydroxyapatite (HA) bio-ceramic is a well-known material in bone tissue engineering and bone defect repair due to its good biocompatibility and bioactivity. Bio-ceramic scaffolds with an interconnected pore network and both porous micro and macroarchitecture are preferred to improve bone cell vascularization and attachment for their growth in all three dimensions. Additive manufacturing (AM) technologies allow the production of scaffolds with defined and reproducible internal structures. Depending on the AM technique, the process basis, methodology, and primary feedstock properties can vary widely [1]. Masked stereolithography (mSLA), also called liquid crystal display (LCD) 3D printing, as part of the VAT photopolymerization category of AM technologies, uses a UV-light source to cross-link a photocurable resin feedstock. This resin comprises monomers, diluent, photoinitiator, photoabsorber, and various additives such as ceramic powders. Ceramic particle properties affect photocurable resins reactivity, rheology, and stability. Particles in the nano to micro-scale, with low specific surface area and quasi-spherical morphology, are usually preferred [2]. However, the production of highly loaded (≥50 wt. %) HA photocurable resins, which would reduce the shrinkage of the green bodies and increase the sintering efficiency, needs accurate tailoring of the particles to obtain the most outstanding performance in terms of slurry viscosity (<5 Pa.s at a low shear rate, 1-10 s^{-1}) [3], and dispersion stability (Turbiscan stability index <2) [4]. Additionally, the design of a debinding-sintering strategy that controls the gas diffusion and avoids the formation of cracks is highly relevant to obtain sintered bio-ceramic scaffolds with dimensional accuracy and suitable mechanical properties.

EXPERIMENTAL METHODS

This communication discusses the preparation of highly loaded resins by tailoring their properties to make them stable and processable in an mSLA apparatus. Starting from a commercial resin Dentifix-3D (High-reactive), the effect of PEG200 as a reactive diluent on its rheology was evaluated. Also, HA particles with a controlled size were produced through their synthesis and comminution via two different milling processes. The properties of the suspensions prepared with three different particle size distributions were assessed to obtain the most outstanding values in terms of rheology and stability before printing. A debinding-sintering process was designed for sintering the printed parts. Several characterizations were performed to evaluate the applicability of the sintered bio-ceramic scaffolds in bone tissue engineering.

RESULTS AND DISCUSSION

The addition of 25 wt. % of PEG200 and the tailoring of hydroxyapatite powders were required to lower the viscosity and increase the particle stability of the suspensions. The debinding-sintering step (with a maximum of 1250ºC) effectively avoided the formation of cracks during the pyrolysis of the resin and sintering of the printed parts. A controlled total porosity of 35 vol. % and compression strength of 4.9 ± 0.3 MPa were obtained for the printed scaffolds with a slow degradation rate due to the high degree of crystallinity and intrinsic stability of the hydroxyapatite phase.

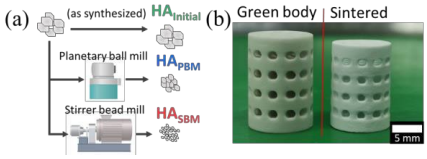

Figure 1. (a) Preparation of the different HA powders under study and (b) HA bio-ceramic scaffolds (before and after the debinding-sintering process).

CONCLUSION

The tailoring of HA particles was crucial for the processability of the highly-loaded ceramic suspensions. Successfully printed HA scaffolds showed promising results (mechanical, macro-, and microstructural properties) for their applications as minor or non-load bearing implants requiring slow resorption properties.

REFERENCES

[1] L.C. Hwa, S. Rajoo, A.M. Noor, N. Ahmad, M.B. Uday, Curr. Opin. Solid State Mater. Sci. 21 (2017) 323–347.
[2] L. Xing-Bang, Z. He, Z. Jing-Xian, D. Yu-Sen, J. Dong-Liang, J. Inorg. Mater. (2019) 13.
[3] F.P.W. Melchels, J. Feijen, D.W. Grijpma, Biomaterials 31 (2010) 6121–6130.
[4] S.Y. Song, M.S. Park, D. Lee, J.W. Lee, J.S. Yun, Mater. Des. 180 (2019) 107960.

ACKNOWLEDGMENTS

This project has received funding from the European Union's Horizon 2020 research and innovation programme under the Marie Skłodowska-Curie grant agreement No 764935.

Novel borosilicate bioactive glass scaffolds for bone implants

Agata Szczodra[1*], Amel Houaoui[1], Susanna Miettinen[1], Jonathan Massera[1]
[1]Faculty of Medicine and Health Technology, Tampere University, Tampere, Finland
[*]agata.szczodra@tuni.fi

INTRODUCTION

Bioactive glass (BAG)-bone substitutes are limited to powders, granules, and putties. Indeed, commercial BAGs e.g., S53P4, demonstrate crystallization tendencies during sintering, thus inhibiting the processing of porous construct. While glasses such as 13-93 have been developed and FDA approved, those glasses, with improved thermal stability, have low reaction rate and bioactivity[1]. To overcome these problems, borosilicate glasses were developed. High boron content was found efficient in producing glasses with fast conversion into hydroxyapatite and with thermal properties allowing sintering into porous 3D scaffolds, with porosity (pore size, interconnection, and overall porosity) adequate for bone tissue engineering. Moreover, B_2O_3 substitution for SiO_2 showed strong ability to stimulate osteogenic commitment and upregulate endothelial markers[2]. However, uncontrolled boron release was also linked with decreased cells attachment and proliferation, in static conditions. Aside from boron, strontium and magnesium have also been used to favor sintering while tailoring the dissolution rate and providing ions beneficial to the bone regeneration. Indeed, the addition of strontium has been shown to stimulate osteogenic response from human bone marrow mesenchymal stem cells[3]. Magnesium broadens the sintering window and consequently suppresses crystallization tendency of glass during processing[4]. Mg also improves bone density and helps to prevent fractures[4]. The aim of the present study was to 1) develop new borosilicate BAGs with tailored release of boron ions, 2) to evaluate their potential for manufacturing 3D porous scaffolds and 3) investigate their effect on viability, proliferation, morphology, and differentiation of Adipose stem cells (ASC).

EXPERIMENTAL METHODS

1. Scaffolds fabrication and characterization

Borosilicate glasses based on S53P4 and 13-93 compositions have been developed: B12.5MgSr (47.12 SiO_2–6.73 B_2O_3–6.77 CaO–22.66 Na_2O–1.72 P_2O_5–5 MgO–10 SrO (mol%)) and 1393B20 (43.68 SiO_2–10.92 B_2O_3–22.10 CaO–7.9 K_2O–6 Na_2O–1.7 P_2O_5–7.7 MgO (mol%)). The scaffolds were prepared by 3D-printing. The ink was made by mixing glass powder (<38 µm) and Pluronic 127 binder solution. After drying and sintering, scaffolds had average dimensions of 5.5mm x 6mm. The bioactivity of these glasses was investigated in Simulated Body Fluid (SBF) during a 2-week incubation.

2. Culture with ASC

To study the cytocompatibility of the scaffolds, Live/Dead assay was carried out. All scaffolds were sterilized and preincubated for 2 days in TRIS followed by 24h in αMEM. Next, scaffolds were seeded with 25.000 ASC and incubated for up to 1 week. Ions released in culture medium was assessed using ICP-OES. ASC proliferation is quantified using Cyquant. Alkaline Phosphatase (ALP) activity has been investigated. Finally, the cytoskeleton and nuclei of the ASC are stained, and cells morphology observed using confocal microscopy.

RESULTS AND DISCUSSION

All developed scaffolds were amorphous post-sintering and demonstrated precipitation of hydroxyapatite upon immersion in SBF. In Figure 1, fluorescent microscope images of ASC incubated with scaffolds for 7 days and stained using live/dead assay are shown. On B12.5MgSr scaffolds, it is observed that the cell density is lower than at the surface of the 1393B20 scaffolds, at 7 days. Cells proliferation and morphology, as well as ALP activity will be correlated to ion release over time in the culture medium.

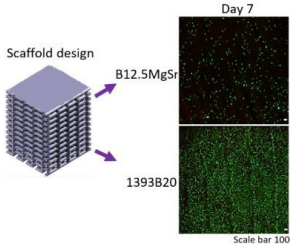

Figure 1. (Left) Design of 3D printed scaffolds. (Right) Live/Dead images of the top of the scaffolds after 7 days of culture with ASC (Scale bar 100µm).

CONCLUSION

Summarizing, B12.5MgSr and 1393B20 novel BAGs were successfully processed into 3D scaffolds with interconnected porosity. However, 1393B20 scaffolds appears to support ASC viability and proliferation more efficiently than the B12.5MgSr scaffolds. In conclusion, these new BAGs, and especially 1393B20 composition, are promising as 3D porous scaffolds for bone applications.

REFERENCES

1. Massera J. *et al*., J. Am. Ceram. Soc. 95:607-613, 2012
2. Qiang F. *et al*., J. Biomed. Mater. Res. 95A:164-171, 2010
3. Naruphontjirakul P. *et al*., Acta Biomater. 90:373-392, 2019
4. Watts S.J. *et al*., Non-Cryst. Solids 356: 517-524, 2010

ACKNOWLEDGMENTS

The authors would like to thank Jane and Aatos Erkko foundation and Academy of Finland for financial support.

New amorphous calcium ortho-/pyrophosphate biomaterial promotes bone repair of critical-sized calvarial defects in rat

Rebecca Landon[1], Maximilien Desbord[2], Robin Siadous[3], Ahmad Moustapha Diallo[1], Nathanael Larochette[1], Hanane El-Hafci[1], Jérémy Soulié[2], Joelle Amédée[3], Christèle Combes[2], Fani Anagnostou[1,3*]

[1] B3OA, CNRS UMR 7052, INSERM U1271, ENVA, Université de Paris, 75010 Paris, France,
[2] CIRIMAT, UMR 5085 INPT-CNRS-UPS, Université de Toulouse, ENSIACET, 31030 Toulouse, France
[3] BIOTIS, INSERM U1026, Université de Bordeaux, 33000 Bordeaux, France
[4] Service of Odontology-Pitié Salpêtrière Hospital, AP-HP et U.F.R. of Odontology, 75013 Paris, France
[*] fani.anagnostou@univ-paris-diderot.fr

INTRODUCTION

In maxillofacial surgery and orthopedics, the treatment of bone defects represents a major public health challenge. Autologous graft remains the "gold standard" treatment, but the insufficient quantity and donor site morbidity restricted their use. Bioactive materials, such as silicate-based bioactive glass (Bioglass®), are among the bone substitutes the most widely used as alternatives, for their osteogenic potential but their resorbability is limited. New amorphous biomaterial compositions containing mainly pyrophosphate and orthophosphate entities have been elaborated by soft chemistry[1]. Their biological interest is linked to the control of the resorption rate (through the orthophosphate/pyrophosphate ratio) by biochemical hydrolysis. The present study aimed to investigate the bone-repair effectiveness, the resorption rate, and the impact on the early bone healing of a gel-derived hydrated amorphous calcium/sodium pyrophosphate-based biomaterial with the chemical formula (Ca2+)1,57 (Na+)0,14 (H+)0,05 (PO43-)0,67 (P2O74-)0,33] (H2O)10,36 (NaPYG_030), (ratio ortho-/ pyrophosphate =3) using a critical-size model in rat calvaria.

EXPERIMENTAL METHODS

NaPYG-030 was synthesized according to a previously published protocole[1] and was tested for cytotoxicity against human mesenchymal stem cells using an MTT assay. To test the tissue response 72 Wistar rats (male 12 weeks old) were randomly distributed (n=6 per group; a total of 12 per time point). Circular 8 mm- diameter bone defects were created on calvaria. Defects were left empty (n=12), or filled either with NaPYG_030 (n=12) or with silicate-based bioactive glass Bioglass® (n=12), used as control. The radiopacity was evaluated *in vivo*, using micro-CT analyses, performed immediately after surgery and on days, 15, 30, and 60. Histological analyses were performed after the sacrifice of the animals at days 30 and 60 post-surgery. Tissue response, bone formation, and material resorption were assessed using non-decalcified histology. Other 36 animals randomly distributed (n=6 per group; a total of 12 per time period, i.e., 7, and 14 days after surgery) were needed to study the expression levels of selected inflammation-, angiogenesis-, and bone-related genes, in the defect's tissue using RT-PCR after animal sacrifice at 7 and 14 days post-surgery.

RESULTS AND DISCUSSION

In vivo follow-up of the defect's radiopacity volume, allowed us to study the kinetics of the residual implanted material and the newly formed bone volume. Results showed differences related to the bone substitute used. On days 30 and 60 post-surgery, the histological analysis showed an absence of inflammation and/or foreign body reaction and newly-formed bone around the particles of both implanted materials. However, while the mineralized tissue was in close contact with the Bioglass® particles, a thin layer of unmineralized tissue was observed at the interphase NaPYG_030-newly formed bone, suggesting an ongoing resorption process. Moreover, compared to the Bioglass®-filled defects, the NaPYG_030 group exhibited a significant ($p < 0.05$) decrease in radiopacity at all time points tested indicating NaPYG_030 resorbability. Moreover, the study of the transcriptional profile of the genes showed that compared to the Bioglass®, in the presence of NaPYG_030 the expression of TNFα, IL-6, and IL-8, ANG, PECAM, and VWF as well as that of ALP, BGLAP, SP7, and Col1A1 was significantly decreased on the day 14 post-surgery.

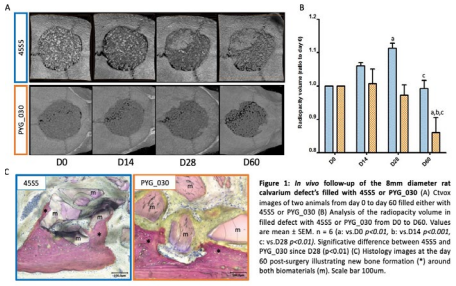

Figure 1: ***In vivo*** **follow-up of the 8mm diameter rat calvarium defect's filled with 4555 or PYG_030** (A) Ctvox images of two animals from day 0 to day 60 filled either with 4555 or PYG_030 (B) Analysis of the radiopacity volume in filled defect with 4555 or PYG_030 from D0 to D60. Values are mean ± SEM. n = 6 (a: vs.D0 *p<0.01*, b: vs.D14 *p<0.001*, c: vs.D28 *p<0.01*). Significative difference between 4555 and PYG_030 since D28 ($p<0.01$) (C) Histology images at the day 60 post-surgery illustrating new bone formation (*) around both biomaterials (m). Scale bar 100um.

CONCLUSION

In conclusion, the results obtained showed the biological performance of a pyrophosphate-based amorphous biomatrial tested in the critical-size defects and indicated that pyrophosphate species may enhance the resorption rate. The NaPyG-30 influenced the early critical events involved in bone regeneration by modulating specifically the expression of genes pertinent to inflammation, angiogenesis and osteogenesis, and exhibited both, efficient bone-forming capacity and resorbability making it an attractive bone substitute to repair defects in the maxillofacial area. Further studies are needed to elucidate if and how pyrophosphate species could provide controlled levels of the inorganic components for mineralization.

REFERENCES

1. Mayen, L. *et al.*, Acta Biomater.103,333-345, 2020

ACKNOWLEDGMENTS

The authors would like to thank l'Agence Nationale de la Recherche (ANR-16-CE19-0013)

Injectable Mesoporous Bioactive Nanoparticles for Bone Regeneration in Osteoporotic Model

Daniel Arcos[1,5*], Natividad Gómez-Cerezo[1,5], Laura Casarrubios[2], María José Feito[2], Melchor Saiz-Pardo[3], Luis Ortega[3], David de Pablo[3], Idoia Díaz-Güemes[4], Blanca Fernández-Tomé[4], Silvia Enciso[4], Francisco M. Sánchez-Margallo[4], M. Vallet-Regí[1,5], María Teresa Portolés[2,5]

[1]Dep. of Chemistry in Pharmaceutical Sciences. IdIS Hosp 12 Octubre. Univ. Complutense, Madrid, Spain
[2]Dep. of Biochemistry and Molecular Biology. IdISSC. Univ. Complutense, Madrid, Spain
[3]Pathology Department, Hospital Clínico San Carlos, Madrid, Spain.
[4]Centro de Cirugía de Mínima Invasión Jesús Usón, NANBIOSIS. Cáceres, Spain.
[5]CIBER de Bioingeniería, Biomateriales y Nanomedicina, CIBER-BBN, 28040 Madrid, Spain
arcosd@ucm.es

INTRODUCTION

One of the most interesting nanotechnology based strategies for the osteoporosis treatment and bone regeneration therapies is the development of new formulations based in mesoporous bioactive glass nanoparticles (MBG-NP)[1]. The small size of MBG-NP facilitates the implantation as injectable platforms[2], so that they could be administered as intraosseous biomaterials by means of minimally invasive surgery. As far as we know, no study has tested the bone regeneration capability of MBG-NP in osteoporotic animal models. In order to evaluate the potential of these nanoparticles for the treatment of defects in osteoporotic bone, we have prepared MBG-NP containing the antiosteoporotic drug ipriflavone (IP). After the *in vitro* study of the expression of inflammatory genes, the MBG-NP were incorporated into hyaluronic acid and intraosseous injected in osteoporotic rabbits, thus evaluating their bone regeneration capability as well as the potential inflammatory adverse effects.

EXPERIMENTAL METHODS

MBG-NPs $75SiO_2$-$20CaO$-$5P_2O_5$ (%mol) MBG-NPs were prepared by hydrolysis and condensation in the presence of poly(styrene)-block-poly(acrylic acid) and CTAB under alkaline conditions[3]. IP was incorporated by the impregnation method, soaking MBG-NP in a saturated solution of IP in acetone. MBG-NP were characterized by SEM, TEM-EDX, N_2 adsorption and FTIR spectroscopy. Expression of eight pro- and anti-inflammatory genes was quantified by QPCR in macrophages treated *in vitro*.

Twelve adult female New Zealand rabbits were used in this study. A laparoscopic bilateral ovariectomy was performed and methylprednisolone sodium succinate was administered during 4 weeks in order to reproduce similar conditions as osteoporosis in humans. MBG-NPs were suspended in hyaluronic acid at the operation room and injected into the rabbit's bone. After 12 weeks of implantation, the bone segments containing the defect were dissected and histologically analyzed.

RESULTS AND DISCUSSION

Figure 1 shows the SEM and TEM images of MBG-NP evidencing the regular and spherical morphology, as well as a porous structure consisting in a large cavity surrounded by a mesoporous shell with radial distribution. N_2 adsorption analysis evidenced a surface area and porosity values of 543 m^2/g and 0.43 cm^3/g, respectively.

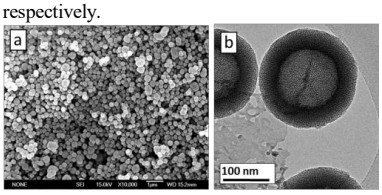

Figure 1. SEM (a) and TEM (b) images of MBG-NPs.

In vitro studies did not show adverse inflammatory effects in terms of gene expression. Figure 2 shows the histological analysis accomplished. Only those defects filled with MBG-NPs clearly show new bone formation. In addition, presence of osteoblast lining and osteoclasts could be also observed No significant differences were observed for MBG-NP loaded with IP, although the presence of this drug induced a slightly higher ossification and trabeculae thickness.

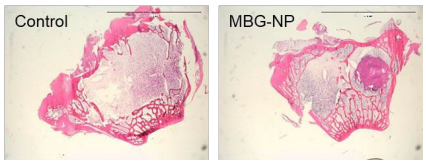

Figure 2. Histological images of control defect (left) and defect filled with injectable MBG-NP

CONCLUSION

Mesoporous bioactive nanoparticles can be incorporated in hyaluronic acid to be injected as filling material in bone defects. This injectable material regenerates bone even under osteoporotic conditions.

REFERENCES

1. Hajiali H. *et al*., Nanoscale. 13: 10266-10280, 2021
2. Wei D. *et al*., Curr. Osteopor. Rep. 14: 239-247, 2016
3. Li Y, et al., Chem. Eur. J. 21: 8038–8042, 2015

ACKNOWLEDGMENTS

This research was funded by the projects MAT2016–75611-R, PID2020-11709RB-I00, Advanced Grant VERDI; ERC-2015-AdG Proposal No. 694160.

Influence of Bioceramic Scaffold Macro-Architecture on Loaded Mesenchymal Stromal Cell Viability and Local Inflammation in a Rat Subcutaneous Model

Alexandra Villard[1], Baptiste Charbonnier[2,*], Manon Maroquenne[1], Guoyan Xian[1], David Marchat[3], Hervé Petite[1], Morad Bensidhoum[1] Delphine Logeart-Avramoglou[1], Esther Potier[1]

[1] Université de Paris, CNRS UMR 7052, INSERM U1271, B3OA, Paris, France
2. Nantes Université, INSERM UMRS 1229, RMeS, Nantes, France
3. Mines Saint-Etienne, Univ Lyon, Univ Jean Monnet, Etablissement Français du Sang, INSERM U1059, Sainbiose, Saint-Etienne, France
[*] baptiste.charbonnier@univ-nantes.fr

INTRODUCTION

Bone tissue engineering focuses on bone repair using osteocompetent cells, mainly mesenchymal stromal cells (MSCs), and biodegradable, porous scaffolds. In this therapeutical strategy, MSCs are loaded into scaffolds devoid of a pre-existing vascular network, and thus encounter an ischemic environment upon implantation. The resulting oxygen and nutrient deprivation can alter both MSC survival and functions, compromising the repair potential of tissue engineered products. Internal mass transport[1] and vascular invasion[2], both regulating nutrient supply and waste removal within the scaffold, can be modulated by the scaffold macro-scale architecture.

The present study aims, therefore, to evaluate the effects of different macro-architectures of porous bioceramic scaffolds on MSC viability and functions (i.e. modulation of local angiogenesis and inflammation) after sub-cutaneous implantation in rats.

EXPERIMENTAL METHODS

Carbonated hydroxyapatite-based scaffolds were produced using a dedicated additive manufacturing technology[3] to fit the anatomic shape of a 5-mm-long, femoral defect in rats. Five porous macro-architectures were tested: two mathematically defined (gyroid structures with macropores of 250 (*G250*) and 800 (*G800*) µm in diameter), two bioinspired (mimicking trabecular bone (*T*) and porous *acropora* coral (*A*) structures), and one reproducing the random porosity (*RP*) of commercial calcium phosphate granules (standard care). Scaffolds were loaded with 1.5 million of eGFP-Luc Lewis rat MSCs and implanted sub-cutaneously in Lewis rats (12-14 weeks old, female). Bioluminescence signal was recorded before and after 7, 10, and 14 days of implantation (n=6-16). At D7 and D14, scaffolds were explanted and analyzed for the expression level of genes involved in the modulation of angiogenesis (VEGF, FGF2, PDGFa, VEGF-R2) and inflammation (CD68, IL1b, IL6, TNFa, iNOS, IL10, TGFb, Arg1, CD206) (n=3-5).

RESULTS AND DISCUSSION

T and *RP* scaffolds showed a better cell retention before implantation. Although *G800* and *T* scaffolds tended to improve MSC viability (estimated with BLI signal) at D7, no significant differences were found between the architectures after either 7, 10 or 14 days of implantation. For all architectures, MSC viability decreased with implantation time, reaching 53.8% of viability relative to D1 for *A* scaffold but falling down to 6.7% for *T* scaffolds after 14 days of implantation.

Expression levels of genes involved in angiogenesis and M0 profile (CD68) were similar for all architectures. *A* scaffolds tended to increase the M1 macrophage profile (trends for IL6 and iNOS, significant difference for TNFa gene expression) at D7, while *T* scaffolds tended to improve the M2 macrophage profile (trend for CD206 and significant difference for TGFb gene expression) at D14 (Fig.1). It is unknown, however, if the architectures are affecting MSC immunomodulatory functions or directly modulating the host response. Experiments with acellular scaffolds are ongoing.

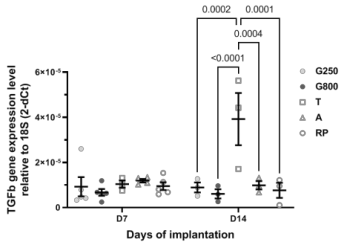

Fig.1. TGFb gene expression levels after 7 and 14 days of implantation. Values are mean +/- SEM.

CONCLUSION

The different tested architectures did not significantly improve MSC viability upon implantation, but could modulate the local inflammatory response. This study suggests that complementary strategies, such as glucose supplementation[4], are needed to further improved MSC survival after implantation in ischemic sites. It also hints that the macro-architecture of bioceramic scaffolds can be tuned to promote a favorable host response toward a pro-healing phenotype and thus improve the bone repair potential of MSC-based tissue engineered products.

REFERENCES

1. Melchels F.P.W. *et al.*, Acta Biomater. 6:4208–17, 2010
2. Magnaudeix A. *et al.*, Acta Biomater. 38: 1789–91, 2016
3. Charbonnier B. *et al.*, Adv Eng Mater. 18:1728-37, 2016
4. Deschepper M. et al., Stem Cells. 31:526-35, 2013

ACKNOWLEDGMENTS

Financial support was received from CNRS PEPS 2017 Archibone.

Synthesis of Octacalcium Phosphate by Co-Precipitation Method

Rajan Choudhary[1,2], Abhishek Indurkar[1,2], Kristaps Rubenis[1,2], Janis Locs[1,2]

[1]Rudolfs Cimdins Riga Biomaterials Innovations and Development Centre of RTU, Institute of General Chemical Engineering, Faculty of Materials Science and Applied Chemistry, Riga Technical University, Pulka St 3, Riga, LV-1007, Latvia

[2]Baltic Biomaterials Centre of Excellence, Headquarters at Riga Technical University, Kalku Street 1, LV-1658, Riga, Latvia

Email: rajan.choudhary@rtu.lv

INTRODUCTION

Octacalcium phosphate (OCP, $Ca_8H_2(PO_4)_6 5H_2O$) has been known as a precursor of biological apatite crystals in the hard tissues. It has been indicated that hydroxyapatite and tri-calcium phosphate possesses inferior osteoconductivity than OCP[1]. The synthesis of OCP is very challenging and time-consuming. Molarity, temperature, pH, stirring rate, and order of reagent addition affect the synthesis of OCP. The formation of undesirable phases is often observed due to variations in these parameters[2].

EXPERIMENTAL METHODS

The current report aims to prepare octacalcium phosphate by co-precipitation method using calcium acetate and phosphate buffer. The Ca/P ratio was taken as 1.33. An optimum amount of sodium hydroxide was added to the reaction mixture to maintain the pH at 6 for four hours at 60 °C. The precipitate was centrifuged, freezed in liquid nitrogen, and lyophilized.

RESULTS AND DISCUSSION

The XRD pattern of the sample was found to be composed of low crystalline OCP (Fig. 1). The characteristic peaks were found to match with the standard octacalcium phosphate pattern [ICDD card no. 00-026-1056] confirming the formation of OCP. The surface morphology of OCP was observed as broken plate-like structures scattered throughout the surface (Fig. 2).

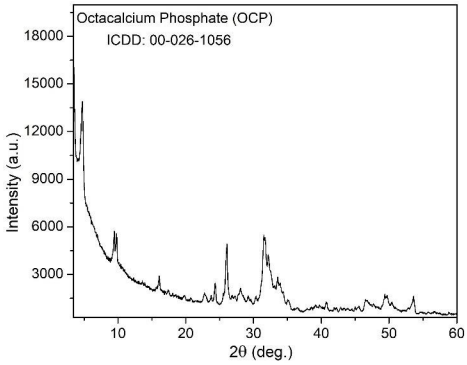

Fig. 1 XRD pattern of prepared octacalcium phosphate

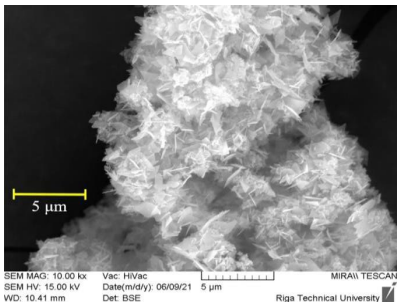

Fig. 2 Scanning Electron Microscopy images of prepared octacalcium phosphate

CONCLUSION

The conditions required for the synthesis of OCP were optimized and OCP can be prepared within 4 hours. The most common method used for the synthesis of OCP is dissolution precipitation which takes at least 2-3 days for completion of the entire process. Thus, current study suggests that the synthesis duration of OCP was reduced from days to hours.

REFERENCES

1. Suzuki O. *et al.,* Dent. Mater. J. 39:187–199, 2020
2. Chow LC. *et al.,* Octacalcium Phosphate. Monographs in Oral Science. Basel, Karger, 18:94-111, 2001

ACKNOWLEDGMENTS

The authors acknowledge financial support from the European Union's Horizon 2020 research and innovation programme under the grant agreement No. 857287.

Functionalized 3D-Printed Silk-Hydroxyapatite Scaffolds for Enhanced Bone Regeneration with Innervation and Vascularization

Vincent Fitzpatrick[1*], Zaira Moldes Martin[1], Anna Deck[1], Ruben Torres[1], Riley Patten[1], Anne Valat[1], David Kaplan[1]

[1]BME department, Tufts University, Medford, Massachusetts, U.S.A.
[*] vincent.fitzpatrick@tufts.edu

INTRODUCTION

The goal of this study was to generate functionalized 3D-printed scaffolds for bone regeneration using silk/hydroxyapatite bioinks and osteoinductive, proangiogenic and neurotrophic growth factors or morphogens for accelerated bone formation. 3D printing was utilized to generate macroporous scaffolds with controlled geometries and architectures that promote osseointegration. We build on the knowledge that the osteoinductive factor Bone Morphogenetic Protein-2 (BMP2) can also positively impact vascularization, Vascular Endothelial Growth Factor (VEGF) can impact osteoblastic differentiation[1], and that Neural Growth Factor (NGF)-mediated signaling can influence bone regeneration[2,3].

EXPERIMENTAL METHODS

We developed and characterized a silk-based bone cement with mechanical properties close to those of bone. We assessed our ability to 3D print this material to generate structures with a controlled geometry, macroporosity, and our ability to adapt the printing process to patient-tailored scaffolds. We investigated the cytocompatibility and osteoconductivity of these constructs. We further assessed functions on the 3D printed construct via the osteogenic differentiation of human mesenchymal stem cells. We also examined the migration and proliferation of human umbilical vein endothelial cells, and the proliferation of human induced neural stem cells.

RESULTS AND DISCUSSION

The silk/hydroxyapatite bioink could be printed with control over geometry, internal architecture and porosity (**Fig. 1**). The scaffolds provided mechanical properties suitable for bone and the materials were cytocompatible, osteoconductive and maintained the activity of the morphogens and cytokines. Synergistic outcomes between BMP-2, VEGF and NGF in terms of osteoblastic differentiation in vitro were identified, based on the upregulation of genes associated with osteoblastic differentiation (Runt-related transcription factor-2, Osteopontin, Bone Sialoprotein). In vivo studies were carried out to assess the biocompatibility and bone regeneration capability of these 3D printed constructs. New designs and internal architectures were exploited using 3D printing, to maximize the mechanical properties of the bone constructs.

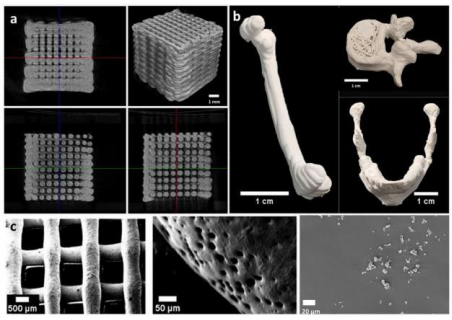

Figure 1: Characterization of the silk-HAP material. (a) Microcomputed tomography of a 3D printed 10 × 10 × 10 mm cube, showing the general aspect of the cube (top right), regular filament distribution and interconnected pores. Scale bar: 1 mm. (b) 3D-printed anatomical structures: femur (left); vertebra (right, top); mandible (right, bottom). Scale bar: 1 cm. (c) Scanning electron micrograph (SEM) of a 3D-printed construct (left), showing control of filament deposition and macroporosity; of the surface of the filament, showing microporosity (center); of the hydroxyapatite (HAP) powder used for the silk-HAP bone cement, showing particle distribution (right).

CONCLUSION

The specific cell responses observed here are key steps towards the development of the next generation of functionalized, 3D printed bone scaffolding to promote multicellular responses in the context of bone tissue system regeneration. These results are expected to have a strong impact in bone regeneration in dental, oral and maxillofacial surgery.

REFERENCES

1. N.C. Keramaris, G.M. Calori, V.S. Nikolaou, E.H. Schemitsch, P. V. Giannoudis, Fracture vascularity and bone healing: A systematic review of the role of VEGF, Injury. 39 (2008)
2. R.E. Tomlinson, Z. Li, Q. Zhang, B.C. Goh, Z. Li, D.L.J. Thorek, L. Rajbhandari, T.M. Brushart, L. Minichiello, F. Zhou, A. Venkatesan, T.L. Clemens, NGF-TrkA Signaling by Sensory Nerves Coordinates the Vascularization and Ossification of Developing Endochondral Bone, Cell Rep. 16 (2016)
3. R.E. Tomlinson, Z. Li, Z. Li, L. Minichiello, R.C. Riddle, A. Venkatesan, T.L. Clemens, NGF-TrkA signaling in sensory nerves is required for skeletal adaptation to mechanical loads in mice, Proc. Natl. Acad. Sci. U. S. A. 114 (2017)

ACKNOWLEDGMENTS

We thank the NIH (P41EB027062 and R01AR068048) for support of this work.

Synthesis of nanosized silicoaluminophosphate (SAPO) zeolites with osteoinductive properties.

Cristian Covarrubias[1], Camila Torres, Miguel Maureira, Rocío Orellana

[1]Laboratory of Nanobiomaterials, Research Institute for Dental Sciences, Faculty of Dentistry, University of Chile, Santiago, Chile.
* ccovarrubias@odontologia.uchile.cl

INTRODUCTION

Novel osteoinductive particles for bone tissue regeneration applications are demanded. Bioceramics such as bioactive glasses are osteoinductive, however most of the ceramics present limited capacity to promote bone cell diferentiation[1]. Zeolites are crystalline and nanoporous ceramic materials scantly explored for bone tissue applications[2]. Chemical composition, nanoporous architecture, particle size and shape of zeolites can be tuned to generate a ceramic with osteoinductive properties.

In this work, the synthesis of silicoaluminophosphate (SAPO) zeolites with osteoinductive properties was studied. The effect of structural parameters such as porous framework type, calcium/lithium modification, size and shape of the zeolite crystals were explored.

EXPERIMENTAL METHODS

Zeolite synthesis.

MeSAPO-34 and MeSAPO-5 zeolite types were hydrothermally synthesized at 200 ºC using a Al_2O_3-P_2O_5-SiO_2-H_2O-MeOx (Me: Li or Ca). As-synthesized zeolites were calcined at 550 ºC for 6 hours. Some zeolites samples were also subjected to cation exchange using Li^+ and Ca^{2+} ions. Structural characterization was performed by XRD and SEM/EDX.

Bioactivity in simulated body fluid (SBF).

The ability of zeolites to promote the formation of apatite in SBF was carried out according to the method reported by Kokubo[3]. Apatite formation was analyzed by ATR-FTIR spectroscopy and SEM/EDX.

Cell culture.

Cell cultures were performed using MC3T3 osteoblast precursor cell line. Cytocompatibility of zeolites particles was assessed using the MTS cell viability kit for 3, 7, and 14 days. The capacity of zeolites to induce osteogenic cell differentiation was evaluated by measuring the alkaline phosphatase (ALP) activity at 7 and 14 days and the gene expression of Runx2 by RT-PCR at 7 days of incubation. Bioactive glass nanoparticles (nBG) were used as osteoinductive bioceramic of reference.

RESULTS AND DISCUSSION

Fig. 1 shows the structural and compositional analyses of the synthesized zeolites. XRD patterns match well with the crystalline structure of SAPO-5 and SAPO-34 with AFI and CHA zeolite type topographies, respectively[4]. Hexagonal (SAPO-5) and cubic (SAPO-34) zeolite crystals have layered morphology of 40 – 170 nm thick and EDX composition constituted by Si, Al, P, O, traces of C, and Ca or Li as modifier element.

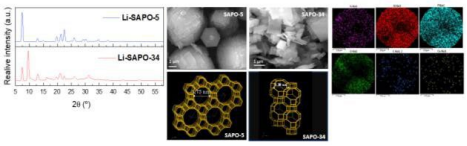

Fig. 1. XRD, SEM and EDX analysis of representative SAPO zeolite synthesis products.

Apatite formation by immersion in SBF was detected by ATR-FTIR only for SAPO-5 zeolites. MTS assays demonstrated that there are not differences in the viability of MC3T3 cells cultured with zeolites as compared to that of control without material. Highest ALP activity was obtained with Ca^{2+} and Li^+ cation exchanged SAPO zeolites (**Fig. 2a**) at 14 days of incubation, which was comparable to those produced by nBG. Preliminary results also show that the expression of Runx2 is specially upregulated with SAPO zeolites modified with Li^+ cations (**Fig. 2b**).

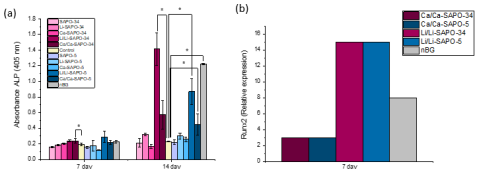

Fig. 2. ALP activity and Runx2 expression of MC3T3 cells cultured with SAPO zeolites and nBG.

CONCLUSION

Nanodimensional SAPO type zeolites promote the formation of apatite in SBF and exhibit osteoinductive properties by stimulating the osteogenic cell differentiation, particularly those modified with Ca or Li as extrafamework cations.

REFERENCES

1. LeGeros R.Z. *et al.*, Chem. Rev. 108:4742-4753, 2008.
2. Bedi R. S. *et al.*, Adv. Funct. Mater.19:3856, 2009.
3. Kokubo T. *et al.* Biomaterials 27: 2907–2915, 2006.
4. Baerlocher Ch. *et al.*, Atlas of Zeolite framework types, sixth revised edition, Elsevier, Amasterdam, 2007, pp. 96-97, 140-141.

ACKNOWLEDGMENTS

The authors would like to thank the National Agency for Research and Development (ANID) (FONDECYT Grant 1211314) in Chile for providing financial support to this project.

Fibronectin Adsorption On Surface-Modified Bioactive Glass S53P4 And Its Implication On Human Adipose Stem Cells Behavior

Virginia Alessandra Gobbo[1*], Amel Houaoui[1], Agata Szczodra[1], Paula Turkki[1], Vesa P. Hytönen[1], Susanna Miettinen[1], Jonathan Massera[1]

[1] Faculty of Medicine and Health Technology, Tampere University, Tampere, Finland
*virginiaalessandra.gobbo@tuni.fi

INTRODUCTION

Bioactive glasses (BGs) are a promising class of biomaterials for applications in bone tissue regeneration. Their unique dissolution/reaction in physiological fluids leads to osteoconductive/ osteoinductive cells response[1]. Moreover, BGs composition can be tailored to further control their reactivity and bioactivity, or to include therapeutic ions[2,3]. To further control their physico-chemical properties, BGs can be superficially treated to expose functional groups or to graft specific molecules of interest. This makes BGs optimal substrates for biomolecule adsorption, with the final goal to improve their biocompatibility or to impart ulterior functionalities to the final device[4,5]. However, despite the wide literature about BGs and their chemical properties, their interaction with proteins, extremely critical for the success of the implant, has not been deeply investigated yet. The control over protein adsorption would enhance the biological response and, consequently, the fate of the implant. The current study aims to investigate how BGs surface physico-chemical properties are influencing protein adsorption kinetics, and how adsorbed proteins on BG surface are affecting cell behavior.

EXPERIMENTAL METHODS

In the current work, S53P4 (FDA approved) was exposed to four different surface pre-treatments: 72 hour-soaking in 0.05 M TRIS, 72 hours-soaking in SBF, APTES grafting and quaternized APTES (Q-APTES) grafting (Figure1).

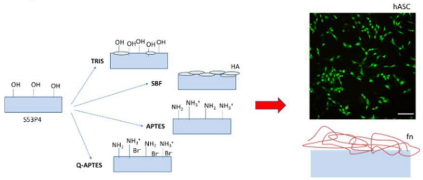

Figure 1. On the left: surface pre-treatments implemented on S53P4. On the right: adsorption of fn on untreated S53P4 and fluorescent image of hASC. The scalebar corresponds to 200 µm.

Change in surface chemistry was investigated by contact angle, zeta potential, XPS, FTIR and EDX/SEM. The impact of surface modification on protein adsorption was studied using fibronectin (fn) as a model protein in static and dynamic conditions. Protein adsorption was assessed by confocal microscopy (static) and change in surface charge (dynamic). Finally, the impact of fn adsorption on S53P4 was evaluated *in vitro*, using human adipose stem cells (hASC). Cells were directly seeded on the samples, and adhesion, proliferation and morphology were analyzed.

RESULTS AND DISCUSSION

Treatment in TRIS led to the formation of surface rich in Si-OH functional groups while incubation in SBF led to the precipitation of a thick hydroxyapatite layer. Treatments with APTES and Q-APTES were successful as demonstrated by XPS analysis, as characteristic nitrogen and bromine peaks were detected.

In static condition, while all surfaces promoted adsorption of fn, surface treated with APTES and Q-APTES showed improved protein adsorption. This was confirmed by a higher fluorescence intensity and a more homogeneous coverage of the silanized surfaces by fn. The dynamic test confirmed the static results. Indeed, the surface charge, at the surface of the functionalized glasses, increased rapidly to a value close to the one of fn ((30.17 ± 4.23) mV), thus demonstrating rapid fn adsorption under flow. However, the dynamic test raises the question of the stability of the APTES-grafted surfaces, when put in contact with the continuous flow of the electrolyte.

Cell culture tends to indicate that adsorbed fn has a positive impact on cell adhesion and proliferation. Experiments are ongoing to assess change in gene expression induced by the functional groups and/or fn.

CONCLUSION

Overall, fn adsorption kinetics was controlled through the surface physico-chemical properties of S53P4. Fn adsorption improved cytocompatibility. Further studies are needed to assess cells behavior on fn-coated samples.

REFERENCES

1. Notingher I. *et al.*, Mater. Charact., 49:255-260, 2003
2. Massera J. *et al.*, J. Non-Cryst. Solids, 425 :52-60, 2015
3. Hupa L. *et al.*, J. Non-Cryst. Solids, 432(A):41-46, 2016
4. Ciraldo F.E. *et al.*, Acta Biomater., 75:3-10, 2018
5. Ferraris S. *et al.*, Applied Surface Science, 475 :43-55, 2019

ACKNOWLEDGEMENTS

This research is part of "PREcision Medicine for mUsculoskeletal Regeneration, prOSthetics, and Active ageing, PREMUROSA". The authors would like to thank H2020-MSCA-ITN-2019 (grant agreement No. 860462) for providing financial support to the project.

Surface modified mesoporous bioactive glass:

effect of silanization on bioactivity and protein interaction

Anita Lucas[1*], Khalil Aneb[1,2], Soizic Chevance[1], Odile Merdrignac[1], Bertrand Lefeuvre[1], Nouha Letaïef - Ounalli[3], Théodore Berthelot[1]

[1] Institut des Sciences Chimiques de Rennes, UMR CNRS 6226, Université de Rennes1, 263 avenue du Général Leclerc, 35042 Rennes, France.

[2] Laboratoire de Génie de l'Environnement, Département de Génie des Procédés, Faculté de Technologie, Université de Bejaia, 06000 Bejaia, Algérie.

[3] Laboratoire de Physico-Chimie des Matériaux, avenue de l'Environnement, Université de Monastir, 5000 Monastir, Tunisie.

* anita.lucas@univ-rennes1.fr

INTRODUCTION

Surface functionalization may be efficient to modify the surface reactivity or the way to associate glass to molecules of potential interest. Silanization allows to bond functional groups to the glass surface. The influence of this surface modification on bioactivity and interaction with protein was investigated.

EXPERIMENTAL METHODS

An amine group was grafted on mesoporous bioactive glass[1,2] by a silanization process using 3-aminopropyltriethoxysilane (APTES, 98%, Alfa-Aesar). The grafting was evaluated using elemental analysis to quantify the weight percentage of nitrogen on the glass.

The bioactivity of the surface modified glass was evaluated by soaking it in a Simulated Body Fluid (SBF) up to 15 days.

The interaction of the glass surface with fibrinogen[3], a blood protein involves in the inflammatory process, was evaluated. Fibrinogen was quantified in the supernatant, after a contact with the glass during 48 hours, using UV spectrometry.

RESULTS AND DISCUSSION

The bioactivity of the glass was maintained and a hydroxyapatite layer was formed at the glass surface after 1 day in SBF as for the non silanized glass.

Results concerning the protein adhesion indicate that silanization induces a delayed adsorption of the protein at the glass surface.

CONCLUSION

The functionalized glass presents the same bioactivity than the initial glass with an original feature concerning the protein adhesion. The silanized glasses is now envisaged as drug-carrier.

REFERENCES

[1] Letaïef N. *et al*. J. non Cryst. Solids, 402: 194-199, 2014
[2] Letaïef N. *et al*. Micropor. Mesopor. Mater., 195: 102-111, 2014
[3] K. Magyari *et al*. Vib. Spectroscop., 62:172-179, 2012

ACKNOWLEDGMENT

The authors would like to thank the Institut des Sciences Chimiques de Rennes (ISCR) for providing financial support to this project.

'Ready-to-use' magnesium phosphate bone cement with advanced degradation rate

Friederike Kaiser[1*], Anna-Lena Preißler[1], Lena Schröter[2], Anita Ignatius[2], Uwe Gbureck[1]

[1]University Hospital of Würzburg, Department for Functional Materials in Medicine and Dentistry, Würzburg, Germany
[2]University Hospital of Ulm, Institute of Orthopaedic Research and Biomechanics, Ulm, Germany
*friederike.kaiser@fmz.uni-wuerzburg.de

INTRODUCTION

Calcium phosphates, e.g. hydroxyapatite, are commonly used as synthetic bone replacement materials due to their high biocompatibility and similarity to natural bone tissue.[1] However, a complete resorption of hydroxyapatite and replacement by bone tissue is rarely observed.[2] Magnesium phosphates such as struvite ($MgNH_4PO_4 \cdot 6H_2O$) are a promising alternative, due to their higher solubility.[3] *In vivo* studies in a sheep model showed an almost complete degradation of a struvite forming cement with a struvite content of ≈40% after 10 months.[4] Building on these findings, we developed in the current study a glycerol-based 'ready-to-use' magnesium phosphate bone cement. Compared to the 'traditional' cold-setting cement, where powder and liquid are mixed in the operating room, this cement can be directly applied in its liquid/moldy form. This shortens the preparation time of the cement during surgery, increases the time window for the application by the surgeon, and reduces the risk of bacteria contamination and the influence of mixing personnel on the cement properties. After implantation, the cement hardens by replacement of the glycerol with water from the surrounding tissue.

EXPERIMENTAL METHODS

The 'ready-to-use' bone cement was prepared by mixing the powders as displayed in Fig. 1 with glycerol at a powder-liquid ratio of 3 gml^{-1}. Directly after mixing in the planetary mixer, or after 4 weeks of paste storage, injection force (n=3) was measured using a universal testing machine (Z010, Zwick Roell, USA) and 5 ml luer lock syringes without needle. Cohesion was also tested shortly after mixing by injecting the paste into 50 ml ultrapure water in a petri dish. Compressive strength (n=10) was determined after hardening of the cement paste in silicon rubber molds (12x6x6 mm) for 1 or 3 days at 37°C in ultrapure water. The pastes were filled in the rubber molds directly after mixing or after 7 days or 3 months of paste storage.

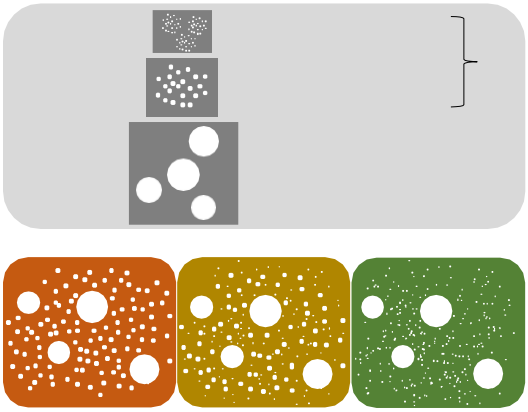

Fig. 1 Composition of the 'ready-to-use' magnesium phosphate bone cement. The percentage refers to the content of the fine trimagnesium phosphate in the powder.

RESULTS

Although the bimodal distribution with only fine trimagnesium phosphate (80% composition) provided the best cohesion, the trimodal particle size distribution (20% composition) showed a clear advantage regarding injection force (Fig. 2). Even after 3 months of storage, the paste still set to a stable bioceramic. The injection force however increased to 113 N after 4 weeks of paste storage. The 20% composition was evaluated regarding *in vivo* biocompatibility in sheeps, the histological evaluation is on-going.

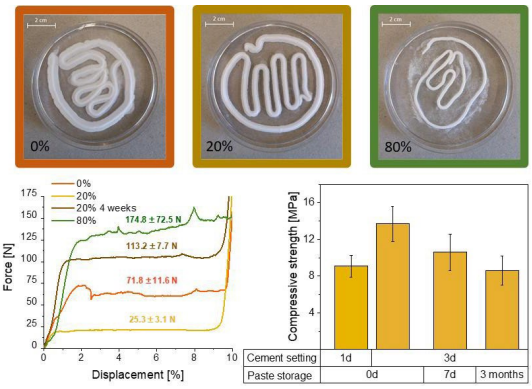

Fig. 2 Cohesion (top), injection force (lower left) and compressive strength (lower right, 20% composition) of the different paste compositions and depending on storage time.

REFERENCES

(1) K. de Groot, *Ceram. Int.* **1993**, *19* (5), 363–366.
(2) C. Mangano et al., *J. Periodontol.* **2008**, *79* (5), 929-933.
(3) M. Nabiyouni et al., *Acta Biomater.* **2018**, *66*, 23–43.
(4) B. Kanter et al., *Acta Biomater.* **2018**, *69*, 352–361.

ACKNOWLEDGEMENT

We gratefully acknowledge funding by the German Research Foundation (GB 1/15-3 and IG 18/11-3). We would also like to thank Isabell Biermann from the Department for Functional Materials in Medicine and Dentistry in Würzburg for the synthesis of the trimagnesium phosphate raw powder.

Decellularized Fibrillar Matrix for Engineering Organotypic Tumor-stroma 3D Biomodels

Vítor M. Gaspar[1], Luís P. Ferreira[1], Luís Mendes[1], Iola F. Duarte[1] and João F. Mano

[1] *CICECO-Aveiro Institute of Materials, Aveiro University, Aveiro, Portugal*
[*] vm.gaspar@ua.pt

INTRODUCTION

Currently available 3D in vitro breast cancer models focus mostly on the independent recapitulation of either cell population interactions or singular ECM-specific moieties[1]. Within this context, decellularized scaffolds provide a new pathway to recapitulate major tumor hallmark characteristics in complex cell-representative coculture models capable of integrating ECM-specific stimuli and bioactive components[2]. Seeking to overcome these disadvantages, herein we developed fibrillar dECM breast tumor-stromal models which recapitulate the cellular and matrix landscape of the human tumor.

EXPERIMENTAL METHODS

ECM-derived from porcine adipose mammary tissues was decellularized, characterized and homogenized into fibrillar micro-fragments suitable for inclusion in the process of microtumor assembly as we recently described[3]. As an initial characterization of the decellularization process, DNA, Collagen GAGs and fibrillar elements size distribution was evaluated. Breast cancer cells (MDA-MB-231) and Breast Cancer Associated Fibroblasts (BCAFs) were directly cultured with conjugated dECM microfibrillar fragments.

RESULTS AND DISCUSSION

Physiomimetic culture of tumor and stroma elements in fibrillar ECM supporting matrix led to the assembly of spherical 3D tumors with, fibrillar dECM spatial distribution in microtumors volume (**Figure 1**).

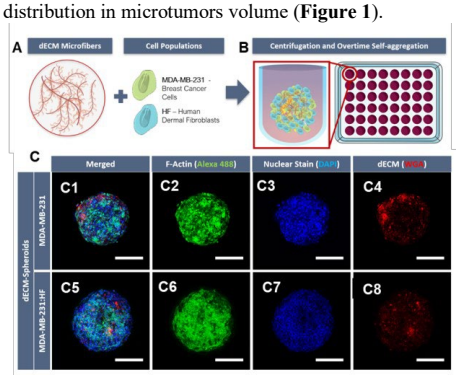

Figure 1. Engineering physiomimetic 3D microtumor-stroma models in fibrillar dECM matrix via superhydrophobic surfaces. Green channel: F-actin. Red channel: Fibrilar dECM. Blue Channel: Nuclei.

Endometabolomics analysis indicated a clear impact of fibriblar dECM inclusion in microtumor-stroma models, with a marked increase in lactate excretion and pyruvate consumption being observed, simulating the metabolic pathways activated in the *in vivo* scenario.

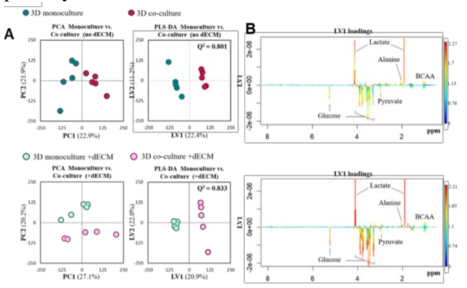

Figure 2. Exometabolomics analysis. (A and B) PCA scores scatter plots, PLS-DA scores scatter plots (middle) and LV1 loadings plots, respectively obtained through multivariate analysis of 1H NMR spectral profiles.

CONCLUSION

Overall, our finding evidence the importance of fibrilar dECM in promoting microtumor-stroma models recapitulation of key disease hallmarks. The herein proposed approach provides a universal methodology for developing more physiomimetic in vitro tumors models that are amenable for high-throughput drug screening. We envision that the modularity of this methodology will further allow the inclusion of other tumor building blocks including tumor-associated macrophages in the future, contributing for the so desired immunization of such models.

REFERENCES

1. Monteiro M. V. et al., Small methods. 5:2001207, 2021.
2. Ferreira, L.P. et al. Trends Biotechnol. 38 (12), 1397-1414, 2021.
3. Ferreira et al.,. Biomaterials 275, 120983, 2021.

ACKNOWLEDGMENTS

This work was developed within the scope of the project CICECO-Aveiro Institute of Materials, UIDB/50011/2020, UIDP/50011/2020/LA/P/0006/2020, financed by national funds through the FCT/MEC (PIDDAC). This work was also supported by (POCI), in the component FEDER, and by national funds (OE) through FCT/MCTES, in the scope of project PANGEIA (PTDC/BTM-SAL/30503/2017) and through a Doctoral Grant (SFRH/BD/141718/2018, L.P.F.) and through a Junior Researcher contract (CEEC/1048/2019, V.M.G.).

Development of a New Preservation Method of Human Amnio-Chorionic Membrane for Bone Regeneration

Paul Galvez[1,2]*, Naïma Ahmed Omar[1], Robin Siadous[1], Xavier Lafarge[3], Loic Sentilhes[4], Sylvain Catros[1,2], Nicolas L'Heureux[1], Jean-Christophe Fricain[1,2], Mathilde Fénelon[1,2]

[1] University of Bordeaux, INSERM, Laboratory BioTis, UMR 1026, F-33076 Bordeaux, France
[2] University hospital, Oral Surgery Department, F-33076 Bordeaux, France
[3] French Blood Establishment (EFS), Aquitaine-Limousin Branch, Bordeaux, France
[4] University hospital, Gynecology-Obstetrics Service, F-33076, Bordeaux, France

*paul.valgez@gmail.com

INTRODUCTION

Due to their biological properties and low immunogenicity, placental membranes (i.e amniotic and chorionic membranes) are widely used as biological scaffolds in the field of tissue engineering. We previously reported the interest of using amniotic membrane to regenerate both non-critical and critical bone defects [1,2]. However, some limitations have been observed due to amniotic membrane thinness making it difficult to handle. In this study, we proposed to combine the chorion with the amniotic membrane because chorion is three to four times thicker than the amnion and contains several growth factors in higher quantities, which can optimize the properties of the membrane for bone tissue engineering applications.

The objective of this study was to develop a simple and reproducible method for decellularization and preservation of amnio-chorionic membrane (ACM) for bone regeneration.

EXPERIMENTAL METHODS

Placentas were recovered after elective cesarean surgery and the ACM was cut out from placenta (n=10). ACM was decellularized using a previously established method (enzymatic method followed by a detergent decellularization method)[3], and was then lyophilized and gamma-sterilized. The effectiveness of the decellularization process was assessed using DAPI staining, DNA extraction and quantification, and separation by agarose gel electrophoresis. ACM was also characterized by scanning electron microscopy and its thickness was measured. Histological analyze was performed for morphological characterization (HES staining). *In vitro* cytotoxicity of ACM was studied by assessing the effects of the DL-ACM soluble extracts on human bone marrow mesenchymal stem cells (hBMSCs) viability and activity. Finally, we evaluated the biocompatibility of ACM in a rat subcutaneous model *in vivo*. Histological analysis was performed on subcutaneous DL-ACM implants one week, one month and two month after the surgery (n=9).

RESULTS AND DISCUSSION

The effectiveness of the decellularization process was validated by DNA extraction and confirmed with separation by agarose gel electrophoresis and HES as well as DAPI staining. The thickness of DL-ACM was significantly increased compared to amniotic membrane. *In vitro*, the preservation method did not confer any indirect cytotoxicity. *In vivo*, DL-ACM was easier to handle compared to amniotic membrane. Histological analysis of explanted samples from the rat indicated a moderate inflammatory reaction. Several preservation methods of ACM have been reported. They usually are time-consuming or not precisely described, and did not rigorously assess the effectiveness of their process. In this study, the effectiveness of the decellularization process was assessed according to previously established validation criteria and its realization time is shorter than the other processes described[4,5].

CONCLUSION

In this study, we developed a simple and reproducible method for effective decellularization of a biocompatible ACM, without cytotoxic effects. Implantation in non-critical bone rat defects will be performed to assess the *in vivo* osteogenic and angiogenic properties of the DL-ACM compared to amniotic membrane.

REFERENCES

(1) Fenelon M. *et al.*, Mater Sci Eng C Mater Biol Appl. 2021 (2) Fenelon M. *et al.,* J Mater Sci Mater Med. 2018 (3) Fenelon M. *et al.,* Mater Sci Eng C. 2019 (4) Crapo PM. *et al*., Biomaterials. 2011 (5) Kakabadze Z. *et al.,* J Surg Oncol. 2016

ACKNOWLEDGMENTS

The authors would like to thank the Department of Science and Technology for Health Bordeaux for providing financial support to this project.

A newly developed ECM scaffold for cardiac tissue engineering is remodeled by resident human cardiac progenitor cells

Anna Maria Sacco[1], Domenico Cozzolino[1], Veronica Romano[1], Immacolata Belviso[1], Giulia Ricci[2], Marcella Cammarota[2], Oriana Casciello[1], Fabrizio Schonauer[1], Cristiano Amarelli[3], Franca Di Meglio[1], Clotilde Castaldo[1*]

[1]Department of Public Health, University of Naples Federico II, Naples, Italy
[2]Department of Experimental Medicine, Università della Campania Luigi Vanvitelli, Naples, Italy
[3]Department of Cardiovascular Surgery and Transplant, Monaldi Hospital, Naples, Italy
[*] clotilde.castaldo@unina.it

INTRODUCTION

Along with structural support, the extracellular matrix (ECM) provides biochemical and mechanical signals that drive cell behavior. During the last decade, the central role played by the ECM in myocardium integrity and homeostasis has been emphasized by cardiac tissue engineering, and cardiac decellularized ECM has rapidly emerged has an attractive biomaterial for regenerative medicine applications. Since cardiac d-ECM availability is severely affected by organ donor shortage, we have recently provided evidence in support of the decellularized human skin (d-HuSk) as a promising biological, and potentially autologous, scaffold material for cardiac tissue engineering. Indeed, d-HuSk has proven capable to support human cardiac progenitor cells (hCPCs) engraftment, survival, and differentiation potential[1]. However, since any scaffold should be considered as a temporary implant that complies with resident cell requirements, the scope of the present study is to evaluate *in vitro* whether d-HuSk is remodeled by cardiac resident cells.

EXPERIMENTAL METHODS

Decellularization and preparation of three-dimensional scaffolds. Human abdominal skin samples from waste material of patients undergoing abdominoplasty (n = 12) were decellularized in a solution containing 1% SDS, 1% Triton-X and antibiotics. The efficiency of decellularization procedure was evaluated by the Hematoxylin and Eosin (H&E) staining and by measuring the residual content of dsDNA. d-HuSk samples were then cryosectioned to prepare 600-µm-thick three-dimensional scaffolds.

hCPC isolation and preparation of hCPC-d-HuSk bioconstructs. hCPCs were isolated from specimens of explanted human hearts (n = 10), seeded on d-HuSk scaffolds, and cultured for two weeks. Afterwards, hCPCs seeded on d-HuSk were induced to myogenic differentiation by the addition of ascorbic acid and VEGF, then d-HuSk-hCPC bioconstructs were cultured for two additional weeks. Induction of differentiation was evaluated by the expression of specific markers by semi-quantitative real-time PCR.

Analysis of hCPC-d-HuSk bioconstruct composition and organization. The composition and organization of both unpopulated and repopulated d-HuSk scaffolds was evaluated by quantitative assays specific for glycosaminoglycan (GAG), collagen and elastin, by immunofluorescence for laminin, fibronectin and tenascin, and by scanning electron microscopy.

All data obtained from quantitative or semi-quantitative analyses were analyzed using Student's two-tailed unpaired t-test and expressed as the mean ± SEM.

RESULTS AND DISCUSSION

The absence of nuclei in H&E staining and the quantification of a residual DNA content well below the accepted threshold of 50 ng/mg of dry tissue (9.138 ± 1.009 ng/mg) confirmed that d-HuSk met the criteria established to satisfy the intent of decellularization. Gene expression analysis revealed the significant down-regulation of genes typical of the early stages of cardiac myocyte differentiation, like TBX3, and up-regulation of late differentiating and mature cardiac myocyte markers, like connexin-43, in hCPCs induced to differentiate. However, the retained expression of markers typical of mesenchymal, vascular endothelial and smooth muscle cells, also showed that hCPCs still consisted of a mixed population including progenitor and precursors of other cardiac cell lineages. As concerns the composition and organization of d-HuSk, the quantitative assays and histological analysis revealed in repopulated d-Husk scaffolds with respect to the acellular d-HuSk a significant decrease of collagen (16.49 ± 1.496 vs 29.42 ± 2.298 µg/mg wet tissue, respectively) and elastin content (26.74 ± 1.241 vs 33.94 ± 1.973 µg/mg of dry tissue, respectively), a significant increase of GAGs (2.434 ± 0.533 vs 1.246 ± 0.175 µg/mg wet tissue, respectively) and a remarkable higher mean intensity of fluorescence for fibronectin and tenascin (6969 ± 177.4 vs 5172 ± 292.3 intensity/pixel^2 and 1210 ± 66.82 vs 820.6 ± 36.64 intensity/pixel^2, respectively), while no statistically significant differences emerged for laminin. Finally, SEM analysis revealed a network of tiny filaments resembling elastic fibers more evident in repopulated d-HuSk scaffolds, whereas the thicker collagen fibers resulted less abundant.

CONCLUSION

Evidence emerging from our study confirms the hypothesis that d-HuSk is actively restructured and remodeled by cardiac resident cells, thus providing additional proof of d-HuSk suitability as a temporary platform for cardiac tissue engineering.

REFERENCES

1. Belviso I. *et al.*, Front. Bioeng. Biotechnol, 8:229, 2020.

Decellularized pancreatic extra-cellular matrix to mimic tumor microenvironment

Sophia Coffy[1*], Anastasia Papoz[1], Patricia Obeid[1], Clémence Pfeil[1] Julia Novion-Ducassou[2], Edouard Girard[3], Gael Roth[3], Xavier Gidrol[1], Amandine Pitaval[1].
[1]Univ. Grenoble Alpes, CEA, Inserm, IRIG, Biomics, F-38000, Grenoble, France
[2]Univ. Grenoble Alpes, INSERM, CEA, UMR BioSanté U1292, CNRS, CEA, FR2048 38000, Grenoble France
[3]Univ. Grenoble Alpes, CNRS, CHU Grenoble Alpes Department of Digestive and Emergency Surgery, Grenoble INP, TIMC-IMAG, Grenoble, France.
[*] sophia.coffy@cea.fr

INTRODUCTION

Pancreatic cancer is a fatal disease, with a survival rate of only 9% 5 years after diagnosis1. This low rate is due to its absence of specific symptoms and sensitive biomarker. New diagnostic tools and treatments are needed, and development of new, appropriate disease models required for this search. To date, most models focus only on cellular aspect and forget the microenvironment, which plays an important function y in pancreatic cancer. The microenvironment, consists in support cells and the extra cellular matrix (ECM). The ECM provides a protein scaffold to cells in tissues, and contains important secreted factors to support cell growth and survival. Its composition and structure change upon carcinogenesis[2,3]. Here we propose to use hydrogels obtained from human and porcine decellularized extracellular matrix as a way to model the pancreatic microenvironment..

EXPERIMENTAL METHODS

Microenvironment: Decellularized extracellular matrices (dECM) from human and porcine pancreases were obtained and used as a hydrogel on which pancreatic cells could grow in 3D and form organoids. Purity and protein content of each hydrogel was determined and the matrisome analysis was performed in order to identify quantitative and qualitative differences in protein contents. To increase the relevance of our model, pancreatic stellate cells (HPaSteC) were further added to the hydrogel we obtained.

Pancreatic organoids and tumoroids: To mimic healthy and tumoral pancreases, different cell lines were used: H6c7, a non tumoral, immortalized pancreatic cell line and PANC-1, a tumoral pancreatic cell line. Pancreatic organoids were characterized by immunofluorescence. We then monitored the effect of the different microenvironments on the relative proportion of organoids (partially differentiated structures) and tumororoids (non-differentiated tumor-like structures).

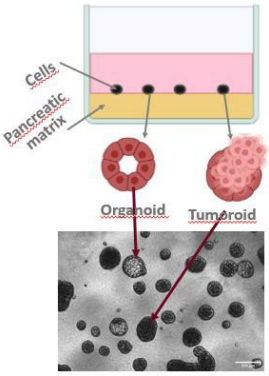

Figure 1.
Schematic representation of the 3D culture method (Top) Representative image of pancreatic cells cultured in hydrogel (Bottom)

RESULTS AND DISCUSSION

Characterization of dECM. We describe the generation of dECM, and further characterized its composition (absence of DNA and lipid, presence of ECM proteins such as collagen). We also perform in depth analysis of the matrisome using mass spectrometry-based proteomics of the various hydrogels mentioned above.
Effect of microenvironment on the generation of pancreatic organoids or tumoroids. We assess the impact of the microenvironment on pancreatic cells with immunolabelling, morphological and phenotypic analysis

CONCLUSION

The human dECM of the tissue under scrutiny is an exquisite representation of the tissue microenvironment. We have shown here that we can generate either organoids or tumoroids in such physiologically relevant microenvironment. Comparing a normal ECM to a tumoral one could help us to better comprehend tumor initiation in pancreas and lead to the discovery of relevant biomarkers for pancreatic cancer diagnosis.

REFERENCES

References must be numbered. Keep the same style.
1. Sung H et al, *CA Cancer J Clin*. 2021;71(3):209-249
2. Liot S et al, *Front Immunol*. 2021;12(April):1-12
3. Frantz C et al, *J Cell Sci*. 2010;123(24):4195-4200

ACKNOWLEDGMENTS

The authors would like to thank the Focus Organoids on Chip for providing financial support to this project.

ESB 2022
32nd ANNUAL CONFERENCE OF THE EUROPEAN SOCIETY FOR BIOMATERIALS

Biological and mechanical characterization of a decellularized porcine esophageal biological matrix

Romane LESIEUR[1,2], Cécile MONFOULET[2], Samantha ROQUES[2], Martine RENARD[2], Agnès DROCHON[3], Denis COLLET[4], Laurence BORDENAVE[1,2,5,] Marlène DURAND[1,2]

[1]BIOTIS U1026 INSERM, Université de Bordeaux, France
[2]CIC1401 INSERM, CHU de Bordeaux, France
[3]Institut de mécanique et d'ingénierie, UMR CNRS 5295, Campus Talence, France
[4]Service de Chirurgie Digestive, CHU de Bordeaux, France
[5]Service de Médecine Nucléaire, CHU de Bordeaux, France
Mail: romane.lesieur.stag@chu-bordeaux.fr

INTRODUCTION

The restoration of digestive continuity after the ablation of a portion of the esophagus is currently ensured by the interposition of a colon segment or by the tubulation of the stomach. The development of a tissue-engineered esophageal substitute is part of the improvement of the surgical treatment of esophageal pathologies. Previous studies[1,2] have focused on the development of a decellularized porcine biological matrix, using a chemical and enzymatic detergent perfusion method[3]. These protocols have been upgraded to ensure sterility and thus avoiding deleterious Gamma rays irradiation. The objective of this study is to characterize both the biological and mechanical properties of this decellularized matrix (DM).

EXPERIMENTAL METHODS

DM design and decellularization process

Esophagi were collected from pigs of 30 kg to 50 kg. The design of a DM is done according to 3 steps: a decontamination process with antibiotics/antimycotics solutions, a decellularization process with the successive perfusion of chemical and enzymatic solutions, and a detoxification process that absorbed chemical residues from the decontamination and decellularization processes.

The decellularization process was performed by perfusing the organs with a controlled flow and rotation in the SYNTHECON system. The flow characterization of the perfusion/rotation system confirms its use in our application. The detersions solutions ensured the removal of the cells and their contents. These phases were separated by rinsing phases.

Biological characterization

Histological analysis

Samples of DM (n=20) were embedded in paraffin, cross-sectioned and stained with hematoxylin eosin saffron (HES). The efficacy of the decellularization process and the histological structure were then analyzed.

Cytotoxicity analysis

BALB/3 T3 cells were seeded in direct contact with the DM (n=6) following ISO 10993-5 standard. Viable cells were counted after neutral red staining.

Mass spectrometry analysis

The identification of the proteins contained in the MD is performed by nanoLC-ESI-MS/MS Fusion Lumos coupling, at the Functional Genomics Center of Bordeaux. The DM were chemically treated in order to be analyzed (n=6). Data are collected via Proteome Discoverer 2.4 / PEAKS and compared according to an adapted database.

Mechanical characterization

Longitudinal traction

Native esophagus (NE) patches are prepared (n=10) as well as DM patches (n=14). The samples were clamped in jaws of a tensile testing machine and pulled at a constant speed until rupture (150 mm/min).

Suturability

NE patches are prepared (n=9) as well as DM patches (n=3). The suture thread and the samples are maintained in clamps that are extended with tensile force until rupture is reached (150 mm/mn).

Burst pressure

The burst pressure test was performed on the Bose Biodynamic Test©. Increasing endoluminal pressures are applied to the DM until burst (n=7).

RESULTS AND DISCUSSION

A total of 40 porcine esophagi were decellularized using our in-house upgraded method. No remaining cells were observed within the stained cross-sections of the matrix. More than 70% of the cells were viable when in contact with the DM, confirming its non-cytotoxic potential. The main collagens and glycoproteins were identified, showing the complex and rich composition of the DM. In traction tests, rupture of the DM (n=14) required the application of an average force of 31.30±3.5 N in comparison to the NE (n=10) for which an average force of 18.11±5.18 N was required. The three MD patches had a mean suture retention force of 5.26±0.43N, which favorably compares to the NE data (2.40±1.25N). Burst testing demonstrated that the MD is compatible with implantation as an esophageal substitute.

CONCLUSION

We characterized biologically and mechanically a DM, with which we can expect to improve clinical outcomes after implantation, in comparison to Luc *et al*. and Arakelian *et al*.

REFERENCES

1. Luc G. *et al*. Biomaterials. 175:1-18, 2018.
2. Arakelian L. *et al.* Tissue Engineering and Regenerative Medicine. 13:2191-2203, 2019.
3. Zambon P.J. *et al.* Methods. 171:3-10, 2020.

Engineering a Cell-derived Extracellular Matrix for Intervertebral Disc Regeneration using CRISPR/dCas9

Catarina Milheiro[1,3*], Raquel Gonçalves[1,2,3], Mário Barbosa[1,2,3], Joana Caldeira[1,2,3]

[1]i3S – Instituto de Investigação e Inovação em Saúde, Porto, Portugal
[2]INEB – Instituto de Engenharia Biomédica, University of Porto, Portugal
[3]ICBAS – Instituto de Ciências Biomédicas Abel Salazar, University of Porto, Portugal

[*] catarina.milheiro@i3s.up.pt

INTRODUCTION

Intervertebral disc (IVD) degeneration is characterized by structural alterations as result of matrix and water depletion[1]. As consequence there is an irreversible loss of function that can lead to serious conditions like disc herniation and low back pain. Current treatments fail to tackle the functionality deficiency and promote regeneration. We propose to recapitulate a fetal-like IVD microenvironment, in mesenchymal stem cells (MSCs), using a CRISPR activating (CRISRPa) system. This will promote the expression of *COL12A1* and *COL14A1*, which are exclusively present in the fetal IVD. We hypothesize that the tailored cell-derived matrix (CDM), from these engineered MSCs, will recapitulate in a reproducible way the fetal IVD microenvironment and consequently have an increased pro-regenerative potential, as demonstrated in other tissues.

EXPERIMENTAL METHODS

Bone-marrow derived human MSCs (BM-MSCs) were collected and transduced with the CRISPR/dCas9-VP64 lentiviral system, targeting *COL12A1* or *COL14A1* promoter regions. An additional and lentiMPHv2 (pHelper) system was used when targeting *COL12A1*. The same vectors were used to transduce an immortalized cell line of human MSCs (iMSCs). Selection with antibiotics was performed to ensure exclusive maintenance of the engineered cell population *COL12A1* and *COL14A1* gene expression levels were evaluated by qRT-PCR. In parallel, optimization of extracellular matrix (ECM) deposition and of a decellularization protocol (based on NH4OH/Triton X-100 and SDS) was performed using iMSCs. Process efficacy was validated by immunofluorescence for deposited ECM (specifically, fibronectin), presence of cell nuclei (DAPI) and cytoskeleton (Phalloidin). DNA content was quantified using the Quant-iT™ PicoGreen™ Kit.
For statistical analysis, Kruskal-Wallis test was applied, followed by Dunn's multiple comparison.

RESULTS AND DISCUSSION

Gene activation of *COL12A1* and *COL14A1* was observed in only 2 out of 5 BM-MSCs donors, and was not statistically significant, suggesting a donor-dependent genome editing variability. In iMSCs (n=2), *COL12A1* mRNA relative expression levels were increased in average 2.12-fold, when the Bn CRISPR vector was combined with a helper plasmid. For *COL14A1* levels, we observed an average increase of 11.7-fold, when using the CRIPSR vector alone. ECM deposition, and preservation after decellularization, was confirmed by fibronectin staining in the NH4OH-based decellularized samples. The same was not observed with the SDS-based protocol. In turn, cell removal was demonstrated by a reduction of nuclear and actin staining in the treated groups, when compared to the non-decellularized control. DNA content showed a sharp decrease with both protocols. Nonetheless, decellularization protocol is still being further optimized to achieve maximal cell removal with high ECM maintenance.

CONCLUSION

The observed variability in terms of BM-MSCs editing efficiency can be explained by variable lentiviral integration rates and sites, as well as natural epigenetic differences between cells. The use of iMSCs emerged as an alternative to overcome senescence and reproducibility issues. Protein analysis by Western Blot and Proteomics are ongoing.
Decellularization experiments indicate that the use of NH4OH enables ECM maintenance, contrarily to the SDS-based procedure. Nonetheless, additional protocol optimizations and further quantitative analysis are being performed. Altogether, the use of a personalized ECM and the recapitulation of a fetal microenvironment constitute a pioneer strategy for IVD function restoration, opening new avenues in the tissue regeneration field.

REFERENCES

1. Molinos M. *et al*, J.R.Soc.Interface. 12, 2015

ACKNOWLEDGMENTS

The authors would like to thank Prof. Silvia Diaz Prado (Universidade da Coruña, Spain) for kindly providing the cell line of iMSCs. We also thank the Centro Hospital Universitario de São João (CHU São João) for the ethical reviewed collection of bone marrow for MSCs isolation. In addition, we would like to acknowledge Fundação para Ciência e Tecnologia (Grant: EXPL/BTM-ORG/0880/2021 and Grant: Fellow_BI/FCT_Proj2020/i3s/11062506/2021), and EUROSPINE/ON Foundation (Grant: 20-165), for the financial support of this project.

Human protein based materials to engineer groundbreaking accurate 3D models for cell culture and tissue engineering

Catarina Custódio[1], Sara Santos[1], Cátia Monteiro[1], Inês Deus[1], Elisa Martins[1], André Lima[1], João Mano[1]

[1] Department of Chemistry, CICECO - Aveiro Institute of Materials, University of Aveiro, 3810-193, Aveiro, Portugal

*catarinacustodio@ua.pt

INTRODUCTION

A physiologically relevant cell culture model is one that mimics the in vivo tissue organization and is physiologically relevant and/or patient-derived and meet the requirements of the pharmaceutical industry. We propose human-based biomaterials prepared from platelet lysates (PL) and the extracellular matrix of the placenta to engineer humanized platforms for cell culture.([1,2,3])

Human placenta based biomaterials result in non-immunogenic platforms with anti-inflammatory and pro-angiogenic properties. PL are rich in growth factors involved in tissue healing and angiogenesis and were herein explored to prepare bioactive hydrogels for cell culture.

We propose human based materials, as innovative, versatile platforms for cell culture, microtissue development and disease modeling. It offers the possibility to be personalised (using the patient's own proteins) according to the end-user needs with high potential for clinical translation.

EXPERIMENTAL METHODS

Placenta was decellularized, solubilized, lyophilized, and milled. Platelet lysates (PLs) were prepared by exposing PRP to freeze-thaw cycles. The placenta extracellular matrix (hPECM)-proteins and PLs were chemically modified using a methacrylation protocol well established in our group.[1] Degree and local of modification were evaluated by mass spectrometry. The methacrylated proteins were processed in the form of a hydrogel upon irradiation with UV light. To prepare the sponges, the hydrogels were freeze dryed.

RESULTS AND DISCUSSION

We have demonstrated the superior bioperformance of such materials compared to classical materials, and their versatility for spheroid invasion, endothelial cell alignment and stem cell culture (Fig. 1). The mechanical properties of the resulting materials can be easily tailored by varying the degree of modification and/or the concentration of the solution.

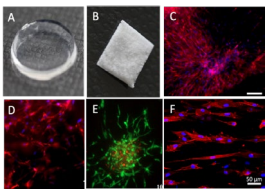

Figure 1 – A)PLMA hydrogel; B) PLMA sponge; C) hASCs seeded in PLMA sponges at 14 days culture without serum; D) hASCs encapsulated in PLMA hydrogels at 7 days culture; E) Viability of MG-63 tumor spheroids at 24 days of culture; F) hBM-MSCs cultured on top of AMMA hydrogels containing topographical cues.

The human based materials have proven to support distinct human derived cell cultures (stem cells, endothelial cells and cardiomyocytes), furthermore, the cells acquired an in vivo-like cell polarity and were able to invade the matrix, forming complex interconnected cellular networks.).

CONCLUSION

Our technology will have a significant impact on the 3D cell culture market and pharmaceutical industry by accelerating drug screening and development reducing associated costs. The competitive advantage of our materials is based on the fact that they contain human biochemical cues (vital for cell function and with a reduction on animal experimentation), are a complete xeno-free solution (avoids contamination), do not gel at room temperature (easier to manipulate) and have tunable mechanical properties (increased stability and versatility).

REFERENCES

1- Santos, S. C., Custódio, C. A., Mano, J. F., Photopolymerizable Platelet Lysate Hydrogels for Customizable 3D Cell Culture Platforms. Adv. Healthcare Mater. 7, 1800849, 2018

2- Deus, I. A., Santos, S. C., Custódio, C. A., Mano, J. F., Designing highly customizable human based platforms for cell culture using proteins from the amniotic membrane. Materials Science and Engineering: C. 2021, 112574.

3- Monteiro, C. F., Santos, S. C., Custódio, C. A., Mano, J. F., Human Platelet Lysates-Based Hydrogels: A Novel Personalized 3D Platform for Spheroid Invasion Assessment. Adv. Sci. 7, 1902398. 2020

ACKNOWLEDGMENTS

European Union (EU) Horizon 2020 for the project InterLynk, Grant agreement: H2020-NMBP-TR-IND-2020, Project ID: 953169 and the Portuguese Foundation for Science and Technology (FCT) through the project BEAT (POCI-01-0145-FEDER-030869). C. Custódio acknowledge the FCT for the individual contract 2020.01647.CEECIND This work was developed within the scope of the project CICECO-Aveiro Institute of Materials, UIDB/50011/2020, UIDP/50011/2020 & LA/P/0006/2020, financed by national funds through the FCT/MEC (PIDDAC).

ESB 2022
32nd ANNUAL CONFERENCE OF THE EUROPEAN SOCIETY FOR BIOMATERIALS

Yarn of Human Amniotic Membrane Can Be Woven into a Vascular Graft with Clinically-Relevant Mechanical Properties.

Agathe Grémare[1,2], Lisa Thibes[1], Maude Gluais[1], Yoann Torres[1], Diane Potart[1], Nicolas Da Silva[1], Nathalie Dusserre[1], Mathilde Fénelon[1,2], Loïc Sentilhes[3], Sabrina Lacomme[4], Isabelle Svahn[4], Etienne Gontier[4], Jean-Christophe Fricain[1,2], Nicolas L'Heureux[1*]

[1] Univ. Bordeaux, INSERM, Laboratory for the Bioengineering of Tissues - BioTis, UMR1026, F-33076 Bordeaux, France
[2] CHU Bordeaux, Odontology and Oral Health Department, F-33076 Bordeaux, France
[3] CHU Bordeaux, Obstetrics and Gynecology Department, F-33076 Bordeaux, France
[4] Univ. Bordeaux, CNRS, INSERM, Bordeaux Imaging Center, BIC, UMS 3420, US 4, F-33000 Bordeaux, France
[*]nicolas.lheureux@inserm.fr

INTRODUCTION

Since synthetic vascular prosthesis perform poorly in small diameter revascularization, biological vascular substitutes are being developed as an alternative. Although their *in vivo* results are promising, their productions involve tissue engineering methods that are long, complex and expensive.[1-3] To overcome these limitations, we propose an innovative approach that combines the human amniotic membrane (HAM), which is a widely available and cost-effective biological raw material, with a rapid and robust textile-inspired assembly strategy.[4]

EXPERIMENTAL METHODS

Fetal membranes were collected after cesarean deliveries at term. Once isolated by dissection, HAM sheets were cut in ribbons that could be further processed, by twisting, into threads. Ribbons were decellularize by trypsin (1.25 g/l) and ethylenediaminetetraacetic acid (EDTA, 0.625 g/l) treatment for two minutes at 37°C. After rinsing in PBS (3x5 min) and distilled water (1 × 5 min), HAMs were placed on an orbital shaker at room temperature for 7h with a decellularization solution (8 mM 3-[(3-Cholamidopropyl)dimethylammonio]-1-propanesulfonate hydrate (CHAPS), 25 mM EDTA, 0.12 M NaOH, and 1 M NaCl in PBS), and then washed with PBS (1 × 5 min) and distilled water (3 × 30 min). HAMs were then cut, air-dried, spooled, and stored at -80°C. Dry or hydrated (distilled water) ribbons were sterilized at room temperature by gamma irradiation (25 kGy, BGS, Germany).

Tensile tests were performed as previously described. [1]

The TEVGs were produced using a basic weaving technique (plain 1/1) with a custom-made circular loom, as previously described.[1]

Significant differences were assessed by two-tailed t-test (two groups compared) or one-way analysis of variance (more than two groups compared) if data had a normal distribution. Otherwise, they were assessed by Mann-Whitney test (two groups compared) or by Kruskal-Wallis test (more than two groups compared). Differences were significant when $p < 0.05$.

RESULTS AND DISCUSSION

Characterization of HAM yarns (both ribbons and threads) showed that their physical and mechanical properties could easily be tuned. Since our clinical strategy will be to provide an off-the-shelf, allogeneic implant, we studied the effects of decellularization and / or gamma sterilization on the histological, mechanical, and biological properties of HAM ribbons. Decellularization had little effect of HAM yarn mechanical properties other than a small increase in strain at failure. However, gamma sterilization of the dried and decellularized HAM caused a decrease in rehydrated yarn diameter, an increase in ultimate tensile strength and a decrease in strain at failure. Gamma irradiation of hydrated (and decellularized) HAM largely avoided these mechanical changes. Furthermore, the process did not interfere with the ability of the matrix to support human umbilical vein endothelial cells to form a confluent monolayer *in vitro*. Finally, HAM-based, woven, tissue-engineered vascular grafts (TEVGs) showed clinically relevant mechanical properties with a burst pressure of over 8000 mmHg (at a diameter of 4.4 mm), suture retention strength of over 5 N, and a transmural permeability of 1 $ml \cdot min^{-1} \cdot cm^{-2}$ (Fig).

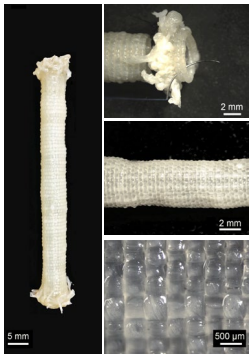

CONCLUSION

This study demonstrates that human, completely biological, allogeneic, small diameter TEVGs with excellent mechanical properties can be produced from HAM, thereby avoiding costly manufacturing strategies based on cell culture and complex bioreactors.

REFERENCES

1. McAllister T.N., *et al.*, The Lancet, 373:1440-1446, (2009).
2. Lawson J.H., *et al.*, The Lancet, 387:2026-2034, (2016).
3. Syedain, Z.H., et al., Sci Transl Med, 9:209 (2017).
4. Magnan L., *et al.*, Acta Biomater, 105:111-120, (2020)

ACKNOWLEDGMENTS

The authors would like to acknowledge Patrick Guitton for his technical help.

Development of protocol for obtaining autologous liquid PRF for local drug delivery systems

Ilze Salma[1,2,4], Lana Micko[1,2,4], Karina Egle[3,4], Arita Dubnika[3,4]

[1]Institute of Stomatology, Riga Stradins University, LV
[2]Department of Oral and Maxillofacial Surgery, Riga Stradins University, LV
[3]Rudolfs Cimdins Riga Biomaterials Innovations and Development Centre of RTU, Institute of General Chemical Engineering, Faculty of Materials Science and Applied Chemistry, Riga Technical University, LV
[4]Baltic Biomaterials Centre of Excellence, Headquarters at Riga Technical University, LV
ilze.salma@rsu.lv

INTRODUCTION

For bone regeneration in oral and maxillofacial surgery different bone graft materials (autologous, allogenic and synthetic) have been used. In recent years platelet-rich fibrin (PRF) has been considered suitable for bone regeneration[1]. PRF is obtained from autologous peripheral blood by the separation of its constituents to produce activated fibrin based biomaterial to accelerate tissue healing. PRF contains high concentration of different platelets and leukocytes derived growth factors[2]. Without adding any modifiers it is a totally autologous material prepared extemporaneously. A wide variety of centrifugation protocols for obtaining PRFs are available in the literature. Centrifugation parameters range from 600 rpm to 1200 or even up to 2400 with the centrifugation time from 3 to 12 or even 16 minutes.
The aim of our study is to develop a protocol for obtaining liquid PRF that polymerizes in about 20-30 minutes and is a suitable matrix for the development of local drug delivery systems.

EXPERIMENTAL METHODS

Written consent was obtained from all volunteers for their blood samples to be used in the research. All donors were free of any infectious disease and did not have any abnormal consumption of nicotine or alcohol. None of the subjects used any drugs. Permission No. 6-2/10/ 53 of the Research Ethics Committee of Riga Stradiņš University has been received for the research.
The blood was drawn with a clinically approved butterfly blood collection method (BC-12, 21 G x 3/4") by medical nurse. Blood of volunteers was collected in 13 mL i-PRF+ tubes. Centrifuge PRF Duo Quattro (rotor radius 100 mm) was used.

RESULTS AND DISCUSSION

Using the classic centrifugation parameters (1300 rpm / 5min or 1300 rpm / 8min) we obtained PRF, which was gel-like already at the beginning. This didn't allow to prepare a scaffold for drug delivery system and use for antibacterial tests.
Gradually reducing speed (till 700 rpm) we got PRF that changes from a liquid state to a solid, forming a three-dimensional fibrin network in about 20 minutes.
After the centrifugation, the upper layer of liquid PRF from each tube was transferred into a cell culture plate for further use in drug release studies. Approximately 1ml of PRF could be obtained from each tube.

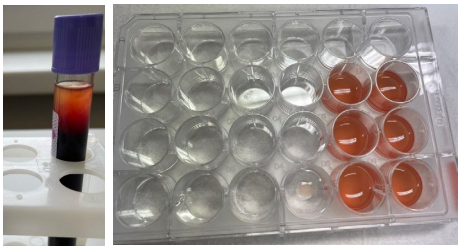

Fig. 1. i-PRF+ tube after centrifugation.
Fig. 2. PRF prepared for drug release studies.

By further reducing the centrifugation time and speed (less than 700 rpm and less than 5 min) obtained PRF did not acquire a gel-like consistency even after 30-40 minutes.
We performed blood cell number estimation by flow cytometry to analyze changes in platelet and leukocyte count in PRF samples at different centrifugation parameters 700 rpm/3 minutes and 700 rpm/5 minutes. Platelet (PLT) count did not change with centrifugation time. The number of leukocytes (WBC) was slightly higher, by centrifuging the samples for 5 minutes compared to 3 minutes.

CONCLUSION

By gradually reducing the speed and spin time, we obtained a PRF that meets our requirements. Based on the results of our research and the data from the literature, we decided to use for our further drug release studies the following protocol: 5 min / 700 rpm (rotor radius 100 mm).

REFERENCES

1. Liu Y et al. Biomed Res Int. 2019 Dec 6; 2019:3295756.
2. Bielecki T et al. Curr Pharm Biotechnol. 2012 Jun; 13(7):1121-30.

ACKNOWLEDGMENTS

This research was funded by the European Union's Horizon 2020 research and innovation program under the grant agreement No 857287 and the Latvian Council of Science research project No. lzp-2020/1-0054 (MATRI-X).

Development Of Customized Nanoparticle-Doped Bioinks For 3D Printed Dynamic Cancer Models

Paula Vázquez-Aristizabal[1,2*], Malou Henriksen-Lacey[2,3], Dorleta Jiménez de Aberasturi[2,3,4], Judith Langer[2,3], Ander Izeta[1,5], Luis M. Liz-Marzán[2,3,4]

[1] Biodonostia Health Research Institute, Tissue Engineering Group, Paseo Dr. Beguiristain s/n, 20014, Donostia-San Sebastián, Spain.
[2] CIC biomaGUNE, Basque Research and Technology Alliance (BRTA), 20014, Donostia-San Sebastián, Spain.
[3] Centro de Investigación Biomédica en Red, Bioingeniería, Biomateriales y Nanomedicina (CIBER-BBN), 20014, Donostia-San Sebastián, Spain.
[4] Ikerbasque Basque Foundation for Science, 48009, Bilbao, Spain.
[5] School of Engineering, Tecnun-University of Navarra, 20009, Donostia-San Sebastián, Spain.
[*] pvazquez@cicbiomagune.es

INTRODUCTION

There is an unmet need for more complex and monitorable cancer models. The development of solid tumor micromodels based on printed decellularized extracellular matrices (dECMs) offers a step in this direction, with the biomolecule-rich matrix of dECM inks allowing cell growth in a three-dimensional (3D) and natural environment[1].

By pre-labelling cells with plasmonic nanoparticles (NPs) exhibiting stable and high intensity surface enhanced Raman scattering (SERS) signals, cell movement can be imaged in situ using Near-Infrared (NIR) light sources which show limited cytotoxicity and good penetration within biological materials[2]. Hence, the combination of dECM scaffolds and tumoroids labelled with SERS-encoded NPs, will allow the monitoring of cells in a more realistic 3D microenvironment, offering the possibility of studying a living system for longer times than other conventional techniques.

EXPERIMENTAL METHODS

Porcine breast and skin tissue were exposed to different chemical, enzymatic and mechanical agents adapted to the nature of each tissue. Decellularization was confirmed by histological analysis and DNA quantification. The resulting matrices were grinded and digested into a hydrogel. Printability was confirmed by extrusion printing and rheological assessment.

Cells lines were cultured under standard conditions and labelled individually before any assay.

RESULTS AND DISCUSSION

Porcine skin and breast tissue have been effectively decellularized and turned into printable dECM inks that exhibit suitable rheological and biocompatible properties. Additionally, complex 3D cellular models have been developed for both melanoma and breast cancer modelling. By incorporating NPs into the formulations and/or into the spheroids, the cells within the microtissues can be imaged.

CONCLUSION

Our results suggest that in vitro tumoroid models grown on 3D printed dECM can be used as a powerful tool in tissue engineering and disease modelling, to make progress towards understanding cellular behavior and drug responses.

REFERENCES

1. Kim BS. *et al*., Chem. Rev. 120(19):10608–10661, 2020
2. Jimenez de Aberasturi D. *et al*. Adv. Funct. Mater. 30(14):1909655, 2020.

ACKNOWLEDGMENTS

PV-A was supported by a fellowship paid by the donation made by Asociación Katxalin in 2019. The authors acknowledge financial support from the European Research Council (ERC-AdG-2017#787510), the Instituto de Salud Carlos III (PI19/01621 and PT20/00030) co-funded by ERDF/ESF, "Investing in your future"; Diputación Foral de Gipuzkoa; and the Department of Health (2020111004; 20BU206) and the Department of Economy and Competitiveness of the Basque Government (KK-2020/00010; KK-2019/00006; KK-2019/00093). This work was performed under the Maria de Maeztu Units of Excellence Program from the Spanish State Research Agency, grant no. MDM-2017-0720.

Development of a purification process for xenogeneic bone matrices using supercritical CO_2 technology

Solène Rota[1,2*], Ludovic Sicard[3]
Justine Perarnaud[2], Michel boissière[2], Raphaël Bardonnet[1], Catherine Chaussain[3], Caroline Gorin[3], Emmanuel Pauthe[2]

[1]BIOBank, Lieusaint, France
[2]BioSan group, ERRMECe Laboratory, CY Cergy-Paris Université, Neuville-sur-Oise, France
[3] Université Paris Cité, Laboratory URP2496 Orofacial Pathologies, Imaging and Biotherapies, Paris, France
[*]solene.rota@outlook.com

INTRODUCTION

Many traumatic or pathological conditions cause significant bone damages that, in many cases, lead to bone tissue unable to heal spontaneously. It is then necessary to use bone grafts capable for guaranteeing the the reconstruction of the damaged tissue [1]. Allogeneic bone tissues are mainly used as an alternative to autografts. However, the availability of this source is limited, mainly due to regulatory constraints. Bone substitutes of animal origin have been developed to face the increasing need of the surgeons. These xenogenic sources are appealing from an economic and regulatory point of view, allowing easier commercialization on a global scale. However, their use is conditioned by the implementation of purification processes guaranteeing their harmlessness and their performance for bone regeneration.

In the present study, we first aimed to identify a source of xenogenic bone displaying ideal biological characteristics, as close as possible to the human bone. Second, we explored the potentialities of the supercritical CO_2 technology for the cleaning and the optimization of the purification of this new source.

EXPERIMENTAL METHODS

A bone matrix of porcine origin was selected and, initially, characterized after application of the Supercrit® [2] process from BIOBank, used for the purification of bone allografts. With the objective of both reducing the aggressiveness of the treatment and preserving the tissue some optimization of the process was proposed. first, adjustments of solvents, concentrations and processing parameters were tested and evaluated by multiple physico-chemical and biochemical characterizations, and biophysical approaches. Animal studies of implantation in a bone site (rat calvaria) were next conducted in order to evaluate, through micro-CT analysis and histology, the capacity of the grafts to regenerate bone tissue and measure the inflammatory reaction.

RESULTS AND DISCUSSION

The animal matrix selected, and purified by the reference Supercrit® process, showed similarities with the human bone. After improvement and adjustment of the purification treatment, biochemical and biological characterizations of the matrices produced confirmed the preservation of the characteristics of the animal bone treated with the new process. The *in vivo* results established that porcine bone matrices treated with the optimized process allowed significantly more efficient repair of critical size bone defects performed in rats at two months upon implantation. At one month, no inflammatory reaction was observed, regardless of the type of treatment.

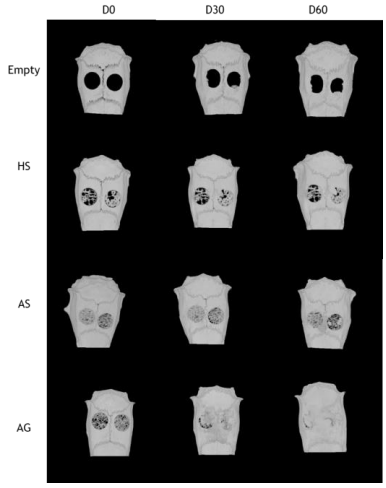

Animal experimentation in bone site (calvaria rat). Micro-CT scan of Animal Goxcrit (AG), Animal Supercrit(AS) Human Supercrit (HS)

CONCLUSION

This work show the interest of supercritical fluid technology for the purification of a bone matrix of animal origin. Additional validations on biocompatibility will however have to be carried out to consider therapeutic applications in humans.

REFERENCES

1. Khan SN et al, J Am Acad Orthop Surg (2005) 13:77
2. Fages J et al. ASAIO J Am Soc Artif Intern Organs (1998);44(4):289-93

ACKNOWLEDGMENTS

The authors would like to thank Remy Agniel of ERRMECe laboratory for microscopical expertise, Coralie Torrens and Brigitte Baroukh of URP 2496 to their histological expertise.
The authors would like to thank BIOBank for providing financial support to this project.

Antibacterial and immunomodulatory decellularized Wharton's jelly scaffold for tissue engineering

Marie Dubus, Loïc Scomazzon, Julie Chevrier, Léa Abou Nassif, Fabien Lamret, Marius Colin, Cédric Mauprivez, Halima Kerdjoudj.

Université de Reims Champagne Ardenne, EA 4691, Biomatériaux et Inflammation en Site Osseux (BIOS), Reims, France.

* marie.dubus@univ-reims.fr

INTRODUCTION

Of all biologic matrices, decellularized tissues have emerged as a promising tool in the field of regenerative medicine. Few empirical clinical studies have shown that human Wharton's jelly (WJ) of the human umbilical cord promotes wound closure and reduces wound-related infections. It was in this scope that we investigated if decellularized (DC)-WJ could be used as an engineered biomaterial.

EXPERIMENTAL METHODS

After stripping the surrounding superfluous tissue (*i.e.* sub amniotic envelop and blood vessels), WJ matrix was treated for 24 h with Triton X-100 and DNase then freeze-dried. The effective removal of both cells and nucleic moieties was assessed by 4,6-diamidino-2-phenylin-dole (DAPI) staining and DNA quantification. Collagen and glycosaminoglycans were quantified. The linear modulus of DC-WJ was monitored in dry and wet conditions through quasi static tensile tests up to failure. Secretion of mediators by human neutrophils, monocytes and differentiated macrophages, cultured in the presence of DC-WJ was evaluated by ELISA. *In vitro* and *in vivo* biocompatibility were evaluated according to ISO/EN 10993 part 5 and ISO/EN 10993 part 6 guidelines, respectively. Antibacterial properties of DC-WJ were then tested against Gram positive and Gram negative bacteria.

RESULTS AND DISCUSSION

Following the full removal of cell membranes and nuclei moieties from Wharton's jelly (WJ) tissue, no major alterations in the ECM components (i.e. collagen, GAG content and growth factors), physical (i.e. porosity and swelling) and mechanical (i.e. linear tensile modulus) properties were noticed [1]. Interestingly, an increase in macromolecules and growth factors release was observed for DC-WJ, assuring thus a suitable bioactive matrix for cell maintenance upon recellularization. Based on the in vitro biocompatibility and stromal cell homing capabilities, DC-WJ provided an ideal substrate for stromal cells adhesion and colonization. Regarding the clinical application of WJ to treat infected wounds, we evaluated the antibacterial effect of DC-WJ on gram positive and gram negative strains. Surprisingly, in comparison with devitalized (DV)-WJ, our results showed bacteriostatic and antiadhesive effect of DC-WJ on *S. aureus*, *S. epidermidis* as well *E. coli* and *P. aeruginosa*. Although DC-WJ activated the neutrophils and monocytes in comparable magnitude than DV-WJ, macrophages modulated their phenotypes and polarization states from the resting M0 phenotype to the hybrid M1/M2 phenotype in the presence of DC-WJ. M1 phenotype was predominant in the presence of DV-WJ. Finally, the subcutaneous implantation of DC-WJ showed a total resorption after three weeks of implantation without any sign of foreign body reaction. Used as a membrane for guided bone regeneration, few bone regeneration evidence was found at the marginal area of the rat calvarial defect after eight weeks of implantation. The limited bone regeneration could be attributed to the immunomodulatory properties in favour of M2 phenotype but also to a lack of sufficient mechanical strength [2] that leads to the membrane collapse into bone defect area.

CONCLUSION

These significant data shed light on the potential regenerative application of DC-WJ in providing a suitable biomaterial for soft tissue regenerative medicine and an ideal strategy to prevent wound-associated infections. An increase in the mechanical features of DC-WJ in hydrated conditions is in progress.

REFERENCES

1. Dubus M et al., Biomedicines 2022, 10, 227.
2. Baldit A et al., Journal of the Mechanical Behavior of Biomedical Materials 2022, 126, 104981.

ACKNOWLEGDMENTS

This work was supported by "Region Grand Est, Fonds Régional de Coopération pour la Recherche-ERMES" and by Interreg France-WallonieVlaanderen "3D4MED" project.

Promising Decellularized Material Derived from Umbilical Cord Displays Extended Antibacterial Properties

Fabien Lamret*, Marie Dubus, Julie Chevrier, Cédric Mauprivez, Halima Kerdjoudj, Marius Colin

Biomatériaux et Inflammation en Site Osseux (BIOS) EA 4691, Université de Reims Champagne Ardenne, 51100 Reims, France.
* fabien.lamret@univ-reims.fr

INTRODUCTION

In the field of regenerative medicine, the potential use of decellularized extracellular matrix has recently raised as an emerging trend. While the medical use of cellularized materials is restricted by legislation and can lead to rejection from the patient, decellularization is meant to avoid these obstacles. Among sources of extracellular matrix, the human umbilical cord appears particularly valuable in terms of technical and ethical considerations. Indeed, abundant Wharton's Jelly (WJ) is extractible from human umbilical cords, and studies have demonstrated its potential application in wound closure and treatments of wound infections. Aiming to develop a legislative compliant medical device from WJ, we proceeded to its decellularization. Previously[1], we highlighted the immunomodulating properties of the decellularized WJ matrix (DWJ) and we initiated preliminary antibacterial tests, with promising results. In this study, we aimed to characterize these antibacterial properties against *Staphylococcus aureus*, first species involved in bone infections as well as in skin and soft tissues infections, and especially against *S. aureus* persistence mechanisms in recurrent infections.

EXPERIMENTAL METHODS

Planktonic growth, biofilm formation and Small Colony Variant (SCV) phenotype induction were conjointly followed in bipartite (DWJ+bacteria) and tripartite (DWJ+bacteria+titanium sample) models through culture methods, biomass staining, and confocal imaging. For each model respectively, three and six biological replicates of the experiments were conducts. We then sought to identify the DWJ post-partum metabolites involved and proceeded to methanol extraction followed by Centrifugal Partition Chromatography (CPC), Nuclear Magnetic Resonance (NMR) and Liquid Chromatography / Mass Spectrometry (LC/MS).

RESULTS AND DISCUSSION

Results confirmed the overall antibacterial properties of DJW, with a strong reduction of the biofilm formation on plastic and titanium (Mean $\log_{10}$ reduction of the number of adhered bacteria: -0.74). In presence of a gentamicin stress inducing bacterial persistence mechanisms, the reduction of the number of adhered bacteria was strongly increased (mean $\log_{10}$ reduction: -1.90; P=0.0152). Interestingly, the presence of DWJ did not induce SCVs formation. The extraction and CPC successfully lead to the isolation of ten fractions. NMR analysis revealed the presence of various compounds, including numerous fatty acids, nucleosides, traces of sterols and steroids and niacinamide. The antibacterial effects of the various fractions obtained, as well as the confocal analysis, are currently under investigation.
The first results highlight the specific antibiofilm effect of DWJ, especially under an antibiotic stress which is typical from infectious microenvironment.

CONCLUSION

DWJ appears as a promising adjuvant to clinically apply on bone sites, especially to avoid biofilm initiation on prosthesis materials or fight persistent infections.

REFERENCES

1. Dubus M. *et al*, Biomedicines. 10(2):227, 2022

ACKNOWLEDGMENTS

This work was supported partially by UmbRegen project and 3D4MED Interreg project.

High Hydrostatic Pressure (HHP) treatment influences apoptosis of porcine cartilage tissue

Nico Brandt[1], Christopher Pohl[1], Charlotte Koppe[1], Andreas Hoene[1], Daniel Behrendt[1], Friederike Poosch[2], Daniel Strüder[2], Michael Schlosser[1]
[1]Department of General Surgery, Visceral, Thoracic and Vascular Surgery, University Medical Center Greifswald, Greifswald, Germany; [2]Department of Oto-Rhino-Laryngology, Head and Neck Surgery, Rostock University Medical Center, Rostock, Germany
*nico.brandt@protonmail.com

INTRODUCTION

Tissue replacement by allogenic materials is of great importance in clinical practice. To ensure optimal transplantation outcome it is of utmost importance to reduce immunogenicity to minimize adverse inflammatory effects in recipients. These adverse effects are mainly triggered by protein and DNA components of foreign cells in the tissue-cell composite. Consequently, a successful method for decellularization is required High Hydrostatic Pressure (HHP) is currently under investigation as a new perspective for application on decellularization and devitalization of tissue. It utilizes pressure levels up to 600 MPa to induce apoptosis in cells, while keeping extremely high matrix integrity with undiminished biomechanical features.Therefore, this in vitro study aimed to determine the most effective levels of HHP for inducing apoptosis in porcine cartilage tissue.

EXPERIMENTAL METHODS

Porcine cartilage samples were extracted post mortem from from three different livestock animals. Following extraction, tissue samples were kept in PBS and HHP treated with either 150 MPa, 300 MPa, 450 MPa or 600 MPa for 10 minutes while untreated cartilage samples were used as control. After treatment all samples were fixated, placed in an embedding medium (TissueTek) and shock frozen in liquid nitrogen. Cryosections of 6 µm thickness were prepared with a Leica CM 3050 S Cryotome. TUNEL staining was used to identify in situ cell death. For quantitative analysis, the stained sections were photographed with a Keyence A-9000 fluorescence microscope and analysed by a custom-made script utilising the QuPath software. In order to compare the apoptosis rates of the different HHP treatments, various statistical tests were applied using the GraphPad Prism software. The Shapiro-Wilk-Test was used to analyse for normality distribution of data. Since data was not normally distributed, multiple group comparison was executed by Kruskal-Wallis-Test.

RESULTS AND DISCUSSION

In general, observed apoptosis rates of cartilage tissue treated with different intensities of HHP revealed significant differences (Figure 1). The untreated control showed a median apoptosis rate of 1.33 % (IQR 0.00 % - 4.63 %). In contrast, samples treated with 150 MPa showed an average apoptosis rate of 17.27 % (2.44 % - 55.24 %) as well as those exposed to 450 MPa reacted with 5.67 % (0.35 % - 27.57%). Samples treated with 150 MPa showed a highly significant increased apoptosis compared to control samples and those treated with 300 MPa and 600 MPa ($p < 0.0001$) and, to a lesser extend compared to 450 MPa ($p = 0.0263$). Interestingly, samples treated with 450 MPa showed a highly significant increase in apoptosis compared to 300 MPa ($p < 0.0001$) and to 600 MPa ($p = 0.0016$), but also a tendency of increased apoptosis compared to untreated control samples ($p = 0.0533$).

CONCLUSION

By morphometric histological analysis, we were able to demonstrate a significant, up to 15% increase of median apoptosis rate in HHP treated cartilage, compared to untreated control samples. Moreover, as previously described in cell culture experiments, a significant increase of in situ cell death in chondrocytes following exposure to 150 MPa HHP treatment could be shown. We were able to confirm this observation in differentiated porcine cartilage tissue sections. In addition, a apoptotic tendency can be observed in samples treated with 450 MPa. In contrast, this effect could not be detected in cell culture, possibly caused by different cell types as well as metabolic-stages or matrix enclosure. Further analyses with higher biological sample numbers are needed to confirm these results and tendencies.

ACKNOWLEDGMENTS

This study was supported by the European Social Fund, HOGEMA project P4 (grant no. ESF/14-BM-A55-0015/18).

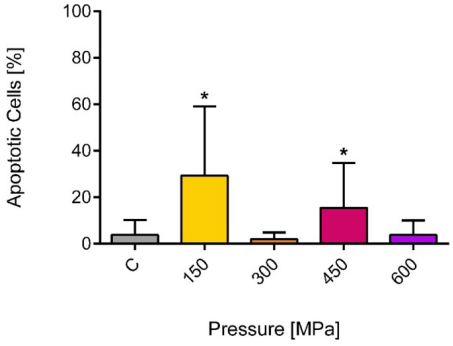

Figure 1 ***Apoptosis rates after High Hydrostatic Pressure (HHP) treatment of cartilage tissue***
HHP treated samples at 150 MPa, 300 MPa, 450 MPa and 600 MPa in comparison to untreated control (C). Data given from three different biological individuals showed a highly significant increase in apoptosis compared to control at 150 ($p < 0.0001$) Cartilage exposed to 450 MPa revealed a tendency of increased apoptosis, when compared to untreated control samples ($p = 0.0533$) and highly significant as well as significant increase compared to samples exposed to other pressure levels.

Co-encapsulation of Macrophages with *Candida albicans* in Porcine Decellularized Adipose Extracellular Matrix Hydrogels

Rosalía Diez-Orejas[1*], Mónica Cicuéndez[2], Andrea García-Lizarribar[3], Laura Casarrubios[4], Alberto Polo-Montalvo[4], María José Feito[4], Francisco Javier Fernández-San Argimiro[3], Nerea García-Urkia[3], Olatz Murua[3], Iratxe Madarieta[3], Beatriz Olalde[3], María Teresa Portolés[4,5]

[1]Departamento de Microbiología y Parasitología, Universidad Complutense de Madrid (UCM), Instituto de Investigación Sanitaria del Hospital Clínico San Carlos (IdISSC), 28040 Madrid, Spain
[2]Departamento de Química en Ciencias Farmacéuticas, UCM, IdISSC, 28040 Madrid, Spain
[3]TECNALIA, Basque Research and Technology Alliance (BRTA), E20009 Donostia-San Sebastian, Spain
[4]Departamento de Bioquímica y Biología Molecular, UCM, IdISSC, 28040 Madrid, Spain
[5]CIBER de Bioingeniería, Biomateriales y Nanomedicina, CIBER-BBN, 28040 Madrid, Spain
[*]rosaliad@farm.ucm.es

INTRODUCTION

Candida albicans is a human commensal fungus that when the host immunocompetence decreases behaves as an opportunistic pathogen rendering invasive infections. Cellular immune response and mostly macrophages are key factors in the resolution of candidiasis. Macrophages exhibit functional plasticity that allows them to polarize towards pro-inflammatory (M1) and anti-inflammatory (M2) phenotypes. The importance of the M1 polarization of macrophages for fungal elimination have been fully addressed.[1] In the present study, Raw 264.7 macrophages were co-encapsulated with *Candida albicans* in ECM hydrogels prepared from porcine decellularized adipose tissue (pDAM) to evaluate the effects of the hydrogel concentration on the macrophage/fungus interaction.

EXPERIMENTAL METHODS

Porcine adipose tissue decellularization and pre-gel preparation: porcine adipose tissue was decellularized following an organic solvent-based methodology, previously published by the group. Powdered pDAM (5-10 mg/ml) was enzymatically digested with pepsin in 0.1 N HCl for 48 h at room temperature. The pH and salt concentration of the digested pDAM was adjusted to 7.4.

Cell encapsulation: Raw 264.7 macrophages and *Candida albicans* expressing a red fluorescent protein were prepared in 150 µl of culture medium (1:1 ratio) and mixed with 300 µl of pDAM pre-gel at three final concentrations (A 10 mg/ml, B 7.5 mg/ml and C 5 mg/ml). Then, 100 µl of the mixture were deposited in glass bottom dishes and maintained at 37 ºC under a 5% CO_2 atmosphere for 1 hour. Then, 2 ml of medium were added and cultured for 3 and 24 h.

Confocal microscopy studies: The samples were fixed with 4% paraformaldehyde, permeabilizated with 0.1% Triton X-100 and, incubated with FITC-phalloidin and with 3 µM DAPI, to stain F-actin filaments in green and cell nuclei in blue, respectively. The samples were examined using a Leica SP2 Confocal Laser Scanning Microscope (Centro de Citometría y Microscopía de Fluorescencia UCM).

Detection of TNF-α: This pro-inflammatory cytokine secreted by Raw-264.7 macrophages was quantified in the culture supernatants after 3 and 24 hours by enzyme-linked immunosorbent assay.

Statistics: Statistical analysis was performed by using the Statistical Package for the Social Sciences (SPSS) version 22 software.

RESULTS AND DISCUSSION

Raw 264.7 macrophages and RFP-*Candida albicans* were successfully encapsulated in pDAM hydrogels at different concentrations. Raw 264.7 macrophages proliferate better in the hydrogel A (10 mg/ml), however *Candida albicans* proliferate better in the less concentrated hydrogel C. The hydrogel concentration also influenced the macrophage defence capability against the fungus. TNF-α secretion by encapsulated macrophages increased, in a time dependent manner, and was significantly higher in macrophages co-encapsulated with *Candida albicans* in the hydrogel C than in the hydrogel A.

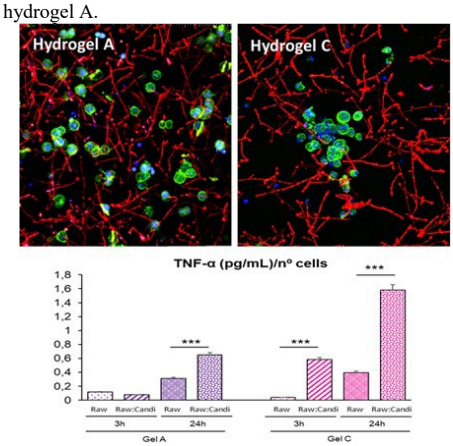

CONCLUSION

The co-encapsulation of macrophages with *Candida albicans* in pDAM hydrogels represents an excellent 3D experimental model to evaluate macrophage-pathogen interactions.

REFERENCES

1. Gao, Q. *et al*., ACS Nano 14:3980-3990, 2020

ACKNOWLEDGMENTS

This work was supported by the European Union's Horizon 2020 Research and Innovation Programme (FETOPEN-2018-2020, NeuroStimSpinal Project, Grant Agreement No. 829060).

Use of tubular plants as vascular models: A feasibility study of decellularization and characterization

Ali Salehi*, Gemma Lucas Salido, Giorgio Cattaneo

Institute for Biomedical Engineering (BMT), Universityof Stuttgart, Stuttgart, Germany
* ali.salehi@bmt.uni-stuttgart.de

INTRODUCTION

Due to the increasing rate of death by heart diseases and stroke, investigation of intravascular implants remains an important issue. Pre-clinical investigation of implants is performed in in-vitro models, that normally do not provide a natural biological test environment and in in-vivo models, that have disadvantages such as high cost, complexity, not reproducibility and ethical concerns. On the other hand, based on recent research[1-5] plant scaffolds as natural, cost-effective, nontoxic substrates with suitable microstructure for the proliferation of human cells are high potential biomaterials. Therefore, we are motivated to use tubular plants as novel biologized vessel models, called "Green Vessels" for cardiovascular research and potentially as novel implants. In this study, we present first results of mechanical and microstructural properties of decellularized selected plans.

EXPERIMENTAL METHODS

A pre-selection among various tubular plants was performed according to the following criteria: geometry and dimensions (inner diameter in the range between 3 and 7,5 mm); stability and integrity before and after decellularization; and withstanding flow (50 rpm) when connected to a peristaltic pump.
A decellularization process was carried out following three consecutive washing steps of 7 cm long plant samples in Hexane (99%) and PBS for six minutes to remove wax cuticles. Afterward, the samples were soaked in a 10% SDS solution for 5 days, and then in 0.1% Triton-X-100 and 10% bleach solution for 2 days. DNA quantification tests were performed for both native and decellularized samples to evaluate complete decellularization using Zymo's Quick-DNA Plant/Seed Miniprep Kit for DNA extraction and a Biotek's Take3 Plate for DNA quantification based on light absorbance.

To characterize mechanical properties of the selected tubular plants, their Young's modulus was measured utilizing tensile tests by INSTRON 34SC-1 machine. To visualize nano/microstructural properties of the inner surface of the tubular plants, SEM and Confocal microscopy images were obtained from both native and decellularized plants. For both experiments, the number of samples ranged between 3-5 per group.

RESULTS AND DISCUSSION

Based on the above-mentioned criteria, four candidates were selected: Green onion (*Allium fistulosum*), Wheat (*Triticum aestivum*), Water spinach (*Ipomoea aquatica*) and Water horsetail (*Equisetum fluviatile*). The four introduced tubular plants could resist the physiological flow and were stable after a complete decellularization.

Comparing DNA amounts in samples before and after decellularization proved effective elimination of plant cells. Mechanical tests showed a reduction of Young's modulus after the decellularizationprocess (16, 21, 280, 2040 MPa) compared to native plants (9, 12, 70, 689 MPa) in Green onion, Water spinach, Water horsetail, Wheat respectively.
SEM images of the selected plants illustrated that each of them owns unique natural microstructures. Confocal imaging for 3D visualization of available patterns on the inner walls showed that plant cell removal left concave spaces non-presented in the non-decellularized natural structure. These patterns can potentially provide a suitable environment for human endothelial cells to adhere and proliferate.

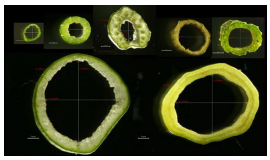

Fig1: Cross-sectional images of the selected plants

Fig.2: Decellularized plant

CONCLUSION

Although all the plants presented higher Young's modulus than human natural vessels, Green onion and Water spinach showed more similar mechanical behavior and further experiments should be carried out to adjust the mechanic of the plants. Collected data of microstructural imaging showed a change in thestructure of the inner wall of plants after decellularization. As a goal, we aim at using these structures as 3D scaffolds for endothelialization to assess the feasibility of biologized plant-based vessels for in vitro research and potentially as tissue-engineeredvessel grafts.

REFERENCES

1. Salehi, A. *et al*., J. Cell Physiol. 236: 5306– 5316, 2021
2. Salehi, A. *et al*., J. Drug Delivery. 63: 102453, 2021
3. Salehi, A. *et al*., Gene. 757:144852, 2020
4. Bai. H. *et al*., ACS Omega. 6,17 11595-11601, 2021
5. Negrini. N. *et al*., Frontiers in B. 8: 723, 2021

ACKNOWLEDGMENTS

We would like to thank the "University of Stuttgart" and "Ministerium für wissenschaft forschung und kunst baden-württemberg" for providing financial support to this project. We thank many institutes of the University of Stuttgart for providing equipment.

Porcine Decellularized Adipose Extracellular Matrix Hydrogels Modulate Proliferation and Pro-inflammatory Response of Encapsulated Macrophages

Mónica Cicuéndez[1*], Andrea García-Lizarribar[2], Laura Casarrubios[3], Alberto Polo-Montalvo[3], María José Feito[3], Francisco Javier Fernández-San-Argimiro[2], Nerea García-Urkia[2], Olatz Murua[2], Iratxe Madarieta[2], Rosalía Diez-Orejas[4], Beatriz Olalde[2], María Teresa Portolés[3,5]

[1]Departamento de Química en Ciencias Farmacéuticas, Universidad Complutense de Madrid (UCM), Instituto de Investigación Sanitaria del Hospital Clínico San Carlos (IdISSC), 28040 Madrid, Spain
[2]TECNALIA, Basque Research and Technology Alliance (BRTA), E20009 Donostia-San Sebastian, Spain
[3]Departamento de Bioquímica y Biología Molecular, UCM, IdISSC, 28040 Madrid, Spain
[4]Departamento de Microbiología y Parasitología, UCM, IdISSC, 28040 Madrid, Spain
[5]CIBER de Bioingeniería, Biomateriales y Nanomedicina, CIBER-BBN, 28040 Madrid, Spain
[*]mcicuendez@farm.ucm.es

INTRODUCTION

Macrophage polarization towards M1 and M2 phenotypes mediates pro-inflammatory and anti-inflammatory processes respectively, which are crucial in the response of the organism to biomaterials.[1] Hydrogels are often used as scaffolds for tissue engineering due to their structural properties similar to extracellular matrix (ECM). Different hydrogel properties such as hydrophobicity may alter macrophage adhesion and biological response.[2] In the present study, Raw 264.7 macrophages were encapsulated in ECM hydrogels prepared from porcine decellularized adipose tissue (pDAM) to evaluate the effects of the hydrogel concentration on macrophage proliferation and secretion of pro-inflammatory cytokines such as TNF-α and IL-6.

EXPERIMENTAL METHODS

Porcine adipose tissue decellularization and pre-gel preparation: porcine adipose tissue was decellularized following an organic solvent-based methodology, previously published by the group. Powdered pDAM (5-10 mg/ml) was enzymatically digested with pepsin in 0.1 N HCl for 48 h at room temperature. The pH and salt concentration of the digested pDAM was adjusted to 7.4.
Cell encapsulation: Raw 264.7 macrophages at a concentration of 450,000 cells in 150 µl of specific culture medium, were mixed with 300 µl of pDAM pre-gel at three final concentrations (A 10 mg/ml, B 7.5 mg/ml and C 5 mg/ml). Then, 100 µl of the mixture were deposited in glass bottom dishes and maintained at 37 ºC under a 5% CO_2 atmosphere for 1 hour for induction of gelation. Afterwards, 2 ml of medium were added and cultured at 37 ºC under a 5% CO_2 atmosphere for 3 and 5 days.
Confocal microscopy studies: Encapsulated cells were fixed with 4% paraformaldehyde, permeabilized with 0.1% Triton X-100 and, incubated with FITC-phalloidin and with 3 µM DAPI, to stain F-actin filaments in green and cell nuclei in blue, respectively. The samples were examined using a Leica SP2 Confocal Laser Scanning Microscope (Centro de Citometría y Microscopía de Fluorescencia UCM). The proliferation rate was calculated considering the number of cells per microliter hydrogel volume.
Detection of TNF-α and IL-6: These pro-inflammatory cytokines secreted by Raw-264.7 macrophages were quantified in the culture supernatants after 3 hours, 24 hours and 5 days by enzyme-linked immunosorbent assay.
Statistics: Statistical analysis was performed by using the Statistical Package for the Social Sciences (SPSS) version 22 software.

RESULTS AND DISCUSSION

Raw 264.7 macrophages were successfully encapsulated in pDAM hydrogels at different concentrations. Confocal microscopy studies evidenced that Raw 264.7 macrophages proliferate better in the hydrogel A (10 mg/ml) than in the less concentrated hydrogel C (5 mg/ml). TNF-α and IL-6 secreted by encapsulated Raw-264.7 macrophages increased in a time dependent manner and were significantly lower in macrophages encapsulated in the hydrogel A than in the hydrogel C.

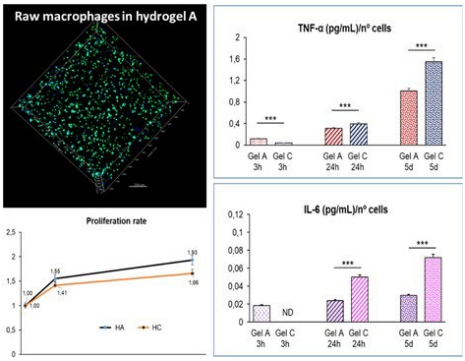

CONCLUSION

These results indicate that the concentration of the pDAM in the hydrogel modulates the proliferation and the pro-inflammatory response of encapsulated macrophages.

REFERENCES

1. Ping J. *et al*., Mol. Immunol. 38:110–120, 2021
2. Xu Z. *et al*., Biochem. Eng. J. 165: 107821, 2021

ACKNOWLEDGMENTS

This work was supported by the European Union's Horizon 2020 Research and Innovation Programme (FETOPEN-2018-2020, NeuroStimSpinal Project, Grant Agreement No. 829060).

Effects of Porcine Decellularized Adipose Extracellular Matrix Hydrogels on Encapsulated Liver, Lung and Kidney Cells

Alberto Polo-Montalvo[1], Mónica Cicuéndez[2], Andrea García-Lizarribar[3], Laura Casarrubios[1], María José Feito[1], Francisco Javier Fernández San Argimiro[3] Nerea García-Urkia[3], Olatz Murua[3], Iratxe Madarieta[3], Rosalía Diez-Orejas[4], Beatriz Olalde[3], María Teresa Portolés[1,5*]

[1]Departamento de Bioquímica y Biología Molecular, Universidad Complutense de Madrid (UCM), Instituto de Investigación Sanitaria del Hospital Clínico San Carlos (IdISSC), 28040 Madrid, Spain
[2]Departamento de Química en Ciencias Farmacéuticas, UCM, IdISSC, 28040 Madrid, Spain
[3]TECNALIA, Basque Research and Technology Alliance (BRTA), E20009 Donostia-San Sebastian, Spain
[4]Departamento de Microbiología y Parasitología, UCM, IdISSC, 28040 Madrid, Spain
[5]CIBER de Bioingeniería, Biomateriales y Nanomedicina, CIBER-BBN, 28040 Madrid, Spain
[*]portoles@quim.ucm.es

INTRODUCTION

Hydrogels are widely used as biomaterials for drug delivery, cell culture and tissue engineering. Owing to their high water content, hydrogels resemble natural tissues and may themselves regulate many cellular functions.[1] Cells in the different tissues produce their own surrounded extracellular matrix (ECM), which determines cell behavior and plays a key role in cell survival, proliferation, differentiation and migration.[2] The encapsulation of cells in hydrogels prepared with ECM would represent the most complete 3D model for understanding how cells respond to different physical and biochemical signals from their natural environment. In the present study, liver (Hep G2), kidney (HK-2), and lung (A549) cells, have been encapsulated in ECM-derived hydrogels prepared from porcine decellularized adipose matrix (pDAM). The effects of the hydrogel concentration on the functionality of these cell types have been evaluated by analyzing the cell morphology, proliferation rate, and lactate dehydrogenase release as plasma membrane damage marker

EXPERIMENTAL METHODS

Porcine adipose tissue decellularization and pre-gel preparation: porcine adipose tissue was decellularized following an organic solvent-based methodology, previously published by the group. Powdered pDAM (5-10 mg/ml) was enzymatically digested with pepsin in 0.1 N HCl for 48 h at room temperature. The pH and salt concentration of the digested pDAM was adjusted to 7.4.
Cell encapsulation: Liver (Hep G2), kidney (HK-2), and lung (A549) cells at a concentration of 450,000 cells in 150 µl of specific culture medium, were mixed with 300 µl of pDAM pre-gel at three final concentrations (A 10 mg/ml, B 7.5 mg/ml and C 5 mg/ml). Then, 100 µl of the mixture were deposited in glass bottom dishes and maintained at 37 ºC under a 5% CO_2 atmosphere for 1 hour to induce gelation. Afterwards, 2 ml of cell type-specific medium were added and cultured at 37 ºC under a 5% CO_2 atmosphere for 3 and 5 days.
Confocal microscopy studies: Encapsulated cells were fixed with 4% paraformaldehyde, permeabilizated with 0.1% Triton X-100 and, incubated with rhodamine-phalloidin and with 3 µM DAPI, to stain F-actin filaments in red and cell nuclei in blue, respectively. The samples were examined using a Leica SP2 Confocal Laser Scanning Microscope (Centro de Citometría y Microscopía de Fluorescencia UCM). The proliferation rate was calculated considering the number of cells per microliter hydrogel volume.
Lactate dehydrogenase (LDH) measurements: LDH activity was measured in the culture medium by an enzymatic method at 340 nm (Bio-Analítica).
Statistics: Statistical analysis was performed by using the Statistical Package for the Social Sciences (SPSS) version 22 software.

RESULTS AND DISCUSSION

The specific morphology of each cell type was observed after encapsulation of liver (Hep G2), kidney (HK-2), and lung (A549) cells in pDAM hydrogels. Lung cells proliferate better in hydrogel A (10 mg/ml), however, kidney and liver cells preferred the less concentrated hydrogel C (5 mg/ml). LDH measurements at 3 and 5 days indicate that there was no damage to the plasma membrane of lung, kidney and liver cells encapsulated in these ECM-derived hydrogels.

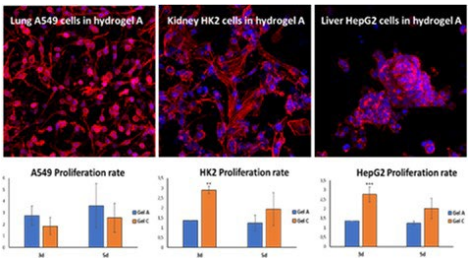

CONCLUSION

The encapsulation of lung, kidney and liver cells in ECM-derived hydrogels prepared from pDAM could be used as an excellent 3D experimental model to evaluate drug metabolism and toxicity.

REFERENCES

1. Wu X. *et al*., Nano Research 11: 5556–5565, 2018
2. Huang G. *et al*., Chem. Rev. 117: 12764-12850, 2017

ACKNOWLEDGMENTS

This work was supported by the European Union's Horizon 2020 Research and Innovation Programme (FETOPEN-2018-2020, NeuroStimSpinal Project, Grant Agreement No. 829060).

Porcine decellularized adipose matrix-based bioinks to fabricate 3D-printed models of the central nervous system

Andrea García-Lizarribar[1*], Lina Papadimitriou[2], Francisco-Javier Fernández-San-Argimino[1], Olatz Murua[1], Iratxe Madarieta[1],Anthi Ranella[2], Beatriz Olalde[1]

[1]TECNALIA, Basque Research and Technology Alliance (BRTA), E20009 Donostia-San Sebastian, Spain
[2]IESL, Foundation for Research and Technology-Hellas (FORTH), Heraklion, Crete, 71003, Greece
[*] andrea.garcia@tecnalia.com

INTRODUCTION

In vitro models of the central nervous system (CNS) aim to depict the neuronal and glial communication pathways in a simplistic way that can be easily monitored and analyzed afterward. In this context, *in vitro* models based on biomaterials brings the opportunity to recapitulate the microenvironment of brain tissue, which comprise different types of neural cells, glial cells and components of the extracellular matrix (ECM). Among them, hydrogels based on decellularized ECMs provide the widest diversity of biomolecules present in native tissues, which better mimic the complexity of tissue microenvironment in contrast to hydrogels based in isolated polymers[1].

The brain anatomy is organized in segments that are connected through the interaction of afferent axons and efferent neural bodies. To recapitulate the architecture of neural pathways, the axonal growth can be oriented towards the direction of a given flux[2] or achieving aligned nanopatterned 3D structures of ECM components[3]. A more controlled and direct way to align the biopolymer chains can be achieved by the shear forces generated during extrusion bioprinting. In this layer-by-layer fabrication, the geometry of the 3D culture can be designed to enhance the connection of different neural compartments. Furthermore, the fabrication of *in vitro* models by additive manufacturing techniques optimizes the time of fabrication and bioink deposition volume in an automated manner.

EXPERIMENTAL METHODS

In this study, we develop highly printable bioinks based on a porcine decellularized adipose matrix (pDAM) for the automated fabrication of *in vitro* models of CNS. The parameters of extrusion bioprinting were configured to promote the directionality of the axons. To achieve cocultures of neural and glial cells, we encapsulate embryonic neuroectodermal cells that are committed to neurons and astrocytes after the priming with retinoic acid (RA).

RESULTS AND DISCUSSION

Differentiated neurons were organized as neural clusters homogeneously distributed in the 3D culture which showed numerous and elongated projections of neurites (**Figure 1**). Though to a lesser extent, bioprinted models cultured on basal medium, without neural differentiation factors, displayed differentiated neurons with considerable growth of neurites. Our results suggested that the pDAM bioink induces the spontaneous differentiation of neural precursor cells. The combination of pDAM bioink with extrusion bioprinting technique promoted the orientation of the neurites toward the printing direction, which could be guided to enhance synaptic events.

CONCLUSION

The intrinsic properties of pDAM bioinks allow the automated fabrication of *in vitro* models of the central nervous system with enhanced differentiation of both neural and glial cells.

These features make the bioprinted model a potential candidate to study biological processes of healthy brain and neurodegenerative diseases *in vitro* in an affordable and straightforward manner.

REFERENCES

1. Cicuéndez, M., *et al*., Int. J. Mol. Sci. 21, 3847-3869, 2020.
2. Odawara, A., *et al*., RSC Advances, 3(45), 23620–23630, 2013.
3. Kamudzandu, M., *et al*., RSC Advances, 5(28), 22053–22059, 2015.

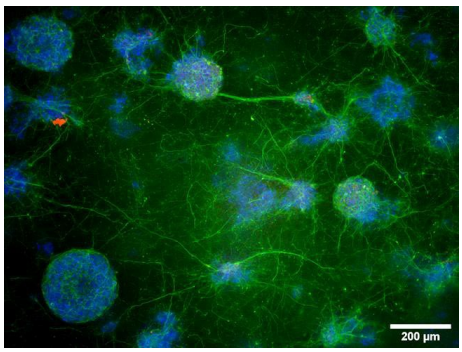

Figure 1. Confocal image of neuroectodermal precursor cells encapsulated in pDAM and cultured for 17 days. Differentiated neurons, astrocytes and nuclei were stained using Tuj1 (green), GFAP (red) and Hoechst (blue) respectively.

ACKNOWLEDGMENTS

This work has been supported by the European Union's Horizon 2020 Research and Innovation Programme (H2020-FETOPEN-2018-2020, NeuroStimSpinal Project, Grant Agreement No. 829060).

Optimization of Cartilage Decellularization to Obtain Functional Extracellular Matrix

Unai Mendibil[1,2,*], Nerea Garcia-Urquia[2], Mikel Azkargorta[3], Felix Elortza[3], Beatriz Olalde[2], Ander Abarrategi[1,4]

[1]Center for Cooperative Research in Biomaterial (CIC biomaGUNE), Donostia-San Sebastian, Spain
[2]TECNALIA, Donostia-San Sebastian, Spain
[3]Center for Cooperative Research in Biosciences (CIC bioGUNE), Donostia-San Sebastian, Spain
[4]Ikerbasque, Basque Foundation for Science, Bilbao, Spain
[*] umendibil@cicbiomagune.es

INTRODUCTION

In recent years, decellularized extracellular matrix (dECM)-derived materials have gained interest as potentially bioactive and regenerative compounds, also in cartilage field. The mainstream in the field is considering that decellularization protocol must be tissue-specific[1], to preserve key tissue-related ECM components[2]. A systematic study to define the best cartilage tissue-specific decellularization method has not been pursued, yet.

The aim of this work is to define an optimal cartilage tissue-specific decellularization method for the production of optimal cartilage dECM, useful as *in vitro* cell culture testing platform and as *in vivo* regenerative material.

EXPERIMENTAL METHODS

Porcine cartilage tissue was isolated and processed in a variety of decellularization techniques. Detergents as SDS and triton X-100, enzymes as DNAse and trypsin-EDTA, and multiple physical methods as freezing cycles and vacuum-assisted decellularization were tested in different combinations and concentrations. After a preliminary characterization step, three custom-designed protocol were selected as good candidates to their in-deed characterization and production of 3D structures.

The samples were characterized by histology and proteomics, among others. The materials were used to create solid foams and the obtained structures were studied. Further on, their *in vitro* biocompatibility and differentiation capacities were tested. In parallel, hydrogels were created, 3D printed and tested in *in vitro* cell culture studies (**Figure 1**).

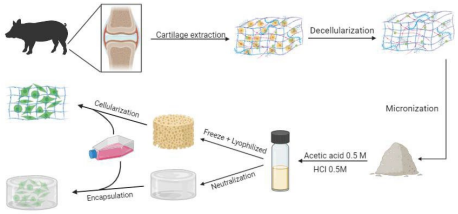

Figure 1: *Schematics of the decellularization and post-processing*

RESULTS AND DISCUSSION

Samples obtained from decellularization protocols were characterized and we observed differences between treatments regarding the obtained final protein composition and structural properties. Besides, only one decellularization treatment allows to generate stable 3D structures once freeze-dried and tested for cell culture conditions. These samples show good biocompatibility in terms of cell proliferation (**Figure 2**) and cartilage differentiation.

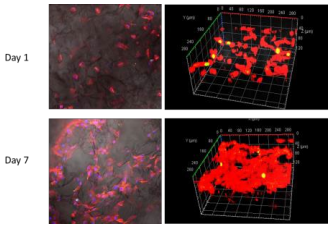

Figure 2: Cartilage ECM scaffolds are biocompatible. *Images show ATDC5 cartilage cell line seeded in cartilage-ECM scaffolds. Cells were incubated for 7 days. At day 1 and day 7 samples were fixed and stained for the detection of proliferative cells (Ki-67, green), Cytosqueleton (Actin, red) and Nuclei (DAPI, blue).*

CONCLUSIONS

We have tested different cartilage tissue decellularization protocols and we have defined a decellularization protocol which preserve the key cartilage ECM molecules, while allows the fabrication of solid-foam 3D structures. Materials are biocompatible and able to support cartilage cell differentiation. Further *in vivo* studies will be performed to define their cartilage regenerative potential.

REFERENCES

1. Mendibil *et al*. International Journal of Molecular Sciences, 2020.
2. Benjamin D. Elder *et al*. Neurosurgery, 2010.

ACKNOWLEDGMENTS

Grant RTI2018-101708-A-I00 and RYC2018-025502-I funded by MCIN/AEI/10.13039/501100011033, by ERDF A way of making Europe and by ESF Investing in your future. Grant MDM-2017-0720 funded by the Spanish State Research Agency. Grant KK-2019/00093 funded by Basque Government. Finally, Grant CICBMG_PhD_05_2019 funded by CICbiomaGUNE and Tecnalia.

3D Bioinspired Hydrogels with Molecularly Imprinted Nanoparticles Sequester Endogenous Growth Factors and Synergistically Direct Stem Cell Fate Commitment

Simão P. B. Teixeira[1,2], Alberto Pardo[1,2,3], Syeda M. Bakht[1,2], Manuel Gomez-Florit[1,2], Rui L. Reis[1,2], Manuela E. Gomes[1,2], Rui M. A. Domingues[1,2]

[1]3B's Research Group, I3Bs—Research Institute on Biomaterials, Biodegradables and Biomimetics of University of Minho, Headquarters of the European Institute of Excellence on Tissue Engineering and Regenerative Medicine, AvePark – Parque de Ciência e Tecnologia, Zona Industrial da Gandra, 4805-017 Barco GMR, Portugal.
[2]ICVS/3B's–PT Government Associate Laboratory, Braga/Guimarães, Portugal.
[3]Colloids and Polymers Physics Group, Particle Physics Department and Health Research Institute, University of Santiago de Compostela, 15782 Santiago de Compostela, Spain
* simao.teixeira@i3bs.uminho.pt

INTRODUCTION

Growth factors (GFs) are a crucial element for tissue regeneration, but their exogenous administration has proven expensive and ineffective. Biomaterial approaches inspired by the extracellular matrix have attempted to sequester GFs, thus regulating their activity and presentation to cell receptors.[1] Our previous work first demonstrated that molecularly imprinted nanoparticles (MINPs) can fulfill these requirements in standard 2D and 3D cell cultures, combining high recognition specificity, stability, and cost-effectiveness.[2] Taking this concept to the next level, here we tested MINPs against transforming growth factor (TGF)-β3, a regulator of tenogenesis, in hydrogel scaffolds with bioinspired ordered microstructures. Our hypothesis is that combined control over biochemical and biophysical stimuli will synergistically contribute to more robust tenogenic commitment of stem cells.

EXPERIMENTAL METHODS

MINPs were synthesized by solid phase imprinting using acryloyl-containing monomers and a TGF-β3 N-terminal epitope as the template. Their affinity and selectivity were assessed by surface plasmon resonance (SPR), Western and dot blots. 50-µm microfibers were produced by cryosectioning of electrospun polycaprolactone meshes. To enable their remote orientation within hydrogels, superparamagnetic iron oxide nanoparticles were synthesized by thermal decomposition and incorporated in the electrospinning solution. Lastly, tenogenic constructs were assembled by enzymatically crosslinking gelatin, encapsulating human adipose tissue-derived stem cells (hASCs), along with microfibers and MINPs. A uniform magnetic field was employed during gelation to unidirectionally align the microfibers.

RESULTS AND DISCUSSION

MINPs showed an outstanding affinity for the template in SPR assays (K_D = 18±13 nM), in the range of some monoclonal antibodies. Comparatively, the interaction between TGF-β3 epitope and MINPs imprinted against biotin was negligible, demonstrating the imprinting effect on the molecular recognition ability of nanoparticles. hASCs remained viable for over 14 days within the constructs, preferentially orientating in line with the microfiber alignment axis (**Fig. 1**). Initial qPCR results reveal a positive correlation between MINP concentration and tendon-associated gene expression markers (*SCX, TNMD, TNC*) in aligned structures, which does not occur in hydrogels with randomly oriented microfibers. Moreover, *ALP* expression (associated with osteogenesis) was downregulated with increasing MINP concentrations, supporting the hypothesis of phenotypic steering toward tenogenesis. Protein synthesis is currently under analysis by immunostaining to reinforce these results.

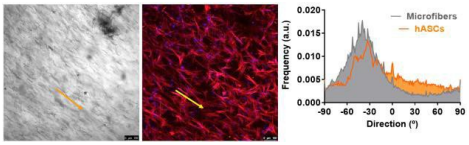

Fig. 1 – Confocal microscopy images of constructs on day 14. Left: brightfield image of magnetic microfibers. Right: fluorescence image of hASCs. Orange arrows represent the peak direction. Histogram shows that hASCs favourably follow the direction of microfibers.

CONCLUSION

Our findings show the potential of molecular imprinting as a cost-effective tool in the tissue engineering kit, allowing an efficient substitution of expensive commercial GFs. Furthermore, we also establish that its coupling with microstructural cues synergistically directs stem cell commitment toward tenogenesis in engineered constructs. Hence, the principles behind this strategy can be applied not only to improve tendon healing after injury, but also for engineering other tissues.

REFERENCES

1. Teixeira, S. *et al*. Adv.Funct.Mater. 30:1909011, 2020.
2. Teixeira, S. *et al*. Adv.Funct.Mater. 31:2003934, 2021.

ACKNOWLEDGMENTS

EU HORIZON 2020 for projects ACHILLES (Twinning-810850) and MagTendon (ERC-2017-CoG-772817); FCT/MCTES for scholarships PD/BD/143039/2018 (S.P.B.T.) and PD/BD/129403/2017 (S.M.B.) under PhD PATH (PD/00169/2013), project SmarTendon (PTDC/NAN-MAT/30595/2017), and individual contracts 2020.03410.CEECIND (R.M.A.D.) and CEECIND/01375/2017 (M.G.F.); Xunta de Galicia for postdoctoral grant ED481B2019/025 (A.P.).

Designing a NanoIntelligent bioartificial pancreas to treat type I Diabetes

Joana Moreira Marques[1;2], Ana Margarida Carvalho[1], Rute Nunes[1;4], José das Neves[1;4], Helena Florindo[3], Domingos Ferreira[2], Bruno Sarmento[1;4*]

[1]i3S - Institute for Research & Innovation in Health, University of Porto, Porto, Portugal
[2]Faculty of Pharmacy of the University of Porto, Porto, Portugal
[3]Faculty of Pharmacy of the Universidade de Lisboa, Lisbon, Portugal
[4]CESPU – Instituto de Investigação e Formação Avançada em Ciências e Tecnologias da Saúde, Instituto Universitário de Ciências da Saúde
[*]Presenting Author: jcmarques@i3s.up.pt

INTRODUCTION

Diabetes mellitus (DM) is one of the biggest health problems nowadays, being estimated that 537 million individuals suffer from DM worldwide[1]. Type 1 DM (T1DM) is a chronic auto-immune disease characterized by insulin insufficient secretion due to β-cells destruction[1]. Since T1DM is not preventable and most of the cases are diagnosed after extensive β-cells destruction[2], definitive cure consists in replacing the destroyed pancreas[3]. However, the number of available donors is limited, in addition to the need of a lifelong immunosuppressive therapy. In this work, we propose the development of an innovative biomimetic pancreas, comprising β- and α-cells differentiated from human induced pluripotent stem cells (hiPSCs) immobilized in a biofunctional matrix, embedding glucose-responsive nanoparticles (NPs) encapsulating a GLP-1 analogue. Glucose sensitiveness will be accomplished by the incorporation of glucose oxidase (GOx) in the system, which oxidizes glucose into gluconic acid, thus transiently decreasing the surrounding pH (↓).

EXPERIMENTAL METHODS

pH-sensitive NPs based on hybrid PLGA/ polymethacrylates matrices were produced by double emulsion technique to encapsulate GLP-1 analogue exenatide (EXN) or semaglutide (SMG). NPs were characterized regarding average size, size distribution and zeta potential by DLS. Association efficiency (AE) and drug loading (DL) were determined by HPLC. EXN and SMG *in vitro* release profiles were assessed at different pH (5.0 and 7.4), while secondary structure stability after release was assessed by circular dichroism. WLS-4D1 hiPSCs were differentiated into β- and α-cells[4,5] and the differentiation efficiency was assessed at different stages by flow cytometry through the expression of key cell markers. Differentiated β-cells functionality was assessed *in vitro* by glucose-stimulated insulin secretion (GSIS) assay. Undifferentiated hiPSCs were immobilized in alginate hydrogel and cell viability was evaluated by resazurin reduction assay.

RESULTS AND DISCUSSION

Different NP formulations showed a monodisperse population (PdI <0.170) with an average size ranging from 130 to 155 nm and zeta potential (ZP) around +25-40 mV for higher polymethacrylates ratios, decreasing up to -7 mV for higher PLGA proportions. EXN and SMG were encapsulated using different DL (between 5% and 15%). For EXN-loaded NPs, AE values ranged from 34% to 49%, while SMG-loaded NPs AE ranged from 50% to 65%, depending on polymers ratios. NPs showed a pH-dependent *in vitro* release profile, despite showing a burst release of around 40% at pH 7.4 and 60-70% at pH 5 after 5 minutes, depending on the peptide. Both EXN and SMG maintained their secondary structure after at least 48h of *in vitro* release, when compared to native structure. Regarding hiPSCs differentiation into β-cells, insulin-positive cells (INS^+) were successfully obtained (99%), despite showing low glucose-responsiveness in the GSIS assay, due to <1% co-expression of NKX6.1 and insulin. Concerning α-cells differentiation, monohormonal glucagon-positive cells (GLU^+) were obtained, as well as a population of polyhormonal GLU^+,INS^+ cells (3.8%). Undifferentiated hiPSCs remained viable 3 days after immobilization in alginate, thus supporting the suitability of the protocol developed for cell immobilization.

CONCLUSION

GLP-1 analog-loaded glucose-responsive NPs were successfully produced and encapsulated peptides retained their secondary structure. Glucagon- and insulin-producing differentiated cells were obtained, even though the last were not fully responsive to changes in glucose levels. Furthermore, the protocol developed for hiPSCs immobilization in alginate can be easily applied to the immobilization of differentiated cells. Currently, an *in vivo* study is being performed to assess the efficacy of the biofunctional system after transplantation in a diabetic mouse model.

REFERENCES

1. International Diabetes Federation, IDF Diabetes Atlas, 10th ed Brussels, Belgium 2021
2. Mannucci E., *et al*., J. Endocrinol. Invest. 37: 477-495, 2014
3. Pellegrini S. *et al*., Acta Diabetol. 53:683-691, 2016
4. Rezania A., *et al*., Nat. Biotechnol. 32:1121-1133, 2014
5. Peterson Q.P., *et al.* Nat. Commun. 11:2241-2241, 2020

ACKNOWLEDGMENTS

The work was funded by the Portuguese Science and Technology Foundation (FCT) (Project PTDC/MED-OUT/30466/2017, POCI-01-0145-FEDER-030466). Joana Marques acknowledges FCT for financial support through the grant PD/BD/145149/2019 (through the PhD Program in Medicines and Pharmaceutical Innovation, i3DU).

ECM mimicking hydrogel scaffolds for liver tissue engineering

Nathan Carpentier[1*], Louis Van der Meeren[2], Andre Skirtach[2], Lindsey Devisscher[3], Hans Van Vlierberghe[4], Peter Dubruel[1], Sandra Van Vlierberghe[1]

[1] Polymer Chemistry and Biomaterials group, Ghent University, Ghent, Belgium
[2] Nano-biotechnology Laboratory, Ghent university; Ghent, Belgium
[3] Gut-Liver Immunopharmacology Unit, Dpt Basic and Applied Medical Sciences, Ghent University, Ghent, Belgium
[4] Hepatology Research Unit, Dpt Internal Medicine and Paediatrics, Ghent University, Ghent, Belgium
[*] Nathan.Carpentier@UGent.be

INTRODUCTION

Annually, millions of people die because of liver failure, while the waiting duration for a donor liver is around 12 months.[1] Herein, we target hybrid 3D-printed scaffolds to serve liver tissue engineering applications.
As starting materials gelatin in combination with a polysaccharide was used to develop printable hydrogels. As polysaccharides dextran (Dex) and chondroitin sulphate (CS) were selected as mimics for the liver extracellular matrix (ECM) to explore their effect on the cell response. Methacrylated gelatin (GelMA) served as benchmark. The hydrogel materials were characterized on 2D-as well as on 3D-level.

EXPERIMENTAL METHODS

Development of Methacrylated gelatin

Methacrylated gelatin (GelMA) was developed by a protocol described before by Van Den Bulcke *et al.*[2] GelMA was subsequent crosslinked using UV-A light in the presence of Li-TPOL as a photo-initiator.

Development of DexNB-GelSH

Thiolated gelatin (GelSH) was developed by a protocol described before by Van Vlierberghe *et al.*[3]
Norbornene-modified (NB) dextran was developed by coupling the hydroxyl groups of dextran with the carboxylic acid groups of 5-Norbornene-2-carboxylic acid using DMAP and DCC. GelSH and DexNB were subsequent crosslinked under the same conditions as GelMA.

Development of CSNB-GelSH

NB modified CS was developed by coupling of the hydroxyl groups of CS with NB carboxylic acid using DMAP and Boc_2O as coupling reagents.
GelSH and CSNB were subsequent crosslinked in the same way as the other two materials.

3D-scaffold development

The different hydrogel materials were processed into hydrogel scaffolds using an indirect printing technique using PLA scaffolds as a sacrificial mold for the hydrogels.

Characterization

The compressive modulus of the whole scaffold was assessed using compression tests, the microscale stiffness was assessed using atomic force microscopy (AFM). The biocompatibility was assessed using an MTS proliferation assay, live-dead staining and a albumin quantification assay.

RESULTS AND DISCUSSION

On a 2D-level, DexNB-GelSH and CSNB-GelSH were superior over GelMA as they mimicked natural liver tissue (NLT) to a greater extent with respect to swelling and mechanical properties. The swelling ratio of GelMA, DexNB-GelSH and CSNB-GelSH were respectively 9.1±0.5 and 9.6±0.5 and 8.7±0.2 which is in line with the swelling of NLT (i.e.10).[4]

AFM measurements revealed superior microscale mechanical properties of the DexNB-GelSH hydrogel compared to the other materials. DexNB-GelSH exhibited a stiffness of (196±24)kPa, CSNB-GelSH of (106±2)kPa and GelMA of (291±11)kPa. NLT exhibits a stiffness of (183±48)kPa. The higher the stiffness, the more the material mimics the ECM of a cirrhotic liver ((411± 63)kPa)[5].

On a 3D-level, DexNB-GelSH scaffolds exhibited a compressive modulus of (4.8±1.6)kPa which is in excellent agreement with that of NLT (i.e. 1–5kPa)[4] as compared to GelMA which resulted in a modulus of (8.5±1.9)kPa and CSNB-GelSH (12.6±1.9)kPa.
So far, the biocompatibility of DexNB-GelSH was assessed and comparable to GelMA. The live-dead staining showed that the cells grew more into clusters on the DexNB-GelSH scaffolds compared to the more spread morphology which the cells exhibited on the GelMA material.

CONCLUSION

DexNB-GelSH and CSNB-GelSH scaffolds are promising hybrid materials to support LTE as they exhibit similar physico-chemical properties compared to NLT, while cell viability and proliferation of the hepatocytes were preserved.
In future research, different cell types such as primary hepatocytes and organoids will be included in the biological evaluation. Furthermore decellularized liver ECM will be incorporated into the hydrogel material in order to improve the cell interactivity and proliferation.

REFERENCES

1. Emek, E. *et al.* Transplant. Proc. 51: 2413-2415, 2019
2. Van Den Bulcke, A. *et al.* Biomacromolecules. 1: 31-38, 2000
3. Van Vlierberghe, S. *et al.* Eur. Polym. J. 47: 1039 – 1047, 2011
4. Mattei, G. *et al.* Acta Biomater. 10: 875–882, 2014
5. Zhao, G. *et al.* J. Surg. Oncol. 102: 482-489, 2010

ACKNOWLEDGMENTS

Nathan Carpentier would like to acknowledge the Research Foundation Flanders (FWO) for providing him with an FWO-SB fellowship (3S99321N).

Hybrid HMSCs-Microcomposite Building Blocks for Bottom-Up Engineering of Bone Tissue

K. Song, Z. Tahmasebi Birgani, P. Habibović, R. Truckenmüller
Department of Instructive Biomaterials Engineering, MERLN Institute for Technology-Inspired Regenerative Medicine, Maastricht University, Universiteitssingel 40, 6229 ER Maastricht, The Netherlands
k.song@maastrichtuniversity.nl

INTRODUCTION

Cell-rich and cell-laden hydrogel-based three-dimensional (3D) assemblies, largely employed in bottom-up tissue engineering (TE) strategies [1-2], may not provide the stiffness and osteogenic-inducing properties required for load-bearing bone TE applications. Therefore, we suggest the use of bioinspired organic-inorganic composite microparticles stiffer than hydrogels as matrix-mimicking building blocks to produce bottom-up modular assemblies for bone TE. To that end, we fabricated a series of poly(lactic acid) (PLA) and nano-hydroxyapatite (HA) microcomposites and used them to form 3D self-assembled hybrid cell-microparticle bone-like spheroids.

EXPERIMENTAL METHODS

A polydimethylsiloxane (PDMS) intermediate mold containing squared protrusions (100 µm*100 µm* 30 µm) was prepared via standard soft lithography and inversely replicated onto a photocurable bifunctional perfluoropolyether-urethane methacrylate, forming non-wettable micromolds. PLA-HA suspensions with PLA/HA ratios of 70/10, 50/30, 30/50 and 10/70 w/w were cast onto the micromolds and later peeled off with a sacrificial poly(vinyl alcohol) film, which was further dissolved in deionized water, releasing free-standing microcomposites. PLA microparticles were prepared as a control. The microcomposites were characterized with Fourier transform infrared spectroscopy (FTIR), Scanning electron microscopy (SEM) coupled with energy-dispersive X-ray spectroscopy (EDS) and laser scanning confocal profilometry. Microcomposites and human mesenchymal stem cells (HMSCs) were co-seeded onto in-house-made low-adherent polycarbonate film-based thermoformed microwells. We recorded the diameter and viability of the hybrid cell-microcomposites with brightfield microscopy and PrestoBlue™ cell viability assay at varying time points. Dead cells, cell nuclei and F-actin cytoskeletal fibers in the spheroids were labelled with LIVE/DEAD™ Fixable Dead Cell Stain, DAPI and Alexa Fluor 647 (phalloidine), respectively, and visualized with a confocal fluorescence microscope (CFM).

RESULTS AND DISCUSSION

Solid microcomposites with good shape fidelity were fabricated (Figure 1A). Increased HA content generally led to microcomposites with higher surface roughness and reduced meniscus profile on the top surface, often seen after solvent evaporation[3] (Figure 1A-C). Microcomposites successfully participated in cell-guided assembly, forming hybrid spheroids, with highest cell viability detected in PLA/HA 10/70 after 5 days. Moreover, microcomposites led to the formation of larger spheroids with irregular shapes, as opposed to spherical and smaller cell-rich spheroids (Figure 2).

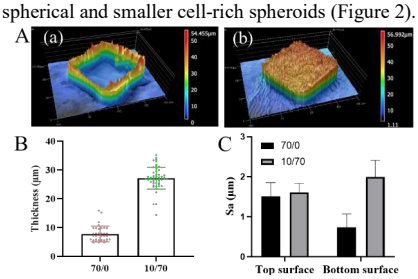

Figure 1. A) Surface profiles of (a) PLA and (b) PLA/HA 10/70 microparticles, their B) average height and C) surface roughness of the top and the bottom surfaces.

CONCLUSION

We developed a series of microcomposites with varying organic/inorganic phase ratios, pre-defined outer shapes and isotropic surface profiles and roughness, which were dependant on the PLA/HA ratio. Preliminary experiments on HMSC-microcomposite spheroid formation were successful and next, we will investigate the osteogenic properties of the hybrid spheroids.

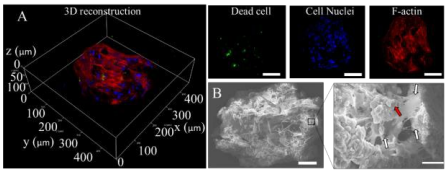

Figure 2. Morphology of Hybrid HMSCs-PLA/HA 10/70 assembly in osteogenic medium for 10 days visualized by (A) 3D CFM (scale bars: 100 µm) and B) SEM (scale bars: 50 µm (left) and 10 µm (right), red arrow: mineral deposit, white arrows: cells).

REFERENCES

1- Advanced Materials 32 (2020) 1903975.
2- Advanced Materials 26 (2014) 2592–2599.
3- Advanced materials 33 (2021) 2007695.

ACKNOWLEDGMENTS

This research was supported by the China Scholarship Council (CSC) from the Ministry of Education of P.R. China, the European Union Interreg Vlaanderen-Nederland project "BIOMAT on microfluidic chip), the Dutch Province of Limburg (program "Limburg INvesteert in haar Kenniseconomie/ LINK"), the NWO Gravitation Program (project "Materials-Driven Regeneration") and the NWO Incentive Grant for Women in STEM (Project "Biotetris").

Multi-Material Approach For The Replacement Of The Temporomandibular Joint

Joanna Babilotte[1*+], Monize Caiado Decarli[1+], Amit Chandrakar[1], Paul Wieringa[1], Lorenzo Moroni[1]

[1]Complex Tissue Regeneration department, MERLN Institute for Technology-Inspired Regenerative Medicine, Maastricht University, Maastricht, the Netherlands
[*] j.babilotte@maastrichtuniversity.nl

[+]Joanna Babilotte and Monize Caiado Decarli contributed equally to this work

INTRODUCTION

Temporomandibular joint (TMJ) disorders impair masticatory function and speaking, reducing patients' quality of life. Even though synthetic TMJ implants are commercially available, only a limited range of sizes can be found, thus not often meeting patient needs. The use of a patient-specific TMJ implant would overcome this limitation[1]. 3D printing technologies are the most appropriate fabrication techniques to provide a high-precision scaffold with a patient-specific design, in a controlled and reproducible way. Due to the complex anatomical structure of TMJ, it is clear that multi-material approaches, that combine different manufacturing techniques, can be very promising.
Here we aimed at developing an innovative scaffold that will meet the biological and mechanical criteria to replace TMJ. The objective of this work was to evaluate one specific combination of a Xantham-gum (XG) hydrogel reinforced with fibrous scaffolds made with polycaprolactone (PCL) or copolymers of polycaprolactone and polylactic acid (PCL-LA).

EXPERIMENTAL METHODS

Fibrous scaffolds were produced by melt-electrowriting (MEW). Polycaprolactone (PCL) and a copolymer of polycaprolactone-polylactic acid (PCL-LA, 30:70 wt%) were used to fabricate ten layers of fibrous scaffolds. PCL scaffolds were manufactured at 105˚C, varying speeds from 10-50 mm/s, 0.3 bar, 5 kV and 4mm height. PCL-LA scaffolds were manufactured at 170˚C, varying speeds from 10-50 mm/s, 0.8 bar, 6 kV and 4 mm height. Multi-layered constructs of XG hydrogel were 3D printed, varying speed from 40-60 mm/s and pressure from 50-70 KPa using smooth flow tapered tip. XG hydrogels were studied with and without stabilization using ionic crosslinking.

The morphology of both produced scaffolds was observed through optical and scanning electron microscopes regarding fibers/filaments size and porosity. The different scaffolds were manually assembled before the crosslinking step. Shear stress tests evaluated the improvement of mechanical properties. The stability of the constructs in culture media for 28 days was also analyzed. Finally, the cell survival and proliferation on both scaffolds were evaluated with human mesenchymal stem cells (hMSCs).

RESULTS AND DISCUSSION

Given the complexity of the TMJ, there is not just one material that could be considered an ideal to replace and restore the function. PCL and PLA are both biocompatible and bioresorbable polymers with great interest in tissue engineering[2].
Regular and well-defined PCL and PCL-LA meshes were obtained using MEW. The range of fibers size obtained was 30-50 µm and the interfiber space was 0.5-1 mm, depending of the parameters used. Increasing the printing speed generally led to reducing the size of the fibers. The interfiber spacing (IFS) also influenced pattern fidelity, reducing the IFS resulted in the misalignment of the fibers.
Multi-layered XG constructs with high shape fidelity were also obtained through 3D printing. The pore size was 3±0.5mm and the line width was 1±0.2mm. The ionically crosslinked XG constructs were stable in cell culture media over 28 days, and porosity was maintained. Both materials were functionalized by photocurable methacrylated (MA) groups to ensure a strong binding, avoid delamination and improve mechanical properties. Alone, usually hydrogel shows too weak mechanical properties for our application. The XG hydrogel will be reinforced with a fibrous scaffold to improve the mechanical properties. It is expected to observe changes depending on the fibrous scaffold structure (pattern and number of layers).
Finally, hMSCs showed good cell viability and survival overtime on the hydrogel and fibrous scaffolds independently. Further investigation on cell differentiation will be performed to explore the benefits of our multimaterial.

CONCLUSION

Overall, based on the hybridization between both processing techniques, employing a multi-material approach, as well as including a double crosslinking strategy, we show a promising approach for interfacial tissue regeneration with improved mechanical properties.

REFERENCES

1. Mehrotra D. *et al*., J. Oral Bio. Cranio. Research 11:334-342, 2021
2. Stefani I. *et al*., Acta Biomat. 36:231-240, 2016

ACKNOWLEDGMENTS

The authors acknowledge the support of the European Union's Horizon 2020 research and innovation program under grant agreement No 953169 (Interlynk).

Organo-mineral 3D-printed scaffolds for bone regeneration

Baptiste Charbonnier[1*], Ségolène Reiss[1], Pierre Corre[1], Pierre Weiss [1]

[1] RMeS Lab, INSERM U1229, Nantes University
[*] baptiste.charbonnier@univ-nantes.fr

INTRODUCTION

Developments in the field of computer-aided design and additive manufacturing have allowed significant improvements in the design and production of ephemeral scaffolds with biologically relevant features to treat bone defects [1]. Their benefits versus standard scaffolds have already been acknowledged. Unfortunately, the clinical and manufacturing workflow to generate personalized scaffolds is still source of inaccuracies which may lead to a poor fit between the implant and patients' bone defects [1]. This may result in drastic consequences on the regenerative outcomes: e.g., poor osteointegration of the scaffold, reduced bone formation, delayed or non-union. Furthermore, most scaffolds display a non-adapted mechanical behavior (e.g., fragility, brittleness, low stiffness), an inappropriate biodegradability rate and a mediocre potential to promote the formation of new vascularized bone tissues. Tackling these issues, organo-mineral scaffolds with evolutive mechanical properties were 3D-printed: from deformable scaffolds after production to stiff scaffolds after implantation

EXPERIMENTAL METHODS

Alpha tricalcium phosphate (α-TCP) and anhydrous trimagnesium phosphate (a-TMP) were used as reactive inorganic powders. They were obtained by heat treatment of apatitic TCP (1360°C-15h, air quenching) and hydrated TMP (1050°C-5h) rods, respectively. Rods were crushed using an agate mortar and pestle and the powder sieved between 20 and 40 µm.As organic phase, 6% w/v hyaluronic acid (2.6 MDa, HTL Biotechnology) was dissolved in a 50% w/w D-glucose solution. Organo-mineral cementitious pastes were prepared by mixing 60 and 50% w/w of reactive α-TCP and a-TMP, respectively. Disks (Ø = 5 mm, h = 1 mm) were printed by robocasting (R-Gen 200, RegenHu) using 25G cones following a rectilinear and gyroid pattern. These macroporous scaffolds were implanted in non-critical calvarial defects (rat model) with or without total bone marrow (N = 6 scaffolds per condition). Animals were euthanized after 7 weeks, and scaffold degradation and bone formation was assessed by micro-computed tomography X (µCT), scanning electron microscopy (SEM, back-scattering) and histology (hematoxylin and eosin & toluidine blue/von Kossa stain). Deep-learning routine were developed for µCT and SEM quantitative analyses. Finally, a real size 3D-printed polymeric model of a cleft lip and palate deformity was used as a proof of concept: a scaffold, 15% larger than the intended defect, was robocasted then inserted within the defect; this simulating a surgical intervention (Fig. 1).

RESULTS AND DISCUSSION

The simulated procedure was a success, with a deformable scaffold that could be inserted into the defect without breaking and adjusted to the edges for an optimized bone-implant contact (Fig. 1).
Bone formation in calvarial defect could be observed for both calcium and magnesium phosphates (CaP & MgP, respectively) – based scaffolds up to their core (Fig. 2); the addition of bone marrow playing a significant role. Scaffold architecture has little influence on bone formation. Significant differences in scaffold biodegradation were observed: while CaP-based scaffold largely remained, MgP-based scaffold could hardly been observed.

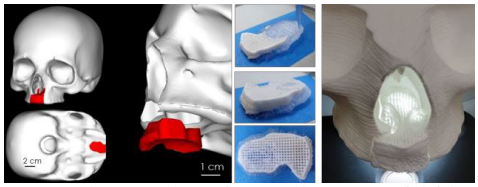

Fig. 1. Real size simulation of a surgical reparation of cleft lip and palate using 3D-printed scaffold 15% larger than the defect

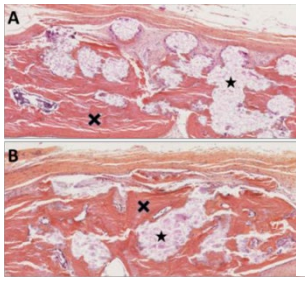

Fig. 2. Histological sections stained by hematoxylin and eosin of A. CaP-based scaffold and B. MgP-based scaffold; both supplemented with bone marrow

⋆ Material x Bone

CONCLUSION

The potential of 3D-printed organo-mineral scaffolds with evolving mechanical properties was demonstrated in this study. Biological response was driven by the inorganic phase composition. Further improvements of material formulations are currently ongoing, taking advantage of this proof of concept.

REFERENCES

References must be numbered. Keep the same style.
1. Charbonnier B. *et al*., Act. Biomat. 121:1-28, 2021

ACKNOWLEDGMENTS

The authors would like to thank the French National Research Agency (ANR-20-CE17-0018) for providing financial support to this project.

Cabbage leaves as 3D platform for in vitro adipose tissue model

Maddalena Bracchi[1], Andrea Fiorati[1,2], Lina Altomare[1,2*]
[1]Dipartimento di Chimica, Materiali, Ing. Chimica 'G Natta' Politecnico di Milano, Milan, Italy
[2]INSTM local unit Politecnico di Milano
[*] lina.altomare@polimi.it

INTRODUCTION

Adipose tissue is histologically characterized as a type of loose connective tissue that, normally, constitutes about 10% of the total body mass. It is highly vascularised and it is the only tissue with unlimited growth throughout adulthood[1]. Until now, different scaffold-based 3D *in vitro* models have been investigated for adipogenesis and adipocyte differentiation, studying both biopolymers, synthetic polymers and their combinations[2]. In recent years, plants have been identified as an alternative source of decellularized scaffolds for their ability to offer a broad range of potential architectures and surface topographies to support mammalian cell growth[3]. In the present study, savoy cabbage (S) and black cabbage (B) were selected and tested as potential scaffolds for scaffold-based 3D in vitro models to study adipose tissue. Their 3D structure, characterized by cavities and their intrinsic vascular structure, could promote cell adhesion, growth and adipocytes differentiation[4].

EXPERIMENTAL METHODS

Different decellularization protocols were performed on black and savoy cabbage leaves, combining mechanical agitation and ultra-sonication on square-based samples (10 x 10 mm^2). SDS solution was used as a decellularizing agent, followed by washing with aqueous $CaCl_2$ solution (100 mM, 4 x 20 mL) washes in $CaCl_2$ solution and water (4 x 20 mL) were performed to remove detergent residues.

Morphological characteristics of samples were investigated by means of stereomicroscope and scanning electron microscopy (SEM). Physical and mechanical characteristics, such as swelling ratio, contact angle and tensile properties, were also evaluated.

Indirect cytotoxicity test was performed according to the ISO 10992: 3T3-L1 murine preadipocytes were seeded on eluate at 1, 3 and 7 days. Cell viability was evaluated by means of Alamar Blue assay.

3T3-L1 preadipocytes were seeded on both savoy and black cabbage ($2x10^5$ cells per sample) and, after 7 days, adipogenic differentiation was induced through immersion in differentiation culture medium[5]. Adhesion and proliferation were evaluated by Alamar blue assay and SEM images, while differentiation was evaluated by Oil Red O test and Nile Red test combined with Hoechst 33258.

RESULTS AND DISCUSSION

Image at stereomicroscope showed that after optimization of decellularization protocol both S and B leaves were clean with no detergent residues, moreover the morphology of the plants is unmodified. SEM images (Figure 1) showed a rough regular geometrical grid structure with stomata without their cells, removed by decellularization process.

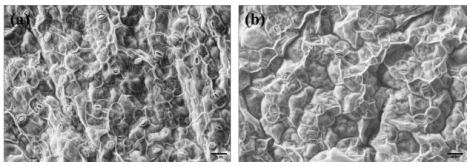

Figure 1 SEM images of S (a) and B (b) at 1000x magnification

Water uptake was measured up to 7 weeks, samples reached a plateau (1581% for S, 2388% for B) of water absorption after 4 and 3 weeks, respectively.

For all time point considered, S and B cabbage leaves showed no residual cytotoxicity, and cells showed more than the 85% of viability.

The SEM imaging, carried out 3 and 7 days after seeding, revealed good cell adhesion to the S and B scaffolds. Metabolic activity measured by Alamar blue assay, increased up to 14 days indicating that both leaves can support cell growth. Finally, Oil Red O staining (Figure 2), performed 14 days after seeding, showed a strong intracellular lipid accumulation typical of adipocytes.

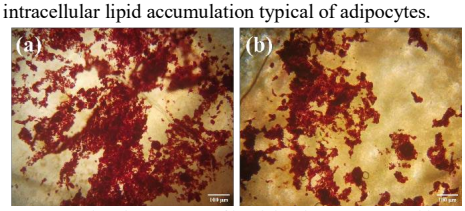

Figure 2 Oil Red O staining of lipid droplets on savoy cabbage (a) and black cabbage (b)

The presence of lipid droplets is confirmed by Nile Red staining, moreover Hoechst staining allowed to highlight numerous nuclei on S and B surfaces.

CONCLUSION

Decellularization protocols have been optimized on cabbage leaves, maintaining the original morphology and the obtained specimens showed no residual cytotoxicity. The obtained scaffold was successfully employed for promote preadipocytes adhesion and their differentiation. Further studies will allow to understand the possibility of exploiting leaves branches as vessels for nutrient diffusion paving the way to the development of a mature tissue.

REFERENCES

1. Mariman E. *et al*., Cell. Mol. Life Sci.67:1277-1292, 2010
2. Van Nieuwenhove I. *et al*., Acta Biomaterialia 63: 37-49, 2017
3. Cheng Y.W. *et al*., ACS Biomater. Sci. Eng. 6:3046-3054, 2020
4. Fontana G. *et al*., Adv Healthc Mater. 6(8), 2017
5. Contessi Negrini N. *et al*., Front. Bioeng. Biotechnol. 8:723, 2020

Multifunctional biomimetic pancreatic cancer cell membrane-camouflaged vitamin E-based prodrug micelles

Miguel Pereira-Silva[1,2,3*]; Alba Ferreirós[4]; Ana Cláudia Paiva-Santos[1,2]; Francisco Veiga[1,2]; Angel Concheiro[3]; Carmen Alvarez-Lorenzo[3]

[1] Department of Pharmaceutical Technology, Faculty of Pharmacy, University of Coimbra, 3000-548 Coimbra, Portugal
[2] REQUIMTE/LAQV, Group of Pharmaceutical Technology, Faculty of Pharmacy, University of Coimbra, 3000-548 Coimbra, Portugal
[3] Departamento de Farmacología, Farmacia y Tecnología Farmacéutica, I+D Farma, Facultad de Farmacia and Health Research Institute of Santiago de Compostela (IDIS), Universidade de Santiago de Compostela, 15782 Santiago de Compostela, Spain
[4] Nasasbiotech, S.L., Canton Grande 9, 15003 A Coruña, Spain
* miguelsilva@ff.uc.pt

INTRODUCTION

Pancreatic cancer (PC) is currently one of the deadliest and most aggressive cancers worldwide, bearing a dismal 5-year survival rate of only 11% [1]. PC is characterized by a desmoplastic and dense stroma barrier and to rapid emergence of a multidrug resistant phenotype to conventional chemotherapeutic agents. Gemzar® is a clinically-approved gemcitabine (GEM) solution widely used in PC treatment, mostly in combination regimens, but evidences poor stability, accelerated clearance and extensive systemic toxicity [2]. Nanoparticles have been receiving increasing attention as advanced drug delivery systems capable to protect and enhance stability of encapsulated drug payloads as well as to enable controlled drug release at target sites [2,3]. In recent years, attention has been paid in developing all-functional nanoparticles bearing intrinsic biofunctionalities, thus able to function as active ingredients. In this work, a strategy was explored to leverage serum stability, blood circulation half-life and PC targeting features of GEM by preparing all-functional polyvinyl caprolactam-polyvinyl acetate-polyethylene glycol graft copolymer /vitamin E succinate (VES)-GEM (VES-GEM) prodrug micelles (Soluplus®/VES-GEM) camouflaged with PC cell membrane (PCCM@M). Soluplus® has multidrug resistance reversal features, and antioxidant, anticancer and p-glycoprotein inhibition properties are ascribed to VES. Further coating with pancreatic cancer cell membrane (PCCM) is expected to work as a biomimetic stealth conferring prolonged blood circulation profile, as a source of antigens to drive immune reactivation of PC microenvironment, and as a display of receptors for improved PC targeting through homotypic mechanisms [4].

EXPERIMENTAL METHODS

Soluplus®/VES-GEM micelles were firstly prepared through solvent evaporation method. BxPC3 cell line was used for PCCM extraction, through hypotonic lysis, sonication and differential centrifugation steps. Aliquots of obtained PCCM pellet suspension (200 µL, 0.5 mg/mL) were added to diluted Soluplus®/VES-GEM micelle dispersions (100 µL, 1 mg/mL of Soluplus®) attaining a 1:1 (w/w) ratio. The resulting product was subjected to ultrasonication (3 min, 3 s on /1 s off). A similar approach was carried out to prepare PCCM nanovesicles. Next, the hydrodynamic size, polydispersity index (PDI) and zeta potential (ZP) of Soluplus®/VES-GEM micelles (M), PCCM nanovesicles (PCCM) and PCCM@M were measured by dynamic light scattering (DLS) (Zetasizer Nano ZS, Malvern Instruments, UK).

RESULTS AND DISCUSSION

Results showed PCCM@M had size= 108.8 ± 3.6 nm, ZP= -13.89 ± 1.49 mV an PDI= 0.306 ± 0.034. When compare to Soluplus®/VES-GEM micelles (M), size increased ca. 15 nm which is in accordance to the average width of cell membranes, and ZP decreased from -2.52 ± 0.25 mV (M) to -13.89 ± 1.49 mV (PCCM@M) typical of cell membranes, which suggests a successful coating with the PCCM (**Figure 1**).

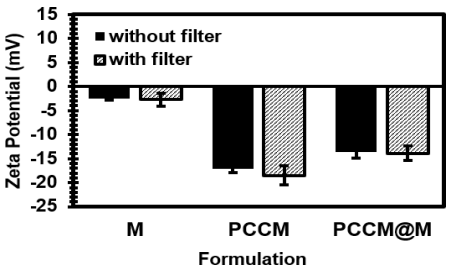

Figure 1. Zeta potential of M, PCCM and PCCM.

CONCLUSION

PCCM-camouflaged Soluplus®/VES-GEM micelles were prepared and characterized regarding size, PDI and ZP. The substantial decrease in ZP of PCCM@M accompanied by slight increase in size suggests successful coating of the micelle core with PCCM.

REFERENCES

1. Rawla, P., *et al*., World J Oncol. 10:10-27, 2019
2. El-Zahaby, S.A., *et al*., J Control Release. 293:21-35, 2019;
3. Xu, Y., et al., Int J Pharm. 495:792-7, 2015
4. Tang, H., et al., Acta Pharm. Sin. B. 2022

ACKNOWLEDGMENTS

The authors would like to thank FCT (grant SFRH/BD/148771/2019) for providing financial support to this project.

Bone Regeneration with Antibiotic Delivery – A New Approach to Osteomyelitis and Infected Joint Replacements

Eoin Barrett[1], Helena Kelly[2], Robert Flavin[3], Gerard Insley[4], Ciara M Murphy [1*]

[1]Anatomy and Regenerative Medicine, Royal College of Surgeons in Ireland, Dublin, Ireland
[2]School of Pharmacy and Biomolecular Sciences, Royal College of Surgeons in Ireland, Dublin, Ireland
[3]Orthopaedics, St. Vincent's Private Hospital, Dublin, Ireland
[4]PBC Biomed, Unit 4D, Western Business Park, Shannon, Co. Clare, Ireland.
[*] ciaramurphy@rcsi.ie

INTRODUCTION

Osteomyelitis and Infected Joint Replacements have been the most challenging problem in Orthopaedics for decades. Whilst there have been huge advances in the development of biomaterial-based bone grafts for orthopaedic applications, healing bone infections remain a major challenge[1]. One approach commonly used by orthopaedic surgeons is the use of calcium sulfate as a biomaterial based delivery platform for local antibiotic release. Calcium sulfate has a relatively rapid reabsorption time, optimal for sustained antibiotic elution. Furthermore, calcium sulfate is biocompatible so its removal via a secondary procedure is not required. However, the rapid rate of resorption outpaces that of bone formation, so whilst it is advantageous as an antibiotic elution platform, it does not have the capacity for functional bone healing[2]. As such, there is a major gap in the market for antibiotic eluting biomaterials to simultaneously treat the infection and facilitate bone regeneration within a defect. We have developed a new class of biomimetic biomaterial call an organo-calcium phosphate bioadhesive (OssStic). This project aims to investigate the ability of this innovative bioactive bone graft as an antibiotic delivery platform.

EXPERIMENTAL METHODS

The potential of OssStic as an antibiotic delivery platform was compared to commercially available calcium sulfate based biomaterial – Osteoset.

Antibiotic loading: OssStic and Osteoset are powder-based materials and antibiotic loading was via mixing in antibiotic solution with the powders. 50 mg/ml vancomycin was mixed with the biomaterial powders. Antibiotic release: Vancomycin release from the biomaterials was detected over 21 days via high performance liquid chromatography. Degradation: OssStic degradation rates was compared to Osteoset as degradation can significantly influence therapeutic release. Both biomaterials were placed in PBS and simulated body fluid (SBF) for 14 days and the % loss in weight was monitored. These two media were chosen as they do not interfere with HPLC detection of antibiotics.

RESULTS AND DISCUSSION

OssStic follows a similar release profile compared to Osteoset over the 21-day period however the release of vancomycin from OssStic was slower. Both initially release a high dose before decreasing gradually over the first 12 hrs. This is due to the antibiotic eluting from the surface of the material initially. As the outer surface degrades, a significant increase is observed again at 24hr that is maintained until day 7 (120hr), after which a significant decrease is observed. Osteoset release drops below the minimum inhibitory concentration (MIC) at day 14 (336 hr) but OssStic continues releasing vancomycin up to day 21 (Fig 1A).

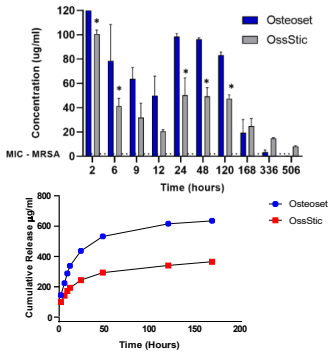

Figure 1: *(A) Vancomycin release from OssStic and Osteoset over 21 days (B) Cumulative release of vancomycin from both biomaterials*

Release data presented as cumulative release shows that OssStic has a lower initial burst release and slower subsequent release compared to Osteoset (Fig. 1B). The OssStic is less susceptible to degradation than the commercially available Osteoset but does have a significant decrease in % mass

CONCLUSION

OssStic proved a significant advance over clinical standard Osteoset, with a more controlled and longer release profile and slower degradation rate that overcomes the challenges associated with current clinical approaches

REFERENCES

1. Hannan *et al*., Semin Plast Surg. 23(2): 132–140. 2009
2. Huan *et al*., Acta Biomater., 3: 952-960. 2007

ACKNOWLEDGMENTS

The authors would like to thank Aleksandra Rulikowska and Jesus Maria Frias Celayeta in TU Dublin - Environmental Sustainability and Health Institute (ESHI) for their contributions on this project

The interplay of collagen/bioactive glass nanoparticle coatings and electrical stimulation regimes distinctly enhanced osteogenic differentiation of human mesenchymal stem cells

Poh Soo Lee [1,2 *], Christiane Heinemann [2], Kai Zheng [3], Revathi Appali [1,6], Jan Krieghoff [5], Aldo R. Boccaccini [4], Ursula van Rienen [1,6,7], Vera Hintze [2].

[1] Institute of General Electrical Engineering, University of Rostock, Rostock, Germany.
[2] Max Bergmann Centre of Biomaterials, Technische Universität Dresden, Dresden, Germany
[3] Jiangsu Province Engineering Research Center of Stomatological Translational Medicine, Nanjing Medical University, Nanjing, China
[4] Institute of Biomaterials, University of Erlangen-Nuremburg, Erlangen, Germany
[5] Institute of Pharmacy, University Leipzig, Leipzig, Germany.
[6] Department of Ageing of Individuals and Society, University of Rostock, Rostock, Germany.
[7] Department of Life, Light and Matter, University of Rostock, Rostock, Germany.

[*] poh_soo.lee2@tu-dresden.de

INTRODUCTION

The unique ion release mechanisms and physical properties of bioactive glass nanoparticles (BGN) to promote cell proliferation, osteogenic differentiation and angiogenesis are attracting great interest in the field of bone tissue engineering [(1)] and also demonstrated in our recent publication on collagen coatings [(2)]. Moreover, the application of electric field (EF) stimulation to enhance osteogenic differentiation in place of conventional biochemical supplements has also gained more attention [(3)]. Interestingly, the interplay of BGN and EF was less investigated and their proficiency to induce / support osteogenic differentiation is unclear. In this study, we aimed to elucidate the synergistic effects of BGN and EF for osteogenic differentiation of human mesenchymal stem cells (hMSC). Further, the influences of continuous versus intermittent EF regimes were also our key interest.

EXPERIMENTAL METHODS

Collagen (Col) coatings with BGN were prepared at a 1:1 (w/w) ratio and air-dried on glass coverslips (Ø 13 mm). hMSC from two donors were investigated and seeded at 10,000 hMSC/cm^2. Coverslip with only Col was used as controls. Next, the coverslips were cultured in cell culture chambers and exposed to either continuous or intermittent EF stimulation regimes (*Fig. 1*) for 28 days on a transformer-like coupling (TLC) system designed to exert pure EF [(3)]. Importantly, the osteogenic differentiation medium was supplemented only with 50 µM ascorbic acid 2-phosphate and 10 mM β-glycerophosphate. Dexamethasone was omitted to show the proficiency of BGN and EF to initiate osteogenic differentiation. Samples were collected every 7 days. ALP activity was used as an indicator for osteogenic differentiation and calcium accumulation for mineralization (n=4). Real-time qPCR (n=3) was performed to determine the gene expression profiles at each condition.

RESULTS AND DISCUSSION

The results from this study showed the potential of BGN to initiate osteogenic differentiation at early time points. Further, the stability of collagen coatings was enhanced when both BGN and EF were applied. By coupling BGN with a continuous (12/12) EF regime, an obvious increase in ALP activity was observed as early as day 7. When coupled with an intermittent (4/4) EF regime, a higher calcium accumulation was documented on day 28 (*Fig. 1*). Further, each EF regime had shown preferences on osteogenic differentiation pathway.

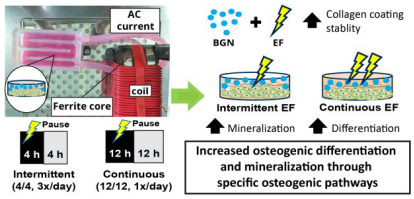

Fig.1: The experimental approach (left) and summarized results (right) of this study.

CONCLUSION

In summary, our results had illustrated the synergistic effects of BGN and EFs in different regimes on osteogenic differentiation that can be further exploited to enhance current bone tissue engineering and regeneration approaches. Further enhancement could be accomplished by doping metal ions to the existing BGN to achieve coatings / scaffolds with tunable electrical conductivity. It would be done with an objective further to enhance osteogenic differentiation through BGN and EFs interplay.

REFERENCES

1. K. Zheng, B. Sui, K. Ilyas, A.R. Boccaccini. *Mater. Horizons.* **8** (2021) 300–335.
2. L. M. Kroschwald, et.al., *Int. J. Mol. Sci.* **22** (2021), 12819.
3. R. Balint, N.J. Cassidy, S.H. Cartmell. *Tissue Eng. Part B Rev.* **19** (2013) 48–57.
4. R. Hess, et.al. *Cell Biochem. Biophys*, **64** (2012), 223–232.

ACKNOWLEDGMENTS

The authors would like to express our utmost gratitude to the Deutsche Forschungsgemeinschaft (DFG, German Research Foundation) regarding DFG SFB 1270/1,2 – 299150580 ELAINE and TRR 67 - 59307082,TRR67, subproject A3 that provided financial support for this study. And Dr. Michael Hacker for his guidance to Mr. Krieghoff on rheology measurements.

Collagen-MWCNTs composite foils from benign solvent– optimization of parameters and physicochemical characteristic

Sebastian Wilk[1*], Michał Dziadek[1,2], Magdalena Ziąbka[1], Katarzyna Cholewa-Kowalska[1], Aleksandra Benko[1]

[1]Faculty of Materials Science and Ceramics, AGH University of Science and Technology, Krakow, Poland
[2]Department of Chemistry, Jagiellonian University, Krakow, Poland
[*] sewilk@agh.edu.pl

INTRODUCTION

Type I collagen is one of the main constituents of the extracellular matrix of all mammalian tissues. Its fibrillar structure strongly influences the cells, maintaining their proper shape and actively aiding in proliferation and differentiation. As such, it is highly interesting for fabricating tissue engineering scaffolds, where biomimetic biopolymers are highly desired[1,2]. Unfortunately, the extraction and further processing of collagen are cumbersome, which results in the high price of extra pure, laboratory-grade material. Moreover, collagen is hard to dissolve, thus highly toxic solvents, like hexafluoroisopropanol (HFIP), are commonly used[2]. It is of high importance to find less-toxic solvents for the commercial processing of collagen.

The aim of this study was to find a benign solvent that is able to dissolve relatively low-priced and commercially available collagen. Another goal was to fabricate and characterize electroconductive collagen-multi walled carbon nanotubes (MWCNTs) composite foils that possibly could improve the regenerative potential of cells.

EXPERIMENTAL METHODS

Collagen (C9879), glycerol (G9012), hydrochloric acid (HCl), and fluoric acid (HF) were bought from Sigma Aldrich. Dimethyl Sulfoxide (DMSO) was supplied by ChemPur. Roti®-CELL PBS was bought from Carl Roth. HFIP was bought from abcr. Highly oxidized and ammonia functionalized multi-walled carbon nanotubes (MWCNTs) were obtained following the protocol established by Benko et al. [3].

3,17 g of collagen was mixed with 60 ml of DMSO/PBS (5:1) with the addition of 317 µL of 1M HCl and 317 µL of 5% HF. For a reference solution, 3,17 g of collagen was dissolved in 60 mL of HFIP. Mixtures were left on a magnetic stirrer for one week at 4 °C until collagen was fully dissolved. After that, solutions were portioned, and glycerol (5% wt./wt.$_{collagen}$) and/or MWCNTs of one type (0,25% wt./wt.$_{collagen}$) were added. All components were mixed until fully homogenized and poured into dishes made from PTFE. Materials were kept in a laboratory dryer for at least one week at 37 °C until all foils were completely dry. Materials were stored at 4 °C.

Morphologies of the obtained materials were characterized by scanning electron microscopy (NOVA NANO SEM 200, FEI). Chemical properties were analyzed by FTIR-ATR spectroscopy (Tensor 27, Bruker). Electrical resistance was measured with the use of an Agilent 34405A multimeter. Mechanical performance was tested by Inspect Table universal testing machine (Hegewald-Peschke).

RESULTS AND DISCUSSION

SEM images revealed that the type of solvent, addition of glycerol, presence of MWCNTs, and the side of drying (Fig 1) are the factors that strongly influence the final material's morphology.

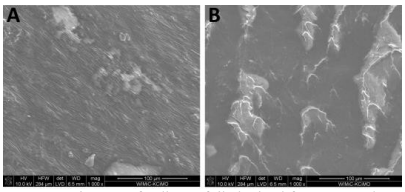

Fig 1. SEM images of collagen foil obtained from DMSO/PBS solvent solution. Significant morphological differences between the "down" (A) and "up" (B) sides can be observed.

FTIR-ATR analysis revealed that bands characteristic of native collagen structure were present in all of the obtained samples. Both glycerol and MWCNTs influenced the mechanical properties of films, affecting their elasticity. Completely dry materials were found to be electrically non-conductive. However, when wetted, materials with the addition of MWCNTs were characterized by a significantly lower resistivity, when compared to other foils.

CONCLUSION

Foils made out of inexpensive and commercially available collagen were successfully obtained from a benign solvent, based on DMSO and PBS. Materials of specifically tailored morphologies and physicochemical properties can be obtained by optimizing the composition and the drying process. Thus, composites for numerous, highly specific applications in tissue engineering and regenerative medicine can be fabricated.

REFERENCES

1. Salvatore L. *et al*., Front. Bioeng. Biotechnol. 9: 644595, 2021
2. Jiang Q. *et al*.,, J Biomed Mater Res Part A, 2013:101A:1237-1247
3. Benko A. *et al*., Mater. Sci. Eng. C vol. 120, 2021, ISSN 0928-4931

ACKNOWLEDGMENTS

This study has been supported by the National Centre for Research and Development under grant no. LIDER/7/0020/L-11/19/NCBR/2020.

Novel Design of Gelatin Microparticles for Anticancer Delivery and Integration with Fibre-based Devices

Samuel Moorcroft[1,2*],Russell Harris[2], Stephen J. Russell[1], Giuseppe Tronci[1]

[1]Leeds Institute of Textiles and Colour, University of Leeds, Leeds, United Kingdom
[2] School of Mechanical Engineering, University of Leeds, Leeds, United Kingdom
[*] S.C.Moorcroft@leeds.ac.uk

INTRODUCTION

Inherent biocompatibility, biodegradability and lack of antigenicity have led to a rise in the adoption of gelatin as a biomaterial used in soft medical devices.[1] Microparticulate controlled delivery systems in particular favour gelatin as a widely available amphoteric scaffold to internalise therapeutic agents that can be delivered locally on-demand. Microparticulate systems can also provide drug release rates dependent on diffusive retardation from the entangled polymer chains and drug protection from external denaturing stimuli. Despite these advantages, gelatin systems suffer from intrinsic issues regarding uncontrollable swelling, rapid biodegradation and limited drug retention *in vivo,*[2] partially due to gelatin's hygroscopic nature and reversible gelation below physiological temperatures. Our previous work demonstrated increased fibroblast tolerability and retained wet-state mechanical competence in UV-cured meshes of photoactive gelatin systems compared to state-of-the-art carbodiimide-crosslinked materials.[3] Building on this platform, we hypothesised that the covalent functionalisation of gelatin could offer a novel route for the development of gelatin microparticles with enhanced size and morphology controllability as well as enhanced integrability on to functional fibre-based devices.

EXPERIMENTAL METHODS

Utilizing a novel emulsion-based system, we demonstrate the fabrication of microparticles using 4-vinylbenzyl chloride (4VBC)-functionalised gelatin that, in the presence of a photoinitiator and UV light, form a water-insoluble covalent network at the molecular scale. Consumption of gelatin's primary amino groups in 4VBC-reacted products was confirmed via Ninhydrin assay, so that a tunable degree of functionalisation was accomplished.

Electrospinning was conducted by the extrusion of a mixture of polycaprolactone polymer with the 4VBC functionalized gelatin microparticles. The particle integrated fibre was collected on a foil collection plate before extraction and imaging using electron microscopy to characterize the resultant mesh composition.

RESULTS AND DISCUSSION

UV-induced molecular network formation afforded gelatin microparticles with decreased size compared to native gelatin-based variants, supporting the presence of covalent crosslinks between gelatin chains and secondary aromatic interactions between 4VBC-crosslinking segments.

In light of these characteristics, aforementioned microparticles could also be delivered onto electrospun meshes indicating their facile integration into macroscopic medical devices aiming at localised and controlled therapeutic delivery capability.

CONCLUSION

We believe that the integrated biocompatibility, drug release capability, and integratability with fibre-based medical devices make 4VBC functionalized gelatin microparticle systems highly appealing for a wide variety of therapeutic applications, e.g. anticancer localised treatments and long-lasting regenerative devices for hard tissue repair.

REFERENCES

(1) Bello, A. B., Kim, D., Kim, D., Park, H., & Lee, S.-H. (2020). Engineering and Functionalization of Gelatin Biomaterials: From Cell Culture to Medical Applications. *Tissue Engineering Part B: Reviews*, *26*(2), 164–180.

(2) Foox, M., & Zilberman, M. (2015). Drug delivery from gelatin-based systems. *Expert Opinion on Drug Delivery*, *12*(9), 1547–1563.

(3) Bazbouz, M. B., Liang, H., Tronci, G. (2018). A UV-cured nanofibrous membrane of vinylbenzylated gelatin-poly(ε-caprolactone) dimethacrylate co-network by scalable free surface electrospinning. *Materials Science and Engineering: C*, *91*, 541–555.

ACKNOWLEDGMENTS

The authors would like to thank the University of Leeds, the Clothworkers Company and the EPSRC (grant code: EP/V009818/1) for providing financial support to this project.

3D printed bone-like scaffolds: design and biological assessment

_Miriam Merco[1], Federico Mochi [2,3], Eleonora Zenobi [2,3], Elisa Scatena[2,3], Antonella Lisi[1], Costantino Del Gaudio [1,2] and Mario Ledda[1]

[1] Institute of Translational Pharmacology, National Research Council, Rome, Italy.
[2]Hypatia Research Consortium, Rome, Italy
[3] E. Amaldi Foundation, Rome, Italy
* miriam.merco@ift.cnr.it

INTRODUCTION

The tailored design of tissue engineered scaffolds is a key topic to be properly addressed in order to elicit a valuable biological response. In this regard, a biomimetic approach can provide the scaffold with specific cues to resemble the natural extracellular matrix (ECM) of the tissue to be healed, starting from the physiological microstructure. Referring to bone applications, the fabrication of devices morphologically similar to the trabecular arrangement can offer an instructive and functional feature to deal with. This expected output can be achieved by means of 3D printing technologies, allowing to control the spatial deposition of the selected materials to reproduce the bone microarchitecture[1,2]. According to this experimental strategy, bone ECM-like scaffolds were fabricated by fused deposition modeling (FDM) and tested by means of human osteosarcoma SAOS-2 cells. These cells have an osteoblast phenotype similar to human primary osteoblasts[3] and were thus seeded on three different models of 3D printed polylactic acid (PLA) scaffolds to evaluate the biocompatibility, bioactivity, and osteoconductive properties.

EXPERIMENTAL METHODS

Scaffold design and fabrication

Three CAD models were designed (Meshmixer 3.5 free software), starting from a box-shaped solid and subtracting a three-dimensional random cluster of spheres to obtain a porous structure. The scaffolds were FDM fabricated, processing a commercial PLA filament. Samples were printed by means of the Raise 3D N2 printer, setting the nozzle temperature at 205 °C and the bed temperature at 60° C. Scaffolds were labelled P1S1, P2S2, and P3S3.

Cell culture and mRNA expression analysis

The human osteosarcoma SAOS-2 cell line was chosen as a well characterized osteoblast model. SAOS-2 cells were seeded on the three scaffolds surfaces and on the PLA sample (CTR) and grown up to 4 days. Total RNA was extracted from the SAOS-2 cells, grown on scaffold surfaces for 4 days and quantification of all gene transcripts was carried out by real-time quantitative polymerase chain reaction (RT-qPCR).

RESULTS AND DISCUSSION

The designed bone-like scaffolds are shown in Fig. 1. The gravimetric evaluation of porosity was (37.3 ± 1.1) %, (45.3 ± 0.2)% and (50.4 ±0.3)% for P1S1, P2S2 and P3S3, respectively, the latter case being in the variability range of human bone samples 4,5.

Figure 1. CAD models of 3D printed bone-like scaffolds

The biocompatibility and osteconductive properties of the scaffolds were studied through the mRNA expression analysis of osteogenic markers, highly expressed in healthy growing Saos-2 cells, such as Osteopontin (OPN), Alkaline Phosphatase, RUNX2 and Osteocalcin (OCN). The mRNA expression study by qRT-PCR assay, showed a statistically significant increase of all four osteoblast differentiation markers in the cells grown on three different type of substrates compared to CTR one.

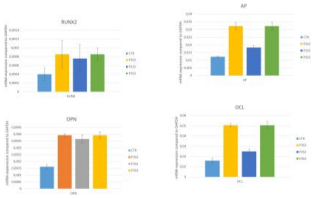

Figure 2 qRT-PCR analysis of the osteoblast differentiation markers.

CONCLUSION

A biomimetic approach was here considered to reproduce ad hoc microarchitectures for bone tissue engineering. Comparing human trabecular bone from different anatomical sites, i.e., skull, mandible, ulna and maxilla, P3S3 resulted to be the most similar scaffold to the physiological case. The results demonstrate that this biomimetic scaffolds do not affect cell viability, but, instead, supports the protein synthesis, proliferation and differentiation process of the growing Saos-2 cell line.

REFERENCES

1. Pecci R. *et al.*, J. Mech. Behav. Biomed. Mater. 103:103583, 2020
2. Ledda M. et al., Int. J. Mol. Sci. 23:5383, 2022
3. Saldana L. et al., Acta Biomater. 7:4210–4221. 2011

ACKNOWLEDGMENTS

This project is supported by "POR FESR LAZIO 2014–2020-Gruppi di Ricerca 2020. Dispositivi biomimetici realizzati mediante stampa 3D per il trattamento di patologie del sistema scheletrico (BioBone3D)", grant number A0375-2020-36493.

Biomimetic approach to decipher proliferation, adhesion and differentiation in neuroblastoma cell lines

João Lopes Cardoso[1], Perrine M'Pemba-Hennebert[1], Paul Machillot[1], Elisa Migliorini[1], Catherine Picart[1,2]

[1] CEA, CNRS, University Grenoble Alpes, BRM ERL 5000, Grenoble, France
[2]CEA, direction of fundamental research, interdisciplinary research institute of Grenoble (IRIG), FRE CNRS, Grenoble, France
joao-carlos.lopescardosofilho@cea.fr

INTRODUCTON

Neuroblastoma is a rare pediatric cancer that develops from the neuronal crest and affects the sympathetic nervous system, contributing to 15% of pediatric oncology deaths. Current therapies are not effective in the long-term treatment of almost 80% of patients with this clinically aggressive disease[1]. From the survivors, there is a high risk of development of other cancers or illnesses as effects of the treatment[2].

The complex biology and diversity of the tumor, together with the reduced population eligible for clinical trials difficult the development of an accurate model for neuroblastoma and, therefore, possible treatments[3].

Biomimetic approaches are prominent techniques to overcome the artifacts introduced by in vitro models and to represent the complex tumor microenvironment[4].

Bone morphogenetic proteins are essential for the development of the neuronal crest, making sense to propose BMPs as potential treatment for neuroblastoma [5]. Indeed, it has been shown that BMP2 and 4 are regulators of cellular proliferation and differentiation of tumoral cells [6]. Also, glycosaminoglycans such as HS have been recently shown to interact with the tumor microenvironment. The application of those molecules embedded in a biomaterial emulating the ECM may take account neuroblastoma's environment and improve in vitro test for anticancer drugs.

EXPERIMENTAL METHODS

The effects of growth factors (BMP2, BMP4, BMP7, BMP9 and TGF-β) are being studied over neuroblastoma cell lines: SH-SY5Y isolated from human bone marrow, and N2A murine tumor. The growth factors are presented both in soluble form or bound to extracellular matrix biomimetic materials. Initially, for setting up experiments, cell proliferation was studied by following confluency for 48H in Incucyte live cell imaging microscope, with images take at each 2H. Using growth factors at a concentration of 20 ng/mL, nuclei count was performed after 4 and 26H of seeding. Same proliferation assays was done over layer-by-layer PLL/PEI/HA films.

RESULTS AND DISCUSSION

We followed-up the proliferation of the two cell lines at different cell concentrations over 48H (Fig 1). We observed that both cell type reduces their proliferation with the increased cell passage.

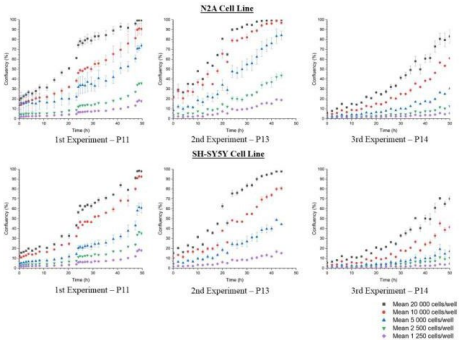

Figure 1: Confluency of cell lines over 48H.

Preliminary results have shown different behaviors for different growth factors and layer-by-layer films of different stiffness. Notably, cell proliferation and viability reduced prominently in softer films for BMPs 2, 4 and 9. In stiffer films, this behavior is less remarkable.

CONCLUSION

SH-SY5Y and N2a cell lines proliferation is different and depends on the passage number. BMP2, 4 and 9 show promising effects over soft films regarding cell proliferation.

The next step is to deeper understand the role of biomimetic surfaces on cancer cells proliferation, adhesion and differentiation by modulating surface stiffness and growth factor grafting.

REFERENCES

1. Tolbert VP et al. Cell and Tissue Research. 2018;372(2):195-209.
2. Peinemann F et al. Cochrane Database of Systematic Reviews. 2017;2017(8).
3. Kaitin KI. Clinical Therapeutics. 2017;39(2):236-237.
4. Nolan JC et al. Cancer Letters. 2020;474:53-62.
5. Mabie PC et al. Multiple Roles of Bone Morphogenetic Protein Signaling in the Regulation of Cortical Cell Number and Phenotype.; 1999.
6. Du Y et al. Differentiation. 2010;79(2):84-92

ACKNOWLEDGMENTS

The authors would like to thank the Prix Line Pomaret-Delalande pour les Maladies Rares de la Fondation pour la Recherche Médicale, IRGA UGA and GlyCON Project for providing financial support to this project.

3D Printing Biomimetic Analogues of Calcium Deposits at Vascular Chronic Total Occlusions Using Computed Tomography Angiography

Muireann O'Reilly[1,2*], Benjamin Brennan[1,2], Hugh G. Manning[3,4], Rachel Beatty[1,3], Peter Dockery[1], Garry P. Duffy[1,2,3]

[1]Discipline of Anatomy and Regenerative Medicine Institute, School of Medicine, College of Medicine, Nursing and Health Sciences, National University of Ireland Galway, Galway, Ireland
[2]CÚRAM, SFI Research Centre for Medical Devices, National University of Ireland Galway, Galway, Ireland
[3]SFI Centre for Advanced Materials and Bioengineering Research (AMBER), Trinity College Dublin and National University of Ireland Galway, Ireland
[4]Additive Research Laboratory (AR-Lab), Trinity College Dublin, Dublin, Ireland
[*] m.oreilly26@nuigalway.ie

INTRODUCTION

~40% of individuals with symptomatic peripheral arterial disease develop vascular chronic total occlusions (CTOs)[1]. CTOs have a complex multi-material anatomy, with a necrotic lipid core capped by fibrous tissue. The core becomes calcified over time, making it difficult to cross with interventional medical devices[2]. While optimal crossing strategies for CTOs have been established[3,4], there are few medical devices that can maintain artery patency long-term. Here, we aimed to develop a novel workflow for creating 3D analogues of CTO components from patient computed tomography angiography (CTA) files. We are particularly interested in calcium deposits, as they present the biggest challenge to successful device crossing and deployment. We aimed to 3D print calcium deposit analogues in resin (to prove the concept) and in other materials that more closely mimic the properties of bone. These patient-specific analogues could be used to create a CTO biomimetic for device design and testing.

EXPERIMENTAL METHODS

Two 2 mm axial lower limb CTA files with evidence of calcification and/or CTO were obtained from University Hospital Galway. Approval was granted by the Galway Clinical Research Ethics Committee. Anonymized scans were opened in the RadiAnt DICOM viewer (Medixant, Poland) and the calcification examined to determine if a true CTO was present, with 3D models of files also rendered for further examination (Fig. 1A). Files with evidence of true CTO were manually segmented in Mimics (Materialise, Belgium) to produce models of the arterial lumen and calcification at the CTO (Fig. 1B). These were exported as STL files and 3D-printed in grey resin at 1X scale (original scale in Mimics) and 1.5X scale (1.5 times the original in all directions) on a Form 3L stereolithography (SLA) printer (Formlabs, MA) (Fig. 1C). The 1X STL files were also printed in LithaLox HP 500, an aluminum oxide material, on a Lithoz CeraFab 7500 printer (Lithoz, Austria) (Fig. 1D).

RESULTS AND DISCUSSION

CTA files were successfully segmented to produce models of calcification and the arterial lumen at the CTO. Both the calcium and lumen models from each file were successfully printed in resin at 1X and 1.5X scale, verifying the 1X scale was sufficient for study purposes. The 1X calcium model was also printed to scale in LithaLox HP 500, which more closely mimics bone.

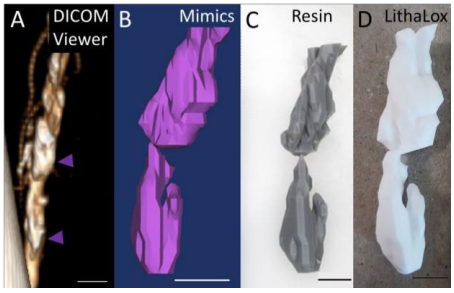

Figure 1: Calcium Models (A, B) and 3D-Printed Analogues (C, D). **Scale Bars:** 10 mm. Purple arrows show calcium.

CONCLUSION

Here, we established a workflow for creating 3D-printed analogues of CTO calcium deposits using patient CTA files. These analogues could be used for creating a biomimetic for device testing. As CTA file resolution was not very high, printed models appeared pixelated. However, we believe they are adequate for biomimetic assembly. The ability to print models using an SLA printer was promising. However, printing on a Lithoz printer does not require support rafts, which enables the preservation of model surface topography, and produces models which better mimic the boney nature of calcium deposits. Here, we printed in an aluminum oxide material. However, Lithoz printers can support mediums like hydroxyapatite bone replacement materials, which may be better mimics. In future, we hope to print in several materials and test the mechanical properties of these to establish which most closely mimics vascular calcifications. We are also exploring molding the arterial lumen model in silicone to begin creating a biomimetic vessel.

REFERENCES

1. Hamur *et al.*, Angiology. 68(2):151-158, 2017.
2. Insull Jr, Am J Med. 122(1):S3-S14, 2009.
3. Saab *et al.*, J Endovasc Ther. 25(3):284-291, 2018.
4. Kondapalli *et al.*, Vasc Med. 23(1):39-45, 2018.

ACKNOWLEDGMENTS

This research was supported in part by Science Foundation Ireland (SFI) and the European Regional Development Fund (ERDF) (Grant no: 13/RC/2073_P2). R.B acknowledges funding from SFI's AMBER Centre through their PhD program (Grant no: SFI/12/RC/2278).

Improving the Biofunctionality of Tubular Bacterial Nanocellulose Hydrogel Scaffolds for Coronary Artery Bypass Grafting by Bioprocessing Strategies

Jörn Hülsmann[1*], Fabian Reuter [2], Martin Beutner [3], Theresa Fraune [1], Viktoria Beck [1], Max Wacker [1], Matthias Hackert-Oschätzchen [3], Claus-Dieter-Ohl [2], Katja Bettenbrock [4], Maximilian Scherner [1], Jens Wippermann [1]

[1]Department for Cardiac Surgery, Otto von Guericke University, Medical Faculty, Magdeburg, Germany
[2]Department Soft Matter, Otto von Guericke University, Magdeburg,
[3] Institute of Manufacturing Technology and Quality Management, Otto von Guericke University, Magdeburg,
[4] Max Plank Institute for Dynamics of Complex Technical Systems, Magdeburg,
* joern.huelsmann@med.ovgu.de

INTRODUCTION

Today, the urgent clinical need for artificial coronary artery bypass grafts still is unmet due to the complex biophysical demands in that highly artificial biological environment. However, defining the biophysical functionality of biomaterials by tailoring biomechanical properties and functional architecture attributes are well studied and technologically progressed but mostly restrained to laborious experimental manufacturing.

In contrast, scaffolds derived by Bacterial Nanocellulose (BNC) biofilms provide simplicity in handling by its natural integrative character regarding form, architecture and biomechanical properties. However, the same character hampers any isolated approaches for improving single characteristics of the resulting hydrogel definition.

In this study, approaches for modular control of biofunctional attributes in BNC tubes by multiparametric template coating and bioprocessing methodology are presented. Thereby it is aimed to improve the density of the luminal polymer-matrix for potential cell adhesion, stress-strain relations for both passive biomechanical function and stimulation of anchored cells and further to implement varying luminal microstructure approaches that allow for guiding flow profiles and cell alignment.

EXPERIMENTAL METHODS

Controlled Komagataeibacter *xylinus* bioreactor cultivation, surface microstructuring of cylindrical small caliber form-templates by external longitudinal grinding and 3D printing, MMR Tech® coating of cylindrical templates by K. *xylinus* bacterial culture broth, Calcoflour White (CFW) cellulose staining, self-established CFW based fluidfilm to biofilm (BNC density) assay, enzymatic cellulose to glucose digestion, enzymatic quantitative glucose assay, tensile testing of BNC tube walls and rings, *in vitro* colonization of BNC tubes by endothelial cells (EC), Arcidine Orange (AO) cell staining, confocal microscopy.

RESULTS AND DISCUSSION

Dynamic K. *xylinus* cultivation by guided oxygen uptake limitation, used for producing inoculums for the template coating process, resulted in working cell densities c_X exceeding the standard static process by 2 orders of magnitude. Fluorometric evaluation of the biofilm dynamics revealed clear indication, that the resulting BNC density increases in direct correlation to the actual c_x values. Increased c_x then resulted in better biomechanical performance of the grafts as shown by tensile testing. Here, stress-strain relations approached typical relations of soft-tissues. Further, confocal imaging gave indication for a denser and smoother BNC polymer matrix for cell adhesion at the luminal side.

Using microstructured form-templates qualitatively changed the wetting and coating behavior. Thereby, previously reported wetting patterns by similarly occurring formation of the BNC biofilm could be reproduced. The area-normalized BNC densities varied for differently designed surface architectures of the form-templates. The resulting luminal hydrogel microarchitecture revealed respectively clear imprints of differently sized and organized groove and ridge profiles according to the templates. This has the potential to tailor hydrogel functionality and mechanical properties.

After *in vitro* colonization, BNC tubes providing longitudinal large range groove structures, potentially allowing for stabilization of laminar flow and wall shear stress stimulation, continuous surface coverage by vital EC´s attached on both, groove cavities and lamellar walls was observed. In angled small-range ridges, potentially allowing for more complex flow profiles, EC´s elongated, arranged and organized according to the lamellar orientation. After perfusion cultivation of repopulated BNC tubes with angled lamellar structures, EC elongation was apparently increased when compared to static controls.

CONCLUSION

Our study shows the feasibility of implementing a variety of biofunctional attributes to tubular BNC scaffolds by simple bioprocessing strategies and by controlling the microfluidic processes on the templates via microstructuring. Thereby, smooth and dense luminal surfaces providing different lamellar microstructure profiles could successfully be realized. These also could be accepted by EC´s and appeared to be functional under perfusion. Further improvement or implementation of more features may be approached by adjusting recipes for cultivation and coating, utilizing feedback from *in vitro* validations.

ACKNOWLEDGMENTS

The authors are thankful for the technical help of Dr. Roland Hartig and Andrea Schütze.

Innovative UV-physical filter based on hybrid Ti-doped hydroxyapatite for eco-sustainable sunscreen formulations

Elisabetta Campodoni[1], Margherita Montanari[1], Chiara Artusi[1], Linda Bergamini[1], Giada Bassi[1], Silvia Panseri[1], Anna Tampieri[1], Alessandra Sanson[1], Monica Sandri[1]

[1]Institute of Science and Technology for Ceramics-National Research Council (ISTEC-CNR), Faenza, Italy

chiara.artusi@istec.cnr.it

INTRODUCTION

The sunlight is essential for our well-being, because it is responsible for regulating the metabolism, immune systems, and for the production of vitamin D essential for healthy bones; however, excessive sun exposure can be dangerous for human health, particularly for skin. In this regard, the use of sunscreen to protect ourselves from solar radiation, especially harmful UVA and UVB rays, is becoming an increasingly important issue[1], to avoid skin photo-aging and the onset of malignant tumours[2]. Furthermore, the more attention for the preservation of the marine environment has brought out the need to develop eco-sustainable materials[3]. With these evidences, this research would propose innovative and eco-sustainable hybrid UV-physical filters composed of hydroxyapatite and biopolymers obtained by a nature-inspired biomineralization process.

EXPERIMENTAL METHODS

Through the biomineralization process, titanium-doped-hydroxyapatite (TiHA) crystals were nucleated on different organic matrices to develop biomimetic physical filters with eco-friendly properties and without photocatalytic effect. The hybrid composites were investigated through chemical-physical (XRD, FTIR, TGA, ICP-OES) and morphological (SEM) analysis. Moreover, the interaction with the UV-VIS radiations (adsorption and reflection spectra) and the photodegradation potential were evaluated. In addition, complete sunscreen formulation tests were performed and the functionality and safety of these new eco-sustainable UV-filters were evaluated by in vitro and in vivo validations test.

RESULTS AND DISCUSSION

The major phase (more than 85 %) is a nanostructured TiHA featured by a micrometric size due to the presence of organic phase on which the apatitic crystal are grown avoiding the penetration into epidermis and, thus, conferring a complete safety for human healthy. Furthermore, the low TiHA crystallinity very close to human bones and obtained through the biomineralization process, allow to create a fully biodegradable material releasing only harmless ions for health and aquatic environment. The results obtained by UV-VIS spectroscopy have shown excellent reflectance and absorption properties of the composites thanks to the presence of Ti ions. Moreover, since titanium is not present in the form of titanium dioxide (TiO_2), as in commercial UV-physical filters, but as Ti(IV) ions, any photocatalytic effect. The photo-stability of the physical filter results in avoiding the photo-degradation of the other ingredients in sunscreen formulations and the generation of radicals and/or reactive species under irradiation, harmful for skin and corals. In addition, the presence of organic matrix allowed an excellent sunscreen formulation and in vitro and in vivo tests have shown a good efficiency and safety results.

CONCLUSION

Effective and eco-sustainable Ti-HA based sunscreens have been developed as new safe physical filters compared to commercial ZnO and TiO_2. Thanks to the introduction of Ti ions within the biomineralization process, it was possible to obtain the partial substitution of both Ca (Ti^{4+}) and P (TiO_4^{4-}) ions into the hydroxyapatite latex, realizing innovative solar filters featured by high biocompatibility, full-biodegradability in sea water with the release of harmless ions for humans and animals, bands of UV radiations absorption/reflection in the desired range and absence of photocatalytic effect. Moreover, complete sunscreen formulation was developed and their efficiency and safety by means of in vitro and in vivo validations was confirmed.

REFERENCES

1. Smaoui S. *et al*., Arabian J. of Chemistry, 10, S1216–S1222, 2017
2. Rünger, T. M., Photodermatology, Photoimmunology & Photomedicine, 15(6), 212–216, 1999
3. Piccirillo, C. *et al.*, J. Mater. Chem. B, 2, 5999–6009, 2014

ACKNOWLEDGMENTS

The authors would like to thank the ProtecTHA project "Innovative solar filters for safer and more eco-sustainable PROTECtion: titanium-apatites (TiHAPol) as physical filters of UV rays" funded by the National Research Council of Italy (CNR), for providing financial support to this project.

In-vitro Studies of 2D Orthopaedic Implants with Cell Instructive Nanotopographies.

Rosalia Cuahtecontzi Delint[1*], Monica P. Tsimbouri[1], Irill Ishak[2], Angela Nobbs[2], Bo Su[2], Manuel Salmeron-Sanchez[1] & Matthew J. Dalby[1].
[1]Centre for Molecular Microenvironment. Institute of Molecular, Cell and Systems Biology. College of Medical, Veterinary and Life Sciences, University of Glasgow, Glasgow, UK.
[2]School of Oral and Dental Sciences, University of Bristol, Bristol, UK.

[*] rosalia.cuahtecontzidelint@glasgow.ac.uk

INTRODUCTION

The demand for total hip (THR) or knee replacements (TKR) has been steadily increasing worldwide due to an ageing population, the rise in obesity, and change to more active lifestyles, which is collectively resulting in an increase in degeneration of cartilage and subchondral bone in joints leading to osteoarthritis. While the success rate of these implants is relatively high, many still fail prematurely within the first 10 to 20 years. The two leading causes of bone implant failure are aseptic loosening (due to poor osseointegration) or infection (due to bacterial infiltration and biofilm formation). Certain topographies and active coatings have shown to be bactericidal. Here, we use high aspect ratio nanospikes to reduce bacterial adhesion[1]. We also use a plasma poly(ethyl acrylate) (pPEA) polymer coating on surfaces to spontaneously organize fibronectin (FN) and to deliver bone morphogenetic protein 2 (BMP2) to improve human mesenchymal stem cells (hMSCs) adhesion and osteogenesis[1] as the nanospikes also lower hMSC adhesion.

EXPERIMENTAL METHODS

Nano-patterned titanium surface were fabricated by changing etching times in sodium hydroxide to yield different structures on the Ti surfaces: 2h etch yielded nanosurface 1 (NS1), and 16h were necessary to form nanosurface 2 (NS2) (Figure 1).

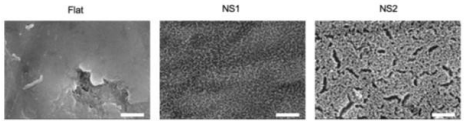

Figure 1. Scanning electron microscope images from Ti surfaces. Flat surface without etching used as control. NS1 etched for 2h, and NS2 etched for 16h.

Plasma polymerised PEA was used to coat the titanium surfaces for 90 seconds at 100W, followed by treatment with 20 µg/mL of fibronectin and 100 ng/mL of BMP2. The viability, and adhesion quality of primary hMSCs was tested using immunofluorescence staining and colorimetric assays. The antimicrobial properties of these coated and uncoated surfaces were challenged using Gram-stained negative bacteria *Pseudomonas aeruginosa*. Additionally, the viability of hMSCs co-cultured with *P.aeruginosa* on the titanium surfaces was evaluated, as well as the ability of the hMSCs to remain attached to the titanium surfaces and their osteogenic differentiation potential.

All assays were done in triplicate and the data obtained was statistically analysed using a students' T-test with two-tailed unpaired samples in Microsoft Excel. Differences between the experimental and control groups were compared.

RESULTS AND DISCUSSION

Nanopatterned titanium surfaces treated with active coatings such as PEA+FN+BMP2 offer great potential to grow viable hMSCs and sustain osteogenic differentiation. Furthermore, both topographies showed significant antibacterial potential, corresponding with previous studies done in high aspect ratio nanospikes.[2] Importantly, this antibacterial potential was not lost with PEA/FN/BMP.2 coating of the features. Moreover, the exposure of hMSCs to bacteria did not cause a significant change in the hMSCs viability or adhesion features in short-term co-culture when the features were coated in PEA/FN/BMP2. The conditions were more favourable for the titanium surfaces with nanopatterns.

CONCLUSION

This study showed the potential for the implementation of nanotopographical surfaces to address both poor osseointegration on bone implants and bacterial biofilm formation. PEA/FN/BMP2 coated topographies offer better support for hMSC adhesion and differentiation versus uncoated surfaces. This finding is of major importance given that primary cells need to be recruited for successful osseointegration. Moreover, biofilm formation was decreased when bacteria was seeded on NS1 and NS2 patterned surfaces which helps hMSCs to colonize the titanium surface. This has clear implication for development of orthopaedic biomaterials.

REFERENCES

1. Damiati L. A. *et al*., Biomaterials. 2022;280:121263.
2. Ivanova E. P. *et al.,* Small. 2012;8(16):2489-2494.

ACKNOWLEDGMENTS

The authors would like to thank the Medical Research Council (MRC) for providing financial support to this project.

Development of bio-inspired protein-based materials as novel anti-corrosive coatings and transparent adhesives

Craig Allan[1*], Gethin Allen[1], Alex Harold[1], Sholeem Griffin[1], Dave Penney[2] and Geertje van Keulen[1]

[1]Institute of Life Science, Swansea University, Swansea, United Kingdom
[2]College of Engineering, Swansea University, Swansea, United Kingdom
[*]Craig.allan@swansea.ac.uk

INTRODUCTION

Streptomyces bacteria are highly versatile micro-organisms, which have been recognised as potent soil, (bio)chemical and (bio)material engineers. *Streptomyces* has served as a source of inspiration for materials development in vitro, based on their ability to modulate in vivo the properties of its own surface and that of its natural environment. Our interdisciplinary projects have developed chaplins, functional amyloid proteins from *Streptomyces* bacteria, into novel nano-thin anti-corrosion coatings and confer strong adhesive properties to hydrophilic non-metal substrates when applied as a bio-composite when chaplin proteins are mixed with a sugar-based biopolymer. The need for more sustainable and innovative solutions to combat corrosion is becoming more important.

This research demonstrates the ability for chaplin proteins to be produced and extracted in a more economical manner over conventional growth and extraction procedures. It also shows how the composition and ratio of protein to sugar polymer has affected the deposition consistency and water contact angle of the coating's surface when deposited on hydrophilic substrates. Our anti-corrosive protein coating and protein-based adhesive applications have great potential for the manufacturing, defence and other industries, including healthcare and biomaterials manufacturing.

EXPERIMENTAL METHODS

To optimise the growth of *Streptomyces* for the extraction of chaplin proteins, alternative buffers and recipes were trialled. Chaplin protein concentrations were determined and compared, as well as microscopic analysis of the growth cycle.

For characterisation of the bio-composite, we have determined the effect of the glycan addition by depositing onto different substrates, both hydrophilic and hydrophobic to determine the water contact angle change. Material topography and performance analyses, using different high-resolution imaging, qualitative and quantitative electrochemistry techniques were used to determine coating thickness and appearance, as well as its elastic, adhesive and functional properties.

RESULTS AND DISCUSSION

By monitoring the growth cycle of the different media iterations, buffer B had a similar growth cycle to the control, unlike Buffer C which did not lead to sporulation of the strain. The spore count and Thioflavin T assay of these sporulating iterations suggests that the modified media with the alternative buffer does lead to sporulation of the strain. This modified media in combination with the buffer can reduce the overall cost of the medium by ~75%. This has been successful at 200mL scale and has been demonstrated within a 2L bioreactor.

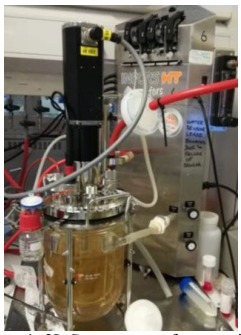

Figure 1: 2L *Streptomyces* fermentation

To test the effects of the glycan addition, increasing amounts were added to the protein sample and allowed to dry onto the substrate before performing goniometry.

In comparison of the protein only and bio-composite samples, there was a 20º improvement observed in the water contact angle over the protein only. It is hypothesised that the glycan assists in the formation of the chaplin fibrils in solution and aids in the coating uniformity.

CONCLUSION

The optimisations made to the growth medium has a significant effect on the economic viability of the process. The barrier properties that chaplin proteins provide could be an alternate corrosion resistance strategy but would require production to be on a larger scale. The research here demonstrates the ability for the growth to be increased whilst providing cost savings.

The addition of the glycan improves the overall water contact angle in comparison to the chaplin only sample and provides a more uniform coating, which in turn is likely to positively affect corrosion resistance performance.

ACKNOWLEDGMENTS

The authors would like to thank the Defence Science and Technology Laboratory for providing financial support to this project.

Recombinant polyelectrolyte-based Complex Coacervates with intrinsically disordered and LCST behavior

Julio Fernández*[1], Carmen Herrero[1], Jaime Caldevilla[1] , Mercedes Santos[1], Matilde Alonso[1], José Carlos Rodríguez[1]

[1]GIR BIOFORGE, University of Valladolid, Valladolid, Spain
* jfernandez@bioforge.uva.es

INTRODUCTION

Polyelectrolyte complex coacervates are formed by the self-assembly and the electrostatic interaction between oppositely charged polyelectrolyte chains[1]. Limited information is available about the assembly of complex coacervates from recombinant proteins, particularly when this takes place from intrinsically disordered polypeptides (IDPs) although it is common knowledge that they play an important role in the natural processes of self-organization and hierarquical emergence of structure and shape in biological systems[1]. To this end, we compare the spinodal decomposition generating self-assembled nano and microstructures of two amphiphilic Elastin-Like Recombinamers with opposite charges in their hydrophilic block and a common neutral and thermally sensitive hydrophobic block. Their mixes at different rates are also studied.

EXPERIMENTAL METHODS

The two diblocks were obtained by recombinant DNA technology[2]. Elastin-Like Recombinamers are artificial polypeptides, which sequences are repeat motifs found in intrinsically disordered regions of tropoelastin. The two ELRs are dissolved in water at 5ºC, and characterized at physiological temperature by different techniques such as nuclear magnetic resonance (NMR), isothermal titration calorimetry (ITC), circular dichroism (CD), differential scanning calorimetry (DSC), dynamic light scattering (DLS) and cryo/transmission electron microscopy (Cryo-TEM/TEM).

RESULTS AND DISCUSSION

The two separated ELRs are characterized by their soluble and unfolded chains at 5ºC, while at 37ºC they self-assemble hydrophobically into spherical micelles with hydrodynamic diameters between 100 and 200 nm. Then, the two dissolved ELRs are mixed each other and the interactions between them are demonstrated by 1D NMR spectrums and their chemical shifts, and quantified by the titration calorimetry data. Those interactions decrease their inverse transition temperatures and reduce the random coil conformations as the molar ratio converge to equal charge numbers. Contrarily to what happens when they are alone, their mixes generates more complex and bigger self-organizing structures. Thanks to the combination of hydrophobic and ion pairing taking place in those co-coacervates, the formation of large micelle structures of much larger size (hydrodynamic diameter ~ 1 µm) with smaller micelles encrusted on their surfaces are the predominant morphological structures. This is more prominent as the system approaches charge neutralization.

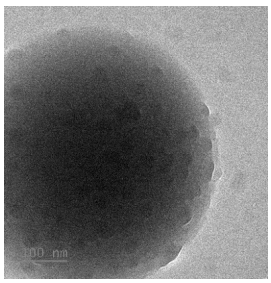

Figure: Cryo-TEM image of Complex Structure resulting from the 1:1 charge molar ratio mixture.

CONCLUSION

The interaction between hydrophobic and Coulomb forces in the mixture of the amphiphilic and thermosensitive IDP models used here conditions the way they self-assemble after the spinodal decomposition phase and segregate their aqueous solutions. As opposed to the simple micellar nanostructures obtained when alone, when mixed, more microstructures of greater complexity are found. These results highlight the importance of the interplay between different self-organizing forces as well as the order-disorder balance in the spontaneous emergence of complex hierarchical IDP structures. These results provide insights into the understanding of the self-organizing nature of biological macromolecules. It is also of interest in the fabrication of supramolecular protein-based materials.

REFERENCES

[1] S. Shah and L. Leon, “Structural dynamics, phase behavior, and applications of polyelectrolyte complex micelles,” *Curr. Opin. Colloid Interface Sci.*, vol. 53, p. 101424, 2021.

[2] J. C. Rodríguez-Cabello, I. G. De Torre, S. Acosta, S. Salinas, and M. Herrero, *Elastin-like proteins: Molecular design for self-assembling*. Elsevier Ltd., 2018.

ACKNOWLEDGMENTS

The authors would like to thank the European Social Fund Plus and Junta of Castile and León (EDU/875/2021), Interreg V España Portugal POCTEP (0624_2IQBIONEURO_6_E), PID2019-110709RB-I00 and RTI2018-096320-B-C22 for providing financial support to this project.

New boron-containing cryogel scaffolds for tissue engineering application

S. Ceylan[1,2], R. Dimmock[2], Y. Yang[2]

[1]*Department of Bioengineering, Faculty of Engineering, Adana Alparslan Türkeş Science and Technology University, Adana, Turkey*

[2]*School of Pharmacy and Bioengineering, Keele University, Stoke on Trent, UK*

INTRODUCTION: Tissue engineering aims to design artificial constructs for regeneration of new tissue. Various biocompatible and biodegradable polymers have been combined with growth factors and biochemical signal molecules into scaffolds to accelerate regeneration process. Cryogelation is a simple method to fabricate scaffolds with interconnected micropores allowing better cell communication and ECM production. Boron has an important role in several metabolic pathways. Besides, 3% boric acid solution has been shown to increase healing rate of deep wounds. In the present study, we fabricated polyvinyl alcohol (PVA), starch and chitosan based cryogels scaffolds with borax (sodium tetraborate decahydrate) as crosslinking agent. The effects of boron amount and PVA molecular weight on PVA/starch-chitosan cryogel scaffolds' mechanical, swollen and biological properties have been investigated.

METHODS: PVA with molecular weight of 30000-70000 and 85000-124000 was used to produce scaffolds. The polymer concentration of PVA/starch-chitosan blend solution was fixed at 3% w/v and the borax amounts of 1, 2, 3, 4 and 5 % (w/w) were added to the polymer mixture for the cryogelation process. The non-destructive imaging devices, Optical Coherence Tomography device and dissection microscope, were used to analyse the cryogels volume change when swollen in PBS. Mechanical properties of the 3D cryogel scaffolds were analysed by tensile machine under compression mode. The cytotoxicity of cryogels and the effect of released chemicals from the scaffolds were evaluated by CCK8 kit and cellular morphology using MG63 osteoblast cell line for 5 day culture.

RESULTS: Most composition formula of PVA/starch-chitosan blends formed stable cryogels. However, the PVA with molecular weight 30000-70000 and borax amount higher than 5 % total polymer amount did not produce stable cryogels. The swollen rate of cryogel depended on borax amount and generally swollen rate decreased with increasing borax amount. Volume change of produced cryogels without borax showed highest value (24.68%) compared to the ones prepared with 1, 2, 3% borax. The Young modulus of cryogels also changes along borax amount with 2% boron scaffolds bearing the highest modulus value of 21.53 KPa. CCK-8 assay showed viable cells presented in scaffolds with slight low cell number/metabolic rate in 3% boron-containing scaffolds. The released chemicals from the scaffolds apparently affected MG63 cells' phenotype. MG63 cells grown in the presence of 1% boron-containing scaffolds exhibited normal proliferation morphology (Fig 1 A); as the borax concentration increased to 2 and 3% in the cryogel, the MG63 cells start to aggregate and differentiate (Fig 1B, C).

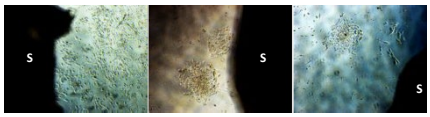

Figure 1: *Microscopic images of cells-cryogels with different contents of borax A) P:S/C- 1% B , B) P:S/C- 2% B ,C) P:S/C- 3% B, (S: scaffold; P: PVA; S: starch; C: chitosan and B: borax) on day 5 culture.*

DISCUSSION & CONCLUSIONS: It can be concluded that all gelated scaffolds had good biocompatibility. Borax amount and PVA molecular weight affected the characteristic properties and cell response of the cryogels with optimizing boron content laid between 2-5% of the total mixture mass.

Keywords: *Boron, Cryogel, Tissue engineering*

ACKNOWLEDGEMENTS: This work was supported by the the "Scientific and Technological Research Council of Turkey" (TUBITAK/2219-1059B191900823) and EPSRC CDT programme, UK.

Osteoinductive porous Ti6Al4V-beta Tricalcium Phosphate Hybrid Scaffolds for Orthopedic Applications

JiaPing Li, Lorenzo Moroni and Pamela Habibovic
(MERLN Institute for Technology-Inspired Regenerative Medicine, Maastricht University, The Netherlands
Jiaping.li@maastrichtuniversity.nl

INTRODUCTION

Titanium (Ti) and its alloys are extensively used to fabricate porous metal implants for primary- and revision total joint arthroplasty owing to their good mechanical and chemical properties and biocompatibility (1). For the long-term success of cementless implants, it is crucial to have fast bone ingrowth around and inside the porous structure to fix the implant. However, the main disadvantage of porous metallic biomaterials including Ti-based ones is that they lack bioactivity. Although bioactive calcium phosphate (CaP) coatings are often applied on the surface of metallic implants to improve their bioactivity, poor interfacial strength between the metallic substrate and the coating as well as the brittleness of the coating itself may result in implant loosening with serious clinical consequences (2). To meet practical requirements of biological fixation and long-term stability, there is a need to manufacture implants that mimic properties of natural bone, are bioactive and thus result in earlier and more pronounced bone ingrowth into the implant (3). The aim of this study is to develop porous Ti-CaP hybrid implants, which allows the combination of the mechanical properties of Titanium with the bioactivity of the ceramic.

EXPERIMENTAL METHODS

Ti6Al4V (Ti) powder with a size below 45 µm (AP&C Inc. Canada) was used. TCP particles having a size below 500 µm (Kuros Biosciences BV, Netherlands) was processed by a ball mill to obtain a size of 63-125 µm. Urea particles with a size of 100-1000 µm were used as porogen. Porous Ti-TCP was prepared by mixing the porogen into Ti with 10 wt%TCP slurry, which was prepared in a 100% ethanol binder solution, and then poured into a plastic mold with a diameter of 8 mm. The resulting Ti-TCP green bodies were first dried, then debinded to remove the porogen and the binder, and finally sintered at 1150 °C under protective argon environment. The structure, chemical composition, and crystallinity of 3D Ti/TCP were analyzed. Mechanical tests were performed. Porous Ti with and without TCP were implanted in the dorsal muscles of mature dogs (male, 2-4 years old, weight 10–15 kg, n = 4 per scaffold) for 12 weeks. Harvested scaffolds were fixed, dehydrated and embedded with MMA. The histological section was made by a diamond saw and stained with 1% methylene blue (Aldrich) and 0.3% basic fuchsin (Aldrich) solutions after etching with HCl/ethanol mixture, then analyzed by light microscope to determine bone incidence.

RESULTS AND DISCUSSION

TCP particles were observed on the surface as well as in the center of the scaffold. The hybrid scaffolds were highly porous; macropores formed by porogen (Fig.1A and 1B), microspores resulting from Ti particle fusion (Fig. 1C), and sub micropores resulting from the presence of TCP particles (Fig.1D) were observed. Chemical analyses proved the presence of TCP in the scaffolds. The compressive strength and Young's modulus of porous Ti-TCP scaffolds were between the values for cancellous bone and cortical bone. In vivo study, in which the scaffolds were implanted intramuscularly in dogs, showed no bone formation on porous titanium scaffolds (Fig.2A and 2B) and ectopic bone formation in the porous Ti6Al4V-TCP scaffolds, showing their osteoinductive potential (Fig. 2C and 2D).

Fig.1

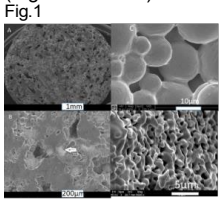

Fig.2

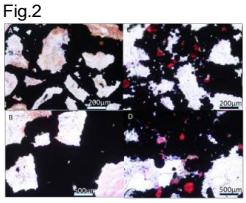

Fig.1 Structure of porous Ti–TCP under SEM
Fig.2 Bone formation on Ti-TCP and no bone on Ti

CONCLUSION

Porous Ti-TCP hybrid scaffolds were successfully fabricated. The porous scaffolds exhibited macropores, micropores, and submicropores in the structure. The compressive strength and Young's modulus were similar as those of natural bone. A preliminary *in vivo* study in an intramuscular model demonstrated that the addition of TCP to the metal alloy improved its bioactivity, showing their osteoinductive potential. These newly developed porous Ti-TCP hybrid scaffolds may improve cementless fixation and long-term patient outcomes in total joint replacement.

REFERENCES

1. Alireza N, Peter D. Hodgson, Cui'e Wen. In: Biomimetics Learning from Nature 2010;21:415
2. Surmenev RA, Surmeneva MA, Ivanova AA. 2014, Acta Biomater.;10 (2):557
3. Lewallen EA, Riester SM, Bonin CA etc, , 2015 Tissue Eng Part B Rev. Apr 1; 21(2): 218

ACKNOWLEDGMENTS

This research has been made with the support of the Dutch Research Council (NWO-AES, Grant #16711). The authors would like to thank the LINK project, INTERREG Northwestern Europe BONE Project (NWE497), and the Gravitation Program "Materials Driven Regeneration"(024.003.013)

Fabrication of Collagen-Hyaluronic Acid Cryogels by Directional Freezing Mimicking the Arcade-Like Structure of Articular Cartilage

Taiyo Yamamoto[1], Rotsiniaina Randriantsilefisoa[1], Christoph Martin Sprecher[1], Matteo D'Este[1*]

[1] AO Research Institute Davos, Clavadelerstrasse 8, 7270 Davos Platz, Switzerland
rotsiniaina.randriantsilefisoa@aofoundation.org

INTRODUCTION

Extracellular matrix macromolecules are building blocks of choice for fabricating constructs recapitulating the characteristics of connective tissues. However, mechanical, and biological properties do not depend only on composition, but also on internal architecture. In this work we introduce a simple and robust method to fabricate constructs based on derivatized extracellular matrix macromolecules with porosity arranged according to the arcade-like structure found in articular cartilage. The method is based on the growth of ice crystals from copper pins at cryogenic temperatures. Double network cryogels based on hyaluronic acid (MeHA) and collagen (CollGTA) were formed approaching cartilage mechanical properties.

EXPERIMENTAL METHODS

The cryogels were produced using a pin plate setup: the method consists in immobilizing copper pins in a poly (methyl methacrylate) (PMMA) plate. The upper part of the copper pins was in contact with liquid nitrogen on one side and with the CollGTA precursor solution contained in wells on the other side. Directly following the freezing of the CollGTA solution, crosslinking with glutaraldehyde was achieved overnight at -20 °C through cryogelation.

The morphological characteristics of the obtained CollGTA-MeHA double networks were investigated by light and scanning electron microscopy.

Mechanical characterization was assessed by unconfined compression on the obtained double networks and on CollGTA and MeHA single network cryogels.

RESULTS AND DISCUSSION

Morphological characterization of the cryogels showed that at the surface close to the pins, the collagen was more closely packed and compacted tangentially to the surface, while in the centre the polymers were more elongated, obliquely oriented, and perpendicular to the surface. Therefore, arranged in an arcade structure. This morphology can be explained by the ice crystal formation occurring during the process: ice crystals nucleated at the surface of the pin and grew outwards over a relatively large distance of over 4 mm, in the range of the thickness of articular cartilage.[1]

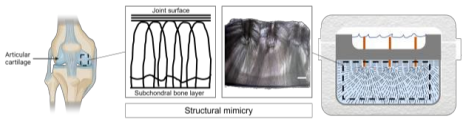

Figure 1. Schematic description of the concept: structural mimicry of cartilage by using a pin setup for directional cryogel formation.

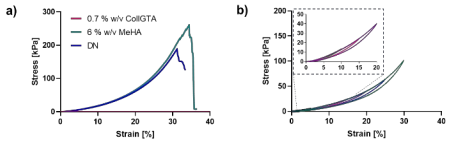

Figure 2. Compressive stress-strain curves of CollGTA, MeHA single network cryogels and CollGTA-MeHA double network cryogels. a) CollGTA and MeHA single networks and the corresponding double-network with a collagen concentration of 0.7 % w/v and MeHA concentration of 6 % w/v. b) Cyclic loading of CollGTA-MeHA (0.7 % w/v and 6 % w/v respectively) to 30% strain in 5% increments.

The compressive stress-strain curves (Fig 2a) indicate that the CollGTA first network exhibited negligible resistance to the stress applied for the whole range of 5-40% strain (Young's modulus: 1.6 Pa). On the contrary, the MeHA alone exhibited a higher elastic modulus (233 kPa) and stress at break (260 kPa). Therefore, MeHA lends its good mechanical properties to the corresponding DN cryogels, which also exhibited a high early elastic modulus (~200 kPa) and a stress at break of ~184 kPa. Given that the elastic compressive modulus of articular cartilage ranges between 240 and 1000 kPa, the compressive modulus of the CollGTA-MeHA cryogels approaches the lower range of articular cartilage moduli.[2]

CONCLUSION

Cryogels displaying architectural properties similar to native articular cartilage were achieved. The constructs possess enhanced mechanical properties compared to the corresponding single collagen network alone. Overall, combining morphological, compositional, and mechanical aspects in mimicking native articular cartilage opens new perspectives concerning tissue substitutes and models with controlled architecture. The present study provides a straightforward and versatile method to introduce complex spatial arrangement in extracellular matrix-based constructs.

REFERENCES

1. S., Fox, A., Bedi & S. A., Rodeo, 2009.
2. B., Barragan, T., Gehrke, & Detamore, 2016; J., Welch, & Winkelstein, 2011; L., Bawolin, & Chen, 2011.

ACKNOWLEDGMENTS

The authors would like to thank AO Foundation for providing financial support to this project.

Hybrid bioinspired coating induces *in vivo* critical-sized defect bone regeneration

Marie Dubus, Loïc Scomazzon, Léa Abou Nassif, Adrien Baldit, Abdelilah Beljebbar, Julien Braux, Cédric Mauprivez, Halima Kerdjoudj

[1]Université de Reims Champagne Ardenne, EA 4691, Biomatériaux et Inflammation en Site Osseux (BIOS), Reims, France
[2]LEM3-UMR-7239, CNRS - Arts et Métiers ParisTech; ENIM, Université de Lorraine, Metz, France
[3]UMR CNRS 7369, BioSpectroscopie Translationnelle BioSpecT, Université de Reims Champagne Ardenne, Reims, France
* halima.kerdjoudj@univ-reims.fr

INTRODUCTION

A multifunctional membrane that kills bacteria and drives bone healing is urgently sought, especially in bone regeneration field. Herein, we used simultaneous spray coating of interacting species process to build a bone inspired coating made of calcium phosphate nano particles and chitosan/hyaluronic acid nanofilm on collagen membrane.

EXPERIMENTAL METHODS

The physicochemical characterizations of the resulting hybrid coating were performed by confocal Raman spectroscopy mapping and high resolution-transmission electron microscopy combined with electron diffraction. Then human mesenchymal stem cells (MSCs) and human monocytes were cultured on those membranes. Biocompatibility and bioactivity of the hybrid coated membrane were respectively evaluated through MSCs proliferation (WST-1 and DNA quantification) and visualization; and cytokine release by MSCs and monocytes (ELISA and endothelial cells recruitment). Antibacterial properties of the hybrid coating were then tested against *S. aureus* and *P. aeruginosa*, and through MSCs/bacteria interactions. Finally, a preclinical *in vivo* study was conducted on rat calvaria bone defect. The newly formed bone was characterized 8 weeks post implantation through µCT reconstructions, histological characterizations, immunohistochemistry analysis, Raman spectroscopy, and second harmonic generation. Biomechanical features of newly formed bone were determined.

RESULTS AND DISCUSSION

Confocal Raman spectroscopy mapping and high resolution-transmission electron microscopy combined with electron diffraction characterization of the resulting coating revealed the presence of dicalcium phosphate dehydrate amorphous mineral structures with rod-*like* shapes exposed on the membrane surface and within the thickness of the membrane. *In vitro* studies revealed that coated membrane possesses excellent bioactivity and capability of inducing an overwhelmingly positive response of stromal cells and monocytes in favour of bone regeneration [1-3]. Furthermore, the coating provides contact-killing properties by disturbing the cell wall integrity of Gram-positive and Gram-negative bacteria. Its combination with stromal cells, able to release antibacterial agents and mediators of the innate immune response, constitutes an excellent strategy for fighting bacteria [4]. A preclinical *in vivo* study was therefore conducted in rat calvaria bone critical size defect. After eight weeks, µ-CT showed that coated membrane induced bone regeneration (two-fold increase in bone volume *vs*. bare membrane (control)). The histological characterizations of calcified and decalcified samples confirmed that the thickness bridging in the bone defect site was significantly higher in the presence of the coating *vs*. control. The majority of the defect region was filled with mature-*like* bone (marked by the presence of osteoblasts, osteocyte lacunae, bone marrow and blood vessels (CD31 positive cells)) with a lamellar-like collagen organization in the dura side, while in the control, bone tissue in-growth pattern was from the peripheral region. Raman spectroscopy analysis performed on freshly explanted specimen revealed higher relative band intensities of phosphate and carbonate in the presence of the coating vs control. Carbonate-to-phosphate ratio was lower while mineral-to-collagen ratios (*i.e*. carbonate-to-collagen and phosphate-to-collagen) were higher in the newly formed bone *vs*. connective tissue in the control group. Taken together these results suggest an increase in the bone mechanical strength of the newly formed bone. Despite an increase in the stiffness of the newly formed bone vs. control, the obtained values of stiffness were lower than those for native bone. This could be attributed to the poor bone remodelling of the calvaria bone, bone site which is poorly mechanically stimulated.

CONCLUSION

These significant data shed light on the regenerative potential of such bioinspired hybrid coating, providing a suitable antibacterial environment for bone regeneration and vascularization.

REFERENCES

1. Rammal *et al*., ACS Appl. Mater. Interfaces. 2017, 9, 12791−12801.
2. Rammal *et al*., Int. J. Mol. Sci. 2018, 19, 3458.
3. Dubus *et al*., Colloids Surf. B Biointerfaces. 2019, 181, 671.
4. Dubus *et al*., Biomater. Sci. 2020, 8, 5763.

Synthetic Biomimicking Lipid Coatings Enhance Hemocompatibility of Silica Microparticles

F.L. Fernandes Gomes[1*], J. van Weerd[2], P. Jonkheijm[3], J. Leijten[1]
[1]Leijten Lab, Department of Developmental BioEngineering, Faculty of Science and Technology, Technical Medical Centre, University of Twente, Enschede, The Netherlands
[2]LipoCoat BV, Enschede, Netherlands
[3]Department of Molecules and Materials, Laboratory of Biointerface Chemistry, Faculty of Science and Technology, MESA+ Institute for Nanotechnology, University of Twente, Enschede, The Netherlands
*f.l.fernandesgomes@utwente.nl

Introduction

Silica is used as a standard substrate for life sciences due to its hydrophilicity and ease of functionalization. Specifically, silica particles have been extensively used in biosensors, drug and gene delivery, protein immobilization, and as protective coatings on inorganic micro- and nanomaterials. However, silica is also known for its high hemolysis rates and subsequent low hemocompatibility.[1] A promising approach to improve this aspect is to use bioinert coatings that mimic the natural cell membrane.

Supported lipid bilayer (SLB) coatings are predominantly applied on silica through vesicle fusion. This method, however, is laborious and incompatible with the use of certain lipids (e.g. cholesterol) at biologically relevant concentrations. Solvent gradient-based methods have emerged as more simple, universal SLB coating alternatives due to their bottom-up approach from single lipid solutions, proven successful in a wider range of substrates and lipid compositions.[2]

In this work, a solvent gradient coating method was devised, refined, and applied to silica microparticles to conduct a hemocompatibility screening of different cell membrane-mimicking lipid coatings. Our results showed that silica particles were successfully coated with various lipid compositions, and that minimal lipid coatings reduced silica hemolysis rates from 70-85% to below 4%. Future studies will focus on more in-depth hemocompatible profile studies.

Methodology

DiagNano™ Green Fluorescent Silica Particles of 5 µm (SiO_2 MPs, CD Bioparticles) were coated through a solvent gradient method. In short, ethanol-based fluorescent solutions of different lipid compositions (Avanti Polar Lipids, Inc.; Sigma-Aldrich; Invitrogen™) were added to SiO_2 MP suspensions in ethanol, and a solvent-buffer gradient was created through the gradual addition of DPBS. Heating and osmotic shock steps were added to facilitate coating formation. Finally, particles were washed and resuspended in DPBS. The coating was studied using a Zeiss LSM 880 (Zeiss). Hemolysis assays were conducted by incubating 0.2 mg/ml suspensions of smaller SiO_2 MPs (0.1 µm, Polysciences Inc.) with freshly isolated human red blood cells at 37ºC for 4 hours.

Results and Discussion

Confocal microscopy images show four different cell membrane-mimicking lipid coatings applied on SiO_2 MPs (Fig.1A) after optimization of some solvent gradient coating method parameters such as DPBS addition rate (Fig.1B). Lower addition rates resulted in higher lipid loading, possibly indicating different coating structures. The effect of other parameters such as solvent and gradient ratio is under testing. Hemolysis tests revealed a clear decrease in hemolysis rate with phosphocholine (PC)-rich coatings, with no significant differences between compositions (Fig.1C). Other biological studies are currently underway to assess any potential bio-responsive differences between formulations.

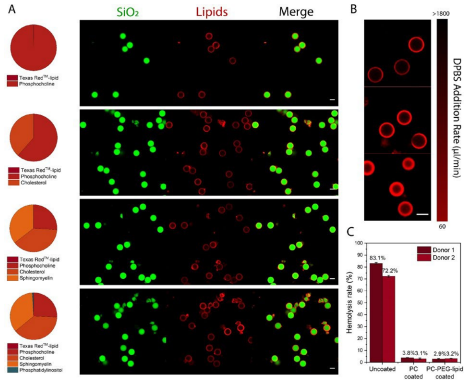

Figure 1. A. *Cell membrane-mimicking coating compositions and application on SiO_2 MPs.* ***B****. Effect of DPBS addition rate on lipid loading.* ***C****. Hemolysis rates of phosphocholine (PC)-coated particles, with and without PEGylated lipids, on small SiO_2 MPs. Scale bar 5 µm.*

Conclusions

A solvent gradient coating method was refined and used to form different cell membrane-mimicking lipid coatings on SiO_2 MPs. Blood assays indicated a substantial improvement of hemolysis rates of the coated materials regardless of lipid formulation. Forthcoming efforts will focus on a more complete biological study of the different biomimicking formulations.

Acknowledgements

F.L. Fernandes Gomes acknowledges the TechMed Donor Service of the University of Twente and all its collaborators and donors. Authors acknowledge financial support from Health~Holland (Project LSHM19074).

References

1. Slowing, I.I., et al. Small, 2009. **5**(1): p. 57-62.
2. Sut, T.N., et al., Applied Materials Today, 2021. **25**: p. 101183.

Design and Production of a Novel HELP-based Component for Antimicrobial Surfaces Functionalization

Laura Colomina[1*], Artemis Stamboulis[2], Pietro Riccio[2], Hanieh Ijakipour[2] and Antonella Bandiera[1]

[1]University of Trieste, Department of Life Sciences, via L. Giorgieri,1, 34127 Trieste, Italy
[2]University of Birmingham, School of Metallurgy and Materials, Biomaterials Research Group, Edgbaston, Birmingham B15 2TT, UK
[*]laura.colominaalfaro@phd.units.it

INTRODUCTION

In the last decades, the transition from conventional synthetic polymers to biomaterials with the potential to better integrate with the biological systems substantially mutated the landscape of tissue engineering and regenerative medicine.

Natural Biopolymers are products of biological systems and fulfil a wide range of essential structural and functional roles. Proteins offer great flexibility due to the significant advances in genetic engineering and biotechnology that opened the way to tailored and customized functional bio-based materials. The thermo-responsive Elastin-like Polypeptides represent a paradigmatic example of this approach since their bio-inspired nature collocate them in-between natural and synthetic compounds of biotic origin, having a regularly repeated structure typical of polymers.

HELP (Human Elastin-like Polypeptide) is the platform developed in our lab and aimed to design and realize innovative biomaterials with advanced functionality [1]. This versatile system can be readily customized by fusing bioactive domains of interest, thus adding new functionality to the final construct. Notably, a simple method for preparing 3D hydrogel matrices based on this recombinant biopolymer has been set up. [2]

To realize innovative biomaterials with antimicrobial properties, we present the new HELP-based construct inspired by the antimicrobial peptide human β-defensin 1. This fusion protein represents a prototype model as a starting point to develop biomimetic components for 3D-printed "smart" implants fabrication.

EXPERIMENTAL METHODS

The synthetic gene of the HELP biopolymer was fused with the coding sequence 47 aa-domain corresponding to the 22-68 region of the hBD1 pro-protein (NM_005218.4) exploiting the unique DraIII / HindIII sites in the expression vector for the in-frame fusion at the C-terminus. The final construct was verified by sequencing and the recombinant product was expressed in the C3037 *E. coli* strain. Purification was carried out exploiting the inverse phase transition properties of the HELP domain. The recombinant fusion protein was analyzed by SDS-PAGE. 4% solution of HhBD1 in 10mM Tris/HCl and pH=8 was treated with microbial transglutaminase to a final concentration of 2µg/µL. The cross-linking was carried out for 30 min at RT.

RESULTS AND DISCUSSION

A biopolymer named HhBD1 (HELP-hBD1) carrying the HBD1 pro-peptide fused with the HELP domain was successfully designed and produced in our lab.

This biopolymer has two unique proteolytic sites for the specific Glu-C and Asp-N endoproteases, to cleave and release both the pro-peptide and the mature peptide (Fig.1).

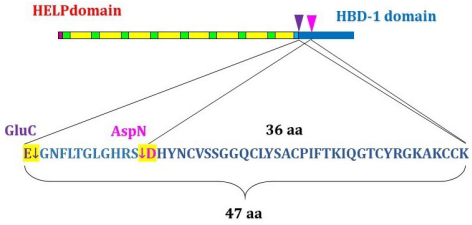

The hydrogel matrices were successfully obtained by the enzymatic crosslinking of HhBD1, indicating that the presence of the bioactive domain does not affect this process. As already demonstrated for the HELP matrix, the HELP domain is expected to be degraded by the elastolytic activity [1]. Thus, we expect that in environments where the inflammatory condition occurs or in the presence of microorganisms that secrete elastolytic enzymes such as *P. aeruginosa,* the bioactive peptides will be released.

CONCLUSION

Our new fusion protein represents an example for the design of novel components and biomaterials that have the potential to release antimicrobial activity. We will exploit the specific endoproteolytic sites to trigger the release of the bioactive domain. The antimicrobial activity towards bacterial strains will be tested for the *in vitro* validation of our model.

REFERENCES

[1] Bandiera, A., et al., (2021) *Biotechnol Appl Biochem.* Aug 25. doi: 10.1002/bab.2245.

[2] Bandiera, A. (2011) *Enzyme Microb. Tech.,* **49**, 347-352.

ACKNOWLEDGMENTS

This research is funded by the Horizon 2020 Innovative Training Network AIMed under the Marie Skłodowska-Curie grant agreement No 861138.

Utility of chitin and chitosan derived from Tenebrio Molitor for biomedical applications

Neda Khatami[1,2*], Pablo Martín-Abad[3], Sandra Camarero-Espinosa[2,4], Ander Abarrategi[1,4]

[1]Center for Cooperative Research in Biomaterial (CIC biomaGUNE), Donostia-San Sebastian, Spain
[2]POLYMAT, University of the Basque Country UPV/EHU, San Sebastián, Gipuzkoa, Spain
[3]University of the Basque Country UPV/EHU, Bilbao, Spain
[4]Ikerbasque, Basque Foundation for Science, Bilbao, Spain
*nkhatami@cicbiomagune.es

INTRODUCTION

Chitin is a natural cationic polysaccharide found in fungus cell walls, crustacean shells, and insect cuticle. Chitosan is a fiber-like polymer derived from chitin and shares some characteristics with various GAGs and hyaluronic acid present in bone and cartilage (1). Both chitin and chitosan are biomolecules of a great potential, possessing versatile biological activities (2).

In our previous study, it was depicted that chitosan derived from the crab source is not batch-to-batch reproducible (3). In this study, we hypothesized that chitin and chitosan from insect origin is highly reproducible and stable and can be used for biomedical applications. In that regard, we aimed to obtain these two polysaccharides from the insect source (Tenebrio Molitor) using different methods and prove they are beneficial for biomedical context.

EXPERIMENTAL METHODS

Chitin powder was derived from Tenebrio Molitor in different developmental stages and using chemical and physical methods. Sodium Hydroxide solution and ultrasound equipment were employed as chemical and physical approaches subsequently. Various times and temperatures were applied in order to achieve an optimal condition for chitin extraction. Resulted chitin powder was characterized using H-NMR, FT-IR, ash content and water content analyses. In the next step, chitosan was obtained by deacetylation of chitin exploiting Sodium Hydroxide. Chitosan deacetylation degree and molecular weight were analysed by H-NMR and a rheometer subsequently.

Obtained chitosan was used to form films incorporated with cells. Afterwards, *in vitro* biocompatibility and immunomodulatory properties of the prepared films were tested.

RESULTS AND DISCUSSION

Chitin and chitosan derived from various sources of Tenebrio Molitor were characterized in terms of their chemical and physical properties and cell-biomaterial interactions. Obtained samples had similar characteristics compared to the reference materials from crab source indicating that Tenebrio Molitor can be a potential source for chitin and chitosan extraction. Cells exhibited satisfactory cell viability and attachment on chitosan films. Moreover, mild immune response was induced by these samples.

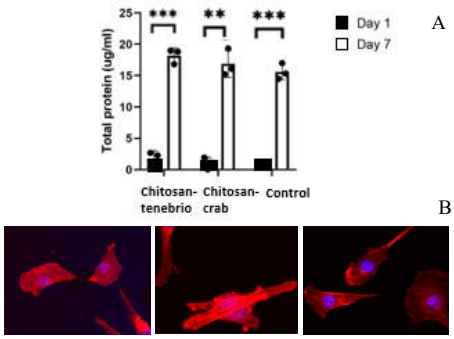

Figure 1: C2C12 Cells on Tenebrio Molitor-derived chitosan show similar behaviour to the control. *Images exhibit* ***A)*** *Bradford assay (for 7 days) and* ***B)*** *Actin and DAPI staining (day 1) of C2C12 cell line seeded on chitosan films derived from Tenebrio Molitor and crab.*

CONCLUSION

Chitin and chitosan were derived from Tenebrio Molitor insect in different developmental stages using different methods. Chitin and chitosan extracted from the insect had comparable properties to the ones from crab. Cell culture studies revealed the suitability of insect-derived polysaccharides as cell culture substrates. Further analyses are required to prove that Tenebrio Molitor is a reproducible source for chitin and chitosan extraction.

REFERENCES

1. Abarrategi A, Civantos A, Ramos V, Sanz Casado JV, López-Lacomba JLJB. Chitosan film as rhBMP2 carrier: delivery properties for bone tissue application. 2008;9(2):711-8.
2. Tharanathan RN, Kittur FS. Chitin—the undisputed biomolecule of great potential. 2003.
3. Abarrategi A, López-Morales Y, Ramos V, Civantos A, López-Durán L, Marco F, et al. Chitosan scaffolds for osteochondral tissue regeneration. 2010;95(4):1132-41.

ACKNOWLEDGMENTS

Grant RTI2018-101708-A-I00 and RYC2018-025502-I funded by MCIN/AEI/10.13039/501100011033, by ERDF A way of making Europe and by ESF Investing in your future. Grant MDM-2017-0720 funded by the Spanish State Research Agency. Grant KK-2019/00093 funded by Basque Government. Grant CICBMG_PhD_03_2021 funded by CICbiomaGUNE and Polymat.

Suitability of octacalcium phosphate-carboxylates in mineralised collagen film production

Katrina J. Staunton[1*], Thomas Kress[2], Melinda J. Duer[2], Ruth E Cameron[1], Serena M Best[1]
[1]Department of Materials Science and Metallurgy, University of Cambridge, Cambridge, UK
[2]Department of Chemistry, University of Cambridge, Cambridge, UK
[*] kjs84@cam.ac.uk

INTRODUCTION

Bone is an inorganic-organic composite material with a hierarchical structure built from mineralised collagen fibrils. A recent bone mineral model proposes carboxylates bridge between the apatitic core of bone mineral platelets, residing in the disordered surface region best described by an octacalcium phosphate (OCP) phase[1]. Novel collagen film production using electrophoretic deposition (EPD)[2], has inspired research into the techniques applicability in producing bone implants. Numerous OCP-carboxylates have successfully been synthesised providing an exciting variety of mineral characteristics that can be selected and adjusted according to the desired properties. The relative stability and ease of handling of the OCP-carboxylates require testing to determine their suitability for mineralised collagen film production.

EXPERIMENTAL METHODS

Synthesis of OCP-CIT: Citric acid solution (250 mM, 55 ml) was maintained at 37 ˚C and pH adjusted to 5.52 using 50% NaOH solution. α-tricalcium phosphate (TCP, 0.8361 g) was added and pH adjusted to 6.50. The suspension was stirred at 200 rpm for 48 hrs.

Synthesis of OCP-LAC: α-TCP (1.28 g) was added to a sodium L-lactate solution (247 mM, 160 ml) maintained at 37 ˚C while stirring. pH was adjusted to 6.50 and maintained using 1 M HCl. The suspension was stirred at 200 rpm for 24 hrs.

Dialysis: Mineral suspensions were either dried or dialysed against DI water or lactate buffer at pH 6.50.

Solid-state Nuclear Magnetic Resonance (NMR): NMR was performed on Bruker 400 MHz proton frequency (9.4 T) Avance spectrometer. $^{13}C\{^{31}P\}$ Rotational Echo DOuble Resonance (REDOR) experiments were performed at magic angle spinning rate of 10 kHz at room temperature after referencing: ^{13}C to glycine at 53.1 ppm and ^{31}P to hydroxyapatite at 2.8 ppm. ^{1}H-^{31}P cross polarisation (CP) used π/2 pulse length 2.50 μs; CP contact time 2000 μs, 70 kHz recycle delay 2.5 s. SPINAL64 decoupling was used during signal acquisition at ^{1}H 100 kHz. REDOR spectra were obtained using a train of ^{31}P 6.5 μs π pulses, 50 μs period, dephasing times of 2.9 ms (OCP-CIT) and 4.9 ms (OCP-LAC). The ^{31}P pulse power was set to zero in the reference spectra.

Microanalysis: CHN combustion and ICP-OES analysis were performed by the Microanalysis service, Department of Chemistry, University of Cambridge.

RESULTS AND DISCUSSION

The lower intensity of the REDOR spectra compared to the reference, alongside their broad peaks confirm citrate and lactate incorporation into the OCP structure (Fig. 1). Microanalysis reveals the number of phosphorous atoms per OCP unit cell is ~11 for OCP-CIT and ~12 for OCP-LAC (Table 1) showing the citrate molecule substitutes for a phosphate ion whereas the smaller lactate ion resides in OCPs hydrated layer. While the carbon content in OCP-CIT halves after dialysis, the REDOR experiment proves the remaining citrate is situated within the structure. However, the dialysed OCP-LAC samples show a significant drop in carbon content, even whilst dialysing against relatively high lactate concentrations (10-60% of synthesis) and is confirmed by the low signal to noise ratio in the REDOR experiment. Citrate, a chelating agent, has a potent affinity for calcium. Comparatively, as a monocarboxylate, lactate has a weaker affinity to calcium and is therefore more easily lost from the structure.

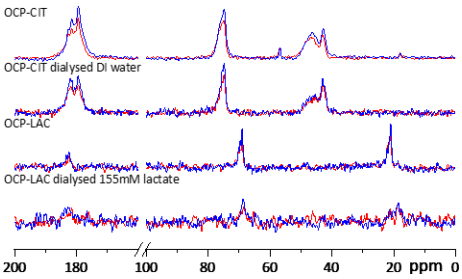

Fig. 1: $^{13}C\{^{31}P\}$ REDOR spectra (red) and reference spectra (blue) of OCP-carboxylates.

Compound	Dialysed against	No. of C/ unit cell	No. of P/ unit cell
OCP-CIT	Before dialysis	8.7	10.9
	DI water	3.7	10.6
OCP-LAC	Before dialysis	2	12.2
	155 mM lactate	1.3	12.2
	77 mM lactate	0.9	12.2
	25 mM lactate	0.6	12.2

Table 1: Microanalysis of OCP-carboxylates, calculated assuming 16 Ca per unit cell.

CONCLUSION

To create mineralised collagen films using a novel EPD technique, first the stability of OCP-carboxylates throughout a dialysis procedure needed to be established. Citrate remains incorporated within the OCP structure, making OCP-CIT the mineral of choice in the production of mineralised collagen films.

REFERENCES

1. Duer, M. J. *J. Magn. Reson.* **2015**, 253, 98–110.
2. Barrett, D. J., et al. *Biofabrication* **2019**, 11 (4), 045017.

ACKNOWLEDGMENTS

Funding by EPSRC Doctoral Training Programme (KJS).

Novel Pulsed Electrodeposition Method for Hybrid Conductive Soft Hydrogel based on PEDOT/Alginate for Versatile Drug Delivery

Aruã Clayton Da Silva[1], Thomas Paterson[1] and Ivan R. Minev[1]

[1]Implantable Bioelectronics Laboratory. Department of Automatic Control and Systems Engineering, Faculty of Engineering, University of Sheffield, Sheffield, UK
*a.dasilva@sheffield.ac.uk

INTRODUCTION

Conductive soft hydrogels offer a promising approach to either delivery specific molecules *in locu* or probe electrical signals from living tissue, being greatly important in bioelectronics applications[1].
In a previous work, our research group proposed a hybrid PEDOT/Alginate conductive soft hydrogel. However, using step potential to obtain the hybrid was very limited due to diffusional limitation at the electrode interface[2].
Herein, we are showing a novel electrodeposition pulsed method to 1) enhance the conductivity of the hydrogel and 2) homogeneously obtain the hydrogel layer. The hybrid conductive soft hydrogel was loaded with model drug for passive and electroactive release studies.

EXPERIMENTAL METHODS

Herein we developed a pulsed electrodeposition method to obtain an enhanced conductivity in the hybrid hydrogel. For this, we prepared the deposition solution containing 1% alginate (w/w), 0.5% calcium carbonate (w/w), 70 mM sodium dodecylsulfate (SDS) and 50 mM 3,4-ethylenedioxythiophene (EDOT). Using a gold wire as electrode, we applied +1.4 V (vs. Ag/AgCl/KCl 3M) for 500 miliseconds, followed by either 10 seconds resting at open circuit potential (OCP) or at 0.0V (vs. Ag/AgCl/KCl 3M). We used the traditional electrodeposition method of applying step potential for a time and just EDOT without alginate for comparison. When the electric potential is applied, it promotes the electrodeposition reaction of EDOT, which triggers other two chemical steps to obtain the alginate hydrogel. This mechanism is known as electrochemical-chemical-chemical (ECC) (**Figure 1**). We characterized its electrical properties by using cyclic voltammetry and electrochemical impedance spectroscopy. For the electroactive release investigation, we added 1 mg/mL of Fluorescein (model molecule for drug delivery) to the solution and encapsulated together with the hydrogel formation.

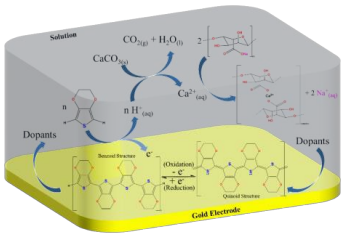

Figure 1. Schematic representation of the ECC mechanism for electrodeposition of PEDOT/Alginate hydrogel.

RESULTS AND DISCUSSION

The pulsed method enabled fine control of hydrogel growth kinetics. From 1 to 120 polymerization pulses it follows order zero ($t_{1/2}$ = 22 pulses), while after 120 pulses it follows first order ($t_{1/2}$ = 252 pulses) growth kinetics. The hydrogel produced using OCP pulsed protocol generated the most electroactive hydrogel. It presented lower total impedance and higher charge storage capacitance. Additionally, we were able to control the crosslinking of the alginate layer to promote either a dense (1.5-3% calcium carbonate) or a loose (0.5-1% calcium carbonate) hydrogel. Based on this step, the alginate layer can be disassembled within 2-3 hours (loose) or resist decomposition for more than 36 hours (dense) in PBS solution. The conductive soft hydrogel can be loaded with Fluorescein for releasing study (**Fig. 2**). In the passive release, we used the conductive property of the hydrogel as a sensor, monitoring the capacitance and correlating it to the passive release of desired molecule, with excellent correlation between the capacitance and the amount of molecule quantified by fluorescence. Furthermore, we demonstrate the electroactive release is fully controlled by electric potential. Full release (100%) when -1.2V and full holding (0%) when +0.8V was applied for 40 minutes. Additionally, intermediate gradient release was achieved by applying pulses at -1.2V was applied for 3, 8 and 30 seconds.

Figure 2. Picture of the PEDOT/Alginate hydrogel loaded with Fluorescein.

CONCLUSION

In the current work we described a novel pulsed method of obtaining a hybrid conductive and soft hydrogel of PEDOT/Alginate.

REFERENCES

1. Yuk, H. *et al*., Chem. Soc. Rev. 48, 1642, 2019.
2. Da Silva, A.C. *et al*., Nat. Comm. In Press (DOI: 10.1038/s41467-022-29037-6).

ACKNOWLEDGMENTS

The authors would like to thank funding from ERC Starting Grant: IntegraBrain (804005).

Cytotoxicity of nitric oxide releasing Pluronic F-127 hydrogel containing silica nanoparticles loaded with cisplatin towards breast cancer cell

Amedea Barozzi Seabra*, Bianca de Melo Santana, Joana Claudio Pieretti, Rafael Nunes Gomes, Giselle Cerchiaro

Center for Natural and Human Sciences, Federal University of ABC, Santo André, Brazil
* amedea.seabra@ufabc.edu.br

INTRODUCTION

Several papers describe promising uses of nitric oxide (NO) in cancer therapies, mainly because NO actuates as a chemotherapeutic sensitizer.[1] However, its action is limited by time, concentration and application site. Due to its short half-life (0.5 s), NO donors with highest stability are used to carry and deliver NO, such as S-nitrosothiols (RSNOs). RSNOs have been incorporated into polymer matrices to enhance the sustained NO release.[2] Furthermore, to improve cancer-targeting therapies, hyaluronic acid (HA) has been used due to its strong affinity to the CD44 glycoprotein, overexpressed in cancer cells membrane.[3] In addition, silica nanoparticles (SiO_2 NPs) have been shown to be an excellent drug carrier, due to their porosity that allows the incorporation of chemotherapeutics, such as cisplatin (SiO_2@CisPt NPs).[4] Thus, the aim of this study was to synthesize, characterize and evaluate the cytotoxicity of NO-releasing Pluronic F-127 hydrogel containing HA and SiO_2@CisPt NPs against breast cancer cells. We hypothesize that the combination of NO and cisplatin in a biomaterial would enhance its toxicity against cancer cells

EXPERIMENTAL METHODS

SiO_2@CisPt NPs: SiO_2 NPs were prepared by sol-gel method.[5] The loading with cisplatin was made as previously reported,[3,5] dispersing 45 mg of SiO_2 NPs and mixing with cisplatin (1:1) for 24 h.

GSNO (RSNO): GSH (1.23 mol/L) was dissolved into HCl (1 mol/L), followed by the addition of an equimolar amount of $NaNO_2$. The nitrosation reaction was carried out for 20 min, in an ice bath, under magnetic stirring and in the dark, leading to the formation of a pink precipitate of GSNO.[6]

Pluronic F-127 hydrogels: All hydrogels were prepared with 25% (w/v) Pluronic F-127 and 0.05% (w/v) of hyaluronic acid (HA).[6] Briefly, 1.25 g of solid Pluronic F-127 (PL) was added to 5.0 mL of PBS, kept at 10 °C overnight, leading to the complete PL dissolution. Then, 2.5 mg of HA was added into PL solution, as well as GSNO (25 mM) and/or silica NPs (0.5 % w/v), in an ice bath, followed by gentle homogenization.

Characterization of materials: Several techniques were used to evaluate the morphology and physical-chemistry of the prepared materials, such as X-ray diffraction (XRD), Dynamic Light Scattering (DLS), Transmission Electron Microscopy (TEM), and Kinetics of NO release from GSNO-containing PL.

In vitro cytotoxicity: The cytotoxicity of the biomaterials was evaluated by MTT assay, using epithelial breast cancer adenocarcinoma MDA-MB-231 cell line. Statistical difference between groups was determinate using Tukey's multiple comparisons test.

RESULTS AND DISCUSSION

SiO_2@CisPt showed an average hydrodynamic size of 318 ± 2.6 nm, polydispersity index of 0.353 ± 0.04 and a zeta potential of -20.2 ± 0.75 mV, indicating stability in aqueous suspension. XRD reveled an amorphous structure for silica NPs and TEM showed that these NPs has spherical shape morphology and are well-distributed, with an average size in solid-state of 158 ± 20 nm. The kinetics of NO release from hydrogel matrix revealed a spontaneous and sustained release of NO at millimolar range for at least 24 h at room temperature. The cytotoxicity of the hydrogel was evaluated against MDA-MB-231, which are highly aggressive, invasive and poorly differentiated, with different groups and concentrations. Results showed a concentration-dependent cytotoxicity (100 to 200 µg/mL in terms of NPs). Interestingly, the combination of GSNO and SiO_2@CisPt halved cell viability when compared to treatments without these compounds over 100 µg/mL, decreasing cell viability by 20% more than others. At 200 µg/mL, this combination led to a critical cell viability of 30%, indicating a synergistic effect between GSNO and SiO_2@CisPt NPs.

CONCLUSION

The hydrogel was prepared successfully, such as its components (NO donor – GSNO and SiO_2@CisPt NPs). The combination between these compounds led to a formation of a biomaterial with a great antitumor action, since it was found to exist a synergistic effect between GSNO and SiO_2@CisPt NPs, highlighting the potential uses of this drug delivery system for anticancer therapies.

REFERENCES

1. Seabra & Duran, Med. Chem. 17:216–223, 2016
2. Seabra *et al.*, British J. Dermatology, 151:977–983, 2004
3. Deng *et al.*, J. Biomaterials, 35:4333-4344, 2014
4. Jeelani *et al.,* Silicon, 1337–1354, 2019
5. Cheng *et al.*, J. Mater. Chem. B, 1–25, 2019.
6. Pelegrino *et al.,* Polymers, 10:452–471 2018

ACKNOWLEDGMENTS The authors would like to thank the Fundação de Amparo À Pesquisa do Estado de São Paulo (Fapesp) (Processes 2020/08566-7; 2018/08194-2), CNPq (404815/2018-9, 313117/2019-5), and Capes.

Dynamic Hydrogel Bioinks for Tissue Regenerative Applications

Tony Feliciano[1*], M.B. Baker[1]
Underline the presenting author's name.

[1]MERLN, Maastricht University, Maastricht, NL
*a.feliciano@maastrichtuniversity.nl

INTRODUCTION

Efforts to engineer tissues and advance regenerative medicine now rely on the recapitulation of both static and dynamic mechanical properties. Via mechanotransduction, natural extracellular matrix (ECM), as demonstrated by its own time-dependent mechanical behavior, can affect cell adhesion, migration, differentiation and gene expression.[1] Similar dynamics are difficult to engineer as most chemisties rely on degradation to enhance cellular takeover. Our 3D Microenviornment hydrogel platform was engineered using reversible dynamic chemistry that can be tuned to match a tissue's microeviroment to improve cell behavior and even prevent fibrotic tissue formation in organoid development.[2,3] Further, the reversibility and viscoelastic flow property enables injection through a needle, a requirement for bioprinting and cell injection applications.

EXPERIMENTAL METHODS

Supramolecular and dynamic/covalent polymers were synthesized and characterized by H-NMR and GPC. Mechanical testing of hydrogels were performed under shear rheology after mixing with variable crosslinkers of different equilibria. Stiffness (G') and stress relaxation property were tuned to meet stiff/soft and non-relaxing/relaxing requirements. Kidney organoids were produced from hiPSCs and encapsulated in these hydrogels by pipetting mixture over a Transwell membrane at day 7+14 of culture. The organoids were cryo-sectioned and immunohistochemistry performed.

RESULTS AND DISCUSSION

Hydrogels made via supramolecular and dynamic/covalent interaction proved to be self-healing, injectable, and have stiffness and stress relaxation properties in physiologically relevant regimes. Organoids cultured in tuned stiffer hydrogels (20kPa) expressed more aSMA than in soft hydrogels (0.1kPa) and fast relaxing hydrogels further reduced EMT markers.

CONCLUSION

Hydrogel materials comprised of supramolecular or dynamic/covalent chemistry not only capture the mechanics of a 3D cell microenviornment but also provide a medium whereby cells can be protected through organoid expansion, injection and delivery applications. These properties also influence cell, aggregate, and organoid behaviors that will be crucial to the development of regenerated tissue.

REFERENCES

1. Guimarães C.F., Gasperini L., Marques A.P., Reis R.L., *Nat. Rev. Mater.,* 5(5), 351-370, 2020

2. Ruiter F.A., Morgan F.L., Roumans N., Schumacher A., Slaats G.G., Moroni L., LaPointe V.L., Baker M.B., *bioRxiv*., 2021

3. Hafeez S., Ooi H.W., Morgan F.L., Mota C., Dettin M., Van Blitterswijk C., Moroni L., Baker M.B., *Gels*, 4(4):85, 2018

ACKNOWLEDGMENTS

AJF and MBB would like to graciously thank NWO's Take-Off grant for providing financial support to this project.

Assessing Jellyfish Collagen Hydrogel for supporting Human Osteoblasts

Swastina Nath Varma[1*], Maryam Tamaddon[1], Andrew Mearns Spragg[2], Pascale V Guillot[3], Chaozong Lui[1]

[1] Institute of Orthopaedic and Musculoskeletal Science, University College London, Royal National Orthopaedic Hospital, Stanmore, London HA7 4LP, UK
[2] Jellagen Pty Ltd, Capital Business Park, G6, Cardiff CF3 2PY, UK
[3] EGA Institute for Womens Health, University College London, UCL Great Ormond Street Institute of Child Health, 30 Guilford Street, London WC1N 1EH UK
[*] t.varma@ucl.ac.uk

INTRODUCTION

Large bone defects can be caused by trauma, disease, surgery or tumour resection where the bone is unable to heal as normal due to the size of the defect or fracture [1-3]. To understand and resolve this clinical problem, regenerative medicine approaches, particularly tissue engineering and the use of biomaterial, have been widely studied and used. A more recent type of collagen that has emerged is jellyfish collagen (Jellagen), which is collagen type 0, non-cytotoxic and biocompatible [4]. In this project, we are investigating whether a jellyfish collagen hydrogel can provide a natural 3D microenvironment for bone formation.

EXPERIMENTAL METHODS

Established quantitative and qualitative methods such as PrestoBlue™ Cell Viability Reagent, Live/Dead ® Viability/Cytotoxicity Kit, DNA quantification, histology and immunostaining have been used to determine whether a jellyfish collagen hydrogel supports human osteoblast viability, proliferation and migration.

RESULTS AND DISCUSSION

The viability test showed that the jellyfish collagen hydrogels maintain cell growth throughout the time-points. Cell proliferation was seen through the Live/Dead images. This was also seen in the H&E staining in addition to the morphology and distribution of osteoblasts across time-points (Figure 1). The immunostaining of collagen 1 (COL1) showed the osteoblasts within the hydrogel at Day 21 (Figure 2).

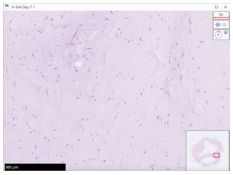

Figure 1. H& E staining of cells within hydrogel at Day 7. The osteoblasts retain their morphology and are even throughout the gel.

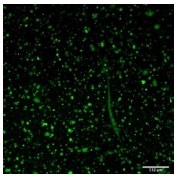

Figure 2. Immunostaining (COL1) of cells within hydrogel at Day 21.

CONCLUSION

The overall PrestoBlue results showed that the hydrogel supported cell viability and to further support this, the Live/Dead images were strong evidence to show that osteoblasts were viable and proliferating both within and on top of the hydrogel. Moreover, it was evident that osteoblasts seeded within the hydrogel were distributed throughout the hydrogel across the 7 day period. This is a promising result that suggests the cells can and will be able to proliferate long-term in a 3D microenvironment. The early experiments of this project have so far shown that a jellyfish collagen hydrogel can support human osteoblasts and encourage their growth over 7 days. Some results have shown that cells are viable within the hydrogel at 21 days. This is a good indication that cells can be cultured for longer. The next step would be to assess bone formation in the hydrogel up to 28 days.

REFERENCES

1. Vidal, L., et al., *Regeneration of segmental defects in metatarsus of sheep with vascularized and customized 3D-printed calcium phosphate scaffolds.* Sci Rep, 2020. 10(1): p. 7068.
2. Winkler, T., et al., *A review of biomaterials in bone defect healing, remaining shortcomings and future opportunities for bone tissue engineering: The unsolved challenge.* Bone Joint Res, 2018. **7**(3): p. 232-243.
3. Majidinia, M., A. Sadeghpour, and B. Yousefi, *The roles of signaling pathways in bone repair and regeneration.* J Cell Physiol, 2018. **233**(4): p. 2937-2948.
4. https://jellagen.co.uk/ Jellagen website

ACKNOWLEDGMENTS

This work was supported by Engineering and Physical Science Research Council (EPSRC) via DTP case programme (Grant No. EP/T517793/1).

Keywords: (3-5 keywords)

collagen, hydrogel, microenvironment, viability, osteoblasts

Development of Functional Composite Hydrogels for Bone Regeneration

Anna Rubina[1,2 *], Inta Kreicberga[1,2], Artemijs Sceglovs[1,2], Kristine Salma-Ancane[1,2]

[1]*Rudolfs Cimdins Riga Biomaterials Innovations and Development Centre of RTU, Institute of General Chemical Engineering, Riga Technical University, Riga, Latvia*
[2]*Baltic Biomaterials Centre of Excellence, Headquarters at Riga Technical University, Riga, Latvia*
[*] anna.rubina@rtu.lv

INTRODUCTION

Bone grafting is the second most commonly used surgical procedure in clinic right after blood transfusion[1]. Traditional treatment for bone regeneration such as autografts has been widely used, but it brings some serious disadvantages, such as infection, pain and the need for additional surgery. Thus, there is a critical need for new therapeutic strategies to repair bone damage caused by traumatic injury or osteoporotic fracture. An ideal bone grafting material should be bioactive, injectable, antibacterial, provides appropriate mechanical properties and act as a drug delivery system[2]. The aim of this study was to develop and investigate bioactive composite hydrogels based on natural biopolymers - hyaluronic acid (HA) and ε-polylysine (ε-PL), as well as strontium ranelate loaded nanosized hydroxyapatite (SrRAN-nHAp).

EXPERIMENTAL METHODS

Bioactive composite hydrogel systems were synthesized by chemical crosslinking using 1-ethyl-3-(3-dimethylaminopropyl) carbodiimide (EDC) and N-hydroxysuccinimide (NHS) crosslinking agents (with ε-PL to HA mass ratio of 50:50 wt%, with EDC to NHS molar ratio of 1:1) (method adapted from [3,4]). SrRAN-nHAp was synthesized by wet chemical precipitation (with 10 wt% Sr) and incorporated into composite hydrogels systems. The molecular structure, phase composition, microstructure, morphology, drug release kinetics of the fabricated composite hydrogels with SrRAN-nHAp to ε-PL-HA mass ratios of 60:40 wt%, 50:50 wt%, 40:60 wt% and 70:30 wt% were investigated. Drug release profile from SrRAN-nHAp and SrRAN-nHAp/ε-PL-HA composite hydrogels was evaluated in PBS at 37ºC for up to 30 days.

RESULTS AND DISCUSSION

The XRD patterns of the lyophilized composite hydrogels revealed existence of hydroxyapatite crystalline phase. SEM micrographs of the lyophilized composite hydrogels revealed homogenous and porous structure. μCT images showed homogenous distribution of SrRan-nHAp powder particles into hydrogel matrix. It was found that cumulative SrRAN release from SrRAN-nHAp was ~ 87% burst release in up to 2 h. In the first 30 days the SrRAN-nHAp/ε-PL-HA composite hydrogels with 70:30 wt% showed the highest release of drug - 36% and composite hydrogels with 40:60 wt% showed the least release of drug - 27%. The composite hydrogel SrRAN-nHAp/ε-PL-HA 40:60 wt% showed a higher swelling degree - up to 525% - than the other composite hydrogels (up to 400%).

CONCLUSION

The developed bioactive composite hydrogels based on ε-PL, HA and SrRAN-nHAp showed promising functionalities for bone regeneration application, such as sustained drug release profile, high porosity and swelling degree, and homogenous SrRAN-nHAp distribution into hydrogel matrix. Further studies on antibacterial activity and cytotoxicity, as well as injectability and rheological properties are required to determine the full biomedical potential of the developed biomaterials.

REFERENCES

1. Wang W., Yeung K. W. K.,"Bone grafts and biometerials substitutes for bone defect repair: A review," *Bioact. Mater.,* vol. 2, issue 4, pp. 224 – 247, 2017
2. Alonso J. M. *et al.,* "Injectable Hydrogels: From laboratory to industrialization," *Polymers*, vol. 13, p. 650, 2021
3. Salma-Ancane K. *et al*., "Effect of crosslinking strategy on the biological, antibacterial and physiochemical performance of hyaluronic acid and ε-polylysine based hydrogels," *Int. J. Biol. Macromol.,* vol. 208, pp. 995 – 1008, 2022
4. Sceglovs A., Salma-Ancane, K., "Novel Hydrogels and Composite Hydrogels Based on Ɛ-Polylysine, Hyaluronic Acid, and Hydroxyapatite," *Key Eng. Mater.*, vol. 850, pp. 242–248, 2020

ACKNOWLEDGMENTS

The authors acknowledge financial support from the Latvian Council of Science research project No. lzp-2020/1-0072 "Injectable bioactive biocomposites for osteoporotic bone tissue regeneration (inBioBone)".
The authors acknowledge financial support from the European Union's Horizon 2020 research and innovation programme under the grant agreement No 952347.

Gelatin-alginate hydrogel enriched by dialdehyde starch or squaric acid as a new bio-ink

Joanna Skopinska-Wisniewska[1*], Marta Tuszynska[2], Łukasz Kazmierski[2], Anna Bajek[2]

[1] Faculty of Chemistry, Nicolaus Copernicus University in Torun, Poland
[2] Faculty of Medicine, Department of Tissue Engineering, The Ludwik Rydygier Collegium Medicum in Bydgoszcz, Nicolaus Copernicus University in Torun, Poland
[*] joanna@umk.pl

INTRODUCTION

Bioprinting is currently an intensively developing method of creating scaffolds for tissue engineering. Solutions of appropriately selected polymers combined with cells are used as bioinks, and the obtained printouts are usually in the form of hydrogels. Mechanical properties, swelling capacity, or susceptibility to degradation of the final constructs can be modified by proper cross-linking of the material[1-3]. However, the addition of cross-linking agents to polymer solution may also modify the properties of the polymer solution. The viscosity of the bio-ink is one of the crucial parameters for the printing process. It determines the flow properties of the fluid and is crucial for optimizing bio-ink extrusion conditions.

The aim of the research was to investigate the influence of the addition of two cross-linking agents, macromolecular dialdehyde starch (DAS) and small-molecular squaric acid (SQ), on the viscosity of gelatin - sodium alginate solution in water.

EXPERIMENTAL METHODS

The solution containing 6% gelatin (G) and 2% sodium alginate (A) was prepared in water. Then 1% (w/w of gelatin) cross-linking agents (starch dialdehyde – DAS1 or squaric acid – SQ1) were added to the mixtures. The viscosity of the solutions was tested using DV-1 Viscosimeter (Brookfield Ametec) at the temperature of 40°C, against spindle 6, shear rate 6 - 60 RPM. Then the hydrogels were cross-linked with 1% $CaCl_2$ solution and the elongation test with the speed of 10 mm/min using Shimadzu EZ-Test_SX was made.

RESULTS AND DISCUSSION

Our research showed that the SQ addition causes viscosity increase, while the use of DAS lowers the viscosity of the gelatin (6%) and sodium alginate (2%) solutions in water (Fig.1.). Moreover, the viscosity of G6_A2 and SQ1 slightly decreases with increase of shear rate, while the parameters of DAS1 solution remain almost unchanged. It was also observed that cross-linking with squaric acid or dialdehyde starch improves the mechanical strength of gelatin-alginate hydrogels. However, these compounds have a different effect on the stiffness of the final hydrogel. Cross-linking with SQ causes significant stiffening of the material, while the use of DAS increases the flexibility of the hydrogel - higher elongation at breaking point and lower Young's modulus are observed.

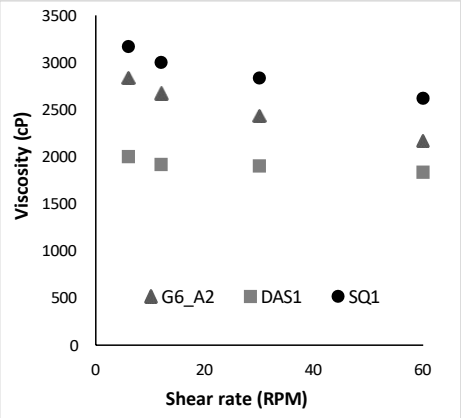

Fig.1. The viscosity of gelatin (6%) and sodium alginate (2%) solutions (G6_A2), with the addition of 1% DAS or SQ in relation to shear rate.

CONCLUSION

Our research indicates that stiffness of the final hydrogel may be related to viscosity of the polymer solution from which it is obtained. Moreover, although both reagents (DAS and SQ) cause the formation of cross-links between the gelatin chains, the size of the cross-linking agent influences the rheological and mechanical properties of the systems. All the tested solutions are suitable for bioprinting and lead to obtaining hydrogels with good mechanical parameters.

REFERENCES

1. Yilmaz B. *et al.*, Bioprinting, 23:e00148, 2021
2. Sanchez E.M. *et al.*, Front.Bioeng.Biotechnol. 8:776, 2020
3. Hu W. *et al.*, Biomat. Sci. 7:843, 2019

ACKNOWLEDGMENTS

The authors would like to thank the National Centre for Research and Development (NCBiR, Poland, Grant no: TECHMATSTRATEG2/407770/2/NCBR/2020) for providing financial support to this project.

Hydrogel properties applied in contact lenses

Barbara Farias-Mancilla[1,2], Romain Jagu[2], Olivier Sandre[1], Simon Harrisson[1]

[1]LCPO UMR5629, Université Bordeaux/ CNRS/ Ecole Nationale Supérieure de Chimie, de Biologie & de Physique 16 Avenue Pey-Berland, 33607 Pessac Cedex, France.

[2]Ophtalmic Compagnie, 33 rue des vanesses 93420 Villepinte, France

barbara.farias_mancilla@bordeaux-inp.fr

Contact lenses are medical devices which help to correct eye defects such as astigmatism, myopia, hypermetropia and presbyopia. They can be classified as daily or extended use[1] and they can be rigid, soft or hybrid, based on their composition.[2] Soft contact lenses are one of the most popular types, due to the comfort that they provide to the user. Soft contact lenses are composed of conventional hydrogels or silicone hydrogels. The main advantage of silicone hydrogels is that they are very hydrophilic which contributes to a higher water content, and also they have a good oxygen permeability.[3,4]

In general contact lenses should provide durability, stability, good vision, comfort and they should be able to allow an appropriate corneal metabolism. All these features depend on the optical (transparency, refractive index), chemical (water content and oxygen permeability)[5] and mechanical (modulus, coefficient of friction)[6] properties of the hydrogel contact lenses. Thus the polymer properties are very important because they will dictate how the contact lens interacts with the ocular surface.[7]

The aim of this research is to develop and study new silicone hydrogel formulations and evaluate the chemical, mechanical and optical properties of contact lenses. Two different crosslinkers were used in the formulations and their main feature is that they possess a high number of hydroxyl groups which contributes to a better hydrophilicity. It is thus expected that these new formulations help to improve the water content of the hydrogel contact lenses. The properties of a commercial formulation of silicone hydrogel contact lenses were also analyzed in order to compare them against our formulations. In all cases, the contact lenses were produced by cast molding at 80 °C.

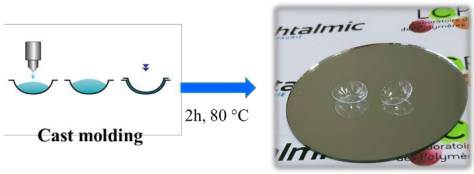

Figure 1. Silicone hydrogel contact lenses production.

REFERENCES

1 S. L. Willis, *et al.*, *Biomaterials*, 2001, **22**, 3261–3272.

2 R. Moreddu, *et al.*, *Adv. Healthc. Mater.*, 2019, **8**, 1900368.

3 B. Pilskalns, *et al.*, *Optom. Vis. Sci.*, 2007, **84**, 334–342.

4 D. Obendorf and M. Wilhelm, *Anal. Chem.*, 2003, **75**, 1374–1381.

5 C. Maldonado-Codina, *Contact lens in practice*, Elsevier, Edinburgh, 2018.

6 T. S. Bhamra and B. J. Tighe, *Contact Lens Anterior Eye*, 2017, 40, 70–81.

7 C. Manicam, *et al.*, *Sci. Rep.*, 2018, **8**, 1–15.

Hydrogels based on chitosan with the addition of copper- and cobalt-doped mesoporous bioactive glasses

Szymon Salagierski[1], Barbara Zagrajczuk[1], Elzbieta Menaszek[3], Michal Dziadek[1,2], Katarzyna Cholewa-Kowalska[1]

[1]Department of Glass Technology and Amorphous Coatings, Faculty of Materials Science and Ceramics, AGH University of Science and Technology, 30 Mickiewicza Av., 30-059 Krakow, Poland;
[2] Faculty of Chemistry, Jagiellonian University, 2 Gronostajowa St., 30-387 Krakow, Poland;
[3] Department of Cytobiology, Faculty of Pharmacy, Jagiellonian University, Collegium Medicum, 9 Medyczna St. 30-688 Krakow, Poland

salagier@agh.edu.pl

INTRODUCTION

Hydrogel materials are extremely attractive for tissue engineering due to their beneficial properties such as high water content, great swelling ability, porous three-dimensional network structure, biocompatibility and the ability to mimic native extracellular matrix with the creation of a cell-friendly environment. Due to their nature, hydrogels are often modified with biologically active components such as antibiotics, drugs or therapeutic ions. In the environment of the human organism, functional components are released from three-dimensional structure and can fulfill their therapeutic tasks. Copper ions Cu^{2+} are responsible for cellular processes such as respiration, neural transmission, and tissue maturation, while cobalt ions Co^{2+} play a key role in forming amino acids, proteins in nerve cells and creating neurotransmitters which are essential for proper functioning of human organism. Moreover both ions can induce the formation of new blood vessels by mimicking hypoxia. The source of ions such as copper or cobalt can be mesoporous bioactive glasses (MBGs) obtained via sol-gel technique. MBGs are well-known for their outstanding surface area and very high porosity, what enhances their bioactivity compared with other bioglasses. Thus, the use of highly porous bioactive glasses with the addition of therapeutic ions (Cu^{2+} and Co^{2+}) as a biologically active ingredient in hydrogel materials can lead to the creation of multifunctional composite materials with properties extremely beneficial for tissue engineering.

MATERIALS

The subject of this study are lyophilized hydrogel materials based on chitosan cross-linked with a functionalized dextran with the addition of mesoporous bioactive glasses. Sol-gel-derived MBGs such as S2 (80 mol% SiO_2, 16 mol% CaO, 4 mol% P_2O_5), copper-doped S2Cu5 (80 mol% SiO_2, 11 mol% CaO, 4 mol% P_2O_5, 5 mol% CuO) and cobalt-doped S2Co5 (80 mol% SiO_2, 11 mol% CaO, 4 mol% P_2O_5, 5 mol% CoO) act as functional components. After preparation, all materials were freeze-dried and in this form subjected to all tests.

EXPERIMENTAL METHODS

The aim of this research was to evaluate the impact of the presence of different MBGs on the physicochemical and biological properties of chitosan-based hydrogels. All materials were incubated in PBS and SBF solutions to test their swelling, degradation and bioactivity. FTIR and SEM/EDS were used to evaluate structural, morphological and chemical changes of materials during incubation in SBF solution. Moreover the ICP-OES analysis was held to access the changes in ion concentration in SBF, while a preliminary *in-vitro* studies of the biological response were carried out on Hs680 fibroblasts.

RESULTS AND DISCUSSION

Obtained results showed that the presence of MBGs doped with copper and cobalt influenced the properties of chitosan-based hydrogel materials. Not only the structural, physicochemical, such as swelling and degradation, but also biological properties tested *in vitro* has changed. Based on the conducted research, it was found that by appropriate selection of mesoporous bioactive glasses it is possible to affect the final properties of hydrogel materials. The obtained materials have promising multifunctional properties and great potential for use in tissue regeneration.

ACKNOWLEDGMENTS

This work was supported by the National Science Centre, Poland, grant nos. 2017/27/B/ST8/00195 (KCK), 2019/32/C/ST5/00386 (MD), and program „Excellence initiative – research university" for the AGH University of Science and Technology.

Characterization of Gelatin Hydrogels for 3D Bioprinting and Tissue Engineering

Ángela Castro María[1], Juan Pedro Fernández,[2] Jennifer Patterson[1]

[1] Biomaterials and Regenerative Medicine and [2] Multifunctional Nanocomposites Groups, IMDEA Materials Institute, Getafe, Madrid, Spain 28906

* angela.castro@imdea.org

INTRODUCTION

3D bioprinting is a biofabrication technique that is booming in biomedical research due to its great potential for generating biocompatible constructs for tissue engineering [1]. Within this area, the use of hydrogels, which are polymeric structures with properties similar to the extracellular matrix, is of great importance, making the development of bioinks based on these materials of great interest. In this work, gelatin and low molecular weight gelatin (LMWG) [2] are chemically crosslinked with genipin, a crosslinker of natural origin, to form the hydrogels while avoiding cytotoxicity problems. The main objective of the present work is to determine whether the LMWG, a material that has not been studied before in this context, presents better processability than the regular gelatin, opening a path to its possible applications in the 3D bioprinting field.

EXPERIMENTAL METHODS

LWMG was prepared as previously described [2]. Hydrogels were prepared from gelatin and LMWG with different polymer concentrations (2 wt %, 6 wt %, and 12 wt %) and the same concentration of crosslinker for all the samples (1 wt%). Swelling and sol-gel fraction studies were carried out, along with mechanical characterization by compression tests in a device of dynamic mechanical analysis (DMA). The morphology of both hydrogel types was characterized by scanning electron microscopy (SEM) using lyophilized and gold-metalized samples. NCTC clone 929, areolar fibroblast (*mus musculus*) from the American Type Culture Collection (ATCC), was used to evaluate the cytotoxicity of the hydrogels, which was measured through a Presto Blue assay. Confocal microscopy of phalloidin and DAPI stained samples and SEM images were used to see the morphology of the cells on the surface of the hydrogels. Finally, a statistical analysis of the data was carried out through an ANOVA test, and a significant difference between the data with a p-value of $p<0.05$ was assumed.

RESULTS AND DISCUSSION

Both hydrogels were successfully made and had good swelling capacities that were inversely proportional to the polymer concentration. The regular gelatin hydrogels had the highest swelling capacity for low polymer concentrations (364 %). In comparison, those of LMWG had a greater swelling capacity for intermediate and high values of polymer concentration (318 % and 254 %, respectively). Regarding the mechanical properties (**Figure 1**), no significant differences between the gelatin and LMWG hydrogels were found for the elastic modulus with values of 0.055±0.009 MPa and 0.080±0.032 MPa in the case of 6wt% and 12wt% LMWG hydrogels and 0.066±0.010 MPa and 0.404±0.102 MPa for 6wt% and 12wt% gelatin hydrogels. On the other hand, preliminary cytocompatibility assays showed high cellular viability at 1 day. Both confocal microscopy and SEM images showed that the cells were able to attach and spread on the surface of the hydrogels (**Figure 1**).

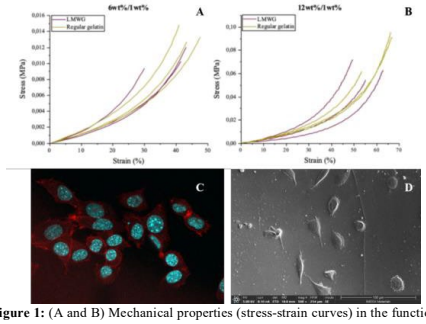

Figure 1: (A and B) Mechanical properties (stress-strain curves) in the function of the polymer concentration (6 wt% and 12 wt%, respectively). (C and D) L929 cells seeded on the gelatin hydrogel surface. (C) Confocal images of DAPI/Phalloidin staining, 60x. (D) SEM images, 500x, scale bar 100 µm.

CONCLUSION

The absence of differences in mechanical properties makes LMWG hydrogels interesting because they are processed at a lower temperature than regular gelatin hydrogels. This makes them easier to handle without adverse effects on the resulting hydrogel properties. The preliminary cytocompatibility tests show good results, but this should be further investigated in the future, including evaluation with tissue-specific cells. Therefore, chemically cross-linked LMWG and gelatin hydrogels prove to be a tool with great potential for possible application as bioinks for 3D bioprinting.

REFERENCES

[1] P. S. Gungor-Ozkerim, I. Inci, Y. S. Zhang, A. Khademhosseini, and M. R. Dokmeci, "Bioinks for 3D bioprinting: an overview," *Biomater. Sci.*, vol. 6, no. 5, pp. 915–946, 2018, DOI: 10.1039/c7bm00765e.

[2] S. Piluso, T. Weigel, A. Lendlein, and A. T. Neffe, "Synthesis and characterization of gelatin fragments obtained by controlled degradation," *Macromol. Symp.*, vol. 309–310, no. 1, pp. 199–204, 2011, DOI: 10.1002/masy.201100054.

ACKNOWLEDGMENTS

Activity financed through the agreement signed between the Community of Madrid (Consejería de Educación, Universidades, Ciencia y Portavocía) and the IMDEA Materials Foundation for the direct award of a grant of 1.937.000,00 euros to finance research activities on SARS-COV 2 and COVID-19 disease financed with REACT-EU resources from the European Regional Development Fund.

Strontium ranelate loaded ε-poly-L-lysine/hyaluronic acid hydrogels

Eleonora Rieksta[1,2], Amanda Vinciune[1], Dagnija Loca[1,2*]

[1]Rudolfs Cimdins Riga Biomaterials Innovations and Development Centre, Institute of General Chemical Engineering, Faculty of Materials Science and Applied Chemistry, Riga Technical University, Riga, Latvia
[2]Baltic Biomaterials Centre of Excellence, Headquarters at Riga Technical University, Riga, Latvia
* dagnija.loca@rtu.lv

INTRODUCTION

Nowadays, osteoporosis is becoming more common, affecting both young and old people. Various medications containing active substances increasing bone density, such as strontium ranelate (SrRan), can be used for the treatment. Hydrogels with anti-inflammatory and antibacterial properties have been a major research topic in the biomedical field for the past decades[1], thus combining antibacterial properties of ε-poly-L-lysine (ε-PL), bioactivity of hyaluronic acid (HA) and anti-osteoporotic properties of SrRan novel injectable polymer hydrogels providing controlled and prolonged drug release at the target site were prepared and analysed[2].

EXPERIMENTAL METHODS

Physically crosslinked HA/ε-PL/SrRan hydrogels (HA:ε-PL ratio of 80:20 wt%, 70:30 wt%, 60:40 wt% and 50:50 wt%) with and without addition of 5 wt% SrRan were prepared and characterized towards the swelling behavior, gel fraction, viscoelastic properties, and drug release kinetics. Viscoelastic properties were evaluated within oscillatory mode at a constant frequency of 1 Hz at 25 °C, with strain varied from 0.01% to 100% (Discovery HR 20, TA Instruments, USA). Swelling ratio was monitored in PBS for 7 days (37 °C and 100 rpm) to evaluate the degradation behavior of prepared hydrogels. To evaluate the hydrogel crosslinking degree, gel fraction was determined by placing the samples in 100 ml of PBS (37 °C and 100 rpm) for 24h. SrRan release rate was evaluated in PBS (37 °C and 100 rpm) and measured using Ultraviolet-visible light spectrophotometry (UV-VIS) at λ=318 nm.

RESULTS AND DISCUSSION

Physically crosslinked hydrogels were prepared combining such oppositely charged polyelectrolytes as HS and ε-PL by their complementary electrostatic attractions[1].

The hydrophilic functional groups in the structure of HA and ε-PL revealed an excellent ability to bind the water molecules. It was found that the hydrogel swelling degree increased with increasing HA content in samples and reached 547 ± 4% for HA/ε-PL 80:20 wt% and 466 ± 29% for HA/ε-PL/SrRan. Obtained results indicated that the maximum swelling degree was reached within the first 24 h and significant influence of SrRan addition on hydrogel swelling was not observed. Furthermore, all obtained hydrogels were characterized with gel fraction ~ 75% regardless of the hydrogel composition. It was found that the storage shear modulus (G') was higher than the loss modulus (G") for all prepared hydrogels, indicating that viscoelastic solid is formed and crosslinking reactions occurs just after the component mixing. All samples had a well-defined linear viscoelastic region up to ε ≈ 10%. The average crossover point of G' and G" was found at ε ≈ 50%, indicating the transition from gel to liquid state. Also, it was found that hydrogels with SrRan additive exhibited higher storage modulus values, than those without SrRan. Finally, obtained results indicated that initial SrRan burst release within first 24 h was ~ 30% and no significant differences in SrRan release kinetics were observed depending on the composition of the hydrogels.

CONCLUSION

Physically crosslinked hydrogels have many advantages, including ease of preparation, excellent biocompatibility, and biomedical safety. According to the results, all prepared HA/ε-PL/SrRan hydrogels are super-swelling materials since they can absorb a large amount of water (>100% of their weight) in a short amount of time[1]. During the research it was established that SrRan addition did not affect the hydrogel swelling behaviour or gel fraction but provided higher stiffness as indicated by the storage modulus.

In the future studies it has been planned to combine the obtained hydrogels with calcium phosphates to mimic the bone inorganic/organic phase composition and to promote the bone regeneration.

REFERENCES

1. K. Salma-Ancane *et al*., Int. J. Biol. Macromol. 208: 995–1008, 2022.
2. E. Tracuma, D. Loca., Key Eng. Mater. 850: 213–218. 2020.

ACKNOWLEDGMENTS

The authors acknowledge financial support from the Latvian Council of Science research project No. lzp-2019/1-0005 "Injectable in situ self-crosslinking composite hydrogels for bone tissue regeneration (iBone)" and European Union's Horizon 2020 research and innovation programme under the grant agreement No. 857287.

Anisotropic conductive shape-memory g-C_3N_4/rGO hydrogel-based nerve guide conduits

Jordi Amagat,[1, 3] Frederik Højbjerg Svejsø[1], Yingchun Su,[1,4] Alice Le Friec,[1] Steffan Møller Sønderskov,[2] Mingdong Dong[2], Menglin Chen[1,2]

[1.] *Department of Biological and Chemical Engineering, Aarhus University, Denmark.*
[2.] *Interdisciplinary Nanoscience Center, iNANO, Aarhus University, Denmark.*
[3.] *Sino-Danish College (SDC), University of Chinese Academy of Sciences, Beijing 101400, China.*
[4.] *School of Electrical Engineering and Computer Science, KTH Royal Institute of Technology, Electrum 229, 16440, Kista, Sweden.*

INTRODUCTION

Peripheral nerve injuries are a common trauma for individuals involved in accidents and diseases. There is a need for alternative approaches such as biomaterial-based therapies, which, with proper design, hold the potential to solve availability problems. Hydrogels, and in particular photo-crosslinked ones, can provide the right maintenance of a physiological environment to the implant site *in vivo*. g-C_3N_4 is an emerging graphene derived semiconductor with visible light adsorption and excellent photocatalytic activity [1]. It can act as a highly efficient photo-initiator and reinforcer to form a N,N-dimethylacrylamide (DMA)-based hydrogel [2]. Moreover, hydrogels with g-C_3N_4 could be crosslinked under visible-light irradiation. Melt electro-writing (MEW) is an emerging technique which consists of the deposition of melted polymer onto a computer-controlled station under a high voltage electric field. MEW scaffolds have already been investigated as topological guidance components for neural cells [3]. Herein, we present the fabrication and neural differentiation guidance of anisotropic, conductive, shape-memory g-C_3N_4/rGO hydrogels as nerve guidance conduit (NGC)

EXPERIMENTAL METHODS

Under 450nm blue light, hydrogels were polymerized via g-C_3N_4 radical formation, inducing polymerization of DMA. MEW channels were produced with a melt electro writing equipment and introduced into the hydrogel via a sacrificial template method. Hydrogels were characterized via SEM, swelling, mechanical and surface charge density analysis. PC12 cells, a model neural cell line, proliferation and cytotoxicity was analyzed via CCK and LDH tests. PC12 differentiation was analyzed via immunohistochemistry and fluorescence imaging. T-tests and ANOVA tests were used as statistical analysis.

RESULTS AND DISCUSSION

Different concentrations of graphene oxide (GO) were incorporated into g-C_3N_4 hydrogels. GO was reduced in situ using ascorbic acid, a mild reducing agent. Morphological analyses showed concentrations of GO didn't affect internal structure or pore morphology. Increased concentrations of GO restricted the swelling ratio and increased surface charge. PC12 cells were grown on top of g-C_3N_4/rGO hydrogels, and showed no cytotoxicity and increased proliferation over 7 days.
After differentiation, PC12 average neurite length was analysed. Neurite length was found significantly longer when hydrogels were loaded with GO, and reduced over 4 days compared to non-loaded and non-reduced ones. Guidance effect was incorporated into the hydrogels via a sacrificial template method using MEW. 3 different channels width were analysed. Finally, a self-folding shape-memory hydrogel was generated via differential crosslinking. Upon wetting, hydrogels could recover their initial cylindrical shape, which hold potential for PC12 encapsulation and their functionality as NGC.

CONCLUSION

An anisotropic, conductive, self-folding g-C_3N_4/rGO based hydrogel system was successfully fabricated and adapted for NGCs.. Neural differentiation was found significantly higher in reduced GO-loaded hydrogels compared to non-loaded hydrogels. Furthermore, hydrogel anisotropy guided enhanced neurite extension was achieved by introducing sacrificial MEW microchannels topography in the hydrogels. Finally, a self-folding hydrogel NGC was obtained by differential crosslinking over the cross-section of the tubular hydrogel. The anisotropic, conductive, self-folding hydrogel NGC could support neural cell differentiation and possess great potential for repairing peripheral nerve injuries.

REFERENCES

1. Tong, Z., et al., ACS Appl Mater Interfaces, 2015. **7**(46): p. 25693-701.
2. Kumru, B., et al., Macromolecules, 2017. **50**(5): p. 1862-1869.
3. Zhang, Z., et al., Biomaterials, 2020. **253**: p. 120108.

ACKNOWLEDGMENTS

The authors would like to thank the Carlsberg Foundation and Sino-Danish Center.

Intravital 3D bioprinting of microfluidic networks for blood guidance in living organisms

Luca Brandolino[*1,2], Anna Urciuolo[2,3], Andrea Maset[1,2], Carmela Ribecco[1,2], Pietro Bellet[1,2], Assunta Fabozzo[5], Gino Gerosa[5], Monica Giomo[1], Nicola Elvassore[1,2,4]

[1]Department of Industrial Engineering, University of Padova, Padova, Italy.
[2]Veneto Institute of Molecular Medicine, Padova, Italy.
[3]Department of Women's and Children's Health, University of Padova, Padova, Italy.
[4]University College London Great Ormond Street Institute of Child Health, London, UK.
[5]Department of Cardiac, Thoracic, Vascular Sciences and Public Health, University of Padua, 35128 Padua, Italy.
[*] luca.brandolino@studenti.unipd.it

INTRODUCTION

Vascular tissue engineering or anastomosis of engineered tissues with host systemic circulation are still unmet challenges. Our inability to further improve the vascular engineering field is associated with a lack of technology able to develop *de novo* micro-vessels into a patient and connect them to the patient's systemic circulation. The state-of-the-art solutions to this problem are mainly based on the paradigm of engineering a vascular construct *in vitro*, and subsequently implant it *in vivo*[1]. However, these approaches showed intrinsic limitations: i) the clinical feasibility has been proved only for vascular graft above 3-4 mm diameter[2]; ii) the generation of a vascular graft requires multiple step - from *in vitro* fabrication to *in vivo* implant - which make this process expensive and time-consuming; iii) the anastomosis of vascular graft with the systemic circulation become an impossible challenge when size is smaller than 1 mm[3]. Here, we show further developed the intravital 3D bioprinting concept, we previously developed[4], for to the generation of vascular networks directly into the tissue of living organisms. In particular, we designed a photo-sensitive polymer that can be crosslinked and de-crosslinked with micrometric spatial resolution. This allows to build hydrogel vascular network with high efficiency directly in living organisms.

EXPERIMENTAL METHODS

As model of vascular anastomosis, we use the femoral artery and femoral vein of GFP + transgenic mice. After injection in the anatomic site of interest the photosensitive-4armPEG solution was crosslinked by using UV light at 365 nm. Infrared light at 800 nm wavelength was used to decrosslinking and generate vascular network. The anastomosis was generated by high-energy laser ablation of blood vessel wall.

RESULTS AND DISCUSSION

First, we developed successfully multiphoton infrared light to decrosslink UV-Vis crosslinked hydrogel resulting in erasing of a selected volume of the hydrogel *in vitro*. Once we achieved this, we fabricated empty microfluidic channels within hydrogel *in vitro*, which were perfusable with fluorescent beads. Then, we translate the technology from *in vitro* to *in vivo*. We developed a surgical procedure, which allowed to deposit biopolymer in close contact with femoral vessels of mice and we fabricated empty microfluidic channels within living animals. We connected microfluidic channels with host vasculature through multiphoton laser ablation. We observed blood cells flowing within the microfluidic channels.

CONCLUSION

We were able to guide blood in three different configurations: i) vein-vein configuration ii) artery-artery configuration iii) artery-vein configuration. This strategy overcomes the paradigm of engineering a vascular construct since microfluidic channels are fabricated and connected with host vasculature directly in situ. Compared to state-of-the art approaches, we can fabricate in a fast way microfluidic channels with high resolution and spatial control and by exploiting multiphoton light we can, directly and immediately after fabrication, create vascular micro-anastomosis, resulting in perfusion of microchannels.

REFERENCES

1. Chen EP et al, Front . Bioeng. Biotechnol. 2021;9:
2. Burkel WE, Med Prog Technol, 1988-1989;14(3-4):165-75
3. MacDonald J, Skull Base, 15(3): 229–240
4. Urciuolo *et al*, Nat Biomed. Eng., 2020;4(9):901-915

ACKNOWLEDGMENTS. Authors would like to thank "CORIS" of the Veneto Region, Italy (LifeLab Program).

Adhesive lignin reinforced hydrogels with conductive PEDOT:HA nanoparticle additives for sensing and electricity generation applications.

Caitriona (Winters)[1*], Mario (Culebras)[2], Maurice (Collins)[1]

[1]Stokes Labs, Bernal Institute, School of Engineering, University of Limerick, Ireland.
[2] 2.Institute of Material Science, University of Valencia
[*]caitriona.winters@ul.ie

INTRODUCTION

Natural polymeric hydrogels are gaining in interest for various biomedical applications such as sensors, biomimetic skin and bioelectrodes due to their high stretchability, biocompatibility and conductivity. Previous studies synthesized polymeric hydrogels that were suitable for sensing applications and capable of generating electricity upon moist air passing through them, reaching voltages of up to 306.6mV[1,2]. Poly(3,4-ethylenedioxythiophene): polystyrene sulfonate (PEDOT:PSS) nanoparticles have been used in biomedical applications to infer conductivity, however, there is concerns relating to its stabilizer, PSS, and its release of acidic product upon degradation in *vivo*[3,4]. This work reports on the successful synthesis of PEDOT nanoparticles using hyaluronic acid (HA) as a stabilizer using oxidative miniemulsion polymerization. This is a green synthesis technique used to improve the bioactivity and hydrophilicity of the resulting nanoparticles. This work initially analyses the characteristics of these nanoparticles and the effect of varying amounts of HA, different molecular weights of HA and differing molar ratios of EDOT:FeTos on the conductive properties of the nanoparticles. It will then incorporate these conductive nanoparticles into a lignin/acrylic acid hydrogel to improve their conductivity for potential use in strain sensing and electricity generation applications. These hydrogels will aim to be adhesive, self-healing, highly stretchable, biocompatible and conductive.

EXPERIMENTAL METHODS

Nanoparticle characterization

PEDOT:HA nanoparticles were synthesized via miniemulsion polymerization. Methods used to characterize the nanoparticles include SEM, TEM, UV-vis, conductivity analysis, Raman Spectroscopy and cytotoxicity testing.

Hydrogel Analysis

Hydrogels will be characterized using swell testing, DMA, DSC, conductivity analysis and SEM spectroscopy.

RESULTS AND DISCUSSION

Stable, conducting PEDOT:HA nanoparticles were successfully synthesized via oxidative miniemulsion polymerization. The conductivity of the nanoparticles showed a general increase with the amount of oxidant added and oxidation levels as well as increased molecular weight of HA. This increase in conductivity could also be due to higher agglomeration occurring in these films.

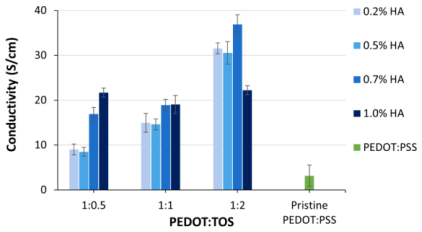

Figure 1 The conductivity of various PEDOT:HA Films compared to pristine PEDOT:PSS

Nanoparticles also show an increase in fluorescence, similar to that of the control, over the course of a three-day cytotoxicity test and show good cell viability *in vitro*. These nanoparticles will then be added to a lignin/acrylic acid hydrogel and the results will be reported in order to determine their potential for strain sensing and electricity generation.

CONCLUSION

From the work above it can be concluded that these PEDOT:HA films show a higher conductivity than that of pristine PEDOT:PSS. The suspensions obtained are stable for several weeks/months and showed good cell viability. It can be concluded that the synthesized hyaluronic acid doped PEDOT nanoparticles show promise as a conductive additive for hydrogel applications. From these findings, this work will determine the optimum addition of conducting PEDOT:HA nanoparticles for use in hydrogel applications such as strain sensing and electricity generation applications.

REFERENCES

1. Fu C. et al., International Journal of Biological Macromolecules. 201:104-110, 2022.
2. Zhang Y. et al., International Journal of Biological Macromolecules. 193(Pt A):941-947, 2021.
3. Asplund et al., Biointerphases, 3: 83-89, 2008.
(4) Mantione et al., Macromolecular Bioscience, 18:1227-1238, 2016.

ACKNOWLEDGMENTS

The authors would like to thank the School of Engineering at the University of Limerick for supporting this work.

Scaffolds that meet the electrochemical balance of the native cartilage for the regeneration of osteoarthritic joints

Garazi Larrañaga-Jaurrieta[1,2], Ander Abarrategui[2], Sandra Camarero-Espinosa[1,3*]

[1]BioSmarTE Lab, POLYMAT, University of the Basque Country UPV/EHU, Donostia / San Sebastián 20018, Gipuzkoa, Spain.

[2]Regenerative Medicine Lab, CICbiomaGUNE, Donostia / San Sebastián 20014, Gipuzkoa, Spain

[3]IKERBASQUE, Basque Foundation for Science, Bilbao, Spain
garazi.larranaga@polymat.eu, sandra.camarero@polymat.eu

INTRODUCTION

Osteoarthritis (OA) is the most common disability affecting over 30% of the population over 65 years old. Characterised by the loss of cartilage mass, can lead to total disability of patients affected by the pathology in areas such as the hips, spine, shoulders and mostly knee. Cartilage owes its mechanical properties to its extra cellular matrix (ECM) that can be modelled as a biphasic system. Collagen provides stiffness to the tissue while glycosaminoglycans (GAGs) are responsible for pressurization upon compression as a result of water entrapment through its negative charges or neat electrical charge[1]. OA is characterized by tissue thinning due to the degradation of the ECM and therefore loss of GAGs that results in an electrochemically unbalanced environment. Being GAGs the key regulators of the loads transmitted to chondrocytes, their loss results in over-stressed cells with a consequent overproduction of growth factors, enzymes and cytokines (i.e. MMPs, ADAMTS, etc.) that further degrade the matrix. Thus, regeneration of the tissue requires the restoration of the neat electrochemical charge of the native tissue.

Here, we fabricated 3D printed chondroprotective scaffolds based on interpenetrating networks (IPNs) that mimic the biphasic character of the tissue and restore the electrochemical balance, promoting the formation of a healthy tissue.

EXPERIMENTAL METHODS

Synthesis of light-printable IPNs: Gelatin methacrylate (GelMA) was synthesised, by the addition of anhydride methacrylate to a gelatin dissolution at 50ºC and basic pH. GelMa with three different degrees of substitution (DS) were prepared. Tyramine-functionalized alginate (Alg-tyr) was prepared via amidation with 4-(4,6-dimethoxy-1,3.5-triazin-2-yl)-4 methylmorpholinium chloride (DMTMM) also with three different DS. To create IPNs, GelMa and Alg-tyr were mixed in different ratios. **Chateracterization:** The effectiveness and DS of the reactions was evaluated by NMR, by the nihydrin colorimetric assay and absorbance. The viscoelastic properties of the individual materials as well as the IPNs were measured by rheology. Alg-tyr crosslinking was carried out via enzymatic reaction with oxygen peroxide (H_2O_2), horseradish peroxidase (HRP) and Eosin Y. This reaction was validated as simple increase in the viscosity after irradiating it with a 505nm diode. Taking into account the importance of liquid absorption, the swelling of both materials and IPNs was measured over 24h. **Modification of the surface charge of Alg-tyr:** The negative charges present on carboxylic groups of alginate were quenched by Steglich esterification with an alcohol and activating agents dicyclohexylcarbodiimide (DCC) and 4-N, Ndymethylaminpyridine (DMAP).

RESULTS AND DISCUSSION

IPNs were created from GelMa and Alg-Tyr. GelMa mimicked the stiff collagen network while Alg-Tyr was used to mimic the electronegativity conferred by GAGs on the native tissue through the carboxylic group of the polymer. The methacrylation reaction of gelatin could be controlled to obtain GelMa with three well differentiated DS, ranging from 30% to 90%. For Alg-tyr instead, low DS were targeted, 5-10%, to retain as many carboxylic groups as possible. Rheology was used to confirm crosslinking of Alg-tyr.

To find the right electrochemical charge that could restore the balance of native cartilage, Alg-Tyr was modified to display different degrees of carboxylation by means of esterification reactions. The efficiency of the esterification reaction was demonstrated by NMR and most importantly by its influence in the viscoelastic properties of the material.

IPNs were finally obtained via 3D printing at two different wavelengths (Figure 1.) of 365 and 505 nm resulting on scaffolds with varying neat electrochemical charge and viscoelastic properties. Moreover, the different electrochemical charge influenced the water uptake ability of our IPNs, as it occurs on the native cartilage, achieving swelling ratios between 40 and 60%.

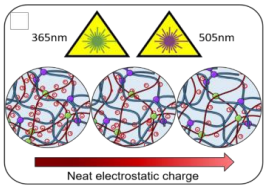

Figure 1. Photocrosslinked IPNs with varying neat electrochemical charge.

CONCLUSION

Summarizing, we have created IPNs with desired mechanical and electrochemical properties for cartilaginous tissue formation *in vitro*. We have also developed a fast curing printing process combining two photocurable polymers to resemble the bi-phasic nature of cartilage.

REFERENCES

1. Camarero-Espinosa, S., *et al.,* Biomaterials Science,

ACKNOWLEDGMENTS

The authors would like to thank the Basque Government for the "Predoctoral Training Program for Non-Doctoral Research Staff 2021-2022" (Grant ref.: PRE_2021_1_0403). This work was supported by the RETOS grant PID2020-114901RA-I00 of the Ministry of Science and Innovation (MICINN).

Non-Swellable Click Hydrogels Solely Composed of A Cold Water Fish Gelatin Polymer Network

Tobias Hammer[1,*], Ke, Yang[2], Markus Rottmar[2], Katharina Maniura-Weber[2], Rene M. Rossi[1], Kongchang Wei[1,2]
[1]Laboratory for Biomimetic Membranes and Textiles,
[2]Laboratory of Biointerfaces
Department of Materials Meet Life, Empa, Swiss Federal Laboratories for Materials Science and Technology
Lerchenfeldstrasse 5, 9014 St. Gallen, Switzerland
[*]tobias.hammer401@empa.ch

INTRODUCTION

Hydrogels represent a promising group of materials for tissue engineering and biomedical applications due to their intrinsic tissue-mimetic characteristics. While swelling is often the leading cause of mechanical weakness, it is attractive yet challenging to develop non-swellable hydrogels, especially from bioactive polymers such as gelatin[1]. Gelatin has been widely employed as the primary component for hydrogels with gelatin methacryloyl (GelMa) being one of the most prevalent modified gelatins used[2]. Commonly, these gelatins are of porcine or bovine origin, but more recently, gelatin from cold water fish skin (fGel) has been discovered as a valuable alternative owing to a number of favourable properties such as lower gelling and melting points as well as lower immunogenicity[3, 4]. Many fGel hydrogels require a co-polymer or lengthy crosslinking protocols for their formation[5]. Herein, we aim to develop fully fGel-based non-swellable hydrogels.

EXPERIMENTAL METHODS

By synthesizing two functional derivatives, namely thiol-functionalized fish gelatin (fGel-SH) and norbornene-functionalized fish gelatin (fGel-NB), stable hydrogels composed solely of fGel were obtained via rapid UV-mediated "click" crosslinking of fGel-SH/fGel-NB mixture at ambient temperature (Fig. 1). The gelation behavior and viscoelasticity were characterized by oscillatory rheological measurements (frequency 1 Hz).

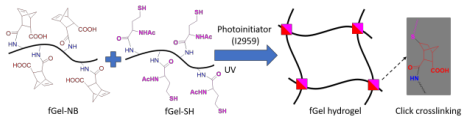

Figure 1. Click crosslinking between fGel-NB and fGel-SH.

RESULTS AND DISCUSSION

The results of the photo-rheological measurements revealed rapid crosslinking, with all the tested formulations reaching their maximum storage modulus (G') shortly after being exposed to UV. Equal ratios of the two polymers (5wt% each) showed the highest G' (Fig. 2). With such a rapid and straightforward fabrication, the hydrogels showed negligible swelling after 8 days within PBS at 37°C ($R_{swelling}$ ~ 4.72 ± 0.74 %). Rheological amplitude sweep confirmed the broad linear viscoelastic region (LVR) with a limit strain (γ) of at least 200% (beyond the maximum stress of the instrument).

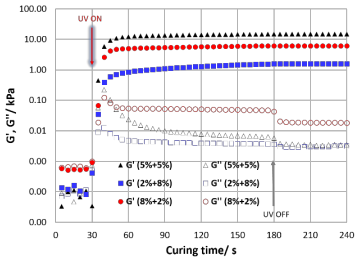

Figure 2. Gelating behaviour of fGel hydrogels with varied formulations, where percentages indicate the fGel-SH and fGel-NB content (wt%) .

CONCLUSION

The hydrogel formulation presented in our work represents a promising biomaterial for tissue engineering and biomedical applications. We were able to fabricate non-swellable hydrogels with good mechanical properties without having to add any further network components that could reduce the biological activity of gelatin. Such click hydrogels form rapidly after only a brief exposure to UV, and give rise to desirable biomechanical properties (non-swellable matrix, broad LVR), as well as biochemical properties originating from fGel (cell adhesive and degradable, low immunogenicity; as supported by literature)[4], thus making them a potentially promising material platform for in vitro 3D cell culturing and in vivo tissue regeneration.

REFERENCES

1. Kamata, Hiroyuki, et al. "“Nonswellable” hydrogel without mechanical hysteresis." *Science* 343.6173 (2014): 873-875.
2. Sakr, Mahmoud A., et al. "Recent trends in gelatin methacryloyl nanocomposite hydrogels for tissue engineering." *Journal of Biomedical Materials Research Part A* 110.3 (2022): 708-724.
3. Levato, Riccardo, et al. "High-resolution lithographic biofabrication of hydrogels with complex microchannels from low-temperature-soluble gelatin bioresins." *Materials Today Bio* 12 (2021): 100162.
4. Yoon, Hee Jeong, et al. "Cold water fish gelatin methacryloyl hydrogel for tissue engineering application." *PloS one* 11.10 (2016): e0163902.
5. Atma, Yoni. "Synthesis and Application of Fish Gelatin for Hydrogels/Composite Hydrogels: A Review." *peptides* 22 (2021): 23.

ACKNOWLEDGMENTS

“The authors would like to thank the Skintegrity.CH and Empa for providing financial support to this project”.

Patterned hydrogels with spatially tunable biophysical and biochemical properties to guide 3D stem cell response and osteogenesis

Claudia A. Garrido[1,2], Daniela Garske[1,2], Shahrouz Amini[2], Georg N. Duda[1], Katharina Schmidt-Bleek[1], Amaia Cipitria[2,3]

[1] Julius Wolff Institut, Berlin Institute of Health, Charité - Universitätsmedizin Berlin, Berlin, Germany
[2] Max Planck Institute for Colloids and Interfaces, Potsdam, Germany
[3]Biodonostia Health research Institute, San Sebastian, Spain

INTRODUCTION

Alginate based hydrogels offer a broad range of materials for regenerative medicine. Structurally patterned materials offer various options for guided cell behavior, such as patterning spatially discretized biochemical, topological, or mechanical properties, or combinations thereof. Patterned materials allow to integrate multiple characteristics in a single material, create interphases or gradients which better mimic the anisotropy found in tissues and endogenous regeneration cascades. Previous studies using orthogonal Diels-Alder and thiol-ene crosslinking of degradable peptides in alginate hydrogels, showed that patterns in 2D affect cell attachment and differentiation[1]. However, to employ the full potential of patterning principles, 3D cell encapsulation in such materials appears mandatory. We hypothesize that the matrix spatial patterning of biophysical cues can modulate cell behavior in terms of morphology, proliferation, and tissue organization. Therefore, this study aims to evaluate cell response in 3D alginate hydrogels with spatial patterns in biophysical and biochemical properties.

EXPERIMENTAL METHODS

Hydrogel synthesis

Single-phase materials were formed using norbornene (N) and tetrazine (T) modified alginate (Diels-Alder reaction, spontaneous non-UV crosslinking) together with matrix metalloproteinase (MMP) sensitive peptide as a degradable crosslinker (thiol-ene reaction, UV-mediated crosslinking). The patterns on the material were formed using a photomask with UV irradiation with stripes of 220µm width.

Mechanical characterization

The variations in the N-T ratio and the concentration of MMP sensitive peptide can tune the mechanical properties and degradability of the material. The materials were mechanically characterized based on the elastic modulus using rheology for single phase materials and microindentation for patterned materials. Degradation studies were performed by evaluating the elastic modulus of single-phase hydrogels with encapsulated cells over 14 days.

3D cell encapsulation

Mouse embryonic fibroblasts (MEFs) were encapsulated in 3D in single phase (UV and non-UV) and patterned materials in hydrogel disks of 5mm diameter and 2mm height. To evaluate cell behavior, cell viability (live/dead staining), cell morphology(DAPI/phalloidin) and proliferative state (Ki67) were evaluated at days 1 and 14.

Statistical analysis

All experiments were conducted with n = 3-4 samples for mechanical characterization and in vitro studies and with n=9 (3 different images from 3 different hydrogels). Origin Software was used for statistical analyses. Comparisons between hydrogels or time points were performed using Student t-test ($p < 0.05$).

RESULTS AND DISCUSSION

The rheology of single-phase showed the potential of this platform, as a broad range of materials with different stiffness can be formed. In order to analyze cell behavior in dependence of the material degradation, it was necessary to design two biomaterials with comparable elastic moduli. We achieved this by tuning the N:T ratio to 1.5 and the MMPsens peptide concentration to 3mg/mL. The microindentation results of the patterned material were consistent with the rheology of the single phases, showing an elastic modulus of ~1.5kPa in the degradable (UV) and ~2kPa in the non-degradable (non-UV) materials.

The 3D encapsulation of mouse embryonic fibroblasts (MEFs) in single-phase materials gels showed high viability (>85%) over the 14 days in bothe phases and a significant increase in cell number in the degradable hydrogels (UV). Cell morphology showed a significant increase in cell area and decrease in circularity indicating cell spreading in degradable hydrogels, whereas the cells in non-degradable materials remained round and with no significant changes in the cell area. The main differences in cell morphology were observed in filopodia formation, as the cells in softer gels had significantly higher filopodia number and length compared to non-degradable hydrogels (Figure 1). The proliferation marker Ki67 was highly expressed in softer gels compared to stiff gels, which is consistent with the significant increase in cell number in degradable hydrogels.

CONCLUSION

The hydrogels showed spatially tunable mechanical and degradation characteristics determined by the crosslinking type. This ongoing work reached the level were cells are surviving within a patterned material and showing differences in cell behavior, thus the foundation was laid to invent a biomaterial that can be used to study the ECM with more relevant cell types. Currently we are investigating 3D encapsulation in patterned materials of (i) human mesenchymal stem cells with the aim to guide osteogenic differentiation, (ii) HUVECs to study angiogenesis and (iii) the effect of patterns in the coculture of hMSCs and HUVECs with the aim to better understand the bone ECM.

REFERENCES

(1) Lueckgen A. et al., Acta Biomaterialia,. 115:185-196, 2020

Cellulose-based Hydrogel Scaffolds for 3D in vitro Cultivation of Human Mesenchymal Stem Cells

Ilias Nikolits[1], Sara Radwan[2], Falk Liebner[3], Dominik Egger[1], Cornelia Kasper[1]

[1]Institute of Cell and Tissue Culture Technology, Department of Biotechnology, University of Natural Resources and Life Sciences, Vienna, Austria
[2]Department of Life Science Engineering, UAS Technikum Wien, Fachhochschule Technicum Wien, Vienna, Austria
[3]Institute of Chemistry of Renewable Resources, Department of Chemistry, University of Natural Resources and Life Sciences, Vienna, Austria

*ilias.nikolits@boku.ac.at

INTRODUCTION

Mesenchymal stem cells (MSCs) are among the most investigated and promising types of cells in regenerative medicine, due to their highly proliferative and multipotent capacities. It is true, that when MSCs are cultured in vitro in traditional 2D culture systems, they gradually lose their differentiation and proliferative potential and their immunogenicity is altered. However, the physiologic functionalities of MSCs can be maintained when cells are cultured in 3D using suitable biomaterials.

In this context, cellulose is an abundant, low-cost, biocompatible and highly tunable material, and therefore represents an excellent biomaterial candidate. Cellulose-based scaffolds can serve as 3D platforms for physiological in vitro cultivation or in vitro modeling.

For this purpose, cellulose-based hydrogel scaffolds were synthesized and their suitability for cell culture applications as well as their mechanical properties were assessed. Materials of different bulk densities were prepared and evaluated for their applicability as scaffold biomaterial by encapsulating human MSCs in these hydrogels and monitoring their viability, metabolic activity, migration and morphology during in vitro cultivation.

EXPERIMENTAL METHODS

Human adipose tissue MSCs were encapsulated in cellulose nanofiber hydrogels of different bulk content concentrations in tissue culture treated well plates. Samples were cultivated for up to 14 days at 21% O_2, 5% CO_2 and 37°C, under static conditions.

RESULTS AND DISCUSSION

Results showed that MSCs can survive, grow and migrate inside the cellulose hydrogels, however, the survival and proliferative capacities of the cells as well as their morphological characteristics correlate with the bulk cellulose content of the hydrogels.

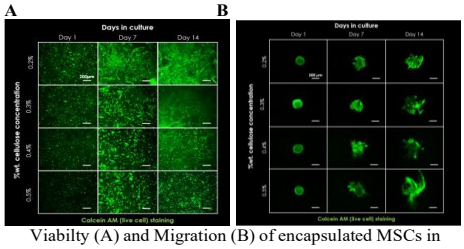

Viabilty (A) and Migration (B) of encapsulated MSCs in cellulose nanofiber hydrogels with different bulk content concentrations, cultivated up to 14 days.

CONCLUSION

In contrast to other cellulose-based hydrogels, the presented hydrogel supports the adhesion, growth and migration of human MSCs. Furthermore, the survival, metabolic activity, growth capacities and morphological characteristics of the MSCs correlate with the bulk cellulose content of the hydrogels.

ACKNOWLEDGMENTS

This project is supported by the Doctoral School "Biomaterials and Biointerfaces (BioMatInt)" of the University of Natural Resources and Life Sciences, Vienna

Generation of "elastic" organotypic skin cultures

Cristina Quílez[1,*], Maria Stojic[1], Maria Luisa López-Donaire[2], Jorge González-Rico[2], Daniel Gracía-González[2], Miguel González Pérez[3], José Carlos Rodríguez-Cabello[3], José Luis Jorcano[1,4], Israel González de Torre[3], Diego Velasco[1,4]

[1] Department of Bioengineering and Aerospace engineering, Universidad Carlos III de Madrid, Leganés, Spain
[2]Department of Continuum Mechanics and Structural Analysis, Universidad Carlos III de Madrid, Leganés, Spain
[3]BIOFORGE (Group for Advanced Materials and Nanobiotechnology), University of Valladolid, CIBER-BBN, 47011 Valladolid, Spain
[4]Instituto de Investigación Sanitaria Gregorio Marañón, Madrid, Spain
[*] cquilez@ing.uc3m.es

INTRODUCTION

Plasma-derived fibrin matrices has been proved to provide a more suitable 3D environment to promote migration, proliferation and differentiation of the skin cells[1]. Plasma-fibrin matrices allow an efficient production of natural collagen by human fibroblasts and a fully autologous process for skin grafting. However, dermo-epidermal equivalents based on plasma-derived fibrin showed low mechanical properties which limit their reproducibility and lifespan. In a previous work[2] elastin was incorporated into the plasma-derived hydrogels to achieve better mechanical and elasticity properties, but *in vitro* studies were not carried out to evaluate their ability to form dermo-epidermal equivalents.

In this work, we propose the generation of "elastic" *in vitro* skin equivalents derived from plasma-derived fibrin and supplemented with elastin for the generation of a new a human plasma-derived bilayered (including dermis and epidermis) skin model. The structure of this "elastic" skin model was biologically and structurally characterized by histological and immunofluorescence methods.

EXPERIMENTAL METHODS

"Elastic" in vitro skin equivalents were prepared following the protocol previuolsy described[2]. Briefly, SKS-N3 was dissolved in plasma supplemented with AmchaFibrin (0.008 wt.%) while SKS-Cyclo was dissolved in 0.9 wt.% NaCl. Molar ratio of SKS-N3 and SKS-Cyclo was 1:1 and prepared solutions were kept at 4 ºC overnight. Plasma-elastin hydrogels were obtained by simply mixing these two solutions at 4 C. Elastin-plasma hybrid hydrogel was prepared with a final fibrinogen and elastin concentration of 1.2 and 3 mg/mL respectively. hFBs (20.000 cells/ml) were encapsulated within the hydrogel and followed by hKCs deposition on top (4,2 $\cdot 10^5$ cells/cm^2) and cultured in the air liquid interface up to 15 days. For structural characterization, samples stained using Hematoxylin and Eosin (H&E) and correct epidermal differentiation was characterized by localization of K5, K10, Involucrin, Loricrin and Filaggring using immunofluorescence.

RESULTS AND DISCUSSION

H&E tinction showed a bilayered skin construct with dermal and stratified epidermal compartment (Figure 1, left). Moreover, correct epidermal differentiation after 15 days in culture was proven by positive expression of the well-known epidermal proteins (Figure 1, right): K5, K10, Involucrin, Loricrin and Filaggring, as well as the presence of Elastin and Col III in the dermal compartment.

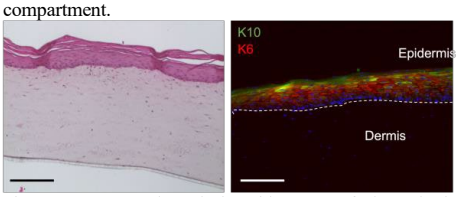

Figure 1: Structural analysis with H&E of the "elastic" organotypic skin equivalent after 15 days in culture (left) and immunofluorescence characterization of K10 (suprabasal layer) and K6 (proliferative activity) (right). Scale bar 300µm.

CONCLUSION

Plasma-derived hydrogels supplemented with elastin prove their ability to generate organotypic skin cultures with a stratified epidermis, proven by the structural immunolocalization of well-known epidermal markers. Moreover, tensile and compression tests of the generated "elastic" organotypic skin constructs are being evaluated and compared to conventional *in vitro* skin constructs to ultimately analyze the effect of the presence of elastin in skin constructs.

REFERENCES

[1.] A. Montero, C. Quílez, L. Valencia, P. Girón, J. L. Jorcano, Diego Velasco. Effect of Fibrin Concentration on the In Vitro Production of Dermo-Epidermal Equivalents. Int J Mol Sci 2021 Jun 23;22(13):6746.
[2.] M. Stojic, et al., Polymers (Basel). 2021 Jul; 13(13): 2114.

ACKNOWLEDGMENTS

The authors are grateful for the funding from the Spanish Government (FPU15-00448, PID2019-110709RB-100, RED2018-102417-T), Junta de Castilla y León (VA317P18. Infrared2018-UVA06), Interreg. V España Portugal POCTEP (0624_2IQBIONEURO_6_E) and Centro en Red de Medicina Regenerativa y Terapia Celular de Castilla y León. This research was also funded by Programa de Actividades de I + D entre Grupos de Investigación de la Comunidad de Madrid, S2018/BAA-4480, Biopieltec-CM; by Programa Estatal de I + D + i Orientada a los Retos de la Sociedad, RTI2018-101627-B-I00; by Programa de Apoyo a la Realización de Proyectos Interdisciplinares de I + D para Jóvenes Investigadores de la Universidad Carlos III de Madrid (project: BIOMASKIN); and by Cátedra Fundación Ramón Areces.

Biologically Active Double Network Hydrogels Based on Chitosan Derivatives and Poly(Vinyl Alcohol) for Regeneration of Cartilage Defects

Patrycja Domalik-Pyzik, Malwina Furgała

Department of Biomaterials and Composites, Faculty of Materials Science and Ceramics,
AGH University of Science and Technology, Kraków, Poland
* pdomalik@agh.edu.pl

INTRODUCTION

The pain and gradually progressing limitation of mobility are the main burdens of osteoarthritis (OA). Each year, an increasing number of people are affected by the OA. Meanwhile, despite the efforts of many scientific groups, the successful regeneration of cartilage tissue remains an unresolved issue. Amongst many therapeutic strategies, those involving hydrogels are one of the most promising ones since those three-dimensional polymeric networks with high water content already possess tissue-like features and can be further tailored to the needs of the cartilage[1,2].

EXPERIMENTAL METHODS

In our study, bioactive high-strength scaffolds based on double network (DN) hydrogels were proposed for the regeneration of partial-thickness cartilage defects. First, chitosan derivatives, i.e. 2-hydroxypropyltrimethyl ammonium chloride chitosan (HACC) and N,O-carboxymethyl chitosan (NOCC), were synthesized synthesized. Then, a double network structure was created through appropriate crosslinking of HACC/NOCC and poly(vinyl alcohol) (PVA) networks. For regeneration of partial-thickness cartilage defects, bi-layered scaffolds were designed with different orientation of collagen fibers to mimic the superficial and middle zone of the native tissue. The physicochemical properties of the obtained materials were assessed. Rheological properties of the hydrogels, as well as structure, morphology, mechanical, surface, and finally biological properties of the scaffolds were investigated.

RESULTS AND DISCUSSION

Chitosan derivative were successfully synthesized. DN hydrogels formed through physical crosslinking of HACC/NOCC and PVA expressed superior mechanical properties. The bi-layered scaffolds were produced to imitate the missing part of the assumed cartilage defect. The use of collagen had a positive effect on cytocompatibility. Increased biological activity was achieved through the introduction of kartogenin.

CONCLUSION

The design of the proposed scaffolds followed biomimetic principles. The developed chitosan derivatives/PVA double network hydrogels modified with collagen and kartogenin have promising properties and can be considered for cartilage tissue engineering.

REFERENCES

1. Wei, W. et al., Bioact. Mater. 6, 998–1011 (2021).
2. Xu, X. et al., Mater. Horiz., 8, 1173-1188 (2021).

ACKNOWLEDGMENTS

This study was supported by the Program "Excellence Initiative – Research University" for the AGH University of Science and Technology.

Synthesis and Characterization of Novel Selanated Hydrogels for Tissue Engineering and 3D Bioprinting

Maria Perez-Araluce[1,2*], Alessandro Cianciosi[3], Tomasz Jüngst[3], Carmen Sanmartín[2], Felipe Prósper[1], Daniel Plano[2], Manuel M Mazo[1]

[1]Tissue Engineering, CIMA University of Navarra, Pamplona, Spain

[2]Department of pharmaceutical technology and chemistry, University of Navarra, Pamplona, Spain

[3]Department for Functional Materials in Medicine and Dentistry, University of Würzburg, Würzburg, Germany

[*]mparaluce@unav.es

Key words: hydrogel, selenium, tissue engineering.

INTRODUCTION

The development of new materials that allow 3D cell culture is necessary to achieve greater similarity to natural tissues. Different biomaterials have been developed for this purpose. They can be divided according to their origin into synthetic materials, that allow their properties to vary according to the needs of a tissue, natural materials that have the benefit of being more biocompatible and more widely available, and semi-synthetic materials that have the advantages of both. Hydrogels have been used as one of the most common tissue engineering scaffolds in the last two decades due to their ability to support a 3D structure, to provide mechanical support for cells, and to simulate the native extracellular matrix. The high-water content of hydrogels can provide an optimal environment for cell survival and a structure that closely replicates native tissues[1]. Also, they can be chemically functionalized to display additional features. Selenium has been shown to have relevant actions due to its antioxidant and anticarcinogenic properties. Recent studies have confirmed a correlation between the decrease of the level of blood plasma Se in patients with acute coronary syndrome and myocardial infarction[2]. Thus, the use of selenated hydrogels could be very beneficial in the field of cardiac tissue engineering. However, no selenated soft materials are currently available that could fulfill the mechanical requirements of the biofabrication of cardiac tissue. The aim of the present work is to collaborate with the development of cardiac tissue engineering strategies by increasing the portfolio of available biomaterials. Specifically, we have chosen to incorporate selenium to the polymeric backbone, and to generate a final 3D bioprintable system capable of photopolymerization.

EXPERIMENTAL METHODS

Chemical synthesis. Different strategies have been developed to introduce selenium into gelatin. Different crosslinking strategies have also been tested to form the hydrogels from the functionalized gelatin. These strategies are based on the Diels-Alder and Michael reactions and can photopolymerize with visible light.

Hydrogel characterization. The methods used for characterization have been NMR, atomic absorption, ninhydrin assays and rheometry.

Cell culture viability assays. The cell lines used were HELAs, mesenchymal stem cells and cardiomyocytes derived from human induced pluripotent stem cells (hiPSCs-CM). The viability assays used were the Alamar Blue test and the Live/Dead® test. hiPSC-CMs were obtained in-house by differentiation through small molecule-based biphasic modulation of the Wnt pathway, followed by lactate-based metabolic selection.

3D bioprinting. A purpose-build extrusion-based bioprinting system was employed, developed by Cocuus. Syringe tip, extrusion and collector speeds, collector temperature and light exposure were tuned for optimal results.

RESULTS AND DISCUSSION

Characterization of the new molecules not only confirms the acquisition of the desired functionality, but also gives insight to their structure. The presence of selenium was confirmed by ^{77}Se-NMR (Fig.1) and quantified by atomic absorption. The synthesized selenated gelatin derivatives are capable of photopolymerizing to form hydrogels (Fig. 2). Rheometry tests have shown that it is possible to vary the mechanical properties of hydrogels by changing the percentage of gelatin, the concentration of photoinitiators or the time of light exposure. Cell viability has been found to be similar to other biomaterials such as GelMA, which is widely used in tissue engineering. We have also been able to verify that it is a material suitable for 3D printing.

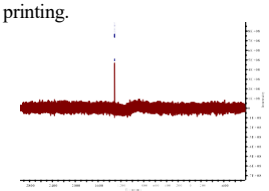

Fig1. Gelatin derivative ^{77}Se-NMR

Fig2. Selenated hydrogels

CONCLUSION

New gelatin derivatives capable of photopolymerizing and generating hydrogels have been successfully synthesized. These hydrogels present similar viability to other materials used in tissue engineering, but also present an additional biological function by incorporating selenium. These hydrogels were also capable of being bioprinted with a 3D bioprinter.

REFERENCES

1. Mantha S. *et al*., Materials (Basel). 12;12(20), 2012

2. Sanmartin C. *et al*., Curr Med Chem.18(30):4635, 2011.

ACKNOWLEDGMENTS

This work was co-funded by FEDER funds, European Union´s H2020 Program under grant agreement No 874827 (BRAVƎ) and Gobierno de Navarra Proyectos Estratégicos IMPRIMED (0011-1411-2021-000096).

A composite Bioink Based on Gelatin/Cellulose Nanofibrils: Overcoming Remaining challenges

Sara Nejati, Luc Mongeau

Deparment of Mechanical Engineering, McGill University, Montreal, Canada
* sara.nejati@mail.mcgill.ca

INTRODUCTION

Gelatin is a promising material for tissue engineering and regenerative medicine applications due to its biocompatibility, biodegradability, and abundance. Despite the advantages of gelatin, its fast gelation at room temperature, poor printability, and weak mechanical properties limits its applications in tissue engineering, particularly for injection and bioprinting purposes [1]. To address these challenges, we introduced cellulose nanofibrils (CNFs) into gelatin-based hydrogels. Nanocellulose has been widely explored for tissue engineering applications and shown to be a promising reinforcement for improving mechanical and rheological properties of biomaterials [2].

EXPERIMENTAL METHODS

Firstly, methacrylated gelatin (GelMA) was synthesized as described elsewhere. Then, 10 %w/w GelMA solutions with different CNF filling content (0.25%, 0.5%, 0.75%, and 1%) were prepared and GelMA/CNF composite hydrogels were prepared by getting samples exposed to UV light. Prepared composites where finally characterized in terms of morphology, gelation time, rheological and mechanical properties.

RESULTS AND DISCUSSION

Proper methacrylation of gelatin was confirmed by FTIR (Figure 2, a). The morphology of the CNFs and GelMA/CNFs composite was observed using TEM and SEM, respectively (Figure 1). The rheological properties of the samples were characterized using a photorheometer and hydrogels' gelation time at room temperature were measured (Figure 1, c, d). The incorporation of CNFs within GelMA-based hydrogels could significantly delay their gelation at room temperature. This is most likely because the physical association of gelatin chains, which is the main mechanism behind the gelation of gelatin at room temperature, can be highly limited by the CNF fibrils. This property is particularly favorable for injection and printing applications, where fast gelation would clog the needle and negatively affect the shape fidelity. Investigation of rheological properties under UV light displayed that although introducing CNFs delayed the gelation time from 26 s to 105 s, the gelation is still fast, meaning that the proposed composite is very promising for in situ forming applications. Also, the incorporation of fibrils quadrupled the maximum storage modulus. Moreover, CNFs improved the mechanical properties of the hydrogel through increasing the yield stress and degree of deformation. Hence, the problem of brittleness and poor mechanical properties of gelatin could be addressed as well.

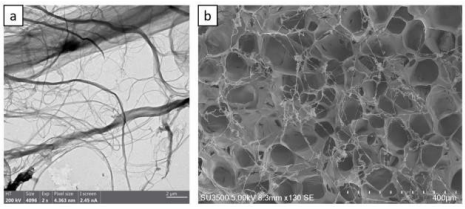

Figure 1: a) TEM of CNFs. b) SEM of GelMA/CNFs

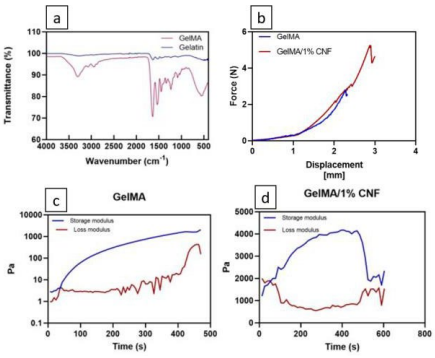

Figure 2: Results of a) FTIR, b) Compression, c and d) rheometry

CONCLUSION

The incorporation of cellulose nanofibrils within gelatin matrix will not only overcome the challenges associated with gelatin-based bioinks, including fast gelation at room temperature, poor printability, and weak mechanical properties, but also will imitate the hydrogel/fiber nature of a true extracellular matrix.

REFERENCES

1. Du H. et al., *Carbohydrate Polymers*, *209*: 130–144, 2019.
2. Jiang Y., *Journal of Materials Science*, *55*(6), 2618–2635, 2020.

ACKNOWLEDGMENTS

This work was supported by the National Institute of Deafness and other Communication Disorders. The content is solely the responsibility of the authors and does not necessarily represent the official views of the National Institute of Health.

Hyaluronic Acid Hydrogels and the release of an Immunomodulating Parasitic Derived Peptide Therapeutic to overcome the Foreign Body Response

Ward, V.[1,2], O'Dwyer, J.[1] , Lalor, R.[3] , Dalton, J.P[3], Duffy, G.P [1,2,4]

[1] Anatomy and Regenerative Medicine Institute (REMEDI), College of Medicine, Nursing and Health Sciences, NUI Galway. [2] SFI Advanced Materials and BioEngineering Research Centre (AMBER), Trinity College Dublin & NUI Galway. [3] Center of One Health (COH) and Ryan Institute, School of Natural Science, NUI Galway. [4] CÚRAM, SFI Research Centre for Medical Devices, National University of Ireland Galway (NUIG) & RCSI, Galway, Ireland

email: v.ward1@nuigalway.ie

INTRODUCTION

Biomaterials are increasingly being investigated and used in medical applications including tissue engineering, regenerative medicine, and drug delivery. Hydrogel-based biomaterials are particularly desirable as they can be delivered in a minimally invasive way and have excellent biocompatibility and tunable degradation properties. Hyaluronic acid (HA) is a natural glycosaminoglycan found in the body which can form hydrogel scaffolds (Fig.1A). As with most biomaterials however, HA hydrogels often cause an undesirable immune response and various strategies are currently being developed to limit this foreign body response.

Peptides drugs derived from parasites are a promising treatment strategy to help overcome the body's immune response to biomaterials. Specific peptides responsible for a parasites immune evasion in a host have been extracted and their specific cellular pathways have been studied. The novel peptide drug SM16-K66 derived from the parasite *Schistosome mansoni* (Fig.1C) is known for its immunomodulating effects and is a promising biotherapy[1]. This peptide has been shown to block Toll-Like-Receptor 4 (TLR4) signaling against lipopolysaccharide bacteria (LPS) and has potential to combat biomaterial induced inflammation. Herein, we aim to optimise a mechanically supportive hydrogel scaffold with SM16-K66 delivery capabilities to achieve a biocompatible scaffold capable of providing mechanical support to tissue.

EXPERIMENTAL METHODS

Hydrogel Characterisation: Tyramine-modified hyaluronic acid (Fig.1A) was purchased at a high molecular weight (HMW), 720-1080 kDa, and low molecular weight (LMW), 240-360 kDa from Contipro. Hydrogels were characterised with a rotational rheometer. Amplitude sweeps were carried out at a 1 Hz frequency and shear strain from 1-500% to obtain the linear viscoelastic region (LVR). Frequency sweeps were performed from 0.01-100Hz at a 10% strain of the LVR to obtain the shear storage modulus (G'), the shear loss modulus (G''), and the complex viscosity. Swelling profiles of hydrogels were obtained from a weighted 24-hour PBS immersion and enzymatic degradation of hydrogels was carried out through a weight analysis and the Ehrlich's reagent assay. **Peptides Bioactivity:** Bone marrow derived macrophages (BMDM) were extracted from C57/Bl6 mice. BMDM were stimulated with LPS to mimic inflammation and the effect of HA hydrogels and SM16-K66 released from HA was investigated. TNF-α concentration in the supernatant was measured using an ELISA.

RESULTS AND DISCUSSION

Characterisation: A 2% HMWHA has softer mechanical properties compared to a 2% LMWHA at the same enzymatic crosslinking (Fig.1B). This is potentially due to the steric hindrance in the HMWHA preventing crosslinking. LMWHA hydrogels recorded higher and more varied mechanical stiffness with a range of crosslinking concentrations. **Bioactivity:** Stiffer hydrogels composed of LMWHA were seen to invoke a higher TNF-α response compared to softer hydrogels (Fig.1D). The SM16-K66-loaded HA reduced the TNF-α levels working similarly to the peptide only treatment.

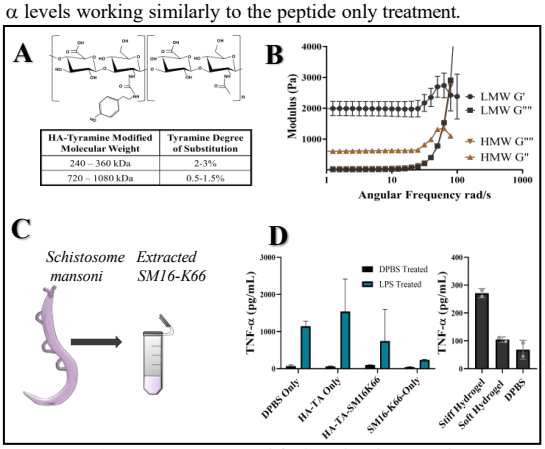

Figure 1:A) HA-Tyramine modified molecular weights with, B) Frequency sweep at different molecular weights. C) Representation of S. mansoni. D)The effect of low molecular weight hyaluronic acid hydrogels mechanical stiffness on macrophages and SM16-K66 treatment.

CONCLUSION

LMWHA hydrogels produced stiffer scaffolds compared to HMWHA. Different stiffness hydrogel models made from LMWHA HA invoked different inflammatory responses in BMDM which will require further investigation. SM16-K66 released from HA reduced TNF-α production indicating its retained bioactivity. This parasitic peptide has future biotherapeutic potential to modulate immune responses to biomaterials.

REFERENCES

1-Shielsid J.*et al*.,J. PLoSNegl Trop Dis,14(7):1-25 2020

ACKNOWLEDGMENTS

I would like to thank the AMBER SFI (SFI/12/RC/2278) for providing financial support to this project.

Immunomodulatory Microgels for Wound Healing Applications

Sepideh Mohammadi[1*], Hossein Ravanbakhsh[1], Sareh Taheri[1], Guangyu Bao[1], Luc Mongeau[1]

[1]Department of Mechanical Engineering, McGill University, Montreal, Canada
[*] sepideh.mohammadi@mail.mcgill.ca

INTRODUCTION

The formation of scars that consist of fibrous connective tissues is a natural consequence of injury when an incisional wound heals in soft tissues. Using biomaterials to control macrophage polarization illuminate a way to combat fibrosis and enhance healing. So far, however, such immunomodulatory scaffolds have lacked interconnected micropores to promote cell ingrowth. Existing materials limitations also include invasive delivery procedures and harsh synthesis conditions that are incompatible with drug molecules.[1] Here, we report hybrid nanocomposite microgels containing interleukin-10 (IL-10) to modulate tissue macrophage phenotype during wound healing.

EXPERIMENTAL METHODS

To synthesize microgels, precursor solutions were prepared by mixing different amounts of IL-10 -loaded Laponite with methacrylated gelatin/methacrylated hyaluronic acid polymer solution. Aqueous droplets were produced using the water-in-oil emulsion technique. Crosslinked beads instantly formed upon the addition of the initiator solution to the emulsion and through redox polymerization.

Fluorescence microscopy of Thp-1 derived macrophages and vocal fold fibroblasts was performed using a confocal laser scanning microscope. The controlled release property of the microgels was assessed by ELISA. An atomic force microscope was used to perform microindentation tests to estimate the microscale Young's modulus of the sample.

A sample size of $N \geq 3$ was used for all tests. Statistical analysis was performed using an unpaired Student's t-test or by one-way or two-way ANOVA.

RESULTS AND DISCUSSION

The intercalation of laponite nanoparticles in the polymer network yields microgels with tissue-mimetic elasticity (Young's modulus in the range of 2 to 6 kPa) and allows the sustained release of IL-10 to promote the differentiation of macrophages towards pro-regenerative phenotypes (Figure 1). The porous interstitial spaces between microgels promote fibroblast proliferation and trafficking. The co-culture of macrophages and fibroblasts treated with transforming growth factor-beta 1 resulted in a 2-fold reduction in collagen-I production for microgels releasing IL-10 compared to the IL-10 free group (Figure 2).

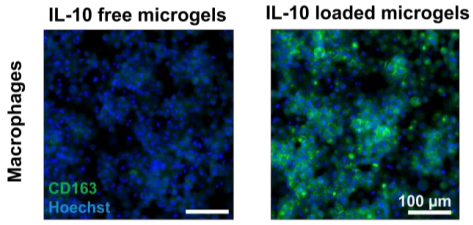

Figure 1. Confocal imaging showing expression of CD163 in co-cultured macrophages after 8 days.

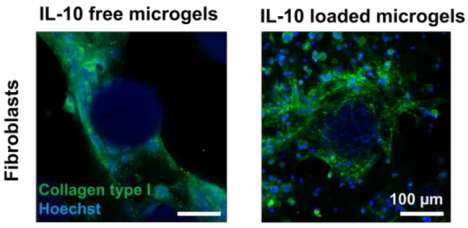

Figure 2. Confocal imaging showing collagen-I secretion by fibroblasts after 8 days of culture on different microgels.

CONCLUSION

This study supports the potential of the new microgels to harness the anti-fibrotic behavior of host macrophages toward regenerative healing. Combined with the microgel injectability, these results present these multifunctional hydrogel beads as a promising cell-instructive system in wound healing applications.

REFERENCES

1. Mohammadi S. et al., Advanced Healthcare Materials. 5:2102366, 2022

ACKNOWLEDGMENTS

This work was supported by the National Institute on Deafness and Other Communication Disorders. The content is solely the responsibility of the authors and does not necessarily represent the official views of the National Institutes of Health. The authors also thank the Advanced BioImaging Facility (ABIF, McGill University) and the Facility for Electron Microscopy Research (FEMR, McGill University) for providing access to their facilities. S.M. thanks McGill Engineering Doctoral Award (MEDA) and Fonds de recherche du Québec - Nature et technologies (FRQNT) - Bourses de doctorat (B2X) for their support.

A New Sequentially Functionalised Collagen I Based Visible Light Crosslinked Hydrogel for Chondrocyte Encapsulation

Ahranee Canden[1*], Hazel Fermor[1,2], Xuebin B Yang[3], Giuseppe Tronci [3,4] and Claire Brockett [1]
[1] Institute of Medical and Biological Engineering, University of Leeds, Leeds UK
[2] Faculty of Biological Sciences, University of Leeds, Leeds UK
[3] School of Dentistry, St; James's University Hospital, University of Leeds, Leeds UK
[4] Clothworkers' Centre for Textile Materials Innovation for Healthcare, School of Design, University of Leeds, Leeds UK
***mnac@leeds.ac.uk**

INTRODUCTION

Autologous matrix-induced chondrogenesis (AMIC) has existed as a therapeutic technology for many years to treat chondral defects. Hydrogels provide a promising platform for such biocompatible materials as they can fill a defect site and exhibit similar physical characteristics as seen by native hyaline cartilage. As a platform, hydrogels are also tuneable, as they can be functionalised to change their mechanical properties or biofunctionality. However, in the case of chondral defects, studying how bone marrow or mesenchymal stem cells (MSCs) behave within these scaffolds, especially with regards to cell survival and differentiation, is imperative to understanding the capabilities of such materials for potential AMIC treatments.

UV-cured 4-vinylbenzyl chloride (4VBC)-functionalised collagen hydrogels have previously been shown to inhibit the activity of matrix metalloproteases (MMPs) in chronic wound healing. Such MMPs are upregulated in the joint space of arthritic tissue and cause further degradation of the cartilage. Thus, it is hypothesised that this hydrogel would promote improved cartilage regeneration by promoting a phenotypic change in chondrocytes from the arthritic, hypertrophic phenotype to a regenerative state.

This study aims to develop a new sequentially functionalised collagen I based hydrogel utilising visible light crosslinking for encapsulation of chondrocytes to assess how cells are able to disperse throughout the gel.

EXPERIMENTAL METHODS

Type I rat tail collagen (RTC) was extracted in-house using a previously established method[1], and sequentially functionalised with both 4VBC and methacrylic anhydride (MA) using a modified version of a previously published method[2]. 2,4,6-Trinitrobenzenesulfonic acid colourimetric assay was performed to assess free amino content and degree of functionalisation[1]. The sequentially functionalised precursor was solubilised in 10 mM HCl solution to reach a final collagen concentration of 8 mg.mL^{-1}. The solution was neutralised using 1M NaOH solution, supplemented with Lithium phenyl- 2,4,6-trimethylbenzoylphosphonate (0.5 wt.% in PBS) and with an immortalised chondrogenic cell ATDC-5 (1.6 x10 ^{5} cells mL^{-1}) and cured for 7 mins at 405 nm light. Scaffolds containing cells were washed in a PBS wash for 2 X 10 mins and then left to grow in the medium for 24h. Cells were observed by confocal imaging using cell tracker green.

RESULTS AND DISCUSSION

The degree of functionalisation of the scaffold showed that the free amine group molar content was reduced initially by 25 mol.% relating to the addition of 4VBC moieties. A 69 mol.% functionalisation was seen following the reaction with MA moieties. The resultant hydrogels produced were uniform with a consistent morphology and size of 5 mm diameter and appeared to maintain the shape; little to no changes in size were seen after 24h in media. Encapsulation of ATDC-5 cells within the scaffolds showed viable cells evenly distributed throughout the scaffold. The cells can be seen to be evenly distributed throughout the hydrogel (Fig 1).

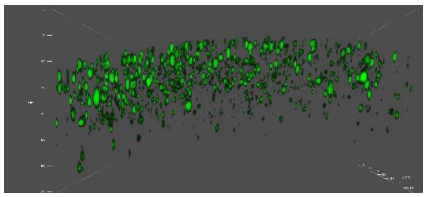

Fig1 Confocal microscopy of ATDC-5 chondrogenic cells following 24 h culture in the 4VBC-MA hydrogel. Cells are stained with CellTracker Green.

CONCLUSION

Here we have presented a method to assess the behaviour of cells within this sequentially functionalised collagen hydrogel. This subsequently will provide a platform to assess the ability of this scaffold to promote differentiation and formation of cartilage tissue from MSCs encapsulated in the scaffold, whilst allowing us to assess the production of new extracellular matrix deposition and differentiation potential of the cells within the 4VBC-MA scaffolds. Assessment of the mechanical swelling properties of the hydrogel will be performed to further understand how different cells behave within the hydrogel for longer durations.

REFERENCES

[1] G. Tronci, S. Russell, D. Wood, *Journal of Materials Chemistry B* 2013, *1*.
[2] H. Liang, J. Yin, K. Man, X. Yang, E. Calciolari, N. Donos, S. Russell, D. Wood, G. Tronci, *Acta Biomaterialia* 2022, *140*.

ACKNOWLEDGMENTS

The authors would like to thank the EPSRC (EP/LO14823/1) for providing financial support to this project.

Nanocomposite Hydrogel of Phosphorous-containing Nanocellulose and Bionanoceramics and Its Impact on the Osteogenic Differentiation of Osteoblasts in Scaffold Cell Culture

Qingbo Wang[1], Özge Karadas[2], Tuomas Näreoja[2, 3, 4], Xiaoju Wang[1, 2]
[1] Laboratory of Natural Materials Technology, Åbo Akademi University, Turku, Finland.
[2] Pharmaceutical Sciences Laboratory, Åbo Akademi University, Turku, Finland
[3] Molecular Biotechnology & Diagnostics, Dept. of Life Technologies, University of Turku, Turku, Finland
[4] Division of Pathology, Department of Laboratory Medicine, Karolinska Institutet, Huddinge, Sweden
*xwang@abo.fi

INTRODUCTION

Biomedical hydrogels are one intriguing profiling area for wood-derived cellulosic nanomaterials and biopolymers, where in lieu of their synthetic counterparts they offer not only sustainability but also many clinically preferred characteristics as biomaterials[1]. Cellulose nanofibers (CNFs) are made by reducing wood cellulose fibers into small elementary fibrils through a top-down method of defibrillation. These nanofibrils are produced in nanoscale diameter and microscale length and typically demonstrate a hydrophilic and stiff gel consistency even at a rather low aqueous concentration (0.5-0.7 wt%), mainly due to physical entanglement and electrostatic repulsion among these tiny but flexible fibers with a high-aspect-ratio. The chemical nature and charge density of surface-modified groups on the CNFs can accommodate application-specific requirements to facilitate cell-biomaterial interactions. In the context of bone tissue regeneration, phosphorous-containing biopolymers have been applied to expedite the biomineralization of damaged bone tissue by stimulating the function of phosphorous groups in natural bones[2]. Inspired by these research findings, it is hypothesized that phosphorous-containing cellulose nanofiber (P-CNF) can be a suitable biomaterial for fabricating a hydrogel matrix with its sufficient rigidity, ECM-mimicking morphology, strong mechanical properties, high water-retention, and capacity for augmented biomineralization.

EXPERIMENTAL METHODS

When fabricating tissue engineering scaffolds, the nanocomposite approach is integrative to increase the bio-relevant functions of the hydrogel and even to embed biological cues in it in order to direct cell response. In our research endeavor, we have engaged the P-CNF as a major constituent in a nanocomposite hydrogel matrix laden together with bioactive glass nanoparticles (BaGNP) of 80SiO2-20CaO. Meanwhile, photoreactive biopolymers, methacrylated gelatin (GelMA) and methacrylated galactoglucomannan (GGMMA) were introduced as auxiliary biopolymers to tune the mechanical stiffness of the hydrogel through the photo-crosslinking of methacryloyls triggered by UV at 405 nm. The as-proposed hydrogel formulation is also printable via hydrogel extrusion 3D printing synchronizing with photocrosslinking. 3D hydrogel printing of this kind is of high efficiency to produce hydrogel constructs with digitally designed geometry. Through a conventional lyophilization process, macroporous but mechanically robust nanocomposite cryogels of P-CNF/GelMA+GGMMA/BaGNP can be conveniently fabricated in clinically relevant shapes.

RESULTS AND DISCUSSION

When immersed in simulated body fluid (SBF), the release of inorganic ions (Si and Ca ions) from BaGNP within the swollen hydrogel can locally induce deposition of the CaP-rich phase along the polymeric matrix composed of the hydrogel. Currently, we are carrying out the cytocompatibility and cell-matrix interaction study by culturing MC3T3-E1 pre-osteoblast cells on these scaffolds. We focus on revealing the impact of the phosphorylation modification in such a biomaterial system on osteogenic differentiation of pre-osteoblasts by evaluating the alkaline phosphatase (ALP) activity, biomineralization, and osteogenic cell differentiation. More results will be presented in detail to ESB 2022.

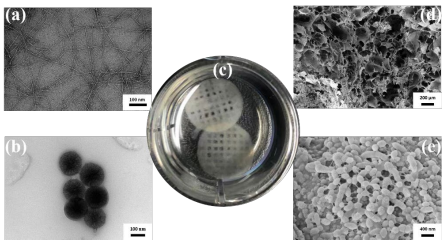

Figure 1. Illustration on (a) TEM image of P-CNF; (b) TEM image of BaGNP of 80SiO2-20CaO; (c) 3D printed hydrogel construct of P-CNF/GelMA+GGMMA/BaGNP preserved in PBS buffer; (d) Cross-section SEM image of a cryogel scaffold of P-CNF/GelMA+GGMMA/BaGNP; and (e) Local deposition of the CaP-rich phase along with the polymeric matrix in the hydrogel scaffold of P-CNF/GelMA+GGMMA/BaGNP immersed in SBF for 7 days.

REFERENCES

1. Wang, X. *et al*., Bioengineering 7:40, 2020
2. Watson, B. M. *et al*., Biomed. Mater., 9: 025014, 2014

ACKNOWLEDGMENTS

The authors would like to thank Academy of Finland (Grant no: 333158) and Jane and Aatos Erkko Foundation for providing financial support to this project.

Swelling Force of Hydrogel Tissue Expander Induces Intestinal Lengthening

Sasza Chyntara Nabilla[1], Ren-Jei Chung[2], Jan T. Czernuszka[1]
[1]Department of Materials, University of Oxford, Oxford, United Kingdom
[2]Department of Chemical Engineering and Biotechnology, National Taipei University of Technology, Taipei, Taiwan
* sasza.nabilla@materials.ox.ac.uk

INTRODUCTION

Crohn's disease (CD) is associated with transmural inflammation in regions throughout the gastrointestinal (GI) tract but is most likely to develop in the ileum or colon. Up to 80% of CD patients require at least one surgical resection within 10 years of diagnosis[1]. A single massive resection or multiple repeated resections lead to short bowel syndrome (SBS). It is the condition when intestinal length remnant less than 180 cm and often disabling malabsorptive condition associated with significant morbidity and mortality[2]. Therefore, a new therapy to address CD is needed. It is well-known that the tissue can grow in response to mechanical force. In this study, the mechanical force generated from hydrogel tissue expander is used to stimulate lengthening and growth of the intestine. VP/MMA hydrogel was placed inside the animal models. The increase in the total amount of intestinal lengthening could be achieved without compromising intestinal function.

EXPERIMENTAL METHODS

VP/MMA hydrogel with the composition ratio of 85:15 wt% (n=3) was chosen for swelling force measurement. It was measured using Denser Mayer Group Instrument with the maximum load of 3 kN. Water was filled into it until the height of the hydrogel was all covered. The hydrogel began to swell and started to detect the force reading. Data were collected every hour until the force reaches an equilibrium state. The ex-vivo study was conducted. Hydrogels were attached perpendicular to the top and bottom sides of the stainless steel (SS) plate. Holes were created in each plate and the intestine was inserted through the holes. Both ends of the intestine were sutured with metal plates. The devices (n=3) were immersed in DI water to allow hydrogel to swell and stretch the intestine. The length of the intestine was measured as a function of time. *In vivo* study was implemented in the Sprague-Dawley (SD) rats with the age of 3–4-week-old. The experiment was divided into three groups such as normal (n=4), isolated-control (n=4), and stretched-intestine (n=4). On postoperative 1 and 7 days, the animal was sacrificed. The final lengths were measured, and the histology of the intestine was observed using H&E staining.

RESULTS AND DISCUSSION

The swelling forces of the VP/MMA hydrogel as a function of time are shown in Figure 1. As time increases, the swelling force shows significantly increased until reaches an equilibrium. The equilibrium swelling force is 4.9 ± 0.14 N. The swelling force is affected by decreasing water-soluble VP content over the stiffer and hydrophobic MMA.

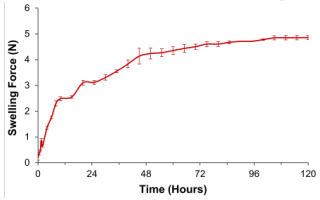

Figure 1. The swelling force of VP/MMA hydrogel as a function of time

The result of the ex-vivo study shows that the stretched intestine lengthens the intestine from 2 mm to 4.1 ± 0.18 mm, 4.3 ± 0.20 mm, and 4.48 ± 0.18 mm on days 0, 1, 3, and 7, respectively. This represents a 2.2-fold increase in length. Successful intestinal lengthening and thickening are observed on days 1 and 7 in-vivo studies. The initial length of the intestine before being stretched is 2.26 ± 0.11 mm. The lengthening ratio of hydrogel on day 1 (n=4) and day 7 (n=4) are 1.27 ± 0.08 and 1.34 ± 0.07, respectively. In contrast, there is no significant change in the isolated-control intestine. H&E staining results show that the normal intestine has an average thickness of 74.34 ± 16.1 µm and 436.5 ± 53.7 µm for muscular and non-muscular layers, respectively. The average thickness of muscular and non-muscularis layers in the stretched segment is increased to 120.4 ± 26.2 µm and 561.2 ± 72.3 µm, respectively, on day 7.

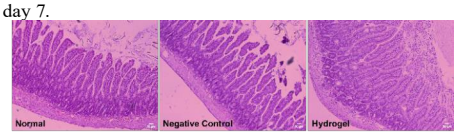

Figure 2. H&E of normal, isolated-control, and stretched-intestine

CONCLUSION

Hydrogel tissue expander device can induce intestinal lengthening through the swelling force generation. The hydrogel device does not compromise bowel function and results in a 2.2-fold increase in intestinal length.

REFERENCES

(1) Farmer RG, Whelan G, Fazio VW. Gastroent. 88:1818-25, 1985
(2) Jon ST, Kishore R.L, John KD, Renee LY, Cindy RB, Alam NL, Gastroint Surg. 8:1069-72, 2003

ACKNOWLEDGEMENT

This work has received support from the National Taipei University of Technology, Taiwan

U Can't Touch This: anti-adhesive PEG hydrogels with improved mechanical properties for blood-contacting devices

Helena P. Ferreira[1,2,3*], Duarte Moura[1,2,4], Andreia T. Pereira[1,2], Patrícia C. Henriques[1,2], Cristina C. Barrias[1,2,3], Fernão D. Magalhães[5], Lorenzo Moroni[6], Inês C. Gonçalves[1,2]

[1] i3S – Instituto de Investigação e Inovação em Saúde, Universidade do Porto, Porto, Portugal [*] helena.ferreira@i3s.up.pt
[2] INEB – Instituto de Engenharia Biomédica, Universidade do Porto, Porto, Portugal
[3] ICBAS – Instituto de Ciências Biomédicas Abel Salazar, Universidade do Porto, Porto, Portugal
[4] FEUP – Faculdade de Engenharia, Dep. Engenharia Metalúrgica e Materiais, Universidade do Porto, Portugal
[5] LEPABE – Laboratório de Engenharia de Processos, Ambiente, Biotecnologia e Energia, FEUP, Porto, Portugal
[6] MERLN – Institute for Technology-Inspired Regenerative Medicine, Maastricht University, Maastricht, Netherlands

INTRODUCTION

Blood-contacting devices (BCD) have a crucial role in the management of cardiovascular diseases, the #1 cause of death worldwide. However, implantable BCD still face issues of thrombosis and infection.[1] Here, we propose the reinforcement of polyethylene glycol (PEG) hydrogels – non-fouling, highly tunable – with graphene oxide (GO) nanomaterials – outstanding mechanical strength – to be used as a bulk material for the fabrication of BCD.[2] Furthermore, we explore the application of PEG/GO composite hydrogels for the additive manufacturing of BCD by extrusion-based embedded 3D printing,[3] particularly recurring to a support bath and different thickeners to increase the viscosity of the inks.

EXPERIMENTAL METHODS

Hydrogels of 15%w/v PEG dimethacrylate (MW 8 kDa), with 0 or 4%w/v graphene oxide (GO; 30%O) were produced by chemical crosslinking, using redox initiators (0.1%APS and 0.1%SMB). The mechanical properties of neat PEG and PEG/GO composite hydrogels were evaluated by tensile tests using a texture analyser. The cytotoxicity of 24h extracts was tested using HUVEC, assessing metabolic activity (resazurin) and morphology (phalloidin/DAPI staining). The anti-adhesiveness was evaluated by directly seeding on top of hydrogels either HUVEC (observed by phalloidin/DAPI staining), human platelets or *S. aureus* (observed by SEM). Envisioning 3D printing of PEG/GO formulations, both inks and support baths were characterized by viscosimetry assays using a Kinexus rheometer. A 22.5% Pluronic F-127 with 0.5%APS+ 0.5%SMB was considered for the support bath. To increase inks' viscosity, we explored: (i) adding redox initiators to the ink and allowing for partial gelation; (ii) adding thickeners (alginate, carboxymethyl cellulose (CMC), polyvinylpyrrolidone, polyvinyl alcohol (PVA) or Kolliphor P407).

RESULTS AND DISCUSSION

The incorporation of 4%GO in PEG hydrogels resulted in composites 6x stiffer, 14x stronger and 1.7x more elastic than neat PEG hydrogels. These PEG/GO composites presented 163kPa Young's modulus, 218kPa ultimate tensile strength and 126% elongation at break. These values are close to mechanical stresses exerted in BCD such as vascular grafts.[4] The extracts obtained from neat and composite hydrogels caused no cytotoxicity on HUVEC (cell viability ~100%), and phalloidin staining revealed a normal morphology (vs. control medium). When seeding HUVEC, platelets or *S. aureus* on top of neat or composite hydrogels, images reveal that none adhered, proving that PEG/GO hydrogels are as anti-adhesive as neat PEG hydrogels.

After validating these material requirements in 2D, we aimed to optimize the production of 3D structures using PEG/4%GO formulation. Because gelation occurs via chemical crosslinking, we hypothesized that a support bath with APS and SMB would allow the diffusion of these redox initiators from the bath to the ink, resulting in gelation. Viscosimetry assays revealed that a Pluronic bath with 0.5% initiators presented a ~160Pa·s viscosity ($1s^{-1}$ shear rate). It was also necessary to increase the PEG/GO ink's viscosity (it was too fluid to be printed). Firstly, we tried adding redox initiators to the ink and allowing for partial gelation, but tuning their concentration (from 0.025% to 0.1%) did not increase the printability window (15-25min), proving this strategy unsuitable. Also, different thickeners were assessed. Viscosimetry assays showed that alginate, PVA and CMC significantly increased ink's viscosity, up to values similar to Pluronic bath (~100Pa·s), proving the potential of these components to improve the extrusion of PEG/GO ink. After producing PEG/4%GO hydrogels in the presence of these thickeners and thorough washing to remove them, we observed that, although all formulations remained anti-adhesive towards blood platelets, hydrogels produced in the presence of alginate and CMC had lower Young's moduli (132 and 79kPa, respect.), while PVA did not affect stiffness (161kPa).

CONCLUSION

We have produced a biocompatible, antithrombogenic, antimicrobial PEG/GO composite hydrogel, with good mechanical properties for load-bearing BCD. PEG/4% GO inks can be improved for 3D printing by addition of thickeners like alginate, PVA or CMC, and potentially be extruded into a Pluronic support bath with crosslinking initiators. Particularly, the inclusion of PVA appears to not affect the antiadhesive or tensile properties of the final PEG/GO composite hydrogels. This work paves way for the use of PEG/GO hydrogels in production of BCD like vascular grafts or heart valves, particularly by extrusion-based embedded 3D printing.

REFERENCES: 1. Jaffer I. *et al.*, Acta Biomater. 94:2-10, 2019; **2**. Ferreira H. *et al.*, Int. J. Mol. Sci. 23:2312, 2022; **3**. Shiwarski D. *et al.*, APL Bioeng. 5, 010904, 2021;**4**. Hasan, A. *et al.*, J. Biomech. 47:1949-1963, 2014

ACKNOWLEDGMENTS
The authors thank FCT and FEDER for projects POCI-01-0145-FEDER-032431 and UIDB/04293/2020, and PhD fellowship 2020.04712.BD.

Biomimetic Hydrogel Formulation via Machine Learning for Bioprinting

Alexander David Stokes, Priscila Melo, Piergiorgio Gentile, Jaume Bacardit, Ana Marina Ferreira.

Schools of Engineering and Computing, Newcastle University Newcastle upon Tyne, UK

a.stokes2@ncl.ac.uk

INTRODUCTION

Hydrogels can provide a suitable 3D environment for chondrocytes to produce new cartilage, though currently, biomimetic hydrogels with adequate load-bearing potential are yet to succeed[1]. This hydrogel mimics the principal components of the chondrocyte's extracellular matrix, glycosaminoglycans and collagen, using chondroitin sulphate (CS) and gelatin (GEL), respectively, with 4-arm polyethylene glycol (PEG) as a spacer agent to provide structural support. The three polymers are chemically crosslinked to form a hydrogel with high mechanical properties. The ideal concentrations and ratios to formulate this new hydrogel are undefined. A Machine learning algorithm is under development to predict the mechanical and rheological properties of potential materials based on varied inputs such as the concentration of polymer precursors. The algorithm should also suggest potential formulations, which can be processed and validated through printing experiments.

In the first stage of this work, it was hypothesised that the concentrations of gel precursors (GEL, PEG, CF) and crosslinker (EDC/NHS) could be tuned with the help of machine learning to produce a bioink processable via extrusion printing, that once optimised can incorporate chondrocytes in attempt to mimic the cartilaginous tissue. The main objectives are:

1. To study the influence of the concentration of gelatin (GEL) and EDC/NHS on the rheological properties of the materials to assess their printability.
2. To determine the compressive strength of casted discs.
3. Feed the experimental data into the machine learning algorithm to optimise it.
4. Tune the formulation of promising materials for bioprinting.

EXPERIMENTAL METHODS

27 different formulations of hydrogel were tested with:

- Mechanical testing: compression under 65% strain until fracture.
- Rheology: 1) flow ramp at 37°C under a wide range of shear rates (0.01-1000s^{-1}); 2) time sweep followed by a temp sweep with settings at 37°C fixed strain 1% and 1Hz for 2h, 25-90°C heating rate 5 °C/min respectively.

In the next stage of this project results from the tests will be fed into a supervised machine learning algorithm, with a leave-one-out cross-validation for the train-test split and linear regression as the regression algorithm. Using the final trained model, we aim to identify the best parameters for which the model predicts ideal and desirable rheological and mechanical properties. Formulation of this new hydrogel will allow the validation of the algorithm's predictions.

RESULTS AND DISCUSSION

Early results on the rheological characterisation show a concentration of GEL in the precursor solution (Fig. 1) resulted in higher viscosity at given shear rates for their respective formulations. This trend was also seen in the increase in EDC/NHS. All materials are shear-thinning. However, their viscosity is too high compared to the literature[2], implying these formulations might not be processable using 0.25 mm nozzles. An increase in nozzle size could prevent clogging but would sacrifice the printing resolution. Therefore, the formulation must be optimised.

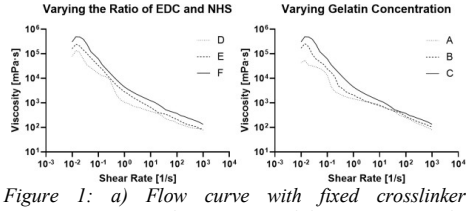

Figure 1: a) Flow curve with fixed crosslinker concentration and ratio, while varying the concentration of GEL, A = 15% [GEL], B = 20% [GEL], C = 25% [GEL] b) fixed GEL and crosslinker concentration, while varying the ratio of EDC and NHS, D = 1:1 EDC:NHS, E = 2:1 EDC:NHS, F = 4:1 EDC:NHS.

Preliminary results from compression testing show that the hydrogel's Young's Modulus can range from 30 to 200 kPa, which is within the desired range for cartilage applications, 100kPa and higher[1].

CONCLUSION

A biomimetic and bioprintable hydrogel is formulated with potential for biocompatibility and chondrogenesis, due to the use of polymers found in the ECM of cartilage and high modulus. A new method of synthesising hydrogels is currently under development using machine learning, with the aim to improve efficiency, and saving costs by reducing material waste. The method is customisable and easily adaptable for the use case of the researcher.

REFERENCES

1. Stokes. *et al*. Biomimetic hydrogels designed for cartilage tissue engineering. Biomaterials Science. 2021;9(12):4246-59.
2. Cuomo F. *et al.* Rheological characterisation of hydrogels from alginate-based nanodispersion. Polymers. 2019 Feb;11(2):259.

Self-synthesizing materials for tissue culture applications

K. Mikhailov[1*], I. Marić[1], L. Yang[2], R. Bron[2], P. van Rijn[2] and S. Otto[1]

[1]Stratingh Institute for Chemistry, University of Groningen, Nijenborgh 4, 9747 AG Groningen, the Netherlands
[2]University Medical Center Groningen, Department of Biomedical Engineering and W. J. Kolff Institute, University of Groningen, Antonius Deusinglaan 1, 9713 AV, Groningen, the Netherlands
*k.mikhailov@rug.nl

Key words: hydrogels, supramolecular chemistry, tissue engineering

INTRODUCTION

Peptide-based hydrogels are important materials in cell culture research due to their close resemblance to the extracellular matrices, which allows their utilization as scaffolds for tissue engineering, wound healing and drug delivery[1,2]. In recent years, hydrogels were successfully applied in a wide variety of materials[1,2]. In this work, we report on the creation of cell-compatible self-synthesizing peptide-based hydrogel scaffolds that can be used in tissue culture applications. Cells as a living material would potentially benefit from a material that also displays life-like character in terms of spontaneous emergence of a highly ordered self-assembled supramolecular structure from a complex mixture of simple molecules. Hence, here we combine a new conceptual hydrogel approach as a cell culture platform.

EXPERIMENTAL METHODS

Oxidation of a peptide building block modified with a thiol-containing moiety at the C-terminus and with a hydrazide moiety at the N-terminus (**1**) results in a dynamic equilibrium of various sized macrocycles upon stirring (Figure 1).

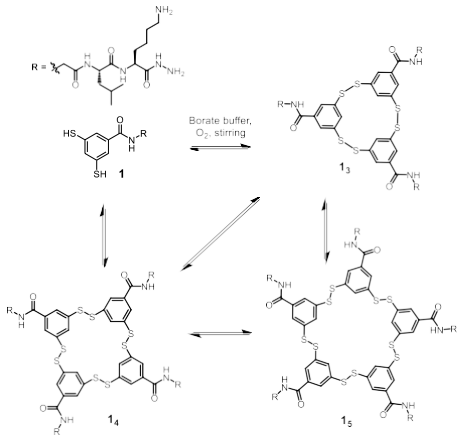

Figure 1. Formation of dynamic combinatorial library

Out of the mixture, only pentamers $\mathbf{1_5}$ stack on each other and form fibers that have hydrazide groups on their surfaces. When the dynamic combinatorial library is dominated by $\mathbf{1_5}$, this network of fibers is cross-linked with a dialdehyde to form a hydrogel. The $\mathbf{1_5}$ fibers can also be modified with aldehyde-containing molecules via the same hydrazone linkage, which opens vast possibilities of hydrogel modifications with bioactive peptides and other moieties.

RESULTS AND DISCUSSION

These novel, innovative hydrogels were used for cell culture experiments to determine their biocompatibility and cell proliferation. Three types of samples were investigated: unmodified hydrogel ($\mathbf{1_5}$) and hydrogels modified with 10 mol % glyoxylyl-functionalized RGD ($\mathbf{1_5}$**-RGD**) and LDV ($\mathbf{1_5}$**-LDV**) peptides. All hydrogels showed cell viability and good spreading in live/dead staining experiments after 24 hours of culturing (Figure 2a, b) [3].

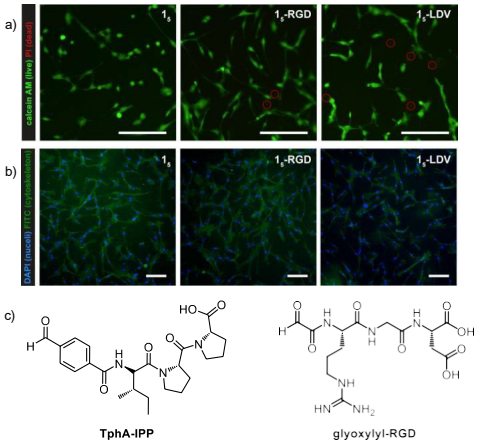

Figure 2. (a) Live/dead staining with calcein-AM (alive cells, green) and propidium iodide (dead cells, red) of hBM-MSCs of the hydrogel samples after 24 h. (b). DAPI (nuclei, blue) and FITC-phalloidin (cytoskeleton, green) staining, after 24 h. Scale bars equal 150 µm. (c) Chemical structures of ***TphA-IPP*** *and* ***glyoxylyl-RGD****.*

To evaluate the properties of the modified hydrogel as a biological scaffold, we are currently investigating the process of osteogenic differentiation on Saos-2 osteoblast-like cells and hBM-MSCs. For this purpose, we have synthesized terephthalaldehydic modified IPP peptide (**TphA-IPP**, Figure 2c), which has a positive influence on osteoblast function [4].

CONCLUSION

Here we show the development of biocompatible and self-synthesizing hydrogel, which can be applied as a tissue engineering scaffold. The osteogenic differentiation studies utilizing these hydrogels as scaffolds are currently in progress.

REFERENCES

1. X. Ding *et al.*, *Adv. Drug Deliver. Rev.*, **2020**, *160*, 78–104
2. J. Li *et al.*, *Soft Matter*, **2019**, *15*, 1704-1715
3. I. Maric, Unpublished results.
4. M.M. Huttunen *et al.*, *J. Nutr. Biochem.*, **2008**, *19*, 708–715

Biopolymer hydrogels for 3D *in vitro* modelling of rheumatoid arthritis synovial tissue

Nora Selicato[1], Antonella Stanzione[1,2], Beatrice Vilardo[3,4], Francesca Scalera[1], Annalisa Chiocchetti[3,4], Alessandro Polini[1], Francesca Gervaso[1]

[1] CNR NANOTEC – Institute of Nanotechnology, Campus Ecotekne, via Monteroni, 73100 Lecce, Italy
[2] Dipartimento di Matematica e Fisica E. de Giorgi, Università Del Salento, Campus Ecotekne, via Monteroni, 73100 Lecce, Italy
[3] Dipartimento di Scienze della Salute, Interdisciplinary Research Center of Autoimmune Diseases-IRCAD, Università del Piemonte Orientale, Novara, Italy
[4] Center for Translational Research on Autoimmune and Allergic Diseases, University of Piemonte Orientale, Novara, Italy
nora.selicato@nanotec.cnr.it; francesca.gervaso@nanotec.cnr.it

INTRODUCTION

Rheumatoid arthritis (RA) is an autoimmune inflammatory disorder, primarily characterized by synovial joint inflammation affecting ~0.5 to 1% of the overall population[1]. There is no cure and, currently, there are not disease-relevant *in vitro* models. To gain deeper insight into its pathogenesis and facilitate the drug screening, advanced *in vitro* models able to mimic the articular joint are required. In this frame, hydrogels are 3D networks able to model the extracellular matrix (ECM) and provide an *in vivo*-like microenvironment.

In arthrisis, inflammatory reaction primarily affects the inner layer of the joint capsule and the sublining layer of the synovial membrane[2] and fibroblast-like synoviocytes (FLSs) or Type-A synovial cells are one of the most important resident cells of the synovial joints. In RA, synovium is characterized by synovial lining hyperplasia, and FLSs play an important role in the pathogenesis of RA[3]. In order to match the synovial tissue composition and to better understand the biomechanical effect of matrix on the synovial cells, two biopolymers (chitosan, Ch, and gelatin methacrylate, GelMA)[4,5] were chosen to prepare two different stimuli (thermo- or photo-) responsive hydrogel systems.

EXPERIMENTAL METHODS

Ch hydrogel was prepared following a previously reported optimized protocol[4]. Gelatin was chemically modified to obtain GelMA and allow its subsequent photo-crosslinking[5]. GelMA hydrogel (10% w/v) was prepared by dissolving GelMa in PBS containing the UV photoinitiator (Irgacure 2959, 0.5% w/v), placing the solution inside a mold and irradiating it with UV light for 4 minutes in order to induce the photopolymerization. Both Ch and GelMA hydrogels were characterized from a physical and chemical point of view by rheometry, mechanical testing (stiffness), morphology (scanning electron microscopy, SEM), swelling and stability/degradation tests in physiological conditions. Then, in order to choose the hydrogel formulation for better mimicking the synovial compartment, commercially purchased primary FLSs were encapsulated at optimal seeding density. The interaction between hydrogels and cells and the biological properties of the hydrogels were evaluated testing viability (live/dead staining) and morphology (DAPI-phalloidin staining) post-encapsulation (t0) and on days 1, 4, 7 after encapsulation.

RESULTS AND DISCUSSION

In order to select the best performing hydrogel between Ch and GelMA, their physico-chemical and biological properties were compared.
From a physico-chemical point of view, the Ch-based hydrogel resulted slightly superior, showing a comparable swelling behavior, higher stability in cell culture conditions at long term (24 days), higher mechanical stiffness in compression and a slightly more marked shear-thinning behavior at room temperature than gelatin-based hydrogel.
From a biological point of view, both Ch-βGP and GelMA showed high viability, indicating no cytotoxic effects of biomaterials up to 7 days of culture. However, from the morphological analysis, FLSs embedded in the Ch-βGP and located in the middle of the hydrogel drop showed a round shape, while FLSs 3D-cultured in GelMA hydrogel showed a spindle shape along the whole depth of hydrogel drop at each time point.

CONCLUSION

FLSs in 3D cell culturing condition, showed high viability with both proposed hydrogels but were able to retain long term their cell morphology in GelMA. Subsequent steps aim to obtain a more relevant disease *in vitro* model, including other resident cells of the synovial joints (as macrophage-like synovial cells) and using RA patient-derived primary cells in order to have a physiopathologically relevant model of RA synovia.

REFERENCES

1. Kerschbaumer A. *et al*., Ann. Rheum. Dis. 79, S744–S759 (2020)
2. Rothbauer M. et al., Lab Chip 20, 1461-1471 (2020)
3. Noss E. H. & Brenner M. B., Immunol. Rev. 223, 252–270, 2008
4. Stanzione A. *et al*., Biomater. Sci. 9, 7492–7503, (2021)
5. Yue K. *et al*., Biomaterials 73, 254–271 (2016)

ACKNOWLEDGMENTS

The authors would like to thank European Union's Horizon 2020 Research and Innovation programme under grant agreement No. 953121 (FLAMIN-GO) for financial support.

UV-Cured Collagen Networks as Building Blocks for Advanced Wound Dressings

Charles Brooker[1*], Giuseppe Tronci[1]
[1]Clothworkers' Centre for Textile Materials Innovation for Healthcare (CCTMIH), School of Design & School of Dentistry, St. James's University Hospital, University of Leeds, Leeds, UK
[*]c.brooker@leeds.ac.uk

INTRODUCTION

In light of its major role in wound healing and tissue remodelling, collagen has been successfully applied in a range of biomedical applications.[1] The selection of collagen tissue source and the formation of covalent networks are key to ensure reproducibility, scalable development, and regulation-friendly clinical translation of new medical devices, e.g. wound dressings. Here, type I collagens from three mammalian sources (bovine, porcine, and murine) were covalently functionalised with 4-vinylbenzyl chloride (4VBC) to form UV-cured hydrogels, and the effect of the molecular characteristics of the raw material on the macroscopic hydrogel properties was studied. The UV-cured collagen network with optimal physical properties was subsequently employed as the building block of a multifunctional wound dressing, integrating wound healing capability, infection responsivity, and on-demand antimicrobial activity.

EXPERIMENTAL METHODS

Type I atelocollagens were covalently functionalised with 4VBC[2] and cured (λ= 365 nm) in the presence of a water-soluble photoinitiator (I2959) to generate a covalently crosslinked hydrogel. Resulting systems were characterised from the molecular scale up to the macroscopic scale via e.g. colourimetric (TNBS) assay, circular dichroism, SDS-PAGE, compression testing, and swelling studies.[3] Following freeze-drying and cytotoxicity assessment, the selected collagen network was employed as a collector for electrospun fibres supplemented with a functional dye, e.g. bromothymol blue (BTB).[4] The resulting prototype was assessed with respect to microstructure, dye loading/release, and environmental responsivity.

RESULTS AND DISCUSSION

The dichroic, electrophoretic, and spectral characteristics of the three native collagen samples were comparable. However, lysine content varied depending on the tissue source and was found to be a critical parameter in realising UV-cured hydrogels with controlled macroscopic properties. The lysine content of porcine atelocollagen ($2.32 \pm 0.04 \times 10^{-4}$ mol·g^{-1}) was lower than that of both bovine atelocollagen ($2.60 \pm 0.19 \times 10^{-4}$ mol·g^{-1}) and extracted rat tail collagen ($2.65 \pm 0.05 \times 10^{-4}$ mol·g^{-1}). The 4VBC-reacted bovine product exhibited a higher degree of functionalisation (F= 21 mol.%) than the porcine variant, and generated UV-cured hydrogels with increased gel content (G= 97 ± 1 wt.%) and compression modulus (Ec= 79 ± 25 kPa), as well as decreased swelling ratio (SR= 1796 ± 239 wt.%). The swelling and compressive properties of the three gels are summarised in Figures 1a and 1b, respectively. The freeze-dried bovine network enabled the deposition of dye-loaded fibres, with high loading efficiencies (≥ 99 wt.%). This result was also supported by the prompt colour change of the construct following incubation in varied pH.

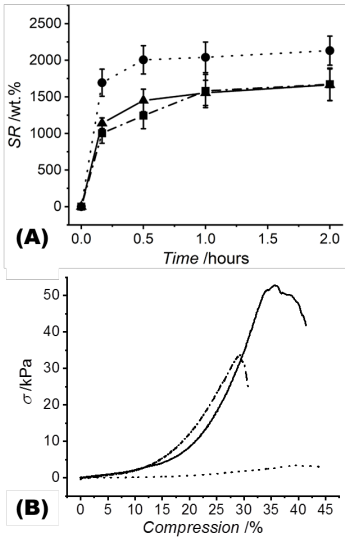

Figure 1. (A) SR profiles of dry UV-cured collagen networks in 10 mM PBS (pH 7.4, 25 °C). (B): Stress-compression curves of UV-cured hydrogels. Black dot, Porcine-4VBC*; black dash dot, Bovine-4VBC*; black solid, Murine-4VBC*.

CONCLUSION

Bovine collagen proved to be a commercially available and chemically viable raw material for the development of water-insoluble hydrogels with controlled swelling properties and increased mechanical compliance. These characteristics were harnessed for the creation of a multi-layer wound dressing prototype, to support antibiotic-free wound management and infection detection.

REFERENCES

1. Sorushanova, A. *et al*. Adv. Mater. 31:1801651, 2019
2. Liang, H. *et al*., Front. Chem. 6:626, 2018
3. Brooker, C. *et al*., Prosthesis 4:1-14, 2022
4. Bazbouz, M.B. *et al*., Sensors 19:991, 2019

ACKNOWLEDGMENTS

The authors gratefully acknowledge financial support from the Clothworkers' Company.

Self-assembling peptide gels for articular patella cartilage repair

James Warren[1,2,3], Raelene Cowie[1], Louise Jennings[1], Ruth Wilcox[1], and Hazel Fermor[1,2]

[1] Institute of Biological and Medical Engineering, University of Leeds, Leeds, UK

[2] Faculty of Biological Sciences, University of Leeds, Leeds, UK

[3]Bragg Centre for Materials Research, University of Leeds, Leeds, UK

J.P.Warren@leeds.ac.uk

INTRODUCTION

Osteoarthritic cartilage is associated with a loss of glycosaminoglycans (GAGs) and reduced biotribological function [1]. There is a clinical need for early intervention treatments to restore cartilage function and delay the progression of degeneration. Chondromalacia patella is softening of the cartilage surface of the patella and is associated with patellofemoral pain.

A self-assembling peptide (SAP) hydrogel, combined with chondroitin sulfate (CS), has shown early promise in restoring GAG content and biomechanical function in degenerate cartilage samples [2, 3].

The aim of this study was to develop an *in vitro* GAG-depleted patella model and assess the biomechanical effects following treatment with a SAP:CS self-assembling hydrogel.

EXPERIMENTAL METHODS

Porcine patellae (4-6 month old) were harvested and subject to 0.1% (w/v) sodium dodecyl sulfate (SDS) washes to remove GAGs from the cartilage. Histological and quantitative biochemical analyses were carried out to assess GAG removal and any changes to the tissue architecture (n=6).

Patellae were GAG depleted and then treated by injection with SAP (~ 6 mM) and CS (10 mg) in Ringer's solution through a 30 G needle in a ~10 mm Ø area. Native, GAG-depleted and treated groups (n=6 per group) were characterised mechanically through indentation. The depleted and treated groups were compared to the native group (Kruskal-Wallis, post-hoc Dunn-Bonferronni, $p<0.05$)

Native and GAG depleted paired patellae and femurs were additionally characterized tribologically through wear testing when undergoing a walking gait profile (n=6 per group). The cartilage surfaces were assessed and compared (Mann-Whitney, $p<0.05$) using the ICRS scoring system, surface damage was illustrated through the application of Indian ink.

RESULTS AND DISCUSSION

The GAG depletion process removed 56±12% of the GAGs within porcine patella cartilage (mean ± 95% C.I.). Histological analysis of GAG depleted samples showed GAG loss with the remaining architecture unaffected.

Mechanically, a significant increase in deformation was seen in the GAG depleted group (n=6, $p<0.001$) compared to native. Treated samples showed significant reduction in normalized deformation (n=6, $p<0.05$) compared to depleted. The injected treatment into GAG depleted cartilage restored the deformation to a level similar to the native group, as shown in Figure 1.

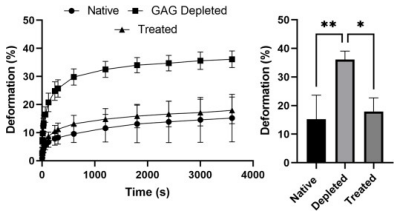

Figure 1. A) Percentage deformation of different patella cartilage states over test duration. B) .Normalised for each sample's cartilage thickness. (n=6, error bars = mean ± S.D) * = p<0.05, **=p<0.001

Wear tests indicated a significant increase in the cartilage damage on the femoral surface of the patellofemoral joint in the GAG depleted group (n=6, $p<0.001$), localised to the medial and lateral regions of the femoral surface with no significant increase in damage on the associated patella surface, as shown in Figure 2.

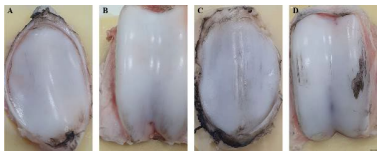

Figure 2. Photographs of cartilage damage following wear testing. A and B) patella and femur from native group. C and D) patella and femur from GAG depleted group.

CONCLUSION

The ~50% reduction of GAGs represented a moderate osteoarthritic patella cartilage model and did not cause observable changes in the tissue architecture or collagen orientation. This loss showed a significant change in the cartilage stiffness response under indentation loading. This same loss transferred to the dynamic wear tests with significant changes in the damage on the femoral counter face associated with the GAG loss. SAP:CS treatment showed promise in restoring cartilage stiffness to treat Chondromalacia patella. Future work will further assess functional repair using the six-axis natural joint simulator

REFERENCES

1 Macri, E. M. *et al*, J. Clin. Med., 9(11):3397, 2020.
2 Barco, A. *et al*, J. Pept. Sci., 24(8-9), 2018.
3 Warren, J. P. *et al*, Adv. Healthcare Mater., 10, 2021.

ACKNOWLEDGMENTS

The authors would like to thank the EPSRC (Grant no: EP/P001076/1) for providing financial support to this project.

Radiopaque Laponite® crosslinked pNIPAM-co-DMAc hydrogel for Tissue Regeneration

Ronak Janani[1], Abdusalam Essa[1], Christine Le Maitre[2], Chris Sammon[1*]

[1]Materials and Engineering Research Institute, Sheffield Hallam University, Sheffield, UK
[2]Biomolecular Sciences Research Centre, Sheffield Hallam University, Sheffield, UK
[*]c.sammon@shu.ac.uk

INTRODUCTION

Degeneration of the intervertebral disc (IVD) is the leading cause for lower back pain worldwide. We have previously reported the development of an injectable Laponite® crosslinked pNIPAM-co-DMAc based hydrogel (NPgel) that undergoes an irreversible rheological transition when cooled to 37°C[1]. NPgel promotes differentiation of stem cells into nucleus pulposus cells without additional growth factors[2,3]. Here we describe incorporation of iohexol into NPgel facilitating visualisation under X-ray during injection. We report the influence of iohexol on the mechanical properties of the NPgel and its *in vitro* impact on human mesenchymal stem cells (hMSCs).

EXPERIMENTAL METHODS

Injection of NPgel (containing 100 mg/mL iohexol) into bovine tails was monitored under X-ray. The physical properties of iohexol-incorporated NPgel were characterised using rheometry and DSC. In addition, the metabolic activity of hMSCs (4x10^6 cells/mL) in NPgel with/without iohexol polymerised for different durations were evaluated using alamar Blue™ over 7 days in cell culture. The release rate of iohexol was determined via USP Dissolution Apparatus 1.

RESULTS AND DISCUSSION

Injection of ≤1000 µl of NPgel into bovine tail was successfully visualised with X-ray imaging (Figure 1). The incorporation of iohexol had a modest impact on the physical properties of the hydrogel, it increased the lower critical solution temperature (LCST) by ~1°C (Table 1) while causing a drop in the storage modulus from 10 kPa to 2 kPa at 1% strain, still well within the physiological range. There was no change in metabolic activity of hMSCs with the addition of iohexol (Figure 2).

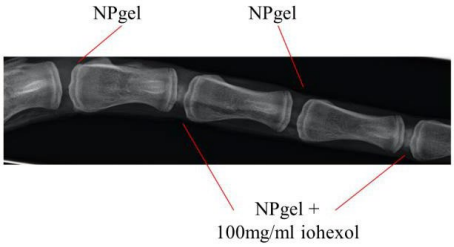

Figure 1: Evidence that iohexol facilitates X-ray visualisation of NPgel post injection into an IVD.

Table 1: DSC of NPgel with and without iohexol to determine the globule to coil transition temperature.

	NPgel	NPgel + 100mg/mL iohexol
DSC T_{onset} (Exo)	37.9	39.5
DSC T_{peak} (Exo)	35.6	37.3
DSC T_{endset} (Exo)	34.2	35.8

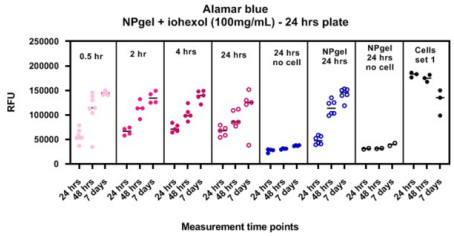

Figure 2: Incorporation of iohexol into NPgel leads to no change in metabolic activity of hMSCs.

CONCLUSION

This study shows the suitability of iohexol for use as the radiopaque agent in NPgel and further supports the use of NPgel as an injectable therapy for IVD regeneration.

REFERENCES

1. Boyes, V. L. *et al.* Polymer. 233:124201, 2021
2. Thorpe, A. A. *et al.* Acta Biomater. 54:212–226, 2017
3. Thorpe, A. A. *et al.* Acta Biomater. 36:99–111, 2016

ACKNOWLEDGMENTS

The authors gratefully acknowledge receipt of funding from Grow MedTech and the European Union's Horizon 2020 Research and Innovation programme (grant agreement no 825925, iPSpine).

Printing versatility of a novel hydrogel material as a key to tissue engineering applications

Martina Meazzo[1], Fabrizio Barberis[2], Catherine Van Der Straeten[1], Peter Dubruel[1]
[1]Ghent University, Ghent, BE, [2]Genova University, Genova, IT, [3] Ghent University Hospital, Ghent, BE
Martina.Meazzo@UGent.be

INTRODUCTION

Tissue engineering (TE) aims to replace and repair damaged tissues. Incorporating the three main TE triad elements (cells, biological factors and scaffolds) needs a good scaffolding technique. Additive manufacturing (AM) techniques are the most common ones.
As any polymer processing technique, AM requires materials that are compatible with the processing technique of choice[1]. Hydrogels have been used as one of the most common materials constituting TE scaffolds over the past two decades due to their ability to maintain a distinct 3D structure, to be printed in different ways, to provide mechanical support for the cells in the engineered tissues, and to simulate the native extracellular matrix.

EXPERIMENTAL METHODS

Starting from a patented polymer family (structure cannot be disclosed), 3D scaffolds were developed using different printing techniques.
The first technology was extrusion-based 3D printing. The parameters that were varied include: the printing temperature (from 50-60°C), the printing speed (50-400 mm/min), the printing pattern (0°/90°, 0°/45°, …) and the photoinitiator (PI) concentration (1-4 mol%).
The second technology was digital light processing (DLP). The required liquid polymer phase was prepared using different hydrogel building block concentrations (ranging from 30–90 % w/v), varying PI concentrations (from 5-20 mol%) and a photoblocker concentration of 1 mol%. The printing parameters varied include: the UV-exposure time (from 3-10 s) and the intensity of the UV-lamps (from 10-30 mW/cm2).
The third technology investigated was indirect rapid prototyping. To obtain a hydrogel scaffold, a sacrificial PLA mould (pore size 400 µm, strut size 250 µm) was printed using a FDM printer (Ultimaker 3) at a printing temperature and speed of 200°C and 20 mm/s respectively. Subsequently the scaffolds were filled with hydrogel precursors. Finally, the PLA mould was dissolved in chloroform.
Before being mechanically tested, using destructive and non-destructive testing (NDT), the efficiency of the UV-cross-linking process of the scaffolds was verified through sol-gel testing. Minimal gel-values of 80-90% are targeted as go/no go criterion for further testing.

RESULTS AND DISCUSSION

Using our newly developed polymer family, reproducible scaffolds were obtained using different technologies. All scaffolds reveal gel fractions exceeding 90%.
In a first part of the mechanical testing, the 3D printed scaffolds (pore size 250 µm, strut size 380-480 µm) were subjected to mono-axial compression using Dynamic Modulus Analysis – DMA as NDT and to DT. The studies showed that the material revealed mechanical properties relevant for various TE applications (i.e. in the range of 0.2-30 MPa depending on the printing composition, the scaffold design and the hydrogel building block concentration).
As the applied extrusion-based technology permitted to vary and investigate different pattern orientations, the results from the (N)DT were used to optimize the 3D printing parameters. The DMA results revealed the complex modulus of the 0°/45°/90°/135° printing pattern to be superior to the other two patterns most likely due to its more isotropic structure (i.e. 8.22 ± 0.2 MPa compared to respectively 5.99 ± 0.3 MPa for 0°/45° and 5.66 ± 0.2 MPa for 0°/90°).
The results obtained from destructive compression static tests were aligned with the DMA results.
DLP printed scaffolds (pore size 250 µm and strut size 400-450 µm) were subjected to DT technique and showed comparable results with scaffolds obtained through the extrusion-based technology.
For the scaffolds obtained by indirect printing, the first goal was to create a negative mould with minimal material waste. For these scaffolds, (N)DT analysis will be performed in the upcoming months and presented during the meeting. Microscopic analysis of the obtained hydrogel scaffolds (pore size 200 µm, strut size 600 µm) already revealed a comparable structure to the scaffolds obtained through extrusion-based printing and DLP.

Figure 1: Indirect moulding set-up. The material is pressed into PLA mould.

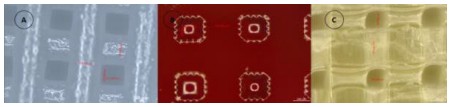

Figure 2: Microscope pictures (magnification 5x: a) extrusion-based scaffold; b) DLP scaffold; c) Indirect moulding hydrogel scaffolds.

CONCLUSION

Our data indicate that applying various printing techniques enable us to develop scaffolds, revealing comparable mechanical properties. This indicates the great versatility of the material under study.

REFERENCES

1. Mhanna R. et al., 'Introduction to Tissue Engineering', Tissue Engineering for Artificial Organs, First Edition, 2017

ACKNOWLEDGMENTS

The research was funded using resources from the research groups involved.

Light and temperature dual-responsive interpenetrating polymer network for mimicking muscle tissue ECM

Antonella Stanzione[1,2], Alessandro Polini[2], Francesca Scalera[2], Giuseppe Gigli[1,2] and Francesca Gervaso[2]

[1] Dipartimento di Matematica e Fisica E. De Giorgi, University of Salento, 73100 Lecce LE, Italy;
[2] CNR-Nanotec, Institute of Nanotechnology, 73100 Lecce, Italy;

INTRODUCTION

Extracellular matrix (ECM) and its crosstalk with resident cells strongly influence cellular behaviour through their mutual exchange of bio-chemical and physical signals[1]. The properties of a complex 3D architecture, such as the ECM, have been proved to play a key role in many cellular processes, such as proliferation, migration and differentiation[2]. Recently, matrix-based 3D culture systems have been successfully proposed[3] to properly model *in vitro* the physio-pathological interactions of organs and tissues. A 3D matrix analogue must possess high biocompatibility and fully reproduce the characteristics of the native tissue in terms of mechanical properties. In this regard, Interpenetrating Polymer Networks (IPN) are particularly attractive because they present a wide range of highly tunable chemical and physical properties. In this study, we propose an IPN composed of chitosan (Ch) and modified gelatin (GelMA), able to respond to two external physical stimuli, i.e. light (UV) and temperature, and achieve physico-chemical properties matching the target application. Here, Ch-GelMA IPNs were designed to mimic the muscle tissue ECM in terms of mechanical stiffness.

EXPERIMENTAL METHODS

A dual-responsive Ch-GelMa IPN hydrogel was obtained by mixing the two following solutions: Ch, final concentration 2% in 0.1M HCl, and GelMa, final concentration 10% in milliQ water, the latter containing also the thermo-inducing gelling agents for Ch (β-glycerophosphate, βGP, and sodium hydrogen carbonate, SHC, final molarity 0.2M and 0.05M respectively[4] and the photoinitiator for UV-crosslinking of GelMA chains (Irgacure 2959 1.25%w/v). The GelMA solution was added to the Ch solution (Ch/GelMA ratio 3:2 v/v) under gentle stirring until a homogeneous solution was obtained. This pre-hydrogel solution was poured into molds and cross-linked by double stimulation, UV for 4 min and T=37°C for 10 min. The Ch-GelMA IPN hydrogel was characterized both physico-chemically (weight loss, swelling, morphology and compression) and biologically, by encapsulating mouse skeletal muscle cells (C2C12, 6 M/mL) and monitoring their viability up to 7 days of culture (by live/dead assay).

RESULTS AND DISCUSSION

The Ch-GelMa pre-hydrogel solution showed a physiological pH suitable for cell encapsulation, it was injectable and underwent a sol-gel transition after exposure to light and temperature stimuli. The obtained Ch-GelMA hydrogels were stable in terms of weight loss up to 3 weeks in culture conditions, presented a high swelling ratio, an interconnected porosity (by SEM analysis) and a high compressive stiffness, in the range of muscle tissues (8-20 KPa). C2C12 cells were homogenously encapsulated within the Ch-GelMA IPN and showed a high viability up to day 7 of culture, as confirmed by the presence of very rare dead cells.

CONCLUSION

In this study, a dual-responsive Ch-GelMA IPN with improved mechanical properties was successfully developed in order to mimic the muscle tissue ECM architecture. The IPN hydrogel resulted suitable for cell encapsulation and 3D culture, being stable up to three weeks. The biological test revealed that the developed IPN supports the C2C12 cell viability by reproducing their native environment. The proposed Ch-GelMA IPN hydrogel may be a good ECM-analogue for 3D *in vitro* models of muscle tissues.

REFERENCES

1. Souza, G. R. et al., *Nat. Nanotechnol.* 2010, *5* (4), 291–296.
2. Baharvand, et al., *Int. J. Dev. Biol.* 2006, *50* (7), 645–652.
3. Härmä, V. et al., *PLoS One* 2010, *5* (5).
4. A. Stanzione, A. Polini, V. La Pesa, A. Quattrini, A. Romano, G. Gigli, L. Moroni and F. Gervaso, *Biomater. Sci.*, 2021, **9**, 7492–7503.

ACKNOWLEDGMENTS

The authors are grateful to the "Tecnopolo per la medicina di precisione" (TecnoMed Puglia) - Regione Puglia: DGR n.2117 del 21/11/2018, CUP: B84I18000540002 and "Tecnopolo di Nanotecnologia e Fotonica per la medicina di precisione" (TECNOMED)-FISR/MIUR-CNR: delibera CIPE n.3449 del 7-08-2017, CUP: B83B17000010001 and the support from the European Union's Horizon 2020 research and innovation programme under grant agreement No.953121 (FLAMIN-GO).

A smart biomaterial platform for 2D-grown hMSC osteogenic differentiation

Valeo Michele[1,2,3*], Remy Murielle[1,2,3], Guee Laura[4], Feuillie Cécile[1,2,3], Chanseau Christel[1,2,3], Marie Sébastien[4], Molinari Michael[1,2,3], Durrieu Marie-Christine[1,2,3]

[1]Université de Bordeaux, Chimie et Biologie des Membranes et Nano-Objets (UMR5248 CBMN), Allée Geoffroy Saint Hilaire - Bât B14, 33600 Pessac, France.
[2]CNRS, CBMN UMR5248, Allée Geoffroy Saint Hilaire - Bât B14, 33600 Pessac, France.
[3]Bordeaux INP, CBMN UMR5248, Allée Geoffroy Saint Hilaire - Bât B14, 33600 Pessac, France.
[4]FGHI, Avenue de l'Europe, 34830 Clapiers, France.

*michele.valeo@u-bordeaux.fr

INTRODUCTION

Mesenchymal stem cells (MSCs) are adult stem cells capable of *in vitro* differentiation into multiple cell lineages of mesodermal origin[1]. Owing to their *in vitro* multipotency and self-renewal ability[2], human mesenchymal stem cells (hMSCs) offer the chance of recreating patient-derived cultures[2], to treat pathological conditions such as bone diseases[3]. Most culture protocols employed to expand and direct *in vitro* the differentiation of hMSCs to bone-forming cells (i.e., osteoblasts) require an osteogenic medium[4]. However, such induction media, when applied to 2D-grown cells in Petri dishes result in poor outcomes, with hMSC of reduced differentiation potential and altered morphology[5].

EXPERIMENTAL METHODS

We aim to design an extracellular matrix (ECM) mimicking scaffold to induce the *in vitro* differentiation of hMSC to osteoblasts, in a rapid and high-yield way, devoid of induction media. We direct the hMSCs differentiation by recapitulating in our material the biochemical and mechanical cues of the ECM, the main component of the stem cell niche, responsible for cell adhesion, proliferation and fate commitment[6,7].

RESULTS AND DISCUSSION

We synthesized a thin, smart hydrogel layer, obtained by cross-linking of polymeric nanoparticles entirely made of lysine (dendrigrafts of lysine, DGLs, from COLCOM SA). Such lysine dendri-grafts are biocompatible and can be prepared in many shapes and surface properties by a generational synthesis (G2-G5), affording nanoparticles of customizable size, surface charge and surface amino-functions density for further bioconjugation[8]. We engineered the hydrogel by optimizing the type and concentration of DGLs and cross-linker, to have the mechanical properties that best induce osteogenic commitment. Among these, natural tissues' viscoelasticity (dissipation of mechanical energy stored during deformation) is crucial to cells spreading and matrix remodelling[11,12]. So, we figure to prepare visco-elastic hydrogels with Young's moduli (E) spanning at least two orders of magnitude and independent stress-relaxation half-times, evaluated by atomic force microscopy nanoindentation. Such technique can be used both to acquire a topographical image, by mapping the hydrogel (fig. 1A) to gauge its roughness; and the E values, which display a narrow, unimodal distribution throughout the surface (fig. 1B). To evaluate the hydrogel water content, we performed swelling experiments in PBS at 4°C. The swelling ratio (g PBS/g polymer) at equilibrium, reached after 48 hours, was dependent upon the DGL's generation (0.25 and 0.15 for G2 and G5, respectively). Afterwards, we functionalized the hydrogel's surface with biomolecules (to favor MSC adhesion and their differentiation into an osteoblastic lineage) to find their optimal density and distribution by fluorescence microscopy. Our bioconjugation strategy involves the covalent coupling of DGLs amino groups with bioactive peptides, tethered to a heterobifunctional PEG chain (MAL-dPEG® 24-NHS ester), to favor their recognition by cells.

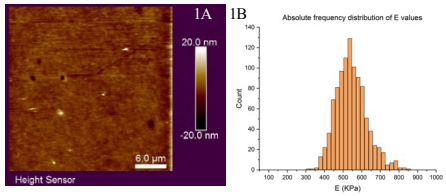

***Fig. 1A (left)**: virgin G5 hydrogel surface mapping by AFM (height image acquired by contact mode, spherical tip probe, 32µm size image), showing an overall smooth surface with few irregularities (holes, crests). **1B (right)**: histogram showing the absolute frequency distribution of E values of the same hydrogel as fig. 1A, probed by nanoindentation in contact mode (n=1017, bin number is the squared root of n).*

CONCLUSION

We will soon seed hMSCs on top of our hydrogel and monitor the differentiation process by immunostaining with fluorescence microscopy quantification and qPCR of both early and late osteogenic markers. Eventually, we will test the osteogenic-inductive performance of our system against current osteogenic media.

REFERENCES

1. Pittenger, M. F. *et al. npj Regen. Med.* **4**, (2019).
2. Han, Y. *et al. Cells* **8**, 886 (2019).
3. Knight, M. N. & Hankenson, K. D. *Adv. Wound Care* **2**, 306–316 (2013).
4. Lee, W. C. *et al. ACS Nano* **5**, 7334–7341 (2011).
5. Tsai, A. C., Jeske, R., Chen, X., Yuan, X. & Li, Y. *Front. Bioeng. Biotechnol.* **8**, (2020).
6. Discher, D. E., Mooney, D. J. & Zandstra, P. W. *Science (80-.).* **324**, 1673–1677 (2009).
7. Guimarães, C. F., Gasperini, L., Marques, A. P. & Reis, R. L. *Nat. Rev. Mater.* **5**, 351–370 (2020).
8. Collet, H. *et al. Chem. - A Eur. J.* **16**, 2309–2316 (2010).
9. Charrier, E. E., Pogoda, K., Wells, R. G. & Janmey, P. A. *Nat. Commun.* **9**, 1–13 (2018).
10. Chaudhuri, O. *et al.* Hydrogels with tunable stress relaxation regulate stem cell fate and activity. *Nat. Mater.* **15**, 326–334 (2016).
11. Prouvé, E. Synthesis of bioactive surfaces for the control of stem cells differentiation. (2021).
12. Prouvé, E., Laroche, G. & Durrieu, M. C. Hydrogels for mesenchymal stem cell behavior study. in *Superabsorbent Polymers* 75–102 (2021).

Differentiation of NSC-34 cells toward motor neuron-like phenotype in a 3D thermosensitive chitosan-based ECM model

Antonella Stanzione[1,2], Alessandro Polini[2], Velia La Pesa[3], Angelo Quattrini[3], Alessandro Romano[3], Giuseppe Gigli[1,2], Lorenzo Moroni[2,4] and Francesca Gervaso[2]

[1] Dipartimento di Matematica e Fisica E. De Giorgi, University of Salento, 73100 Lecce LE, Italy;
[2] CNR-Nanotec, Institute of Nanotechnology, 73100 Lecce, Italy;
[3] IRCCS San Raffaele Scientific Institute, Neuropathology Unit, Institute of Experimental Neurology and Division of Neuroscience, 20132 Milan, Italy;
[4] Complex Tissue Regeneration, Maastricht University, 6229 ER Maastricht, The Netherlands
antonella.stanzione@unisalento.it;

INTRODUCTION

Motor neuron diseases (MNDs) encompass a heterogeneous group of neurological disorders defined and characterized by degeneration of motor neurons[1]. Amyotrophic Lateral Sclerosis (ALS) is the most severe form, involving both lower and upper motor neurons leading to muscle weakness, respiratory failure and, ultimately, death[2]. To date, there are no valid therapeutic treatments for ALS, and the classical experimental models fail in faithfully reproducing the pathological mechanisms behind them. In this regard, the use of three-dimensional (3D) culture systems, such hydrogels, which more closely reproduce the native *in vivo* environment[3], can be a promising approach. The 3D environment, indeed, strongly influences cell fate and morphology, playing a key role in all cellular processes such as proliferation, differentiation, migration and dead[4]. In this study, we tested the ability of thermosensitive chitosan-based hydrogels to support neuroblastoma/spinal cord hybrid cell (NSC-34) differentiation towards a motor neuron-like morphology.

EXPERIMENTAL METHODS

Low molecular weight chitosan (Ch) powder was dissolved in 0.1 M HCl solution. The obtained Ch solution was mixed (3:2 ratio) with the gelling agent solutions (GA), β-glycerophosphate (βGP) and sodium hydrogen carbonate (SHC). GA solutions were added drop by drop to cold Ch solution, up to final concentration of 0.2M and 0.05M for βGP and SHC, respectively. After mixing, the hydrogels were injected into molds and heated at 37 ° C for 2 hours to induce the thermal sol-gel transition. Two formulations of hydrogel were characterized: Ch+βGP and Ch+βGP+SHC.

RESULTS AND DISCUSSION

Both formulations were injectable at r.t. and presented a sol-gel transition by increasing the temperature to 37°C. Rheological temperature sweep test (5-55°C) showed that hydrogels storage modulus G' drastically increased as temperature reached 30°C, demonstrating that both hydrogels were thermosensitive. The degradation kinetics revealed a high stability of the hydrogels in culture conditions, higher for Ch+βGP+SHC formulation that was stable in weight up to 3 weeks. Mechanical compression test revealed that Ch+βGP+SHC is stiffer than Ch+βGP, but still in the range of "soft" biological tissues (1–10 KPa). The biological characterization demonstrated that NSC-34 cells have a high viability up to 7 day of culture and can be efficiently differentiated to motor neuron-like phenotype adopting standard protocols[5], as observed after cell staining with a neuronal maker (neurofilament-H). Both hydrogels allowed NSC-34 cells to acquire the typical neuron-like morphology characterized by an elongated cell shape and the development of long neurites.

CONCLUSION

In this study we proposed an optimized protocol for the preparation of thermosensitive chitosan-based hydrogels that allowed to obtain a bubble-free system. Both formulations showed optimal chemical-physical properties with a mechanical stiffness in the range of "soft" biological tissues. Biological analyses conducted with motor neuron-like NSC-34 cells revealed that the system is able to support not only cell growth and viability but also their differentiation. The proposed hydrogels are suitable as ECM-like biomaterials for 3D *in vitro* models of motor neuron diseases.

REFERENCES

1 D. W. Mulder, L. T. Kurland, K. P. Offord and M. Beard, *Neurology*, 1986, **36**, 511–517.
2 L. C. Wijesekera and P. N. Leigh, *Orphanet J. Rare Dis. 2009 41*, 2009, **4**, 1–22.
3 A. Birgersdotter, R. Sandberg and I. Ernberg, *Semin. Cancer Biol.*, 2005, **15**, 405–412.
4 J. Nicolas, S. Magli, L. Rabbachin, S. Sampaolesi, F. Nicotra and L. Russo, *Biomacromolecules*, 2020, **21**, 1968–1994.
1 . Maier, J. Böhm, M. Dahm, S. Brück, C. Beyer and S. Johann, *Neurochem. Int.*, 2013, **62**, 1029–1038.

ACKNOWLEDGMENTS

The authors are grateful to the "Tecnopolo per la medicina di precisione" (TecnoMed Puglia) - Regione Puglia: DGR n.2117 del 21/11/2018, CUP: B84I18000540002 and "Tecnopolo di Nanotecnologia e Fotonica per la medicina di precisione" (TECNOMED) - FISR/MIUR-CNR: delibera CIPE n.3449 del 7-08-2017, CUP: B83B17000010001 and the support from the European Union's Horizon 2020 research and innovation programme under grant agreement No. 953121 (FLAMIN-GO).

Biofabrication of Atherosclerotic Plaques to Develop Ex-Vivo Stenotic Artery Model

Ravipati Priusha[1*], Federica Potere[1], Sara Mantero[1], Giancarlo Pennati[1]

[1]LaBS, Department of Chemistry, Materials and Chemical Engineering 'Giulio Natta', Politecnico di Milano, Milan, Italy

[*]ravipatipriusha@polimi.it

INTRODUCTION

Peripheral artery disease (PAD) is the narrowing or occlusion of arteries due to formation of plaques composed of cholesterol, calcium, collagen, and smooth muscle cells within the arterial wall[1]. Preclinical testing of the drug delivery devices or therapeutics designed to treat PAD are often performed in ex-vivo models involving the use of healthy animal arteries without accounting for the in vivo presence, composition, and mechanical properties of the atherosclerotic plaque[2]. Nevertheless, mimicking the plaque compositions and mechanical properties is very important to allow better understanding and to aid in better designing and evaluating drug delivery vehicles. This work is focused on mimicking American heart association classification (AHA) type VII and VIII plaques that are predominantly observed in superficial femoral artery (SFA), and that are majorly composed of calcium deposits and fibrotic tissue/collagen respectively[3]. We aim to reproduce human type VII and type VIII plaques in porcine arteries by designing injectable hydrogels, using gelatin and gelatin-based composite materials. Injectable plaques with different mechanical properties can be obtained by tuning the polymer, crosslinker and calcium salt concentrations to create stenosis in ex-vivo porcine artery. Gelatin, a hydrolyzed form of collagen, is chosen due to its chemical similarity to the sclerotic tissue of the plaque.

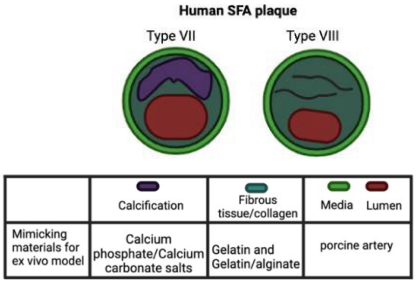

Figure 1: Rationale for materials choice to biofabricate human SFA type VII and VIII mimicking plaques.

EXPERIMENTAL METHODS

0.5% – 10% w/v Gelatin and Gelatin-alginate solutions are prepared. Gelatin is dissolved in distilled water under continuous stirring at 60°C for 15 minutes, followed by addition of alginate (only for gelatin-alginate gels) at 37°C. To prepare type VII plaques, different concentrations of calcium carbonate and calcium phosphate salt forms are added to the solutions. Internal crosslinking is performed for gelatin and gelatin-alginate solutions with glutaraldehyde (GA) and glucono-δ-lactone (GDL) respectively. Type VIII plaque is mimicked using Gelatin gels without calcium salts. Gelling time and injectability of the various hydrogel solutions are being assessed. The swelling properties and stability of the hydrogels in saline/PBS at 37°C are being studied by checking the weights at different time points for up to 72 hours. A mechanical analysis of the hydrogels and porcine arteries with injected hydrogel is currently ongoing. Preliminary tests were performed to assess that feasibility of injecting the developed hydrogels in porcine arteries (provided by a local abattoir). Hematoxylin and Eosin (H&E) staining of the artery with injected hydrogel is being performed.

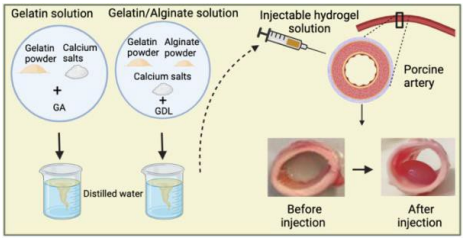

Figure 2: Preparation of injectable hydrogels to create type VII plaques in porcine arteries.

RESULTS AND DISCUSSION

The performed preliminary tests demonstrated that the injection of hydrogel solutions into the porcine arterial wall is feasible, and that a plaque within the wall can be created (Figure 2). The location of the plaque within the artery wall is being confirmed by H&E. However, methods to control the shape and size of the obtained plaque are necessary and will be developed in the future. Gelatin-based injectable hydrogels are expected to be obtained with different mechanical stiffness.

CONCLUSION

Artificial plaques are created with compositions mimicking human atherosclerotic plaques in SFA using simple materials. This groundwork can be exploited to mimic various other AHA types of plaques such as fatty plaques by introducing cholesterol or other lipids into the hydrogels. This ex-vivo atherosclerotic model will be further developed to achieve different types of calcifications that can be used to assess the performance of drug coated balloons (DCB).

REFERENCES

1. Bentzon JF. et al., Circ Res. 114(12):1852-1866, 2014
2. Anbalakan K. et al., *Eur J Pharm Biopharm*. 158:72-82, 2021
3. Herisson F. et al., Atherosclerosis. 216(2):348-354, 2011

ACKNOWLEDGEMENTS

This project has received funding from the European Union's Horizon 2020 research and innovation program under grant agreement No 956470.

Insight into the repercussions of magnetically oriented PEG microgels regarding structure, fiber properties and cell behavior in collagen hydrogels

Ana Luísa Castro[1,2,3*], Sitara Vedaraman[5,6], Mário A. Barbosa[1,2,3], Raquel M. Gonçalves[1,2,3], Laura De Laporte[4,5,6]

[1]i3S - Instituto de Investigação e Inovação em Saúde, Universidade do Porto, Portugal;
[2]INEB - Instituto de Engenharia Biomédica, Universidade do Porto, Portugal;
[3]ICBAS - Instituto de Ciências Biomédicas Abel Salazar, Universidade do Porto, Portugal;
[4]DWI—Leibniz Institute for Interactive Materials, Aachen, Germany;
[5]Department of Advanced Materials for Biomedicine, Institute of Applied Medical Engineering, RWTH Aachen University, Aachen, Germany;
[6]Department of Technical and Macromolecular Chemistry, RWTH Aachen University, Aachen, Germany
*luisa.castro@i3s.up.pt

INTRODUCTION

Designing novel *in vitro* tissue constructs, which replicate native cells and its extracellular matrix (ECM) organization *in vivo*, is the aim of tissue engineering. Biofabricated scaffolds using collagen type I – one of the major and most important ECM components – which accurately resemble *in vivo* features, have been widely explored. One focus of such constructs is to provide the right architectures to grow aligned tissue [1].

Mimicking tissue-oriented organization *in vitro* has been extensively studied in recent years, with both natural and synthetic materials in combination with external magnetic fields to establish anisotropic conditions [1-3]. More specifically, magneto-responsive polyethylene glycol (PEG) based microgels embedded inside a bulk gel (Anisogel) have reported to impart unidirectional cues that promote oriented cell growth. [2].

In this study, we translate the Anisogel technology to provide *in vitro* anisotropy in collagen scaffolds to achieve collagen fiber alignment and influence cellular responses, depending on the dimensions and amounts of magneto responsive, anisometric PEG microgels.

EXPERIMENTAL METHODS

PEG microgels (µgel) are designed and fabricated in an anisometric rod-shape, following a previously established protocol using mold-based soft lithography [2]. Collagen hydrogels precursor solutions (3.2 mg/ml) are prepared, mixed with PEG µgel (Col-PEG-µgels) and allowed to gel by a pH switch with NaOH at 37ºC for 60 minutes. In the presence of an external magnetic field (70 mT), different µgel sizes, aspect ratios, and concentrations are explored to enable µgel orientation inside the collagen hydrogel precursor solution. Fibrillogenesis kinetics and mechanical properties of the hydrogels are evaluated by measuring the optical density over time and the rheological properties for all Col-PEG-µgels conditions. Fiber orientation and diameters are assessed using confocal reflectance microscopy (CRM). Normal human dermal fibroblasts (NHDF) are used for cell behavior evaluation inside the Col-PEG-µgels hybrid hydrogels. The orientation of cellular actin and its ECM production are analyzed.

RESULTS AND DISCUSSION

The addition of PEG µgels did not impair the collagen fiber formation as observed by turbidimetric analysis of fibrillogenesis, nor compromise the collagen mechanical properties (storage modulus, control group without µgels: 136.4 ± 13.2 Pa; Col-PEG-µgels: 95.21 ± 53.6 Pa to 314.4 ± 190.8 Pa) with no significant difference between the subgroups. A preferential alignment of collagen fibers is observed in formulations containing µgels with larger cross-sections and lengths (2,5 and 5 vs 10 µm width and 25 and 50 vs 100 µm length). Fiber diameters are quantified using an in-house developed software tool to evaluate possible alterations induced by PEG µgels and the magnetic field on the collagen fibers. Confocal microscopy reflection micrographs revealed that NHDF cells cultured with µgels with dimensions 2.5x50 µm (width x length), 5x50 µm, and 10x100 µm exhibit oriented actin signals starting from day 1. After 7 days of culture, the control group and Col-PEG-µgels hydrogels with smaller PEG microgels sizes (2,5 and 5 µm diameter) show matrix stiffening to a large extent due to the contractile forces imparted by the cells resulting in loss of actin orientation. Interestingly, in Col-PEG-µgels hydrogels containing 10x100 µm PEG microgels, actin orientation in cells is retained and matrix stiffening is observed only to a smaller extent. Currently, evaluation of aligned ECM production and the mechanical properties of the cellular hydrogels are measured using nanoindentation.

CONCLUSION

Our results point us towards the optimal conditions to establish a 3D unidirectional collagen hydrogel suitable for different tissue engineering applications. The anisotropy imparted by the PEG µgels is accompanied by collagen fiber alignment and NHDF cells have shown to orient parallel to this physical guidance. Further studies will allow for a better understanding of the impact of anisotropy in hydrogels on cell behavior and ECM production, which is important to achieve functional tissue-like structures.

REFERENCES

[1] Dewle, A., et al. (2020). "Multifarious Fabrication Approaches of Producing Aligned Collagen Scaffolds for Tissue Engineering Applications." ACS Biomaterials Science & Engineering.

[2] Omidinia-Anarkoli, A., et al. (2017), "An injectable hybrid hydrogel with oriented short fibers induces unidirectional growth of functional nerve cells" Small.

[3] Rose J.C., et al. (2017) "Nerve Cells Decide to Orient inside an Injectable Hydrogel with Minimal Structural Guidance" Nano Lett.

ACKNOWLEDGMENTS

AL Castro acknowledges Fundação para a Ciência e a Tecnologia (FCT) for the PhD Grant (SFRH/BD/147300/2019). S.Vedaraman and L De Laporte thank the support from universities of excellence funding line (Grant no. EXS-PFLS010) RWTH, Aachen.

Chemically-modified natural hydrogels for the design of double network 3D printed scaffolds

Ugo D'Amora[1*], Alfredo Ronca[1], Luigi Ambrosio[1]

[1]Institute of Polymers, Composites and Biomaterials, National Research Council, Naples, Italy
[*] ugo.damora@cnr.it

INTRODUCTION

Over the past years, natural polymers have highlighted a great potential in the biomedical field due to their excellent physico-chemical, mechanical and biological properties. Furthermore, their use is attracting a wide research interest as they can work as suitable bioinks for 3D bioprinting of site-specific and customizable structures, offering the possibility to control the design in terms of porosity, interconnectivity and mass transport properties[1]. Furthermore, to improve the mechanical properties, a double network (DN) approach can be also employed. Indeed, DN hydrogels have widely demonstrated to be an interesting class of interpenetrating polymer networks with improved mechanical behavior[2]. Previous studies have already shown methacrylated hyaluronic acid (MEHA), and methacrylated gellun-gum (GGMA) as valuable candidates for soft tissue engineering applications[3]. However, their low mechanical properties and low residence time were still a limitation.
In this study, two different DN scaffolds were analyzed in terms of physico-chemical, morphological and mechanical properties. The first DN scaffold was characterized by MEHA, as first network, and a synthetic polymer, poly(ethylene glycol) diacrylate (PEGDA), as second one. A fully natural DN scaffold was also obtained by combining GGMA, as a tightly crosslinked polyelectrolyte first network, and methacrylated gelatin (GEMA), as soft and neutral second polymer network.

EXPERIMENTAL METHODS

HAs (M_w=~340 kDa), GG (low acyl, Gelzan) and GE (Type A, 300 bloom) were methacrylated by reaction with methacrylic anhydride (MA) to obtain MEHA, GGMA and GEMA, respectively. Different molar ratios of MA to HAs, GG or GE were used to obtain materials characterized by different degrees of substitution (DS). The materials were studied by attenuated total reflect Fourier transform infrared (ATR-FTIR) and nuclear magnetic resonance (NMR) to assess the success of the functionalization. MEHA and GGMA bioinks were also optimized in terms of rheological behavior. Indeed, the modification was able to confer a shear thinning behavior for the extrusion-based process. MEHA (2%w_t/v) and GGMA (4%w_t/v) were dissolved in deionized water (dH_2O) containing Irgacure 2959 (0.1 w_t%). Finally, 3D scaffolds were produced by processing MEHA and GGMA using a 3D bioprinter "In vivo Rokit" (Rokit Healthcare Inc.). Afterwards, DN scaffolds were obtained by interpenetrating MEHA/PEGDA and GGMA/GEMA. The porous scaffolds MEHA or GGMA (1st network) were dipped in the PEGDA or GEMA (2nd network) solution for 4 days. The extracted samples were exposed to UV light, washed in dH_2O and stored at 4°C. Morphological and mechanical performances were evaluated by scanning electron microscopy (SEM) and dynamical mechanical analysis (DMA), respectively. Swelling and stability tests were also performed in physiological conditions.

RESULTS AND DISCUSSION

NMR and ATR-FTIR highlighted the peaks related to the introduced methacrylate moieties confirming the success of the functionalization reaction of all the materials. MEHA and GGMA scaffolds were able to retain their well-ordered structure without collapse in the Z direction. Furthermore, as confirmed by SEM, both DN structures maintained their structure with a homogenous porosity and lateral pores clearly visible. However, the DN approach influenced the size of the pores, which resulted smaller with thicker lateral walls. Mechanical properties of DN scaffolds showed almost a 10-time increase of the storage modulus, if compared to neat structures. DN scaffolds highlighted increased stability in physiological conditions as result of a more compact interpenetrated polymer architecture with a tailored swelling ratio.

CONCLUSION

The main goal of this study was to demonstrate the feasibility of tailoring the viscoelastic properties of chemically modified HAs and GG as bioinks for the production of 3D morphologically-controlled scaffolds. A DN approach has been considered using a PEGDA and GGMA solution. The scaffolds showed enhanced stability, improved mechanical properties, without significantly altering their morphological architectures.

REFERENCES

1. Petta D. *et al., Biofabrication* 12:p.032001, 2020.
2. D'Amora U. *et al., J. Biomed. Mater. Res. A 106*:3079-3089, 2018.
3. Zhang L. *et al. RSC Adv.* 10:32183-32192, 2020.

ACKNOWLEDGMENTS

The authors would like to thank the POR FESR 2014 - 2020 - Accordi regionali di insediamento e sviluppo delle imprese - bando 2019 in attuazione dell'art. 6 della L.R. N. 14 /2014 Sviluppo di approcci PERsonalizzati nel trattamento del Piede Diabetico mediante utilizzo di stampante 3D (PERPD-3D).

Designing a new *in situ* forming injectable hydrogel based on Schiff base linkages as platform for tissue engineering applications

Roberta Pappalardo[1*], Monica Boffito[1,2], Rossella Laurano[1], Valeria Chiono[1,2], Gianluca Ciardelli[1,2]

[1] Politecnico di Torino, Department of Mechanical and Aerospace Engineering, Turin, Italy
[2] Istituto per i Processi Chimico-Fisici, Consiglio Nazionale delle Ricerche, Pisa, Italy
[*] roberta.pappalardo@polito.it

INTRODUCTION

Injectable hydrogels represent promising systems for tissue engineering (TE) applications thanks to their high-water content and the capability of encapsulating and transferring their payload to the surrounding tissues. The former provides a physiologically similar environment to the native extracellular matrix, while the latter allows the delivery of therapeutic agents (e.g., drugs or biomolecules) to the target site in a minimally invasive manner[1]. To achieve this purpose, injectable hydrogels should possess adequate rheological properties and quickly achieve a complete developed gel state after injection. *In situ* forming hydrogels through the Schiff-base crosslinking exploit the advantages of chemical hydrogels (i.e., fast gelation time and favorable stability under physiological conditions) without any toxic chemical crosslinking agent required for their preparation. Furthermore, these hydrogels possess favorable properties (e.g., high reactivity, self-healing ability, pH-responsiveness) that make them suitable for designing injectable drug delivery systems[2]. In this scenario, in this contribution we designed new *in situ* forming injectable hydrogels based on Schiff base linkages exploiting the versatility of polyurethanes (PURs) as constituent materials. The optimized synthesis processes led to two water-soluble PURs bearing primary amino groups along each polymeric chain and aldehyde end groups, respectively. Then, a Schiff base-based hydrogel was designed and characterized to assess its key physico-chemical properties.

EXPERIMENTAL METHODS

A high molecular weight PUR bearing a huge amount of amino groups, referred to as NHE3350, was synthesized through a one-step polymerization procedure, by reacting poly(ethylene glycol) (M_n 3500 Da, PEG3350) as diol, 1,6-hexanediisocyanate (HDI) as diisocyanate and N-Boc serinol as chain extender. NHE3350 was subjected to an acidic treatment to remove Boc protecting groups, thus exposing primary amines. The deprotected PUR, referred to as SHE3350, was characterized by size exclusion chromatography (SEC), infrared (IR) and proton nuclear magnetic resonance (^{1}H NMR) spectroscopies, and Orange II sodium salt colorimetric assay. A low molecular weight PUR with aldehyde end groups was also synthesized by end-capping an isocyanate-terminated prepolymer based on PEG and HDI using 4-hydroxylbenzaldehyde[3]. The resulting material, coded as PEG-dial, was characterized by SEC, IR and ^{1}H NMR spectroscopies. Then, hydrogels were prepared by simply mixing SHE3350 and PEG-dial solutions (primary amines/aldehyde groups 1:1 molar ratio) at room temperature and finally characterized in terms of gelation time and rheological properties (e.g., strain and frequency sweep test, strain test). Injectability and self-healing ability were also qualitative evaluated using 2.5 ml syringes equipped with needle of different diameters (e.g., G18 and G21).

RESULTS AND DISCUSSION

The optimized synthesis processes led to two PURs with suitable physico-chemical properties for the realisation of hydrogels based on Schiff base linkages. NHE3350 PUR showed a high molecular weight (M_n 30 kDa) and a narrow molecular weight distribution (polydispersity index= 1.8). In addition, the complete cleavage of the Boc protecting groups present along NHE3350 chains was confirmed by ^{1}H NMR spectroscopy and the exposed primary amines were quantified to be around 10^{19} units/g of SHE3350, as calculated through the Orange II sodium salt colorimetric assay. The success of PEG-dial synthesis was proved by the appearance of the signal ascribed to the proton bound to the carbonyl carbon at 9.8 ppm and the appearance of a new absorption band at 1720 cm^{-1}, in its ^{1}H NMR and IR spectra, respectively. Finally, SHE3350/PEG-dial hydrogels were prepared by homogeneously mixing their aqueous solutions and the resulting mixtures transformed into hydrogels within few minutes, proving the formation of the dynamic covalent Schiff base linkages between the primary amines and aldehyde groups exposed by the constituent polymeric materials. Qualitative and rheological characterizations proved the formation of fully developed gel networks with easy injectability and self-healing properties.

CONCLUSION

In this contribution, we reported the successful synthesis of two water-soluble PURs (i.e., SHE3350 and PEG-dial) characterized by suitable molecular weight and amount of exposed chemical functionalities (i.e., primary amines and aldehyde groups, respectively) for the preparation of rapid *in situ* forming hydrogels based on Schiff base linkages (i.e., gelation within few min). The attractive properties of these injectable hydrogels can be exploited to design new therapeutic platforms for TE applications.

REFERENCES

1. Lee J.H. *et al.,* Biomater Res, 22:27, 2018
2. Xu J. *et al.*, Molecules, 24(16):3005, 2019
3. Rahmani S. *et al.*, Polym. Bull., 78:2887-2909, 2021

ACKNOWLEDGMENTS

The authors acknowledge Dr. Claudio Cassino (Università del Piemonte Orientale "A. Avogadro", Italy) for ^{1}H NMR analyses.

Monophasic Hyaluronic Acid-Silica Hybrid Hydrogels with Tunable Mechanical Properties for Articular Cartilage Applications

Huijun Zhang[1*], Aldo R. Boccaccini[1]
[1]Institute of Biomaterials, Friedrich-Alexander-Universität Erlangen-Nuremberg, Erlangen, Germany
[*] huijun.zhang@fau.de

INTRODUCTION

Articular cartilage has limited regeneration capacity due to lack of innervation, vascularisation and low number of chondrocytes. Cartilage degeneration will cause inflammation, pain, and movement limitations, leading to osteoarthritis. One way to treat this disease is autologous matrix-induced chondrogenesis (AMIC). AMIC is a technique that combines microfracture and an exogenous scaffold[1]. Therefore, it is vital to fabricate scaffolds with customized sizes, shapes and mechanical properties for this method. These scaffolds should also support cell attachment, proliferation, and migration to achieve cartilage regeneration. Hydrogels have been widely researched for cartilage tissue regeneration, because their similar properties to the extracellular matrix (ECM). In particular, hyaluronic acid (HA), an FDA approved injection polymer and component of the ECM, is a great candidate for 3D printing hydrogels scaffolds[2]. However, crosslinked HA scaffolds have poor mechanical properties and thus their stiffness is too low to function in cartilage area. HA-silica hybrids are developed to stiffen HA. Inorganic silica and organic HA interpenetrate and bond covalently with each other at molecular level to develop a monophasic hydrogel. In this study, we develop a stiff and stable hydrogel by forming covalent bonds between HA and 3-glycidopropyltrimethoxysilane (GPTMS).

EXPERIMENTAL METHODS

Hydrogel Preparation. 15% (w/v) HA solution was mixed with GPTMS at different molar ratios (50, 100, 200, 300, and 400). Then 1% BDDE (crosslinker) was added and the solution was stirred at 40 °C for 4 hours. The sol solution was transferred to a silicon mold with a diameter of 8 mm and height of 4 mm for further characterization.

Nuclear magnetic resonance (^{1}H NMR). After reaction of HA and GPTMS for 4 hours, the sol solution was freeze dried and dissolved in D_2O for ^{1}H NMR characterization.

Swelling and Degradation Test. The swelling and degradation ratio of the hydrogels were characterized by determining the weight changes before and after immersed in DPBS for 4 weeks (n=3).

Mechanical Properties. The compressive strength and Young's modulus were assessed through a mechanical testing machine (Instron model 5967, Instron, UK) with a 1 kN compression plate by compressing the samples to 70% of their original height.

Rheological properties. Rheological measurements were conducted using a Discovery HR-3 rheometer (New Castle, USA) with three loading modes (compression, tension, torsional shear) at different frequencies and strains.

Cell Viability. WST-8 assay and Live/Dead staining were used to evaluate NIH-3T3 cell behaviour on hybrid hydrogels (n=3).

Statistical Analysis. Statistical differences were determined by GraphPad Prism 8.4.3 using the two-way ANOVA method.

RESULTS AND DISCUSSION

Liquid state ^{1}H NMR confirmed the successful reaction between HA and GPTMS. Swelling test indicated that increasing GPTMS concentration and adding higher molecular weight HA result in a lower swelling ratio and increased stability. All the HA-G hydrogels could be compressed to a 70% height of the original cylinder samples without any fracture. Young's modulus increased from 0.15 kPa to 1.43 kPa as the GPTMS ratio increased from 50 to 400, showing that a denser and stronger cross-linking network could be established. HA hybrid hydrogels markedly increased their storage modulus from 60 kPa to 130 kPa when the GPTMS concentration was increased. This is because the higher crosslinking density and the branching of the silica structure give higher support to the material. We also observed that the gap between storage and loss modulus was larger and the compression-tension asymmetry was enlarged by increasing GPTMS concentration. It means that a higher GPTMS concentration also limits the flexibility of the matrix and 3D network. There is no sign of cell viability decrease as the GPTMS concentration increases, indicating that the developed HA-G hybrid is a biocompatible hydrogel.

CONCLUSION

In this work, monophasic stiff HA-GPTMS hybrid hydrogels were synthesized and characterized. The relationship between the molar ratio of HA-GPTMS and the mechanical and rheology properties were evaluated. With an increased molar ratio, a stiff and stable hydrogel was created. These hybrid materials are biocompatible and should be capable of supporting cartilage cell adhesion and proliferation. Therefore, these materials have great potential for articular cartilage applications.

REFERENCES

1. Giannini, S. *et al*., Injury 2010, 41, 1196.
2. Jeong, S.H. *et al.*, Biomacromolecules 2016, 17, 841-851.

ACKNOWLEDGMENTS

The authors would like to thank the Chinese government CSC Scholarship for a scholarship. The authors also acknowledge Dr. Silvia Budday for allowing access to the rheometer and Dr. Weiqing Mao for assistance with NMR test".

Spatial-controlled coating of proangiogenic proteins on 3D porous hydrogels guides endothelial cell behaviors

Chau Le Bao[1,2*], Helen Waller[3], Daniel Peters[3], Jeremy Lakey[3], Didier Letourneur[1], Frédéric Chaubet[1,2], Teresa Simon Yarza[1]
[1]INSERM U148, Université Paris Cité, X Bichat Hôpital, 75018 Paris, France
[2]Université Sorbonne Paris Nord, Galilée Institute, 93430 Villetaneuse, France
[3]Newcastle University, Newcastle upon Tyne NE1 7RU, United Kingdom
[*] chau.lebao@univ-paris13.fr

INTRODUCTION

Vascularization of 3D hydrogels (HGs) remains a major challenge in tissue engineering and a key prerequisite for *in vitro* angiogenesis. Porous HGs are ideal candidates for vascularization strategies as they facilitate nutrient and oxygen diffusion, thus enabling cell migration[1]. Numerous studies have shown that the addition of channels inside a porous scaffold can facilitate cell growth and rapid vascularization, resulting in enhanced tissue formation[1]. Furthermore, the presence of proangiogenic peptides on hydrogels have also been shown to promote cell adhesion, proliferation, sprout formation, and lumen formation[2]. In this work, porous HGs with preformed microchannels were developed and functionalized with a novel bioengineered protein polymer, capsular antigen fraction 1 (Caf1), which was inserted with cell-adhesive motifs[3]. The proteins were grafted on hydrogels via electrostatic interactions.

EXPERIMENTAL METHODS

HG synthesis: Pullulan-dextran HGs (named PUDNA) were synthesized using a patented method[4] based on the addition of porogens and a freeze-drying step. Microchannels within HGs were formed by mechanical removal of suture filaments. **HG functionalization via electrostatic interactions:** Briefly, varying amount of DEAE-Dextran (D), (up to 20 wt%; ζ = +29.5 mV) was added to the standard gel formula. These gels were referred to as PUDNA-D20. In parallel, a solution of Caf1 (1-2 mg/mL; pI = 4.56; ζ = -23.5 mV) was prepared in DI water. HGs were coated in the protein solution via syringe vacuum-induced method, followed by incubation in protein solution at RT for 2h, prior to freeze-drying to ensure selective coating of the channel. Coated HGs were named PUDNA-D20C. **Cell culture and seeding into 3D scaffolds:** Human umbilical vein endothelial cells (HUVECs) were cultured in EGM-2. Cell loading was performed using the syringe vacuum-induced method. **Cell metabolic activity:** Resazurin assay was performed for cell metabolic activity quantification. Seeded scaffolds were transferred to a 96-well plate and incubated with 0.5 mL of resazurin for 3h at 37ºC. **Cell morphology:** Cellularized scaffolds (up to 14 days in culture) were fixed and permeabilized using standard protocol. Then samples were incubated with DAPI and Phalloidin-TRITC. Cell morphology and behaviors were observed using confocal microscopy.

Statistical analysis: All experiments were carried out at least in triplicates. Statistical analysis was performed using ANOVA One-way test. Statistical significance was indicated as * $p < 0.05$.

RESULTS AND DISCUSSION

Cell spreading was only observed in location where the bioactive protein Caf1 polymer was coated (channel vs. pores). These results suggest the spatial controllability of our coating method. Increase in initial surface charge of the HG resulted in enhanced quantity of cell-adhesive proteins, with the best cell behavior outcomes for D20% (PUDNA-D20C). After 7 days in culture, adhered HUVECs with elongated morphology were observed only in the coated channel (Figure 1A), together with an increase in cell metabolic activity compared to those seeded on non-coated scaffolds (Figure 1B). After 14 days, cells started to leave the channel and migrated to the surrounding pores (Figure 1A), suggesting angiogenic behaviors.

CONCLUSION

The functionalized porous HGs promoted angiogenic behaviors of ECs where cell adhesion, proliferation, and migration were observed. By spatial-controlled coating of proangiogenic proteins on the HGs we could modulate cells behaviors in the scaffolds. Our results strongly suggest that these hydrogels can be used as prevascularized scaffolds for tissue engineering applications.

REFERENCES

1. Kang Y. *et al.* Regen. Med., 705–715, 2018.
2. Dellaquila *et al.* Adv. Sci., 2021.
3. Roque A. *et al.* Adv. Mater., 2014.
4. Labour MN. *et al.* Int. J. Mol. Sci., 2020.

ACKNOWLEDGMENTS

The authors would like to thank the "Recherche Hospitalo-universitaire" Innovations for Liver Tissue Engineering (RHU iLite) (Grant no: ANR-16-RHUS-0005) for providing financial support to this project.

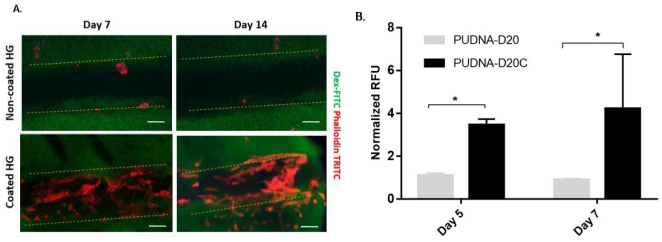

Figure 1. A.Confocal microscopy images of HUVECs on non-coated HGs and coated HGs after 7 and 14 days in culture. Scale bar: 100 µm; Yellow dash line represents the limit between the channel lumen and the HG's porous region; B. Cell metabolic activity after 5 and 7 days in culture on non-coated (grey) vs. coated (black) scaffolds.

Injectable collagen/MSCs microspheres for pulmonary tissue regeneration

Francesca Della Sala[1*], Gennaro Longobardo[1,2], Mario di Gennaro[1,3], Luigi Ambrosio[1], Assunta Borzacchiello[1]
[1]Institute of Polymers, Composite and Biomaterials (IPCB), National Research Council (CNR) of Italy, Viale J.F. Kennedy 54, 80125 Naples, Italy
[2]University of Naples Federico II, Naples, Italy
[3]University of Campania "Luigi Vanvitelli", Via Vivaldi 43, 81100, Caserta, Italy
[*]francesca.dellasala@cnr.it.

INTRODUCTION

Pulmonary pathologies, acute and chronic, are the third cause of worldwide deceases. They are commonly associated with aberrant repair processes and anomalous remodelling of the lung extracellular matrix (ECM), leading to a damage of alveolar epithelial surface and permanent alteration of respiratory functions. To date, beyond palliative procedures relieving patient's symptoms, there are no other effective treatments for lung injured epithelia. Mesenchymal stem cells (MSCs) intravenous or intratracheal administration is seen as potential treatment in regenerative medicine for lung diseases, indeed, MSCs modulate the inflammatory and remodeling processes, proliferation and differentiation into alveolar epithelial cells and restore alveolo-capillary barriers[1]. Moreover, MSCs can secrete soluble factors, eliciting a regenerative response from surrounding cells, to create a microenvironment for tissues regeneration. However, the anomalous remodeling of lung ECM can hinder tissue repair and correct homing of MSCs[2]. Stem cells suspension in saline solution is an ascertained delivery approach, but the limitation is an immediate loss of most injected cells due to the backflow via injection path. Moreover, cell viability may result compromised, especially since MSCs are responsive to anchorage dependent survival-apoptosis regulation[3]. Thus, a delivery system shielding and creating a temporary home for cells can improve their residence time at the delivery site. Therefore, the aim of this work was to develop new delivery strategies for MSCs by encapsulating them in ECM-like microspheres based on Collagen (COLL) suspended in a solution of Hyaluronic Acid (HA) for the regeneration of lung tissue.

EXPERIMENTAL METHODS

COLL gels were prepared by diluting COLL stock solutions [2.4 mg ml^{-1}] with 10× PBS (8:1) and adjusting pH to 7.2 adding NaOH. MSCs were seeded at different density in COLL gel (mCOLLs) to obtain different final diameters d≤ 250-µm. Gel solution was microextruded to obtain mCOLLs/MSCs and place at 37°C to induce fibrillogenesis. Then, diameter was monitored up to stabilization at different cell density and in different culture media (αMEM, α/Low Molecular Weight (LMW) HA, SAGM, SAGM/LMWHA) by morphological analysis. MSCs viability in mCOLL/MSCs was evaluated at different HA concentration in cell media (Alamar Blue test). Morphology was evaluated by confocal microscopy, marking cells' actin cytoskeleton with green Phalloidin and nuclei with DAPI. Differentiation in Alveolar Type II (ATII) cells was evaluated qualitatively by immunofluorescence after 21 days, by marking surfactant protein (SP) C antibody. Alongside, Elisa kit was performed to quantify the expression of SPC, specific marker of pulmonary differentiation, along with SPA, B and D, as well as the expression of VGEF angiogenesis markers for tissue regeneration.

RESULTS AND DISCUSSION

Diameters' observation showed a faster stabilization for mCOLLs seeded with 10^6 than 10^5 cell/ml, in particular for the ones cultured in αMEM (4 days). Cell viability test (Fig1) gave an excellent response, with cellular metabolism significantly increased in microspheric systems, as HA concentration increased due to improved interaction with dissolved HA. Data were also corroborated by the morphological analysis, showing the achievement of the complete stabilization of the diameter. ATII cell differentiation (Fig1) strongly occurred in mCOLLs suspended in SAGM/LMWHA, due to the recognition of a lung ECM-like surrounding for cell differentiation. Quantitative data were supported by a qualitative observation of SPC marker at confocal microscopy. Angiogenesis marker was observed, asserting mCOLLs' potentiality to induce an effective lung regeneration.

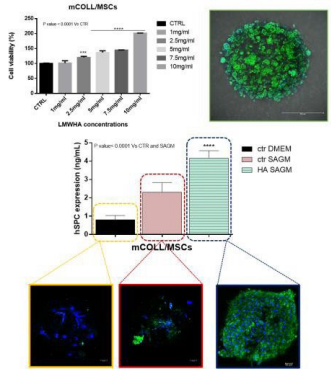

Figure 1: mCOLLs viability and morphological analysis. Quantitative expression of SPC by Elisa kit test and confocal microscopy of differentiated ATII cells. Scale bar: 50 µm.

CONCLUSION

Results showed good cells viability of mCOLLs/MSCs systems and good differentiability in in pulmonary lineage. Moreover, when they were suspended in lung media implemented with LMWHA, differentiation ability of the MSCs was furtherly enhanced.

REFERENCES

1. Della Sala F., *et al*., Polymers 13(17) (2021) 2928.
2. A. Borzacchiello, *et al*., PCT. Patent No. W0/2020 123982 A1 (2019)
3. Chan, T. *et al., Biomaterials*, ***28***(31), 4652-4666, 2007

ACKNOWLEDGMENTS

The authors would like to thank the project ADViSE Antitumor drugs and vaccines from the sea" CUP B43D18000240007

Cellulose based Injectable bio-composites for Bone Tissue Regeneration

Angelo Sciullo[1], Andrea Fiorati[1,2], Maria Grazia Raucci [3], Lina Altomare [1,2*]
[1]Dipartimento di Chimica, Materiali, Ing. Chimica 'G Natta' Politecnico di Milano, Milan, Italy
[2]INSTM local unit Politecnico di Milano
[3] Institute of Polymers, Composites and Biomaterials (IPCB) National Research Council (CNR)- Naples, Italy
[*] lina.altomare@polimi.it

INTRODUCTION

Hybrid hydrogels combine the positive properties of organic and non-organic materials, allowing a reduction of the drawbacks of both. They result particularly feasible for many biomedical applications (*e.g.,* bone regeneration) [1]. Cellulose and its derivatives, like TEMPO-oxidized nanofibers (TOCNFs) [2], are particularly interesting, considering their high availability and low cost [3]. Calcium phosphates (CaP) and graphene oxide (GO) used as fillers allow mechanical enhancement and bioactivity of the gel while introducing antibacterial activity [4]. For these reasons, biocomposite, injectable hydrogels for bone regeneration were designed starting from cellulose processed by TEMPO-oxidation and CaP with GO [5]. In this work we optimize the oxidation steps to reduce intrinsic cytotoxicity and increase chemical stability. Then we evaluate the contemporary mineralization of the hydrogel and osteogenic differentiation of 3T3-E1 pre-osteoblasts.

EXPERIMENTAL METHODS

Cellulose from cotton linters (SigmaCell S6790-100G, Type 101, Sigma Aldrich) was oxidized by means of TEMPO-mediated oxidation. A batch of the obtained powder was further oxidized using $NaClO_2$ for aldehyde elimination. Oxidized cellulose was used to produce 4% w/w TOCNFs dispersions. Different amounts of CaP and CaPGO particles (synthetized at the IPBC-CNR, Naples), were embedded in the dispersion obtaining injectable hydrogels with 3.56% w/w cellulose and 1, 2, and 4% w/w CaP or CaPGO. The produced composites were characterized in terms of swelling behaviour, rheological properties, injectability, morphology by SEM images, and composition (XRD). Biomimetic mineralization assays using a polymer-induced liquid precursor process were carried out for bioactivity assessment. Moreover, cytotoxicity and cytocompatibility of the gel were evaluated by Alamar Blue assay using 3T3-E1 murine pre-osteoblasts. Finally, *in-vitro* assays were performed to evaluate the contemporary mineralization of the gel and osteogenic differentiation of 3T3-E1 pre-osteoblasts; differentiation was assessed by means of alkaline phosphatase (ALP) activity quantification.

RESULTS AND DISCUSSION

TEMPO-oxidation introduces high amounts of carboxylates on the cellulose fibrils, but with significant depolymerization and poor chemical stability of the material. Aldehyde oxidation provides higher stability and cytocompatibility of the produced gels. Hydrogels do not show significant weight loss in the first 28 days. Moreover, their bioactivity is proven by the deposition of a mineral layer on cellulose fibrils, as underlined by XRD diffractograms (Figure 1), in which peaks related to CaP increase with the mineralization time. Produced materials show useful rheological properties (viscosity under 200Pa s, storage modulus under 400 Pa) and a high degree of thixotropicity. The increase in inorganic fraction allows an improvement of mechanical properties, while a more visible shear-thinning behaviour appears. These rheological behaviours are affordable for injectability purposes; indeed, all hydrogels need forces lower than 8 N to be extruded from a 18G needle.
Gels are non-cytotoxic, showing viability rates higher than 70% in any case, except the gels with inorganic fraction of 4% w/w; they also show good cytocompatibility, higher for CaPGO-filled composites.

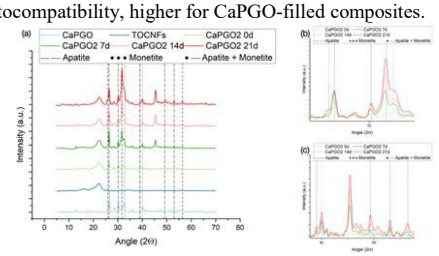

Figure 1: (a) XRD diffractograms of TOCNFs dispersion, CaPGO powder and CaPGO2 hydrogel at 0, 7, 14, 21 days of mineralization; (b,c) zoom-in

CONCLUSION

Injectable bio-composites were successfully obtained embedding both CaP and CaPGO particles. The obtained materials show appropriate swelling behavior and bioactivity, and satisfactory mechanical properties, while maintaining their easy injectability. *In-vitro* biological assays demonstrate the materials are non-cytotoxic when the inorganic fraction is kept reasonably low, and allow cell adhesion, proliferation and differentiation when specific environmental conditions are present. The designed materials are therefore good candidates for bone regeneration.

REFERENCES

1. Sanchez C. *et al*., Chem. Mater., 13;10:3061-3083, 2001
2. Pierre G *et al.*, Carbohydr Polym., 165:71-85, 2017
3. Orpea, M and Voicu, S.I., Carbohydr Polym., 247:116683, 2020
4. Matharu, R.K., *et al.*, J. Colloid Interface Sci., 571:239-252, 2020
5. Fiorati A. *et al.*, Materials, 14:4511, 2021

ACKNOWLEDGMENTS

The authors would like to thank the PRIN program ACTION (Grant no: 2017SZ5WZB) for financial support.

Advancements in the Production of Self-Esterified-Hyaluronan Hydrogels And Their Potential in Tissue Regeneration

E. Bedini[1], E.Cassese[2], A.D'Agostino[2], M. Cammarota[2], C. Schiraldi[2], A. La Gatta[2]
[1]Department of Chemical Sciences, University of Naples Federico II, Italy
[2]Department of Experimental Medicine, School of Medicine, University of Campania "Luigi Vanvitelli", Italy

INTRODUCTION

Hyaluronan (HA) is widely exploited for tissue healing purposes however, HA-based formulations can exert their benefits for short time intervals due to the high rate of HA turn-over in vivo. In this regard, esterified-HA derivatives are of particular interest: they are water-insoluble and undergo hydrolysis under physiological conditions, releasing HA. Therefore, they are expected to act as HA reservoirs allowing for active biopolymer concentration, at the injury site, for prolonged time. An ideal device should be easy to produce in diverse forms (sponge, film, powder) to meet specific clinical demands, and should progressively release HA with defined and tunable molecular weight (MW) distribution; the latter feature is highly desirable considering that HA biological effects are related to the biopolymer chains' length. Currently available devices (HA-benzyl esters and self-esterified HA) proved effective in the clinical practice however, they are produced through time-consuming and complex procedures involving HA dissolution in organic solvents and steps performed under conditions degrading HA, thus hampering the control of the MW of the biopolymer released [1]. Efforts to set up more convenient procedures, using a water-soluble carbodiimide (EDC) have been reported but formation of acyl-urea by-products was observed [1]. Here, we aimed to evaluate the use of the EDC in association with 1-hydroxybenzotriazole (HOBt), combined with heterogeneous reaction conditions, for producing self-esterified HA networks. The EDC/HOBt system has been widely used for the coupling of amines to HA but was never reported for HA self-esterification. We reasoned that the proposed protocol would be a simplified procedure potentially overcoming the limits related to the conventional ones.

EXPERIMENTAL METHODS

HA samples with M_w=230-250kDa, M_w/M_n=1.6-2.0 (powder or sponges obtained by freeze-drying) were used. Several hydrogels were prepared at RT using 2-100% molar ratio of activating system (EDC/HOBt) to HA carboxylate groups. Products were characterized by NMR and SEC-TDA analyses to accomplish structural characterization and to evaluate the extent of HA insolubilization as well as the hydrodynamic parameters of the water-soluble fraction, including the MHS curves providing conformational information. The 3D-architecture of the sponges, before and after reaction, was observed by SEM. The treated sponges were also analyzed for the hydration degree and the mechanical behavior in physiological medium. The HA release in PBS was evaluated by monitoring HA solubilization and hydrodynamic parameters over incubation time. The HA released from the materials was tested for the ability to prompt wound healing in an *in vitro* scratch test using a primary human keratinocytes/fibroblasts co-culture and a time-lapse videomicroscopy station [2].

RESULTS AND DISCUSSION

The SEC-TDA data demonstrated that, when treated with increasing amounts of EDC/HOBt, HA initially increased its MW while exhibiting more compact conformation, then it became progressively water-insoluble up to 100% (wt%). The NMR data demonstrated that no by-products were formed. The sponges' 3D-architecture was preserved during reaction indicating that, unlike the conventional protocols, the polymer can be first processed to the desired form and then chemically modified. The sponges showed decreasing water up-take and increasing storage modulus when increasing the EDC/HOBt amount, confirming the possibility to tune the hydrogel biophysical properties by varying the extent of modification. Under physiological conditions, HA was progressively released from the matrices and the rate was slower at increasing modification extent. Furthermore, SEC-TDA data also demonstrated that the final released product is HA with the same MW distribution as the starting polymer. Thus, the developed protocol permitted to tune the released HA MW simply varying the size of the HA prior to chemical modification. Released HA proved to prompt Wound Healing in the *in vitro* model used.

CONCLUSION

Self-esterified HA matrices were successfully produced using a procedure that overcomes conventional protocols. Indeed, it allows chemical stabilization with high control of the molecular weight of the released HA whilst avoiding the formation of by-products and simplifying the synthetic approach and the processing with respect to current technologies. These results, along with the proved potential of the matrices to prompt *in vitro* wound healing, suggest the materials as interesting candidates for HA-based active wound dressing devices and, in general, for devices supporting tissue regeneration.

REFERENCES

[1] Schantè et al. Carbohydrate Polymers 85:469 (2011)
[2] D'Agostino et al. BMC Cell Biology 16 (2015)

Tuning of mechanical properties in photopolymerizable gelatin-based hydrogels for *in vitro* intestinal epithelial models

Regina Pamplona[1*], Sandra González-Lana[2,3], Ignacio Ochoa[3,4,5], Rafael Martín-Rapún[1,4], Carlos Sánchez-Somolinos[1,4]

[1] Aragón Institute of Nanoscience and Materials (INMA), CSIC-University of Zaragoza, Zaragoza, Spain
[2] BEONCHIP S.L., Zaragoza, Spain
[3] Aragón Institute of Engineering Research (I3A), University of Zaragoza, Zaragoza, Spain
[4] CIBER in Bioengineering, Biomaterials and Nanomedicine (CIBER-BBN), Spain
[5] Institute for Health Research Aragón (IIS Aragón), Zaragoza, Spain
[*] reginapc@unizar.es

INTRODUCTION

The mechanical microenvironment is a critical factor in the evolution of colorectal cancer (CRC) [1]. In order to set and study different scenarios, hydrogels have emerged as versatile biomaterials with a huge potential to behave as two- and three dimensional *in vitro* models owing to their unlimited functionalization possibilities. Gelatin methacryloyl (GelMA)- based hydrogels are of particular interest due to the peptidic backbone which provides cell adhesion sites [2] and the on-demand photopolymerization alternatives to create covalently crosslinked networks. In addition, photo-induced thiol-based reactions own many of the advantages of click chemistry, including robustness, simplicity and the formation of homogeneous networks [3]. Thus, it is highly relevant to develop a platform of bioscaffolds with different chemical composition and tunable stiffness in order to generate *in vitro* intestinal epithelial models for the study of CRC.

EXPERIMENTAL METHODS

In the present work, two types of biomaterials have been prepared and characterized: GelMA hydrogels were generated through UV-photopolymerization and GelMA-SH hydrogels followed a "mixed-mode" mechanism combining radical photopolymerization and thiol-ene step-growth reaction. Swelling properties, pore size and stiffness are reported for hydrogels prepared in PBS. In addition, hydrogels have also been prepared in DMEM and characterized in terms of swelling behaviour and stiffness. In order to check the biological relevance of these biomimetic materials, *in vitro* cell culture experiments were performed by seeding Caco-2 cells on the surface of four different substrates. Cell viability, adhesion and proliferation were reported. Lastly, immunofluorescence staining and SEM imaging were performed. Between three and five replicas were fabricated for mechanical characterization and cell culture experiments.
Student's t-tests were used to determine significant differences. Non-normally distributed populations were analyzed with the Mann-Whitney method.

RESULTS AND DISCUSSION

First of all, gelatin was successfully functionalized achieving almost 85% of amines derivatized into methacrylamide groups. UV irradiation of GelMA and GelMA-SH mixtures in PBS led to hydrogels exhibiting similar stiffness but with different curing times. Besides, the thiol click chemistry was found to be an effective tool to easily tune mechanical properties. GelMA-30, GelMA-150, SH-10 and SH-30 were the selected scaffolds to perform a deeper characterization study. While the crosslinking strategy and the irradiation time had no significant effect on hydrogels morphology, it was observed that thiol-ene systems showed higher swelling properties. Hydrogels prepared in DMEM exhibited markedly different values of Young's Modulus compared to PBS although the swelling trend was similar.
Regarding cell experiments, Caco-2 cells showed the best substrate adhesion after 24h on GelMA-150 whereas they hardly adhered to SH-10 scaffolds. A good cell proliferation was achieved in GelMA-30, GelMA-150 and SH-30 since the three conditions supported a confluent monolayer at day-14. Finally, SEM imaging of cell-seeded hydrogels showed a proper apical-basal polarization of cells according to a villus-forming monolayer, exposing structural differences among the different substrates.

CONCLUSION

This research describes a precise stiffness modulation of covalently crosslinked GelMA-based hydrogels by varying the photoirradiation time. A platform of bioscaffolds with different chemical composition and stiffness values covering a wide range from healthy tissue to cancerous stages, have been prepared. 2D *in vitro* studies showed successful cell viability, proliferation and polarization of Caco-2 cells-seeded hydrogels. This work demonstrates the formation of adequate epithelial models and stablishes the basis for future studies focused on more complex stroma models and deeper epithelium characterization.

REFERENCES

1. Liu, C. *et al*., Onco. Targets. Ther. 13:2747-2755, 2020
2. Yue K. *et al*., Biomaterials 73:254-271, 2015
3. Hoyle C.E. and Bowman C.N., Angew. Chemie – Int. Ed. 49:1540-1573, 2010

ACKNOWLEDGMENTS

Funding for this work was provided by the Spanish "Ministerio de Ciencia, Innovación y Universidades (MCIU)" through AEI/FEDER(UE) project PID2020-118485RB-I00; Gobierno de Aragoń project LMP221_21, FEDER (EU); through the "Fondo Social Europeo" (DGA E15_20R and E47_20R). RPC acknowledges Gobierno de Aragón for a predoctoral fellowship (2017-2021).

Gelatin modified with alkoxysilanes (GelmSi): a new hybrid polymer dedicated to bioengineering applications

Matthieu Simon* [1], Marie Maumus [1,2], Baptiste Legrand [3], Lilian sole [1], Marjorie Dufaud [1], Christian Jorgensen [1], Danièle Noël [1], Gilles Subra [3]

[1] IRMB, University Montpellier, INSERM, CHU Montpellier, Montpellier, France
[2] Bauerfeind, Montpellier, France
[3] IBMM, University Montpellier, CNRS, ENSCM, Montpellier, France

* matthieu-simon@chu-montpellier.fr

INTRODUCTION

The world of tissue engineering and regenerative medicine is booming and there is a strong need to develop innovative biomaterials as closest as possible to native extracellular matrix which allow the embedment of cells, their growth and differentiation towards determined tissues. ECM extracts such as Matrigel™ and Geltrex™, but also collagen-based hydrogels are extensively used in cell culture and tissue engineering thanks to high biocompatibility and bioactivity. However, they are impaired by some limitations including a poor control of their composition (for ECM extracts), a limited range of processing temperature, a low mechanical tunability and they cannot be easily chemically modified. On the other hand, easily processible scaffolds, such as polyethylene glycol and polysaccharide derivatives, natively lack bioactive components necessary for cell adhesion. Interestingly, the methacrylate gelatin[1] (GelMA) meets most of these specifications. However, its use requires exposure to UV light that generate free radicals which can be deleterious to the integrity of the cells.

EXPERIMENTAL METHODS

GelmSi intermediate was synthetized, purified and then characterized by UV-Vis, nuclear magnetic resonance (NMR), circular dichroism (CD), Energy-dispersive X-ray spectroscopy (EDS). Then, we carefully studied the sol-gel transition during this polymerization process by testing of the GelmSi hydrogel formation and viscoelasticity (G') over time. Finally, a protocol to encapsulate the cells into the hydrogel was developed followed by cell viability assays.

RESULTS AND DISCUSSION

In such a context, we developed a new matrix called "GelmSi" with biological and mechanical properties comparable to GelMA, but with an innocuous setup for initiation of the gelation process for bioengineering or medical applications thanks to the introduction of alkoxysilane moieties on gelatin. This chemical modification allows the formation of a chemical network in physiological conditions, and more importantly, in a fully chemoselective and biorthogonal manner. Siloxane bonds increases the mechanical properties and thermal stability of the gelatin making it fully compatible with cell encapsulation and cell culture at 37 °C. Moreover, this hybrid matrix allows the straightforward incorporation of silylated molecules during the network formation[2-6] (e.g. dye, drugs, biomolecules etc.). Importantly, we developed a synthesis protocol with a perfect control of the constituent of the matrix and an excellent batch-to-batch reproducibility.

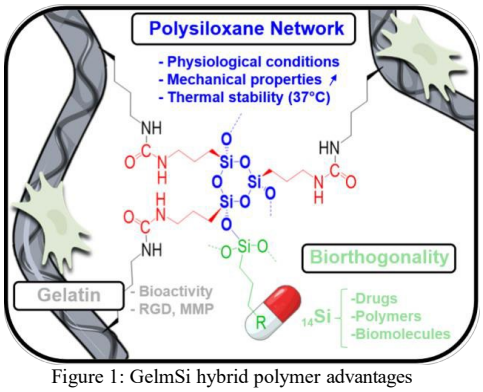

Figure 1: GelmSi hybrid polymer advantages

CONCLUSION

Together, these features open broad perspectives for many bioengineering applications, particularly where gelatin is already involved such as, for example, 3D bioprinting, tissue engineering, development of nanoparticles for drug or siRNA delivery and controlled drug release applications.

REFERENCES

1. V.D.Bulcke. *et al*., Biomacromolecules 1:31–38, 2000
2. Echalier, C. *et al.,* Chem. Mater 28:1261–1265, 2016
3. Montheil, T. *et al.,* ACS Omega 5:2640–2647,2020
4. Ciccione, J. *et al.,* Chem. Mater. 28:885–889, 2016
5. Jebors, S. *et al.,* J. Mater. Chem. B 1:2921–2925, 2013
6. Xu, Z *et al.,* Nanoscale 7:5859–5868, 2015

ACKNOWLEDGMENTS

The authors acknowledge the tissue engineering facility CARTIGEN supported by the FEDER/Region Occitanie program, the Montpellier University Hospital, and the University of Montpellier This work was also party founded by ANR (Agence Nationale de la Recherche) Legogel program ANR-16- CE18-0003.

Programmable DNA-Crosslinked Hydrogels as Adaptive Matrices for 3D Cell Culture

Yu-Hsuan Peng[1,2], Krishna Gupta[1,2], Syuan-Ku Hsiao[1,2], Dr. André Ruland[2], Dr. Günter K. Auernhammer[3], Prof. Carsten Werner[1,2], Dr. Elisha Krieg[1,2*]

[1]Technische Universität Dresden, Germany
[2]Institute for Biofunctional Polymer Materials, Leibniz-Institut für Polymerforschung Dresden e. V., Germany
[3]Institute of Physical Chemistry and Polymer Physics, Leibniz-Institut für Polymerforschung Dresden e. V., Germany
*krieg@ipfdd.de

INTRODUCTION

Materials that enable rational design and precise dynamic control over their properties are important for a wide range of applications. Hydrogels that consist of self-assembling DNA-based components are particularly interesting, since the molecular-scale programmability of DNA self-assembly can be used to modulate macroscopic material behavior[1,2,3]. Yet, DNA-based hydrogels typically require large concentrations of synthetic DNA, oftentimes resulting in prohibitively high material cost and potential undesired effects when in contact with living cells or tissues. We herein report a programmable, inexpensive, and cytocompatible soft material based on novel DNA crosslinker modules and DNA-grafted poly (acrylamide-co-acrylic acid) chains[4,5].

EXPERIMENTAL METHODS

i. Computational design of oligonucleotides

Using oligo simulation tool NUPACK, we designed the DNA crosslinker sequences and predicted their thermodynamic behaviors.

ii. Rheological characterization

The mechanical properties of gels were characterized by oscillatory rheology with a cone-plate geometry (MCR301, Anton Paar). The measurements were performed with three independent repeats.

iii. Extrusion printing

The formed gels were extruded by using BioScaffolder (GeSiM) with a disposable syringe.

iv. Cell viability assay

Mesenchymal stem cells (MSCs) were embedded and imaged with live-dead staining on the fluorescence confocal microscope after 2 days of culture. Three independent samples were examined in both 3D and 2D culture.

v. Enzymatic degradation quantification

The degradation rate of oligonucleotides in the presence of nucleases and its inhibitors was detected by qPCR.

RESULTS AND DISCUSSION

A novel crosslinking approach with combinatorial DNA crosslinker libraries (CCLs) promotes gelation at very low DNA concentration (0.13 wt% - 0.22 wt%). The material's stress-relaxation time (τ) can be tuned over a wide range (τ = 1 – 1000 s) via the DNA crosslinker sequence, mimicking the range of stress-relaxation behavior of living tissues. The temperature-dependent gelation time can be controlled by additional modules that predictably alter the non-covalent crosslinking reaction kinetics. The mechanical stiffness of the gels are comparable to basement membrane-like matrices that are commonly used in 3D cell culture. The DNA hydrogels are cytocompatible, exhibit rapid self-healing, and are suitable for extrusion printing. These features support the usage as a bio-ink for printing complex 3D tissue structures. The degradation of the gel under mild cell-compatible conditions can be promoted or inhibited via enzymes and other additives, allowing extended 3D cell culture for up to 8 days and subsequent release of cells.

CONCLUSION

These results highlight the unique programmability of DNA-crosslinked hydrogels. Using DNA-based cell culture matrices, the complex mechanical interactions of cells with their environment can be reproduced, observed, and dynamically modified. For the first time, the stress relaxation of the material can be adjusted without changing the biochemical properties of the material backbone or the medium. A high crosslinking efficiency can be achieved with relatively small amounts of DNA in this system. Thus, on one hand, these materials are less expensive, and on the other hand, the risk of stimulating unwanted reactions of the cells is reduced. In the future, the function of the materials can be extended by additional modules (e.g. sensor modules) via sequence-controlled self-assembly in various combinations. Taken together, the programmable DNA-crosslinked hydrogel paves the way to smart adaptive systems, expanding the toolbox for tissue engineering and other biomedical applications.

REFERENCES

[1] Simmel, F. C. & Schulman, R. MRS Bulletin 42, 913 (2017).
[2] Gačanin, J., Synatschke, C. V., Weil, T., Adv. Funct. Mater. 30, 1906253 (2020).
[3] Ohira, M., Katashima, T., Naito, M., et al. Adv. Mater. 2108818 (2022).
[4] Krieg, E. & Shih, W. M. Angew. Chem. Int. Ed. 57, 714 (2018).
[5] Krieg, E., Gupta, K., Dahl, A., Lesche, M., Boye, S., Lederer, A. & Shih, W. M. Commun Biol 3, 369 (2020).

ACKNOWLEDGMENTS

The authors would like to thank the Bundesministerium für Bildung und Forschung (BMBF) NanoMatFutur (Grant no: 13XP5098) for providing financial support to this project.

Collagen/hyaluronan polyionic complexes as a new building block to develop a novel bioink to model the intervertebral disc

Stéphanie De Oliveira[1], Gregor Miklosic[2], Matteo D'este[2], Sébastien Grastilleur[3], Joëlle Véziers[3] & Christophe Hélary[1]
[1] Laboratoire de Chimie de la Matière Condensée de Paris, Paris, France
[2] AO Research Institute, AO Foundation, Davos, Switzerland
[3] Regenerative Medicine and Skeleton Laboratory, Nantes, France
stephanie.de_oliveira@sorbonne-universite.fr

INTRODUCTION

Intervertebral disc (IVD) degeneration is not completely understood yet and requires the development of novel 3D in vitro models to test new treatments. As IVD is mainly composed of collagen and glycosaminoglycans, a novel bioink consisting of type I collagen and tyramine functionnalized hyaluronic acid (THA) have been developed in this study to design IVD models by 3D printing. It has been shown that these two biopolymers aggregate and form polyionic complexes (PIC) when mixed together. In this study, we have investigated the PIC formation thanks to a physicochemical study and found the best formulation to get a homogeneous 3D printable hydrogel which can be used to model IVD.

EXPERIMENTAL METHODS

The effects of pH (HCl concentration from 10^{-1}M to 10^{-3}M) and ionic strength (chloride sodium concentration of 0 and 400mM) on PIC formation were investigated. The solutions were observed by CryoSEM to detect the collagen/THA interactions. Then, collagen and THA gelation were triggered. Collagen fibrillogenesis was induced by pH rise with ammonia vapors to form a physical hydrogel. THA crosslinking was conducted using either Horse Radish Peroxidase (HRP) with H_2O_2 or eosin Y with green light. The hydrogel ultrastructure, mechanical and thermal properties were characterized by Differential Scanning Calorimetry, Scanning Electron Microscopy and Rheometry.

RESULTS AND DISCUSSION

Collagen/THA solutions with a hydrochloric acid concentration of 10^{-1}M were homogeneous. For the other pH conditions, PIC were observed with a perturbated ultrastructure observed in CryoSEM. By adding salt, PIC formation was inhibited leading to a colloidal solution. After collagen gelling, small PIC and homogeneous hydrogels were observed when NaCl was added. Their ultrastructure consisted of collagen fibrils as seen in *Figure 1A*. However, THA seemed to weaken the mechanical properties of the collagen network measured by rheometry (*Figure 1B)*.

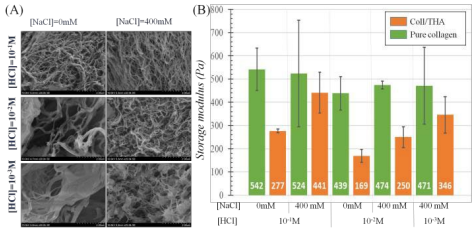

Figure 1: Impact of THA on (A) the ultrastructure and (B) the storage moduli of collagen/THA hydrogels.

In a second time, fibrillated hydrogels were crosslinked using HRP/H_2O_2 to trigger THA gelling. Unfortunately, storage moduli of hydrogels did not increase, suggesting the absence of gelation by HRP/H_2O_2. As an alternative, THA gelling was triggered by the eosin Y/green light system. The latter seemed to enhance the storage modulus for the formulations using [HCl] at 10^{-2}M and 10^{-3}M (*Figure 2)*. Last, THA gelling was performed prior to collagen fibrillogenesis but mechanical properties were very low.

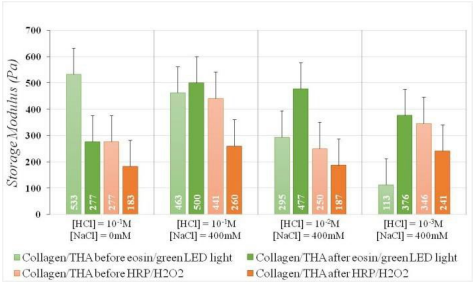

Figure 2: Impact of the THA crosslinker on the storage moduli of collagen/THA hydrogels measured by rheometry.

CONCLUSION

Taken together, the condition using salt and 10-2M HCl seems to be the most appropriate to develop a collagen/THA bioink because it lowers the PIC formation and allows for the hydrogel formation. Collagen gelling needs to be performed first followed by the THA one using green light and eosin Y. This procedure could be useful for 3D printing in order to design an in vitro model of IVD.

ACKNOWLEDGMENTS

Conducted within the scope of the INDEED project, funded by the Swiss National Science Foundation (189310) and French National Research Agency (ANR-19-CE06-0028).

Basic characterization of gelatin_κ-carrageenan hydrogels as potential novel biomaterials for biomedical application

Marta Tuszyńska[1*], Joanna Skopińska-Wiśniewska[2], Jakub Marchewka[3], Piotr Jeleń[3], Maciej Bik[3], Anna Bajek[1]

[1]Faculty of Medicine, Department of Tissue Engineering, The Ludwik Rydygier Collegium Medicum in Bydgoszcz, Nicolaus Copernicus University in Torun, Poland
[2]Faculty of Chemistry, Nicolaus Copernicus University in Torun, Poland
[3]Faculty of Materials Science and Ceramics, AGH University of Science and Technology, Krakow, Poland
[*]marta.tuszynska96@gmail.com

INTRODUCTION

Hydrogels are promising biomaterials for innovative biomedical applications due to their biocompatibility, excellent permeability, and similarity to the native extracellular matrix. Over the past decades, hydrogels have attracted special attention in the field of tissue engineering, wound dressing, and treating injuries that are practically difficult to access [1]. The κ-carrageenan derived from red algae, *Acanthophora spicifera*, belongs to hydroxyl and sulphate groups. κ-Carrageenan in presence of potassium ions forms strong, rigid gels applicable as novel biomaterials in biomedical research [2]. Gelatin is a biopolymer that has been combined with κ-carrageenan. Gelatin is a protein obtained by partial denaturation of collagen. It has many advantages, including excellent biocompatibility, biodegradability, and non-immunogenicity [3].
The aim of this study was the characterization of non-crosslinked and crosslinked gelatin_κ-carrageenan gels.

EXPERIMENTAL METHODS

Both gelatin and κ-carrageenan were dissolved in water and then mixed in different volume ratios to finally obtain a solution of 6% gelatin and 2% κ-carrageenan (G6_Car2) in one mixture. KCl solutions of two different concentrations were prepared, 1% and 5%. Then gels were immersed in potassium chloride solutions (G6_Car2_KCl1 and G6_Car2_KCl5).
Materials were characterized based on SEM images, FT-IR spectrum, and contact angle measurements. The morphology images of lyophilized G6_Car2 biomaterials were obtained, by a scanning electron microscope (SEM) manufactured by Phenom XL, ThermoFisher Scientific. The chemical structure of hydrogels was analyzed by FT-IR spectroscopy using Vertex 70v Bruker spectrometer and DRIFT technique, where the sample was heated 1°C/min up to 80°C and then cooled down 1°C/min to 25°C. Finally, the contact angle of gelatin_κ-carrageenan gels was measured using Krüss DSA25E Drop Shape Analyzer.

RESULTS AND DISCUSSION

The results obtained in SEM imaging showed that all hydrogels possess a 3-D porous structure, with pores of irregular shape and heterogenic size. Surprisingly, the pore size increased after using a more concentrated of KCl solution. The avg. pore size was 176,67 µm (G6_Car2), 145,67 µm (G6_Car2_KCl1) and 214,33 µm (G6_Car2_KCl5). According to the obtained data, the FT-IR DRIFT spectra of unmodified and cross-linked gels confirmed the presence of absorption bands characteristic to gelatin and κ-carrageenan. The temperature increase up to 80°C did not cause any significant changes in the hydrogel structure, except the water loss. All the materials remained solid. The water contact angles were lower than 90° for all the hydrogel surfaces. The lowest contact angle was noted for G6_Car2_KCl1 hydrogel. Thus, this indicates that this material is the least hydrophilic of tested gels. The material not immersed in KCl solution performed as the most hydrophilic, suggesting the influence of the potassium ions on the wettability of the material.

CONCLUSION

The basic characterization of the tested materials, was obtained. It was proven, that the non-cross-linked material is the most hydrophilic, and its structure is less stable compared to the cross-linked gels. Cross-linker immersion is an important step to form sustained gelatin_κ-carrageenan hydrogels. The higher the concentration of KCl solution, the more stable structure, was obtained. The hydrogel cross-linked with 5% KCl has an appropriate porous structure and is the most stable gel during the temperature increase. Thus, this hydrogel is the most promising for further biomedical research.

REFERENCES

1. Pettinelli N. *et al*., Int. J. Pharm. 589, 2020
2. Muthulakshmi L. *et al*., Mater. Chem. Phys. 258, 2021
3. Li H. *et al*., Carbohydr. Polym. 198: 261–269, 2018

Chemically Crosslinked Hyaluronic Acid-Chitosan Scaffolds for Potential Application on Cartilage Regeneration

Sandra Escalante[1,2], José Becerra[1,2], Julio San Román[2,3], Mª Rosa Aguilar[2,3], Iván Duran[1,2], Luis García-Fernández[2,3,*]

[1]Laboratory of Bioengineering and Tissue Regeneration-LABRET, Department of Cell Biology, Genetics and Physiology, Málaga (Spain)
[2]Centro de Investigación Biomédica en Red, Bioingeniería, Biomateriales y Nanomedicina (CIBER-BBN.) Madrid (Spain).
[3]Instituto de Ciencia y Tecnología de Polímeros. Consejo Superior de Investigaciones Científicas (ICTP-CSIC). Madrid (Spain).
* luis.garcia@csic.es

INTRODUCTION

Articular cartilage is an avascular tissue that lines the ends of bones in diarthrodial joints, serves to support, acts as a shock absorber, and facilitates joint's motion in low friction. Damage to these tissues is usually associated with traumatic injuries or age-associated processes that often lead to discomfort, pain and disability in patients.
Human articular cartilages are composed of a dense extracellular matrix and chondrocytes. One of the major components of this extracellular matrix is hyaluronic acid. The combination of hyaluronic acid with other natural polymers to prepare hydrogel scaffolds may be potentially useful in many tissue engineering applications, including cartilage regeneration.
We proposes the synthesis of hydrogels based on hyaluronic acid and chitosan by a new strategy of synthesis using di-isocyanates to obtain an interpenetrated network of chitosan and hyaluronic acid for cartilage repair.

EXPERIMENTAL METHODS

Hyaluronic acid-chitosan (HACh) hydrogels were synthesized using L-lysine diisocyanated as crosslinker. In order to improve cartilage regeneration the hydrogels were loaded with chondroitin sulphate (HAChCS).

Biocompatibility

Cytotoxicity in vitro assays (MTT) and cell adhesion tests (Alamar Blue) were performed on the hydrogels using different cell lines to corroborate the biocompatibility of the hydrogels.

Cell differentiation and chondrogenesis assay

Histological analysis of scaffolds seeded with mesenchymal stem cells were performed to visualized proteoglycan production with Alcian Blue.

RESULTS AND DISCUSSION

The toxicity of lixiviates coming from the different scaffolds was evaluated on hOBs and hACs (Figure 1 (a) and (b)). Cell viability on hACs was not affected on the first days. After 7 days, there is significant differences in the viability in comparison with the control but in general, the cell viability is higher than 90 %. In the case of hOBs cell viability increase in contact with scaffolds lixiviates.
Cell proliferation (Figure 5 (c) and (d)).increase over time for all the systems but is lower in the scaffolds that in the control. This difference is due to the surface of the scaffolds, the cells needs more time to adhered on an irregular surface, but after the first days the cell growing on the surface significantly increase with the time. The presence of CS on the scaffold improve cell proliferation.

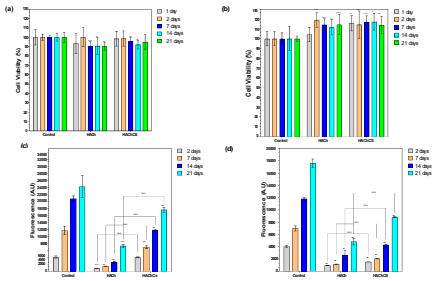

Figure 1 (a) and (b). Cell viability of hACs (a) and hOBs (b) cultures with HACh and HAChCS scaffolds lixiviates. **(c)** and **(d)** Cell proliferation values of hACs (c) and hOBs (d) seeded on HACh and HAChCS scaffolds.

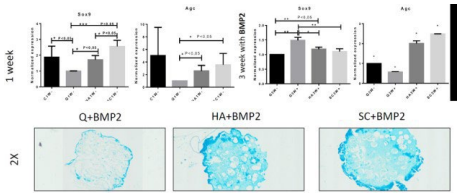

Figure 2. Expression analysis of SOX9, aggrecan and osteocalcin and microscopic images of the histological stain with Alcian Blue.

Expression analysis of skeletal differentiation markers determined that HAChCS promoted sox9 expression during initial differentiation stages, and an increase in the cartilage structural component aggrecan, both signs of a healthy cartilage. Histology staining of cartilage proteoglycans by Alcian Blue confirmed presence of mature chondrocytes and cartilage matrix.

CONCLUSION

The results support that the HAChCS scaffold promotes chondrogenic differentiation and its potential for cartilage regeneration.

ACKNOWLEDGMENTS

This work was supported by the Ministry of Science, Innovation and Universities (Spain) (PID2020-114086RB-I00 and PID2020-117255RB-100-VASCUBONE). This research work was performed in the framework of the Nanomedicine CSIC HUB (ref202180E048) and L. García-Fernández and M.R. Aguilar are members of the SusPlast+ platform from the CSIC.

Characterization and Mechanical Properties of AgNPs/Gelatin/PEGDA Hydrogels for Wound Dressing

Tuğçe Şener Raman, Stefan G. Mayr, Bernd Abel, Agnes Schulze

Leibniz-Institute of Surface Engineering (IOM), Permoserstrasse 15, 04318 Leipzig, Germany
E-mail: tugce.senerraman@iom-leipzig.de

INTRODUCTION

Hydrogels are one of the candidates with the most potential to mimic the native skin microenvironment, due to their porous and hydrated molecular structure. Also, they can be applied as a dressing to support the regeneration and healing of the injured skin [1]. Hydrogels can be subdivided into two main groups, natural and synthetic, based on the material used for their fabrication. Natural polymers such as gelatin mimic the natural dermal extracellular matrix and can be therefore easily employed for wound dressings, but it has insufficient and uncontrollable mechanical properties and high degradation rate [2-3]. While hybrid hydrogels overcome this problem, they possess both suitable mechanical properties and strong biocompatibility, and biodegradability compared to natural hydrogels and synthetic hydrogels as a single polymer material. Additionally, to increase the antimicrobial properties of hydrogels silver nanoparticles could be implemented which are the most adopted antibacterial agent. Silver nanoparticles (AgNPs) in combination with hybrid hydrogels can be the basis of the new generation of antimicrobial materials [4].

EXPERIMENTAL METHODS

In this study, Gelatin/PEGDA hybrid hydrogels with AgNPs in various concentrations were synthesized with an electron beam to provide biocompatibility, high mechanical strength, and sterilization required for wound dressing. The reason why electron beam polymerization was preferred in the study is to promise high efficiency as well as precise and fast crosslinking while not inducing cytotoxicity.

I

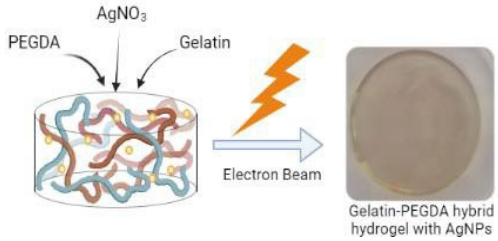

Figure 1. Schematic illustration of synthesized AgNPs/Gelatin/PEGDA hydrogels by electron beam

RESULTS AND DISCUSSION

It was investigated how the mechanical structures of synthesized Gelatin/PEGDA hybrid hydrogels with AgNPs at different concentrations of AgNPs and applied electron beam irradiation at various doses affect the mechanical structure of these hydrogels. For determining the mechanical properties of the hydrogels, rheology properties, swelling ratio, and crosslinking ratio measurement were investigated. The degree of crosslinking of the hydrogels was found to increase with an increase in the irradiation dose. In swelling test, it was determined that increased AgNPs concentration and irradiation dose in hydrogels affected the swelling properties of hydrogels significantly. Moreover, toxicity studies revealed AgNP size and concentration-dependent effects. Therefore, the release of AgNPs and AgNPs size in hydrogels were detected at various irradiation doses and AgNPs concentrations to control the cytotoxicity of AgNPs.

CONCLUSION

Synthesized Hybrid hydrogels have higher mechanical stability than Gelatin. Additionally, electron irradiation demonstrated the ability to precisely tune the hybrid hydrogel properties by the selection of dose and AgNPs concentrations.

REFERENCES

1. Tavakoli S. *et al*., Biomolecules, 8:1169-10, 2020.
2. Zhao X., *et al*., Adv. Healthc. Mater. 5:108-118, 2016,
3. Wisotzki E. I., *et al*., J. Mater. Chem. B, 2:4297, 2014.
4. Varaprasad K., *et al*., J Mater Sci Mater Med, 11: 4369, 2011.

ACKNOWLEDGMENTS

T. Sener Raman is grateful for a scholarship from the Republic of Turkey, Ministry of National Education.

Engineering Hydrogels with Tunable Mechanical Properties for Targeted Stem Cell Differentiation

Cristina Lopez-Serrano[1,2,3,4,5], Murielle Remy[3,4,5], Christel Chanseau[3,4,5]. Andrée-Anne Guay-Bégin[1,2], Jean Ruel[6, 2], Cécile Feuille[3,4,5], Michael Molinari[3,4,5], Gaétan Laroche[1,2], Marie-Christine Durrieu[3,4,5]

[1] Laboratoire d'Ingénierie de Surface, Département de génie des mines, de la métallurgie et des matériaux, Université Laval, Québec, Canada, [2]Axe Médecine Régénératrice, Centre de recherche du CHU de Québec-Université Laval, Hôpital St-François d'Assise, Québec, Canada, [3]Université de Bordeaux, Chimie et Biologie des Membranes et Nano-Objets (UMR5248 CBMN), Pessac, France, [4]CNRS, CBMN UMR5248, Pessac, France, [5]Bordeaux INP, CBMN UMR5248, Pessac, France, [6]Département de Génie mécanique, Université Laval, Québec, Canada
cristina.lopez-serrano@u-bordeaux.fr

INTRODUCTION

Successful tissue engineering strategies depend on an accurate replication of key characteristics of the cell environment. Traditionally, the focus has been put on chemical signals, which consist in interactions between cell receptors and ligand molecules. Over the past decades, mechanobiology has emerged as a key field in bioengineering. It is now known that cells detect and respond to the mechanical properties of their surroundings. Accordingly, the in vitro differentiation of stem cells is affected by the stiffness of the substrate on which they are cultured[1]. Later studies have demonstrated that cell behaviour is dependent, not only on the elastic modulus, but also on the viscoelastic mechanical properties of the matrix[2–4].

Mesenchymal Stem Cells (MSCs) are adult multipotent stem cells, widely used in tissue engineering since they can differentiate towards various lineages, and thus are suitable in many applications. However, it is challenging to tightly control this differentiation process to obtain a single type of cell, bone cells for instance. It is necessary to further define the effect of matrix elasticity and viscoelasticity in 2D versus 3D cell cultures, as well as the interplay between these mechanical characteristics and the presence of bioactive molecules such as adhesion or differentiation peptides. In this context, our research challenge is to develop a material that encompasses the optimal properties to obtain osteogenic differentiation of MSCs.

METHODS AND RESULTS

To address this objective, polymer-based hydrogels are synthesized in a biologically relevant range of stiffnesses. To do that, solutions of poly(ethylene glycol) diacrylate (PEGDA, M.W=4kDa) at different concentrations are photocrosslinked under UV light to form a reticulated polymer network. Their macroscopic elastic and viscoelastic properties are measured though uniaxial compression testing and dynamic mechanical analysis (DMA). A material with different elastic modulus but comparable viscoelastic behaviour has been fabricated (Fig. 1). Atomic Force Microscopy (AFM) will be used to measure the surface mechanical properties at the nanoscopic and microscopic level.

Previous research has shown that the bifunctionalization of materials with both adhesion and differentiation peptides boosts the osteogenic potential of hMSCs [5]. For this reason, hydrogels will be covalently grafted with RGD and BMP-2 mimetic peptides. Tagging the peptides with a fluorescent dye enables to assess the homogeneity and density of grafted domains using fluorescent microscopy. Osteogenic differentiation of hMSCs will be evaluated via immunofluorescence staining and qPCR.

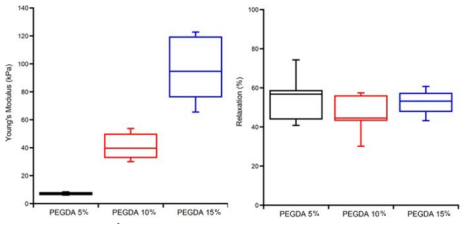

Figure 1: Young's modulus (a) and relaxation percent (b) for different PEGDA concentrations

CONCLUSION

Further work will focus on the fabrication of PEG-based 3D scaffolds with similar characteristics in terms biofunctionality and mechanical properties in order to compare the cellular response between 2D and 3D cultures. Different techniques for 3D porous scaffold fabrication are considered, including laser-assisted 3D printing and porogen leaching using gelatin microspheres.

REFERENCES:

1. gler, A. J., Sen, S., Sweeney, H. L. & Discher, D. E. Matrix Elasticity Directs Stem Cell Lineage Specification. *Cell* **126**, 677–689 (2006).
2. audhuri, O., Cooper-White, J., Janmey, P. A., Mooney, D. J. & Shenoy, V. B. Effects of extracellular matrix viscoelasticity on cellular behaviour. *Nature* **584**, 535–546 (2020).
3. uvé, E. *et al.* Evaluating Poly(Acrylamide-co-Acrylic Acid) Hydrogels Stress Relaxation to Direct the Osteogenic Differentiation of Mesenchymal Stem Cells. *Macromolecular Bioscience* **21**, 2100069 (2021).
4. uvé, E. *et al.* Interplay of matrix stiffness and stress relaxation in directing Mesenchymal Stem Cells osteogenic differentiation. *Bioactive Materials* (2022).
5. em, I. *et al.* RGD and BMP-2 mimetic peptide crosstalk enhances osteogenic commitment of human bone marrow stem cells. *Acta Biomaterialia* **36**, 132–142 (2016).

Development of a Structured Fluid Spray to Prevent Oral Scarring in Epidermolysis Bullosa Patients

Thomas E. Robinson[1*], Richard J.A. Moakes[1], Iain L.C. Chapple[2], Adrian H.M. Heagerty[3], Anthony D. Metcalfe[1], Liam M. Grover[1]

[1]Healthcare Technologies Institute, University of Birmingham, Birmingham, UK
[2]School of Dentistry, University of Birmingham, Birmingham, UK
[3]Institute of Inflammation and Aging, University of Birmingham, Birmingham, UK

[*] T.E.Robinson@bham.ac.uk

INTRODUCTION

Epidermolysis bullosa (EB) is a group of genetic conditions that can cause blistering and scarring often with minimal trauma. While the effect on the external skin is the most visually apparent, blistering and scarring can also affect the skin of the mouth (called mucosa), leading to problems with eating and oral hygiene. The purpose of this study was to develop a new oral spray, which would provide good coverage of the oral mucosa, and a long retention time to allow any loaded anti-fibrotics to act. Many existing sprays have material properties similar to water, which allows them to spray well but leads to poor mucoadhesion when *in situ*. To overcome this issue, we investigated utilising polymers to increase the viscosity, elasticity, and specific mucoadhesion of our anti-fibrotic sprays.

EXPERIMENTAL METHODS

The viscosity and other rheological properties of the materials were assessed using a rheometer with a double-gap geometry. Sprayability was assessed by first mixing rhodamine-6G (0.001%) into the sample, spraying from a set distance onto firm paper, scanning the pattern with a fluorescence scanner, and analyzing the image using ImageJ software. Mucoadhesion was measured by applying the materials to a mucin-gelatin gel, and measuring the time taken for them to flow a set distance, or rheologically using this gel as the bottom plate. Collagen fibrillogenesis was measured by mixing cold collagen with the material, and observing the increase in absorption over time and collagen fibrils form. An *in vitro* scarring model was established by exposing dermal cells to transforming growth factor beta, inducing a scar like response. The materials were mixed into the media, and their ability to prevent scarring measured immuno-histochemically.

RESULTS AND DISCUSSION

An initial study showed that gellan, a bacterially derived polysaccharide, covered a relatively large area when sprayed and could be formulated into sprayable formulations in 3 ways; as a dispersion, as a solution, and as a fluid gel, a hydrogel which undergoes shear during gelation to produce gelled particles in an interstitial phase. Solutions were found to spray well in the dilute regime, although at a certain polymer concentration the spray area suddenly decreased. Interestingly, this did not correlate precisely with the onset of structuring, which occurred at slightly higher polymer concentrations. However, by increasing the salt concentration and moving into the gelled regime (at sufficiently high polymer concentrations), a large spray area could be maintained even at high viscosity, thought to be due to the gel particles depleting polymer interactions within the interstitial phase.

To probe this further, gellan was compared to carrageenan, another polysaccharide with potential anti-fibrotic efficacy. Here it was shown that sprayability did not correlate with viscosity, but was instead related to viscoelastic relaxation time (Figure 1).

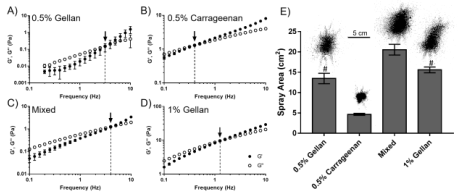

Figure 1: Frequency sweeps of gellan and carrageenan (A-D), showing that the crossover point (the inverse of the viscoelastic relaxation time) is directly related to spray area (E).

The functional characteristics of the sprays were then evaluated. Gellan was found to be more mucoadhesive than carrageenan, owing to its high density of hydroxyl groups. Polymers were assessed for their ability to inhibit collagen fibrillogenesis, and interestingly all polyanions tested inhibited this process above a certain concentration, however a neutral polymer gave no effect. The next step in this project will thus be to test the anti-fibrotic properties of the formulations in the developed *in vitro* scarring model.

CONCLUSION

Viscosity is not a direct predictor of sprayability in structured fluids systems. This knowledge can be used to create new formulations that spray well, but have the material characteristics to provide extended mucoadhesion and thus therapeutic effectiveness. By loading anti-fibrotic agents into these sprays, a new device can be created to lessen the oral effects of EB.

ACKNOWLEDGMENTS

The authors would like to thank the DEBRA UK for providing financial support to this project.

Self-assembling peptide hydrogels for nucleus augmentation of the intervertebral disc

Matthew Culbert[1*], James Warren[1], Hazel Fermor[1], Paul Beales[2], Ruth Wilcox[1]

[1]Institue of Medical and Biological Engineering, University of Leeds, UK
[2]School of Chemistry, Astbury Centre for Structural Molecular Biology and Bragg Centre for Materials Research, University of Leeds, UK
[*]cm14mpc@leeds.ac.uk

INTRODUCTION

Lower back pain affects 80 % of adults and has estimated costs up to 1 – 2 % of GDP[1,2]. Current surgical treatments include spinal fusion but outcomes are poor with reoperation required in 20% of patients[3]. Nucleus augmentation is the delivery of a biomaterial into the nucleus of a degenerated intervertebral disc with the aim of restoring the biomechanical properties of the disc. Self-assembling peptides (PEP) can be used with glycosaminoglycans (GAG) to form a PEP-GAG hydrogel and tuned to improve the biocompatibility and mechanical properties for use as a nucleus augmentation material. This work focuses on the non-charged polar amino acids (serine and/or glutamine) in the peptide sequence and their effect on the material properties.

EXPERIMENTAL METHODS

All samples contained peptide (20 mg/ml) with or without chondroitin sulfate (136 mg/ml). All hydrogel samples were maintained at room temperature for 24 hours before testing.

Differential scanning calorimetry (DSC) was run from 20 – 80 °C, held at 80 °C and then run from 80 – 20 °C.

Small amplitude oscillatory shear rheology was used to assess mechanical properties of different gels and different delivery needle designs. The linear viscoelastic region (LVER) was determined for each PEP-GAG hydrogel and material properties within the LVER were investigated.

Contact, extract, and filter diffusion assays were used to assess PEP-GAG hydrogel cytotoxicity with L929 and BHK cells.

Peptide samples were made at a range of concentrations in D_2O to determine the critical concentration for self-assembly using ^1H NMR (500 MHz).

CryoSEM and FIB-SEM images were obtained using FEI – Helios G4 CX Dual beam FIBSEM.

RESULTS AND DISCUSSION

As the end polar amino acid changes from ser-ser to glu-ser to glu-glu the c* was found to decrease as a result of the increased number and strength of intermolecular hydrogen bonding. An increase in absorption energy was also seen in the DSC data. When combined with GAGs the hydrogel rheology data showed that increasing glutamine content increased the phase angle. When injected down different needle length, gauges and designs there was a slight reduction in gel stiffness (G') when the design was changed but the stiffness was still within the required clinical range.

CryoSEM images showed that all three PEP-GAG hydrogels were able to form fibrous networks.

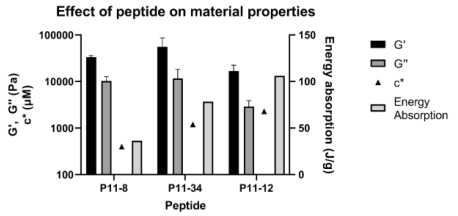

Figure 1 – c and energy absorption of peptides. Mechanical properties of PEP-GAG hydrogels.*

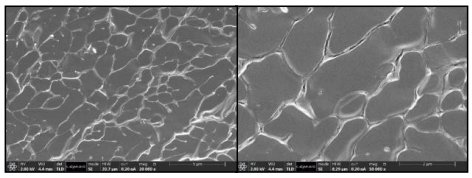

Figure 2 – CryoSEM images of P11-34-GAG hydrogel.

Cytotoxicity testing of different PEP-GAG hydrogels showed some slight cytotoxicity in the indirect and extract assays. Changing the peptide counterion from TFA showed that HCl resulted in a significantly higher cell viability in the extract assay.

CONCLUSION

Changing the end polar amino acid between glutamine and serine allows for tuning of the material properties whilst maintaining a low level of cytotoxicity. The mechanical properties as determined by rheology suggest that the PEP-GAG hydrogels are suitable for nucleus augmentation. The clinical delivery system was found to deliver the gels within the required stiffness range and provides the advantages of minimizing damage to the annulus fibrosus and enabling simultaneous delivery of the two components.

REFERENCES

1. Kent, P.M. *et al*, Chiropr. Osteopat. 13:13, 2005.
2. Philips, C.J. *et al*, Expert. Rev. Pharmacoecon. Outcome Res. 6:591-601, 2006.
3. Gillet, P. J Spinal Disord Tech. 16:338-345. 2003.

ACKNOWLEDGMENTS

The authors would like to acknowledge Stuart Micklethwaite and LEMAS for their support obtaining cryoSEM and FIB-SEM images.

The authors would like to thank the UK EPSRC (Grant no: EP/L014823/1) for providing financial support to this project.

Evaluation of enzymatic *in-situ* Crosslinking for the development of soft tissue engineering matrices

Sonja Kuth[1*], Aldo R. Boccaccini[1]

[1]Institute of Biomaterials, Friedrich-Alexander-Universität Erlangen-Nuremberg, Erlangen, Germany
[*] sonja.kuth@fau.de

INTRODUCTION

When developing hydrogels for biomedical applications various processing details must be considered. Next to the choice of hydrogel material itself, the crosslinking characteristics play an important role for the success of the developed matrix with regard to biocompatibility, stability and ideal mechanical properties. Hyaluronic acid (HA) is a biodegradable, biocompatible and non-immunogenic polysaccharide native to the human body extracellular matrix (ECM).[1] Upon oxidation, aldehyde groups are formed in the OHA chain, enabling a covalent crosslinking to amino groups of proteins, such as gelatin.[1] Gelatin (GEL) is synthesized from collagen, which is an abundant polymer in the mammalian body.[2] Various crosslinking options are available for HA and GEL, many of them however include toxic reagents or environmental conditions harmful to cells. (Microbial) transglutaminase (mTG) is an enzyme native to the human body inducing an amide crosslink between collagen amino groups.[3] In this work, different approaches to include mTG in OHA/GEL crosslinking will be developed and compared. The best possible concentration of mTG in the hydrogel matrix was determined by measuring degradation behavior, mechanical properties, and release of gelatin from the crosslinked samples.

EXPERIMENTAL METHODS

Hydrogel crosslinking. OHA/GEL hydrogels were crosslinked using two different protocols. Post crosslinked OHA/GEL was prepared following a previous protocol by mixing OHA and GEL in a ratio of 1:1 and initiating thermal gelation at room temperature. A crosslinking solution containing mTG was added on top of the sample. After crosslinking, the solution was removed and the samples were stored in saline. For the crosslinking of *in-situ* crosslinked samples two different concentrations of mTG were added to OHA first, which was then mixed with GEL to achieve a final concentration of 1:1 (OHA:GEL). *In-situ* crosslinking occurred at room temperature.

Release of GEL from crosslinked samples. The release of GEL from the crosslinked samples was measured over an incubation period of 28 days and compared for both crosslinking approaches (n=6).

Degradation of crosslinked hydrogels. The degradation of the differently crosslinked hydrogels was determined by measuring the change of wet weight (n=6) and mechanical properties (n=4) over 28 days of incubation at cell culture conditions. For measurement of mechanical properties parallel plate compression was employed.

Statistical analysis. Statistical analysis was performed by analysis of variances. For the comparison of the mean values, the Tukey post hoc analysis was used.

RESULTS AND DISCUSSION

In all experiments *in-situ* crosslinked samples showed superior properties compared to post-crosslinked ones. The degradation rate *of in-situ* crosslinked hydrogels was significantly reduced indicating a higher density and more homogenous distribution of crosslinking bonds compared to the post-crosslinked samples. Similar results were shown by the mechanical analysis where stiffness was reduced more rapidly in the post-crosslinked hydrogels. The results were confirmed by the protein release study where a lower amount of gelatin was released from the *in-situ* crosslinked samples, indicating a denser and more homogenous crosslinking of gelatin by this crosslinking protocol. Cell viability tests confirmed no negative effects on cell viability by the *in-situ* added mTG. In a direct cell test a slightly lower cell viability was found for the mTG samples compared to the mTG free control.

CONCLUSION

By comparing the two different techniques of crosslinking OHA/GEL samples by mTG, the *in-situ* protocol was found to be superior in terms of crosslinking homogeneity, structural integrity and consistency of mechanical properties during incubation. This crosslinking protocol therefore provides improved requirements for soft tissue engineering applications

REFERENCES

1. Pandit, A.H. *et al.*, Int J Biol Macromol. 137, 853, 2019.
2. Xiao, Z. *et al.*, PeerJ. 5:e3665, 2017.
3. Yung, C.W. *et al.*, Wiley Periodicals, Inc. J Biomed Mater Res 83A: 1039–1046, 2007

ACKNOWLEDGMENTS

The authors thank the FAU Emerging Fields Initiative (EFI) on "Novel Biopolymer Hydrogels for Understanding Complex Tissue Biomechanics" for financial support during this project.

Phenolic agent as an addition to alginate-based hydrogels for 3D printing and drug delivery approaches

Faina Bider[1*], Marta Miola[2], Enrica Vernè[2] and Aldo R. Boccaccin[1]

[1]Institute of Biomaterials, Friedrich-Alexander-Universität Erlangen-Nuremberg, Erlangen, Germany
[2]Applied Science and Technology Department, Politecnico di Torino, Torino, Italy
[*]faina.bider@fau.de

INTRODUCTION

Tissue Engineering (TE) involves the development of regenerative scaffolds following the combination of cells and biomaterials, which should mimic human tissue functions and structure [1].

Sodium alginate, a natural polymer derived from brown algae, is a widely used hydrogel material to design inks for 3D bioprinting and several medical applications, including TE and drug delivery systems. The oxidation of alginate leads to alginate di-aldehyde (ADA), which enables the covalent bonding to the free NH_2-groups in proteins like gelatin (GEL) resulting in ADA-GEL via Schiffs base formation [2].

The formation of biofilms following bacteria adhesion could lead to the loss of function or failure of the 3D printed scaffolds [3]. For that reason, the addition of an antibacterial agent to hydrogel bioinks is a reasonable approach to prevent risk of infections. Ferulic acid (FA) is a natural phenolic phytochemical, which can be extracted from the plant cell walls and is well known for its antioxidant, anticancer and antibacterial properties [4].

The main aim of this study was to develop ADA-GEL bioinks containing FA. The most suitable concentration of FA in ADA-GEL hydrogels was determined in terms of antibacterial properties, cell viability, release capability, printability, degradation behavior and mechanical (stiffness).

EXPERIMENTAL METHODS

FA was added to ADA/GEL in three different concentrations (0.1%, 0.15% and 0.2% (w/v)). Printing was performed with a pneumatic 3D printed (BioX CELLINK). FA release from 3D printed ADA-GEL-FA scaffolds was measured via UV-Vis spectroscopy. Furthermore, the influence of FA on degradation/swelling and mechanical properties of ADA-GEL hydrogels was investigated. Antibacterial tests were performed using a S. epidermidis strain (ATCC 14990) and a colony forming unit test. Moreover, antioxidant properties and the phenolic content were examined. A direct cell viability study was performed with MG-63 cells to determine possible anticancer properties of the bioink. MC-3T3-E1 cells were used in order to investigate cell viability of ADA-GEL-FA hydrogels.

RESULTS AND DISCUSSION

Direct cell viability testing showed a decrease of cell viability of MG-63 cells in the presence of FA. A high cell viability was shown for MC-3T3-E1 cells up to a FA concentration of 0.15% (w/v). However, a decrease with 0.2% (w/v) FA was observed, which could be due to a pH drop due to the acid content. The highest release of FA was measured from ADA-GEL-0.15%FA 3D printed scaffolds. This might be due to limited solubility of FA in non-organic solvents in high concentrations (0.2% (w/v)). Antibacterial results revealed that with higher FA concentration an increase of antibacterial effect could be observed. Moreover, an antioxidant investigation confirmed the antioxidant effect of FA and the presence of phenolic rings could be seen.

CONCLUSION

The study developed FA containing ADA-GEL bioinks. The superior concentration of FA within ADA-GEL hydrogels was determined. It was concluded that the middle FA concentration (0.15% (w/v)) was the best in terms of finding the balance between high cell viability and good antibacterial properties. Due to promising properties of FA in hydrogels, the present hydrogels will most likely gain more attention in TE and drug delivery approaches.

REFERENCES

1. Khademhosseini A. *et al.*, Nat. Protoc. 11: 1775-1781, 2016
2. Reakasame S. *et al.*, Macromol. Biosci. 20: 1-14, 2020
3. Coelho C.C. *et al.*, Mater. Sci. Eng. C. 97: 529-538, 2019
4. Kumar N. *et al.*, Biotechnol. Reports. 4: 86-93, 2014

ACKNOWLEDGMENTS

Faina Bider would like to acknowledge KMM-VIN for supporting the collaboration between PoliTo and FAU (KMM-VIN fellowship program).

Natural polymer-based bioinks for *in situ* bioprinting

Nicola Contessi Negrini[1], Alexandros Makrypidis[1], Dominic Wales[2], Muhsincan Sesen[1], Adam Celiz[1]
[1]Department of Bioengineering, Imperial College London, London, UK
[2]Hamlyn Centre, Institute of Global Health Innovation, Imperial College London, London, UK
*n.contessi-negrini@imperial.ac.uk

INTRODUCTION

Classical bioprinting strategies (*i.e.*, external scaffold pre-fabrication, *ex vivo* culture, clinic supply, and *in vivo* implant) are currently hindering clinical application of bioprinted scaffolds, due to the time-consuming and complex "fabrication-to-application" route. Portable devices for direct writing *in vivo* bioprinting can be manually used by surgeons to directly print scaffolds on injured body sites, greatly simplifying bioprinting procedures and allowing to tailor the shape of the printed scaffold to the injured tissue[1]. Few examples are described in literature, due to challenges in developing bioinks suitable for *in situ* bioprinting and in engineering easy-to-handle portable printers[2], including complex printing devices and bioinks that require post-curing procedures (e.g., UV radiation). Here, we develop new bioinks that spontaneously crosslink after mixing hydrogel precursors and a new microfluidic printer head that can be used to print the ink to simplify the device handling and potential surgical procedures.

EXPERIMENTAL METHODS

Alginate (il-6G, Mw = 56000, KIMICA Corporation, ALG) and gelatin (type B, gel strength = 240-270 g, Rousselot Biomedical, GEL) were respectively modified using carbodiimide chemistry with norbornene (ALG_Nb)[3] and tetrazine (GEL_Tz)[4], targeting comparable degrees of modification. ^{1}H NMR spectroscopy was performed to measure the degree of modification of gelatin and alginate derivatives. Hydrogels (GELALG_2, GELALG_4, and GELALG_6) were then prepared by mixing different concentrations of ALG_Nb and GEL_Tz precursors (2, 4, and 6% w/v). After mixing, the evolution of the rheological properties of the hydrogels (storage modulus G', loss modulus G", and time required for crosslinking t_{cross}; n = 3) were tested by rheometry (Netzsch Kinexus Ultra+). After crosslinking, hydrogels were immersed in PBS at 37 °C to test their stability and swelling (n = 6). As a separate experiment, hydrogel precursors were loaded in two separate syringes and injected into a microfluidic passive mixer by syringe pumps. The resolution of the printed structures was qualitatively evaluated to test the potential of the hydrogels as bioinks. Data are represented as mean ± standard deviation and analyzed by ANOVA ($p<0.05$).

RESULTS AND DISCUSSION

ALG and GEL were functionalized with norbornene (ALG_Nb) and tetrazine (GEL_Tz), as evidenced by the appearance of their characteristic signals in the NMR spectra. The degree of modification calculated based on the NMR spectra for both ALG_Nb and GEL_Tz is approximatively 0.1 mmol/g. Hydrogels were successfully prepared by mixing ALG_Nb and GEL_Tz precursors at different concentrations (Fig 1A).

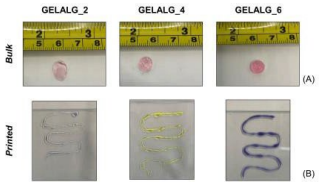

Figure 1. Bioortoghonal crosslinking of (A) bulk and (B) printed hydrogels.

Depending on the concentration, the crosslinking kinetics vary (Fig 2). G' values increase for all hydrogels after mixing, indicating ongoing crosslinking. Hydrogels prepared with higher concentrations reached higher G' values at plateau (80-2000 Pa; GELALG_6 > GELALG_4 > GELALG_2) and crosslinked faster (60-85 min: GELALG_6 < GELALG_4 < GELALG_2). Hydrogels are stable in aqueous environments at 37 °C, confirming their crosslinking. Hydrogels prepared with lower concentrations are characterized by higher weight variation (2000-4000%; GELALG_2 > GELALG_4 > GELALG_6), suggesting the formation of a looser hydrogel network absorbing a higher mass of water. Hydrogel precursors were loaded in two separate syringes, injected into a microfluidic mixer, and manually printed in predefined patterns. All formulations can be extruded, indicating the possibility of printing them in defined shapes. Printed hydrogels show qualitatively good printing resolution (i.e., good shape fidelity replicating the pattern), and spontaneously crosslinked after mixing and printing, suggesting their potential use as bioinks for manual *in situ* 3D bioprinting (Fig 1B).

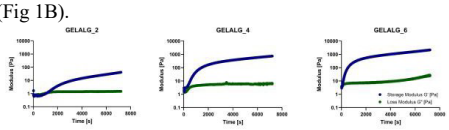

Figure 2. Evolution of inks rheological properties during crosslinking.

CONCLUSION

Hydrogels were prepared by bioorthogonal crosslinking between ALG_Nb and GEL_Tz. The crosslinking kinetics of the hydrogels was tuned by varying concentration and hydrogel precursors were successfully extruded and bioprinted by using a hand-held printing device prototype.

REFERENCES

1. Keriquel *et al.*, Biofabrication 2:014101, 2010
2. O'Connel *et al.*, Biofabrication 8:015019, 2016
3. Desai *et al.*, Biomaterials 50:30-37, 2015
4. Contessi Negrini. *et al.*, ACS Biomater. Sci. Eng. 7:4330-46, 2021

ACKNOWLEDGMENTS

Dame Julia Higgins Engineering Postdoc Collaborative Research Fund 2021.

Extracting ready-to-use silkworm sericin: finding the best starting point

Anabela Veiga[1,2,3], Filipa Catro[2], Fernando Rocha[2], Blanca Vazquez[3,4], Luis Rojo[3,4] and Ana L. Oliveira[1]

[1]Universidade Católica Portuguesa, CBQF - Centro de Biotecnologia e Química Fina – Laboratório Associado, Escola Superior de Biotecnologia, Rua Diogo Botelho 1327, 4169-005 Porto, Portugal
[2]Laboratory for Process Engineering, Environment, Biotechnology & Energy, Dep. of Chemical Engineering, Faculty of Engineering of Porto, R. Dr. Roberto Frias, 4200-465 Porto, Portugal
[3]Instituto de Ciencia y Tecnología de Polímeros ICTP-CSIC, C. Juan de la Cierva, 3, 28006 Madrid, Spain
[4]Centro de Investigación Biomédica en Red de Bioingienería, Biomateriales y Biotecnología CIBER-BBN, Instituto de Salud Carlos III, Calle Monforte de Lemos S/N, 28029 Madrid, Spain
*s-anveiga@ucp.pt

INTRODUCTION

To develop silk-sericin (SS) 3D structures such as hydrogels, SS is usually concentrated using different procedures such as rotavapor, lyophilization, dialysis and evaporation. Although evaporation in a heating plate is challenging to control, this technique is simple and allows to obtain high concentrations [1]. Lyophilization has been used in different works to improve control over the concentrations used. However, this process is reported to induce β-sheet conformation which can cause a blockage of hydrogel permeability and mechanical constrain [2]. Rotavapor is also used to concentrate silk-sericin, nevertheless studies do not usually report all the relevant experimental parameters used such as precise evaporation temperature and pressure. In similarity, only limited information about dialysis is available in the literature. In the present study, the abovementioned concentration techniques were optimized based on the best available evidence and compared.

EXPERIMENTAL METHODS

SS was obtained using extraction in boiling water. Afterwards, different concentration techniques were performed: 1) SS1: controlled evaporation; 2) SS2: rota-evaporation (BUCHI Rotavapor™ RII) at 40°C, 500 mbar and 120 rpm; 3) SS3: lyophilization, in which the SS solution was frozen in LN_2 and freeze-dried under vacuum; 4) SS4: SS concentrated against a 20 wt.% PEG solution (Sigma-Aldrich, 20 KDa), using a dialysis membrane (Spectra/Por™ pre-wetted RC tubing MWCO: 3.5 kD). The concentrated SS solutions were analyzed by Circular Dichroism (CD), FTIR (Spectrum Two FTIR PerkinElmer), XRD (D8 Advance de Bruker) and Cryo-SEM (JEOL JSM 6301F/ Oxford INCA Energy 350/ Gatan Alto 2500).

RESULTS AND DISCUSSION

The CD spectra of SS1-4 have strong negative bands around 200 nm assigned to the random coil conformation and a weak negative band around 220 assigned to the β-structure, characteristic of SS extracted in boiling water [3]. The presence of these conformations was corroborated by FTIR through the deconvolution of amide I peak. The FTIR spectrum of SS4 resulted in a change in the amide I/II ratio. This was associated with a change in secondary structure due to the increase in β-sheet conformation. In XRD, a diffraction peak with broad intensity at 2θ = 28 and at 40 indicates the poor crystallinity of the SS-solutions, characteristic of random coil conformations and of the presence of high polar amino acids. Again, peaks for SS concentrated by dialysis were slightly sharper, indicating an increase in crystallinity when compared to the other concentration methods, which corroborates the presence of higher β-sheet content. The presence of different types of porosity was also verified for this condition in Cryo-SEM, one of them apparently with a higher orientation degree. The longer concentration period during dialysis has favored the molecular self-assembly of silk sericin, which explains the differences registered. On the other hand, the proposed method of lyophilization using cryogenic temperature was able to freeze and dry the silk maintaining its amorphous structure. In this particular case it was possible to obtain a ready-to-use dry material which was easy to re-dissolve.

CONCLUSION

For the first time, a study was carried out on comparing different SS concentration methods on its physicochemical characteristics and further processability. The results show that our so-called cryo-lyophilization does not change the properties of the protein. Thus, this methodology in particular has high potential to generate a ready-to-use powder which can be easily sterilized and processed. Concentration by dialysis, on the other hand, leads to the formation of a more rigid structure with higher β-sheet amount. This study constitutes an important step to ensure the best silk characteristics at the starting point before further development, according with the processing goal.

REFERENCES

[1] Baptista-Silva S. *et al.*, *ACS Biomater. Sci. Eng.*, vol. 7, no. 4, pp. 1573–1586, 2021. [2] Arango M. C. *et al.*, *Mater. Res. Express*, vol. 6, no. 9, 2019. [3] Cho K. Y. *et al.*, *Int. J. Biol. Macromol.*, vol. 32, no. 1–2, pp. 36–42, 2003.

ACKNOWLEDGMENTS

This work was financially supported by National Funds through FCT under the project UIDB/50016/2020 (CBQF), LA/P/0045/2020 (ALiCE), UIDB/00511/2020 and UIDP/00511/2020 (LEPABE); and was carried out in the framework of the COST Action CA18125 "Advanced Engineering and Research of aeroGels for Environment and Life Sciences" (AERoGELS), funded by the European Commission. AV gratefully acknowledges doctoral scholarship [2020.08683.BD] from FCT and ERASMUS + from ESB-UCP. BV and LR are members of Technological Interdisciplinary Platform SUSPLAST+

Dual-Functional Polysaccharide Microgels Modulated by Therapeutic Metal Ions

Andrea Lončarević[1*], Karla Ostojić[2], Teodoro Klaser[3], Inga Urlić[2], Anamarija Rogina[1]

[1]Faculty of Chemical Engineering and Technology, University of Zagreb, Zagreb, Croatia
[2]Department of Biology, Faculty of Science, University of Zagreb, Zagreb, Croatia
[3]Department of Physics, Faculty of Science, University of Zagreb, Zagreb, Croatia
[*] aloncarev@fkit.hr

INTRODUCTION

In recent years, chitosan-based materials modified by therapeutic metal ions gained much attention in regenerative medicine and tissue engineering due to the synergy of polymer's biocompatibility and bioactivity of metal ions. Chitosan is a biocompatible, biodegradable and non-toxic cationic polysaccharide[1] whose properties can be modulated by complexation with therapeutic metal ions such as cupric (Cu^{2+}) or zinc (Zn^{2+}) ions.[2,3] Cu^{2+} ions are well known for stimulating the proliferation and differentiation of human endothelial and mesenchymal stem cells, while Zn^{2+} ions promote bone formation by enhancing osteoblast differentiation.[4] Furthermore, the complexation interactions between Cu^{2+} or Zn^{2+} ions with amino and hydroxyl groups,[5] leads to stable complex hydrogels. Combining biologically active ions with pH-responsive chitosan microspheres could generate multifunctional carriers and delivery systems. Still, there is no work focused on synthesis of Cu^{2+}/Zn^{2+}-chitosan complexes as microgels, i.e. in the form of microspheres. The aim of this work was to prepare and investigate the composition, morphology and cytotoxicity of Cu^{2+}/Zn^{2+}-chitosan complexes and their ability to form microgels using electrohydrodynamic atomization process.

EXPERIMENTAL METHODS

Chitosan (CHT) with the degree of deacetylation of 83.2 % (Chitoscience Chitosan 85/200, Heppe Medical Chitosan GmbH) was used. Zinc acetate dihydrate and copper acetate monohydrate were used as precursors for Zn^{2+} and Cu^{2+} ions, respectively. The Cu^{2+}/Zn^{2+}-chitosan hydrogels were prepared by mixing 1 wt.% CHT solution with metal precursor solutions, followed by gelation with 5 wt.% NaOH solution. The final concentration of Cu^{2+} and Zn^{2+} ions in prepared complex solutions was ranging from 0 to 5 mmol/L. Prepared bimetallic-chitosan complex solutions were denoted as Cu5/Zn0-CHT Cu3/Zn2-CHT, Cu1/Zn4-CHT and Cu0/Zn5-CHT. Obtained hydrogels were extensively washed with distilled water, frozen and lyophilized to obtain dry materials which were characterized by ATR-FTIR spectroscopy and XRD analysis. The samples' morphology and elemental analysis were investigated by scanning electron microscopy (SEM) with energy-dispersive X-ray spectroscopy (EDS), while their cytotoxic activity was evaluated on HEK293 cells by MTT assay for 72 hours. To obtain materials in the form of microgels, the electrohydrodynamic process was conducted at solution flow rate of 5 mL/h, the voltage of 22.5 kV and needle tip-to-collector distance of 10 cm. After neutralization in NaOH, microspheres were washed and dried in acetone.

RESULTS AND DISCUSSION

Bimetallic-chitosan hydrogels were successfully prepared by gelation of Cu/Zn-chitosan complex solutions. Visual assessment of hydrogels in their native wet state indicated stable structure of Cu5/Zn0-CHT Cu3/Zn2-CHT and Cu1/Zn4-CHT hydrogels, while Cu0/Zn5-CHT hydrogel was disintegrated during the washing step. The addition of Zn^{2+} ions decreased the stability of hydrogels which imply that Cu^{2+} ions are mostly responsible for stronger complexation reactions with functional groups of chitosan's chains. Such observation was confirmed by FTIR spectra which indicated physical interactions between metal ions and polymer. Furthermore, X-ray diffraction patterns of dry materials showed the changes in the intensity and width of diffraction maximum characteristic for chitosan in $c(Cu^{2+})$-depended manner indicating the changes in chitosan crystallinity caused by cupric ions. Furthermore, X-ray diffraction patterns did not show any presence of Cu or Zn species. The MTT assay indicated cytotoxic activity at higher copper concentration, while the addition of zinc ions resulted in good cytocompatibility. Prepared Cu/Zn-CHT complex solutions were then successfully transformed into spherical microgels by electrohydrodynamic atomization resulting in stable microspheres with average diameter of 65 – 95 μm.

CONCLUSION

In this work, stable complex hydrogels based on chitosan with two different therapeutic metal ions were successfully prepared. Obtained Cu/Zn-CHT materials showed porous microstructure without formation of Cu or Zn inorganic phase. The MTT assay indicated that the cytotoxicity of materials can be modulated by the addition of Zn^{2+} ions. Furthermore, prepared Cu/Zn-chitosan complexes could be promising systems for microspheres production as potential bioactive carriers.

REFERENCES

1. Nie J. et al., Sci. Rep. 6:36005, 2016
2. Gritsch L. et al., J. Mater. Chem. B 7:6109-6124, 2019
3. Gamboa-Solana C. D. C. et al., Polymers (Basel) 13:3861, 2021
4. Mouriño V. et al., J. R. Soc. Interface 9:401-419, 2012
5. Guibal E., Sep. Purif. Technol. 38:43-74, 2004

ACKNOWLEDGMENTS

This work has been supported by the Croatian Science Foundation under the project UIP-2020-02-6201.

Alginate-Based Biocomposites Hydrogels Reinforced with Natural Polymers Used in Tissue Engineering: Structural and Physicochemical Properties

Alexandra Feraru[1,2,*], Zsejke-Réka Tóth[1], Klára Magyari[1,4], Lucian Baia[1,3]

[1]Interdisciplinary Research Institute on Bio-Nano-Sciences, Babeș-Bolyai University, Cluj-Napoca, România
[2]Doctoral School of Physics, Babeș-Bolyai University, Cluj-Napoca, România, Faculty of Physics, Babeș-Bolyai University, Cluj-Napoca, România
[3]Faculty of Physics, Babeș-Bolyai University, Cluj-Napoca, România
[4]Department of Applied and Environmental Chemistry, Faculty of Science and Informatics, University of Szeged, Hungary

*elena.feraru@ubbcluj.ro

INTRODUCTION

The primary purpose of this study is to develop innovative formulations of alginate-based biocomposite hydrogels reinforced with micro-fibrillated cellulose, micro-crystalline cellulose, and Gum arabic. The first step to put in practice such a desideratum is to obtain such structures, optimize their compositions, and characterize the morphological, structural, and biological performances of the chosen bio-nano-composites by taking into consideration the reported requirements and progresses in the field. Three particular cases are in the spotlight for this research: epithelial tissue regeneration, bone tissue regeneration[1], and targeted drug release. The development of polymer-based hydrogels seems to be a suitable alternative to cover the design features of biomaterials such as biocompatibility, nontoxic, biodegradability, and mechanical properties. However, they are strongly dependent on composites' structure and physicochemical properties.

EXPERIMENTAL METHODS

Microfibrillated cellulose (MCC), microcrystalline cellulose (FC), and Gum arabic (GA) were used as reinforcing polymers in the hydrogel-alginate matrix. Different ratios of MCC and FCC were added into NaOH/urea/H_2O solvent under vigorous stirring that was kept in the freezer for 24 h. Then, sodium alginate solution was gradually mixed into the cellulose solution with continuous vigorous stirring to obtain the sodium alginate/MCC and sodium alginate/FC hydrogel. The shape of the bead structures was controlled with a syringe by extruding the droplets in a solution of $CaCl_2$ (4%). Crosslinking using calcium chloride solution was used to modify hydrogel composites' chemical and physical properties.

A similar methodology was followed in the case of Gum arabic samples, the only difference being the solvent used; ionic liquid at below temperature for cellulose and ultrapure water at room temperature for Gum arabic. In vitro bioactivity was assessed 7 days after introducing the samples into the simulated body fluid (pH 7.4) at 37C°.

RESULTS AND DISCUSSION

Our results cast a new light on the ratio of the two biopolymers in the alginate matrix composition as well as on structural and morphological properties of the hydrogels based biocomposites. The characterization of biocomposites in terms of structural and morphological properties, swelling capacity, biocompatibility and / or cytotoxicity revealed different behaviors of hydrogels, both in the process of biocomposite formation and in vitro evaluation.

It is worth mentioning that the general properties can be customized by changing the ratio between alginate, cellulosic biopolymers and Gum arabic. Hydrogels with optimized variables indicated a satisfactory result attesting to bioactivity after immersion in simulated biological fluid, the evidence being consistent with morpho-structural indicators. The newly obtained hydrogels can be promising structures for the development of biomedical engineering materials.

CONCLUSION

In the present study, we report the results of an investigation on the optimization of protocols used in the design and advanced characterization of hydrogels based on innovative biopolymer composites and provide detailed descriptions of the morphological, structural and biological parameters that influence the properties of hydrogels.

REFERENCES

1. Radu A Popescu. *et al*., *J Tissue Eng Regen Med*. 12, 2112–2121 (2018)

ACKNOWLEDGMENTS

“This work was supported by a grant from the Ministry of Research and Innovation, CNCS - UEFISCDI, project number PN-III-P1-1.1-TE-2019-1138, within PNCDI III. I gratefully acknowledge the financial support received from the Babeș-Bolyai University, Ph.D. fellowship.”

Gellan Gum-Based Hydrogels for Extracellular Vesicles Delivery in Regenerative Medicine

Franco Furlani[1], Rossi Arianna[1], Bassi Giada[1], Montesi Monica[1], Silvia Panseri[1*]

[1] National Research Council of Italy - Institute of Science and Technology for Ceramics (ISTEC-CNR), Faenza (RA), Italy
[*] silvia.panseri@istec.cnr.it

INTRODUCTION

Hydrogels are highly hydrated networks consisting of a solute (*e.g.* a polymer) and a solvent (*i.e.* water) and are able to mimic the native extracellular matrix (ECM) [1] and to provide a controlled released of different payloads, including biologically active compunds[2]. Injectable hydrogels can be fabricated by using different polymers, including gellan gum (GG), a biocompatible bacteria-derived polysaccharide[3].

Extracellular vesicles (EVs) are lipid bilayer-delimited particles naturally produced and secreted by cells. EVs derived from mesenchymal stem cells (MSCs) play an important role in cell physiology, cell-cell communication, and immunomodulation. EVs are promising for regenerative medicine[4], but their therapeutic effect *in vivo* is reduced due to their rapid clearance and short half-life[5].

In the present work, we develop a novel delivery system consisting of a gellan gum-based hydrogel crosslinked with spermidine, a biocompatible agent able to enhance the hydrogel stability and endowed with anti-inflammatory properties[6], to achieve a controlled release of EVs derived from human adipose mesenchymal stem cells (hA-MSC). We then evaluated the cross-talk between the EVs e different cells such as hA-MSC, rat hippocampal neural stem cells (rH-NSC), and human skin fibroblast (WS1).

EXPERIMENTAL METHODS

Gellan gum-based hydrogels were fabricated by using as crosslinking agent spermidine (weight ratio between polymer and spermidine between 1:10 and 1:40). The resulting system was also implemented with hyaluronic acid (HA) (weight ratio between GG and HA from 1:4 to 1:1). The interaction between the different molecules was investigated by FTIR-ATR analyses. The resulting samples were characterized using rheology to evaluate the gelation time and mechanical properties. Mechanical performance was also investigated by compression tests by Dynamic Mechanical Analyses (DMA). Additionally, the stability and the swelling ability of hydrogels were investigated up to 21 days by weighting samples after the incubation in physiological-like conditions.

EVs were isolated from hA-MSC by an ultracentrifugation protocol[7] and loaded within the hydrogels[8]. To evaluate hydrogel biocompatibility a preliminary screening on rH-NSC, WS1 and hA-MSC was performed analyzing cell viability by Presto Blue assay at different timeframes up to 7 days. The cell viability was also confirmed by Live/Dead assay. Additionally, the cell morphology and spreading ability were investigated by fluorescent microscopy analyses (after nuclei and cytoskeleton labelling) at different timeframes up to 7 days. Finally, MSCs-derived EVs release from the hydrogel, and the resulting cross-talk effect was tested by real-time PCR.

RESULTS AND DISCUSSION

Hydrogels showed a dependence of gelation time, stability, mechanical properties, and swelling degree on their composition. Specifically, the presence of higher sperimidine concentrations (i) enhanced the stability, (ii) reduced the swelling ability, (iii) reduced the gelation time and (iv) enhanced the mechanical resistance of resulting hydrogels. Additionally, hydrogels were able to release EVs in a controlled manner.

Hydrogels exhibited good biocompatibility without affecting cell viability and morphology of all the screened cell cultures. MSCs-derived EVs were homogenously embedded into the hydrogel without negatively affecting the gelation kinetic and they were released in a sustained manner. Additionally, EVs maintained their structure and bioactivity enhancing the cell viability.

CONCLUSION

In the present work, we developed a biocompatible hydrogel system based on gellan gum and spermidine. These hydrogels were able to provide a controlled release of EVs overcoming issues that normally are faced *in vivo*. In fact, they might prolong the retention of EVs and maximize the localized benefit *in situ*. The resulting system displayed good biocompatibility on human fibroblasts, hA-MSC, and rH-NSC and is a promising system for several regenerative medicine applications.

REFERENCES

1. Tibbitt M. *et al.*, Biotechnology and Bioengineering, 103:655-663, 2009
2. Grimaudo, M. A. *et al.*, Acta Biomater., 140:88–101, 2022
3. Das, M. *et al.*, J. of Drug Deliv. Sci. and Tech., 56:A101586, 2020
4. Elsharkasy, O. M. *et al.*, Adv. Drug Deliv. Rev., 159:332-343, 2020
5. Imai, T. *et al.*, J. Extracell. Vesicles, 4:26238, 2015
6. Liu. R. *et al.*, Free Radic. Biol. Med., 161:339-350, 2020
7. Momen-Heravi, F., Methods Mol. Biol., 1660:25-32, 2017
8. Holkar, K. *et al.*, ACS Biomater. Sci. Eng., 7(6):2687-2700, 2021

Elaboration of Injectable Thermosensitive Hydrogels Based on Infernan: a Marine Glycosaminoglycan-Mimetic Exopolysaccharide for Tissue Engineering.

Arnaud Fillaudeau[1*], Agata Zykwinska[1], Corinne Sinquin[1], Laetitia Marchand[1], Stéphane Cuenot[2], Sylvia Colliec-Jouault[1]

[1]Ifremer, Laboratoire Ecosystèmes Microbiens et Molécules Marines pour les Biotechnologies, Centre Atlantique, Nantes, France.
[2] Nantes Université, CNRS, Institut des Matériaux Jean Rouxel, IMN, Nantes, France.

* Arnaud.Fillaudeau@ifremer.fr

INTRODUCTION

Exopolysaccharides (EPS) secreted by bacteria from deep-hydrothermal vents of the Ifremer collection have structures and/or properties similar to glycosaminoglycans (GAG), essential components of connective tissues[1]. One of them, called Infernan (GY785 EPS)[2] has shown high potential in cartilage[3-5] and bone[6] regeneration. With increasing demand of mini-invasive therapies, we intend to design injectable and thermoresponsive hydrogels based on biologically active EPS for tissue engineering applications. In this context, the aim of this study was to graft a synthetic thermosensitive polymer, poly(N-isopropylacrylamide) (pNIPAM) onto Infernan backbone and to evaluate the mechanical properties of the resulting hybrid hydrogels.

EXPERIMENTAL METHODS

A commercial pNIPAM (20,000 g/mol) was grafted on the native high-molecular weight (HMW) EPS (weight average MW 1,000,000 g/mol) and on its medium-molecular weight (MMW) derivative (weight average MW 400,000 g/mol) through EDC/NHS chemistry.

The successful grafting of the pNIPAM was confirmed by three complementary techniques: ATR-FTIR spectroscopy, HPSEC-MALS chromatography and colorimetric assays. The lower critical solution temperature (LCST) as well as the mechanical properties of hydrogels were then assessed by rheology.

RESULTS AND DISCUSSION

The pNIPAM was successfully grafted on the backbone of the native HMW EPS and on its MMW derivative using EDC/NHS chemistry. The percentage of pNIPAM-NH_2 grafted on the EPS carboxylic groups varied from 5% to 40% with decreasing EPS/pNIPAM molar ratio. EPS molecular weight had not a major impact on grafting density.

The thermosensitive gelling behavior of these hybrid polymers was then evaluated at different concentrations ranging from 5% to 10% in DMEM culture cell medium.

Rheological measurements were then performed to determine the sol-gel transition temperature and mechanical properties of resulting EPS/pNIPAM hydrogels. LCST varied from 25°C to 28°C, independently from the percentage of pNIPAM grafted on the EPS backbone. However, the LCST was lower for the native HMW EPS compared to MMW EPS. Storage modulus (G') at 37°C varied from 10 kPa to 250 kPa, depending on the pNIPAM grafting density and EPS molecular weight. The variation of hybrid polymer concentrations also enables to modulate the mechanical properties of hydrogels.

CONCLUSION

The development of these injectable, thermosensitive and bioactive hydrogels is promising for further applications in tissue regeneration in particular as cell scaffolds. Their impact on cell viability and proliferation will be studied.

REFERENCES

1. Delbarre-Ladrat C. *et al*., Front.Chem. 2:1-15, 2014
2. Roger O. *et al*., Carbohydrate Research. 339: 2371-2380, 2004
3. Rederstorff E. *et al*., Acta Biomater. 5:2119-2130, 2011
4. Rederstorff E. *et al*., J Tissue Eng Regen Med. 11:1152-1164, 2017
5. Merceron C. *et al.,* Stem Cells. 30:471-480, 2012
6. Gélébart P. *et al.,* Carbohydr. Polym. 284:119191, 2022

Fine-tuning the hydrogels porosity: a reliable strategy for controlling the drug delivery features

Ioana A. Duceac, Sergiu Coseri

Department of Polyaddition and Photochemistry, Petru Poni Institute of Macromolecular Chemistry, Iasi, Romania
duceac.ioana@icmpp.ro, coseris@icmpp.ro

INTRODUCTION

Fine-tuning materials for controlled drug delivery can be an efficient approach to address the issues related to conventional drug administration (e.g., repeated administration, low efficacy, side effects and toxicity). Therefore, the aim of this research opportunity is achieving a drug delivery system based on a polysaccharide material that does not only functions for loading and releasing a specific therapeutic compound, but also exhibits properties such as biocompatibility or antibiotic activity, rendering in a challenging research subject. [1]

EXPERIMENTAL METHODS

The material design and preparation had as a starting point chitosan porous beads, which have been subsequently subjected to surface modification with pullulan derivatives.

This choice was endorsed by the fact that these are easily obtained and versatile materials.

Two coating strategies have been explored – more precisely, physical or chemical surface modification, respectively. Consequently, two types of selective oxidation reactions were employed for pullulan chemical functionalization. The TEMPO-mediated oxidation leads to the introduction of carboxyl groups at the primary hydroxyl moieties. By comparison, the periodate oxidation yields in the transformation of secondary hydroxyl groups into aldehyde moieties.

Thus, chitosan beads have been tuned by coating via the amino groups either by electrostatic interactions with 6-carboxy pullulan, or by imide bonds with 2,3-dialdehyde pullulan, respectively.

RESULTS AND DISCUSSION

Complementary structural analysis has proven that the intended polymeric networks have been obtained.

Hydrogel beads surface and internal morphology have been studied by scan electron microscopy and revealed a significant reduction is pore size – from microns to nanometers. Further surface and porosity studies were performed to investigate in depth the synthesized materials.

The drug delivery performance – specifically, drug loading and release studies-, of the prepared materials were studied using various model drugs with different types of chemical structures and pharmacological actions. The results indicated that the loading efficiency and the release behaviour are strongly dependent on the hydrogel porosity, as expected.

The release mechanism was analysed by fitting different equations on the experimental data. To that aim, the Matlab software was used. After a literature study concerning the characterization of drug delivery systems, seven empirical mathematical models that are frequently reported were chosen: zero and first order equations, Higuchi model, the power law (Korsmeyer-Peppas & Ritger-Peppas model), Peppas-Sahlin model, Weibull and Gompertz equations [2-7]. The drug release kinetics are best described by the first order equation and by the Weibull model. This result is correlated with a typical behaviour of release of a soluble drug from a porous matrix.

CONCLUSION

The reported findings suggest that the fine-tuning of hydrogels porosity was successfully achieved using as starting materials chitosan beads and as coating polymer oxidized pullulan derivatives. This approach led to multiple changes in network and surface properties have resulted in materials with great properties, and therefore are a promising toolkit for controlled drug delivery.

REFERENCES

1. J. Li, D.J. Mooney, Nature reviews, 2016, 16071, 1-17.
2. I.A. Duceac, L. Verestiuc, C.D. Dimitriu, V. Maier, S. Coseri, Polymers, 2020, 12, 1473.
3. R. Dwivedi, A.K. Singh, A. J. Dhillon, Sci. Adv. Mater, 2017, 2, 45–50.
4. R.W. Korsmeyer, R. Gurny, E. Doelker, P. Buri, N.A. Peppas, Int. J. Pharm., 1983, 15, 25–35.
5. P.L. Ritger, N.A. Peppas, J. Control. Release, 1987, 5, 37–42.
6. T. Higuchi, J. Pharm. Sci., 1961, 50, 874–875.
7. T. Higuchi, J. Pharm. Sci. 1963, 52, 1145–1149.

ACKNOWLEDGMENTS

This work was supported by a grant of the Romanian Ministry of Research and Innovation, CNCS - UEFISCDI, project number PN-III-P2-2.1-PED-2019-0169, acronym “HISENSE”, within PNCDI III.

A smart bioprintable Gellan Gum/Lignin hydrogel for cartilage regeneration

Maria A. Bonifacio[1#], Stefania Cometa[2#], Andrea Cochis[3], Annachiara Scalzone[4], Piergiorgio Gentile[4], Alessandro C. Scalia[3], Lia Rimondini[3], Piero Mastrorilli[5], Elvira De Giglio[1*]

[1]Department of Chemistry, University of Bari, Bari, Italy
[2]Jaber Innovation s.r.l., Rome, Italy
[3]Center for Translational Research on Autoimmune and Allergic Disease, CAAD, Department of Health Sciences, University of Piemonte Orientale UPO, Novara, Italy
[4]Newcastle University, School of Engineering, Newcastle upon Tyne, United Kingdom
[5]DICATECh Department Politecnico di Bari, Bari, Italy
[*] elvira.degiglio@uniba.it

INTRODUCTION

Recent developments in tissue engineering are directed towards advanced biomaterials with highly performing properties allowing the sustainable exploitation of renewable sources[1]. Lignin has been already blended to several polymers as a bio-compatibilizer, enhancing thermal resistance, interfacial and mechanical properties of the resulting composites[2]. Injectable hydrogels based on gellan gum modified with lignocellulose nanofibrils have been proposed for biomedical applications[3]. In this work, a composite hydrogel, based on a blend of two gellan gums with different acyl content embedding lignin, was developed for the first time aimed to the regeneration of cartilage tissue. This easily bioprintable and eco-friendly hydrogel evidenced an intriguing combination of suitable chondrogenic activity and mechanical features useful for printability.

EXPERIMENTAL METHODS

High- and low-acyl gellan gums (GG_H and GG_L) have been dissolved in hot water at 1.2% and 0.8% w/v, respectively. Meanwhile, lignin aqueous solution (0.1, 0.2 or 0.4%w/v) has been prepared. Lignin solution has been added to the dissolved gellan gums and magnetically stirred. Finally, hydrogels have been crosslinked with magnesium ions[4] (Bonifacio et al., 2018). Gellan gums hydrogels without lignin (GG_{HL}) have been prepared as controls. Hydrogels were characterized by means of XPS and SS-NMR analyses and radical scavenging activity was tested *in vitro* on DPPH and ABTS radicals. Cytocompatibility and chondrogenic activity have been *in vitro* assessed on immortalised hMSCs cultivated into 3D-hydrogels by means of metabolic assays, live/dead fluorescent imaging, chondrogenic genes up-regulation by real-time PCR and extracellular matrix deposition by histological staining. Finally, the bioink encapsulating hMSC allowed manufacturing 3D-porous constructs for cartilage regeneration.

RESULTS AND DISCUSSION

The physico-chemical characterizations established that no chemical interaction between lignin and the polysaccharides was detected. Lignin achieved up to 80% of ascorbic acid's radical scavenging activity *in vitro* on DPPH and ABTS radicals. Lignin exploitation resulted cytocompatible as the viability of hMSCs 3D-seeded onto scaffolds resulted comparable to the lignin-free control hydrogel (>70% viable cells, $p>0.05$). Moreover, the 0.4% lignin composites significantly improved the hMSC 3D-constructs chondrogenesis bringing to a significant ($p<0.05$) up-regulation of the aggrecan (Fig.1a), collagen type II (Fig.1b), and SOX 9 (Fig.1c) chondrogenic genes. Finally, cellularized 3D constructs were manufactured via 3D bioprinting (Fig.1d).

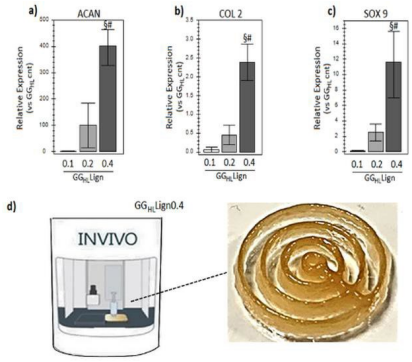

Figure 1: Up-regulation of chondrogenic genes in a dose-dependent manner (a-c). Bioprinting process of concentric cellularized cylindrical structures (d).

CONCLUSION

A new gellan gum-based hydrogel formulation was developed in order to prepare 3D-printed scaffolds for the regeneration of cartilage tissue. This challenging matter has been achieved by the incorporation of lignin to the polysaccharide blend. The bioprinted hydrogel did not adversely affect the encapsulated hMSC, allowing cell proliferation and showing its unique biological features for creating a physiological milieu for cell growth.

REFERENCES

1. Iravani S. *et al.* Green Chem., 21:4839-4867, 2019.
2. Sen S, *et al.* Green Chem., 17:4862-4887, 2015.
3. Kouhi M. *et al.* Mat. Sci. Eng. C, 115:111114, 2020.
4. Bonifacio M.A. *et al.* Carb. Pol., 198:462–472, 2018.

[#]These authors equally contributed to the work

Electrohydrodynamics based functional nanofibers electrically stimulate neuron regeneration

Christoph Müller[1], Menglin Chen[1*]

[1]Department of Biological and Chemical Engineering, Aarhus University, Aarhus, Denmark
[*] menglin@bce.au.dk

INTRODUCTION

Alongside the widely studied pathways of biochemical regulation by chemokines, cytokines and growth factors, one often-overlooked but significant influence over the behavior of biological systems is electrical signaling. Voltage gradients among all somatic cells (not just excitable nerve and muscle) control cell behavior, and the ionic coupling of cells into networks via electrochemical synapses allows them to implement tissue-level patterning decisions, which is called developmental bioelectricity. Electrical modulation is therefore a potential target for many new therapies for a range of diseases and biological functions.
We have pioneered various new techniques to enable artificial, biomimetic, nanofibrous scaffold substrates to mediate cell behavior using electrical stimulation. Anisotropy, photocatalytic stimulation and assembly process as three design parameters for the neuron guide conduits were addressed here for peripheral nerve regeneration.[1]

EXPERIMENTAL METHODS

After optimizing the topographical patter, the MEW patterned PCL scaffolds were firstly treated by 1,6-hexamethylenediamine /isopropyl alcohol solutions for 8 h at 37 °C to achieve surface amino functionalization. Then, the modified PCL scaffolds were immersed in a GO colloidal dispersion for 1h and subsequently protonated g-C_3N_4 dispersion for 1h. Scanning electron microscopy (SEM), atomic force microscopy (AFM), Raman spectroscopy, X-ray photoelectron spectroscopy (XPS) and fluorescence microscopy were used to characterize the modifications. The neurite outgrowth on the PCL-GO-C3N4 scaffolds under mono- chromatic light irradiation (450 nm) was studied. Finally, based on the anisotropic micropatterned structures, NGCs assembly for implantation were explored.

RESULTS AND DISCUSSION

MEW PCL scaffolds with rectangular anisotropic patterns (1–2, 1–3) promoted significant longer average neurite extension length than those with isotropic 1-1 pattern. After the surface functionalization of g-C_3N_4 nanoparticles (Fig. 1a,b) by electrostatic interaction (Fig. 1c), The blue fluorescence originated from g-C_3N_4 was observed (Fig. 1d, e). The PCL-GO-C_3N_4 scaffolds were then used for stimulating PC12 cells differentiation under a blue LED light irradiation (450 nm). As shown in Fig. 1g-i, after differentiation for 7 days, cells cultured under light irradiation exhibited greater neurite outgrowth than those without stimulation. Lastly, combining a thermo-responsive PNIPAM membrane with geometry defined MEW micropatterns in a bi-layer system provided a spontaneously-forming Neural guidance conduit.

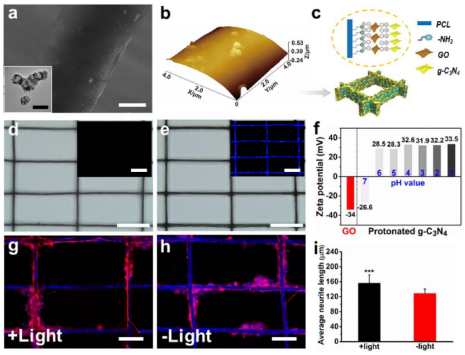

Fig. 1 Effect of photocatalytic stimulation initiated by g-C3N4 decorated polymeric scaffolds on neurite outgrowth. (a) SEM and (b) AFM images of a single PCL-GO- C3N4 fiber. The inset shows a typical TEM image of g-C3N4 nanoparticles. Scale bars: 5 µm in SEM image and 200 nm in TEM image. (c) Scheme diagram of PCL-GO-C3N4 scaffold. Bright field and fluorescence images (the insets) of (d) PCL-GO and (e) PCL-GO-C3N4 fibers, using 360 nm light excitation. Scale bars: 200 µm. (f) Zeta potential of the GO colloids, and protonated g-C3N4 dispersed in DI water at various pH values. Immunofluorescence images of PC12 cells differentiated on PCL-GO- C3N4 scaffold for 7 days (g) with and (h) without light stimulation. Cells were stained with TUJ1 (red) and Hoechst (blue). (i) Average neurite length analysis of cells cultured on PCL-GO-C3N4 scaffold with/without light treatment.

CONCLUSION

In this work, anisotropy, photocatalytic stimulation and assembly process as three design parameters for the NGCs were addressed for peripheral nerve regeneration. Unitedly addressing the three aspects, MEW based NGCs may possess great potential for repairing peripheral nerve injuries.

REFERENCES

1. Zhang Z. *et al*., Biomaterials. 253, 120108, 2020

ACKNOWLEDGMENTS

The authors would like to thank the Carlsberg Foundation (Grant no: CF19-0300) for providing financial support to this project.

Nutlin-loaded ultrasound-activated piezoelectric nanovectors: Modulation of anti-angiogenic activity

Ozlem Sen[1*], Attilio Marino[1], Carlotta Pucci[1], Gianni Ciofani[1]

[1]Istituto Italiano di Tecnologia, Smart Bio-Interfaces, Viale Rinaldo Piaggio 34, 56025 Pontedera, Italy
[*]ozlem.sen@iit.it

INTRODUCTION

Angiogenesis refers to vessel growth, and plays an essential role in embryonic development, wound healing, and many diseases including cancer metastasis[1]. In conventional therapies, the aim is targeting and blocking the activity of pro-angiogenic factors. Recently, a new strategy has been proposed in cancer nanomedicine, based on nanomaterials that can remotely respond to external stimulation (*e.g.*, ultrasound -US-)[2].

In this work, we show how the angiogenic activity of hCMEC/D3 (human cerebral microvascular endothelial) cells is inhibited by exploiting apolipoprotein E-functionalized nutlin-3a-loaded piezoelectric polymeric nanoparticles (ApoE-Nut-PNPs). that can respond to US remote stimulation (Figure 1)[3].

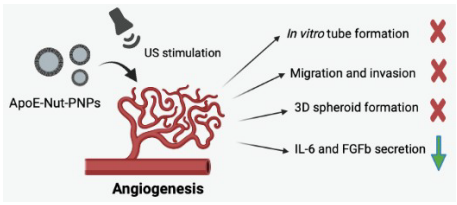

Fig 1. Schematical representation of the study.

EXPERIMENTAL METHODS

Nutlin-3a loaded poly(vinylidene fluoride-co-trifluoroethylene) (P(VDF-TrFE)) nanoparticles (Nut-PNPs) were prepared and functionalized with ApoE peptide, as previously described[4]. After morphological characterization of the nanoparticles, the biocompatibility was tested *via* WST-1 and hemolysis assays. Cellular internalization of the nanovectors was tested by using confocal microscopy. *In vitro* endothelial tube formation assay was performed by considering 8 experimental groups with or without US stimulation. Migration and invasion assays were tested using transwell inserts and a 3D spheroid invasion assay. Angiogenesis-related cytokines production has been assessed using an ELISA kit. Statistical analysis was evaluated by using ANOVA (analysis of variance) and then followed by Fishers *post-hoc* test.

RESULTS AND DISCUSSION

The sizes of the nanoparticles were found to be 66 ± 22 nm, 76 ± 16 nm, 62 ± 20 nm, and 56 ± 12 nm for ApoE-PNPs, ApoE-Nut-PNPs, PNPs, and Nut-PNPs, respectively, while the ζ-potential values are -21.6 ± 0.7 mV, -18.3 ± 0.6 mV, -20.8 ± 0.9 mV, and -18.4 ± 0.8 mV. The release of Nut resulted to be 12.5 ± 0.3% at pH 4.5 upon US stimulation. The experiments were carried out by using a 500 µg/mL of nanoparticles that corresponds to Nut 21.5 µM. As depicted in Figure 2A, the total mesh area significantly decreased in ApoE-Nut-PNPs + US treatment (231463 ± 28310 µm^2, $p < 0.05$). 3D spheroid invasion assay was performed in the presence of glioblastoma cancer cell migration cues on Matrigel matrix. Figure 2B shows fewer cells invaded out of 3D spheroids in ApoE-Nut-PNPs + US stimulated cultures (area = 130067 ± 31247 µm^2, $p < 0.05$), which is in agreement with the transwell invasion assay. We have also profiled 8 angiogenesis-related cytokines, and IL-6 and FGFb resulted significantly down-regulated after ApoE-Nut-PNPs + US stimulation. The decrease of FGFs and IL-6 levels is considered promising to inhibit tumor progression, being a strong connection between angiogenesis and inflammatory processes[5].

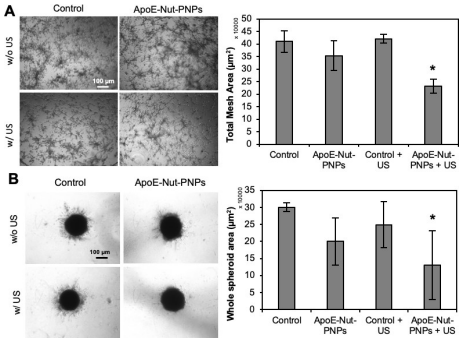

Fig 2. Results of **A)** *in vitro* tube formation and **B)** 3D spheroid invasion assays on Matrigel-coated plate.

CONCLUSION

In this study, ApoE-functionalized nutlin-3a-loaded piezoelectric nanoparticles were synthesized and remotely controlled to inhibit angiogenesis. The obtained findings confirm that ApoE-Nut-PNPs have an *in vitro* anti-angiogenic behavior by inhibiting endothelial cells migration and invasion, vessel formation, and secretion of cytokines related to angiogenesis. In addition, the therapeutic efficacy of the free drug was enhanced by exploiting the prepared piezoelectric nanovectors after US stimulation. Altogether, this study shows that piezoelectric nanoparticles can be exploited as feasible therapeutics to inhibit tumor-induced angiogenesis.

REFERENCES

1. Saeed BA. *et al.,* Int. J. Nanomed. 14:5135-5146, 2019
2. Racca L. *et al*., Nano-micro Lett. 13:1–34, 2021
3. Sen O. *et al.,* Materials Today Bio 13:100196, 2022
4. Pucci C. *et al.,* Acta Biomater. 139:218-236, 2021
5. Aguilar-Cazares D. *et al.,* Front. Oncol. 9:1399, 2019

ACKNOWLEDGMENTS

We would like to acknowledge the financial support of the ERC (European Research Council, grant agreement 70961).

Hydrothermally and Plasma Treated Ti_6Al_4V for Antibacterial Surfaces

Niharika Rawat[1*], Metka Benčina[2], Ita Junkar[2], Aleš Iglič[1]

[1]Laboratory of Physics, Faculty of Electrical Engineering, University of Ljubljana, Ljubljana, Slovenia
[2]Department of Surface Engineering, Jožef Stefan Institute, Ljubljana, Slovenia
niharika.rawat@fe.uni-lj.si

Implant-associated infection (IAI) is a matter of concern for various implant procedures in the biomedical field. IAI often leads to implant removal, revision surgery in some cases even amputation which ultimately increases the medical cost. Therefore there is an increased demand to develop biomaterials with improved surface properties, which would prevent bacterial infections and by this decrease associated medical costs due to lower amount of revision surgeries. For this purpose various surface modification techniques, for instance, electrochemical anodization, hydrothermal treatment, etc. have been proposed to enhance the antibacterial property of metallic materials used as implants. The surface modification of metallic materials often leads to changes in physico-chemical properties such as morphology, surface chemistry and wettability which influences on antibacterial properties of the surface. In the present contribution, TiO_2 nanostructures have been synthesized by hydrothermal method on the surface of Ti_6Al_4V which was pre or post- treated with low pressure gaseous plasma. The morphology wettability and surface chemistry of as-prepared samples were analysed by scanning electron microscopy (SEM), water contact angle analysis (WCA) and X-ray photoelectron Spectroscopy (XPS). The antibacterial effect of the prepared nanostructured surface was studied against *Escherichia coli* (*E.coli*). It was observed that colony forming unit per milliliter (CFU/mL) of *E. coli* was significantly reduced in the case of hydrothermally treated surfaces in comparison to untreated samples. The same effect was also observed for additionally plasma-treated surfaces.

RESULTS AND DISCUSSION

The results of WCA analysis (Figure 1) on hydrothermal (HT), hydrothermal and plasma treated (HT+P) and plasma treated followed by hydrothermal treatment (P+HT) show that the surfaces were fully hydrophilic as the water drop covered the surface. For freshly prepared samples surface was fully wettable (i.e. 0^0) until 1 week. Even after 4 weeks, samples were still hydrophilic. For HT sample, even after a month, the contact angle was about 5^0. For HT+P and P+HT contact angle was about 12^0 which was much lower than the untreated Ti_6Al_4V sample with the contact angle of about 80^0. From SEM images (Figure 1), we can say that compared to the untreated surface the treated surfaces exhibited different morphologies. In the case of only HT the surface consists of feather like micro-nano structures that is interconnected with nanowire like morphology. When this HT-treated disc is pre or post-treated with plasma the morphology becomes more grass-like; containing nanoflake structures that are intertwined. From XPS analysis, it was observed that after hydrothermal treatment of Ti_6Al_4V, the concentration of Ti and O increased from 2.8 to 16% and 27.2 to 48.7% respectively. Similar was observed for pre-plasma treated surfaces, while the plasma treated HT sample exhibited higher oxygen content.

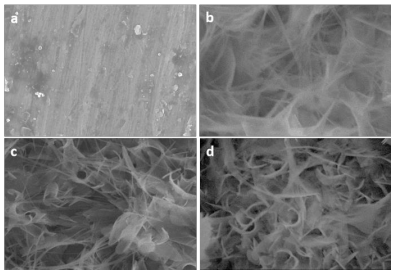

Figure 1: SEM images of Ti_6Al_4V discs (a) untreated (b) HT (c) HT+P (d) P+HT.

From Figure 2, we can state that after surface nanostructuring significant decrease in bacterial growth was observed. In the case of HT, HT+P and P+HT there was more than 90% reduction in bacterial growth as compared to the untreated sample. The reason for this could be that micro–nanofeatures restrict the surface area available for bacterial attachment by entrapping an air layer (bubbles) between the intertwined nano-topographical features leading to the development of an antibiofouling effect.

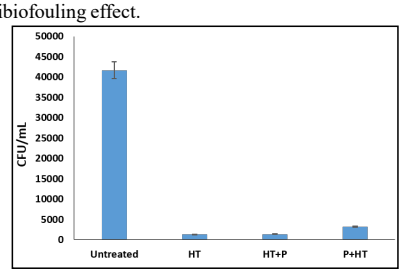

Figure 3: CFU/mL of E. coli bacterial culture on the surface of treated (HT, HT+P, P+HT) and untreated Ti_6Al_4V discs.

CONCLUSION

The present work studied the antibacterial behavior of *E. coli* on TiO_2 nanosurface fabricated via hydrothermal method and plasma treatment on Ti_6Al_4V discs. It was shown that HT treatment leads to the formation of interwoven nanowires on the surface whereas pre or post treatment with plasma leads to the formation of cross-sectioned nanoflakes. *E. coli* cultured on all three surfaces i.e. HT, HT+P and P+HT showed a significant reduction in CFU/mL. This could be due to the increased concentration of titanium and oxygen on the hydrothermal surface, which provides the unique characteristics of the surface. An increase in oxygen concentration could lead to the formation of an oxygenated layer that limits the bacterial interaction to the surface preventing biofilm formation, while the freshly plasma treated surfaces could increase the release of ROS from the TiO_2 layer which could initiate cell death mechanism. This work discusses the prospects of a novel methodology that could help limit the implant-associated infections which are related to biofilm formation on the implant surface.

Synthesis of Cerium Oxide Nanoparticles in Microfluidic Reactors

Konstantinos Tsachouridis[1], Antonios Anastasiou[1]

Department of Chemical Engineering, University of Manchester, Manchester, UK, M13 9PL

email: konstantinos.tsachouridis@postgrad.manchester.ac.uk

INTRODUCTION: Although the global nanomaterials market witnessed robust growth during the last decades and is expected to reach 16.8 $B by the end of 2022, there are few barriers that constrain the further development. These are revolving around two main questions: **a)** how do we achieve consistent properties of nanoparticles? **b)** how we achieve continuous processes and sustainable production by minimizing required energy and raw materials?

Microfluidics can be the potential answer to these problems. It is well known that in microreactors we have strict control of operating conditions, enhanced transport phenomena and minimum use of raw materials. At the same time scaling up is a straightforward procedure by just increasing the number of the required devices (numbering up). In this work we will demonstrate the synthesis of cerium oxide nanoparticles in microfluidic reactor (MRs). Cerium oxide nanoparticles (CONs) cover 5% of the global market due to their broad spectrum of engineering applications. They have excellent physio-chemical properties and some of their applications include catalysis, biomedical engineering while they are also used as additives in fuels.

EXPERIMENTAL METHODS: A segmented flow microreactor was selected in order to avoid fouling. The continuous phase is a low viscosity oil (PMDS), immiscible to water. The two aqueous solutions of the reactants form microdroplets and are the segmented phase where the reaction takes place.

Computational Fluid Dynamics (CFD) was utilized to simulate droplet formation and decide for the optimal geometrical characteristics and operating conditions of our microreactor. The MRs was designed in AutoCAD and then fabricated using a resin 3D printer. Flow experiments followed where microdroplets were monitored with a high-speed camera. CONs that will be used as a reference were first synthesized using the chemical precipitation method (p-CONs) [1], and then characterised using XRD, DLS and TEM.

RESULTS AND DISCUSSION: One of the biggest challenges during the design of the microreactor was to determine the appropriate geometrical characteristics (aspect ratio of the inlets) and flow conditions in order to achieve the formation of merging droplets from the two liquids of the two side inlets. This is required for the reactants to come in contact and the reaction to occur (Fig.1). Our results were in accordance to what is reported in literature [2], that in order to achieve merging droplets low Ca and Re numbers are required (<0.05) while ideally the aspect ratio of the side inlets to the main channel should be 1.5. Based on these results, a cross junction microreactor was designed in AutoCAD with the width of the main channel to be 500 μm and the one at side inlets 750 μm. The design was imported to a 3D-printed using a clear resin for fabrication (BV-007 acrylate polymer). To verify our simulations the formation of oil/water droplets in the MR using a microscope with the high-speed camera was investigated. Adjustments on the parameters of our microfluidic system were required to facilitate a proper merging-droplet regime (reducing Ca number). The experiments of CONs synthesis in the microreactor are currently in progress.

For having them as reference nanoparticles were also synthesised using chemical precipitation method. These were characterized with X-ray diffraction for their crystallographic structure and their chemical composition. All of the CeO_2 peaks from the database's reference are matching our samples, with the more characteristic peaks found at 28.5, 33.0, 47.4 and 56.3 deg. thus confirming the p-CONs synthesis. After DLS (Mastersizer3000) we found that the particle size ranges from 10 to 70 nm depending on the residence time of the reaction.

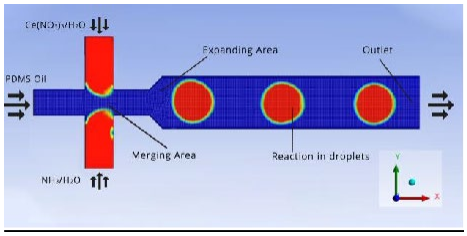

Fig.1 Droplet formation study in microreactor with CFD.

CONCLUSION: A segmented flow microreactor has been designed for the synthesis of CONs. After CFD simulations and experiments with a high-speed camera the appropriate Re and Ca numbers to obtain merging droplets have been identified. Comparisons between CONs obtained from the microfluidic reactor and through conventional synthesis routes is in progress.

REFERENCES:

1. Wang, W., et al., A surfactant and template-free route for synthesizing ceria nanocrystals with tunable morphologies. Journal of Materials Chemistry, 2010. **20**(36): p. 7776-7781.
2. Ngo, I.-L., et al., A numerical study on the dynamics of droplet formation in a microfluidic double T-junction. Biomicrofluidics, 2015. **9**(2): p. 024107.

ACKNOWLEDGMENTS: "The authors would like to thank the Horizon 2020 funded project I-SMarD for providing financial support to this work".

Development of nanovectors for targeted delivery of p38 MAPK inhibitors to dendritic cells

Jinge You[1*], Andrew Jackson[2], Poulam Patel[2], Giuseppe Mantovani[1], Cameron Alexander[1]

[1]School of Pharmacy, University of Nottingham, Nottingham, United Kingdom
[2]School of Medicine, University of Nottingham, Nottingham, United Kingdom
[*] Jinge.You@nottingham.ac.uk

INTRODUCTION

Dendritic cells (DCs) are antigen-presenting cells which play an important role in tumour immunity. However, the function of DCs can be suppressed due to specific conditions found in the tumour microenvironment.[1,2]

Previous studies suggested that p38 inhibitors (p38i) can reverse dysfunction of tumour patient-derived dendritic cells *in vitro*.[3,4] However, in addition to DCs, p38 is also expressed by a plethora human cells, thus treating patients with p38i may potentially lead to undesired off-target effects. Therefore, to improve drug efficacy and reduce side-effects *in vivo*, this work aimed at developing sugar-based nanovectors targeting lectin endocytic DC receptors for delivery of p38i to DCs.

EXPERIMENTAL METHODS

2-(3-chloro-4-hydroxybenzamido) ethyl acrylate (CHB), 2-(((butylthio)carbonothioyl)thio)propanoic acid, and VA-044 were dissolved in 1.0 mL of water/DMSO, deoxygenated by argon bubbling for 15 minutes and stirred at 70 °C and for 2 h. PolyCHB intermediate was precipitated by pouring the reaction mixture into water. PolyCHB and 2′-acrylamidoethyl-α-D-mannopyranoside (ManAA) were dissolved in 1.0 mL of water/DMSO, deoxygenated by argon bubbling for 15 minutes and stirred at 70 °C and for 2 h. CHB-*b*-ManAA diblock copolymer was purified by dialysis against water.

CHB-*b*-ManAA based nanoparticles were prepared by the nanoprecipitation method. Briefly, PBS (4 mL) was added dropwise to of a 10 mg/mL solution of polymers (with or without 2 mg/mL coumarin 343-4-Morpholineethyl ester (CME)) in DMSO (1.0 mL). The mixture was then transferred into a dialysis bag (3.5 kDa, MWCO) and dialyzed against 2 L of PBS pH 7.4 at room temperature for 16 hours with 4 buffer exchanges.

Cytotoxicity experiments were carried out using monocyte derived DCs with PrestoBlue assay.

RESULTS AND DISCUSSION

Amphiphilic CHB-*b*-ManAA block copolymers were designed to self-assemble under aqueous condition. Mannose was chosen as the recognition element of choice as DCs often display mannose-binding endocytic receptors, such as DC SIGN and CD206. PolyCHB block was designed to be both hydrophobic and weakly acidic to improve loading of hydrophobic drugs with amine functionalities by ionic interactions. Importantly for our study, BIRB796 p38i is a hydrophobic molecule with a basic tertiary amino group.

^{1}H NMR and GPC results confirmed the identity and narrow molecular weight dispersity of our CHB-*b*-ManAA amphiphilic block copolymers. DLS analysis of the resulting self-assembled CHB_m-*b*-$ManAA_n$-based nanoparticles, with or without incorporated CME, showed narrow size distribution. UV-Vis analysis indicated high efficiency of p38 inhibitors-mimic fluorescent probe incorporation (encapsulation efficiency (EE) = 64%, loading capacity (LC) = 11.3%). No toxicity was observed in cytotoxicity experiments for 24 hours, at 10^{-5}-10^{-1} mg/mL polymer concentration range.

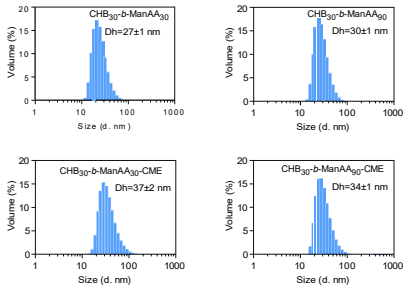

Figure 1. DLS analysis of self-assembled structures of CHB_{30}-*b*-$ManAA_{30}$, CHB_{30}-*b*-$ManAA_{90}$, CHB_{30}-*b*-$ManAA_{30}$-CME (LC= 11.3%) and CHB_{30}-*b*-$ManAA_{90}$ (LC= 7.1%) self-assembled aggregates, PBS pH 7.4

CONCLUSION

To date, we have synthesized a family of CHB-*b*-ManAA amphiphilic diblock copolymers. And stable CHB-*b*-ManAA based nanoparticles were successfully prepared, which showed high drug loading efficiency and no obvious cytotoxicity. Therefore, CHB-*b*-ManAA polymers are potential materials for delivery of p38i to dendritic cells.

REFERENCES

1. Pinzon-charry, A. *et al.* Immunology and Cell Biology 83:451–461, 2005
2. Zong, J. *et al.* Cancer Immunol. Immunother. 65:821–833, 2016
3. Adhikaree, J. *et al.* Oncoimmunology 8:1–12, 2019
4. Franks, H. A. *et al.* Int. J. Cancer 134:575–586, 2014

ACKNOWLEDGMENTS

Thank University of Nottingham for funding.

Synthesis and Characterization of Cerium Oxide Nanoparticles for Surface Coating of Titanium Implants

Maria-Eleni Ioannou[1*], Georgia K. Pouroutzidou[1,2], Ioannis Tsamesidis[1], Iason Chatzimentor[1], Eleni Likotrafiti[3], Jonathan Rhoades[3], Eleana Kontonasaki[1]

[1]School of Dentistry, Faculty of Health Sciences, Aristotle University of Thessaloniki, 54124 Thessaloniki, Greece
[2]School of Physics, Faculty of Sciences, Aristotle University of Thessaloniki, 54124 Thessaloniki, Greece
[3] Department of Food Science and Technology, International Hellenic University, 570 0154124 Thessaloniki, Greece
*marilenaioannou@dent.auth.gr

INTRODUCTION

Nanotechnology is a known and advanced science for the last 60 years and concerns the use and production of materials at the nanoscale level. Nanoparticles (NPs) are defined as small particles with at least one dimension being less than 100 nm[1]. This tiny size contributes in new properties relative to the same particles in larger sizes[2]. Various methods have been used for the synthesis of nanoparticles which fall into two browed categories top-down and bottom-up[3]. A very interesting element of the periodic table is Cerium (Ce) which belongs to the lanthanide group, that exists uniquely in two oxidation states, Ce^{+3} and Ce^{+4} and has a broad range of applications and properties[4]. CeO_2 exhibits antioxidant and extraordinary electrochemical properties[3]. It acts as a catalyst and behaves as a scavenger of Reactive Oxygen Species (ROS) and free radicals[5]. Its FCC structure helps in the neutralization of free radicals and provides oxygen storage capacity (OSC)[3]. In this study the synthesis and characterization of CeO_2 nanoparticles were performed aimed for surface coating of titanium implants. Hemocompatibility evaluation was also performed.

EXPERIMENTAL METHOD

Synthesis of Ce-NP: Synthesis of CeO_2 nanoparticles was performed with the sol-gel method. Cerium nitrate hexahydrate 1, 2, 3, 4 and 5g, gelatin 0.2 g, ammonia solution and d.d water 20ml were used to obtain five different samples (S1, S2, S3, S4, S5 based on cerium nitrate quantity). Finally, each sample was dried and heated at 550 ºC for 1h.

Characterization: The physicochemical properties of the synthesized nanoparticles were evaluated with Fourier Transformation Infrared Spectroscopy (FTIR), X-ray diffraction (XRD) and Scanning Electron Microscopy (SEM) techniques. Hemolytic activity in contact with human red blood cells (RBCs) was also investigated. Diluted RBCs were prepared in PBS and were treated with different concentrations of NPs (12.5 up to 1000 μg/ml) for 24 hours at 37 °C. The absorbance of hemoglobin at 541 nm was measured with a plate reader, from supernatants after centrifugation at 2000 rpm for 1 minute. The percent of hemolysis was calculated as follows: Hemolysis % = [(sample absorbance-negative control)/ (positive control-negative control)]x100. Antimicrobial activity experiments against *St. aureus* and *E.coli* were performed using eluates of Ce-NPs. A suspension of 5 mg/mL Ce-NP was prepared in ultrapure water, sterilized by uv and left on a rotary shaker for 24 h at room temperature. The solid material was removed by centrifugation and the antimicrobial activity of the eluate was determined with Bioscreen.

RESULTS AND DISCUSSION

The FTIR spectra presented several characteristic peaks which are attributed to the presence of CeO_2 and XRD revealed the presence of CeO_2 crystalline phase. Particles diameter measured from SEM micrographs were approximately 140nm-300nm (Fig.1). The amount of cerium affected the morphology and size. However, the NPs with the largest amount of cerium presented the smallest particle size and best size distribution. All NPs did not induce hemolysis in concentrations lower than 500 μg/mL. Ce-NPs with 1 and 2g of cerium nitrate presented hemolysis at the highest concentration. Increasing the amount of cerium nitrate (3, 4 and 5g) no hemolytic effect was observed even at the highest concentrations, indicating better hemocompatibility. Some slight inhibition of *St. aureus* growth was observed with Ce-NP eluates, but *E. coli* was unaffected.

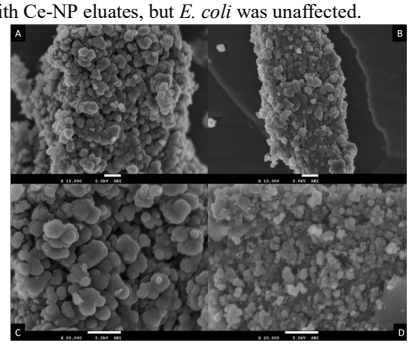

Fig. 1. SEM micrographs of synthesized materials. S1 (A, C) and S5 (B, D).

CONCLUSION

Ce-NPs were successfully synthesized by the sol-gel method. Hemolytic activity showed that the higher the concentration of the cerium additive, the better the blood compatibility was.

REFERENCES

1. Khan I. *et al.*, Arab J Chem. 12:908-931, 2019
2. Thakur N. *et al.*, J Nanobiotech. 17:1-27, 2019
3. Singh KRB. *et al.*, RSC Adv. 10:27194-27214, 2020
4. Tumkur PP. *et al.*, Nanomanufact. 1:176-189, 2021
5. Darroudi M. *et al.*, Ceram Int. 39:6917-6921, 2013

Amphiphilic Nanogels for the Delivery of Hydrophobic Compounds

Clara López-Iglesias[1,2*], Alexandra Gruber[2], Ante Markovina[2], Nithiya Nirmalananthan-Budau[3], Ute Resch-Genger[3], Daniel Klinger[2]

[1]Department of Pharmacology, Pharmacy and Pharmaceutical Technology, I+D Farma (GI-1642), iMATUS and IDIS, Universidade de Santiago de Compostela, Santiago de Compostela, Spain
[2]Institute of Pharmacy, Department of Biology, Chemistry and Pharmacy, Freie Universität, Berlin, Germany
[3]Biophotonics Division, Federal Institute of Materials Research and Testing, BAM, Berlin, Germany
[*] claralopez.iglesias@usc.es

INTRODUCTION

Most new potential therapeutics are hydrophobic, including a high number of natural compounds with promising antibiotic, anti-inflammatory and pro-regenerative properties (e.g. curcumin and berberine)[1]. Nanogels (NGs) are promising carriers for drug delivery due to their colloidal size, flexible structure and biocompatibility, but their hydrophilic character limits the loading of hydrophobic compounds[2]. Providing NGs with partial hydrophobicity by introducing a certain number of hydrophobic groups into the structure can be a strategy to overcome this limitation[3]. However, deeper understanding of the interaction of the hydrophobic cargo with the overall hydrophilic network is needed to adjust the structure to each specific molecule. In this work, a library of amphiphilic nanogels was synthesized, and the structure-cargo interactions were deeply studied by spectroscopic methods and loading tests.

EXPERIMENTAL METHODS

Synthesis of the amphiphilic NGs

Briefly, crosslinked particle precursors based on poly(pentafluorophenylmethacrylate) were prepared via miniemulsion polymerization. The NG precursors were later functionalized by substitution of the pentafluorophenyl esters with a mixture of a hydrophilic and different hydrophobic amines and purified by dialysis. The resulting nanogels were measured by dynamic light scattering (DLS) and observed by transmission electron microscopy (TEM).

Fluorescence studies

NGs functionalized with different hydrophobic groups and suspended in water were loaded with a solvatochromic dye (nile red, NR) at different concentrations. Emission spectra and quantum yield (QY) values were determined. Spectra deconvolution was carried out with Origin Pro software to determine the proportion of aggregated and non-aggregated species.

Load content evaluation

A determined set of NGs were loaded with a set of drugs and dyes with different hydrophobicity, using the same initial drug concentration. The aqueous suspensions of loaded NGs were freeze-dried and particles were resuspended in acetonitrile or DMSO to analyze their drug content using HPLC or UV/Vis spectroscopy, respectively.

RESULTS AND DISCUSSION

The prepared nanogels presented hydrodynamic diameters of 115 nm and narrow particle size distributions, with good colloidal stability in water.

Spectroscopic analysis of the nanogels loaded with different concentrations of NR revealed a strong influence of NR concentration on its interaction with the hydrogel. At the lowest concentrations, NR was molecularly dispersed in the network and high QY were obtained, showing changes in the peaks of maximum emission that could be correlated with the different polarities of the hydrophobic groups. However, as NR concentration increased inside the particles, the emission spectra showed a secondary peak appearing at higher wavelength that correlated with the apparition of aggregated species, and low QY values were obtained in all cases.

The loading studies showed no influence of the hydrophobicity of the loaded substances on the loading capacity of the nanogels, suggesting that other properties need to be considered to predict NG-cargo affinity.

CONCLUSION

In this work, a set of NGs with different amphiphilic characters and similar colloidal features was synthesized from the same particle precursors. The NGs were able to load hydrophobic cargoes with a disposition that was dependent on the concentration of cargo, and spectroscopic studies were a useful tool to study the microenvironment of the loaded substances inside the NG network.

REFERENCES

1. Wang G. *et al*., Expert Opin Drug Deliv. 12:1475-1499, 2015.
2. Larrañeta E. *et al*., J Funct Biomater. 9:13, 2018
3. Gruber A. *et al.*, Polym Chem. 9:5553-5632, 2018

ACKNOWLEDGMENTS

This work was partially funded by the DFG (Deutsche Forschungsgemeinschaft/German Research Foundation) (KL 3152/2-1, project number: 430915250). N.N.-B. acknowledges financial support from the Federal Institute for Materials Research and Testing (BAM) within the funding program "Menschen, Ideen" (MI, type III project). C.L.-I. acknowledges Xunta de Galicia for a postdoctoral fellowship [ED481B 2021/008].

Dual-functional nanofibers for light neural stimulation and nerve growth factor release

Jordi Amagat[1, 3], Natasja Porskjær Christensen[1], Yingchun Su[1,4], Alice Le Friec[1] , Menglin Chen[1,2]

[1.] *Department of Biological and Chemical Engineering, Aarhus University, Denmark.*
[2.] *Interdisciplinary Nanoscience Center, iNANO, Aarhus University, Denmark.*
[3.] *Sino-Danish College (SDC), University of Chinese Academy of Sciences, Beijing 101400, China.*
[4.] *School of Electrical Engineering and Computer Science, KTH Royal Institute of Technology, Electrum 229, 16440, Kista, Sweden.*

INTRODUCTION

Neurons, as electroactive cells, can respond to electrical signals. Electrical stimulation has widely been used and has shown to influence processes such as migration, proliferation, and axonal outgrowth. Electrospun nanofibrous structures produced in electrospinning strategies can closely mimic the natural extracellular matrix and serve as a reliable in vivo-like environment for 3D in vitro experiments. Indirect electrical stimulation, in particular photostimulation, could provide an alternative to direct stimulation through the use of photocatalysts. To avoid UV-derived cell death, g-C_3N_4 as a promising semiconductor photocatalyst in the visible-light range has gained great attention. g-C_3N_4 was reported combining with GO for indirect stimulation of PC12 differentiation, and the blue-light stimulated cells grown on top of g-C3N4 coated scaffolds show longer neurites compared to non-stimulated cells [1].

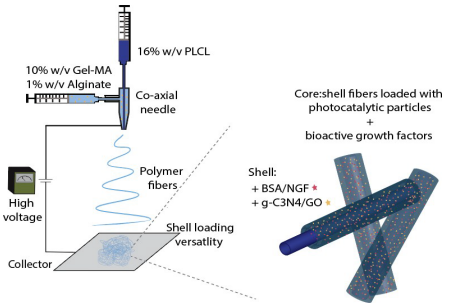

Scheme 1: Ilustration of the overall idea for generation of dual function electrospun coaxial nanofibers.

Herein, we explored PLCL-NGF-BSA/GelMA-g-C3N4-GO coaxial nanofibers for Nerve Growth Factor (NGF) release from the core and photostimulation for neural differentiation from the shell. The neural photostimulation, and enhanced release of NGF via light stimulation in 3D culture were designed (Scheme 1).

EXPERIMENTAL METHODS

Electrospun nanofibers were produced via coaxial electrospinning. Nanofiber morphology was analysed with SEM and TEM. Injectability tests were performed with a surgical needle and imaged with fluorescence microscopy. PC12 cells, a model neural cell line, proliferation and cytotoxicity was analyzed via CCK and LDH tests. PC12 differentiation was analyzed via immunohistochemistry and fluorescence imaging. Bidaily light stimulation was performed with a 450nm light. NGF release was measured via an ELISA kit. T-tests and ANOVA were used as statistical analysis.

RESULTS AND DISCUSSION

Different concentrations of g-C3N4 and graphene oxide (g-C_3N_4/GO) and NGF were successfully incorporated into both shell and core of electrospun nanofibers. Due to the lubricant properties of the hydrogel shell, scaffolds could be injected through a needle and retain photocatalytic particles. Both loaded scaffolds showed no cytotoxicity and allowed proliferation of PC12 cells. In addition, when PC12 cells were differentiated on top of light stimulated loaded g-C_3N_4/GO nanofibers, showed an increased neurite length compared to non-stimulated nanofibers. Coaxial nanofibers also provided the structures to release NGF into the media and trigger neurite differentiation of PC12 cells. ELISA showed that upon 30 days of culture, an 8.3% of NGF could be released into the media. In addition, combination of light stimulation and NGF loaded nanofibers enhanced the release of NGF into the media over the same period of time.

CONCLUSION

In the present study, the versatility of coaxial PLCL/GelMA electrospun nanofibers was presented with dual-function for g-C3N4 based photocatalytic wireless electrical stimulation and NGF release. Upon visible light stimulation g-C3N4-GO-loaded nanofibers could enhance the neurite outgrowth of PC12 cells after 10 days culture, compared to non-stimulated ones. In addition, coaxial nanofibers could also support and enhance the differentiation of PC12 cells with a sustained release of functional NGF over 30 days in culture. Finally, combining both approaches led to an increase of NGF release upon light stimulation. The versatile coaxial electrospun fibers could support neural differentiation and sustained growth factor release and thus hold great potential to be used for repairing nerve injuries in the future.

REFERENCES

1. Zhang, Z., et al., ACS Appl Mater Interfaces, 2017. **9**(40): p. 34736-34743.

ACKNOWLEDGMENTS: The authors would like to thank the Carlsberg Foundation and Sino-Danish Center.

Targeting photothermal therapy to endometriotic cells overexpressing CD44

Cristina Volpini[1,2,3*], Nora Bloise[1,2,3], Mattia Dominoni[4], Fabio Barra[5,6], Valerio Gaetano Vellone[7,8], Barbara Gardella[4,9], Simone Ferrero[5,6], Livia Visai[1,2,3*]

[1]Molecular Medicine Department (DMM), Centre for Health Technologies (CHT), UdR INSTM, University of Pavia, Pavia, Italy
[2]Medicina Clinica-Specialistica, UOR5 Laboratorio di Nanotecnologie, ICS Maugeri, IRCCS, 27100 Pavia, Italy
[3]Interuniversity Center for the promotion of the 3Rs principles in teaching and research (Centro 3R), University of Pavia Unit, Italy
[4]Department of Clinical, Surgical, Diagnostic and Paediatric Sciences, University of Pavia, Pavia, Italy.
[5]Academic Unit of Obstetrics and Gynecology, IRCCS Ospedale Policlinico San Martino, Genova, Italy
[6] DINOGMI, University of Genova, Italy
[7]Anatomia Patologica Universitaria, IRCCS Ospedale Policlinico San Martino, Genova
[8]Dipartimento di Scienze Chirurgiche e Diagnostiche Integrate (DISC), Università di Genova
[9]Department of Obstetrics and Gynecology, Fondazione IRCCS Policlinico San Matteo, Pavia, Italy
*cristina.volpini01@universitadipavia.it

INTRODUCTION

Endometriosis is an estrogen-dependent inflammatory condition that affects women in their reproductive period and is associated with diagnostic delay, reduced quality of life, and loss of work productivity. It's defined as the presence of endometrial glands and stroma outside the uterine cavity, predominantly, but not exclusively, in the pelvis.[1] In the last years, the growing knowledge of different molecular pathways involved in endometriosis development paved the way for investigating new therapeutic approaches.[2] Since endometriosis and cancer share many pathophysiological features, some fundamental principles of cancer nanomedicine can be adapted to develop novel nanoparticle-based strategies for the treatment and imaging of endometriosis.[3] The study aims to evaluate an active targeting of CD44 (transmembrane glycoproteins) overexpressing endometriosis cells by using gold nanoparticles with star shape conjugated with antiCD44 antibody (Au@antiCD44) with and without photothermal therapy (PPT).

Keywords: gold nanoparticles, endometriosis, photothermal therapy

EXPERIMENTAL METHODS

Gold nano-stars (GNS) were synthesized, pegylated (PEG), and characterized using Transmission electron microscopy (TEM), Dynamic Light Scattering (DLS), and UV-Vis spectrophotometry. The conjugation between PEG-GNSs and anti-CD44 antibody was carried out using the Maleimide chemistry. The conjugated GNSs were characterized using UV-visible spectroscopy absorption studies, DLS, Bicinchoninic Acid (BCA), and dot blot analyses.
Viability (MTT) studies with/without laser treatment were performed to verify the efficiency of PEG-GNSs against three different cell lines: CD44 overexpressing cells (z12 cells) and compared to CD44 low expressing cells (Thesch) and normal fibroblast cell line (NIH-3T3).

RESULTS AND DISCUSSION

The UV-Vis spectra displayed a plasmon resonance band in the range of 750-950 nm, which can be suitable for performing PTT in deep tissues. Next, anti-CD44 antibody conjugated PEG-GNSs were prepared and characterized using DLS and UV-Vis spectroscopy. The conjugation increased particle size reduced negative zeta potential, and UV-Vis absorption spectrum shifted with respect to PEG-GNSs. The antibody's presence on the surface of the conjugated nanoparticles was also assessed by dot blot (direct) and BCA (indirect) studies. The photothermal activity of PEG-GNS was observed by *in vitro* studies on the three different cell lines, as previously indicated.

CONCLUSION

The conjugated Au@antiCD44 could be a new therapeutic approach in endometriosis disorder exploiting the GNSs-mediated photothermal activity on the endometriotic cells. Further investigations on 2D *in vitro* models are needed. 3D *in vitro* models and *in vivo* studies are required to assess the toxicity and efficacy of this PTT nanoplatform against endometriotic cells overexpressing CD44.

REFERENCES

1. Vercellini P. *et al*., *Nat. Rev. Endocrinol.* 10, 261–275, 2014.
2. Ferrero, S. *et al*., Drugs, 78(10): p. 995-1012, 2018
3. Moses, A.S., et al., Small, 17(7): p. e2004975, 2021. Smith G. *et al*., J. Biomech. 2:5-11, 2011

ACKNOWLEDGMENTS

The authors would like to thank the Italian Ministry of Health, BANDO RICERCA ENDOMETRIOSI (Grant no: ENDO-2021-12371975) for providing financial support to this project".

Cell-penetrating peptide-modified nanoparticles for enhanced adipocyte uptake

Suim Choi[1], Yurim Bae[1], Keuen Yong Lee[1*]

[1]Department of Bioengineering, Hanyang University, Seoul 04763, Republic of Korea
[*] leeky@hanyang.ac.kr

INTRODUCTION

Obesity has become a global health issue because it causes many complications, such as type 2 diabetes, fatty liver, gallstones, and several cancers.[1] Although pharmacotherapy has been widely used to treat obesity, conventional approaches did not specifically target adipocytes for the treatment of obesity and diet-induced conditions.[2] Polymeric nanoparticles have been widely exploited as drug delivery cargos.[3] Herein, we suggest a use of poly(lactic-co-glycolic acid) (PLGA) nanoparticles loaded with calcium carbonate ($CaCO_3$) for endosomal pH-responsive gas-generation. Additionally, the surface of the nanoparticles was modified with nona-arginine (R_9) peptide to enhance the cellular uptake. The effect of peptide modification of $CaCO_3$-loaded PLGA nanoparticles on the uptake by adipocytes and adipose-derived stem cells (ADSCs) was investigated. The endocytic pathway and resultant gas generation from the nanoparticles under endosomal conditions were also investigated *in vitro*.

EXPERIMENTAL METHODS

Preparation of nanoparticles. PLGA nanoparticles containing $CaCO_3$ as a gas-generating nanoparticles (GNP) were prepared by the water-in-oil-in-water (W/O/W) double emulsion and solvent evaporation method. As a control, PLGA nanoparticles without $CaCO_3$ were prepared (PNP). R_9 peptide was covalently conjugated to the surface of GNP via carbodiimide chemistry (R_9-GNP, R_9-PNP).

Characterization of nanoparticles. The mean diameter, size distribution, and zeta potential of nanoparticles were determined by dynamic light scattering. The conjugation of R_9 peptide to GNP was confirmed by Fourier-transform infrared spectroscopy (FT-IR) and ^{1}H nuclear magnetic resonance (NMR) spectroscopy

***In vitro* cell viability.** The viability of 3T3-L1 adipocytes and ADSCs treated with nanoparticles was evaluated by the MTS assay. The uptake of R_9-modified PLGA nanoparticles by 3T3-L1 adipocytes was observed by confocal microscopy.

RESULTS AND DISCUSSION

The size and its distribution of nanoparticles were assessed by the dynamic light scattering method. The mean diameter of PNP and GNP were 218 nm and 220 nm, respectively, with a narrow size distribution. The size of R_9-GNP was slightly increased compared to that of GNP. The surface charge of GNP was increased when R_9 peptide was introduced to GNP due to the positive arginine residues in the peptide. The conjugation of R_9 peptide to GNP was confirmed by FT-IR spectroscopy and ^{1}H NMR spectroscopy. No significant decrease in the viability of 3T3-L1 adipocytes and ADSCs was observed when the cells were treated with PNP and R_9-PNP. However, the viable cells were significantly decreased when R_9-GNP was used compared with those treated with GNP. Enhanced cellular uptake of Alexa 488-conjugated R_9-PNP was observed by confocal microscopy compared to Alexa 488-conjugated PNP.

CONCLUSION

GNP was prepared and modified with R_9 peptide. R_9-GNP showed enhanced cellular uptake by both undifferentiated and differentiated adipocytes. These nanoparticles generated carbon dioxide gas at acidic pH. Accordingly, R_9 -GNP could be a useful delivery system to adipocytes and ADSCs for the treatment of obesity and diet-induced conditions. Cell penetrating peptide-mediated delivery of functional polymer nanoparticles may also be useful for various diseases.

REFERENCES

1. Sibuyi, N.R.S., International Journal of Nanomedicine, 2018. 13: 7915.
2. Haas, B., Diabetology & Metabolic Syndrome, 2012. 4(1): 1-11.
3. Deirram, N., Macromolecular Rapid Communications, 2019. 40(10): 1800917.

ACKNOWLEDGMENTS

This study was supported by a National Research Foundation of Korea (NRF) grand funded by the Korean government (MSIT) (NRF-2020R1A2C1012199).

Surface-functionalized polymer nanoparticles for localized fat reduction

In Young Lee[1], Yu Rim Bae[1], Eun Ju Jeong[2], Kuen Yong Lee[1*]

[1]Hanyang University, Seoul 04763, Republic of Korea
[2]Supernova bio, Inc., Seoul 04385, Republic of Korea
[*] leeky@hanyang.ac.kr

INTRODUCTION

Polymeric nanoparticles have been widely exploited for the treatment of various diseases, and the surface modification of the nanoparticles has often been used to enhance the therapeutic efficacy and reduce the side effect.[1] Here, we hypothesized that polymer nanoparticles could be exploited as a potential adipocytolytic system via targeted delivery. We also hypothesized that gas-generation from the delivered polymeric nanoparticles could be beneficial for the membrane disruption of adipocytes. In this study, poly(lactic-*co*-glycolic acid) (PLG) nanoparticles loaded with calcium carbonate mineral were prepared as gas-generating nanoparticles under acidic endosomal conditions.[2] The surface of the nanoparticles was modified with functional peptides to achieve receptor-mediated endocytosis by adipocytes.[3] Various properties of nanoparticles were investigated, including size, shape, and amount of gas-generation The cytotoxicity of the nanoparticles was tested *in vitro*. The efficacy of the nanoparticles as an adipocytolytic agent was also evaluated using a high-fat diet-induced obesity mouse model.

EXPERIMENTAL METHODS

Materials. PLG (MW 6,400 g/mol, 0.15–0.25 dL/g) was purchased from Lactel Absorbable Polymers (USA). Calcium carbonate ($CaCO_3$) was purchased from Sigma-Aldrich(USA). A peptide with the adipocyte-targeting sequence (ATS) was supplied by Peptron (Korea).

Preparation of nanoparticles. PLG nanoparticles containing $CaCO_3$ core were prepared by a double emulsion method. ATS peptide was then chemically coupled to the surface of the nanoparticles via carbodiimide chemistry.

Size and size distribution of nanoparticles were investigated by dynamic light scattering. The loading content of $CaCO_3$ was determined using a calcium colorimetric assay kit.

***In vitro* cell viability.** The cytotoxicity and intracellular uptake of nanoparticles by 3T3-L1 adipocytes were investigated *in vitro*.

***In vivo* efficacy test.** C57BL/6 mice (5 weeks old) were purchased from Orient Bio (Korea). The proportion of a high-fat diet was gradually increased, and mice were fed only a high-fat diet with 60 kcal% fat. When the body weight reached approximately 42 g, each sample was subcutaneously injected into the left side of the inguinal fat pad (50 mg/kg, single injection).
Tissues extracted from the mice were placed into paraffin blocks. Tissue blocks were cut into 5 μm thickness and stained with hematoxylin and eosin (H&E).

RESULS AND DISCUSSION

Surface-functionalized polymer nanoparticles were successfully synthesized (mean diameter = 227 nm), and conjugation between nanoparticle and peptide was confirmed by ^{1}H NMR spectroscopy. Chemical modification of nanoparticles with the peptide did not significantly affect the characteristic of the nanoparticles. Their size distribution was significantly changed at acidic pH, indicating carbon dioxide (CO_2) gas generation from the nanoparticles. Enhanced intracellular uptake of ATS-modified nanoparticles by adipocytes substantially decreased the cell viability due to CO_2 gas generation from the nanoparticles. ATS-modified nanoparticles were also useful for fat reduction when subcutaneously injected into the inguinal fat pad of the mouse without significant loss of body weight and systemic side effects.

CONCLUSION

This study reports a new strategy to reduce localized adipose tissue using polymer nanoparticles. ATS-modified gas-generating nanoparticles were useful as a targeted delivery vehicle to adipocytes, and CO_2 gas released from the nanoparticles disrupted the adipocyte membrane. These functional polymeric nanoparticles may be promising as a safe and effective adipocytolytic agent for further therapeutic exploration.

REFERENCES

1. Elsabahy, M. *et al*., Chem Rev, 115 (19), 10967-11011, 2015.
2. Maleki Dizaj, S. *et al*., Expert Opin Drug Deliv, 12 (10), 1649-1660, 2015.
3. Won, Y. W. *et al*., Nat Mater, 13 (12), 1157-1164, 2014.

ACKNOWLEDGMENT

This work was supported by the National Research Foundation of Korea (NRF) grant funded by the Korean government (MSIT) (NRF-2020R1A2C1012199).

Carbon dioxide gas-generating PEG-based micelles for adipocytolysis

Chunggoo Kim[1], Minju Kim[1], Kuen-Yong Lee[1*]

[1]Department of Bioengineering, Hanyang University, Seoul, Republic of Korea
[*] leeky@hanyang.ac.kr

INTRODUCTION

Obesity is one of the key factors of the metabolic syndrome, which is related to type 2 diabetes and cardiovascular diseases.[1] Additionally, demand for localized fat reduction to get slim and healthy body is increasing to date.[2] Although liposuction remains the most popular method for the reduction of subcutaneous fat, this approach may cause severe side effects such as pain, edema, and bruise. Here, we propose the use of poly(ethylene glycol) (PEG)-based micelles that can generate carbon dioxide gas as an adipocytolytic agent for the reduction of subcutaneous fat. PEG-based amphiphilic polymers containing the carbonate linkages were synthesized and used to form micelles. Structural changes in the PEG-based amphiphilic polymers significantly influenced the generation of carbon dioxide gas from the micelles. Nona-arginine peptide, a representative cell-penetrating peptide, was introduced to the surface of the micelles for effective intracellular delivery. This micelle system could have the potential as an adipocytolytic agent for reduction of localized fat deposit.

EXPERIMENTAL METHODS

Methoxypoly(ethylene glycol) (mPEG) (M_n = 5,000 g/mol) was reacted with 2-amino-2(hydroxymethyl)-1,3-propanediol through a CDI-mediated reaction. After 2 h, the solution was dialyzed against distilled water using dialysis membrane (molecular weight cut-off, 1000g/mol). mPEG-tri-arm-octyl chloroformate (mPEG-T-OC) was synthesized by acyl halide reaction using mPEG-T and octyl chloroformate. The final product was acquired by repeated precipitation with diethyl ether at 0 ℃. Synthesis of amphiphilic polymer was verified by Fourier transform-infrared (FT-IR) spectroscopy.

Nona-arginine (r9) peptide was conjugated to O-(2-aminoethyl)poly(ethylene glycol) (M_n = 5,000 g/mol) by EDC-NHS reaction. Then, r9-PEG was reacted with octyl chloroformate through acyl halide reaction.

Micelles were prepared from amphiphilic PEG-based polymer by the solvent evaporation method. Amphiphilic polymer was dissolved in dichloromethane, and the organic solvent was evaporated using a rotary evaporator. After of the formation of thin polymer film on the surface of vial, addition of distilled water induced micelle formation.

RESULTS AND DISCUSSION

The formation of amide bond through the CDI reaction was confirmed by FT-IR spectroscopy. The peaks for the amide bond of PEG-T were observed at 1650 cm^{-1}. The peaks corresponding to the carbonate linkage between PEG-T and OC were found at 1750 cm^{-1} and 1650 cm^{-1}. The modification of PEG with r9 peptide was confirmed at 1580-1650 cm^{-1}.

Carbon dioxide gas generation from the micelles was monitored by ultrasound imaging technique over time. PEG-based micelles dispersed in PBS were loaded in empty space of 5% agarose gel, and images were captured at the predetermined time. Generation of carbon dioxide was observed for 12 h after fabrication of micelles.

In vitro cytotoxicity of gas-generating micelles was evaluated by an MTS assay using differentiated 3T3-L1 adipocytes. The r9-PEG-OC micelles were more efficient for reduction of the number of adipocytes compared to PEG-OC micelles. In addition, r9-PEG-T-OC micelles reduced the viability of adipocytes more than r9-PEG-OC micelles, indicating the effectiveness of structural modification in PEG-based amphiphilic polymers.

CONCLUSION

In this study, PEG-based micelles generating carbon dioxide gas was synthesized and proved to be promising as an adipocytolytic agent. Furthermore, the amphiphilic polymer was designed to contain 3 carbonate linkages for the increase of gas generation. The generation of carbon dioxide was confirmed by ultrasound imaging, and reduction of adipocyte induced by adipocytolytic agent was verified by *in vitro* cytotoxicity test. Introduction of r9 peptide to micelles, as well as structural changes of the polymer with multiple carbonate linkage enhanced the ability of PEG-based micelles to reduce adipocytes. This approach to developing gas-generating nano-micelles may provide a new strategy for the reduction of local fat deposits.

REFERENCES

1. Despres, J. P. and I. Lemieux., Nature, vol. 444, no. 7121, pp. 881-87, 2006
2. Kennedy, J. *et al.*, J Eur Acad Dermatol Venereol, vol. 29, no. 9, pp. 1679-88, 2015

ACKNOWLEDGMENTS

This research was supported by a grant from the National Research Foundation of Korea (NRF) funded by the Ministry of Science and ICT (NRF-2020R1A2C1012199).

New sensitive sericin nanocarriers designed by living polymerization for cancer management

Ionut-Cristian Radu[1*], Catalin Zaharia[1], Madalina Necolau[1], Eugeniu Vasile[2], Andreea Vadureanu[1]

[1]Advanced Polymer Materials Group, University Politehnica of Bucharest, Bucharest, Romania
[2]University Politehnica of Bucharest, Bucharest, Romania

[*] radu.ionucristian@gmail.com

INTRODUCTION

Nanotechnology has been attending much attention since 1980s and has been adapted into many engineering fields. In particular, nanotechnology has led to the significant progress in a biomedical field such as controlled drug/gene delivery, tissue engineering, imaging of specific sites and probing of DNA structure. Among nanomaterials, nanoparticles have been contributing to the progress in this field. In particular, therapies using nanoparticles have widely been achieved for the treatments of cancer, diabetes, allergy, infection or inflammation. Nanoparticles have gained a high interest in therapeutic applications due to the fact that nanoparticles exist in the same size domain as proteins. Their large surface areas can also allow for displaying a large number of surface functional groups such as ligands. Furthermore, they have a rapid absorption and release behavior provided by high abilities of their diffusion and volume change. In addition, the particle sizes and surface characteristics of nanoparticles can be tailored or controlled [1, 2].

One of the main administration methods of the nanoparticles is injection into blood stream. When drugs- or genes-loaded nanoparticles are injected into bodies, they cross epithelial barriers and circulate in the blood vessels before reaching the target site. Escape of nanoparticles from the vascular circulation then occurs in either continuous or fenestrated tissues. At continuous vascular endothelium in healthy tissues, nanoparticles escape from the bloodstream via paracellular pathway, intracellular process or transmembrane transport. The drug accumulation into desired cells is a major problem researched in the literature by point of view of active targeting and amount quantifying [2, 3].

EXPERIMENTAL METHODS

In this study we propose the design of a new smart drug delivery carrier by assembling of modified silk sericin molecules. The silk sericin biofunctionalization involves silk sericin grafting modification with side synthetic chains of poly-(2-acrylamido-2-methylpropane sulfonic acid- co-N-isopropyl acrylamide) [Poly-(AMPSA-co-NIPAM)]. The protein engineering biofunctionalization proposes two pathways: un-controlled modification based on ammonium cerium nitrate grafting and a controlled live living polymerization based on atom transfer radical polymerization (ATRP). The two synthesis pathways generate complex macromolecular structures able to exhibits a sensitive thermal behavior and a sensitive ionic behavior. Therefore, the resulted protein-based nanocarriers respond to external stimuli such as temperature or pH due to the chemical tailoring. There are proposed various ratio between the two monomers in different synthesis conditions.

RESULTS AND DISCUSSION

The nanoparticles were obtained by direct nanoprecipitation in non-solvent at different parameters. The nanocarriers were morphologically characterized by SEM, DLS while drug release and encapsulation tests were carried out to show the release profiles. Furthermore, the nanocarriers are tested on a 3D microfluidic platform in order to simulate the flow and interaction within a blood vessel. The 3D microfluidic device contains microfluidic channels with dimensions up to 500 microns and a polymeric membrane.

CONCLUSION

In conclusion, we reported the development of new polymeric self-assembled nanocarriers with thermal and ionic sensitivity for cancer management. The drug delivery system is able to load and control the release of the specific drugs based on the propriate chemical features. The nanocarriers functional testing approach is a new concept which may be a powerful tool in the future for carries testing within cancer therapy and management.

REFERENCES

1. C. Dalwadi, G. Patel, Application of Nanohydrogels in Drug Delivery Systems: Recent Patents Review, Recent Patents on Nanotechnology, **9**, 17-25 (2015)
2. J. Zhang, H. Chen, L. Xu, Y. Gu, The targeted behavior of thermally responsive nanohydrogel evaluated by NIR system in mouse model, Journal of Controlled Release, **131**, 34-49 (2008)
3. S. K. Nitta, K. Numata, Biopolymer-Based Nanoparticles for Drug/Gene Delivery and Tissue Engineering, Int. J. Mol. Sci., **14**, 1629-1654 (2013).

ACKNOWLEDGMENTS

This work was supported by a grant of the Ministry of Research, Innovation and Digitization, CNCS/CCCDI – UEFISCDI, project number **PN-III-P1-1.1-PD-2021-0478.**

Wound dressing based on nanofibers from hyaluronic acid and hyaluronic acid derivative

Štěpán Vondrovic[1]*, Adéla Kotzianová[1], Petr Šulc[1], Dagmar Čožíková[1], Jaromír Kulhánek[1], Vojtěch Pavlík[1], Tomáš Prát[1], Hana Vágnerová[1], Vendula Jones[1], Ondřej Žídek[1], Vladimír Velebný[1]

[1]Contipro a.s., Dolní Dobrouč, Czechia
*stepan.vondrovic@contipro.com

INTRODUCTION

Using nanofibrous materials for wound healing is very promising yet still challenging. The dressing is usually a composite made of several layers, with a specific role to ensure proper moisture of the wound, breathability, low adhesiveness to the wound, and prevention of the infection. One of the benefits that nanofibers have is the ability to easily incorporate antimicrobial drugs, which provide an anti-infection effect. In this work, we focused on the preparation of the wound dressing with two biologically active substances – hyaluronic acid, which plays an important role in wound healing processes, and a hyaluronic acid derivative with an antimicrobial effect[1]. These two biologically active ingredients represent the active nanofibrous layer of the dressing, which readily dissolves after contact with wound fluids and forms a protecting gel.

EXPERIMENTAL METHODS

The presented wound dressing consists of a nanofibrous layer based on antimicrobial hyaluronan chloramide (HA-Cl), low molecular weight hyaluronic acid (LMW-HA) and polyethylenoxide. Nanofibers were prepared by electrospinning technology (4SPIN Lab, Contipro a.s.) and laminated to a wound contact layer and an absorbent layer. The complete wound dressing was sterilized with ethylene oxide (EtOX). The morphology of nanofibers was studied by SEM. Residual solvents and residues after EtOX sterilization were determined by GC-MS. The amount of LMW HA was determined by HPLC and the amount of HA-Cl by iodometric titration. The wound dressing was analyzed for the presence of bacterial endotoxins by the monocyte activation test (MAT). "*In vitro*" testing was used for the evaluation of the safety of this composition. The effect of the wound dressing extracts on the viability of 3T3 fibroblasts and migration of HaCaT keratinocytes was assessed as well as the potential for skin irritation where the model of the human epidermis was used. The potential for skin sensitization of wound dressing extract was assessed by the dendritic cell activation test. The safety of the nanofiber layer was evaluated "*in vivo*" using a mouse model of an excisional acute wound.

RESULTS AND DISCUSSION

We prepared nanofiber layer containing low molecular weight hyaluronic acid, hyaluronan chloramide and polyethylenoxide. The large format electrospun nanofibrous layers were laminated to the wound contact layer and the absorbent layer. The lamination did not affect the nanofibrous structure (fig. 1). The nanofiber structure and the content of the active ingredients did not change after sterilization and no EtOX residues and residual solvent were found. The uniform distribution of LMW HA and HA-Cl in nanofibrous mats was confirmed by HPLC and titration. The safety of the wound dressing was evaluated by in vitro tests without any negative results. Furthermore, the tested nanofiber layer was well-tolerated when applied to acute mouse excisional wounds (fig. 2).

CONCLUSION

A new wound dressing with the active nanofibrous layer and homogenous content of bioactive components was produced using the semi-production electrospinning device. The results obtained so far have demonstrated the safety of the bioactive layer and promising results for future development.

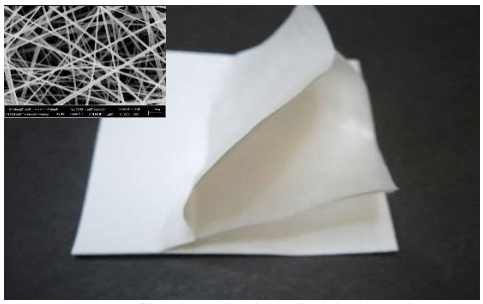

Fig. 1. The nanofiber layer laminated to the wound contact layer and the absobent layer

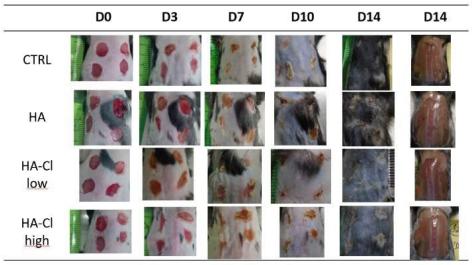

Fig. 2. The application of nanofiber layer with HA-Cl to acute mouse excisional wounds

REFERENCES

1. Buffa, R. *et al*., Carbohydr. Pol. 250:116928, 2020

Modular Colloidal Gels for Focalized Delivery of Immunomodulatory Therapeutics

Leandro Gonçalves[1*], Pedro Lavrador[1], Vítor M.Gaspar[1], João F.Mano[1]

[1] CICECO –Aveiro Institute of Materials, Department of Chemistry, University of Aveiro, 3810-193, Aveiro, Portugal
[*] leandrogoncalves@ua.pt

INTRODUCTION

Colloidal gels (CGs) represent unique biomedical platforms comprised of nanoparticle building blocks that self-assemble via inter-nanoparticle interactions into higher order 3D multifunctional systems.[1] In these modular platforms, because nanoparticles can operate as reservoirs for both hydrophobic and hydrophilic bioactive molecules, the high nanoparticle content of CGs can be leveraged for designing long-term bioactive depots intended for advanced tissue engineering strategies.[2]

Gathering on this, we design a fit-to-shape moldable and injectable CG system that self-assemble into macrosized 3D constructs (Fig. 1), presenting autonomous multi-particle shedding upon injection. The biomedical versatility of these bioinstructive platforms is demonstrated by loading CGs with anti-inflammatory Quercetin flavonoid to attenuate pro-inflammatory activated macrophages.

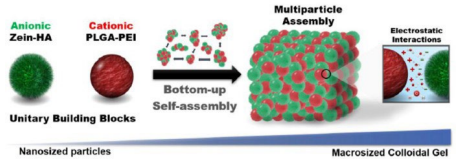

Fig. 1. Bottom-up assembly of nanostructured colloidal gels. Two complementary nanosized building blocks, (i) anionic Zein-HA nanogels and (ii) cationic PLGA-PEI nanoparticles, can self-assemble into macrosized 3D structures under aqueous conditions via interparticle electrostatic interactions. Nanoscale building blocks are combined into higher order multiparticle assemblies, ultimately producing macrosized colloidal gel platforms.

EXPERIMENTAL METHODS

Cohesive CGs were manufactured by centrifugation of colloidal suspensions of complementary nanoparticulated building blocks (anionic Zein-HA nanogels and cationic PLGA-PEI nanoparticles). The resulting colloidal gels were molded into different shapes in in-house produced circular molds. To produce bioactive CGs, Zein-HA nanogels were loaded with Quercetin and, for cellular assays, prostate cancer cells and LPS activated THP-1 derived macrophages were employed to evaluate the anti-inflammatory and anti-tumoral potential of the different platforms.

RESULTS AND DISCUSSION

An optimized nanoprecipitation protocol enabled the successful one-step formulation of surface-engineered cationic PLGA-PEI and anionic Zein-HA nanocarriers with low polydispersity index and oppositely charged zeta-potential. Such building blocks were combined and compacted under centrifugation, rapidly producing macroscopic nanostructured CG constructs with homogeneous distribution of nanoparticle species throughout the network, as showcased by confocal imaging upon loading of hydrophobic fluorophores (Figure 2). Rheological studies investigating viscosity as a function of shear rate demonstrated that CGs exhibit shear-thinning behavior and fit-to-shape properties. Moreover, this nanoparticulated supra-assembled platform showed efficient loading of bioactive molecules (i.e. flavonoids), while whilst maintaining their original physicochemical properties. Upon CGs direct contact with M1-Macrophages, a dampening of the pro-inflammatory response was observed.

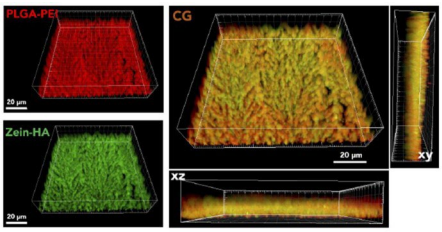

Fig. 2. Confocal laser scanning microscopy of a colloidal gel with fluorescently-labelled unitary building blocks, DiD-loaded PLGA-PEI nanoparticles (red channel), and DiO-loaded Zein-HA nanogels (green channel), respectively. Orthogonal projections in merged channel showcase near complete overlap (yellow-coloured), evidencing homogeneous distribution of both nanoparticle species throughout the colloidal gel network.

CONCLUSION

In conclusion, we developed a highly modular and nanostructured CG supra-assembled 3D platform with enhanced physicochemical and mechanical features for focal therapeutics and particles delivery. Overall, this enhanced supra-assemblies demonstrate valuable properties for operating as delivery systems for localized bioinstruction of endogenous microenvironments.

REFERENCES

1. Diba, M et al., Adv. Mater. 2017, 29, 1604672.
2. Freitas, B., *et al.*, Appl. Mater. Interfaces 2020, 12, 31282.

ACKNOWLEDGMENTS

This work was developed in the scope of project CICECO-Aveiro Institute of Materials (UID/CTM/50011/2019). FCT is acknowledged for funding individual fellowships (SFRH/BD/141834/2018, PL) and (CEECIND/01410/2018, VMG).

Electrospun Silica Nanofibres as Multifunctional Substrate for Regenerative Medicine and Drug Delivery

Miroslava Rysová[1*], Hana Tománková[1], Markéta Schaabová[1], Šárka Hauzerová[1,2], Pavel Kejzlar[1], Alena Ševců[1,2]

[1]Institute for Nanomaterials, Technical University of Liberec, Liberec, Czech Republic
[2]Department of Chemistry, Technical University of Liberec, Liberec, Czech Republic
[*]miroslava.rysova@tul.cz

INTRODUCTION

Over the last decades, electrospun nanofibres were proven to be interesting material applicable in regenerative medicine and drug delivery, possessing number of unique properties including high specific surface area, high porosity and small pore size. Properties such as chemical and mechanical stability, biocompatibility and degradation kinetics then depend on chemical composition, crosslinking or possibly functionalization. While polymer nanofibres may exhibit serious disadvantages including swelling in moist environment and during degradation or low surface functionality or limited bioactivity, inorganic nanofibres represent a family of nanofibres unlimited by these factors and potent for medical applications[1]. Silica nanofibres, being member of this family, combine traditional properties of nanofibres based on their structure and advantages of inorganic bioactive material. Their mass and/or surface can be modified by various methods[2,3]. The aim of this paper is to outline overview of properties and performance of silica nanofibres as biocompatible, biodegradable, and easy to modify high performance material for regenerative medicine and drug delivery.

EXPERIMENTAL METHODS

Silica nanofibres were prepared by sol-gel method and needle-less electrospinning, which led to formation of nanofibrous matrix of 5 – 30 g/m^2 and mean fiber diameter 180 – 850 nm depending on the applied spinning conditions. Biocompatibility was tested *in vitro* on several model cell lines including 3T3-A31 fibroblasts, Hacat keratinocytes, Vero cells, Caco-2 cells and HepG2 hepatocyte-like cells, and human blood erythrocytes in compliance to ISO 10993. Biodegradation of silica nanofibres was evaluated *in vitro* under simulated conditions (37 °C, SBF). Silica release into the SBF was measured using ICP-MS. Impact of degradation on the surface morphology was evaluated by electron microscopy (SEM). Surface availability for chemical functionalization and its impact on relevant properties, such as fibrous morphology, was tested. Surface functionalization, applicable in surface charge modification and further drugs conjugations, was performed by silanization process using selected organosilanes. The grafted functional groups were quantified and visualized via specific staining. Impact on interactions with biological systems was evaluated *in vitro*.

RESULTS AND DISCUSSION

Silica nanofibres were confirmed to possess multitissue biocompatibility *in vitro*. Fast degradation under simulated conditions *in vitro* was observed with surface erosion appearing after 24 hours in simulated body fluid (SBF) with limited swelling and sustained integrity of the nanofibrous matrix. Silica released upon degradation in form of orthosilicic acid, was confirmed to have a concentration-dependent beneficial impact on cellular viability and proliferation, which is known effect provided silica nanomaterials in general. Successful grafting of functional groups by silanization of surface silanols was confirmed without relevant impact on the fibre morphology or integrity. Positive impacts of the silanization process on biocompatibility, surface charge and drug conjugation capacity were verified.

CONCLUSION

The electrospun silica nanofibres represent interesting novel biocompatible and bioactive nanomaterial with capacity to promote tissues regeneration through its degradation products. Moreover, the unique degradation mechanism reminiscent of Stöber silica degradation mechanism was revealed. The high specific surface available for surface functionalization can be applied in drug and bioactive molecules delivery for specific wound healing and tissue regeneration stimulation.

REFERENCES

1. Makova V. *et al.* Polymers 12(1):2006, 2020
2. Steinerova M. *et al.* Mat. Sci. Eng. C 121:111792, 2021
3. Danilova I *et al.* Fib. and Tex. 21(2):3-11, 2014

ACKNOWLEDGMENTS

The authors would like to thank to the Project of Ministry of Education, Youth and Sports of the Czech Republic and the European Union - European Structural and Investment Funds in the frames of Operational Programme Research, Development and Education - project Hybrid Materials for Hierarchical Structures (HyHi, Reg. No. CZ.02.1.01/0.0/0.0/16_019/0000843) for the financial support provided for this research.

DNA Modified MSN Films as Versatile Biointerfaces to Study Stem Cell Adhesion Processes

X. Zhang, S. van Rijt
Department of Instructive Biomaterials Engineering, MERLN Institute for Technology-Inspired Regenerative Medicine, Maastricht University, P.O. Box 616, 6200 MD Maastricht, the Netherlands
xingzhen.zhang@maastrichtuniversity.nl

INTRODUCTION

Stem cells, with an inherent ability to self-renew and the potential to differentiate into specialized cells, have great potential in the regenerative medicine field. However, an ongoing challenge in their clinical translation is control over their behavior once transplanted. In their natural environment, stem cell fate is regulated by their interaction with extracellular matrix (ECM), mainly through integrin-mediated cell adhesion. Integrin-mediated adhesion not only provide stem cells anchoring points but also directs their fate such as stem cell differentiation and self-renewal. As such, integrin-mediated stem cell adhesion processes are an important field of study to understand, predict and control stem cell behaviors. 2D biointerfaces that selectively present ECM ligands can be used as valuable tools to study and improve our understanding on stem cells adhesion processes. Mesoporous silica nanoparticles (MSNs) have promising characteristics to develop 2D biointerfaces, which include high surface area, mesoporous structure and high control over their size and shape. In this project, we aim to develop a new type of biointerface based on DNA functionalized mesoporous silica nanoparticles (MSN-DNA) to study stem cell adhesion.

EXPERIMENTAL METHODS

MSN-ssDNA synthesis and characterization: MSN-NH2 were synthesized based on a sol-gel co-condensation process [1]. To create the DNA modified MSN, MSN-NH2 were modified with a Mal-PEGn-NHS linker (n=6, 8 or 12) to form MSN-L. Then, a thiol functionalized ssDNA was grafted onto the PEG linker modified MSN (MSN-L) by thiol-maleimide reaction. DNA functionalized MSN (MSN-ssDNA) with varying PEG linker length were developed in the study and designated as MSN-L_6-ssDNA, MSN-L_8-ssDNA, MSN-L_{12}-ssDNA. MSN and MSN-ssDNA were characterized with Transmission electron microscopes (TEM).

MSN-dsDNA-RGD film preparation: To create the films, concentrated MSN-ssDNA nanoparticle suspension was spun over a plasma-treated coverslip. MSN-ssDNA films were characterized with Scanning electron microscope (SEM) and Water contact angle (WCA). Then, cell adhesion tripeptide RGD was conjugated to a complementary DNA strand, which could specifically bind to MSN-ssDNA to create MSN-dsDNA-RGD films. Finally, the morphology of human mesenchymal stromal cells (hMSC) on fabricated MSN films was analyzed by DAPI and phalloidin staining.

RESULTS AND DISCUSSION

TEM images show that MSN-NH2, MSN-L_6 and MSN-L_6-ssDNA have a spherical shape and a porous structure. DNA surface modification resulted in a less visible porous structure. SEM showed that DNA modified MSN could be homogenously spin coated to form a continuous layer of nanoparticles over the glass substrate. The WCA measured on nanoparticles coated glass was lower than that measured on plasma treated glass, which indicated an increase in surface hydrophilicity due to hydrophilic PEG linker and DNA modification. Fluorescent microscopy images showed that MSN-dsDNA-RGD films could promote hMSCs adhesion and spreading, whereas MSN-dsDNA films without RGD resulted in poor cell spreading with round morphology, and low cell adhesion (Fig.1). In addition, we showed that cell adhesion to the films is PEG length-dependent.

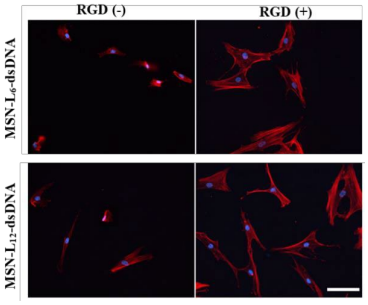

Fig.1 Representative fluorescence micrographs of hMSC cultured on MSN-L-dsDNA films with and without RGD for 1 day. Scale bar represents 100 µm.

CONCLUSION

In conclusion, DNA can be successfully surface grafted to MSN using various PEG linkers. MSN modified with PEG and ssDNA can be spin coated to create homogenous, stable and biocompatible films, which can be used as a novel and versatile 2D biointerface to study ligand-induced stem cell adhesion processes.

REFERENCES

[1] Journal of the American Chemical Society 2009, 131, 11361.

Black Phosphorus-based 2D material with selective effects on Healthy and Cancer cell behavior

Ines Fasolino[1*], Alessandra Soriente[1], Maria Caporali[2], Manuel Serrano-Ruiz[2], Maurizio Peruzzini[2], Luigi Ambrosio[1], Maria Grazia Raucci[1]

[1]Institute of Polymers, Composites and Biomaterials – National Research Council (IPCB-CNR) Mostra d'Oltremare pad.20 - Viale J.F. Kennedy 54, 80125 Naples, Italy.
[2]Institute of Chemistry of Organometallic Compounds – National Research Council (ICCOM-CNR), via Madonna del Piano 10, 50019 Sesto Fiorentino, Italy.

*e-mail: ines.fasolino@cnr.it

INTRODUCTION

In recent years, numerous studies support the use of Photodynamic Therapy (PDT) as minimally invasive curative approach with a selective cytotoxic activity toward cancer cells.[1] In this context, a relatively new member of the bi-dimensional family, exfoliated black phosphorus (2D BP) has been largely applied thanks also to the great advantage of being in vitro and in vivo biocompatible and biodegradable[2], with a lower cytotoxicity, high mechanical properties, optical properties and topological features than other 2D materials. Moreover, 2D BP has shown a good effectiveness as photodynamic therapy agent for cancer treatment because of its capability to produce singlet oxygen and its ability to act as photosensitizer.[3] Hence, we have studied the biological properties of 2D BP comparing biological response of healthy and cancer cells derived from bone and prostate tissues on 2D and 3D cell culture models.

EXPERIMENTAL METHODS

2D BP was obtained through liquid exfoliation. 2D BP effect on healthy (bone=HOb; prostate=PNT-2 cell lines) and cancer (bone=SAOS-2; prostate=PC-3 and LNCAP cell lines) cell behaviors was evaluated w/o near-infrared light (NIR)-irradiation by investigating cell viability, oxidative stress (nitrites, ROS, GPX-3, Iron levels, p53 expression) and inflammatory marker expression (COX-2, pro and antinflammatory interleukins) from quantitative and qualitative points of view on *in vitro* 2D cell culture model. Furthermore, 2D BP effect in terms of cell proliferation, morphology and antiproliferative marker expression was also evaluated on 3D in vitro model obtained by culturing 3 different cancer cell lines (PC-3, LNCaP and SAOS-2) on Matrigel® matrix. Statistical analyses were undertaken using GraphPad Prism®, version 6.00. Data were compared using a Student's t-test, a one-way ANOVA, with a Bonferroni post-test.

RESULTS AND DISCUSSION

The main goal in cancer therapy is to protect healthy tissue surrounding tumor microenviroment.

Our results showed 2D BP (5-75 µg/mL) inhibited bone and prostate cancer cell proliferation, meanwhile promoted healthy cell survival in vitro by modulating oxidative stress and immune response with and without NIR-irradiation. These results were confirmed by analyses on cell morphological features that showed a good density and spreading in the case of healthy cells (HOb and PNT-2) after the interaction with 2D BP. Conversely, after the same exposure to 2D BP, cancer cells (SAOS-2 and PC-3) showed a collapsed cell shape thus indicating cell-suffering condition. 2D BP solution (5-75 µg/mL) injected in 3D in vitro tumor decreased cell proliferation of PC-3, LNCaP and SAOS-2 cells grown on Matrigel after 72 hours of 2D BP treatment. In addition, 72 hours of exposure to 2D BP induced P53 (oncosoppressor) expression in PC-3, LNCaP and SAOS-2 cells.

CONCLUSION

Our investigations suggested that 2D BP exerts a selective antiproliferative effect on cancer cells. Indeed, 2D BP was capable to inhibit in vitro bone and prostate cancer cell survival. Simultaneously, 2D BP protects healthy bone and prostate cells through the control of oxidative stress and immune response. All these results open the door to the development of 2D BP based anticancer therapies to apply in different tumors.

REFERENCES

1. Fasolino I. *et al*., Sci. Rep. 11:5856, 2021. Doi: 10.1038/s41598-021-85310-6.
2. Latiff N. M. *et al*., Eur. J., 21:13991-13995, 2015;
3. Raucci M. G. *et al*., Appl. Mater. Interfaces. 11:9333-9342, 2019.

ACKNOWLEDGMENTS

This study has been supported by Ministry for Education, University and Research (MIUR) through funds provided by PRIN2017 - ACTION (N. 2017SZ5WZB). The authors also thank Mariarosaria Bonetti for lab technical support & data elaboration and Dr. Roberta Marzella for support to project management.

Fabrication of PLGA nanoparticles by droplet microfluidics for the sustained release in tumour microenvironment

Xue Bai[1], Sam Butterworth[1], Annalisa Tirella[1,2]

[1]Division of Pharmacy and Optometry, School of Health Science, FBMH, University of Manchester, Oxford Road, Manchester M13 9PT, United Kingdom
[2]BIOtech Research Center, Department of Industrial Engineering, University of Trento, Via delle Regole 101, 38123 Trento, Italy
xue.bai-5@postgrad.manchester.ac.uk

INTRODUCTION

Poly-(D, L-lactide-co-glycolide) (PLGA) is a biocompatible, non-toxic FDA-approved polymer used in many biomedical applications, such as implants or nanoparticles (NPs) [1]. Microfluidics is an alternative method for the fabrication of polymeric NPs, having the advantages of an easy, robust and reproducible fabrication thanks to the control of processing parameters, allowing the fabrication of particles uniform in size and shape [2,3]. This study uses a systematic approach for the fabrication of PLGA NPs using microfluidics, investigating the effect of process parameters on size, size distribution and surface charge of products. Target values for PLGA NPs for the sustained release of chemotherapeutics in the tumour microenvironment [4,5] were identified as: size range 100-150 nm, PDI < 0.2, Surface charge (ζ-potential) of -15 mV.

EXPERIMENTAL METHODS

The automated microfluidic system (Dolomite, Royston UK) equipped with a 5-input chip was used in the study. Process parameters used in the study are: flow rate ratio (FRR, dispersed phase/continuous phase ratio at the mixing point), total flow rate (TFR), and composition of the dispersed phase. 1% (w/v) polyvinyl alcohol (PVA) in water was selected as continuous phase, whereas PLGA in acetonitrile was used as dispersed phase. The following parameters were selected to study their effect on particle size and shape: FRR (i.e. 1/39, 1/19, 1/9, 1/4, 1/1.5), TFR (i.e. 40 µL/min, 100 µL/min, 200 µL/min, 400 µL/min, 800 µL/min), and PLGA concentration (i.e. 2.5 mg/mL, 5 mg/mL). All preparations were performed at 25 °C. Size, poly dispersity index (PDI) and ζ-potential were measured using dynamic light scattering. Reported data represents the mean of three independent experiments.

RESULTS AND DISCUSSION

The size of PLGA NPs increases with FRR, while TFR and PLGA concentration are kept constant. This is because higher flow rate of the dispersed phase could decrease the compactness of nanoparticles [6]. The smaller NPs are obtained with FRR=1/39 and PLGA concentration of 2.5 mg/mL, with average Z-size 17±2 nm and PDI 0.391±0.057. At higher FRR (i.e. 1/1.5), and TFR (200 µL/min), the size of NPs is 10-times higher: 188±7 nm, PDI 0.145±0.021. We found also that PLGA concentration influences the size of obtained NPs: at higher PLGA concentration (5 mg/mL) corresponds the higher particle size (Z-size 212±3 nm, PDI 0.112±0.025, FRR 1/1.5, TFR 200 µL/min). This is because the higher quantity of PLGA monomers lead to slower solvent diffusion and therefore larger particles [6].

ζ-potential of all PLGA NPs is negative, with ζ-potential ranging from -5 mV to -25 mV due to the presence of uncapped end carboxyl groups of the polymer present on NPs' surface. With higher FRR (i.e. more PLGA, less PVA) more negative values of ζ-potential are measured.

Of note, with constant FRR and PLGA concentration, while varying TFR values, not significant difference in size and PDI are observed. Similarly, ζ-potential values don't vary by changing TFR.

CONCLUSION

In this study, we investigated the effect of process parameters on the physicochemical properties of PLGA NPs. A robust method for the fabrication of PLGA nanoparticles was established, with identification of fabrication parameters to obtain nanoparticles with target size of 100-150 nm (PDI < 0.2), and ζ-potential around -15 mV. The next step will be the fabrication of NPs with PLGA-drug conjugate (FK866, anti-cancer drug) for sustained release in the tumour microenvironment.

REFERENCES

[1] S. Alkahtani, S. Alarifi, G. Albasher, M. Al-Zharani, N. H. Aljarba, M. H. Almarzoug, N. M. Alhoshani, N. S. AL-Johani, H. Alothaid, A. A. Alkahtane, *Oxid. Med. Cell. Longev.* **2021**, *2021*, 5834418.
[2] J. P. Martins, G. Torrieri, H. A. Santos, *Expert Opin. Drug Deliv.* **2018**, *15*, 469.
[3] S. Garg, G. Heuck, S. Ip, E. Ramsay, *J. Drug Target.* **2016**, *24*, 821.
[4] M. Gaumet, A. Vargas, R. Gurny, F. Delie, *Eur. J. Pharm. Biopharm.* **2008**, *69*, 1.
[5] J. D. Clogston, A. K. Patri, in *Charact. Nanoparticles Intend. Drug Deliv.* (Ed.: S.E. McNeil), Humana Press, Totowa, NJ, **2011**, pp. 63–70.
[6] L.-H. Hung, S.-Y. Teh, J. Jester, A. P. Lee, *Lab. Chip* **2010**, *10*, 1820.

ACKNOWLEDGMENTS

I wish to acknowledge Dr. Leonidas Gkionis for technical support of the project.

Investigations on the Influence of the PEG Chain Length on the Properties of Magnetic Nanoporous Silica Nanoparticles

Timo Herrmann[1*], Janin Reifenrath[2], Jessica Meißner[3], Peter Behrens[1,4]

[1]Institute for Inorganic Chemistry, Leibniz University Hannover, Hannover, Germany
[2]Clinic for Orthopedic Surgery, Hannover Medical School, Germany
[3]Institute for Pharmacology, Toxicology and Pharmacy, University of Veterinary Medicine Hannover, Foundation, Germany
[4]Cluster of Excellence Hearing4all, Hannover, Germany
[*] timo.herrmann@acb.uni-hannover.de

INTRODUCTION

The number of implant-associated infection, which can occur at many different implantation sites rises, as the number of implantations is rising. To avoid the disadvantages of a conventional treatment, a selective treatment of implant-associated infections by a special drug targeting system is developed.[1,2] In this system a combination of a magnetizable implant, drug-loaded magnetic nanoporous silica nanoparticles (MNPSNPs) and an external magnetic field are used. An external magnetic field is applied at the site of the infected implant, which is additionally enhanced by the implant itself. After injection, drug-loaded superparamagnetic NPSNPs travel to the implant site and should accumulate there due to the strong magnetic field; finally, they release the loaded drug. With this method of implant-directed magnetic drug targeting, the drug dosage required for an effective treatment can be significantly reduced, compared to other drug delivery methods or a systemic treatment.[1,2]
To reduce the immunogenic reaction of the MNPSNPs, the particles can be PEGylated. A PEG (polyethyleneglycol) functionalization is known to evoke a so-called stealth effect, where the interaction between the nanoparticles and the phagocytic cells is weakened. To achieve this stealth effect, the chain length of the PEG moiety is essential. In general, it is observed, that a longer PEG results in a better stealth-effect.[3,4]

EXPERIMENTAL METHODS

The preparation of the magnetic nanoporous silica nanoparticles was performed in two steps. First the superparamagnetic iron oxide core was synthesized by co-precipitation from iron(II)- and iron(III)-chloride solutions in the presents of oleic acid. Next, the silica shell was condensed around the core using a sol-gel approach. After calcination a nanoporous magnetic material was obtained. PEG chains with different chain lengths were equipped with triethoxysilyl groups. The covalent attachment of the so-modified mPEG chains to the silica surface was performed by reacting triethoxysilyl-modified PEG with the silanol groups on the surface of the magnetic silica nanoparticles.

RESULTS AND DISCUSSION

The synthesised MNPSNP showed a diameter of 108 nm ± 10 nm as determined by TEM images. Furthermore, the unfunctionalized particles show a high BET surface, pore diameter and pore volume. After the functionalization, the typical absorption bands in the IR spectra can be observed, indicating a successful functionalization. This was further verified by physisorption measurements. Here, the BET surface area decreased when the chain length of the PEG moiety increased. An exception is the functionalization with the longest mPEG chain, where the BET surface area increased again. This behaviour can be explained by thermogravimetric measurements. These show a lower total amount of the longest PEG chain on the surface of the MNPSNPs, so that fewer adsorption sites are blocked, resulting in a higher BET surface area. That for the longest mPEG the attached amount is lower is presumably be due to entropic hindrance of the long monofunctionalized polymer chain.

CONCLUSION

In this work magnetic nanoporous silica nanoparticles were successfully synthesized and functionalized with PEG moieties of different chain length. The influence of the chain length largely follows the expectation. An exception is the functionalization with the longest PEG chain. Further research shall focus on the drug delivery behavior and the test of the stealth properties.

REFERENCES

1. H. C. Janßen *et. al*, J. Nanobiotechnology 18:14, 2020.
2. H. C. Janßen *et. al*, J. Nanobiotechnology 16:96, 2018.
3. M. D. Howard *et. al*, J. Biomed. Nanotechnol. 4:133, 2008.
4. A. S. Karakoti *et. al*, Angew. Chem. Int. Ed. 50:1980, 2011.

ACKNOWLEDGMENTS

This work was funded by the DFG (Project number 280642759) in a joined project with the Hannover Medical school and the University of Veterinary Medicine Hannover. The authors would like to thank the LNQE (Laboratory of Nano and Quantum Engineering) for using their TEM equipment.

Synthesis and morphological & structural characterization of metal oxides and their behavior in biological medium

Zsejke-Réka Tóth[1,*], Lenuța Nastasia Răzvanță[2], Alexandra Feraru[1,3], Emilia Licarete[1], Lucian Baia[1,4], Klára Magyari[1,5]

[1]Nanostructured Materials and Bio-Nano-Interfaces Center, Interdisciplinary Research Institute on Bio-Nano-Sciences, Babeș-Bolyai University, Cluj-Napoca, Romania
[2]Faculty of Chemistry and Chemical Engineering, Babeș-Bolyai University, Cluj-Napoca, Romania
[3]Doctoral School of Physics, Faculty of Physics, Babeș-Bolyai University, Cluj-Napoca, Romania
[4]Faculty of Physics, Babeș-Bolyai University, Cluj-Napoca, Romania
[5]Department of Applied and Environmental Chemistry, Faculty of Science and Informatics, University of Szeged, Szeged, Hungary
*zsejke.toth@ubbcluj.ro

INTRODUCTION

Cerium oxide nanoparticles are one of the most studied metal oxides, which have unique properties (could change their oxidative state in different environmental medium). The reason of these unique properties is that cerium is the most presented rare-earth element on the Earth[1]. Cerium (IV) oxide (CeO_2) is applied in different field of science, such as in biological process, electrochemistry, and in environmental application. Cerium (IV) oxide could be synthesized in several synthesis method[2]: hydrothermal crystallization, precipitation method, and green synthesis method. The synthesis temperature influences the material crystallinity and the shape of the sample[3]. Sodium hydroxide (NaOH) could also have an effect on the morphology of the samples. Thereby, the main aim of this work was to synthesize CeO_2 by using different concentrations of NaOH. Further, our interest was focused on both analyzing the behavior of the obtained CeO_2 in biological medium and investigating the character of the materials cell viability.

EXPERIMENTAL METHODS

Cerium (IV) oxide nanomaterials were synthesized by hydrothermal synthesis method[3]. As a cerium source, cerium (III) nitrate hexahydrate was used and the effect of the different concentrations of the sodium hydroxide (C_{NaOH}= 2 M, 4 M, 6 M and 8 M) was investigated on the crystal structure of the CeO_2. No calcination step was used after the heat-treatment. Bioactivity of the samples was analyzed by soaking of the samples into simulated body fluid (SBF) for 1 and 3 days. The morphological and structural properties of the obtained nanomaterials were analyzed by UV-Vis spectrophotometer (JASCO-V650), transmission electron microscope (Hitachi S-4700 microscope) and X-ray diffractometer (Shimadzu XRD 6000). The cell viability of the samples was analyzed on Human keratinocytes cells (HaCaT, Cell Line Service, Germany).

RESULTS AND DISCUSSION

The cubic crystallographic structure[1] was confirmed by XRD measurements. The hydrothermal crystallization of CeO_2 nanocrystals resulted in partially amorphous crystals, without calcination step.

The influence of the concentration of the sodium hydroxide was also confirmed by XRD, thus the crystallographic plane ratio of 111/220 decreased with the increased of the concentration of the NaOH. Thereby, we can assume that the NaOH is responsible for the appearance of 220 crystallographic planes. After soaking into SBF the structural and morphological parameters of the samples have a slightly difference, thereby bioactivity could be also assumed, which could also affect the cell viability of the samples.

Figure: Graphical abstract of the study

CONCLUSION

Nanostructured CeO_2 materials were partially amorphous, their crystalline structure being modified by using different amounts of NaOH. The samples crystallinity was also influenced by soaking the samples into SBF for 1 and 3 days.

REFERENCES

1. Shan Y. *et al.*, Sep. Purif. Technol, 250:117181, 2020.
2. Rajeshkumar S. *et al.*, Biotechnol. Rep., 17:1-5, 2018.
3. Mai H.-X. *et al.*, J. Phys. Chem. B 109: 24380-24385, 2005.

ACKNOWLEDGMENTS

The authors would like to thank the Ministry of Research and Innovation, CNCS – UEFISCDI (project number: PN-III-P1-1.1-TE-2019-1138, within PNCDI III). K. Magyari acknowledges the financial support of János Bolyai Research Scholarship of the Hungarian Academy of Sciences BO/00066/19/7.

Intranasal delivery of mixed Nano-Micelles for Enhanced Glioblastoma Targeting Gene Therapy

Youngki Lee, Junkyu Ha, Minkyung Kim, Minhyung Lee

Department of Bioengineering, College of Engineering, Hanyang University, Seoul 04763, Korea
E-mail address: leeyg1992@gmail.com

INTRODUCTION

Glioblastoma is the leading cause of the death worldwide with growing importance in graying society. Blood brain barrier (BBB) limit entrance of the molecules which is challenging for development of drug. Transferrin receptor (TfR) overexpressed both in glioblastoma and BBB is a strong candidate for targeting therapy[1]. In this research, transferrin receptor peptide was modified with cholesterol (T7c). Unlike naïve transferrin receptor peptide (T7), hydrophobic moiety provides micelle structure above certain concentration. In addition, anti-miR-21 widely known for its therapeutic effect against various cancer[2] was also modified with cholesterol (AMO21c). Taken together, AMO21c/T7c co-micelle was prepared and administrated intranasally[3] to orthotopic rat glioblastoma model as studied previously4. Tumor size was evalulated with Nissl staining and high reduction was observed compared to AMO21c/T7 and lipofectamine groups. MTT assay elucidate that AMO21c/T7c co-micelle due to its biocompatibility, showed only minimum cytotoxicity compared to AMO21c/lipofectamine. In conclusion, intranasal delivery of co-micelle AMO21c/T7c induce therapeutic effect against glioblastoma.

EXPERIMENTAL METHODS

1. MTT assay

C6 cells were seeded on 96 well plate in a density of 5 x 10^3 per well in 10% FBS containing DMEM. After 24hr, medium was replaced to fresh DMEM and prepared materials with scrambled sequence AMO21 (scrAMO21c) at different doses were treated. Medium was replaced again after 4hr and incubated for another 20 hr. Then, 10 ul of 3-[4,5-dimethylthiazol-2-yl]-2,5-diphenyltetrazoliumbormide was treated to each wells and incubated for 4 hr. Medium was removed and 100 ul of DMSO was treated to dissolve formazan crystals. The absorbance at 570 nm was measured using a microplate reader. Cell viability (%) was calculated according to the following equation: Cell viability (%) = $(OD_{570(sample)})$/average of $OD_{570(control)}$) ×100. Statistical analysis was performed by parametric ANOVA followed by a Newman-Keuls test.

2. Nissl staining

Paraffin embedded brain tissues were cut into 5 um thick sections and stained with 0.1% cresyl violet. Then, sections were destained with 70 % ethanol, 10% acetic acid and dehydrated with 100% ethanol and xylene. Images were obtained and measured tumor size using Image J software. Statistical analysis was performed by non-parametric Mann-Whitney U test to compare diffrences between groups.

RESULTS AND DISCUSSION

As shown in Figure 1, both naked scrAMO21c and AMO21c/T7c co-micelle showed cell viability above 80% whereas lipofectamine was decreased under 60%. This elucidate biocompatible non-toxic characteristic of scrAMO21c/T7c which might prevent damage to normal brain tissue.

To evaluate *in vivo* anti-cancer effect, rat orthotopic glioblastoma model was prepared. In Figure 2, AMO21c reduced tumor size compared to control, however only AMO21c/T7c showed statistically significant effect.

In conclusion, AMO21c/T7c might be and drug for glioblastoma.

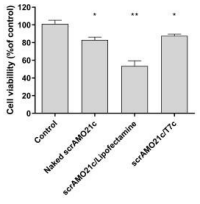

Fig1. MTT assay

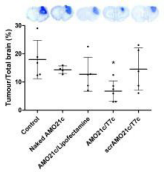

Fig2. Nissl staining

CONCLUSION

This research showed preparation of therapeutic co-micelle against glioblastoma through simple modification with cholesterol. Peptides and oligonucleotide along with cholesterol modification showed only minimum toxicity, whereas conventional cationic carrier induce high cytotoxicity. Moreover, adequate physical characteristics allowed administration through intranasal route which resulted in reduction of tumor size. In conclusion, AMO21c/T7c might be effective therapy for glioblastoma.

REFERENCES

1. Li, s. et al., Mol. Pharm., 18 (3), 1480-1485, 2021
2. Aloizou, A.-M. et al., Toxicol. Rep.7:1514-1530, 2020
3. Erdő, F. et al., Brain Res. Bull 143:155-170, 2018
4. Ha, J. et al., Nanoscale. 13: 14745-14759, 2021

ACKNOWLEDGMENTS

This work was supported by the Individual Basic Science & Engineering Research Program (NRF-2019R1A2C1089560) through the National Research Foundation funded by the Ministry of Science and ICT in Korea.

Green Synthesis of AgNP using Snail Slime

Maria Francesca Di Filippo[1*], Valentina Di Matteo[1], Silvia Panzavolta[1]

[1]Department of Chemistry, University of Bologna, Bologna, Italy
[*] maria.difilippo5@unibo.it

INTRODUCTION

In recent years, research has been increasingly interested in the development of nanomaterials with tailored properties for applications in the biomedical and pharmaceutical fields, for drug delivery and biosensing. In particular, innovative therapies in the field of wound healing started using nanomaterials, as they are able to provide antibacterial and anti-inflammatory activity, and to regulate the production of extracellular matrix, promoting cell proliferation and differentiation. Silver nanoparticles (AgNPs) have been found to have exceptional antimicrobial, antibacterial, antifungal and antiviral properties[1] compared to silver ions solutions. However, the reduction or co-precipitation processes used in the synthesis of nanoparticles use hard conditions and organic solvents, with the production of toxic by-products. Therefore, recent studies have focused on the research of biocompatible procedures and methods, which support the use of natural extracts for the rapid and green synthesis of nanoparticles. Snail slime is a natural extract that contains a complex mixture of substances as glycoproteins, collagen, allantoin and glycolic acid and its use has already demonstrated to be effective in the synthesis of gold nanoparticles.[2] In the present work, snail slime has been used in the synthesis of AgNPs: the main compounds contained in the slime act as reducing and stabilizing agents, allowing the synthesis of AgNPs through the reduction of Ag(I), from a solution of $AgNO_3$, to Ag(0). AgNPs are hence synthesized using a single step reaction, avoiding the use of additional and toxic agents, and employing aqueous solutions.

EXPERIMENTAL METHODS

The snail slime used in this project was supplied by 'lumacamadonita' (Palermo, Italy) and extracted from *Helix Aspersa* snails by means of a cruelty-free machine that allows to obtain the product with a pH between 5 and 7. Prior to use, the slime was subjected to dialysis by means of a membrane with a cut-off of 12-14 kDa.
The synthesis of AgNPs was carried out at room temperature and kept under stirring for 48 hours, when a change in color occurred. Reference samples were prepared using gelatin and glucose as stabilizing and reducing agents, as described in the literature.[3]
All the obtained nanoparticles were fully characterized and stored in the dark at room temperature.

RESULTS AND DISCUSSION

Besides the well-known cosmetic use of snail slime from *Helix Aspersa* snails due to its rejuvenating and emollient properties, in this work it was employed as reducing agent and stabilizing agent for silver nanoparticles formation. Its use allowed the production of AgNPs trough a green and sustainable synthesis.

UV-Vis analyses showed the typical absorption band centered at about 420 nm and related to AgNPs, confirming their actual formation in presence of snail slime.

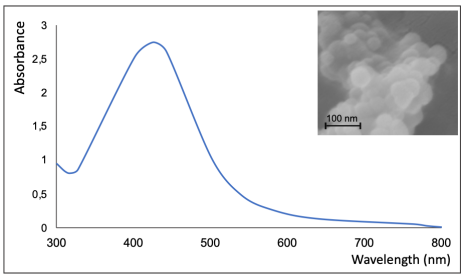

Figure 1. UV-Vis spectrum and SEM image of AgNPs (bar= 100nm).

The obtained AgNPs are spherical and stable up to three weeks: they tend to form agglomerates as a function of time and concentration of Ag.
Dynamic Light Scattering (DLS) measurements revealed average nanoparticle diameters between 30 and 50 nm, further confirmed by Electron Transmission Microscopy (TEM). Moreover, antibacterial tests revealed the effectiveness of the synthesized AgNPs to inhibit the bacterial growth both on Gram+ and Gram- bacterial strains, which comparable to the values of the reference samples. Cell biocompatibility and cytotoxicity studies are ongoing.

CONCLUSION

The snail slime from *Helix Aspersa* snails has been used for the synthesis of AgNPs through a green approach and a complete characterization of the obtained AgNPs was performed. Their antibacterial activity was effective against both Gram+ and Gram- bacterial strains. Biocompatibility cell studies are ongoing.

REFERENCES

(1) Khan SU, et al., Nanosilver: New Ageless and Versatile Biomedical Therapeutic Scaffold. *Int. J. Nanomedicine* **2018**, *13*, 733–762.
(2) Gubitosa J, et al., Biomolecules from Snail Mucus (Helix Aspersa) Conjugated Gold Nanoparticles, Exhibiting Potential Wound Healing and Anti-Inflammatory Activity. *Soft Matter* **2020**, *16* (48), 10876–10888.
(3) Darroudi M, et al., Green Synthesis and Characterization of Gelatin-Based and Sugar-Reduced Silver Nanoparticles. *Int. J. Nanomedicine* **2011**, *6* (1), 569–574.

Piezoelectric nylon-11 nanoparticles as innovative anti-cancer nanovectors

Ozlem Sen[1*], Melis Emanet Ciofani[1], Gianni Ciofani[1]

[1]Istituto Italiano di Tecnologia, Smart Bio-Interfaces, Viale Rinaldo Piaggio 34, 56025 Pontedera, Italy
[*]ozlem.sen@iit.it

INTRODUCTION

Breast cancer is the most commonly diagnosed cancer in female patients. Despite the advanced research in the last decades, the exploration of new strategies in therapy is strongly required, mainly because of the inability of delivering an adequate amount of chemotherapy drugs[1]. Nanotechnology suggests the exploitation of biocompatible and biodegradable systems, which can improve the bioavailability of drugs at the targeted area[2]. Recently, an innovative approach has been proposed in cancer nanomedicine based on the use of nanomaterials that can remotely respond to external irradiation such as ultrasound[3]. In this context, piezoelectric nanomaterials featuring the capability of converting mechanical energy to electricity represent great potential in cancer therapy, due to the non-invasive and remote delivery of electrical cues affecting cell fate by enhancing drug release or/and regulating the invasion and migration pathways[3,4]. Nylon is a polyamide bioplastic, and it is known that odd-numbered nylons (*e.g.*, 7, 9, and 11) present satisfactory piezoelectric properties[5]. No biomedical applications have been developed so far: here, we propose to exploit nylon-11 nanovectors to improve the therapeutic outcome in cancer angiogenesis treatment, by exploiting an indirect electric stimulation mediated by the mechanical excitation of the nanoparticles.

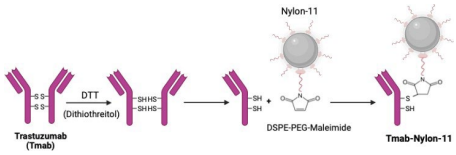

Figure 1. Schematic representation of nanovector functionalization.

EXPERIMENTAL METHODS

Nylon-11 nanoparticles were prepared by a simple anti-solvent method[5] with some modifications. Briefly, 25 mg of nylon-11 were dissolved in 1 mL of formic acid under 80°C for 30 min while stirring. Then, the solution was added to 2 mL of MilliQ water including 10 mg of 1,2-distearoyl-*sn*-glycero-3-phosphoethanolamine-poly(ethylene glycol) (DSPE-PEG) and 2 mg of DSPE-PEG-maleimide. Trastuzumab (Tmab) was conjugated to the nanoparticles as shown in Fig. 1, and successful binding was confirmed by sodium dodecyl sulfate-polyacrylamide gel electrophoresis (SDS-PAGE) and bicinchoninic acid (BCA) assay. Size distribution and ζ-potential of nanoparticles were investigated with a Nano Z-Sizer, while their morphology was analyzed using scanning electron microscopy (SEM). The stability of the particles up to 30 days was monitored by using dynamic light scattering (DLS) measurements. Biocompatibility of the Tmab-nylon-11 nanoparticles was tested using WST-1 assay on human brain capillary endothelial cells (HCMECs). Statistical analysis was evaluated by using ANOVA (analysis of variance), followed by Fisher's *post-hoc* test.

RESULTS AND DISCUSSION

SEM imaging suggests the formation of spherical-shaped particles for nylon-11 and Tmab-nylon-11 nanoparticles (representative images reported in Fig. 2A and 2B, respectively). The sizes of nylon-11 and Tmab-nylon-11 nanoparticles respectively resulted 193.9 ± 3.5 nm and 182.1 ± 0.9 nm (Fig. 1C), while the ζ-potential 7.4 ± 0.8 mV and 11.1 ± 0.5 mV. After synthesis, the particles were stored at 4°C, and the long-term stability has been monitored using DLS and ζ-potential measurements. The results showed that the nanoparticles remained stable up to 30 days after preparation. Finally, biocompatibility data showed that the particles are safe up to 250 µg/mL on HCMECs after 24 h of incubation.

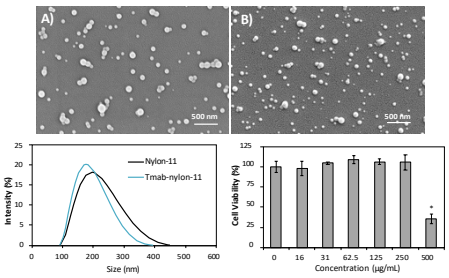

Figure 2. Representative SEM images of **A)** nylon-11 **B)** Tmab-nylon-11 nanoparticles. **C)** Size distribution of the nanoparticles. **D)** Biocompatibility results for Tmab-nylon-11 nanoparticles.

CONCLUSION

Piezoelectric nylon-11 nanoparticles were successfully synthesized by a simple anti-solvent method, and decorated with trastuzumab to improve the therapeutic efficiency. The obtainment of biocompatible, stable, and monodisperse polymeric piezoelectric nanoparticles is a first step towards innovative approaches in cancer nanomedicine.

REFERENCES

1. Boix-Montesino P. *et al.,* Adv. Drug Deliv. Rev. 173:306-330, 2021
2. Pucci C. *et al.*, Ecancermedicalscience. 13, 2019
3. Sen O. *et al.,* Materials Today Bio 13:100196, 2022
4. Jin Y. *et al.,* RSC Adv. 10:20405-20413, 2020
5. Ma B. *et al.,* J. Mater. Chem. B. 7:1847-1854, 2019

ACKNOWLEDGMENTS

The authors acknowledge the financial support of the AIRC (Project Code: 26590).

Tannic acid – Iron-based Nanocomplexes: a Natural Derivative to Fight Oxidative Stress

Carlotta Pucci[1*], Gianni Ciofani[1]

[1]Smart Bio-Interfaces, Istituto Italiano di Tecnologia, Pontedera (Pisa), 56025 Italy
[*]carlotta.pucci@iit.it

INTRODUCTION

Intracellular enzymes balance the amount of reactive oxygen species (ROS), produced by our metabolism. Their excessive accumulation induces oxidative stress, damaging cellular components and activating cell death mechanisms.[1] Oxidative stress is linked to age-related conditions and neurodegenerative disorders.[1] Naturally derived antioxidants could help counteracting oxidative stress: tannic acid, a polyphenol found in wine, coffee, tea, and in some fruits, is a promising candidate.[2] However, natural antioxidants are prone to oxidation and enzymatic degradation in biological fluids,[1] and free tannic acid can precipitate plasma proteins and chelate metal ions in our body.[3]

In this work, we exploited the metal chelating properties of tannic acid to form nanosized hydrophobic complexes with iron ions (Fe^{3+}) coated with a biocompatible phospholipid (1,2-distearoyl-sn-glycero-3-phosphoethanolamine-poly(ethylene glycol) (DSPE-PEG)) to improve stability in biological media and to favor the intracellular accumulation of high tannic acid payloads.

EXPERIMENTAL METHODS

DSPE-PEG-coated tannic acid – Fe^{3+} nanoparticles (L-TAFe NPs) were prepared by nanoprecipitation and characterized by dynamic light scattering (DLS), transmission electron microscopy (TEM), thermogravimetric analysis (TGA), Fourier-transform infra-red (FTIR), UV/Vis and Raman spectroscopy, while the scavenging activity was assessed with different assays. The *in vitro* biocompatibility was tested on human primary skin fibroblasts. L-TAFe NPs uptake was studied with confocal and Raman microscopy and flow cytometry. Their protective effect against oxidative stress induced by a pro-oxidant (tert-butyl hydroperoxide, TBH) were evaluated both *in vitro* on human primary skin fibroblasts (CellROX™, WST-1, Live/Dead™) and *in vivo* on planarian worms (*Dugesia japonica)* and compared to conventional antioxidants (*e.g.,* tannic acid, L-ascorbic acid, N-acetyl-L-cysteine).

RESULTS AND DISCUSSION

L-TAFe NPs were found to be a nanoscale network with an average hydrodynamic diameter of 201 ± 4 nm, with a negative ζ-potential (-29 ± 1 mV). L-TAFe NPs were stable over time in several conditions, proving their suitability for biological applications. UV/Vis spectroscopy of L-TAFe NPs showed a charge transfer band at ≈ 550 nm, typical of the bis-complex. Combining ICP and TGA data, the iron and tannic acid content in L-TAFe NPs were estimated to be 5.4 and 87 wt%, respectively. Therefore, L-TAFe NPs represent a good way to deliver high tannic acid payloads.

L-TAFe NPs displayed good biocompatibility in a wide range of concentrations and a high internalization rate in fibroblasts (98 ± 2% of the cells internalized L-TAFe NPs after 24 h). L-TAFe NPs were able to efficiently scavenge TBH-induced intracellular ROS. TBH-treated cells showed ROS levels (5.69 ± 0.83)-fold higher than control cells, while in cells pretreated with L-TAFe NPs before the pro-oxidant insult, ROS levels were similar to those observed in control cells, proving their *in vitro* antioxidant activity. The ROS scavenging effect of L-TAFe NPs was superior to that of free tannic acid, L-ascorbic acid, and N-acetyl-L-cysteine, showing how the encapsulation in nanoparticles increases the stability and favors the cellular uptake of tannic acid. Since oxidative stress induces cytotoxicity, the protective effect of L-TAFe NPs against the damages of acute oxidative stress was evaluated. TBH-treated fibroblasts underwent a reduction in cell viability (62 ± 6% with respect to controls); however, cells pretreated with L-TAFe NPs showed a higher cell viability (79 ± 4%). The Live/Dead™ assay corroborates this result, suggesting a promising protective effect of L-TAFe NPs against oxidative stress-induced damages *in vitro*. L-TAFe NPs antioxidant action was also tested *in vivo* on planarian worms. Treatment with L-TAFe NPs was effective in reducing TBH-elicited mortality on planarians.

CONCLUSION

L-TAFe NPs formulation method presented in this work allows encapsulating a high amount of tannic acid and guarantee long-term stability in several conditions. L-TAFe NPs are biocompatible, possess strong antioxidant activity, and can counteract oxidative stress-related toxicity, both *in vitro* and *in vivo*. This work offer a new potential application for tannic acid – Fe^{3+} complexes, paving the way for the use of nature-derived antioxidants for the treatment of oxidative stress-related diseases.

REFERENCES

1. Martinelli, C. *et al.* Adv. Healthc. Mater. 9:1901589, 2020.
2. Daré, R.G. *et al.* Free Radic. Biol. Med. 160:342-355, 2020.
3. Pinto, A.F. *et al.* Eur. J. Pharm. Sci. 138:105018, 2019.

ACKNOWLEDGMENTS

This work was partially supported by the European Space Agency (ESA) (Grant Nr. 4000130094/20/NL/MH/ac).

Synthesis and characterization of ZnO nanoparticles carrying nitric oxide donor for potential biomedical applications

Amedea Barozzi Seabra[1*], Isabella Martins Lourenço[1], Joana Claudio Pieretti[1], Bruna Moreira Freire [1], Bruno Lemos Batista[1], Gerson Nakazato[2], Marcelly Chue Gonçalves[2]

[1]Center for Natural and Human Sciences (CCNH), Federal University of ABC (UFABC), Santo André, São Paulo, Brazil
[2]Biological Sciences Center, Department of Microbiology, Londrina State University, Londrina, Paraná, Brazil
[*]amedea.seabra@ufabc.edu.br

INTRODUCTION

In recent years, nanomaterials for biomedical purposes have received great attention mainly as drug delivery, anticancer and antibacterial drugs.[1] Interestingly, zinc oxide nanoparticles (ZnO NPs) are the most used metal oxide NPs for commercial purposes because they have antimicrobial and optical properties due to the strong possibility of ZnO to absorb UV light.[2] Numerous works describe the promising applications of nitric oxide (NO) in biomedical applications, as it is a potent antimicrobial and vasodilator agent.[3] However, its action becomes limited by the time factor, application site and concentration. Due to the short half-life of NO (0.5 s), NO donors, such as S-nitrosothiols (RSNOs) have been using in biomedical applications.[4] In this work, the NO donor, S-nitrosoglutathione (GSNO), which belongs to the class of RSNOs, was synthesized and incorporated into hydrothermally synthesized ZnO NPs. GSNO-ZnO NPs were characterized by different techniques and their antibacterial activity was evaluated.

EXPERIMENTAL METHODS

ZnO NPs: Were prepared by the hydrothermal method[5]. A mass of 2.195 g of zinc acetate dihydrate was dissolved in 30 mL of deionized water, followed by dropping of NaOH. The final suspension was poured into a hydrothermal reactor for 10 h at 170 °C.

GSNO: Glutathione (1.23 mol/L) was dissolved in HCl (1 mol/L), followed by the equimolar addition of $NaNO_2$. The nitrosation reaction was kept in an ice bath, under magnetic stirring and protected from light for a period of 20 min, resulting in a pink coloured of GSNO precipitate.

GSNO-ZnO NPs: The incorporation of GSNO was carried out by dispersing 10 mg of ZnO NPs in 10 mol/L of GSNO under magnetic stirring for 1 h.

Material characterization: Different techniques were used to evaluate the physicochemical characteristics of the prepared material, such as dynamic light scattering (DLS), x-ray diffraction (XRD), transmission electron microscopy (TEM), Fourier transform infrared spectroscopy (FTIR), inductively coupled plasma mass spectrometry (ICP-MS), kinetics of NO release incorporated in ZnO NPs and antibacterial activity (MIC and MBC) tested with *Escherichia coli*, *Staphylococcus aureus* and *Klebsiella pneumoniae*.

RESULTS AND DISCUSSION

ZnO NPs showed a hydrodynamic size of 280.5 ± 0.006 nm and a polydispersity index (PDI) of 0.342 ± 0.062 mV at pH 7.5, indicating good stability in aqueous suspension. GSNO-ZnO NPs had a hydrodynamic size of 350.5 ± 0.800 nm and a PDI of 0.503 ± 0.121 mV. XRD revealed the crystal structure of ZnO NPs indicated by refractive indices. TEM images revealed that the GSNO-ZnO NPs have mostly hexagonal morphology with the presence of clusters, with an average size of 118 ± 43 nm. The FTIR demonstrated the functional groups of ZnO in the synthesized NPs. The release kinetics showed a sustained release of NO for 12 h, 37 ºC. The ICP-MS showed that the total amount of Zn^{2+} released from the NPs did not show significant variations. Antibacterial activity demonstrated synergistic effect of ZnO NPs allied to GSNO against *Staphylococcus aureus* and *Klebsiella pneumoniae* at a concentration from 0.05 mg/mL to 0.2 mg/mL for ZnO NPs and 0.6 mg/mL to 3 mg/mL for GSNO.

CONCLUSION

ZnO NPs were successfully synthesized and characterized. Moreover, the NO donor, GSNO was incorporated into ZnO NPs. The combination of NO donor and ZnO NPs showed superior antibacterial activity against bacteria of great medical relevance, compared with ZnO NPs and GSNO individually applied, highlighting the potential use of this nanosystem in biomedical application.

REFERENCES

1. Jiang *et al*., Bioinorg Chem Appl, 1565-36332018, 2018
2. Bhat *et al*., Russ. J. Plant Physiol, 68:559–568, 2021
3. Singha *et al.*, J Biomed Mater Res Part A 107A:1425–1433, 2019
4. Seabra *et al.*, British J. Dermatology, 151:977–983, 2004
5. Wang *et al*., Materials Letters, 55–58, 2016

ACKNOWLEDGMENTS

The authors would like to thank CNPq (404815/2018-9, 313117/2019-5), CAPES, and Fundação de Amparo À Pesquisa do Estado de São Paulo - FAPESP (Process nº: 2020/08566-7, 2018/08194-2).

Sumac (*Rhus coriaria*) Extract Loaded Polymeric Nanosheets for Controlled Transdermal Drug Delivery

Melis Emanet[1,2,3‡], Mayu Okuda[4], Özlem Şen[1‡] Shinji Takeoka[3,4*], Gianni Ciofani[1,3*]

[1]Smart Bio-Interfaces, Istituto Italiano di Tecnologia, Pontedera (Pisa), Italy
[2]Sabanci University Nanotechnology Research and Application Center (SUNUM), Sabanci University, Istanbul, Turkey
[3]TGU Unit for Energy and Nanomaterials, Waseda University, Tokyo, Japan
[4]Department of Life Science and Medical Bioscience, Waseda University, Tokyo, Japan

melis.emanetciofani@iit.it

INTRODUCTION

In healthy physiological conditions, living organisms possess a variety of antioxidant mechanisms to scavenge over-produced reactive oxygen species (ROS). However, under pathological conditions, endogenous antioxidant systems may not be adequate to eliminate the excessive rate of oxidants,[1] and thus, a continuous exogenous antioxidant income is required.[2] In this regard, sumac (*Rhus coriaria*) extract is a good candidate for therapeutic applications, because of its high content of antioxidant polyphenolic compounds.[3] In this work, extract-loaded nanosheets (PCL_Ext_PDLLA) have been exploited for loading and controlled release of sumac extract envisioning transdermal drug delivery applications.[4]

EXPERIMENTAL METHODS

Sumac extract has been obtained by solvent extraction method (Figure 1A) and evaluated for evaluation of polyphenolic compounds content and total antioxidant capacity. Polymeric nanosheets have been thereafter prepared through a layer-by-layer spin coating of polycaprolactone (PCL), sumac extract (Ext), and poly(D,L-lactic acid) (PDLLA) (MNT-TOP-8; 4000 rpm and 20 s) (Figure 1B). The PCL layer has been plasma-treated to develop a hydrophilic surface and thus improve the extract loading efficiency. The characterization of the nanosheets has been performed by scanning electron microscopy (SEM), contact angle measurement, and tensile and adhesion tests; the antioxidant capacity assay has been exploited for the measurement of the extract release. All measurements have been statistically analyzed by ANOVA test.

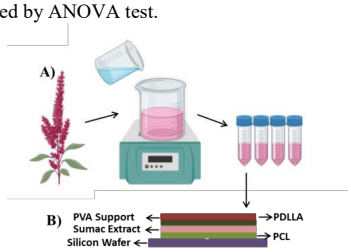

Figure 1. *Schematic representation of sumac extraction (A) and of the sumac extract-loaded nanosheets preparation (B).*

RESULTS AND DISCUSSION

As depicted in Figure 2A, the total polyphenolic content of the sumac extract was evaluated as tannic acid equivalent, and 1200 µg/mL of sumac extract was found equivalent, in terms of polyphenolic groups content, to 964 µg/mL of tannic acid. Concerning antioxidant capacity, 240 µg/mL of sumac extract was found equivalent to 18.425 ng/mL of Trolox (Figure 2B). Concerning mechanical properties, the evaluation of PCL_PDLLA and PCL_Ext_PDLLA film resistance showed an increment of tensile stress of about 100% in the presence of extract (Figure 2C). SEM imaging suggested the presence of a relatively uniforme surface (Figure 2D), while the contact angle resulted to be 52 ± 5° (Figure 2E).

Finally, drug release investigation showed a well-sustained release of sumac extract up to 72 h, at both neutral and acidic pH values (Figure 2F).

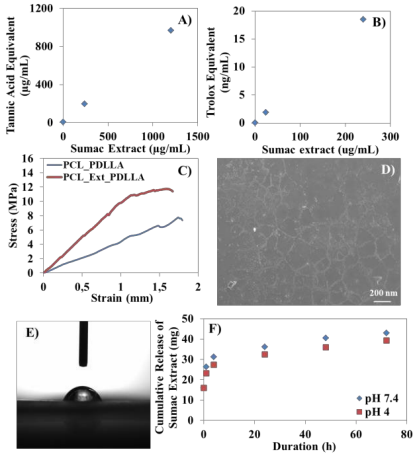

Figure 2. *Folin-Ciocalteu phenolic group analysis (A) and antioxidant capacity quantification (B) of sumac extract. Tensile stress measurements (C), representative SEM image (D), and contact angle measurement (E) of nanosheets. Extract release analysis from nanosheets (G).*

CONCLUSION

Collected data confirm strong antioxidant properties of sumac extract, and its suitability as oxidative stress scavenger. Moreover, for the first time in the literature, we showed the possibility to efficiently load such extract in polymeric nanosheets, envisioning important applications in transdermal drug delivery.

REFERENCES

[1] Z. Rong-zhen, et al. *J Integr Agric.* 12, 1826 (2013)
[2] D. P.Xu, et al. *Int. J. Mol. Sci.* 18, 96 (2017)
[3] M. Kosar, et al. *Food Chemistry.* 103, 3 (2007)
[4] T. Fujie, et al. *Nanobiotechnology.* 68, (2014)

Gold@Silver-Gold nanorattles as potential catalysts for biosensing

Flavia Gontijo da Silva[1], Pedro Camargo[1]

[1]Department of Chemistry, University of Helsinki, Helsinki, Finland

INTRODUCTION

Biosensing is an important tool for the diagnosis and treatment of several diseases, with the development of effective sensors leading to a fast and reliable detection of biomolecules. Hence several nanostructures have been vastly studied to improve biosensing devices and techniques[1]. Au NPs have been in the center of biosensing research due to their unique features, such as easy surface functionalization, optical and electronic properties that can be used to intensify biosensing signals and compatibility to most biological media. However, studies have showed that the catalytic activity of these particles is low compared to the enzymes usually used in biosensing[2]. In order to overcome the catalytic limitations of Au NPs, we aimed to synthesize gold@silver-gold nanorattles (Au@AgAu NRs), which present a core-void-shell structure that should lead to improved catalytic and optical properties[3]. We expect that this morphology design will lead to a better interaction with biomolecules, allowing these NRs to be used for biosensing applications.

EXPERIMENTAL METHODS

Gold nanospheres seeds were prepared by the citrate reduction approach, followed by the deposition of silver by seeded growth. Finally, the Au@Ag core-shell particles were submitted to a galvanic replacement reaction to for the Au@AgAu nanorattles. Sequentially, the nanostructures were physiochemically characterized by UV-vis spectroscopy, Scanning Electron Microscopy (SEM), Transmission Electron Microscopy (TEM), High-angle Annular Dark-field Scanning Transmission Electron Microscopy (HAADF-STEM) and Atomic Emission Spectroscopy (AES). Finally, the potential of these particles for biosensing applications was evaluated using the 3,3′,5,5′-Tetramethylbenzidine (TMB) oxidation in the presence of H_2O_2 as a model reaction. The reactions were done with the concentration of TMB and H_2O_2 being kept constant at 750 uM and 0.6 M, respectively and pH 4.5 over 20 minutes. The activity of the NRs was measured by evaluating the increase in absorbance in the UV-vis spectra over time. In addition, the catalytic activity of Au NPs and Au@AgAu NRs was compared by keeping the metal loading constant for both materials.

RESULTS AND DISCUSSION

The synthesis of Au NPs led to a bright red suspension that turned orange with the formation of Au@Ag core-shell particles and brownish after the galvanic replacement step, to form the Au@AgAu NRs. The change in color was also evidenced in the UV-VIS spectra, that showed a hypsochromic shift and broadening of the NRs spectrum compared to the Au NPs, indicating the presence of Ag in the shell. In addition, electron microscopy images showed that spherical Au NPs with an average diameter of 15.0 ± 1.7 nm and Au@AgAu NRs of around 31.2 ± 3.4 nm in outer diameter, with uniform size distribution, were synthesized (Fig. 1). HRTEM confirmed that the core-void-shell structure was obtained (Fig. 1b).

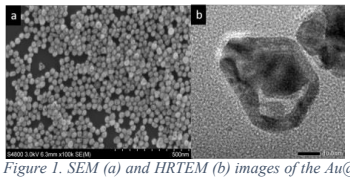

Figure 1. SEM (a) and HRTEM (b) images of the Au@AgAu NRs.

Following the morphological studies, the NRs were used as catalysts for the TMB oxidation as a model reaction. Preliminary results demonstrated that the synthesized NRs were active for the TMB oxidation, since there is an increase in absorbance over time (Fig. 2a). In addition, when compared to the original Au NPs, Au@AgAu NRs showed a catalytic activity 150 times higher (Fig. 2b). This significant increase in activity is due to the increased surface area of NRs and a synergic effect of the core and shell towards the reduction of H_2O_2 to form the radical species responsible for the oxidation of TMB.

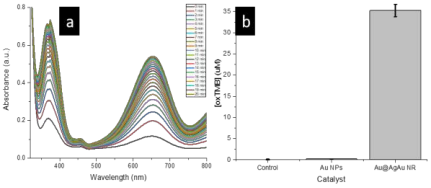

Figure 2 UV-vis spectra over time for TMB oxidation with Au@AgAu NRs (a). Comparison of the concentration of oxTMB when Au NPs and NRs were used as catalysts (b).

CONCLUSION

In this work prepared Au@AgAu nanorattles that showed a significantly higher catalytic activity for TMB oxidation when compared to Au NPs. This demonstrated the potential of the nanorattle morphology for biosensing purposes. A more detailed investigations on catalytic activity and structure-performance relationships is in progress.

REFERENCES

1. Naresh V. *et al*., *Sensors* **21**, 1109, 2021
2. Ye H. *et al., ChemNanoMat* **5**, 860–868, 2019
3. Ahlawat M. *et al*., *ChemNanoMat* **5**, 625–633 2019

ACKNOWLEDGMENTS

The authors would like to thank the Jane and Aatos Erkko Foundation, Academy of Finland, the Fortum and Neste Foundation, and the University of Helsinki for the financial support.

Dual-crosslinked degradable elastomer with self-healing properties

Mathilde Grosjean[1*], Louis Gangolphe[1,2], Frédéric Bossard[2], Xavier Garric[1], Benjamin Nottelet[1]

[1]Department of Polymers for Health and Biomaterials, IBMM, University of Montpellier, Montpellier, France
[2]LRP, Grenoble INP, Université Grenoble Alpes, Grenoble, France
[*] mathilde.grosjean@umontpellier.fr

INTRODUCTION

A wide array of chemically crosslinked degradable elastomers based on synthetic polyesters have been investigated for tissue engineering applications in the past years[1]. These elastomers present various advantages such as a rubber-like behavior matching with those of the soft tissues, and an ability to preserve 3D structure over their degradation[2]. Among the various chemical strategies available to develop 3D networks, photo-crosslinking is an efficient strategy due to its fast reaction time, easy implementation and low thermal energy production[3]. However, one major drawback is the inability to be healed after damage or breaking. This can be overcome by supramolecular networks whose polymer chains are linked via dynamic and/or reversible non-covalent bonds, that act as crosslinks which bring self-healing properties to the material. Hydrogen bonds are the most widely studied reversible non-covalent bonds due to their ability to quickly create bonds with high strength and excellent reversibility[4]. In this study, our objective was to combine the high mechanical properties and degradation properties of chemically photo-crosslinked elastomers, with the self-healing properties of hydrogen-bonds supramolecular networks. To this aim, a degradable 8-arm star-shaped PEG-*b*-PLA block copolymer was designed and functionalized with either methacrylic and/or catechol groups. Various degradable dual-crosslinked elastomers were then designed and the mechanical properties, self-healing efficiency, and biodegradability were evaluated.

EXPERIMENTAL METHODS

1. Preparation of elastomers

Star-shaped copolymers were synthesized by ROP before being functionalized with methacrylate and/or catechol groups. Elastomer films were prepared by solvent evaporation of polymer solutions containing defined amounts of methacrylate and/or catechol copolymers and exposed to UV light for 5 minutes per side.

2. Mechanical properties

The mechanical properties were assessed through tensile test at room temperature on dog-bone strips (10x2mm) with an Instron 3344 testing machine equipped with a 500 N load cell at a deformation rate of 10 $mm.min^{-1}$.

3. Self-healing study

The samples were cut in two pieces thanks to a razor blade. Then, the pieces were put together, pressed for 5 seconds and heated at 37°C in an oven for different times.

RESULTS AND DISCUSSION

The influence of the methacrylate/catechol (MC/CT) ratio on the tensile properties was investigated. It was demonstrated that the amount of catechol improved the elongation but decreased the stress at break. Indeed, elongation and stress reached 539% and 10.7 MPa for MC/CT 100/0 respectively, against 932% and 1.8 MPa for MC/CT 0/100. MC/CT 75/25 was selected as the best compromise with intermediate values between MC/CT 100/0 and MC/CT 0/100 (798% and 3.4 MPa) and interesting self-healing properties. The self-healing abilities were studied at 37°C. The samples were cut and put together for different times. The self-healing efficiency (SHE) was calculated by comparing the values of elongation and stress at break of the healed samples to the original ones. SHE increased with time and MC/CT 75/25 was totally recovered after 60 minutes (Figure 1). SHE reached 100% of the elongation at break and 120% for the stress, which reflects the properties improvement through the dynamic reorganization of the network.

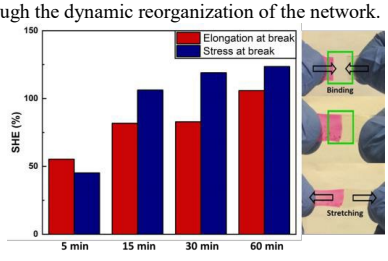

Figure 1. Evolution of SHE with time of MC/CT 75/25 and images of self-healing of a cutting film

CONCLUSION

In this work, we designed dual-crosslinked elastomers thanks to methacrylate and catechol functionalized star-shaped PEG-PLA copolymers. The resulting elastomers exhibit mechanical properties that are compatible with soft tissue applications and self-healing properties at 37°C. Moreover, the elastomers showed to be degradable *in vitro*. Therefore, we demonstrated that our strategy is an elegant approach to design, from a single copolymer type, degradable biomaterials combining both rubber-like behavior and self-healing properties.

REFERENCES

1. Gangolphe L. *et al*, Mater. Today Chem. 12:209-221, 2019
2. Ye H. *et al*., Chem. Soc. Rev. 47:4545-4580, 2018
3. Ifkovits J.L. *et al*., Tissue Eng. 13:2369-2385, 2007
4. Yan X. *et al*., Chem. Soc. Rev. 41:6042, 2012

ACKNOWLEDGMENTS

This work was supported by ANR2016-BIOSCAFF (ANR-16-CE09-0024), ANR2019-OPENN (ANR-19-CE19-0022-02) and Institut Carnot Balard Cirimat (Corol).

Supramolecular network of poly(ε-caprolactone) and poly(ethylene oxide) biomaterials with efficient thermo- and moisture-sensitive shape-memory.

Jérémie Caprasse, Thomassin Jean-Michel, Riva Raphaël, Jérôme Christine*

CERM, University of Liège, CESAM-RU, Allée du Six Août, 13, 4000 Liège, Belgium

* C.Jerome@ulg.ac.be

INTRODUCTION

Covalent networks of poly(ε-caprolactone) (PCL) are shape-memory polymers (SMP) widely studied for smart medical devices thanks to their biocompatibility, degradability and efficient thermally triggered shape-memory properties, i.e. high fixity of the temporary shape and high recovery of the permanent shape[1]. As an answer to the increasingly demanding biomedical field, we aim at providing to such PCL SMP an additional shape transition triggered by the presence of water at constant temperature. For this purpose, a hydrophilic component, namely poly(ethylene oxide) (PEO) has been introduced in the PCL network.

EXPERIMENTAL METHODS

The chain-ends of 4-arm PCL and PEO stars were functionalized by maleimide and furan respectively. The functionalization degree was determined by ^{1}H-NMR. The network was formed by mixing both types of stars in stoichiometric amount in a mini-extruder at 105°C followed by annealing in a mould at 65°C during 48h. The network was characterized by swelling experiment in $CHCl_3$ and its crystallinity by differential scanning calorimetry (DSC). The thermal-triggered shape-memory properties were quantified by dynamic mechanical analysis (DMA), and the water-triggered ones were qualitatively tested upon immersion in water at room temperature. Finally, the hydrolytic degradation of the material was studied in phosphate buffer at 37°C.

RESULTS AND DISCUSSION

In the present work, a covalent PEO/PCL hybrid network was formed by Diels-Alder reaction between PCL and PEO stars purposely end-capped by maleimide and furan respectively (**Figure 1a**). After melt-blending of these cross-reacting stars and post-curing, the resulting material shows high crosslinking density, as demonstrated by the low swelling (1000%) and high insoluble fraction (96%) in $CHCl_3$, a good solvent of both stars. This network exhibits excellent thermal triggered shape-memory properties with fixity and recovery both above 95%. Moreover, by immersion in water and drying at room temperature, it is possible to trigger a second shape transition by the water swelling of the PEO component of the network (**Figure 1b**).

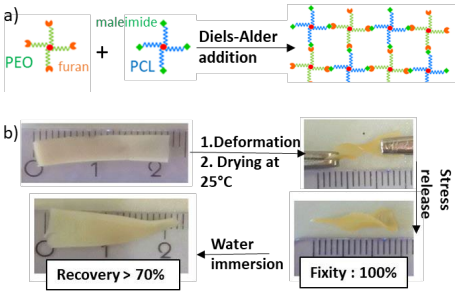

Figure 1. PEO/PCL hybrid network a) synthesis pathway b) water-triggered shape memory

Results obtained by DMA evidenced that there is no decrease of the PEO/PCL network properties after immersion during one month in PBS.

CONCLUSION

PEO/PCL hybrid networks have been successfully obtained by Diels-Alder addition of four-arms PCL and PEO stars bearing maleimide and furan moieties, respectively.

These networks present excellent thermal and water shape-memory properties and keeping good mechanical properties. Interestingly, multiple shape memory is achieved by fixing a first temporary shape with the temperature and a second by hydration and drying. These networks are thus very promising to design medical devices of complex shapes exhibiting in vivo self-deploying properties.

REFERENCES

1. Defize, T. *et al. Macromol. Rapid Commun.* **32**, 1264–1269 (2011).

ACKNOWLEDGMENTS

The IN FLOW project is being carried out within the context of the Interreg V-A Euregio Meuse-Rhine programme, with EUR 2,1 million coming from the European Regional Development Fund (ERDF). With the investment of EU funds in Interreg projects, the European Union directly invests in economic development, innovation, territorial development, social inclusion and education in the Euregio Meuse-Rhine.

The physicochemical and antibacterial properties of chitosan-based materials modified with phenolic acids irradiated by UVC light

Beata Kaczmarek-Szczepańska[1]*, Marcin Wekwejt[2], Lidia Zasada[1], Anna Pałubicka[3], Ewa Olewnik-Kruszkowska[4]
[1]Faculty of Chemistry, Department of Biomaterials and Cosmetics Chemistry, Nicolaus Copernicus University in Torun, Poland
[2]Department of Biomaterials Technology, Faculty of Mechanical Engineering and Ship Technology, Gdańsk University of Technology, Gdańsk, Poland
[3]Specialist Hospital in Kościerzyna, Department of Laboratory Diagnostics and Microbiology with Blood Bank, Kościerzyna, Poland
[4]Physical Chemistry and Physicochemistry of Polymers, Faculty of Chemistry, Nicolaus Copernicus Univer-sity in Torun, Poland
*beata.kaczmarek@umk.pl

INTRODUCTION

Bacterial, viral, and fungal infections often re-sult from lack or improperly performed decontamination processes, which remains in contradiction to the existing standards and regulations. Inadequate tools, air, and various surfaces used when dealing with sterile tissues are the sources of pathogens[1].
In this study, we have made an attempt to determine the influence of UVC light on the properties of thin films obtained from chitosan modified by different phenolic acids: ferulic, caffeic, and tannic acid.

EXPERIMENTAL METHODS

Chitosan was dissolved in 0.1 M acetic acid at 2% concentration. Phenolic acids were also dissolve in 0.1 M acetic acid, at 1% concentration, each compound separately. A chitosan solution was mixed with a magnetic stirrer with 10vol/vol% phenolic acid solutions addition. Mixtures (40 ml) were then placed in plastic holders (10 cm x 10 cm) to evaporate the solvent (room conditions, 72h). Thin films were exposed to UVC light at 254 nm wavelength (ULTRAVIOL NBV 15 lamp, intensity: 18 W/m2) for 1 and 2h. Films were irradiated in the distance of 5 cm from the lamp. Samples without the UV exposure were left as control.

A Scanning Electron Microscope (SEM; LEO Electron Microscopy Ltd, England) was used to observe the bacteria adhered to the material surface. In the both analyses, films were sputter-coated with gold, prior to the observation.

Bacterial growth inhibition was checked by measuring the cultured bacterial broth turbidity according to McFarland standards[2] with an assumption that there is a direct relation between the solution turbidity and the number of bacteria, and 1 McFarland index (iMS) corresponds to 3×10^8 CFU/mL. Two bacterial strains were used for the tests: Staphylococcus aureus (ATCC 25923) and Escherichia coli (ATCC 35218), selected as various Gram groups representatives.

RESULTS AND DISCUSSION

Scanning Electron Microscope (SEM)

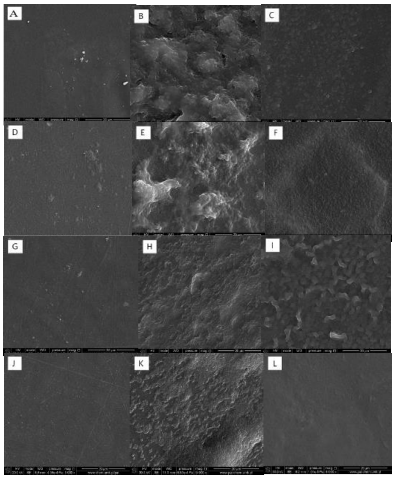

Figure 1. Comparison of bacterial adhesion to the films surface after 14 days of incubation in a bacterial suspension for films irradiated for 2h: CTS (A-C), CTS+FA (D-F), CTS+CA (G-I), CTS+TA (J-L) as control (A, D, G, J), *Staphylococcus aureus* (B, E, H, K), *Escherichia coli* (C, F, I, L).
The addition of phenolic acids into chitosan films does not significantly improve the *S. aureus* growth inhibition, and bacteria multiply at a similar rate.

CONCLUSION

Films with phenolic acids showed better antimicrobial activity against both, Gram-positive and Gram-negative bacteria.

REFERENCES

1. McDonell G. *et al.*, J. Hospital Inf 85:268–273, 2013
2. Zapata A.. *et al.*, Carbohyd Polym 2:100024, 2021

ACKNOWLEDGMENTS

The authors would like to thank the Nicolaus Copernicus University in Torun (Grant no: 282/2021 IDUB) for providing financial support to this project.

Chitosan-based films enriched by caffeic acid with poly(ethylene glycol)

Beata Kaczmarek-Szczepańska[1]*, Adrianna Sosik[1], Anna Małkowska[1], Lidia Zasada[1], Marta Michalska-Sionkowska[2]
[1] Nicolaus Copernicus University in Toruń, Faculty of Chemistry, Department of Biomaterials and Cosmetics Chemistry, Gagarin 7, 87-100 Toruń, Poland
[2] Nicolaus Copernicus University in Toruń, Faculty of Biological and Veterinary Sciences, Department of Environmental Microbiology and Biotechnology, Lwowska 1, 87-100 Toruń, Poland
*beata.kaczmarek@umk.pl

INTRODUCTION

Designing and obtaining bioactive materials is one of the main challenges science is currently facing. Polymer-based materials have been studied for decades. However, there is still a need to search for various modifiers which will improve the physicochemical properties of the material and enhance their bioactivity[1]. Polysaccharides have also been extensively studied as packaging materials, which is also within the scope of their potential applications[2].

The aim of the study was to investigate the chitosan/caffeic acid mixture as a raw complex for the preparation of thin films. Moreover, poly(ethylene glycol) was additionally used as a stabilizer.

EXPERIMENTAL METHODS

Chitosan, caffeic acid, and poly(ethylene glycol) were dissolved in 0.1M acetic acid, separately, at a concentration of 1%. CA solution was heated to completely dissolve the compound. The CTS solution was mixed with the CA solution in the weight ratios of 80/20 and 50/50. Then, 10 and 20 wt% of a PEG solution were added. Thin films were obtained by solvent evaporation under room conditions (size: 10 x 10 cm; thickness 0.13 ± 0.02).

DPPH radical scavenging assay

Antioxidant properties of the films were determined using the DPPH reagent (2,2-Diphenyl-1-picrylhydrazyl, free radical, 95%; Alfa Aesar, Germany)[3]. Samples (1 cm 1 cm) of each film were placed in a 12-well plate and filled with 2 mL of a DPPH solution (250 µM solution in methyl alcohol). They were left without exposure to light for 0.5h. After incubation, a spectrophotometric measurement was made at 517 nm (UV-1800, Shimadzu, Switzerland). The antioxidant activity was calculated from the formula:

$RSA\% = (Abs_{DPPH} - Abs_{PB}) / Abs_{DPPH} * 100\%$

Dehydrogenase activity

A dehydrogenase activity test was performed using CellTiter 96 AQ One Solution Cell Proliferation Assay (Promega, Germany) according to the manufacturer's guidelines. 20 µL of a reagent was added to 100 µL of the cell suspension after contact with the materials (10 mm x 10 mm). The samples were incubated at 37°C for 1.5-2 h depending on a the bacterial strain. Absorbance was measured at 490 nm.

RESULTS AND DISCUSSION

Results of antioxidant activity analysis and dehydrogenase activity are shown below.

Table 1. Antioxidant activity (RSA%) of films based on chitosan and caffeic acid modified by PEG

Specimen	RSA [%]
80CTS/20CA	92.77 ± 0.12
80CTS/20CA+10%PEG	90.10 ± 1.97
80CTS/20CA+20%PEG	64.59 ± 3.21
50CTS/50CA	95.11 ± 0.24
50CTS/50CA+10%PEG	91.34 ± 2.24
50CTS/50CA+20%PEG	90.73 ± 2.70

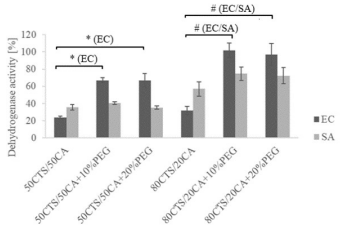

Figure 1. Dehydrogenase activity of S.aureus (SA) and E.coli (EC) suspension after 2h of contact with the materials (n=4; * significantly different from 50CTS/50CA $p<0.05$; (# significantly different from 80CTS/20CA $p<0.05$).

CONCLUSION

80CTS/20CA+10%PEG showed antioxidant activity in the range 91.34%, and the highest dehydrogenase activity. Thereby, it may be considered as a packaging material with antibacterial properties and can be classified as technologically advanced.

REFERENCES

1. Wei W. *et al.*, Bioact. Mater. 6: 998-1011, 2021
2. Nechita P. *et al.*, Coatings 10:566, 2020
3. Zhang W. *et al.*, J. Phys. Chem. C 121: 18635–18642, 2017

ACKNOWLEDGMENTS

The authors would like to thank the Nicolaus Copernicus University in Torun (Grant no: 282/2021 IDUB) for providing financial support to this project.

Supramolecular polymers for the design of modular multivalent antibacterial vaccines

Yuqing Wang[1], Moritz Urschbach[1], Riem Attariya[2], Tobias Bopp[2], Edgar Schmitt[2], Pol Besenius[1*]

[1]Department of Chemistry, Johannes Gutenberg- University Mainz, Germany
[2]Institute of Immunology, University Medical Center Mainz, Germany

INTRODUCTION

Peptide secondary structures can be harnessed to design monomers capable of self-assembling into nano-scaled supramolecular structures in aqueous media.[1,2] Decorating the surface with immunogenic molecular patterns results in pathogen-mimicking entities and potential vaccine candidates.[3] In the context of antibacterial vaccines, oligosaccharide structures derived from the bacterial polysaccharide capsule can be introduced as B cell epitopes.[4] The challenge remains in the generation of a T cell mediated immune response. Therefore, a co-stimulation of B cells with Th cells is mandatory, which we aim to achieve using a co-presentation of different epitopes and immunostimulating agents at the surface of multicomponent supramolecular polymers.

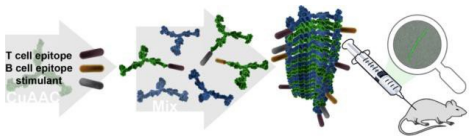

EXPERIMENTAL METHODS

Oligoethylene glycol-decorated C_3-symmetric peptide amphiphiles were synthesized according to procedures from previous studies. Oligosaccharide antigen derivatives against different serotypes of S*treptococcus pneumoniae* were synthesized from protected precursor building blocks by solution-phase oligosaccharide synthesis. T cell epitope p30 was synthesized from commercial and modified amino acids using a solid-phase peptide synthesizer. Subsequently, B cell and T cell epitopes were conjugated to the C_3-symmetric peptide amphiphiles, and the resulting compounds were purified *via* size-exclusion chromatography. All molecules were characterized *via* nuclear magnetic resonance spectroscopy and mass spectrometry.
The self-assembly behavior of the supramolecular monomers obtained from the synthesis were investigated by circular dichroism (CD) measurements. In addition, transmission electron microscopy (TEM) images of the nanostructures were accomplished.

RESULTS AND DISCUSSION

Glycoconjugate vaccines have achieved huge success in protecting humans from different bacterial infections. Nevertheless, the commercially available polysaccharide-based and glycoconjugate pneumococcal vaccines consist of isolated saccharides from cultured bacteria and fail to cover all the invasive serotypes. Polysaccharides in their native form are not capable to induce T cell-dependent immune response.[4]
In this work, a fully synthetic supramolecular antibacterial vaccine platform is presented that overcomes the cellular impurities from cultured bacteria and allows the co-presentation of B and T cell epitopes as well as other immunostimulants. Oligosaccharide antigens against different serotypes of *Streptococcus pneumoniae* were synthesized and introduced as B cell epitopes. As T cell epitope, a small fragment from highly immunogenic tetanus toxin (p30) was chosen. These epitopes were conjugated to supramolecular monomers and mixed in aqueous solution to yield a polymeric vaccine formulation.
The self-assembly of functionalized supramolecular monomers with non-functionalized monomers was investigated using CD spectrometry. The formation of filament-like supramolecular polymers was observed in TEM images.

CONCLUSION

Oligosaccharide- and p30-decorated C_3-symmetric peptide amphiphiles were synthesized as monomers for supramolecular vaccines. By mixing with non-functionalized monomers in aqueous media, nanorod-like supramolecular polymers containing different epitopes were formed. This approach shows potential of multivalent presentation of B cell and T cell epitopes for the development of supramolecular antibacterial vaccine platform.

REFERENCES

1. Spitzer D. *et al.*, Angew. Chem. Int. Ed. 57:11349, 2018.
2. Krieg E. *et al.*, Chem. Rev. 116:2414, 2016.
3. Straßburger D. *et al.*, ChemBioChem 19:912, 2018.
4. Seeberger P. *et al.*, Chem. Rev. 121:3598-3626, 2021.

ACKNOWLEDGMENTS

The authors would like to thank the Fonds der Chemischen Industrie (Kekulé-Fellowship) and by the European Research Council (ERC CoG SUPRAVACC 819856) for providing financial support to this project.

Validation of a New Surgical Management Strategy for Open-Book Pelvic Lesions.

Robert Beya[1*], Cyril Breque[1], Jérôme Danion[1], Elodie Château[1], Jean-Pierre Faure[1], Tanguy Vendeuvre[1], Denis Oriot[1], Jean-Pierre Richer[1], Guillaume Herpe[2], Rémy Guillevin[2], Thierry Hauet[3].

[1] Anatomy Biomechanics Simulation Lab, Research Institute, University, Poitiers, France.

[2] DACTIM-MIS Radiology, Research Institute, University, Poitiers, France.

[3] INSERM U1082 – IRTOMIT, Research Institute, University, Poitiers, France.

*robert.beya@univ-poitiers.fr

Keywords: human pubic ligament, characterization, quasi-static tests.

INTRODUCTION

The treatment of choice for the open-book pelvic lesion with a gap of more than 2.5 cm is a screwed plate[1]. However, the occurrence of failure of this material[2] has led some authors to clinically perform an endo-button repair with success[3]. Works were published to compare this dynamic device with screwed plates[4].

The aim of this cadaveric study was to validate the new surgical management strategy for human pubic ligament lesions by evaluating its mechanical properties.

EXPERIMENTAL METHODS

Seven pelvises fresh frozen from Donors were submitted to CT scan for determining inclusion criteria (normal pelvis), exclusions criteria (abnormalities) and bone density. Three models in prospective and randomized design were defined for non-destructive and destructive tests: A (native), B (open book B1) and C (repaired). In C, three semi-rigid devices with threads, tapes and a steel strapping wire. Two groups of assemblies were carried out such as parallel and crossed endo-buttons. Tinus Olsen machine has been coupled to a stereovision system for uniaxial quasi-static tests. The Deformations measurements no contact (Deftac) 3D was used[5]. Whole system was calibrated beforehand, allowing to have a maximum stress of 2500 N and a 3D reference working marker. The Excel and Student T test were used for evaluating the results.

RESULTS AND DISCUSSION

Displacements and deformations were elevated for parallel endo-buttons (Figure 1) and steel strapping wire than in crossed (Figure 2), all $p < 0.05$).

Figure 1.

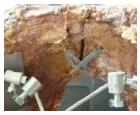

Figure 2.

Figure 1: anatomical result of parallel endo-button

(● 1a: pelvic gap, ● ● 1b: parallel endo-button).

Figure 2:● anatomical result of a cross assembly of endobutton with tapes.

But no breakage observed. The advantage of our mechanical model was that the specimen can be used in different groups, which is statistically more interesting while minimizing the use of bodies given to science. In osteoporosis, parallel assembly of endo-button with threads behaved like a butter thread (Figure 1).

CONCLUSION

We suggest a cross assembly with an increase in the tapes width of the endobuttons.

REFERENCES

1. Tile M. *et al.,* J. Bone Joint Surg. Br. 70, 1–12. 1988.

2. Eastman JG. *et al.,*Injury. 47(8), 1707-1712.2016.

3. Chen L. *et al.*J., Acta Orthop. Belg.79, 54–59, 2013.

4. Böhler C. *et al.,* Injury. 53, 339-345, 2022.

5. Bremand F. et al. Photomechanics, 171-177, 1995

Ethic Declarations respected. No conflict of interest.

Acknowledgements to all bodies donors and their families, our monitors, all members of the ABS Laboratory and the Radiology Service of the Poitiers University.

Design of Nitrile-functionalised Poly(2-oxazoline)s as Novel and Versatile Platform for Drug Delivery System

Zihnil A. I. Mazrad,[a,#] Baptiste Schelle,[a] Joseph A. Nicolazzo,[a] Meike N. Leiske,[a] Kristian Kempe[a,b]*

[a]Drug Delivery, Disposition and Dynamics, Monash Institute of Pharmaceutical Sciences, Monash University, Parkville, VIC 3052, Australia

[b]Materials Science and Engineering, Monash University, Clayton, VIC 3800, Australia

* kristian.kempe@monash.edu, #zihnil.mazrad@monash.edu

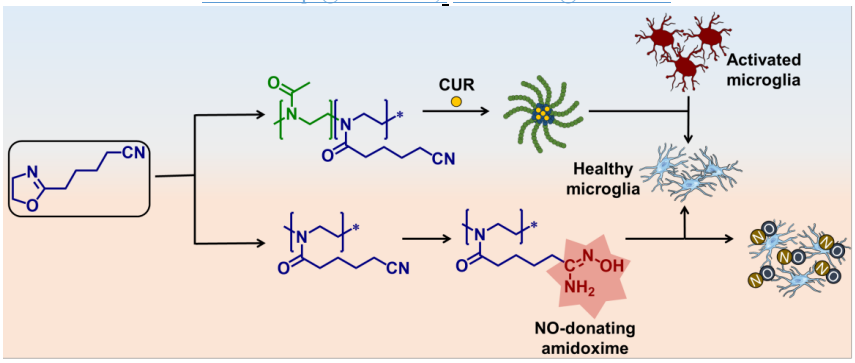

Figure 1. (a) Design of polymer from 2-(4-nitrile-butyl)-2-oxazoline for drug delivery system

INTRODUCTION

In recent years, polymers bearing reactive groups have received extensive attention due to their ability to incorporate active compounds and targeting moieties for biomedical application.[1] Several functional polymer platforms have been explored, which allow for the preparation of materials with tailored physicochemical and biological properties via post-polymerisation modifications (PPM). However, many functional groups are not compatible with the initial polymerisation because of their reactivity. The nitrile group is a highly interesting and relatively inert functionality, which has mainly received attention in radical polymerisations.[2] Here, we introduce a nitrile-functionalised 2-oxazoline monomer (2-(4-nitrile-butyl)-2-oxazoline; BuNiOx) and report its compatibility with the cationic ring-opening polymerisation as well as identify their suitability for applications in the biomedical research field.

EXPERIMENTAL METHODS

Polymers based on BuNiOx were designed with regard to the planned application (Figure 1): Homopolymers were synthesised and modified for optimal *in vitro* NO-release studies. Block copolymers of BuNiOx and 2-methyl-2-oxazoline (MeOx) were selected for the fabrication of micelles to encapsulate curcumin (CUR) *via* thin hydration method. Statistical copolymers of BuNiOx with the hydrophilic MeOx or the thermoresponsive EtOx were synthesised to study the temperature responsiveness of these materials. Here, statistical copolymers were chosen rather than a diblock system to avoid the formation of nanostructures upon increasing temperature.

RESULTS AND DISCUSSION

We have successfully synthesised a nitrile-functionalised 2-oxazoline monomer (2-(4-nitrile-butyl)-2-oxazoline; BuNiOx) and report its compatibility with the cationic ring-opening polymerisation. The versatility of nitrile-functionalised poly(2-oxazoline)s (POx) is also presented. To this end, diverse (co)polymers are synthesised and are shown to efficiently encapsulate the hydrophobic drug CUR in aqueous solution. The nitrile-functionalised POx/CUR formulation efficiently reduced inflammation in an activated BV-2 microglia model. Furthermore, the availability of the BuNiOx repeating units for PPM with hydroxylamine to yield amidoxime (AO)-functionalised POx is demonstrated. The AO-functionalised POx were shown to release nitric oxide (NO) in concentration dependent manner intracellularly in BV-2 microglia.

CONCLUSION

In conclusion, our findings reveal nitrile functionalised POx as a promising and robust platform for the design of polymer therapeutics for a wide range of applications.

REFERENCES

(1) Gauthier, M. A.; Gibson, M. I.; Klok, H. A. Synthesis of Functional Polymers by Post-Polymerization Modification. *Angew. Chem. Int. Ed. Engl.* **2009,** *48*, 48-58.

(2) Adegbola, T. A.; Agboola, O.; Fayomi, O. S. I. Review of Polyacrylonitrile Blends and Application in Manufacturing Technology: Recycling and Environmental Impact. *Results in Engineering* **2020,** 7, 100144.

ACKNOWLEDGMENTS

Z.A.I.M wishes to acknowledge Monash Graduate Scholarship.

Preparing biocompatible oligomers

Cordula Hege[1,2], Amy Stimpson[2], Helena Henke[1,2], Adam Dundas[1,2], Chris Fox[3], Derek Irvine[1,2*]

[1]Centre for Additive Manufacturing (CFAM), University of Nottingham, Nottingham, United Kingdom
[2] Chemical and Environmental Engineering/Faculty of Enginering, University of Nottingham, Nottingham, United Kingdom
[3] Access to Advanced Health Institute (AAHI), Seattle, USA
*corduld.hege@nottingham.ac.uk

.

INTRODUCTION

Oligomers can be useful for medical application like vaccine adjuvants. Methacrylic polymers are known to be widely tolerated in vivo, so they are widely used in biology and medicine. Due to that mainly methacrylic monomers were used to prepare the oligomers.

EXPERIMENTAL METHODS

Catalysed-chain transfer polymerisation (CCTP) an effective method to prepare oligomers. However, normally cobalt catalysts are used for that. As cobalt is toxic, this disadvantageous for medical applications. Iron is abundant in nature, with that more sustainable and it has a higher biocompatibility. Mainly the catalyst was prepared *in situ*. For that iron bromide and dimethyl glyoxime or diphenyl glyoxime were added as ligands. Different catalyst concentrations were used.

RESULTS AND DISCUSSION

The level of control is influenced by the reaction conditions, as well as the used monomers. One needs a higher amount of iron to control the reaction, than one would need for cobalt-catalysed reactions.
Still, iron catalysts were found to be a possible replacement for cobalt catalysts to perform CCTP. They allow to prepare reproducible, biocompatible oligomers. Further work will be done to optimise the conditions

CONCLUSION

Replacing the cobalt catalysts for iron catalysts in the CCTP will allow using this efficient method to prepare oligomers for medicinal and biological samples.

ACKNOWLEDGMENTS

This work was supported by both the National Institute of Allergy and Infectious Diseases, National Institutes of Health, Department of Human and Health Services under grant R01AI135673 and the EPSRC (EP/P031684/1) which supported the polymer mechanistic studies. Its contents are solely the responsibility of the authors and do not necessarily represent the official views of NIH/NIAID. They would also like to thank Professor Vernon Gibson for his discussion on iron based CCTP during prior collaborations with DJI.

Fully peptide-based nanomaterials by Aqueous Ring-Opening Polymerization Induced Self-Assembly (ROPISA) of N-Carboxyanhydrides

Hannah Beauseroy[1*], Chloé Grazon[1], Ségolène Antoine[1], Elisabeth Garanger[1], Sébastien Lecommandoux[1], Colin Bonduelle[1]
[1]Laboratoire de Chimie des Polymères Organiques UMR CNRS 5629, Univ. Bordeaux, Bordeaux INP, F-33600 Pessac, France.
[*] hannah.beauseroy@u-bordeaux.fr

INTRODUCTION

Peptide-based polymers are an emerging class of scaffolds adopting biomimetic behaviour by taking advantage of the wide variety of naturally available amino acids.[1] For instance, elastin-like polypeptides (ELPs), obtained by recombinant protein production, are thermosensitive polymers that hold many promises for biomedical applications and nanomedicine.[2] So far, the most economical and efficient process to prepare polypeptides is a one-step process based on the ring-opening polymerization (ROP) of N-carboxyanhydride monomers (NCA). We recently combined this ROP methodology to polymerization-induced self-assembly (PISA), a promising concept that enables both the synthesis of amphiphilic block copolymers and the formation of nano-objects at high solid content in a single step.[3] Using α-amino-polyethylene glycol (PEG-NH_2) as macromonomer in aqueous conditions, we successfully protected the NCA monomers from hydrolysis through a spontaneous *in situ* self-assembly that we named ROPISA.[4] We present here the synthesis of fully peptide nano-objects using this ROPISA process by using ELP as alternative macroinitiator. We made a proof-of concept study comparing the nanomaterials obtained from PEG-NH_2 and ELP with γ-benzyl-L-glutamate NCA (BLG-NCA) as a monomer.

EXPERIMENTAL METHODS

Typical synthesis of nanoparticles made of PEG-*b*-PBLG.[4] 2.7 mL of an ice-cooled solution of $NaHCO_3$ 0.05M containing the initiator PEG_{5k}-NH_2 (100mg, 0.02 mmol, [M]/[I] = 19) was added to the BLG-NCA powder (100 mg, 0.38 mmol) under a strong agitation (τ_s = 7%). The reaction is left to stir 1) first in an ice-cold water bath; 2) then at room temperature overnight. The opalescent dispersion obtained was then transferred to a 3.5kDa dialysis membrane and dialyzed against deionized water for 2 days. The nanoparticles were then observed by atomic force microscopy (AFM). An aliquot was dried to also characterize the copolymer by size exclusion chromatography (SEC).

Typical synthesis of nanoparticles made of ELP-*b*-PBLG. The synthesis was conducted in the same way by replacing PEG with ELPM40 (17035g.mol^{-1}).[5]

RESULTS AND DISCUSSION

In line with our recent work,[4,6] ROPISA of PEG with BLG-NCA led to well-defined amphiphilic copolymer with low dispersity as confirmed by SEC analyses (M_n=10100 g.mol^{-1}, $Đ$=1.09). The study of the nanoparticles produced upon ROPISA was achieved by AFM. Self-assembly was influenced by the secondary structure of the polypeptide, which tends to form α-helices when it reaches a length of 8–12 amino-acids.[6,7] As a result, an homogeneous population of needles-like nano-objects averaging 60nm long and 6nm in diameter were observed by AFM (Figure 1A). This first ROPISA was achieved at a 7 wt% solid content using a PEG concentration that was slightly above its CMC.

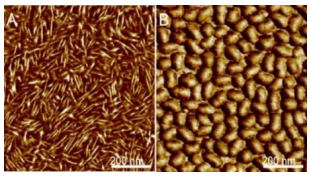

Figure 1: AFM images of needle and cocoon-like nanoparticles obtained upon aqueous ROPISA. (A) PEG-*b*-PBLG, (B) ELP-*b*-PBLG

We then achieved ROPISA from ELPM40. Since the CMC of ELP is ten times lower than that of PEG, the process was performed at 0.7 wt%. At this solid content, ELP aggregation was prevented and well-defined copolymers were obtained (SEC analysis: M_n=21900 g.mol^{-1}, $Đ$=1.03). AFM imaging showed unexpected cocoon-like nano-objects of about 40nm long, revealing the influence of the macroinitiator on the morphology (Figure 1B). This second morphology is hypothetically explained: i) by the larger size of the ELP hydrophilic block that could impose an increased interfacial curvature during self-assembly, ii) by possible H-bond interactions between ELP and BLG units.

CONCLUSION

In summary, we reported the one-pot synthesis and formulation of fully peptide-based nano-objects by using ELP in an original ROPISA process, This contribution highlights the robustness and versatility of ROPISA, enabling polymerization of different monomers[6] from different macroinitiators. As such, the use of ELP paves the way to a wide range of other macroinitiators.

REFERENCES

(1) Song, Z. *et al*., *Chem. Soc. Rev.* **2017**, *46* (21), 6570–6599.
(2) Le, D. H. T. *et al*., *Mol. Syst. Des. Eng.* **2019**, *4* (3), 545–565.
(3) Penfold, N. J. W. *et al*., *ACS Macro Lett.* **2019**, *8* (8), 1029–1054.
(4) Grazon, C. *et al*., *Angew.Chem.Int.Ed.*, **2020**, *59* (2), 622–626.
(5) Petitdemange, R. *et al*., *Biomacromolecules* **2017**, *18* (2), 544–550.
(6) Grazon, C. *et al*., *Polym. Chem*., **2021**, *12*, 6242–6251
(7) Goodman, M. *et al*., *Proc Natl Acad Sci U S A* **1969**, *64* (2), 444–450.

ACKNOWLEDGMENTS

The authors would like to thank the Agence Nationale de Recherche (ANR) (Grant No. ANR-20-CE06-0020-01) for providing financial support to this project.

Conducting Films Based on Biopolymers

Zdenka Capáková[1*], Daniela Jasenská[1], Věra Kašpárková[1], Jirí Pacherník[2]

[1]Centre of Polymer Systems, Tomas Bata University in Zlin, Zlin, Czechia
[2]Faculty of Science, Masaryk University, Brno, Czechia
[*] capakova@utb.cz

INTRODUCTION

Conducting polymers are well suited for the biomedical applications, where they can be used as stimuli-responsive components. Their combined electronic and ionic conductivity is fundamental for the communication with biological objects[1]. Among conducting polymers, polyaniline (PANI) is at the center of attention thanks to its easy synthesis, stability, reasonably high conductivity, and unique redox characteristics[2]. However, PANI itself possesses a quite high cytotoxicity[3]. However, it's composites with biomacromolecules should increase their cytocompatibility. Here, the component of extracellular matrix – sodium hylauronate (SH) and biocompatible, biadogradible and antibacterial polysaccharide – chitosan (CH) have been used for the preparation of conducting films. The physico-chemical and biological characteristics were determined. The cytocompatibility was studied using human induced pluripotent stem cells (hiPSCs).

EXPERIMENTAL METHODS

Films preparation

Films were prepared *in situ* in the colloidal mode according to procedure described previously[4]. Briefly, aniline hydrochloride and ammonium persulfate were dissolved in solution of SH or CH. Resulting solution was poured on the supports (polystyrene dishes and glass slides). The polymerization was completed within 4h for SH and the resulting films were designed as PANI-SH. In case of CH, polymerization takes 12h. Here, the procedure was repeated for two times to obtain thicker films and the films were assigned as PANI-CH.

Physico-chemical characterization

Contact angle measurements and determination of surface energy, FTIR analysis, atomic force microscopy (AFM; maximum surface heigh – Sz; surface roughness – Sa), and conductivity were involved to determine physico-chemical properties of prepared films.

Biological properties

For the determination of biological properties protein adsorption tests, the antibacterial testing and the cytocompatibility of hiPSCs (cell lines Neod1 and M67) were employed.

RESULTS AND DISCUSSION

Material characteristics are crucial for all biomaterial surfaces as they determine cells' fate on them. Composite films showed smoother topography compare to neat PANI film (Fig. 1). The presence of biopolymers did not decrease the conductivity which was comparable with the native PANI films.

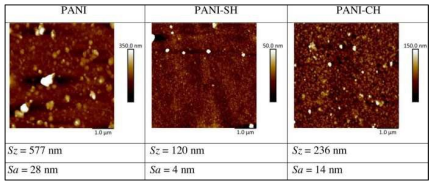

Fig. 1. AFM images of PANI, PANI-SH and PANI-CH.

The comprehensive biological tests suggest composite films as a suitable material for biomedical applications. The proteins were able to adsorb onto film surfaces. The sample PANI-SH also exhibited an outstanding antibacterial effect against the common gram-negative specie E. coli. Moreover, composite films exhibit unique properties in terms of their cytocompatibility with HiPSCs. Both used cell lines were able to adhere and proliferate on the surfaces. Further, the differentiation protocol led to cardiomyogenesis accompanied by the formation of spontaneously beating clusters of cardiomyocytes. The presence of cardiomyocytes was also confirmed by immunohistochemistry by the detection of cells positive to cardiomyocyte-specific sarcomeric α-actinin within cells growing on the films. The presence of beating clusters serves as the marker of the absence of embryotoxicity Thus, it is evidence that tested composite films do not induce embryotoxic effects.

CONCLUSION

Composite films of PANI and biopolymers afford an effective way how to prepare functional surfaces for the biomedical applications. The novel composite films revealed a range of excellent properties, especially great cytocompatibility, the absence of embryotoxicity, and reasonably good conductivity, comparable with pristine polyaniline.

The combination of studied properties such good conductivity, antibacterial activity and mainly great cytocompatibility with hiPSC opens wide application potential of these biopolymer-based composites.

REFERENCES

1. Capáková Z. *et al*., Mater. Sci. Eng. C. 113:110986, 2020
2. Bober P. *et al*., RSC Adv. 62:50328-50335, 2015
3. Humpolíček P. *et al*., Mater. Sci. Eng. C. 91:303-310, 2018
3. Kašpárková V. *et al*., Carb. Pol. 219:423-430, 2019

ACKNOWLEDGMENTS

This work was supported by OP RDE by the project The Development of Capacity for Research and Development of TBU in Zlin – CZ.02.269/0.0/0.0/16_028/0006243.

Woven PLA-PLA and PLA-PCL composites for biomedical applications

Carolina Pereira L. Costa[*] [1,2], Guillermo Domínguez[1,3], Jimena de la Vega[1], Cristina Pascual-González[1], Mónica Echeverry Rendón[1], Carlos González[1,3], Javier Llorca[1,3]

[1]IMDEA Materials, Universidad Carlos III de Madrid, Madrid, Spain
[2] RWTH Aachen University, Institut für Textiltechnik (ITA), Aachen, DE
[3] Department of Materials Science, Polytechnic University of Madrid, Madrid, Spain
[*] carolina.pereira@imdea.org

INTRODUCTION

Polylactide (PLA) and polycaprolactone (PCL) are biodegradable polymers, approved by US Food and Drugs Administration for medical purposes[1]. Textile structures, which can cover very wide ranges of degradation times, mechanical properties as well as the porosity, can be manufactured from these materials. As a result, they can be used in different biomedical applications associated with tissue regeneration, including bone, cartilage, ligaments, and skin. This investigation was aimed to assess the mechanical properties, degradation rate and biocompatibility of composites manufactured with PLA/PCL woven textiles consolidated by compression molding.

EXPERIMENTAL METHODS

Commingled yarns of high and low melting temperature PLA (PLA_{HM}-PLA_{LM}) were weaved (Narrow weaving Jakob Müller NH2 53) to produce a PLA-PLA dry fabrics. Laminates following the $[0°]_n$ stacking sequence were hot-pressed (Fontijne Grotnes, model TP400, the Netherlands) at 155°C with 2 MPa for 10 minutes. The same procedure was used to manufacture PLA-PCL materials in which PLA-PCL commingled yarns were mixed in a ratio of 1 to 3 to produce the woven fabric. To obtain the PLA-PCL composite panels, the later fabric was hot-pressed at 110°C with 2MPa and for 10 minutes. The melting point T_m and the glass transition temperature T_g were evaluated for PLA-PLA and PLA-PCL yarns by differential scanning calorimetry (DSC). The results were used to optimize the consolidation pressure and temperature cycle parameters used for the composite panels. The porosity of the consolidated textiles was analyzed by tomography inspections (GE Nanotom).
Regarding the mechanical behavior, uniaxial tensile tests were carried out following the guidelines presented in ISO/DIS52-4 and ISO 13934-1 standards. Following the ISO 13781, *in vitro* accelerated degradation tests in phosphate buffered saline (PBS) fluid at 50°C and pH 7.2 were performed. Changes in molecular weight, pH, and mass were monitored to analyse degradation. For biocompatibility evaluation, indirect (use of extracts) and direct tests were carried out with pre-osteoblast MC3T3 cells following the ISO 10993-5 and 10993-12 standards.

RESULTS AND DISCUSSION

The PLA-PLA and PLA-PCL dry woven fabrics presented an interconnected structure with a porosity of around 35 %. The PLA-PLA consolidated composite did not show relevant values of porosity; on the other hand, PLA-PCL composites had a highly porous structure because the quantity of PCL, that resulted to be the matrix, was not enough to wet the reinforcement (PLA). In terms of mechanical performance, the results obtained can be seen in the table I.

Table 1- Mechanical performance of the performed structures.

Materials	Ultimate strength (MPa)	Young modulus (GPa)
PLA-PLA composite	30	4
PLA-PCL composite	17.3	1.3
PLA-PCL weave	19	0.13

Concerning the cytotoxicity of PLA-PLA, the composite was biocompatible, a percentage of viability of 71%; the other composite, PLA-PCL, had the mitochondrial activity of 84% after the two dilutions (25% of the extract). The dry wovens, PLA-PLA and PLA-PCL, were subjected to the same cytotoxicity tests and presented 76 % (25% of the extract) and 83% (12,5% of the extract) mitochondrial activity. Such differences can be endorsed to the higher surface area ratio of the dry textiles compared with the consolidated composites. Lastly, the accelerated degradation test showed that after 45 days, the pH of the PBS solution dropped significantly and the weight of the samples. Sample debris was observed and indicated that, at this stage, the samples lost their mechanical integrity.

CONCLUSIONS

The present study shows that it is possible to tailor the properties of the materials by altering the manufacturing process parameters. By tuning the materials properties, it is possible to use them in a wider range of biomedical applications. Ongoing work will focus on the assessment of the biocompatibility and degradation of the material.

REFERENCES

1. Yao et al., Biomaterials 2017, 115.

ACKNOWLEDGMENTS

The authors would like to thank the European Union's Horizon 2020 research and innovation programme (Grant no: 813869) for providing financial support to this project.

Poly(ester urethane)s with Tunable Properties for the Additive Manufacturing of Tissue Engineering Scaffolds

Arianna Grivet-Brancot[1,2,*], Monica Boffito[1,3], Leonardo Mortati[4], Carla Divieto[4], Simona Bronco[3], Gianluca Ciardelli[1,3]

[1]Department of Mechanical and Aerospace Engineering, Politecnico di Torino, Torino, Italy
[2]Department of Surgical Sciences, Università di Torino, Torino, Italy
[3] Istituto per i Processi Chimico-Fisici, Consiglio Nazionale delle Ricerche, Pisa, Italy
[4]INRIM – Istituto Nazionale di Ricerca Metrologica, Torino, Italy
[*] arianna.grivet@polito.it

INTRODUCTION

The increasing use of innovative fabrication techniques in the medical field (e.g., additive manufacturing (AM)) has raised the need to develop biomaterials with specific characteristics to meet highly demanding technological and application-related requisites. In particular, biomaterial properties must combine printing requirements in terms of thermal and rheological properties with proper surface characteristics to promote tissue repair and regeneration. Moreover, the final construct mechanical properties at the macro- and micro-scale should match as much as possible those of the native tissue to trigger the correct biological response. To address all these issues, poly(urethane)s can be an interesting solution because of their LEGO-like chemical structure, that permits to tune their characteristics by changing the building blocks. In this work, novel poly(urethane)s (PURs) were developed starting from a poly(ester) diol, poly(ε-caprolactone) (PCL), a well-known poly(ester) commonly used in the biomedical field. The use of different chain extenders was exploited to adjust the thermal, mechanical and surface properties of the final polymers to open the way towards their use for different applications in the tissue engineering field.

EXPERIMENTAL METHODS

PUR synthesis was adapted from a previously developed protocol[1], using PCL-diol (2000 Da), 1,6-hexamethylene diisocyanate, and aliphatic chain extenders (i.e., 1,4-butanediol, 1,8-octanediol, 1,12-dodecandiol). Chemical characterization was conducted through Size Exclusion Chromatography (SEC) and Infrared (IR) spectroscopy. Differential Scanning Calorimetry (DSC), Thermogravimetric Analysis (TGA) and rheology were used to evaluate PUR suitability for Fused Deposition Modeling (FDM). Atomic Force Microscopy (AFM) measurements were performed on PUR samples obtained by spin coating to investigate polymer microstructure. Tensile tests were performed on solvent casted films to assess polymer mechanical properties at the macroscale, while indentation-type atomic force microscopy (IT-AFM) was used for microscale properties. Degradation kinetics of PUR films was also investigated in hydrolytic and enzymatic conditions.

RESULTS AND DISCUSSION

PUR synthesis was confirmed by IR spectroscopy and an average molecular weight of 30-40 kDa was detected for all PURs, independently of the chain extender. DSC and TGA analyses showed that all PURs could be processed with common AM techniques, but the presence of secondary crystalline phases, due to the PUR hard phase, became evident for longer chain extenders. Rheological results also showed a solid-to-liquid transition temperature increase with hard phase crystallization. From AFM measurements (Fig.1), the influence of the chain extender length on PUR microstructure was evidenced: the PUR hard phase was able to crystallize in more ordered lamellar crystals with a longer chain extender, while the shortest chain extender (i.e., 1,4-butanediol) resulted in a PUR with bigger crystals mostly due to PCL dispersed in an amorphous matrix. IT-AFM testing showed that the Young Modulus (E) varied within a wide range of values, thus confirming the presence of hard and soft phases in the microstructure. This difference was also evidenced in the mechanical properties at the macroscale: although the E value was in this case similar among the three PURs, the presence of a more ordered crystalline structure in the PUR with the longest chain extender (i.e., 1,12-dodecandiol) resulted in a more brittle material, while the lower phase separation between hard and soft segments in the PUR with 1,8-octanediol produced an evident plastic deformation. Finally, degradation in accelerated enzymatic conditions proved to be faster where PCL crystals where more prominent (i.e., PUR with 1,4-butanediol).

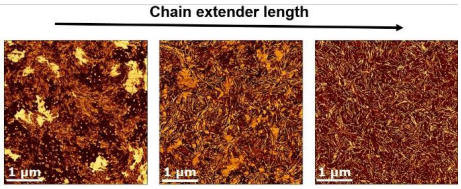

Fig. 1: AFM images of the microstructure of the three PURs.

CONCLUSION

A group of PCL-based PURs was successfully developed using different building blocks. Their suitability for scaffold production through AM was assessed and the possibility to tune PUR properties by changing one of the building blocks' characteristics (i.e., chain extender length) was evaluated to target different tissue engineering applications.

REFERENCES

1. Sartori S. *et al.*, React Funct Polym 73, 2013

Films of Covalently Crosslinked Hyaluronan as Resorbable Implants

Jiří Mrázek[1*], Jana Bažantová[1], Kristina Nešporová[1], Eva Kriváková[2], Martina Bajerová[2], Lukáš Kubala[2], Josef Chmelař[1]

[1]Contipro a.s., Dolní Dobrouč, Czechia
[2]Institute of Biophysics, Academy of Sciences of the Czech Republic, Brno, Czechia
[*] jiri.mrazek@contipro.com

INTRODUCTION

Crosslinked hyaluronan (HA) is an attractive material for tissue engineering applications due to its generally high biocompatibility and biodegradability. Here we present self-supporting films prepared from hyaluronic acid derivative with an aldehydic group in the position (6) of the glucosamine (HAOX; fig. 1). This modification allows simple crosslinking of the polymer with diamine linkers. Films with different degradation rates can be prepared by varying the crosslink density. We designed the films as resorbable implants.

EXPERIMENTAL METHODS

The hyaluronan derivative HAOX with a Mw of 0.8 MDa and a degree of substitution of 8 %, was prepared in-house[1]. Films of HAOX crosslinked with O,O′-1,3-Propanediylbishydroxylamine (POA) were prepared by solution casting[2,3]. The target thickness of dry film was set to 15 µm. Films were characterized by electron microscopy, swelling ratio, thickness homogeneity and in-vitro enzymatic degradation assay. Elastic modulus of hydrated films was evaluated by nanoindentation. Film properties before and after ethyleneoxide sterilization were compared. Film samples (15×15 mm) were then implanted into the abdominal cavity of C57Bl/6J mice to evaluate their safety and in-vivo degradation.

RESULTS AND DISCUSSION

Transparent and homogeneous films of crosslinked HAOX were successfully prepared (fig. 1). The ratio R of the amine groups of POA to the aldehyde groups of HAOX was varied from R = 0 to 1. The swelling ratio decreased with increasing R from over 5000 % to 500 %. The fully crosslinked film (R = 1) induced fibrotic reactions in-vivo, probably due to its high elastic modulus in hydrated state (0.8 MPa). To achieve optimal properties for the intended film application, low R ratios leading to much softer films (< 100 kPa) were needed. Films without crosslinker (R = 0) were fully resorbed after one day. Only gel-like remains of the film with R = 0.03 were present five days after implantation while fragments of the film with R = 0.1 were still found after 28 days, but without any adverse reaction (Fig. 2).

CONCLUSION

We prepared films from covalently crosslinked oxidized hyaluronan that can be used as resorbable implants. Unlike films from native hyaluronan which dissolve immediately after contact with wet surface, even the HAOX films without added crosslinker dissolve gradually, allowing convenient manipulation during implantation. Film in-vivo degradation time could be tuned from hours to weeks by varying the crosslink density. However, the film toughness should be kept comparable to the toughness of surrounding tissues to prevent mechanical irritation.

ACKNOWLEDGMENTS

Supported by the European Regional Development Fund – proj. INBIO (No. CZ.02.1.01/0.0/0.0/16_026/0008451)

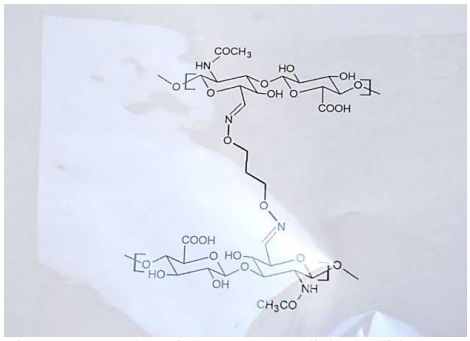

Fig. 1. Formula of HAOX crosslinked with POA photographed through a clear HAOX film 15 µm thick.

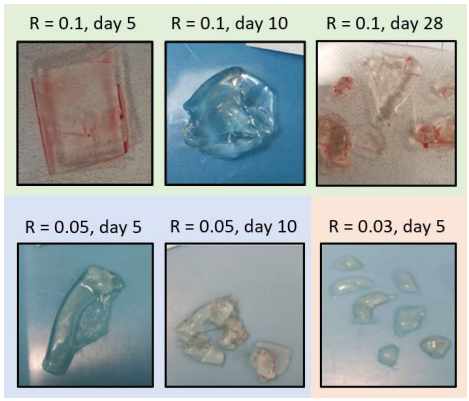

Fig. 2. Samples of HAOX films tested in-vivo extracted at various time points. Ratio of amino groups of the POA to the aldehyde groups of HAOX is indicated.

REFERENCES

1. Šedová P. *et al.*, Carbohydr. Res. 371:8-15, 2013
2. Chmelař J. *et al.*, Carbohydr. Pol. 224:115162, 2019
3. Mrázek J. *et al.*, Int. J. Bio. Macromol. 191:201, 2021

One-step generation of alginate-based hydrogel foams using CO2 simultaneously for foaming and gelation

Imene Ben Djemaa*[1,2], Stéphane Auguste[2], Leandro Jacomine[1], Malgorzata Tarnowska[2], Wiebke Dreckhan-Andreatta[1], Sébastien Andrieux[1]

[1]Bas-Rhin/ Institut Charles Sadron, University of Strasbourg, Strasbourg, France
[2] Côte-d'Or/Urgo Research Innovation and Development, Chenôve Cedex, France

*E-mail: imen.ben-djemaa@etu.unistra.fr

INTRODUCTION

The reliable generation of hydrogel foams remains an important challenge in a wide range of sectors including biomedical[1] or food[2] sectors. Using the example of alginate-calcium bicarbonate foams whose gelation relies on the pH-dependent solubility of the calcium bicarbonate, we introduce here a novel foaming method that uses CO_2 simultaneously for foaming and for acidification of the alginate solution to trigger gelation[3]. Diffusion and dissolution of the CO_2 from the foam bubbles into the alginate solution induces an interface-driven acidification of the pre-gelling solution (Figure 1). This allows a good matching of the foaming and gelation timescales via tuning the CO_2 content in the foaming gas, a very important criterion for an effective "liquid foam templating"[4]. We show that using this approach, gelled foams of different relative densities can be reliably generated in a simple one-step process.

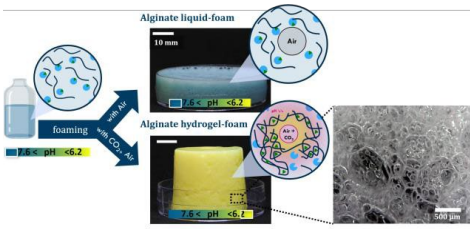

Figure 1: Illustration of our new one-step method for generating alginate-$CaCO_3$-based hydrogel foams using CO_2 for foaming and gelation. Foams with different foaming gases containing a pH-indicator dye (bromothymol blue): on top, a foam with pure air retains its initial blue colour (pH > 7.6) and remains liquid after pouring in a petri dish. On the bottom, a foam with CO_2/air= 50/50 changes colour from blue to yellow (revealing pH decrease down to ≤ 6.2) and retains the cylindrical structure of its container after being taken out.

EXPERIMENTAL METHODS

The foaming solution is composed of alginate (low viscosity alginate purchased from Alfa Aesar) mixed with $CaCO_3$ and the non-ionic surfactant Disponil APG 425. We produced the foams using the double-syringe technique which consists in mixing the foaming solution with the selected gas by repeatedly pushing between two syringes through a constriction[5]. We follow the acidification macroscopically using a pH responsive indicator. We investigate the role of CO_2 on foam ageing via foam stability measurements, and on the foam structure via optical macroscopy. Finally, we use interfacial rheology to put in evidence the gelation process initiated by the dissolution of the CO_2 from the bubble surface.

RESULTS AND DISCUSSION

We first show that, using the pH-dye indicator, introducing CO_2 to the gas phase induces homogeneous acidification (i.e., gelation). The hydrogel foams show a good resistance to compression. By tuning the CO_2 content in the foaming gas, we show that gelled foams of different relative densities can be reliably generated in a one-step process. This route has also proven to provide efficient stabilisation against all foam ageing mechanisms. Finally, interfacial rheology shows a fast gelation kinetics, with a gelation front following the diffusion front of CO_2.

CONCLUSION

We report, for the first time, the generation of alginate-based hydrogel foams using the foaming gas as the gelation trigger in a simple one-step process. We also show that interfacial rheology allows to put in evidence the interface-driven gelation. Both approaches, gas-initiated gelation and interfacial rheology for their characterization, can be transferred readily to other types of gases and formulations.

REFERENCES

1. J. Baxter *et al*., J. Cardiothorac. Surg. 15:1–8, 2020.
2. L. Ma *et al*., Adv. Mater. Interfaces, 6 :1900417, 2019.
3. S. Andrieux, W Drenckhan. FR3102364/ WO2021084200, 2019.
4. I. Ben Djemaa *et al.,* ACIS, 294 : 102479, 2021.
5. T. Gaillard et al., Int. J. Multiph. Flow, 96 : 173-187, 2017.

ACKNOWLEDGMENTS

We acknowledge discussions with Dr Laurent Apert, Dr François Schosseler, and Algaia team.
We acknowledge funding from an ERC Consolidator Grant (agreement 819511 - METAFOAM), from URGO supported by CIFRE ANRT (agreement n° 2019/1150) and from the Interdisciplinary Institute HiFunMat of the University of Strasbourg, CNRS and Inserm (ANR-10-IDEX-0002 and SFRI STRAT'US ANR-20-SFRI-0012).

Protein-based Nanoformulations Loaded with Active Principles For The Management of Brain Tumors

Catalin Zaharia[1*], Ionut-Cristian Radu[1], Mircea Teodorescu[1], Bianca Galateanu[2], Madalina Necolau[1], Ariana Hudita[2], Eugenia Tanasa[3]

[1]Advanced Polymer Materials Group, University Politehnica of Bucharest, Bucharest, Romania
[2]Department of Biochemistry and Molecular Biology, University of Bucharest, Bucharest, Romania
[3]University Politehnica of Bucharest, Bucharest, Romania

[*] zaharia.catalin@gmail.com, catalin.zaharia@upb.ro

INTRODUCTION

The field of nanotechnology has developed rapidly in the last decade with a major impact on the biomedical field[1]. Various nanoparticles including gold, magnetic, lipid and polymeric are prepared and targeted on brain cancer diagnosis and therapy[2]. Brain tumors are life-threatening conditions characterized by low survival rate and a high annual incidence of primary malignant brain tumors. Among them, Glioblastoma remains one of the most lethal cancers in humans with a median survival after maximal therapy of less than two years after first diagnosis. Despite improvements in the past few decades with intraoperative surgical techniques, chemotherapy, and radiation therapy, predictable curative treatment for glioblastoma is not fully developed. Some unconventional therapies including immunotherapy, gene and photodynamic therapy are potential adjuvant treatments for brain tumors. Referring to nanotechnology, this involves the design, synthesis, and application of materials with at least one dimension in the size range of 1–100 nm. Nanoparticles (NPs) have large surface to volume ratios that leads to high loading capacity. At the same time, NPS have shown to improve drug solubility, prolong blood circulation half-life, and control drug-release. Modern polymeric nanocarriers can be designed and developed by combining protein engineering tool with top techniques of polymer growth. Therefore, living/controlled radical polymerization is a powerful tool able to shape novel polymeric nanoformulations based on proteins.

EXPERIMENTAL METHODS

Novel sericin-based nanoformulations have been developed based on the grafting functionalization of silk sericin with synthetic side chains (Poly(2-dimethylamino ethyl methacrylate)). Silk sericin had a macroinitiator role while the synthetic chains generate the side chains such as a brush-like structure. The sericin was firstly modified with an alkyl halogen to provide the growing sites for the poly(2 dimethylamino ethyl methacrylate) chains. In this respect, atom transfer radical polymerization (ATRP) was employed. The polymerization technique can control the growth of the side chains resulting in a brush-like structure. Furthermore, the grafted sericin was used to prepare small size polymeric nanocarriers by nanoprecipitation. In this regard, solutions of grafted silk sericin were precipitated into a non-solvent to generate self-assembled polymeric structures. Drug loading (ganciclovir, ribavirin) and release tests were performed by drug dissolution into the grafted silk sericin media followed by the self-assembling step. The morphological investigation is a key procedure to reveal the nanocarriers' size, size distribution and shape as major characteristics. These important features and differences between the nanocarriers generated by the two synthesis conditions were shown through SEM and DLS. These nanocarriers were further tested for their *in vitro* biocompatibility and cytotoxic potential effect on human glioblastoma cells cultured in a modern microfluidic device. The biological investigations performed in this view highlighted the cells viability and proliferation potential under the treatment of the cells with pristine nanocarriers, drug-loaded nanocarriers as compared with a reference treated with the simple drug and with an untreated sample. These investigations were done using fluorescence microscopy and spectrophotometric assays such as MTT and LDH activity measurements.

RESULTS AND DISCUSSION

Silk sericin-based nanoformulations have shown narrow size distribution with low size and significant differences considering the synthesis conditions. The drug release tests revealed an expected behavior considering the pH conditions. The biological assessment revealed that the pristine nanocarriers did not display cytotoxic effects on the cells, while the drug loaded delivery systems exerted similar toxic effects as the drugs alone.

CONCLUSION

In conclusion, we reported here the development of novel protein-based nanocarriers able to deliver various drugs with potential benefits for the central nervous system cancer management (glioblastoma). The nanocarriers were successfully investigated in terms of morphology, size distribution, drug release behavior and biological assessment. Further *in vivo* tests will be employed to check the efficiency of drug-loaded sericin nanocarriers on the treatment of glioblastomas.

REFERENCES

1. Ramos A.P. *et al.*, Biophys Rev. 9(2):79-89, 2017.
2. Gregory J.V. *et al.*, Nature Communications 11:5687, 2020.

ACKNOWLEDGMENTS

This work was supported by a grant of the Ministry of Research, Innovation and Digitization, CNCS/CCCDI – UEFISCDI, project number PN-III-P4-ID-PCE-2020-1448, within PNCDI III.

Towards Thymidine-based Low Molecular Weight Oleogelators (LMWO) biomaterials

Arthur Klufts-Edel[1*], Bérangère Dessane[1], Fanny Caffin[2], Philippe Barthélémy[1], Christophe Piérard[2], Sylvie Crauste-Manciet[1], Valérie Desvergnes[1]

[1]Equipe ChemBioPharm, INSERM U1212, UMR 5320 CNRS-Université de Bordeaux, Acides nucléiques : Régulations Naturelles et Artificielles (ARNA), 146 rue Léo Saignat, Bat. Pharmacie 3ième tranche, 4ième étage 33076 Bordeaux cedex, France
[2]Département Toxicologie et Risques Chimiques, Institut de Recherche Biomédicale des Armées, 1 Place Général Valérie André - B.P. 73 91223 Brétigny-sur-Orge Cedex, France

[*]arthur.klufts-edel@u-bordeaux.fr

INTRODUCTION

Nature offers a wide range of hybrid molecules all with an incredible richness of properties. Among them, nucleolipids (NLs)[1] contain one nucleoside part (or nucleotide) and one fatty chain linked by a covalent bond making them amphiphilic. Several synthetic biocompatible and biodegradable NLs were found to display astounding self-assembly abilities upon weak interactions allowing the formation of numerous supramolecular networks including gels.[2] They have been investigated for many applications and draw growing attention in drug delivery for release control and rise formulation's stability.[3] Supramolecular oleogels[4] (continuous oily phase) have received less interest than hydrogels (continuous aqueous phase) and yet, they represent a major issue in medicine to convey lipophilic drugs which are numerous in the pharmacopoeia. Previous work[5] have shown that the incorporation of a hydrophobic group on a thymidine skeleton allows its solubility in oil medium by increasing the lipophilicity. Based on macroscopic observations, we have performed a rational synthetic approach to study the relationship between structure and gelation ability.

EXPERIMENTAL METHODS

^{1}H NMR and ^{13}C NMR were recorded on a Bruker Avance 300 (^{1}H: 300 MHz, ^{13}C: 75.46 MHz) spectrometer using residual $CHCl_3$ as an internal reference (7.26 ppm) and at 293 K unless otherwise indicated. Fourier transform infrared (FT-IR) spectra were recorded on a PerkinElmer FT spectrometer Spectrum two (UATR two). High resolution mass spectra (HRMS) data were recorded on a microTOF spectrometer equipped with orthogonal electrospray interface (ESI). Rheological measurements were performed on a Kinexus® Pro+ rheometer (Malvern Instruments Ltd., Orsay, France) with steel cone-plate geometry (angle: 1°, diameter: 20 mm).

RESULTS AND DISCUSSION

We successively studied - the influence of the nature of the covalent bond, - the influence of the nature of the hydrophobic group (especially the influence of groups which can generate π-stacking), as well as - the influence of the length of the carbonated fatty chain.

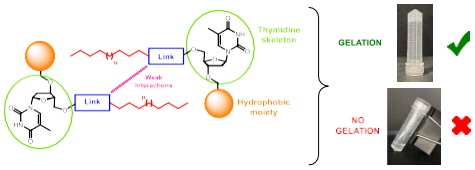

The first elements of a structure/gelling capacity rationalization could be formulated and will be presented herein. The resulting Thymidine-based supramolecular biomaterials will also be described.

CONCLUSION

A better understanding of the gelation process at a molecular level is crucial to rationalize the design and the conception of LMWO materials and would be of major interest for the development of innovative formulations for drug delivery.

REFERENCES

1. Rosemeyer H. *et al*., Chem. Biodivers. 2:977-1062, 2005
2. Baillet J. *et al.* Adv. Mater. 30:1705078, 2018
3. Weiss R.G. J. Am. Chem. Soc. 136:7519-7530, 2014
4. Dassanayake, L.S.K. *et al.* Current Opinion in Colloid Interface Science 16:432-439, 2011
5. Cunha A. *et al.*, ACS Omega 5:5815-5823, 2020 ; Brouillard M. *et al.* Front. Chem. 9:736554, 2021

ACKNOWLEDGMENTS

ESB is thanked for organization of this event. The authors would like to thank INSERM, CNRS and University of Bordeaux for their support. Arthur Klufts-Edel warmly thanks AID («Agence de l'Innovation de la Défense») for PhD fellowship.

3D Printable Supramolecular Self-Assembling β-Sheet Peptide and Tyramine-Modified Hyaluronan Hydrogels with Immunomodulatory Properties

Jacek K. Wychowaniec[1*], Charlotte J.C. Edwards-Gayle[2], Ezgi Irem Bektas[1], David Eglin[3], and Matteo D'Este[1]

[1]AO Research Institute Davos, Clavadelerstrasse 8, 7270, Davos, Switzerland
[2] Diamond Light Source, Harwell Science and Innovation Campus, Fermi Avenue, Didcot, OX110DE, United Kingdom
[3] Mines Saint-Étienne, Univ Lyon, Univ Jean Monnet, INSERM, U1059 Sainbiose, Saint-Étienne, France

* jacek.wychowaniec@aofoundation.org

INTRODUCTION

Delayed or severed tissue regeneration is often caused by compromised immune system[1]. One solution to tackle this issue is to design immunomodulatory biomaterials that support tissue regeneration by reprogramming immune system to a pro-regenerative state[2]. It has been shown that high molecular weight (>1000 kDa) hyaluronic acid (HA) can re-polarize macrophages to an M2 pro-regenerative phenotype, whereas low molecular weight HA leads to retention of a pro-inflammatory M1 phenotype[3]. Designing functional materials that incorporate immunomodulatory effects, biocompatibility and allow stable long-term polarization of macrophages is of high interest in tissue engineering and 3D bioprinting[2].

EXPERIMENTAL METHODS

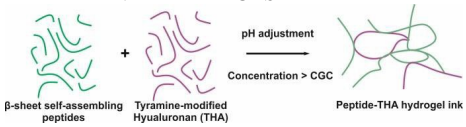

***Figure 1**. Schematic representation of the peptide-THA hydrogel formation.*

Here we designed a selection of hydrogels built from self-assembling β-sheet forming peptides[4] and immunomodulatory tyramine-modified HA (THA)[5], that can be processed by 3D micro-extrusion printing (**Fig. 1**). A selection of peptide sequences was based on the alternation of hydrophobic and hydrophilic amino acids: **DABACABACD** (**A**: hydrophobic residue: **F** phenylalanine or **Y** tyrosine, **B**/**C**: hydrophilic residue e.g.: **K** lysine or **E** glutamic acid), stemming from the known parental **FEFKFEFK** sequence and it subsequent modifications[4]. Self-assembly and gelation of all designed sequences were evaluated using oscillatory rheology, Fourier transform infrared spectroscopy (FTIR) and small angle X-ray scattering (SAXS). THA of two molecular weights (280 kDa and 1640 kDa) was synthesized as previously described[5]. The successful THA synthesis was confirmed using ^{1}H-NMR and UV-Vis spectroscopy.

RESULTS AND DISCUSSION

A parametric study was carried out on the designed selection of **DABACABACD** peptides to verify the effect of rational peptide sequence modification on final physicochemical properties of composite hydrogels. **D** residues were rationally varied between hydrophobic (**Y**) or hydrophilic (**E**) amino acids to modulate the interactions ability of formed β-sheet edges and shell with other peptide fibres and THA. All parental peptides self-assemble into semi-flexible networks and hydrogels above critical gelation concentration in the region of 2.5-5 mM, display characteristic high β-sheet content and controllable rheological properties (**Fig 2.**).

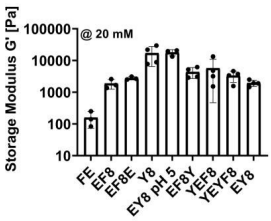

***Figure 2**. Storage modulus (G') for different designed peptide hydrogels measured at 0.2% strain and 1 Hz frequency.*

CONCLUSION

Self-assembly and rheological properties of both peptide and peptide-THA hydrogels can be controlled by the choice of primary peptide sequence, fabrication technique and final crosslinking mechanisms including enzymatic (HRP, H_2O_2) and visible green light crosslinking using Eosin. By controlling the crosslinking mechanisms, concentration and ratio of peptide to THA, overall viscoelasticity can be modulated. Selection of hydrogels were characterised by shear-thinning behaviour and rapid recovery allowing extrusion-based fabrication of scaffolds for immunomodulatory tissue engineering.

REFERENCES

1. Shan, B. *et al*. *Nature Immunology* **2017**, *18*, 519.
2. Walsh, C. M. *et al*. *Pharmacology & Therapeutics* **2021**, 108043.
3. Rayahin, J. E. *et al*. *ACS Biomaterials Science & Engineering* **2015**, *1* (7), 481-493.
4. Wychowaniec, J. K. *et al*. *Biomacromolecules* **2020**, *21* (6), 2285-2297.
5. Loebel, C. *et al*. *Biomacromolecules* **2017**, *18* (3), 855-864.

ACKNOWLEDGMENTS

This work was supported by the European Union's Horizon 2020 (H2020-MSCA-IF-2019) research and innovation programme under the Marie Skłodowska-Curie grant agreement 893099 — ImmunoBioInks.

Electrospun PNIPAAm-based fibers for pH- and thermo-responsive localized drug release

Adriana Gonçalves[1], Miguel Castilho[2, 3], João Paulo Borges[1], Paula I. P. Soares[1]

[1] CENIMAT | i3N, Department of Materials Science, NOVA SST, Caparica, Portugal
[2] Department of Biomedical Engineering, Technical University of Eindhoven, Eindhoven, the Netherlands
[3] Department of Orthopedics, University Medical Center Utrecht, Utrecht, the Netherlands
* aml.goncalves@campus.fct.unl.pt

INTRODUCTION

Poly(N-isopropylacrylamide) (PNIPAAm) is a biocompatible polymer that exhibits a negative temperature response with a lower critical solution temperature (LCST) of around 32 ºC. The transition temperature of PNIPAAm, along with the conformational change that comes with it makes this polymer particularly interesting for biomedical applications such as controlled drug release, biosensing and tissue engineering [1]. An important and requirable characteristic of thermosensitive polymers for applications in biomedical applications is the possibility of tuning the LCST to values near or above physiological temperature. In the present work we hypothesize that PNIPAAm copolymerization with hydrophilic monomers, like acrylic acid and acrylamide, can be used to increase its transition temperature. To test this hypothesis we explored the use of RAFT polymerization to synthetize different PNIPAAm based copolymers. Reversible addition fragmentation transfer (RAFT) polymerization (Fig. 1) was used, since it provides well-defined polymers with targeted molecular weights and narrow molecular weight distributions [2].
Finally, the produced PNIPAAm based copolymers with a LCST near physiological temperature were used as fiber template in electrospinning technique to produce thermoresponsive fibrous scaffolds for drug delivery applications.

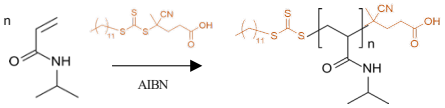

Figure 1 - Scheme of RAFT polymerization of PNIPAAm.

EXPERIMENTAL METHODS

PNIPAAm based copolymers were synthesized by RAFT polymerization. NIPAAm was used as a monomer and acrylic acid (AAc) and acrylamide (AAm) were used as co-monomers. 2,2'-Azobis(isobutyronitrile) (AIBN) and 4-cyano-4- [(dodecylsulfanylthiocarbonyl) sulfanyl] pentanoic acid (CDTP) were used as an initiator and chain transfer agent (CTA), respectively. Different monomer ratios were studied. Electrospinning technique was used to produce pH- and thermosensitive fibers using the previously obtain copolymers and the membranes were later crosslinked to increase their water stability.

RESULTS AND DISCUSSION

pH- and temperature-responsive copolymers were designed and prepared by reversible addition fragmentation transfer polymerization. Successful copolymerization with AAc and AAm was confirmed through FTIR and ^{1}H NMR analysis. The LCST of PNIPAAm based copolymers in different pH mediums was determined. PNIPAAm-AAm copolymers showed an increase in the LCST with the increase in AAm content, independent of the pH value of the medium. In contrast, PNIPAAm-AAc copolymers showed a pH-dependent thermosensitive behavior where the transition temperatures rises with AAc content at pH 6.5 and 7.4 but it decreases at pH 4.5. pKa of acrylic acid is 4.7, which means that at lower pH values (e.g 4.5) most of the carboxylic groups of AAc are protonated. This leads to a higher hydrophobicity of AAc segments in a more acidic medium, therefore, lowering the LCST [3]. Stress test were performed to evaluate the mechanical parameters of the membranes. The swelling ability of the membranes was also evaluated in different pH medium.
Contact angle assays were performed with different pH solutions and showed a decrease in the hydrophilicity of the surface of the membrane when heated to temperatures above their LCST, confirming the pH- and thermoresponsive behavior of the fibers.

CONCLUSION

PNIPAAm based thermoresponsive copolymers were successfully synthesized via RAFT polymerization. The LCST of PNIPAAm was tuned to temperatures near human body temperature through the copolymerization with hydrophilic monomers such as acrylic acid and acrylamide. The obtained copolymers were successfully electrospun and gave rise to pH- and thermoresponsive fibers which opens great opportunities for controlled and localized drug release.

REFERENCES

[1] A. Gonçalves, F. V. Almeida, J. P. Borges, and P. I. P. Soares, Gels **7**, (2021).
[2] K. Nieswandt, P. Georgopanos, M. Held, E. Sperling, and V. Abetz, Polymers (Basel). **14**, (2022).
[3] X. Gao, Y. Cao, X. Song, Z. Zhang, C. Xiao, C. He, and X. Chen, J. Mater. Chem. B **1**, 5578 (2013).

ACKNOWLEDGMENTS

This work is co-financed by FEDER, European funds, through the COMPETE 2020 POCI and PORL, National Funds through FCT—Portuguese Foundation for Science and Technology and POR Lisboa2020, under the project POCI-01-0145-FEDER-007688, reference UIDB/50025/2020-2023. Adriana Gonçalves acknowledges the Portuguese Foundation for Science and Technology (FCT) for the PhD grant with reference 2021.06558.BD.

Nano-doped piezoelectric hydrogels and low-intensity pulsed ultrasound boost the chondrogenic differentiation of human adipose tissue-derived stromal cells

Leonardo Ricotti[1,2,*], Diego Trucco[1,2,3], Lorenzo Vannozzi[1,2], Andrea Cafarelli[1,2], Cristina Manferdini[3], Elena Gabusi[3], Paolo Dolzani[3], Yasmin Saleh[3], Marta Columbaro[4], Gina Lisignoli[3]

[1] The BioRobotics Institute, Scuola Superiore Sant'Anna, Pisa, Italy
[2] Department of Excellence in Robotics & AI, Scuola Superiore Sant'Anna, Pisa, Italy
[3]SC Laboratorio di Immunoreumatologia e Rigenerazione Tissutale, Istituto Ortopedico Rizzoli, Bologna,Italy
[4]Direzione Scientifica, IRCCS Istituto Ortopedico Rizzoli, Bologna,Italy
[*] leonardo.ricotti@santannapisa.it

INTRODUCTION

In the field of cartilage tissue engineering, the development of scaffolds capable of providing an instructive biomimetic environment to effectively drive mesenchymal stem cells (MSCs) differentiation remains a major challenge, at present[1]. Hydrogels have emerged as promising biomaterials for this purpose, due to their biocompatibility and ability to mimic the tissue extracellular matrix. However, new solutions are needed to effectively direct the differentiation of MSCs, especially the ones derived from the adipose tissue (ASCs), which are poorly effective in engrafting and reconstituting the deteriorated cartilage tissue[2,3].

In this study we investigated the chondrogenic differentiation of ASCs embedded in a novel hydrogel doped with graphene oxide (GO) nanoflakes and piezoelectric barium titanate nanoparticles (BTNPs), periodically stimulated with low-intensity pulsed ultrasound, using a dedicated set-up enabling a precise control of the energy dose at the target.

EXPERIMENTAL METHODS

Human adipose mesenchymal stromal cells at $2 \cdot 10^6$ cells/mL were embedded in a 3D VitroGel RGD® hydrogels (TheWell Bioscience), without nanomaterials (controls) or doped with 25 µg/mL of GO nanoflakes and 50 µg/mL of BTNPs.

Hydrogel properties were tested in terms of: (1) rheological properties and printability; (2) injectability; (3) adhesion force to the cartilage tissue, performed on ex vivo bovine cartilage samples; (4) degradation time in PBS, PBS + lysozime (120 µg/mL to simulate an inflamed environment) and in synthetic synovial fluid.

The hydrogels were exposed to LIPUS stimulation (frequency: 1 MHz, intensity: 250 mW/cm^2, duty cycle: 20%, pulse repetition frequency: 1 kHz, stimulation time: 5 min) every 2 days, until day 10 of culture. Samples were chondrogenically differentiated for 2,10 and 28 days. At each time point cell viability (Live&Dead), cytotoxicity (LDH), gene expression of collagen type 2 (COL2), aggrecan (ACAN), SOX9, and collagen type 1 (COL1), electron microscopy, histology and immunohistochemistry (COL2, aggrecan, SOX9, and COL1) were evaluated.

RESULTS AND DISCUSSION

Results highlighted an alginate-like nature of the hydrogel, with piezoelectric BTNPs having a diameter of ~ 60 nm (Figure 1a). Rheometric measurements highlighted a shear-thinning behavior (Figure 1b). However, the hydrogel resulted poorly printable. Injectability was good, with force values compatible with ISO 7886-1:2018 (Figure 1c). Interestingly, the nanomaterials increased considerably the hydrogel adhesion to the cartilage tissue (Figure 1d). The hydrogel completely degraded in 3 months (Figure 1e).

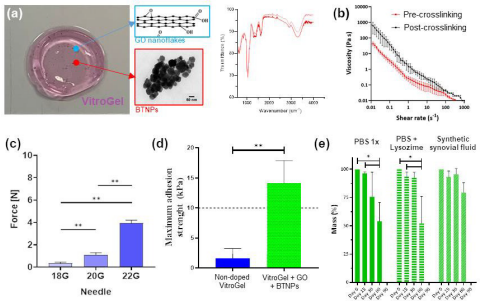

Figure 1: Results of the nano-doped hydrogel characterization.

Ultrasound stimulation considerably boosted the chondrogenic differentiation of ASCs laden in 3D piezoelectric hydrogel: COL2 (Figure 2), aggrecan and SOX9 were considerably overexpressed, while the fibrotic marker COL1 decreased, compared to control samples (non piezoelectric hydrogels and piezoelectric hydrogels not stimulated with LIPUS).

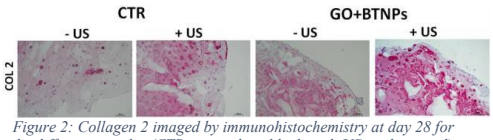

Figure 2: Collagen 2 imaged by immunohistochemistry at day 28 for the different samples (CTR = non-doped hydrogel, US = ultrasound).

CONCLUSION

These results suggest that the ultrasound stimulation of ASCs encapsulated in piezoelectric hydrogels represents a promising paradigm for cartilage regeneration.

REFERENCES

1. Gaharwar A.K. *et al*., Nat. Rev. Mater. 5: 686-705, 2020
2. Martin I. *et al*., Sci. Transl. Med. 11: eaat2189, 2019
3. Zha K. *et al*., npj Regen. Med. 6: 1-15, 2021

ACKNOWLEDGMENTS

This work received funding from the European Union's Horizon 2020 research and innovation program, grant agreement No 814413, project ADMAIORA (AdvanceD nanocomposite MAterIals fOr in situ treatment and ultRAsound-mediated management of osteoarthritis).

Biocompatible DLP resins with programmable shape memory

A.A. Aldana*, T. Kuhnt, R. Marroquin-Garcia, L. Moroni, M. Baker

Department of Complex Tissue Regeneration, MERLN Institute for Technology Inspired Regenerative Medicine, Maastricht University, P.O. Box 616, 6200 MD Maastricht, The Netherlands

a.aldana@maastrichtuniversity.nl

INTRODUCTION

Among the additive manufacturing techniques, light-based fabrication like Digital Light Processing (DLP) results in high-resolution and fast printing times. DLP has been recently explored in regenerative medicine owing to high accuracy to print complex scaffolds like vascular branches [1, 2]. However, the development of customizable biodegradable and biocompatible resins remains a bottle-neck. On the other hand, shape memory polymers (SMPs), with the capability to change the shape in response to an external stimulus, have a great potential for applications in biomedical devices such as vascular grafts and cardiovascular stents [3]. The development of SMPs may open up new possibilities for designing novel devices such as tissue scaffolds, sensors, minimally invasive procedures, self-tightening degradable sutures, drug delivery systems, among others. Here, we aim to explore novel biodegradable copolymers for modulating the shape memory properties of printed structures, using the body temperature as a triggered stimulus.

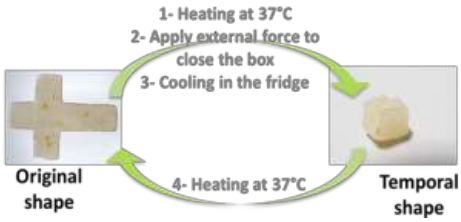

Figure 1. ***Copolymers could change their shape at body temperature****. Scheme of heat-cold-warm cycle.*

EXPERIMENTAL METHODS

Copolymers with different copolymer composition were synthesized and characterized. To evaluate the effect of end groups on shape memory properties, two different end-capping acrylates were explored. Photopolymerizable copolymers were characterized by nuclear magnetic resonance (^{1}H-NMR and ^{13}C-NMR), gel permeation chromatography (GPC) and differential scanning calorimetry (DSC). For DLP printing, resins were prepared by adding a photoinitiator. Open box structures (original shape) were printed and the shape memory properties were explored by a cold-warm cycle. An external force was applied to get the desired configuration (closed box, temporary shape) and it was fixed by cooling. The shape recovery was explored in a water bath at 37°C.

RESULTS AND DISCUSSION

A series of 4 copolymers was synthesized and characterized. The copolymer composition, degree of polymerization and molecular weight were determined by ^{1}H-NMR. The degree of acrylation was 42% and 76% for method 1 and 2, respectively. The molecular weight for the samples were around 4000 Da. GPC analysis showed that copolymers presented dispersities in the range of 1.1 to 1.6. According to DSC data, the melting point of all photocrosslinked resins was around 35°C. The cold crystallization peak (in the range of -17 to 8°C) was also observed on all samples, which is attributed to the larger amount of amorphous monomer disrupting crystallization. All printed structures were capable to adopt a temporal shape (close box) after cooling and recover their original shape after heating. The differences in composition affect the recovery time at 37°C, being faster with higher amount of amorphous monomer in the copolymer. Furthermore, the shape recovery was also tested at 40 and 50°C. The higher temperature resulted in the faster shape recovery. We were able to show simple delivery of a payload from within the 3D printed objects, triggered by body temperature.

CONCLUSION

The synthesis of the copolymers has allowed us to explore these DLP polymerizable resins with programmable shape memory. So far, the printed structures have shown quick shape recovery, even more than one cycle, at body temperature. The current results lend these cytocompatible, biodegradable polymers well to further in vitro and in vivo testing of DLP printed scaffold for soft and medium-soft tissue regeneration.

REFERENCES

1. Mota C., *et al.*, Chemical Reviews, 120, 19, 10547-10607, 2020.
2. Chartrain N.A., *et al.,* Acta Biomaterialia, 74, 90-111, 2018.
3. Chan B.Q.Y., *et al.*, ACS Applied Materials & Interfaces, 8, 16, 10070-10087, 2016.

ACKNOWLEDGEMENTS

This research has been made possible with via support of NWO (Innovation Fund Chemistry, project "DynAM" under project agreement 731.016.202), and the Dutch Ministry of Economic Affairs.

Firefly-Bioinspired Hydrogels with Redox-responsiveness as Cell-encapsulating Injectable Matrices

Minye Jin[1,2,3*], Alisa Gläser[1], Supun W. Mohotti[1], Julieta I. Paez[1,3]
[1] INM – Leibniz Institute for New Materials. Campus D2-2, 66123, Saarbrücken, Germany.
[2] Chemistry Department, Saarland University. 66123, Saarbrücken, Germany.
[3] University of Twente. Drienerlolaan 5, 7522 NB, Enschede, The Netherlands.
[*]m.jin-1@utwente.nl

INTRODUCTION

Cell-encapsulating hydrogels are biomaterials used as extracellular matrix mimics for basic study of cell function, high-throughput drug screening, and delivery of therapeutics. To facilitate their adaptability for diverse applications, there is a need for hydrogel crosslinking strategies that are smart, flexible, and user-friendly. Recently, firefly-bioinspired hydrogels for 3D cell culture based on the coupling reaction between cyano-benzothiazole (CBT) and cysteine (Cys) groups were reported[1]. These hydrogels showed good cyto-compatibility and high mechanical and biochemical tunability. However, this initial molecular design showed some limitations that complicated its formulation as injectable matrices. This is relevant to expand the use of these hydrogels into therapeutic delivery scenarios. Thus, the aim of this work is to develop firefly-inspired hydrogels further as injectable and stimuli-responsive materials. It is envisioned that the incorporation of redox-triggering property to the design of poly(ethylene glycol) (PEG) hydrogel networks is the key to solve the mentioned limitations (Fig. 1a). When macromers denoted as PEG-Cys(SR), bearing protected Cys groups, are mixed with PEG-CBT macromers; no gel formation occurs because the protecting group at the Cys blocks its reactivity. Upon the addition of a biocompatible reductant, the protecting group is cleaved, exposing a Cys group, and the crosslinking reaction is triggered on demand. In this work, the relevant molecular and environmental parameters, necessary to trigger the onset of gel formation and to achieve biomaterials with tailorable properties, are investigated.

EXPERIMENTAL METHODS

4-arm, 10 and 20 kDa PEG-CBT[1] and PEG-Cys(SR) (R=Et, tBu)[2] macromers were synthesized. Tris(2-carboxyethyl)-phosphine (TCEP), dithiothreitol (DTT) and glutathione (GSH) were used as biocompatible reactants. PEG (3-10 wt%) and reductant solutions (12-40 mM) were prepared in HEPES buffer, pH 7-8 at mild temperature (25-37ºC); and used for hydrogel preparation. The effect of molecular parameters (structure of the Cys protecting group, reductant type) and environmental parameters (pH and temperature), over gelation kinetics and final mechanical strength of the hydrogels was investigated by shear rheology, before and after swelling. Gel cytocompatibility was studied by encapsulating human mesenchymal stem cells (hMSCs) for 1 day and analysing cell viability via live/dead assay.

RESULTS AND DISCUSSION

Redox-triggerable hydrogels were prepared under physiological conditions, demonstrating controlled onset of the crosslinking reaction and efficient gelation kinetics. Rheological results revealed tunable gelation times, spanning from ca 15 s to ca 15 min, which is convenient for injectability purposes. Gelation rate depended on the choice of molecular and environmental parameters of the system. At the molecular level (Fig. 1b), a smaller protecting group at the Cys site and a stronger reductant, resulted in faster-curing gels. Environmental parameters such as higher pH and higher temperature, also lead to faster-curing materials. Gel mechanics was not affected upon variation of protecting group, reductant, or pH; whereas it was impacted by temperature. Moreover, hydrogels showed good cyto-compatibility, evidenced by high cell viability of encapsulated hMSCs (Fig. 1c). Finally, preliminary experiments, where a mixture of both PEG precursor solutions was injected into a reductant-containing bath enabled high control of the gelation onset, indicating that this platform is promising as injectable and extrusion-based bioprinting formulations.

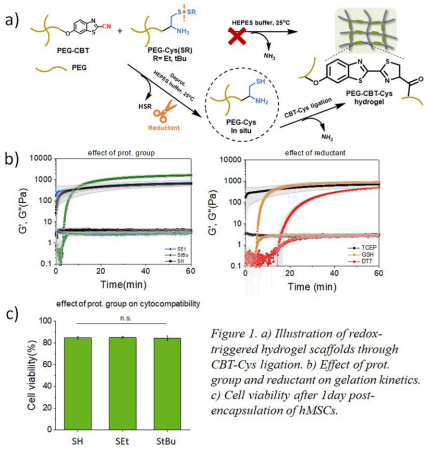

Figure 1. a) Illustration of redox-triggered hydrogel scaffolds through CBT-Cys ligation. b) Effect of prot. group and reductant on gelation kinetics. c) Cell viability after 1day post-encapsulation of hMSCs.

Firefly-bioinspired hydrogels with redox-triggerable properties were developed, thus expanding their application versatility as injectable biomaterials. The molecular and environmental parameters to control materials properties were elucidated. These matrices are expected to become valuable for tissue engineering.

REFERENCES

1. Jin, M. *et al*., ACS Appl. Mater. Interfaces 14, 5017-5032, 2022.
2. Liang, G. *et al.*, Nat. Chem. 2, 54-60, 2010.

ACKNOWLEDGMENTS

The authors thank DFG's support (proj. no. 422041745).

Stimuli-responsive face mask-based on electrospun nanofibers

Mohammad Ali Haghighat Bayan[1*], Chiara Rinoldi[1], Paweł Nakielski[1], Filippo Pierini[1]

[1]Institute of Fundamental Technological Research, Polish Academy of Sciences, Warsaw, Poland
[*] mbayan@ippt.pan.pl

INTRODUCTION

Environmental pollutants and pathogens have been made issues for human health, especially in the recent pandemic situation.[1] Filtering facepieces are the most common way to protect inhalation from ambient pollutants. Available protective devices have some issues that can be solved to present a higher shield against harmful matters and provide smart features.[2]

The main problem of surgical masks is the low efficiency of filtration. Furthermore, reusability and disinfection properties can also be achieved by proposing stimuli-responsive capability, like the photothermal antimicrobial surface.

EXPERIMENTAL METHODS

Electrospray of Au nanorods

The electro-spraying technique deposited Au nanorods (NRs) over the face masks. The alcosols of Au NRs were prepared in different concentrations. The ratio of gold NRs colloid in the utilized solutions varied from 1:5 to 1:50 volume ratio. Optimization of the Au NRs concentrations was carried out by employing laser irradiation and studying the effect of the laser.

Fabrication of Electrospun face mask

To create a nanofibrous layer over the commercial surgical face mask, a solution of 12% (v/v) of polyacrylonitrile (PAN) in N, N-dimethylformamide was electrospun. The thickness of the electrospun layer is optimized by implementing a filtration efficiency test and scanning electron microscope to achieve the desired structure. PAN 10 and PAN 20 refer to 10 and 20 minutes of electrospinning over the face mask.

RESULTS AND DISCUSSION

Filtration Efficiency

The filtration efficiency of the filtering facepieces was performed by the use of NaCl aerosols (0.3 am). This analysis was conducted to compare the commercial face masks filtration with the modified masks (Figure 1a). Electrospun PAN nanofibers layer leads to a decrease in the pore sizes of the mask compared to the commercial masks (Figure 1b). The proposed structure of the masks showed an impressive enhancement in the performance of the protective devices.

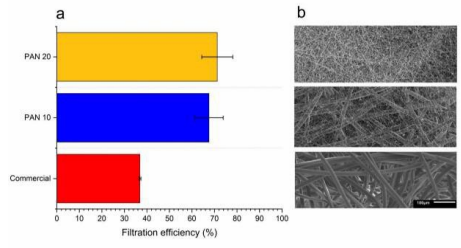

Figure 1. Distinctive features and structures of the produced face masks. a) Filtration efficiency test of the electrospun face masks shows two times increase in the efficiency. b) SEM images of the different obtained masks` structures (microscope images located in front of the corresponding diagram).

Photothermal Activity

Stimuli-responsivity of fabricated electrospun gold treated face masks investigated by a thermo-optical setup (Figure 2a). After electro-spraying Au NRs over the mask, upon laser exposure, the plasmonic photo-responsivity drives to increase the outer layer's temperature (ΔT=20°C; Final T: 45°C - Figure 2b). The analysis of the response of the smart masks to the laser beam was conducted over the different concentrations of the Au NRs (Figure 2c).

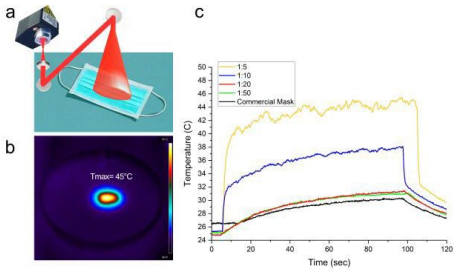

Figure 2. Photo-responsive electrospun masks, a) Schematic of triggering laser to the sample. b) Thermographic image of the heat generation of the mask. c) Monitoring the temperature of the face masks with the different concentrations of the Au NRs by triggering the laser.

CONCLUSION

The study demonstrated that electrospun nanofibers could double the filtration efficiency over the commercial face mask. Also, by employing Au NRs, it made out that the electrospun mask will turn into a smart photo-responsive protective equipment that can potentially eliminate the pathogens. This new characteristic may lead to on-demand sterilizable masks that can be fruitful in the pandemic situation.

REFERENCES

1. Utkal A *et al*., Environmental Research. 203:111839, 2022
2. Kumar, P et al., Applied Materials & Interfaces. 13: 12912-12927, 2021

ACKNOWLEDGMENTS

This work was supported by the National Science Centre grant no. 2020/38/E/ST5/00456.

Study of Dual Cross-linking of Alginate Based Hydrogels for Biomedical Application

Michel Habib[1*], Steve Berthalon[1], Audrey Tourrette[2], Tahmer Sharkawi[1], Sebastien Blanquer[1]
[1]ICGM, Univ Montpellier, CNRS, ENSCM, Montpellier, France
[2]CIRIMAT - UMR5085, University Toulouse III, Toulouse, France
[*] michel.habib@umonpellier.fr

INTRODUCTION

Alginate hydrogels are interesting candidates for medical applications due to their versatility and biocompatibility[1]. They are commonly obtained by either physical crosslinking in Ca^{2+} rich solutions or by photo-crosslinking after chemical modification[2]. However, very limited literature reports the influence of the dual crosslinking (chemical and physical) on the alginate hydrogels properties.
In this work, we investigate the properties of the double crosslinked alginate hydrogels in terms of swelling, mechanical self-healing properties as well as a mean to induce shape deformation.

EXPERIMENTAL METHODS

1) Chemical modification and hydrogel preparation
Chemical modification is done on two sodium alginate sources: high and low molecular weight.
Methacrylated alginates with different degrees of methacrylation (DM) were obtained by reacting sodium alginate with methacrylic anhydride under vigorous stirring. The finale methacrylated alginate is obtained after precipitation in acetone, dialysis against water and freeze-drying. The DM is calculated from ^{1}H-NMR.
Hydrogels were obtained by curing the pregel mixture (modified alginate and the photoinitiator) under UV irradiation.
2) Swelling behavior and mechanical testing
The swelling behavior of the hydrogels was studied in different medias (water, PBS) as function of the DM. Tensile testing was used to determine the stiffness of the hydrogel networks.
3) Dual crosslinking and self-healing
The reversible dual crosslinking was observed by cycling swelling between $CaCl_2$ and EDTA solutions. It is also used as a tool to induce self-healing and shape morphing. Tensile testing and lapshear were used to determine the efficienctiveness of the self-healing property.
4) Biocompatibility was tested using Fibroblast L929 cells.

RESULTS AND DISCUSSION

1) Degree of methacrylation
The DM defined as the number of methacrylate groups per sugar moiety can be tuned by varying the equivalent of methacrylic anhydride added or by adjusting the reaction time.
2) Swelling behavior and mechanical testing
After UV irradiation of the modified alginate, it was observed that both the equilibrium swelling degree and the mechanical properties are observed to be dependent on the DM. Where, higher DMs lead to lower swelling degrees and improve the stiffness of the system.
3) Dual crosslinking and self-healing
Upon submerging in Ca^{2+} solution, the dual crosslinking can be observed by the shrinkage of the hydrogels in addition to an improvement in the mechanical properties. The reversibility of the ionic crosslinking can be attained by altering between $CaCl_2$ and EDTA solutions over several cycles.

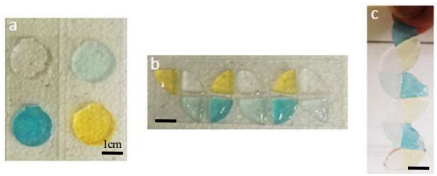

Figure 1. Self-healing test of Alg-MA hydrogels; (a) different coloured hydrogels (b) cut in quarters and (c) self-healed in snake-like architecture suspended in air. Scale bare = 1cm.

The reversible ionic crosslinking can be used as a mean to induce self-healing in alginate hydrogels. When a hydrogel is cut, the pieces can be rearranged and fixed (healed) to obtain more complex architectures as shown in figure 1. Lapshear and tensile testing confirms the effectiveness of the self-healing.
The difference in the swelling behaviour between the chemical crosslinked hydrogel and the dual-crosslinked one can be used to trigger a 3D deformation. By patterning a chemical hydrogel strip with ionic crosslinking at specific sections, folding, twisting or curling motions can be obtained.
4) Application
Given the biocompatibility of the alginate hydrogels, they have great potential for wound dressing or therapeutic tissue engineering.

CONCLUSION

The ability of alginate to complex with multivalent ions can be used as a mean to introduce a secondary reversible crosslinking. This dual crosslinking was seen to be a simple and viable tool to add a self-healing property in alginate hydrogels, to tune their swelling and mechanical properties and to induce shape deformation.

REFERENCES

1. Teng, K. *et al*., ACS Biomater. Sci. Eng. 2021, 7, 1302−1337
2. Hasany, M. *et al*., Applied Materials Today 2021, 24, 101150.

ACKNOWLEDGMENTS

The authors would like to thank Institute Carnot Chimie Balard Cirimat (ICCBC) for providing financial support.

Black phosphorus-incorporated hybrid nanomaterials as a theragenerative platform for bone tissue engineering

Ashkan Bigham [1], Ines Fasolino [1], Carmen Valente [2], Gabriele Turacchio [2], Maria Caporali [3], Luigi Ambrosio [1], Maria Grazia Raucci [1]

[1]Institute of Polymers, Composites and Biomaterials, National Research Council (IPCB-CNR), Naples, Italy

[2]Institute of Endocrinology and Experimental Oncology "G. Salvatore" -National Research Council (IEOS-CNR), Naples - Italy

[3]Institute of Chemistry of Organometallic Compounds -National Research Council (ICCOM-CNR), Sesto Fiorentino - Italy

ashkan.bigham@ipcb.cnr.it

INTRODUCTION

Biomaterials endowed with therapeutic and regenerative (theragenerative) properties are of particular interest recently[1]. Black phosphorus (BP) nanomaterials have shown very promising potential in cancer therapy through their intrinsic anticancer activity through arresting G2/M phase leading to apoptosis, photothermal therapy (PTT), and photodynamic therapy[2,3]. Bioactive glass (BG)-based biomaterials are very reputable in bone tissue regeneration with stimulating effects on osteogenesis[4]. The present study has focused on designing a new organic-inorganic theragenerative biomaterial through a two-step synthesis strategy for bone cancer therapy and regeneration.

EXPERIMENTAL METHODS

The carrier composed of Pluronic F127, bioactive glass, and BP nanosheets was synthesized through sol-gel method and then exposed to microwave irradiation. The samples then have undergone drying in an incubator followed by being rinsed with deionized water. The hybrids were characterized through SEM, TEM, Raman spectroscopy, NMR, FTIR, and XRD.

RESULTS AND DISCUSSION

Since oxidation weakens BP's photothermal properties, it turned out that the hybrid was successfully obtained with no oxidation of encapsulated BP. The microwave irradiation led to turning BP nanosheets into BP quantum dots (BPQDs). Moreover, it increased the chemical stability of hybrid and homogeneously distributed calcium ions throughout the structure. The hybrid with various concentrations were put against osteosarcoma cells; the existence of BP led to anticancer activity while the same concentration without BP had no cytotoxicity. Moreover, the PTT potential of BP and BPQDs-loaded hybrids was assessed *in vitro* through exposing to NIR irradiation. The generation of heat as the result of light irradiation even reinforced the anticancer activity of the hybrids.

CONCLUSION

A novel theragenerative platform was synthesized without affecting the BP optical properties. The hybrid selectively inhibited cancer cells proliferation thanks to sustain release of BP nanomaterials while stimulating the healthy cells growth. In overall, this hybrid can be a promising theragenerative candidate for bone cancer therapy and regeneration.

REFERENCES

1. B. Chen, et al. Advanced Functional Materials. 30:2002621, 2020.
2. W. Zhou, et al. Angewandte Chemie International Edition. 58:769–774 2019.
3. M.G. Raucci, et al. ACS Applied Materials and Interfaces. 11:9333–9342 2019.
4. E. Sharifi, et al. Advanced Science. 9:2102678 2022.

ACKNOWLEDGMENTS

Funds provided by Progetto MIUR PRIN2017–ACTION, Grant N. 2017SZ5WZB.

Methylcellulose-based responsive hydrogels for controlled delivery of silver nanoparticles

Lorenzo Bonetti[1], Andrea Fiorati[1,2], Agnese D'Agostino[1,2], Carlo Maria Pelacani[1], Roberto Chiesa[1,2], Silvia Farè[1,2], Luigi De Nardo[1,2]

[1]Department of Chemistry, Materials and Chemical Engineering "G. Natta", Politecnico di Milano, 20131, Milan, Italy
[2]National Interuniversity Consortium of Materials Science and Technology (INSTM), Florence, 50121, Italy
* lorenzo.bonetti@polimi.it

INTRODUCTION

Cellulose-silver nanoparticles (AgNPs) composites have recently gained significant consideration. In fact, the distinctive properties of cellulose (e.g., biodegradability, biocompatibility, and non-toxic nature)[1] can be combined with the possibility of cellulose to act as a surface capping agent when the metal nanoparticles are embedded into it[2,3].
On this topic, methylcellulose (MC) has been reported to produce MC–silver nanocomposite films[2,3]. However, the possibility of a stimulus-responsive delivery of AgNPs from MC films has never been explored before. Here, MC–AgNPs nanocomposite films were obtained via a one step *in situ* synthesis process. The obtained films were crosslinked with citric acid (CA)[4] and characterized. Furthermore, the possibility of a pH-triggered release of AgNPs from the nanocomposite films was evaluated with the aim of developing systems with enhanced antibacterial activity in alkaline conditions (e.g., infected chronic wounds).

EXPERIMENTAL METHODS

MC hydrogels (8 % w/v in 50 mM Na_2SO_4) were prepared and crosslinked with CA at three different crosslinking degrees (CLDs): low (MC-L), medium (MC-M), and high (MC-H)[4]. Pristine hydrogel (MC) was used as control. The thermo- and pH-responsiveness of the samples was assessed by swelling and rheological tests, carried out on the samples swollen in normal saline solution (NSS) at different pH (4, 7, 12) and temperatures (25, 37, 50 °C). MC-H samples were further investigated due to their remarkable pH-responsive behavior. ^{1}H-NMR spectrometry was exploited to disclose the mechanism of pH-responsiveness. Afterwards, MC–H-AgNPs nanocomposite films were prepared via AgNPs in situ synthesis using MC as capping agent[2]. The shape, size, and distribution of AgNPs were assessed by TEM and UV-vis measurements. Lastly, the possibility of pH-triggered release of AgNPs from the obtained films was assessed by ICP and UV-vis measurements.

RESULTS AND DISCUSSION

Swelling tests at pH 4 (***Fig. 1A***) revealed a decrease in the swelling rate (SR) of the samples by increasing the CLD[4]. Conversely, at pH 12 (***Fig. 1B***) all the samples displayed no differences in terms of SR as a function of the CLD. Rheological tests confirmed, from a mechanical point of view, the results obtained via swelling/degradation tests: samples swollen at pH 12 displayed a significant reduction in G', which was more marked as the CLD increased. These characterizations disclosed the possibility to exploit pH variations to control the fate of the crosslinked MC samples.

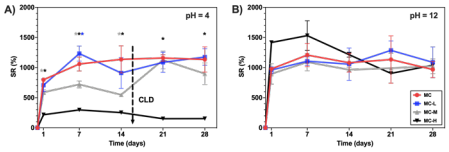

Fig. 1 *– SR (%) vs. time of MC samples in NSS, at 37 °C, at A) pH = 4 and B) pH = 12.*

Given their distinctive pH-responsiveness, MC-H samples where further investigated. ^{1}H-NMR spectrometry revealed that the pH responsiveness of MC-H samples was ascribable to alkaline hydrolysis (at pH 12) of the ester bonds in the crosslinked samples. Therefore, MC-H samples were selected as potential platforms for the pH-triggered release of AgNPs. MC-H-AgNPs samples were thus prepared, obtaining AgNPs with a diameter of 12.2 ± 2.8 nm (***Fig. 2A***) exploiting MC as a surface capping agent[1].
Interestingly, a selective release of AgNPs in the swelling media was confirmed by UV-vis measurements, displaying a characteristic resonance peak at 410 nm[2] at pH 12 (no peak was detected at pH 4). In addition, ICP analyses confirmed a selective Ag release, which was found to be ~ 10 times higher at pH 12 than at pH 4 (***Fig. 2B***).

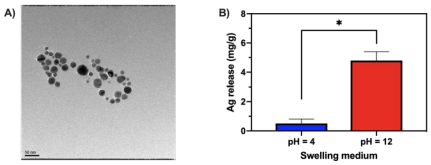

Fig. 2 *– A) AgNPs image (scalebar = 50 nm) and B) Ag release (mg_{Ag}/g_{MC}) from MC-H-AgNPs samples as a function of pH obtained by ICP analyses.*

CONCLUSION

MC–AgNPs nanocomposite films were here disclosed as potential candidates for the controlled delivery of AgNPs. Such systems could provide a distinctive advantage for those applications where an antibacterial activity is desirable at alkaline pH (e.g., infected chronic wounds).

REFERENCES

1. Klemm D. *et al.*, Angewandte chemie international edition. 44.22: 3358-3393, 2005
2. Maity D. *et al.*, Carbohydr. Polym. 90.4:1818-1825, 2012
3. Kolarova K. *et al.*, Jpn. J. Appl. Phys. 56.6S1: 06GG09, 2017
4. Bonetti L. *et al.*, Soft Matter 16: 5577-5587, 2020

3D-printing of Smart Hybrid Multifunctional Bioinks and their Application in Disease Modelling

Uxue Aizarna-Lopetegui[1], Carlos Renero-Lecuna[1,2], Clara García-Astrain[1,2], Luis Liz-Marzán[1,2,3], Malou Henriksen-Lacey[1,2], Dorleta Jiménez de Aberasturi[1,2,3]

[1]CIC biomaGUNE, Basque Research and Technology Alliance (BRTA), 20014 Donostia-San Sebastián, Spain.
[2]Centro de Investigación Biomédica en Red de Bioingeniería Biomateriales, y Nanomedicina (CIBER-BBN), 20014 Donostia-San Sebastián, Spain.
[3]Ikerbasque Basque Foundation for Science, 48009 Bilbao, Spain.
*uaizarna@cicbiomagune.es

INTRODUCTION

3D printing of biomaterials combined with living cells and stimuli-responsive materials can be used to fabricate complex in vitro models which mimic the natural environment, thereby aiding our understanding of the underlying mechanisms of native tissue functions and pathophysiology[1,2]. In this work we explore the design of organic-inorganic hybrid printable inks comprising polymers/hydrogels with embedded gold nanorods (AuNRs). Specifically, we chose AuNRs with a Localized Surface Plasmon Resonance (LSPR) at ca. 780 nm, in resonance with an 808 nm laser which thus allows local plasmonic heating effects to take place upon irradiation. The combination of plasmonic AuNRs with thermoresponsive polymers thus offers the possibility to tailor the local heating of the nanocomposite material by changing AuNR concentration or irradiation properties, resulting in an ink which can undergo physical contractile and expansion changes. Our aim is to mimic the physical changes to which arterial cells are exposed during the pulsatile blood flow process. Finally, endothelial cells contained in bioinks can be 3D printed with a controlled spatial distribution on top of our hybrid inks, thereby achieving a 3D arterial model in which physical forces can be modeled.

EXPERIMENTAL METHODS

Hybrid ink formulations based on N-Isopropylacrylamide (NIPAm) - Poly(ethylene Glycol Diacrylate) (PEGDA), dissolved in solutions containing AuNRs of varying concentrations, were synthesized to form a stimuli-responsive layer. The cell-containing bioink was constructed from gelatin methacryloyl (GelMA)-alginate based biocompatible formulations to provide a matrix for living cells. 3D bioprinting of multilayer constructs was achieved using a multi-headed 3D Discovery bioprinter (RegenHU, Switzerland) (Figure 1). Each bioink formulation was characterized in terms of rheological and structural properties, printability, and cell viability. Stimuli response experiments were carried out using a multi-modal 808 nm laser.

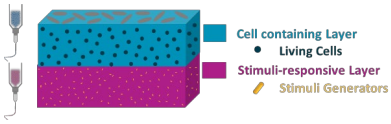

Figure 1: Schematic representation of multilayered 3D bioprinted systems based on the stimuli-responsive nanocomposite material and a cell containing bioink.

RESULTS AND DISCUSSION

AuNRs were synthesized using previously reported methods[3] and incorporated into a NIPAm based thermoresponsive ink for the fabrication of the stimuli-responsive ink. By pulsing the laser source, a fast and reversable change in temperature, in the biological range of 20 - 40°C, could be induced in the hybrid ink. The hybrid ink was biocompatible and continued to show thermoresponsive properites after printing of bioinks ontop. All bioinks tested were compatible with the tested cell lines, presenting a homogenous cell distribution with high cell viability and stability after printing (≤ 3 weeks). The rheological properties revealed that all the studied formulations showed a typical yield stress-like response at low applied strains with a dominant (elastic) solid-like response, characteristic of hydrogel-based materials. Structural characterization of the inks was performed by Scanning Electron Microscopy (SEM), confirming a uniform porosity, which is essential for the adequate diffusion of oxygen and nutrients in biological samples.

CONCLUSION

Multilayer models based on smart-hybrid living bioinks that present appropriate rheological properties with a highly porous structure were fabricated by 3D-printing. The introduction of plasmonic AuNPs within polymeric networks provides the system with multifunctionality including responsiveness to external stimuli. The living bioinks composed of GelMA-Alginate are biocompatible and provide a suitable environment for cell growth, up to at least 3 weeks.

REFERENCES

1. Skylar-Scott MA. *et al*., Sci. Adv. 5(9), 2019
2. Zhu K. *et al.,* Adv. Funct. Mater. 27(12), 2017
3. Scarabelli L. *et al*., J. Phys. Chem. Lett.6(21), 2015

ACKNOWLEDGMENTS

Financial support was provided by the the Spanish State Research Agency (Project PID2019-108854RA-I00), European Research Council (ERC-AdG-2017# 787510) and the European Commission (EUSMI). This work was performed under the Maria de Maeztu Units of Excellence Program from the Spanish State Research Agency – Grant No. MDM-2017-0720. Uxue Aizarna would like to thank the Basque Government for a predoctoral fellowship (PRE-2021-1-0041).

Topography-induced modulation of cell behaviour by alumina ceramic textiles

Deepanjalee Dutta[1], Titinun Nuntapramote[1], Kurosch Rezwan[2], Dorothea Brüggemann[1]

[1]Institute for Biophysics, University of Bremen, Otto-Hahn-Allee 1, 28359 Bremen, Germany
[2] Advanced Ceramics, University of Bremen, Am Biologischen Garten 2, 28359 Bremen, Germany
*ddutta@uni-bremen.de

INTRODUCTION

Substrate topography as well as changes in the physical microenvironment of cells play a major role in cell adhesion and cytoskeletal changes, thereby influencing intracellular signaling and other cellular properties.[1] In particular, scaffold porosity is known to influence cellular integration into a host tissue, which is especially important for wound healing. Therefore, we studied how 3T3 fibroblasts and HaCaT keratinocytes interact with microporous alumina textiles as a potential scaffold material for wound repair.

EXPERIMENTAL METHODS

Alumina textiles (Zircar Ceramics Inc., USA) were cleaned by 5 min immersion into piranha solution and stored dry after washing with deionized water.

To study the metabolic cell activity on the textiles, adherent NIH 3T3 mouse fibroblasts and HaCaT keratinocytes were used. After 24h, 72h and 120h of cultivation, presto blue assay was performed in triplicates for each substrate type.

For subsequent cell morphology analysis, actin filaments and cell nuclei were stained with iFluor phalloidin 647 (AbCam) and Hoechst (NucBlue Live ReadyProbes Reagent, Thermo Fisher Scientific) for 30 min, respectively, mounted and imaged using an inverted fluorescence microscope (Ti-E− V5.30, Nikon, Tokyo, Japan). The morphology of the textiles and the fixated cells was further studied with SEM using previously described method.[2]

For immunostaining of fibronectin and E-cadherin, cells were grown for 72h. Then the cells were fixed by 30 min fixation in 4% PFA, permeabilized with 0.1% TritonX-100, and blocked by non-specific binding blocking buffer (0.3M glycine and 1% BSA in 1X PBS), for 1hr. Then, the respective primary antibody was applied and incubated overnight at 4°C. Thereafter, the respective second antibody was used for 1hr at 4°C in the dark. The samples were then stained with Hoechst for 15 mins and imaged with our inverted fluorescence microscope.

RESULTS AND DISCUSSION

The ceramic textiles supported the adhesion of keratinocytes and fibroblasts up to 120h in culture and growth on textiles was comparable to the growth on standard tissue culture (TC) plates. For HaCaTs, on microporous alumina textiles a distinct difference in morphology was observed compared to standard TC plates and alumina-coated glasses. On alumina textiles, HaCaTs exhibited an elongated cell shape while they grew in clusters on both reference substrates. Moreover, the unique woven topography of the alumina textiles induced visible changes in the actin cytoskeleton, as observed by phalloidin staining. SEM analysis further revealed that HaCaTs had formed multiple contact points along the filaments of the alumina textiles hence inducing changes in the cell morphology and adhesion pattern. Fibroblasts also adhered well to microporous alumina textiles and grew along individual filaments yet with minimal changes in their morphology compared to TC plates and alumina coated glass. Inspired by the differences in HaCaT morphology, further analysis of protein expression in keratinocytes on alumina textiles revealed upregulation of fibronectin expression followed by downregulation of E-cadherin. 3T3 fibroblasts on the other hand showed negligible changes in protein expression. The observed differences in the expression of cell-specific maker proteins in HaCaTs indicate that topography-induced changes in cell adhesion might be related with the epithelial-mesenchymal transition (EMT) of epithelial cells, which could be beneficial in respect to tissue regeneration during wound healing. In the future, it will be highly interesting to explore if inorganic ceramic textiles can trigger beneficial cell signaling pathways in addition to supporting cell growth.

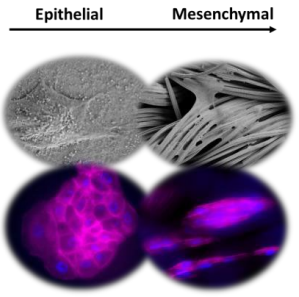

Figure 1: Topography-induced changes in cell behavior by alumina textiles.

CONCLUSION

In summary, our results suggest that microporous alumina textiles, although being an inorganic biomaterial, are very attractive scaffolds for skin tissue engineering. In the future, the observed topography-driven induction of possible EMT-like behavior of keratinocytes on alumina textiles could potentially promote native wound repair mechanisms.

REFERENCES

1. Mihalko, E. P. *et al.,* ACS Biomaterials Science and Engineering 4, 1149–1161,2018.
2. Dutta, D. *et al*., ACS Appl. Bio Mater. 4, 2, 1852–1862,2021.

ACKNOWLEDGMENTS

We acknowledge funding via the Emmy Noether Program (grant no 267326782) and the RTG MIMENIMA (GRK 1860) of the German Research Foundation.

Zinc loaded L-Carnosine biofunctionalized polyacrylonitrile nanofibers with a wound healing potential

Shahin Homaeigohar[1*], Farnaz Ghorbani[2], Aldo R. Boccaccini[2]

a: School of Science and Engineering, University of Dundee, Dundee DD1 4HN, United Kingdom. (Shomaeigohar001@dundee.ac.uk)
b: Institute of Biomaterials, Department of Materials Science and Engineering, University of Erlangen-Nuremberg, 91058, Erlangen, Germany.

INTRODUCTION

The multifunctionality of bionanohybrids is a promising research topic that employs advantage of the synergistic assembling of biopolymers with inorganic nanoscaled solids. Here, this extraordinary ability of bionanohybrids is employed to create a novel wound dressing material. Zn nanoparticles are biosynthesized by L-Carnosine ligands immobilized onto hydrolyzed polyacrylonitrile (PAN) nanofibers (NFs) to form a hierarchical NF biohybrid with wound healing potential. While the NFs act as a biomimetic scaffold for skin tissue regeneration, Zn and L-Carnosine (β-alanyl-L-histidine) support the wound healing process. Carnosine performs as a physiological pH buffer and ion-chelating agent (particularly for Cu (II) and Zn (II)) [1]. Moreover, it has shown to offer a wound healing effect thanks to its promising antioxidant, anti-inflammatory, and anti-neoplastic properties [1,2]. Zn also acts the cofactor of metaloprotein thus is crucial for regeneration of the extracellular matrix (ECM) of skin. It also regulates the auto debridement process and migration of keratinocytes, two vital prerequisites for wound healing [3]. Cooperatively, Zn-Carnosine/PAN NFs are believed to show a high potential for wound healing.

EXPERIMENTAL METHODS

Polyacrylonitrile (PAN) nanofibers (NFs) were electrospun from a PAN/DMF solution (8 wt.%) (feed rate= 1 ml/h and 20 kV). The NFs were hydrolyzed by 1N NaOH to be chemically functionalized [4]. Later, they were biofunctionalized by immersion into a L-Carnosine/PBS (5 mg/ml) solution overnight. Lastly, the biofunctionalized NFs were immersed in an aqueous solution of $ZnCl_2$ overnight to allow for biosynthesis of Zn nanoparticles. The biohybrid NFs were characterized with respect to morphology and surface composition and chemistry.

RESULTS AND DISCUSSION

Figure 1a shows the morphology of the biohybrid NFs whereon distinct Zn-carnosine composed zones are apparent. EDX analysis, Figure 1b, confirms the formation of Zn rich areas on the surface of the NFs, as reflected in several Zn peaks. The histidine moiety of L-carnosine dipeptide (β-alanine-histidine) can potentially chelate Zn^{2+} ions [2]. Moreover, as seen in Figure 2, amine and carboxyl groups of Carnosine can be involved in biosynthesis of the Zn phase. The dips related to such functional groups disappear after chelation of Zn^{2+} ions. It is worthy to note that the hydroxylated PAN NFs can firmly hold Carnosine ligands through hydrogen bonding between OH and amine groups of hydrolyzed PAN and Carnosine, respectively. Esterification of hydroxyl and carboxyl groups of hydrolyzed PAN and Carnosine, respectively, is also plausible. Such possibilities have already been proven in our earlier study on Bovine Serum albumin biofunctionalized PAN NFs [4].

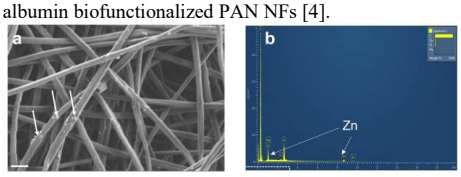

Figure 1: a) SEM micrograph showing the morphology of Zn-Carnosine/PAN NFs (the scale bar represents 1 µm)(the arrows mark the presence of Zn-Carnosine rich areas), b) EDX analysis verifies the biosynthesis of Zn nanoparticles across the NF mat.

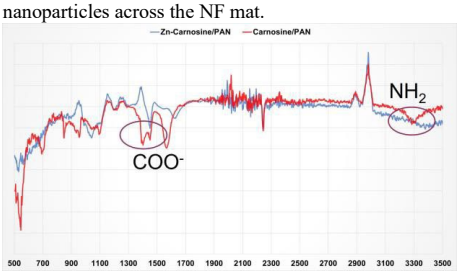

Figure 2: ATR-FTIR spectra imply the disappearance of characteristic dips of Carnosine (amine and carboxylate), most likely due to Zn coordination.

CONCLUSION

In this study, we devised a bionanohybrid comprising PAN NFs surface decorated with Carnosine ligands enabling biosynthesis of Zn rich areas. Such a hierarchical nanostructure benefits from wound healing effect of Zn and Carnosine as well as robustness and reliable physicochemical properties of the polymeric NFs. Cooperatively, the components as a bionanohybrid allow for biomimicry and stimulate the cellular activity within the wound milieu. Such promising features can lead to better wound healing conditions for the wounds treated by Zn-Carnosine/PAN NFs.

REFERENCES

1. Sonamuthu, J. *et al.* Int. J. Bio. Macromol. 153: 1058-1069, 2020.
2. Tsai, SJ. *et al.* J. Agric. Food. Chem., 58: 11510-11516, 2011.
3. Rath G. *et al.* Mater. Sci. Eng.: C, 58: 242-253, 2016.
4. Homaeigohar, S. *et al.* Mater. Sci. Eng. C. 116: 111248, 2020.

Tribological Properties Of The Lubricated Interface Between Hydrogel Fibres and Bone Tissue

Deyo Maeztu Redin[1,2], Paul Guillot[1,2], Vladislav A. Yastrebov[1], Laurent Corté[1,2]

[1] Centre des Matériaux, CNRS UMR 7633, Mines Paris, PSL University, Évry, France
[2] Molecular, Macromolecular Chemistry and Materials, CNRS UMR 7167, ESPCI Paris, PSL University, Paris, France
[*] juan-deyo.maeztu-redin@minesparis.psl.eu

INTRODUCTION

Fibrous materials are the preferred option for repairing and replacing stiff, anisotropic tissues like ligaments and tendons.[1] Depending on the kinematics of the joint and the implant positioning, these textile grafts can come in contact with other tissues, producing friction and wear. In the case of the anterior cruciate ligament, wear caused by friction against adjacent tissues represents a major cause of failure for both tendon grafts and synthetic implants.[2,3] At the time of contact, the graft can be in an elongation and torsion state. Therefore, it is of great interest to characterise and understand how the friction and wear may be affected by the deformation state of the fibres. Here, we investigate the tribological behaviour of poly(vinyl alcohol) (PVA) hydrogel fibres that can reproduce the tensile response of ligament tissues.[4] For that, we devised an experimental set-up allowing us to adjust the tension of a single fibre immersed in water and to measure the friction forces created upon contact with cortical bone tissue. We combined this experiment with microscopic observations and characterised how the coefficient of friction (COF) and the wear damage depend on the fibre tensile strain.

EXPERIMENTAL METHODS

PVA fibres (Solvron, Nitivy Ltd. 45 dtex, diameter 85 µm) were used and immersed in water for 8 h to produce hydrogel PVA fibres (diam. 120±10µm, water content 50±5 wt%). Tribological measurements were carried out with a CETR UTM-3M0 tribometer. A custom-made chamber was used to perform friction in a water bath (Figure 1a). In each experiment, one single fibre was held on a sample carrier and prestretched to a given tensile strain ranging from 0% to 70%. Contact with a 3 mm radius cylindrical pin made from bovine tibial cortical bone was made by lowering the pin to a fixed height (12 mm) below the fibre axis. This creates an additional strain of 4%. Sinusoidal reciprocating movement of 3 mm amplitude and 2 Hz frequency was imposed. Tangential (F_T) and normal (F_N) forces were recorded and the dynamic COF computed as the ratio of these signals at maximal speed. Wear surfaces were observed by scanning electron microscopy (SEM) and the reduction in fibre diameter within the contact area was measured by image analysis.

RESULTS AND DISCUSSION

We represented the friction behaviour by plotting F_T/F_N as a function of the displacement. These friction cycles are shown in figure 1b for 4%, 34% and 64% tensile strain. For the lowest tensile strain (4%), the contact is almost frictionless as indicated by the non-dissipative hysteresis loop. As we increase the tensile strain, the COF increases and the friction cycle takes a parallelogram-like shape. These results show that an increase in the fibre tension increases the energy dissipated by friction. From these cycles, we extracted a dynamic COF and found that it increases linearly with increasing fibre strain (figure 1c). Such dependence suggests that the resulting wear stronly depends on the tensile state of the fibre during contact. Wear was evidenced by SEM observations after different number of cycles, as shown in figure 1d for 34% tensile strain. At this fixed tensile strain, we found that the diameter reduction increases linearly with the number of cycles (figure 1e).

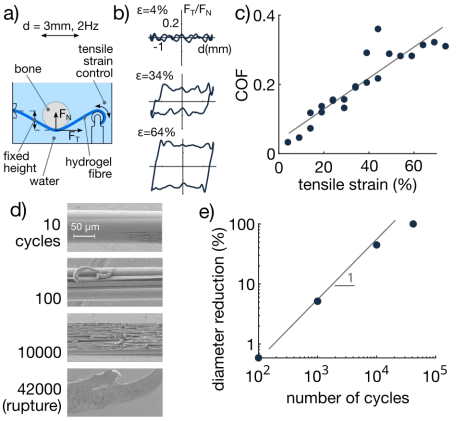

Figure 1: a) Experimental setup b) Friction cycles at ε=4%, 34% and 64% c) Dynamic COF as a function of fibre tensile strain (line shows linear fit) d) SEM images of the wear surfaces for different number of cycles at tensile strain of 34% e) Fibre diameter reduction with number of cycles (tensile strain 34%)

CONCLUSION

With this work, we show that the tensile strain of hydrogel fibres greatly affects its friction behaviour and could amplify the extent of wear. These results and methodology provide design and implantation guidelines to improve the wear-resistance of implants.

REFERENCES

1. Laurent C. *et al.,* J. Cell. Immunother. 4:4-9, 2018
2. Poddevin N. *et al.*, J. Biomed. Mater. Res. 38:370-381, 1997
3. Schützenberger S. *et al.,* Knee Surgery, Sport. Traumatol. Arthrosc. 29:2880-2888, 2021
4. Bach J.S. *et al.,* J. Biomech. 46:1463-1470, 2013

ACKNOWLEDGMENTS

We thank Y. Auriac and M. Simoes for technical support. Financial support from Mines Paris and Carnot Mines (Carnot 2019-SGM5) is acknowledged.

Poly (!-caprolactone) process parameter optimized nanofibers promote the growth of 3T3 human cells

Andre Mathias Souza Plath[1], *Helen Greutert*[1], *Serena Rosa Alfarano* [2], *Daniel Abbott* [3], *Raffaele Mezzenga*[2], *Victor Mougel, and Stephen J. Ferguson*[1]

[1] Institute for Biomechanics, Department of Health Sciences and Technology, ETH Zurich, Zurich, Switzerland

[2] Laboratory of Food and Soft Materials, ETH Zurich, Zurich, Switzerland.

[3]Department of Inorganic Chemistry, ETH Zurich, Zurich, Switzerland

Keywords: Nanofibers, scaffolds, wound-healing.

*andre.souzaplath@hest.ethz.ch

INTRODUCTION

Electrospinning is a nanomaterials fabrication technique that produces cost-effective high surface-to-area biomaterials. Electrospun materials are versatile extracellular matrix (ECM) mimicking materials with tunable fiber diameters for a wide range of applications. The ECM is a fibrous natural structural and mechanical support that provides cells with biological, physical, and chemical signaling. In the literature, poly (!-caprolactone) (PCL) electrospun materials have shown good cell compatibility for human fibroblasts, cartilage, mesenchymal stem cells, and other tissues. The optimization of nanofiber topology and diameter is strongly related to the envisioned applications of nanofibrous mats. In previous works, fiber diameter influenced mechanotransduction and the cell differentiation path. Herein, we sought to obtain with an experimental design uniform, reproducible cytocompatible nanofibers based on a binary system and a fixed content of weight per volume of poly (ε-caprolactone) for a versatile set of applications.

EXPERIMENTAL METHODS

Mats were electrospun using an experimental design varying the acetic acid content, voltage, distance to the collector, and flow rate (Figure 1). The experiments were planned with a 2^4 factorial design using the software JMP Pro 14.0. Surface morphology was assessed with scanning electron microscopy with a voltage of 3kV in the samples previously coated with an 80/20 Platinum-Palladium alloy. Spectroscopy (FTIR-ATR and XPS) studies were conducted on the surface of the electrospun mats to assess chemical alterations after the solubilization and electrospinning of the polymers. FTIR spectroscopy was performed for 16 scans and a resolution of 4 cm^{-1} from 4000 to 600 cm^{-1}. X-ray photoelectron spectroscopy was performed with 200W power and HR spectra were deconvoluted with OriginPro 2021 using Shirley Background to minimize χ^2. Cell viability, proliferation, and morphology were examined at day 5 for 3T3 fibroblasts seeded at 5000 cells/cm^2.

RESULTS AND DISCUSSION

Within the range, most solutions were electrospinnable, but most of them presented jet splitting, conglutination, thus, low reproducibility. The nanofibrous mats had an average fiber diameter within the 124 to 289 nm range. These results are compatible with reported pure PCL electrospun in a Formic/Acetic acid binary solvent by Ekram (2019). Two process parameters also yielded beads-on-string mats. Process parameters have shown increasing acetic acid content and collector distance promote finer nanofibrous structures. Contrary to the initial hypothesis, electrospinning voltage increase did not promote finer nanofibers. We report here microscopy images of sample 11, the most reproducible parameter produced, that was also characterized for its surface chemistry and cell viability. FTIR-ATR and XPS characterizations showed no significant hydrolysis of the ester bonds in PCL after solubilization in the Formic or Formic/Acid solvent system, an important parameter that impacts the mechanical properties of the mats. Finally, the nanofibrous electrospun mats were characterized according to their cytocompatibility. Cell staining of 3T3 fibroblast cells with DAPI and phalloidin showed cell viability, spreading, and proliferation after 5 days. The actin filaments, stained with Alexa Fluor 568, showed a significant spreading of the actin filaments and the clustering of cells.

RUN	DISTANCE (CM)	VOLTAGE (KV)	FEED RATE (ML.H^{-1})	ACETIC ACID (VOL.%)	FIBER DIAMETER (NM)
1	12	18	750	0	173 ± 17
2	12	12	325	30	171 ± 14
3	12	18	325	0	289 ± 40
4	16	12	750	30	180 ± 10
5	16	18	750	30	*
6	12	12	750	30	124 ± 13
7	12	12	750	0	*
8	16	12	750	0	*
9	16	18	325	30	265 ± 37
10	16	18	750	0	076 ± 12**
11	12	18	325	30	156 ± 13
12	16	12	325	30	173 ± 15
13	16	12	325	0	*
14	16	18	325	0	046 ± 05 **
15	12	18	325	30	182 ± 20
16	12	12	325	0	*

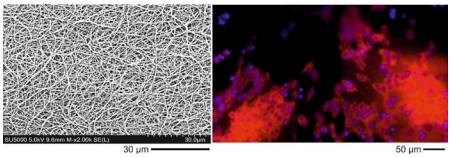

Figure 1. Electrospinnability of the tested conditions (not spinnable, ** beads-on-string), SEM, and inverted microscopy images of 3T3 cells on day 5 for sample 11 (5000× and 20× magnification, respectively.*

CONCLUSION

Distance to the collector and acetic acid content were the most significant parameters affecting uniformity of nanofiber mats. Applications are envisioned for fibroblast compatible materials such as artificial blood vessels and wound dressings. Other tissue engineering applications can be proposed upon the conjugation of other macromolecules to the electrospun surfaces.

ACKNOWLEDGMENTS

This project has received funding from the European Union's Horizon 2020 research and innovation program under the Marie Skłodowska-Curie grant agreement No 956004. We also thank ScopeM and partner laboratories for the characterizations.

Optimization of composition and spinning process of copper-chitosan fibers for the production of cytocompatible antibacterial and knittable monofilaments

Renaud Passieux[1,2,3*], Marie Vandesteene[2], Martine Renard[3], Guillaume Sudre[1], Alexandra Montembault[1], Ali Haddane[1], Agnès Hagège[4], Laurence Bordenave[5], Laurent David[1]

[1]Ingénierie des Matériaux Polymères (IMP), Univ Lyon, Université Claude Bernard Lyon 1, CNRS, UMR 5223, F-69622, Villeurbanne, France
[2]MDB Texinov, F-38110, La Tour du Pin, France
[3]CIC-IT, Université de Bordeaux, INSERM, CHU de Bordeaux, PTIB Hôpital Xavier Arnozan, F-33600 Pessac France
[4]Institute of Analytical Sciences (ISA), Univ Lyon, Université Claude Bernard Lyon 1, CNRS, UMR 5280, Villeurbanne F-69100, France
[5]BIOTIS , Université de Bordeaux, INSERM, U1026, F- 33000 Bordeaux, France
*renaud.passieux@univ-lyon1.fr

INTRODUCTION

We processed chitosan fibers[1] as monofilaments for biomedical textiles, leveraging the capability of chitosan to chelate metallic cations[2] in order to enhance its mechanical properties and antibacterial activity[3], but not at the expense of cytocompatibility.

EXPERIMENTAL METHODS

A wet spinning process was set to produce fibers from dopes consisting of chitosan solutions formulated with $CuCl_2$, with various glucosamine to Cu^{2+} molar ratios (r_{Cu2+}). Different draw ratios were applied during the spinning process. The formulation ratios were found very close to the final composition ratios in the fibers, determined by ICP-MS. The cytocompatibility on fiber samples was assessed by *in vitro* live-dead assays on mouse fibroblasts cells (balb 3T3) by a direct contact method (ISO 10933-5/ 12). The antibacterial activity of the fibers was evaluated by two different tests, *i.e.* evaluation of the inhibition of the bacterial proliferation in suspension and in agar gels entrapping the samples (ISO 20645:2004). We used two strains, *Staphylococcus epidermidis* (S.e) and *Escherichia coli* (E.c). Finally, the "knittability" of fibers was evaluated by conventional tensile test to evaluate the uniaxial tenacity of fibers (Te_U). A specific tensile test, using a knitting needle as fixed clamp, yields the tenacity at needle (Te_N).

RESULTS AND DISCUSSION

We found a first optimal r_{Cu2+} ratio by comparing the cytocompatibility and antibacterial properties of different fibers (see figure 1). Fibers produced with a ratio r_{Cu2+}= 0.01 (CTS-Cu0.01) were in the tradeoff windows ('zone of interest') for combined cytocompability and antibacterial activity.

Tensile tests using knitting needles were used to evaluate the textile tenacity of different fibers. CTS-Cu0.01 fibers Fibers spun with τ_{tot}=1.6 were shown to exhibit the optimal properties and were successfully knitted using industrial machines in humid conditions (Comez DNB/EL-32, MDB Texinov, La Tour du Pin, France).

CONCLUSION

We found an optimal formulation for chitosan fiber containing Cu^{2+} ions for r_{Cu2+}~0.01.

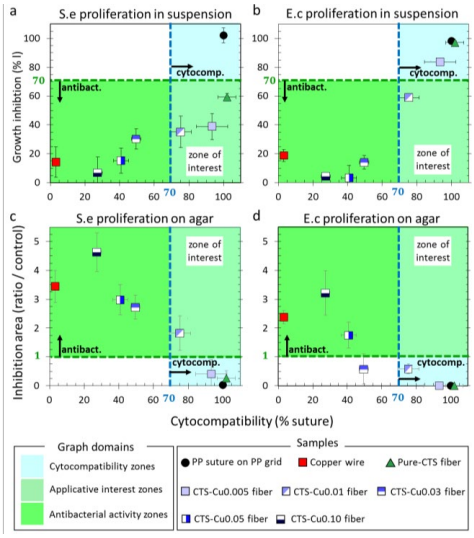

Figure 1. Antibacterial activity and cytocompatibility for *S.epidermidis* and *E.coli*. proliferation in suspension (a, b) or on agar gels (c, d), evaluated for different chitosan/Cu^{2+} fibers.

such fibers exhibited antibacterial activity on *S.epidermidis* cultured either in suspension or on agar gels, while maintaining cytocompatibility, but showed less antibacterial activity on *E.coli*. CTS-Cu0.01 was shown to be a suitable candidate for biomedical implant applications requiring knitted monofilaments.

REFERENCES

1. Passieux R *et al.*, ACS Biomater Sci Eng. 2022 doi: 10.1021/acsbiomaterials.2c00079
2. Guibal, E. Sep. Purif. Technol. 38: 43–74, 2004, doi: 10.1016/j.seppur.2003.10.004
3. Gritsch, L., *et al.* Carbohydr. Polym. 179:370–378, 2018. doi: 10.1016/j.carbpol.2017.09.095

ACKNOWLEDGMENTS

We thank ANRT for the Cifre grant (CONVENTION CIFRE N° 2016/0416) that was given to RP and MDB Texinov. We are very grateful to MDB Texinov for the financial support of this study.

Mechanical and structural properties of textile-like biodegradable membranes fabricated by under-extrusion 3D printing

Léa Dejob[1] and David Eglin[1]
Corresponding Author: lea.dejob@emse.fr

Mines Saint-Étienne, Univ Lyon, Univ Jean Monnet, INSERM, U1059 SAINBIOSE, Saint-Étienne F-42023 France

INTRODUCTION

A wide range of clinical issues can be addressed by biomedical textiles. While external uses include wound dressings or bandages for instance, implantable textiles can serve for general surgery, orthopedic, cardiovascular and plastic surgeries, or tissue engineering [1-2]. Yet, textile manufacturing is complex and alternative process to produce textile-like membranes would be beneficial to explore new designs and material compositions. Recently, under-extrusion fused deposition modeling (FDM) printing has been reported for the production of quasi-textiles [3]. However, impact of the manufacturing conditions on the membrane features was not fully explored. In this study, influence of these parameters on the membrane mechanical and structural properties is evaluated.

EXPERIMENTAL METHODS

Membranes of poly(lactic acid) were printed by FDM (Stream 20Pro MK2, Volumic 3D) and imaged by optical microscopy (Zeiss Axio Vert.A1). Their mechanical properties were investigated in tensile mode (INSTRON 3343, steady speed of 5 mm/min, 170x22 mm specimens, n=2).

RESULTS AND DISCUSSION

Textile-like membranes were produced by under-extrusion regime in FDM, a technique were the extrusion multiplier (EM), a parameter related to the volume of melt polymer extruded per time unit, is optimized to obtain a non-continuous filament deposition [3]. Varying the printing speed and extrusion multiplier values was found to impact on the membrane tensile properties (Figure 1.A,B). When these parameters were set to their optimal values (best mechanical properties), a membrane with regular porosity was obtained (Figure 1.C). The porous architecture of the membrane was also influenced by the printing speed, as lowering the later induced an axial elongation of the open pores. On a mechanical point of view, the membrane obtained at 40 mm/s with an extrusion multiplier of 0.8 showed a Young Modulus 2.5 higher compared to a commercial PET woven mesh that is used in surgical and medical device applications.

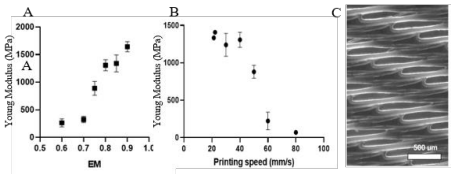

Figure 1. Apparent Young modulus of the membranes obtained at a constant A) printing speed (40 mm/s) and B) extrusion multiplier (EM=0.8). C) Optical microscopy of the membrane obtained at 40 mm/s, EM=0.8

CONCLUSIONS

Controlling the under-extrusion FDM printing of PLA enables the production of thin (<0.3 mm) and flexible membranes with potential applications as biomedical textiles. This easy manufacturing process is also versatile, and will therefore be applied to different biocompatible and biodegradable materials in future studies.

REFERENCES

1. G. Li *et al.,* Adv. Health.Mat, 2015
2. S. Thadepalli, Materials today: proceedings, 2021
3. J. Forman *et al.*, UIST 20, 2020

ACKNOWLEDGMENTS

This project has received funding from European Union's Horizon 2020 research and innovation programme under grant agreement No.952150 (BoneFix).

Enhanced Osteointegration of an Artificial Ligament Through a Tailored Local Osteoinductive Product Delivery

Cedric Zobrist[1*], Salim Hamidi[2], Feng Chai[2], Mehdi Daoudi[3], Stephanie Degoutin[1], Stéphane Noël[3], Nicolas Blanchemain[2], Bernard Martel[1]

[1] CNRS, INRA, ENSCL UMR8207, UMET – Unité Matériaux et Transformations, Université de Lille, Lille, France
[2] INSERM, CHU Lille, U1008 – Controlled Drug Delivery Systems and Biomaterials, Université de Lille, Lille, France
[3]Cousin Surgery, Wervicq-Sud, France
[*] cedric.zobrist@univ-lille.fr

INTRODUCTION

Tear of the Anterior Cruciate Ligament (ACL) is one of the most common knee injuries, which lead frequently to a surgery for recovery, due to the poor capacity of self-healing of the ligament[1]. The standard ACL reconstruction (ACLR) procedure uses an auto- or allograft harvested from the hamstring or patellar tendon. An alternative is to do the ACLR with a synthetic graft, which is introduced during the surgery through tunnels drilled in the tibial and the femoral bone to reproduce the natural anchoring of the ligament[2]. Although those ligaments provide high biomechanical properties, their poor biocompatibility can cause the widening of the bone tunnels due to a loose connection between the new ligament and the bone[3]. Hence, the solution we propose here is modify the ends of the artificial ligament with a core-sheath structure including a core braid loaded with bioactive glass (BG) and an overbraid with a windowed pattern that prevent the leak of bioactive glass and allow the osteoinduction through. This structure is designed to induce an optimal anchoring of the ligament in the neobone formed inside and outside the core-sheath ligament. The first goal of this study was to ensure the reliability of the protocol of BG incorporation to the device. The second goal was to induce biomineralization and to evaluate different sheath braid patterns to see how they allow the external growth throughout the windowed structure. Furthermore, we will also evaluate the cytotoxicity towards osteoblast cells.

EXPERIMENTAL METHODS

Preparation of the core functionalized core braid

Poly(vinylpyrrolidone) (PVP) was used to immobilize the BG on the core braid. In a typical procedure, the PET braid (from Cousin Surgery) was immersed in a PVP/BG solution in ethanol, and roll-padded. The PVP concentration was optimized to provide high sedimentation time of the BG particles and a minimum loss of the solution during the roll-padding of the braid.

Overbraiding of the core braid

Pristine and functionalized core braids were overbraided with a 16- or 24- spindles braiding machine. The 16-spindle overbraid was used as a tight non-windowed pattern reference. Two other patterns were overbraided using the 24-spindle machine, with a windowing ratio of 33% and 50%.

Biological evaluation of the samples

Biomineralization of each core-sheath braid has been realized by plunging them into a simulated body fluid solution (SBF). At 3,5 and 7 days, three samples of each braid were taken out of the solution, rinsed and dried for a SEM/EDS and XRD observation. Cytotoxicity evaluation of the samples after the cleansing and the sterilization was made (n=6) on osteoblast-like cells, MC3T3-E1

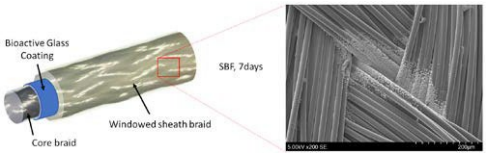

RESULTS AND DISCUSSION

The BG uptake by the braid was optimal with a PVP concentration of 6% wt, which is slightly over the entanglement concentration of the polymer. BG was homogenously spread along the braid with a 0,3 wt% load precision. Moreover the load percentage can be tailored by the number of roll-padding cycles. The biomineralization study shows that all the overbraid patterns allows the mineral deposit inside the core-sheath structure, but only the windowed ones allow the mineralization to occur on the outside face of the device. A further analysis of the cristals shows that they are a mix of hydroxyapatite and tricalcium phosphate phases, both of them are known to be osteoinductive. Finally, the *in vitro* evaluation of the braids showed that the device wasn't cytotoxic. That means that our new core-sheath functionalized braid is non-cytotoxic and is able to produce osteoinductive mineral deposition, especially around the windows of the overbraid, which should allow the bone matrix to grow tightly around the device.

CONCLUSION

This study is a first proof of concept for enhancing the biocompatibility of artificial ligaments through an innovative design. The next step will include an *in vivo* evaluation on an animal model.

REFERENCES

1. Cabaud H. *et al.*, Am. J. Sports Med. 7(1), 18–22, 1979
2. Sommer C. *et al.*, Knee Surg. Sports Traumatol. Arthrosc, 8(4), 207-213, 2000
3.Taketomi S. *et al.*, Arthrosc. J. Arthrosc. Relat. Surg.37(8), 2564-2566, 2021

ACKNOWLEDGMENTS

This study has been made possible through the European Regional Development Fund. The authors thank Dr Nils Becker from Ferro GmbH, who provided us a sample of their bioactive glass.

Strong Polycaprolactone fibers with modified morphology as a building block for Tissue Engineering of slowly healing tissue

Benedict Bauer[1*], Caroline Emonts[1], Rokaya Annan[1], Thomas Gries[1]

[1] Institut für Textiltechnik, RWTH Aachen University, Aachen, Germany
[*] benedict.bauer@ita.rwth-aachen.de

INTRODUCTION

Tissue engineering of tendons and ligaments is considered a promising alternative for autografts, allografts or permanent synthetic prostheses. However, the requirements for an appropriate scaffold are extremely high, including mechanical, degradation-related, and cell biological aspects. Especially, the mechanical strength and its retention during the degradation (~50% after 24 weeks are required) pose a challenge for many scaffold materials to date. In this study, melt-spun and highly-oriented Polycaprolactone (PCL) fibers are evaluated as a promising scaffolding material.

EXPERIMENTAL METHODS

Highly-oriented PCL fibers were fabricated from PCL pellets (Sigma–Aldrich, USA, M_n = 80,000) using a single screw melt spinning plant (Fourné Maschinenbau, Germany). Circular as well as snowflake-shaped monofilaments were melt spun utilizing respective spinneret geometries. Fiber morphology was investigated optically. Yarn count (n=3) was determined in accordance with DIN EN 13392. The mechanical properties were tested in uniaxial tensile tests (n=30) according to DIN EN ISO 2062. Additionally, fibers were exposed to phosphate buffer saline (PBS) and 37°C for up to 24 weeks and tested mechanically (n=30).

RESULTS AND DISCUSSION

Melt spun PCL monofilaments were produced while systematically varying spinning process parameters as draw ratio and spinneret geometry. Draw ratios ranged between 5.58 and 9.25. With increasing draw ratio, the tensile strength of the resulting filaments increased from 35.58 cN/tex (~ 409 MPa) to 68.76 cN/tex (~ 785 MPa) while the elongation at break decreased from 98.76% to 23.72%, respectively.

This is attributed to the increased macromolecular orientation induced by the drawing process. Simultaneously, the yarn count decreased from 458.58 ± 5.06 dtex to 271.03 ± 0.40 dtex.

Two different fiber cross-section geometries were investigated using a circular as well as a snowflake shaped spinneret geometry. Compared to the circular fiber morphology, snowflake-shaped fibers exhibited slightly reduced tensile strength which is in accordance with the results presented by Babaarslan et al.[1] and our earlier works. However, the snowflake geometry exhibits significantly higher specific surface area and a potential means to facilitate cell growth by providing growth guidance along the fiber axis.

In a long-term in vitro hydrolysis study in PBS at 37°C, the strength retention during the degradation process was investigated for circular and snowflake shaped fibers. Both fiber morphologies showed a similar strength retention (~ 80%) after 24 weeks.

CONCLUSION

In this study, PCL fibers with superb tensile strength were produced via melt spinning underlining the potential of highly-oriented PCL fibers for use in tissue engineering of tissue with extreme mechanical demands such as tendons and ligaments. Snowflake-shaped filaments may offer a potential means to facilitate cell growth by providing growth guidance. Circular as well as snowflake-shaped PCL fibers exhibited more than sufficient strength retention during a 24-week in vitro degradation study to provide mechanical stability for slowly healing tissue. In textile fabrication methods such as braiding, weaving or knitting three dimensional, porous scaffolds with excellent properties can be produced from the presented fibers. Further studies will address especially cell adhesion and proliferation.

ACKNOWLEDGMENTS

The authors would like to thank the German Federal Ministry for Economic Affairs and Energy for funding the research project within the framework of the Central Innovation Program for SMEs (Hexa+, KK5055913RU0).

REFERENCES

1. Babaarslan O. *et al.*, Fiber Polym, 14:146-151, 2013

3D-Braided PCL Scaffolds for Ligament Tissue Engineering

Caroline Emonts[1*], Benedict Bauer[1], David Wienen[1], Thomas Gries[1]

[1] Institut für Textiltechnik, RWTH Aachen University, Aachen, Germany
[*] caroline.emonts@ita.rwth-aachen.de

INTRODUCTION

Tendons and ligaments have a limited ability to regenerate. With an incidence of 1:3500, injuries to the anterior cruciate ligament (ACL) are among the most common injuries of the knee joint. Worldwide, the number is estimated at one million cruciate ligament ruptures per year. Current surgical repair techniques are based on tissue replacement with autograft. One of the main problems associated with the use of autograft is the need for additional surgery with possible infection of the donor site and pain. Today's synthetic cruciate ligaments are rarely used because they cannot permanently withstand the mechanical stress in the knee. Deficits exist in terms of fatigue strength, friction resistance and biological compatibility.
Tissue engineering offers a new approach to regenerate a functional ligament by using a three dimensional scaffold which enables mechanical stability and cell ingrowth.
Textile scaffolds can provide a 3D structural design, and their manufacture is reproducible and scalable. In addition, braided scaffolds can be designed for efficient loading and high strength while providing a high porosity for cell ingrowth.
The aim of this study is to investigate long-term degradable scaffolds based on poly-ε-caprolactone (PCL) for ACL replacement using the 3D-hexagonal braiding technique.

EXPERIMENTAL METHODS

The 3D-hexagonal braiding technique offers a high degree of geometric freedom and thus the possibility to develop new scaffold architectures. Five different scaffolds based on different braiding geometries are each investigated at three braiding points.
The influence of different braiding parameters regarding the maximum tensile load, elongation and stiffness are evaluated by tensile test. The tensile testing is performed in physiological length of the ACL (n=5) as well as according to standard testing norm (n=5). Furthermore, the critical morphological parameters for tissue engineering like porosity and pore size are characterized by µ-CT scans.

RESULTS AND DISCUSSION

The braided scaffolds reach tensile forces between 1522 N and 1986 N with an elastic elongation between 33.5% and 45.4%. Thus, all scaffolds match the tensile forces of the native ACL (734-1730 N) and are in the same elongation range as the native ACL with 37%.

The braid geometry and the height of the braid position significantly influence the elastic strain, the absolute stiffness as well as the elastic maximum tensile force of the braids. A higher position results in lower elastic strain due to the more linear orientation of the fibers. The stiffness of the braids can be adjusted to the values of the native human cruciate ligament by further modification of the braiding parameters, as well as increasing the number of filaments.
Porosity and pore size are crucial factors for cell ingrowth and tissue regeneration. Especially 3D braids provide an interconnected pore structure and possible guidance structure for cells. A porosity of at least 80% with an interconnected pore structure can be achieved with all scaffolds.

CONCLUSION

The current study has demonstrated the potential of 3D-braided PCL-based scaffolds for tendon or ligament replacement specifically for the anterior cruciate ligament. By further modification of the parameters, the application can be extended to other tendons and ligaments such as the medial and lateral knee ligaments as well as the rotator cuff. Further studies will evaluate the degradation behavior, as well as the cell behavior on the scaffolds.

ACKNOWLEDGMENTS

The authors would like to thank the German Federal Ministry for Economic Affairs and Energy for funding the research project within the framework of the Central Innovation Program for SMEs (Hexa+, KK5055913RU0).

Photo-crosslinkable gelatin-based bio-inks as strategy towards patient-specific breast reconstruction

Lana Van Damme[1,2], Phillip Blondeel[2*], Sandra Van Vlierberghe

[1] Polymer Chemistry & Biomaterials Group, Centre of Macromolecular Chemistry (CMaC), Department of Organic and Macromolecular Chemistry, Ghent University, Krijgslaan 281, S4-Bis, 9000 Ghent, Belgium
[2] Department of Plastic & Reconstructive Surgery, Ghent University Hospital, Corneel Heymanslaan 10, 2K12, 9000 Ghent, Belgium
[*] lana.vandamme@ugent.be

INTRODUCTION

There exists a clear clinical need for adipose tissue reconstruction strategies to repair adipose tissue defects which outperform the currently available approaches, such as breast implants, micro-surgical free tissue transfer and lipofilling. The development of biomimetic materials able to promote cell proliferation and adipogenic differentiation has gained increasing attention in the context of adipose reconstructive purposes. Thiol-norbornene crosslinkable gelatin-based materials were developed and benchmarked to the current commonly applied methacryloyl-modified gelatin (GelMA) with different degrees of substitutions focussing on bottom-up tissue engineering. [1]

EXPERIMENTAL METHODS

Modification of Gelatin. Norbornene-modified gelatin (GelNB) was developed based on a protocol described earlier by Van Hoorick et al. [2] Methacryloyl-modified gelatin (GelMA) was developed according to the protocol described by Van Den Bulcke et al.[3]

Physico-chemical characterization

A rheometer (Physica MCR-301; Anton Paar) was used to evaluate the gelation kinetics of the hydrogels. The gel fraction, mass swelling ratio and enzymatic degradation was assessed on punched-out hydrogel films (8 mm diameter).

In vitro assays

The cytocompatibility of the encapsulated cells was tested in triplicate through a live/dead viability assay using calcein-acetoxymethyl (Ca-AM) and propidium iodide (PI) at day 1, 3, 7 and 14. To quantitively assess the differentiation of the cells into the adipogenic lineage, secretome analysis, a triglyceride assay and Bodipy/DAPI staining were performed at day 7 and 14.

In vivo assays

Scaffolds (both sham scaffolds and scaffolds containing adipose derived stem cells) were implanted sub-mammary in mice and assessed through contrast enhanced µCT imaging, one month post implantation. Following 12 weeks of implantation, ex vivo histology will be performed through a H&E staining.

Statistical analysis

Statistical analysis was performed using a unifactorial analysis of variance (ANOVA). Two values were considered statistically significant when the P-value was <0.05.

RESULTS AND DISCUSSION

The developed hydrogels resulted in similar physico-chemical properties (gel fractions >90% and mass swelling ratio ~13). The mechanical properties of the hydrogels could be tuned by incorporating more or less crosslinkable functionalities or using different crosslinking techniques (i.e. step-growth ~15kPa vs chain-growth ~30kPa). The biocompatibility (viability >85%) as well as differentiation potential of encapsulated adipose tissue-derived stem cells were analysed and showed superior adipogenic differentiation in the thiol-ene constructs. The elasticity of the hydrogels plays a key role in the cell differentiation potential, especially in cell-laden hydrogels and scaffolds. [4] A hydrogel offering an elasticity equivalent to physiological conditions should thus offer a mechanical cue toward the encapsulated ASCs to differentiate into the adipogenic lineage. Indeed, it can be observed that the softest material, namely GelNB55/SH75, resulted in significantly greater differentiation at both time points. This could be observed based on all assays. Initial in vivo data already showed good vascularisation throughout the construct one month post-surgery via contrast-enhanced µCT imaging. Additional in vivo experiments are currently ongoing assessing the differentiation potential and neovascularisation via ex vivo histology of constructs implanted sub-mammary in mice.

CONCLUSION

It can be concluded that the mechanical properties of a biomaterial are of utmost importance with respect to differentiation into the adipogenic lineage. The mechanical cues of GelNB55/SH75 were superior over the other investigated hydrogels. Photo-crosslinkable thiol-ene systems thus offer a promising strategy toward adipose tissue engineering through cell encapsulation compared to the widely used GelMA.

REFERENCES

1 Van Damme, L. *et al. Biomacromolecules* 22, 2408–2418 (2021)
2 Van Hoorick, J. *et al. Macromol. Rapid Commun.* 39, 1–7 (2018)
3 Van Den Bulcke, A. I. *et al. Biomacromolecules* 1, 31–38 (2000)
4 Engler, A. J. *et al. Cell* 126, 677–689 (2006)

ACKNOWLEDGMENTS

The authors would like to thank Tim Courtin for his help with recording the ^{1}H NMR spectra. L.V.D. would like to acknowledge the Research Foundation Flanders (FWO) for providing FWO-SB fellowships (1S85120N). Prof. Blondeel and Prof. Van Vlierberghe would also like to thank FWO for providing them with an FWO fellowship (3S039319)

Characterization and Modeling of Functional Gradients for Enabling Tough Biomimetic Devices

Mauricio C. Saldivar[1*], Robin P.E. Veeger[1], Quentin Grossman[2], Astrid Cantamessa[2], Davide Ruffoni[2], Eugeni L. Doubrovski[3], Mohammad J. Mirzaali[1], Amir A. Zadpoor[1]

[1]Department of Biomechanical Engineering, Faculty of 3mE, Delft University of Technology, Delft, The Netherlands
[2]Mechanics of Biological and Bioinspired Materials Laboratory, Department of Aerospace and Mechanical Engineering, University of Liège, Liège, Belgium
[3]Faculty of Industrial Design Engineering, Delft University of Technology, Delft, The Netherlands
[*]m.cruzsaldivar@tudelft.nl

INTRODUCTION

Functional gradients (FGs) are among the most common structural elements that Natural materials have evolved to survive perilous environments[1]. Their presence enhances the mechanical performance of multifunctional structures by releasing interfacial stresses through the systematic transition of mechanical properties (*e.g.,* power, exponential)[2]. Today, voxel-based additive manufacturing techniques allow mimicking such FGs due to its point-wise freedom for depositing both hard (mineral-like) and soft (collagen-like) phases across space[3]. However, the non-linear transition in mechanical properties between both phases depends on the voxels' hard material fractions (ρ) and spatial distributions, where no models have been introduced to estimate their behavior. Therefore, it is fundamental to derive and validate such models, enabling the realization of fully tuned biomimetic devices with enhanced toughness.

EXPERIMENTAL METHODS

We used a Polyjet 3D printer (Stratasys, USA) for manufacturing an FG with a linear ρ transition discretized by randomly depositing the hard-soft voxels (Figure 1A). We performed nanoindentation experiments with a Hysitron TI 950 Triboindenter (Bruker, USA) to measure the elastic modulus response of the FG. Then, we used a simplified model obtained from the literature to characterize its behavior, which takes the form[4]:

$$E/E_H = \rho^b + E_S/E_H$$

where b is a fitting parameter and E, E_H, and E_S are the elastic moduli of the composite, hard, and soft material, respectively. We validated this model by designing two intervertebral discs (IVDs) and testing them under quasi-static compression. The first one was designed with a non-graded interface between its hard-soft connections. In contrast, the second IVD was graded, and its hard material distribution averaged the same elastic response as the first design. We hypothesized that the graded IVD would have an improved toughness before critical failure.

RESULTS AND DISCUSSION

The nanoindentation results denoted an elastic modulus transition that variated non-linearly (Figure 1B), similar to what has been reported in the literature[3]. Besides, the parameterized model (b = 2.06) adequately followed the non-linear behavior of the experimental data with a high correlation (R^2 > 97%) across three different orders of magnitude. These outcomes indicate that the proposed model is an excellent candidate for tunning the hard-soft composite's response since only a single parameter is necessary to describe their entire behavior.

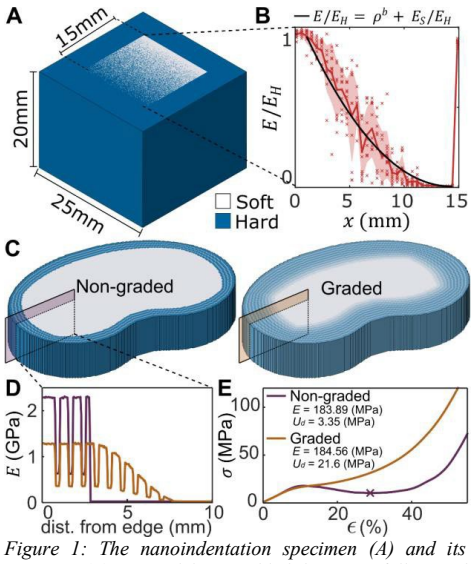

Figure 1: The nanoindentation specimen (A) and its response (B). Its modeling enabled designing fully tuned IVDs (C-D), where the graded one was tougher (E).

The proposed model enabled discretizing and manufacturing IVDs with functions of elastic modulus that resemble those of their lamellae (Figure 1D). The resulting average elastic modulus of both IVDs was nearly identical (Figure 1E), validating the accurate performance of the parameterized model. Furthermore, the graded design enabled a better distribution of stresses across the IVD, resulting in a hardening-like response with an improved toughness compared to the critical yielding of the non-graded design.

CONCLUSION

These findings prove that the introduced model enables the design of fully-tuneable biomimetic devices with only a single relation, where the application of FGs enhanced their overall non-linear performance.

REFERENCES

1. Liu Z. *et al.*, Prog. In Mat. Sci. 88:467-498, 2017
2. Naleway S. *et al.*, Adv. Mat. 37:5455-5476, 2015
3. Mirzaali M. *et al.*, Comp. Struct. 237:111867, 2020
4. Davies W. *et al.*, J. Phys. D: Appl. Phys. 4:1325, 1971

ACKNOWLEDGMENTS

This project is part of the Idea Generator (NWA-IDG) research programs NWA.1228.192.206 and NWA.1228.192.228.

Micellar Nitric Oxide-Releasing Hydrogels for DLP-Based 3D Printing

Mateus P. Bomediano, Murilo I. Santos, Giovanna J.V.P. dos Santos, Laura C.E. da Silva, Marcelo G. de Oliveira*

[1]Institute of Chemistry, University of Campinas, UNICAMP, Campinas, SP, Brazil
*mgo@unicamp.br

INTRODUCTION

3D printing of hydrogels is increasingly being explored in the field of biomaterials, especially when considering the customized printing of hydrogel prostheses for cartilage tissue replacement[1]. In this case, in addition to biocompatibility, the hydrogels must possess appropriate elastic properties. Recently, we demonstrated the 3D printability of supramolecular hydrogels comprised of chemically cross-linked poly(acrylic acid) (PAA), interpenetrated by a micellar network of Pluronic F127 micelles, containing cellulose nanocrystals, capable of releasing nitric oxide (NO)[2]. The interest in NO release by prostheses is motivated by the potential beneficial actions that NO can provide, including improved and faster tissue integration, along with microbicidal and angiogenic actions[3,4]. In the present study, we developed a novel photocrosslinkable micellar PAA/F127 hydrogel for 3D printing via Digital Light Processing (DLP), though the. Incorporation of preformed polyvinyl alcohol (PVA) in the intermicellar space.

EXPERIMENTAL METHODS

3D-printable resins were comprised of 30 wt% acrylic acid, 0.26-0.32wt% N,N'-methylenebisacrylamide, 7.6-20wt% Pluronic F127, 1-2wt% poly(vinyl alcohol), 0.08wt% Irgacure 818 and 0.01wt% SUDAM I. Hydrogel constructs were 3D printed in a MoonRay D75 DLP printer (75 µm minimum pixel size/100 µm printing step size). S-nitrosoglutthione (GSNO) (20-130 nmol/g) was incorporated through absorption from solution. Compression tests were performed in a TA.XT Plus Texture Analyzer. Cryo-TEM micrographs were obtained in a transmission electron microscope TALOS F2000. GSNO charge and real-time NO release were measured by chemiluminescence in a NOA, Sievers 280i (GE Analytical Instruments). Numerical results are the average of triplicates.

RESULTS AND DISCUSSION

The AA/micellar F127/PVA resins showed good printability and fidelity to the computational model (Fig. 1a-d). Mechanical compression/decompression tests showed that the presence of 2 wt% PVA significantly reduces the hysteresis and Young's modulus of the PAA/F127 hydrogels. This effect can be attributed to the plasticizing action of the interpenetrated PVA chains, which is exerted through intermolecular hydrogen bonding interactions among PVA hydroxyls, terminal F127 hydroxyls at the crowns of the F127 micelles, and the protonated carboxyl groups of PAA. The presence of F127 micelles in two different micelle packings was confirmed by Cryo-TEM (Fig. 1 e-f). PAA/F127/PVA hydrogels charged with GSNO were shown to release NO spontaneously under hydration, at rates which can be modulated by the GSNO charge.

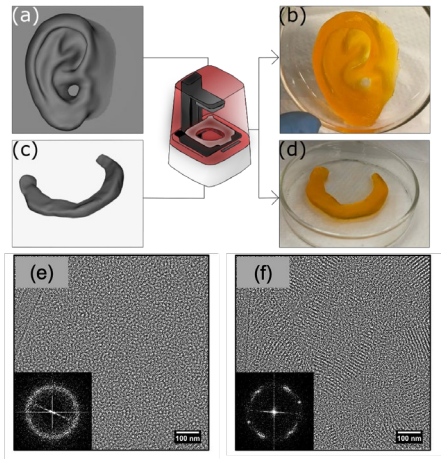

Fig 1. 3D models of ear (a) and knee meniscus(c) and the corresponding DLP-3D printed constructs (b) and (d) of PAA/F127/PVA hydrogel. Cryo-TEM micrographs of F127 7.6%/PVA hydrogel (e) and F127 22%/PVA hydrogel (f).

CONCLUSION

The incorporation of PVA improves the elastic behavior of 3D-printed PAA/F127 hydrogels, by reducing their plastic deformation in the compression process. PAA/F127/PVA hydrogels loaded with S-nitrosoglutathione (GSNO) release NO locally in a dose-response manner, upon hydration. PAA/F127/PVA/GSNO hydrogels have potential for the 3D-printing of customized cartilage replacement constructs, with enhanced biocompatibility and mechanical properties.

REFERENCES

1. Picheth GF. *et al*. J. Colloid Interf. Sci. 576:457-467, 2020
2. Santos MI. *et al*., Soft Matter. 17:6352–6361, 2021
3. de Oliveira MF *et al*., Bioprinting. 22:e001373, 2021
4. de Oliveira MG. Basic & Clin. Pharmacol. & Toxicol. 119:49-56, 2016

ACKNOWLEDGMENTS

The authors would like to thank the São Paulo Research Foundation (FAPESP) (Grants no: 2016/02414-5, 2017/04615-0, 2018/14142-5 and 2019/07325-9) for financial support.

Effect of Storage and Reuse on powder properties for powder bed fusion – laser beam of WE43 magnesium alloy

Giulio Pietro Cavaliere[1*], Francesco D'Elia[1], Pelle Mellin[2], Cecilia Persson[1]

[1] Department of Materials Science and Engineering, Uppsala University, Uppsala, Sweden
[2] Swerim AB, Kista, Sweden
[*] giulio.cavaliere@angstrom.uu.se

INTRODUCTION

Processing magnesium (Mg) alloys through Powder Bed Fusion–Laser Beam (PBF–LB) gives the possibility of realizing patient-specific biodegradable implants for fracture fixation and healing of large bone defects. Mg-RE (rare earth) alloys and specifically WE43 (Mg-$Y_{3.7\text{-}4.3wt\%}$ -$RE_{2.4\text{-}4\text{-}4wt\%}$-$Zr_{0.4wt\%}$), have shown promising results in this field with a slower degradation rate than most other Mg alloy systems [1]. At the present moment, the cost of production of Mg-based powder for PBF-LB is an important factor that limits the scalability of the process. Furthermore, recycling possibilities are of utmost importance in our endeavor for a sustainable world, in particular when it comes to rare earth elements. Hence, it is important to understand the potential of Mg alloy powders for recycling in order to reduce costs and improve the sustainability of the PBF-LB process. Studies on Hastelloy X[2] and $AlSi_{10}Mg$[3] have shown that recycled powders have substantially different characteristics compared to the virgin one. For instance, increases in particle size, a significant loss in particle sphericity, and decreases in flowability were observed for the recycled powders. Also, the printed products displayed a higher porosity, larger size defects and a higher surface roughness. However, the effect of reuse and storage on WE43 powder remains to be investigated. The aim of this study is to increase the understanding of the effect of powder reuse and storage for WE43 in order to tune the process parameters to obtain the best possible properties of the printed samples.

EXPERIMENTAL METHODS

The PBF-LB WE43 powder properties were characterized in virgin, stored and recycled conditions. The spreadability of the powder was evaluated using a TQC Sheen automatic film applicator. In addition, the flowability and apparent density of the powders were measured using both a Hall and a Gustafsson flowmeter. Finally, the particle size distribution and morphology were evaluated using SEM. The different powder conditions were then used as feedstock for PBF-LB printing bulk WE43 specimens in an EOS 100 system and the porosity of the samples compared.

RESULTS AND DISCUSSION

Preliminary results show an increase in both powder size and amount of irregular shaped particles for the recycled powder in comparison to the virgin condition. This resulted in poorer spreadability and lower values of flowability for the recycled powder. In turn, when used as feedstock, the recycled powder generated bulk specimens with increased levels of porosity and an overall poorer quality compared to samples printed with virgin powder feedstock.

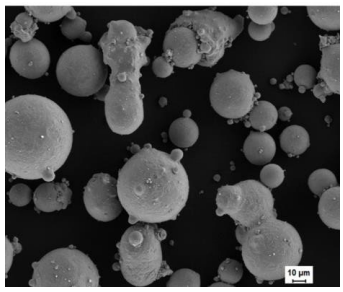

Fig.1 SE-SEM image of virgin gas atomized WE43 powder. (Nilsson et al.,2022)

CONCLUSION

The preliminary findings from this study suggest that storage and reuse have a detrimental effect on the properties of WE43 powder, thereby impacting the overall density of the printed specimens. Further investigation is needed to address the potential for accommodating such changes in powder properties through tailoring of PBF-LB processing parameters. The goal is to enable the use of recycled powders for production of high quality WE43 Mg alloy specimens.

REFERENCES

1. Nilsson et al., *Materials* **2022**, *15* (2), 417.
2. He et al., *Addit. Manuf.* **2022**, *55*, 102840..
3. Weiss et al., *JOM* **2022**, *74* (3), 1188–1199.

ACKNOWLEDGMENTS

This Project has received funding from the European Union´s Horizon 2020 research and innovation program under the Marie Skłodowska-Curie grant agreement No. 956004.

ESB 2022
32nd ANNUAL CONFERENCE OF THE EUROPEAN SOCIETY FOR BIOMATERIALS

Preparation of elastomeric polyurethane photo-curable resins for stereolithography 3D printing

P. Navarrete-Segado[1*], J. P. Fernández-Blázquez[1], A. Castro[1], A. Camacho[1], J. Patterson[1]

[1]Biomaterials and Regenerative Medicine Group, IMDEA Materials Institute, C/Eric Kandel, 2, 28906, Getafe, Madrid, Spain
[*]pedro.navarrete@imdea.org

INTRODUCTION

Polyurethanes (PUs), block copolymers composed of alternating soft and hard blocks or segments, have a large diversity of chemical compositions and have been widely used in biomedical fields, for soft tissue regeneration. This is due to their cellular compatibility and their tuneable flexibility and mechanical properties achieved by varying their monomers' types and content. Aliphatic isocyanates (as hard segment) and polyethylene glycol (PEG, as soft segment) are commonly used in PUs design due to their enhanced biodegradation kinetics, hygroscopic base properties, and microbe resistance [1]. The production of PU elastomeric constructs with complex and reproducible internal structures has become feasible thanks to additive manufacturing (AM) technologies [2]. Stereolithography (SLA) 3D printers use a UV-light source to cross-link a photocurable resin feedstock layer by layer. PU photocurable resins, which generally include a photoinitiator for initiation of the cross-linking reaction, monomers or oligomers as main components, reactive diluents, and photoblocker, have to be carefully formulated. It is then of high importance to control their reactivity and rheological properties to be compatible with the SLA 3D printers and achieve high resolution printed parts [3]. The goal of this study was to prepare and characterize a PU resin capable of achieving printed features less than 200 µm.

EXPERIMENTAL METHODS

A mixture of PEG-400 with 0.25 wt% of dibutyltin dilaurate catalyst was mechanically agitated in a three-neck round-bottom flask under Ar atmosphere before adding hexamethylene diisocyanate (HDI) dropwise. Then, 2-hydroxyethyl methacrylate (HEMA) was added to produce the biodegradable methacrylate terminated PU oligomer (PUMA) through a solvent-free, two-step polymerization process. A mole ratio of 1:1.5:1 was used for the main reagents PEG-400:HDI:HEMA. Polypropylene carbonate was added as a reactive diluent to decrease the viscosity. The physicochemical properties of the compounds were investigated using Fourier transform infrared spectroscopy (FTIR), gel permeation chromatography (GPC), nuclear magnetic resonance (NMR), and viscosity measurements. For SLA printing, a photoinitiator (TPO-L) and a photoblocker (sodium copper chlorophyllin) were added to complete the resin.

RESULTS AND DISCUSSION

To follow up on the reaction, aliquots were taken time to time from the vessel, and these were analysed by FTIR to find the correct time for adding the reagents and confirm the structure. Through the NMR and GPC analyses(Mp = 2536 Da) it was observed that a chain extension occurred even if it was limited by increasing the ratio of isocyanate to hydroxyl functionality. Further attempts will be performed to try to reduce it. A viscosity of 451 cps was obtained for the final resin, which makes it suitable for its use in an SLA 3D printer. The amounts of TPO-L and sodium copper chlorophyllin were monitored to be able to print layers with a thickness of 50µm. A resin XP2 Validation Matrix model was printed for calibration purposes, obtaining flexible objects with high-resolution features (Figure 1).

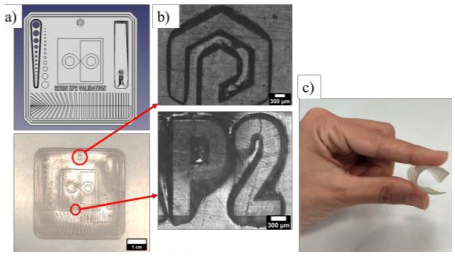

Figure 1. a) XP2 Validation Matrix model and below the printed specimen (scale bar = 1 cm), b) optical microscope images of the features (scale bars = 300 µm), c) demonstration of the flexibility.

CONCLUSION

In this communication, we present the synthesis, characterization, and printing of PU-based photocurable resins. The easy chemical modification of the monomers could be employed to alter the physical and chemical properties of the resin, for example, through the addition of multifunctional crosslinkers. This type of resin has high potential for use in the creation of 3D in vitro tissue models. As next steps, the mechanical properties and the biocompatibility of 3D-printed objects will be studied to evaluate the possible resin implementation in applications involving living cells.

REFERENCES

[1] M.F. Sonnenschein, Polyurethanes: Science, Technology, Markets, and Trends, John Wiley & Sons, Inc, Hoboken, NJ, 2014.
[2] A. Farzan, S. Borandeh, N. Zanjanizadeh Ezazi, S. Lipponen, H.A. Santos, J. Seppälä, European Polymer Journal 139 (2020) 109988.
[3] F.P.W. Melchels, J. Feijen, D.W. Grijpma, Biomaterials 31 (2010) 6121–6130.

ACKNOWLEDGMENTS

Activity financed through the agreement signed between the Community of Madrid (Consejería de Educación, Universidades, Ciencia y Portavocía) and the IMDEA Materials Foundation for the direct award of a grant of 1.937.000,00 euros to finance research activities on SARS-COV 2 and COVID-19 disease financed with REACT-EU resources from the European Regional Development Fund."

3D-Printed Biodegradable Hybrids for Bone Regeneration Applications

Haffsah Iqbal[1], Athanasios Skandalis[1], David R. Sory[2], Yu-Chien Lin[1], Theoni K. Georgiou[1], Julian R. Jones[1,*]
[1]Department of Materials, Imperial College London, London, UK
[2]Faculty of Medicine, National Heart & Lung Institute, Imperial College London, London, UK
h.iqbal18@imperial.ac.uk

INTRODUCTION

Organic-inorganic class II hybrids have synergistic properties of their components while acting as a single-phase material. Class II hybrids have covalent bonds between an organic (functionalized polymer) in a sol-gel system. Biodegradable silica/poly(ε-caprolactone) (PCL) hybrids have been prepared, in which hydroxyl groups at either end of the PCL polymer chains were modified with a triethoxysilyl group (TEOS)[1], but mechanical properties were low. Poly(methylmethacrylate-*co*-3-(trimethoxysilyl) propyl methacrylate)-SiO_2 hybrids have been investigated in bone regenerating biomaterials because of their promising mechanical properties, but biodegradation has been limited[3]. The aim here was the synthesis of ABA biodegradable copolymers containing with PCL as biodegradable entity along with methyl-methacrylate (MMA) and trimethoxysilyl) propylmethacrylate (TMSPMA) as monomer. The polymer-TEOS hybrid system was optimized as ink for the preparation of 3D-printed scaffolds. The effect of polymer MW on the mechanical strength and degradation was investigated.

EXPERIMENTAL METHODS

The ABA-type biodegradable triblock copolymers used in this study were synthesized by a combination of ROP and RAFT polymerization methodologies, and they were molecularly characterized by GPC and ^{1}H-NMR for MW and composition. The copolymers were used as the organic phase for the preparation of 3D-printed (extrusion printing) class II glass-polymer hybrid scaffolds *via* the sol-gel method. The scaffolds were characterized for mechanical properties, morphology (SEM, microCT), biodegradability and *in vitro* toxicity.

RESULTS AND DISCUSSION

P(MMA-*co*-TMSPMA)-*b*-PCL-*b*-P(MMA-*co*-TMSPMA) well-defined triblock copolymers with molecular weights ranging from 14000-27000 g.mol^{-1}, as derived from GPC measurements, were successfully synthesized. The copolymers were later utilized as hybrid sol ink for direct extrusion printing. Gelation time of the hybrid ink increases as Mw increases. Subsequently the use of lower Mw polymer led to better control of printing. SEM imaging of the 3D-printed scaffolds showed a well interconnected pore channel structure (Fig. 1). The qualitative pore inter-connectivity was confirmed *via* microCT. Uniaxial compression and cyclic loading measurements of 3D-printed scaffolds exhibited promising mechanical properties of 7-9Mpa, which is within the range of those of the trabecular bone. In vitro bioactivity of the hybrid structures was evaluated through incubating them in simulated body fluid (SBF) which shows the ability of the materials to form HA layers on their surface. The *in vitro* degradation studies revealed a weight loss of 18-23% over the period of 3 months. Cytotoxicity studies by MTT metabolic assay (Fig. 1) passed ISO standards, with viability of h-BMSC (Bone marrow-derived mesenchymal stem cells) exposed to hybrid scaffolds at>87% to that of the control media.

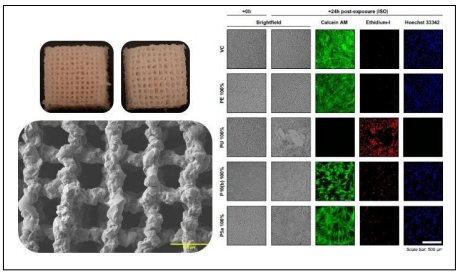

Fig. 1: Photos (top left), SEM image (bottom left) of the 3D-printed scaffolds; brightfield and fluorescent micrographs (right) of h-BMSCs cultured with media conditioned by the scaffolds for 24 h.

CONCLUSION

A novel, biodegradable hybrid ink containing P(MMA-*co*-TMSPMA)-*b*-PCL-*b*-P(MMA-*co*-TMSPMA) triblock copolymers as the organic phase was successfully prepared. Direct ink writing led to the construction of 3D printed scaffolds with interconnected porous structures with pore size of 250-300 µm. Optimal printability was observed with polymers with Mw around 15000 to 17000 g.mol^{-1}. The porosity and mechanical properties of the scaffolds were within the range of the trabecular bone. *In vitro* studies showed bone regeneration ability of the scaffolds. Based on these results, material shows promising properties for the potential use for bone regeneration application.

REFERENCES

1. Rhee *et. al*., Biomaterials. 25(7-8):1167-1175, 2004
2. Rhee *et. al*., Biomaterials. 30 (20), 3444-3449, 2009
3. Chung *et. al.,* Chem. Mater. 28(17):6127-6135, 2016

ACKNOWLEDGMENTS

"The authors would like to thank **The Punjab Educational Endowment Fund (PEEF) Pakistan** for providing financial support to this project".

Additive manufacturing of zirconia-based ceramics by laser stereolithography for jawbone implants applications

S. Fournier[1], G. Baeza[1], J. Chevalier[1], H. Reveron[1],
[1] *Univ Lyon, INSA Lyon, UCBL, CNRS, MATEIS, UMR5510, 69621 Villeurbanne, France*

Ceramic laser stereolithography (SLA) offers the degree of design freedom and resolution required in the development of complex and dense ceramic pieces, such as structural biomedical implants. This additive manufacturing technique allows producing medical prostheses with complex geometries, tailored architectures, high dimensional resolution and smoother surface finish. Moreover, to enhance bone integration, it is possible to precisely control the location and/or geometry of pores and surface structuring.

SLA of ceramics is based on a layer-by-layer polymerization of pastes that are composed of ceramic particles and photopolymerizable monomers. During SLA, thin 2D-layers of paste are successively exposed to laser irradiation following a given pattern defined by the sliced CAD file (computer-aided design) of the piece to be manufactured. Multifunctional monomers polymerization and consecutive layers curing zones superposition ensure the mechanical strength of the 3D-printed ceramic. Finally, debinding and sintering steps permit to obtain a high-density ceramic part from this polymerized printed object. The SLA process can be controlled by adjusting printer parameters (laser power, layer thickness, laser scanning speed, hatch spacing…) and/or paste characteristics (photosensibility of the resin, size and content of ceramic particles, organics additives…). In general, the printer manufacturer provides the ceramic pastes, as well as the optimized printing parameters to be used.

Our study aims to understand the underlying phenomena involved at each step of the processing of a ceramic part by laser stereolithography. This knowledge will allow us to optimize the process in order to fulfil all the requirements for zirconia-based biomedical devices, such as mechanical resistance, reliability, phase stability and biointegration.

As ceramics are usually brittle materials, their reliability can be improved by decreasing the size and number of defects created at each step of the additive manufacturing process. In this context, we will discuss here the effect of: I) the paste rheology and ageing II) the laser parameters used for photopolymerization and III) the printing and post-printing procedures on the creation of defects.

SLA pastes have a high content of ceramic particles (ca. 50 vol.%) making their mechanical response to scraping quite difficult to rationalize without a fine structural analysis. To address this question, we conducted rheological investigations in order to: 1) provide quantitative parameters describing the “printability” of the paste 2) characterize the paste ageing behaviour and its possible reuse over a year and 3) understand the restructuring of ceramic particles under shear stresses.

Besides, the laser energy received per volume element was estimated in order to better understand the effects of printing parameters and laser patterning on the photopolymerization of the paste. The monomer conversion and solidification were investigated by FT-IR, NMR and compared to Jacob’s equation results.

SLA printed samples have been submitted to DSC and ATG tests in order to understand phenomena involved during debinding. Laser parameters and heating cycles were optimized to fully densify zirconia-based ceramics.

Another possibility we explore in order to increase the reliability of SLA-printed parts is to use ductile Ce-TZP-based composites. A Ce-TZP-composite SLA paste was developed, printed and post-treated thermically leading to dense ceramics which showed promising mechanical properties despite the presence of some printing defects still produced during the SLA process. Zirconia phase transformation induced plasticity demonstrated its ability to increase the resistance of ceramic parts to microstructural inhomogeneities, layer decohesion and/or other defects.

We finally close this discussion by showing some previous results on zirconia bone integration and projected work on ultra-fast laser surface modification for enhancing bone-cell adhesion to zirconia-based biomedical implants manufactured by SLA.

Effect of Graphene-Based Nanomaterials on Photocurable PLA Resin: Study of Curing Depth and Optimization of Exposure Time on LCD 3D Printing

Eva Paz[1*], Sara Lopez de Armentia[1], Mariano Jiménez[1], Juan Carlos del Real[1], Nicholas Dunne[2]

[1] Institute for Research in Technology/Mechanical Engineering Dept., Universidad Pontificia Comillas, Madrid, Spain
[2]School of Mechanical and Manufacturing Engineering, Dublin City University, Dublin, Ireland
[*] eva.paz@comillas.edu

INTRODUCTION

The effect of different graphene-based nanomaterials (GBN) on the thermal curing of polymers has already been widely studied. Two tendencies were found[1,2]: (i) the presence of nanofillers accelerated the polymerization process by increasing thermal conductivity or catalyzing the reactions thanks to its oxygenated groups; (ii) nanofillers reduced the curing reaction rate due to the steric hindrance, or the increase in viscosity which hindered the mobility of the reactive species. Photocurable resins have gained great interest due to the population of 3D printing techniques based on UV polymerization. The effect of the GBN in the curing of this kind of resins have been hardly studied. These manufacturing techniques have gained a great attention for biomedical applications and some new biocompatible and bioactive resin formulations have been recently developed. GBN have been extensively used to improve mechanical properties of polymeric materials and also have demonstrated biological properties as antimicrobial activity or osteoconductivity. This work aims to study the effect that the addition of GBN to a photocurable resin, with biomedical applications, used for LCD 3D printing, have over the photopolymerization process and therefore, over the printing process.

Photopolymerization process is mainly governed by two parameters: the penetration depth of the curing light and the energy needed to polymerize. Jacob's working curve is widely used in literature as a basic procedure for testing and characterizing photocurable resins[1]. If curing depth is not large enough, delamination may occur. To avoid it, exposure time could be increased. However, over-curing could occur, leading to a detriment in printing accuracy. In this work, the effect of GBN on curing depth was study and exposure time was optimized following the study reported by Barkane et al. [3].

EXPERIMENTAL METHODS

Materials: PLA resin was eResin PLA Bio-Photopolymer Resin White, supplied by Shenzhen eSUN Industrial Co., Ltd. (Shenzhen, China). Three different Graphene-Based Nanomaterials (GBN) were used in this study: Graphene (G) (Avanzare), Graphene Oxide (GO), and Graphite Nanoplatelets (GoxNP) (Nanoinnova).

Sample preparation: GBN were dispersed with ultrasonication by probe (US) combined with mechanical stirring (MS): 10' US + 60' MS + 10' US.

Jacobs' working curve: Liquid mixtures were exposed to UV light for different times. Cured surfaces were cleaned with IPA and thickness was measured. Jacobs' working curve is described by Eq. 1.

$$CC_{dd} = DD_{pp} \cdot llll \frac{EE_0}{EE_{cc}} \quad (1)$$

Being C_d the cured depth, E_0 the energy of the light at the surface and E_c the "critical" energy to start the polymerization. D_p is the depth where the penetrating light intensity falls 1/e.

Optimal exposure time: Intensity of the peaks corresponding to C=O and C=C were measured with Tensor 27 Spectrophotometer (Bruker). $I_{C=O}/I_{C=C}$ was represented as a function of exposure time. A linear relationship is found, but the slope changed at a certain point. Optimal curing time can be calculated as the intersection point of the lines with different slope[3].

Thermal characterization: Samples with different exposure times were obtained by LCD printing and T_g was calculated by DSC 882e (Mettler Toledo).

RESULTS AND DISCUSSION

In all cases, the addition of GBN to PLA resin reduced E_c and D_p, affecting the photocuring process. The more notable effect on the D_p reduction was observed in the case of G, probable caused by a reduction on the light penetration due to its opaqueness against UV wavelength.

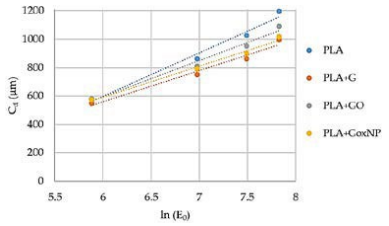

Figure 1. Jacobs' working curves

The reduction of E_c could be due to a catalytic effect of GBN. When optimal exposure time was studied, this catalytic effect was also found and the optimal time were reduced, especially in the case of GO.

Table 1. Optimal exposure time

	PLA	PLA +G	PLA +GO	PLA +GoxNP
Optimal time (s)	9.26	4.64	2.43	5.09

CONCLUSION

GBN catalyzed the polymerization of PLA thanks to its structure and oxygenated groups but also impact on the UV light penetration. This effect could modify the printing process and should be take into consideration to optimize the printability of this kind of materials.

REFERENCES

1. Rehman S. *et al.*, Termochim. Acta. 694: 178785, 2020
2. Paz E. *et al.*, Mater. 12 (19): 1-14, 2019
3. Barkane A. *et al.*, Polym. Degrad. Stab. 181: 109347, 2020

Development of Zirconia Toughened Alumina Composites Reinforced with Carbon Phases for Application as Femoral Heads of Hip Prostheses

Vivian Inês dos Santos[1,2,*], Bruno Alexandre Pacheco de Castro Henriques[1], Márcio Celso Fredel[1], Laurent Gremillard[2]

[1]Mechanical Engineering Department, Federal University of Santa Catarina, Florianópolis, SC, 88040-900, Brazil
[2]Univ Lyon, CNRS, INSA Lyon, UCBL, MATEIS, UMR5510, 69100 Villeurbanne, France
[*] vivian.inds@gmail.com

INTRODUCTION

Increasing longevity has been intensifying the number of hip replacements and the need for hip prostheses with improved lifespan. In this concern, the durability of these medical devices is strongly related to their mechanical properties, in particular to their wear resistance and, in the case of ceramics, their mechanical reliability (fracture toughness). To enhance these mechanical properties, this project studied the reinforcement of ATZ (alumina toughened zirconia) with oriented carbon phases (nanotubes (CNTs) or nanofibers (CNFs)) achieving orientation through the printing method of direct ink writing (DIW).

EXPERIMENTAL METHODS

The suspensions for the DIW printing were mixed and homogenized in a Speed Mixer DAC 150.1 FVZ-K planetary mixer (FlackTeck Inc.) in 150 mL PE containers. A deflocculant (Darvan 821-A, 1.0 wt%) was added to water and mixed at 800 rpm for 90 s and 1500 rpm also for 90 s. Then, the binder (Pluronic® F-127, 25 wt% in relation to the liquids) was incorporated into the suspension that underwent the same mixture procedure, this time under vacuum. The suspension was then cooled in a refrigerator at 4 °C for 10 min. Subsequently, the ATZ powder (33 vol%) was added to the suspension with zirconia grinding balls (1 and 2 mm in diameter) to facilitate the mixing procedure. After mixing again with the same procedure, either the multi-walled carbon nanotubes (MWCNTs) or the carbon nanofibers were introduced into the suspension in the contents of 0.01 to 2.0 wt% (0.01, 0.03, 0.05, 0.1, 0.5, 1.00 and 2.00 wt%). After mixing, the suspension was put in a sieve container in the Speed Mixer to remove the balls from the suspension. The final suspension was stored in 5 mL syringes.

The printing procedure was conducted with the aid of the Robocad 5.1 software in a Robocasting printer (3D Inks LLC, Stillwater, OK, USA). The parts were printed at 25 °C under a humid atmosphere of 75% RH to avoid premature drying of the parts. The printing support was a glass plate with a very thin coconut oil layer deposited on its surface to minimize the stresses during drying. The nozzle diameter was varied during the study to ensure the proper orientation of the CNTs/CNFs.

A complete rheological evaluation optimized the composition and studied the influence of each component of the suspension on its viscosity, yield stress and hysteresis behavior. The influence of the different process parameters on microstructural properties (such as the CNT/CNF orientation) and mechanical properties was determined. Sintering was performed by the Spark Plasma Sintering (SPS) method.

RESULTS AND DISCUSSION

The optimized deflocculant content was shown to be 1.0 wt%, a value that was utilized for all the suspensions produced. The maximum solid content of the suspension was determined to be 47 vol%. The rheological evaluations showed that the addition of the highest CNT/CNF content (2.0 wt%) resulted in the displacement in the suspension behavior equivalent to a 3 vol% increment in solid content. A study of the microstructural features of the printed components was conducted, including the characterization of the defects and the orientation of the nanotubes/fibers.

CONCLUSION

The present study highlighted the influence of the presence of strong reinforcement phases such as CNTs and CNFs in ceramic matrices, which are typically known for their low fracture toughness. It was shown that control of the orientation of the nanotubes/fibers by the process parameters is possible and that this aspect influences the mechanical properties of the composites. The results found are of great interest to a field such as that of hip prostheses in which the lifespan of the components is highly dependent on their mechanical behavior.

ACKNOWLEDGMENTS

The authors would like to thank the Higher Education Personnel Improvement Coordination (CAPES-Brazil) for providing financial support to this project, by means of the Project CERCA (Carbon-phase Reinforced Ceramic Composites for biological applications, COFECUB/CAPES (936/19)).

Hybrid Resins for the 3D Printing of Nitric Oxide-Releasing Blood Contacting Devices

Laura C. E. da Silva[1], Elizaura H. C. Silva[1], Giovana B. Romano[1], Marcelo G. de Oliveira[1*]

[1]Institute of Chemistry, University of Campinas, UNICAMP, Campinas, SP, Brazil.
[*] mgo@unicamp.br

INTRODUCTION

Poly(2-hydroxyethyl methacrylate) (PHEMA) is a hydrophylic polymer widely used in the biomedical field due to its biocompatibility and wear resistance[1]. Pluronics are atoxic triblock copolymers which are able to form supramolecular micellar arrangements that confer flexibility and drug delivery control[2]. The insertion of triethoxysilyl groups at the hydroxyl groups of PHEMA and Pluronics allows the in-situ formation of polysilsesquioxane (PSS)[3] that confers thermal and mechanical stability and may promote drug delivery control. Nitric oxide (NO) is an endogenous radical species involved in vasodilation, angiogenesis and endothelialization. The NO delivery from biomaterials is usually obtained from S-nitrosothiols (RSNO) incorporation[4]. Herein we developed novel hybrid photocurable resins that contain PHEMA, F127 and in-situ generated PSS. These resins are useful for producing blood contacting devices through 3D printing via Digital Light Processing (DLP). The S-nitrosoglutathione (GSNO) incorporation on the 3D constructs allowed the spontaneous NO release mediated by hydration.

EXPERIMENTAL METHODS

The hybrid 2-triethoxysilylethyl methacrylate (HEMA-TES) and ditriethoxysilyl-Pluronic F127 (TES-F127-TES) precursors were produced as described elsewhere[3]. Three different hybrid resins were produced. The PHEMA-PSS was obtained by mixing HEMA-TES with HEMA and acidified water. PHEMA-PSS-F127 was obtained by including 7.5 wt% of TES-F127-TES into the previous mixture (reducing HEMA content) and PHEMA-PSS-F127-DMA was obtained by substituting TES-F127-TES by a dimethacrylate-terminated F127 (F127-DMA) produced according to Van Hove et al.[5]. All resins were 3D printed using a PhotonS (Anycubic) LCD-DLP 3D printer, washed and post-cured in a wash and cure chamber (Anycubic), submerged in a 10 mM GSNO solution for 30 min and freeze-dried to produce NO-releasing 3D constructs. Real-time NO release was measured by chemiluminescence in a NOA, Sievers 280i (GE Analytical Instruments). Numerical results are average of triplicate measurements

RESULTS AND DISCUSSION

3D printable hybrid resins were produced from the hydrolysis and condensation reaction in acidified media of the HEMA-TES hybrid monomer in the absence or presence of chain-end modified Pluronics (TES-F127-TES or F127-DMA) to generate polysilsesquioxane nanoparticles in situ. All resins were stable at 8 °C for at least 24 months and were able to withstand at least 5 printing processes in commercially available LCD-DLP 3D printers without loss of reactivity. Fig 1. shows a representative 3D construct obtained from these resins, along with scanning electron micrographs (SEM) of their top surface, showing the high fidelity to the CAD model. The Pluronic F127 addition significantly reduced the model fidelity, however, the TES-F127-TES substitution by F127-DMA recuperated it significantly. All 3D constructs were able to sustain constant NO release for at least 10 hours in ranges within the beneficial NO actions[4]. PHEMA-PSS showed a rate of approximately 2.1 nmol min^{-1} g^{-1} while PHEMA-PSS-F127 and PHEMA-PSS-F127-DMA showed approximately 0.7 nmol min^{-1} g^{-1} rates, highlighting F127 participation on the NO release control.

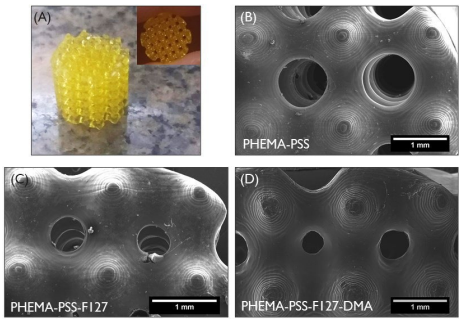

Fig 1. (A) Representative 3D construct. Top view on the inse). (B-D) SEM of the top surface of the 3D constructs built from each hybrid resin.

CONCLUSION

Hybrid 3D printable resins were obtained with good stability and printability, resulting in 3D constructs with good model fidelity and NO-releasing properties. The incorporation of chain-end functionalized Pluronics reduced model fidelity and NO release control.

REFERENCES

1. Wirth DM *et al.*, ACS Appl, Mater, Interf., 12:19033 – 19043, 2020.
2. Wanka G *et al.*, Macromolecules, 27:145–4159, 1994.
3. Da Silva LCE *et al.*, Soft Matter, 14:1709-1718, 2018.
4. de Oliveira MG. Basic & Clin. Pharmacol. & Toxicol. 119:49-56, 2016.
5. Van Hove AH. *et al.*, J. Vis. Exp., 80:e50890, 2013.

ACKNOWLEDGMENTS

The authors would like to thank the São Paulo research Foundation (FAPESP), grants 2016/02414-5 (MGO); 2018/14142-5 (LCES) and 2020/16804-5 (GBR), and the National Council for Scientific and Technological Development, grant 142065/2021-8 (EHCS).

Digital Light Processing of biocompatible acrylate-endcapped poly(ε-caprolactone)-based resins into porous shape memory scaffolds towards minimally invasive breast reconstruction

Coralie Gréant[1], Bo Van Durme[1], Lana Van Damme[1], Sandra Van Vlierberghe[1]
[1]Polymer Chemistry & Biomaterials Group – Centre of Macromolecular Chemistry (CMaC) – Department of Organic and Macromolecular Chemistry, Ghent University, Krijgslaan 281, S4-Bis, 9000 Ghent, Belgium
*coralie.greant@ugent.be

INTRODUCTION

According to estimations of the Global Cancer Observatory, worldwide, over 2.2 million women were diagnosed with breast cancer in 2020[1]. While most of these women require surgical removal of the affected breast tissue, breast reconstruction following mastectomy remains a challenge[2]. Conventional reconstruction techniques, using synthetic prostheses or autologous tissue, are often accompanied with risks and complications. Therefore, regenerative adipose tissue engineering is of great interest as it aims to shift reconstruction strategies from tissue replacement to autologous tissue regeneration. In the present work, a novel approach is envisaged to enable minimally invasive, patient-specific breast reconstruction based on 3D printed shape memory PCL-scaffolds.

EXPERIMENTAL METHODS

Bifunctional PCLs with two different molar masses were synthesized using ethylene glycol as initiator. Next, these PCLs were converted into photocrosslinkable acrylate-endcapped urethane-based polymers (AUPs), which were characterized physico-chemically by ^{1}H NMR spectroscopy, differential scanning calorimetry (DSC) and thermogravimetric analysis (TGA). These PCL-AUPs were used as a basis for a photo-sensitive resin using TPO-L as photo-initiator, Tartrazine as photo-absorber and 1-methyl-2-pyrrolidine (NMP) as solvent. (Photo-)rheology was performed to identify the maximal AUP concentration and to gain insights in the photocrosslinking kinetics. Gel fraction and swelling ratio experiments were performed on crosslinked discs. Next, DLP printing experiments were performed on a LumenX printer. The obtained scaffolds were characterized via light microscopy and scanning electron microscopy. Finally, *in vitro* biocompatibility assays were performed via an indirect cytotoxicity assay at 24h, 72h and 7 days in culture media using adipose-derived stem cells. Lastly, preliminary shape memory experiments were performed.

RESULTS AND DISCUSSION

^{1}H NMR indicated successful polymerization of PCL resulting in molar masses of 2000 and 6000 g mol^{-1} (i.e. PCL-2k and PCL-6k) as well as successful endcapping into AUPs, with acrylate contents of 0.43 and 0.15 mmol g^{-1} for PCL-2k AUP and PCL-6k AUP, respectively. DSC experiments indicated that PCL-2k AUP exhibited the most favorable melting temperature (i.e., corresponding to shape memory trigger) below body temperature (T_m = 35.2°C). Furthermore, the synthesized materials exhibited excellent thermal degradation properties (T_d above 250°C).

Subsequently, these materials were used as a basis for a photo-sensitive PCL-2k AUP-based resin. Rheological evaluation allowed to identify the maximal AUP concentration, while maintaining a viscosity below 3 Pa.s, whereas photorheology measurements were performed to gain insight in the photocrosslinking kinetics upon variation of the TPO-L concentration. Furthermore, gel fraction and swelling tests were performed on crosslinked discs, resulting in values above 70% and below 7%, respectively. Based on this set of experiments, an optimal resin composition could be identified suitable for DLP printing.

Finally, the photo-sensitive resin was DLP processed into porous scaffolds with a pore size of 1000 µm x 1000 µm and a strut size of 200 µm, as an appropriate porous architecture will enable adipose tissue infiltration and regeneration within the scaffold. Light microscopy and scanning electron microscopy analysis confirmed that the pore and strut features were close to the target values.

In vitro biocompatibility assays were performed via an indirect cytotoxicity assay in culture medium using adipose-derived stem cells. The medium, containing any leached components, was placed on top of the seeded cells to assess biocompatibility through a live/dead staining and MTS assay. This indicated that all assessed formulations were considered biocompatible (i.e. >70% viability).

Lastly, a crucial aspect in this project is the shape memory behavior of the final scaffolds. To this end, preliminary proof-of-concept experiments indicated a reproducible shape shift around body temperature (i.e. 37°C). This is promising towards the minimally invasive approach of the developed strategy. Additionally, the materials proved fully biodegradable in accelerated degradation assays. More in depth analysis of this shape memory behavior as evaluated by shape fixity and strain recovery, as well as the mechanical characterization of the scaffolds, is currently ongoing.

CONCLUSION

As a result, the developed biocompatible, degradable porous shape memory scaffolds can be considered promising candidates towards minimally invasive, patient-specific adipose tissue engineering.

REFERENCES

1. International Agency for Research on Cancer 2021. GLOBOCAN 2020, https://gco.iarc.fr/
2. S. Winocour and V. Lemaine, “Hypoplastic breast anomalies in the female adolescent breast,” Semin. Plast. Surg., vol. 27, no. 1, pp. 42–48, 2013.

ACKNOWLEDGMENTS

The authors would like to acknowledge the Research Foundation Flanders (FWO) and the Interreg program MATMED for financial support under the form of the research grant G056219N and Interreg NWE 5B (2014-2020) project no. NWE764, respectively.

PATIENT-SPECIFIC PRINTING OF CONDUCTIVE BIPHASIC PEDOT:PSS-HYALURONIC ACID SCAFFOLDS FOR SPINAL CORD REPAIR.

Woods, I.[1*], Leahy, L.[1], Phair, W.[1], Dervan, A.[1], O'Brien, FJ.[1,2]

[1] Tissue Engineering Research Group, Dept. of Anatomy & Regenerative Medicine, Royal College of Surgeons in Ireland, Dublin, Ireland

[2]Advanced Materials Bio-Engineering Research Centre (AMBER), Trinity College Dublin & Royal College of Surgeons in Ireland, Dublin 2, Ireland

[*]IanWoods@rcsi.ie

INTRODUCTION

Due to the complex pathophysiology of spinal cord injury (SCI) and the poor intrinsic healing potential of the damaged cord, effective treatments for functional repair are lacking. Electrical stimulation can enhance neural regeneration and there is increasing focus on the use of conductive biomaterials to deliver this novel therapeutic approach (1). However, these materials exhibit poor processability - making the manufacture of conductive scaffolds with the complex geometries necessary for SCI repair a challenging proposition. To resolve this issue, it was hypothesized that an indirect printing technique using sacrificial moulds modelled on high resolution MRIs of spinal cords (2) could be used to produce anatomically correct architectures, while addition of a neurotrophic biomaterial would enhance axonal growth through the scaffold. As part of a 2-step process, a conductive PEDOT:PSS architecture mimicking the anatomy of cord axonal tracts was produced and then filled with a neurotrophic hyaluronic acid material (HyA)(3). The resulting biphasic scaffold exhibits a complex conductive architecture alongside a neurotrophic material for enhancing axonal regeneration.

EXPERIMENTAL METHODS

PEDOT:PSS and HyA-filler materials were used to coat glass coverslips (n=4) and the resulting films were used as a substrate for the culture of SH-SY5Y neuronal cells. Following 3 and 7 days of culture, respectively, cellular proliferation & morphology were analysed using a picogreen assay and immunohistochemistry.

A high resolution MRI data set of the human spinal cord was used to produce anatomically correct models of the human spinal cord (Fig.1 (A)). Meshmixer (Auto-desk) was used to produce a 3D model of the cervical spinal cord (C3) with manual tracing of axonal tracts throughout (Fig 1. (A)). An Ultimaker-2 (Ultimaker, NL) was used to 3D-print sacrificial PVA moulds of the axonal tract model.

The PVA moulds were filled with a PEDOT:PSS solution, freeze-dried and the PVA mould dissolved in diH20. The polymer frame scaffolds were then dried & heat treated in a vacuum oven. Hydrazide-modified hyaluronic acid gels were prepared through crosslinkage of 3mg/ml hyaluronic acid solution using adipic acid hydrazide and EDC, as previously described (3), and the PEDOT:PSS frames were filled with the HyA-filler material. A directional freeze drying protocol was then used to produce macroporous scaffolds with aligned pores. The conductivity of the PEDOT architectures was analysed using a sourcemeter (Keithley) and the pore structure was analysed using SEM microscopy.

RESULTS AND DISCUSSION

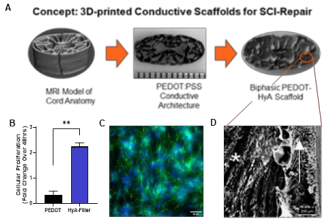

Figure 1. Manufacture of Biphasic PEDOT:PSS/HyA scaffolds for SCI-repair. (A) 3D modelling and the 2-step manufacturing process. (B) Neuronal proliferation is significantly higher on HyA Filler. (C) F-actin labelling of SH-SY5Y neurons on HyA-filler exhibit dense neurite networks (scale bar = 50 µm). (D) SEM of pore structure (*=HyA, Arrow=PEDOT:PSS, scale bar=200µm).

A comparison of the biocompatibility of the HyA-filler with PEDOT:PSS indicated that cellular proliferation significantly increased on the HyA substrates (Fig 1. (B)) & that neurons exhibited excellent biocompatibility (C). The conductivity of the frame material was indicated to be ~0.26 ±0.7 S/m. Following fabrication of biphasic scaffolds, SEM analysis indicated the successful production of an aligned pore structure (D) throughout the HyA-filled axon tracts. The use of indirect printing allowed the production of conductive polymer scaffolds with complex anatomically relevant geometries. However, the conductance of the biphasic scaffold structure is limited by the surface area of the conductive architecture.

CONCLUSION

The biphasic nature of the scaffold combines the conductivity of PEDOT:PSS with the neurotrophic properties of the HyA-filler and overcomes a significant challenge for the application of conductive materials for spinal cord injury.

REFERENCES

(1) Zhao, Y., et al. (2020) Biomaterials 255;120164
(2) Calabrese, E., et al. (2018) Neuroimage Clin. 27;18:963-971.
(3) Woods, I. et al., (2021) Adv. Healthc. Mater. (Nov) 16:e2101663

ACKNOWLEDGMENTS

Authors would like to thank the following funding bodies; AMBER & IRFU Charitable Trust - Grant No. 2349A
IRC Fellowship – Grant No. GOIPD/2021/262

Combining Melt Electrowriting with other 3D printing techniques towards regenerative implants

Max von Witzleben*, David Kilian, Alina Zeinlova, Marlene Ihler, Emily Steyer, Tilman Ahlfeld, Anne Bernhardt, Anja Lode, Michael Gelinsky

Technische Universität Dresden, Faculty of Medicine, Center for Translational Bone, Joint and Soft Tissue Research, Dresden, Germany
*Max.von_Witzleben@tu-dresden.de

INTRODUCTION

In the additive manufacturing process of melt electrowriting (MEW), a molten polycaprolactone (PCL) jet is stabilized by high voltage to deposit micrometer fibers in an arrayed pattern to produce highly defined scaffolds. While this can mimic the extracellular matrix and control cell-scaffold interaction in a determined manner, the maximum scaffold height is limited to a few millimeters. For translational research, it means that thin membranes such as the tympanic membrane (TM) can be mimicked in an appropriate way, but MEW is less suitable for larger, hierarchical constructs. This problem is addressed by combining MEW with other additive manufacturing techniques, e.g. fused deposition modeling (FDM) or extrusion printing. On the one hand, these techniques can be employed to fabricate sacrificial structures to induce a three-dimensional morphology in otherwise flat structures through the shape memory effect of PCL. On the other hand, they can be combined in an alternating manner to produce heterogeneous hierarchical scaffolds. Furthermore, the occurring irritation of the otherwise homogeneous electric field due to the presence of additional structures on the print bed significantly complicates accurate deposition of MEW fibers with a consistent diameter. Yet, in order to understand the interaction of the different possible materials and the necessary requirements for the printing process, we have combined a number of different manufacturing processes in one printing process with MEW. This resulted in the fabrication of several implants for different tissue types such as bone, tendon, TM and vessels.

EXPERIMENTAL METHODS

All printing techniques were performed on one GeSiM BioScaffolder 3.1 combined with a MEW module. PCL fibers were deposited on sacrificial pyramids made of silicone to imitate the funnel-shape of the TM. The impact of different pyramid designs on fiber diameter and placement was evaluated. Subsequently, we applied these parameters to the fabrication of composite scaffolds of calcium phosphate cements (CPC) + PCL, embroidery scaffolds + PCL, and alginate-methylcellulose (Alg-MC 3/9 wt%) + PCL. All scaffold types were then mechanically investigated either with tensile- or compression tests. Moreover, the biocompatibility with the respective tissue-specific cell types was analyzed.

RESULTS AND CONCLUSION

To improve the mimicry of the natural TM with a synthetic replica, the shape memory effect of the PCL was exploited. In order to achieve a homogeneous fibre diameter and an aligned fibre placement, the modification of the electric field due to the pyramids had to be considered. Thus, not only material choice, occurring edges and peaks, but also the gradient of the pyramids mainly influenced the fibre diameter. By choosing a suitable gradient, a selective placement of edges in the sacrificial structure and an appropriate distance from nozzle to placement location, a homogeneous fibre diameter without major fibre pulsing and -beading could be achieved. The fibre placement was optimized in such a way that the fabricated scaffolds mimicked not only the morphological and the structural but also the acousto-mechanical properties of the TM.

Upon transfer of these findings to bone replacement scaffolds, porosity significantly influenced fibre deposition. When the PCL fibres were deposited parallel to the CPC strands, the strands deflected the fibres from their intended deposition location. Conversely, the more perpendicular the fibres were deposited to the CPC strands, the more accurate the deposition was. In this way, open-pore scaffolds in clinically relevant defect sizes (> 3 cm) could be realized by an alternating combination of PCL microfibers with printed CPC. Moreover, this minimal addition of PCL content improved the mechanical properties in such a way that fragments of CPC occurring under load did not dislocate but were fixed by the fibres. Furthermore, a PCL mesh printed larger than the CPC scaffold would provide a suturing option and thus allow a better fixation of the scaffold during surgery.

In another study, PCL microfiber structures were deployed on embroidered scaffolds to optimize cell-scaffold interaction in view of tendon replacement. This resulted in directed cell growth on the scaffolds even without mechanical stimulation. Additional collagen coating increased the biocompatibility of the composite scaffolds and provided more uniform and rapid cell growth.

The addition of PCL fibres to vascular grafts of Alg-MC was challenging as the Alg-MC dried during the time consuming printing process of the fibres. Appropriate adjustment of the printing parameters not only resulted in an ordered fibre pattern and a homogeneous fibre diameter, but also increased the mechanical robustness of the scaffolds in a suitable manner to allow the scaffolds to be sewn to tissue without negatively affecting the perfusion properties.

Synthesis and Characterization of collagen based bio-ink for 3D printed meniscus with improved mechanical properties

Alfredo Ronca[1*], Ugo D'Amora[1], Carla Zihlmann[2], Niklaus Stiefel[2], Anna Abbadessa[3], Anna Guilford[4], Luigi Ambrosio[1*]

[1]Institute of Polymers, Composites and Biomaterials – National Research Council of Italy, Viale Kennedy, 54; Mostra d'Oltremare – Pad. 20 80125 Napoli, Italy.
[2] Geistlich Pharma AG (Geistlich), Bahnhofstrasse 40, CH-6110 Wolhusen, Switzerland.
[3] University of Santiago de Compostela (USC), Av. Barcelona s/n, Campus Vida ES-15782 Santiago de Compostela Spain.
[4] Tissue Click Ltd (TC) C3c The Knoll Business Centre, Old Shoreham Road, Hove BN3 7GS Brighton and Hove UK
*alfredo.ronca@cnr.it

INTRODUCTION

Current approaches for meniscus repair focus on the combination of scaffolds acting as substrates of relevant cell populations involved in meniscal healing that can be supplemented with growth factors to increase the healing potential induced by cells. Among the different biomaterials, polymeric hydrogels exhibit a high cell biocompatibility and tunable properties to modulate the release of bioactive molecules or cells [1,2]. In this work, two different strategies have been adopted for the synthesis of a biodegradable bio-ink for meniscus regeneration. In the first approach, double network (DN) hydrogels were prepared through the synergic use of methacrylated hyaluronic acid (MEHA) and polyethylene glycole diacrylate (PEGDA). The second approach, instead, entailed the synthesis of bio-ink based on medical grade collagen blend. Successively both bio-inks have been characterized from mechanical, morphological and biological point of view and they have been optimized for 3D printing process. Moreover, due to the importance of the suture pull out force during the surgery different strategies have been adopted to increase these properties.

EXPERIMENTAL METHODS

Hyaluronic acid sodium salt (HAs, M=~340 kDa, Bloomage Freda Biopharm Co. Ltd., Shandong, China) was modified to graft photoactive polymerizable groups by reacting with methacrylic anhydride (ME) as previously reported (1). DN three-dimensional (3D) scaffolds were synthesized by two-step reaction procedure. Briefly, MEHA hydrogels were immersed in PEGDA/Irgacure solution (20 %) for four days. The soaked samples were successively photocrosslinked for 180 seconds by UV radiation (2). In parallel bio-inks with different collagen fiber sizes and concentrations (w/w) 5%, 10%, 15%, and 20% at pH 3.5 were prepared and optimized in terms of viscosity and injectability properties. The collagen concentration of 12.5% has been selected and it was used for further experiments due to their printability and shape retention. Both bio inks have been characterized in terms of mechanical properties, internal morphology, printability and, shape retention after printing. Moreover, zonal functionalization has been realized by using loaded PLGA microparticles, PhenoDrive-Y and PhenoDrive-U biomimics (Tissue Click, UK) to induce different vascularization stimuli inside the scaffold. The biological effect of the biomimics as well as the distribution of microparticles have been evaluated.

RESULTS AND DISCUSSION

In order to find a suited material for a meniscal implant, a MEHA, MEHA-PEDGA double network as well as a collagen bio-ink have been prepared. DN hydrogel did not show the appropriate properties in terms of suturing. A collagen bio-ink has been optimized in terms of printability and processed by "In Vivo Rokit 4D" to obtain 3D porous scaffold. Morphological analysis by SEM performed on the collagen-based scaffold revealed that collagen scaffolds were able to maintain their 3D porous structure after printing and lyophilization, with a good shape fidelity. PLGA microparticle loaded collagen bio-ink was successfully printed and particles were homogenously distributed in the matrix. Moreover, the presence of PhenoDrive-Y and PhenoDrive-U inside the collagen blend improved cell viability and proliferation. However, since collagen alone does not fulfil the minimal target of 10N for the suture pull out test, a collagen blend consisting collagen/Poly(vinyl alcohol) and Collagen/Polyvinylpyrrolidone have been developed and tested.

CONCLUSION

In order to find a suitable material for a meniscal implant, a MEHA/PEGDA based double network (DN) hydrogel as well as a medical grade collagen bio-ink have been prepared. DN hydrogel did not show the appropriate properties in terms of suturing. Preliminary tests showed that collagen blend improves mechanical properties without altering its printability and 3D shape fidelity. While preliminary biological results showed that the functionalization with particles and biomimics improve of cell viability and proliferation.

REFERENCES

1. D'Amora U et al. Regen Biomater. 2019;6(5).
2. Ronca A, et al. Materials (Basel). 2018;11(12).

ACKNOWLEDGMENTS

The project leading to this application has received funding from the European Union's Horizon 2020 research and innovation programme under grant agreement No 814444 (MEFISTO).

Influence of anodic oxidation on the biocompatibility of Ti6Al4V implants made by the SLM method

Ada Orłowska[1*], Janusz Szewczenko[1], Wojciech Kajzer[1], Karolina Goldsztajn[1], Marcin Basiaga[1]

[1]Department of Biomaterials and Medical Devices Engineering, Faculty of Biomedical Engineering, Silesian University of Technology, 41-800 Zabrze, Poland
[*] ada.orlowska@polsl.pl

INTRODUCTION

The aim of the study was to determine the effect of surface modifications using anodic oxidation on the spine cage implant produced by the SLM method. The use of incremental methods to produce permanent implants makes it possible to create an element with an open structure which allows the implant to overgrow with tissue. Although 3D printing has been successfully used in the manufacture of clinically used implants [1], and the process of modification of biomaterials, i.e. Ti6Al4V, is widely researched [2], there is little research into the effect of modifications applied to conventionally processed biomaterials on the biocompatibility of SLM implants.

The study was conducted with the use of a proprietary spine cage implant intended for the treatment of discopathy in the c4-c5 segment with an open structure based on a diamond mesh with high porosity (porosity ~ 65%, pore size 600 µm) [3]. The mechanical resistance of the implant to physiological loads has been verified with the use of FEM and strength tests (static compression test). The implant was made of Ti6Al4V at ChM sp.z o.o. in Bialystok

EXPERIMENTAL METHODS

The tests were carried out on samples in their original state and anodically oxidized (U = 97 V, t = 2 min) in a Titan Color solution (phosphoric acid + sulfuric acid). The tests included studies of the corrosion potential and determination of the mass density of metal ions (Ti, Al, V) for the incubation solution (PBS). Additionally, microscopic observations were performed to determine the actual pore size, helium pycnometry to determine the actual porosity, and SEM observations to compare the implant surface before and after modification. The microscopic and SEM observations were made on the outer layers of the implant and in its central part (after cutting the sample). The studies were carried out on freshly prepared implants and after 2, 4 and 6 weeks of incubation in PBS at 37° C.

RESULTS AND DISCUSSION

The microscopic examination showed a smaller pore size than the designed value. The actual pore diameter was 450-500 µm compared to 600 in the model. Helium pycnometry showed a decrease in the designed porosity from 65% to 44% of the actual porosity. Referring to the literature data, this difference is acceptable, and the obtained pores are within the optimal size range for the conditions of bone tissue overgrown. Observations did not reveal any differences between the pores on the surface of the implant and in its central part.

Comparing SEM images, anodically oxidized implants were characterized by greater smoothness, however, these differences were visible at the nanoscale.

Corrosion tests showed that anodic oxidation allowed to obtain a positive corrosion potential (~ 400 mV), which is very beneficial for the potential bone overgrowth of the implant. For comparison, the samples in the initial state had a potential of ~ 0mV. The samples in the initial state achieved the lowest value of the corrosion potential after 2 weeks (~ -470mV). Longer incubation resulted in a slight increase in potential (~ -415 mV after 6 weeks). The decrease in the corrosion potential of the oxidized samples was greater and remained at a constant level for all measurement groups (~ -550 mV).

The study of the mass density of metal ions permeating into the environment showed a decrease by 15-30% in the concentration of all ions for the anodized samples in relation to the samples in the unmodified state.

CONCLUSION

Surface modifications with the use of anodic oxidation have a positive effect on the biocompatibility of Ti6Al4V implants produced by the SLM method. Further research is being carried out to optimize the surface modification of this type of implants.

REFERENCES

1. McGilvray K.C. *et al*., The Spine J. 18:1250-1260, 2018
2. Diamanti M.V. *et al.*, J Appl Biomater Biomech. 9:55-69, 2011
3. Tamiguchi N. *et al.*, Mater Sci Eng C, 59: 690-701, 2016

Photocurable Resin for 3D Printed Metamaterials towards Biomedical Applications

Valentina Cirillo*, Estelle Collin, Débora Castel, David Moreau, Marie Malafosse, Maria Pereira

Tissium, Paris, France

*vcirillo@tissium.com

INTRODUCTION

Three-dimensional (3D) Printing, also known as additive manufacturing technique, is used to create a product in a consecutive layering sequence, making possible to produce complex structures when compared with conventional manufacturing techniques. It is one of the most sought-after technologies for the engineering field and medical applications with continuous extending limits.[1]

High-performance 3D printing materials are key for the advancement and practical applications of emerging 3D printing technology.[2] In the biomedical field, there is a strong need of biocompatible 3D printable materials to create 3D printed medical devices.

TISSIUM has developed a synthetic vascular sealant that received the CE mark for clinical use in Europe. Based on the same proprietary polymer (designated poly (glycerol sebacate) acrylate, or PGSA), a photocurable resin was evaluated to produce 3D printed biocompatible metamaterials via digital light processing (DLP). PGSA is based on the acrylation of a tough biodegradable elastomer, poly- (glycerol sebacate) (PGS). PGS is known to have robust mechanical properties and *in vitro* and *in vivo* biocompatibility.[3] The following acrylation step allows to obtain a versatile photocurable biocompatible ink for 3D printing that could be deposited layer-by-layer into complex auxetic and non-auxetic shapes with tuneable mechanical and physico-chemical properties. Here, we investigated the tunability of PGSA resin, varying its chemistry, the processing parameters and the 3D printed architectures in order to 3D print biocompatible metamaterials open to a wide range of applications in the tissue engineering and biomedical fields, such as deployable scaffolds for soft tissue implants or deployable nasal stent with minimally invasive delivery.

EXPERIMENTAL METHODS

PGSA resins were 3D printed using a DLP printer (3D Systems, USA) at 405 nm wavelength. Models were designed by SolidWorks and sliced through the printer software 3D Sprint. After the 3D printing process, the parts were washed in solvent, dried under vacuum to eliminate residual solvent and post-cured. Printing parameters were tuned to obtain desired mechanical and physico-chemical properties. Qualitative evaluation of parts morphology, mechanical and physico-chemical characterizations were performed to assess the impact of the different printing parameters used. Based on those results, graded scaffolds with tunable mechanical property gradients were 3D printed in form of cellular square lattices of holes with a unit cell size of 2 mm. Mechanical response in compression was evaluated using using a dynamometric machine (Instron 3340). PGSA auxetic patterned structures were also 3D printed to fabricate deployable nasal stent as proof of concept. Auxetic pattern width and repetition units were varied. Minimally invasive delivery within the middle turbinate in a human nose model was considered.

RESULTS AND DISCUSSION

Mechanical tests showed that the introduction of acrylate groups into the PGS backbone facilitated an additional level of control of the mechanical properties, with PGSA stiffness increasing with the degree of acrylation. In addition to PGSA polymer programmability and tunability via chemical synthesis, we tested the assumption that the printing conditions and parameters influenced the 3D printed parts, in particular their mechanical properties, by affecting the nature of the polymeric network. As an example, it was proved that modulating the exposure time to the light during the printing process, it was possible to tune PGSA stiffness. The stiffness tunability coupled with lattices designs allowed the production of graded structures exhibiting unprecedented mechanical properties under compression. Indeed, it was possible to obtain a lattice with stiffness gradients in the printing direction. This macroscopic mechanical tunability and the polymer biocompatibility could enable PGSA lattice metamaterials to adapt to various tissue environments, making them promising scaffold candidates for tissue implants.

PGSA was also used to fabricate 3D printed deployable nasal stent for minimally invasive delivery. Thanks to the auxetic 3D printed pattern and the PGSA elasticity, the 9 mm stent was folded to a small volume and inserted into a tube, delivered in a human nose model, then expanded to be well opposed to the tissue of the middle turbinate.

CONCLUSION

The high tunability of TISSIUM proprietary polymer lies in the possibility to influence its properties by altering its chemical structure, by changing 3D printing parameters and designs. This represents a unique combination of factors influencing the final devices properties to obtain 3D printed biocompatible metamaterials, that can be manufactured, industrialised, and commercialised.

REFERENCES

1. Rastogi P. *et al.,* Chem. Eng. J. 366:264-304, 2019
2. Guo Y. *et al.,* J. Mater. Chem. A 5:16307-16314, 2017
3. Nijst C.L.E. *et al.,* Biomacromolecules. 8:3067-3073, 2007

How Simple Surface Treatments Modify Primary Human Osteoblast Response to Additively Manufactured Titanium Scaffolds

Edgar B. Montufar[1,*], Anna Diez-Escudero[2], Adelia Kashimbetova[1], Karel Slameska[1], Ladislav Čelko[1], Nils P. Hailer[2]

[1]Central European Institute of Technology, Brno University of Technology, Brno, Czech Republic
[2]Department of Surgical Sciences, Uppsala University Hospital, Uppsala, Sweden
[*] eb.montufar@ceitec.vutbr.cz

INTRODUCTION

Titanium has high specific strength, low elastic modulus, high corrosion resistance and it is biocompatible, having important applications in medicine. Moreover, the additive manufacturing of titanium enables to produce patient-specific implants and scaffolds with superior control of pore network to promote bone ingrowth and reduce the stiffness of the implant, preventing stress shielding. Besides, several surface treatments have been developed to improve the osseointegration of titanium implants. However, there is limited information of the effects on post-surface treatments on the osteoblast response to titanium scaffolds. Therefore, the aim of this work was to study the *in vitro* behaviour of human osteoblasts (hOb) on robocast titanium scaffolds, either modified by surface alkali treatment or chemically functionalized with gelatine instead of expensive and instable proteins and peptides.

EXPERIMENTAL METHODS

Titanium scaffolds (11 mm in diameter and 4 mm in height) were fabricated by robocasting, using an ink of c.p. titanium powder and gelatine as a binder. The scaffolds were fabricated in air, with a nozzle of 610 µm, following an orthogonal deposition pattern, with the distance between filaments of 550 µm (60 % of porosity). The scaffolds were sintered in argon after removal of the binder. The scaffolds were cleaned and then alkali treated by immersion in 5M NaOH solution at 60 °C for 24 h and subsequently heat treated at 600 °C for 1 h. For functionalization, the clean scaffolds were passivated in HNO_3, silanized in APTES, coupled with glutaraldehyde, and functionalized with type B bovine gelatine.
hOb were isolated from human femoral heads removed by medical reasons after approval of the Swedish ethical review authority (2020-04462). Sterile scaffolds were seeded with $5x10^4$ cells/scaffold and cultured under static conditions up to 21 days. Cell proliferation was quantified by lactate dehydrogenase assay, hOb morphology, matrix deposition and maturation were studied by scanning electron microscopy (SEM), alkaline phosphatase (ALP) assay, Sirius Red and Alizarin Red staining and quantification, and fluorescence immunostaining of nucleus, cytoskeleton, collagen I and osteocalcin (OC).

RESULTS AND DISCUSSION

Fig. 1 shows the surface of the scaffolds. The same smooth and wavy surface was observed in non-treated (Ti) and gelatine functionalized (gel-Ti) scaffolds. Eosin staining and XPS analysis of the surface confirmed the presence of gelatine in the later. The surface of the alkali treated scaffolds (alk-Ti) showed submicrometric porous features over the wave surface, having a crystalline composition of titanium dioxides, rutile and anatase.

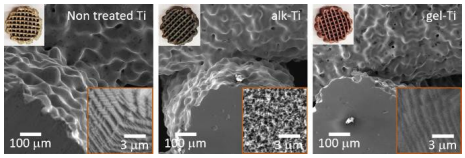

Fig. 1. SEM images of the scaffolds' surfaces and optical images after eosin staining.

The proliferation and viability of hOb was similar on all the scaffolds. Fig. 2 shows that collagen expression was significantly higher, while ALP activity and OC expression were lower on alk-Ti than on the other scaffolds. The highest OC expression was observed on gel-Ti scaffolds. SEM images and Sirius Red staining showed that the cells on alk-Ti were enveloped in a collagen matrix, whereas the cells were clearly recognizable by their morphology on Ti and gel-Ti (Fig. 2), suggesting that the proteins observed by immunostaining have not been yet exocytosed. In congruence, the hOb cultured on gel-Ti showed spherical features under SEM, which may be vesicles containing proteins since nodules of mineralization were not detected by EDX chemical analysis.

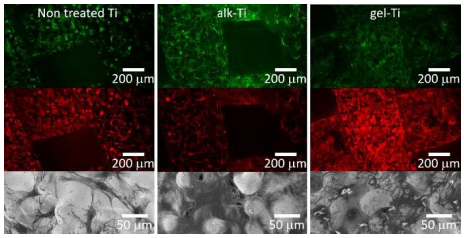

Fig. 2. Immunostaining of collagen I (top, green), OC (centre, red), and SEM images (bottom) of the cells after 21 days of culture.

CONCLUSION

Simple surface treatments significantly modify the hOb response to titanium scaffolds, allowing the selective regulation of bone matrix deposition and maturation *in vitro* without the aid of growth factors.

ACKNOWLEDGMENTS

This work was supported by MEYS - Czech Republic (LTAIN19112). AK acknowledges the Brno PhD talent scholarship.

Establishing a new photo-crosslinkable poly(ε-caprolactone)-based material for tubular melt electrowritten constructs with predefined architecture and tunable mechanical properties

Michael Bartolf-Kopp[3], Nele Pien[1,2], Laurens Parmentier[1], Jasper Delaey[1], Lobke De Vos[1], Diego Mantovani[2], Sandra Van Vlierberghe[1], Peter Dubruel[1], Tomasz Jungst[3]

[1] Polymer Chemistry & Biomaterials Research Group, Centre of Macromolecular Chemistry (CMaC), Ghent University, Krijgslaan 281 S4bis, 9000 Gent, Belgium, [2] Laboratory for Biomaterials and Bioengineering, CRC-I, Laval University, Pavillon Pouliot, Québec G1V 0A6, Canada, [3] Department of Functional Materials in Medicine and Dentistry, Institute of Biofabrication and Functional Materials, University of Würzburg and KeyLab Polymers for Medicine of the Bavarian Polymer Institute (BPI), Pleicherwall 2, 97070 Würzburg, Germany

Michael.bartolf-kopp@fmz.uni-wuerzburg.de

INTRODUCTION

Addressing the necessity of various tubular constructs for medical application has increased in recent years. Several methods try to meet the demand of different lengths and diameters as well as geometrical features such as bifurcations while remaining biocompatible. One of these areas of high demand is the clinical application of artificial vascular grafts in the small diameter category (<6mm), which is limited by factors like rapid graft occlusion, for example due to increased thrombus formation. Due to this, autografts are still the gold standard in vascular grafting surgeries and a need for novel approaches in manufacturing of artificial small diameter vascular grafts is required.

A promising technology to utilize for manufacturing of synthetic tubular grafts is tubular melt electrowriting (MEW). MEW can be used to fabricate filigree and highly ordered geometries with different mechanical properties. These can range from conventional box structures, as known from many additive manufacturing processes, to elaborate geometries like intertwined hexagons and sine waves. Further, certain modifications also allow for special features like klick mechanisms and widening under compression.

One benefit of MEW constructs is the absence of solvents during manufacturing. This limits the overall processable amount of materials compared to solution electrospinning (SES). In recent works, the catalogue of processable materials grows steadily with different intrinsic characteristics like photo-crosslinkability and piezoelectric conductivity[1]. One of these materials is a modified PCL backbone with the name of AUP20k[2].

EXPERIMENTAL METHODS

In our recent work[3], we investigated and characterized the physico-chemical properties of acrylate-endcapped urethane-based (AUP) PCL (AUP20k) to introduce a UV inducible network into the material, even after processing with MEW at elevated temperatures.

DSC/TGA as well as H-NMR and FT-IR have been utilized to confirm the successful modification of the PCL backbone. A custom build MEW device with tubular collector has been used for assessment of MEW processability and fabrication of the tubular AUP20k constructs.

A post-process GPC was employed to analyze blend compositions and constructs were tested circumferentially on an uniaxial testing device to evaluate mechanical properties of constructs.

RESULTS AND DISCUSSION

The material was shown to be processable and retaining its reactivity to UV irradiation, though featuring a very brittle behavior. Blending with medical grade PCL allowed for alterations of the overall mechanical properties while still conserving the crosslinking functionality that enabled further modification post processing. Cyclic mechanical tensile testing illustrated mechanical parameters comparable to blood vessels frequently used in autograft transplantations.

CONCLUSION

Overall, the modification of PCL via urethane crosslinking molecules to introduce acrylate groups onto PCL showed a potential and rather simple pathway of modifications for a novel material, processable via MEW and allowing for post processing modification to finetune mechanical properties of the constructs.

REFERENCES

References must be numbered. Keep the same style.
(1) Kade J.C. et al., Adv. Healthc. Mater. 10 (2021)
(2) Dubruel P. et al., Patent WO 2017/005613. 2017.
(3) Pien N. and Bartolf-Kopp M. et al. Macromol. Mater. Eng. 2022 (in revision)

ACKNOWLEDGMENTS

The authors would like to thank the following institutions for financial support that benefitted this work: Vanier Canada Graduate Scholarship, Research Foundation Flanders (FWO) (K201221N), Deutsche Forschungsgemeinschaft (DFG) (project number 326998133-TRR 225 - subproject Z01) and (INST 105022/58-1 FUGG), European Union for support on printing strategies (European Fund for Regional Development - EFRE Bayern, Bio3D-Druck project 20-3400-2-10). European Union's Horizon 2020 research and innovation program (874827).

Biocompatibility of Ti-Nb and Ti-Zr-Nb alloys generated by means of laser additive manufacturing

Felipe Arias-González[1*], Alejandra Rodríguez-Contreras[2,3,4], Miquel Punset[2,3,4,5], José María Manero[2,3,4], Óscar Barro[1], Mónica Fernández-Arias[1], Fernando Lusquiños[1,6], Francisco Javier Gil[7] and Juan Pou[1,6]

[1]LaserOn Research Group, CINTECX, School of Engineering, UVIGO, Vigo, Spain
[2]BBT Research Group, Materials Science and Engineering Department, UPC, Barcelona, Spain
[3]Institut de Recerca Sant Joan de Déu, Barcelona, Spain
[4]Barcelona Research Center in Multiscale Science and Engineering, UPC, Barcelona, Spain
[5]UPC Innovation and Technology Center, UPC, Barcelona, Spain
[6]Galicia Sur Health Research Institute (IIS Galicia Sur). SERGAS-UVIGO, Vigo, Spain
[7]School of Dentistry, UIC, Sant Cugat del Vallès, Spain
[*] felipeag@uvigo.es

INTRODUCTION

Laser Directed Energy Deposition (LDED) is an Additive Manufacturing (AM) process to build a component by delivering energy and material simultaneously[1,2]. A laser beam is employed to melt the material that is selectively deposited on a specified surface, where it solidifies. The feedstock material is supplied in the form of particles or wire. LDED can be employed to process any material that can be melted, such as metals and some ceramics[3,4]. This technology is particularly suitable for producing low volumes of near net shape products.

The objective of this work is to evaluate the feasibility of the LDED technique to produce biomedical Ti-Nb and Ti-Zr-Nb alloys ranging from 0 wt% Zr to 35 wt% Zr from elemental powders. Samples with different compositions are characterized to analyze the in-vitro biocompatibility.

EXPERIMENTAL METHODS

Laser Directed Energy Deposition (LDED) technique with elemental powders (Ti, Nb and Zr) as feedstock materials was employed to produce in situ Ti-Nb and Ti-Zr-Nb samples with different compositions. Samples were generated employing a high-power diode laser. The powders were carried by argon and coaxially injected in the molten pool by a coaxial laser head. The whole process was carried out in a controlled atmosphere, inside a chamber with a low oxygen content (O_2 < 50 ppm) to avoid the oxidation in the molten pool.

Human osteosarcoma SaOS-2 cells were used to assess the in vitro biocompatibility of the laser-deposited Ti-Nb and Ti-Zr-Nb alloys compared to the cp-Ti grade 2 control. Previously, the surfaces of the materials were treated with SiC paper to obtain a surface with a similar roughness in all the samples (Ra = 2.0 ± 0.4 µm). This roughness value is of the same order of magnitude as that of real implants after shot blasting.

RESULTS AND DISCUSSION

Cell count after 24 h of culture showed a lower number of SaOS-2 cells on cp-Ti grade 2 compared to the laser-deposited alloys. The adhesion of osteoblasts-like cells was 6-, 11-, 7-, 10-, and 7-fold higher on the Ti-12Nb, Ti-37Nb, Ti-57Nb, Ti-34Zr-15Nb, and Ti-35Zr-25Nb alloys, respectively (Figure 1). These significant differences between the cp-Ti grade 2 control and the laser-deposited alloys may be related to the presence of more biocompatible alloying elements, such as Nb and Zr.

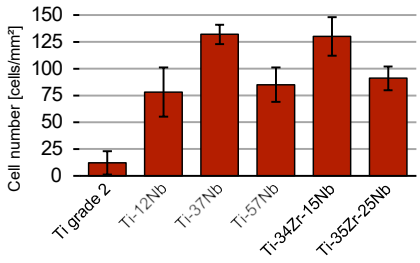

Figure 1. Measured cell number (Error bars represent standard deviation).

CONCLUSION

The feasibility of the Laser Directed Energy Deposition technique to produce in situ biomedical Ti-Nb and Ti-Zr-Nb alloys ranging from 0 wt% Zr to 35 wt% Zr from elemental powders has been demonstrated. Laser-deposited Ti-Nb and Ti-Zr-Nb alloys have an outstanding in-vitro biocompatibility and they are promising materials for orthopedic and dental applications.

REFERENCES

1. Arias-González F. *et al.,* Additive Manufacturing 1st Edition, 121–157, Elsevier, 2021.
2. Saboori A. *et al.,* Appl. Sci. 7:883, 2017.
3. Comesaña R. *et al.,* Sci. Rep. 5:10677, 2015.
4. Arias-González F. *et al.,* Metals 11:1205, 2021.

ACKNOWLEDGMENTS

This research was partially funded by SOADCO S.L. (Escaldes Engordany, Andorra), by the Spanish Government (RTI2018-098075-B-C21), by Xunta de Galicia (ED431C 2019/2; ED481B-2021-113), by Generalitat de Catalunya (2017 SGR-1165) and by the EU through the European Regional Development Funds (MINECO-FEDER, EU). The authors wish to thank the technical staff from CACTI (UVigo), Barcelona Research Center in Multiscale Science and Engineering (UPC) and CCiTUB (UB) for their technical assistance with the characterization techniques. Technical assistance of Mr. A. Abalde (UVigo) is also acknowledged.

3D Printing of an Electroconductive Scaffold for the Promotion of Axonal Regrowth after Spinal Cord Injury

Liam M. Leahy[1,2], Ian Woods.[1,2], Javier Gutierrez-Gonzalez.[1,2,4], Michael G. Monaghan[2,3], Adrian Dervan[1,2], Fergal J. O'Brien[1,2,3]

1 Tissue Engineering Research Group, Dept. of Anatomy & Regenerative Medicine, RCSI, Dublin, Ireland, 2 Advanced Materials and Bioengineering Research Centre (AMBER), RCSI and TCD, Dublin, Ireland, 3 Trinity Centre for Biomedical Engineering and 4. School of Chemistry, TCD, Dublin, Ireland

INTRODUCTION

Spinal cord injury (SCI) induces paralysis by severing the long axons of neurons and recovery is inhibited by poor axon regrowth rates. As neural cells are electroactive, electrical stimulation (ES) may present a promising method of promoting axonal regrowth when applied in conjunction with electroconductive (EC) biomaterials[1]. EC polymers hold promise for such applications, but as thermosetting materials they are difficult to develop into complex 3D structures. This manufacturing barrier must be overcome to develop scaffolds with precise, controllable architectures that could efficiently deliver ES to target regrowth of motor and sensory axons for SCI repair.

This work focused on developing novel EC scaffolds for spinal cord injury by coating 3D-printed polycaprolactone (PCL) with EC polypyrrole (PPy) and assessing its suitability as a substrate for neuronal growth.

EXPERIMENTAL METHODS

PCL scaffolds consisting of multiple interlocking 'axon' channels were extrusion 3D-printed (Allevi 2 printer). PPy was then polymerised *in situ* to form an EC coating[2] on the porous PCL construct Electroconductivity was measured via the 4-point method and surface morphology and coating thickness were assessed using SEM (N=3). The biocompatibility was tested by seeding SH-SY5Y neurons on PPy/PCL films and measuring metabolic activity and total cellular DNA (N=3-5, n=3). Neurons were also immunostained for beta-III tubulin, and imaged using a Nikon 90i fluorescent microscope to determine neurite outgrowth (N=3, n=3). Images were analysed using ImageJ.

RESULTS & DISCUSSION

A method was developed to successfully coat complex 3D-printed PCL structures with a biocompatible, EC PPy layer (Fig 1A, B). These scaffolds are produced via a simple two-step process, comprising traditional extrusion printing and in situ polymerisation, without requiring complex fabrication methods. SEM images of coated films (Fig 1C) show that PPy forms a network of particles over the PCL surface. Conductivity of the PPy coating was 15 ± 5 S/m, rendering the scaffold suitably electroconductive for biological applications. The conductivity of the PPy coating is more than 30 times higher than that of the central nervous system grey matter, potentially allowing for efficient direction of electrical stimulation[3]. In cultures of SH-SY5Y neurons on 2D PCL and PPy/PCL films, metabolic rate and total cellular DNA increased significantly

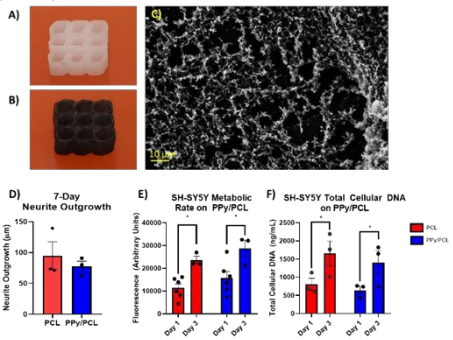

Figure 1 –Images of an uncoated (A) and PPY coated (B) PCL scaffolds. C) SEM image of PPY-coated PCL Surface. SH-SY5Y neurite outgrowth (D), cell metabolic rate (E) and total cellular DNA (F) on PCL and PPy/PCL samples.

($p<0.05$) in both groups between day 1 and 3 (Fig 2E,F), with no significant difference in either metric between groups, showing that the PPy coating is a suitable substrate for neural proliferation. Neurons cultured on both film types for 7 days exhibited robust neurite outgrowth and typical morphology with no significant difference in cell number or neurite length (Fig 2D) between groups, confirming neuronal viability.

CONCLUSION

This study describes the production of biocompatible, 3D EC scaffolds with complex architectures for SCI repair. By coating 3D-printable PCL with EC PPy, the issue of processing EC polymers is avoided, allowing printing of structures with precise, controlled geometries and porosities before coating them with PPy to optimise their electroconductive properties. The neuronal culture results indicate that PPy/PCL is biocompatible, supports neuronal growth and is a suitable substrate for the growth of neurons. The high electroconductivity of the PPy coating renders the PPy-coated PCL suitably conductive for electrical stimulation of neurons.

REFERENCES

1. Bertucci *et al.*, Brain Res. Bull., 152: 265-284, 2019
2. Olvera *et al.*, Adv. Func. Mater., 30: 1909880, 2020
3. McCann *et al.*, Brain Topogr., 32: 825-858, 2019

ACKNOWLEDGEMENTS

Research was funded by Irish Rugby Football Union Charitable Trust and Science Foundation Ireland Advanced Materials and Bioengineering Research (AMBER) Centre (SFI/12/RC/2278_P2).

3D Printed PLA Scaffolds with Double Porosity for Bone Tissue Engineering

Matteo Pitton[1], Davide Pellegatta[1], Davide Vandoni[1], Nicola Contessi Negrini[1], Silvia Farè[1,2]
[1] Department of Chemistry, Materials and Chemical Engineering G. Natta, Politecnico di Milano, Milan, IT
[2] National Interuniversity Consortium of Materials Science and Technology - INSTM, Florence, IT
* matteo.pitton@polimi.it

INTRODUCTION

Conventional additive manufacturing techniques allow to fabricate scaffolds with a single level of porosity, obtained by spacing printed filaments during the printing process (e.g., fused deposition modelling, FDM) [1]. However, a single level of porosity only allows for cells colonization and tissue ingrowth in the designed porous structures, with limited infiltration inside the filaments [2,3]. Herein, we developed a novel technology to print double-porous poly(lactic acid), PLA, scaffold for bone tissue engineering by combining FDM technique, to obtain the conventional porosity of 3D printed scaffolds, and a chemical blowing agent (CBA), to obtain microporous 3D printed filaments. The CBA, incorporated into PLA extruded filaments, is activated when the activation temperature is reached, generating microscopic porosities on the filaments surface.

EXPERIMENTAL METHODS

PLA (Shenzhen Cadit Plastic Material Co., Ltd) and CBA (Sigma-Aldrich) were extruded by using a twin extruder (FSMC2140, TSA Industrial s.r.l) in form of printable filaments, after an optimization step testing different CBA concentration (0, 1, 3, 5, 7.5 and 10 w_{CBA}/w_{PLA}). Extrusion temperature was kept lower than the one of CBA degradation. The extruded filaments were the printed by FDM (Sharebot Next Generation, Sharebot NG, Nibionno, Italy) in 0/90° patterned scaffolds, at 240°C (T > TCBA-degradation), to activate CBA and form microporosity in the filaments. Scaffolds morphology was characterized by SEM, pore size and distribution by optical microscopy, surface hydrophilicity by static contact angle, in vitro degradation by swelling tests (dH_2O, 37°C), CaP nucleation by immersion in simulated body fluid (1.5 SBF, 37°C), compressive properties by mechanical tests, cytotoxicity (L929) and cytocompatibility (MC3T3-E1) by in vitro tests. Cells morphology was observed via SEM and cell viability and metabolic activity measured by Alamar Blue and ALP assay, respectively.

RESULTS AND DISCUSSION

SEM (Figure 1) showed a correlation between CBA content and induced microporosity. 1 and 3% CBA scaffolds were discarded for limited obtained pores; 5% CBA scaffold showed the lowest number of pores (18.2±7.6 pores/0.8mm) with the smallest diameter (23.46±16.60 µm); 7.5% samples had the highest number of pores ($p<0.05$); 10% samples had the largest diameter (10-90 µm), but less pores than 7.5% samples.

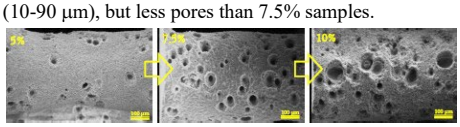

Figure 1. Surface of the filaments printed with 5, 7.5, and 10 wt% of ACA.

Since a different porosity can influence the mechanical strength to external loads, the tested scaffolds exhibited elastic modulus values similar to other dual porous scaffolds described in literature (2-8 MPa) [3]. The elastic moduli (E5%, E10% and E80%) decrease by increasing the ACA content and therefore the surface porosity. This trend was also observed for the maximum stress (Figure 2). From the obtained results, it is possible to identify a threshold value that determined a significant variation of the mechanical behavior, and it was observed when increasing the ACA content from 5 to 7.5 wt%.

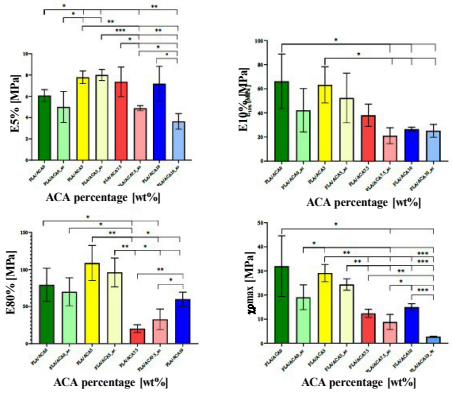

Figure 2. Mechanical properties of scaffolds printed by varying the ACA content.

Degradation tests showed a significant ($p<0.05$) weight loss for 10% CBA scaffolds, due to the higher content of pores and to the surface roughness that increases the contact area between the fluid and the surface of the samples, accelerating the degradation process. The 1.5SBF treatment enlightened the ability of scaffolds to promote CaPs nucleation. SEM micrographs showed CaP deposits characterized by the spherical nano-needle morphology typical of calcium-phosphate. In vitro cytotoxicity test showed high viability (around 100%) for all scaffolds. AlamarBlue and ALP demonstrated good osteoblast cells behavior.

CONCLUSION

FDM and CBA were coupled to fabricate double-porous PLA scaffolds. The optimal CBA content (i.e., 7.5%) was found and it allowed obtaining promising results in terms of generated microporosity, without compromise the mechanical properties and degradation kinetics.

REFERENCES

1. Grémare A. *et al*., J Biomed Mater Res Part A. 106:887, 2018.
2. Naddeo F *et al*., Compos Part B Eng. 115:60, 2017.
3. Yoo CJ *et al*., IOP Conf Ser Mater Sci 229, 2017.

ESB 2022
32nd ANNUAL CONFERENCE OF THE EUROPEAN SOCIETY FOR BIOMATERIALS

The impact of Residual Stresses formed during PBF-LB on the Biodegradability of Magnesium alloys

Lisa Larsson[1*], Hanna Nilsson-Åhman[1,2], Tuerdi Maimaitiyili[2], Cecilia Persson[1]

[1]Department of Materials Science and Engineering, Uppsala University, Uppsala, Sweden
[2]Swerim AB, Stockholm, Sweden
[*]lisa.m.larsson@uu.se

INTRODUCTION

The high degradation rate of magnesium (Mg) alloys is one of the main obstacles to its use in biodegradable implants. New manufacturing techniques, such as powder bed fusion – laser beam (PBF-LB) allows for tailoring of the microstructure[1], including the residual stress formation. This is important since residual stresses formed during PBF-LB can have an effect on the degradation behavior of Mg alloys. So far, no studies have characterized the residual stress in Mg alloys processed using PBF-LB. Here, the influence of PBF-LB process parameters on the formation of residual stress in the printed parts were investigated using non-destructive neutron and synchrotron techniques.

EXPERIMENTAL METHODS

Magnesium rare-earth metal alloy WE43 (Mg-4wt%Y-3wt%Nd-0.5wt%Zr, NMD GmbH) samples were printed in an EOS M100 machine with gas-atomized spherical powder with particle size 23-60 µm. The influence of process parameters, namely hatch distance (40 µm, 50 µm and 60 µm) and laser scan strategies (67º rotation or 90º rotation, i.e. x-y, between consecutively scanned layers) on the residual stress formed in the printed samples was studied. Additionally, the influence of build size and build direction was also investigated (Table 1). The residual stress measurements were performed by neutron imaging and diffraction at PSI, Switzerland, to map the strain in the complete sample, and synchrotron diffraction at DESY, Hamburg, to characterize the local residual stress.

Table 1: Matrix of the sample nomenclature for the 25 mm³ cubes (left), and for the 80 mm x 25mm x 25mm cuboids (right), with arrows indicating the build direction.

	h40	h50	h60
67°	1	2	3
x-y	4	5	6

	h50
67°	7
67°	8
x-y	9

RESULTS AND DISCUSSION

The results showed that the residual stresses formed during the PBF-LB process are affected by the choice of scan strategy during printing. The 67º scan strategy produced larger difference in residual stress in the pieces, as compared to the x-y scan strategy. Using different process parameters throughout the part could hence provide a chance of tailoring the degradation behavior in the final piece. The residual stresses formed in the surface zone of the printed parts were found to be tensile, and especially towards the edges of the samples in the build direction (Point S in Fig. 1). As described in literature, these tensile residual stresses are known to be present in the surface zone of PBF-LB parts[2], and can negatively affect the degradation of metallic materials[3].

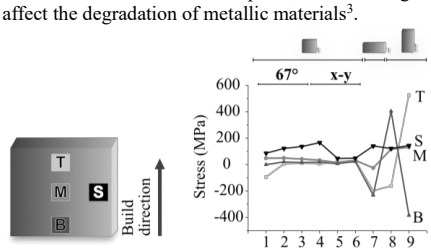

Fig 1. Illustration of the measurement sites of the synchrotron diffraction experiment with the corresponding residual stress data, showing the influence of process parameters on the residual stress in the longitudinal direction.

An increased build size increased the residual stresses formed in the as-built samples to a level close to the yield strength of the material. A way of reducing the amount of tensile residual stresses in the surface zone, in an attempt to reduce degradation and circumvent cracking of the final part, is surface treatments such as laser shock peening. This induces compressive stress in the outside layers and could further help improve the degradation behaviour of magnesium produced by PBF-LB.

CONCLUSION

The residual stresses formed during the PBF-LB process were successfully mapped in the biodegradable Mg samples using non-destructive neutron and synchrotron techniques. The tensile residual stresses found in the surface zone of the printed parts are likely instigators of higher degradation rates, and the results from this study show that the choice of process parameters during PBF-LB is key to reducing the residual stresses in the printed parts.

REFERENCES

1. Marattukalam, J.J. *et al.,* Mat. & Des., 193, 2020
2. Li, C. *et al.*, Procedia CIRP, 71, 2018
3. Esmaily, M. *et al.*, Addit. Manuf., 35, 1, 2020

ACKNOWLEDGMENTS

The authors would like to thank the Swedish Foundation for Strategic Research (SSF) within the Swedish national graduate school in neutron scattering (SwedNess), and VINNOVA's Competence Centre in Additive Manufacturing for the Life Sciences AM4Life (2019-00029) for providing financial support to this project.

Designing and Evaluating Tailorable 3D-printed Metamaterials for Lower Limb Prostheses

Vasja Plesec[1*], Gregor Harih[1]

[1]Faculty of Mechanical Engineering, University of Maribor, Slovenia
[*] vasja.plesec@um.si

INTRODUCTION

In the development of transtibial and transfemoral prostheses, researchers have focused primarily on the shape of the socket itself. The socket is rectified according to the geometry and condition of the residual limb based on the prosthetist's experience and knowledge, resulting in a subjective process that is both lengthy and inconsistent. However, not much has been done to develop new materials for the socket-liner system that would further improve fit, comfort, and safety. Previous studies have shown that by manipulating the design parameters of metamaterials, mechanical properties of the structure can be adjusted to enhance ergonomics between biological tissue and the product[1]. In practise, metamaterials are already successfully used in footwear or personal and sports protective equipment applications[2]. The use of cellular or lattice-like structures in prosthetics is already being explored, but the structures are not yet established in clinical use[3]. Therefore, our research has focused on the development and evaluation of different metamaterials for the socket-liner system. The study includes numerical analyses with models of the samples and a generic transtibial prosthesis, as well as mechanical tests on 3D-printed samples.

EXPERIMENTAL METHODS

To improve a socket liner system, one must determine the best balance between comfort and stability for a given case. The structure should remain rigid up to a specific pain pressure threshold (PPT) to maximise stability, but just before reaching this limit, it should deform to provide a higher contact area and a more uniform contact pressure distribution for improved comfort. PPT determines when a structure should deform, and this depends on both the location on the residual limb and the individual.

We have developed a cellular structure with hyperelastic material properties – linear elastic behaviour initially, followed by a plateau, which starts with the deformation of the cell walls under nearly uniform stress. Finally, when the intercellular space is fully deformed, the structure's stiffness increases exponentially to provide stability. The design parameters of the cellular structure, such as wall thickness, cell size and structure type, were adjusted in the ANSYS software package to achieve the desired material properties. Based on the numerical analysis samples were 3D printed. Compression tests were performed to obtain a stress-strain (suspension) diagram for each structure type. In addition, we compared the newly developed cellular socket-liner system to conventional liners and sockets using a previously developed numerical transtibial model based on arthrometric measurements. Two loading cases were analysed: donning of the prosthesis and vertical loading representing a one- or two-legged stance.

RESULTS AND DISCUSSION

Using numerical tools we designed a structure, that started to deform in the reported rage of PPT (50-250kPa). By manipulating the design parameters of the metamaterials, we determined at what pressure the plateau began. The compressive tests confirmed the successful customisation of the material parameters for the socket-liner system.

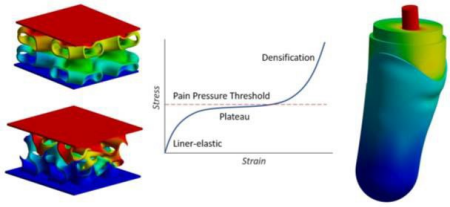

Figure 1: FEM analysis of cellular samples, schematical stress-strain diagram and numerical transtibial model

A relative comparison with conventional prostheses shows that metamaterials can minimise stress concentration through a more uniform distribution of contact pressure, which could improve comfort while maintain stability. The structure can be adjusted according to the condition and shape of the residual limb to find the best balance between pressure distribution and relative displacement for a given case. Numerical simulations and experimental tests demonstrate the adaptability of the structure to control the onset of the plateau.

CONCLUSION

The results show that by adjusting the material parameters of metamaterials, an enhanced response can be achieved, improving the socket-liner system. Future work will include the fabrication and testing of a full-size 3D printed socket-liner prototype and a direct comparison with a conventional prosthesis.

REFERENCES

1. Cupar A. *et al*., Int J. Ind Ergo. 82:1-7, 2021
2. Soe S. *et al*., Int J. Adv ManufTechnol. 79:1975-1982, 2015
3. Brown N. *et al*., J. Biomech Eng. 143(5):051001, 2021

ACKNOWLEDGMENTS

The authors acknowledge the financial support from the Slovenian Research Agency (research core funding No. P2-0063).

3D Screen printing technology for silicones in biomedical applications

Vedrana Tadić Krippendorf [1*], Luisa Ungelenk[1], Nicolle Schwarz [1]

[1]Axenoll 3D Printing GmbH, Jena, Germany
[*] v.tadic-krippendorf@axenoll.com

INTRODUCTION

3D bioprinting technologies are rapidly growing and are currently transforming the biomedical field. However, limitation in speed, scaling out and scaling up are the main challenges to overcome[1]. 3D screen printing technology is a novel approach to 3D printing. It is possible to print a wide variety of material classes with this technology. With the aid of a screen-printing screen and a squeegee its strength lies in the process of applying pastes layer by layer. It allows printing of dozens to hundreds of items per screen in parallel. It is applicable for research as well as for batch production (Figure 1A)[2,3]. The simplified printing process can be described as follows: i) paste is pressed in a screen-printing process through a screen-mesh with a defined layout, followed by a curing step; ii) a layer-on-layer printing is repeated until the series of 3D pieces are manufactured. Our technology enables production of items with fine geometries (lines with < 100 µm), such as channels, closed cavities, and free-standing overhangs[2]. We are focused on tissue engineering applications, screening chips, cell-culture scaffolds, and other biomedical applications. Here, we wanted to demonstrate printing possibilities of the 3D screen printers for silicones in biomedical application.

EXPERIMENTAL METHODS

Silicon pastes were made from Elastosil, a two-component, Pd-catalysed, addition cross-linking silicon rubber curing at room temperature with addition of thixotropic additive, pigment paste and vulcanisation inhibitor. This material was used as a mock-up for soft biocompatible materials. All chemicals were obtained from Wacker, Germany, and the silicone pastes were formulated according to recommendations by Wacker. The silicon paste was printed by an EX 301 3D screen printer from Exentis Group AG, Stetten, Switzerland.

RESULTS AND DISCUSSION Silicon was printed in different geometries using the 3D screen printing technology Here you can see various silicone nets with different geometries (Figure 1: B, C, D). Depending on the application and desired properties of the components, different silicones can be formulated and used. By adjusting process parameters such as temperature, it is possible to 3D screen print silicones and produce filigree components for biomedical applications.

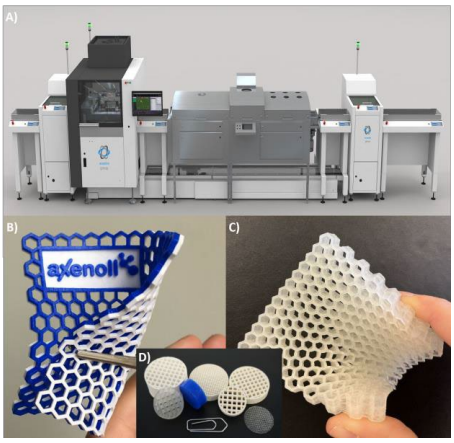

Figure 1: A) Inline production unit with (from left to right)**:** lift, 3D printing station, transport, drying station, transport, and lift. **B)** Printed flexible silicone mesh with two-coloured honeycomb mesh to demonstrate possibilities of printing different paste on top each other (blue and white). **C)** Printed flexible silicone honeycomb mesh with a high of 1.1cm. **D)** Silicon Scaffolds.

CONCLUSION

With the innovative 3D screen technology, it is possible to print silicones with different properties into different geometries. Because of low screen costs, component optimizations can be realized quickly and cost-effectively through rapid design changes. Thanks to the modular design of the systems, it is possible to transfer development processes into industrial production processes without changing technologies.

REFERENCES

References must be numbered. Keep the same style.
1. Smith G. *et al*., J. Biomech. 2:5-11, 2011

In vitro biological evaluation and degradation study of a 3D-printed polyurethane stent-graft for customized endovascular repair of abdominal aortic aneurysm

Marie-Stella M'Bengue[1,2,*], Thomas Mesnard[1,3], Mickaël Maton[1], Valérie Gaucher[2], Nicolas Tabary[2], Maria-José García-Fernandez[1], Jonathan Sobocinski[1,3], Feng Chai[1], Bernard Martel[2], Nicolas Blanchemain[1]

[1]Univ.Lille, INSERM, CHU Lille, U1008 – Advanced Drug Delivery Systems (ADDS), F-59000 Lille, France
[2]Univ.Lille, CNRS, INRAE, Centrale Lille, UMR 8207 – Unité Matériaux et Transformations (UMET), F-59000 Lille, France
[3]Institut Coeur Poumon, Hospital Center University of Lille (CHU Lille), 2 avenue Oscar Lambret, 59000 Lille, France

[*] marie-stella.m-bengue@univ-lille.fr

INTRODUCTION

Long-term success of endovascular aortic repair (EVAR) intervention is strongly determined by the appropriate selection and sizing of stent-graft (SG). Aiming at patient-specific treatment of abdominal aortic aneurysms (AAA) with challenging vessel morphologies, a 3D-printed (3DP) prototype of aortic SG, was custom-made using a medical grade biocompatible elastomer: thermoplastic polyurethane (TPU) (1). Before implantation study in a physiological environment, the cytocompatibility, hemocompatibility and degradation/stability of the prototype in its final form were investigated *in vitro* in the present study. It will help validate the design and art of elaboration of this 3DP-SG prototype, and accelerate the development and introduction of mature products to market.

EXPERIMENTAL METHODS

Firstly, the cytotoxicity of 3DP-SG samples was assessed, according to ISO10993-5, via 72-hour extraction method. Then, the cytocompatibility test was carried on the 3DP-SG samples by direct contact with human pulmonary microvascular endothelial cells (HPMEC) for 3 and 6 days. The cell viability in both tests was assessed by alamarBlue® assay. Hemocompatibility of 3DP-SG was evaluated, according to ISO10993-4, through direct contact for 1h with fresh whole blood (from a healthy human donor): the potential hemolytic property of material was assessed by detecting the presence of hemoglobin in the blood serum via UV-visible spectroscopy at 541 nm; the material surface after contacting with blood was observed using scanning electron microscopy (SEM). Moreover, the *in vitro* degradability of TPU was investigated, according to ISO10993-13, by incubating test materials in two different types of media, to simulate the real-time degradation occurring in a physiological environment. Briefly, 3DP-SG samples were incubated in PBS (pH 7.4) and in $3_{v/v}$ % H_2O_2 to simulate, respectively, degradation by hydrolysis and oxidation in real time. During 12-month incubation, at preset time points (1, 3, 6 and 12 months) the material was characterized by diverse physico-chemical analytical techniques (size exclusion chromatography (SEC), differential scanning calorimetry (DSC), tensile tests, infrared spectroscopy (FTIR) and water contact angle measurements) to monitor the evolution of the bulk and surface properties. All tests were performed at least in triplicate and compared by *p*-value.

RESULTS AND DISCUSSION

In extraction test, survival rate of HPMEC cells for test samples was 102±6%, showing no cytotoxicity. Via 3- and 6-day direct cell-material contact, the viability of growing cell on the samples (80±3% and 71±2%, respectively) were superior to 70% of control. Hemolysis test, with < 5% of hemolysis, proved that the prototype in its final form leads no hemolytic risk. SEM evidenced that, after contact with blood, there were very few adhered but non-activated platelets on the material surface. Concerning *in vitro* real-time degradation test, after 3 months, differences of the samples' bulk properties were detected in both PBS and 3% H_2O_2. Notably, it was manifested by SEC with a significant increase (11-12%, $p<0.05$) of molecular weight and by DSC with a decrease of glass transition temperature of the soft phase in TPU as well as decreasing enthalpies of melting and crystallization. The surface properties of samples were also found changing after 3 months: peak height of the H-bonded C=O stretching vibration at 1700 cm^{-1} increased whereas that of the non-H-bonded C=O stretching vibration at 1730 cm^{-1} decreased. In addition, a new peak of an O-H stretching vibration emerged at 3500 cm^{-1}. All these implicit the formation and/or the increase of hydrogen bonds between the hard segments to form hard domains, which are well dispersed in the soft phase of TPU (2). However, such microstructural changes did not provoke any measurable degradation of the mechanical properties of the samples.

CONCLUSION

The developed 3DP-SG has been shown *in vitro*, by this study, non-cytotoxic and well cytocompatible, non-hemolytic and non-thrombogenic. After 3-month incubation in PBS or 3% H_2O_2 solution, changes in bulk and surface properties of material were indeed observed but not detrimental to its integrity with regard to its application. Therefore, this 3DP prototype is ready for further *in vivo* evaluation.

REFERENCES

1. Mrad O. *et al.*, Rad. Phys. Chem. 79:93−103, 2010.
2. Miller J. *et al.*, Macromolecules. 18:32−44, 1985.

ACKNOWLEDGMENTS

This research was funded by University of Lille Nord-Europe, I-SITE Scholarship, sustained program FEDERATE (call for project *EXPAND*).

Hydrogel Manufacturing via novel 3D Screen Printing Technology

Authors: Luisa Ungelenk[1], Dana Elster[1], Vedrana Tadić Krippendorf[1] and Nicolle Schwarz[1]

[1]Axenoll 3D Printing GmbH, Jena, Germany
*l.ungelenk@axenoll.com

INTRODUCTION

As an innovative and future-oriented technology company, Axenoll develops and implements projects for the 3D printing of biomaterials for applications in the medical and biotechnological sector. Our process is the only fast and gentle mass 3D printing process on the market to produce biotechnological and/or medical products[1]. Within the additive manufacturing process, 3D screen printing belongs to the subgroup of material extrusion processes. The process combines all the advantages of classic 2D screen printing. Instead of applying a single layer of material, entire components are built-up in large numbers and with high resolution over numerous layers. The process allows printing on various substrates such as paper, ceramics, plastic, metal and wood and is characterized by a high technical level. Our technology enables substrate-free production of items with fine structures (lines with < 100 µm), such as channels, closed cavities, and free-standing overhangs[2]. It combines high productivity with the highest precision for a variety of materials. It is also possible to combine and print different materials with each other. Support structures are not required. Compared to the classic additive manufacturing processes, components can be manufactured in small to medium batch sizes as well as in large series for mass production. Here we want to show the possibility to print hydrogels by 3D screen printing.

EXPERIMENTAL METHODS

Hydrogels were based on 6 % gelatin (AppliChem) dissolved in water. In addition, 2.5 % sodium alginate (Sigma-Aldrich) were added and stirred for 1-2 h to generate a complete dilution. The gelatin-alginate paste was printed by an EX 301 3D screen printer from Exentis Group AG, Stetten, Switzerland. Printer settings such as squeegee speed, height increment for screen elevation, off-contact distance, and drying temperature were kept constant. Items were printed on a ceramic substrate plate (w, l, h = 300, 300, 5 mm). To stabilize the printed hydrogels a cross-linking was induced by calcium chloride.

RESULTS AND DISCUSSION

Hydrogels were printed in various geometries using the 3D screen printing technology. The geometries were defined by the screen, which is shown in figure 1 (honeycomb with web width of 1 mm, coil structure with web width of 2 mm and circles with a web width of 1 mm). The printed hydrogels (Fig. 2) can be easily removed from the plate. Then, the structure was stabilized via treating with calcium chloride to induce a cross-linking. After sterilization with UV-light or 70% ethanol, the hydrogels can be used directly or dried and stored for later use. The geometric complexity of the printed pieces can be increased by changing to screens with different layouts.

Fig.1: Screen with different geometries. Screen with defined layout of the screen-mesh. The printing paste is pressed through the bright openings and the red part is covered with photopolymer.

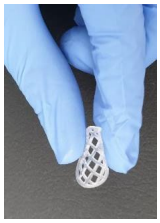

Fig.2: Printed hydrogel. Printed flexible hydrogels with web structure.

CONCLUSION

3D screen printing offers the possibility to design and change the geometries for the products quick, flexible and cost-effective in comparison to commercially available technologies such as injection moulding[2]. Moreover, the same screens can be used for printing at development units and as well as at batch production units. Thus, scaling up is fast and uncomplicated. We showed that natural biomaterials such as gelatine and alginate are suitable materials for the 3D screen printing technology to print items such as hydrogels.

REFERENCES

1. Axenoll 3D Printing GmbH. *Axenoll 3D Bioprinting*. 2020 [cited 2020 17 Aug].
2. Dressler, M. and S. Vasic, *3D-Siebdruck: Filigrane keramische Bauteile in Großserie.* Keramische Zeitschrift, 2019. **71**(5): p. 52-55.

Arburg Freeformer Process Optimization for Manufacturing Biodegradable Ureteral Stents

Leonardo Engler[1,2,3*], Noel Gately[2], Ian Major[1], Janaina Crespo[3], Declan Devine[1].

[1] Material Research Institute, Technological University of the Shannon: Midlands Midwest, Athlone, Ireland
[2]Applied Polymer Technologies, Technological University of the Shannon: Midlands Midwest, Athlone, Ireland
[3]Programa de Pós-Graduação em Engenharia e Ciência dos Materiais, University of Caxias do Sul, Brazil.
[*]A00278634@student.ait.ie

INTRODUCTION

Ureteral stents are one of the most crucial medical devices used when a patient needs any urological interventional procedure. However, adverse side effects such as discomfort, dislodgment, encrustation, and infection occur in more than 80% of long-term cases. Biodegradable polymeric stents, which dissolve after fulfilling their function are a great alternative of use, as a further removal procedure is not necessary[1]. A novel approach uses state-of-the-art technology to design and print polymeric stents using a Freeformer 300-3X. The Additive Manufacturing technology is capable of printing directly from polymeric granules and has the ability to utilize up to three different materials at the same time. This allows the production of parts with different densities from the same material, controlling droplet deposition rate, surface roughness, porosity, and layer thickness. This work aims to develop and evaluate a biodegradable ureteral stent (BUS) using a polymeric matrix of polylactic acid (PLA), reinforced with Halloysite nanotubes (HNT).

EXPERIMENTAL METHODS

The material compounding was performed by using a Prism twin-screw extruder with 16 mm diameter screws, 25/1 (L/D). The profile temperature used was kept at 200/190/180/150/100 ºC, from the die to the feeder. PLA/HNT batches were compounded varying the HNT content by 0, 1, 3, 5, and 10% wt. and the thermal, analytical, and mechanical properties of these materials were assessed to verify their feasibility for the following 3D manufacturing of polymeric stents. Additionally, tensile bars were printed following the ISO 527, varying the printing orientation (XY and XZ axes), as well as the filling pattern, starting from 0º and 45º and adding 90º for the subsequent layer, now described as PLA+ and PLA-X, respectively.

RESULTS AND DISCUSSION

Polymer viscosity analysis indicated a decrease from 11.6 to 8.6 g/10min on MFI values as the HNT content added to the compounds increased, for PLA and PLA/HNT10, respectively. Whereas previous studies using these compounds have shown an increase in the mechanical properties such as Young's Modulus and Stress at Break[2,3].

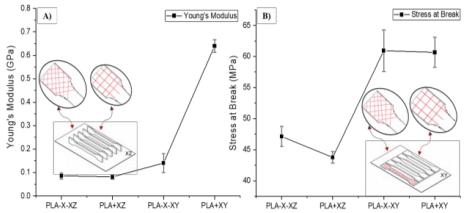

Figure 1: Tensile results of PLA specimens printed with different printing orientations and filling pattern: Young's Modulus in (A) and Stress at Break in (B).

Additionally, the tensile results have shown similar behavior for PLA tensile specimens printed in different axes orientations and printing angles, as seen in Figure 1, the XY orientation promotes the highest mechanical properties. Moreover, the Strain at Break results indicate the axis orientation influences the flexibility of the material, decreasing this property in XY compared to XZ, this behavior is probably because droplets printed in XY direction are more packed than in XZ[4].

SEM-EDX analysis has shown some agglomerates on samples containing HNT and it tends to increase as the %wt. of HNT on the compounds increase (Figure 2), further analysis will determine the HNT dispersibility on the material before the stent printing. WAXD results confirm PLA is mainly amorphous, although, the addition of HNT increases its crystallinity. DSC analysis of printed parts on XY and XZ presented, respectively, a crystallinity of 44.2 and 45.1%, a higher value, compared to the extruded PLA (X_c = 41.6%).

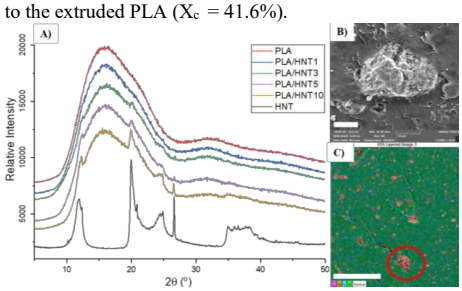

Figure 2: WAXD analysis in (A), SEM (bar = 10µm) in (B), and EDX (bar = 100µm) in (C); both (B) and (C) corresponds to PLA/HNT10.

CONCLUSION

The current methodology achieved satisfactory results to 3D print and evaluate successfully a BUS. Therefore, additional tests regarding the mechanical properties and the degradation rate of the printed stents are required to qualify the BUS as an implantable medical device.

REFERENCES

1. Ahlinder A. *et* al. Polym Degrad. 181:109372, 2020
2. Venkatesh C. *et al.* J Polym Eng. 6273:1-10, 2021
3. Venkatesh C. *et* al. In: Proc Manufac. 38:17-24, 2019
4. Peng F. *et al.* ACS Appl Polym. 1:275-285, 2019

ACKNOWLEDGMENTS

This publication has emanated from research conducted with the financial support of the Enterprise Ireland under the Capital Call 2019 Grant Nº CE 20190068 and Applied Polymer Technology Gateway Project Nº TG-2017-1014.

Investigation of Porous Materials for the Release of Hydrogel-bound Drugs made by Fused Filament Fabrication (FFF) and Melt-Electrospinning (MES)

Carsten Linti[1*], Andreas Scherrieble[1], Michaela Schön[1], Carla Siegle[1], Götz Gresser[1], Michael Doser[1]

[1]Deutsche Institute für Textil- und Faserforschung Denkendorf DITF, University, City, Country
[*] carsten.linti@ditf.de

.

INTRODUCTION

Drug delivery systems (DDS) are becoming increasingly important in medicine. They are used to release drugs in a targeted and controlled manner at the desired site of application e.g. for preventing inflammatory reactions and influencing cell growth. Porous structures are successfully used in several medical applications like tissue engineering (TE) or DDS. Thereby, the pore morphology influences migration, proliferation and differentiation of cells[1]. Furthermore, porous interconnecting structures filled with hydrogel-bound drugs are an interesting system for DDS[2] especially if a thermoresponsive hydrogel enables a controlled release of drugs.

EXPERIMENTAL METHODS

The processing of polymer compounds in fused filament fabrication (FFF) and melt electro-spinning (MES) into porous fibers and porous materials is investigated by using polymer compounds containing water-soluble components. The compositions used in this study are: PA6/PEO [80/20 and 90/10], PLA/CoPET [80/20], PLA/PVA [80/20], PLA/PVP [70/30]. A modified 3D printer German RepRap x350pro (Feldkirchen, Germany) with high voltage source between nozzle and collector plate on print bed allowed melt electrospinning. Samples were manufactured with both FFF and MES and washed in demineralized water. Pore structures are analyzed by scanning electron microscopy (SEM) and analysis, the fibre diameter distribution of the electrospun non-woven are determined by MAVIfiber2d.

As a model for drug release, small plates (30mm x 30mm x 1mm) were printed by FFF with the PA6/PEO 80:20 filament. After washing the pores were filled with the hydrogel gellan gum (GG) or poly(N-isopropylacrylamid) (PNIPAM) as thermoresponsive gel using a vacuum assisted process. The inter-connectivity of the pores was examined with fluorescein isothiocyanate-labeled GG and assessed using fluorescence microscopy (FM). Horseradish peroxidase (HRP) is added to the GG and PNIPAM as a model drug for the release experiments. Released HRP is measured via a chemiluminescence reaction with luminol (microplate reader CLARIOstar, BMG Labtech).

RESULTS AND DISCUSSION

The tests show that porous structure and pore size as a result of the washout process. (Fig.1). The FM recordings indicate that the plates were successfully filled with GG (Fig.2 left). First results confirm HRP release dependent on pore volume (Fig. 2 right).

Porous 3D-printed small plates were successfully produced, filled with HRP-containing hydrogel and the time-dependent HRP-release of plates containing PNIPAM at temperature between 25 and 35°C was determined.

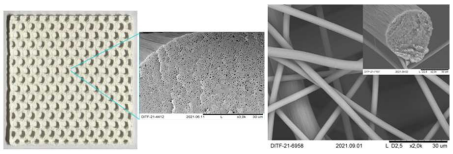

Figure 1: left: FFF printed porous PA6 plate and SEM of plate cross-section; right: SEM of MES PA6 non-woven and fiber cross-section

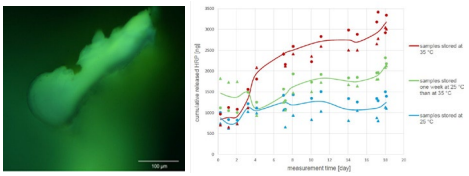

Figure 2: left: FM image of pores filled with fluorescein isothiocyanate-labeled GG; right: time-dependent HRP-release of small plates containing PNIPAM at temperature between 25 and 35°C

CONCLUSION

The suitability of four polymer compounds for manufacturing porous structures with a 3D printer either by FFF or MES could be demonstrated. FFF is suitable for the controlled and reproducible generation of macroscopic pore structures by leaching of water-soluble polymers. Absorbable as well as non-absorbable compounds have been used for FFF. Porous 3D-printed plates were successfully produced, filled with a hydrogel-bound drug (HRP) and the relationship between pore morphology and release rate was determined. The results suggest that the 3D-printed structures are suitable as DD systems. This allows to further studies to functionalise additively manufactured, personalised devices as well for implants as for extracorporeal use.

REFERENCES

1. Sgarminato, V. *et al*., J. BIOMEDICAL MATERIALS RESEARCH. Part B, APPLIED BIOMATERIALS. pp.10 (pp.1-10), 2020
2. Dohle, E. *et al.*, Tissue engineering. Part C, Methods 26 (9), S. 475–484, 2020

ACKNOWLEDGMENTS

Special thank goes to Martin Hoss for the preparation of the compound filaments for FFF and to Ingo Windschiegel for the help with MAVIfiber2d.

3D printing of PEGDA hydrogel scaffold by photopolymerization on LumenX. In vitro and in vivo biocompatibility.

Julien Clauzel[1*], Lorenne Robert[1], Nina Colitti[1], Maylis Combeau[1], Carla Cirillo[1], Wafae Labriji[1], Franck Desmoulin[1], Isabelle Loubinoux[1]

[1] Toulouse NeuroImaging Center (ToNIC), INSERM, University Paul Sabatier, UPS, Toulouse
[*] julien.clauzel@inserm.fr

INTRODUCTION

After a severe traumatic brain injury, spontaneous regeneration of the lesioned area is usually minimal. The partial functional recovery that can be observed is mainly accounted for by neural plasticity, that is, reorganisation of the non-damaged neural networks[1]. To improve the biological response and favor the regeneration, we chose to focus on engineering a cellular microenvironment that will provide a mechanical support inside the injured area: a scaffold. In order to guide the long axonal regrowth process, the scaffold must last several months in the brain. Here we report a feasibility study of a scaffold made of PEGDA, a slowly degrading hydrogel, 3D printed by photopolymerisation with the bioprinter LumenX (CellInk).

EXPERIMENTAL METHODS

We tested two types of poly(ethylene glycol) diacrylate : PEGDA200 and PEGDA500, which were bought directly from CellInk. 200 and 500 indicate their young's modulus in kPa, which is dependent on their molecular weight. We printed the scaffolds by photopolymerization with a LumenX printer, developed by the same company. This printer uses the digital light processing (DLP) technology, with a voxel size of 50 µm. Geometric fidelity, thickness of the structure and swelling of the hydrogel were assessed via microscopic observation. In-vitro testing was conducted to assess cell adhesion on the printed PEGDA structures. We used SH-SY5Y progenitor neural cells. Handling of the scaffolds was done with tools sculpted with a Dremel on PTFE rods.
In vivo testing was performed in the brain of rats 13 days after a malonate injection to simulate an acute brain injury[2]. The scaffolds were 5mm large, and MRI data were acquired to evaluate non-invasively the host response with a 7T Brucker Pharmascan.

RESULTS AND DISCUSSION

The **printing** required no specific skill asides from CAD design. We found that the Fusion CAD software is not tailored to manage complex shapes with hundreds of repetitions of the same pattern, and we made the necessary adjustments with Python code.
We were able to print patterns 150-200µm thick. The main limiting factor was the mechanical fragility of the structure. The print removal blade provided with the printer was too thick, tearing the scaffold apart, and we designed a thinner one. Handling with tweezers damaged the structure. To avoid that, we added a handle on the top of the scaffold, using a shepherd's crook shaped tool to pick it. The structure was then only submitted to its own weight. The handle was an ogive arch centered above the center of mass of the scaffold in order to stay vertical. Specific tools were also made for surgery in PTFE, a polymer than can resist the high temperatures of an autoclave sterilization process.
In vitro testing with cells seeded on the printed structures showed as expected a weak cell adhesion. Swelling of PEGDA200 and PEGDA500 were respectively 30% and 15% in distilled water. The transparency of PEGDA200 allowed microscopic observation. Coating with polylysine or polyornithine plus laminine to improve adhesion was made.
In vivo experiments on two rats induced a strong inflammatory response with encapsulation by macrophages seen on histology 2 months after. In the PEG200 case, an abscess formed and grew rapidly, no bacteria were observed on HE staining, and a Gram staining is ongoing for confirmation. The high water content of the hydrogel allowed for a non-invasive observation and follow-up with an MRI scan.

CONCLUSION

We were able to easily print scaffolds with complex 3D shapes in PEGDA, a biocompatible and bioresorbable hydrogel. Increasing the resolution of the printed patterns and the porosity required to craft new tools to handles the scaffold without damaging them. In the future, it would be interesting to print them with a resin suitable for surgery.
In vitro, the printed structures showed no adverse effects on the neural progenitor cells. In vivo, inflammatory response was strong.
In conclusion, 3D printing by photopolymerization is becoming more and more accessible, but finding the right material is still a challenge.

REFERENCES

1. Cirillo C. *et al*., J. Cereb Blood Flow Metab. 40(1)3-22, 2020
2. Le Friec A. *et al*., Transl Stroke Res, 12(1) :98-11, 2020

ACKNOWLEDGMENTS

The authors would like to thank the Agence d'Innovation de Défense and the INSERM for providing financial support to this project.

Optimization of titanium spinal cages to maximize synthetic graft content in composite implants

Salim Ghandour[1*], Per Isaksson[1], Cecilia Persson[1]

[1]Dept. of Materials Science and Engineering, Uppsala University, Uppsala, Sweden
[*]salim.ghandour@angstrom.uu.se

INTRODUCTION

Spinal fusion is the gold standard for treating patients with degenerative disc disease [1]. Titanium alloys and PEEK are the two most common materials used to manufacture cages for spinal fusion, used to maintain disc height while the vertebrae fuse. Other materials, such as morselised bone, may be added to the cage to enhance the bioactivity. A monetite-based calcium phosphate has (as a composite implant in combination with titanium) shown potentially osteoinductive properties [2] and may be a synthetic alternative to bone graft. Maximizing the ratio of calcium phosphate to titanium could be desirable to maximize bone ingrowth and fusion. Further, the calcium phosphate can be incorporated into the cage and stored ahead of surgery. The aim of this study was to topologically optimize cervical spine implants to incorporate a bioactive but mechanically weak material such as calcium phosphate.

EXPERIMENTAL METHODS

An outer geometry was established based on the shape of cervical vertebrae, with a height representing a typical distance between two cervical vertebrae in a healthy spine, as recommended by ASTM F2077. All quasi-static simulations were performed with the commercial finite element code Ansys (2020).

An isotropic material behaviour was assumed for the Ti-Al6-V4 (Laserform Ti Grade 23 A) with a Poisson's ratio of $v = 0.3$. The elastic modulus was estimated from tensile testing of additively manufactured samples (power bed fusion with laser beam (PBF-LB) using an EOS 100, EOS GmbH, Germany), according to ASTM E8/E8M, as this would be the future method for producing the titanium cages. Samples were printed in both the vertical and horizontal direction, to test for isotropy in the printed material.

In the simulations, the bottom and top faces were bonded to stiff plates. Four different loading scenarios were investigated: compression, flexion-extension, axial rotation, and a flexion-extension with a compression preload [3].

To optimize global stiffness, an algorithm based on [4] was applied with an effective stress limit of 0.35 GPa (corresponding to the estimated fatigue life of Ti-Al6-V4 [5]). Feature sizes were also limited to 1-2 mm to construct a semi-porous cage.

RESULTS AND DISCUSSION

The titanium tensile tests showed no significant difference between the different printing directions, with estimated elastic moduli of 112.5 ±4.9 GPa and yield stress of 1.17 ± 0.05 GPa (**Fig. 1**). These values are well within the range for Ti-Al6-V4 alloys where the elastic modulus range from 90-117 GPa.

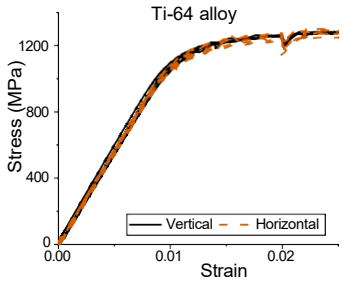

Fig. 1 Stress-strain curves portraying tensile test results for vertically and horizontally printed samples in Ti-64.

The resulting geometry from the topology optimization portrayed a semi-porous structure with cavities where synthetic graft can be placed. The final optimized geometry had 75% volume reduction and a maximum effective stress of about 160 MPa in all loading scenarios. Since the resulting stresses are significantly lower than the limit set in the optimization algorithm, there may be potential for a further decrease of material.

Future work includes incorporating the calcium phosphate in the verification, geometries for surgical tools and experimental validation using ASTM F2077 and more complex loading scenarios.

CONCLUSION

Preliminary cage designs, minimizing the amount of titanium while optimizing the global stiffness, were manufactured to investigate the structure's mechanical behaviour under different load cases. The results imply that there is room for further material reduction. Future work includes experimental validation and more complex geometrical features.

REFERENCES

1. S.M. Kurtz *et al.*, Elsevier Inc., 2006
2. O. Omar *et al.*, Proceedings of the National Academy of Sciences of the United States of America, 2020.
3. M.M. Panjabi *et al.*, Spine (Phila. Pa. 1976). 26:2692 2700, 2001
4. M.P. Bendsøe, O. Sigmund, Topol. Optim. 2004
5. M. Benedetti *et al.*, Procedia Struct. Integr. 2:3158–3167, 2016

ACKNOWLEDGMENTS

This research has received funding from the European Union's Horizon 2020 research and innovation programme under the Marie Skłodowska-Curie grant agreement No 812765.

Surface free energy dominates the biological interactions of post processed additively manufactured Ti-6Al-4V

Victor M. Villapún[a*], Luke N. Carter[a], Christian Schröder[b], Paula E. Colavita[b], David A. Hoey[c,d], Mark A. Webber[e,f], Owen Addison[g], Duncan E.T. Shepherd[h], Moataz M. Attallah[i], Liam M. Grover[a], S. Cox[a]

[a]School of Chemical Engineering, University of Birmingham, Edgbaston B15 2TT, United Kingdom, [b]School of Chemistry, CRANN and AMBER Research Centres, Trinity College Dublin, College Green, Dublin 2, Ireland, [c]Trinity Biomedical Sciences Institute, Trinity College, Trinity Centre for Biomedical Engineering, Dublin, Ireland, [d]Dept. of Mechanical Manufacturing and Biomedical Engineering, School of Engineering, Trinity College, Ireland, [e]Quadram Institute Bioscience, Norwich Research Park, NR4 7UQ, [f]Norwich Medical School, University of East Anglia. Norwich Research Park, NR4 7TJ, [g]Faculty of Dentistry, Oral and Craniofacial Sciences, King's College London, London, SE1 9RT, [h]School of Engineering, University of Birmingham, Edgbaston B15 2TT, UK, [i]School of Materials and Metallurgy, University of Birmingham, Edgbaston B15 2TT, UK

*v.m.villapun@bham.ac.uk

INTRODUCTION

Although the complication rate in prosthetic joint 'replacements is low, solely in the United States, the annual costs of revision surgeries were estimated to be $1.62 billion in 2020 [1]. As the population grows older, the number of orthopaedic interventions with such devices is expected to exceed 5 million worldwide by 2021 [2]. As such, there is a critical need to develop devices with minimal failure rates. Limited biocompatibility of the native material, aseptic loosening and infection are the main reasons for implant revision [3, 4]. To alleviate and prevent such outcomes it has been recognized that a device must be biocompatible and/or bioactive and to have anti-infective properties. In this regard, additive manufacturing (AM) has been the lead disruptor in orthopaedic device manufacture driven by the ability to produce customized implants that may improve osseointegration, reduce stress shielding, incorporate therapeutically loaded materials or reduce magnetic resonance imaging (MRI) artifacts [5-10]. However printed metal parts still present surface and microstructural defects, which may compromise mechanical and biological interactions. This has made physical and/or chemical post processing techniques essential for metal AM devices, albeit limited fundamental knowledge is available on how alterations in physicochemical properties influence AM biological outcomes posing a risk to their successful implementation.

EXPERIMENTAL METHODS

Herein, powder bed fusion Ti-6Al-4V samples were post processed with three industrially relevant techniques: polishing, passivation, and vibratory finishing. These surfaces were thoroughly characterized in terms of roughness, chemistry, wettability, surface free energy and surface zeta potential. These results were then correlated with attachment and biofilm formation of *S. epidermidis* and adhesion, proliferation and mineralization of SAOS-2 osteosarcoma cells

RESULTS AND DISCUSSION

Treated samples displayed a relatively smooth surface and similar roughness with chemical modification methods influencing the surface contract angle. Specifically, polished and passivated surfaces were found to be highly hydrophilic while vibratory finished and stainless-steel displayed a near hydrophobic behaviour. Variations in *S. epidermidis* colonisation were mostly driven by wettability and surface free energy, indicating a reduced attachment and proliferation on hydrophobic or low acid-base, γAB, substrates. Further analysis through the DLVO and XDLVO colloidal models did not correlate with bacterial adhesion, further supporting the need of more complex theories for cell/surface interactions. In contrast to the differences in bacterial attachment, similar metabolic activity was observed for SAOS-2 cells deposited on all analysed samples albeit a significant increase in total protein adsorption displayed by passivated and vibratory finished surfaces. Furthermore, mineralisation on Ti-6Al-4V AM substrates was heavily influenced by post processing selection, showcasing a direct correlation with the total surface free energy and its acid-base component.

CONCLUSION

These results indicate that surface free energy has a fundamental effect on the biological outcome of metallic surfaces, which could be used to guide the development of future medical devices. Nevertheless, the heavy reduction in S. epidermidis and lower mineralization brought by lower total surface free energy or acid-base component suggest that the chemical modifications achieved through single post processing methods may not be enough to optimize medical devices. As a consequence, it seems plausible that a combination of different physicochemical processes would be required to ensure limited bacterial proliferation while maximizing mammalian cell interactions for optimal biological interactions.

REFERENCES

References must be numbered. Keep the same style.

[1] Gepreel, M.A.H.N. et al, J. Mech. Behav. Biomed. Mater. 20 407-415, 2013.
[2] Murr, L.E. et al, J. Mater. Res. Technol. 9 1087–1103 2020.
[3] Mediaswanti, K. J. Nanotechnol. 6 2016.
[4] Bernard, L. et al, J. Antimicrob. Chemother. 53(2) 127-129, 2004.
[5] Lowther, M. Addit. Manuf. 28 565-584, 2019.
[6] Hedayati, R. J. Biomed. Mater. Res. B 106 386-398, 2018.
[7] Deing, A.et al, Int. J. Biomater. 8 8, 2014.
[8] Maietta, S. et al, J. Healthc. Eng. 9, 2019.
[9] Burton, H.E. et al, Mater. Sci. Eng. C 94 901-908, 2019.
[10] Carter, L.N. et al, Acta Biomater. 107 338-348, 2020.

ACKNOWLEDGMENTS

The current research is part of the Process Design to Prevent Prosthetic Infections (PREVENTION) and "Invisible Customisation - A Data Driven Approach to Predictive Additive Manufacture Enabling Functional Implant Personalisation" projects. The EPRSC (Grant codes EP/P02341X/1 and EP/V003356/1) and Science Foundation Ireland (Grant code SFI12/RC/2278 2) is acknowledged for financial support

3D Printing of Hybrid Gradient Scaffolds for Native Tissues Reconstruction

M.K. Włodarczyk-Biegun[1,2,*], Pavan Kumar Gudeti[2], Piotr Zieliński[1], Rency Geevarghese[2], Magdalena Gładysz[1], Frendion Marchena[1], Xixi Wu[1], M. Koch[3], Joanna Żur-Pińska[2], Z. Zhang[4], A. Krushynska[4], M. Kamperman[1]

[1] Polymer Science, University of Groningen, Nijenborgh 4, 9747 AG Groningen, The Netherlands
[2] Biotechnology Center, Silesian University of Technology, Krzywoustego 8, 44-122 Gliwice, Poland
[3] Leibniz Institute for New Materials, Campus D2 2, 66123 Saarbrücken, Germany
[4] Computational Mechanical and Materials Engineering, University of Groningen, Nijenborgh 4, 9747 AG Groningen, The Netherlands
*m.k.wlodarczyk@rug.nl; Malgorzata.Wlodarczyk-Biegun@polsl.pl

INTRODUCTION

Native tissues are highly organized structures with an intricate cellular microenvironment. They are typically non-homogeneous, with a gradient in the architecture and biochemical composition. This complexity makes it challenging to produce biomimetic scaffolds using traditional manufacturing processes. However, recently, 3D printing has emerged as a suitable tool to construct complex 3-dimensional objects with great flexibility over the design and high spatial precision of material placement.

Therefore, this project aimed to develop polymeric fibrous scaffolds for tissue engineering, resembling the structure of native tissues, with well-controlled mechanical and biological properties. We have used a novel melt electrowriting (MEW) approach and 3D extrusion bioprinting to construct models of different hierarchical tissues, such as hard-soft tissue interfaces, skin, and human trabecular meshwork (HTM).

EXPERIMENTAL METHODS

Printing of medical-grade polycaprolactone (PURASORB PC 12, Mw ~55,000) was performed with Melt Electrowriting printer (Spraybase, Ireland, Bioscaffolder, GeSiM). Scaffolds with different designs (varied pore shapes and sizes, different number of layers), including gradients, were printed and visualized with scanning electron microscopy (SEM). The mechanical properties of the scaffold were assessed in tensile mode and modeled using COMSOL software. The relation between the scaffold's architecture and mechanical properties was evaluated. Cells (fibroblast and primary HTM cells) were seeded directly on the scaffolds or encapsulated in the gel co-deposited with MEW meshes. The biological response was analyzed based on SEM imaging and immunofluorescent staining.

RESULTS AND DISCUSSION

Different designs (homogeneous and gradient) of the fibrillar scaffolds were proposed and successfully printed (see Figure 1). Some of the geometrical features were closely mimicking the native architecture of particular tissues (e.g., tendon or HTM). Mechanical testing revealed the influence of the design on the mechanical properties of the scaffolds. The developed computational model allowed for good prediction of scaffolds' mechanical performance. Additionally, the MEW scaffolds enclosed in the hydrogel matrix were characterized by higher stiffness and toughness.

Fibroblasts and primary HTM cells attached to the scaffolds, proliferated, spread, bridged the pores, and maintained their phenotype. Cell behavior was influenced by the orientation of the MEW fibers.

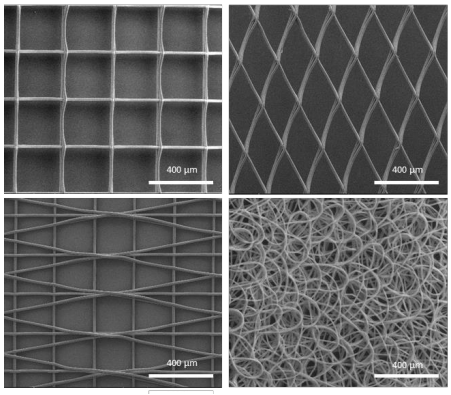

Fig.1. SEM images of exemplary printed designs using the MEW approach.

CONCLUSION

We have shown that 3D bioprinting, specifically the MEW technique, together with hydrogel deposition, is a suitable tool to produce small-scale scaffolds with great precision. The designs can be tailored to specific applications. The proposed approach enabled the reconstruction hierarchical structure of hard-soft tissue interfaces, HTM, and skin. Such hybrid scaffolds with complex biomimetic architecture will serve in the future as implantable systems or an in-vitro testing model. The computational modeling will facilitate the designing and production process.

ACKNOWLEDGMENTS

MKWB is supported by NWO Veni Grant (VI.Veni.192.148), NAWA Polish returns grant (PPN/PPO/2019/1/00004/U/0001), and NCN OPUS grant (2020/37/B/ST5/00743)

Influence of laser power on the corrosion of an additively manufactured Mg-$Y_{3.9wt\%}$-$Nd_{3.0wt\%}$-$Zr_{0.49wt\%}$ alloy

Hanna Nilsson Åhman[1,2], Clarence Wahman[1], Pelle Mellin[2], Cecilia Persson[1]
[1]Department of Material Science and Engineering, Uppsala University, Uppsala, Sweden
[2]Swerim AB, Kista, Sweden
Hanna.nilsson-ahman@swerim.se

INTRODUCTION

Bone has great capability for self-healing. Small fractures heal without any need for outer intervention. However, for large bone defects, the bone needs help to regrow. The standard is to use autografts or allografts, but lack of availability and risk of donor site morbidity calls for development of readily available graft materials[1].

Magnesium (Mg) alloys were first evaluated for their use in orthopedic fixtures already in the beginning of the 1900's, though their implementation has been hampered by excessive corrosion rates[2]. Powder extruded Mg-Y-Nd-Zr alloys have successfully been implemented for orthopedic fixtures since 2013, but larger, more complex implants have yet to be developed[3].

Powder Bed Fusion – Laser Beam (PBF-LB) is an advanced additive manufacturing technique, allowing for the production of complex lattices structures, designed for increased biocompatibility. Nevertheless, the corrosion rates of Mg alloys processed by PBF-LB remains too high[4].

Thus, with an ultimate goal of lowering the corrosion rates, this study aimed to gain a greater understanding of the influence of the process parameter laser power, on the corrosion behavior of Mg-$Y_{3.9wt\%}$-$Nd_{3.0wt\%}$-$Zr_{0.49wt\%}$.

EXPERIMENTAL METHODS

Cylindrical samples (ø5×10 mm) were produced by PBF-LB (EOS M100, EOS GmbH, Germany), using Mg-$Y_{3.9wt\%}$-$Nd_{3.0wt\%}$-$Zr_{0.49wt\%}$ powder (NMD GmbH, Germany) with a size fraction of 23-64 µm. Three sample groups with different laser powers (60W, 70W, 90W) were printed. The other parameters were kept constant (layer height = 20µm, laser scanning speed = 1100 mm/s, and hatch distance = 50µm). The samples were cut from the build plate using dry cutting, and washed in ethanol in an ultrasonic bath for 10 min. The surface roughness was measured (Alicona Infinity Focus SL, Bruker, U.S.), and the microstructure was evaluated with optical microscopy (OM) (Leica DM, Leica Microsystems GmbH, Germany), scanning electron microscopy (SEM) (Sigma 300, Zeiss, Germany), electron diffraction spectroscopy (EDS) (Oxford Instruments, UK) and X-ray diffraction (XRD) (Bruker D8 Discover, Bruker, U.S.).

The corrosion properties were evaluated on as-built samples by immersion in Dulbecco's Phosphate Buffered Saline solution (DPBS D8123, Sigma-Aldrich, U.S.), over a period of 28 days, investigating the volumetric hydrogen evolution, mass change as well as the change in ion concentration in the corrosion media.

RESULTS AND DISCUSSION

The sample printed with 60W exhibited the largest surface roughness (Fig. 1 a). The 60 W samples also contained internal pores measuring >100 µm. The Mg-rare earth intermetallic phases and Y_2O_3 flakes previously observed in Mg-Y-Nd-Zr processed by PBF-LB[4], were present in all samples. However, no difference with regards to their amount, size nor distribution could be found between the samples.

The results from the hydrogen evolution are presented in Fig. 1b), showing an increased hydrogen evolution, and thus an increased corrosion rate, with higher laser power. The ion release and mass change followed the trend. These results were unexpected, as larger surface roughness and higher porosity typically leads to higher degradation rates.

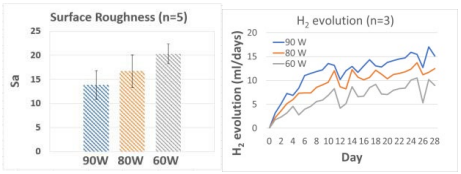

Figure 1: a) Surface roughness of the as-built samples. b) Hydrogen evolution for the as-built samples.

The higher degradation rates of the 90 W samples were probably due to Mg evaporation as a result of a higher energy input. This would lead to an increase in the amount of intermetallic inclusions precipitating. The higher energy input could also have resulted in growth of the precipitates, increasing their cathodic activity and consequently the corrosion rate of the material.

Further work should investigate if change in other process parameters, such as scanning speed and hatch distance would result in similar trends.

CONCLUSION

A higher laser power gave a higher degradation rate of an Mg-$Y_{3.9wt\%}$-$Nd_{3.0wt\%}$-$Zr_{0.49wt\%}$ alloy processed by PBF-LB, despite also resulting in lower surface roughness and a denser bulk material, likely due to an increased relative amount of intermetallic particles in the material.

REFERENCES

1. Valtanen, R. *et al.* Injury 52:72–S77, 2021
2. Witte, F. Acta Biomater. 23:28–40, 2015
3. www.syntellix.de/en/products/technology.html
4. Suchý, J. *et al.* J. Manuf. Process. 69:556–56, 2021

ACKNOWLEDGMENTS

The authors are grateful for assistance by Lena Thorsson (Exmet AB), and financial support from the Swedish Foundation for Strategic Research (FID17-0028), and Vinnova (2019-05259 and 2019-00029).

Influence of TPMS-based Architecture of Hydroxyapatite Scaffolds on Osteoinduction and Osteoconduction

Ekaterina Maevskaia[1*], Julien Guerrero[1], Franz E. Weber[1,2]

[1]University of Zurich, Center of Dental Medicine, Oral Biotechnology & Bioengineering, Zürich, Switzerland
[2]CABMM, Center for Applied Biotechnology and Molecular Medicine, University of Zurich, Zurich, Switzerland
*ekaterina.maevskaia@zzm.uzh.ch

INTRODUCTION

Lately, triply periodic minimal surface (TPMS) structures attracted the attention of researchers in different fields due to their high mechanical properties[1], a great value in the surface to volume ratio[2], and lightweight[3]. Besides, those structures present interconnectivity of pores and a strong tortuosity similar to trabecular bone[4] making them of first interest in bone tissue engineering. The goal of this study was to investigate the influence of the architecture of TPMS-based scaffolds *in vitro* on human bone marrow stromal cells (hBMSCs) growth and differentiation, but also *in vivo* on osteoconduction and osteoinduction after implantation in rabbits calvaria defects.

EXPERIMENTAL METHODS

The scaffolds were designed using nTopology software and fabricated using CeraFab 7500 printer from the hydroxyapatite-based slurry LithaBone HA 400. Scaffolds with three types of TPMS rchitecture were produced: Diamond, Gyroid, and Primitive (**Fig. 1**).

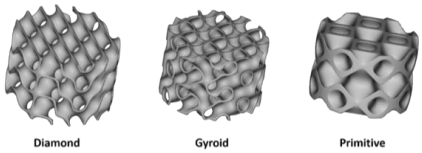

Fig. 1. 3D models of the TPMS-based scaffolds.

To study the influence of scaffold architecture on cell proliferation, hBMSCs were seeded on the fabricated materials and cultured for 21 days in a control medium or osteogenic medium.
Thereafter, an Alamar Blue assay was performed to study cell metabolism. Furthermore, DNA measurement was conducted using the CyQUANT® assay. Additionally, RT-qPCR was used to investigate the osteogenic differentiation of hBMSCs. The expression of the following genes was studied: *ALPL*, *COL1A1*, *RUNX2*, *OPN*, *OCN*, and *CAV1*. To normalize our data, *GAPDH* and *18S* were used as reference genes.
To study osteoconduction and osteoinduction *in vivo*, µCT analyses were performed to measure and quantify bone neo-formation with our three types of fabricated scaffolds after 4 weeks of implantation.

RESULTS AND DISCUSSION

After analysis of the DNA content at Day 5, Day 12, and Day 21, the seeding efficiency within fabricated scaffolds was calculated. We observed a higher seeding efficiency in Gyroid compared to Diamond, with the lowest for Primitive scaffolds. Nevertheless, all fabricated scaffolds showed an increase in cell number and cell metabolism (**Fig. 2**) over culture time. Those results could be connected in regards to the lower tortuosity of Primitive scaffolds in comparison with Diamond and Gyroid structures, retaining a lower amount of cell after the initial seeding.

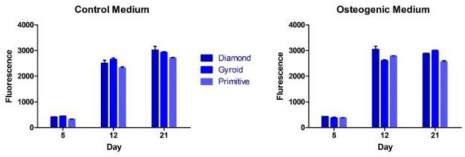

Fig. 2. Evolution of cell metabolism over culture time.

The results of the RT-qPCR showed that the expression of most osteogenic related genes was higher for cells cultured in the osteogenic medium, but without significant difference between the fabricated scaffolds. However, for *RUNX2*, *COL1A1*, and *OCN* the lowest expression was observed for hBMSCs cultured within Gyroid architecture.
Concerning the *in vivo* results, µCT analysis revealed that Diamond and Gyroid structures present a higher volume of mineralized tissue infiltration within the fabricated scaffolds after 4 weeks of implantation.

CONCLUSION

According to the RT-qPCR analysis, we could assume that Gyroid scaffolds possess the least osteogenic potential *in vitro* after 21 days of cell culture with hBMSCs. However, the usage of Primitive leads to the least cells amount. Additionally and after investigating the effect of the TPMS structures *in vivo*, we can claim that Gyroid and Diamond architectures are related to deeper and wider mineralized tissue ingrowth after 4 weeks of implantation in rabbit calvaria defects that indicate their higher osteoconduction properties.

REFERENCES

1. Qureshi Z.A. *et al*., Int. J. Heat Mass Transf. 170:121001, 2021
2. Guerreiro R. *et al*., Symmetry 12:596, 2020
3. Wang H. *et al*., Engineering Structures 252:113640, 2022
4. Liu F. *et al*., Materials 13:2589, 2020

ACKNOWLEDGMENTS

This work was supported by the Swiss National Science Foundation through a grant to FEW (310030_197128).

CO_2 laser-based powder reactive sintering towards bioactive glasses

Louis CHAIGNEAU[1], Agnès NOVELLA[2], Coralie DESBORDES[1], François CHEVIRÉ[1,]

Damien BRÉZULIER[2], Ronan LEBULLENGER[1]

[1] Univ Rennes, ISCR, CNRS-UMR 6226, Eq. Verres & Céramiques, F-35000 Rennes

[3]Univ Rennes, ISCR, CNRS-UMR 6226, Eq. Verres & Céramiques, CHU Rennes, Pôle Odontologie, F-35000 Rennes

louis.chaigneau@univ-rennes1.fr

Traditionally, glass synthesis is performed by melting-quenching or sol-gel processes [1]. This work describes a new method to produce bioactive glass using a CO_2 laser as the unique heat source, from soda-lime silicate glass beads and/or oxide precursors. The formulations chosen for this study are all in the bioactive area of the Hench triangle, including the 45S5® composition [2]

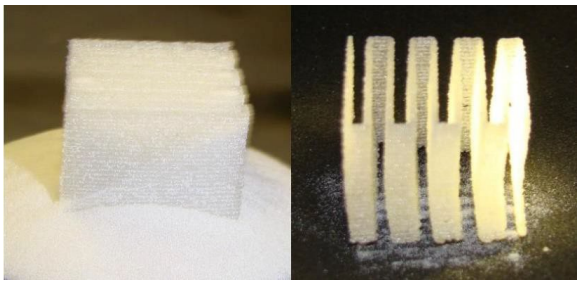

Figure 1. Scaffold made by powder bed fusion with CO2 laser of glass beads

Thermal stability by DSC, crystallisation by XRD, insertion and dispersion of the inserted elements by SEM/EDX as well as the quality of the produced objects will be studied as a function of the granulometry of the glass beads used, the machine parameters (Power, scan velocity, hatch spacing) and the raw materials batch composition. The biocompatibility of CO_2 laser sintered samples is evaluated by cytotoxicity tests and their behaviour in Simulated Body Fluid (SBF) medium. Under ideal conditions, the interest will be to build a complex 3D object while synthesizing a glassy structure.

References

[1] G,Kaur, G Pickrell, N Sriranganathan, V Kumar, Journal of Biomedical Materials Research Part B: Applied Biomaterials, 104, 2016, p. 1248-1275

[2] L.L Hench, Journal of Materials Science: Materials in Medicine, 17, 2006, 967-978

Fused filament fabrication of PLA/bioglass composite and enhancement of these mechanical properties with gold coating thin film of bioglass powder

Louis CHAIGNEAU[1], Aurélien PERROT[2], Jean-François COULON[2], Damien BRÉZULIER[3],

François CHEVIRÉ[1], Ronan LEBULLENGER[1]

[1] Univ Rennes, ISCR, CNRS-UMR 6226, Eq. Verres & Céramiques, F-35000 Rennes

[2] ECAM Rennes - Louis de Broglie, Campus de Ker Lann – 35170 Bruz, France

[3]Univ Rennes, ISCR, CNRS-UMR 6226, Eq. Verres & Céramiques, CHU Rennes, Pôle Odontologie, F-35000 Rennes

ronan.lebullenger@univ-rennes1.fr

Abstract :

Due to the ageing of the population, the synthesis of biomaterials and the optimization of their physico-chemical characteristics are at the heart of many research projects in regenerative medicine. The emergence of 3D printing techniques has rapidly led to the manufacture PLA-bioglass composite scaffolds using the FFF (Fused Filament Fabrication) technique. However, this composite presents some problems including a lower mechanical strength than the two compounds alone, probably due to the ionic salting-out induced by the bio-glass. This study aims to counter this phenomenon by coating the bio-glass particles with a thin layer of gold. The 3D composite objects will then be characterized mechanically and biologically to ensure that the bioactive character of the composite is preserved.

Keywords: biomaterials, additive manufacturing, bioglass, PLA, gold coating

Evaluating the use of synthetic self-assembling peptides to 3D bioprint in vitro cartilage tissue models

Patricia Santos Beato[1*], Aline Miller[2], Andrew Pitsillides[3], Ryo Torii[4], Deepak Kalaskar[5].
[1]Biochemical Engineering, University College London (UCL), London, UK.[2]Chemical Engineering, University of Manchester, Manchester, UK.[3]Comparative Biomedical Sciences, The Royal Veterinary College, London, UK.[4]Mechanical Engineering, University College London (UCL), London, UK.[5]Division of Surgery and Interventional Sciences, University College London (UCL), London, UK. *patricia.beato.19@ucl.ac.uk

INTRODUCTION

Cartilage pathologies remain a challenge in the field of orthopedic medicine, with diseases such as osteoarthritis remaining without a cure. Development of reliable disease models is a key to improve our understanding of these pathologies. However, conventional tissue engineering techniques, such as scaffold top cell seeding, to develop cartilage constructs *in vitro* have encountered multiple issues such as lack of structural control and heterogeneous cell distribution. 3D bioprinting has been used as an alternative approach to overcome these limitations, enabling the manufacturing of intricate structures with a controlled and homogeneous cell deposition. Most cell-laden materials used to 3D bioprint cartilage, such as gelMA[1] or hyaluronic acid[2], are animal-derived. With the goal of taking the next step towards a more sustainable and ethical scientific approach, synthetic polymers are an alternative to biologically derived materials to 3D bioprint cartilage.

In this research, we present the use of a commercial self-assembling peptide as a potential material for 3D bioprinting cartilage tissue *in vitro* models, and its initial evaluation in terms of how the 3D bioprinting process affects the ability of primary human chondrocytes to produce cartilage with this material.

EXPERIMENTAL METHODS

Alpha 1 Peptigel (Manchester Biogel, UK) was mixed with human primary chondrocytes and 3D bioprinted into cylindrical structures (1 mm tall, 5 mm diameter) using the BIOX 6 bioprinter (Cellink, Sweden). These were cultured using chondrogenic growth media (Cell Applications, San Diego, CA) for 21 days, incubated at 37°C in a humidified atmosphere with 5% pCO_2.

Cell viability, cell proliferation, and histological assessments were performed. Specific cartilage markers such as Sox-9, collagen II, and aggrecan expression were assessed through immunochemistry and quantitative ELISA methods. The results were compared to a 3D chondrocyte cell pellet control.

RESULTS AND DISCUSSION

Human primary chondrocytes embedded in Alpha 1 Peptigel showed high cell viability (>75%) after LIVE/DEAD staining; as well as maintenance of cell numbers after day 7 and up to 21 days of culture, assessed through DNA quantification, showing a cartilage-like behavior where cells do not proliferate. The 3D control on the other hand showed a decrease in cell viability and a decrease in cell number over 21 days potentially due to the hypoxic conditions experienced in the cell pellet core.

Regarding cartilage-specific markers, Alpha 1 based *in vitro* cartilage models showed high Sox-9 expression from as early as day 0, indicating that chondrocytes presented a chondrogenic phenotype, which is lost in 2D cell culture expansion[3]. Collagen II and aggrecan expression was firstly observed at day 7 and strongly expressed up to day 21. The expression of collagen II and aggrecan indicated that these cells had matured and produced extracellular matrix later in the culture post-printing. These markers were also observed in the 3D pellet control, which confirmed expected 3D control behavior[4]. These cell viability results as well as the specific cartilage marker expressions shown in Alpha 1 based constructs are similar to the results observed with other hydrogels, such as gelMA, in cartilage 3D bioprinting[1,2].

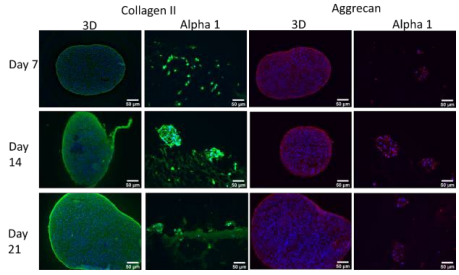

Figure 1. Collagen II (green) and Aggrecan (red) expression in human primary chondrocyte cell laden Alpha 1 and 3D cell pellet control images across days 7, 14 and 21; cell nuclei shown in blue (DAPI). Scale bar show 50 µm.

CONCLUSION

This study highlights the potential of the Alpha 1 self-assembling peptide as a non-animal derived bioink for 3D bioprinting of *in vitro* human cartilage tissue models. Human primary chondrocytes embedded in 3D bioprinted structures show specific cartilage marker expression as well as high cell viability. Future application of this model could include cartilage-specific disease modelling, such as osteoarthritis.

REFERENCES

[1.] Costantini M. et al. Biofabrication. 8(3):035002, 2016
[2.] Antich C. *et al*., Acta biomaterialia. 106:5-114-23, 2020
[3] Benia P.D. *et al.* Cell. 15:4- 1313-1321, 1978
[4] Khajeh S. *et al.* Biologia. 73(7) 715-726. 2018

ACKNOWLEDGMENTS

The authors would like to thank the Engineering and Physical Sciences Research Council (EPSRC) (EP/S021868/1) and Manchester BIOGEL (Manchester, UK) for providing financial support to this project.

Clickable Dynamic Bioinks

Pierre Tournier,[1] Nathan Lagneau,[1] Boris Halgand,[1] François Loll,[1] Jérôme Guicheux,[1] Catherine Le Visage,[1] Vianney Delplace[1,*]

[1]Université de Nantes, Oniris, CHU Nantes, INSERM, Regenerative Medicine and Skeleton, RMeS, UMR 1229, F-44000, France
[*]vianney.delplace@univ-nantes.fr

INTRODUCTION

Bioprinting is a booming technology, with broad applications in tissue engineering and regenerative medicine.[1] It holds the promise of fast and straightforward access to any type of living tissues, with tailored composition and architecture. Yet, while bioprinters have quickly evolved, the field of printable biomaterials is much behind. The main challenge consists in designing cell-containing materials, i.e., bioinks, that can flow for printability, and yet possess the desired composition and mechanical properties after printing. To date, most advanced strategies have revolved around the use of printing baths[2-3] and photocrosslinking[4-5], with inherent limitations; and a simple and universal bioink strategy remains to be found.

EXPERIMENTAL METHODS

To address this challenge, we hypothesized that a dynamic covalent hydrogel, which is printable, can be chemically modified with reactive groups to allow the adjustment of a construct composition and mechanical properties after printing. More specifically, post-printing modifications can be performed by the simple addition to the culture medium of a diffusible molecule (e.g., covalent crosslinker, adhesive peptide) modified with a reactive group complementary to the one grafted onto the hydrogel network. The post-printing reaction has to meet the criteria of click chemistry (i.e., mild conditions, no byproducts, no purification), overall providing what we called « clickable dynamic bioinks ». Using hyaluronic acid (HA) as a polymer of interest, we first developed and characterized a new class of dynamic covalent bioinks based on boronate ester crosslinking. Then, taking advantage of the strain-promoted azide-alkyne cycloaddition (SPAAC) as a click reaction, we investigated the feasibility of various post-printing modifications (e.g., composition, stiffness, adhesion), assessed by fluorescent labelling, rheological and mechanical measurements, and/or cell behavior.

RESULTS AND DISCUSSION

For the first time, we demonstrated that boronate ester crosslinking can be used for the design of printable hydrogels, with appropriate shear-thinning, absence of swelling, long-term stability, and tunable viscoelastic properties (G' of 80 to 2500 Pa, at 1 Hz). We showed that these hydrogels are cytocompatible (>90% cell viability) with various cell types (i.e., fibroblasts, MSCs, chondrocytes), and that they can prevent cell sedimentation in a cartridge for days, circumventing a common issue in bioprinting. These new bioinks allowed us to design constructs of various shapes and volumes (tested up to 10 layers). Regarding post-printing modifications, we first showed that the construct composition can be easily modified with various molecules of interest (chondroitin sulfate, low molecular weight HA, gelatin). This technique also allowed to increase the construct rigidity (G' increased from 200 to 1200 Pa) upon the addition of a desired crosslinker, or trigger cell adhesion upon the addition of a reactive adhesive peptide (e.g., RGD-azide). Of major value, we finally showed that these post-printing modifications can be controlled in time and space.

CONCLUSION

Clickable dynamic bioinks constitute a simple and versatile bioprinting tool that combines printability and tailorable composition and mechanical properties in a most unique fashion. It paves the way toward 4D bioprinting, with virtually unlimited tissue engineering applications.

REFERENCES

1. Sun et al., Biofabrication. 2020, 6;12(2):022002.
2. Hinton et al., Sci. Adv. 2015;1:e1500758
3. Hull et al., Adv. Funct. Mater. 2020, 2007983
4. Ouyang et al., Adv. Mater. 2017, 29, 1604983
5. Bernal et al., Adv. Mater. 2019, 1904209

ACKNOWLEDGMENTS

The authors would like to thank the Nantes Excellence Trajectory program (NExT Junior Talent 2018, VD), and the Marie-Sklodowska Curie Actions (BABHY-CART project, GAP-846477; VD) for their financial support.

Development of optically-tuned bioresins for the rapid volumetric bioprinting of liver organoid-laden metabolic biofactories

Paulina Núñez Bernal[1*], Manon Bouwmeester[2], Jorge Madrid-Wolff[3], Marc Falandt[2], Sammy Florczak[1], Núria Ginés Rodriguez[1], Yang Li[1], Gabriel Größbacher[1], Roos-Anne Samsom[2], Monique van Wolferen[2], Luc van der Laan[4], Paul Delrot[5], Damien Loterie[5], Jos Malda[1,2], Christophe Moser[3], Bart Spee[2], Riccardo Levato[2,1]

[1] Department of Orthopedics, UMC Utrecht, Utrecht, the Netherlands
[2] Department of Clinical Sciences, Faculty of Veterinary Medicine, Utrecht University, Utrecht, the Netherlands
[3] Laboratory of Applied Photonics Devices, École Polytechnique Fédéral Lausanne (EPFL), Lausanne, Switzerland
[4] Department of Surgery, Erasmus MC-University Medical Center, Rotterdam, the Netherlands
[5] Readily3D SA, EPFL Innovation Park, Lausanne, Switzerland
[*] p.nunezbernal@umcutrecht.nl

INTRODUCTION: Developing advanced *in vitro* platforms for biomedical research is a key challenge in tissue engineering, which bioprinting promises to tackle allowing the precise patterning of cell-laden biomaterials into hierarchical architectures. Volumetric bioprinting (VBP) is a novel light-based biofabrication technique that overcomes challenges posed by conventional bioprinting approaches, through the layerless biofabrication of viable and complex cell-laden structures at high printing speeds[1]. Given the requirement of high cell densities to create functional tissue mimics, in light-based printing, strategies to overcome the light-scattering effect of intracellular organelles are needed to ensure high-resolution prints. In this study, an optically engineered bioresin was developed to pattern morphologically undisrupted organoids into complex centimeter-scale assemblies. Patient-derived human liver organoid-laden structures were printed to create advanced *in vitro* models that recapitulate liver functions involved in systemic homeostasis and detoxification.

EXPERIMENTAL METHODS: In VBP, visible light back-filtered projections of a 3D object are directed on a volume of cell-laden bioresin (gelatin methacryloyl with visible-light photoinitiator lithium phenyl-2,4,6-trimethylbenzoyl-phosphinate). The photosensitive resin is then crosslinked in a spatially controlled fashion. Resolution in the presence of a hepatic cell line and patient-derived liver organoids was enhanced via supplementation of iodixanol, a refractive index-matching compound. Optically-tuned resins were used to print high hepatic organoid densities (>10^7cells/mL). Organoid viability and hepatic differentiation post-VBP were tested and compared to extrusion bioprinted (EB) constructs. Organoid-laden, mathematically-derived architectures with different structural properties were printed at high resolution and cultured under dynamic perfusion to evaluate ammonia metabolism.

RESULTS AND DISCUSSION: VBP-printed 3D constructs were fabricated in tens of seconds, achieving the highest resolutions reported to date (41.5±2.9µm positive and 104.0±5.5µm negative features). Iodixanol concentration was optimized to match the refractive index of intracellular components of single cells and organoids, ensuring comparable resolution between cell-free and cell-laden prints. Compared to EB-printed structures, where shear forces resulted in organoid fragmentation and lower viability (73.2±1.2%), VBP-printed organoids showed high viability (93.3±1.4%), undisrupted morphology and displayed apicobasal polarity post-printing. Complex gyroid-like structures with different pore architectures were printed within 16-20s and showed tunable permeability and surface-area-to-volume ratio. When cultured in a dynamic perfusion system, these structures exhibited enhanced rates of ammonia metabolism (33.5±5.8-24.3±1.4nmol $mg_{total\ protein}^{-1}$) compared to static controls (12.7±0.3nmol $mg_{total\ protein}^{-1}$), as well as shape-dependent changes in the metabolic rate of the embedded organoids.

CONCLUSION: This study demonstrated the contactless bioprinting of complex and mechanically fragile biological structures (liver organoids) via VBP. Via refractive index-matching, an optically-tuned gelMA resin enabled high-resolution printing of cell-laden structures, obtaining previously unachievable feature sizes. Organoids displayed high viability and metabolism, as well as hepatic differentiation capacity post-printing. The dynamic culture of convoluted VBP-printed structures was demonstrated through architectures that could modulate organoid function in a printed shape-dependent fashion. The combination of organoid technology with the ultra-fast printing times and freedom of design offered by VBP shows promise for the development of new predictive platforms for *in vitro* disease modeling and drug screening research.

REFERENCES

1. Bernal, P.N. *et al*., Adv. Mater. 1, 1904209, 2019

ACKNOWLEDGMENTS: This project received funding from the European Research Council (ERC) under the European Union's Horizon 2020 research and innovation programme (grant agreement No. 949806, VOLUME-BIO) and from the European's Union's Horizon 2020 research and innovation programme under grant agreement No 964497 (ENLIGHT).

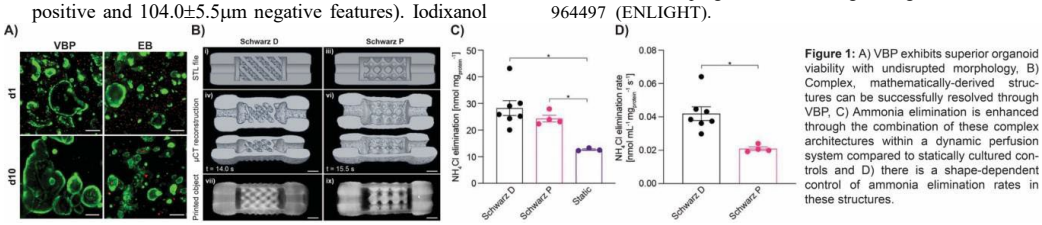

Figure 1: A) VBP exhibits superior organoid viability with undisrupted morphology, B) Complex, mathematically-derived structures can be successfully resolved through VBP, C) Ammonia elimination is enhanced through the combination of these complex architectures within a dynamic perfusion system compared to statically cultured controls and D) there is a shape-dependent control of ammonia elimination rates in these structures.

Development of modified nanocrystalline cellulose based bioinks

Clara M García Sáez[1], María Arevalo[1] Itciar González[2], Francisco J Parra Ruiz[1], Luis M Rodríguez-Lorenzo[1]
[1]ICTP-CSIC, Madrid Spain [2] ITEFI-CSIC, Madrid Spain
luis.rodriguez-lorenzo@ictp.csic.es

INTRODUCTION

Cancer modeling has been of special interest since it paves the way for easing and modulating preclinical research model conditions. 3D modeling of equivalent tumor environments is required for the development of new therapies [1].

3D bioprinting is one of the most promising approaches to create in vitro 3D biomimetic models with relevant physiological characteristics for cancer research, however one of the main limitations of bioprinting is the lack of a consensus in the optimal conditions to be used for each specific application [2]. The development of tumor specific bioinks is one of the mayor challenges for the bioprinting of cancer models.

The objective of this project is the preparation and selection of the suitable components for preparing PANC-1 laden bioinks.

EXPERIMENTAL METHODS

The components used for the bioink were Sodium alginate (SA) (Sigma-Aldrich), nanocrystalline cellulose (CNC) (Forest Products Laboratory (University of Maine, EE.UU.), 2,2,6,6-tetramethylpyperidine-1-oxyl (TEMPO) (TCI Chemicals, EE.UU), TEMPO-CNC, methylcellulose (MC) (Methyl cellulose, viscosity 4,000 cP,M0512-500 G, Sigma-Aldrich), and human plasma CR Region de Murcia. CNC-Ox was obtained in a TEMPO mediated single step oxidation reaction. Materials were characterized by colorimetry, Z potential and FTIR and MAS-NMR spectroscopies.

Bioinks optimization. The proposed ink is composed of 3% SA and several percentage of either CNC, CNC-Ox or MC in human plasma. Every procedure is accomplished under sterility conditions inside a laminar flow cabinet. Fresh frozen human plasma (obtained in compliance with the standards of the American Association of Blood Banks) is thawed at 37ºC and mixed first with SA under stirring, and then MC with a spatula. Thereafter, PANC-1 cells, cultured in 10% FBS 1% L-Glu 1%Pen/Strep RPMI medium at 37ºC and 5% CO2. After mixing the cells with the ink a final concentration of 5·105 cells in each of the printed constructs is obtained. Ink's mechanical properties are rheologically characterized on rheometer ARG2 (TA instruments) with a sandblasted parallel plate D = 25 mm geometry at 37ºC before, during, and after gelation event upon addition of 1.5% CaCl2 crosslinker. **3D Bioprinting.** Cell-laden bioink solution is loaded into a 5 mL cartridge, then stored at RT for stabilization of bioink rheological properties. Pneumatic extrusion Inkredible 3D printer (Cellink) is used for dispensing the hydrogel ink through a conical nozzle (D = 410 µm). Cylindrical constructs of D = 15 mm are printed in 6Pculture well plates. Printed hydrogels are crosslinked for 20 min with 1.5% $CaCl_2$; it is then removed, replaced with fresh medium, and incubated at 37ºC 5% CO2. Cellular survival and proliferation are assessed with a Live/Dead viability kit (ThermoFisher Scientific#L3224) constructs are imaged using a confocal microscope (Leica TCS SPE, Wetzlar, Germany).Viability is screened at 1,4 and 7 days post-printing.

RESULTS AND DISCUSSION

CNC-Ox was obtained from a TEMPO-mediated surface reaction which increased the negative charge from CNC. The reaction can be easily monitored with a colorimetric asssay as displayed in the following fig. Also, CNC-ox displays a carbonyl band at 1738 cm-1 and a band at 180 ppm,in addition of the CNC bands, on the FTIR and 13C-MAS-NMR spectra respectively.

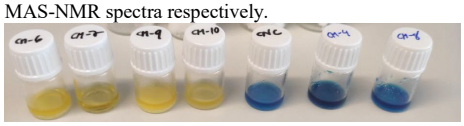

CNC containing inks present a more pronounced shear thinning behavior than MC containing inks but both present a similar recovery capacity. CNC crosslink ability is superior and produce more stable constructs and higher storage modules.

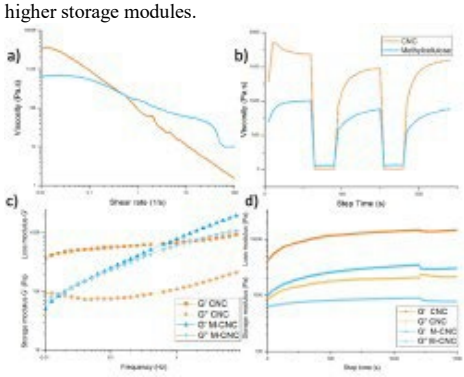

Also while MC containing inks start degrading after 7 days, CNC containing inks start maintaing their integrity for at least 15 days. Embedded PANC-1 cells survive and proliferate within the printed constructs after at least 7 days of culture. Viability at day 1 suggests that the printing process was barely detrimental for cells. A week after, cells remain alive and proliferate.

CONCLUSION

CNC and CNC-OX containing inks has shown lower viscosity and great printability, in comparison with MC containing inks. Cytocompatibility, structural integrity, and consistent mechanical properties are observed as well. Chemical modification of CNC is a promising route for developing a new family of bioactive bioinks.

REFERENCES

[1] Zhang et al ACS Biomat Scie Eng 2, 1710, 2016
[2] N. Cubo, et al , Biofabrication 9, 015006 (2016)

Development Of Biomaterial Inks For The 3D Bioprinting Of Anisotropic Cardiac Patches

Aurelia Poerio[1*], Jean-Philippe Jehl[1], Mélanie Lovera-Leroux[1], Solenne Fleutot[1], João F. Mano[2], Franck Cleymand[1]

[1] Institut Jean Lamour UMR 7198 CNRS / Université de Lorraine, Nancy, France
[2] Department of Chemistry, CICECO, University of Aveiro, 3810-193, Aveiro, Portugal
[*] aurelia.poerio@ univ-lorraine.fr

INTRODUCTION

The heart has a limited capacity of regeneration. Once cardiomyocytes are damaged, for example after myocardial infarction, they are replaced by non-contractile fibrotic scar tissue. The loss of contractile capacity of cardiomyocytes leads to disfunctions of the heart and its pathological remodeling which causes, eventually, heart failure[1]. A promising approach for preventing pathological remodeling is the application of cardiac patches able to compensate and/or repair the damaged tissues. The main limitation for the development of cardiac patches is the recapitulation of the mechanical characteristics of the heart. In fact, once a patch is applied, it should be able to support the heart beating without limiting it and without losing its mechanical properties after each cardiac cycle. The aim of this study was to determine the mechanical characteristics of the ventricular region of the heart and to evaluate candidate biomaterials with the suitable mechanical characteristics. 3D bioprinting is then employed to reproduce the anisotropic structure of the heart walls.

EXPERIMENTAL METHODS

In a first step we characterized the myocardial wall of pig cardiac tissue by performing nanoindentation measures[2]. In the second step we developed inks for 3D bioprinting based on natural biomaterials (i.e. chitosan, gelatin, natural gums and alginate) and performed nanoindentation measures in order to find the suitable values of elasticity, similar to the ones obtained from the real tissue. Subsequently, we optimized the bioprinting of the developed inks and evaluated several properties of 3D printed constructs such as their ability to release a model proteins, their internal morphology and their rate of degradation.

RESULTS AND DISCUSSION

Variations in the stiffness of the myocardial tissue analyzed by nanoindentation reveal the local orientation of cardiac fibers[2] as shown in Figure 1. Through measurements of the Young's modulus (on tissue slices of the long axis of the left ventricle) we were able to identify the radial or longitudinal orientation of the myofibers as well as their intermediary orientation.

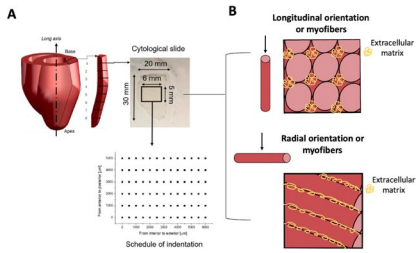

Figure 1: A) Schematization of the tissue slices obtained from the left ventricle of pig hearts and of nanoindentation mapping (Figure reused from ref[2]). B) Representative images showing the direction of the indentation (arrows) and the two opposite myofiber orientations: longitudinal (corresponding to lower values of Young's modulus) or radial (corresponding to higher values of Young's modulus) respectively in the top and bottom images.

The results obtained from this first study allowed us to evaluate candidate biomaterials for the 3D bioprinting of anisotropic patches which follow the myofibers orientation. We developed biomaterial inks which have similar mechanical properties either with the longitudinal or radial orientation of the myofibers. We optimized the bioprinting and evaluated the degradation rate of 3D printed scaffolds and their ability to release proteins (as models of growth factors). The myofiber orientation is then reproduced using the technology of 3D bioprinting.

CONCLUSION

Heart functions are assured by the local fiber structure. By knowing the orientation of the myocardial fibers and their local elasticity we can develop anisotropic patches having mechanical characteristics similar to that of the heart.

REFERENCES

1. Mei and Cheng. Front. Cardiovasc. Med. 7:610364, 2020
2. Jehl *et al.* Journal of the Mechanical Behavior of Biomedical Materials, Volume 119, 104492. 2021

AKNOWLEDGMENTS

This work was supported by the French PIA project "Lorraine Université d'excellence", reference ANR-15-IDEX-04-LUE. The work was also developed in the framework of the CARDIOGEL project, supported by the Chaire Gutenberg of JFM and the CARE FEDER PROJECTS.

Towards superior *in vitro* intestinal models exploiting gelatin-based biomaterial inks

Anna Szabó[1*], Ágnes Dobos[1], Indi Geurs[2], Koen Dewettinck[2], Pedro F. Costa[3], Sandra Van Vlierberghe[1]

[1]Polymer Chemistry and Biomaterials Group, Centre of Macromolecular Chemistry (CMaC), Department of Organic and Macromolecular Chemistry, Ghent University, Ghent, Belgium
[2]Department of Food Technology, Safety and Health, Food Structure & Function Research Group, Ghent University, Coupure Links 653, Gent 9000, Belgium
[3]Biofabics Lda, Porto, Portugal
[*]anna.szabo@ugent.be

INTRODUCTION

Intestinal tissue engineering has been emerging recently as gastrointestinal diseases are becoming increasingly widespread. In 2017, the second most commonly diagnosed cancer type in Belgium was colorectal cancer [1]. To gain superior understanding regarding the nature and treatment of these diseases, *in vitro* intestinal models with superior *in vivo* mimicry are a strict necessity. In addition, these models can be exploited in the food and pharmaceutical industry for the evaluation of the nutritional value of food supplements[2] and the efficiency of novel drugs.

The development of an adequate *in vitro* intestinal model is challenging due to its complexity. The goal of the present work was to create a construct with sufficient permeability towards nutrients and drugs (equilibrium permeability within 24 hours), whilst obtaining suitable mechanical properties (G' < 10 kPa[3]) and a close morphological mimic of the intestinal architecture[4]. To this end, a gelatin-methacryloyl-aminoethyl-methacrylate (gel-MA-AEMA)-based biomaterial ink was exploited as starting material for digital light processing (DLP).

EXPERIMENTAL METHODS

Development of 2D hydrogel constructs

Film casting has been utilized to prepare different gel-MA-AEMA-based 2D hydrogel constructs. To provide sufficient permeability, Tween20® has been exploited as porogen. The mechanical properties were determined via oscillatory rheology on film-casted hydrogel constructs.

Development of gel-MA-AEMA-based biomaterial ink

To determine the optimal biomaterial ink composition, *in situ* rheological evaluation of the formulations was carried out to evaluate their crosslinking kinetics. The most promising inks were subsequently tested for their printing potential on a LumenX+ (CellInk) 3D printer.

Permeability studies of the hydrogel constructs

A static diffusion setup was exploited to determine the permeability towards Lucifer Yellow (LY) through the hydrogel constructs.

Morphological evaluation of the hydrogel constructs

To evaluate the pore size and 3D morphology of the hydrogel constructs, scanning electron microscopy (SEM) and cryo-SEM have been utilized.

***In vitro* biocompatibility assay of the hydrogel constructs**

A live-dead staining (calcein-AM, propidium iodide, PI) of seeded Caco2 and HT29-MTX cells in co-culture (10:1) was performed.

RESULTS AND DISCUSSION

Mechanical evaluation of the 2D hydrogel constructs

The mechanical properties of the hydrogel constructs were below the G' < 10 kPa limit.

Permeability studies of the 2D and 3D hydrogel constructs

The Tween20®-based hydrogel constructs exhibited a higher permeability constant compared to the non-porous structures within a 24-hour time-frame for LY.

Morphological and biological evaluation of the 3D printed hydrogel constructs

The morphological analysis of the 3D hydrogel constructs showed that a well-defined porous structure was achieved in the presence of Tween20® and that the biomaterial ink was utilizable to 3D print villi-like structures (see Figure 1).

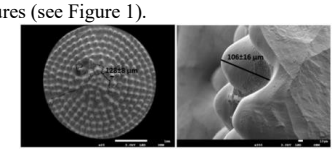

Figure 1. Morphological analysis of a 3D printed gel-MA-AEMA-based construct with cryo-SEM.

The film-casted and 3D printed porous versus non-porous hydrogel constructs showed excellent biocompatibility towards a co-culture of Caco2 and HT29-MTX cells (according to ISO 10993-5-2009).

CONCLUSIONS

A novel gel-MA-AEMA-based biomaterial ink has been successfully developed for digital light processing 3D printing and was exploited for the processing of a 3D villi-like soft hydrogel scaffold. Both the 2D and 3D hydrogel constructs were successfully combined with a co-culture of Caco2 and HT29-MTX cells indicating the potential of the model.

REFERENCES

1. Colorectal cancer Belgium. - https://www.healthybelgium.be/en/health-status/non-communicable-diseases/cancer.
2. Fish-AI - http://fish-ai.eu.
3. Deptuła P. *et. al.*, ACS Biomater Sci Eng. 6(10): 5620–5631, 2020.
4. Dosh R. H. *et. al.*, Tissue Eng - Part B Rev. 24(2):98-111, 2018
5. Van Hoorick J. et. al., Biomacromolecules. 18(10):3260-3272, 2017

ACKNOWLEDGMENTS

This project has received funding from the European Union's Horizon 2020 research and innovation programme under grant agreement No 828835.

Bioprinted Gellan gum/Kappa-carrageenan Scaffolds for Soft Tissue Engineering

Konstantinos Loukelis [1,2], Varvara Platania [1,2], Nikos Koutsomarkos [1], Maria Chatzinikolaidou [1,2]

1 Department of Materials Science and Technology, University of Crete, 70013 Heraklion, Greece
2 Foundation for Research and Technology Hellas (FORTH)-Institute of Electronic Structure and Laser (IESL), 70013 Heraklion, Greece
* mchatzin@materials.uoc.gr

Keywords: bioink, vascularization, bioprinting, gellan gum, kappa-carrageenan

INTRODUCTION

Kappa-carrageenan is a natural linear polysaccharide derived from red seaweed with remarkable biocompatible properties [1, 2]. Gellan gum is another biomaterial produced by the bacterium Sphingomonas paucimobilis, which promotes the cell adhesion and proliferation capacity of different cells [3, 4]. In the recent years, a variety of different research studies in tissue engineering and regenerative medicine focus on the construction of bioinks, which are structures comprising cells and other cellular constituents combined with biocompatible materials [5]. Our current work is based on the fabrication of a bioink containing kappa-carrageenan and gellan gum, whose biocompatibility and gelling capabilities [2,3] make them prime candidates for 3D bioprinting applications.

EXPERIMENTAL METHODS

Two different blend compositions were prepared by mixing 4% w/v gellan gum (GG) with either 1.5% or 2% w/v kappa-carrageenan (K) in deionized H_2O at 90 °C for 4 h to allow for efficient homogenization. The produced blend compositions are designated as GG-K1.5 and GG-K2 and used as inks. Subsequently, after cooling them at room temperature for 5 min, the blends were mildly mixed with a cell suspension of $3x10^6$ cells/ml at a ratio of 10:1 blend volume to cell suspension volume, and the bioinks were loaded into extrusion cartridges for the 3D bioprinting process by means of a bioprinter (Inkredible+, CellInk). The produced bioinks were crosslinked by using a 2.5% w/v potassium chloride solution to enhance the gelling profile of both polysaccharides and were then placed in alpha-MEM culture medium and stored in a humidified incubator at 37 °C. Live/dead assay has been conducted with L929 fibroblasts to determine the cell viability and proliferation inside the bioink on days 1 and 7. Biodegradation studies have been performed on days 0, 7, 14 and 21 to assess the bionks' degradation rate in the presence of cells. Rheological analysis has been carried out to deduce the printability and the mechanical properties of the scaffolds including dynamic strain sweep (DSS), dynamic frequency sweep (DFS), recovery capability and viscosity of the developed bioinks. Ongoing experiments evaluating functional endothelial markers including VE cadherin in bioinks with Wharton's jelly mesenchymal stem cells are in progress.

RESULTS AND DISCUSSION

Live/dead assay indicated a cell viability of 90% for both scaffold compositions on day 1, while between days 1 and 7, a three-fold increase in cell number has been observed. No significant differences were detected between the two compositions regarding their biocompatibility. Additionally, the GG-K1.5 bioink depicted a biodegradation rate of 19% and 37% on days 7 and 21 respectively. The GG-K2 bioink exhibited lower biodegradation values of 15% on day 7, and 26% on day 21. Both blends display shear-thinning behaviour, a necessary characteristic for extrusion bioprinting. From the DSS tests, the yield points of the blends were calculated. The GG-K1.5 blend showed a yield point at 18.4 kPa, and the GG-K2 blend at 27.6 kPa. The loss tangent provides information about the ratio between the viscous and the elastic portion of the viscoelastic deformation behaviour. Both blends shared similar ranges for this parameter, 0.07-0.11 for the GG-K1.5 and 0.08-0.12 for the GG-K2 composition. A crucial condition for extrusion bioprinting is the material's ability to rapidly recover from the applied shear stress. The recovery after 10 seconds was measured at 97% for the GG-K1.5, and at 94% for the GG-K2 blend.

CONCLUSION

Two different bioink compositions containing kappa-carrageenan and gellan gum were fabricated through 3D extrusion bioprinting and promoted the growth of fibroblasts. Physicochemical and preliminary biological investigations confirm the constructs' suitability for 3D bioprinting for soft tissue engineering.

REFERENCES

1. Campo V. *et al.,* C. Polymers. 77(2):167–180, 2009
2. Liu J. *et al.,* C. Polymers. 121:27–36, 2015
3. Muthukumar T. *et al.,* Molecules. 10,24(24):4514, 2019
4. Sumi L. *et al.,* Inter. J. Biol. Macromol. 158:452–460, 2020
5. Hospodiuk M. *et al.,* Biotech. Adv. 35(2):217–239, 2017

ACKNOWLEDGMENTS

This research was funded by the Hellenic Foundation for Research and Innovation (H.F.R.I.) project number HFRI-FM17-1999.

3D bioprinted cross-linked gelatin-alginate hydrogel matrices for biomedical purposes

Adam Mirek[1,2], Habib Belaid[1*], Vincent Cavaillès[3], Mikhaël Bechelany[1]

[1]Institut Européen des Membranes, Université de Montpellier, Montpellier, France
[2]Nalecz Institute of Biocybernetics and Biomedical Engineering, Polish Academy of Sciences, Warsaw, Poland
[3]Institut de Recherche en Cancérologie de Montpellier, Université de Montpellier, Montpellier, France

[*]habib.belaid@umontpellier.fr

INTRODUCTION

Three-dimensional printing is a very broad concept involving a lot of different techniques. They all have one thing in common – making it possible to get a real structure from a computer 3D model prototype from almost any material[1]. This technique offers a flexibility in product design, e.g. for medicine (3D printed implants[2,3]) or pharmacy (unique dosing forms, personalized drug dosing, complex drug release profile[4]). One of the 3D printing techniques, which has gained significant interest in these both fields, is 3D bioprinting that has been developed intensively since the beginning of 2010s. It is used to fabricate biomedical parts for different purposes: advanced tissue engineering, drug delivery and drug screening, wound dressings, and cancer research. The most common 3D bioprinters use bioextrusion. In this technique the material known as a bioink is deposited directly on a dish (collector) creating any previously designed 3D model. One of the most challenging stages of 3D bioprinting is undoubtedly bioink development due to the fact that it must fulfill certain conditions. One of the most common and the easiest to operate bioinks is gelatin-alginate hydrogel[5].

EXPERIMENTAL METHODS

The present study aimed to combine 3D bioprinting technology (Figure 1.) with different cross-linking techniques to develop a novel stable biodegradable 3D bioprinted gelatin-alginate hydrogel matrix for potential biomedical application (e.g. cell culture scaffolds, drug delivery systems).

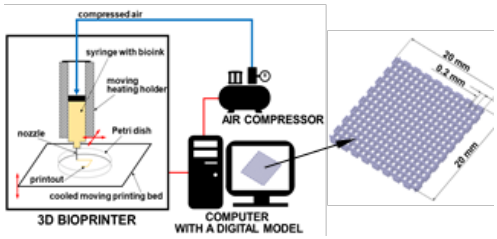

Figure 1. The scheme of 3D bioprinting setup with a digital 3D mesh matrix design.

RESULTS AND DISCUSSION

The influence of the crosslinking method on the hydrogel properties, stability and structure was examined using scanning electron and optical microscopy, Fourier transform infrared spectroscopy, differential scanning calorimetry and thermogravimetric analysis. Research included tests of hydrogel equilibrium swelling ratio and its degradation. Subsequently, biological properties of prepared drug-loaded matrices were studied. Antibacterial activity on *S. Aureus and P. aeruginosa* bacteria and cytotoxicity test on HaCAT cells were performed.

CONCLUSION

This work is a coherent and comprehensive description of the use of a gelatin-alginate hydrogel as a bioink in 3D bioprinting. It presents the bioprintout cross-linking methods and a detailed description of their various properties (important from the point of view of potential use as wound dressings). Such a material can be potentially applied in biomedical engineering, especially as controlled drug delivery systems

REFERENCES

1. G. Poologasundarampillai et al., J. 3D print. Med. 43-7, 2017
2. H. Belaid et al., Mater. Sci. Eng. C. 110595, 2020
3. S. Nagarajan et al., Bioprinting, e00140, 2021
4. A. Ali et al., IntechOpen, 1-13, 2020
5. T. Gao et al., Biofabrication, 034106, 2018

Bottoms-Up Bio-printing of cellularized porous PLGA micro-scaffolds to enhance cell proliferation, viability and migration

Adrien Rousselle[1,2], Youri Arntz[1,2] and Dominique Vautier[1,2]

[1]Inserm U1121; [2]University of Strasbourg

arousselle@unistra.fr

INTRODUCTION

Extrusion bio-printing is the most direct and inexpensive method for printing three-dimensional cell models. This technique provides interesting solutions for generating more complex architectures than the already existing 3D models but still has significant drawbacks. Indeed, printing complex structures induces a high cellular death rate due in part to shear stress, which can induce the apoptosis or inability of the deposited cells.[1] One of the commonly applied solution to these problems is the use of soft hydrogels having little mechanical strength, however implying a lack of structural integrity of the printed designs[2].

A previous study designed PLGA micro-scaffolds, without coatings, used only in hand bio-printing and reported to increase cell viability[3]. This study lacks the printing with an automatic bio-printer.

In our study, we produced hyper porous micro-scaffolds of PLGA, reducing the shear stress experienced by printed cells, and developed two viscous photocrosslinkable hydrogels composed of hyaluronic acid and collagen. These hydrogels enabled us to construct complex 3D structures with multiple cell types by machine bio-printing with our micro-scaffolds.

EXPERIMENTAL METHODS

We developed a method of producing porous PLGA with a simple double emulsion. We enhance the cell adhesion of the particles surface by adding two types of coating, a polylysine (PLL) coating and a collagen coating. With these micro-scaffolds, we put in place a cell culture method using our micro-scaffolds to improve cell proliferation before printing by acting as micro-carriers. We combined these cellularazied micro-scaffolds with a bottom up method of bio-printing of complex 3D structures and integrated them into various types of bio-inks, engineered either for the maximum survival of cells or for the construction of highly complex 3D structures. Ultimately, these micro-scaffolds are capable of protecting the cells during the bio-printing process by absorbing most of the shear stress inherent to all extrusion bio-printing. We also printed more complex structures, composed of structured layers of mesenchymal and cancerous cells, thus constituting an organoid. The observation in time of the movement of cells inside the organoid allowed us to quantify the interaction and migration of cells with and without our micro-scaffolds.

RESULTS AND DISCUSSION

We produced PLL and Collagen coated PLGA micro-scaffolds with an average size of 100 µm in diameter with a porosity of 25-45 %. Our results show an augmentation up to 400% of cell proliferation when cultured with the micro-scaffolds. The viability after printing is augmented with the use of our micro-particles, with a survival rate between 85 and 91% with our particles and between 75 and 83% without the micro-scaffolds. When printing more complex structures with co-cultures of tumorous cells with mesenchymal cells, the presence of our micro-scaffolds increase the migration of stem cells towards the tumorous cells.

CONCLUSION

The overall results offer new insights regarding bio-printing and cellular proliferation and migration in response to the presence of PLGA micro-scaffolds. Our new process promotes high cell productivity and viability before and during bio-printing. The use of our micro-scaffolds makes it easier, faster and more efficient to produce three-dimensional cellular structures and to analyze the interactions of cells in 3D environments

REFERENCES

1. Boularaoui S.*et al*., *Bioprinting* 20, 2020
2. Malda *et al., Advanced Materials* Vol.20, 2013
3. Tan Y *et al., Nature Scientific Reports*, 2016

ACKNOWLEDGMENTS

Financial support was received from Région Grand Est (MIPPID 4D), framework of the Regional Cooperation Fund Research.

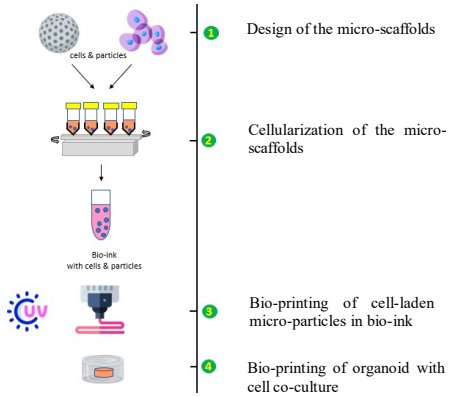

Figure 1: Bio-printing with cellularized PLGA micro-scaffolds

In vivo application of silica-derived inks for bone tissue engineering: a 10-years systematic review

Nicolas Touya[1], Ayako Washio[2], Chiaki Kitamura[2], Yasuhiko Tabata[3], Raphael Devillard[1,4,5], Olivia Kérourédan[1,4,5]

[1] INSERM, U1026 BIOTIS, University of Bordeaux, France
[2] Division of Endodontics and Restorative Dentistry, Department of Science of Oral Functions, Kyushu Dental University, 2-6-1 Manazuru, Kokurakita-ku, Kitakyushu 803-8580, Japan
[3] Laboratory of Biomaterials, Department of Regeneration Science and Engineering , Institute for Frontier Life and Medical Sciences, Kyoto University , Kyoto , Japan.
[4] Faculty of Dentistry, University of Bordeaux, France
[5] CHU de Bordeaux, Services d'Odontologie et de Santé Buccale, France
E-mail: olivia.kerouredan@u-bordeaux.fr

INTRODUCTION

Bone defects, whether due to trauma or surgery, are estimated to affect hundreds of millions people every year, being a major health issue. Although bone graft remains the gold standard therapy, the demand outmatches the supply. A critical need for efficient, sustainable, patient customizable, handy and affordable substitute materials for bone repair is still an ongoing quest.

Silicon has been widely used for medical applications (1,2) and gained a rising potential in hard tissue engineering: easily available, and suitable for malleable preparations, silicon-derived materials crossed the path of additive manufacturing (3,4). Still emerging, this field covers various technologies, including 3D printing and biofabrication processes. In bone tissue engineering, spatially organizing elements to sustain the mechanical functions of bone is one of the most critical needs. Therefore, current research is heavily focused on developing suited materials that bring a satisfying answer on those two levels, exhibiting robust mechanical properties with a high biocompatibility and strong regenerative potential (5). Thus, in the scope of identifying the most efficient materials for bone tissue engineering, investigations of silicon-derived materials were extensively conducted.

Of the numerous materials and strategies assayed, some printable silicon-containing formulations went through the *in vitro* characterization to evaluate their *in vivo* bone repair potential. Thus, this systematic review proposes to state the last decade of *in vivo* applications based on (bio)printed silicon strategies for bone tissue engineering.

EXPERIMENTAL METHODS

The systematic review was conducted according to the Preferred Reporting Items for Systematic Reviews and Meta-Analysis (PRISMA) guidelines, using the Population, Intervention, Comparison, and Outcome (PICO) methods to define the search strategy. The protocol has been registered in PROSPERO database

The following focused question was defined: "Which silica-based bioink/ink formulations have been shown effective for bone tissue regeneration?"

Three electronic databases were screened: MEDLINE (PubMed), Scopus and Web of Science.

The following search combination was used:

((silic*[Title/Abstract]) AND (print*[Title/Abstract]) AND (bone[Title/Abstract])) NOT (silicone[Title/Abstract]) AND ((in vivo[Title/Abstract])

The methodological quality of the studies included was assessed by two independent reviewers, using the SYRCLE's risk of bias tool (SYRCLE's RoB tool) for animal studies, developed by the Cochrane collaboration and completed by the ARRIVE guidelines.

RESULTS AND DISCUSSION

Our searching algorithm provided ~100 articles among the 3 databases. After a first refinement by two reviewers, half of them were removed from the study. Interestingly, more than half of the articles were published recently (2019 or later).
65% of articles used an extrusion strategy associated to heat sintering to create scaffolds based on bioceramics. Although different models of bone defect were assessed, rabbit was the first choice as animal model for the reviewed studies (60% of total), and femoral defect was preferentially chosen by investigators (50% of total).
Often, the different materials were functionalized by various elements such as pro-angiogenic or pro-osteogenic molecules and ions. In the presented studies, in spite of large discrepancies between approaches and inks compositions, authors mainly observed significant improvements of *in situ* mineralization, vascularization, with osteogenic related gene expression, and a better engraftment at the tissue interface and material remodeling, replaced by neo-formed mineralized tissue.

CONCLUSION

Despite being known for decades, the use of silica-derived materials with printing devices for bone tissue applications tremendously increased those past few years. Various strategies have been employed, however most of studies relied on osteoconductive scaffolds. Even though many *in vivo* models were created to assess bone regeneration, the femoral critical size defect appeared to remain the gold-standard strategy. Overall, the use of silica-derived materials improved the bone repair and legitimately stands as a promising addition to ink formulations for bone substitutes.

REFERENCES

(1) Vallet-Regí M *et al.*, Open Biomed Eng J. 2008
(2) Hench L.L. *et al.*, Journal of Biomedical Materials Research, 1971
(3) Götz W. *et al.*, Pharmaceutics, 2019
(4) Zhou X. *et al.*, Journal of Biomedical Materials Research, 2017
(5) Qu H., Materials Today Communications, 2020

Engineering cell responsive extracellular matrix bioinks for bioprinting shape-morphing tissues

Ankita Pramanick [1*], Abhay Pandit [1], Andrew Daly [1,2]
[1] CÚRAM - Science Foundation Ireland Research Centre for Medical Devices,[2] Biomedical Engineering - National University of Ireland Galway
[*] a.pramanick1@nuigalway.ie

INTRODUCTION: During embryonic development, organs emerge through highly dynamic processes driven by complex shape-transformations that sculpt their final shape, composition, and function[1]. Despite this, existing approaches to organ bioprinting employ static hydrogels that are not capable of supporting morphogenetic shape changes essential for their evolution into functional tissues. This is a significant limitation preventing progress in bioprinting research[2-3]. To overcome this limitation, we hypothesised that by varying the bioink extracellular matrix (ECM) composition, tissue shape-morphing behaviour can be modulated. The objective of this research is to develop an ECM bioink composed of collagen-hyaluronic acid that undergoes contractile shape-morphing behaviour driven by cell-generated forces.

METHODS

Bioink formation: The bioink was prepared by mixing collagen (3 mg/ml) and hyaluronic acid (4wt%, MW 50-90 kDa). The rheological properties of the ink were analysed using shear rheology, where viscosity was measured as a function of shear rate (0 to 100 1/s). Human cardiac fibroblasts were then added to the bioink at a 1-2 million/ml concentration. Cells were pre-labelled with a fluorescent cell tracker (green-CMFDA) to enable visualisation of the printed structures using an inverted confocal microscope.

Suspension bath bioprinting: The bioink was extruded into a 3D support bath using an Allevi™ 2 bioprinter (Fig 1a). The support bath was formed using agarose microparticles jammed into viscoelastic suspension with shear-thinning properties (Fig 1a). A curved filament design was created in the support with extrusion performed at a speed of 7 mm/s and a pressure of 4 PSI (30G needle). The bioprinted samples were then cultured for 14 days within the support bath using alpha-MEM, and Glutamax supplemented with 10% FBS and 1% penicillin-streptomycin (37°C, 20% pO_2).

Imaging and statistical analysis: All fluorescent and SEM image processing was performed using ImageJ software, and shape changes were quantified by measuring the cross-sectional area of the samples. Statistical analysis was performed between groups using Graphpad Prism™ for a two-way ANOVA test.

RESULTS AND DISCUSSION: The addition of hyaluronic acid significantly increased viscosity and resulted in shear-thinning properties (Fig 1a). This enabled controlled extrusion of bioink filaments within the support bath at high spatial resolution (~200µm) (Fig 1b). The bioprinted filaments underwent significant shape changes within the suspension bath during culture, with the curved filaments gradually morphing into a straight line over fourteen days (Fig 1b). Quantification of tissue shape changes demonstrated 60-80% bulk contraction after seven days (Fig 1c). Interestingly, by varying the ECM composition, the extent of tissue shape-morphing can be modulated, with the inclusion of hyaluronic acid promoting higher levels of tissue contraction (Fig 1c). Further, it was evident that filament shape-morphing was driven by active cell-generated tractions forces arising from interactions with the collagen network, with increases in cell density and cell spreading evident over the culture period (Fig 1d, e).

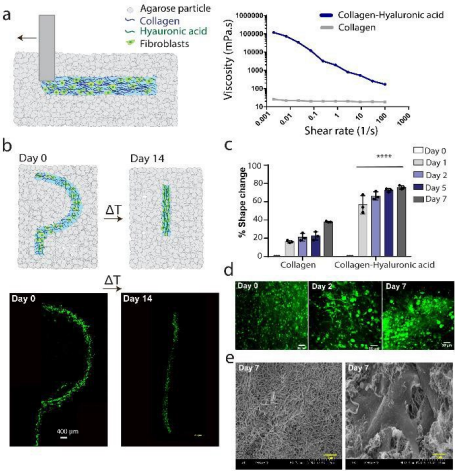

Figure 1 (a) Schematic demonstrating bioprinting of shear-thinning collagen/hyaluronic acid bioinks into a granular suspension bath, including rheological characterisation demonstrating shear-thinning properties. **(b)** Bioprinting of curved filaments within the suspension and subsequent tissue shape-morphing over 14 days. Scalebar 200µm. **(c)** Quantification of tissue shape changes with varied ECM composition. **** denotes significance compared to collagen only samples at the same timepoint. Two-way ANOVA, P<0.001. **(d)** Cell proliferation and spreading over seven days of culture. Scalebar 50 and 200 µm. **(e)** (left) SEM images of the collagen network and (right) cell interactions with the collagen network on day 7. Scalebar 5 µm.

CONCLUSION: We have developed an ECM based bioink that undergoes robust shape-morphing behaviour driven cell-generated traction forces. Importantly, it is possible to modulate this behaviour by varying the ECM composition. The platform holds enormous potential for bioprinting dynamic tissues that undergo programmable shape-morphing behaviours to sculpt their final shape and design.

ACKNOWLEDGEMENTS: Science Foundation Ireland (SFI) and was co-funded under the European Regional Development Fund under grant number 13/RC/2073_P2. Ankita Pramanick was supported by NUI Galway College of Science and Engineering Postgraduate Research scholarship.

REFERENCES:

1. Campàs. *et al*., Nature Methods 11:183-189, 2014
2. Morley. *et al*., Nature Communications 10:1-9, 2019
3. Davidson. *et al*., Science Advances 7:1-14, 2021

A versatile 3D bioprinted pancreas tumor model for new anticancer drug development

Claire Godier[1*], Zakaria Baka[1], Abhik Mallick[1], Varvara Gribova[2], Éric Gaffet[1], Halima Alem-Marchand[1]
[1] Institut Jean Lamour (IJL), UMR 7198 CNRS, Université de Lorraine, Nancy, France
[2]CRBS UMR 1121 INSERM, Unistra, Strasbourg, France
[*] claire.godier@univ-lorraine.fr

INTRODUCTION

While relevant in vitro cancer models are crucial to efficiently develop new anticancer molecules, it is becoming now well established that two-dimensional cell cultures are far from reflecting the complexity and diversity of in vivo tumors and their environment. Three-dimensional cell cultures are interesting alternatives due to their better ability to simulate cell-cell interactions and oxygen and nutrient gradients found in vivo. In this area, 3D bioprinting is considered as a promising approach to establish reproducible and robust 3D tumor models. Indeed, 3D bioprinting is a computer assisted process that generates 3D cell constructs with a well-defined architecture and a high reproducibility. Moreover, this technology makes it easy to associate several cell types in a single model to better simulate the cell diversity inherent to in vivo tumors.

EXPERIMENTAL METHODS

In this work, 3D bioprinting was used to build a pancreatic tumor model containing cancer cells and cancer-associated fibroblasts (CAFs) encapsulated in a gelatin-alginate hydrogel. The hydrogel composition was first optimized to ensure good printability at 37°C and a low extrusion pressure to minimize cell damage. Once the hydrogel optimized, it was used to encapsulate cells at a final density of 1 million cell.mL^{-1}. The resulting "bio-ink" was then used to bio-print tumor-like constructs. These bioprinted tumor models were further characterized to assess the viability and the morphology of the encapsulated cells. The cell membrane integrity was assessed through Live-Dead labelling and confocal imaging. Alamar Blue assay and WST-1 assay were preformed to evaluate cell metabolic activity and proliferation. Annexin V/PI labeling and flow cytometry analysis were also conducted to quantify the proportion of apoptotic cells within the bioprinted tumors. For further assessing cell morphology and distribution within the tumor models, bioprinted structures were fixed and 5 µm thickness sections were realized for hematoxylin and eosin (H&E) staining.

RESULTS AND DISCUSSION

The first results that we have first were the viability at the 1st day, 4th day and 7th day. The higher part of the cells are alive until the 7th day and we notice that we have more cells than the first day. It is also confirmed by the WST-1 assay and AlamarBlue Asssay which shows that the metabolic activity is still working during this period.

The HSE staining also show that cells are growing in the synthetic matrix.

For the moment, all the results are not known because of the need to purchase the experiments.

CONCLUSION

Through these experiments, we could demonstrate that our bioprinted structures show high viability and maintained cell metabolic activity even 15 days

after bioprinting. More interestingly, this work demonstrates that our bioprinted structures can easily be subjected to routinely used viability and histology assays making them very interesting as in vitro models for new anticancer drug development.

REFERENCES

1. Vadivelu *et al*.,Micromachines. 8(4), 2017
2. Augustine *et al.,* Traditional Oncology, 14(4), 2021

ACKNOWLEDGMENTS
Authors should acknowledge any person, or funding agency that has made a significant contribution to the work.

Zwitterionic Microgel Bioink as a Strategy to Inhibit Foreign Body Response to Bioprinted Implants

Maryam Asadikorayem[1], Frantisek Surman[1], Patrick Weber[1], Marcy Zenobi-Wong[1]

[1] Department of Health Sciences and Technology, ETH Zurich, Zurich, Switzerland
* maryam.asadikorayem@hest.ethz.ch

INTRODUCTION

Foreign body response (FBR) to implanted materials is a pervasive problem for almost all biomaterials developed for biomedical applications [1]. Zwitterionic hydrogels have recently drawn tremendous attention in this regard, due to their ultra-low fouling properties, enabling them to effectively inhibit FBR *in vivo* [2, 3]. However, their application in tissue engineering has been limited, due to their unfavorable cell-biomaterial interactions and restricted versatility [4]. In this work, we have developed a macroporous zwitterionic hydrogel which not only has *in vivo* biocompatibility due to the pure zwitterionic nature of the hydrogel, but also is an optimal scaffold for cell encapsulation due to its macroporosity. Moreover, this hydrogel system is based on zwitterionic microgels having inherent injectability and printability which makes it a versatile biomaterial for numerous tissue engineering applications.

EXPERIMENTAL METHODS

Bulk zwitterionic hydrogels are produced via photopolymerization of zwitterionic monomers, carboxybetaine acrylamide (CBAA) and sulfobetaine methacrylate (SBMA), as well as a tyramine acrylamide functional comonomer, using gelatin methacryloyl as the crosslinker. Microgels are produced via mechanical fragmentation of bulk hydrogels using grids with a 50-150 µm mesh size. The microgel solution is mixed with cells, and secondarily crosslinked using horseradish peroxidase enzyme and H_2O_2 resulting in a macroporous zwitterionic hydrogel. Bioprinting of cell laden hydrogel as well as *in vitro* chondrogenesis is studied using primary human chondrocytes as a cell model. *In vivo* performance of both acellular and cell-laden hydrogels is assessed using an immunocompromised animal model.

RESULTS AND DISCUSSION

Macroporous zwitterionic hydrogels were developed by mechanical fragmentation of bulk hydrogels and secondary enzymatic crosslinking. This macroporous hydrogel has 15-20% void space depending on microgel size, allowing for cell migration and proliferation as well as facilitated diffusion. *In vitro* experiments showed more than 90% cell viability and incorporation of SBMA monomers showed positive effect on cell metabolism as well as matrix secretion (Figure.1). The cell-laden microgel bioink showed optimal shear thinning and shear recovery properties required for extrusion printing with high shape fidelity. *In vivo* experiments showed biocompatibility as well as lower FBR and immune cell infiltration compared to non-zwitterionic controls.

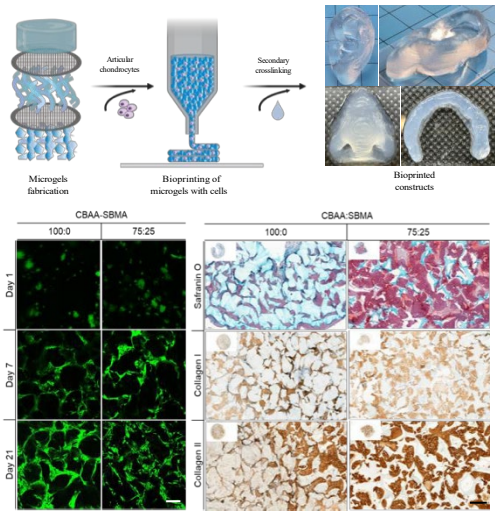

Figure 1. Top) Schematic representation of zwitterionic microgels preparation and bioprinting, and macroscopic images of bioprinted constructs. **Bottom)** Live-dead and histology images of infant human chondrocytes encapsulated (10M/ml) in zwitterionic microgel scaffold (sized with 100 µm mesh) and cultured for 21 days in chondrogenic media. Scale bar: 200 µm.

CONCLUSION

In this study we presented a novel macroporous zwitterionic hydrogel system, with excellent biocompatibility and inherent printability. This novel scaffold is optimal for encapsulation of cells and has *in vivo* biocompatibility, inhibiting FBR as well as immune cell infiltration. This versatile and highly biocompatible platform strategy shows great promise for utilizing zwitterionic materials for multiple tissue engineering applications

REFERENCES

1. Kämmerling L. et al., Journal of Immunology and Regenerative Medicine. 12, 100040, 2021
2. Zhang L. et al, Nat. Biotechnol. 31 (6), 553-556, 2013
3. Dong D. et al., Sci. Adv. 7 (1), eabc5442, 2021
4. Li B. et al., Sci. Adv. 6 (22), eaba0754, 2020

ACKNOWLEDGMENTS

The authors would like to thank the Swiss National Science Foundation (project number 192656 to MZW). for providing financial support.

3D bioprinting of GelMA/hydroxyapatite bio-inks to engineer bone tissue models for the preclinical investigation of new prosthetic implants

Gianluca Ciardelli[1],* Rossella Laurano[1], Roberta Pappalardo[1], Valeria Chiono[1], Monica Boffito[1]

[1]Department of Mechanical and Aerospace Engineering, Politecnico di Torino, Torino, Italy
* gianluca.ciardelli@polito.it

INTRODUCTION

The benefits provided to patients by biomedical implants in terms of pain reduction, mobility and quality of life are incommensurable. Additionally, with the increasing life expectancy and the aging of the world population, the number of implanted prostheses increases every year. In such a dynamic and economically convenient scenario, research groups and leading companies in the field are currently focusing their efforts on the design of a new generation of implants with the potential to reduce the risk of undesired tissue responses (e.g., loosening phenomena) while promoting tissue integration and regeneration, and increasing patient quality of life. However, with the advancement of biomedical research and the development of a new generation of implantable devices, the set-up of standardized and reliable preclinical characterization tools is becoming an urgent need. *In vivo* animal models currently represent the gold standard for medical device testing. However, they often fail in the proper replication of the real human physio-pathological scenario and their use is subjected to many ethical and economic concerns. In this regard, the design of 3D bioengineered models of the bone tissue represents a significant advancement, overcoming the limitations of already used models (e.g., lack of repeatability and standardization, difficult comparisons among already published works), with additional advantages in terms of ethical and economic issues. In this perspective, in this contribution we report the design of a 3D bioprinted bone tissue-mimicking construct by combining bio-ink engineering with the huge versatility of extrusion-based additive manufacturing technologies (i.e., bioprinting). In detail, the bio-ink formulation was first optimized using gelatin methacryloyl (GelMA) and inorganic rod-like nano-hydroxyapatite (nHA). Then, 3D bioprinted structures were designed to reproduce the cortical and cancellous bone tissues.

EXPERIMENTAL METHODS

GelMA with 99% degree of methacryloylation (DoM) was synthesized by reacting gelatin (type A from porcine skin) with methacrylic anhydride (MA) (1 $ml/g_{gelatin}$).[4] GelMA was characterized by infrared (IR) and proton nuclear magnetic resonance (^{1}H NMR) spectroscopies, and the Ninhydrin colorimetric assay. Composite formulations were then designed by solubilizing GelMA in aqueous media containing a photo-initiator (phenyl-2,4,6-trimethylbenzoylphosphinate, LAP) and adding nHA as a disperse phase. Complete rheological and photo-rheological (365 nm, 10 mW/cm^2) characterization was performed. Hydrogel cytocompatibility was assessed according to the ISO 10993-5:2009, meanwhile their potential as cell carriers for the 3D bioprinting of cellularized structures was preliminary tested with NIH-3T3 fibroblasts. CAD models and printing process were finally optimized to 3D bioprint multi-layered *in vitro* models to hold prosthesis prototypes.

RESULTS AND DISCUSSION

GelMA with 99% DoM was successfully synthesized as assessed through IR and ^{1}H NMR spectroscopies and the Ninhydrin colorimetric assay. nHA addition did not alter the typical thermo-responsiveness of GelMA aqueous solutions, with similar gelation onset temperatures and kinetics. Differently, nHA effectively worked as a reinforcement phase within the gel network, leading to significantly improved mechanical properties in GelMA/nHA composite formulations compared to GelMA ones. Moreover, nHA addition did not have detrimental effects on the printing process of the ink: GelMA/nHA exhibited high printability under mild conditions and good shape fidelity to the CAD models. The developed formulations were cytocompatible according to the 10993-5:2009 regulation and exhibited proper rheological properties to avoid cell sedimentation and death during printing. Moreover, the photo-crosslinking process turned out to be cell-friendly and the encapsulated cells spread and proliferated up to 7 days of cell culture. Lastly, a fine CAD model optimization was performed to replicate both the cortical and the cancellous bone tissues and to define the optimal pore size in terms of biological performances.

CONCLUSION

In this work, GelMA/nHA bio-ink formulations were optimized mimicking the composite nature of the bone tissue. The designed thermo-sensitive and photo-curable bio-inks proved to be promising formulations to 3D bioprint *in vitro* bone tissue models with proper geometrical features to hold prosthesis prototypes and allow the investigation of implant-cell interactions at the interface.

REFERENCES

1. Sun M. Polymers 2018;10:1290.

ACKNOWLEDGEMENTS

This work was supported by the EU Horizon 2020 research and innovation program (EVPRO, grant # 814495). The content of this abstract reflects only the author's view, and the Commission is not responsible for any use that may be made of the information it contains. The authors thank Dr. C. Cassino for ^{1}H NMR analyses.

Designing a blueprint for 3D bioprinting of vascular networks

Nehar Celikkin, Dario Presutti, Marco Costantini

Institute of Physical Chemistry, Polish Academy of Sciences, Warsaw, POLAND
* ncelikkn@ichf.edu.pl

INTRODUCTION

Vascular networks are crucial for circulation through the organs to support their function; they are also one of the main focus and biggest challenges of tissue engineering. In the absence of a vascular network, the diffusion of the nutrients into engineered tissues is unfortunately limited only to couple hundreds of micrometers. These vessels are classified based on their extracellular matrix composition, thickness of their lateral layers and their diameter. In the last decade, various 3D manufacturing technologies were employed to engineer vascular networks, trying to recapitulate both their functionality as well as their complex architectures[1,2].

A microfluidic extrusion nozzle that enables multi-ink deposition –greatly outperforming conventional extrusion nozzles in terms of bioink spatial resolution deposition – and biomimetic biomaterial inks that provide proper mechanical stability are two main pillars of ensuing vascular network constructs. Here, a particular attention is paid to the assembly of perfusable vascular networks, for the future integration of the proposed strategy into more complex *in vitro* tissue models.

EXPERIMENTAL METHODS

- **Preparation of biomimetic biomaterial inks**

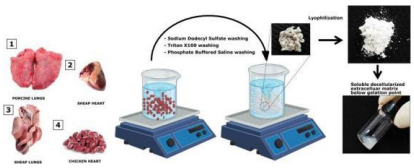

Figure 1. Experimental desing of decellularization of highly vascularized native tissues (created in Biorender.com)

- **Rhelogical characterization of the different dECM inks**

For the rheological characterization of samples the rotational rheometer Kinexus Pro (Malvern Panalytical Ltd) was used. The viscosity was measured by rotation using cone-plate geometries, a cone diameter of 50 mm with an angle of 1 ° at 15°C. To measure the viscoelasticity of samples, oscillation by parallel plate geometry with a diameter of 20 mm at 37°C was used. The gelation point was determined at 4-40°C range with 5°C/min temperature step.

- **Design of the multi-ink extrusion microfluidic nozzle** [3]

The system was obtained by combining a microfluidic chip bearing a Y-junction (2 inlets, 1 outlet). The microfluidic device was fabricated by micro-milling, engraving microfluidic channels into two 5-mm-thick poly-carbonate sheets. The chip outlet was connected to the inner needle (25 G) of the coaxial needle system.

RESULTS AND DISCUSSION

The soluble decellularised matrix gels from porcine lung (PLUNG), sheep heart (SHEART), sheep lung (SLUNG) and chicken heart (CHEART) have all demostrated shear thinning and thermo-responsive characteristics which are highly favourable feature for 3D bioprinting applications. The soluble decellularised matrix gels have exhibited solid-like characteristics (indication of gelation) above their gelation temperature (37 °C). Moreover whereas the dECM sheep lung has demostrated significantly most elastic behaviour, dECM sheep heart has demostrated significantly least elastic behaviour.

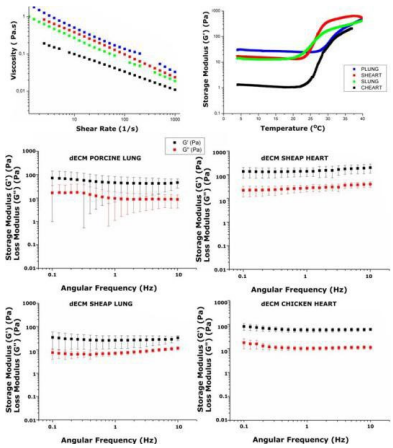

Figure 2. Rheological characterization of soluble dECM

CONCLUSION

We have achieved multi-scale and multi materials biomimetic vascular networks via 3D extrusion-printing based on a microfluidic nozzle allowing to sequentially deposit different bioinks with unprecedented spatial resolution.

REFERENCES

(1) Kinstlinger, Ian S., et al. Nature Protocols 16.6 (2021): 3089-3113.
(2) Liu, Xin, et al. bioRxiv (2021).
(3) Costantini, Marco, et al. Biomaterials 131 (2017): 98-110.

ACKNOWLEDGMENTS

This study is also supported by the National Science Centre Poland (NCN) within PRELUDIUM 19 Project No. 2020/37/N/ST5/03272 to NC.

Printing cell spheroids using laser-assisted bioprinting

Charles Handschin[1*], Nathalie Dusserre[1], Chantal Medina[1], Marie-Laure Stachowicz[1], Léo Comperat[1], Julie Guillermet[2], Hugo de Oliveira[1], Jean-Christophe Fricain[1,3]

[1]Inserm, BioTis U1026, Université de Bordeaux, Bordeaux, France
[2] UMR 1037, CRCT, Inserm F-31037, Toulouse, France
[3]Services d'Odontologie et de Santé Buccale, CHU Bordeaux F-33076, Bordeaux, France

[*] charles.handschin@inserm.fr

INTRODUCTION

Laser assisted bioprinting (LAB) is recognized to be one of the most precise bioprinting technologies, associated with a high throughput and high survival rate. Several studies have demonstrated the ability of LAB to generate well organized microdroplets of bioink with a high cell density[1,2]. Here we exploited the LAB technology to produce small cell spheroids inside a biocompatible hydrogel and we followed the cell maturation over time[3]. In particular, we explored the potential from this methodology to produce a model of 3D pre-microvascularization with a high spatial resolution. We also implement a method to create acini pancreatic spheroids from murine primary culture in order to generate a model for cancer studies.

EXPERIMENTAL METHODS

The laser assisted bioprinter used for these experiments was already described in previous studies[1]. It includes a nanosecond laser (30 ns pulse duration, 1064 nm, 7W) functioning at 1kHz. Typical pulse energy used in this study were in the range from 30 µJ to 100 µJ. Human umbilical vein endothelial cells (HUVEC), expressing a Red Fluorescent Protein, were cultured, trypsinized and concentrated at 70.10^6/mL to create the bioink for the pre-microvascularization experiments. 33 µL from this bioink were spread on a cartridge consisting on a 30 mm diameter glass plate, previously coated with a thin gold layer. The bioink was printed on 150 µL of 5 % (w/v) methacrylated gelatine (GelMa) spread on the surface of a 30 mm diameter glass plate and containing human skin fibroblasts (HSF). LAP was used as photoinitiator at 0.2 % (w/v).

Concerning the exocrine pancreatic cancer model experiments, acini were extracted from mice pancreas and loaded in 2.5 % (w/v) GelMa + 0.2 % LAP with a concentration varying between 1 and 5 million/mL. The resulted bioink was printed on the same biopaper than for HUVEC experiments and a second layer of 5 % (w/v) GelMa + 0.2 % LAP was added to stabilize the structure.

RESULTS AND DISCUSSION

HUVEC printing:

Printing parameters were adjusted to control the depth of the spheroid deposition inside the GelMa. We firstly assessed the spheroid volumes as a function of laser energy. We showed that we were able to control the size of the bioprinted spheroids. We then studied the cell maturation as a function of the HSF concentration (5, 10, 15, 20 and 25 millions/mL). In order to facilitate the analysis of the maturation, we firstly printed simple lines of spheroids. By analysing the number and the directionality from the vascularisation branches over the maturation, we observed than the highest concentration in HSF were more suitable to preserve the shape of the printed geometries.

Acini printing:

High concentrated acini spheroids were deposited on a mesh grid pattern. Pattern with more than 10 x 10 spheroids were successfully printed. After 14 days of culture, we showed than acini were alive and expressed phenotypic markers in accordance with the mice initial transgenic phenotype. As a function of acini concentration in the bioink, we found than we were able to vary the size of the spheroids (from single acini to 100 µm diameter). Such adjustments were helpful depending the markers we tried to obverse (specified to one acini or to the population).

CONCLUSION

We have explored the potential of the laser assisted bioprinting to generate cell spheroids encapsulated in methacrylated gelatine. The methodology we have established enable us to deposit the spheroids in a controlled way and with a diameter size varying between a few tens of micrometres to 100 µm. We show than we were able to control the cell maturation over time. We make a proof of concept with HUVECs, by printing pre-microvascularized structures with high spatial resolution and on murine primary acini from exocrine pancreas for cancer and toxicology models.

REFERENCES

1. Guillemot F *et al.*, Acta Biomaterialia 6, 2494–2500, 2010
2. Koch L. *et al.*, Biofabrication 10 035005, 2018
3. Hakobyan D. *et al.,* Biofabrication 12 035001, 2020

Hyaluronan-Collagen Composite Bioink for the Printing of Nucleus Pulposus-Like Structures

Gregor Miklosic[1,2*], Stéphanie De Oliveira[3], Sébastien Grastilleur[4], Christophe Hélary[3], Stephen J. Ferguson[2], Matteo D'Este[1]

[1]AO Research Institute Davos, Davos, Switzerland
[2]Institute for Biomechanics, ETH Zürich, Zürich, Switzerland
[3]Sorbonne Université, CNRS, UMR 7574, Laboratoire de Chimie de la Matière Condensée de Paris, Paris, France
[4]Inserm, UMR 1229, RMeS, Regenerative Medicine and Skeleton, Université de Nantes, ONIRIS, Nantes, France
[*] gregor.miklosic@aofoundation.org

INTRODUCTION

Despite its high prevalence, debilitating effect on patients, and significant financial burden on the healthcare system, intervertebral disc (IVD) degeneration is still insufficiently understood and treated. This is in part due to the lack of adequate models. In vitro models are oversimplistic, whereas animal models display important biological, compositional, and biochemical interspecies differences. Bioprinting, offering precise and reproducible control over the cell microenvironment, is a promising avenue towards the fabrication of superior three-dimensional in vitro models, capable of reproducing the disc's heterogeneous composition, structure, and mechanical response. As a step towards a full IVD model, we developed a bioink suitable for the fabrication of structures resembling the gel-like nucleus pulposus (NP) in its center.

EXPERIMENTAL METHODS

A tyramine derivative of hyaluronic acid (THA, 30 mg/ml) was combined with type I collagen (20 mg/ml) to form a composite capable of gelation via pH increase, enzymatic oxidation, and visible-light crosslinking. A homogeneous extrudable gel was obtained via shear-induced fragmentation of collagen as it undergoes pH-change triggered fibrillogenesis, followed by enzymatic gelation of the THA with hydrogen peroxide (3.5 ppm) and horseradish peroxidase (0.1 U/ml). Further strengthening of the gel was achieved upon exposure to green light in the presence of photoinitiator eosin Y (0.2 mg/ml). Gelation, elastic recovery, as well as the shear-, strain-, and shear rate-dependent responses were studied rheologically. Response to compression was evaluated with an incremental stress-relaxation test. Lattice-based structures were printed as a proof of concept. Cell compatibility was assessed via embedding of bovine nucleus pulposus cells in cast gels.

RESULTS AND DISCUSSION

We observed good bioink extrudability prior to light crosslinking, and a peak storage modulus of 4.6 kPa after exposure to green light (Figure 1A & 2A). Flow was observed under high strains, followed by recovery of elasticity when the strain was decreased (Figure 1B). Shear thinning of the material was also confirmed (Figure 1C). In equilibrium under compression, the light crosslinked gels exhibited a 5.3 kPa linear-region modulus (Figure 1D). Embedded NP cells demonstrated good viability and proliferation up to day 5 of culture (Figure 2B).

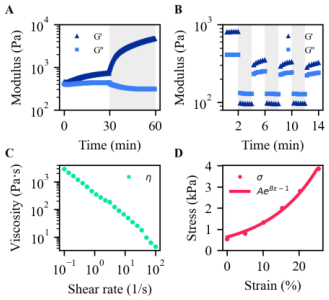

Figure 1: Shear and compressive properties of the bioink after enzymatic (A, B, C) and light (A, D) crosslinking. A) Oscillatory time sweep in shear, showing material gelation, with light exposure period shaded. B) Cyclic intervals of 0.1% / 300% (shaded) oscillatory shear strains. C) Rotational shear rate sweep. D) Equilibrium compressive stress under progressively increasing strains, fit to an exponential model.

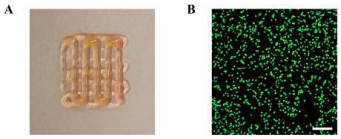

Figure 2: A) 2-layer lattice extruded with a 25G needle. B) Bovine NP cells in cast gels at 5 x 10^6 cells/ml, demonstrating proliferation and good viability at day 5. Stained with calcein AM (green, live) and ethidium homodimer-1 (red, dead).

CONCLUSION

We present a bioink with rheological and compressive properties within the range of healthy human NP. To our knowledge, this is also the first bioink simultaneously composed of biochemically suitable components representative of native NP, and approaching the high concentrations observed in tissue. This work brings us a step closer to better, reproducible, and representative 3D printed IVD models, and the promise of new insights into the treatment of disc degeneration.

ACKNOWLEDGMENTS

Conducted within the scope of the INDEED project, funded by the Swiss National Science Foundation (189310) and French National Research Agency (ANR-19-CE06-0028).

3D Bioprinted Prevascularised Oral Soft Connective Tissue Substitutes for Gingival Tissue Engineering

Rawen Smirani[1*], Chantal Médina[2], Hugo Oliveira[2], Adrien Naveau[1]

[1]Univ. Bordeaux, INSERM, Laboratoire Bioingénierie Tissulaire (BioTis), U1026, CHU Bordeaux, Bordeaux, France
[2] Univ. Bordeaux, INSERM, ART BioPrint, Laboratoire Bioingénierie Tissulaire (BioTis), U1026, Bordeaux, France

[*]rawen.smirani@u-bordeaux.fr

INTRODUCTION

Despite an efficient regenerative potential, gingival tissue loss is frequent and needs a surgical increase of tissue quantity and/or quality[1]. Autologous graft is the gold standard but possesses three disadvantages : morbidity and limited quantity of tissue among the donor site and a slow vascular connection of the graft to the recipient site. 3D bioprinting is a promising tissue engineering technique because it enables precise cell positioning and large-scale production. Moreover, it could address the critical issue of graft vascularisation as initial survival of large tissue substitutes depends on the quick development of adequate blood supply[2-3]. The aim of this research was to produce a gingival connective tissue substitute that contains pre-vascularisation, using extrusion-based bioprinting (EBB) and which was validated *in vitro* and *in vivo*.

EXPERIMENTAL METHODS

The model contained: cells that were human gingival fibroblasts (hGF) from explant primary cultures and human umbilical vein endothelial cells (HUVEC); a composite hydrogel made of collagen and hyaluronic acid methacrylates (HAMA/CollMA)[4] to get the closest to native gingival extracellular matrix while permitting cell printing and viability; and no bioactive molecule in addition to those in culture media. The 3D Discovery micro-extrusion bioprinter (RegenHU) was used. Bioprinted substitutes were cultivated in vitro during at least 28 days without bioreactor. Cell viability, activity, characterisation (flow cytometry and immunocytochemistry) and preformed vessels quantification were performed. *In vivo* validation was performed on nude athymic mice with a subcutaneous implantation in the dorsal area of either a 14 day-precultured and prevascularised substitute (test group) or a 14 day-precultured substitute without prevascularisation (control group). Vessel quantification was performed at 7 and 14 days post-implantation.

RESULTS AND DISCUSSION

The development of hGF/HUVEC cocultures allowed to discover unusual properties of some fibroblasts which displayed a perivascular cell behaviour[5]. This made possible the organisation and stabilisation of the pseudo-vessel networks *in vitro* for at least 30 days. High cell viability following bioprinting was observed and pseudo-vessel networks interconnection increased throughout time in vitro, showing high vessel stability without bioreactor. *In vivo* experiments aimed at evaluating the vascularisation capacity and functionality of the performed pseudo-vessels by lumen formation and successful connection to the host murine vasculature.

CONCLUSION

Connective substitutes containing a pre-vessel network that remains throughout time without bioreactor were obtained using EBB. The study findings validate a faster and more efficient connection to the host vasculature with the pre-vascularised 3D bioprinted substitutes. The next step could be to complexify the constructs to get closer to clinical applications.

REFERENCES

1. Global Burden of Disease Study 2016. Lancet 390, 1211, 2017.
2. Laschke, M.W. et al. Tissue Eng 12, 2093, 2006.
3. Novosel, E.C. et al. Adv Drug Deliv Rev 63, 300, 2011.
4. Oliveira H. et al. Bioprinting 22, e00134, 2021.
5. Smirani R. et al. Tissue Eng Regen Med, 2022.

CONCEPTION OF PHOTOPOLYMERISABLE, DEGRADABLE AND BIOACTIVE POLYMERIC INK FOR MENISCUS REGENERATION

Mathilde MASSONIE[1], Coline PINESE[1], Benjamin NOTTELET[1], Matthieu SIMON[2], Gilles SUBRA[3] and Xavier GARRIC[1]

[1] Department of Polymers for Health and Biomaterials, IBMM UMR 5247, University of Montpellier, CNRS, ENSCM, Montpellier, France
[2] Bio-impression platform CARTIGEN, IRMB, CHU of Montpellier, Montpellier, France
[3] Department of Amino Acid, Peptides and Proteins, IBMM UMR 5810, University of Montpellier, CNRS, ENSCM, Montpellier, France

INTRODUCTION

Nowadays, 3D printing techniques are giving rise to new processing strategies. Photopolymerisation offers new advances with high-definition techniques like 2 photon polymerisation (2PP), which allows photo-triggered crosslink with micro to nanometric resolution. CAD-customized implants are plebiscited for repairing complex default especially for physiogically microstrutured tissues like meniscus. However, for this tissue a good balance with both mechanical and bioactive properties need to be found. Indeed, if various polymeric inks exist, very few of them has shown good tissue regeneration and physiological shear/compression resistance properties. Therefore, in this project we have developed biocompatible and degradable inks designed to closely match physiological properties to meet clinical requirements. The objective of this project is to synthesize and functionalize photocrosslinkable macromolecules using tyramine a biocompatible photocrosslinker. We synthesized different Tyramine-star-PLA in order to modulate the mechanical properties of printed matrix. Tyramine-Gelatin was also used in the composition of the ink to improve cell adhesion and proliferation properties. The composite ink was printable in 2PP[1] and offers an excellent compromise between mechanical and biological properties or highly resolving matrixes.

EXPERIMENTAL METHODS

Poly (D,L-lactic acid) was synthetized using ring opening polymerisation using various initiator such as pentaerythritol, dipentaerythritol tripentaerythritol initiator to obtain 4-, 6- and 8-arms-PLA respectively. The molar ratio Initiator/ Monomer have been fixed to 5,55 10^{-1}. Thereafter, chain extremities of polymers were functionalised with tyramine, using hydroxyl activation with nitro-phenyl chloroformate [2] to obtain Tyr- 4-, 6- and 8-arms-PLA.

On the other hand, we functionalized gelatin with tyramine [3] (Tyr-Gelatin) using EDC/NHS carboxyl activation and then added it directly in the polymeric ink in DMSO at the ratio (m/m, gelatin/ polymer): 0, 10, 25, 50, 75, 100. After irradiation (525nm), inks were characterised through gel fraction, degradation, mechanical and biological tests (cytocompatibility, chondrocyte adhesion and proliferation). Finally, we used 2-photon superresolutive impression to create microstructures and we characterized these with SEM, fluorescence confocal microscopy and AFM.

RESULTS AND DISCUSSION

The synthesis step led to star-PLA with arm's length of 6 800, 5 000 and 4 000 $g.mol^{-1}$ of PLA for 4-, 6- and 8-arms -PLA respectively.

Then, functionalization with tyramine resulted in Tyr- 4-, 6- and 8-arms-PLA with functionalisation rates of 55%, 65% and 75% respectively.

The ink was prepared and directly photocrosslinked at 525 nm. Afterward, gel fraction of the crosslinked materials increased with the number of arms with 10%, 50% and 70% of gel fraction for film composed of Tyr-4-, 6- and 8-arms-PLA respectively. This suggests the higher the number of functionalities, the more crosslinking occurred. This is directly corelated to the mechanical properties that showed higher Young Modulus for Tyr-6- and 8-arms-PLA (250-300MPa) compared to Tyr-4 arm-PLA (150 MPa).

In order to improve the biological properties of the ink, we added Tyr-Gelatin at different ratio. The presence of gelatin significantly improved the cross-linking quality of the ink (gel fraction increased from 60% to 70% with gelatin-10%) and the adhesion and proliferation of chondrocytes on the printed matrix. However, mechanical properties were decreased with the increase of gelatin content.

Finally, 2PP polymerization with the composite ink led to highly resolutive object which structures were preserved after solvent removal. The 3D printed scaffolds were non-cytotoxic.

CONCLUSION

Finally, we have conceived a degradable, biocompatible polymeric PLA-gelatin ink which was successfully photo-crosslinked with visible light (525 nm) thanks to tyramine crosslinking. Super resolutive printing allows to form microstructured objects which address directly to cell scale. The modular character of the ink (modifiable composition) and the highly resolving printing allow the creation of cartilage regeneration matrices with very high potential.

REFERENCES

1 Loebel C. *et al.,* Biomacromolecules,16,2624-2630 2015
2 Park *K.M.et al.*, J. Mater. Chem, 21,13180, 2011
3 Li Z. *et al.*, Acta Biomater., 13 :88-100, 2015

Highly Concentrated Collagen for 3D Bioprinting of Stable Structures

Milena Savioli Lopes[1*], Josefin Blell[1], Volodymyr Kuzmenko[1], Itedale Namro Redwan[1]

[1] CELLINK Bioprinting AB, Gothenburg, Sweden
[*]msl@cellink.com

INTRODUCTION

It has proven difficult to 3D print complex structures using collagen due to its low viscosity and lack of biomechanical stability[1]. Therefore, to facilitate the use of collagen in bioprinting native-like tissue models, one can increase the collagen concentration to ensure its structural stability post-printing[2]. In this study, we present two versions of collagen-based ready-to-print bioinks from Advanced BioMatrix: Lifeink 200 and Lifeink 220 with high collagen concentrations of 35 mg/mL and 70 mg/mL, respectively. Both bioinks showed excellent printability and cell affinity as immortalized renal proximal tubule epithelial cells (RPTECs) were able to easily stretch, migrate and form extensive cell networks during 14 days of culture.

EXPERIMENTAL METHODS

Lifeink 200 and Lifeink 220 were printed using CELLINK's BIO X bioprinter with a controlled printhead temperature set at 8°C. In addition, the collagen bioinks were mixed with RPTECs to demonstrate the collagen's ability to enhance soft-tissue growth.

RESULTS AND DISCUSSION

Figure 1 illustrates the printability of collagen bioinks using BIO X bioprinter equipped with the Temperature-controlled Printhead. Lifeink 200 was printed with 3 layers (Figure 1A) and Lifeink 220 with 13 layers of height equaling 5 mm (Figure 1B). Based on the results, Lifeink 200 can be used as a bioink for creating softer structures, while Lifeink 220 represents an excellent bioink for more complicated and precise constructs. We observed high printing fidelity of both ready-to-print bioinks and no signs of clogging during the printing process.

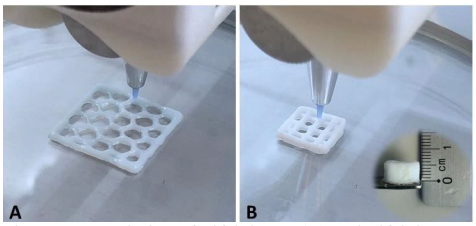

Figure 1. 3D printing of Lifeink 200 (A) and Lifeink 220 (B) using CELLINK´s BIO X bioprinter.

For the bioprinted RPTECs, there was a clear cell stretching in all directions at day 7 and day 14 in both bioinks (Figure 2A). The similarity between both bioinks in terms of cell behavior indicates that neither hinder the growth nor the movement of the RPTECs. Being evenly distributed in collagen bioink before printing, the cells were able to migrate to the borders of the constructs, also lining the natural voids inside as shown in immunohistochemistry (IHC) images (Figure 2B).

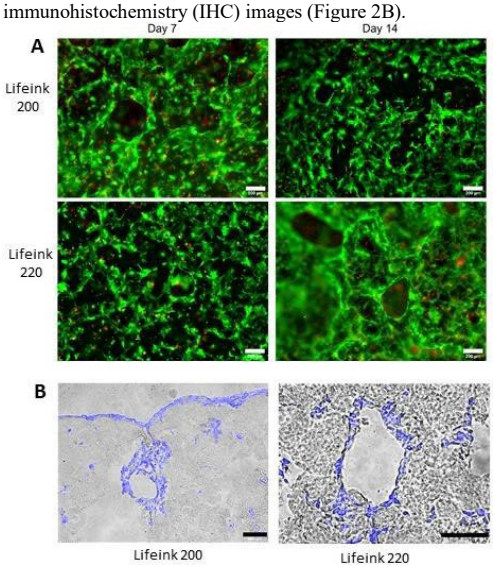

Figure 2. Morphology of bioprinted RPTECs in collagen bioinks. A) Representative images of the bioprinted cells stained with calcein AM and propidium iodide. Scale bars = 200 µm. B) Representative images of the printed constructs stained with DAPI (blue) merged with bright field (gray) after IHC, day 14. Scale bars = 100 µm.

CONCLUSION

We present two versions of highly concentrated ready-to-print collagen bioinks from Advanced BioMatrix. Lifeink 200, can be used for printing soft tissue constructs of a few layers height, while Lifeink 220, can be used for printing multi-layered complex constructs with slightly stiffer texture. We also 3D bioprinted both bioinks with immortalized RPTECs. We could detect cell stretching and cell network formation, as well as high cell migratory ability in the collagens. This work highlights the possibility of bioprinting stable structures using collagens that would enable different cell types to remodel and move through the matrix, allowing for the fabrication of native-like soft tissue models.

REFERENCES

1. Hospodiuk M. et al., Biotechnol Adv. 2:217-239. 2017
2. Rhee S. et al., ACS Biomater Sci Eng. 10:1800-1805. 2016

Newly Polydopamine Guanosine-derived supramolecular hydrogels to improve stability and viscosity properties in 3D printed scaffolds for soft tissue regeneration

Maria Merino-Gómez*[1,2], María Godoy-Gallardo[1,2], Román A. Perez[1,2]

[1]Bioengineering Institute of Technology (BIT), Universitat Internacional de Catalunya (UIC), Sant Cugat del Vallès, Spain
[2]Basic Science Department, Faculty of Medicine and Health Sciences, Universitat Internacional de Catalunya (UIC), Sant Cugat del Vallès, Spain
* mmerino@uic.es

INTRODUCTION

Currently, when soft tissue is damaged, gold standard treatments involves patient grafting although it can be problematic either due to lack of tissue, increased risk of infection or the need of several surgeries. To overcome these disadvantages, tissue engineering has gain special attention as an alternative treatment in addition to 3D printing as it can provide strict control of geometry and porosity. Among the different synthetic materials, guanosine (G) can form planar G-quartet structures able to build 3D nanofibrous G-quadruplex (G4) where addition of K^+ ions are able to stabilize the structure and produce G4-hydrogels. However, only a small number of successful systems based on G4-hydrogels have been reported to date because their use as an ink in 3D printing is limited due to lack of long-term stability[1,2]. We hypothesize that addition of polydopamine (PDA) into the hydrogel obtained by self-polymerization of dopamine (DA) will result in hydrogels both with enhance life-time stability and viscosity properties of our previous G4-hydrogels as PDA has an extraordinary adhesive ability able to form coatings on all types of materials[3]. Moreover, PDA enhances cell adhesion and proliferation of various cell types, which might provide the hydrogel better osteogenic properties and angiogenesis.

EXPERIMENTAL METHODS

For PDA G4-hydrogel formation previously synthesized G4-hydrogels based in G, boric acid, and potassium hydroxide were mixed with DA (0.01 - 0.05 mmol) at 80 °C for 30 minutes and cooled down for gelation. PDA standard curve by fluorescence was evaluated to determine the amount formed into the hydrogel. Printability properties were studied by semi-quantitative filament fusion and collapse test. Additionally, degradability in complete medium and an indirect cell viability assay in rMSCs of different dilutions of the medium was analyzed at 24h. Nanofibrillar structure and mechanical properties were then evaluated by scanning electron microscopy and rheology assays respectively to compare it with control G4-hydrogels. Cell morphology and viability was also assessed at 24h of rMSC seeded onto the printed PDA G4-hydrogels using confocal laser scanning microscopy and live-cell mapping.

RESULTS AND DISCUSSION

We synthesized newly PDA G4-hydrogels, where PDA concentration inside the hydrogels was determined through fluorescence. Hydrogels with 0.02 mmol DA showed better printability results with more define filaments, although all concentrations had good printability properties. Importantly, while all tested PDA G4-hydrogels showed cell viability of ~80% after 24h in the indirect cell viability assay only those with 0.01 and 0.02 mmol of DA were stable for up to 7 days where hydrogel filaments were more differentiated in contrast with G4-hydrogels. SEM analysis revealed nanofibrillar structures in the hydrogel networks of 0.02 mmol DA G4-hydrogel, evident of successful G4-quadruplex formation, and rheological testing confirmed good thixotropic properties. Finally, a cell viability of ~80% after 24 hours was determined for rMSCs seeded onto the 0.02 mmol PDA G4-printed hydrogels.

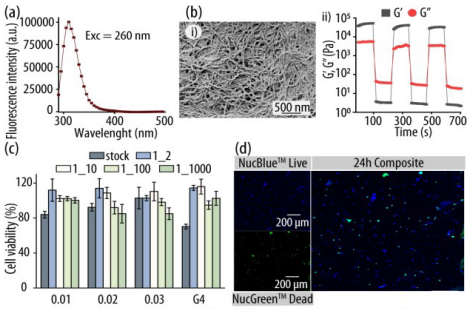

(a)Fluorescence scan of polydopa (b) i)Nanofibrillar structure of PDA G4-hydrogel taken by scanning electron microscope ii)Dynamic step-strain sweep test experiment of PDA G4-hydrogel. Black and red indicate storage modulus (G') and loss modulus (G") respectively (c)Indirect cell viability assay in rMSCs at 24h of different dilutions of the medium with different PDA concentrations. (d)Fluorescence microscopic images showing cell viability assay of rMSC into PDA G4-hydrogels.

CONCLUSION

We developed a novel printable hydrogel based on PDA G4-hydrogel. Those made with 0.02 mmol DA showed good printability and thixotropic properties and its structure was more stable than control G4-hydrogels, while no cytotoxicity was observed. Thus, this PDA G4-hydrogel formulation represents an excellent candidate to have an effect in osteogenic differentiation of MSCs and the maturation of osteoclasts.

REFERENCES

1. Biswas A. *et al.*, Chem. Commun. 54:1778-178, 2018
2. Plank. T.N. *et al.,* Chem. Commun. 52:5037-40, 2016
3. Godoy-Gallardo, M. *et al.,* Int. J. Mol. Sci. 21:6418, 2020

ACKNOWLEDGMENTS

"This study was supported by the Government of Catalonia (2017 SGR 708), the Spanish Ministry by Ramón y Cajal fellowship (RYC2018-025977-I) and predoctoral fellowship from UIC".

Production of Cartilaginous Substitutes using 3D Bioprinting and Development of Innovative Adapted Bioinks.

Océane Messaoudi[1#], Christel Henrionnet[1#], Laurent Grossin[1], Pierre Gillet[1,4], Didier Mainard[1,2], Laurent Galois[1,2], Damien Loeuille[1,3], Christophe Marquette[5], Astrid Pinzano[1]*
# equal contribution
[1] UMR 7365 CNRS-UL, IMoPA, Vandœuvre-Lès-Nancy, France
[2] Service de Chirurgie Orthopédique, Traumatologique et Arthroscopique, CHRU Nancy, Nancy, France
[3] Service de Rhumatologie, CHRU Nancy, Vandœuvre-Lès-Nancy, France
[4] Laboratoire de Pharmacologie, Toxicologie et Pharmacovigilance, CHRU Nancy, Vandœuvre-Lès-Nancy, France
[5] Platform 3D Fab, University of Lyon, CNRS, INSA, CPE-Lyon, ICBMS, UMR 5246, Villeurbanne Cedex, France
* astrid.pinzano@univ-lorraine.fr

INTRODUCTION

Currently, no therapy used in clinical practice allows the regeneration of native articular cartilage tissue. In the field of cartilage tissue engineering, the method of 3D bioprinting by bioextrusion is booming. Bioextrusion is based on the deposition of a continuous filament of bioink that can contain both biomaterials, cells and biomolecules. It turns out to be the most suitable for the production of naturally stratified tissues such as cartilage[1] . The different layers can thus be reconstructed from different bioinks and cells chosen so as to obtain a cartilage substitute close to native cartilage *in vitro*. Different compounds can be added to the bioink such as collagen, naturally present in cartilage, without changing its printing capacity. Given the limited availability of autologous chondrocytes and their rapid dedifferentiation, the most commonly used cells are mesenchymal stem cells (MSCs). They have great proliferation and differentiation capacities. In particular, they can differentiate into chondrocytes under the induction of chondrogenic factors such as TGF-β1.
The objective was to develop an innovative strategy to produce a stratified cartilage substitutes using 3D bioprinting, bone marrow MSCs (BM-MSCs) and a dedicated bioink for the treatment of focal cartilage lesions. We studied the effect of collagen enrichment in order to obtain bioinks adapted to the cartilage layers.

EXPERIMENTAL METHODS

MSCs were isolated from human bone marrow following total hip arthroplasty. Cells are then cultured until the 2nd passage, pre-differentiated at passage 3 and seeded in a dedicated bioink at a cell density of 10^6 cells/mL in order to approximate cell density observed in healthy cartilage[3]. Cartilage substitutes were produced using a bioextrusion printer and alginate / gelatin / fibrinogen bioink (size of substitutes: 1 cm in length, 1 cm in width, and 4 mm in thickness). Chondrogenesis was induced by adding TGF-β1 (10 ng/mL) to the culture medium for 28 and 56 days. The safety of the printing process was evaluated by the mitochondrial activity assay (MTT test). The chondrogenic properties of MSCs and the quality of the extracellular matrix were evaluated by analysis of gene expression, histology and immunohistochemistry. We then studied the effect of adding different amounts of type I collagen to the bioink (0, 0.5, 1 and 5 mg/syringe of bioink) on the chondrogenic differentiation capacities of MSCs.

RESULTS AND DISCUSSION

The mitochondrial activity measurement results show no cellular toxicity of the bioprinting process over the long term with maintenance of the substitutes structure. The gene expression analysis showed that the chondrogenic markers (*COL2A1, SOX9, ACAN, COMP*) are significantly more expressed with TGF-ß1, associated with a significant synthesis of proteoglycans and type II collagen.
Secondly, we showed that a small amount of type I collagen (0.5 and 1 mg) induced a beneficial effect on the chondrogenesis of BM-MSCs induced by TGF-ß1 resulting in increase in chondrogenic markers associated with a decrease in the expression of osteogenic markers. Moreover, with a low amount of collagen, the synthesized extracellular matrix is richer in type II collagen after 56 days of culture. Conversely, the enrichment of the bioink with the highest amount of type I collagen (5 mg) causes an increase in hypertrophic markers and a decrease in the synthesis of matrix constituents associated with an increase in the rate of calcifications within the substitutes.

CONCLUSION

The present study demonstrated a promising approach for cartilage engineering using 3D bioprinting. Our innovative bioink combining alginate, gelatin, and fibrinogen allows the generation of cartilaginous substitutes. First, we reproduced the structure of the chondral intermediate zone, with round cells in abundant ECM. Then, we showed that the low concentration of type I collagen as an additive was attractive for the production of the upper cartilage layers, whereas the higher concentration of 5 mg might be more suitable for the calcified cartilage layer.

REFERENCES

1. Fricain J.-C. *et al.* Med Sci. 52–59, 2017
2. Tricomi B.J.*et a*l, Ann. N. Y. Acad. Sci. 115–124, 2016
3. Henrionnet C. *et al.* Stem Cells International, 2020

ACKNOWLEDGMENTS

This work was supported by “Direction Générale des Armées (DGA), Grant/Award Number: ANR-16-ASTR-0021”; “Fondation de l’Avenir pour la Recherche Médicale Appliquée, Grant/Award Number: AP-RM-16-042”; and “Université de Lorraine - Région Alsace-Champagne-Ardennes-Lorraine 2016, Grant/Award Number: AAP-002-037. A Ph.D. scholarship has been granted by the Fondation pour la Recherche Médicale (FRM).

Production of Multifunctional Wound Dressings by using Newly Developed Antibacterial, Antioxidant, and Anti-inflammatory Biomaterial Ink for Wound Healing Applications

Irem Unalan[1], Aldo R. Boccaccini[1]

[1]Institute of Biomaterials, Friedrich-Alexander-Universität Erlangen-Nürnberg, 91058 Erlangen, Germany

* irem.unalan@fau.de

INTRODUCTION

In recent years, the three-dimensional (3D) printing method using extrusion technology has emerged as a convenient, versatile, and affordable technique for fabricating 3D-printed hydrogel [1,2]. Due to their highly hydrated microenvironment, printability, mechanical behavior, and similarity to native ECM, these hydrogels are increasingly in demand as wound dressings [3]. However, biological properties, including antibacterial, antioxidant, anti-inflammatory, and cell affinity qualities, need to be improved for wound healing applications. Essential oils (EOs) which are plant-derived compounds, particularly clove (CLV), have been investigated for wound healing applications due to their multifunctional properties such as antibacterial, antioxidant, and anti-inflammatory activity [4]. This study aimed to develop natural phytotherapeutic agents-based innovative strategies to fabricate multifunctional 3D-printed hydrogels in wound healing approaches.

EXPERIMENTAL METHODS

The current work focused on improving poor structural integrity and stability properties of sodium alginate (ALG) using the thickeners, and stabilizers properties of the xanthan gum (XAN), while minimizing bacterial infections and oxidative stress by incorporating CLV as a natural phytotherapeutic agent. For this approach, CLV-incorporated ALG-XAN 3D-printed hydrogels were fabricated by using three axes moveable bioplotter (type BioScaffolder 3.1, GeSIM, Großerkmannsdorf, Germany) via the "ScaffoldGenerator" software of the bioplotter.

RESULTS AND DISCUSSION

The results showed that blending ALG with XAN increased the viscosity of the inks and additionally enhanced the printability and shape fidelity of the ALG biomaterial ink, which was also confirmed by filament fusion and filament collapse assays. SEM was used to analyze the surface morphology, and the results illustrated that the addition of CLV did not influence the morphology of the 3D-printed hydrogels. The functional groups and total phenolic (TP) content of 3D-printed hydrogels were confirmed by ATR-FTIR analysis and TP content assay, respectively. Moreover, the release results indicated that the ALG-XAN 3D-printed hydrogels are potential drug carriers due to the 28 -days sustainable releasing profile of CLV. On the other hand, antioxidant activity in terms of DPPH free radical scavenging activity assay indicated that incorporating CLV enhanced the antioxidant property of ALG-XAN 3D-printed hydrogels. The antibacterial activity of the 3D-printed hydrogels was tested with *S. aureus* and *E. coli* bacteria. The results demonstrated that CLV- incorporated 3D-printed hydrogels declined the bacterial growth of both bacteria type. Additionally, the *in vitro* cytotoxicity results showed that the incorporation of CLV has no toxic effect on normal human dermal fibroblast (NHDF) cells. Lastly, the anti-inflammatory properties of the CLV-incorporated 3D-printed hydrogels were investigated using Raw 264.7 macrophage-like cells and confirmed by Nitrite/Nitrate colorimetric kit.

CONCLUSION

In conclusion, incorporating CLV into ALG-XAN 3D printed hydrogels can serve as competitive multifunctional wound dressings in wound healing applications, including treatment of wound infections and oxidative stress, as well as improving cell-material interaction.

REFERENCES

1. Paxton N. *et al.*, Biofabrication. 2017. doi:10.1088/1758-5090/aa8dd8
2. Ribeiro A. *et al.,* Biofabrication. 2018. doi:10.1088/1758-5090/aa90e2
3. Koehler J. *et al.,* Eur Polym J. 2018. doi:10.1016/j.eurpolymj.2017.12.046
4. Unalan I. *et al.,* Curr Opin Biomed Eng. 2021. doi:10.1016/j.cobme.2021.100261

ACKNOWLEDGMENTS

"The authors would like to thank the Deutscher Akademischer Austauschdienst (DAAD) [Research Grants—Doctoral Programs, Section ST21, 91652927] for providing partially financial support to this project".

How structural microheterogeneities control bioink macroelasticity, printing quality and cell viability

Bruna R. Maciel[1*], Alisa Grimm[2], Sonja Haase[2], Xenia Kempter[2], Ute Schepers[2], Claude Oelschlaeger[1], Norbert Willenbacher[1]

[1] Institute of Mechanical Process Engineering and Mechanics, Karlsruhe Institute of Technology (KIT), Karlsruhe, Germany
[2]Institute of Functional Interfaces, Karlsruhe Institute of Technology (KIT), Karlsruhe, Germany
[*] bruna.maciel@kit.edu

INTRODUCTION

Bioink rheological properties, including bulk elasticity, yield stress and shear-thinning, have to be considered for successful 3D bioprinting[1,2], as they can all affect the printing quality and cell viability. Here we investigated an aspect present in biological tissues which has hardly been considered so far, namely the impact of bioink microstructural and micromechechanical heterogeneities on printing process, particularly cell viability, resolution and shape fidelity of the printed construct. Experiments with different bioink systems demonstrate that the presence of microstructural heterogeneities strongly controls the hydrogel bulk elasticity and yield stress as well as printing quality. This allows for establishing a correlation between microscopic structural features, macroscopic flow properties and the printing process.

EXPERIMENTAL METHODS

Bioinks of different composition have been investigated: alginate (pre-) crosslinked with calcium salts, mixtures of gelatine/PVA and gelatine/nanosilicate clay (Laponite). Classical rotational rheometry has been used to characterize macromechanical properties, namely the elastic plateau modulus G_0 and the yield stress. Multiple particle tracking (MPT) based microrheology[3] has been used to characterize structural micromechanical properties. The bioinks were printed with an extrusion based 3D printer without cells for printability evaluation and with HepG2 cells for cell viability analysis.

RESULTS AND DISCUSSION

Pure gelatin gels show a homogeneous microstructure independent of the solvent used (water or DMEM). In contrast, for (pre-) crosslinked gels and mixtures, MPT measurements reveal a heterogeneous structure on the µm-scale with formation of viscous inclusions within a highly elastic matrix in both water and in cell culture medium. Viscosity, size and spatial distribution of these inclusions have been characterized. Additionally, we observed that gels with the higher degree of heterogeneity exhibit a higher macro elasticity which contributes with layer stacking property of 3D printed constructs. However, excessively large micro heterogeneities often reveal a negative impact in the hydrogel yield stress and therefore in the printed line width. The bioinks have been 3D-printed and a correlation between micro heterogeneities and printing quality of multi-layered constructs has been established. Finally, an analysis of the impact of different crosslinking densities spatially varying in the hydrogel on the viability of HepG2 cells has been conducted. Viability analysis suggests that structural microheterogeneities protect cells from shear stress while printing.

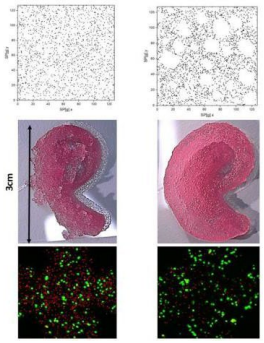

Figure 1 – Microstructural heterogeneities, 3D printing quality and cell viability assay for gelatin/PVA bioinks

CONCLUSION

Experiments suggested that bulk rheological properties such as elasticity and yield stress as well as printing quality were affected by the microstructural heterogeneities. These results will help to better understand the relationship between the bioink´s microstructure before printing and cell viability after printing, as well as feature size and shape fidelity of 3D printed objects.

REFERENCES

1. Maciel B. R. *et al*. Chem. Ing. Tech. 94:1-10, 2022
2. Lee J. *et al*., Biofabrication. 12:035018, 2020
3. Hafner J. *et al*., Acta Biomaterialia 111:254-266, 2020

Aqueous Two-Phase Enabled Low Viscosity 3D (LoV3D) Bioprinting of Living Matter

Malin Becker[1], Jeroen Leijten[1]
[1] Leijten Lab, Dept. of Developmental BioEngineering, TechMed Centre, University of Twente, Enschede, The Netherlands
Contact of presenting author: m.l.becker@utwente.nl

INTRODUCTION

Embedded bioprinting is a promising additive manufacturing technique that permits the fabrication of large-scale, freeform, complex 3D tissue constructs. During the development of new (bio)inks, the shape-stability of extruded strands plays a major role. To stabilize the strand after extrusion, while allowing for smooth extrusion with limited pressures, shear thinning inks are commonly employed. For these inks, the printing resolution is dictated by nozzle diameter[1], while shear stresses within the nozzle during extrusion determine cell viability[2], which thus limits bioprinting resolution and speed. Here, we report on a low viscosity 3D (LoV3D) liquid printing approach, which is enabled by the innovative use of an aqueous-two phase system (ATPS). LoV3D allows for the highly rapid bioprinting with high cell viability, while allowing for continuous on-the-fly tuning of filament diameter, which ranges from millimetric down to single cell resolution using a single nozzle in a nozzle-diameter independent manner.

EXPERIMENTAL METHODS

Alginate was functionalized with tyramine (TA) groups via DMTMM coupling to form a photo crosslinkable embedding bath. For 3D printing of several inks, a Cellink Inkredible+ printer was combined with a syringe pump to allow for printing at set speeds and extrusion rates. Various mammalian cell types including 3T3 mouse fibroblasts were used to investigate LoV3D's cytocompatibility.

RESULTS AND DISCUSSION

The suitability of a variety of established (bio)polymer solutions for loV3D printing was confirmed and Dex-TA/PEG as well as Alginate-TA/PEG were chosen as model systems. The formation of a stable ATPS interface was substantiated by establishing the binodal curves of these systems. The use of low viscous solutions allowed for strand elongation (thinning) with increased printing speeds (Figure 1a). Comparing reported print diameters in literature for various nozzle sizes, we determined that LoV3D printing offers a substantially higher resolution printing regime, which can be equally accessed with all tested nozzle diameters (Figure 1b). The unique thinning of printed low viscosity strands was utilized to create prints with diameters ranging over two orders of magnitude down to single-cell resolution, all achievable with a single nozzle (Figure 2a). Conventional complex shapes such as spirals, tubes and grids could readily be created (Figure 2b,c) To investigate the influence of viscosity dependent shear stresses within the printing nozzle on cell viability, we combined simulation based data with extrusion experiments. Here, we were able to establish, that for a wide range of flow rates, low viscosity inks do not show any significant reduction of cell viability, while higher viscosity inks reduced the viability with increasing flow rates down to 50% (Figure 2d). Further, incorporation of cells within a sacrificial ink allowed for a one-step print and seed approach. Here, the liquid/liquid interface during printing facilitated additional surface modification, where covalent bonds between coating and channel wall could be formed more-effectively for ATPS liquid/liquid as compared to conventional solid/liquid interfaces.

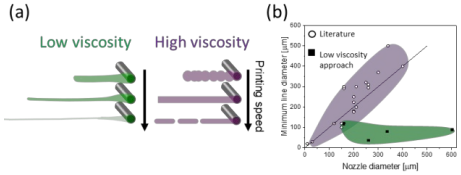

Figure 1: Filament thinning opens up a new high resolution printing regime. (a) Schematic filament shape of low and high viscosity aqueous solutions at different printing speeds and set extrusion rate. (b) Line diameters reported in literature with different nozzle sizes as compared to experimental data with low viscosity inks.

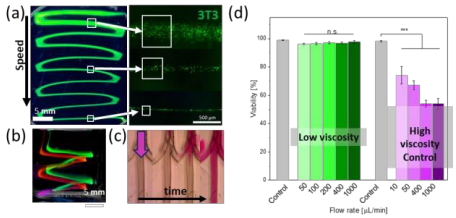

Figure 2: Low viscosity bio-inks allow for high cell viability while enabling high resolution and channel interconnection of prints. (a) Printing with increased speed thins filaments and decreases filament diameter down to single-cell resolution. (b) Multi-material 3D printing demonstrated with a printed spiral shape. (c) 3D printed perfusable branched capillary networks. (d) Cell viability after extrusion through a 25G nozzle at various flowrates.

CONCLUSION

In this study, we introduce loV3D bioprinting as a highly versatile and rapid bioprinting technique, which is inherently compatible with a wide range of biomaterials and crosslinking strategies, while offering on-the-fly tunable high resolution prints without compromising printing speed or cell viability. Future studies will focus on the cell incorporation within the channels, aiming for the creation of perfusable multiscale vascular networks.

REFERENCES

1. Jin Y. *et al*., Mater. Sci. Eng., C. 80:313-325, 2017
2. Murphy, S.V. *et al.*, Nat. Biotechnol., 8:773-785, 2014

ACKNOWLEDGMENTS

Financial support was received from the European Research Council (ERC, Starting Grant, #759425) and the Dutch Research Council (NWO, Vidi Grant, #17522).

In vitro and in vivo characterization of a novel tricalcium silicate-based ink for bone regeneration using Laser-Assisted Bioprinting

Nicolas Touya1, Mathilde Devun1, Charles Handschin1,4, Sophia Casenave1,2,3, Naïma Ahmed Omar1, Alexandra Gaubert5, Nathalie Dusserre1,4, Hugo De Oliveira1,4, Olivia Kérourédan1,2,3, Raphaël Devillard1,2-3

1INSERM, U1026 BIOTIS, University of Bordeaux, France;
2Faculty of Dentistry, University of Bordeaux, France;
3CHU de Bordeaux, Services d'Odontologie et de Santé Buccale, France ;
4ART BioPrint, INSERM U1026, Bordeaux, France;
5INSERM U1212, UMR CNRS 5320, F-33076, University of Bordeaux, France
E-mail: nicolas.touya@u-bordeaux.fr

INTRODUCTION

Grafts aside, current therapeutic solutions employed to overcome bone loss still fail to reproduce native tissue physiology. Among bioprinting strategies, Laser-Assisted Bioprinting (LAB) offers the highest resolution, allowing to design micrometric patterns in a contactless manner (1). Until now, no LAB- associated ink succeeded to provide a reproducible ad integrum bone regeneration on a murine calvaria critical size defect model (2). As a first step toward this goal, a novel approach is proposed here, using the CE approved BioRoot RCS® (essentially tricalcium silicate, zirconium oxyde and calcium chloride) as a mineral addition to a collagen1-enriched ink compatible with LAB. Already described with other models (3) and based on literature evidence, this mineralized ink (MI) was supposed to favorize cell osteogenic differentiation (4) and polarization/migration (5). Here, the Stem Cells from Apical Papilla (SCAPs) were chosen as cell model. The present study aimed to use this mineralized bioink as a new substrate to promote bone repair using in situ LAB.

EXPERIMENTAL METHODS

1- Rheological characterization

Linear Viscoelastic Region, determination of elastic (G') and viscous (G'') moduli, GelSol temperature and shear-thinning behavior of new formulation were studied

2- *In vitro* assessment

Metabolic, migration and differentiation assays were performed over SCAPs for biocompatibility and osteogenic potential.

3- *In vivo* evaluation

Mouse calvaria critical size (3mm) bilateral bone defects were created and different printing approaches were tested. After 2 months, vascularization and in situ mineralization were characterized

RESULTS AND DISCUSSION

After a few assays of printability over different substrates, 1:10 preparation (0.5g.ml-1) candidate was chosen for its consistency in pattern fidelity outcome. the SCAPs in presence of MI exhibited similar levels of resazurin reduction as control, suggesting that the formulation of MI was cytocompatible for SCAPs. Regarding migration properties, cell speed was found to be enhanced by the presence of MI. 2D cell spreading behavior was not affected by the presence of MI printed as a 'confining fence' around SCAPs, but also showed that cells were not specifically attracted to MI. From the results obtained, it is strongly hypothesized that the leachate released by the set ink homogeneously within culture supernatant triggered rise in cell motility without influencing cell mobility. The in vitro cytotoxic effect of the MI observed on HUVECs did not seem to affect the in vivo neo-vascularization process, as the vessel density found at the cicatricial tissue was equivalent to the control condition without MI. Using MI, regardless of the quantity delivered in situ in the critical size defect, did not led to a significant higher level of mineralization of the cicatricial tissue compared to control. The quantity of MI deposed to fill the entire volume of the defect (pipette deposit) was more efficient to induce tissue mineralization than LAB associated quantity of MI, suggesting a dose/effect of MI. Two MI-SCAPs associated printed patterns were studied. Although not significant regarding the number of animals tested, a large difference in the median value between the two patterns in the BVF outcome were noticed.

CONCLUSION

This study confirmed the necessity, when developing a new ink, to consider all aspects of the formulation: rheological impact, *in vitro* characterization and *in vivo* evaluation according to the aimed model. Thus, we designed an original ink formulation candidate based on BioRoot RCS®, oriented towards tissue mineralization and compatible with LAB requirements. This study suggested that, in spite of great compatibility with its associated laser bioprinter, a potential for bone tissue engineering supported by literature evidence, with the ability to deliver in situ microliters or nanoliters of active compounds thanks to Laser-Assisted Bioprinting, this ink formulation was not successful to demonstrate a strong regenerative potential in a mouse calvaria critical defect model. *In vivo* results illustrated hurdles that have to be overcome to conciliate mechanical and biological objectives. Standardized protocols and models, at each level of development (*in vitro* and *in vivo*), could be defined to allow comparison regardless biofabrication approaches used. However, the results obtained here strengthened the ink development approach, and helped to assess multiple hypothesis. Further studies shall focus on improving the ink by adjusting its formulation

REFERENCES

(1) Kérourédan O. *et al.*, Biofabrication 11, 2019
(2) Keriquel V. *et al.*, Sci Rep 7, 2017
(3) Siboni F. *et al.*, International endodontic journal 50, 2017
(4) Yongjuan C. *et al.*, PloS one 10, 2015
(5) Aspenström P., (BBA) Molecular Cell Research 1742, 2004

ACKNOWLEDGMENTS

We thank Dr. H. Boeuf (Inserm U1026 Biotis) for the generous gifts of UBx-SCAP cells (N1, N2, N3 and N4). The authors also thank Dr. S. Al-Bourgol (Alphanov), his team and Alphanov facility for hosting the SEM/EDS experiments with their TECSAN device.
This work was supported by grants from « Fondation des Gueules Cassées », Paris – France, « Fondation de l'Avenir », Paris – France, « Institut Français pour la Recherche Odontologique », and « Société Odontologique de Paris » (Bourse Michel Degrange).

Eliminating the Trade-Off between Printability and Biomimicry in 3D Bioprinting

Rachel C. Irlam[1*], Gema Dura[2], Jeremy H. Lakey[3], Helen Waller[3], Ana Marina Ferreira[4] and David A. Fulton[1]

[1] Chemistry, Newcastle University, Newcastle-Upon-Tyne, UK
[2] Departamento de Química Inorgánica, UCLM, Spain
[3] Biosciences Institute, Newcastle University, Newcastle-Upon-Tyne, UK
[4] School of Engineering, Newcastle University, Newcastle-Upon-Tyne, UK
[*] rachel.irlam@newcastle.ac.uk

INTRODUCTION

3D bioprinting has the potential to revolutionise 21st century medicine, emerging as the approach of choice for engineering structurally complex living tissues from a patient's own cells. Realising the full potential of 3D bioprinting, however, relies upon the development of a 'bioink' that guides tissue formation or regeneration. This bioink, which consists of live cells supported within a hydrogel matrix, must display both printability and biomimicry. Current hydrogels prize printability but often possess little to no inherent biomimicry. This work aims to develop a **next-generation bioink featuring both printability and biomimicry**.

We have developed a revolutionary new hydrogel based on Capsular antigen fragment 1 (Caf1, **Fig. 1a**).[1] This a protein polymer expressed by the bacteria *Yersinia pestis* and, on account of its structural similarity to fibronectin, its hydrogels display exceptional levels of biomimicry.[2] Caf1 is amenable to mutagenesis, meaning we can also modify its structure to feature cell-adhesion motifs. Using this, we have shown that Caf1 hydrogels can successfully be used for cell culture.[3]

Herein, we aimed to encapsulate human bone marrow mesenchymal stem cells within 3D Caf1 hydrogels and demonstrate their survival and proliferation for up to 21 days. We also assessed the printability of the hydrogels and attempted to culture human stem cells on the resulting constructs.

EXPERIMENTAL METHODS

Cell culture: After expansion, human bone marrow mesenchymal stem cells were harvested and mixed with 30 mg/mL Caf1 polymer solutions ($1x10^6$ cells/mL). An equal volume of 8-Arm PEG-SG crosslinker solution (30 mg/mL) was added to the protein-cell mix and 100 µL aliquots were added to wells of a 96-well plate to gelate. Cells were monitored at different time points for viability, proliferation and differentiation.

3D bioprinting: A Rokit Invivo bioprinter was used with a 10 mL syringe, 27 gauge needle and syringe temperature of 37 °C.

RESULTS AND DISCUSSION

Using an extrusion-based bioprinter, Caf1 hydrogels could be successfully 3D printed into stable constructs of differing shapes (**Fig. 1b,c**). As well as this, stem cells could be encapsulated within 3D Caf1 hydrogel networks and were observed to survive and proliferate for up to 21 days (**Fig. 1d**).

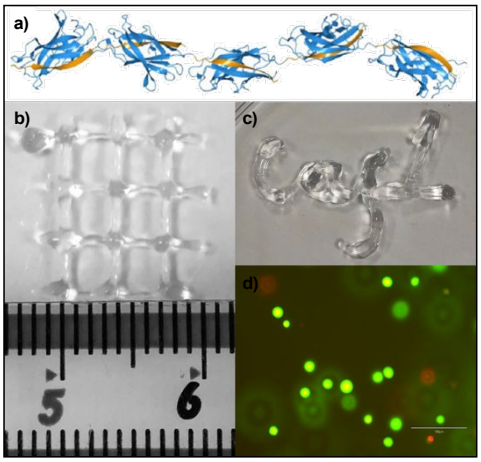

Figure 1: *a) Representation of the Caf1 structure, b) Caf1 hydrogel (3%) 3D-printed into a single-layered grid, c) 3D-printed 'Caf1' and d) live/dead assay (day 3) of cells encapsulated within a Caf1 hydrogel.*

CONCLUSION

We have developed Caf1-based hydrogels that are printable, as well as favourable for cell culture. This elimination of the trade-off between printability and biomimicry could enable generation of biological structures with unprecedented levels of sophistication.

REFERENCES

[1] Dura, G. *et al.,* Mat. Sci. Eng. C, 93: 88-95, 2018.
[2] Dura, G. *et al*., Chem, 6: 3132-3151, 2020.
[3] Dura, G. *et al.,* Biomater. Sci., 9: 2542-2552, 2021.

ACKNOWLEDGMENTS

The authors would like to thank the EPSRC for funding the research and the Bioimaging facility at Newcastle University for access to the confocal microscope.

Synthesis of aligned hollow polymeric microfibers by coaxial electrospinning for the development of 3D *in vitro* models in perfusion bioreactors

M. Mantecón-Oria[1,2,*], M.J. Rivero[1], O. Tapia[3], A. Urtiaga[1,2] and N. Diban[1,2]

[1]Departamento de Ingenierias Química y Biomolecular, Universidad de Cantabria, Santander, Spain
[2]Instituto Marqués de Valdecilla (IDIVAL), Santander, Spain
[3]Universidad Europea del Atlántico (UNEATLANTICO), Santander, Spain
[*]@manteconma@unican.es

INTRODUCTION

In recent years, there has been a growing interest in developing novel functional materials to support cell outgrowth in biomedical applications. In this regard, electrospinning techniques are presented as one of the best alternatives to generate scaffolds that mimic the extracellular matrix emulating *in vivo* microenvironment. It has been proven that the alignment of the electrospun fibers provide topographical and biophysical cues that guide cellular morphogenesis[1,2]. Moreover, highly porous electrospun mats could be easily colonized by multiple cell types to reconstruct 3D cell structures. However, non-vascularized 3D cell systems rapidly suffer nutrients (O_2) shortage.

This work proposes the incorporation of aligned hollow microfibers in a perfusion bioreactor to mimic artificial vascularization with simultaneous cellular guidance for 3D cell cultures. This study presents the tune-up and selection of the working variables to prepare biocompatible polyacrylonitrile (PAN) hollow microfibers by electrospinning with adequate alignment, and preliminary cell tests.

EXPERIMENTAL METHODS

Polymer PAN solutions in dimethylformamide (DMF) at concentrations 10, 12, and 13 wt% were prepared. PAN solutions were extruded through a single needle with a syringe pump at different flowrates within 1 to 3 mL h^{-1}, and the distance between the needle and the collector was tried from 7 to 18 cm. The speed of the rotary collector was set at 252, 435 and 1168 rpm. The morphology and diameter of the fibers were analyzed by scanning electron microscopy (SEM).

With the previously selected working conditions (12 wt% of PAN, 2.12 mL h^{-1} of flowrate, 18 cm of distance, 1168 rpm of rotation speed), coaxial electrospinning using a coaxial needle of 0.83 mm ID and 1.83 OD was performed. Polyethylene glycol (PEG) solutions in DMF at concentration of 12 and 18 wt%, and flowrates between 0.71 to 2 mL h^{-1}, were extruded in the core of the fibers. Finally, the effect of extruding the polymer solutions in horizontal or vertical mode on the hollow formation of the microfibers was also evaluated.

Culture tests using C2C12 rat myoblasts were performed and the effect of the influence of the microfiber alignment on the C2C12 myotube differentiation was analyzed.

RESULTS AND DISCUSSION

Figure 1 shows the surface and cross section of the best results of aligned hollow microfiber membranes synthetized by coaxial electrospinning attained at using a 12 wt% of PAN in the polymeric solution and 18 wt% of PEG in the core solution with a flowrate of 0.71 mL h^{-1}, 18 cm of distance, 1168 rpm of collector speed and extruding the polymer solutions in vertical mode.

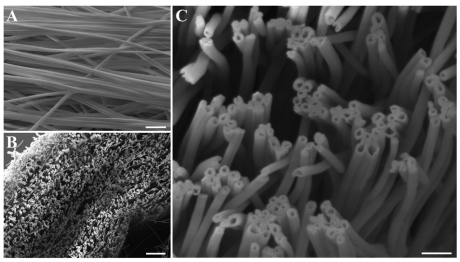

Figure 1. SEM images of aligned hollow microfiber PAN membranes: A) surface, and B, C) cross section. Scale bar: A) 10 µm, B) 50 µm, and C) 5 µm.

These working conditions allowed uniform alignment and centered hollow microfibers, with average external and internal diameters of 1.5 ± 0.1 µm and 0.6 ± 0.1 µm, respectively, and average bulk porosity of 87.3 ± 1%. The complete removal of the PEG, immersing the synthetized membranes in ultrapure water baths, was confirmed by thermogravimetric analysis.

Cell culture results showed C2C12 cells aligned with the hollow microfiber membranes and primary differentiation into myotubes.

CONCLUSION

This study presents the tune-up of different processing variables to attain aligned and centered PAN hollow microfiber membranes synthetized by coaxial electrospinning technique with potential to become 3D structural scaffolds in perfusion bioreactors.

Future work will focus on testing nutrients transport properties of these membranes and co-culture studies e.g., of neuronal and muscle cell lines.

REFERENCES

1. Y. Guo, et al. *Biochem. Biophys. Res. Commun.* **2019**, 516
2. S.-H. Park, et al. *ACS Appl. Mater. Interfaces*. **2016**, 8

ACKNOWLEDGMENTS

Grants PCI2018-092929 and PID2019-105827RB-I00 funded by MCIN/AEI/10.13039/501100011033/ supported this research. M. Mantecón-Oria acknowledges FPU grant (19/02324) awarded by the Spanish Ministry of Science and Innovation.

3D membrane of electrospun fibers for cell culture

Bénédicte Fromager[1], Julien Cambedouzou[1], David Cornu[1]
[1]Institut Européen des Membranes, Univ Montpellier, ENSCM, CNRS, Montpellier, FRANCE
*benedictefromager8@gmail.com

INTRODUCTION

Cell therapy, which is organ or tissue regeneration from injection and growth of stem cells, raises a lot of hope for treatment of diseases. However, the direct injection does not work out so well. Thus, biocompatible membranes, allowing stems cells to growth and differentiate, are needed. 3D membranes of electrospun fibers have been developed by both IEM and INM. Their application extends from drug screening to cell therapies. In fact, this scaffold is purely synthetic, reproductible, low cost to produce and fibers show fluorescence properties. Moreover, it is inert, biocompatible, it can be sterilized and inserted into well plates. Studies[1-2] have shown that migration and growth of stem cells can be studied realistically since fibers imitate extracellular medium.

EXPERIMENTAL METHODS

3D nanofiber matrix

Nanofibers were produced by electrospinning a solution of 10% w/w Polyacrylonitrile (Sigma Aldrich) in DMF (Sigma Aldrich). A voltage of 20kV and a flow rate of 2.4 ml/h were applied. Multi-walled carbon nanotubes (MWCNT, Nanocyl) were added in the electrospun solution. After overnight drying at room temperature, the nanofibers were put in a chamber furnace for heat treatment. Before biological use, the matrixes were cut and sterilized in a classical autoclave.

FTIR

ATR-FTIR Spectrum was recorded on Nexus Spectrum.

Scanning electron microscopy (SEM)

Scanning electron micrographs were captured of sample mounted onto SEM stubs with carbon tape (HITACHI S-4800, 2keV, 5mm working distance).

Tomography Electron Microscopy

Samples were embedded in LR White resin and cut with an ultramicrotome Leica UC7. TEM analyses were performed on a JEOL 2200FS microscope, equipped with a field emission gun (FEG) and an in-column Omega-type energy filter, operated at 200 kV. Images were acquired on an CCD Gatan UltraScan 4000 camera.

DiameterJ[3]

DiameterJ algorithm was used to analyze SEM images of 500 resolution.

Cell culture and migration assay

GBM cells were cultured in U-bottomed 96-well plates (25 000 cells/well) in DMEM/F12 medium supplemented with glucose, glutamine, insulin, N_2, Epidermal Growth Factor and Fibroblast Growth Factor. After 24h, they were dissociated and put on nanofiber matrixes. After 15 minutes, 500 µl of DMEM/F12 medium supplemented with fetal bovine serum (0.5%), fungizone and B27 were added. They were put in incubator at 37°C, 5% CO_2. After 5 days, medium was removed and washed with PBS twice. Then, cells were fixed with formaldehyde solution (1%) in PBS and permeabilized with triton (0.5%)/serum (5%) solution in PBS. After 30 min in incubator, nuclei were colored in Hoechst (1/1000). Fibers were then placed on slides, dried, recovered by mounting liquid and another slide above, left overnight in fridge and analyzed by epifluorescence microscopy.

RESULTS AND DISCUSSION

The study of spectrum before and after heat treatment shows that PAN has undergone aromatization and dehydrogenation. The functional groups on the surface enable the formation of hydrogen bond between nanofibers and cell surface, which make the matrix biocompatible, and will enable us to coat the nanofibers with biomolecules such as MEC proteins.

With the parameters chosen, we obtain a membrane composed of 0.716±0.046 µm diameter nanofibers and pores of 27.11±3.302 µm². As showed in previous study[2], the morphology of nanofibers, the dimension of pores and the constitution of the mesh enable cells to infiltrate, migrate and proliferate.

To better understand the impact of MWCNT on mechanical properties, we analyzed membranes with TEM. The comparison between TEM images of fibers without MWCNT and those with 0.05% MWCNT shows that MWCNT are all inside the fibers and towards their lengthwise. Over the 195 sections of fibers, 19 contained MWCNT. They are well incorporated within PAN solution and kept through electrospinning process.

The analysis of fibers with DiameterJ showed that neither the diameter and mesh hole area nor the orientation are significantly impacted by MWCNT.

Results show that GBM migration is maximal when they are cultured on nanofibers matrixes containing 0.0015% MWCNT. Moreover, we can see that migration is directional, following fibers orientation. These results show that GBM can migrate in the nanofibers.

CONCLUSION

We produced a 3D nanofiber matrix whose physical and chemical property can be modified and studied independently to produce an environment mimicking *in vivo* ECM. Moreover, it is suitable for cell culture. Thus, it represents a relevant tool to study ECM role in cell migration, proliferation, and differentiation.

REFERENCES

1. Saleh A. *et al*., Sci. Rep. 14612, 2019
2. Marhuenda E. *et al*., J. Experimental & Clinical Cancer Res., 2021
3. Hotaling NA. *et al*., Biomaterials 61:327–38, 2015

Microstructured Electrospun Scaffold Composed of PVA And Marine Biopolymers and Its Effect on Muscle Cells

Dragica Bezjak[1], Nicole Orellana[1], Cristian Acevedo[1,2], Tomas P. Corrales[2]
[1]Centro de Biotecnología, Universidad Técnica Federico Santa María, Valparaíso, Chile.
[2]Departamento de Física, Universidad Técnica Federico Santa María, Valparaíso, Chile.
dragica.bezjak@usm.cl

INTRODUCTION

Electrospinning is a technique used for tissue engineering due to its simplicity, ability to modify the surface and the possibility of using various biomaterials[1]. In this work, electrospun scaffolds were produced for muscle cell growth. Muscle is composed of elongated multinucleated cells aligned with each other[2], with this in mind, the electrospun surface scaffold was fabricated with parallel microchannels to align the cells. A new mixture of poly (vinyl alcohol) (PVA) was enhanced with marine biopolymers, such as fish gelatin (Ge) and chitosan (Ch). PVA is a polymer used in biomedical applications for its biocompatibility[3], Ge contains RGD-sequences that promote cell adhesion[4] and Ch is a biodegradable polymer with positive charges which can interact with negative charges of cell membrane[5]. In this work, the effect of the scaffold microstructure and composition was evaluated on cell morphology.

EXPERIMENTAL METHODS

Duralumin collectors with microchannels of 400 µm width and a periodicity of 500 µm, were fabricated (Fig. 1A). Solution mixtures of 10% (w/w) PVA, 0.9% (w/v) fish gelatin and 0.6% (w/v) chitosan (PVA-Ge-Ch) were prepared. Electrospinning was carried out using this mixture over the duralumin collector to fabricate scaffolds. SEM images of the produced scaffold are shown in Figure 1 (B-C). Then, our cells were cultured on the scaffold at a density of $2.5 \cdot 10^5$ cells/cm^2 for 3 days with DMEM high glucose medium with L-glutamine and 10% fetal bovine serum.

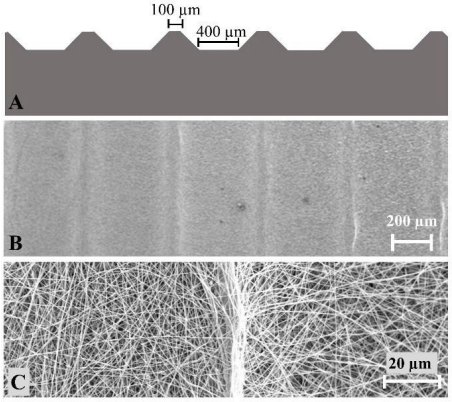

Figure 1: A) Design of the microstructured electrospinning collector. B) Scaffold surface. C) Nanofibers obtained over the microstructured collector.

RESULTS AND DISCUSSION

The morphology of the cells changed considerably when they were seeded on PVA-Ge-Ch scaffolds, in contrast to pure PVA scaffolds (Fig. 2). When the cells were seeded on pure PVA, the cells do not spread throughout the scaffold and tend to form sphere-like clusters, where the elongated shape of muscle cells was not observed. However, when cells were cultured on PVA-Ge-Ch scaffolds, it is observed that the cells spread throughout the material and that they have an elongated shape, in some cases they are multinucleated, which indicates that the mixture enhances the cell development.

Regarding the microstructured scaffolds, we observed little effect on cell growth when pure PVA was used. However, in the mixture, the microstructure allows the cells to grow in the microchannels, with an orientation perpendicular to the microstructures.

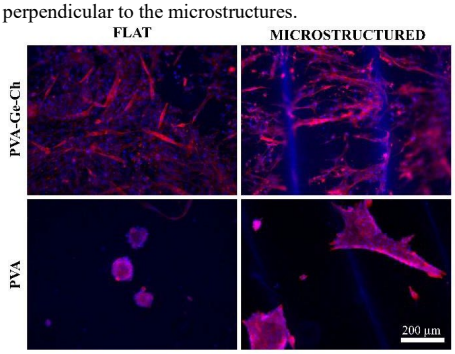

Figure 2: Muscle cell morphology in microstructured and flat scaffolds, fabricated with PVA-Ge-Ch and PVA alone.

CONCLUSION

These results indicate that the PVA-Ge-Ch electrospun mixture is a potential biomaterial that could be used in the development of muscle skeletal tissue engineering.

REFERENCES

1. Sung-Kang M. *et al*., Bioengineering. 7,99, 2020.
2. Chal J. *et al*., Development. 144, 2104-2122, 2017.
3. Paradossi G. *et al*., J. of Materials Science. 14, 687-691. 2003.
4. Yamada S. *et al*., BioMed Research International. Vol.2014.
5. Croisier F. *et al*., European Polymer Journal. 49 780–792. 2013.

ACKNOWLEDGMENTS

FONDECYT Grant 1190100 (ANID, Chile)
Conicyt-Max Plank Grant MPG190023 (ANID, Chile)
Doctoral Scholarship ANID 21211207.

Surface topography and roughness analysis of the laser-treated powder metallurgy prepared Ti-graphite composite for application in dental implantology

Peter Šugár[1], Richard Antala[1*], Jana Šugárová[1], Jaroslav Kováčik[2]

[1]Institute of Production Technologies, Faculty of Materials Science and Technology, Slovak University of Technology, Trnava, Slovakia
[2]Institute of Materials and Machine Mechanics, Slovak Academy of Sciences, Bratislava, Slovakia
[*] richard.antala@stuba.sk

INTRODUCTION

Titanium (Ti) and its alloys are one of the most used materials in either orthopaedic or dental implantology. They are used as commercially pure (cp) Ti with different degrees of purity, as multi-component metallic alloys, or as Ti metal matrix composites (TiMMCs) reinforced with different types of particles or whiskers. TiMMCs represent a novel generation of biomaterials with superior properties and cost-effective methods of fabrication. To minimalize the mismatch between Young's modulus of Ti-based materials and the bone, there is a strong effort to develop this kind of materials with defined porosity through powder metallurgy way[1]. The bio-functionalities of implant surfaces that influence implant–tissue interaction and the osseointegration process, can be enhanced through surface integrity parameters, such as surface topography, surface roughness, surface chemistry, surface energy, and wettability[2]. From the topography point of view, a surface with grooves or depressions having the same size as the cells, i.e. about 30 µm or larger, is more preferred for cell colonization[3].

In this study, the laser surface treatment of low-temperature powder metallurgy processed Ti – graphite composite without using a shielding atmosphere was investigated and the surface topography and roughness parameters influencing the osseointegration process were evaluated and compared with the results of the study[4], where Ar shielding atmosphere was used.

EXPERIMENTAL METHODS

The Ti – graphite composite with 15 vol. % of graphite flakes was prepared using the vacuum low-temperature extrusion method with a final density in the range from 4.1 to 4.15 g.cm^{-3} and porosity of 2.44 % ± 0.15 %. The square-shaped surfaces of 6 mm side length were laser machined using a Yb-doped fibre nanosecond laser working at 1064 nm wavelength by combining different levels of pulse energy and lateral laser spot distances leading to the different total energies delivered to the material per illuminated area, which was in the range from 0.5 mJ to 20 mJ. The samples were ablated in two layers without a shielding atmosphere followed by surface topography and surface roughness analysis. The surface profile parameters (Ra, Rq, Rv, Rp, Rsk, Rku, and Abbott-Firestone curve characteristics) were elaborated and reported according to ISO 21920-2:2021 standard. The One-Way ANOVA analysis and Tukey Post-Hoc Test were used for statistical analysis of the evaluated data applying Minitab v. 17 software.

RESULTS AND DISCUSSION

The mean value of the skewness Rsk for surface irradiated with a lower level of the transmitted energy is positive, and vice versa for surface irradiated with higher energy is negative. It means, that both surface profiles have symmetrical height distribution. The surface with positive Rsk is more porous while the surface with negative Rsk is rougher. The distribution curve of the laser-treated surfaces is platykurtic (Rku < 3; the profile consists of relatively few flat hills and dales). Only in the case when the transmitted energy of 5 mJ is used, the surface profile is leptokurtic (Rku > 3; the profile consists of relatively many sharp hills and dales). The highest values of the Ra, Rz, Rp and Rv were observed in the cases when the highest values of lateral overlaps of the laser pulses were used. When the value of the lateral laser spot overlap decreased, the amplitude parameters of the surface profile also decreased. The positive values of kurtosis Rku in combination with the skewness Rsk values near zero indicate a fluctuating topography with a high value of the hills density. The highest value of the energy used in the experiment resulted in the steeper shape of the Abbott-Firestone curve.

CONCLUSION

The obtained results confirmed the strong influence of the laser energy on the topography and roughness parameters. The lower amount of the transmitted energy resulted in the surface profile with few low, wide dales and higher hills with a rugged surface. The surface profile which consists of relatively many narrow (sharp) hills and many low dales, where the dales dominate over the hills was documented when higher-level energy was used. The highest energy resulted in higher values of the Rv, Rku and a highly negative value of Rsk.

REFERENCES

1. Fang Z Z. *et al*. Int. Mater. Rev. 63:7, 407-459
2. Hanawa T.Front. Bioeng. Biotechnol. 7:170, 2019.
3. Gnilitskyi I. *et al*. Biol. Med. 21:102036, 2019
4. Šugár P. *et al*., Materials. 14:6067, 2021.

ACKNOWLEDGMENTS

This research was supported by the research project VEGA 2/0135/20. The authors would like to thank the Ministry of Education, Science, Research and Sport of the Slovak republic for providing financial support to this project. The authors would also like to acknowledge dr. Barbora Bočáková for her laser surface modification technical assistance.

Tubular Constructs as Small Diameter Vascular Grafts and Tissue Models

Michael Bartolf-Kopp[1], Alessandro Cianciosi[1], Csaba Gergely[1], Tomasz Jungst[1*]

[1]Department for Functional Materials in Medicine and Dentistry, University of Würzburg, Würzburg, Germany
[*] tomasz.juengst@fmz.uni-wuerzburg.de

In the human body, tubular structures are abundant and appear in different architectures. Examples are the vascular or lymphatic systems. To mimic the hierarchy of natural tissues to improve the performance of biofabricated constructs, tubular geometries are highly relevant. Potential transplants should not only mimic the macroscopic structure and shape but also the microarchitecture of the tissue they replace in a way that supports cell function and helps improving the performance of the implant. Besides the architecture, it is also important to take the biomechanics of the tissues into account. In terms of blood vessels, concerning their macroscopic shape, one could see them as tubular constructs with a defined diameter. A closer look reveals that they have multiple layers. Those layers are composed of different extracellular matrix components and cell types. In addition, the orientation of the cells and the extracellular matrix tailor their unique mechanical properties. If one wants to mimic the hierarchy of a blood vessel, multi-layered tubular scaffolds need to be produced.

This presentation is demonstrating how melt electrowriting (MEW) combined with solution electrospinning can be used to generate hierarchical tubular constructs with biomimetic architectures and adjustable mechanical properties.

To produce bi-layered constructs, first a nonwoven was electrospun onto a tubular collector with varying diameters (1.0-3.0 mm). This construct was transferred to the MEW device to generate a second medial layer on top of the nonwoven. The geometry and the deposition pattern of tubular constructs made by MEW was tailored to influence the mechanical properties of the scaffolds. In addition, also different combinations of materials were used to influence the over-all properties of the grafts. Besides polycaprolactone (PCL) also poly[(L-lactide-co-ε-caprolactone)-co-(L-lysine ethyl ester diisocyanate)-block-oligo(ethylene glycol)-urethane] (PEU) was used and different combinations of PCL and PEU were processed. Mechanical testing revealed that the addition of PEU made the grafts more elastic and more comparable to natural blood vessels. In vitro experiments in co-culture conditions using human endothelial colony (hECs) forming cells on the luminal side and human multipotent mesenchymal stromal cells (hMSCs) on the outer part of the scaffolds were used to compare the performance of the scaffolds to grafts made from PCL only[1,2]. In vitro experiments were conducted in static and dynamic conditions.

Combining different materials and fabrication methods to produce tubular grafts enables to adjust their mechanical properties. The findings made in this project might enable the fabrication of biomimetic and functional grafts for small diameter blood vessel replacement.

REFERENCES

1. Jungst *et al.*, Advanced Functional Materials. 29, 2019
2. Pennings *et al.*, Biofabrication. 12, 2019

ACKNOWLEDGMENTS

This work has been supported by the European Research Council consolidator grant Design2Heal, contract #617989, and the DFG State Major Instrumentation Programme for funding the Zeiss Crossbeam CB 340 SEM (INST 105022/58-1 FUGG).

Ultrafiltration impact in the enzymatic activity of lysozyme

Ariane de Espindola[1*], Patrick Dutournié[1], Arnaud Ponche[1]

[1] Institut de Science des Matériaux de Mulhouse, Université de Haute-Alsace, Mulhouse, France
[*] ariane.de-espindola@uha.fr

INTRODUCTION

Proteins are examples of macromolecules present in living systems from bacteria to human beings. In human bodies, proteins are present in muscles, hair, nails, organs and skin, playing functions as hormones, enzymes, oxygen carriers, antibodies, muscle messenger, among others. Considering protein importance for human health, it is crucial to have external sources in the case of body low production rate or disease treatment and that is the reason why the interest for protein use as food supplement, vaccines, antibiotics and biopharmaceutical enzymes increased in the last two decades. [1,2]

High quality product is required for the final customer, which implies the processing of proteins through purification, fractionation, concentration, mixing, heating and pumping. These processes could induce changes in protein conformation resulting on its biological activity loss.[3,4]

EXPERIMENTAL METHODS

Lysozyme aqueous solution was filtrated with a tubular mono channel ultrafiltration titania membrane with a commercial cut-off of 1 kDa (TAMI membranes). The pressure varied from 4 to 12 bar. Samples of retentate (part of the solution in the tank feed) and permeate (solution that passed through the pores) of each pressure were studied according to its enzymatic activity. The enzymatic assay was evaluated by a turbidity test at 450 nm using the bacteria *Micrococcus Lysodeikticus* as the substrate. The whole assay was done 3 times in triplicate and the results are presented as an activity index that is defined as the ratio between sample activity and the reference (untreated lysozyme).

RESULTS AND DISCUSSION

Initial hydrodynamic properties of the studied membranes are presented in figure 1. Results indicated that membrane M3 with lower hydraulic permeability has the smaller pores.

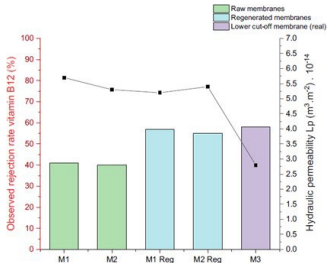

Figure 1: Initial membrane performances: selectivity (histogram, red axis) and hydraulic permeability Lp (black squares, right axis) for the studied membranes.

The membranes with bigger pores (M1 and M2) didn't present any influence in the antibacterial action of lysozyme. On the other hand, membranes with small pores as M3 caused a decrease of the lysozyme enzymatic activity against *Micrococcus Lysodeikticus* with increasing pressure as observed in figure 2.

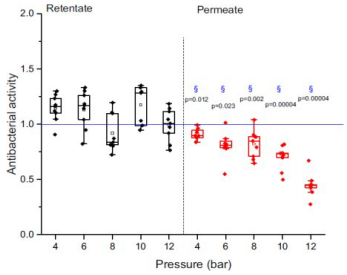

Figure 2: Lysozyme antibacterial activity for retentates (black) and permeates (red) for solution filtered with membrane M3.

CONCLUSION

Antibacterial activity loss was directly proportional to the applied pressure for the membrane with small pores (M3). The results indicate that membrane real cut-off should be taken into account when processing proteins to avoid activity decrease due to denaturation caused by shear forces and chemical interactions in the pores.

REFERENCES

1. Thomas E. *et al*., Heliyon. 5:1508, 2019
2. Miron S. M. *et al.*, Comp. Rend. Chim. 22: 198-205, 2017.
3. Wang W., Int. Journ. Pharm. 185:129-188, 1999.
4. Saxena A. *et al.*, Adv. in Col. And Int. Sci. 145:1-22, 2009.

Electrospun PCL coated with Collagen/Hydroxyapatite for Bone Tissue Engineering

M.G.Bartley[1*], K.A.Hing[2], K.E.Tanner[3]

School of Engineering and Materials Science, Queen Mary University of London, London, E1 4NS,UK

*m.g.bartley@qmul.ac.uk

Introduction

Bone tissue is susceptible to damage caused by trauma and disease resulting in bone loss and bone defects. Autologous bone grafts have been frequently used for bone regeneration however there are drawbacks such as limited bone supply, donor site morbidity and a long recovery time [1]. To address this limitation and the clinical demand for bone grafts, biodegradable bone graft substitutes have been developed. We therefore developed an electrospun polycaprolactone (PCL) scaffold that has been immersed in a collagen and hydroxyapatite coating. The microstructure of electrospun fibres were analysed using Scanning Electron Microscopy (SEM). The cytocompatibility of these electrospun scaffolds was further investigated using the SaoS-2 osteosarcoma cell line.

Experimental Methods

15% (wt/v) PCL was prepared by dissolving PCL pellets in chloroform PCL solutions were loaded into a 10ml Luer-lock syringe with a 16 gauge straight blunt needle 3.7 mm long. Fibres were electrospun onto a rotating collector spinning at 800 rpm with a flow rate of 6ml/hr at 20.5kV and the needle tip to collector distance was kept at 30cm.

For the 70wt% HA 30wt/v% collagen (Col/HA) coating two types of HA fillers were used: Spray dried HA in the form of nanoscaled needles (HA1) and sintered HA with a smoother topography (purchased from Plasma Biotal Ltd UK). Pepsin soluble collagen type I in 0.01 M HCL (purchased from Collagen Solutions Ltd UK) was also used. PCL samples were first sterilised in 70% ethanol then immersed samples in Col/HA and dried overnight at room temperature. For collagen coated samples the same process was repeated. Uncoated PCL material were used as controls.

Saos-2 cells were cultured in Dulbecco's Modified Eagle's medium (DMEM) supplemented by 10% foetal bovine serum (FBS) and 1% penicillin/streptomycin and incubated at 37°C at 5% CO_2. Using non-coated 24 well plates, Saos-2 cells were seeded at a density of 800,000 cells/ml directly onto sterilised PCL material.

Results and Discussion

SEM micrographs show the differences in particle morphology between HA1 and HA2 (Figures 1 A-E). The surfaces of HA1 particles (Figure 1C) show nanoscale needle projections and rough appearing topography. Meanwhile, HA2 particles exhibit a much smoother surface (Figures 1E).

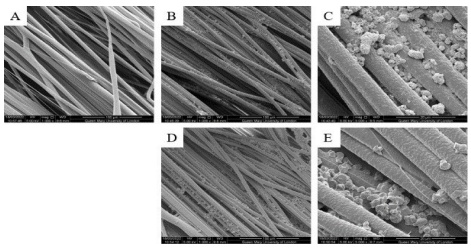

Figure 1: SEM micrographs of A, PCL fibres uncoated, B&C, PCL fibres coated with Col/HA1, D&E, PCL fibres coated with Col/HA2. (Figures A,B&D marker bars=100µm, Figures C&E 20=µm).

Within the first day of incubation the cells attached to PCL fibres using filopodial extensions. Cells appeared to have a spherical shape and smooth surface appearing adhered to the surfaces of individual and multiple PCL fibres.

Conclusions

Introducing a collagen and HA coating to PCL fibres maintained the morphology and diameter of PCL fibres. SEM micrographs further showed a good distribution and integration of HA1 and HA2 particles on the surface and in between PCL electrospun fibres. Electrospun PCL fibres produced uniform and aligned fibres which may encourage the attachment and elongation of Saos-2 cells along their surfaces.

References

[1] Sheikh, Z., Najeeb, S., Khurshid, Z., Verma, V., Rashid, H. and Glogauer, M., (2015). Biodegradable materials for bone repair and tissue engineering applications. *Materials*, *8*(9), pp.5744-5794.

Keywords- Electrospinning, Collagen, Hydroxyapatite, Polycaprolactone

Melt Electrowriting of an Organic-inorganic Hybrid Doped with a Natural Plasticizer Agent

Nafise Elahpour[1], Cedric Bossard[1], Nora Abdellaoui[1], Édouard Jallot[1], Jonathan Lao[1*]

1Université Clermont Auvergne, CNRS/IN2P3, LPC, F-63000 Clermont-Ferrand, France
*Jonathan.lao@clermont.in2p3.fr

INTRODUCTION

Melt Electrowriting (MEW) has emerged since almost 20 years ago as a high resolution additive manufacturing technique, enabling highly ordered, controllable and microscale three-dimensional geometries o be fabricated with a variety of polymers[1]. The fine structure printed yields a very high specific surface area, which is suitable for cellular adhesion and proliferation. However, MEW has so far mainly use to print polymers. Organic-inorganic hybrids, defined as materials mixing intimately organic-inorganic conetworks, own highly viscous rheological properties which make them challenging to 3D print using MEW. We propose in this study the introduction of curcumin, a natural polyphenol from the ginger family and acting here as a naturally derived plasticizer[2], inside a bioactive glass (BG)-polycaprolactone (PCL) hybrid material, to facilitate its processing using MEW.
To the best of our knowledge, it is the very first time the melt-electrowriting of a bioactive glass-polymer hybrid is reported along with its in vitro apatite forming ability.

EXPERIMENTAL METHODS

Homogeneous hybrids containing 68 wt. % PCL, 30 wt.% BG and 2wt% curcumin were synthesized using the sol-gel process[3]. Curcumin was dissolved with PCL in THF and then the mix was added to a BG sol, designed to yield a 75 wt.% SiO_2 and 25 wt.% CaO inorganic network. After drying, a fine powder was obtained and processed for MEW. A 200 micrometer nozzle was used to extrude the melt and direct-write the hybrid. Then the best set of parameters were obtained with the changing of voltage, temperature and pressure according to the viability and homogeneity of struts. Scaffolds were immersed in SBF (Simulated Body Fluids) to investigate their bioactivity. ICP (Inductively Coupled Plasma spectrometry) and PIXE (Particle-Induced X-ray Emission) analyses were used to evaluate the in-vitro apatite-forming ability. TGA and DSC analyses were done to evaluate the thermal properties of curcumin-doped hybrid.

RESULTS AND DISCUSSION

Scaffolds with fine structures were printed with struts diameter varying between 83.5 and 105.5 micrometers. This is a 3- to 5-fold increase in printing resolution compared to conventional 3D FDM printing techniques commonly used to fabricate bioceramics scaffolds. When immersed in SBF, the MEW scaffolds quickly formed calcium phosphate (CaP) precipitates. The formation of the latter was not limited to the surface of the struts, but extended to the entire volume of the struts, as demonstrated by PIXE chemical mapping of cross sections of the scaffolds.

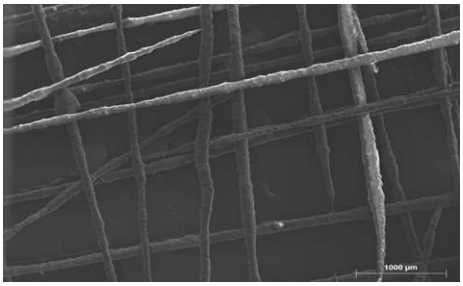

Figure 1: SEM micrograph of PCL-BG-Cur melt electrowritten hybrid scaffold.

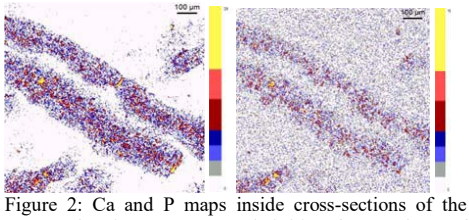

Figure 2: Ca and P maps inside cross-sections of the MEW-printed PCL-BG-Cur hybrids after 3 days of immersion in simulated body fluids.

CONCLUSION

The feasibility of writing very fine-structured organic-inorganic hybrid scaffolds was proved for the first time. The local and systemic apatite forming evaluations prove the gradual calcium phosphate precipitation and deposition throughout the scaffold struts. Despite being written in a very small dimension, the homogeneity of the hybrid is well preserved making this material a good candidate for bone tissue engineering applications.

REFERENCES

1. Dalton PD, J. Cobme. 2: 49-57, 2017.
2. Saltos JA. et al., J. RSC Adv. 4 : 54725-54728, 2014.
3. Bossard C. et al., J. Biomed. Glasses. 4 :108-122, 2018.

ACKNOWLEDGMENTS

The authors would like to thank CNRS for support through the MITI project for providing financial support to this project.

Electrospun Thermally Treated PVA/Gellan Gum Membranes for Bone Tissue Engineering

Konstantinos Loukelis [1,2], Danai Papadogianni [1,2], Maria Chatzinikolaidou [1,2]

1 Department of Materials Science and Technology, University of Crete, 70013 Heraklion, Greece
2 Foundation for Research and Technology Hellas (FORTH)-Institute of Electronic Structure and Laser (IESL), 70013 Heraklion, Greece
* mchatzin@materials.uoc.gr

INTRODUCTION

Gellan gum (GG) is a natural polysaccharide used in tissue engineering applications due to its biocompatible and cell adhesion promoting character [1]. Polyvinyl alcohol (PVA) is a hydrophilic synthetic biodegradable polymer that also demonstrates a cytophilic behavior [2]. An important aspect that governs both biomaterials is their ability to fully dissolve in water, which is crucial for in vivo conditions. Among the tissue engineering fabrication techniques, electrospinning is considered as one of the low-cost and most effective methods for nanofibrous scaffold fabrication [3]. Taking into account the aforementioned properties of these two biomaterials, our current work focuses on the electrospinning of PVA/gellan gum blends of various compositions to develop mechanically stable membranes that promote bone tissue growth.

EXPERIMENTAL METHODS

To prepare the electrospun nanofibrous mats, a 10% w/v PVA stock solution and three solutions of gellan gum with the concentrations of 0.75, 1, and 1.25% w/v were prepared in deionised water (dH_20) at 90°C for 3 h. Subsequently, the PVA solution was mixed with each one of the individual gellan gum stock solutions in a volume ratio of 1:1, and the blends were left under stirring at 90°C for approximately 5 h. The three resulting blends, PVA-0.75% GG, PVA-1% GG, and PVA-1.25% GG were supplemented with two drops of the non-ionic surfactant Span 80, in order to lower their surface tension and allow for uniform electrospinning. The three solutions were electrospun from a 5 ml syringe with controlled flow rate at 0.4 ml/h at a horizontal distance of 12 cm between the metallic needle (20 G) tip and the anode at a voltage of 11–13 kV. The produced fibrous mat was extracted from an aluminum foil sheet and placed in an oven at 120°C for 1 h to completely dry, allowing for the esterification between the hydroxyl groups of PVA and the glucuronic acid's carboxyl groups of gellan gum to take place. This heat procedure strengthens the nanofibrous mats [4] providing them with high hydrolysis resistance in aqueous biological environments. The electrospun mats were also investigated under scanning electron microscopy (SEM). Moreover, FTIR spectroscopy was conducted to ensure the various blends' chemical composition integrity. MC3T3-E1 pre-osteoblasts have been used to determine the scaffolds' biological response, including cell viability, morphology, proliferation, and measurement of alkaline phosphatase activity as well as calcium mineralization levels.

RESULTS AND DISCUSSION

SEM analysis of the produced nanofibrous mats depict fine, elongated fibers without significant presence of beads, with similar diameters of approximately 55-65 nm for all three compositions.

All biological assays were performed at three different time points. TCPS polystyrene coated wells seeded with MC3T3-E1 acted as control in all experiments. Cell viability assessment was conducted at days 3, 5, and 7. No significant differences were observed between days 3 and 5, but a higher increase in cell viability was evident at day 7. All three electrospun fibrous mat concentrations depicted similar biocompatibility profiles and comparable to the TCPS control, while the PVA-1% GG slightly exceeded the other two compositions. The ALP activity (days 3, 7, and 14) and calcium mineralization (days 7, 14, and 21) protocols exhibited similar trends, with a significant increase between the first two time points, respectively. All compositions had comparable values to those of the TCPS, but the PVA-1% GG indicated the highest values compared to the other two concentrations. In addition, SEM images of cells on nanofibrous mats display strongly adhered cells forming a dense cell layer on the mats.

CONCLUSION

Electrospun nanofibrous mats comprising PVA and varying gellan gum concentrations were produced and thermally crosslinked in order to create mechanically stable and biocompatible membranes that promote cell viability, adhesion, proliferation, and differentiation to mature osteoblasts.

REFERENCES

1. Sumi L. *et al.,* Inter. J. Biol. Macromol. 158:452-460, 2020
2. Xu M. *et al.,* J. Biomat. Sci. Polymer Ed. 1-21, 2020
3. Pham Q.P. *et al*., Tissue Eng 12(5):1197-1211, 2006
4. Franco R.A. *et al.,*J. Nanomater, 1–9, 2012

ACKNOWLEDGMENTS

This research was funded by the Hellenic Foundation for Research and Innovation (H.F.R.I.) project number HFRI-FM17-1999, and the European Union's Horizon 2020 research and innovation program under grant agreement No. 814410.

Processing of fast-gelling hydrogel precursors in microfluidics by electrocoalescence of reactive species

Talika Alina Neuendorf[1*], Nicolas Hauck[1], Max Julius Männel[1], Lucas Vogel[1], Ping Liu[2], Enno Stündel[1], Yixin Zhang[2], Julian Thiele[1]

[1]Leibniz Institute of Polymer Research Dresden, Dresden, Germany
[2] B CUBE Center for Molecular Bioengineering, Technische Universität Dresden, Dresden, Germany
[*] neuendorf@ipfdd.de

INTRODUCTION

Microscopic hydrogels, also referred to as microgels, find broad application in life and materials science. To further promote their application in cell biology, e.g., in mechanobiology[1,2], where homogeneous hydrogel microenvironments are essential for reproducible force sensing, uniform hydrogels obtained from fast-gelling precursors are of great interest. A well-established technique for fabricating uniform microgels is droplet microfluidics. Here, optimal mixing of hydrogel components is crucial to yield uniform microgels with respect to their morphology, mechanics, and distribution of functional moieties. However, processing highly reactive polymer precursors is challenging due to the risk of instantaneous, uncontrolled gelation causing microchannel blockage and device failure[3].

EXPERIMENTAL METHODS

Microfluidic flow cell fabrication

We employ photo- and soft lithography to manufacture PDMS-based microfluidic flow cells, followed by subsequent electrode integration by filling selected microchannels with a low-melting-point solder.

Microfluidic fabrication of microgels

Hydrogel precursor particles are fabricated using droplet microfluidics. Droplet coalescence is induced via electrode activation using a custom-built power source. The hydrogelation is based on covalent crosslinking via thiol-Michael addition reaction or on non-covalent self-assembly via supramolecular or ionic crosslinking. The resulting microgels are transferred into water by emulsion breaking.

Microgel characterization

For size determination, bright-field images of the resulting emulsion droplets and microgels are analyzed manually using ImageJ[4]. To evaluate spatial uniformity of the resulting microgels, a fluorescent dye is incorporated into the hydrogel network. The dye's distribution is revealed by mid-plane images of the microgels via 3D confocal microscopy.

RESULTS AND DISCUSSION

We address the challenges of processing reactive polymer precursors by utilizing microflow cells with integrated electrodes, enabling fast addition and mixing of hydrogel network precursors on demand through emulsion coalescence. As depicted in Figure 1, two populations of surfactant-stabilized aqueous droplets – the first containing the material basis of the microgel and the second containing another gel-forming or crosslinking component are formed at two consecutive microchannel junctions and merged via electric field-induced temporary thin-film instability.

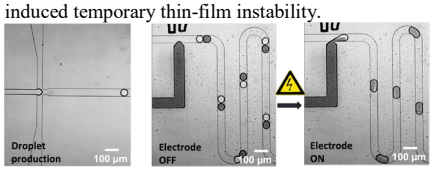

Figure 1: Droplet formation of two aqueous droplet species and formation of droplet pairs (Left and Middle). Electrode activation leads to coalescence between the droplet pairs, followed by fast convection-based droplet mixing by passage through a meander-shaped microchannel (Right).

Using this method, covalently crosslinked microgels via thiol-Michael addition reaction of PEG-thiol and PEG-maleimide, and supramolecularly or ionically crosslinked microgels via non-covalent assembly of dextran sulfate and peptide-lipid-starPEG or sodium alginate and calcium chloride, respectively, are fabricated. All types of hydrogels yield the desired isotropic microgels with high spatial uniformity of the microgel volume as confirmed utilizing 3D confocal microscopy.

CONCLUSION

Using our approach, hydrogel systems that are otherwise challenging to process into uniform droplets and microgels by conventional droplet microfluidics become processable. To demonstrate its versatility, we fabricate microgels with uniform shape and composition based on fast hydrogelation via thiol-Michael addition reaction or via non-covalent self-assembly by supramolecular or ionic crosslinking[5].

REFERENCES

1. Wagner K. *et al.*, Soft Matter 15:9776-9787, 2019
2. Kühn S. *et al.*, Adv. Funct. Mater. 30:1908857, 2020
3. Neubauer J. W. *et al.*, ACS Appl. Mater. Interfaces. 11:26307-26313, 2019
4. Rueden C. T. *et al.*, BMC Bioinf. 18:529, 2017
5. Hauck N. *et al.*, Soft Matter 17:10312-10321, 2021

ACKNOWLEDGEMENTS

The authors would like to thank the German Research Foundation (DFG, Research Training Group 1865: Hydrogel-based Microsystems), and the European Research Council (ERC) under the European Union's Horizon 2020 research and innovation program (Grant agreement No. 852065).

Peptide Mediation of Nanoparticles To Cross The Blood-Brain Barrier – A Platform For Brain Drug Delivery

Catarina I. P. Chaparro[1,2*], Marco Cavaco[2], Miguel Castanho[2], João Paulo Borges[1], Vera Neves[2], Paula I. P. Soares[1]

[1]CENIMAT/i3N (Centro de Investigação em Materiais), NOVA School of Science and Technology (FCT-NOVA), Almada, Portugal
[2]Instituto de Medicina Molecular, Faculdade de Medicina da Universidade de Lisboa, Lisboa, Portugal
* c.chaparro@campus.fct.unl.pt

INTRODUCTION

Poly(lactic-co-glycolic) acid (PLGA) nanoparticles enhance drug pharmacodynamics and bioavailability, and when loaded with superparamagnetic iron oxide nanoparticles (SPIONs) they can act as contrast agents for magnetic resonance image (MRI)[1]. These characteristics make them attractive for brain imaging and therapy. However, the application of nanoparticles (NPs) for brain drug delivery is hindered by the presence of the blood-brain barrier (BBB). The BBB is a natural defense against circulating toxic and infection agents that also prevents most therapeutic compounds from reaching the brain. BBB peptide shuttle (BBBpS) are small peptides that engage adsorptive mediated transport (AMT) across the BBB and allow brain uptake[2]. In this work, we propose SPIONs-loaded PLGA nanoparticles functionalized with a BBBpS as a platform for brain drug delivery.

EXPERIMENTAL METHODS

SPIONs-loaded PLGA NPs were produced through simple-emulsion solvent evaporation according to a modified procedure reported by Kandasamy et al.[3]. The size of the nanoparticulate system was confirmed by DLS and TEM techniques, while the zeta potential was measured by ELS. Iron content of SPIONs encapsulated in NPs was determined using 1,10-phenanthroline colorimetric method through UV/VIS spectrometry. To test the activity of NP we first investigated the interaction with human brain endothelial cells (BEC) that make up the BBB. NP internalization in BEC was evaluated through flow cytometry and fluorescence microscopy.

RESULTS AND DISCUSSION

The nanoparticles produced have a size range of 110-145 nm (Figure 1 (A)) and iron content of SPIONs of 80%. In the functionalization step, 15% of fluorescently labeled BBBpS was conjugated to NPs surface, resulting in alteration of size and charge. The size increasing in 60 nm and zeta potential from -21.2 ± 0.6 before functionalization, to -4.2 ± 1.2 after functionalization. The increase in charge was expected due to the presence of cationic BBBpS at NPs surface. Internalization of NPs by BEC reveal that BBBpS promotes internalization, with an increase of 6-fold in BBBpS modified NP, in comparison with naked NP, at 24 h (Figure 1 (B)). Also, time-course evaluation of NP internalization reveals a plateau at 12 h, suggesting an equilibrium between endocytosis and exocytosis. Given the results obtained, we are now studying the translocation efficiency of these NPs when conjugated, or not, with the BBBpS through the BBB *in vitro* model.

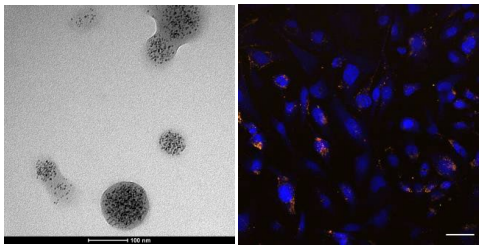

Fig. 1. (A) TEM image of SPIONs-loaded PLGA NPs and **(B)** Confocal microscopy of NPs conjugated with BBBpS and internalized in BEC. Nuclei are stained with Hoechst (blue), labeled NPs appear in yellow and labeled BBBpS appear in red.

CONCLUSION

We have successfully synthesized magnetic-polymeric nanoparticles tailored with a BBBpS for brain uptake. Morphological and stability characterization allowed us to move for *in vitro* evaluation of NPs through flow cytometry and fluorescence microscopy where we could find that NPs-BBBpS conjugation improves brain cells uptake. We will further test these NPs in *in vitro* models of the BBB and *in vivo* brain uptake with the purpose of supporting those novel hybrid nanoparticles as a new strategy for brain drug delivery.

REFERENCES

1. Chaparro C, *et al.*, 6th IEEE Port. Meet. Bioeng. ENBENG 2019 - Proc., 2019
2. Neves V, *et al.*, ACS Chem. Biol. 12, 1257-1268, 2017
3. Kandasamy G, *et al.*, J. Mol. Liq. 293:1-16, 2019

ACKNOWLEDGMENTS

This work is funded by FEDER funds through the COMPETE 2020 Program and National Funds through FCT—Portuguese Foundation for Science and Technology under the project POCI-01-0145-FEDER-007688 (Reference UID/CTM/50025), and by Grants Nos. SFRH/BD/148588/2019 and PTDC/BTM-MAT/2472/2021 funded by the Portuguese Funding Agency, FCT IP.

Milk-Derived Extracellular Vesicles for siRNA Delivery into Intestine Mimicking Caco-2 Cells

Josepha Roerig[1*], Franziska Mitrach[1], Maximilian Schmid[1,2],
Michael C. Hacker[1,2], Christian Wölk[1], Michaela Schulz-Siegmund[1]

[1]Pharmaceutical Technology, Institute of Pharmacy, Medical Faculty, Leipzig University, Germany
[2]Institute of Pharmaceutics and Biopharmaceutics, Heinrich-Heine-University Duesseldorf, Germany
[*] josepha.roerig@medizin.uni-leipzig.de

INTRODUCTION

Extracellular vesicles (EVs) are cell-derived nanostructures, which gain increasing interest for their role as natural RNA carriers. We would like to exploit EVs for the oral delivery of therapeutic RNA. Therefore, EVs must fulfill: (1) stability in the gastrointestinal system, (2) bioavailability, and (3) loading with RNA.

We have chosen bovine raw milk as a source for EVs, as these survive the harsh conditions of the gastrointestinal system[1]. To assess the suitability of EVs for oral RNA delivery further, this work aims to study EV uptake and transport across the intestinal barrier *in vitro*. Currently, low RNA loading efficiencies limit the therapeutic use of milk EVs. Therefore, we explore novel strategies to load EVs with siRNA and test the functional siRNA delivery in Caco-2 cells.

EXPERIMENTAL METHODS

EV Isolation and Analysis

Raw milk was centrifuged and loaded onto a Sephacryl S-500 (Cytiva, USA) column. The presence of EVs was evaluated by antibody detection of marker proteins, electron microscopy, and nanoparticle tracking analysis.

EV and Liposome Uptake into Caco-2 Cells

Enterocyte-like Caco-2 cells were incubated with stained EVs (5 µM Vybrant DiO, 20 µM CellTrace CFSE, or 10 µM SYTO®). For comparison with liposome uptake, cells were incubated with the same particle number of DPPC-Chol (70/30 mol/mol) liposomes. Cell uptake was analysed by confocal microscopy (Leica, Germany).

EV Transport across the Caco-2 Monolayer

Caco-2 cells grown on 3 µm PET inserts were used for transport studies. Stained EVs were added to the donor compartment and fluorescence measured in the acceptor compartment to calculate the transport rate (P_{app}).

siRNA Loading and Functional Delivery

Fusion with non-cationic liposomes, dehydration-rehydration, and dual asymmetric centrifugation were compared for EV loading with either siRNA complexed with calcium phosphate nanoparticles[2] or free siRNA. Encapsulation efficiency and loading capacity were calculated using fluorescently labelled siRNA (Quiagen, Netherlands). To test the functional delivery in Caco-2 cells, AllStars Hs Cell death siRNA (Quiagen, Netherlands) was used instead. Cell viability was measured three days after transfection using RotiTest® Vital (Roth, Germany).

RESULTS AND DISCUSSION

Milk EVs were isolated using size-exclusion chromatography and analysed according to the MISEV2018 guidelines[3]. Cell uptake was compared to liposomes (DPPC/Chol) in intestinal cells. Three different EV labelling approaches showed comparable results by microscopic evaluation after 15 min to 6 hours, indicating a fast EV internalization into Caco-2 cells (Fig. 1, white arrows). Liposomes rather remained attached to the cell surface (Fig. 1, blue arrows). As well, the EV transport rate across the Caco-2 barrier was quantified as $P_{app} = 2.4 – 6.5 \cdot 10^{-6}$ cm/s.[4]
Strategies to load EVs were adapted from liposome loading including fusion, dehydration-rehydration, and dual asymmetric centrifugation. Cationic transfection reagents that alter the EV membrane were avoided. Loading efficiencies were sufficient to functionally deliver siRNA. As a proof-of-concept, cell-death siRNA decreased the cell viability of Caco-2 cells dose-dependently.

CONCLUSION

In conclusion, size-exclusion chromatography offers a reproducible method to isolate milk-derived EVs. The fast uptake of EVs in intestinal Caco-2 cells as well as their beneficial properties compared to liposomes make them promising for oral drug delivery purposes. The systematic investigation of siRNA loading approaches and the functional siRNA delivery in Caco-2 cells will set a basis to further investigate milk EVs for oral delivery of therapeutic nucleic acids.

REFERENCES

1. Grossen P. *et al*. Eur J Pharm Biopharm 158:198-210, 2021
2. Mitrach, F. et al. Pharmaceutics 14(2):326, 2022
3. Théry, C. *et al*. J Extracell Vesicles 1:1535750, 2018
4. Roerig J. *et al*. Eur J Pharm Biopharm 166:61-74, 2021

ACKNOWLEDGEMENTS

We are grateful to C. Vissiennon and L. Schiller (Medical Physics and Biophysics, Leipzig) for their expertise with Caco-2 cells, to H. Kalwa (Clinical Pharmacology, Leipzig) for access to CLSM imaging, and to G. Hause (Biozentrum, Halle) for the TEM images.

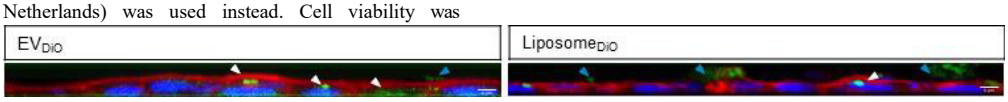

Figure 1. z-stacks of Caco-2 cells incubated with DiO (green) labelled EVs (left) and liposomes (right) are shown.

Influence of the structure of regioselectively oxidized polysaccharides on the anticancer-drug delivery

Lukáš Münster,[1*] Zdenka Capáková,[1] Ivo Kuřitka[1], Jan Vícha,[1]

[1]Centre of Polymer Systems, Tomas Bata University in Zlín, Zlín, Czech Republic.
[*]munster@utb.cz

INTRODUCTION

Polysaccharides have been investigated as potential anticancer-drug carriers due to their natural origin, biocompatibility and large potential for modifications.[1] They are however notoriously known for their structural diversity and lack of suitable functional groups, which complicate their drug delivery capability. Regioselective oxidation of polysaccharides to corresponding dicarboxy polysaccharides (DCPs)[2–4] provides a unique opportunity to remedy this issue. Sequential periodate/chlorite oxidation introduces two –COOH groups per each oxidized unit, which are capable to conjugate platinum(II) complexes, while preserving the main structural features of source polysaccharides intact. Hence, we performed selective two-stage oxidation of four structurally different polysaccharides (cellulose, dextrin, dextran and hyaluronate), loaded them with the equivalent amount of cisplatin (CP), and compared their properties as drug carriers. Fig. 1 shows the structures of source polysaccharides and corresponding DCPs.

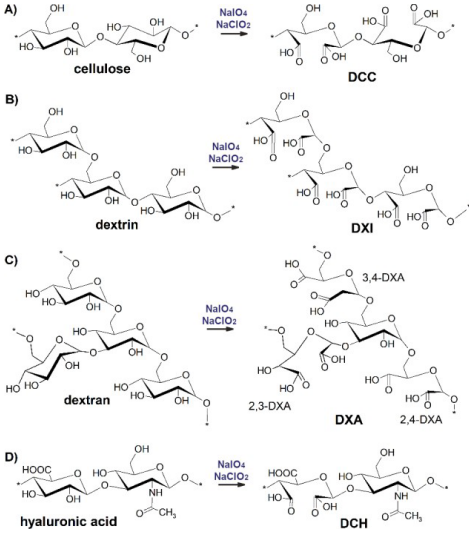

Fig. 1 Structures of investigated polysaccharides and their respective dicarboxy derivatives.

EXPERIMENTAL METHODS

Cellulose, dextrin, dextran (Sigma Aldrich, Co.), and sodium hyaluronate (Contipro, Czech Republic) were regioselectively oxidized by periodate at C2 and C3 (primary oxidation), and formed –CHO groups were converted to –COOH by chlorite (secondary oxidation). Prepared derivatives were characterized (NMR, GPC, FT-IR, DFT etc.), loaded with CP, and compared in the terms of drug loading efficacy, carrier capacity, drug release rates, cellular uptake and cytotoxicity against malignant (MCF-7) and healthy (NIH/3T3) cell lines.

RESULTS AND DISCUSSION

i) The drug loading capacity and binding efficacy depend on –COOH group density in the carrier structure.
ii) The drug loading efficacy is mainly affected by the conformation of binding sites determining the mode of drug binding (bidentate vs monodentate).
iii) The mode of drug binding governs the release kinetics (monodentate binding - faster release of CP-DXA, see Fig. 2 A). The higher carrier molecular weight and branching reduce the initial release rate.
iv) Polysaccharides composed of oxidized glucopyranose units have similar cytotoxicity, while the carrier based on hyaluronate is considerably less cytotoxic.
v) The main structural factors influencing the cytotoxicity of the CP-carrier conjugates are bidentate binding and branching.
vi) The cellular uptake of platinum from conjugates roughly correlates with the drug release kinetics and is also influenced by the CD44 expression (see Fig 2 B).

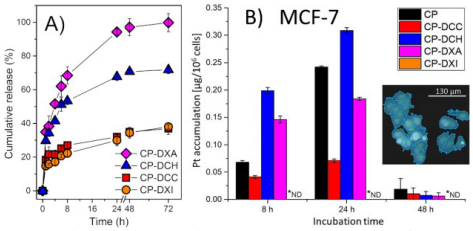

Fig. 2 A) CP release; B) MCF-7 CP cellular uptake.

CONCLUSION

The oxidized cellulose (DCC) was found to be the most cytotoxic of all compounds tested, including free CP. The oxidized hyaluronate (DCH) showed the highest accumulation in cancer cells, which was correlated to the expression of CD44 receptors. Both derivatives are thus excellent candidates for further research.

REFERENCES

[1] G. Huang et al., *Curr. Pharm. Des.* **2015**, *21*, 3692–3696.
[2] K. Khomyakov et al., *Polym Sci U.S.S.R.* **1965**, *7*, 1140–1145.
[3] J. A. Sirviö et al., *Carbohydr Polym* **2014**, *114*, 73–77.
[4] L. Münster et al., *Carbohydr Polym* **2021**, *257*, 117562.

ACKNOWLEDGMENTS

This work was supported by the OP RDE project The Development of Capacity for Research and Development of TBU in Zlín CZ.02.2.69/0.0/0.0/16_028/0006243 and by the Ministry of Education, Youth and Sports of the Czech Republic project DKRVO RP/CPS/2022/007.

Self-assembling amphiphilic cyclodextrin-based nano-sized delivery systems for hydrophobic drugs

Sarah Vogel-Kindgen[1*], Felix Brettner[1], Maike Windbergs[1]

[1]Institute of Pharmaceutical Technology, Goethe-University Frankfurt, Frankfurt am Main, Germany
[*] vogel-kindgen@em.uni-frankfurt.de

INTRODUCTION

Encapsulation of drugs into nano-sized drug delivery systems (DDS) has intensively been investigated as a promising strategy to improve the treatment efficacy of severe diseases. DDS do not only have the potential to protect drugs from biodegradation, to improve their solubility and to control the release, but may also be designed to overcome biological barriers or to target specific tissues and cells to enhance the drugs` therapeutic efficacy. However, encapsulation of hydrophobic drugs into nano-sized DDSs is challenging. Naturally occurring cyclodextrins (CDs) are cyclic oligosaccharides obtained by the enzymatic digestion of starch, constituting biomaterials approved by the Food and Drug Administration (FDA) and commonly used for pharmaceutical applications. They have been shown to increase drug solubility and stability, control drug release, enhance drug absorption, and improve drug permeation through biological barriers. Grafting aliphatic chains onto natural CDs renders them amphiphilic and enables the self-assembly into nano-sized DDSs. Amphiphilic CD derivatives are usually prepared by aminations, esterifications or etherifications of primary and secondary hydroxyl groups of the natural CDs. Thus, a wide variety of derivatives can be obtained depending on the choice of linker and grafted aliphatic chain.
In this study, we synthesized a library of amphiphilic CD derivatives and investigated the influence of CD chemical structure on self-assembly and encapsulation of a pharmaceutically challenging model drug with low aqueous solubility and low permeability.

EXPERIMENTAL METHODS

A library of amphiphilic CD derivatives was synthesized (Scheme 1) starting from natural β-CD. Substitution and purity of the derivatives was assessed by mass spectrometry, nuclear magnet resonance spectroscopy and attenuated total reflection infrared spectroscopy.

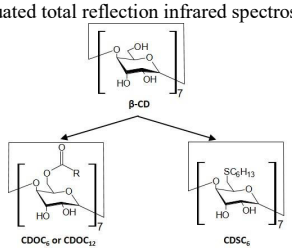

Scheme 1: Synthesis routes of amphiphilic CD derivatives.

Drug-free and drug-loaded self-assembled nanocarriers were prepared by nanoprecipitation of a solution of the CD derivatives in organic solvent into aqueous solution. For drug-loaded carriers, CD derivatives and the model drug were co-dissolved in the organic solution. Formulations were characterized in terms of surface morphology, size distribution, surface charge, and encapsulation efficiency. Cytotoxicity of CD formulations was evaluated using human monocytes.

RESULTS AND DISCUSSION

All amphiphilic CD derivatives were obtained with yields >70% and successful syntheses were confirmed by ^{1}H-NMR and ^{13}C-NMR. The introduction of the aliphatic chains enhanced the amphiphilic properties of the natural CDs and enabled the self-assembly into uniform and stable nanocarrier systems (Fig. 1A and B). The hydrophobic model drug was successfully encapsulated into the nanocarriers with encapsulation efficiency between 60 and 85%, depending on the individual CD derivatives (Fig. 1C).

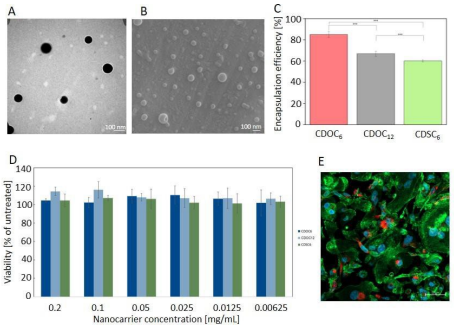

Figure 1: Transmission electron (A) and scanning electron (B) micrographs of amphiphilic CD nanocarriers. Encapsulation efficiency of the model drug into CD nanocarriers (c). Cell viability of monocytes after treatment with nanocarriers (D). Cellular uptake of CD nanocarriers (E) (blue: cell nuclei, green cell cytoskeleton, red nanocarriers).

Most importantly, amphiphilic CD derivatives were non-toxic for human monocytes (Fig. 1D) and were taken up by the cell in high quantities (Fig. 1E).

CONCLUSION

Based on their versatile chemistry, amphiphilic CDs provide a platform for designing self-assembling nanocarriers with tailor-made control over physicochemical properties and drug encapsulation. Thus, amphiphilic CD derivatives pose a high potential to become potent carrier systems for a wide variety of drugs associated with delivery challenges so far.

ACKNOWLEDGMENTS

The authors would like to thank the German Federal Ministry for Education and Research (Grant no: 03ZU11096A) for providing financial support to this project.

Design of a biodegradable bone cement for the treatment of bone fractures induced by breast cancer metastases

Orlane Jouanneau[1*], Marilyn Kajdan[2], Carole Barou[1,2], Vincent Cavaillès[2], Mikhael Bechelany[1]

[1]Institut Européen des Membranes, IEM, UMR 5635, Univ Montpellier, ENSCM, CNRS, 34730 Montpellier, France
[2]Institut de Recherche en Cancérologie de Montpellier, IRCM, U1194, INSERM, Univ Montpellier, ICM, 34298 Montpellier, France
* orlane.jouanneau@gmail.com

INTRODUCTION

During the development of a primary tumor, malignant cells undergo a series of genetic and epigenetic changes. These changes allow cancer cells to enter into the systemic circulation (blood or lymph vessels) and eventually find another site where cell implantation and growth is promoted. This is the origin of cancer metastasis. In the case of breast cancers, a large proportion (20 to 30%) lead to bone metastases[1], which weaken the bone tissue and increase the risk of fractures. When a fracture occurs, a bone substitute material is used to fix the damaged tissue and to provide a mechanical support.

In the present work, we aim to introduce in the material an anticancer agent (ACA) able to block the proliferation of metastatic breast cancer cells and to stimulate bone formation. The bioavailability of the ACA chosen being low due to its poor water-solubility, high doses of the agent need to be administrated increasing the risk of side effects.

The main objective of this work is to develop and characterize a new biodegradable cement having the potential to improve drug targeting and mechanical properties by the addition of functionalized polymer-based nanofibers fibers. Indeed, fibers are characterized by a high specific area leading to a high assimilation of drugs presenting poor-solubility.[2]

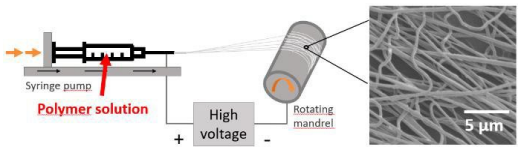

Figure 1. Schematic representation of the electrospinning process and SEM images of electrospun nanofibers.

EXPERIMENTAL METHODS

Biopolymer-based ACA loaded nanofibers were fabricated by electrospinning (Figure 1), which presents many advantages (inexpensive, easy to use, and high production yields). These nanofibers were incorporated homogeneously within the solid mineral phase at different ratios. Rheological properties (setting time, injectability, etc.) and physicochemical properties (cohesiveness, etc.) were evaluated. More specifically toughness of the fiber-reinforced cement was evaluated using a standard three-point flexural test after immersion in PBS for 72h. The kinetics of *in vitro* drug release from the fibers was evaluated by UV-spectrometer.

RESULTS AND DISCUSSION

The surface morphology of electrospun nanofibers is represented in **Figure 1**. SEM images showed that bead-free, well defined and uniform fibrous nanofibers were obtained. After crushing at a microscopic scale, the electrospun fibers were integrated at different ratios into the mineral phase. No significant changes on the setting time and chemical composition (XRD analysis) of the cement were observed. At a low weight fraction, fibers improved the toughness of the cement by more than 3-fold without compromising their rheological and physicochemical properties.

Figure 2 showed the profile of the *in vitro* ACA release from the loaded nanofibers. A burst release was observed on the first days; this is due to the drug adsorption on the surface of the fibers. It was followed by a slower and sustained released over 8 weeks. Incorporation of fibers into the cement matrix should provide a better drug-controlled release over a longer period.

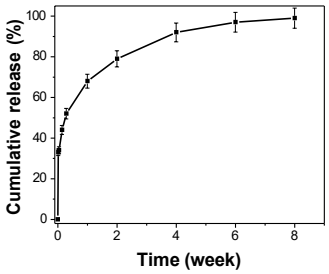

Figure 2. *In vitro* release kinetics of the ACA drug loaded into nanofibers.

CONCLUSION

This work shows the great potential of functionalized fibers-reinforced cement to overcome their brittleness. An ACA was successfully incorporated into electrospun nanofibers providing a drug delivery over 8 weeks. A study in order to characterize drug release over the cement is in progress.

In vitro cytocompatibility is ongoing to evaluate the efficiency of the biomaterial using two human cell lines i.e. MCF-7 breast cancer cells and hFOB 1.19, fetal osteoblast.

REFERENCES

1. Pulido C. *et al*., Ecancermedicalscience, 715, 2017.
2. Dzierzkowoska E. *et al*., Engineering of Biomaterials 149, *10-14*, 2019.

ACKNOWLEDGMENTS

The authors would like to thank Occitanie région for providing financial support to this project.

Localization of Oral Device Solid Tablet Deposition in Canine and Human Gastric Ex Vivo Tissues

Kristina Rivera[1], Maria Pereverzina[1], Mette Poulsen[1], Lise Lotte Gluud[2], Drago Sticker[1], Stephen Buckley[1]

[1]Novo Nordisk A/S, 2760 Måløv, Denmark [2]Hvidovre Hospital, 2650 Hvidovre, Denmark

INTRODUCTION

Large molecules, such as proteins and peptides, must be delivered subcutaneously or intravenously to enable absorption and achieve a relevant therapeutic dose. Treatment for chronic diseases, such as Rheumatoid arthritis, Hemophilia, and Diabetes, require monthly, weekly, or multiple injections per day of biologics. Apart from chronic illnesses, administration via hypodermic needles is also necessary for vaccines and steroid treatments. To alleviate the need for needle injections, a platform technology was previously developed as an ingestible self-orienting millimeter-scale applicator (SOMA) oral device that facilitates either solid or liquid active pharmaceutical ingredient (API) delivery into the bloodstream via the gastric tissue wall[1,2]. Currently, the SOMA is being used in preclinical studies to define appreciable solid API deposition inside the gastric epithelium. As part of the preclinical evaluation of injectable API tablet efficacy for drug delivery, we generated a novel method to investigate solid tablet delivery into canine and human ex vivo gastric tissues from API loaded oral devices.

EXPERIMENTAL METHODS

Gastric tissues were isolated from cadaver canine stomachs, and human stomach biopsies were collected from patients undergoing sleeve gastrectomy for weight loss that would otherwise be routinely discarded. Solid tablets were compressed from a mixture of 1% carbon black nanoparticles mixed with sorbitol powder. After assembling the oral device with the black tablets, canine and human gastric pieces were dissected from same-day isolations and devices were activated on small tissue samples (**Fig. 1**). Following device activation, tissues were frozen in minus 20°C for approximately 30 minutes, before large (0.5 mm) tissue sections were obtained using a tissue trimming microtome blade. Brightfield microscopy was used to review each tissue section.

RESULTS AND DISCUSSION

The location of the tablet containing carbon black was found within the tissue sections, and a representative image was collected for each tablet deposition (**Fig. 2**). The images were processed to analyze the carbon black tablet location within each gastric tissue layer and compare penetration depth for each parameter changed within each oral device design. We generated new data showing successful solid tablet delivery into the submucosal space within gastric tissue layers in both canine and human ex vivo samples.

CONCLUSION

This method of rapid histology allows for new iterations of oral devices to be tested on relevant gastric tissues with same day image turnaround. Rapid histology avoids the need for long histological processing times. Identification of the tablet location within the gastric tissue layers confirms both successful device functionality and API delivery via penetration of the outer wall (epithelium). Knowledge of ex vivo tissue tablet delivery location can potentially be used to predict drug delivery success in preclinical in vivo studies and, furthermore, accelerate optimization cycles for intragastric drug delivery.

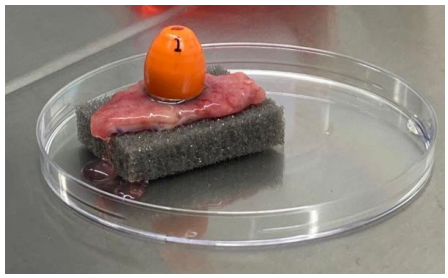

Figure 1. SOMA device activation on ex vivo human gastric tissue sample.

Figure 2. Canine gastric tissue with tablet containing carbon black inside submucosal space following rapid histology sectioning and imaging.

REFERENCES

1. Abramson, A., *et al.*, Nat. Biotechnol., 40: 103-109, 2022
2. Abramson, A., *et al.*, Science, 363: 611-615, 2019

ACKNOWLEDGEMENTS

KR, MP, MP, DG, and SB are employees of, and this work was supported by, Novo Nordisk A/S.

Luminescent Silica Nanoparticles for Monitoring Drug Delivery

Grace Ball[1*], Menisha Manhota[1], Asier R. Muguruza[1], Maria Odyniec[1], Sarah Keuhne[2], Damien Walmsley[2], Zoe Pikramenou[1]

[1]School of Chemistry, University of Birmingham, Birmingham, UK
[2]School of Dentistry, University of Birmingham, Birmingham, UK

[*]gxb194@student.bham.ac.uk

INTRODUCTION

Improving drug delivery systems is an integral part in combatting disease particularly cancer and infections where drug doses are ineffective for different mechanisms of action, notably traditional chemotherapeutic agents present poor specificity and off-target toxicity. Antibiotic resistance also presents a huge problem in todays' society, where worldwide approximately 1.27 million people die annually due to bacterial infections that are resistant to antibiotics.[1] Nanomaterials provide a scaffold for attachment of multiple agents for drug delivery but also for detection to track delivery. Improvement in drug delivery using nanomaterials can be attributed to a greater site-specific delivery and controlled release of the drug which can decrease the required dose.
Our approach is to use nanoparticles with luminescent metal complexes for detection due to their unique properties including photostability and long luminescence lifetimes for detection.[1,2] We have used nanoparticles to also carry the drug either by attachment[3] or encapsulation.[4]

EXPERIMENTAL METHODS

1) Development of luminescent metal complexes for attachment onto nanoparticles 2) One pot nanoparticle synthesis with encapsulated drugs 3) Monitoring drug release using spectroscopic and analytical methods

RESULTS AND DISCUSSION

Development of ruthenium and iridium complexes for attachment and inclusion to silica nanoparticles has previously allowed tracking of nanoparticles in flow.[5] We have now introduced a method of encapsulation of antimicrobial agents into the silica framework. Developed particles present a non-mesoporous network, preventing unwanted drug leakage that can be seen in traditional mesoporous silica nanoparticles. Particles allowed simultaneous antimicrobial release and luminescent tracking in bacterial cells.

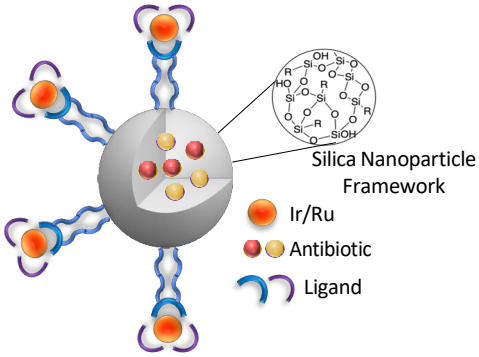

Figure 1: Depiction of silica nanoparticles with encapsulated antibiotics and grafted luminescent metal complexes on the surface

CONCLUSION

Silica nanoparticles are ideal for triggered release of antibiotics, allowing site specific release, whilst detection using luminescent metal complexes allows local detection and spatialisation of the agents.

REFERENCES

1. Antimicrobial Resistance Collaborators, Lancet, 2022, 399, 629-655
2. A. N. Dosumu, S. Claire, L. S. Watson, P. M. Girio, S. A. M. Osborne, Z. Pikramenou, and N. J. Hodges, JACS Au, 2021, 1, 174-186
3. S. M. King, S. Claire, R. I. Teixeira, A. N. Dosumu, A. J. Carrod, H. Dehghani, M. J. Hannon, A. D. Ward, R. Bicknell, S. W. Botchway, N. J. Hodges, and Z. Pikramenou, J. Am. Chem. Soc., 2018, 140, 10242-10249
4. A. B. Caballero, L. Cardo, S. Claire, J. S. Craig, N. J. Hodges, A. Vladyka, T. Albrecht, L. A. Rochford, Z. Pikramenou, and M. J. Hannon, Chem Sci., 2019, 10, 9244-9256
5. D. J. Lewis, V. Dore, N. J. Rogers, T. K. Mole, G. B. Nash, P. Angeli, and Z. Pikramenou, Langmuir, 2013, 29, 14701-14708

ACKNOWLEDGMENTS

The authors would like to thank the EPSRC (SONATA project, GB, MO), Sci-Phy DTC (MM), MIBT (AM) for providing financial support to this project

In vitro study of poly(lactic acid) block copolymers with poly(hexylene succinate) as microparticles for long-acting injectables of risperidone drug

Iouliana Chrysafi[1*], Stavroula Nanaki[2], Eleni Pavlidou[1], Dimitrios N.Bikiaris[2]

[1]Department of Physics, Aristotle University of Thessaloniki, Thessaloniki, Greece
[2]Department of Chemistry, Aristotle University of Thessaloniki, Thessaloniki, Greece
[*] iochrysa@physics.auth.gr

INTRODUCTION

Long Acting Injectables (LAIs) are drug delivery systems that are administered intramuscularly, creating a "depot" of drug, which is released at a controlled rate. As a result, the needed concentration of the drug is available in the human body. Poly (lactic acid) and specifically poly(glycolic acid) are used in medicine due to their biocompatibility and non-toxicity[1]. PLGA is currently used in the commercial form of risperidone drug delivery system, but its slow hydrolysis (7-8 days until the start of its release) is a major disadvantage. Therefore, during the first week of administration, co-administration of risperidone tablets is required to achieve the desired concentration of the drug[2]. In order to overcome those disadvantages, new poly(lactic acid)/poly(hexylene succinate) (PLA-b-PHSu) block copolymers were synthesized in different PLA/PHSu ratios[3] as matrices for the encapsulation and delivery of risperidone. PHSu is a promising non-toxic, biodegradable, and biocompatible polyester that will enhance the desired properties of PLA. In this work, risperidone loaded microparticles were formed by spray-drying, and their in vitro study was held. Moreover, the structure and the surface of the prepared microparticles were studied by Scanning Electron Microscopy.

EXPERIMENTAL METHODS

Microparticles were prepared by spray-drying with a Mini Spray-Dryer B-290. The solutions for spray-drying were obtained by completely dissolving 5 g of each polymer and 0.85 g of Risperidone in 200 mL of dichloromethane (DCM). For the in vitro release studies, a Distek Dissolution apparatus was used, equipped with an autosampler, using the basket method. Microparticles, placed into suitable dialysis tubing cellulose, were inserted into the dissolution baskets, while the dissolution analysis was performed at 37 ± 1 °C with a rotation speed of 50 rpm. At predefined time intervals, 2 mL of aqueous solution was withdrawn from the release media and analyzed for risperidone content by HPLC. The drug loading and the drug entrapment efficiency of microspheres were calculated. Risperidone content was assayed using a Shimadzu Prominence HPLC system. Chromatographic analysis was performed with a C18 column at 25 °C. The structure of the synthesized microparticles and risperidone was observed by Scanning Electron Microscopy (SEM). Microphotographs were taken from the surface area with a Scanning Electron Microscope from Jeol.

RESULTS AND DISCUSSION

Microparticles were prepared by spray-drying and SEM microphotographs revealed their spherical shape. The microparticles exhibited sizes ranging between 5 and 12 μm, while their surface showed pores attributed to the rapid evaporation of the solvent. Although the drug loading is decreased as the content of PHSu increases, it is considered high enough due to the smaller size of microparticles compared to other studies[4]. The copolymers presented increased entrapment efficiency (EE) (73.16%) compared to the one from typical o/w procedure (36.51%) because the formed microparticles during spray-drying are not subjected to other processes, while EE decreases as the content of PHSu increases. As for the dissolution study, the release of risperidone takes place in two stages; the initial burst is due to the pore formation on the microparticles' surface, while the controlled release is attributed mainly to the diffusion of risperidone between the formed channels. PLA-b-PHSu90/10 and 80/20 microparticles showed enhanced release profiles reaching 90 and 100% release in 15 and 12 days respectively (Figure 1).

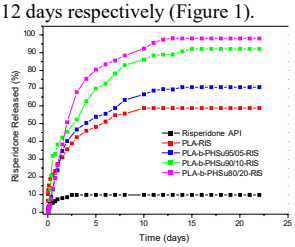

Figure 1. Dissolution rate of Risperidone from prepared microparticles.

CONCLUSION

PLA-b-PHSu microspheres containing risperidone have been successfully prepared by spay-drying with their structure being confirmed by SEM. The drug loading and the entrapment efficiency decreased, as the content of PHSu in the copolymers increased. Concerning the risperidone release, as the content of PHSu increased, a higher percentage of RIS was released, with PLA-b-PHSu80/20 releasing 100% of RIS after 12 days.

REFERENCES

1. E. Balla et al., Polymers (Basel). 2021;13(11):1822-1872.
2. S. Nanaki et al., Pharmaceutics. 2018;10(3):130.
3. I. Chrysafi et al., Thermochim. Acta, vol. 698, no. November 2020, p. 178883, 2021.
4. S. Nanaki et al. J Pharm Sci. 2018;107(11):2891-2901.

Silk fibroin based dexamethasone and cannabidiol delivery systems

Andra Grava[1,2], Arita Dubnika[1,2]

[1]*RTU Rudolfs Cimdins Riga Biomaterials Innovation and Development Centre, Faculty of Materials Science and Applied Chemistry, Riga Technical University,*
[2]*Baltic Biomaterials Centre of Excellence, Headquarters at Riga Technical University, Riga, Latvia*
* andra.grava@rtu.lv

INTRODUCTION

Modern biomaterials are becoming increasingly complex to meet a number of properties. A combination of silk fibroin (SF) and calcium phosphate (CaP) have several benefits for bone regeneration[1]. The composite consists of organic and inorganic phase, which mimics the natural bone. By adding gelatin (G) and horseradish peroxidase (HRP)/ hydrogen peroxide (H_2O_2) a hydrogel can be created[2]. These hydrogels can be a matrice for development of sodium dexamethasone phosphate (DEX) and cannabidiol (CBD) novel drug delivery systems. DEX improves bone regeneration and prevents inflammation[3], however CBD has anti-oxidant, anti-inflammation and pain relief properties [4].The aim of this study is to compare various compositions of SF/CaP as well as two different drug loaded hydrogel effect on cell viability.

EXPERIMENTAL METHODS

The first step to hydrogel preparation is SF/CaP *in situ* synthesis. In 10 mg/mL SF CaO is suspended and 2M H_3PO_4 is added dropwise till the pH reaches 6 and 10. Gelatin (G) is added to the fresh slurry and set aside to bloom. The mixture is then heated at 70°C until G dissolves. 1 mL of suspension is transferred to 24 well plate for hydrogel preparation, where 5 mg of DEX is added. To crosslink the hydrogel, HRP and H_2O_2 is mixed in via pipetting. The prepared samples are put in the incubator at 37°C for 5 days. Obtained samples are frozen and lyophilized for 72h. Structure and morphology of the hydrogels was tested. Furthermore, drug loaded hydrogel effect on cell viability was evaluated.

Prior to indirect cytotoxicity tests, lyophilized DEX samples were sterilized at 105°C in an autoclave. Hydrogels with CBD were prepared by immersing the hydrogel in 10 µM CBD/ethanol solution for 2 hours. One whole sample was put in 5 mL full cell medium. Extracts were completely taken off after 6h, 24h and 48h and diluted to 1:10 and 1:100, which were applied on 3T3 mouse fibroblast cells after incubation of freshly seeded cells overnight. For analysis the dilutions were left on cells for 24h after each time point. The cell viability was tested with Neutral red assay (NR).

RESULTS AND DISCUSSION

The obtained cytotoxicity results with NR test show that none of the hydrogels with or without drugs are cytotoxic. Dilutions of the extracts obtained after 6 hours at pH6 showed a higher cell viability for the hydrogel synthesized with DEX (89%-92%) than for the hydrogel with CBD (75%-78%), whereas at pH 10, CBD (80%-112%) showed a slightly higher cell viability than DEX (101%-103%). After 24h and 48h the cell viability increases above 100%, which indicates that the drug loaded system increases cell proliferation. SEM images of DEX loaded hydrogels with hydroxyapatite are shown in figure 1. On the surface of the hydrogel, hydroxyapatite is formed, which increases water absorption[5].

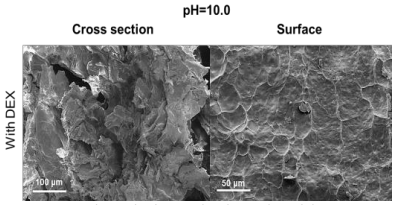

Fig. 1. SF/CaP/G/HRP hydrogels with DEX.

The swelling degree for SF/CaP/G/HRP hydrogels with HAp (pH10) showed high swelling degree - 956.3 % (4 hours), on the other hand hydrogel with HAp/brushite mix (pH6) started to degrade after 1 hour and swelled for 99.5%. Gel fraction (GF) results showed that hydrogel with pure HAp (pH10 had the highest – 107.23% ± 25.69% GF, however HAp/brushite containing matrix (pH6) insoluble material part was only 56.41% ± 12.13%.

CONCLUSION

In situ synthesized and enzymatically crosslinked hydrogels have a high potential of becoming novel scaffolds for bone regeneration due to their similarity to natural bone. *In vitro* results show that the obtained hydrogels are not cytotoxic after 48-hour tests and can even increase cell proliferation with DEX and CBD. Further studies on hydrogel effect on osteoblasts growth should be conducted to evaluate the designed matrix potential in bone regeneration.

REFERENCES

1. Zakharov et al., *Inorg. Mater.* **2017**, *53* (3), 333–342. https://doi.org/10.1134/S0020168517030128.
2. McGill et al., *Acta Biomater.* **2017**, *63*, 76–84. https://doi.org/10.1016/j.actbio.2017.09.020.
3. Kim et al., **2015**, *94*, 28–40. https://doi.org/10.1016/j.addr.2015.06.003.
4. Koch et al., *Int. J. Pharm.* **2020**, *589* (August), 119812. https://doi.org/10.1016/j.ijpharm.2020.119812.
5. Varaprasad et al., *RSC Adv.* **2018**, *8*, 18118–18127. https://doi.org/10.1039/C8RA01887A.

ACKNOWLEDGMENTS

The authors thank the M-era.Net 2 project "Bioactive injectable hydrogels for soft tissue regeneration after reconstructive maxillofacial surgeries" (INJECT-BIO) under agreement No. ES RTD/2020/14 and the European Union's Horizon 2020 research and innovation programme under the grant agreement No 857287 for financial support.

Hypoxia-mimicking fibrin matrix via factor XIII catalyzed transpeptidation of deferoxamine - *a clinically translatable strategy for augmenting fracture healing*

Norein Norein[1], Ayan Samanta[2], Jöns Hilborn[3]

[1]Department of Chemistry – Ångström Laboratory, Macromolecular Chemistry, Uppsala University, Uppsala, Sweden
[2]Department of Chemistry – Ångström Laboratory, Macromolecular Chemistry, Uppsala University, Uppsala, Sweden
[3]Department of Chemistry – Ångström Laboratory, Macromolecular Chemistry, Uppsala University, Uppsala, Sweden
*norein.norein@kemi.uu.se

INTRODUCTION

A major obstacle for a successful bone union is impaired vascularization at the fracture site.[1] To increase the union rate, we designed an injectable fibrin-based hydrogel loaded with deferoxamine (DFO), a potent angiogenic stimulant. DFO induces new blood vessel formation by upregulating the HIF-1α pathway through iron chelation. However, due to its short half-life and rapid clearance, maintaining DFO at the callus site remains a challenge.

Donneys, A. *et al.* have demonstrated that DFO added to the bone defect site by direct injection or by an implantable formulation of DFO conjugated to hyaluronan matrix promotes angiogenesis and subsequent bone formation. They showed, in a radiation-treated rat mandible model, that HA-DFO treated mandibles exhibited a 91% union rate as compared to irradiated controls (20% bone union rate).[2] However, hyaluronan lacks dimensional stability and shows strong swelling in vivo.[3] Furthermore, the formulation involves toxic crosslinking chemistry and a lengthy preparation protocol.

Fibrin hydrogel is well-documented and is commercially available as a hemostatic sealant and FDA-approved tissue glue. It is also the first scaffold that a cell encounters as it performs its role in healing wounds. The fibrin network develops from three plasma components; fibrinogen, thrombin and factor XIII. Thrombin initiates the polymerization of fibrinogen to produce a fibrin matrix. Then, factor XIII, a plasma transglutaminase, stabilizes the clot structure by catalyzing isopeptide bonds between glutamine and lysine residues in the fibrin matrix. The use of N-terminal transglutaminase is a strategy pioneered by Hubbell's group and has been used to directly attach growth factors such as VEGF and BMP-2 to a fibrin backbone.[4]

We hypothesized that factor XIII would covalently attach the primary amine in DFO to the glutamine residues in the fibrin matrix through a transglutaminase catalyzed transpeptidation attachment and thereby retaining DFO in the matrix.

EXPERIMENTAL METHODS

Fibrin gels with and without DFO were prepared in transwell inserts with a 5 µm pore size. To simulate a direct injection, DFO was allowed to diffuse freely through the 5 µm pores. After polymerization and crosslinking for 10 minutes at 37°C, the inserts were placed in wells containing 1 ml saline solution (0.9%). The release rates of DFO were obtained by removing 250 µl from each well and mixing with 50 µl $FeCl_3$ (aq) to achieve a final $FeCl_3$ concentration of 3 mM. The Fe^{3+} ions are chelated by DFO and the complex has an absorbance at 430 nm. The concentration of released DFO was then determined by UV/Vis spectroscopy.

RESULTS AND DISCUSSION

Initial results show that >50% of DFO is retained in the fibrin matrix as compared to the simulated direct injection. Furthermore, soaking Fibrin-DFO in $FeCl_3$ solution visually demonstrated that DFO grafted to the matrix was able to chelate Fe^{3+}. The amount of grafted DFO was confirmed by degrading the matrix followed by UV/Vis spectroscopy.

CONCLUSION

We have developed a facile method for attaching deferoxamine to a fibrin matrix via factor XIII mediated functionalization for local iron chelation. The reduced local concentration of free iron induces the formation of new blood vessels which has been shown to augment fracture healing.

REFERENCES

1. Schenker M. *et al.,* Angiogenesis in bone regeneration. (2011)
2. Donneys, A. *et al.,* Implantable hyaluronic acid-deferoxamine conjugate prevents nonunions through stimulation of neovascularization. (2019)
3. Engstrand T. *et al.,* Alveolar bone healing accompanied by severe swelling in cleft children treated with bone morphogenetic protein-2 delivered by hydrogel. (2013)
4. Helgerson S. *et al.,* Fibrin-based biomaterials to deliver human growth factors. (2003)

Nanodelivery of Urocortin-1 as a Chondroprotective Agent against Post-Traumatic Osteoarthritis

Zara L Smith[1], Annalisa Tirella[2,3*], Paul Townsend[4], Stephen Richardson[1]

[1]Division of Cell Matrix Biology & Regenerative Medicine, University of Manchester, Manchester, UK
[2]DIII, University of Trento, Trento, Italy
3. Division of Pharmacy and Optometry, University of Manchester, Manchester, UK
[4]Faculty of Medicine and Biological Sciences, University of Surrey, Guildford, UK
[*]annalisa.tirella@unitn.it

INTRODUCTION

Post-traumatic osteoarthritis is a significant concern in today's society, accounting for 12% of all osteoarthritis presentations[1], and with increasing numbers of young people suffering from damage performed during high intensity sporting participation (ACL tears, meniscal injury, etc.)[2]. Chondrocytes subject to traumatic impact will perpetuate the opening of calcium ion channel, *Piezo1*, leading to intracellular calcium influx and eventually, cell death[3]. Urocortin-1 (UCN-1) has been shown to retain the closed conformation of *Piezo1*, preventing cell death by calcium influx[3] and therefore avoiding eventual ECM degradation that would ordinarily result in osteoarthritis. This project aims to produce the first disease-modifying osteoarthritis drug (DMOD) for the prevention of post-traumatic osteoarthritis. In this study, we aim to show the effect of successful UCN-1 controlled delivery on preserving cell viability by the reduction of intracellular calcium as a potential therapy for post-traumatic osteoarthritis.

EXPERIMENTAL METHODS

Liposomes were formulated using a 5-input microfluidics chip with 10 mg ml^{-1} DMPC/3 mg ml^{-1} cholesterol against HEPES saline buffer (pH 7.4) with/without the addition of UCN-1. Chitosan-hyaluronic acid nanocolloids were produced using 0.69 mg ml^{-1} chitosan/1.5 mg ml^{-1} hyaluronic acid. UCN-1 was added by % weight.
Characterisation of nanoparticles were performed using dynamic light scattering (DLS) and transmission electron microscopy (TEM).
Human chondrocyte cell line (C28/I2) and impacted (500 g, 4 cm) porcine cartilage explants were used for experimentation. LDH (CytoTOX, Thermo Fisher), resazurin reduction (Sigma Aldrich, UK) and live/dead (Thermo Fisher, UK) assays were performed following manufacturer's guidelines. Staining for intracellular calcium and Hoechst were both performed at 1 µM, and Biotracker ATP (Merck, UK) at 10 µM. ANOVAs with Tukey post hoc tests were used to identify significance.

RESULTS AND DISCUSSION

Parameters Yield Stable Nanoparticles
Nanocolloids showed replicable size and polydispersity index (PDI) results within groups (0-40% wt. UCN-1). Peak splitting during DLS measurements and high PDI values, indicated particle aggregation, confirmed by TEM (*Fig. 1*). Actual nanoparticles measured approximately 250 nm and 100-130 nm for nanocolloids (*Fig. 1*) and liposomes respectively (n=3).

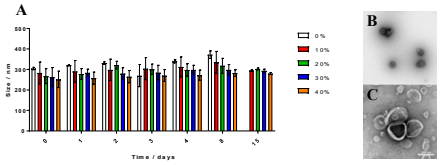

Fig. 1. TEM images of nanocolloids (B) and liposomes (C)(empty).Graph shows nanocolloid sizes over time (A).

Nanoparticles have Low Toxicity
Empty liposomes and nanocolloids were suspended in increasing ratios of suspension:media to test the toxicity of the delivery vehicles. They were delivered to C28/I2 cells and incubated as described (n=5), before testing with and LDH assay. Interestingly, cells experienced less toxicity with increasing concentrations of nanocolloid, though the opposite was true for liposomes. Neither vehicle displayed any obvious toxic response.

UCN-1 Nanodelivery to Cartilage Explants
Liposomes (25 µg ml^{-1} UCN-1) and nanocolloids (15% wt. UCN-1) were incubated with porcine cartilage explants (n=3) following traumatic impact. Explants showed higher viability when treated with nanocolloids which reduced intracellular calcium following UCN-1 delivery (*Fig. 2*).

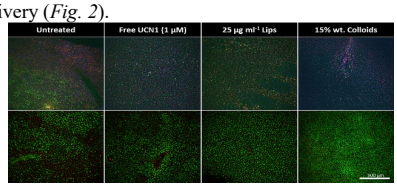

Fig. 2. Imaging of cells within porcine cartilage explants following traumatic impact. (top row) Intracellular calcium (green) and live cells (red) are displayed, and cells were counterstained with Hoechst (blue). (bottom row) viability using Live/dead staining shows live (green) and dead (red) cells. Scale bar represents 500 µm.

CONCLUSION

Traumatic impact appears to increase intracellular calcium and reduce viability, which can be avoided by the delivery of UCN-1, where nanocolloids show the most promise. This indicates the requirement for further development of UCN-1 as a DMOD.

REFERENCES

[1]Thomas AC *et al.* (2017) *J Athl Train.* **52**:491-496.
[2]Wang LJ *et al.* (2020) *Arthritis Res. Ther.* **22**:no.57.
3Lawrence KM *et al.* (2017) *Sci. Rep.* **7**(1):5147.

ACKNOWLEDGEMENTS

Funding by EPSRC/University of Manchester (EP/T517823/1) and use of CQ1 imaging system (Henry Royce Institute for Advanced Materials (EP/R00661X/1, EP/S019367/1, EP/P025021/1, EP/P025498/1)). Imaging of nanoparticles was performed by Aleksandr Mironov at the University of Manchester FBMH EM Centre.

RGD-Integrin Interactions as a Facile Approach to Tether Ligands onto the Surface of Extracellular Vesicles for Targeted Drug Delivery Applications

Antoine Karoichan[1], Maryam Tabrizian[1,2]

[1] Faculty of Dental Medicine and Oral Health Sciences, McGill University, Montreal, QC, Canada; [2] Department of Biomedical Engineering, McGill University, Montreal, QC, Canada

antoine.karoichan@mail.mcgill.ca

Introduction: Extracellular vesicles (EVs) have emerged as ideal candidates for drug delivery vectors. Secreted by almost all cells and having various important physiological functions, these membrane-bound nanovesicles offer higher biocompatibility and intrinsic bioactivity compared to synthetic nanoparticles.[1] Several proteins decorate the surface of EVs and they have been garnering increasing interest as means to drive forward the targeting and retention of EVs; such proteins can be exploited to functionalize the EVs with targeting and other functional ligands.[2] Integrins are one class of these surface proteins that have been reported common across many EVs.[3] Integrins are known to bind Arg-Gly-Asp (RGD) peptides with strong affinity, and some studies started exploring RGD-functionalized hydrogels to deliver EVs and increase their bioavailability.[3] Alternatively, this study aims to investigate the potential of functionalizing RGD-conjugated ligands to the surface of EVs through integrin binding for targeted drug delivery applications.

Methods: EVs from conditioned media of THP-1 monocytes were isolated through PEG precipitation. Isolated EVs were characterized through NTA analysis, TEM, and western blotting for EV markers CD63 and CD81. RGD conjugated gold nanoparticles (RGD-AuNP) were then formed as described by Yin *et al.* and allowed to incubate with the EVs to promote RGD-integrin binding.[4] TEM was used to observe if binding occurred. Lastly, RGD-AuNP functionalized EVs (RGD-AuNP-EVs) will be loaded with fluorescent quantum dots and added to the culture media of different cells at a concentration of $1x10^8$ particles per well of a 24-well plate. After 16h, the uptake of RGD-AuNP-EVs will be observed through fluorescent microscopy and TEM.

Results and Discussion: Preliminary isolation experiments yielded $2x10^9 \pm 10^7$ particles/mL with a mean size of 109.1 nm. This corresponded to a 13.8 µg/mL protein concentration measured by BCA assay. Negative-stain TEM demonstrated the typical "cup-shape" morphology of EVs, with their presence further confirmed by positive western blot signals for CD63 and CD81.

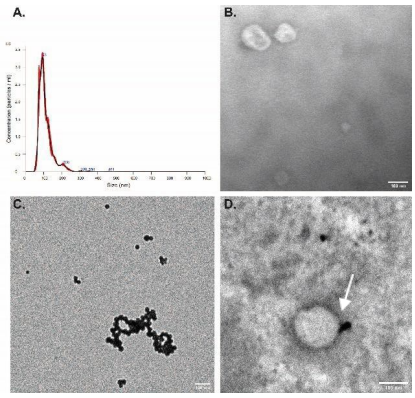

Figure 1: (A) Raw NTA data showing EVs concentration per size; (B) Negative-stain TEM image of EVs, scale = 100 nm; (C) RGD-AuNPs, scale = 100 nm and (D) Binding of RGD-AuNPs to EV surface, scale = 100 nm.

Gold nanoparticles were chosen to easily visualize and determine successful RGD-integrin interaction on the surface of EVs. After 60 minutes incubation with EVs, some of the AuNPs were observed on the surface of EVs. The current work consists of further optimizing and testing the RGD binding to the EVs surface and confirming that this binding would not affect EV uptake by various cell types, particularly by chondrocytes and osteoblastic cells for potential bone targeted applications.

Conclusion: This study offers insight into a time and cost-effective approach to functionalize EVs with targeting ligands by taking advantage of their native proteomic properties and bring them closer towards clinical use in targeted drug delivery.

Acknowledgements: The authors would like to thank the Canada Research Chair in Regenerative Medicine and Nanomedicine and CHRP for providing financial support to this project.

References: 1. Murphy D.E. *et al.*, Nano Lett. 21: 1888–1895, 2021; 2. Herrmann I.K. *et al.*, Nat. Nanotechnol. 16: 748–759, 2021; 3. Zhang C. *et al.* ACS Nano 14: 12133-12147, 2020; 4. Yin H. *et al.* RSC Adv. 4: 9078-9085, 2014

Ferrostatin-Nanotherapeutic Materials for Neurodegeneration Applications

Joshua P. Morrow[1], Zihnil Mazrad[1], Ashley I. Bush[2], and Kristian Kempe[3]*

[1]Drug Delivery, Disposition and Dynamics, Monash Institute of Pharmaceutical Sciences, Monash University, Parkville, VIC 3052, Australia
[2]Melbourne Dementia Research Centre, The Florey Institute for Neuroscience and Mental Health, The University of Melbourne, Parkville, Victoria 3052, Australia
[3]Materials Science and Engineering, Monash University, Clayton, VIC 3800, Australia
Joshua.Morrow1@monash.edu, Kristian.Kempe@monash.edu*

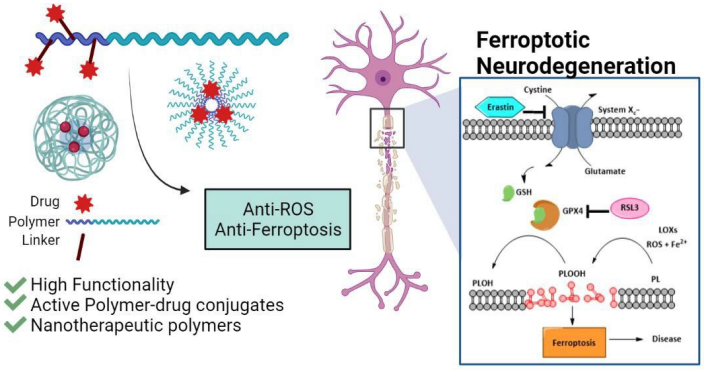

INTRODUCTION

A strong link between neurodegeneration and a form of non-apoptotic iron induced cell death pathway, ferroptosis, can be ameliorated with potent radical scavengers such as ferrostatins (Fer-1). However, currently Fer-1 suffers from low water solubility, poor biodistribution profiles and low clinical success, and to date, no Fer-1 polymer-drug conjugates to improve these qualities exist for testing as an anti-ferroptosis therapeutic. Here, we endeavour to improve ROS scavenging and drug PK profiles in vitro using a ferroptosis model cell line and report on the synthesis and characterization of a library of water-soluble Fer-1 polymer-drug conjugates (PDCs).

EXPERIMENTAL METHODS

Synthesis of the PDC nanomaterials was done by cationic ring opening polymerization (CROP) of water-soluble 2-oxazoline monomers which produced defined copolymers, with high functionality, desirable physiochemical properties and low dispersity. A number of structure property relationships were elucidated through varying components of the PDC design and tested via an AlamarBlue cell viability assay, in RSL3 induced ferroptotic rat neuron cell line.

RESULTS AND DISCUSSION

Most POx-Fer-1 conjugates were effective against RSL3-induced ferroptotic cells in vitro. Polymer chain length, choice of hydrophilic monomer, drug weight percent per polymer chain and drug linkage type to the polymer side chains were all crucial elements effecting PDC activity.

CONCLUSIONS

Our findings uncover synthetic opportunities to advance next generation anti-ferroptosis nanomaterials for as yet incurable neurodegenerative diseases.

REFERENCES

1. Masaldan, S., Bush, A. I., Devos, D., Rolland, A. S., & Moreau, C. (2019). *Free Radical Biology and Medicine*, *133*, 221-233.
2. Ekladious, I., Colson, Y. L., & Grinstaff, M. W. (2019). *Nature reviews Drug discovery*, *18*(4), 273-294.

ACKNOWLEDGMENTS

J.P.M. wishes to acknowledge the support received through the Australian Government Research Training Program. Z.A.I.M wishes to acknowledge the Monash Graduate Scholarship. K.K. gratefully acknowledges the award of an ARC Future Fellowship (FT190100572) from the Australian Research Council (ARC). A.I.B. is supported by the Australian National Health and Medical Research Council.

The bacterium *Magnetospirillum gryphiswaldense* improves the accumulation of surface-adsorbed nanoparticles into the core of 3D cancer models

Radu Alexandru Paun[1,4], Reza Rasouli[1], Daciana C. Dumut[2,4], Danuta Radzioch[2,3,4], Maryam Tabrizian[1,5]*

[1]Department of Biomedical Engineering, [2]Department of Medicine, [3]Department of Human Genetics, [4]Research Institute of the MUHC, [5]Faculty of Dentistry and Oral Health Sciences, McGill University, Montréal, Canada
* maryam.tabrizian@mcgill.ca

INTRODUCTION

Despite significant advances in nanotherapeutics, cancer remains one of the leading causes of death worldwide.[1] One of the major drawbacks of nanoparticle-mediated treatment of solid tumors remains their low accumulation (~0.7% of injected dose) and poor penetration from the circulation deep into cancerous lesions.[2] Once nanoparticles (NPs) pass the tumor endothelial barrier, only a negligible fraction of NPs is delivered to cancer cells due to limited interstitial transport further hindered by the surrounding stroma and immune cells.[3] It was shown previously that magnetotactic bacteria, using magneto-aerotaxis, can improve the intratumoral transport and distribution of NPs conjugated onto the bacterial surface via external magnetic field guidance.[4] While this could be a promising therapeutic approach for localized non-resectable cancer, it remains a limitation for late stage metastatic disease since the protocol of magnetic guidance into metastases has not yet been developed. *M. gryphiswaldense* MSR-1 is a highly motile bacterium with an unexplored potential of targeting and colonizing metastatic tumors.[5] Herein, we show that nanoliposomes (LP) can passively adsorb onto the surface of MSR-1 bacteria, which subsequently direct LP accumulation into the core of 3D tumor spheroid models.

EXPERIMENTAL METHODS

Nanoliposomes were synthesized using the ethanol injection method. A phospholipid mixture containing DSPC/DSPE-PEG$_{2000}$-COOH/CH was dissolved in absolute ethanol and injected into rapidly stirred water. Fluorescent nanoliposomes (fLP) were made by adding 1% DHPE tagged with sulforhodamine 101. The passive adsorption of LP onto the bacterial surface was performed by incubating 10^{10} LPs with 10^8 CFUs of MSR-1 bacteria in PBS at 25°C for 1 hour. SEM images were obtained after fixing the bacteria, which were then deposited onto a glass slide, dehydrated, dried at critical point, and sputter coated with Pl. Fluorescent bacteria were obtained by tagging them with DMTMM-activated rhodamine B in PBS at 25°C for at least 1 hour. 3D spheroids were obtained by culturing YUMM 1.7 cells in low-retention U-bottom 96-well plates until a compact spheroid was formed. Spheroids were treated with PBS, 10^9 fLPs, 10^7 CFU of fluorescent bacteria, or 10^9 fLPs plus 10^7 non-fluorescent bacteria. The fold change in spheroid core fluorescence intensity was calculated by normalizing the core intensity (100 µm from the edge) to the total intensity of the spheroid. All experiments were carried out independently in triplicates, and Brown-Forsythe and Welch's One-Way ANOVA with Dunnett 3T's correction was performed to assess the statistical significance between groups at 95% confidence.

RESULTS AND DISCUSSION

LPs adsorb onto the surface of bacteria (Fig. 1A-B) at approximately 100 nanoparticles per bacterium. This interaction appears stable enough to change the nanoparticles' distribution profile in a 3D melanoma spheroid model. There is an increased accumulation of fLPs into the spheroids' core (1.331-fold increase) when they are added with the bacteria versus a more concentrated signal towards the periphery of the spheroids when they are treated with fLPs alone (0.33-fold decrease, Fig. 2C-D), suggesting the bacteria can target and accumulate in the core of spheroids, and could improve drug-loaded LP delivery into tumors in vivo.

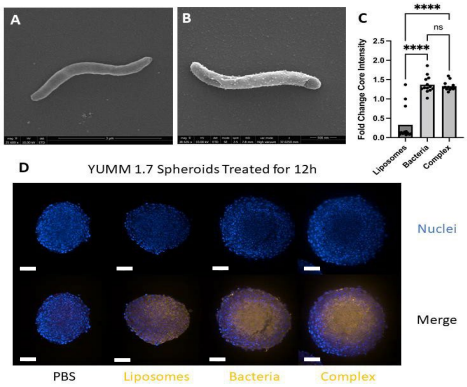

Figure 1. (**A**) SEM micrograph of bacteria in PBS and (**B**) in the presence of PEGylated nanoliposomes. (**C**) Fold change in spheroid core intensity when treated with fluorescent nanoliposomes, fluorescent bacteria, or fluorescent nanoliposomes with non-fluorescent bacteria. Points represent individual spheroids; scale bar = 100 µm; data are plotted as mean ± SD, n=13-15. (**D**) Representative confocal images of 4% PFA-fixed spheroids. Nuclei are stained with Hoechst 33342.

CONCLUSION

These results suggest that MSR-1 bacteria can effectively transport surface-bound LPs deeper into tumor tissue and point towards a potentially novel drug delivery method for the treatment of late-stage metastatic cancer.

REFERENCES

1. Ahmad F.B. *et al*., JAMA. 235(18) :1829-1830, 2021
2. Wilhelm S. *et al.* Nat Rev Mat. 1 :16014, 2016
3. Dai Q. *et al*. ACS Nano. 12(8) :8423-8435, 2018
4. Felfoul O. *et al*. Nature Nanotech. 11 :941-947, 2016
5. Benoit M. *et al*. Clin Cancer Res. 15(16) :5170-7, 2009

ACKNOWLEDGMENTS

Authors would like to thank the Canada Research Chair in Nanomedicine and Regenerative Medicine (TIPS-CRC-232667) for financial support.

Trehalose-based Nucleolipids as nanocarriers for autophagy modulation: an *in vitro* study

Anthony Cunha[1,2*], Alexandra Gaubert[1], Julien Verget[1], Marie-Laure Thiolat[2], Philippe Barthélémy[1], Laurent Latxague[1], Benjamin Dehay[2]

[1] Univ. Bordeaux, INSERM U1212, CNRS UMR 5320, ARNA, ARN: Régulations Naturelle et Artificielle, ChemBioPharm, 146 rue Léo Saignat, 33076 Bordeaux CEDEX, France
[2] Univ. Bordeaux, CNRS, IMN, UMR 5293, F-33000 Bordeaux, France
[*] anthony.cunha@inserm.fr

INTRODUCTION

The Autophagy Lysosomal Pathway is one of the most important mechanisms for removing dysfunctional cellular components. Increasing evidence suggests that alterations in this pathway play a pathogenic role in Parkinson's disease, making it a point of particular vulnerability[1]. Numerous studies have proposed nanotechnologies as a new approach for delivering active substances, such as trehalose whose neuroprotective effect has been shown to reduce proteins aggregates[2], within the central nervous system to treat and diagnose neurodegenerative diseases[3]. A promising formulation leverages the unique properties of trehalose based-nucleolipids (GlycoNucleoLipids GNL) as bioinspired therapeutic amphiphilic carriers co-formulated with biocompatible and non-toxic PLGA nanoparticles (NPs) to improve the drug protection, the targeting efficiency and the cellular internalization[4]. In addition, PLGA NPs has also demonstrated neuroprotective properties in the case of Parkinson's disease treatment[5]. In this context, the aim was to propose the development of a novel pharmaceutical technology for the treatment of neurodegenerative diseases. We designed a GNL nanosystem by combining this small natural autophagy enhancer molecule named trehalose and an amphiphilic nucleolipid conjugate.

EXPERIMENTAL METHODS

The GlycoNucleoLipids, was designed using click chemistry (CuAAC) and esterification reactions. The GNL skeleton, composed of a sugar (trehalose), a nucleoside (thymidine or adenine), and a lipidic chain, was then chemically modified to afford a GNL derivative displaying increasing polarity. NPs were prepared using the rapid mixing method and the obtained nanosystems were characterized by DLS, IR and UV. The NPs were tested *in vitro* on human neuronal cells (BE(2)-M17) using western blot analysis and immunofluorescence assays.

RESULTS AND DISCUSSION

An amphiphilic molecule, named GNL, was synthesized and formulated into two different spherical nanosystems, GNL based SLNs (120.4 ± 1.4 nm) and GNL loaded PLGA NPs (167.2 ± 2.4 nm). These nano-objects were stable for at least 20 days at 4°C and 10 days at 37°C. The successful encapsulation of GNL inside PLGA NPs was confirmed by IR and UV-Visible spectroscopies (DL 15% and EE 96%). Cytotoxicity evaluation of GNL-loaded PLGA NPs and GNL-based SLN on human neuronal cells showed that GNLs were biocompatible at low concentration after 24 h and 48h of exposure. The uptake of fluorophore-loaded PLGA NPs into cells indicated that PLGA NPs are successfully internalized, highlighting the potential of these PLGA NPs as drug delivery systems. Moreover, immunoblotting and transfection assays suggested that GNL-based nanosystems improved biological activity of trehalose (two-fold) compared to molecular trehalose, thereby significantly modulating autophagy.

CONCLUSION

These promising results suggested that GNL-based nanovectors can enhance the uptake of trehalose into neurons and thus trehalose activity. Moreover, the combination of PLGA and trehalose-based GNLs in NPs has two advantages: i) a potential synergistic action of the trehalose and PLGA and ii) vectorization of the nano-objects. Therefore, further *in vitro* studies will be carried out in a PD cellular model (M17 cells overexpressing α-synuclein or BE(2)-M17 cells with depletion of lysosomal type 5 P-type ATPase (ATP13A2)) and further characterization, in particular autophagy flux experiments associated with GNL-based nanosystems will be assessed. GNL-loaded functionalized NPs will be developed and *in vivo* assays will be performed to evaluate their ability to cross the BBB and target neurons of interest, notably in order to modulate the pH and lysosomal activity.

REFERENCES

1. Dehay B. *et al*., Mov. Disord. 28:725-732, 2013
2. Korolenko T.A. *et al*., Cells. 10:2557-2577, 2021
3. Naqvi S. *et al*., Front. Neurosci. 14:1-26, 2020
4. Cunha A. *et al*., Pharm. 13:1042-1066, 2021
5. Arotcarena M.L. *et al*., Aging Cell. 00:e13584, 2022

ACKNOWLEDGMENTS

This research was funded by Le ministère de l'Enseignement supérieur, de la Recherche et de l'Innovation (France) and by Le collège des écoles doctorales (appel doctorat interdisciplinaire 2018). This study received financial support from the French government in the framework of the University of Bordeaux's IdEx "Investments for the Future" program / GPR BRAIN_2030. This work was supported by grants from ANR-21-CE18-0025-01 NOVEL, Fondation de France (number 00066525) and an IDEX Emergence Grant number OPE-2018-410 (B.D.).

Preliminary Toxicology Studies Of Polyoxazolines Intended For Cancel Imuno-Theraphy

Bianca Palade[1], Valentin Vasile[1], Constantin Vlad Tofan[1], Catalin Tucureanu[1], Emilian Ghibu[2], Nicoleta Doriana Banu[2], Florica Adriana Jerca[2], Iuliana Caras[1], Aurora Salageanu[1], Valentin Victor Jerca [2], Elena-Diana Giol[1*]

[1]National Medico-Military Institute for Research and Development, Bucharest, Romania;
[2]Centre of Organic Chemistry "C.D. Nenitescu", Romanian Academy, Bucharest, Romania

[*]diana_giol@yahoo.com, giol.diana@canatcuzino.ro

INTRODUCTION

The aim of the present work is the developing an innovative platform for tumor drug delivery based on poly(2-isopropenyl-2-oxazoline) (PiPOx) and doxorubicin (DOX) as chemo-immuno therapeutic agent. PiPOx emerged as a novel and versatile platform to develop advanced functional materials, showing high potential to be used in the development of biomaterials. The versatility of PiPOx polymer consists in its hydrophilic, the fact that it can be synthesized with well-defined characteristics via anionic polymerization, and can be easily modified by ring opening addition reactions in the presence of various reactive groups, thus, enabling the possibility to be used to conjugate hydrophobic drugs, such as DOX, which is a well-known drug used in chemotherapy. Although previous studies have demonstrated the potential of PiPOx for these applications, the cytotoxicity and cytokine profiles of this type of polymer as a function of the molar mass has not been investigated.

EXPERIMENTAL METHODS

Cytotoxicity of PIPOx with various molecular masses was tested on L929 murine fibroblasts in 96 well-plates, following the guidelines of ISO 10993-5:2009. Life-dead and MTT assays were applied to PIPOx polymers. The cytokine profiles of TNF-α and IL-6, know pro-inflammatory markers, were investigated on RAW264.7 macrophages.

RESULTS AND DISCUSSION

In the present study PIPOx polymers of various molecular weights including 55, 90, 128, 172 and 290 mer units were synthesized and submitted to in vitro investigations. Preliminary cytotoxicity of all polymers at concentrations ranges of 2.5 mg/mL to 80 mg/mL on L929 murine fibroblasts, together with pro-inflamatory cytokine markers were evaluated. All investigations were performed in comparison with golden standard, polyethyleneglycol.

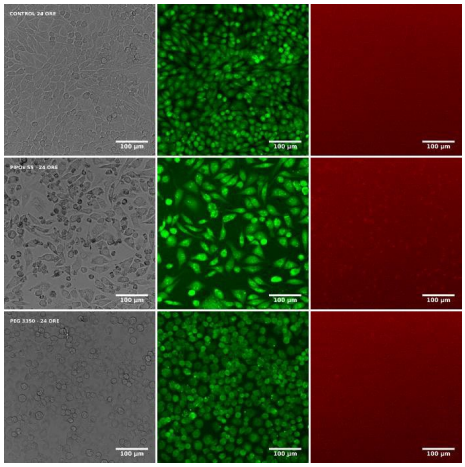

Figure 1. Images of live-dead assay on L929 murine fibroblast cells stimulated for 3 h with a solution of 80 mg/mL concentration of PIPOx 55. Alive cells are visualized as green post Acridin Orange staining, while dead cells are visualized as red. Bar scale is 100 µm.

CONCLUSION

The successful synthesis of PIPOx polymers with controlled properties and various molecular masses was performed and their non-cytotoxicity was proven up to a concentration of 40 mg/mL.

Albupad project: Protein based biomaterials for the delivery of anti-tumoral active ingredients

Jordan Beurton [1], Eya Aloui [1], Philippe Lavalle [2], Benoit Frisch [1]

[1] Laboratory of Design and Application of Bioactive Molecules (CAMB) – Biovectorisation - UMR 7199, University of Strasbourg, France
[2] Biomaterials and BioEngineering - Inserm UMR_S 1121, University of Strasbourg, France

* jbeurton@unistra.fr

INTRODUCTION

The Albupad project is about the development of protein based biomaterials showing plastic behaviors and tunable features (shape, size, porosity…). These materials are obtained through the salt assisted compaction of albumin. They can be loaded with active ingredients to create implantable devices for a drug delivery purpose. The Albupad materials can outperform and replace synthetic implantable polymers by providing a higher biocompatibility and an easier green production process. The biocompatibility of unloaded human albumin-based implants has already been demonstrated *in vivo*, in a humanized mouse model. The study presented here focuses on the adaptation of the Albupad technology for the delivery of anti-tumor molecules. Doxorubicin, a DNA intercalant, is a highly suitable active ingredient for this type of application [1]. Indeed, this molecule represents a reference treatment for several types of cancer such as breast or esophagus cancer. However, this active principle generates a strong systemic toxicity and suffers from a lack of specificity [2]. Thus, the development of localized delivery systems would reduce the risks related to doxorubin and increase the efficiency of these treatments.

EXPERIMENTAL METHODS

Materials formulation

The membranes were obtained by salt-assisted compaction of albumin solution containing doxorubin.

Materials characterization and study of doxorubicin release kinetics

Materials characterization was performed by quantification of the doxorubicin loading rate at the end of the formulation process. The release kinetics of doxorubicin was studied by incubating the materials in PBS (0.15 M, pH = 7.4) at room temperature for 30 days. The quantification of doxorubicin was performed by spectrofluorimetry with an excitation wavelength of 495 nm and by monitoring the emission wavelength at 595 nm

In vitro evaluation of anti-tumor efficiency

The cytotoxicity of doxorubicin loaded materials was studied with two models from human colon (HCT 116) and mammary (MCF-7) cancerous cell lines. Cells were seeded directly on the membranes and viability was determined after 48 hours of contact by the measurement of metabolically active cells.

RESULTS AND DISCUSSION

Doxorubicin loaded materials were formulated and characterized. The highest loading rate achieved corresponded to the presence of 3000 doxorubicin molecules per albumin forming the material. The release kinetics of doxorubicin was studied as a function of its loading rate and the material formulation process. Two different delivery profiles were identified, one with moderate flux and long-term release (>30 days) and the other with a higher flux and shorter release time (≈ 30 days). The study of direct and indirect cytotoxicity of doxorubicin-loaded materials was performed on two human cancerous cells strains (HCT-116 and MCF-7). The efficiency of the materials was found similar to the one of free doxorubicin, demonstrating that the release of active doxorubicin is allowed by our system.

Finally, an *in vivo* study aiming to demonstrate the therapeutic efficiency of peri-tumoral implants is underway on a mouse model with orthotopic tumors.

CONCLUSION

In conclusion, this work presents a new process to form biodegradable and highly biocompatible implantable materials. The application of this technology to the delivery of anti-tumor molecules was achieved, the therapeutic efficacy of these new biomaterials was demonstrated with *in vitro* and is being studied *in vivo.*

REFERENCES

References must be numbered. Keep the same style.

1. Thorn, C *et al*., *Pharmacogenet. Genomics 21:*440–446,2011
(2) Hanna, A. D *et al*., *Mol. Pharmacol.* **2014**, *86:*438–449,2014.

ACKNOWLEDGMENTS

The authors would like to thank SATT Conectus Alsace for providing financial support to this maturation project.

Gelatin-coated microneedles as advanced corticosteroid delivery systems towards a painless treatment for hypertrophic scars

Anna Szabó[1], Dr. Ignace De Decker[2], Dr. Stan Monstrey[2], Dr. Karel Claes[2], Dr. Phillip Blondeel[2], Sandra Van Vlierberghe[1]

[1]Polymer Chemistry and Biomaterials Group, Centre of Macromolecular Chemistry (CMaC), Department of Organic and Macromolecular Chemistry, Ghent University, Ghent, Belgium
[2]Ghent University Hospital Burn Center - Department of Plastic, Aesthetic and Reconstructive surgery
*anna.szabo@ugent.be, ignace.dedecker@ugent.be

INTRODUCTION

Deep dermal and full thickness burn injuries often result in hypertrophic scarring, which is characterized by chronic dermal inflammation and expresses in rigidity, erythema and contracture. The scars often require injection of corticosteroids to reduce excessive collagen formation caused by the chronic inflammation, while such injections are reported to be painful for patients.

To provide a painless sustained release of corticosteroids in the hypertrophic scars, coated microneedles (MNs) can offer a solution[1]. It is important to direct the drug delivery towards the upper dermis, therefore the design requires a 300-1000 µm-long microneedle-design[2].

Another key specification is a mechanically roboust structure to puncture through the stratum corneum (one needle should bear 0.058 N at 500 µm displacement[3]). To achieve this goal, an acrylate-endcapped urethane-based poly-ε-caprolactone (AUP-PCL) microneedle structure has been created[4]. To provide long-term drug delivery, a gelatin-methacryloyl-aminoethylmethacrylate-based (gel-MA-AEMA) hydrogel coating[5] has been applied on the AUP-PCL structures. Due to the tunability of the hydrogel properties, the sustained relase of the corticosteroids can be fine-tuned.

EXPERIMENTAL METHODS

Moulding of the MNs

The silicone moulds utilized for MN development have been kindly provided by Smicna Pte. Ltd. AUP-PCL (MM 530 g/mol) was vacuum-moulded at 55 °C, in the presence of 2 mol% photo-initiator (Irgacure2959) followed by photo-crosslinking exploiting UV-A light.

Gelatin coating of the MNs

To provide a suitable coating on the AUP-PCL constructs, the MNs were treated with gel-MA-AEMA solutions (1, 2.5, 5, 10 w/v% aqueous gel-MA-AEMA) in the presence of 2 mol% photoinitiator (Lithium phenyl-2,4,6-trimethylbenzoylphosphinate, Li-TPO-L) for 24 hours followed by a chemical crosslinking step exploiting UV-A light. To enable visualization of the coating, a coomassie-blue staining has been utilized.

Morphologycal analysis of the MNs

Optical characterization of the moulded constructs was executed with optical (OM) and scanning electron microscopy (SEM).

Mechanical evaluation of the MN structures

Compression testing of the non-coated and coated MN constructs was performed at a speed of 0.5 mm/min.

Ex vivo skin permeation studies

Residuary skin from a subcutaneous mammectomy was harvested and penetrated with a gel-MA-AEMA coated AUP-PCL microneedle patch, followed by histological analysis.

RESULTS AND DISCUSSION

Morphological analysis of the MNs

The OM images have shown an adequate microneedle-length (908 ± 7 µm) and morphology. Moreover, a successful gel-MA-AEMA coating was observed on the AUP-PCL constructs.

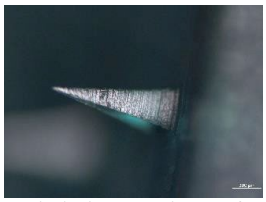

Figure 1. Optical microscopy image of a gel-MA-AEMA-coated AUP-PCL MN construct.

Mechanical evaluation of the MN structures

The compression tests have shown that both the coated and non-coated MN constructs excess the minimum force requirement (0.058 N/needle) at 500 µm displacement (0.090 N/needle for uncoated AUP-PCL MNs, 0.140 ± 0.02N/needle for coated MNs).

Hystologycal analysis of in vitro skin tissue after MN treatment

The histological analysis of the skin sample showed clear epidermal-dermal penetration at a regular distance interval. Optical microscopy confirmed the removal of the coomassie-blue stained gel-MA-AEMA post-insertion.

CONCLUSION

An AUP-PCL-based, gel-MA-AEMA coated MN system has been developed, which can successfully penetrate the epidermis. What is more, the coatings (2.5, 5 w/v% gel-MA-AEMA) can be localized in the epidermis after the patch removal from the ex vivo skin tissue, therefore a local, long-term drug delivery could potentially be realized. In the future, the corticosteroid-release of the MN system will be further investigated.

REFERENCES

1. Tan C. *et. al.*, Dermatology therapy. 9:601–611, 2019
2. Waghule T. *et. al.*, Biomedicine & Pharmacotherapy. 109:1249-1258, 2019
3. Davis S. P. *et al.*, J. Biomech. 37(8):1155-1163, 2004
4. Houben *et. al.*, 2017, WO 2017/005613 Al
5. Van Hoorick J. et. al., Biomacromolecules. 18(10):3260-3272, 2017

Hyaluronic acid based multifunctional nanostructured devices in cancer therapy

Mario di Gennaro[1,2], Antonio Fabozzi[3], Francesca Della Sala[1], Gennaro Longobardo[1,4], Luigi Ambrosio[1], Assunta Borzacchiello[1]

[1]Institute of Polymers, Composites and Biomaterials, National Research Council, (IPCB-CNR), Viale J.F. Kennedy 54, 80125 Naples, Italy
[2]Department of Environmental, Biological and Pharmaceutical Sciences and Technologies, University of Campania "L. Vanvitelli", 81100 Caserta, Italy
[3]Altergon Italia s.r.l, Zona Industriale ASI, Morra De Sanctis (AV), 83040 Italy
[4]Department of Chemical, Materials and Production Engineering, University of Naples "Federico II", 80125, Naples, Italy

*bassunta@unina.it

INTRODUCTION

Hyaluronic Acid (HA) is a hydrophilic, not sulfated glycosaminoglycan, naturally occurring in mammalian tissues, that performs different biological functions, among which the joint lubrication and the ability to bind the cell surface glycoprotein CD44, that is overexpressed in many kinds of tumor cells, are the most relevant. In addition, HA exhibits reactive functional groups, such as the glucuronic acid carboxylic acid, that can be easily grafted with molecules of pharmaceutical interest[1]. In particular, the chemical modification of polysaccharides by using natural origin prodrugs is considered an effective strategy to prepare new materials with improved therapeutical efficacy. Curcumin, for instance, is a diarylheptanoid obtained from turmeric, known for its anti-tumoral, anti-oxidant, anti-inflammatory properties, whose employment is limited by its reduced water solubility[2]. Curcumin conjugation to HA was demonstrated to improve it water solubility ad its bioavailability, and to obtain an amphiphilic derivative that spontaneously arranges in micelles. HA-Cur was used in literature to prepare micelles for the targeting release of Doxorubicin. Anyway, micelle-based drug delivery systems often exhibit some critical problems, such as low loading capacity and low stability in physiological conditions. To overcome these issues, the ability of HA-Cur to stabilize poly(lactic-co-glycolic acid (PLGA)-based nanoparticles (NPs) was evaluated. PLGA is a hydrophobic FDA approved polymer, used in literature for the preparation of NPs for chemotherapy drug delivery[3]. In this work, conjugate was synthetized and a method for the preparation of HA-Cur/(PLGA) core shell NPs was optimized.

EXPERIMENTAL METHODS

Curcumin was conjugated to HA (803 kDa) adapting a reaction reported in literature for the modification of lower MW HA. The substitution degree of the conjugated was evaluated by NMR spectroscopy, and the critical aggregation concentration of the amphiphilic polymer was quantified with surface tension measurements. HA-Cur/PLGA NPs were prepared by means of nanoprecipitation using a bulk method and a microfluidic method. The preparation was optimized in order to obtain stable over time NPs. Size, morphology and stability of NPs were analyzed by means of Transmission Electron Microscopy (TEM), Dynamic Light Scattering (DLS) and ζ-potential experiments. The arrangement of the curcumin moieties was assessed with Static Light Scattering (SLS) and UV-Vis spectroscopy. NPs were loaded with a chemotherapy drug (e.g. Irinotecan, Doxorubicin) and the drug entrapment efficiency and the drug release kinetics were examined through UV-Vis.
In vitro biological responses, such as cytotoxicity (Alamar blue assay) cell morphology (Confocal microscopy) and ant-inflammatory level expression of Interleukin-10 (IL-10) (ELISA kit), has been evaluated on Fibroblast cell (L929).

RESULTS AND DISCUSSION

A HA-Cur conjugated with a 6% substitution degree and CAC 42.1 µg/mL was obtained. The NPs preparation method optimized by preparing NPs with a HA-Cur solution at a concentration 10, 5 and 3 times below the CAC. The physical chemical and morphological analysis by means of TEM, DLS and ζ-potential allowed to individuate the NPs prepared with HA-Cur at 3 times below CAC as the more stable over ten days. The drug was loaded with efficiency comparable to that obtained for other PLGA-based core-shell systems reported in literature.

CONCLUSION

HA-Cur conjugated was synthetized using HA 803 kDa. The conjugated polymer was employed to prepare core-shell HA-Cur/PLGA NPs for the targeted chemotherapy drug delivery. The preparation method of NPs was optimized to obtain stable drug loaded NPs.

REFERENCES

References must be numbered. Keep the same style.

1. Huang G *et al.*, Int. J. Biol. Macromol. 125:478-484, 2019
2. Li J *et al.* Food Res. Int. 69:202-208, 2015
3. Giarra, S. *et al.*, Carbohydr. Polym. 140:400-407, 2016

ACKNOWLEDGMENTS

The authors would like to thank the ADViSE project (CUP: B43D18000240007) for providing financial support to this project.

Microfluidic-Assisted Nanoprecipitation of Hyaluronic Acid Core-Shell Nanoparticles for Cancer Therapy

A. Fabozzi[1*], F. Della Sala[2], M. Barretta[2], M. di Gennaro[2], N. Solimando[1], M. Pagliuca[1], L. Ambrosio[2], A. Borzacchiello[2]
[1]Altergon Italia S.r.l., Morra De Sanctis (AV), Italy
[2] National Research Council, Institute for Polymers, Composites and Biomaterials, Naples, Italy
[*] a.fabozzi@altergon.it

INTRODUCTION

Hyaluronic acid (HA), a naturally-occurring anionic polysaccharide, is widely employed in active tumor targeting research, especially to decorate nanoparticles (NPs) for their ability to bind CD44 receptor, overexpressed in a variety of cancer cells. Physico-chemical properties of NPs such as size and size distribution are fundamental parameters influencing considerably nanobiointeractions[1]. In literature, a manufacturing technique to generate spherical NPs such as nanoprecipitation with subsequent solvent evaporation, bulk method (BM), has been described[2]. Unfortunately, the BM, does not lead to gain reproducibility in physicochemical properties of NPs, as size distribution, polidispersion index (PDI) and consequently *in vitro* and *in vivo* drug delivery tests. Newly continuous-flow nanoprecipitation assisted by microfluidic systems, in contrast to conventional NPs synthetic methods, are widely investigated for their unique properties in which the nucleation and growth steps for the NPs formation can be separated as a function of distance from the position where solution mixing occurs to obtain an absolute control of the particle size[5]. In this work, blank and irinotecan-loaded (Iri) spherical NPs composed of poly(lactic-co-glycolic acid) (PLGA) have been formulated and coated with HA by means of microfluidic (MM), and presents the investigation of the structural by means of Transmission Electron Microscope (TEM), dynamic by means of Dynamic light scattering (DLS), ζ-potential and biological properties of resulting NPs, including cell uptake and citotoxicity on L929 cells.

EXPERIMENTAL METHODS

Spherical blank and Iri-loaded NPs were prepared by a nanoprecipitation–assisted by MM. Briefly, for the NPs organic phase ((O) PLGA (RG504H) 50:50) and poloxamers (PP) (PF68/PF127) (1:0.3:0.3) powder were solubilized at 1.25% (w/w) in acetone and 10 µl of nile red (1 mg ml^{-1}) were added; while the water phase was composed HA (803 kDa) at 0.08% (w/w) and in which 3 ml of a mixture of PP was added, respectively. In particular, PLGA/PP solution was introduced in the internal channel of micromixer chip having 12 mixing phases and pumped at 100 $\mu L \cdot min^{-1}$ and a solution of HA, was used in the external channels at 1000 $\mu L\ min^{-1}$ to set a flow ratio (i.e., internal flow/external flow) equal to 0.1. In the case of drug-loaded NPs, Iri (1 mg) was solubilized in the O. NPs sizes and ζ-poitential were evaluated by DLS, and morphologies by TEM. Drug entrapment efficiency (DEE) was evaluated by UV-vis and *in vitro* release kinetic of Iri by spectrophotometric assay. *In vitro* cell uptake of IRI-loaded NPs was performed on L929 cells.

RESULTS AND DISCUSSION

The TEM micrographs revealed that the HA/PLGA/PP NPs show a regular spherical shape with a diameter *d* of ~118 nm. On the contrary, from the inspection of TEM micrographs of HA/PLGA/PP a dimensional distribution with a diameter $160<d\ (nm)<200$ with an irregular shape is observed, respectively). The above results clearly highlight that the MM is a simple way of preparing NPs with a small size and controlled morphology. Single peaks and the PDI lower than 5% have been found in all NPs size distributions. The addition of HA in the BM synthesis of NPs resulted into ζ potential value of ~−55.1 mV for HA/PLGA NPs, and ~-47.8 mV for NPs, synthesized by MM. A less marked decrease of ζ potential trend of NPs synthesized by MM is likely due to the lower surface area exposed by NPs. Moreover, it was observed, for HA/PLGA/PP NPs synthesized by MM, a higher yield (92.4%) than those synthesized by BM (61.2%). Furthermore, the DEE was found to be 87.8% for NPs synthesized by MM, which is higher than DEE obtained for the HA/PLGA/PP NPs synthesized by a BM (64.3%). *In vitro* assay release profiles of Iri for HA/PLGA/PP NPs showed that IRIN is released in less than two weeks. Cell uptake studies of spherical HA/PLGA/PP NPs synthesized by both MM and BM performed on L929 cell line revealed that in both cases, internalization increases with exposure time, reaching a plateau after approximately 24 h. Furthermore, from the analysis of biological assays it is clear that the HA/PLGA/PP internalizationis higher than those NPs fabricated by BM, especially evident in the longer times of exposure. This trend of biological assay can be due to the small dimension of NPs produced by MM.

CONCLUSION

We developed a novel spherical blank and Iri-loaded HA/PLGA/PP NPs by means of microfluidics. *In vitro* assays of HA/PLGA/PP NPs revealed that the spherical NPs, fabricated by MM allow better internalization than spherical NPs fabricated by BM on the L929 and HS578T cells. The obtained results highlight the potential application of novel spherical HA/PLGA/PP NPs for cancer therapy.

REFERENCES

1. A. Fabozzi, *et al.,* Polym. Chem., 12, 6667-6687 (2021).
2. M. Nowa, *et al*. Bioeng Transl Med., 10153, 5 (2020).

ACKNOWLEDGMENTS

The authors acknowledge the research project "ADViSE DRUGS AND ANTI-TUMORAL VACCINES FROM THE SEA-POR CAMPANIA FESR 2014-2020"

Amphiphilic Anionic Oligomer-Stabilized Calcium Phosphate Nanoparticles for siRNA Delivery via Convection-Enhanced Delivery

Franziska Mitrach[1], Maximilian Schmid[1], Heike Franke[2], Alexander Ewe[3], Achim Aigner[3], Christian Wölk[1], Michael C. Hacker[1,4], Michaela Schulz-Siegmund[1]

[1]Pharmaceutical Technology, Institute of Pharmacy, Medical Faculty, Leipzig University, Germany
[2]Rudolf-Boehm-Institute for Pharmacology & Toxicology, Medical Faculty, Leipzig University, Germany
[3]Rudolf-Boehm-Institute for Pharmacology & Toxicology, Clinical Pharmacology, Medical Faculty, Leipzig University, Germany
[4]Institute of Pharmaceutics and Biopharmaceutics, Heinrich-Heine-University Düsseldorf, Germany
* franziska.mitrach@medizin.uni-leipzig.de

INTRODUCTION

Convection-enhanced delivery (CED) represents a promising technique to deliver nanoparticles (NP) through the narrow interstitial spaces of the brain via a pressure gradient [1]. However, delivery of NP via CED requires a particle size below 100 nm as well as low zeta potentials [2]. In this study, we investigated calcium phosphate nanoparticles (CaP-NP) intended for delivery of siRNA to brain cancer cells. To circumvent CaP aggregation, we introduced a new terpolymer o14PEGMA1:1:2.5_NH_3 for stabilization suitable for CED application [3]. This terpolymer provides a fatty alcohol to improve interfacial activity, short PEG chains for steric stabilization as well as maleic anhydrides that allow for high affinity to Ca(II) and oligomer labeling in the hydrolyzed state [3].

EXPERIMENTAL METHODS

- ***Preparation of CaP-NP:***

Stabilized CaP-NP were prepared by using co-precipitation with simultaneous siRNA loading. For this, a Ca^{2+} solution containing 2.5 M $CaCl_2$ and 1 µM siRNA was mixed with a 3.75 mM PO_4^{3-} solution. To kinetically control aggregation, 10 or 40 µM stabilizer were added to PO_4^{3-} solution and complexed for 30 min.

- ***Size & Zeta potential measurements:***

Particle size measurements were performed by using Nanoparticle Tracking Analysis (NTA). Zeta potential was measured using Litesizer 500 in combination with Univette Low Volume (Anton Paar) for measurement of high conductivity samples.

- ***Oligomer & siRNA binding to CaP-NP:***

For determination of oligomer binding to CaP-NP, oligomer was labeled with Cy5-amine via maleic anhydrides using covalent modification. FITC-labeled siRNA was used to determine siRNA binding to CaP-NP. Unbound siRNA or oligomer were separated via centrifugal filter units and determined using a plate reader.

- ***Survivin siRNA silencing efficiency:***

Silencing efficiency was determined in F98 rat glioblastoma cells using survivin as molecular target. Survivin gene expression levels were determined using quantitative real-time PCR. Cell viabilities were determined using WST-8 assay. To analyze apoptosis induction upon survivin silencing, Annexin V/PI-staining as well as Caspase 3/7 assay were performed.

RESULTS AND DISCUSSION

NTA determined particle sizes revealed that a stabilizer concentration of 40 µM provided narrowly distributed siRNA-loaded CaP-NP with an average size of 50 nm and a zeta potential of about + 2 mV. Particle size remained stable for only 5h probably as a consequence of the comparably short PEG chains of 950 Da. Since NP are easily prepared by a simple mixing reaction, we considered this stability sufficient for application. By concept, PEG chain molecular weight of 950 Da was selected to balance colloidal stability with efficient cellular uptake.

Quantification of FITC-siRNA and Cy5-labeled oligomer in the flow-through of an ultrafiltration separation showed nearly quantitative siRNA and stabilizer binding to the CaP-NP. Stabilizer and siRNA remained associated with the NP even in presence of serum proteins. Analysis of siRNA silencing in rat brain cancer cells using survivin as a molecular target showed a decrease to 20% survivin expression for oligomer-stabilized CaP-NP compared to control groups which further resulted in a significantly decreased cell viability. Annexin V/PI-staining and Caspase 3/7 assay indicated a successful induction of apoptosis by CaP-NP mediated survivin silencing. We further performed first biocompatibility testings by using tissue slice cultures from mice brains.

CONCLUSION

This study demonstrates that the newly developed terpolymer o14PEGMA(1:1:2.5)_NH_3 is able to stabilize CaP-NPs with a size of less than 100 nm and an almost neutral zeta potential. Stabilized by the terpolymer, siRNA-loaded CaP-NPs were able to efficiently silence survivin in rat brain cancer cells and induce apoptosis upon survivin silencing.

REFERENCES

1. Metha A.M. *et al.*, Nanotherapeutics 18: 358-372, 2017
2. Shi M. *et al.,* J Nanobiotechnol 16: 77, 2018
3. Mitrach, F. *et al.,* Pharmaceutics, 14(2): 326, 2022

ACKNOWLEDGMENTS

We would like to the thank the European Regional Development Fund Saxony (EFRE) and the Sächsische Aufbaubank for funding this project. We further thank the Center for Biotechnology & Biomedicine Leipzig (BBZ) for administrative support.

Electrospun Materials for Local Delivery of Docetaxel and Cabazitaxel Intended for Urooncology

Joanna Jaworska[1*], Mateusz Stojko[1], Jakub Włodarczyk[1], Monika Musiał-Kulik[1], Janusz Szewczenko[2], Janusz Kasperczyk[1]

[1]Centre of Polymer and Carbon Materials, Polish Academy of Sciences, Zabrze, Poland

[2] Department of Biomaterials and Medical Device Engineering, Silesian University of Technology, Zabrze, Poland
[*]@jjaworska@cmpw-pan.edu.pl

INTRODUCTION

Docetaxel is the first-generation taxane that plays a key role in prostate cancer treatment. Cabazitaxel is a novel, second-generation taxane with a promising anticancer activity that shows activity in both docetaxel-sensitive and docetaxel-resistant tumors [1].

Electrospun materials attract attention in the local delivery of different anticancer drugs [2]. It is a convenient method for obtaining soft, flexible materials that can be easily implanted. Very important features that make this technique unique are the high porosity of the electrospun material and its large specific surface area. It results in high drug loading capacity and might be beneficial in the local delivery of the anticancer drug.
In the study, bioresorbable polymeric materials loaded with docetaxel or cabazitaxel have been prepared using electrospinning. The aim of the incorporation of the taxanes into electrospun biodegradable fibers was to design materials for local delivery of chemotherapeutics intended for the prostate tumor therapy.

EXPERIMENTAL METHODS

Pol(lactide-co-glycolide), poly(glycolide-caprolactone), poly(lactide-trimethylene carbonate), poly(lactide-glycolide-caprolactone) were synthesized in bulk by the ring-opening polymerization (ROP). Obtained polymers were dissolved in CH_2Cl_2 (Avantor S.A., Poland) and then mixed with docetaxel or cabazitaxel (LC Laboratories, US). Nonwoven materials were obtained with TL-Pro-BM electrospinning unit (Tong Li Tech, China)- polymer solutions were dosed to the spinning nozzle through a PTFE capillary (2ml/h), by using PHD Ultra 4400 syringe pump (Harvard Apparatus, US). Drug release was investigated under in vitro conditions at 37◦C in PBS at pH 7.4 or pH=6.8 for 14 or 90 days with High Performance Liquid Chromatography (VWR-Hitachi/LaCh-romElite®) equipped with a LiChrospher® RP-18 column (250 mm × 4 mm, 5 µm) and LiChrospher® RP-18 guard column (4 mm × 4 mm, 5 µm). The mobile phase consisted of acetonitrile and water (60:40, v/v). Flow rate was set to: 1 ml/min. Docetaxel and cabazitaxel were detected at a wavelength of 227 nm. The amount of incorporated PTX in the nonwoven was measured using extraction method [3].

RESULTS AND DISCUSSION

Fibers morphology

Drug delivery systems were designed as soft, flexible materials, easy for implantation. SEM images of obtained electrospun taxane delivery systems present fibers with different morphology depending on the kind of polymer and drug (Fig.1).

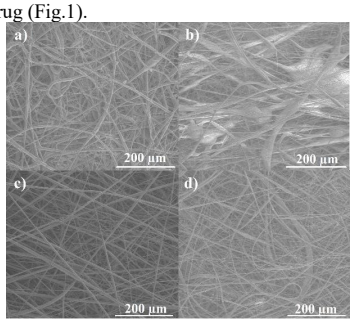

Fig. SEM images of electrospun drug delivery systems: a) PLGA/PGCL+CTX; b) PLGA/PGCL+DTX; c) PLGA+DTX; d) PLGCL+DTX

Drug release

For all nonwoven materials, a different release rate was observed. During 14 days the fastest release of **docetaxel** was observed in the case of PLGA/PGCL+DTX and was nearly 60%; in the case of PLGCL+DTX, it was 32% of DTX, whereas in the case of PLTMC/PLGA+DTX it was 24%. For PLTMC/PLGA+DTX, suspension of the drug release was observed after 3rd day which is a huge disadvantage. **Cabazitaxel** was incorporated in PLGA/PGCL fibers and its release was nearly 17% during 14 days. A stable release of drugs during chemotherapy is important thus, PLGA/PGCL+CTX system seems to be the most promising.

CONCLUSION

Various polymeric materials loaded with the docetaxel or cabazitaxel have been prepared. Electrospinning which was used as a processing method allowed to obtain flexible materials for the implantation. The most promising results were achieved for PLGA/PGCL+CTX system since stable and slow release of the drug was detected what is important in the chemotherapy.

REFERENCES

1. Sun, B. *et al*. Nano Res. 11: 5193–5218, 2018.
2. Zhu, Y. *et al*. Tissue Eng Part A. 27(9-10): 536-548, 2021
3. Jelonek, K. *et al*. Mater. Lett., 214: 220-223, 2018

ACKNOWLEDGMENTS

The work is the result of the research project No. 2020/04/X/NZ7/00016 funded by the National Science Centre

Everolimus Loaded Polyethylene Oxide Films as a Potential Drug Delivery System for Drug-Eluting Balloons

Mohammad AKRAMI-HASAN-KOHAL, Tahmer SHARKAWI
ICGM, Univ Montpellier, CNRS, ENSCM, Montpellier, France
mohammad.akrami-hasan-kohal@umontpellier.fr

INTRODUCTION

Atherosclerosis, the accumulation of plaque in the coronary and peripheral blood arteries that causes obstruction (stenosis), is the primary cause of cardiovascular disease in millions of individuals each year [1] (Fig. 1). Drug-eluting balloons (DEB) can be used to deliver an anti-proliferative drug through an inflated balloon toward the vessel wall, resulting in effective, rapid, and homogenous delivery of the drugs. A key component of balloon technology is the concept of targeted drug delivery, which aids in the speedy healing of vessel walls while also inhibiting the proliferation of smooth muscle cells [2, 3]. Existing DEBs deliver the drug directly from the balloon surface or through several carriers. Numerous studies have demonstrated that a large proportion of the drug is washed out in the bloodstream at the time of balloon tracking, resulting in a subtherapeutic dosage of a drug administered at the place of treatment [4]. The purpose of this study is to investigate Everolimus (EV) loaded PEO films as a controlled drug delivery carrier for DEBs.

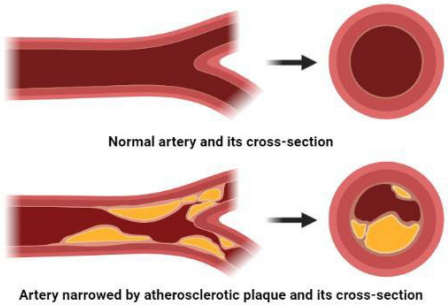

Fig. 1. A schematic view of the normal artery and artery narrowed by atherosclerotic plaque and cross-sections. Created with BioRender.com

EXPERIMENTAL METHODS

Balloon material specimens were coated with everolimus (EV) loaded PEO films. PEO (1% (W/V)) was first dissolved in deionized water. Afterward, a solution of EV in ethanol was prepared by sonicating EV for 5 min three times. The prepared EV solution was added dropwise to the PEO. Balloon material specimens were then dip-coated in the drug-polymer solution and dried. The prepared films were characterized using scanning electron microscopy (SEM), Fourier transform infrared spectroscopy (FTIR), and differential scanning calorimetry (DSC) to observe the morphology of surfaces as well as the cross-sections, the shifts that appeared in the chemical structure, and the changes in crystallinity of the EV loaded PEO and control PEO films, respectively. Moreover, Liquid Chromatography Mass Spectrometry (LC – MS/MS) was used for the drug-elution studies.

RESULTS AND DISCUSSION

The results of the SEM and FTIR demonstrated that the prepared EV– PEO films were homogeneous and that the EV was molecularly dispersed in the PEO matrix during the development procedure. Additionally, the DSC analysis revealed that the PEO crystallinity had not been influenced by the addition of EV to the mixture. Moreover, it has been found that EV-loaded PEO coatings were able to release the drug effectively (Fig. 2).

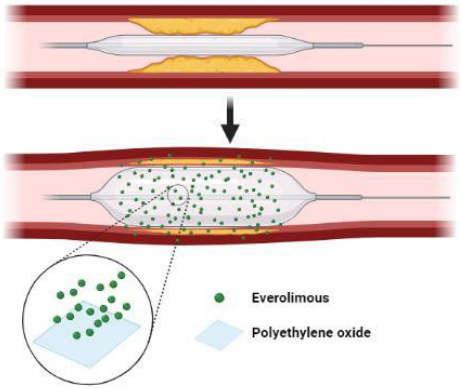

Fig. 2. The concept of Everolimus loaded polyethylene oxide films as a potential drug delivery system for Drug Eluting Balloon (DEB). Created with BioRender.com

CONCLUSION

This study shows the feasibility of using PEO as drug-loaded coatings for DEBs; Strategies to decrease early drug loss at the time of balloon tracking and rapidly distribute the drug during balloon inflation and treatment can thus be proposed for optimizing current designs of drug delivery platforms for DEB.

REFERENCES

1. Woolford, S.E., et al., Int. J. Pharm., 2019. 554: p. 312-321.
2. Bukka, M., et al., Biomed Mater, 2018. 13(3): p. 032001.
3. Iyer, R., et al., Int. J. Pharm., 2019. 554: p. 212-223.
4. Anderson, J.A., et al., Acta Biomater., 2016. 29: p. 333-351.

ACKNOWLEDGMENTS

This project has received funding from the European Union's Horizon 2020 research and innovation program under grant agreement No 956470.

Development of degradable self-rolledpatches for drug release

Sidzigui OUEDRAOGO[1], Mathilde GROSJEAN[2], Arnaud PONCHE[1], Laurent PIEUCHOT[1], Valeriy LUCHNIKOV[1], Noëlle MATHIEU[3], Benjamin NOTTELET[2], Karine ANSELME[1]

[1] UMR 7361/UHA, Institut de Science des Matériauxde Mulhouse (IS2M), Mulhouse, France ;
[2] UMR 5247, Institut des Biomolécules MaxMousseron (IBMM), Montpelier, France ;
[3]Institut de Radioprotection et de Sûreté Nucléaire (IRSN), Paris, France
sidzigui.ouedraogo@uha.fr

INTRODUCTION

A specific innovative treatment is needed to address the Pelvic Radiation Disease (PRD). Current treatments are symptomatic and not curative while some, like systematic drugs, induce systematic side effects. To achieve an efficient therapeutic solution and minimize systemic toxicity, a specific local treatment targeting the inflamed mucosa areas is proposed. We develop a degradable self-rolled patch that could be applied locally by colonoscopy without surgery. This innovative biomaterial is based on the combination of degradable hydrogel and elastomeric layers (Fig.1A). The association of two different layers confers tunable mechanical and bio-resorption properties to the patchand allows the unidirectional release of anti-inflammatory drugs (AI) such as Budesonide and Prednisolone toward the ulcerated zone after its unrolling. Here we report the patch building methodology and its characterization.

EXPERIMENTAL METHODS

The patch encompasses biocompatible polyesters. Star block copolymer poly (ethylene glycol) core and poly(lactide) (PEG-PLA) with end chains functionalized with methacrylic groups are used for the films' formation. The copolymers solutions are poured in plates to produce bilayer patch after UVcross-linking (Fig.1B). Attenuated total reflection Fourier transform infrared spectroscopy (ATR-FTIR) was used to characterize the difference between the top and bottom surfaces of the film. The rolling was achieved by swelling the bilayer films (square or rectangular) in a PEG solution with different molecular weights and concentrations (e.g. linear PEG 1000 at 10% w/v in water) (Fig.2A). We explored the swelling ratio and mechanical properties. The drug delivery capacity of the patch was evaluated, by quantifying the amount of Budesonide and Prednisolone release by Reverse Phase – High Performance Liquid Chromatography (RP-HPLC) coupled to UV light detection. Moreover, the biocompatibility of the mentioned constructs was evaluated using rat adipose tissue derivate mesenchymal stemcells.

RESULTS AND DISCUSSION

We report an approach for the fabrication of fully degradable tubes based on polyester bilayers. Crosslinking is achieved under UVexposure 365 nm and without photoinitiator. We show that the thickness of the obtained patch, can be controlled by adjusting the concentration of the polymer solution. It can be well tuned, ranging fromseveral to hundreds of micrometers. We also report that the number of windings, the inner and the external diameter of the self-rolled patch is a function of the total bilayer thickness.

The similar nature of the two layers enhances their right cohesion. Indeed, the scanning electron microscope (SEM) images of the bilayer tube show a good compatibility and interfacial cohesion (Fig.2C) between the elastomeric and the hydrogel layer. *In vitro* release study confirmed that the device can release AI drugs (Fig.2D). First synthetized PEG-PLA monolayers hydrogels films are able to release 48µg (16%) of Prednisolone on the 300µg used in drug loading medium.

CONCLUSION

Degradable and biocompatible patches were successfully produced by association of two PEG-PLA based films. The bilayer films are able to enroll and achieve our final requirements. Ongoing work focuses on the optimization of amount of drug released and the patch self-unrolling to facilitate its deployment after the placement in the colon *in vivo*.

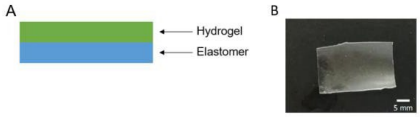

Figure 1: A- Schematic illustration of bilayer patch structure model. B- Synthetized drug delivery system (30 mm × 15 mm × 0.16 mm)

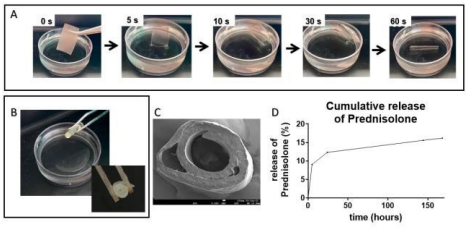

Figure 2: A- Snapshots to show the self-rolling of the PEG PLA bilayer film in a 10% (w/v) 1kDa PEG solution. The flat bilayer film enrolls forming a tube with the hydrogel layer on the exterior. B- PEG-PLA bilayer self-rolled tube 4 mm diameter. C- SEM image of cross-section of enrolled bilayer PEG-PLA tube. D-Cumulative release of Prednisolone fromPEG-PLA hydrogel film.

REFERENCES

1. Andreyev, J. *Lancet Oncol.* 8, 1007–1017 (2007).

ACKNOWLEDGMENTS

The authors would like to thank the French National Research Agency (ANR) (contract n° ANR-19-CE19-0022-03) for providing financial support to this project.

Development and characterization of pNIPAM-based microgels for drug delivery within dentoalveolar tissue engineering strategies

Mehdi Salar Amoli [1,2,*], Huimin Yang [1], Resmi Anand [1,3,4], Mostafa EzEldeen [2,5], Merve Kübra Aktan [6], Annabel Braem [6], Reinhilde Jacobs [2,7], Veerle Bloemen [1,3,6]

[1] Materials Technology TC, Campus Group T, KU Leuven, Leuven, Belgium
[2] Imaging and Pathology Dept., KU Leuven and Oral and Maxillofacial Surgery, University Hospitals Leuven, , Leuven, Belgium
[3] Prometheus, Division of Skeletal Tissue Engineering, KU Leuven, Leuven, Belgium
[4] Inter University Centre for Biomedical Research, Mahatma Gandhi University Campus at Thalappady, Kottayam, India
[5] Oral Health Sciences Dept., KU Leuven and Paediatric Dentistry and Special Dental Care, University Hospitals Leuven, Belgium
[6] Department of Materials Engineering (MTM), KU Leuven, Leuven, Belgium
[7] Department of Dental Medicine, Karolinska Institutet, Stockholm, Sweden
* mehdi.salaramoli@kuleuven.be

INTRODUCTION

Maintaining an optimal concentration of growth factors and signaling molecules can have a significant effect on the outcome of tissue engineering strategies, as they can affect cellular activities such as differentiation or proliferation[1]. This is especially important in tissue engineering strategies aimed at heterogeneous structures such as dentoalveolar tissues. Consequently, several release systems have been developed to be incorporated in tissue engineering strategies such as bioprinting, to circumvent the short half-life of such molecules, enhancing their availability without the need for incorporation of an excessive amount[2,3]. Among such strategies, use of poly-n-isopropylacrylamide (pNIPAM) based microgels is widespread considering their highly controllable properties and thermoresponsive behavior[4,5]. However, these microgels are mainly used for stimuli responsive release systems[2], while in tissue engineering, often a sustained release of different agents is required. In this study, novel microgels based on pNIPAM have been synthesized, systematically characterized, and optimized for sustained delivery of such molecules in tissue engineering strategies.

EXPERIMENTAL METHODS

Novel pNIPAM-methylcellulose microgels have been synthesized through a one-step precipitation polymerization process at 45 °C using a TEMED/APS redox initiatior system. A 23 factorial set of experiments was designed to evaluate the effects of (i) material ratio, (ii) concentration of methylene bis acrylamide (MBA) as the crosslinker and (iii) presence of sodium dodecyl sulfate (SDS) as surfactant during synthesis, on final properties of the microgels. The microgels were characterized in terms of their chemical structure through Fourier-transform infrared spectroscopy (FTIR) and nucleic magnetic resonance (NMR), their size through Dynamic light scattering (DLS), and their volume phase transition temperature (VPTT) through spectrophotometry. Genipin, a natural compound known to promote odontoblastic differentiation of dental pulp stem cells [6], was used as a model drug to be encapsulated in the microgels. The loading capacity of the microgels was evaluated through a "breathing-in" method followed by centrifugation and spectrophotometry, and the release profile in phosphate-buffered saline (PBS) at 37 °C was determined through spectrophotometry. Factorial statistics were applied to determine the most important parameters affecting the microgel properties. Additionally, possible cytotoxicity of these microgels on dental pulp stem cells (DPSCs) was evaluated through live/dead staining and DNA quantification.

RESULTS AND DISCUSSION

The results confirmed successful copolymerization of pNIPAM and methyl cellulose and formation of microgels based on the copolymer. Moreover, the DLS results demonstrated a microgel diameter ranging from approximately 150 nm to 400 nm at 37 °C, where the presence of surfactant did not affect the size to any significant extent at this temperature. However, an increase in the crosslinker concentration resulted in microgels with a larger average diameter. Furthermore, Genipin, as the model drug, was loaded with different efficiencies in the microgels. Statistical analysis determined the crosslinker concentration to have a significant effect on loading efficiency, with a high crosslinker concentration resulting in a statistically significant increase in loading of the drug onto the microgels. Expectedly, this increased crosslinker concentration resulted in a sustained release of the drug at 37 °C over one week. Moreover, the volume phase transition temperature of the microgels ranged from 35 °C to 42 °C in PBS, close to the physiological temperature making them suitable for different applications, including sustained release within tissue engineering. Furthermore, DPSCs exposed to microgels for one week demonstrated high viability in all microgel formulations, while the ones synthesized without surfactant resulted in a higher viability, not statistically different compared to the control groups.

CONCLUSION

Taken together, the results of this study, obtained through a systematic analysis of parameter effects, can serve as a solid basis for development of drug delivering pNIPAM-methylcellulose microgels for dentoalveolar tissue regeneration.

REFERENCES

1. Lee K et al. J R Soc Interface. 8(55):153–70.
2. Qu M et al. Adv Healthc Mater. 9(7):1901714.
3. Rajam M et al. Int J Pharm. 410(1):145–52.
4. Chen Y et al. J Appl Polym Sci. 124(6):4678–85.
5. Witte J et al. Soft Matter. 15 5:1053–64.

ACKNOWLEDGMENTS

Supported by the Research Council of KU Leuven grant number (C24/18/068).

Inhalable polyanhydride microparticles for delivery of hydrophobized gentamycin to treat bacterial pulmonary infections

Konrad Kwiecień[1*], Karolina Knap[1*], Katarzyna Reczyńska-Kolman[1], Daria Niewolik[2], Katarzyna Jaszcz[2], Elżbieta Pamuła[1]

[1]Department of Biomaterials and Composites, University of Science and Technology, Cracow, Poland
[2] Department of Physical Chemistry and Technology of Polymers, Silesian University of Technology, Gliwice, Poland
[*] kkwiecien@agh.edu.pl

INTRODUCTION

Conventional therapies of pulmonary bacterial infections – oral or intravenous administration of antibiotics – to be effective require high antibiotic doses which, on the other hand, may cause severe side effects and the development of antibiotic resistance. The possible solution of the problem is to use biodegradable microparticles (MPs) with a short degradation time as inhaled antibiotic delivery systems [1]. Poly(sebacic anhydride) (PSA) and its copolymers are considered materials for such purposes, as they degrade quickly mostly due to erosion. This work aimed to obtain PSA and its copolymers MPs loaded with hydrophobized gentamycin (gentamycin bis(2-ethylhexyl) sulfosuccinate, GentAOT) to increase the drug loading capacity. This study also aimed to characterize the surface properties of MP as well as to assess their compatibility with human lung epithelial cells and germicidal properties on multidrug resistant bacteria.

EXPERIMENTAL METHODS

PSA was obtained from sebacic acid via polycondensation. GentAOT was obtained by ion exchange reaction from gentamycin sulfate with sodium bis(2-ethylhexyl) sulfosuccinate (Both form Merck). MP were manufactured using solid-in-oil-in-water (S/O/W) emulsification, where S: GentAOT in a different weight ratios; O: PSA or its copolymers dissolved in dichloromethane (DCM); W: water solution of poly(vinyl alcohol) (PVA). GentAOT was dispersed in polymer solution using ultrasounds. MP were obtained by adding the oil phase to the water phase and evaporation of the organic solvent under constant stirring. Then, MPs were washed in MilliQ water to get rid of surfactant residues, and freeze-dried. MPs were observed using both optical and scanning electron microscopes (SEM) to assess their microstructure. Diameter size (Z-ave), polydispersity index (PdI), and zeta potential (ζ) were characterized via dynamic light scattering (DLS), while GentAOT encapsulation efficiency and drug loading by using OPA assay. Cytocompatibility was evaluated using AlamarBlue assay and live/dead fluorescent staining on A549 and BEAS-2B human lung epithelial cells after 24 h contact with MPs dispersed in Dulbecco modified Eagle's medium (DMEM) at different concentrations in the range of 1-1000 µg/ml. The germicidal properties of GentAOT-loaded MPs were evaluated on methycilin-resistant Staphylococcus aureus (MRSA ATCC BAA 1681).

RESULTS AND DISCUSSION

The efficiency of ion exchange (gentamycin sulfate to GentAOT) measured in OPA assay showed almost complete effectiveness (> 99%). The obtained MPs were round, of regular shape, and their surface was smooth. The diameters of the MPs were mostly within the range of 1-2 µm and their surface was charged negatively – the values varied between -10 to -20 mV. Encapsulation effectiveness and drug loading were superior in comparison with unmodified gentamycin. In vitro tests of MPs without the addition of GentAOT showed no cytotoxic effect at low concentrations. Kirby-Bauer tests confirmed that ion exchange process causes no loss of germicidal properties. Surprisingly, GentAOT showed slightly wider inhibition zones than unmodified gentamycin.

CONCLUSION

The results of this study show that gentamycin may be effectively modified to a hydrophobic form to enable high encapsulation efficiency and drug loading within the MPs from hydrophobic polymers. This approach could be useful, especially due to cytocompatibility of the MPs only in relatively low concentrations. The obtained MPs had the right size range and morphology for pulmonary administration, however the exact capability of reaching the deep regions of lungs is yet to be evaluated by the cascade impactor.

REFERENCES

[1] A. K. Thakur, D. K. Chellappan, K. Dua, M. Mehta, S. Satija, and I. Singh, "Patented therapeutic drug delivery strategies for targeting pulmonary diseases," Expert Opin. Ther. Pat., vol. 30, no. 5, pp. 375–387, 2020.

ACKNOWLEDGMENTS

This study was supported by National Science Centre, Poland (project No 2019/35/B/ST5/01103) and by the Program 'Excellence Initiative – Research University' for the AGH University of Science and Technology.

Development and optimization of a Drug Delivery System based on alginate microspheres

Delia Catalano[1], Sophia Dalfino[1], Matteo Pitton[1*], Silvia Farè[1,2]
[1]Department of Chemistry, Materials and Chemical Engineering "G. Natta", Politecnico di Milano, Milan, Italy
[2]INSTM, National Consortium of Materials Science and Technology, Local Unit Politecnico di Milano, Milan, Italy
*matteo.pitton@polimi.it

INTRODUCTION

Conventional therapies are nowadays considered gold standard for pathologies treatments. However, such treatments exhibited some typical drawbacks, which lead to find out new alternative therapies. For this purpose, Drug Delivery Systems (DDS) have recently gained interests, since allowed to control the rate of drug delivery and to locally release therapeutics agents *in situ*. Herein, we developed a DDS based on microspheres (MS) made of alginate, well-known for its low cost, biocompatibility, and biodegradability. Alginate MS were extruded by extrusion dripping and extrusion parameters were finely optimized. Then, MS were encapsulated with curcumin, an anti-tumoral drug [1], to assess their effect on breast cancer cells.

EXPERIMENTAL METHODS

Alginate MS were obtained by an optimized system based on extrusion dripping. A syringe pump forced alginate flowing through a coaxial needle ($d_{external}$ = 20 G, $d_{internal}$ = 26 G) with selected rates. MS formation was also promoted by a coaxial laminar air flow. Extruded droplets fell in a stirring (200 rpm) $CaCl_2$ bath and alginate MS were consequently obtained by chemical crosslinking. Alginate DDS was optimized by tuning the following extrusion parameters: flow pump (20, 30, 40 mL h^{-1}), air pressure (0.5, 0.75, 1 bar), alginate (i.e., 2, 3, 4, 5 % w/V) and $CaCl_2$ bath concentration (i.e., 100, 450, 900 mM). Obtained MS were analyzed by stereomicroscope, and promising MS formulations were defined if average diameter, Ø, resulted < 1.5 mm and circularity, Cir, resulted > 0.6 [2, 3]. Selected alginate MS were then tested for *in vitro* stability in physiological-like (pH = 5.3) or tumoral-like (pH = 5.3) environment and weight percentage variation was calculated. MS loaded with curcumin were morphologically characterized, and drug encapsulation efficiency (EE%) was evaluated. Drug delivery release kinetics was assessed both at pH 7.4 and 5.3. Drug release of the optimized DDS was evaluated by seeding on TCPS MCF-7 breast cancer cells, allowing them to grow for 24 h. Then, curcumin-loaded and pristine alginate MS were added in the wells. AlamarBlue assay was performed to investigate cell metabolism after 4, 24, 48, 72, 168 h of cells-MS contact.

RESULTS AND DISCUSSION

Optimizing extrusion process enlightened average diameter, Ø, directly depended both on alginate concentration and coaxial laminar flow pressure. By increasing air flow, alginate MS Ø decreased ($p < 0.05$), since droplets were dripped more rapidly. Instead, higher alginate concentration was, average diameters increased ($p < 0.05$), due to the increase in solution viscosity. Selected optimal alginate MS formulations resulted A3-C450-0.5 and A3-C900-0.5 (A = alginate concentration, C = $CaCl_2$ bath concentration, 0.5 = air pressure), since parameter combinations (i.e., Ø and Cir) showed Ø < 1.5 mm and Cir > 0.6. Moreover, statistically significant differences were not detected in morphology, once curcumin was loaded into these alginate MS. *In vitro* stability of the selected formulations showed no significant differences ($p > 0.05$) in weight variations in both physiological-like and pathological-like environments. This result suggested that alginate crosslinking in 450 mM $CaCl_2$ bath allowed an efficient alginate MS crosslinking. In the same manner, EE% resulted higher ($p < 0.05$) for lower $CaCl_2$ bath concentration (i.e., 450 mM), since an instantaneous surface crosslinking (i.e., 900 mM) did not led to a complete drug encapsulation [4]. Then, differences ($p < 0.05$) were observed by comparing swelling kinetics in the two environments (i.e., 7.4, 5.3), since degradation rate resulted faster (t = 130 h) at pH 7.4 than at pH 5.3 (t = 1008 h). Acidic environment promoted a lower but prolonged drug release in a pathological-like environment, which well matched the final work aim (i.e., drug release in tumoral environment). Lastly, *in vitro* biological tests showed MCF-7 cancer cells increased their metabolism if cultured in contact with pristine alginate MS, as expected. Otherwise, cell metabolism largely decreased ($p < 0.05$) if MCF-7 were cultured in presence of curcumin-loaded alginate MS, which revealed good efficiency in anti-tumoral treatments (Figure 1).

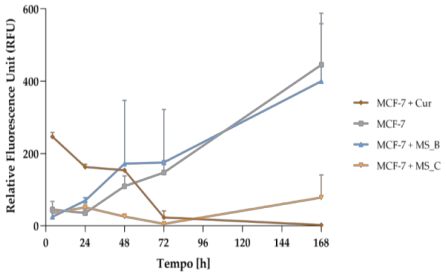

Figure 1 – Cell metabolism (RFU) of MCF-7 cells seeded on TCPS and cultured in contact with MS alginate microspheres.

CONCLUSION

An efficient DDS was here successfully developed. Extrusion dripping parameters were widely investigated, and *in vitro* stability, encapsulation efficiency, degradation kinetic and biological tests demonstrated the good performance of these two formulations.

REFERENCES

1. Sookkasem A. *et al., RSC Advances*, 8753-8756, 2015
2. Lee B. B. *et al., Chemical Engineering and Technology*, 1627-1642, 2013
3. Lin S. F. *et al., PLOS ONE*, vol. 11, no.4, 2016
4. Rastogi R. *et al., International Journal of Pharmaceutics*, 71-77, 2007

Poly(sebacic acid) microparticles loaded with azithromycin as pulmonary drug carriers

Karolina Knap[1], Katarzyna Reczyńska-Kolman[1], Konrad Kwiecień[1], Daria Niewolik[2], Katarzyna Jaszcz[2], Elżbieta Pamuła[1]

[1] AGH University of Science and Technology, Department of Biomaterials and Composites, Kraków, Poland
[2] Silesian University of Technology, Department of Physical Chemistry and Technology of Polymers, Gliwice, Poland
* kknap@agh.edu.pl

INTRODUCTION

Recurrent bacterial lung infections are difficult to treat due to increasing bacterial resistance to antibiotics. Novel inhalable drug carriers can potentially improve treatment efficacy via increased drug bioavailability and reduction of bacterial exposure to antibiotics [1].

The most desirable polymeric carrier for pulmonary drug delivery is one that is hydrophobic and degrades linearly over time in an aqueous environment. Promising candidates for pulmonary drug delivery are polyanhydrides. Polyanhydrides are undergoing uniform surface degradation into non-toxic metabolites that are non-mutagenic, non-cytotoxic and non-inflammatory [2].

The aim of the study was to manufacture microparticles (MP) and microparticles loaded with azithromycin (MP+AZ) based on poly(sebacic acid) (PSA). MP and MP+AZ were characterized in terms of size, morphology, degradation in aqueous environment and cytocompatibility.

EXPERIMENTAL METHODS

The MP based on PSA loaded with azithromycin were manufactured using oil-in-water (O/W) emulsification/solvent evaporation method, where O: PSA (or PSA+AZ) dissolved in dichloromethane (DCM); W: water solution of poly(vinyl alcohol) (PVA). The size of MP was characterized using dynamic light scattering (DLS), while the morphology of MP was evaluated by scanning electron microscope (SEM). Degradation of MP was evaluated using immersion in phosphate buffered saline (PBS) and incubation at 37°C for 96 h. MP morphology and mass changes as well as pH of PBS as a function of incubation time were assessed. Cytotoxicity of MP was evaluated in contact with adenocarcinoma human alveolar basal epithelial cells (A549) and human bronchial epithelial cells (BEAS-2B). The cells were cultured in Dulbecco's modified Eagle's medium (DMEM). The cells were seeded in 96-well plates at 10 000 cells/well and was incubated for 24 h before the treatment of microparticles suspension. The A549 and BEAS-2B cells were treated suspensions MP and MP+AZ in medium in concentration 50 µg/ml and incubated for 24 h. The viability of cells was analyzed using resazurin reduction assay and live/dead staining.

RESULTS AND DISCUSSION

The average hydrodynamic diameters were 1.41 µm ± 0.09 µm and 1.05 µm ± 0.33 µm, for MP and MP+AZ, respectively, which are believed to be suitable for inhalation [1]. The MP and MP+AZ before degradation were spherical with smooth surface. After degradation morphology of MP and MP+AZ changed into more flake-like shapes with wrinkled surface. During degradation pH of PBS decrease was observed and reached 5.8 for MP and 5.7 for MP+AZ after 96 h. Decrease in pH relates to microparticles degradation and release of carboxylic acids which acidify PBS [3]. The mass of MP changed in the course of time. At the beginning the mass of MP and MP+AZ slightly increased, which was related to water absorption and hydrolytic degradation of anhydride bonds [3]. After 96 h mass of MP and MP+AZ decreased to around 50% of their initial mass. The MP and MP+AZ were not cytotoxic for A549 and BEAS-2B cells. The viability of A549 and BEAS-2B cells incubated in MP and MP+AZ suspensions were 111% and 95% of the control, respectively.

CONCLUSION

The obtained MP had optimal size and morphology for pulmonary delivery. The addition of azithromycin did not affect degradation rate and cytocompatibility of MP. The MP based on PSA are promising carriers for pulmonary delivery of antibiotics for the treatment of bacterial infections in the lungs. However, it is necessary to evaluate the aerodynamic properties, drug release and antibacterial activity of MP and MP+AZ.

REFERENCES

[1] H. Douafer, V. Andrieu, and J. M. Brunel, "Scope and limitations on aerosol drug delivery for the treatment of infectious respiratory diseases," J. Controlled Release, vol. 325, pp. 276–292, Sep. 2020, doi: 10.1016/j.jconrel.2020.07.002.

[2] J. P. Jain, S. Modi, A. J. Domb, and N. Kumar, "Role of polyanhydrides as localized drug carriers," J. Controlled Release, vol. 103, no. 3, pp. 541–563, Apr. 2005, doi: 10.1016/j.jconrel.2004.12.021.

[3] D. S. Katti, S. Lakshmi, R. Langer, and C. T. Laurencin, "Toxicity, biodegradation and elimination of polyanhydrides," Adv. Drug Deliv. Rev., vol. 54, no. 7, pp. 933–961, Oct. 2002, doi: 10.1016/S0169-409X(02)00052-2.

ACKNOWLEDGMENTS

This study was supported by National Science Centre, Poland (project No 2019/35/B/ST5/01103) and by the Program 'Excellence Initiative – Research University' for the AGH University of Science and Technology.

Bioadegradable Polydepsipeptide Based-Microparticles as Drug Delivery Systems

Zoé Garisoain[1*], Tobias Burton[1], Olivia Giani[1], Julien Pinaud[1], Emmanuel Belamie[1]

[1]*ICGM, Univ Montpellier, CNRS, ENSCM, Montpellier, France*
* zoe.garisoain@umontpellier.fr

INTRODUCTION

Aliphatic polyesters such as polylactic acid (PLA), polyglycolic acid (PGA), and polycaprolactone (PCL) are widely employed materials for biomedical applications.[1] However, the hydrophobicity and crystallinity of PLA and PCL, as well as the rapid degradation of PGA, severely limits their use in a homopolymer form. On the other hand, by containing both amide and ester bonds, polydepsipeptides (PDPs) combine the mechanical properties of polyamides and the degradation capacities of polyesters, making them very attractive for tissue engineering and drug delivery.[2] In essence, PDPs are the simple alternation of α-amino acids (AAs) and α-hydroxyacids. Such polymers have been shown to degrade slowly over several weeks in aqueous environments. Depending on the initial AA employed to prepare the cyclic monomer they originate from, *i.e morpholine*-2,5-diones (MDOs), PDP's mechanical and biodegradable properties can be tuned to fit the requirements of the desired application. The aims of this study are to synthesize PDP(Leu) via a rapid and controlled method and to elaborate microparticles of leucine-based PDP's (PDP(Leu)) as drug delivery systems.

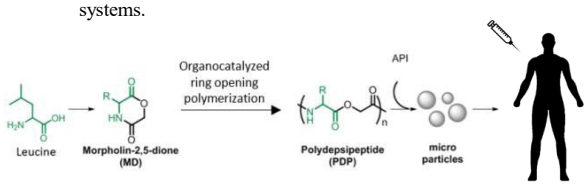

Fig.1. Synthetic pathway to PDP(Leu) microparticles

EXPERIMENTAL METHODS

Synthesis of PDP(Leu)

MDOs are not commercially available and are obtained *via* a two-step synthetic pathway.[3] PDP's are usually synthesized either via polycondensation or via ring opening polymerization of MDOs using $Sn(oct)_2$ as a catalyst. Here, PDP(Leu) was synthesized via organocatalyzed ring opening polymerization of 3S-(Isobutyl) morpholine-2,5-dione using DBU and thiourea as catalysts and benzyl alcohol as an initiator at 40°C.[4]

Formulation of microparticles

Microparticles were prepared by an emulsion solvent-evaporation technique using a 5% PVA in water and a 5% solution of PDP(Leu) in dichloromethane. The size, morphology and texture were analyzed by SEM.

RESULTS AND DISCUSSION

Synthesis of PDP(Leu)

To optimize the formulation and to achieve precise molecular control, various amounts of a thiourea co-catalyst were tested. A range of PDPs with average molecular weights between 8.1 and 25.2 kDa were thus produced with narrow distributions (Đ = 1.13−1.18).

Formulation of microparticles

Microspheres with diameters in the 10-100 µm range were obtained by the emulsion solvent-evaporation technique. This size range is interesting for the sustained release of an encapsulated drug.

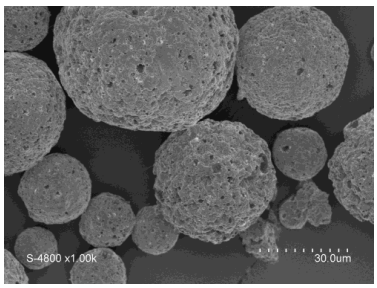

Fig.2. SEM image of PDP(Leu) microparticles

CONCLUSION

Leucine-based Polydepsipeptides with various molecular weight were successfully synthesized and formulated into microparticles. These microparticles could be used as drug delivery system by loading active pharmaceutical ingredient (ongoing experiments). Furthermore, the size of the microparticles allows the use of conventional needles for various administration.

REFERENCES

1. Doppalapudi S. *et al.*, Polym. Adv. Technol. 25, 427-435, 2014
2. Fonseca A. C.*et al.*, Progress in Polymer Science, 39, 1291-1311, 2014
3. Smelcerovic. *et al.*, Amino Acids, 46, 825-840, 2014
4. Burton T. F. *et al.*, Macromolecules, 53, 6598-6607, 2020

ACKNOWLEDGMENTS

This work was subsidized by both the Ministère de l'Enseignement Supérieur, de la Recherche et de l'Innovation (MESRI) and the Centre National de la Recherche Scientifique (CNRS)

Nanoplatforms based on Platinum-Conjugated Graphene Oxide as Drug Delivery System for Glioblastoma and Breast Cancer

Elena Giusto[1], Franco Furlani[1*], Arianna Rossi[1,2], Ludmila Zarska[3], Darren Fergal Beirne[4], Giada Bassi[1,5], Andrea Ruffini[1], Monica Montesi[1], Diego Montagner[4], Vaclav Ranc[3], Silvia Panseri[1]

[1] National Research Council of Italy - Institute of Science and Technology for Ceramics (ISTEC-CNR), Faenza (RA), Italy
[2] University of Messina, Messina (ME), Italy
[3] Regional Centre of Advanced Technologies and Materials, Palacký University Olomouc, Czech Republic
[4] Maynooth University, Dublin, Ireland
[5] University of Chieti, Chieti (PE), Italy

[*] franco.furlani@istec.cnr.it

INTRODUCTION

Glioblastoma is a very aggressive type of cancer with a very poor life expectancy for patients and breast cancer often metastasizes into the liver, lungs, brain, and, in 70% of cases, to bones[1,2]. Chemotherapy is largely used to treat cancer and it is based on the use of molecules targeting the high cancer cell proliferation metabolism[3]. Platinum (Pt) and three of its isoforms (cisplatin, carboplatin, and oxaliplatin) are some of the most successful metal-based drugs to cure breast cancer and glioblastoma[4,5]. Despite Pt-based chemotherapeutics being effective, their side effects (high degradation before entering the cells, the off-target organs toxicity, and cell resistance) remain great drawbacks[6-9]. In this work, it was developed a Graphene Oxide (GO) nanoplatform functionalized with Pt as a promising smart delivery system that could increase the Pt cellular uptake reducing the Pt amount needed for cancer treatment and consequently the side effects.

EXPERIMENTAL METHODS

GO nanoplatforms were treated with 8-arm polyethylene glycol-amine (PEG) that permits to load Pt on the platform (GO-PEG-Pt) and an extensive *in vitro* screening was performed on two breast cancer cell lines with aggressive nature that lead to metastatic behavior (MDA-MB 231 and MDA-MB 468) and two glioblastoma cell lines (U87 and U118). The bioactivity of GO-PEG-Pt compared to Pt-free (15 µM, 30 µM, and 60 µM) was analyzed looking at the effect on cellular uptake (ICP-OES), viability (MTT Assay), morphology (DAPI and actin staining), and migration up to 72 hours (Scratch Assay).

RESULTS AND DISCUSSION

The cell viability was significantly lower in MDA-MB 468 and U118 cells at 30 µM for GO-PEG-Pt group compared to Pt-free (<75%), and even the cell morphology seemed to be compromised. These results were highly related to the cellular uptake of GO-PEG-Pt which is significantly higher compared to Pt-free after 24 hours. This data confirmed that our nanoplatform promotes drug delivery directly inside the cells. In addition, GO-PEG-Pt mostly affected the cell migration compared to Pt-free, in particular, MDA-MB 231 showed a migration reduction of 60%, and this could be a great advantage in reducing the metastasis process.

CONCLUSION

This study demonstrated that the combination of Pt onto PEG-functionalized nano-sized GO provided numerous advantages for tumor therapy such as minimizing toxicity, enhancing the cellular uptake, and consequently we could reduce the side effects because a lower amount of Pt is necessary.

REFERENCES

1. Feng, Y. *et al.*, Genes Dis., 5(2):77-106, 2018
2. Dymova, M.A. *et al.*, Int. J. Mol. Sci., 22(12):6385, 2021
3. Schirrmacher, V., Int. J. Oncol., 54:407–19, 2019
4. Taghavi, M.S. *et al.*, In Vitro Cell. Dev. Biol.-Animal, 49:465–472, 2013
5. Martín, M., Clin. Breast Cancer, 2(3):190-208, 2001
6. Bersini, S. *et al.*, J. Biomaterials, 35:2454–61, 2014
7. Lei, S. *et al.*, Cancer Commun., 12:4413, 2021
8. Rajaratnam, V. *et al.*, Cancers, 12(4):937, 2020
9. Liang, Y. *et al.*, Semin. Cancer. Biol., 60:14–27, 2020

ACKNOWLEDGMENTS

The authors would like to thank the Nano4Tarmed project (H2020-WIDESPREAD-2020-5, grant no: 952063) for providing financial support to this project.

Development of a Nanocomposite Coating for Implant-Associated Local Drug Delivery from Neural Electrodes

Mosaieb Habib[1,3*], Tim-Joshua Strauß[1], Kim Kreisköther[1], Jennifer Harre[2,3], Arne Schierz[1], Thomas Lenarz[2,3], Athanasia Warnecke[2,3], Peter Behrens[1,3]

[1] Institute of Inorganic Chemistry, Leibniz University Hannover, Hannover, Germany
[2] Department of Otorhinolaryngology, Head and Neck Surgery, Hannover Medical School, Hannover, Germany
[3] Cluster of Excellence "Hearing4all"
[*] mosaieb.habib@acb.uni-hannover.de

INTRODUCTION

Platinum is currently used as an electrode material in neural electrodes, such as in the cochlear implant (CI). In addition to stimulating neurons through the electrode contacts, it is also important to restore and maintain healthy conditions in the cochlea. By provision of neuroprotective substances, neuronal growth factors, anti-inflammatory drugs or antibiotics, it is possible to restore the balance in the inner ear and thus stabilize the remaining nerve cells, the spiral ganglion neurons. Furthermore the outgrowth of neurites from these cells can be induced to improve the electrode-nerve contact and increase signal resolution.[1] For optimal application, these drugs should be released locally, for example with an implant-associated local drug delivery system. Due to the inertness of the materials from which the cochlea electrode is made - platinum and silicone - the construction of such a systemis not trivial.

To nevertheless achieve a local implant-associated drug delivery, we devised a novel nanocomposite material of nanoporous silica nanoparticles (NPSNPs) embedded in the pores of nanoporous platinum (NPPt) which can be employed as a coating on the platinumsurfaces of the CI electrode.[2] NPPt exhibits high conductivity and favorable electrochemical properties. NPSNPs embedded in the pore system of platinum provide large surface area, permanent porosity and high versatility in terms of easily tunable surface properties to achieve high drug loading.[3,4]

EXPERIMENTAL METHODS

A hard template approach was used to fabricate the NPSNP@NPPt material on the surface of the platinum, in which 100 nm sized silica-polystyrene core-shell nanoparticles served as templates. Platinum was electrolytically deposited between the particles and the polystyrene was removed via extraction.

The composite coating was characterized by means of scanning electron microscopy (SEM), krypton physisorption measurements, cyclic voltammetry and electrochemical impedance spectroscopy. Release experiments were performed with the dye methylene blue. Cell culture investigations with fibroblasts and spiral ganglion cells were conducted to investigate the cytocompatibility of the novel material.

RESULTS AND DISCUSSION

SEM investigations showed the successful synthesis of the desired structure of the nanocomposite (figure 1). The material exhibits good electrochemical properties and enhanced surface area due to the nanoporous silica nanoparticles. The release experiments indicate a higher loading and release of methylene blue. Cell culture studies with the new material show good cytocompatibility.

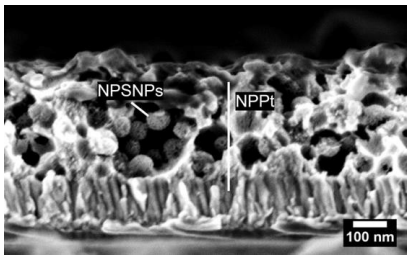

Figure 1. Scanning electron micrograph of the novel nanocomposite material, composed of nanoporous silica nanoparticles embedded in the pore systemof platinum.

CONCLUSION

The novel nanocomposite material combines the favourable properties of both nanoporous platinum and nanoporous silica nanoparticles, specifically the excellent electrochemical behaviour of NPPt and the high specific surface area, large pore volume and amenability to surface modifications of the NPSNPs. Current work is focused on chemically modifiying NPSNPs to introduce specific surface functionalities that enable efficient drug loading and controlled delivery.

REFERENCES

1. Shibata S. B. *et al*., Hear. Res. 281:56–64, 2011.
2. Behrens P. *et al*., Hybrid system with nanoporous nanoparticles in a noble metal structure and process for the production thereof and its use. German Patent published (2019): SW 102018118092.6. International Patent published (2020): WO2020021075A1.
3. Williams S. *et al*., J. Mater. Sci. Mater. Med. 26:125, 2015.
4. Schmidt N. *et al*., PLoS ONE 13: e0194778, 2018.

ACKNOWLEDGMENTS

This work was funded by the Deutsche Forschungsgemeinschaft (DFG, German Research Foundation) under Germany's Excellence Strategy within the Cluster of Excellence EXC 2177/1 "Hearing4all" (Project ID 390895286).

Hyaluronic Acid-based stabilizer to improve skin penetration of actives

Paula Zamora[1], Aitziber Lopez[1], Natividad Diaz[1], Hans-Jürgen Grande[1], Iraida Loinaz[1] Damien Dupin[1]

[1] Fundación CIDETEC, Parque Científico y Tecnológico de Gipuzkoa, P° Miramon, 196, 20014 Donostia-San Sebastián, Spain

* pzamora@cidetec.es

INTRODUCTION

Nanoemulsions are a very trendy drug delivery system to transport and deliver actives or drugs. However, most surfactant required for oil-in-water emulsions are from petroleum-based and lack sustainability [1]. Here, hyaluronic acid (HA), well-known for being biodegradable, biocompatible, nontoxic, non-immunogenic was slightly modified and used as stabilizer for oil-in-water emulsions. Poorly-water-soluble active pharmaceutical ingredients or cosmetics ingredients were encapsulating, and their stability and synergy activity were improved, thanks to the HA based surfactants.

METHODS

Hyaluronic acid functionalization

Hyaluronic acid was modified with methacrylate groups that confers hydrophobic regions and so, increases surface activity. Synthesis were performance with different reagents, molar ratio and purification methods in order to obtain tailored degree of substitution, characterized by ^{1}H-NMR as well as functionalization kinetic. Surface tension variations of aqueous modified polymer solutions were measured with a tensiometer.

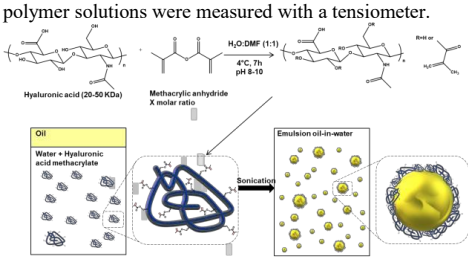

Figure 1: Hyaluronic acid functionalization and its use as oil-in-water emulsion stabilizer

Emulsion characterization

Water-in-oil emulsions were prepared using sonication processes. The effect of process conditions (amplitude, pulse, time, temperature, etc.) were varied with the aim of getting stable emulsions in the nano-range. Droplet size was measured by means of Dynamic Light Scattering (DLS), Laser Diffraction (LD) and electron microscopy. How emulsifier concentration, degree of substitution and oil phase affect emulsion stability were studied.

In vitro studies

Relevant cell lines such as immortalized epidermal human keratinocytes (HaCaT) and Human Dermal Fibroblasts (HDF) were used to study cytotoxicity. Cell viability of both Methacrylate Hyaluronic Acid at different concentrations in solution and diluted emulsions were measured using Cell-Titer Glo reagent.

Ex vivo efficacy testing

Reconstructed Human Epidermis (RHE) and dermis skin model were used to study the safety and efficacy of the system. Skin irritation tests based on OECD 439 guideline were performed with modified polymer and emulsion system. By confocal microscopy, skin penetration was studied. For this purpose, oil phase was labelled using fluorophore. Emulsion was obtained after sonication and applied in RHE skin models (30 µL). Free labelled actives were used for comparative purposes.

RESULTS AND DISCUSSION

Synthesis of methacrylate hyaluronic acid (HA-MA) with controlled degree of substitution between 30 and 120% was achieved. HA-MA was used as stabilizer to produce oil-in-water emulsions. The most stable emulsions were obtained for HA-MA with high degree of substitution (≥80%), low surface tension (c.a. 50 mN/m) at 90/10 water/MCT oil and 10 or 15% of HA-MA based on oil phase. Emulsions with droplet size around 200-600nm, as judged by DLS, were stable during at least 100 days. Both HA-MA and emulsions demonstrated to be non-cytotoxic towards HaCaT and HDF, as well as non-irritant on RHE, with more than 80% viability after 48h of exposition. Preliminary encapsulation studies showed that hydrophobic vitamins, i.e. E and A, could be easily encapsulated. Biodistribution studies on RHE demonstrated that HA-MA stabilized emulsion allowed Nile red (as model molecule) to reach deeper layer of the epidermis. After 4 hrs, the dye was localized 40 microns deep into the epidermis, reaching stratum Spinosum, whereas the nonencapsulated dye remained mostly in the stratum corneum, only reaching a few microns depth. Thus, enhanced active performances could be anticipated from a better penetration in the epidermis.

CONCLUSION

HA-MA was produced with controlled degree of functionalization and proved to be an efficient stabilizer for oil-in-water emulsions.

In vitro and *ex vivo* studies demonstrated the safety of the whole system. Finally, increase bioavailability of encapsulated drug, as judged by skin biodistribution studies, makes HA-MA based nanoemulsions a promising candidate to improve active performances.

REFERENCES

1. WO2021122942A1 "NATURAL ORIGIN STABILIZER FOR OIL IN WATER EMULSIONS"

ACKNOWLEDGMENTS

The authors thank the Diputación Foral de Gipuzkoa (2020-CIEN-000035-01.) for providing financial support to this project.

Smart encapsulation technologies for topical application based on bioinspired emulsifiers

Aitziber Lopez[1*], Natividad Diaz[1], Hans-Jürgen Grande[1], Iraida Loinaz[1], Oihane Vesga[2], Irati Aldalur[2], Maialen Irastorza[2], Elisabeth Garanger[3], Sébastien Lecommandoux[3], Damien Dupin[1]

[1] Fundación CIDETEC, Parque Científico y Tecnológico de Gipuzkoa, P° Miramon, 196, 20014 Donostia-San Sebastián, Spain
[2] EMISSARY Cosmetics S.L., Parque Científico y Tecnológico de Gipuzkoa, P° Miramon, 196, 20014 Donostia-San Sebastián, Spain
[3] Laboratoire de Chimie des Polymères Organiques (LCPO), Université de Bordeaux - CNRS - Bordeaux-INP, ENSCBP, 16 avenue Pey Berland, 33607 Pessac, France

[*] aitziberlopez@cidetec.es

INTRODUCTION

With an expected expansion at GAGR of 8% during 2016-2024[1], the development of new encapsulation technologies that enhance ingredients/drug performance has become an important market for topical administration industry. Technologies that can, not only improve the stability of sensitive molecules, but also be triggered by specific skin needs are highly demanded from a sustainable perspective. Here, new smart delivery systems based on bioinspired emulsifiers have been developed: stimuli responsive polypeptide-based emulsifiers[1].

EXPERIMENTAL METHODS

Active ingredient encapsulation and emulsion characterization

Emulsions were prepared using high pressure homogenization processes. The effect of process conditions (homogenization time, pressure, etc.) were varied with the aim of getting stable emulsions in the nano-range. Droplet size was measured by means of Dynamic Light Scattering (DLS), Laser Diffraction (LD) or electron microscopy. Encapsulation efficiency and active ingredient stability was measured by analytical methods such as HPLC. Biodegradability was measured following OECD 301 guideline.

In vitro/ex vivo efficacy testing and safety

Relevant cell lines, Reconstructed Human Epidermis (RHE) skin models and ex-vivo explants were used to study the safety and efficacy of the compositions. In addition, to skin irritation or skin sensitization tests based on OECD 439 and 422 guidelines, the anti-inflammatory and other bioactive properties such as the antioxidant activity or collagen production was analysed. Antioxidant activity was measured by analysing the inhibition of Reactive Oxygen Species (ROS) in HaCaT cells. Anti-inflammatory properties were measured by damaging ex vivo skin explants and analysing the production of certain cytokines by ELISA methods. Skin penetration was studied by confocal microscopy. For that purpose, both stabilizers and active ingredients were labelled using reactive fluorophores such as DY-405 or cyanine 5.5. Doubly labelled emulsions were produced by sonication and applied in RHE skin models (30 µL) for different time scales. Free labelled actives were used for comparative purposes.

RESULTS AND DISCUSSION

Both oil-in-water and water-in-oil emulsions were produced to encapsulate a great variety of actives with an encapsulation efficiency close to 100%. Droplet size ranged from 100 till 350 nm and emulsions were stable under the conditions described in the ISO/TR 18811/2018. Encapsulated compositions demonstrated to be safe, among others, in terms of skin irritation and sensitization. Compositions were classified as readily biodegradable. Both antioxidant and anti-inflammatory properties were improved by a minimum of twice thanks to encapsulation. This improvement on efficacy was attributed to the enhanced light and temperature stability of sensible cosmetic actives and to a deeper penetration of the actives through skin.

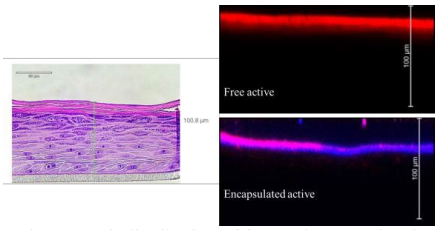

Figure 1. Biodistribution of free and encapsulated actives analysed by confocal imaging.

CONCLUSION

The bioinspired polypeptide-based emulsifiers have demonstrated to be very effective in the encapsulation of both hydrophobic and hydrophilic cosmetic active ingredients. In addition, to be biodegradable, these new emulsion compositions have demonstrated to increase the performance of encapsulated actives thanks to an improved stability and deeper skin penetration.

REFERENCES

1. Delivery Systems In Personal Care Market. Persistance Market Research. 2015.

ACKNOWLEDGMENTS

The authors thank the Spanish Government (SNEO-20201318) for providing financial support to this project.

[1] Lecommandoux, S. *et al*. WO2019068936A1.

Development of a drug delivery system based on silica nanoparticles and silicone

Luisa Vanessa Steingrube[1,3*], Arne Klaus Schierz[1,3], Jennifer Harre[2,3], Athanasia Warnecke[2,3], Thomas Lenarz[2,3], Peter Behrens[1,3]

[1]Institute of Inorganic Chemistry, Leibniz University Hannover, Germany
[2]Nose-Threat Clinic, Hannover Medical School, Germany
[3]Cluster of Excellence Hearing4all, Hannover, Germany
[*] luisa.steingrube@acb.uni-hannover.de

INTRODUCTION

For those who are affected, hearing loss implicates significant challenges. If the hearing loss is a consequence of the loss of hair cells, the implantation of a cochlear implant is the treatment of choice. This implant stimulates the remaining spiral ganglion neurons. One critical issue is the loss of signal transmission which is a consequence of the relatively large gap between the electrode and the remaining neurons. For a better acoustical experience, an improvement of the electrode nerve contact is necessary.[1] For this purpose, a growth factor-based drug delivery system is developed which will be established on the cochlea electrode. This system is based on nanoporous silica nanoparticles (NPSNPs). On these particles the growth factors neutotrophin-3 (NT-3) and brain derived neurotrophic factor (BDNF) are attached. These proteins should support the survival rate of the neurons and guide them among a concentration gradient.[2,3]

The installation of a drug delivery system on cochlear electrodes is generally challenging due to the inert materials used (platinum/silicone). Therefore, a novel procedure to attach the NPSNP on silicone is also being developed using coating of covalently bonded polymers.[4]

EXPERIMENTAL METHODS

In a first step NPSNPs were synthesized via an adapted method by QIAO *et al.*[5] and afterwards modified with (3-aminopropyl)triethoxysilane (by stirring in toluene.

The growth factors were attached on the particle surface via incubation in a 1 $\mu g \cdot mL^{-1}$ solution. To test the release behavior, the particles were stored at 37 °C. The released amount of protein was quantified via enzyme-linked immunosorbent assay (ELISA).

To attach NPSNPs on silicone, a polymer coating is created by UV mediated radical reaction.[4] The polydimethylsiloxane (PDMS) was incubated in an acetone/benzophenone solution, then in an aqueous acrylamide solution. It was irradiated at 365 nm under a nitrogen atmosphere directly in the solution or after a further drying step.

RESULTS AND DISCUSSION

The NPSNPs were characterized before and after modification. Thermogravimetric measurements show a higher mass loss for the modified particles compared to the non-modified NPSNPs which is attributed to the organic functionalization on the surface. Furthermore, the BET-surface area decreased, possibly due to pore partial blocking. Additionally, it is confirmed that the modification process has no influence on the particle morphology by TEM.

Quantification via ELISA confirmed that the immobilization of BDNF and NT-3 was successful and reversible. Modification with APTES causes a delay in the release, which may be due to the stronger interactions between the modified particles and the proteins. There is no evidence that the modification has an impact on the total released amount of NT-3, while the released amount of BDNF varies with modification.

In general, a higher amount of NT-3 (up to 325 ng after 35 days) was determined in the release solutions compared to BDNF (up to 95 ng after 37 days).

The contact angles of pure silicone and polymer coatings were analyzed to characterize the hydrophobicity. It decreased from 117° for pure silicone up to 62°. Furthermore, the coatings were characterized with the SEM and polymer layers could be observed.

CONCLUSION

NPSNPs were successfully synthesized and modified with amino groups. Moreover, these particles were able to reversibly bind NT-3 and BDNF on their surface.

The modification showed no significant influence for the NT-3 release but the release of BDNF was higher with the amino modification. In the future a combined release of both growth factors is aimed. For this, the amino modified particles should be preferred.

The change in hydrophobicity shows that the surface properties of silicone can be changed by a polymer coating which is an important achievement for the installation of the drug delivery system.

Considering these results in context, they jointly form the basis for a composite material that can be used as a cochlear implant-associated drug delivery system.

REFERENCES

[1] N. Schmidt, J. Schulze, D. P. Warwas, N. Ehlert, T. Lenarz, A. Warnecke, P. Behrens, *PloS one* **2018**, e0194778.

[2] K. Moore, M. MacSween, M. Shoichet, *Tissue engineering Part A* **2006**, *2*, 267–278.

[3] A. K. Wise, R. Richardson, J. Hardman, G. Clark, S. O'leary, *The Journal of comparative neurology* **2005**, *487*, 147–165.

[4] D. Keskin, T. Mokabbar, Y. Pei, P. van Rijn, *Polymers* **2018**.

[5] Z.-A. Qiao, L. Zhang, M. Guo, Y. Liu, Q. Huo, *Chem. Mater.* **2009**, *21*, 3823–3829.

ACKNOWLEDGMENTS

This work was funded by the Deutsche Forschungsgemeinschaft (DFG, German Research Foundation) under Germany's Excellence Strategy - EXC 2177/1 - Project ID 390895286.

A Fibre-based Neuronal Guidance Scaffold for the Inner Ear: Delivery of Neurotrophin-3 and Decoration with Laminin

Monika Seegers[1,3*], Jennifer Harre[2,3], Thomas Lenarz[2,3], Athanasia Warnecke[2,3], Peter Behrens[1,3]

[1] Institute of Inorganic Chemistry, Leibniz University Hannover, Hannover, Germany
[2] Department of Otorhinolaryngology, Head and Neck Surgery, Hannover Medical School, Hannover, Germany
[3] Cluster of Excellence Hearing4all, Hannover, Germany
[*] monika.seegers@acb.uni-hannover.de

INTRODUCTION

Hearing loss is a major health problem of today's society. In case of sensorineural hearing loss, the most effective therapy is the implantation of a cochlear implant. However, a critical issue is that the distance between the electrode of the cochlear implant and the spiral ganglion neurons (SGNs) is relatively large which results in a loss of signal transmission. Therefore, an improvement of the electrode-nerve contact for enhanced auditory impression is needed.[1] To achieve this, a neuronal guidance scaffold and drug delivery system which is established on the cochlear implant is designed. This scaffold is made of biodegradable polymer fibres. The fibres shall be decorated with growth factors (brain-derived neurotrophic factor (BDNF), neurotrophin-3 (NT-3)) which are released from the fibres to increase the survival of the SGNs and to stimulate the outgrowth of neurites. In addition, the fibres are coated with components of the extracellular matrix (laminin, heparan sulphate (HS)) to offer growing neurites a favourable environment for their extension to the electrode.[2]

EXPERIMENTAL METHODS

Aminolysis of polymer fibres

The fibres (Glycolon®, Resorba Medical GmbH) were aminolysed according to WILLE *et al.*[2] to generate free amino groups on the surface. For this, ethylenediamine was bound to the surface using the coupling agents *N*-hydroxy succinimide (NHS) and *N,N'*-dicyclocarbo-diimide (DCC). The fibres were characterised by SEM and FTIR.

Attachment of biomolecules

HS was attached to the fibres according to WILLE *et al.*[2] using 1-ethyl-3-(3-dimethylaminopropyl) carbodiimide (EDC) and NHS.

NT-3 was attached to fibres with and without HS. The incubation took place with 1 µg ml^{-1} NT-3 in phosphate-buffered saline (PBS) containing 0.1 % bovine serum albumin (BSA) for 24 h at 4 °C. For a release of NT-3 the samples were stored at 37 °C for different periods. Then the supernatants were removed and replaced by fresh medium.

For covalent attachment of laminin, the fibres were incubated in a MES solution containing EDC, NHS and 10 µg ml^{-1} laminin for 24 h and 4 °C. After washing, the fibres were placed in a special holder and cell culture investigations were carried out. For this, spiral ganglion explants of cochleae of neonatal Sparague-Dawley rats were placed on the fibres. After a fluorescent staining, the SGNs and neurites were investigated.

RESULTS AND DISCUSSION

After the aminolysis the fibres had a rough surface due to the harsh conditions during this treatment. FTIR measurements verified the amino-modification.

The release curves in *Figure 1* show that the release of NT-3 is more continuous when the fibres have been coated with HS previously. There is a release of approximately 7 ng ml^{-1} NT-3 after 35 days. Without HS, the release diminishes after 14 days when ca. 4 ng ml^{-1} have been set free.

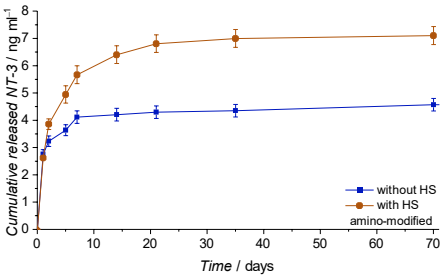

Figure 1:Release of NT-3 from amino-modified fibres coated with (orange) and without (blue) HS after 70 days.

The cell culture investigations showed that explants with SGNs can grow on laminin-coated fibres. They form extended neurites which grow preferably along the fibre, thus using the fibre as a guidance structure.

CONCLUSION

The release experiments showed that it is possible to release NT-3 from the fibres. The cell culture investigations showed promising results with regard to the use of these fibres as a neuronal guidance scaffold for SGN neurites.

REFERENCES

1. Schmidt N. *et al.*, PLoS One, 13(3):e0194778, 2018
2. Wille I. *et al.*, Front. Bioeng. Biotechnol. 10:1-19, 2022

ACKNOWLEDGMENTS

This work was supported by the Deutsche Forschungsgemeinschaft (DFG, German Research Foundation) under Germany's Excellence Strategy – EXC 2177/1 – Project ID 390895286.

Multi-stimuli Responsive Protein Nanoparticles for Controlled Drug Delivery in Cancer Therapy

Juan Gonzalez-Valdivieso[1*], Alessandra Girotti[2,3], Javier Arias[2,3], Moonsoo Jin[1]

[1]Molecular Imaging Innovations Institute (MI3), Weill Cornell Medicine, New York, USA
[2]Smart Biodevices for NanoMed Group, University of Valladolid, Valladolid, Spain
[3]Institute of Biology and Molecular Genetics, Valladolid, Spain

[*]juan.gonzalez.valdivieso@uva.es

INTRODUCTION

Cancer is a general term for a large group of diseases, whose causes, characteristics and occurrence can vary, characterized by the aberrant growth of cells able to divide uncontrollably and infiltrate and disrupt normal body tissues. Cancer has a major impact on society across the world and, in fact, there were 19.3 million new cases in 2020 worldwide[1]. Moreover, the number of new cases per year is expected to rise to 29.5 million by 2040[1]. Poor drug accumulation and adverse side effects are some of the most important problems of current cancer treatments[2]. To overcome this, novel biomaterials constitute a promising approach aiming to develop nanocarriers with improved therapeutic efficacy. Elastin-Like Recombinamers (ELRs) highlight due to their cell-friendly behavior, thermal sensitivity and lack of immunogenicity[3]. We report herein a novel drug delivery nanosystem comprising a small peptide inhibitor of Akt kinase within an ELR scaffold for cancer therapy.

EXPERIMENTAL METHODS

By recombinant DNA technology, the nanoparticles were designed based on an amphiphilic backbone with multiple bioactive sequences[3]. Nanoparticles were characterized by Dynamic Light Scattering, Transmission Electronic Microscopy and Atomic Force Microscopy. The effect of ELR nanoparticles on cell viability was evaluated *in vitro*. *In vivo* biodistribution was determined by IVIS (*in vivo* imaging system) and Positron Emission Tomography – Computed Tomography (PET/CT) Scanning.

RESULTS AND DISCUSSION

The Results and The physicochemical characterization showed that ELR polymers were able to self-assemble into monodisperse nanoparticles with a mean diameter of 72nm when temperature was increased above 16°C. The nanoparticles also showed high stability over time and their size and surface charge were not altered under physiologic conditions. *In vitro* assays evidenced high cytotoxicity in GBM248 cells, with time- and dose-dependent trend. Systemic administration of nanoparticles in tumor-bearing mice showed high tumor uptake and absence of side effects in critical organs, such as heart, liver, kidney or spleen.

CONCLUSION

Hence, these findings indicate that our complex nanosystem allows us to achieve selective controlled release of chemotherapeutic molecules in cancer cells as well as avoid normal healthy tissues. Thus, this complex approach has a promising potential for cancer therapy.

REFERENCES

1. https://www.iarc.who.int/
2. Shi J. *et al*., Nat. Rev. Cancer 17:20-37 2017
3. Gonzalez-Valdivieso J. *et al*., Biomacromolecules 20: 1996-2007 2019

ACKNOWLEDGMENTS

The authors would like to thank the MINECO (Grants no: PCIN-2015-010, MAT2015-68901-R, MAT2016-79435-R and MAT2016-78903-R), and the JCyL (Grant no: VA317P18) for providing financial support to this project.

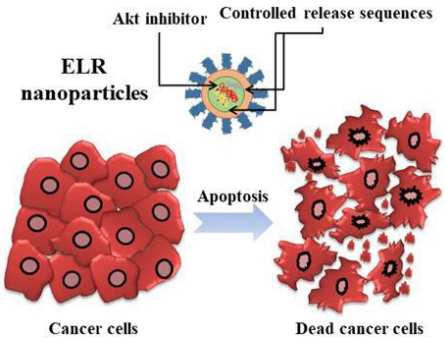

Figure 1. Scheme of self-assembling nanoparticles carrying an Akt inhibitor as an accurate drug delivery system validated *in vitro* and *in vivo*.

Platinum-conjugated Graphene Oxide as Nanoplatform to Enhance Drug Delivery in Osteosarcoma

Elena Giusto[1], Giada Bassi[1,2], Ludmila Zarska[3], Eoin Moyinihan[4], Arianna Rossi[1,5], Andrea Ruffini[1], Monica Montesi[1], Diego Montagner[4], Vaclav Ranc[3], Silvia Panseri[1*]

[1] National Research Council of Italy - Institute of Science and Technology for Ceramics (ISTEC-CNR), Faenza (RA), Italy
[2] University of Chieti, Chieti (PE), Italy
[3] Regional Centre of Advanced Technologies and Materials, Palacký University Olomouc, Czech Republic
[4] Maynooth University, Dublin, Ireland
[5] University of Messina, Messina (ME), Italy

[*] silvia.panseri@istec.cnr.it

INTRODUCTION

Osteosarcoma is the most common type of bone cancer diagnosed especially in children and young adults[1]. A combination of chemotherapy, radiotherapy and surgery is commonly used to treat this type of cancer[2,3]. In detail, chemotherapy is based on the use of molecules targeting the high cancer cell proliferation metabolism such as Platinum (Pt)-based drugs that binds nuclear DNA upon overpassing the cell membrane, causing its damage and the arrest of the cancer cell cycle at G2/M transition phase, leading to apoptosis[4-7]. Despite Pt chemotherapeutics are the most potent used anticancer drugs, their side effects (high degradation before entering the cells, the off-target organs toxicity, and cell resistance) remain great drawbacks[8-11].

EXPERIMENTAL METHODS

In this study, we synthetized Graphene oxide (GO)-based nanoplatforms as smart delivery systems of Platinum-based drug. In order to reduce GO cytotoxicity in health cells while promoting its cellular uptake in cancer cells, and to allow Pt loading on GO, 8-arm polyethylene glycol-amine (PEG) was used. The bioactivity of GO-PEG-Pt platforms were compared to Pt-free (15 µM, 30 µM, and 60 µM) on three osteosarcoma cell lines (MG63, U2 and SAOS-2). The in vitro analysis of cellular uptake (ICP-OES), viability (MTT assay), morphology (actin and DAPI staining) and migration (scratch test) was performed.

RESULTS AND DISCUSSION

A preliminary study showed that GO-PEG was not toxic for cells at any concentration tested compared to cells only. A significant cell viability reduction was detected at 30 µM GO-PEG-Pt for all cell lines compared to Pt-free, reaching 70% cell mortality in MG63 (p value $\leq$ 0.0001) and SAOS-2 (p value $\leq$ 0.001). Morphological analyses showed a round-shape cell morphology and cell number reduction in the presence of GO-PEG-Pt respect to Pt-free in a dose dependent trend. Cellular uptake of GO-PEG-Pt was significantly higher after 24h for SAOS (p value $\leq$ 0.05) and MG63 (p value $\leq$ 0.0001) cell lines than Pt-free. The cell migration was lower in Go-PEG-Pt than Pt-free in MG63 and U2 with overall more than 60% migration inhibition over time at 30 µM concentration.

CONCLUSION

The results confirmed that GO-PEG-Pt platforms work as promising anticancer delivery systems. In fact, all the three osteosarcoma cell lines showed higher susceptibility to GO-PEG-Pt in terms of lower metabolic activity and lower migration rates due to the higher GO-PEG-Pt uptake compared to Pt-free.

REFERENCES

1. Tang, Q.L. *et al.*, Cancer Lett., 113:121, 2011
2. Xiao, X. *et al.,* J Exp Clin Cancer Res, 37:201, 2018
3. World Health Organization – Cancer, 2021
4. Hulvat MC., Cancer Incidence and Trends. Surg. Clin. North Am. W.B. Saunders, 2020
5. Schirrmacher V., Int J Oncol., 54:407–19, 2019
6. Johnstone TC, *et al.* Chem. Rev. American Chemical Society, 3436–86, 2016
7. Gmeiner WH *et al.,* Nanotech. Rev., 3:111–22, 2014
8. Bersini S, *et al.* J Biomaterials 35:2454–61, 2014
9. Lei S *et al.,* Cancer Commun. 1–12, 2021
10. Rajaratnam V. *et al.,* Cancers, 2020
11. Ottaviani G. JN., Cancer Treat Res., 152:33, 2019

ACKNOWLEDGMENTS

The authors would like to thank the Nano4Tarmed project (H2020-WIDESPREAD-2020-5, grant no: 952063) for providing financial support to this project.

Development of Trimagnetic Nanoparticles for Targeted Magnetic Hyperthermia of Prostate Cancer Cells

Valentin Nica, Attilio Marino, Carlotta Pucci, Gianni Ciofani

Center for Materials Interfaces, Italian Institute of Technology, Pontedera, Italy
* valentin.nica@iit.it

INTRODUCTION

Magnetic fluid hyperthermia (MFH) is a promising technique for cancer therapy proved by successfully human clinical trials[1]. The heating efficiency of magnetic nanoparticles (MNPs) can be enhanced by tuning the surface and shape anisotropy, the degree of spin disorder, and exchange anisotropy at the interface between the magnetic phases[2]. Trimagnetic NPs (TMNPs) are a new class of nanovectors that may be successfully applied in many types of cancer such as glioblastoma multiforme, prostate cancer, esophageal cancer or pancreatic cancer.

EXPERIMENTAL METHODS

Shaped-anisotropic TMNPs have been synthesized by thermal decomposition of metallic complexes using one-pot synthesis of bi-magnetic NPs (BMNPs) and subsequent seed-mediated growth route. The structural and morphological properties have been revealed by X-ray diffraction (XRD), and transmission electron microscopy (TEM). Scanning TEM-energy dispersive X-ray technique (STEM-EDX) and X-ray photoelectron spectroscopy (XPS) results confirmed the formation of TMNPS. PC-3 Caucasian prostate adenocarcinoma cell line was used for *in-vitro* intracellular hyperthermia. For cell targeting, the PEGylated TMNPs have been functionalized with a cell-penetrating peptide CTGTPARQC (LN1). Magnetic hyperthermia has been performed *in vitro* at ν=100 kHz and B=20 mT.

RESULTS AND DISCUSSION

In this study, we used a magnetically soft-soft-hard highly dispersible TMNPs (Fe_3O_4@$Mn_{0.5}Zn_{0.5}Fe_2O_4$@$CoFe_2O_4$, further denoted as SSH) (Fig. 1) for targeted magnetic hyperthermia of prostate cancer cells.

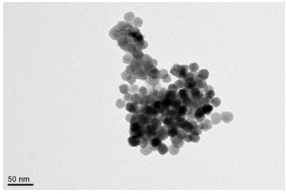

Fig. 1 TEM image of trimagnetic nanoparticles.

The SSH specific absorption rate (SAR = 69 W/g) is higher than its corresponding BMNPs (Fe_3O_4@$Mn_{0.5}Zn_{0.5}Fe_2O_4$, SAR = 45 W/g) with respect to their volume. The specific saturation magnetization values at room temperature was found as 79 emu/g (SSH) and 62 emu/g (BMNPs), respectively.

The WST-1 cell viability assay has demonstrated that the system does not significantly induce cell toxicity compared to the control counterpart at concentrations up to 350 µg/ml. The flow cytometry results have shown that the 99% and 100% of the cells are positive for the LN1-SSH at 24 h and 72 h of incubation, respectively, demonstrating a high internalization rate. Magnetothermal stimulation of PC-3 cells has been carried out by using the LN1-SSH at the highest safe concentration (350 µg/ml). Three different experimental conditions have been performed: non-treated control cells (Control), cultures stimulated with AMF only, and cultures exposed to AMF after 24 h of pre-incubation with LN1-SSH. The AMF treatment has been applied daily for 90 min at 100 kHz and 20 mT over 3 days. The cytotoxicity tests revealed a significantly lower metabolic activity of cells treated with LN1-SSH+AFM (72% decrease) compared to non-treated controls. The AMF stimulation on cells non-incubated with nanoparticles was not able to induce any significant effect on cell viability, therefore indicating the safety of the stimulation protocol.

CONCLUSION

A new magnetic nanovector with enhanced SAR has been developed for hyperthermia therapy of cancer. The system consists of PEGylated TMNPs which were further conjugated with a cell-penetrating peptide (LN1) to facilitate intracellular uptake. The cell viability assays on PC3 cells show that conjugated nanoparticles (LN1-SSH) do not induce significant alteration of the metabolic activity up to 350 µg/ml concentration of MNPs, which was considered the optimal condition for further studies. Flow cytometry results demonstrated that 100 % of the cells are positive for the conjugated nanoparticles after 72 h of incubation. Magnetic-mediated hyperthermia has proven to be efficiently applied for the treatment of PCa cells.

REFERENCES

1. Cihoric N. *et al.*, Int.J. Hyperther. 31:609-614, 2015.
2. López-Ortega A. *et al.* Phys. Rep. 553:1-32, 2015.

ACKNOWLEDGMENTS

The authors would like to thank to Simone Luciello for electron microscopy measurements. The project leading to this application has received funding from AIRC and the European Union's Horizon 2020 research and innovation programme under the Marie Skłodowska-Curie grant agreement No 800924.

Incorporation and Effect of Lidocaine Hydrochloride on Octacalcium Phosphate

Ilijana Kovrlija[1], Clara Barbut[1], Janis Locs[1,2], Dagnija Loca[1,2]
[1]Rudolfs Cimdins Riga Biomaterials Innovation and Development Centre, Institute of General Chemical Engineering, Faculty of Materials Science and Applied Chemistry, Riga Technical University, Pulka 3, Riga, LV-1007, Latvia
[2] Baltic Biomaterials Centre of Excellence, Headquarters at Riga Technical University, Riga, Latvia
* ilijana.kovrlija@rtu.lv

INTRODUCTION

In recent years, employment of octacalcium phosphate (OCP, $Ca_8(HPO_4)_2(PO_4)_4x5H_2O$) as a drug delivery system (DDS) has become a trending topic[1]. Additionally, the ever increasing need for reducing the pain immediately after implantation has prompted the idea of combining OCP and some well researched local anesthetics. With its uncommon structure, made of an interlaying apatite layer and a hydrated layer, OCP offers a new spectra of possibilities in terms of different drug incorporations. In the light of that goal, lidocaine hydrochloride (lidocaine, LidHCl) has been used as a model drug[2]. Even though the range of OCP loaded drugs is expanding, the in situ incorporation of lidocaine, through the hydrolysis of α-tricalcium phosphate (α-TCP), has not been tested so far. Thus the aim of the current study was to examine the influence of LidHCl, and subsequently, to analyze the drug release rate during a chosen time period.

EXPERIMENTAL METHODS

100 mg of α-TCP were added into 50 mL of 0.0016 M H_3PO_4 solution, simultaneously with 50 mg of LidHCl. The reaction was maintained for 24 h at room temperature, under continuous stirring, and monitoring of pH. The attained products were centrifuged at 3000 rpm, washed with deionized water and dried overnight at 37 °C. In order to confirm the OCP phase, X-ray powder diffraction (XRD) and Fourier transform infrared-attenuated total reflectance (FTIR-ATR) were employed. Lidocaine release profile was determined by infusing the drug loaded OCP in three different media – sodium chloride (NaCl), phosphate buffered saline (PBS), and deionized water with acidic pH. The samples were analyzed after 24 hours, 48 hours and six days. LidHCl content in dissolution medium was verified using ultraviolet–visible spectroscopy (UV/VIS) at λ = 209 nm

RESULTS AND DISCUSSION

Phase composition of the synthesized, drug loaded OCPs, was confirmed by the XRD, with characteristic maxima aligning to the theoretical structure of OCP (specific reflection at approximately 4.7, 9.8 and 32 degrees 2θ[3]), however minor variations were visible. Chemical composition of the powders was corroborated with FT-IR, where representative attributes of OCP were observed in all the spectrums (absorption bands typical of PO_4^{3-} stretching vibration in the regions 1075–1017 cm^{-1}, 962 cm^{-1} and at 600 and 560 cm^{-1}, moreover, bands at 1120, 916, and 860 cm^{-1} due to HPO_4^{2-} stretching were present[4]). Nonetheless, specific markings of LidHCl, for both the XRD pattern and FT-IR spectra, were not observed[5]. OCP/LidHCl exhibited drug release of around 150 ±10 µg/mL in the first day, while at the last time point the amount of the released lidocaine was approximately 14 µg/mL, throughout all the dissolution media. The most efficient drug release was noted for the deionized water with acidic pH.

CONCLUSION

The undertaken study provided the confirmation that OCP has been successfully employed as a drug delivery vehicle for lidocaine hydrochloride. In order to test the most efficient release rate, different dissolution media were tested and compared. With an eye toward the maximum exploitation of the OCP as a DDS, further research is needed.

REFERENCES

1. Kovrlija, I.; Locs, J.; Loca, D. Octacalcium Phosphate: Innovative Vehicle for the Local Biologically Active Substance Delivery in Bone Regeneration. Acta Biomater. 135, 27–47, 2021.
2. Gautier, H.; Chamblain, V.; Weiss, P.; Merle, C.; Bouler, J. M. In Vitro Characterisation of Calcium Phosphate Biomaterials Loaded with Lidocaine Hydrochloride and Morphine Hydrochloride. J. Mater. Sci. Mater. Med., 21 (12), 3141–3150, 2010.
3. Brown, W. E.; Mathew, M.; Tung, M. S. Crystal Chemistry of Octacalcium Phosphate. Prog. Cryst. Growth Charact. , 4 (1–2), 59–87, 1981.
4. Fowler, B. O.; Marković, M.; Brown, W. E. Octacalcium Phosphate. 3. Infrared and Raman Vibrational Spectra. Chem. Mater., 5(10), 1417–1423 1993.
5. Powell, M. F. Lidocaine and Lidocaine Hydrochloride. Anal. Profiles Drug Subst. Excipients 1986, 15 (C), 761–779.

ACKNOWLEDGMENTS

This project has received funding from the European Union's Horizon 2020 research and innovation programme under the Marie Skłodowska-Curie grant agreement No 860462 and from the European Union's Horizon 2020 research and innovation programme under the grant agreement No 857287 (BBCE).

Dense collagen-based hydrogels loaded with anti-sclerostin antibodies enhance critical size bone defect repair

Ludovic Sicard[1,2,*], Sophie Maillard[1], Catherine Chaussain[1,2], Thibaud Coradin[3].

[1]URP2496, Université de Paris, Paris, France
[2]Bretonneau Hospital, APHP, Paris, France
[3]Sorbonne Université, CNRS, Chimie de la Matière Condensée de Paris, UMR 7574, Paris, France
[*] ludovic.sicard@aphp.fr

INTRODUCTION

Tissue engineering (TE) strategies based on cellularized scaffolds is a promising approach to restore bone defects but may not be effective for large bone defect or patients with systemic conditions. Additional administration of bioactive molecules offers the possibility to further improve the repair process. In this context, we have previously shown enhanced bone repair in mice with calvaria critical size bone defects using dense collagen hydrogel (DCH) seeded with murine dental pulp stem cells (mDPSC) and intravenous injection of anti-sclerostin antibody (anti-Scl Ab). The same positive outcome was obtained with DCH seeded with *Sost* knock-out mDPSC, suggesting that local inhibition of sclerostin is as efficient as the systemic inhibition.[1] Based on these data, we aim at developing DCH-derived scaffolds enclosing and delivering anti-Scl Ab. Electrostatic interactions between antibodies and scaffolds are key to control their release kinetics[2]. Adding chitosan, a cationic polysaccharide, to collagen should allow to tune such interactions.

EXPERIMENTAL METHODS

DCH-chitosan (10 and 20 %) mixed scaffolds were prepared using the plastic compression process[3]. After addition of $BaSO_4$, hydrogels volume was measured by micro-X-ray computed tomography (Micro-CT). Rheological properties of DCH were studied by frequency sweeps. Antibody release kinetics study were performed using DCH and DCH-chitosan containing 0, 0.2 or 2 $mg.mL^{-1}$ anti-Scl Ab. Released antibody concentration was measured by ELISA.

An *in vivo* experiment was designed to assess the efficiency of anti-Scl Ab-loaded DCH (APAFIS agreement # 24,297). A 3.5 mm critical size defect was surgically created in the parietal bone of 10-week-old male WT mice. The defects were subject to the following conditions: left empty, DCH alone and DCH with 0.2 $mg.mL^{-1}$ or 2 $mg.mL^{-1}$ anti-Scl Ab. Bone formation was assessed by Micro-CT at 1 and 2 months and by immuno-chemistry. Analysis was performed using non-parametric tests. Significance was defined as a p-value lower than 0.05.

RESULTS AND DISCUSSION

Significant difference was found between the volume of uncompressed hydrogels at 10% and 20 % chitosan ($p<0.5$), whereas no difference was found after compression. No difference was found either in storage or loss modulus of compressed hydrogels. Antibody release kinetics were significantly slowed down upon chitosan addition ($p<0.05$) but the slowest release was obtained at 10 % chitosan. This suggests that chitosan has no significant impact on the structure of the DCH whereas, in contrast, it impacts anti-Scl Ab release. The 10 % content may correspond to optimal electrostatic interactions between antibodies and the scaffold.

Significantly improved bone formation was observed in mice at 1 and 2 months with antibody loaded DHC when compared with no DCH or DCH alone ($p<0.05$). These results show that local neutralization of sclerostin by antibodies entrapped within the scaffold improves bone formation.

CONCLUSION

Anti-sclerostin antibody loaded collagen-based hydrogels are promising biomaterials to repair critical-size bone defects. Improved repair can be expected if antibody delivery is tuned. Chitosan is a good candidate additive for this purpose. Modification of its properties (molecular weight, acetylation degree) should allow for further optimization of the scaffold.

REFERENCES

1. Maillard S. *et al*., Acta Biomater. 140:178, 2022
2. Schweizer D. *et al*. Biomacromolecules 14:75, 2013
3. Chicatun F. *et al*. Biomacromolecules 12:2946, 2011

ACKNOWLEDGMENTS

We thank Mereo Bio-Pharma for providing the Setrusumab, BPS804, and D. Ferri-Angulo (LCMCP) for rheological tests.

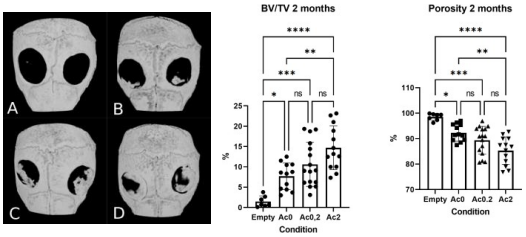

Fig.1 *On the left, CT-scan of mice calvaria at 2 months, A: Empty defect, B: DCH alone, C: DCH+0.2 $mg.mL^{-1}$ Ab, D: DCH+2 $mg.mL^{-1}$ Ab. In the center, comparison of the Ratio Bone volume/Trabecular volume (BV/TV) at 2 months. On the right, comparison of the bone porosity at 2 months. Empty: empty defect, Ac0: DCH alone, Ac0.2: DCH+0.2 $mg.mL^{-1}$ Ab, Ac2: DCH+2 $mg.mL^{-1}$ Ab. * $p<0.05$, ** $p<0.001$, *** $p<0.0001$, **** $p<0.00001$*

Redox-dependent drug delivery by hyaluronic acid-based hydrogels for local tumor therapy of malignant melanoma

Rebecca Rothe[1,2*], Yong Xu[3], Johanna Wodtke[1], Sebastian Meister[1], Yixin Zhang[3], Jens Pietzsch[1,2] and Sandra Hauser[1]
[1] Helmholtz-Zentrum Dresden-Rossendorf, Institute of Radiopharmaceutical Cancer Research, Department of Radiopharmaceutical and Chemical Biology, Dresden, Germany
[2] Technische Universität Dresden, Faculty of Chemistry and Food Chemistry, School of Science, Dresden, Germany
[3] B CUBE Center for Molecular Bioengineering, Technische Universität Dresden, Dresden, Germany
[*] r.rothe@hzdr.de

INTRODUCTION

Besides cardiovascular diseases, cancer disorders are the most frequent causes of death, with malignant melanoma being one of the four most common tumor neoplasms. The median survival for highly metastatic, unresectable stage IV malignant melanomas is only eight months[1] and these tumors are often treated palliatively with aggressive therapies causing partly severe side effects. However, the melanoma cells quickly become resistant to the systemically applied drugs. Thus, it is a concern of cancer research to develop and validate new local tumor therapy strategies for solid tumor entities. In this context, injectable hydrogels are promising drug delivery systems (DDS) for therapeutic applications due to their basic biocompatibility, biodegradability, and minimal invasive administration[2]. In a previous study, a non-covalent hydrogel platform with tunable degradation, structure-dependent molecule release as well as appropriate angiogenic and regenerative tissue responses was established[3]. As these hydrogels fulfilled the clinically relevant criteria mentioned above, subsequently, the most suitable hydrogel composition was developed further towards tumor therapeutic applications. Two cytostatic drugs were introduced into the physical hydrogel system based on different incorporation techniques. Drug release should be triggered by reactive oxygen species (ROS) in the tumor microenvironment (TME) and resulted in significant antitumoral effects in a murine melanoma-bearing model underlining the efficacy of this local DDS.

EXPERIMENTAL METHODS

The modular physical hydrogels comprised a starPEG backbone with coupled repetitive lysine-alanine peptide linkers ($(KA)_7$). Sulfated hyaluronic acid (sHA) being modified with ferrocene (FeCp2) ensured non-covalent hydrogel assembly. First, the hydrogels were investigated in immunocompetent hairless SKH-1 mice regarding their biocompatibility and biodegradability. Following these *in vivo* studies, resected tissue samples were characterized molecular biologically *ex vivo* in terms of fibrous encapsulation, inflammation and vascularization. Second, the hydrogels were loaded with doxorubicin (Dox) and paclitaxel (Plx) based on ionic interactions and entrapment within a FeCp2-formed hydrophobic core, respectively. Tumor growth and hydrogel degradation were investigated in a syngeneic murine allograft model, specifically B16F10 melanoma-bearing C57BL/6J mice, and quantified using T2-weighted magnetic resonance tomography. Statistical analysis was performed using two-way ANOVA (Bonferroni *post-hoc* test) by GraphPad Prism software.

RESULTS AND DISCUSSION

Malignant melanomas are characterized by a high redox potential. For redox-dependent drug delivery in terms of tumor therapeutic applications, a FeCp2-containing sHA-based hydrogel system was developed and two cytostatic drugs were introduced into the hydrogel network as described in the experimental methods. The ROS-induced oxidation of FeCp2 and the associated change in hydrophilicity concomitantly trigger Plx release in the local TME. Further, Dox can increase the local ROS level and thus contributes to a targeted Plx release and chemotherapy. In the SKH-1 mouse model, swelling around the hydrogel was visible within 24 h after subcutaneous injection, potentially due to the hygroscopic properties of FeCp2. The accumulation of tissue fluid caused a minor hydrolytic cleavage of the hydrogel network, but the hydrogel volume remained stable over one month hereinafter. Regarding biocompatibility, neither fibrotic nor inflammatory tissue reactions occurred, confirming the suitability of the hydrogel system for further investigations in the murine tumor model. Thereby, the drug-loaded ROS-responsive hydrogel significantly delayed tumor growth compared to the drug-free hydrogel, PBS, and SOC (standard of care) controls and led to a doubling of the relative survival probability of the tumor-bearing mice (figure 1).

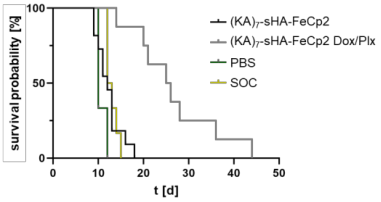

Figure 1: Hydrogel-based tumor therapy. Relative survival probability shown as Kaplan-Meier curve calculated by exponential growth model. n = 8-10, MW + SD.

CONCLUSION

The intratumorally applied ROS-responsive hydrogel system substantially contributed to the deceleration of tumor growth in the murine melanoma model. Further detailed mechanistic clarification may support the transfer of the efficient therapeutic approach to treatment concepts for other solid tumor entities.

REFERENCES

1. Liu Q. *et al*., Adv. Drug Deliv. Rev. 127:208-221, 2018
2. Xu X. *et al*., Mater. Horiz. 8(4):1173-1188, 2021
3. Rothe R. *et al*., Biomaterials. 269, 120637, 2021

Design of a fully-resorbable electronic device for neural stimulation and monitoring

Simon Regal[1,2], Maxime Leprince[2,3], Pascal Mailley[2], Napoleon Torres-Martinez[1], David Ratel[1], Fabien Sauter-Starace[1], Rachel Auzely-Velty[3], Isabelle Texier[2*]

[1]University Grenoble Alpes, CEA, LETI-Clinatec, F-38000 Grenoble, France;
[2]University Grenoble Alpes, CEA, LETI-DTBS, F-38000 Grenoble, France;
[3]University Grenoble Alpes, CERMAV, F-38400 St-Martin d'Heres, France;
* isabelle.texier-nogues@cea.fr

INTRODUCTION

At the interface between living tissues and inert electronics, bioelectronic devices require flexible and biocompatible materials. Additionally, the advent of fully-resorbable transient devices would open the way to new medical possibilities for mid-term post-surgical wound monitoring, on-demand electrically controlled drug delivery, or electro-sensitive tissue engineering[1]. With their mixed ionic/electronic conductivity and tunable mechanical, electrical, electrochemical, and biological properties, conductive polymers are materials of choice for the design of the conductive electrodes of such transient devices. Herein, conductive resorbable materials based on sulfated hyaluronan modified by phenyl-boronic moieties (HAS-PBA) as dopants of poly(3,4-ethylenedioxy)thiophene (PEDOT) were designed and characterized. They were further integrated in a fully-resorbable device dedicated to the implantation in the cortex of rats for stimulation and recording.

EXPERIMENTAL METHODS

EDOT was chemically polymerized in the presence of HAS-PBA, obtained in two steps with quantitative yield and minimal polymer chain degradation, to yield the conductive PEDOT:HAS-PBA ink[2]. The bioelectronic device consisting of poly (lactic-co-glycolic acid) (PLGA) films, molybdenum (Mo) conductive tracks and PEDOT:HAS-PBA electrodes for tissue contact was fabricated using usual microfabrication techniques. PLGA films (50% glycolic acid, 20 µm thick) were prepared by drop casting on plasma-treated glass surfaces. The conductive tracks were either laser-cut in a 10 µm-thick molybdenum sheet or obtained by sputtering of a 500 nm thick layer through a negative mask. Therefore, 200 µm width Mo tracks were either pick-and-placed or sputtered on a first PLGA film, then encapsulated within a second film comprising laser-made electrode openings. Finally HAS-PBA:PEDOT material was deposited in the openings to constitute the electrodes (1.2 mm Ø) in contact with biological tissues (Fig. 1).

RESULTS AND DISCUSSION

To achieve suitable PEDOT dopant properties, HA was sulfated (HAS) to increase its acidity and global negative charge, and phenylboronic acid (PBA) moieties were introduced to enhance hydrophobic interactions with PEDOT domains. A synergy was observed between the sulfate and the PBA aromatic groups to enhance the material conductivity that reached 1.57 ± 0.2 S/cm in physiological conditions[2].

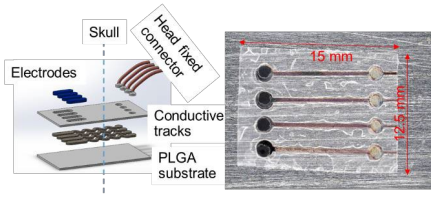

Fig. 1: Left: exploded view of an illustrative device. Right: example of device (15x12.5 mm) with laser-cut Mo tracks.

Mo and PLGA were selected as respectively electrical track and support/encapsulating materials due to their biocompatible and resorbable properties. Electrical impedance spectroscopy (EIS) measurements showed that the PEDOT:HAS-PBA layer reduced the electrode impedance (4 kΩ at 1 Hz), providing a better interface than Mo metal (15 kΩ at 1 Hz).

CONCLUSION

The new conductive PEDOT:HAS-PBA ink appeared as perfectly biocompatible, disintegrable, and exhibited excellent conductive and electrochemical properties. It therefore constitutes a material of choice for contact electrodes in the design of a fully resorbable bioelectronic device. The developed prototype will be implanted in rat cortex for electrical stimulation and recording, and to further explore its resorbability properties.

REFERENCES

1. Bettinger *et al.*, Adv. Mater. 22(5):651-655, 2010
2. Leprince *et al.*, Carbohydrate Pol., submitted.

ACKNOWLEDGMENTS

This work is part of the STRETCH project founded by the French National Research Agency (ANR) (ANR-18-CE19-0018). LETI-DTBS and CNRS-CERMAV are supported by the ANR in the framework of Arcane Labex (CBH-EUR-GS, ANR-17-EURE-0003) and Glyco@Alps (ANR-15-IDEX-02) programs.

Electroactive MXene Accommodating Intraocular Lens Design

Emma J. Ward[1,2,3,4], Cyril Crua[2], Marcus K. Dymond[1], Joseph Lacey[3], Yury Gogotsi[4], Susan Sandeman[1]

[1]School of Pharmacy and Biomolecular Sciences, University of Brighton, Brighton, BN2 4GJ, UK
[2]Advanced Engineering Centre, University of Brighton, Brighton, BN2 4GJ, UK
[3]Rayner Intraocular Lenses Limited, The Ridley Innovation Centre, Worthing, BN14 8AQ, UK
[4]A. J. Drexel Nanomaterials Institute, and Department of Material Science and Engineering, Drexel University, Philadelphia, PA 19104, USA

Introduction

Accommodative intraocular lenses (IOLs) are a recent development in IOL technology. Whilst approaches to lens accommodation, including axial displacement and shape-changing mechanisms, demonstrate advancements in the field, no current clinically available accommodative IOL has been successful in restoring the eye's adaptive focus capabilities[1]. The new class of nanomaterial, MXene, exhibits great potential for wearable optoelectronic applications due to their unique combination of properties, such as high conductivity, optical transparency, flexibility, biocompatibility, and hydroxide/oxide like surface chemistry of these two-dimensional transition metal carbides and/or nitrides[2]. Here, the suitability for use in an accommodative IOL mechanism was investigated. By exploiting these optoelectronic characteristics, MXene was used in an accommodative IOL design with a nematic liquid crystal (LC) and through the application of an electric field, the average direction of the LCs molecules led to a change in refractive index, thus focus position on the development of a truly accommodative IOL.

Methods

MXene ($Ti_3C_2T_x$) was synthesised through liquid exfoliation of the MAX phase precursor with lithium fluoride and hydrochloric acid. The $Ti_3C_2T_x$ solution was spin-coated onto IOL substrates and characterised optoelectronically using UV-Vis spectroscopy and a four-point probe technique. Following the demonstration of refractive index modulation in the presence and absence of an electric field, whereby $Ti_3C_2T_x$ was coated onto solid substrates and a nematic LC residing between, the $Ti_3C_2T_x$/LC mechanism was fabricated into a lens design. $Ti_3C_2T_x$ was spin-coated onto the inner surfaces of the lens, and then alignment layers of polyvinyl alcohol (PVA) were applied. The alignment predetermines the initial orientation of the LC molecules. LC was introduced to the lens through capillary forces and wires connected to the external power supply. A test model was established to evaluate the lens' performance. The test model consisted of a camera, various optical targets, a light source, a power supply and a pulse generator. The camera and power supply were required to trigger simultaneously to accurately evaluate the timings. The targets included a Ronchi ruling, a slanted edge modulation transfer function (MTF) target and a siemens star. A range of voltages were applied to the lens and the results were imaged.

Results and Discussion

$Ti_3C_2T_x$ was synthesised and spin-coated onto IOL substrates to form a transparent, flexible, and conductive electrode. The optoelectronic evaluation found the sheet resistance of the coating to range from 0.2 – 1.0 kΩ sq^{-1} with transmittance in the visible region ranging from 50 % to 80 % and following manual deformation, the conductivity of the coating was retained. The proof-of-concept design demonstrated the potential of the $Ti_3C_2T_x$/LC mechanism for accommodative IOL design when the $Ti_3C_2T_x$ coating actuated the modulation of the refractive index that when combined with a lens could provide a change of focus. The $Ti_3C_2T_x$/LC lens was constructed and successfully switched between the LC's ordinary and extraordinary refractive indices in the presence and absence of an electric field. The lens responded to the application of the field within 0.2 seconds, this change in refractive index resulted in changes in the lens's focus position and spatial resolution, presenting a tuneable, fast switching and reversible accommodative IOL mechanism.

Conclusion

This investigation shows the synthesis, characterisation, and processing of $Ti_3C_2T_x$, for use in an optoelectronic evaluation demonstrating the suitability for use in an ophthalmic device. Moreover, the electroactive $Ti_3C_2T_x$/LC mechanism displays the potential for MXenes as transparent conductive electrodes in accommodative IOL technology and ocular devices.

References

[1] Alió, A. J. L., et al., *Eye and Vision* **2017**, *4*.

[2] Naguib, M, et al, *Advanced Materials* **2011**, *23*, 4248.

Acknowledgements

Funded by a Medical Research Council Industrial CASE Training Grant [MR/P01589/1]

Self-healable and Stretchable Sensors for Human Motion Monitoring

Morteza Alehosseini[1], Tiberiu Gabriel Zsurzsan[2], Jon Spangenberg[3], Firoz Babu Kadumudi[1] and Alireza Dolatshahi-Pirouz[1]
[1]Department of Health Technology, Technical University of Denmark, 2800 Kgs, Lyngby, Denmark
[2]Department of Electrical Engineering, Technical University of Denmark, 2800 Kgs, Lyngby, Denmark
3Department of Mechanical Engineering, Technical University of Denmark, 2800 Kgs, Lyngby, Denmark
mortea@dtu.dk

INTRODUCTION

Wearable health monitoring devices due to the variety of qualities that they offer have become the prime focus in modern health care. These bioelectronic devices are flexible, skin conforming, portable, durable, highly sensitive, and can provide real-time monitoring.
They have proved to be highly useful in numerous cases such as patients going through the rehabilitation process, in the evaluation of the post-surgery performance of athletes, translation of sign language for individuals with inability to hear, early diagnosis and prognosis of certain illnesses such as Parkinson disease and also in sports performance and human-machine interfaces for robotics[1]. The strain sensors can also be widely applied in sports performance and human-machine interfaces for robotics. Flexible wearable sensors are the key point for monitoring motion and physiological signals and daily activity. The current studies on flexible and stretchable strain sensors have hardly succeeded to cover the important characteristics of the next generation of wearable electronics for rehabilitations[2]. These features involve low cost, high sensitivity, high elasticity, self-healing capability, and multi-functionality. Personalized cheap and accurate wearable electronics for human motion monitoring can help patients and doctors for rehabilitation.

EXPERIMENTAL METHODS

Here a sensitive, self-healable, and elastic strain sensor is developed by embedding nanomaterials along with a conductive polymer, PEDOT PSS. The sensors are sensitive to strain, pressure, and temperature and can achieve high stretchability up to 600% and great durability due to the self-healing properties.

RESULTS AND DISCUSSION

The electrical properties, sensitivity, and mechanical properties of the materials were tested at different strains. The conductivity of the materials goes up to 10^-3 S/cm while showing sensitivity to different temperatures between 15°C to 60°C based on the mechanical test. It can heal itself more than 95% in less than 3min. Sensitivity to pressure was measured too and it shows significant changes in conductivity when a wide range of pressures from 1KPa to 1MPa was applied to the sensor.

CONCLUSION

In this study, we developed a low cost and accurate and self-healable sensor for healthcare monitoring. We expanded the functionality of the material to also monitoring temperature of the body. This sensing material was also highly durable because of self-healing properties.

REFERENCES

1. Sepehr T. *et al*., Adv Science. 6: 1801664, 2019
2. Firoz B.K. *et al*., Adv Science. 6: 1801241, 2019

Foreign Body Reaction: Cartography of Macrophage Activation in a Model of Material Implantation in Rat Subcutaneous Tissue

Arvind Rathore[1], Simon Hemour[2], Vincent Raimbault[3], Helene Boeuf[1], Claudine Boiziau[1*]

[1]INSERM, Univ. Bordeaux, BioTis Laboratory, Bordeaux, France
[2]IMS, CNRS, Univ. Bordeaux, Talence, France
[3]CNRS, LAAS, Toulouse, France

INTRODUCTION

Foreign body reaction is a long-described process that occurs upon implantation of medical devices (IMDs). Fibrosis is a common reaction observed with non-degradable IMDs, which can prevent their proper functioning, as in the case of implanted biosensors. Macrophages (either tissue resident or bone marrow-derived circulating monocytes) are main organizers of inflammatory reaction, wound healing, and tissue remodeling; commonly classified into two main categories, pro-inflammatory "M1" and anti-inflammatory "M2", their exact role and regulation in scar formation remain to be better understood[1].

EXPERIMENTAL METHODS

A printable and biocompatible resin, DL260, was designed to tightly associate to a gold electrode, and prevent its breakage due to animal movements. It was subcutaneously implanted in rats for a period of 3 weeks. After sacrifice and dissection, tissues were cryopreserved and immunofluorescence was used to characterize the cells.

RESULTS AND DISCUSSION

The protection of electrode by the resin was confirmed by X-ray imaging follow up. After 3 weeks, we isolated tissues surrounding the material, and treated them for histology analyses. Only a limited fibrosis occured. As expected based on previous experiments, macrophages were detected around the device; markers of the pro-inflammatory M1 phenotype were detected in contact with the biomaterial, colocalized with the myofibrobastic marker alpha-SMA, whereas immuno-modulatory M2 macrophages were dispersed in the tissue. To get a better information on the foreign body reaction, other markers were analyzed: markers of autophagy were differentially expressed in the tissue. Proteins associated with inflammasome activation were hardly detected.

CONCLUSION

A cartography of macrophage activation phenotypes will be presented, in relation with the collagenous matrix density. The association between autophagy activation and inflammasome regulation remains to be better characterized.

REFERENCES

1. Aussel A. *et al*. Biomed. Mater. 14:025009, 2019.

ACKNOWLEDGMENTS

This project has received funding from the European Union's Horizon 2020 research and innovation programme under the Marie Skłodowska-Curie grant agreement No 813006, from the Agence Nationale de la Recherche (ANR-16-CE19-0001-01) and was also supported by the LabEx AMADEus (ANR-10-LABX-42)

Functionalized silica-based sensors for real-time viral screening

Perrine Robin [1*], Lucas Mayoraz [1], Céline Journot [1], Davide Staedler [2], Francesco Bertoni [3], Igor Stefanini [4], Sandrine Gerber-Lemaire [1]

[1]Institute of Chemical Sciences and Engineering, Ecole Polytechnique Fédérale de Lausanne, Lausanne, Switzerland;
[2]TIBIO Services, Scitec Research SA, 1007 Lausanne, Switzerland;
[3]Institute of Oncology Research, Scuola universitaria professionale della Svizzera, Bellinzona, Switzerland;
[4]Institute of Systems and Applied Electronics, Scuola universitaria professionale della Svizzera, Bellinzona, Switzerland.
* perrine.robin@epfl.ch

INTRODUCTION

The emergence of the coronavirus disease in 2019 (COVID-19) highlighted the need for rapid, accurate and massive virus detection techniques to control the widespread of infectious diseases. Epidemic-causing mosquito-borne viruses such as Dengue, Zika or Chinkungunya, are under tight surveillance by sanitary organizations, as may be next to emerge on the global stage[1]. In Europe, although those viruses' circulation is up to now limited, concerns have been raised about the recent emergence of Tiger mosquitos[2]. Monitoring potential arboviruses in the mosquitoes' established populations is of great interest for European health organizations to stay one step ahead. We suggest an approach to address the limitations of current detection procedures using a low-cost and highly responsive biosensor, which would remove the need for biomedical personnel and advanced laboratory infrastructures. The biological samples could be taken from humans or any viral hosts and be processed to detect a variety of viruses. Most viral detection techniques require the immobilization of biomolecules on a sensor surface. Silica-based materials are ideal sensor platform due to their inexpensiveness, ease of functionalization and good temperature and mechanical stability[3].

EXPERIMENTAL METHODS

Catechol-based linkers were designed and used to introduce various chemical functions at the surface of borosilicate slides. Different methods such as dip coating and spin coating have been assessed as functionalization techniques. X-ray Photoelectron Spectroscopy and water-contact angle were used as characterization techniques to evaluate the efficiency of these techniques. The chemical functions introduced at the surface of the platform will be later used for the conjugation of a polymeric layer, followed by the attachment of single-strand DNA (ssDNA) probes at the surface. Copper-free click chemistry will be especially studied to covalently attach the ssDNA on the platform.

RESULTS AND DISCUSSION

We herein disclose a surface conjugation strategy for the immobilization of ssDNA probes on silica-based based slides. Catechol-based linkers inspired by mussels' adhesion mechanism were used to introduce various chemical functions on borosilicate slides. Dip-coating and spin-coating methods are under study to optimize the functionalization of borosilicate with the synthetized linkers. The introduced chemical functions will be used for post functionalization steps with polymer and ssDNA, as illustrated in Figure 1. Copper-free click chemistry will be especially investigated to conjugate the DNA probes to the surface. Due to its biorthogonality, we expect this strategy to improve the orientation of the probes at the surface.

The resulting sensing platforms will be assessed for SARS-CoV-2 and Zika detection. Fluorescence and bioimpedance measurements will be used for the detection of the hybridization events between the viral RNA strands from the biological samples and the immobilized ssDNA strands.

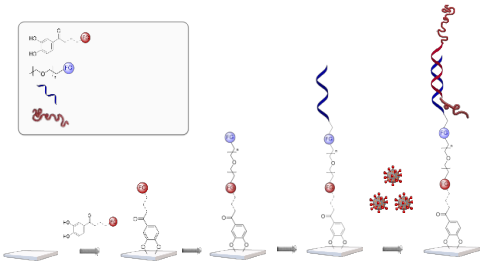

Figure 1: A biomimetic approach for the preparation of ssDNA functionalized glass slides and their application for impedimetric or fluorescence detection of viruses.

CONCLUSION

A three-layer biomimetic surface conjugation strategy is studied to obtain non expensive sensing platforms. As the orientation and density of the ssDNA probes at the surface of the sensor are known to play a major role on the efficacy of hybridization events, variation of size, and functionality of the polymers as well as adjuvants will be investigated for optimal sensor sensitivity.

REFERENCES

1. Kading R. *et al*., Trop. Med. Infect. Dis., 5:142, 2020.
2. Ryan S. *et al*., PLoS Negl Trop Dis., 13:e0007213, 2020.
3. Wittmann C. *et al*., Immobilisation of DNA on chips II. Springer, 2005

ACKNOWLEDGMENTS

We are grateful for financial support by the Swiss Confederation in the form of an Innosuisse grant 38934.1 IP-LS and the Swiss National Science Foundation via a NRP 78 grant 4078P0_198265.

Use of Mixed Iridium and Titanium Oxides for pH Sensing in Biomaterials

Jitrenka Jiru[1*], Vojtech Hybasek[1], Jaroslav Fojt[1]
[1] Department of Metals and Corrosion Engineering, Faculty of Chemical Technology, University of Chemistry and Technology in Prague, Prague, Czech Republic
[*] jiruj@vscht.cz

INTRODUCTION

With all tissue interventions, there is a risk of infection and this risk is increased in the case of implant use. Not only is the patient's health compromised and burdened with prolonged treatment, but the financial cost associated with treatment is also increased. Especially the detection of a delayed infection is a difficult task despite current methods, as clinical manifestations must occur. By the time bacteria adhere to the implant surface, it is already difficult for the patient's immune system to prevent the formation of a biofilm on the surface. The main infectious agents associated with implants include *Staphylococcus aureus*, *S. epidermidis*, *Pseudomonas aeruginosa*, and *Streptococcus* species. All of these microorganisms produce acidic products during their metabolic processes, which affect the pH of the surrounding tissue[1]. The possibility of sensing the pH around the implant could be a promising indicator of initial infection and could lead to faster application of the treatment and thus increase its effectiveness[2].

In this context, it would be best if a pH sensor was directly part of the implant. The most common alloys used for implant fabrication are titanium alloys. Titanium and its alloys are characterized by a passive TiO_2 surface layer, which can be modified by anodic oxidation to form a nanotubular structure. These oxides exhibit an almost Nernstian response (0.059 V/pH). Other metal oxides can be used to enhance their response, including IrO_2[3,4].

EXPERIMENTAL METHODS

In this work, Ti-6Al-4V samples were used as the base material for the prepared sensors. Anodic oxidation was realized in an electrolyte containing 1 mol/L $(NH_4)_2SO_4$ and 0.2 wt% NH_4F at room temperature. Experiments were carried out using a standard three electrode setup with platinum gauze as a counter electrode, the sample as the working electrode, and a silver/silver chloride (3 mol/L KCl) reference electrode (SSCE). The electrochemical measurements consisted of a potential ramp from the open circuit potential to the end potential 20 V/SSCE with a 100 mV/s sweep rate and subsequently by holding the potential at the end potential for 2000 s. After that, the samples were cleaned with distilled water and ethanol in an ultrasonic bath and dried with acetone. Iridium oxide was deposited on TiO_2 nanotubes from electrolyte which contained 0.2 mmol/L $IrCl_3.H_2O$, 1 mmol/L $H_2C_2O_4.2H_2O$, and 5 mmol/L K_2CO_3. The solution was then aged at 37 °C for 4 days and stored at 4 °C until used. The deposition was done using potentiostatic mode, E = -0.4 V/SSCE, t = 7200 s. Energy dispersive spectroscopy (EDS) was used to confirm the presence of iridium on the surface of the sample. Surface characteristics were obtained by X-ray photoelectron spectroscopy (XPS).

All electrochemical measurements were carried out at 37 °C in physiological solution (9 g/L NaCl) with equilibrium oxygen concentration buffered with biological buffer TES (N-Tris(hydroxymethyl)methyl-2-aminoethanesulfonic acid, 5.9 g/L). Measuring cells with the physiological solution were prepared with pH ranging from 7.6 to 5.5, adjusted with NaOH solution. The electrochemical response of the prepared systems with deposited IrO_x on changes of pH was studied. Open circuit potential (E_{OC}), polarization resistance and electrochemical impedance spectra were measured.

RESULTS AND DISCUSSION

Using EDS, the presence of Ir was confirmed and XPS determined 50 wt% of Ir on the surface in the form of oxides.

After evaluating all available results from electrochemical measurements, the open circuit potential monitoring proved to be the most suitable method for monitoring the pH change. Our pH-sensitive system achieved near-Nernstian response, 0.054 V/pH, when the surrounding pH was decreased. When the increase in pH was measured, the response of the system was 0.050 V/pH. The results of the measurement of open circuit potential at different pH are shown in Fig.1.

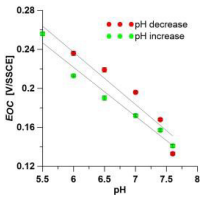

Fig.1: Dependence of open circuit potential on pH change, 37 °C

CONCLUSION

Our sensor appears to be a promising candidate for detecting pH changes caused by infection around the implant. Repeated measurements with more dynamic pH changes showed that the TiO_2/IrO_x mixed oxide system retains its properties and is capable of detecting the change rapidly.

REFERENCES

1. Busscher H.J. *et el.*, Sci Transl Med. 4(153):153rv10, 2012
2. Wang H. *et al*., ACS Biomater Sci Eng. 6(1):727-38, 2020
3. Manjakkal L. *et al*., Progress in Materials Science, 109, 2020
4. Deusenbery C. *et al*., ACS Infect Dis., 7(4):695-720, 2021

ACKNOWLEDGMENTS

This research was funded by Czech health research council, grant number NU20-06-00424.

Development Of A Cardiac Bio-prosthesis

Jean-Philippe Jehl[1*], Aurelia Poerio[1], Mélanie Lovera-Leroux[1], Solenne Fleutot[1], João F. Mano[2], Franck Cleymand[1]

[1] Institut Jean Lamour UMR 7198 CNRS / Université de Lorraine, Nancy, France
[2] Department of Chemistry, CICECO, University of Aveiro, 3810-193, Aveiro, Portugal
[*] jean-philippe.jehl@ univ-lorraine.fr

INTRODUCTION

New therapeutic approaches, such as regenerative medicine and tissue engineering are being developed to compensate or even replace damaged tissues. One of the attempts of tissue engineering is to reproduce as closely as possible the mechanical behavior of the tissue to be treated[1]. Biomaterials applied to the epicardium have been studied intensively in recent years for different therapeutic purposes[2]. Their mechanical influence on the heart, however, has not been clearly identified. Most biomaterials for epicardial applications are manufactured as membranes or cardiac patches that have isotropic mechanical behavior, which is not well suited to myocardial wall motion. In this work, an approach linking the mechanical characterization of healthy heart tissue with its microstructure was carried out. To this end and in order to avoid the degradation of the material properties due to its drying out and/or de-vascularization, an experimental protocol was defined to perform the measurements in a context close to its physiological environment. The cardiac tissue was thus characterized through the estimation of Young's modulus in two main directions by spherical indentation.

EXPERIMENTAL METHODS

The samples used in this study were extracted from five healthy pig hearts provided by the School of Surgery of the University of Lorraine. Ethical approval for the study was obtained from our university's ethics committee (committee number: 201922016556026) and then further validated by the French Ministry of Higher Education. Heart samples cut to 10-µm thickness were stained with DAPI (D9542,Sigma-Aldrich), for the nuclei, and Phalloidin (P5282, Sigma-Aldrich), for the actin, as permanufacturer's instructions. Imaging was performed using fluorescent microscopy (Moticam 3000, Motic). The mechanical properties of the specimen were determined using an ultra nanoindenter (ANTON-PAAR, Peseux, Switzerland).

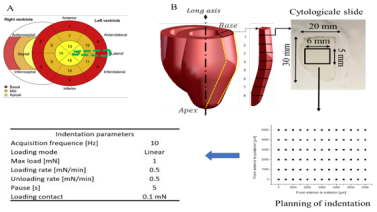

RESULTS AND DISCUSSION

The principal novelty of this study is that we found a simple method describing representative fiber orientation calculated within detected Young's modulus. In fact, the existing computational models describing fiber orientation are based on imaging observation (CT, RMI or histology), while the mechanical behaviour detection was apart. On the basis of the mechanical characterization of the myocardium, a model of the mechanical behaviour of a bio-prosthesis has been defined. A first membrane prototype has been produced and tested on small animals.

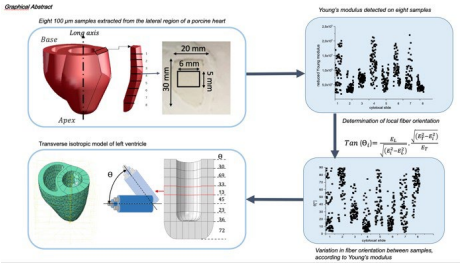

CONCLUSION

The mechanical performance of cardiac tissue is related to local fiber structure. The formula that we propose outlines, for the first time, a way to describe the elasticity of cardiac tissue and underlying fiber orientation. Building off CT imaging, we created a computational model that can accurately simulate the diastole phase of the LV. By modelling LV wall motion during passive diastole filling, our understanding of volume changes and the local deformation of the epicardium will be vastly improved, which will guide advances in the manufacturing of biomaterials for epicardial applications.

AKNOWLEDGMENTS

The authors wish to acknowledge the Nancy Lorraine School of Surgery, France, for their valuable collaboration, along with CARE & ASCATIM FEDER PROJECTS (University of Lorraine).

REFERENCES

References must be numbered. Keep the same style.
1. Weinberger, F. *et al*. Circ Res 120, 1487–1500.
2. Gaetani, R. *et al*. Biomaterials 61, 339–348.

Injectable hydrogels for microRNA delivery to promote direct cell reprogramming in cardiac regeneration

Elena Marcello[1,2,3], Letizia Nicoletti[1,2,3],Camilla Paoletti[1,2,3] and Valeria Chiono[1,2,3]

[1]Department of Mechanical and Aerospace Engineering, Politecnico di Torino, Torino, Italy
[2]Centro 3R, Interuniversity Center for the Promotion of the 3Rs Principles in Teaching and Research, Italy;
[3]POLITO Biomedlab, Politecnico di Torino, Turin, Italy;
[*]elena.marcello@polito.it

INTRODUCTION

Cardiac regeneration post- myocardial infarction (MI) represents a worldwide clinical challenge due to the poor regenerative capabilities of heart tissue. After MI, cardiac extracellular matrix undergoes significant remodeling leading to the formation of a fibrotic scar populated by cardiac fibroblasts (CFs), non-contractile cells. Regenerative medicine approaches are currently being explored to replenish the population of cardiomyocytes (CMs) and re-establish the functionality of injured myocardium. In particular, the direct reprogramming of CFs into induced CMs using a combination of four micro-RNA (miRNA), named miRcombo, has shown encouraging results both *in vitro* and in mouse models[1]. MiRcombo encapsulation in lipoplexes (LPs) can highly improve miRNA cell uptake and transfection efficacy. Furthermore, LPs embedding into an injectable hydrogel could improve their *in situ* delivery to the pathological cardiac tissue. Algysil LVR, an alginate-based material, has been investigated in clinical trials to favor cardiac tissue remodeling after MI[2]. However, Algysil LVR is not cell adhesive and is a permanent device due to alginate poor *in vivo* degradability. To overcome these hurdles, an oxidised formed of alginate, alginate dialdehyde (ADA), was herein explored as a delivery system[3].
In this work, an ADA-based injectable hydrogel was developed able to encapsulate and release miRNA-loaded LPs. To improve hydrogel cell adhesive properties, hydrogel composition was optimized through functionalization with a chemically-modified gelatin (Gel-M).

EXPERIMENTAL METHODS

ADA was prepared by partial oxidation of alginate with sodium metaperiodate and characterized using MAS solid-state NMR spectroscopy and via the iodine–starch test to determine the degree of oxidation[3]. ADA hydrogels were obtained by ionic crosslinking with calcium ions using a double syringe mixing system and characterized rheologically. Novel LPs containing miRNA were prepared *via* spontaneous electrostatic interaction and physically encapsulated in the ADA hydrogels[4]. Release studies of a Cy5-siRNA-loaded LPs from ADA hydrogels were conducted in distilled water at 37°C and estimated by plate reader analysis.
A modified gelatin (Gel-M), able to react with ADA was produced and characterized for its functionalization degree by 2,4,6-Trinitrobenzene Sulfonic Acid (TNBS) assay[5]. ADA/Gel-M hydrogels were prepared varying the polymers weight ratios (%w/w) (from 70-30 to 30-70, ADA: Gel-M), keeping constant the final polymer concentration (%w/v). Adult human CFs (AHCFs) were cultured on ADA/Gel-M hydrogels for 1 and 7 days, and the adhesion of DAPI-stained cells was evaluated by fluorescence microscopy. The analysis of the release of miRNA-loaded LPs from ADA/Gel-M hydrogel is in progress.

RESULTS AND DISCUSSION

ADA with an oxidation degree of 40% was produced from alginate with an average yield of 75%. The presence of aldehyde groups was confirmed by ATR-FTIR and ^{13}C MAS NMR spectroscopy. Tailored calcium ions and polymer concentrations allowed to obtain physical hydrogels with viscoelastic properties similar to Algysil LVR. Novel miRNA-loaded LPs were entrapped into ADA hydrogels without altering rheological properties. Cy5-siRNA, a model fluorescent oligonucleotide loaded in LPs was completely released from the hydrogel in 24h. To improve cell adhesive properties of ADA hydrogels, Gel-M was prepared with an average yield of 80% and with an average degree of functionalization of 14%. Injectable hydrogels with different viscoelastic properties were developed exploiting the possibility to create chemical crosslinking between ADA and Gel-M. Biocompatibility studies with AHCFs showed that the incorporation of Gel-M significantly increased CFs adhesion compared to ADA-based materials.

CONCLUSION

A novel strategy for cardiac regeneration was investigated based on the *in situ* delivery of miRNA-loaded LPs through ADA-based injectable hydrogels to promote myocardial regeneration. The incorporation of Gel-M into the hydrogel matrix supported CFs adhesion. We are currently investigating the release of miRNA-loaded LPs from this novel ADA/Gel-M matrix.

REFERENCES

1. Paoletti C, *et al.* Front Bioeng Biotechnol.,529,2020
2. Cattelan, G. *et al*., Front Bioeng Biotechnol, 8, 2020
3. Sarker, B *et al.*, J. Mater. Chem. B, 2:1470-1482, 2014
4. Nicoletti *et al.*, Nanomed.: Nanotechnol. Biol. Med., under submission.
5. Heo *et al*., ACS Appl. Mater. Interfaces, 12:20295-20306,2020.

ACKNOWLEDGMENTS

The authors would like to thank the European Research Council (ERC) under EU H2020 research and innovation program (BIORECAR; 772168) for providing financial support to this project.

Fabrication and characterisation of lactate releasing PLGA particles for cardiac regeneration

Christopher James[1,2], Barbara Blanco, PhD[1,2], Soledad Perez-Amodio, PhD,[1,2,3] Prof. Elisabeth Engel Lopez[1,2,3]

[1] Institute of Bioengineering Catalunya (IBEC), The Barcelona Institute of Science and Technology, Barcelona, Spain
[2] CIBER en Bioingenieria, Biomateriales y Nanomedicina, CIBER-BBN, Madrid, Spain
[3] IMEM-BRT group· Departament de Ciència i Enginyeria de Materials, Universitat Politecnica de Catalunya, Barcelona, Spain

INTRODUCTION

Systemic or local delivery of lactate in mice with ischemic wounds has been shown to increase reparative angiogenesis through endothelial progenitor cell recruitment and increased deposition of extracellular matrix leading to accelerated wound healing and reduced skeletal muscle atrophy.[1] Recent work by our group also showed that lactate promoted neuronal stem cell/progenitor maintenance and cardiomyocyte dedifferentiation (preprint).[2,3] Lactate releasing polymers, specifically poly(lactic-co-glycolic) (PLGA), have been widely adopted for various uses within medicine. Tuning the polymer length and the ratio of lactic to glycolic acids within the PLGA used to synthesise particles, as well as the method for fabrication (e.g., polymer concentration, ultrasonication intensity and time) used allows tuning of their size and biodegradation rate, and so their lactate release profile.[4] In this project we designed, fabricated, and assessed the potential of PLGA particles for local release of lactate at biologically relevant levels (6 mM) within an implantable scaffold for cardiac regeneration.[2]

EXPERIMENTAL METHODS

The well-defined synthesis method, water-oil-water emulsion, was used to fabricate low and high molecular weight PLGA particles loaded with lactate and stabilised with cryoprotector (sucrose) that were then characterised: their size, polydispersity index (PDI) and zeta potential via direct light scattering (DLS), lactate release and lactate loading via a commercial kit (Nzytech). Those with the greatest lactate release were studied for a cytotoxic effect on human dermal fibroblasts (hDFs) via MTT assay (Roche).

RESULTS AND DISCUSSION

PLGA particles with sizes 200-600 d.nm **(Figure 1)** that release up to 1.74 mM of lactate per mg in a week have been achieved. Synthesis efficiency reached a maximum of 87%, due to an interference with the formation of the particles, the greater the mass of L-lactic acid added in the synthesis step the less efficient the process. Loading efficiencies reached a maximum of 98%. In preliminary indirect studies the particles are non-toxic (**Figure 2**).

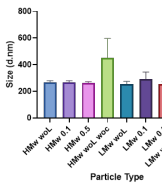

Figure 1: PLGA particle sizes measured by DLS. (HMw: high molecular weight polymer, LMw: low molecular weight polymer, 0.1/0.5: volume of L-lactic acid solution added to 2 mL PLGA (50 mg/mL), woc: without cryoprotector)

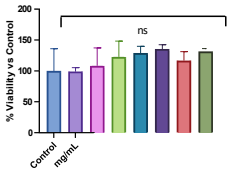

Figure 2: Human dermal fibroblast cytotoxicity of low molecular weight PLGA particles loaded with lactate after 7 days degradation.

CONCLUSION

As these particles release sufficient lactate and are non-toxic, further assessment of their efficacy at promoting angiogenesis is currently under investigation.

ACKNOWLEDGEMENTS

This work was supported by the Spanish Ministry of Science and Innovation (MICINN) through the National Research Agency (AEI) and European Regional Development Funds (ERDF/FEDER), project BIOCARDIO ref. RTI2018-096320-B-C21"and CERCA Program/Generalitat de Catalunya

Bibliography

1. Porporato, P. E. *et al.* Lactate stimulates angiogenesis and accelerates the healing of superficial and ischemic wounds in mice. *Angiogenesis 2012 15:4* **15**, 581–592 (2012).
2. Ordoño, J., *et al*. Lactate promotes cardiomyocyte dedifferentiation through metabolic reprogramming. *bioRxiv* 2020.07.21.213736 (2020) doi:10.1101/2020.07.21.213736.
3. Álvarez, Z. *et al.* Neurogenesis and vascularization of the damaged brain using a lactate-releasing biomimetic scaffold. *Biomaterials* **35**, 4769–4781 (2014).
4. Ochi, M., *et al*. Influence of PLGA molecular weight distribution on leuprolide release from microspheres. *International Journal of Pharmaceutics* **599**, 120450 (2021).

Tailored tubular collagen scaffolds through ice-templating for arterial replacement

Isabelle Martinier[1], Minaine Bouabdallah[1], Florian Fage[1], Alessia Castagnino[2], Abdul Barakat[2], Francisco M. Fernandes[1], Léa Trichet[1]

[1] Laboratoire de Chimie de la Matière Condensée de Paris (LCMCP), Sorbonne University, Paris, France
[2] Laboratoire d'Hydrodynamique (LADHYX), Ecole Polytechnique, Palaiseau, France
* isabelle.martinier@sorbonne-universite.fr

INTRODUCTION

Pathologies such as phlebitis, stroke, arteriopathy or pulmonary embolism originate from blood vessel occlusion. This phenomenon arises from a combination of factors leading to mechanical forces and hemostasis imbalance, which ultimately result in clotting and formation of a thrombus[1]. Current solutions to treat arterial occlusion rely on drug therapy or vascular grafting. However, there is a deadlock in the case of small diameter vessels for which traditional vascular grafts lead to recurrence of the occlusion[2]. Differently from traditional grafts, those capable of replacing small arteries should display radically different properties: a porous tubular structure and a native-like composition. These characteristics should favor cell infiltration, ensure device biointegration and lead to mechanical performances similar to those of native arteries.

In the present study, we propose a method that enables to recreate the above-mentioned properties using the main protein found in the arterial wall, type I collagen. Control over the macro and mesostructure of the collagen materials, respectively the tubular shape and the porous network, is achieved using a top-down approach named ice templating. At the nanoscale, we recapitulate the native tissue fibrillar motifs by bottom-up assembly of collagen through topotactic fibrillogenesis[3]. Combining these two approaches in the elaboration of collagen based-materials, opens an effective pathway to develop biomimetic materials with wide applications in clinical surgery: vascular, thoracic, dermal, ocular…

EXPERIMENTAL METHODS

Highly concentrated collagen filled molds are dipped in liquid nitrogen. During freezing, ice crystals grow and segregate collagen towards the interstices formed in between the crystals, reaching a higher local concentration. Ice crystals are subsequently thawed at 0°C to reveal the pores, while collagen fibrillogenesis is simultaneously induced by ammonia vapors.
Different ice growth kinetics were promoted to tailor the mesostruture by varying the freezing parameters. The implications were analyzed by scanning electron microscopy and confocal microscopy, and the phase segregation was modeled by differential scanning calorimetry.
The parameters were confronted to the biological and mechanical properties.

RESULTS AND DISCUSSION

Many factors play a role in the resulting porosity of the collagen scaffolds. Fine-tuning spatial pore distribution leads to pore sizes ranging from 20 to 130 µm, and generates an interface similar to arterial layer junctions, which position inside the tube wall can be adjusted (Figure 1).

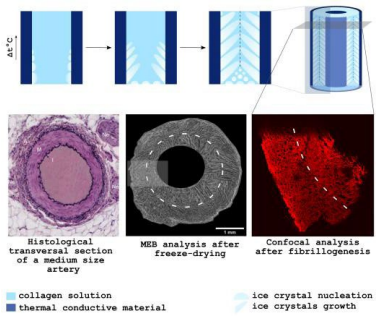

Figure 1. Generation of double-layered collagen scaffolds using highly conductive molds.

The results of the ice-templating modeling indicate that a high local concentration of 100-200 mg/mL is reached, propelling this material as the first substitute reaching the collagen concentration of native tissues.
Finally, we assessed the implications of the structural and compositional features on cell diffusion and proliferation rates (human umbilical endothelial cells and smooth muscle cells), and on mechanical properties (elongation, storage modulus) under pulsatile flow on dedicated devices. We will also discuss the possibility of a coating on the luminal surface by extracellular matrix proteins, in order to foster endothelialization.

CONCLUSION

The versatility of the materials fabrication method allowed to attain the suitable physiological characteristics for an arterial replacement. The promising results direct the future experiments towards *in vivo* testing.

REFERENCES

1. Qiu Y. *et al*., The biophysics and mechanics of blood from a materials perspective. 2019;4(5):294-311. doi:10.1038/s41578-019-0099-y.
2. Carrabba M, Madeddu P. Current strategies for the manufacture of small size tissue engineering vascular grafts. *Front Bioeng Biotechnol*. 2018;6(APR):1-12. doi:10.3389/fbioe.2018.00041
3. Rieu C. *et al*., Topotactic fibrillogenesis of freeze-casted microridged collagen scaffolds for 3D cell culture. *ACS AMI* 2019, 11, 16, 14672–14683. - doi.org/10.1021/acsami.9b03219.

Integration of Mesenchymal Stem Cell-Derived Fibroblast Loaded Hydrogel over the Tubular Scaffold to Mimic the External Layer of Blood Vessel

Gozde Ervin Kole[1,4*], Halime Kenar[2,4], Vasif Hasirci[1,2,4], Deniz Yucel[1,3,4]

Acıbadem Mehmet Ali Aydınlar University (ACU), [1]Graduate School of Health Sciences, Department of Medical Biotechnology, [2] Faculty of Engineering, Department of Medical Engineering, [3] School of Medicine, Department of Histology and Embryology, [4] ACU Biomaterials Center, Istanbul, Turkey
[*]gozdeervin@gmail.com

INTRODUCTION

Cardiovascular diseases are the leading cause of death worldwide[1]. Although the large diameter (>6 mm) blood vessel replacement is performed with synthetic vascular grafts, substitution of small-caliber vessels still remain a challenge since synthetic grafts and autografts' mechanical properties do not match with the native arteries[2]. Tissue engineering could be a promising approach to develop vessel substitutes by mimicking the structural properties of the native tissue. The native blood vessel wall consists of three tunics, starting from the lumen side, tunica intima, tunica media, and tunica adventitia[3]. In vascular tissue engineering studies, most of the tubular constructs were composed of two layers imitating the tunica intima and tunica media. However, the external layer, tunica adventitia that protects blood vessel from overstreching was not commonly integrated to the design of tubular construct[4]. In this study, it was aimed to integrate mesechymal stem cell (MSC)-derived fibroblasts loaded, collagen-based hydrogel around the tubular polymeric scaffold, as an external layer mimic.

EXPERIMENTAL METHODS

In the previous studies conducted by our group, multilayer tubular polymeric scaffold was fabricated by dip-coating and electrospinning. The lumen side was seeded with human umbilical cord vein endothelial cells (HUVEC), while the electropun mats was supported with Wharton's Jelly (WJ) MSC derived smooth muscle cells. In the current study, it was inteded to cover the outer surface of this construct with cell-loaded hydrogel by conserving its tubular form. For that purpose, a cylindrical mold was designed by computer-aided design program (Sketchup), and then fabricated using polylactic acid (PLA) by 3D printing. Hydrogel solution was prepared by mixing 10X DMEM, 2.8 M NaOH, 7.5% $NaCO_3$, 1X DMEM, 5 mg/mL atelocollagen (dissolved in 0.1 M acetic acid) and cells. WJ MSC were differentiated into fibroblast using induction medium containing TGF-β, IGF, basic FGF, ascorbate-2-phosphate, and insulin. After placing the tubular construct into mold, the cell carrying hydrogel solution was injected into the mold, and then it was incubated at 37 ºC in CO_2 incubator for 45 min for the gelation. The hydrogel-integrated tissue substitute was transferred into well plates, and cultured at 37 ºC in CO_2 incubator. The cell viability was determined with LIVE/DEAD assay, and cell behaviour within the tissue substitute was investigated with Confocal Laser Scanning Microscopy (CLSM) after phalloidin-DAPI staining for actin organization and nucleus, respectively.

RESULTS AND DISCUSSION

It was revealed that WJ-MSCs differentiated into fibroblasts displayed expression of fibroblast markers, vimentin and collagen type III. For hydrogel integration, PLA-based cylindrical mold was fabricated successfully by 3D printing. Then, cell-loaded hydrogel integration over tubular scaffold was achieved using the mold (Fig. 1A). It was observed that the cell-loaded hydrogel was combined tightly with multilayer tubular polymeric scaffold by conserving the tubular shape of the construct as intended. The hydrogel layer was measured as 400 µm in thickness. The results of LIVE/DEAD assay showed that cells were alive within collagen-based hydrogel and they were homogeneouly distributed within hydrogel by forming external layer of the vascular substitute (Fig.1B).

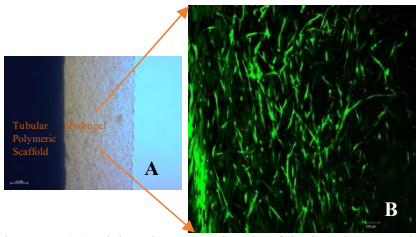

Figure 1. (A) Light microscopy image of hydrogel over polymeric tubular scaffold (B) Confocal micrograph of cells (green) on the external layer of the construct after LIVE/DEAD assay.

CONCLUSION

The external layer, fibroblast-loaded hydrogel was successfully integrated aroud the tubular construct to mimic tunica adventita of blood vessels. A vascular substitute consist of multilayers to imitate three tunics of blood vessel could be a promising new approach in vascular tissue engineering to improve the structural integrity and performance tissue equivalent.

REFERENCES

1. WHO. Cardiovascular diseases (CVDs), 2021.
2. Seifu, D et al., Nat Rev Cardiol. 10, 410–21 ,2013.
3. Ross M.et al., Histology Text and Atlas Correlated Cell and Molecular Biology. 6th Edition, 2011.
4. Holzapfel GA. et al., Am J Physiol Heart Circ Physiol. 1;315(3):540-49, 2018.

ACKNOWLEDGMENTS

This study was supported by The Scientific and Technological Research Council of Turkey (TUBITAK) SBAG 118S587 and TUBITAK 2211-A/BIDEB. The authors acknowledge ACU Biomaterials Center for the use of equipments and facilities.

Biohybrid Miniaturized Valves based on Elastin-like Recombinamers

Sergio Acosta[1], Fernando Gonzalez-Perez[2], Stephan Rütten[3], Alexander Kopp[4], Heinz-Werner Henke[5], Philipp Bruners[6], Caroline Emonts[7], Thomas Gries[7], J. Carlos Rodríguez-Cabello[2], Stefan Jockenhoevel[1,8], Alicia Fernández-Colino[1*]

[1]Department of Biohybrid & Medical Textiles (Biotex), AME –Institute of Applied Medical Engineering, Helmholtz Institute, RWTH Aachen University, Aachen Germany.
[2]G.I.R. BIOFORGE, CIBER-BBN, University of Valladolid, Valladolid, Spain.
[3]Electron Microscopy Facility, Uniklinik RWTH Aachen, Aachen, Germany.
[4]Meotec GmbH, Aachen, Germany.
[5]Innovative Tomography Products GmbH, Bochum, Germany.
[6]Klinik für Diagnostische und Interventionelle Radiologie, Universitätsklinikum Aachen, Aachen, Germany.
[7]Institut für Textiltechnik Aachen (ITA), RWTH Aachen University, Aachen, Germany.
[8]AMIBM-Aachen-Maastricht-Institute for Biobased Materials, Maastricht University, The Netherlands.
acosta@ame.rwth-aachen.de

INTRODUCTION

The development of valve implants able to work properly under the demanding conditions of the cardiovascular system remains a significant challenge.[1,2] In this regard, advanced materials and fabrication approaches are required to manufacture clinically relevant implants in this area. Here, we exploit the inherent properties of the elastin-like recombinamers (ELRs) for creating cell-instructive devices for enhanced *in vivo* performance. We propose a biohybrid approach to develop "off–the–shelf" miniaturized valve replacements with potential application in the venous circulation and the field of pediatric cardiology

EXPERIMENTAL METHODS

Bioactive ELRs, i.e. protease-sensitive, cell-adhesive or low-fouling, were recombinantly produced and subsequently chemically derivatized with azide and cyclooctyne groups for bioorthogonal click chemistry. Small-diameter valves (6-12 mm) were manufactured by means of electrospinning, layer-by-layer deposition, and injection molding, thus combining ELRs with technical components, including warp-knitted textiles and electrospun TPU nonwoven meshes. The mechanical performance of the biohybrid scaffolds was then evaluated by biaxial tensile testing and by measuring the burst strength. Additionally, the hydrodynamic valve performance of the resulting valves was validated in a pulse duplicator bioreactor system for the generation of physiological pressure/flow conditions. The hemocompatibility was assessed by platelet adhesion and hemolysis studies. Primary human endothelial cells and promonocytic cells were seeded on the constructs, and cellular behavior was analyzed by immunohistochemistry, ELISA, and confocal microscopy.

RESULTS AND DISCUSSION

Biohybrid tubular scaffolds composed of ELRs and textile technical components were successfully fabricated and subsequently fashioned into a miniaturized cell-free valve following the single point attached commissures (SPAC) method.[3] The hydrodynamic testing in a pulsatile bioreactor demonstrated excellent hemodynamic valve performance, with minimal regurgitation and pressure drop. In addition, the biohybrid valve implants showed enhanced hemocompatibility. They not only prevented platelet activation and aggregation but also promoted attachment and proliferation of primary human endothelial cells *in vitro.*

CONCLUSION

This work provides an insight into the development of "off-the-shelf" small valves that synergistically combine the hemocompatibility of the ELRs with the mechanical stability of technical components. After upcoming preclinical trials in a sheep model, these bioengineered valves may offer a clinically relevant solution for the treatment of chronic venous insufficiency or congenital heart diseases.

REFERENCES

References must be numbered. Keep the same style.
1. Smith G. *et al*., J. Biomech. 2:5-11, 2011
1 Fernández-Colino A. et al., Tissue Eng. Part B Rev., 27,3:253-265, 2020.
2 Etnel J. R. G. et al., J. Thorac. Cardiovasc. Surg., 151: 143-152, 2016.
3 Weber M. et al., Tissue Eng. Part C. Methods, 20:265, 2014.

ACKNOWLEDGMENTS

This work was supported by The Ministry of Economics, Affairs, Innovation, Digitalization, and Energy of the State of North-Rhine-Westphalia, the Federal Ministry of Education and Research of Germany (BMBF), and the European Union in the framework of the European Regional Development Fund (EFRE-0801314).

Developing next generation biodegradable coronary artery stents

Katarzyna Somszor[1], Onur Bas[2], Fatemeh Karimi[1,3], Stephanie Allison-Logan[1,3], Thomas McKenzie[3], Qiang Fu[3], Tara Shabab[2], Navid T. Saidy[2], Andrea J. O'Connor[1], Greg Qiao[3], Amanda Ellis[3], Dietmar Hutmacher[2], Daniel E. Heath[1*]

[1]Department of Biomedical Engineering, University of Melbourne, Parkville, Australia
[2]School of Mechanical, Medical, & Process Engineering, Queensland University of Technology, Brisbane, Australia
[3]Department of Chemical Engineering, University of Melbourne, Parkville, Australia

Daniel.Heath@unimelb.edu.au

INTRODUCTION

Coronary artery stents are lifesaving devices, with millions of devices implanted annually. Current stents are metallic and permanent.[1] However, permanent stenting is not required as the blood vessel can heal within 1-2 years after intervention. As such, biodegradable stents are receiving significant research attention. Despite their promise, the first clinically available biodegradable stent – Abbot Vascular's Absorb Bioresorbable Vascular Scaffold – was removed from the market in 2017 due to higher rates of late-stage thrombosis.[2] The failure of the first generation of stents was in part due to poor material selection and device design. Specifically, the weaker polymeric stents required thicker struts (~150!m) compared to permanent metal stents such as Synergy or Xience that have a strut thickness of ~80!m. These thicker struts resulted in pro-thrombogenic changes in blood flow, contributing to failure of the device.[3]

In this work, we explore several methods of improving biodegradable stent technology. First, we created polycaprolactone-reduced graphene oxide (PCL-rGO) nanocomposites with increased strength to enable fabrication of stents with thinner struts. We then explored the customizable fabrication of stents with melt electrowriting (MEW). Finally, we synthesized amphiphilic core-crosslinked star polymers that would allow sustained delivery of hydrophilic anticoagulant drugs from the bulk of the device during degradation.

EXPERIMENTAL METHODS

PCL-rGO nanocomposites were made with 0.1, 0.3, 0.6 or 1.0 wt% rGO, and tensile and compressive properties of the nanocomposites were assessed.

The nanocomposites were printed into stent-like structures using MEW. The ability to create tubular and stent-like structures with customizable architectures, thin struts, and increased strength was illustrated.

Core-crosslinked star polymer amphiphiles were synthesized and characterized through an arm-first approach. The stars have a hydrophilic core of PEG and a hydrophobic corona of PCL to facilitate loading of hydrophilic drugs into the core of the polymers and even distribution of the drug carriers throughout the bulk of the PCL device. Controlled elution of the model drug heparin was assessed.

RESULTS AND DISCUSSION

PCL-rGO nanocomposites exhibited superior mechanical properties compared to pristine PCL, and PCL-rGO nanocomposites with 0.1wt% rGO exhibited the best printability. Melt electrowritten fibres of 0.1wt% composites exhibited a 2.5-fold increase in Young's modulus and a 1.5-fold increase in ultimate tensile strength, potentiating the fabrication of mechanically robust stents with thinner struts. Additionally, we illustrated that MEW allows the fabrication of customisable stent-like structures with struts as thin as 60!m, potentiating the fabrication of customised stents.[4] We then synthesized a family of core-crosslinked star polymer amphiphiles, illustrated the ability to load heparin (a model anticoagulant drug) into the stars, showed that the drug carriers could be loaded into PCL with high loading density, and illustrated controlled and extended release of the heparin from the PCL, potentiating the ability to locally deliver an anticoagulant from the stents during the degradation process.[5]

CONCLUSION

These results address many of the biomaterial challenges associated with the first generation of biodegradable stents and could aid in the development of clinically successful devices. First, we increase the strength using PCL-rGO nanocomposites to allow fabrication of devices with thinner struts. Second, the ability to generate customizable stent-like structures using the emerging fabrication technique of melt electrowriting was illustrated. Finally, the ability to deliver drugs from the bulk of the device during degradation was established.

REFERENCES

1. Ho, *et al*., Metals. 6(7):168, 2016
2. Jinnouchi, *et al.,* Nat. Rev. Cardiol. 16(5):286, 2019.
3. Foin, *et al*., Int. J. Cardiol. 177(3):800-08, 2014.
4. Somszor, *et al*., ACS Macro Letters. 9:1732-39, 2020.
5. Somszor, *et al*., Biomacro. 22:2554-62, 2021.

ACKNOWLEDGMENTS

We gratefully acknowledge the support of the University of Melbourne and an Australian Government Research Training Program Scholarship (Melbourne International Research Scholarship). This work was funded in part by the Australian Research Council (FT190100280 and IC160100026). The authors also thank the Materials Characterization and Fabrication Platform (the University of Melbourne) for access to infrastructure and equipment.

Silk Fibroin Tubular Scaffolds: Towards the Development of an Aortic Heart Valve Replacement

Amanda Schmidt[1,2*], Alicia Fernández-Colino[1], Alex Greenhalgh[2], Stefan Jockenhoevel[1], Martin Frydrych[2]

[1]Department of Biohybrid & Medical Textiles (BioTex), AME-Institute of Applied Medical Engineering, Hemholtz Institute, RWTH Aachen University, Aachen, Germany
[2]Spintex Engineering, Oxford, UK
[*] a.schmidt@rwth-aachen.de

INTRODUCTION

Heart valve disease's incidence is increasing worldwide with the steady ageing of the population[1]. Latest research on tissue-engineered valves is focused in overcoming limitations associated with current commercial valve replacement. Promising results were obtained in the development of prosthesis reinforced by synthetic polymeric fibres, and a bioactive scaffold[2]. However, synthetic polymeric materials were shown to increase the stiffness of the heart valve leaflets. Extensive studies have already recognized silk fibroin as a promising biomaterial for tissue-engineered applications[3]. Spintex Engineering has demonstrated promising mechanical and biological functions of a native-like fibroin material. Thus, this study proposes development of silk tubular scaffolds, to be designed as per single point attached commissures (SPAC) approach[2], as a preliminary step towards the development of a native-inspired silk heart valve for *in-situ* tissue regeneration.

EXPERIMENTAL METHODS

Bespoke equipment was developed for the manufacturing of silk hydrogel tubes by depositing silk native-like dope onto the surface of a rotating mandrel. The formation of silk hydrogel was tested by a variety of assembly methods, including crystallisation induced by ethanol at various concentrations, and UV crosslinking through the integration of Riboflavin (RB) into the silk solution, as per pre-defined methods[4]. Tensile tests (Zwick Roell, Zwicki, 20N Load Cell) were performed on the radial and circumferential directions of hydrogel samples. Storage stability tests were performed on EtOH 70% crystallized samples, with and without crosslinking, through regular tensile tests on the radial direction (n=3 for each test day) over the period of 15 days. The structures were pre-sterilized through autoclaving, and stored in PBS at 4ºC.

RESULTS AND DISCUSSION

Tensile test results showed an average of maximum tensile strength of 0.45±0.11 MPa for crosslinked and non-crosslinked samples of the silk hydrogel structure, when tested in the radial direction. These values are shown to be adequate in comparison to the radial direction of native's tissues[5]. Circumferential hydrogel strength is expected to be tuned according to circumferential native tissues properties, with the integration of a biomimetic load-optimised Spintex's silk fibre reinforcement. The inclusion of RB crosslinking significantly enhanced the overall smoothness and thickness consistency across the tubular structures.

Young's Modulus, derived from stress and strain curves, was found to be around 2.05±0.8 MPa for all radial hydrogel samples, which is comparable to native's modulus of 2 MPa in the radial direction[5]. After 15 days in PBS at 4℃ storage, autoclaved hydrogel samples' maximum tensile strength was found to be around 0.42±0.03 MPa for both crosslinked and non-crosslinked samples, resulting in 41% and 21% reduction in strength, respectively.

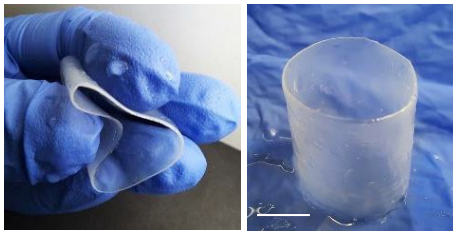

Figure 1. Tubular Silk Hydrogel Scaffold (Scale bar 10 mm).

CONCLUSION

Results show the successful manufacturing of hydrogel tubular structures from Spintex's native-like silk fibroin. Mechanical characterization indicate that tensile properties of the constructed hydrogel are in line with native aortic valve's results. Future work will focus on the integration of a load-optimised silk fibre reinforcement into the tubular structure, leading to the development of a biomimetic silk aortic valve prototype.

REFERENCES

1. Iung B. *et al.,* CJS. 30(9):962-970, 2014
2. Moreira R. *et al*., Tissue Engineering-Part C: Methods. 21(6):530-540, 2015
3. Kasoju N. *et al.,* Adv Healthcare Materials. 1(4):393-412, 2012
4. Brif A. *et al*., Biomaterials Science and Engineering. 6(1) :705-714, 2020
5. Hasan A. *et al.,* Journal of Biomechanics. 47(9):1949-63, 2014

ACKNOWLEDGMENTS

This project has received funding from the European Union's Horizon 2020 research and innovation programme under Marie Skolodowska-Curie grant agreement ID: 956621.

Characterisation of a gelatin release system for the electrophoretic deposition of seamless collagen tubes for use as vascular grafts

Jack W. Bonfield*, David J. Barrett, Ruth E. Cameron, and Serena M. Best
Department of Materials Science and Metallurgy, University of Cambridge, UK
* jwb63@cam.ac.uk

INTRODUCTION

Collagen is a biocompatible, bioresorbable, and bioactive protein which has extensive tissue engineering applications.[1] Using Electrophoretic Deposition (EPD), charged collagen particles held in suspension can be deposited onto cylindrical electrodes, dried, and removed to produce seamless, free standing collagen tubes for use as vascular grafts.[2] The development of a cell-compatible release layer is necessary for release of complex membranes after deposition. Gelatin is candidate release layer derived from denatured collagen which shares many of its properties as a biomaterial. It can be cast onto an electrode a film which dissolves in water at 37°C. This study characterises the effect of impurities and salts in gelatin release layers on relevant EPD parameters including deposition current, electrode gas evolution, and deposit homogeneity.

EXPERIMENTAL METHODS

Collagen slurry preparation: 1wt% insoluble type I collagen from Bovine skin (Devro medical) was rehydrated in 0.05 M acetic acid, homogenised, and dialysed against deionised (DI) water.

Cast gelatin coating: Gelatin from bovine skin (Sigma) was dissolved in DI water at 37°C. Gelatin suspensions were prepared at concentrations of 10 wt% and 0.5 wt% and were either non-dialysed (N-D), dialysed (D) for 72 hours (h), or D for 144 h against DI water. 5 ml gelatin suspension was cast onto a flat 316L steel electrode.

EPD film deposition: 0.5 cm EPD cell consisting of two 316L steel electrodes separated by silicone rubber spacers. Collagen membranes were deposited onto the gelatin coated electrode using a direct voltage of 30 V for 10 minutes. Membrane was dried and removed by dissolving gelatin in DI water at 37°C. Isolated collagen membrane was rinsed and dried.

Current measurements: Current measurements were taken using Keysight B2901A S/MU and software.

RESULTS AND DISCUSSION

The current values measured during EPD of collagen onto N-D 10 wt% gelatin release layers were significantly higher than for depositions onto 0.5 wt% N-D release layers (Figure 1). FTIR analysis of the N-D gelatin identified the presence of salts, and for the 10 wt% release layer this increase in salt concentration led to an increase in conductivity of the collagen suspension, corresponding to higher current values. Images of the collagen membranes produced during each deposition are shown in Figure 2, with a higher porosity visible in the membrane deposited onto the 10 wt% gelatin. The porosity was likely caused by the nucleation of bubbles on the electrode due to electrolysis, and was characterised by visual inspection and SEM. Increased current values led to higher levels of porosity in the membranes. The salt concentration in the gelatin release layers was varied by dialysing gelatin against DI water for 72 h.

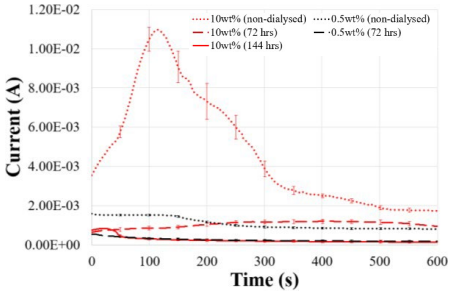

Figure 1. Averaged current vs time graph for EPD of 1 wt% collagen onto N-D and D 10 wt% and 0.5 wt% gelatin release layers.

The current values measured during EPD of collagen onto D 10 wt% and 0.5 wt% gelatin release were lower than for N-D conditions and subsequently the homogeneity of the collagen films increased. For 0.5 wt% gelatin release layers, a completely homogeneous collagen film was deposited. FTIR analysis of the D 10 wt% gelatin showed traces of salts remaining, which accounts for the higher current values and some porosity in the deposited collagen membranes. 10 wt% gelatin was then D for 144 h, and the current values were found to follow the same trend as the current for 0.5 wt% gelatin D for 72 h. The collagen membranes produced from these depositions were homogenous and non-porous.

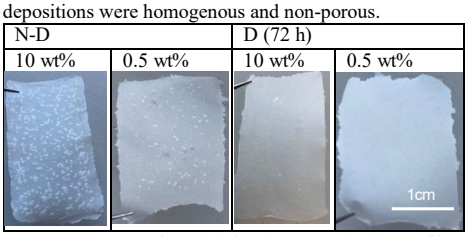

Figure 2. Images of the dried and removed collagen films produced during EPD onto N-D and 72 h D gelatin release layers of 10 wt% and 0.5 wt%.

CONCLUSION

Control of release layer salt concentration is key in allowing for homogeneous and defect free collagen deposition. Lower levels of dialysis led to high deposition currents, changes in deposition behaviour, and a significant increase in gas bubble nucleation and deposit defects.

REFERENCES

1. Barrett, D. J., et al. Biofabrication **2019**, 11 (4), 045017.
2. Linley, M. D., **2020**, PhD Thesis, University of Cambridge, Cambridge.

Acknowledgements: EPSRC DTP grant (JWB). ERC PoC Regen-Membrane (DJB + REC).

Weaving From Cell-Assembled extracellular Matrix Yarn: Towards Better Tissue-Engineered Vascular Grafts

Gaëtan Roudier[1*], Marie Hourques[1], Nicolas Da Silva[1], Maude Gluais[1], Nicolas L'Heureux[1]

[1]BioTis Inserm U1026, University of Bordeaux, Bordeaux, France
[*] gaetan.roudier@inserm.fr

INTRODUCTION

Vascular grafts are implanted daily, whether it is as leg or coronary bypasses or as arteriovenous shunts. Autologous blood vessels are the gold standard but have limited availability while synthetic materials are prone to thrombosis, intimal hyperplasia and infections[1, 2]. To overcome these limitations, our team produced a biological Tissue-Engineered Vascular Graft (TEVG) woven from yarn of Cell-Assembled Extracellular Matrix (CAM). This textile-based approach is very versatile because it gives fine control over the geometric and mechanical properties of the TEVG. The goal of this study is to establish how changes in production parameters (e.g.: yarn count, yarn density, etc.) affect the properties of the TEVG (e.g.: mechanical properties, wall thickness, luminal surface profile, etc.).

EXPERIMENTAL METHODS

CAM sheets were produced by sheep dermal fibroblasts seeded in 225 cm^2 flasks and cultured in DMEM/F-12 with 10% FBS and 0.5 mM Na L-ascorbate. Threads were cut with a custom motorized device composed of rolling blades spaced at the desired width (5 mm). Woven grafts were assembled on a circular loom and composed of a series of longitudinal threads, called "warp", and a circumferential one that spiraled along the length of the vessel, the "weft". The latter was made of two threads twisted together at 5 revolution/cm. The effects of yarn thickness and warp count (number of longitudinal threads) were tested. The influence of weft thread production parameters and its tension during weaving were also studied. Transmural permeability, suture retention strength, compliance and burst pressure were evaluated. Geometrical properties including TEVG inner diameter, wall thickness and graft luminal surface profile were assessed macroscopically and by X-ray microtomography. For each condition, n=3 TEVGs were woven.

RESULTS AND DISCUSSION

A lower yarn thickness decreased wall thickness and suture retention strength. A lower warp count had the same effect on wall thickness, while the compliance increased linearly with a decrease in warp count. In addition, the surface profile, which may have an impact on cellular infiltration, blood compatibility and blood flow, was influenced by both parameters. Narrower weft ribbons decreased weft diameter which resulted in thinner walls, TEVGs with lower strength and decreased waviness. Finally, a lower tension in the weft during weaving resulted in a significantly higher compliance while burst pressure was decreased.

CONCLUSION

We have demonstrated the influence of a number of parameters on the geometric, surface profile and mechanical properties of a TEVG woven from CAM yarn. Investigation of the influence of weft twist is underway to improve our control over the properties of the TEVG, focusing on increasing its compliance. These results are helping to build a toolbox that will allow the production of the TEVG with the most relevant properties for implantations as an arteriovenous graft in sheep.

REFERENCES

1. Klinkert, P. *et al*. *Eur. J. Vasc. Endovasc. Surg.* **27**, 357–362 (2004).
2. Rotmans, J. I. *et al*. *Can. J. Cardiol.* **22**, 1113–1116 (2006).

ACKNOWLEDGMENTS

The authors would like to thank the European Research Council for providing financial support to this project.

Physical and biological behaviour of flowable fiber reinforcedcomposite compared to alternative bulk filling composites

Nina Attik[1,2*], Pierre Colon [1,3], Rémy Gauthier[4], Charlène Chevalier[1], Brigitte Grosgogeat[1,2,5], Hazem Abouelleil[1,2*]

[1] Université de Lyon — Université Claude Bernard Lyon 1, UMR CNRS 5615, Laboratoire des Multimatériaux et Interfaces, Lyon, France
[2] Université de Lyon, Université Claude Bernard Lyon 1, Faculté d'Odontologie, Lyon, France
[3] Assistance Publique-Hôpitaux de Paris, Hôpital Rothschild, Service d'Odontologie, Université de Paris, Faculté dentaire, Paris, France
[4] Université de Lyon — Université Claude Bernard Lyon 1, CNRS, INSA Lyon, MatéIS, France
[5] Hospices Civils de Lyon, Service d'Odontologie, Lyon, France

INTRODUCTION

Many developments have been undertaken to overcome dental composite shortcomings, most notably the development of bulk-fill composites that can be inserted and polymerized in large cavities. They are considered to have higher physical and mechanical properties allowing them to endure high stresses due the masticatory forces. Fiber reinforcement of dental composite is another improvement that was introduced to enhance dental composite restorations toughness and fracture resistance[1]. On the other hand, potential toxicity and polymerization shrinkage stress of dental composites continue to shade some concern on their use. Clinically, bulk composites are mainly indicated for deep and large cavities, highlighting the importance for surveying their biological behaviour. The same holds true regarding the polymerization shrinkage stress. It is known that a higher configuration factor (C-factor) is generally associated with a higher polymerization stress[2]. Hence, stress occurrence during polymerization is an important parameter to investigate. The aim of this study was to assess the mechanical and biological behaviour of a flowable bulk-fill composite with fibers compared to bulk filling composites.

MATERIALS AND METHODS

EverX Flow™ (EXF, GC Corporation), Filtek™ Bulk Fill Posterior Restorative (FBF, 3 M) - one conventional bulk-fill composite, and SDR® flow+ (SDR, Dentsply) - one flowable bulk composite without fibers, were characterized. Composite samples light-cured with a LED device were evaluated in terms of flexural strength, flexural modulus (ISO 4049), fracture toughness (ISO 20795-1), and Vickers hardness. Polymerization stress was evaluated using a test setup that was intended to magnify the stress produced in an enclosed cavity. While, polymerization volumetric shrinkage s was investigated by Archimedes' principle according to ISO 17304:2013. *In vitro* biological assessment was achieved using primary human gingival fibroblast cells (HGF). Alamar Blue assay at 1, 3, and 5 days of contact to the 3 tested composite extracts was used to assess the metabolic activity (ISO 10993) and confocal imaging to evaluate cell morphology. Data were submitted to One-Way analysis of variance (ANOVA) and independent *t*-test ($\alpha = 0.05$).

RESULTS AND DISCUSSION

FBF showed statistically higher flexural modulus and Vickers hardness than EXF and SDR. However, EXF showed statistically higher K_{IC} than FBF and SDR. EXF had the statistically highest shrinkage stress values and FBF the lowest. Archimedes volumetric shrinkage showed significantly lower values for FBF as compared to theother two composites. At day 1, slight cytotoxic effect was observed for the three composites. At day 5, an enhancement of metabolic activity was observed in cells treated with EXF extracts. The higher fracture toughness results of fiber reinforced composite, means that it has a lower propensity to undergo crack initiation during loading. Which could predict the longevity of the restoration in the oral cavity[3]. The lower stress developed during SDR polymerization compared to EXF may be associated with its lower modulus. Generally, composites containing fibers have been shown to undergo higher stresses during polymerization than conventional composites[4]. It has been assumed that this effect of fibers is due to a modification of polymerization kinetics of the polymeric matrix[4]. The results obtained in the current study shows, that the tested fiber reinforced composite EXF had less deleterious effect than FBF and SDR on primary gingival cells viability mostly at day 3. This trend remains at day 5 with an enhancement of the metabolic activity in the presence of EXF (Figure 1).

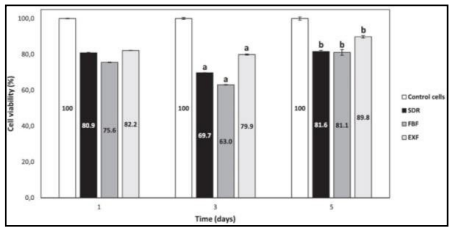

Figure 1: Metabolic activity of HGF subjected to the composite extracts after 1, 3 and 5 days. Lower case letters identify groups with statistical differences ($p < 0.05$): a compared with control cells and b compared with control cells in comparison with day 3.

Despite the limitations of the current *in vitro* study, the HGF metabolic activity enhancement at 5 days indicated a less cytotoxic effect. This result could suggest EXF use in large and deep cavities in contact with pulp tissue. Moreover, EXF had a significantly higher fracture toughness validating its potential use as a restorative material in stress bearing areas.

REFERENCES

1. Soares *et al*. Dent Mater. 2018;34(4):587-97.
2. Fok and Aregawi. Dent Mater. 2018;34(4):649-56.
3. Heintze *et al*. Dent Mater. 2017;33(3):e101-14.
4. Shouha and Ellakwa. J Biomed Mater Res B Appl Biomater. 2017;105(7):1930-7.

ACKNOWLEDGMENTS

The dental companies GC, 3 M and Dentsply are gratefully acknowledged for the generous donation of the tested dental composites. The SEM and CLSM studies were supported respectively by the Centre Technologique des Microstructures (CTμ) and Centre d'Imagerie Quantitative Lyon-Est (CIQLE).

Critical aspects of Ti-based bulk metallic glasses for dental implant manufacturing

Laurabelle Gautier[1], Benoît Ter-Ovanessian[1], Claire Gaillard[1], Damien Fabrègue[1], Jérôme Chevalier[1]

[1] 1 MATEIS UMR CNRS 5510, INSA Lyon, Université Claude Bernard Lyon 1, 7 Av. Jean Capelle, F-69621, Villeurbanne, France

*laurabelle.gautier@insa-lyon.fr

INTRODUCTION

Since two decades, Bulk Metallic Glasses (BMG) are often described as very promising materials for biomedical applications. They may indeed exhibit astonishing mechanical and corrosion properties, especially when they are processed in the form of very small samples. The $Ti_{40}Cu_{36}Zr_{10}Pd_{14}$ grade for example has already been proved to be biocompatible and presents a yield strength up to 2GPa[1]. This, in addition to a theoretical improvement of corrosion resistance related to its amorphous nature, would open the door to minimally invasive implants and small dental products. However, we have recently shown that crystalized casting defects (often referred as spherulites) in this specific composition have a detrimental influence on the mechanical and electrochemical properties[2]. They are particularly numerous and large in several milimeters bulk samples, which are relevant to produce dental implants or dental products. While the exact origin of the spherulites has not yet been determined, their morphology, chemistry, crystallography based on Cu-Ti binary diagram and a growth mechanism have been studied in details[2]. It is hypothesized that if the microstructure (content and size of such spherulites) of this BMG can be better controlled through processing it can lead to a significant improvement in the mechanical properties and corrosion resistance. It was therefore the aim of this work to explore the effect of processing on the presence and the features of spherulites and their effect on mechanical and corrosion properties.

EXPERIMENTAL METHODS

The $Ti_{40}Cu_{36}Zr_{10}Pd_{14}$ bulk amorphous rods used for the experiments were obtained by classic suction copper mold casting from high purity raw metals (Copper, Titanium, Zirconium and Palladium) under high purity Argon atmosphere. Different casting parameters were investigated such as melts number before casting, arc intensity and hydrogen enriched atmosphere. The BMG rods have then been characterized by XRD, DSC, SEM and TEM. The mechanical properties were studied by compressive, tensile and four points bending tests. The electrochemical measurements were conducted in NaCl 0.9% solution at 37°C with Ag/AgCl as reference electrode and Graphite as counter electrode.

RESULTS AND DISCUSSION

In general, mechanical characterisation showed very poor reproducibility except for compressive tests which are less sensitive to casting defects (and not relevant for the real use). Failure was often correlated with the presence of a big spherulite near the sample surface. Nevertheless, the Yield Strength of this BMG is really high around 2GPa (but without any plasticity in mode I). It is believed that the spherulites could be associated to un-melted areas in the alloy during the casting process. Even with an increase of the arc intensity or a large number of fusions, the statistical analysis did not show a significant difference in distribution in spherulite's number and size. The electrochemistry experiments showed that the spherulite/amorphous matrix interface appears to be particularly prone to dissolution. The complex spherulite's microstructure showed several phases with specific orientation relationships which helps to propose a growth scenario.

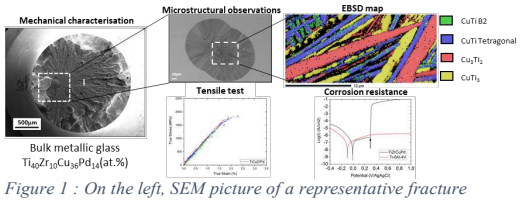

Figure 1 : On the left, SEM picture of a representative fracture surface which illustrates the presence of casting defects in $Ti_{40}Cu_{36}Zr_{10}Pd_{14}$ BMG under tensile test. On the right, EBSD map with the identified phases. On the bottom, stress-strain curves of tensile test and potentiodynamic curves in NaCl 0.9%(compared to TA6V as reference material).

CONCLUSION

The TiCuZrPd grade that has been portrayed as most promising for biomedical applications and particularly for dental implants exhibits casting defects. To date, and despite numerous attempts, we have not been able to avoid them or adjust their size in order to increase ductility and avoid pitting corrosion. This constitutes a key point to further explore for this material to become a robust candidate in biomedical applications in the near future.

REFERENCES

1. Liens A, Etiemble A, Rivory P, et al. On the potential of Bulk Metallic Glasses for dental implantology: Case study on Ti 40 Zr 10 Cu 36 Pd 14. *Materials*. 2018;11(2). doi:10.3390/ma11020249

2. Gautier L, Liens A, Ter-Ovanessian B, et al. Impact of spherulite-type crystalline defects on the mechanical and electrochemical properties of TiCuZrPd metallic glasses. *Materialia*. Published online February 12, 2022:101353. doi:10.1016/j.mtla.2022.101353

ACKNOWLEDGMENTS

The authors would like to thank the 'Agence National de la Recherche' (ANR) and its funding within the framework of the ANR-TNT-18-CE91-0005.

Synergistic combination of Calcium and Cerium ions doping in silica-based mesoporous nanoparticles for periodontal regeneration applications

Anna Theocharidou[1], Georgia K. Pouroutzidou[1,2], Ioannis Tsamesidis[1*], Maria Bousnaki[1], Anastasia Beketova[1], Eleana Kontonasaki[1]

[1] School of Dentistry, Faculty of Health Sciences, Aristotle University of Thessaloniki, 54124 Thessaloniki, Greece
[2] School of Physics, Faculty of Sciences, Aristotle University of Thessaloniki, 54124 Thessaloniki, Greece
[*] itsamesidis@auth.gr

INTRODUCTION

Periodontitis is one of the most common inflammatory diseases and the leading cause of tooth loss in adults. It is characterized by progressive destruction of the supporting complex of the teeth. Periodontal tissue regeneration strategies include regenerative surgery as well as the use of a variety of grafting materials and growth factors[1.] Mesoporous nanoparticles (MSNs) with cerium and calcium ions could contribute to control over bacterial contamination and enhance the capability of vascularization, eliminating the chance of bone loss. The aim of this study was the toxicity evaluation of the newly synthesized NPs in direct contact with primary Human Periodontal Ligament Cells (hPDLCs) and their hemolytic behavior.

EXPERIMENTAL METHODS

The synthesis of Ca and Ce doped silica-based mesoporous nanoparticles (SiCaCe MSNs) was performed using the Sol-Gel technique[1]. The synthesis was conducted using tetraethyl orthosilicate (TEOS) as a silicon source and Cetyltrimethylammonium bromide (CTAB) as a mesoporous agent in an alkaline environment as shown in Table 1(in 12 pH value).

Sample	CTAB/TEOS	pH
SiCaCe 1	*0.10*	*12*
SiCaCe 2	*0.20*	*12*
SiCaCe 3	*0.30*	*12*

Table 1. Synthesis parameters for MSNs.

Biological evaluation: hPDLCs were established from human biopsies of periodontal ligament tissues from a healthy donor and enzymatic dissociation method was followed for the isolation of the cells. CD34, CD45, CD73, CD105, CD146 and STRO-1 antibodies, were used for the cell characterization[2]. Cell viability was evaluated with the MTT 3-(4,5-dimethylthiazol-2-yl)-2,5-diphenyltetrazolium bromide) assay at different concentrations (125, 250 and-500μg/ml). Their hemolytic activity was evaluated in contact with human red blood cells at various concentrations (125-1000μg/ml). The absorbance of hemoglobin at 541 nm was measured with a plate reader, from supernatants after centrifugation at 2000 rpm for 1 minute. The percent of hemolysis was calculated as follows: Hemolysis % = [(sample absorbance - negative control)/ (positive control -negative control)]x100.

RESULTS AND DISCUSSION

The double negative CD34-, CD45- cells expressed STRO-1 at 97% and those cells were positive for CD146 at 98,2%. CD45 and CD34 expression was not observed on the cell surface of the 83,7% cultured cells population. The hPDLCs in direct contact with MSNs presented the characteristic presented biocompatibility that reached above 80% compared to positive control at the 1st day of incubation for all materials and concentrations, without presenting a distinct dose response (Fifure 1). However, after 3 days of incubation, a significant increase in OD was observed for all the materials especially at higher concentrations. This finding suggests that all MSNs were effective in promoting cell proliferation in a dose dependent manner. Further studies will be performed to assess their osteogenic capacity. The hemocompatibility assay revealed no hemolytic effect at any tested concentration.

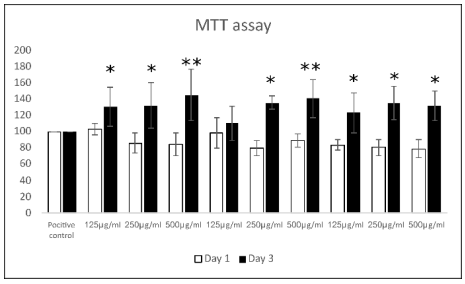

Figure 1. MTT assay results after 1 and 3 days of culture with hPDLCs.*=p<0.05, **=p<0.001 compared to positive control (cells without MSNs).

CONCLUSION

The novel Ce/Ca doped MSNs can be considered as promising candidates as bioactive fillers in composite materials and scaffolds for bone tissue engineering.

ACKNOWLEDGMENTS

This work is supported by European Union's Horizon 2020 research and innovation programme under grant agreement No 953128, project: Smart, Multifunctional Dental Implants: A solution for peri-implantitis and bone loss.

REFERENCES

1. Pouroutzidou G.K. et al. Int. J. Mol. Sci. 2021, 22, 1–25, doi:10.3390/ijms22020577.
2. Kumar S et al. Dent. Clin. North Am. 2019, 63, 69–81, doi:10.1016/j.cden.2018.08.005.

RNAseq analysis reveals divergent molecular events that direct hBMSCs toward fibrosis or bone regeneration: importance of inflammation regulation

Laura Coquelin[1*], Gabriel Windels[1*], Najat Raddi[1$], Luciano Vidal[2$], Cecile Lefevre[3$], Marie Tiffany[1], Nora El Jahrani[1], Mathieu Manassero[4], Hélène Rouard[1], Hakim Hocini[3] and Nathalie Chevallier[1]

[1] IMRB U955-E10, Inserm, Unité d'Ingénierie et de Thérapie Cellulaire-Etablissement Français du Sang, Université Paris-Est, Créteil, France
[2] UMR-1238, INSERM, laboratoire « Sarcomes osseux et remodelage des tissus calcifiés », Université de Nantes, Nantes, France
[3] IMRB U955, Inserm, Vaccine Research Institute, Université Paris Est-Créteil, France
[4] B3OA UMR 7052, CNRS, Inserm, Université Paris Diderot; Ecole Nationale Vétérinaire d'Alfort, Paris, France
[*] Co-first authors
[$] Co-second authors

nathalie.chevallier@efs.sante.fr

INTRODUCTION

Human bone marrow mesenchymal stromal cells (hBMSCs) associated to biomaterials are currently used in clinic for bone repair. Although results are positive, bone formation kinetics are heterogeneous between patients (1, 2). In order to understand the cell heterogeneity and to optimize the development of this therapy, it is necessary to better understand the cellular and molecular mechanisms induced by hBMSCs.

EXPERIMENTAL METHODS

To assess cell heterogeneity, cells from 50 donors were amplified and grafted in combination with HA/bTCP biomaterial subcutaneously in an immunodeficient mouse model and analyzed by histology after 6 weeks. These results were then confirmed using an orthotopic model. To understand why the cells have different bone potential, cells from different donors were transplanted subcutaneously and analyzed i) for cell survival at 24 hours and from 1 to 6 weeks, and ii) for their mechanism of action by RNAseq analysis at 8 hours, 1 and 2 weeks after transplantation. iii) Mice depleted in neutrophils by an anti-Ly6G were also used.

RESULTS AND DISCUSSION

Our results confirmed that the bone potentials of the cells is donor-dependent with bone gradient going from no or very low bone (NB), medium bone (MB) and high bone (HB) potential and these differences were confirmed by using an orthotopic model. To understand this heterogeneity, we focused on the behavior of hBMSCs and observed that hBMSCs with high bone potential were associated with higher cell survival and proliferation after *in vivo* transplantation. To determine their mechanism of action and to understand how cell survival is controlled, RNAseq analysis was performed. Our results show that cells with reduced bone potential have a higher expression level of pro-inflammatory cytokines at 8h post-graft, which is associated with a higher inflammatory response. We then confirm that the long-term survival of hBMSCs depends in part on their ability to regulate neutrophil activation. Furthermore, our RNAseq analysis at 1 and 2 weeks highlights that long-term survival of hBMSCs is associated with increased bone formation only if hBMSCs are able to evolve towards osteoblastic differentiation. Our hypothesis is that bone differentiation allows hBMSCs to synthesize paracrine factors necessary for chemoattraction and osteoblastic and osteoclastic differentiation of neighboring cells.

CONCLUSION

Overall, our results indicate that the low bone potential of the cells is mainly due to the fact that hBMSCs strongly induce an inflammatory response leading initially to their elimination by neutrophils. On the other hand, our results indicate that the high bone potential of the cells is due to their ability to survive, proliferate and evolve towards osteoblastic differentiation. This osteoblastic differentiation appears to be a prerequisite for hBMSCs to synthesize the paracrine factors necessary for chemoattraction as well as osteoblastic and osteoclastic differentiation of neighboring cells, otherwise fibrous tissue formation is observed. As we have shown that inhibition of the neutrophilic response improves the survival of hBMSCs as well as bone formation, we propose that anti-inflammatory treatment in parallel with transplantation should further improve the clinical protocol.

REFERENCES

1. Gómez-Barrena E, et al. Biomaterials. 2018 Mar 19. doi: 10.1016/ j.biomaterials. 2018.03.033
2. Gómez-Barrena E, et al. Injury. 2020 Apr;51 doi: 10.1016/j.injury.2020.02.070.

ACKNOWLEDGMENTS

Authors acknowledge Sanae Zazou, Miryam Mebarki and Tisserand Pascaline for their technical contribution. The authors would like to thank the European H2020 Maxibone (Grant no:779322) and the EFS for providing financial support to this project.

Supersaturated Ion Solutions for Dentin Mineralization

Timo Peltola[1*], Mona Gibreel[2], Laleh Solhi[3], Eero Kontturi[3], Lippo Lassila[2], Pekka Vallittu[2], and Eija Säilynoja[1,2]

[1]Research Development and Production Department, Stick Tech Ltd – Member of GC Group, Turku, Finland
[2]Department of Biomaterials Science and Turku Clinical Biomaterial Center -TCBC
Institute of Dentistry, University of Turku, Turku, Finland
[3]Department of Bioproducts and Biosystems, Aalto University, Espoo, Finland
[*] timo.peltola@gc.dental

INTRODUCTION

Collagen and minerals constitute the main components of human dentin. The mineral layer is, unfortunately, destroyed during the caries treatment procedure. Thus, the remineralization of dentin is of great significance for the restoration of demineralized dentin.

The preliminary idea for this research was to develop supersaturated ion solutions with mineralization property for treatment of dentine bonding surface and dentinal tubules. Essential factors for mineralization are an optimal surface structure together with free calcium and phosphate ions originating from the surrounding tissue, environment or released from the material itself. The aim of this study was to investigate the ability to mineralize dentin with supersaturated ion fluids.

EXPERIMENTAL METHODS

The mineralization effect was determined for different solutions: supersaturated calcium phosphate (CaP) solution, tetrahydroxysilane sol, carboxylated nanocellulose (CNC) solution, and a combination of them (1:1:1).

Test specimens (n=6) were prepared as follows: a 2 mm dentin discs were acid etched with phosphoric acid gel (37%) for 30 sec, followed by surface treatments with experimental solutions for 30 sec or no surface treatment (control). Dried discs were immersed in simulated body fluid (SBF)[1] for 10 days and SBF was changed every second day. Scanning electron microscopy (SEM) examination was done after SBF immersion (top view and longitudinal cross-sections) to determinate the treated dentin surface structure.

RESULTS AND DISCUSSION

The formed precipitation was the thickest and went deepest inside the dentinal tubules of the dentin surface treated with the combination of tetrahydroxysilane, CNC, and CaP solution (Figure 1), compared to the other treatment solutions.

In the second phase, the precipitation was analyzed by energy-dispersive X-ray spectroscopy (EDS). As seen in Figure 2, silica penetrates inside the dentin tubules with a maximum depth of 30 µm depth. Calcium and phosphorus analysis also confirmed the presence of other elements near the surface besides Ca or P ions, which can be seen as black areas. Silica can be seen as orange areas in the image of Si element.

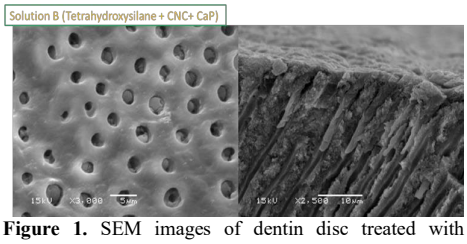

Figure 1. SEM images of dentin disc treated with tetrahydroxysilane, CNC, and calcium phosphate after 10 days in SBF.

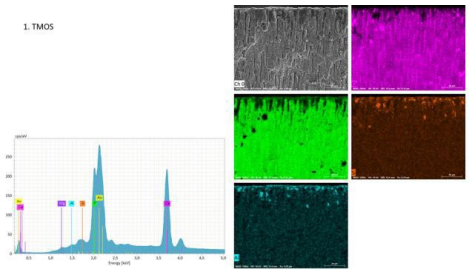

Figure 2. Elemental EDS analysis for the tetrahydroxysilane treated dentin surface.

CONCLUSION

All the three studied solutions (tetrahydroxysilane, supersaturated calcium phosphate, and CNC solutions) showed promising ability to mineralize the dentine surface and dentinal tubules. The combination of these three solutions showed the best results in terms of the ability to mineralize dentin. After these promising results, the next step would be to evaluate how these data can be applied in practice for enhancing sealing and bonding of resin composite to dentine.

REFERENCES

1. ISO 23317:2014 - Implants for surgery -- In vitro evaluation for apatite-forming ability of implant materials.

ACKNOWLEDGEMENTS

Financial support by Academy of Finland project no. 321598 is acknowledged. This work is a part of the Business Finland project Biobased smart materials at biomaterials interface.

HYDROGEL BASED NANO-DELIVERY SYSTEM FOR ONE SHOT REGENERATIVE THERAPY OF PERI-IMPLANTITIS

Lily Paillat[1], Marika Mosina[2,3], Maud Viallon[4], Estelle Bray[1], Liga Stipniece[2,3], Pascale Chevallier[4], Gildas Réthoré[1], Alexis Gaudin[1], Pierre Weiss[1], Assem Soueidan[1], Diego Mantovani[4], and Janis Locs[2,3]

[1] Nantes Université, Oniris, CHU Nantes, INSERM, Univ Angers, Regenerative Medicine and Skeleton, RMeS, F-44000 Nantes, France
[2] Rudolfs Cimdins Riga Biomaterials Innovations and Development Centre of RTU, Institute of General Chemical Engineering, Faculty of Materials Science and Applied Chemistry, Riga Technical University, Pulka Street 3, LV-1007 Riga, Latvia
[3] Baltic Biomaterials Centre of Excellence, Headquarters at Riga Technical University, Kalku Street 1, LV-1658 Riga, Latvia
[4] Laboratory for Biomaterials and Bioengineering, Laval University and CHU de Quebec Division of Regenerative Medicine, Quebec, QC, Canada

INTRODUCTION

Dental implant is a routine treatment in daily dental practice and is becoming more widespread among practitioners as the years progress. However, due to permanent exposure to the infective threats, peri-implantitis affects 20% of individuals with implants and leads to peri-implant soft tissue inflammation and alveolar bone loss. Unfortunately, the use of antibiotics as treatment protocol leads to antibiotic resistant bacterial strains and still have no long-term efficiency. In this context, the use of inorganic antibacterial agents (metal ions, nanoparticles) emerged as a promising alternative to prevent peri-implantitis. Here, we proposed to develop an innovative composite by combining two hydrogels with distinct properties. (i) A resorbable hydrogel loaded with biphasic calcium phosphate (BCP) and gallium-containing hydroxyapatite nanoparticles (GaHAp) to provide pro-regenerative and antibacterial properties, (ii) a slowly-degradable hydrogel-based membrane to prevent the ingrowth of epithelial soft tissue around the implant. For this project we intend to optimize, characterize, assess the cytocompatibility and determine anti-bacterial effect of our innovative composite.

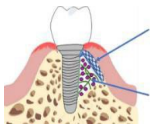

Bone level : Slowly resorbable Hydrogel-based membrane

Gum level : Resorbable hydrogel + BCP + GaHAp

EXPERIMENTAL METHODS

Gallium substituted hydroxyapatite was synthesized via wet chemical precipitation. Phase composition, specific surface and ion release were determined. Silanized hyaluronic acid (Si-HA) hydrogel with gallium containing HAp was synthetized by mixing Si-HA solution with NaOH, then with a specific acidic buffer and BCP granules before let jellify 2 days at 37°C. The hydrogel-based membrane was formed by a sol-gel reaction between a basic solution of silanized hydroxypropyl methylcellulose (Si-HPMC) and acid solution of chitosan. Gallium salt and GaHAp cytotoxicity were assessed in vitro using indirect (conditioned medium) and direct contact assays.

RESULTS AND DISCUSSION

We observed a great calcium phosphate precipitation with 4%wt GaHAp and a complete release of gallium within 30 days. Moreover, while the specific surface was decreased by the sterilization process, GaHap size was increased. Both hydrogels were characterized, and we determined that addition of chitosan didn't modify Si-HPMC hydrogel mechanical properties and that Si-HA hydrogel viscosity is influenced by GaHAp concentration. More tests (enzymatic degradation, ion release) are now required to select the best formulation of each hydrogel to permit the study of the Si-HA-GaHAp hydrogel effect on the bone regeneration and modulation of inflammation. Using gallium salt, we showed that Ga^{3+} is non-cytotoxic until 100 µg/mL for all investigated cell types. Moreover, all tested concentrations of Hap are not cytotoxic, whereas 80 and 800 µg/mL of Ga^{3+} in GaHAp leads to L929 and OKF6 death respectively. Finally, the antibacterial effect of GaHAp have to be determined on three bacteria strains implicated in peri-implantitis pathology.

CONCLUSION

We have successfully synthetized and characterized GaHAp and determined their cytocompatibility on three cell types. We also confirmed that the Si-HA hydrogel formulation allowed the mixing with GaHAp. Our perspectives are to assess biocompatibility and biofunctionality in vivo using rat and rabbit calvaria bone defect model.

ACKNOWLEDGMENT

The authors are grateful to the EuroNanoMed III, fonds de recherche du Québec, Canada, Latvijas Zinatnes Padome/valsts izglitibas attisbas agentura, Latvia, and Agence Nationale de la Recherche, France, for their financial support and HTL for Si-HA hydrogels delivery.

Immunomodulatory Maresin-1 Loaded Zein Nanoparticles to Induce Pro-Regenerative Microenvironments

Ana Beatriz Sousa[1,2,3*], Cláudia Martins[1,2,4], Bruno Sarmento[1,2,5], Mário Adolfo Barbosa[1,2,3] and Judite Novais Barbosa[1,2,3]

[1]i3S – Instituto de Investigação e Inovação em Saúde, Universidade do Porto, Rua Alfredo Allen 208, 4200-135 Porto, Portugal
[2]INEB – Instituto de Engenharia Biomédica, Universidade do Porto, Rua Alfredo Allen 208, 4200-135 Porto, Portugal
[3]ICBAS – Instituto Ciências Biomédicas Abel Salazar, Universidade do Porto, Rua de Jorge Viterbo Ferreira 228, 4050-313 Porto, Portugal
[4]FEUP – Faculdade de Engenharia da Universidade do Porto, Rua Dr. Roberto Frias s/n, 4200-465 Porto, Portugal
[5]CESPU – Instituto de Investigação e Formação Avançada em Ciências e Tecnologias da Saúde, Rua Central de Gandra 1317, 4585-116 Gandra, Portugal
[*] anabsousa@i3s.up.pt

INTRODUCTION

The incidence of chronic wounds is escalating worldwide. The associated healing process is especially problematic in population that are aging and show increased morbidity[1]. The search for strategies that will improve tissue repair is at the cutting edge of regenerative engineering.

The main goal of this research work is to develop an innovative strategy consisting of zein monodisperse nanoparticles loaded with maresin-1 to induce a pro-regenerative microenvironment that will accelerate wound healing, ultimately providing an effective strategy for the rapid healing of wounds.

Zein is an insoluble prolamin protein that is extracted from corn that was approved in 1985 by the FDA. The utilization of zein was reported for several applications such as a platform for drug delivery and for tissue engineering[2].

Maresin-1 is a potent immunoresolvent, biosynthesized in inflammatory exudates to control inflammation via stimulating resolution programs through limiting polimorphonuclear (PMN) leukocytes infiltration and enhancing macrophage uptake of apoptotic PMNs, the hallmark of pro-resolving mechanisms and critical for the inflammatory response to switch off [3].

EXPERIMENTAL METHODS

The Dolomite Microfluidics® chip was used as platform to load maresin-1 into zein nanoparticles. The organic phase consisted of a mixture of 1% (w/v) of zein and maresin-1 in 70% ethanol , whereas the aqueous phase consisted of Milli-Q water. The nanoparticles were produced by flow-focusing the organic central stream with the aqueous outer fluid. The final solution was magnetically stirred for 3h at room temperature and centrifuged for 15 minutes through a filter device with a molecular weight cutoff of 100kDa at 2000g. Liquid suspensions of unloaded and maresin-1 loaded zein nanoparticles were stored at 4°C for 30 days after production. The particle size, size distribution, and zeta-potential were assessed, as well as the amount of maresin-1 recovered. The ability of maresin-1 loaded zein nanoparticles to affect the cell viability was assessed in both primary human macrophages (isolated from healthy blood donors) and primary human dermal fibroblasts. The capacity of these nanoparticles to affect macrophage polarization was also evaluated.

RESULTS AND DISCUSSION

Zein nanoparticles, both empty and encapsulated with maresin-1, presented average diameter values in the range of 150–190 nm, narrow size distribution (polydispersity index < 0.2), and zeta potential of around + 20 mV. Aqueous suspensions of zein NPs were stable for at least 1 month when stored at 4 °C. Maresin-1 alone and maresin-1-loaded zein nanoparticles presented low cytotoxicity to human macrophages and fibroblasts. Moreover, its effect did not alter cell morphology. The effect of the nanoparticles on cell proliferation and macrophage polarization is being evaluated.

CONCLUSION

Maresin-1 loaded zein nanoparticles were successfully produced. The newly developed nanoparticles were not cytotoxic to both human macrophages and fibroblasts. In addition, normal cell morphology was maintained up to 7 days of culture.

REFERENCES

1. Sorg H. *et al*., Eur. Surg. Res., vol. 58, no. 1–2, pp. 81–94, 2017.
2. Abdelsalam A.M. *et al*., Pharmaceutics, 13(9): 1354, 2021.
3. Chiang N. *et al*., J Clin Invest., 129(12):5294-311, 2019.

ACKNOWLEDGMENTS

The authors would like to thank Norte Regional Operational Program: Structured R&D&I Projects – Unorte.pt. HEALTH-UNORTE; NORTE-01-0145-FEDER-000039 for providing financial support to this research work.

Photoemission investigation executed for modified CoCr alloys used in prosthetic dentistry

Anna Zięboowicz[1*], Jerzy Kubacki[2*], Bogusław Zięboowicz[4]

[1] Department of Biomaterials and Medical Device Engineering, Silesian University of Technology, Zabrze, Poland
[2] Silesian Centre for Education and Interdisciplinary Research, University of Silesia, Chorzów, Poland
[3] Department of Engineering Materials and Biomaterials, Silesian University of Technology, Gliwice, Poland
[*] anna.ziebowicz@polsl.pl

INTRODUCTION

A wide range of solutions and access to modern materials and technologies contribute to changes in the field of prosthetic restorations. There are quite meaningful data on the corrosion and toxicity of CoCr alloys for their use in restorative materials such as dental prostheses. In this paper the electronic structure was determined for 50 nm thick zirconium oxide layer [1] deposited on disk of CoCr prepared by casting, additive manufacturing (direct metal laser sintering, DMLS) and milling (CADCAM). The surfaces have been prepared in accordance with the principles of construction of removable skeletal dentures.

EXPERIMENTAL METHODS

The photoemission studies XPS (X-ray Photoemission Spectroscopy) were performed on PHI5700/660 Physical Electronics (USA) spectrometer using Al Kα monochromatic X-ray source with energy 1486.6 eV. All photoelectron spectra were calibrated against the peaks of $Au4f_{7/2}$ at 83.98 eV, $Ag3d_{5/2}$ at 368.27 eV and $Cu2p_{3/2}$ at 932.67 eV of binding energy. The photoemission investigations were executed for "fresh" and cleaned surface. The cleaning procedure was performed in vacuum by Ar+ ion beam with energy E=0,7 keV by time 1 minute. The test of the surfaces of the film was carried out at take-off angle 45°. The electron float gun was used for the compensation of positive surface charge, which may appear on the insulator materials' surface. The XPS measurement was carried out for the core lines of O1s, Zr3d, C1s, and valence band region. Atomic concentration calculations and fitting process were performed with the use of MULTIPAK software.

RESULTS AND DISCUSSION

The survey spectra of ZrO_2 films obtained from "fresh" and after cleaning procedure samples consists a photoemission and auger peaks corresponded to the following electronic levels of zirconium and oxygen.

The presence of the strong C1s peak observed for "fresh" surface is related to its the natural contamination by the aliphatic forms of carbon. The substantial amount of carbon molecules was removed after ions sputtering. The influence of gently ion beam treatment on the electronic structure in dependence of substrate was showed for the valence band region in the follow part.

Application of cleaning procedure remove of carbon contamination level successful approximately five-six times. The obtained values of the Zr/O ratio for all samples is about 0.5 what indicate on well stoichiometry of the film and good chemical quality. The Zr3d doublets and O1s core lines were presented in Figure 1.

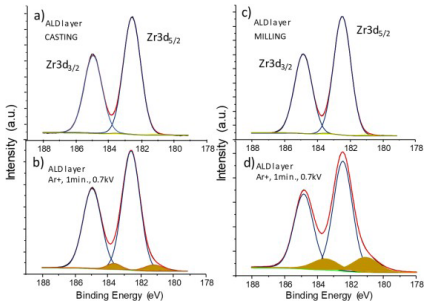

Figure 1. The Zr3d (a) (c) core lines and O1s (e) (g) electronic states obtained for "virgin" and (b) (d) (f) (h) after applied cleaning procedure in UHV conditions ALD films deposited onto two various substrate. Deconvoluted core line obtained for the film deposited on DMLS substrate was presented in [1].

CONCLUSION

The spectra of presented the electronic levels consists Zr4p, O2s and Zr4d-O2p hybridization states. Additional energy states present for the etched surfaces have been compared with the result obtained for the ceramic form of ZrO2 for which the gap is above 4eV [2]. The recorded photoemissions from additional electron states in the energy gap are differs for the films deposited on various substrates. The induced density of states corresponds to the amounts of the defects in ZrO_2 layers. There is the highest for the MILLING substrate and the lowest for the CASTING substrate. This may be related to the adhesion of the films to the substrate and its roughness.

REFERENCES

1. Ziebowicz A. *et al*., Materials 14:1079, 2021
2. Roy M. *et al*., Adv. Colloids and Surfaces B. Biointerfaces. 156:194-202, 2017

Skeletal anchored palatal expanders: primary stability analysis of three different configurations

Matteo Schiaffino[1], Marco Migliorati[1], Alberto Lagazzo[2], Fabrizio Barberis[2]

[1]Orthodontics Department, Genoa University School of Dentistry, Genoa, Italy
[2]Department of Civil, Chemical and Environmental Engineering (DICCA), Genoa University, Genoa, Italy
* matteo.schiaffino@gmail.com

INTRODUCTION

The treatment of young adults and adults with transverse skeletal deficits of the upper jaw, in which skeletal maturation is too advanced to use tooth-borne solutions, is represented by miniscrew assisted rapid palatal expansion (MARPE). However, since this is an innovation of recent development, the scientific evidence to support it is not yet sufficient and there are many configurations and variables to be taken into account[1]: type of mini screw (shape and size), choice of insertion site of the mini screws and their inclination[2], number of mini screws (2 or 4), connections to the expansion screw and type of expansion screw used to make the expander (figure 1).

The purpose of this study is to analyze some of these variables by measuring the primary stability of three different configurations of skeletal anchored expanders, through an ex vivo investigation.

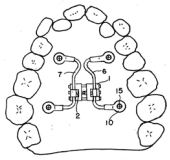

Figure 1: Basic elements of MARPE: 1-2: expansion screw; 7-6: miniscrew-expander connection arms; 15: miniscrew.

EXPERIMENTAL METHODS

The study focused on the comparison of three configurations: 4 TADs and 1 expansion screw (1), 4 TADs and 2 expansion screws (2), and 2 TADs and 1 expansion screw (3). Configuration number 2, having two expansion screws in an asymmetrical position, was tested on both side A and side B. The devices were tested on pork ribs stored at -19°C and thawed 24 hours prior to testing.

The miniscrews OrthoEasy®Pal (8 x 1.7 mm) were inserted by an experienced operator after which CBCT and scanbody scanning was taken.

The application of the expansion devices was performed by the same operator (2 step protocol).

Through the use of a DMA equipment, the primary stability of the devices was carried out by measuring the force through trasducer and the displacement through a laser vibrometer[3]. The test was performed at a frequency range set from 2 to 100 Hz in 1 Hz steps, while the proportionality constant of the laser was set at 80 micron/V displacement. The length of the connection arms was made with a digital gauge.

Finally, cortical thickness and bone density were measured with Horos Mobile Software®.

RESULTS AND DISCUSSION

The results showed higher stability (lower values) in configuration 1, with a lower average distance between the axis of the TAD and the axis of the expansion screw (5.8 mm). The least stable configuration (0. 85 µm/N) was 2B, with an average connection arms length of 9.4 mm, despite the bone into which it was inserted presented the greatest cortical thickness and medullary density[3].

	Primary stability (µm/N)	Average connection arms lenght (mm)	Cortical thickness (mm)	Medullary density (HU)
1	0,41	5,75	0,65	217
2	A)0,65 B)0,85	A) 8,10 B) 9,35	1,72	280
3	0,63	7,75	0,5	192

CONCLUSION

It is inferred that the primary stability is inversely proportional to the length of the device connection arms. This means that not only are the characteristics of the bone and mini screws important, but the connecting elements can also play a primary role in the success of a palatal expansion.

REFERENCES

1. Walter A. et al., Design characteristics, primary stability and risk of fracture of orthodontic mini-implants: pilot scan electron microscope and mechanical studies. Med Oral Patol Oral Cir Bucal. vol 18(5), 804-10, 2013
2. Lee H.K. et al., Stress distribution and displacement by different bone-borne palatal expanders with micro implants: a three-dimensional finite-element analysis. European Journal of Orthodontics. 531–540, 2014
3. Migliorati M. et al., Orthodontic miniscrews: an experimental campaign on primary stability and bone properties. European Journal of Orthodontics. 1–8, 2014.

Tridimensional In Vitro Models for Dental Implant Research: A Systematic Review

Authors: Ghannaa Shayya*, C. Benedetti, L. Chagot, ML Stachowicz, O. Chassande, H. De Oliveira, R. Siadous, S. Catros[1]

1- Inserm BioTis, Laboratory for the Bioengineering of Tissues, University of Bordeaux, 146 Rue Léo Saignat, 33000 Bordeaux, France

* ghannaashayya@gmail.com

INTRODUCTION

Dental implants have been clinically used for almost five decades with high success rates. Those implant systems became a standard care methodology, enabling the rehabilitation of the maxillofacial and oral area. Regarding dental implants it was suggested that there are more than 1300 different types of implants in the market with different materials, shapes, connection interfaces, dimensions, and surface characteristics. This enormous number deserves great scientific attention in order to optimize research models that efficiently characterize various implants' parameters. On the other hand, the major clinical issue observed with dental implants is the development of peri-implantitis, which is an infectious/inflammatory disease resulting ultimately in peri-implant bone resorption and implant loss. This requires the construction of specific study models to better understand the development of such disease and to evaluate novel therapeutic approaches.

In vitro research models currently available in implant dentistry are limited into 2D experiments which are reproducible and well adapted to evaluate a single parameter but do not reproduce the complexity of clinical settings. On the other hand, the in vivo research models using animals offer similar histological and anatomical features to humans, and tissue healing can be close to a clinical situation but those models are usually accompanied with ethical concerns and their outcomes could not be extrapolated to humans due to certain interspecies variabilities. This makes the development of a novel in vitro dental implant model of critical importance in order to combine the advantages of the in vitro and in vivo models currently available.

The aim of this systematic review of literature was to cover the in vitro tridimensional complex models available for research in implant dentistry.

EXPERIMENTAL METHODS

In order to accomplish the aim of the review, a comprehensive search of the literature present on Scopus and Pubmed databases was done using the key words «dental implant osseointegration in vitro » and « dental implant integration in vitro» and utilizing specific inclusion and exclusion criteria.

RESULTS AND DISCUSSION

We had finally included 24 articles in this review with a publication date range between 2005 and 2021. In those articles, the tridimensional models were designed to study the tissue-implant interface behavior in both bone and gingival soft tissue. The articles focused on simulating implant integration, evaluating the effect of different conditions on implant integration efficiency, or developing an infection model for implant integration process. The methods executed in those articles involved implant material, scaffolds, and cells organized in a specific 3D structure. The 3D models developed were able to simulate the process of dental implant osseo- and soft tissue- integration and to give results that are comparable with conventional in vitro and in vivo models. However, none of the considered articles did develop 3D in vitro models were an artificial living bone and gingiva were reconstructed and combined in a same platform, which would represent a more reliable and realistic model for dental implant evaluation

CONCLUSION

The number of articles covering novel in vitro models that mimic the implant integration is relatively limited which indicates that this is an emerging field highly dependent on the progress made in the field of biotechnology and tissue engineering and that further investigation is needed to enhance the reproducibility of the developed 3D models.

Comparison of Commercially Available Collagen-Based Membranes GTR/GBR

Federico Barrino[1*], Valentina Vassallo[1], Chiara Schiraldi[1] and Annalisa La Gatta[1]

[1]Department of Experimental Medicine, University of Campania "Luigi Vanvitelli", Via L. De Crecchio 7, 80138 Naples, Italy
[*] federico.barrino@unicampania.it

INTRODUCTION

Polymeric barrier membranes are widely used in reconstructive periodontal surgery to enhance periodontal/bone regeneration[1]. Both non-resorbable and resorbable membranes are available[2]. Collagen-based devices are the most widely used among the latter: they typically provide excellent biocompatibility while showing the same efficacy as non-resorbable products[3,4]. A huge number of collagen-based devices differing for collagen origin and processing/stability are currently on the market[5]. Several reports, investigating specific properties of some membranes, are available in the literature. However, a "whole" comparison of diverse types of collagen devices, considering all the biophysical and biochemical features potentially affecting *in vivo* performance, is still lacking. Availability of these data could support clinicians to optimize the use of these products also providing valuable information for the development of new highly performing similar devices. To this aim, here, we present a rather complete in vitro characterization of four type of collagen devices, highlighting similarities and differences in chemical structure, superficial morphology, porosity, swelling properties, stability in physiological medium and to collagenase.

EXPERIMENTAL METHODS

Membranes used: 1) Collagen from Achille tendon (Bioactiva®); 2) Collagen from cortical lamina (Bioactiva®); 3) Collagen from pericardium equine (Bioactiva®); 4) bilayer collagen membrane (Bio-Gide®). Samples swelling under physiological conditions (PBS, pH 7.4, 37°C) was analyzed by means of gravimetric measurements. Resistance to collagenase was evaluated by monitoring the mass loss and collagen solubilization (spectrophotometric measurements) during incubation with 4U/mL collagenase Membrane porosity was determined by a fluid replacement method using ethanol. Chemical analyses were carried out by Fourier transform infrared spectroscopy (FT-IR) and the scanning electron microscope (SEM) was employed to observe morphology of the surface. Biocompatibility test and analyses of specific biomarkers both at gene and protein level were performed on primary cells isolated from human bone seeded on the membranes for 7 days.

RESULTS AND DISCUSSION

Analysis of the FTIR spectra confirms the presence of the classic collagen peaks. The spectra of the Bioactiva® membranes are comparable, while the Bio-Gide® membrane shows additional peaks potentially due to various substances that are used to induce cross-linking within collagen membranes. All membranes rapidly absorbed water and reached equilibrium in PBS after 2 minutes. in particular, the pericadium membrane increased by ≅ 10 times the dry weight.

All membranes degraded in the presence of collagenase confirming resorbability. Samples 1 and 4 degraded faster than samples 2 and 3. The porosity result is different; each membrane has a different surface. These data are also confirmed by the SEM images. The pericardium has a very porous surface compared to the others. Bio-Gide® shows a different double layer. The biological tests proved that all the membranes sustained the cells growth and the expression of specific bone phenotype biomarkers. In this context, the membrane 1 and the membrane 4 resulted the most performant.

CONCLUSION

In conclusion, collagen-based materials are better than synthetics or non-resorbables. Data collected up to now highlight differences among the membranes mainly in term of structure.

In particular, the membrane 3 exhibits the highest water sorption and the membrane 2 the greater stability. Based on the porosity and SEM analyses, the product 4 is expected as the one most occlusive to cells. From the first analyses, the pericardial collagen membrane was found to be the best clinical choice. Finally, the biological data showed that none of tested membranes was cytotoxic. Membranes improved the expression of bone biomarkers thus suggesting a biochemical effect in bone regeneration beside the role as barrier membranes.

KEY WORDS

Membranes; collagen; bone and tissue regeneration.

REFERENCES

1. Florjanski W. *et al*., Polymers, 11(5), 782, 2019
2. Bottino MC. *et al*., Dental materials. 28.7:703-721, 2012
3. Steigmann L. *et al*., Biomedicines. 8(12), 636, 2020
4. Spinell T. *et al*., Dental Materials. 35(7), 963-969, 2019
5. Li ST. *et al*., Science, Technology, Innovation. 1-5, 2015

Preclinical evaluation of an injectable composite material for sinus lift, including implant placement

Sylvain Catros[1,2*], Mathilde Fénelon[1,2], Sandrine Auget[3], Jean-Christophe Fricain[1,2], Laurent Bidault[3], Joëlle Amédée[1], Didier Letourneur[3,4]

[1]Inserm U1026, University of Bordeaux, Tissue Bioengineering, U1026, F-33076 Bordeaux, France
[2] CHU Bordeaux, Oral Surgery Department, F-33076 Bordeaux, France
[3]SILTISS SA, Zac de la Nau, F-19240 Saint-Viance, France France
[4]Inserm U1148, LVTS, X. Bichat Hospital, University Paris Diderot F-75018 Paris & Institut Galilée, University Paris13, 93430 Villetaneuse, France

[*] sylvain.catros@u-bordeaux.fr

INTRODUCTION

Insufficient bone height in the posterior maxilla following teeth extraction is a frequent situation in implant dentistry. Pre-implant surgery is thus indicated and specific biomaterials are needed. Current reference biomaterials in this indication are mostly particles of bovine origin, with several limitations and side effects.
A novel synthetic material was developed using pullulan-dextran and hydroxyapatite and it was designed to be injectable. It is also radiolucent and becomes radio-opaque when mineralization occurs [1].
The aim of this preclinical study was to evaluate dental implant stability and osseointegration in the sinus lift model in the sheep, after filling the maxillary sinus defect by a novel bone substitute, using a delayed implantation procedure.

EXPERIMENTAL METHODS

The test material was a composite injectable material, made of pullulan-dextran and hydroxyapatite (Glycobone®, Siltiss, France). The control material was BioOss® (Geistlich). Anthogyr® dental implants were used. We have used the sinus lift model in the sheep (lateral window). The surgeries were conducted under general anesthesia, using an extraoral approach. During the first surgery, six sheeps were submitted to a bilateral sinus lift augmentation, using the test or the control article; after filling the subantral space, no membrane was placed and the tissues were sutured in 2 layers. After 6 months healing, one dental implant (Anthogyr®) was inserted into each grafted area (Second surgical procedure). 3 months later, euthanasia of all animals was done and the samples were collected for subsequent analyses. The characterization methods included implant torque of insertion, implant stability quotient (ISQ,Ostell®), microscanner and histomorphometric observations.

RESULTS AND DISCUSSION

All animals survived the different surgical procedures and no local or general surgical complications occurred. During implant placement in the regenerated area, the insertion torque was 44 N/cm-1 in the test group and 46 N/cm-1 in the control group; the ISQ was 74 for the test group and 73 for control group after implant placement.

At the end of experiment, the ISQ reached 78 in the test group and 77 in the control group. Qualitative histological analyses revealed a slightly higher mucosa inflammation in test samples. Micro-scanner and histological analyses have shown that Total Mineralized Area (TMA) and Bone-to-implant contact (BIC) were similar in both groups.

The novel composite injectable material Glycobone® was as least as efficient as the control material (BioOss®) in the sinus lift model in the sheep. The test material led to a similar bone formation around dental implants using a delayed approach for sinus grafting and implant placement.

CONCLUSION

Further experiments will include a clinical study where the Glycobone® will be used for sinus lift. The material possesses interesting handling properties compared to existing particles biomaterials and its radio opacity increases with time, thus providing an efficient tool to follow bone formation.

REFERENCES

1: Fricain et al Dent Mater. 2018 Jul;34(7):1024-1035.

ACKNOWLEDGMENTS

The authors acknowledge Anthogyr® company for providing dental implants. The study was founded by Siltiss® and the in vivo experiments were conducted at Namsa®, France.

Effect of pH on Fluoride Release from Dental Glass Ionomer Cements

Torbjørn Knarvang, Jan T. Samuelsen, Else Morisbak and Morten Syverud.

Nordic Institute of Dental Materials, Oslo, Norway
tok@niom.no

INTRODUCTION

Glass Ionomer Cements (GICs) are widely used materials in restorative dentistry. All GICs contain a basic glass and an acidic polymer liquid which set by an acid-base reaction. Although the composition may vary, all GICs contain calcium-aluminiumfluorosilicate, water, polycarboxylic acid and tartaric acid[1]. Glass ionomer sealants prevent caries through a steady fluoride release over a prolonged period. Fluoride release is considered one of the important advantages of glass-ionomer cements.

We have previously shown that release of elements like Sr, Si and Al from GICs depend strongly on pH. The purpose of the current study was to compare the effect of pH on fluoride release from commonly used GICs.

EXPERIMENTAL METHODS

Five commonly used GIC were tested. Specimens of GIC materials (areal 2.4 cm^2) were made in "Teflon" molds and cured according to the manufacturer instruction. The specimens were stored in a dark humidification chamber at 37 ºC for 24 h before they were soaked in 2.4 ml TRIS-buffer with varying pH (1M, pH = 4, 6 and 7), and stored at 37 ºC for 7 days. The extracts were transferred to new tubes and stored at 4 ºC until ion determination.

Al, Si and Sr were analyzed by ICP-OES at Sheffield Analytical Services.UK

Fluoride concentrations were analyzed by using a fluoride ion selective electrode (ISE). Release of fluoride in acidic conditions occurs with complexation. Fluor must be found as free fluoride ions and for that reason TISAB buffer (Total Ionic Solubility Adjustment Buffer) is added. The mission of TISAB is to complex bound ions like Fe^{3+}, Al^{3+} that may interfere on the measurement. This condition is fulfilled if the pH of the samples is higher than 5.2

RESULTS AND DISCUSSION

The release of Al, Sr and Si increased with increasing acidity (up to 5-fold increase from pH = 7 to pH = 4; total > 300 µg/cm^2 at pH = 4), as our previous studies have shown. Leakage of fluoride from GIC was seen in a similar pattern. Fluoride release in buffer at pH = 4 were up to 3-fold higher than at pH = 7. The highest fluoride release was 45µg/cm^2

CONCLUSION

The current study showed that the release of several elements, including fluoride, increased strongly with moderate increase in acidity (pH = 7 - 4). Beverages like fruit juices and soft drinks normally range from a pH = 2.5 - 4.5[2]. Hence, the rate of the fluoride release and possibly GIC degradation is likely to depend on food and drinking habits.

REFERENCES

1. Acidity and titrable acidity of different soft drinks and beverages in Norway. Mariann A. Birkeland, Catrine B. Andreassen, Zouhir E. Allouni and Nils R. Gjerdet, Nor Tannlegeforen Tid. 2011; 121: 700-4.
2. A Review of Glass-Ionomer Cements for Clinical Dentistry. Sharanbir K. Sidhu and John W. Nicholson, J Funct Biomater. 2016; 7(3)

Glass-ceramics with zirconia in silica matrix: the effect of the concentration and microstructure

Le Fu[1], Håkan Engqvist[2], Wei Xia[2*]

[1]School of Materials Science and Engineering, Central South University, Changsha, China
[2]Department of Materials Science and Engineering, Uppsala University, Uppsala, Sweden
[*] wei.xia@angstrom.uu.se

The abstract may not contain more than 5000 characters (including spaces) and does not exceed the two columns of one page.

INTRODUCTION

It's always a challenge of developing better materials to replace our damaged teeth, which are the strongest tissue in our body. Glass ceramic (GC) material is one of the dominant materials which have been used for dental restoration, i.e. crown and bridge.[1] One of the well-known glass-ceramics is lithium disilicate based GC, which has balanced strength and translucency, but the strength should be improved.[1-2] Zirconia based full ceramics have better flexural strength and toughness, but the translucency is not good, or has no translucency.[1-2] The question is if we can find a material that could combine the translucency of GC and the strength of zirconia ceramics. Our previous study has shown a new GC with zirconia in silica matrix, which has a good translucency and very high flexural strength and roughness.[3-4] It seems a good combination of GC and ceramics for dental applications. In this study, we tried to find the effect of zirconia concentration and microstructure on the appearance and aiming mechanical strength.

EXPERIMENTAL METHODS

The GC raw powders were synthesized by a sol-gel process. The chemicals were purchased from sigma without any purification. Yttrium was added in high concentrations of zirconia in the silica matrix. All GC samples have been sintered by SPS. The crystal phase was analyzed by XRD. The flexural strength was analyzed by a universal mechanical tester. The toughness was tested by the indentation method. The translucency was analyzed via a UV-Vis device. SEM was used to observe the surface and cross-section. The microstructure was done by TEM. A TEM tomography was done to study its 3D structure. APT (Atomic probe tomography) was used to analyze the chemical compositions and atomic structure at a 3D level.

RESULTS AND DISCUSSION

The content of zirconia in the silica matrix was studied. It was varied from 30% to 80% in molar ratio. We could see that the flexural strength and roughness of the GCs could be enhanced when the zirconia content increased, but not always. The results showed 65% of zirconia gave the highest values. When the content of zirconia was higher than 65%, the monoclinic phase formed, therefore the Y has been added to stabilize the tetragonal phase of zirconia, but did not help the strength significantly. The translucency of GCs was good, and increased when the zirconia content decreased. The growth of zirconia crystal size and the phase compositions have been studied when the zirconia content and the heat treatment changed. The phase transformation is size-driven since it's in nanoscale. 3D TEM tomography showed zirconia nanocrystals aligned in a certain area and formed nanofibers on a 3D scale. APT analysis reveals the distribution of yttrium and the chemical composition of the zirconia/silica heterophase interface in the Y doped GCs. A special core−shell structure, with a thin Zr/Si interfacial layer as a shell and a ZrO2 solid solution as a core, was confirmed.

CONCLUSION

The zirconia concentration and the microstructure of the zirconia/silica GCs determine the translucency and mechanical strength. There is a threshold of zirconia concentration regarding the mechanical strength. The regionally ordered structure contributes to the excellent combination of translucency and flexural strength of the GCs.

REFERENCES

1. Fu L. et al, Materials, 13: 1049, 2020
2. Zarone F. et al, BMC Oral Health, 19: 134, 2019
3. Fu, L. et al, J. Eur. Ceram. Soc., 37: 4067–4081, 2017
4. Fu, L. et al, J. Eur. Ceram. Soc. 36: 3487–3494, 2016

ACKNOWLEDGMENTS

The authors would like to thank Swedish Research Council (VR, 2020-04341), STINT (CTS 21: 1704), and National Natural Science Foundation of China (52102084) for providing financial support to this project.

Development of a personalised 3D bioconstruct for oral maxillofacial critical bone defect application

Ana Catarina Costa [1,2,3], Patrícia Mafalda Alves[1,2,4], Cristina Barrias[1,2,5], Fernando Jorge Monteiro[1,2,3], Christiane Salgado[1,2]

[1]Instituto de Investigação e Inovação em Saúde (i3S), Universidade do Porto, Porto, Portugal
[2]Instituto Nacional de Engenharia Biomédica (INEB), Porto, Portugal
[3]Faculdade de Engenharia, Universidade do Porto, Porto, Portugal
[4]Faculdade de Medicina dentária, Universidade do Porto, Porto, Portugal
[5]Instituto de Ciências Biomédicas Abel Salazar (ICBAS), Universidade do Porto, Porto, Portugal
*csalgado@ineb.up.pt

INTRODUCTION

There is an increase in oral cavity cancer that can lead to surgery requiring restoration of large defects in ca. 300,000 new cases/year [1] and the bone invasion rate can reach 58% [2]. Tumour removal will be generate critical bone defects and promoting major problems to patients, causing dysfunctionalities, affecting speech articulation and oral competences (i.e., mastication, swallowing, breathing) [3]. The gold standard surgical treatment for reconstructing segmental bone defects remains the use of bone autografts, but increased the patient morbidity (second surgery). But, in the first year, the failure rate of the grafts (over 5 cm) could reach 75% [4]. Commercially available products have a lack of the complex bone structure (architecture and porosity) resulting in biomechanically inferior bone tissue repair. The association of novel biomaterials and cell-therapies in tissue engineering strategies could offer new strategies to promote osteo-mucosa healing. This work had focused on the development of an osteoinductive hydrogel loaded with human dental MSC (single cells or spheroids) and injected within a 3D composite construct.

EXPERIMENTAL METHODS

Human dental follicle MSC (hDFMSC) were isolated from dental follicles (Ethical approval: 50/CEUP/2018) To produce spheroids, ell suspensions were loaded into non-adhesive hydrogel micro-moulds and allowed to settle [5]. Spheroids were collected after 1, 3, 7 and 10 days and characterized at different levels: spheroid size/compaction, cell metabolic activity/viability/organization, MSC osteogenic differentiation, ECM immunostaining (osteopontin - OPN).

The OPN solution (100 µg/mL) and fibrinogen solution (20 mg/mL) was mixed to the thrombin/$CaCl_2$ solutions (final rate: Fb/OPN/Tb – 5/0.01/2). Spheroids and single cells (hDFMSC) were suspended with the fibrionogen/OPN at $5x10^5$ cells and mixed with Tb/$CaCl_2$ solution and injected within the Coll/nanoHA scaffold. The gelation process was finished at 37ºC for 30 minutes. Dental MSCs single cells/spheroids ability to differentiate into osteoblastic lineage was evaluated (ALP activity, qPCR and ECM mineralization). The different hydrogels were characterized by rheometer and after injected within the scaffold (DMA).

CBA nude mice received 3 subcutaneous implants (Scaffold+gel+single cells, scaffold+gel+spheroids and scaffold+gel) as described before [7]. Bioluminescence imaging of luciferase-expressing dFMSCs allowed longitudinal cell tracking (IVIS Lumina) from 1 to 15 days (every 3 days). Animals were euthanized after 28 days and processed for histology and immunostaining.

RESULTS AND DISCUSSION

The incorporation of fibrin a modified hydrogel with a Coll/nanoHA scaffold biomaterial showed an improvement in the final mechanical strength and but improved the final mechanical strength, maintaining its elasticity of the graft. Fibrin gel is a versatile biomaterial extensity applied for bone tissue repair due to network structure, mechanical properties, and stability. Mechanically, the OPN incorporation within the 3D composite scaffold did not negatively affect the strength, but improved the osteogenic differentiation with time culture, increase their capacity in producing new bone ECM. The mice model of subcutaneous implants for ectopic bone formation allowed the evaluation of transplanted hDFMSCs in terms of proliferation and migration. After 4-week the single cell-loaded scaffold enhanced animal tissue ingrowth and angiogenesis. Importantly enough, newly formed extra cellular matrix stained for human OPN and a bone tissue-like structure with calcium deposition was also observed (Alizarin red). hDFMSCs were observed the periphery of the scaffold. Although, spheroids were found agglomerated within the implant. The animal tissue ingrowth was progressively decreasing from the scaffold's periphery toward the center.

CONCLUSION

This 3D bioconstruct provided the necessary pro-regenerative effect to modulate the biological response and could precisely fit the bone defect with fine-tuned adjustment to the surrounding original structure and promote the oral osteo-mucosa tissue regeneration.

REFERENCES

1. https://www.who.int/news-room/fact-sheets/detail/oral-health
2. McGregor AD, *et al*. Head Neck Surg, 10:294-301, 1988.
3. Rodriguez ED, *et al*. Plast Reconstr Surg, 120103S–117S, 2007.
4. Pogrel MA, *et al*. Journal of Oral and Maxillofacial Surgery, 55:1200 – 1206, 2016.
5. Bauman E, *et al*. Scientific Reports 8: 230, 2018.
6. Rodrigues SC, *et al*. J. Biomed. Mater. Res. Part A 101:1080–1094, 2013.
7. Salgado CL, *et al*. Front. Bioeng. Biotechnol. 8:724, 2020.

ACKNOWLEDGMENTS

The authors would like to thank the FCT/MCTES for CS's contract as Assistant researcher (CEECINST/00091/2018/CP1500/CT0019).

Effect of Irradiation Distance on Flexural Strength, Dentin Bond Strength, and Degree of Conversion of Resin Composites Polymerized with High-irradiance Light Curing Units

Sun-Young Kim[1*], Hyun Ju Kim[2], Soram Oh[3]

[1]Department of Conservative Dentistry, Seoul National University, Seoul, Korea
[2]Department of Periodontics, Seoul National University Dental Hospital, Seoul, Korea
[3]Department of Conservative Dentistry, Kyung Hee University, Seoul, Korea
[*]denkim@snu.ac.kr

INTRODUCTION

The dental resin composites have excellent esthetic and mechanical properties because they have a tooth-like color and are similar or superior to the strength of dentin or enamel[1, 2]. The optimal conversion of monomers into polymers initiated by light curing is essential to imbue an adequate clinical performance to resin composites.[3, 4] The purpose of the present study is to investigate the effect of increased irradiation distance on the flexural strength (FS), dentin micro-shear bond strength (μSBS), and the degree of conversion (DC) of bulk fill flowable, conventional flowable, and packable resin composites.

EXPERIMENTAL METHODS

The dental resin composites tested were Surefil® SDR™ (SDR), Filtek Z350 XT Flowable Restorative A2 shade (Z3F), and Filtek Z350 XT Universal Restorative A2 shade (Z3P). The light curing unit used in this study was Elipar DeepCure-L (tip diameter 10 mm) with 1470mW/cm^2 according to the manufacturer's data.

For the FS test, bar-shaped specimens were prepared using a custom-made silicon mold (8 mm ξ 2 mm ξ 2 mm). The mold was filled with resin composites, covered with a polyester strip, and gently pressed using a glass slide to remove excess material. Samples were light cured at four different curing distances (0, 2, 4, and 8 mm) from the sample's top surface (n = 15). Specimens were subjected to three-point bending tests. The load cell was 2 kN, and the distance between the two supporting rods was 5 mm. The load was applied at the center of each specimen's top surface using a third rod (2 mm diameter) until fracture was recorded.

For μSBS test, the flattened occlusal dentin was etched with 32% phosphoric acid for 15 s and rinsed. After blot drying the etched surface of the occlusal dentin, dental adhesives were applied and light-cured for 10 s. A cylinder-shaped resin composite prepared by filling a polyethylene tube (0.8 mm in diameter and 2 mm high) with the resin composite was attached to the adhesive-applied dentin surface. The samples were light-cured for 20 s at four different irradiation distances (0, 2, 4, and 8 mm) from the samples' top surface (n = 15). The bonded-tooth samples were mounted to a universal testing machine allowing a force vector to be parallel to the bonded surface. A stainless-steel orthodontic wire with a 0.2 mm diameter was used to apply the shear force to the bonding interface of the sample. The fracture load was recorded and divided by the area of the bonded surface (0.4 mm ξ 0.4 mm ξ π) to calculate the μSBS.

DC was measured by using Raman spectroscopy on the top and bottom surfaces of disk specimens (2-mm thick) (n = 3). For further investigation on whether extended irradiation times could restore the values for reduced irradiance, additional Z3P specimens were prepared, light-cured at 8-mm distances for 40 s and 60 s, and tested for FS, μSBS, and Raman spectroscopy. Statistical analyses were performed by two-way and one-way ANOVA.

RESULTS AND DISCUSSION

Both the FS and DC of Z3P cured at an 8-mm distance were significantly lower than those cured at 0, 2, 4 mm distances ($p < 0.05$), while the FS and DC of Z3F and SDR were not significantly influenced by increased distance. The μSBSs of the three resin composites were reduced by increased irradiation distance. The FS, μSBS, and DC values of Z3P light-cured at 8 mm for 40 s were comparable to the FS, μSBS, and DC values of Z3P cured at 0 mm for 20 s.

According to these overall results, our null hypothesis that there would be no significant difference in DC, FS, and dentin bond strength according to increased irradiation distance was rejected. Our results show that increased irradiation distances can have a significant effect on the FS, DC, and dentin bond strength of resin composites even with high-irradiance LCUs.

CONCLUSION

Increasing irradiation distance to 8 mm can have a negative influence on mechanical performances including the FS, DC, and dentin μSBS of resin composites polymerized with high-irradiance light curing units. Therefore, even with the use of a high-irradiance LCU, compensatory extended irradiation times beyond the manufacturer's recommendation are suggested in cases involving the restorations of long irradiation distance such as deep proximal boxes or the pulpal walls of root canal–treated teeth.

REFERENCES

1. Lempel E. et al. Dent Mater. 35:1308-18, 2019.
2. Rasines Alcaraz MG et al., Cochrane Database Syst Rev. 3:CD005620, 2014
3. El-Askary FS et al., Am J Dent. 25:97-102, 2012
4. Finan L et al., Dent Mater. 29:906-12, 2-13, 2013

ACKNOWLEDGMENTS

"The authors would like to thank the National Research Foundation of Korea, (Grant no: NRF-2018R1A5A2024418, and NRF-2020R1A2C1007725) for providing financial support to this project".

First Principles Modelling of Enamel Erosion and Remineralisation

Palwinder Kaur[1*], Helen Chappell[2], Maisoon Al-Jawad[1]

[1]School of Dentistry, University of Leeds, Leeds, UK
[2]School of Food Science and Nutrition, University of Leeds, Leeds, LS2 9JT, UK
[*]dnpka@leeds.ac.uk

INTRODUCTION

Erosion of dental enamel is becoming a significant problem, affecting ~30% of adults in Europe and most school pupils[1]. Dental erosion is a multifactorial condition characterised by progressive loss of hard dental tissue without bacterial involvement. The current treatment for enamel erosion is conventional dental restorations, which lacks the tooth's biological and mechanical properties and requires further interventions in the future.

Several experimental studies have been conducted to understand the mechanism behind enamel erosion, and efforts have been made to restore these defects[2]. However, experimental data from these studies are limited in providing detailed elemental information about the demineralised and remineralised enamel. For this reason, theoretical methods have become an essential part of hydroxyapatite and mineral studies. First-principles modelling has the advantage of being able to highlight the effects of a specific ionic species introduced into the lattice structure. The information obtained from the computational modelling regarding the crystallographic characterisation of normal and diseased enamel will be crucial for understanding the microstructure of erosion lesions and the mechanisms of remineralisation. This will lead to tailoring of treatment options for enamel erosion and better management of enamel surface loss.

EXPERIMENTAL METHODS

We employed the first principles Density Functional Theory (DFT) plane-wave code, CASTEP, to carry out structural optimizations of enamel. The starting structure of hydroxyapatite (HA) was based on the formula $Ca_{10}(PO_4)_6(OH)_2$, obtained from Wilson *et al*[3]. This structure was used to create a geometry optimized two-unit cell model. A convergence tested cut-off energy of 800 eV, and a k-point spacing of 0.09 eV $atom^{-1}$ were employed. Substitutions at PO_4^{3-} and Ca^{2+} were made to produce a realistic enamel composition of $Ca_{19}Na(PO_4)_{11}CO_3(OH)_4$.Further elemental substitutions including Sr^{2+} and F^- were then made to assess the thermodynamic stability of these structures.

RESULTS AND DISCUSSION

To study the type-B (PO_4^{3-} substitution by a CO_3^{2-} group and one M^+ ion), a series of calculation were conducted with a two-unit cell HA structure. All combinations of Na+ at all Ca^{2+} sites were studied. In the most favourable defect structure (Figure 1), we observed that the substitutional carbonate and monovalent (Na+) ion were located closely together.

The structure became less energetically stable when their separation within the unit cell was increased. (Figure 2).

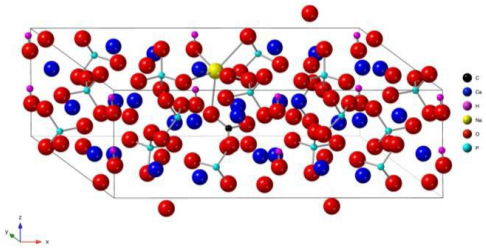

Figure 1. Lowest energy hydroxyapatite structure with B-type carbonate defect, created by replacing a PO_4^{3-} group by a CO_3^{2-} group and one Ca^{2+} ion by a proximate Na^+ ion.

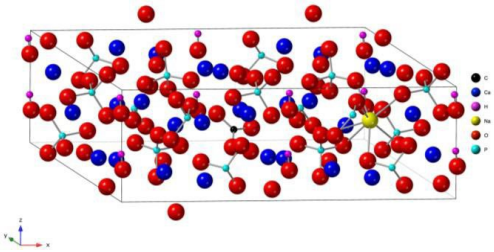

Figure 2. Least stable energy hydroxyapatite structure with B-type carbonate defect, created by replacing a PO_4^{3-} group by a CO_3^{2-} group and one Ca^{2+} ion by a Na^+ ion at a distance.

CONCLUSION

In this study, we employed first principles methods to study the effect of substituting different ions in the HA lattice. The presence of additional ions in tooth enamel is thought to cause a reduction in crystallinity and increase the dissolution of enamel. Our future work involves calculations of different HA structural defects and translating the findings into the laboratory to obtain a demineralisation and remineralisation model.

REFERENCES

1. Skalsky J. *et al.,* J. European Academy of Paediatric Dentistry. 9:23-31, 2018.
2. Behroozibakhsh M. *et al.,* Scientific reports. 5, 15194, 2015
3. Wilson R. *et al.,* American Mineralogist. 84:1406-1414,1999.

ACKNOWLEDGMENTS

This project is funded by a UKRI EPSRC Industrial CASE award in partnership with GlaxoSmithKline (Studentship: 2603494).

Development and characterisation of Ca-doped coatings for dental implants to optimise the initial bone regeneration processes

Iñaki García-Arnáez[1], Francisco Romero-Gavilán[2], Andreia Cerqueira[2], Félix Elortza[3], Mikel Azkargorta[3], Julio Suay[2*], Mariló Gurruchaga[1], Isabel Goñi[1]

[1]Faculty of Chemistry, University of the Basque Country (UPV/EHU), Donostia, Spain
[2]Department of Industrial Engineering Systems and Design, Universitat Jaume I, Castellón, Spain
[3]Proteomics Platform, CicBiogune, Derio, Spain
[*] suay@uji.es

INTRODUCTION

Calcium is an element commonly used in the field of bone tissue engineering for the development of biomaterials due to its functions related to bone metabolism and the coagulation process. The presence of Ca ions conditions the tissue/material interface, affecting protein deposition in the biomaterial and cellular responses.

Development of new biomaterials is a complex process. Unfortunately, the poor correlation between *in vitro* and *in vivo* experimentations complicates the design of such biomaterials. For this reason, new characterization methodologies are needed.

Thus, this work aims to understand, through different proteomic studies, the effect of Ca onto doped biomaterials and to verify the *in vitro-in vivo* correlation.

EXPERIMENTAL METHODS

The acid catalysis sol-gel route was employed to synthetize the different coatings, from the combination of MTMOS and TEOS alkoxysilane precursors. This material was functionalized with 0.5, 1, 2.5 and 5%wt $CaCl_2$. Ti discs were coated with prepared materials by dip-coating. Physicochemical parameter as roughness, topography, wettability and the Ca^{2+} kinetic release were determined. *In vitro* was assessed with human osteoblast and TPH-1 monocytes macrophage cells. The *in vitro* proteomic assay was conducted by incubating the samples with human serum for 3 h and the *in vivo* proteomic assay was performed with a rabbit model. Finally, elutions were analyzed using LC- MS/MS.

RESULTS AND DISCUSSION

The sol-gel synthesis was performed correctly and the successful obtaining of coatings can be confirmed through chemical and morphological characterization. *In vitro* tests revealed an overexpression of both pro-inflammatory markers IL-1b and TNF-α on Ca-enriched coatings respect the base material on macrophage cells. Furthermore, the incorporation of Ca induced a decreased expression of osteogenic markers ALP and COL1 on osteoblasts. Ca-doped biomaterials displayed a remarkable increase on the attachment of coagulation-related proteins in the *in vitro* (PLMN, THRB, FIBA, VTNC) and *in vivo* (FBLN1, SERPING1) proteomic assays, as well as a higher affinity to proteins involved on inflammatory (C1QC, CO5, CARD6) and anti-osteogenic functions (FBN1, AHSG).

CONCLUSION

These new sol-gel materials able to release Ca^{2+} show interesting effects through *in vitro* and *in vivo* proteomic analysis, which were consistent with *in vitro* results. In addition, proteomics also revealed a higher adhesion of a cluster of proteins related to the coagulation system. These types of proteomic analyses show a good correlation between *in vitro* and *in vivo* experimentations. Moreover, together with *in vitro* tests, they have the potential to be useful for the development of new biomaterials.

ACKNOWLEDGMENTS

This work was supported by MICIU [RTC-2017-6147-1], MINECO [PID2020-113092RB-C21], University of the Basque Country under [MARSA21/07], and the Universitat Jaume I under [UJI-B2021-25]. The authors would like to thank the company GMI-Ilerimplant for producing the titanium discs.

Compositional Differences in *In-Vivo* Biofilm Formed on Bracket Materials: A Prospective Pilot Study

Jin Beom Kim[1*], Jung-Sub An[2], Sug-Joon Ahn[1]

[1]Department of Orthodontics, School of Dentistry, Seoul National University, Seoul, Republic of Korea
[2]Department of Orthodontics, Seoul National University Dental Hospital, Seoul, Republic of Korea
[*] gim3165@naver.com

INTRODUCTION

The common side effects of fixed orthodontic treatment are enamel demineralization and gingival inflammation, which is caused by the accumulation of pathogenic oral biofilm around the orthodontic appliances[1]. Differences in biofilm formation according to the bracket material was analyzed previously, but there was a limitation in mimicking the oral environment as it was performed in *in-vitro* condition[2]. The purpose of this study was to investigate the differences in the *in-vivo* biofilms formed on various bracket materials in the oral cavity.

EXPERIMENTAL METHODS

Intraoral appliances preparation

Plaster dental casts were fabricated from 10 healthy volunteers by taking alginate impressions. A customized intraoral appliance capable of inserting and removing bracket material specimens was fabricated using pressure molding ethylene vinyl acetate sheets (Bioplast, Scheu-Dental GmbH, Iserlohn, Germany) (**Figure 1**).

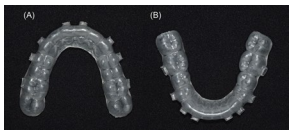

Figure 1. The customized maxillary **(A)** and mandibular **(B)** appliances used in this study.

In-vivo biofilm formation

Three widely used bracket materials were used in this study: metal (stainless steel), ceramic (monocrystalline alumina), and plastic (polycarbonate). The bracket specimens were prepared in a size similar to the commercial brackets (3 mm x 4 mm x 2 mm). The split-mouth design was used to mount the specimens to the specific labial slot of the intraoral appliances to simulate 8 tooth positions: maxillary central incisors, maxillary canines, maxillary first premolars, maxillary first molars, mandibular lateral incisors, mandibular canines, mandibular first premolars, and mandibular first molars (**Figure 1**).

Each participant was instructed to wear the appliance with specimens for 12 hours after toothbrushing at night. The specimen was removed from the appliance, transferred to a cornical tube, and washed using phosphate-buffered saline (pH 7.2). After the biofilms were detached from the specimen using sonication, the resulting cell suspension was subjected to DNA extraction. The experiment was independently repeated 20 times.

Microbial and surface analyses

The amounts of total bacteria, *Streptococcus mutans*, and *Porphyromonas gingivalis* was quantitatively analyzed using real-time polymerase chain reaction. A two-way analysis of variance was used to determine differences in bacterial adhesion to the specimens with respect to their position and material type. Scanning electronic microscopic (SEM) images were taken to analyze the surface morphology of each bracket material.

RESULTS AND DISCUSSION

The SEM images demonstrated that the ceramic has the most irregular surface, but the metal has the smoothest surface (**Figure 2**).

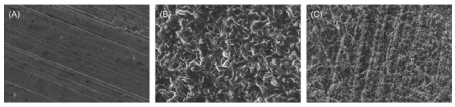

Figure 2. Scanning electronic microscopic images of bracket material surfaces (3000x magnification): **(A)** metal, **(B)** ceramic, and **(C)** plastic.

There was no significant difference in adhesion amount of total bacteria, *S. mutans*, and *P. gingivalis* among the different positions. The amounts of total bacteria and *P. gingivalis* adhesion were not significantly different among the materials, whereas *S. mutans* adhesion was higher to the ceramic than to the metal ($P < 0.05$), indicating the biofilm formed on the ceramic was more cariogenic than those formed on metal. The difference in *S. mutans* adhesion may be due to the difference in surface morphology and bacterial ecology. The rough surface of the ceramic is considered to create a suitable environment for adhesion of the early colonizer, such as *S. mutans* during the initial biofilm formation. However, *P. gingivalis*, which is an obligate anaerobe, is a late colorizer and is difficult to persist in an aerobic environment as in this experiment.

CONCLUSION

Considering higher adhesion of *S. mutans* to ceramic than to metal without significant difference in adhesion of total bacteria and *P. gingivalis* among materials, the results of the present study suggest that the biofilm formed on the ceramic bracket is more likely to be cariogenic than that on the metal bracket.

REFERENCES

1. Mylonopoulou IM. *et al*., Am. J. Orthod. Dentofacial. Orthop. 160:648-658, 2021
2. Papaioannou W. *et al*., Int. J. Dent. 2012:471380, 2012

ACKNOWLEDGMENTS

The authors would like to thank HUBIT (Anyang-si, Gyeonggi-do, Republic of Korea) for kindly providing their materials.

In vivo evaluation of 3D printed, degradable and defect specific composite scaffolds for maxillary bone defects

Paula Korn[1], Margarete Korn[2], Richard Richter[3], Corina Vater[3], Winnie Pradel[4], Martina Rauner[5] Anja Lode[3], Tilman Ahlfeld[3]

[1] Department of Oral and Maxillofacial Surgery, Charité - Universitätsmedizin Berlin, Corporate Member of Freie Universität Berlin, Humboldt-Universität zu Berlin, and Berlin Institute of Health, Berlin, Germany
[2] Faculty of Medicine, TU Dresden, Dresden, Germany
[3] Centre for Translational Bone, Joint and Soft Tissue Research, University Hospital Carl Gustav Carus and Faculty of Medicine, TU Dresden, Dresden, Germany
[4] Clinic for Oral and Maxillofacial Surgery, University Hospital Carl Gustav Carus and Faculty of Medicine, TU Dresden, Dresden, Germany
[5] Division of Endocrinology, Diabetes, and Bone Diseases, Department of Medicine III, University Hospital Carl Gustav Carus and Faculty of Medicine Faculty of Medicine, TU Dresden, Dresden, Germany

paula.korn@charite.de

INTRODUCTION

Maxillary bone defects often requiring augmentation procedures. The clinical standard are autologous bone grafts, nevertheless this might be associated with a donor site morbidity and there is a scientific need to search for alternatives (1,2). 3D Printing of defect specific bone grafts is one option, especially if there is an adequate scaffold resorption with ongoing healing time and support of local bone formation. Aim of the study is the development of a defect specific and biodegradable scaffold combining calcium phosphate cement (CPC) and bioactive mesoporous glass (MBG). Additionally *in situ* tissue engineering was planned to increase the osteogenesis within the defect.

EXPERIMENTAL METHODS

The scaffolds were printed using a strontium CPC paste with or without particles of MBG. They measured 3.3 mm in diameter, 0.48 mm in height and had macro pores with a 60° geometry. To enable *in situ* tissue engineering *in vivo* later, hypoxia conditioned medium (HCM) was produced *in vitro* due to cultivation of mesenchymal stroma cells (rMSC) at 1% oxygen. Afterwards some CPC/MBG scaffolds were loaded with HCM. All kind of scaffolds were characterized *in vitro* and biomechanically. Then an application into artificial maxillary defects in a rat model (n=48) followed for three experimental groups named CPC, CPC/MBG and CPC/MBG+HCM. After healing periods of 6 and 12 weeks *ex vivo* analysis in terms of microCT and histology were performed to quantify the remaining defect width and osteogenesis within the defect

RESULTS

The *in vitro* resulted revealed a homogenous proliferation of rMSC on the scaffold surface within 28 days, whereas especially for the CPC/MBG+HCM group a dense cellular network was detectable. Biomechanically an increase in Young´s modulus and compressive strength were measurable for these scaffolds, too. All groups exposed an ongoing bone formation within the healing time. After 6 weeks the results of bone formation with regard to the initial defect size were 6.3% (± 2.6%) for CPC, 9.1 % (± 2.7%) for CPC/MBG and 10.2 % (± 5.8%) for CPC/MBG+HCM. After 12 weeks a percentage of bone formation of 9.9 % (± 5,3) for CPC, 11.8 % (± 7.3) for CPC/MBG and 17.4 % (± 8.7%) for the composite of CPC/MBG+HCM. The microCT showed an increased degradation of scaffolds containing MBG compared to pure CPC.

CONCLUSION

The degradation of CPC scaffolds can be improved by combining it with MPG. Additionally, local bone formation in a maxillary critical size defect was increased if the scaffolds containing HCM to enable *in situ* tissue engineering. Clinically, these composite scaffolds might be a future alternative for autologous bone grafts as they were for example applied in alveolar cleft patients.

REFERENCES

[1]Korn P. *et al.,* Application of tissue-engineered bone grafts for alveolar cleft osteoplasty in a rodent model. Clin Oral Investig. 2017 Nov;21(8):2521-2534.
[2]Korn P. *et al.,* 3D Printing of Bone Grafts for Cleft Alveolar Osteoplasty- In vivo Evaluation in a Preclinical Model. M.Front Bioeng Biotechnol. 2020 Mar 25;8:217.

ACKNOWLEDGMENTS

The study was founded in terms of an AO Trauma Deutschland research grant for junior scientist.

Tuning the Physical Properties of Collagen/Hyaluronan Hydrogels to favor Mesenchymal Stem Cells Differentiation into NP Cells: A Step forwards Intervertebral Disc Regeneration

Antoine Frayssinet [1], Esther Potier [2], Gervaise Mosser [1], Christophe Hélary[1] *

1. Sorbonne University, CNRS, UMR 7574 – Chemistry of Condensed Matter Laboratory - F-75005 Paris, France
2. Université de Paris, CNRS – Hôpital Lariboisière - B3OA - F-75005 Paris, France

* christophe.helary@sorbonne-universite.fr

INTRODUCTION

Back pain is a major burden of the 21st century as 90% of the world population will be affected during their life time. In half of cases, this disease is associated with intervertebral disc (IVD) degeneration. The regular treatment is based on antipain treatment and physiotherapy. When the pain is too great, surgery is required (discectomy, spinal fusion). Novel strategies relying on stem cell injection have been tested. Unfortunately, the outcomes are disappointing because of cell leakage and incomplete differentiation. Nowadays, a consensus exists on the necessity to encapsulate stem cells within a hydrogel to maintain them in situ and favor their differentiation. As cell behavior depends on biochemical and physical environment, a biomimetic hydrogel would promote IVD regeneration. Nucleus Pulposus is a highly hydrated tissue working as hydraulic shock absorber. Glycosaminoglycans give a high degree of hydration whereas collagen II gives resistance and allows for cell adhesion. With the aim of developing novel biomimetic hydrogels, collagen/hyaluronic acid composites were developed to mimic the structure and the mechanical properties of Nucleus Pulposus. For this purpose, we first studied the impact of the HA content on the hydrogel physical properties. Then, the potential of the different formulations to differentiate mesenchymal stem cells (MSCs) into NP cells was analyzed in detail.

EXPERIMENTAL METHODS

HA functionalized with tyramine groups (HA-Tyr) was mixed with collagen and gelled using Horse Radish Peroxidase and H_2O_2 at pH 7.4. With a constant collagen concentration (0.4%), the HA-Tyr content was increased up to 2 % to create a platform of Collagen/HA-Tyr hydrogels with different properties. The hydrogel structure, the mechanical properties and the degree of hydration were analyzed. Mesenchymal stem cells were encapsulated within the different hydrogel types and cultivated over 28 days. The impact of MSCs on hydrogel stability, metabolic activity and cell morphology were analyzed. Last, the gene expression of Aggrecan, Collagen I and II was quantified by real time PCR.

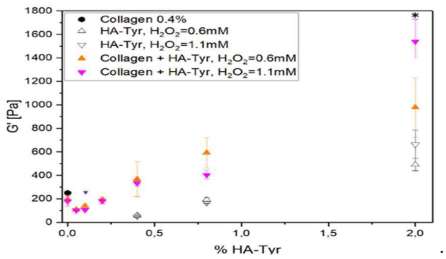

Figure 1: Mechanical properties of Collagen/HA-Tyr hydrogels evaluated by rheology.

RESULTS AND DISCUSSION

The physico-chemical study showed the impact of the HA-Tyr content on the hydrogel physical properties. At low HA-Tyr content (less than 0.4 %), the composite behaviour was driven by collagen. Hydrogels exhibited a fibrillary network and were characterized by low mechanical properties (Figure 1). From 0.8% HA-Tyr, the mechanical properties and the hydration degree increased to reach those of NP (G'= 1.5kPa) when 2% HA-Tyr and 1.1 mM H_2O_2 were added. Below 0.4% HA-Tyr, encapsulated cells contracted hydrogels after one week in culture (Figure 2). From 0.8%, hydrogels, MSCs did not contract hydrogels and their mechanical properties were stable over the time course of the experiment. With a high HA-Tyr content, cells did not proliferate, suggesting their commitment towards differentiation. At low content, MSCs spread and adopt a fibroblast like morphology (Figure 2). On the opposite, cells encapsulated within hydrogels at high HA-Tyr content were more rounded and resemble NP cells. The gene expression quantification showed that MSCs orientated towards a NP cell phenotype. When 2% HA-Tyr was used, cells highly expressed NP cells markers such as Aggrecan and Collagen II, and weakly expressed Collagen I. In contrast, cells encapsulated in hydrogels with a low HA-Tyr content weakly expressed these NP cell markers.

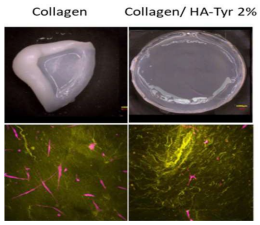

Figure2: Macroscopic view of hydrogels (top) and cell morphology (bottom) after 28 days in culture.

CONCLUSION

Taken together, these results show that Collagen/Hyaluronan Composite Hydrogels with a high HA-Tyr content (2%) mimic the physical properties of the Nucleus Pulposus and promote the differentiation of MSCs into NP cells. Hence, these hydrogels could be useful for IVD regeneration.

.

ACKNOWLEDGMENT: This research has been supported by Agence Nationale de la Recherche (ANR) - grant number: ANR-19-CE06-0028.

Vacuum induction casted MgZnCa alloy based biodegradable bone plate

Manisha Behera[1*], Rajashekhara Shabadi[1], Feng Hildebrand[2] Cosmin Gruescu[1] and David Balloy[1]

[1]UMR 8207-UMET-Unité Matériaux et Transformations, Université de Lille, Lille, France
[2]INSERM U1008- "Controlled Drug Delivery systems and Biomaterials", Faculté de Médecine, Université de Lille, Lille, France
* manisha.behera@univ-lille.fr

INTRODUCTION

Permanent implants have served as potential help in the field of orthopedics. But in case of metallic implants like stainless steel, titanium, etc., there is a large difference of elastic modulus from natural bone, leading to stress shielding effects[1] during bone healing. Furthermore, these implants require secondary clinical intervention for surgical removal of implant, irrespective of implant success or failure. The effectual solution to this challenge is the use of biodegradable implants. As bone is a load-bearing organ, metals are a suitable choice of implant material. Magnesium (Mg) will serve as a revolutionary implant material due to its high specific strength, similar elastic modulus to bone, excellent biocompatibility (as it is a part of bone mineral composition and is involved in various metabolic processes) and biodegradability. However, the rapid degradation of Mg in chlorine environment causes large release of ions which affects implant degradation with bone healing rate.[2]

This work depicts the usage of alloying with carefully chosen elements in order to control the biodegradability, advanced casting technique, and thermo-mechanical processing to overcome this challenge of Mg application in biomedical field. In this study, we have used Zinc (Zn) and Calcium (Ca) as our alloying elements with varied percentages. The vacuum induction melting technique was used to fabricate the alloys. The reasons behind are the limitations faced in conventional casting of Mg like gas entrapment, use of SF_6, non-uniform composition, etc.[3,4] This study establishes a correlation between alloying concentration, melting technique, microstructural evolution and corrosion behavior. All the above properties will play a significant role in serving our MgZnCa alloy as a better cytocompatible orthopedic implant than the existing bone implants.

EXPERIMENTAL METHODS

The optimized MgZnCa alloy was prepared by mixing the Mg (99.9 wt%), Mg-12%Zn master alloy and Mg-15%Ca master alloy in Vacuum induction melting (VIM) machine and by thermo-mechanical processing thin plates were obtained. The material fabrication and processing schematic is depicted in Figure 1. The material characterization techniques include EDS mapping for chemical composition, XRD for phase analysis, optical microscopy for microstructural studies, EDSB mapping for texture evolution, mechanical testing, electrochemical corrosion studies and degradation studies in SBF solution.

RESULTS AND DISCUSSION

The initial cross-sections of the cast ingots illustrate absence of gas porosity in the cast parts. This helped to carry out the further heat treatment and hot-rolling of the cast parts. Elemental analysis revealed uniform mixing of the alloy elements in the Mg matrix, which is quite unlikely in conventional casting process. As low melting point and high volatility of Zn can cause deviation in the alloy composition which usually happens in conventional casting. Pouring the molten liquid into appropriately heated mold along with vibration mode prevents non-equilibrium solidification of the melt and hence prevent formation of secondary phases (like precipitates). Absence of secondary phase was confirmed by EDS mapping and XRD analysis. Presence of secondary phases or precipitates can be a potential gateway for galvanic corrosion, where the secondary phases act as cathode and the α-Mg matrix act as anode. Corrosion potential of MgZnCa alloy by VIM is nobler than the pure Mg. Experimental results showed that the biodegradation of the optimized alloy in SBF solution has better degradation performance in comparison to as-cast Mg.

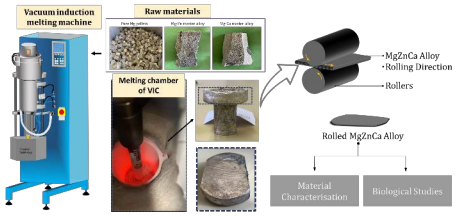

Figure1: Material fabrication and process schematic.

CONCLUSION

This work demonstrated the effect of using the advanced vacuum induction melting technique on the material performance of the Mg alloys. Additional thermo-mechanical processing of the MgZnCa alloy enhanced both mechanical and corrosion property of the system. This new alloy composition can then be tested for *in-vitro* biological studies for biological validation.

REFERENCES

1. Rafia, M.L. *et al*., J. Ortho.Research *39*(6), 1174-1183, 2020
2. Zeng R. *et al*., Adv. Engg. Mat. 8:3-14, 2008.
3. Luo A. A., J. Mag. Alloys 1:2-22, 2013.
4. Wang G. *et al*., Mat. Res. Express 7, 2020.

ACKNOWLEDGMENTS

Authors would like to acknowledge the help offered by Damien Creton during thermo-mechanical processing of the material. The authors would like to thank funding 'Magnesium based Nano Composites for Orthopedic Applications' MAGNACOM, project under the aegis of Programme for Early Stage Researchers in Lille 2020-2023

Platelet-derived Extracellular Vesicles Show Therapeutic Effects on a 3D Tendon Disease Model

Ana Luísa Graça[1,2], Rui M. A. Domingues[1,2], Isabel Calejo[1,2], Manuel Gómez-Florit[1,2] and Manuela E. Gomes[1,2]

[1]3B's Research Group, I3Bs – Research Institute on Biomaterials, Biodegradables and Biomimetics, University of Minho, Headquarters of the European Institute of Excellence on Tissue Engineering and Regenerative Medicine, AvePark, Parque de Ciência e Tecnologia, Zona Industrial da Gandra, 4805-017 Barco, Guimarães, Portugal;
[2]ICVS/3B's–PT Government Associate Laboratory, Braga/Guimarães, Portugal;

INTRODUCTION

Tendon diseases are common clinical problems that can dramatically affect the quality of life of individuals across the demographic spectrum. Current clinical approaches do not tackle the etiology of the disease, underlined by an unresolved inflammatory scenario that provokes hypercellularity, neovascularization, and a dysregulation of the critical balance between extracellular matrix (ECM) remodeling proteases and their inhibitors. In this regard, extracellular vesicles (EVs), a diverse group of nanosized membrane enclosed particles actively released by all types of cells with key roles in communication, are being considered as very attractive therapeutic agents to trigger repair/regenerative processes in injured tissues. Thus, herein, the therapeutic potential of EVs derived from platelets was evaluated using a pre-establish 3D tendon disease in vitro model.

EXPERIMENTAL METHODS

First, bioengineered tendon disease models consisting of Electrospun isotropic nanofibrous scaffolds coated with cell-laden hydrogels encapsulating human tendon-derived cells (hTDCs), were produced. Then, different platelet-derived EVs populations were isolated by differential centrifugation, added to hTDCs culture media, and their influence in cells phenotype and ECM remodeling was assessed over culture time.

RESULTS AND DISCUSSION

As expected, after 14 days of culture, a disease-like phenotype was observed in hTDCs of the miniaturized 3D tendon units. We verified that although EVs do not have a remarkable influence in hTDCs morphology, these are able to influence their biological response. Interestingly, the addition of EVs reestablish the expression of tendon related markers like MKX, SCX, and TNMD in diseased hTDCs and decreasing the expression of osteogenic and fibrotic markers. Moreover, EVs increased the expression of different ECM components such as COL31A and DCN, and the expression of MMP-3, important factors in the balance between the synthesis and degradation of tendon ECM. Moreover, the presence of EVs was found to modulate the inflammatory response, as demonstrated by an increase of anti-inflammatory mediators, like IL-4, which might contribute to blunt the inflammatory processes occurring in damaged tissue.

CONCLUSION

Overall, we showed that platelet-derived EVs have a positive influence on tendon cells cultured on a disease-like in vitro model, not only by increasing the expression of healthy tendon cells markers and promoting ECM remodeling, but also by increasing the expression of anti-inflammatory cytokines. The beneficial effects of these vesicles are worthy to be explored in further studies to provide more insights on how EVs interact with tendon cells, becoming a promising therapeutic tool for tendon injuries recovery.

ACKNOWLEDGMENTS

The authors acknowledge ERC CoG MagTendon grant agreement 772817; EC Twinning project Achilles 810850; FCT for PhD grant PD/59/2013 and PD/BD/135255/2017, Post-Doc grant SFRH/BPD/112459/2015, CEECIND/01375/2017 and 2020.03410.CEECIND.

Multifunctional Hyaluronic acid-based viscosupplementation devices with intrinsic anti-inflammatory properties

Mario di Gennaro[1,2], Francesca Della Sala[1], Gennaro Longobardo[1,4], Maurizio Pagliuca[3], Nicola Solimando[3], Luigi Ambrosio[1], Assunta Borzacchiello[1]

[1]Institute of Polymers, Composites and Biomaterials, National Research Council, (IPCB-CNR), Viale J.F. Kennedy 54, 80125 Naples, Italy
[2]Department of Environmental, Biological and Pharmaceutical Sciences and Technologies, University of Campania "L. Vanvitelli", 81100 Caserta, Italy
[3]Altergon Italia s.r.l, Zona Industriale ASI, Morra De Sanctis (AV), 83040 Italy
[4]Department of Chemical, Materials and Production Engineering, University of Naples "Federico II", 80125, Naples, Italy

*mariodigennaro5@gmail.com

INTRODUCTION

Synovial Fluid (SF) is responsible for functional properties of articular fluids, protecting joints by mechanical stress and lubricating cartilage. SF is altered as result of damage or diseases e.g. ostroarthritis, causing pain and loss of flexibility. The worsening of SF properties is associated to the reduction of hyaluronic acid (HA) molecular weight (MW). HA is a naturally occurring glycosaminoglycan, and the main macromolecular component of most connective tissues'ECM[1]. A common approach to restore SF viscoelastic properties consists in intra-articular injections of formulations containing HA (viscosupplementation)[2]. These HA-based devices are affected by low thermal stability, and by impossibility to be loaded with hydrophobic anti-inflammatory drugs e.g. Diclofenac Sodium (DF), that are used to manage symptomatic pain. DF is generally administrated orally, resulting in low drug absorption and systemic side effects. To overcome these drawbacks, in this work, multifuncional HA-based viscosupplementation devices with higher thermal stability, antioxidant and intrinsic anti-inflammatory properties and able to deliver locally anti-inflammatory drugs such as DF, were produced and characterized. To this aim HA was formulated with omega-3 and -6 fatty acids (FA) and α-tocopheryl acetate (VE). FA are polyunsaturated fatty acids naturally occurring in SF, commonly administrated orally in osteoarthritis management. VE is a lipophilic compound possessing high antioxidant properties that plays a fundamental biological role as a chain-breaking antioxidant for protecting cell membranes from oxidative damage.

EXPERIMENTAL METHODS

FA/VE emulsion was prepared by dissolving the components with Pluronic F-127 (PF-127) and Pluronic F-68 (PF-68), two amphiphilic FDA-approved polymers, used as surfactant in Ethanol. After the formation of the emulsion, HA 1490 kDa was added to reach 2% w/w concentration. The rheological and tribological properties were evaluated, before and after sterilization in autoclave (121 °C, 20 minutes), in order to assess their viscoelastic properties and their thermal stability. The antioxidant properties of the materials were examined by the DPPH assay, and the DF loading efficiency was evaluated by UV-Vis Spectroscopy *In vitro* biological responses, such as cytotoxicity (Alamar blue assay) cell morphology (Confocal microscopy) and ant-inflammatory level expression of Interleukin-10 (IL-10) (ELISA kit), has been evaluated on Fibroblast cell (L929).

RESULTS AND DISCUSSION

The optimized systems exhibited rheological behavior of entangled polymer solutions, typical of SF viscoelastic behaviour i.e. the material behaves as viscous fluid at low frequencies and has an elastic behaviour at frequency higher than the cross-over frequency. The rheological parameters, i.e. the elastic (G') and viscous modulus (G'') were comparable to those of commercial viscoupplementation agents. The values of G' at 1 Hz and of the crossover frequency before and after autoclave, were almost similar, indicating an improved thermal stability. From rheological results a rheological synergism among the components was observed, suggesting an interaction that stabilises HA macromolecular network. Tribological experiments showed how VE and FA improved the lubricating properties of the formulation. The DPPH assay showed how VE and FA conferred to the system antioxidant ability. The Alamar blue assay and the cell morphological analysis revealed the iocompatibility of the formulation. The materials were demonstrated to have intrinsic anti-inflammatory activity by ELISA kit results. The DF release from the material was assessed being sustained over time in order to guarantee the local delivery of the drug,

CONCLUSIONS

HA-based viscosupplementation agent containing FA and VE was formulated and optimized. The material exhibited rheological and tribological properties comparable to those of commercial agents, improved thermal stability and intrinsic anti-inflammatory properties. Furthermore, the HA based formulation was able to load and sustainably release DF.

REFERENCES

1. Necas J., *et al*., Vet. Med. 53(8):397-411, 2008
2. Kim T.H. *et al.*, Tissue Eng. Regen. Med. 15(3):263-274, 2018

Biotechnological chondroitin as novel biopolymer for tissue regeneration: the natural -like polysaccharide compared to the crosslinked one in human chondrocytes in vitro cultures

Valentina Vassallo[1], Celeste Di Meo[1], Annalisa La Gatta[1], Donatella Cimini[1], Emiliano Bedini[2], and Chiara Schiraldi[1]*

[1]Department of Experimental Medicine, University of Campania "Luigi Vanvitelli", Via L. De Crecchio 7, 80138 Naples, Italy
[2]Dept. Chemical Sciences, University of Naples Federico II, Via Cinthia 4, I-80126 Naples, Italy

* chiara.schiraldi@unicampania.it

INTRODUCTION

Osteoarthritis (OA) is a very common pathology characterized by pain and progressive degradation of articular cartilage. Currently, one of the most diffuse treatments is viscosupplementation, using injective intrarticular gels, or pharmaceutical, nutraceutical treatments based on glycosaminoglycans, such as hyaluronic acid (HA) and chondroitin sulfate (CS). Recently, also an unsulfated chondroitin, namely biotechnological chondroitin (BC) was manufactured through tailor-made biotechnological processes [1]. Despite being unsulfated, BC proved similar and eventually superior biological effects in comparison to CS, in different OA *in vitro* models [2,3].

In this research work, BC was chemically modified in order to obtain a cross-linked chondroitin (XBC), to improve mechanical properties and increase the resistance to enzymatic degradation, with respect to the natural, linear counterpart. The biophysical, mechanical and biochemical characterization was performed in comparison to BC. Finally XBC and BC were tested in an OA *in vitro* model based on human pathological chondrocytes.

EXPERIMENTAL METHODS

XBC was prepared following a patented heterogeneous crosslinking reaction, using 1,4-butanediol diglycidyl ether (BDDE), as previously described by our group [4] The extent of chemical modification was assessed by Nuclear magnetic resonance (NMR).

that the crosslinked BC was analysed by size exclusion chromatography coupled to triple detector (SEC-TDA-laser scattering, Intrinsic viscosity and refractive index) to accomplish a complete hydrodynamic characterization. Mark-Howink Sukurada curves were also derived. In addition, flow curves and mechanical spectra were obtained using an Anton Paar Physica MCR 301 rotational rheometer equipped with a double-gap concentric cylinders' geometry (DG26.7). . Stability towards hydrolysis and enzymatic degradation was studied by incubating samples under physiological conditions at 37°C in the presence of Bovine testicular hyaluronidase (BTH) at increasing concentrations (1-50 U/mL) at increasing incubation time. hours respectively, In addition, resistance to ABC chondroitinase (10U/mL) was evaluated up to 24hours. . Finally, human pathological chondrocytes were cultivated *in vitro* with BC or XBC (2 mg/mL) for 7 and/or 14 days. Cell proliferation was assayed by CCK-8 test and the expression of specific biomarkers of chondrocyte phenotype and related to the inflammatory/degradative process was evaluated at gene and protein level by quantitative reverse transcription PCR (qRT-PCR), western blotting analyses (WB) and Immunofluorescence (IF).

RESULTS AND DISCUSSION

The mechanical study showed a different performance between the two samples; for instance, the newtonian plateau of dynamic viscosity was evident for BC with a zero-shear viscosity value of about 0.03Pa·s, while ashear thinning behavior was present for XBC in the whole range of interest (0.1-1000s^{-1}). High resistance to the BTH attack was found for both samples, and a significative molecular weight (Mw) reduction was achieved only with 50U/mL. The enzymatic degradation by ABC chondroitinase, instead, revealed sensitivity for both the linear and crosslinked BC. Specifically, the residual fractions with Mw above 50kDa was 35% for XBC, while BC resiuidual average MW was below 20KDa after 24h of treatment. Moreover, the chemical modification of BC resulted not toxic for the human pathological cells. In fact, both BC and XBC sustained the chondrocytes proliferation. In addition, the expression of specific chondrocytes biomarkers (collagen II and aggrecan) was prompted by both as showed by qRT-PC, WB and IF. Interestinly, not only BC but also XBC were effective in the reduction of pro-inflammatory cytokines (IL-6, PTX-3 and NF-kB) and matrix degradation correlated biomarkers, such asmetalloproteasesMMP-13) and complex oligomeric matrix protein (COMP-2).

CONCLUSION

This experimental set-up showed that the chemical modification improved the mechanical features of BC based gels. The cross-linked BC was effective in counteracting the inflammation/degradative process ongoing in pathological articular cells. However, further experiments also using stem cells are in progress to better assess the potential application of this innovative modified injectable glycosaminoglycan alone or in combination to HA in the management of OA.

KEY WORDS

Unsulfated biotechnological chondroitin, BDDE crosslinking, osteoarthritis, chondrocytes, collagenII.

REFERENCES

1. Schiraldi C et al. Appl Microbiol Biotechnol. 2010;87(4): 1209-1220.
2. Stellavato A et al. J Cell Biochem. 2016;117(9):2158-2169.
3. Russo R et al Int J Mol Sci. 2020;21:3746.
4. De Rosa et al. 2013 WO2013164782 (A1)

Construction of a Multilayer Scaffold for Osteochondral Tissue Engineering

Deniz Basoz[1,4*], Vasif Hasirci1[1,2,4], Deniz Yucel[1,3,4]

Acıbadem Mehmet Ali Aydınlar University (ACU), [1]Graduate School of Health Sciences, Department of Medical Biotechnology, [2] Faculty of Engineering, Department of Medical Engineering, [3] School of Medicine, Department of Histology and Embryology, [4] ACU Biomaterials Center, Istanbul, Turkey
[*]denizbasoz@gmail.com

INTRODUCTION

Osteochondral tissue is a composite structure consisting of articular hyaline cartilage, calcified cartilage, and subchondral bone layers[1]. Since articular cartilage is an avascular tissue and has a low regeneration capacity, recurring or traumatic injury of articular cartilage may result in osteochondral damage[2,3]. The ideal osteochondral scaffold should be designed considering the physical, mechanical and biological properties of the native tissue. In order to mimic the bone and cartilage parts of osteochondral tissue, biphasic scaffolds were commonly produced by combining two separate constructs by gluing, sewing or applying pressure[4]. The disadvantage of these methods is the delamination of two parts due to the formation of a weak interphase. The aim of this study is to construct a multilayer scaffold having structural and mechanical integrity by using 3D printing. The scaffold consists of the bone, calcified cartilage and cartilage zones of osteochondral tissue. In addition, the surface of the cartilage part of 3D printed scaffold is covered with fibrous, electrospun mat to mimic the superficial layer of articular cartilage.

EXPERIMENTAL METHODS

The multilayer scaffold model was designed by computer-aided design programs (Sketchup, Blender) keeping in mind that the pore size of the cartilage part is to be higher than that of the bone part. The scaffold was fabricated by 3D printing of poly(ε-caprolactone) (PCL). The PCL powder was melted at 100^0C in the metal syringe, and the molten polymer was extruded with the parameters of 100 psi, 4mm/s speed and 4mm layer height. In addition, a fibrous mat was fabricated by electrospinning using 20% (w/v) PCL solution in chloroform. This electrospun mat was then fixed onto the surface of cartilage mimic. The final construct was treated with oxygen plasma to improve its hydrophilicity and reactivity. Then, the 3D printed bone phase of the scaffold was coated with β-tricalcium phosphate to impart osteoconductivity. The morphology and pore size of the scaffold were examined with SEM. Mechanical properties of the scaffold parts were determined by compression tests.

RESULTS AND DISCUSSION

The 3D printed scaffold had two layers with different porosities, and an intermediate seamless layer without porosity as intended (Fig. 1). SEM micrographs showed that the 3D printed fibers were straight, and uniform sized. It was observed the pore size of bone and cartilage mimics were 439.85±27.79 µm and 937.99±25.12 µm, respectively. The pore size and pore interconnectivity were appropriate for cell attachment and proliferation. The electrospun mesh with random fibers was attached on the cartilage surface to provide smooth movement on the articular joints and for tissue ingrowth. Mechanical test results showed that the compression strengths of the bone phase, cartilage phase and the whole construct were 62.08±9.3, 38.99±5.3 and 80.19±22.9 MPa respectively.

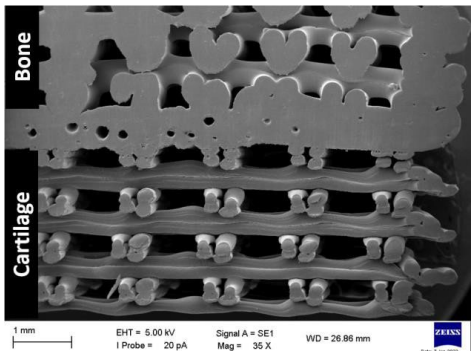

Figure 1. SEM image of cross-section of the 3D printed osteochondral scaffold

CONCLUSION

The multilayer scaffold, composed of bone and cartilage phases including an intermediate calcified cartilage phase could be 3D printed, and an electrospun fibrous mesh to serve as a superficial layer was integrated with 3D printed construct successfully. The multilayer construct appears to be suitable as a scaffold to be used in osteochondral tissue engineering, and therefore, it would be a promising implant for *in vivo* studies.

REFERENCES

1. Tamaddon M. et al., Bio-des. Manuf. 1, 101–114, 2018
2. Datta P. et al., Int. J. Bioprint. 3(2), 007, 2017
3. Tamaddon M. et al., Bio-Des. Manuf. 1(2), 101-14, 2018
4. Mellor F. et al., J J. Biomed. Mater. Res. Part B 108(5), 2017-30, 2020

ACKNOWLEDGMENTS

The authors acknowledge Acıbadem Mehmet Ali Aydınlar University for funding this study and ACU Biomaterials Center for the use of equipments and facilities.

Preparation and Characterization of 3D printed Poly (l-lactic-co-glycolic acid)-Strontium doped Tricalcium Phosphate bone scaffolds

Sam Tiplady[1*], Alex Lennon[1], Eneko Larrañeta[2], Fraser Buchanan[1], Krishna Manda[1]
[1]School of Mechanical and Aerospace Engineering, Queen's University, Belfast, UK
[2]School of Pharmacy, Queen's University, Belfast, UK
[*] stiplady01@qub.ac.uk

INTRODUCTION

Life expectancy in Europe is on the rise, creating significant healthcare challenges associated with ageing[1]. Patients who display fragility fractures are increasing, often caused by osteoporosis, which is more common in over 50s. 10% of fractures result in critically sized defects, requiring a therapeutic aid to achieve full healing[2]. However, the current 'gold-standard' treatment, autografts, has limitations and the need for synthetic scaffolds to overcome these issues is clear. Research has moved towards bioresorbable scaffolds that provide temporary mechanical stability and promote osteogenesis before resorbing into the body leaving behind a fully healed defect. The next generation of orthopaedic scaffolds require innovative composite materials and improved preparation and fabrication methods to address these challenges. **This research aims** to fabricate a 3D printed composite Poly (*l*-lactic-co-glycolic acid)-strontium doped β-tricalcium phosphate (PLGA-SrTCP) scaffold for the repair and regeneration of bone and carry out characterisation testing.

EXPERIMENTAL METHODS

SrTCP powders were fabricated using an aqueous precipitation method[3]. Synthesised powders were cryo-milled and characterised for morphology and particle size using an SEM and particle size analyser. Crystallite size, μ-strain, chemical fingerprint and chemical composition were characterised using XRD, ATR-FTIR and ICP, respectively. The synthesised powders, 20wt%, were mixed with PLGA, (85:15)(PLG 8531 Corbion), using a Rondol freezer mill**. The composite powders** were characterised for chemical composition (wt %) and morphology using an SEM and TGA. Finally, the composite powders, ~5.5g, were printed using a syringe-based printer (GeSim Bioscaffolder, Germany) to create 10x10x6mm **bone scaffolds**, with a pore-size of 550μm and porosity ~60%. Morphology, filler dispersion, thermal and mechanical properties are being characterised using an SEM, AFM, μ-CT, DSC, TGA and compression testing (Zwick Roell).

RESULTS AND DISCUSSION

SrTCP powders were fabricated and characterised using XRD, ATR-FTIR and SEM with EDS. Rietveld refinement of XRD, using Profex software, and FTIR results show peaks and phases consistent with Sr-TCP. Phase quantification shows composition of Sr-TCP of 96% showing limited contaminants of KPO_4 and β-CPP. Characteristic morphology is indicated by SEM, and particle size analysis shows an average particle size of 37μm with all particles below 100μm. Uniform distribution of filler has been achieved, as shown in SEM imaging of both scaffolds and powders, figure 1 (b,iv & vi). Fabricated PLGA and composite scaffolds show consistent architecture, pore sizes of 588μm and 515μm (calculated using ImageJ) respectively, as shown by SEM and optical microscope imaging. Preliminary TGA studies show the composition of composite scaffolds consistent with the methodology, and uniform distribution throughout the scaffold.

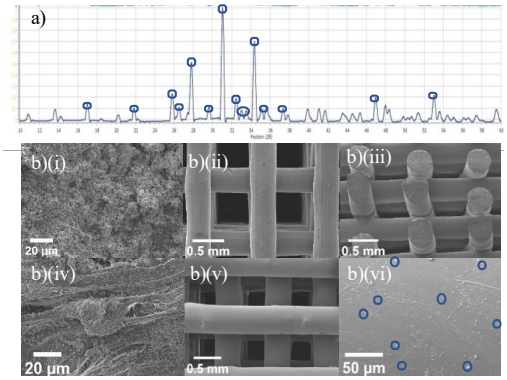

Figure 1 - a) XRD diffraction results of SrTCP, key characteristic peaks (○circled b) SEM imaging (i) SrTCP, (ii) PLGA (top view), (iii) PLGA (side view), (iv) Composite powders, (v) Composite scaffold, (vi) Composite scaffold strand (○ showing some examples of TCP within polymer matrix)

CONCLUSION

A successful method for fabricating SrTCP, composite powders, and scaffolds has been achieved. It has been shown that the syringe-based printing can be used to create reproducible, patient specific, homogenous, composite scaffolds suitable for critical sized defects. Further study will indicate SrTCP filler's effect on the thermal and mechanical properties of the scaffold and therefore the materials suitability in treating critically sized defects.

REFERENCES

1. Wang H. et al, The Lancet, 396(10258), 2020
2. Zimmermann, G. et al, European Instructional Lectures, 10, 2010.
3. Le Gars Santoni, B., et al., J. of the European Ceramic Society, 41(2), 2021.

ACKNOWLEDGMENTS

The authors would like to thank the Department for the Economy of Northern Ireland for funding this research.

Innovative modified gelatin and unmodified chondroitins based scaffolds for cartilage regeneration

Valentina Vassallo[1*], Anastasia Tsianaka [2], Nicola Alessio[1], Jana Grübel [2], Marcella Cammarota[1], Günter E.M. Tovar[2,3], Alexander Southan [2] and Chiara Schiraldi[1]

[1]Department of Experimental Medicine, University of Campania "Luigi Vanvitelli", Via L. De Crecchio 7, 80138 Naples, Italy
[2] Institute of Interfacial Process Engineering and Plasma Technology IGVP, University of Stuttgart, Nobelstraße 12, 70569 Stuttgart, Germany
[3] Fraunhofer Institute of Interfacial Engineering and Biotechnology IGB, Nobelstraße 12, 70569 Stuttgart, Germany.

[*] valentina.vassallo@unicampania.it

INTRODUCTION

Due to its high similarity to the extracellular matrix (ECM), gelatin is frequently considered as a good basis for the developing of scaffolds with applications in cartilage tissue regeneration. However, poor mechanical properties and sensitivity to enzymatic degradation stimulated the scientific community to improve strategies to modify gelatin (enzymatically or chemically) in order to obtain better performing hydrogels [1]. Often, these networks are coupled to glycosaminoglycan (GAGs), in particular, gelatin-methacryloyl (GM) hydrogel is mostly used combined to hyaluronan or chondroitin sulfate (CS). In this experimental set-up, innovative photocross-linked hydrogels based on GM and unsulfated biofermentative chondroitin (BC) were obtained and compared to GM coupled to extractive CS. The biophysical, biochemical and mechanical characterization was assessed to compare GM hydrogels to the heteropolysaccharide containing networks. Moreover, human mesenchymal stem cells (MSCs) were seeded on the obtained scaffolds and cultivated in vitro up to 21 days in order to evaluate differentiation towards the chondrocyte phenotype in relation to materials composition.

EXPERIMENTAL METHODS

GM was prepared with tenfold (GM10) molar excess of methacrylic anhydride (MAAnh) with respect to a nominal amino group content of 0.35 mmol·g^{-1} as previously reported [2]. Then, the hydrogel consisting in: a) 10% (w/w) GM10; b) 10% (w/w) GM10 with 2.5% (w/w); c) BC, or 10% (w/w) GM10 with 2.5% (w/w) CS were obtained, after mixing and subsequent photo-initiated radical cross-linking. After that, hydrogel yield was evaluated, swelling was studied in physiological condition, BC and CS release was analysed using capillary electrophoresis (HPCE). In addition, the rheological characterization was obtained using a Physica Modular Compact MCR301 Rheometer and stability towards hydrolysis and enzymatic degradation (under physiological conditions at 37°C until 21 days and with collagenase solution (3U/mL) for 3 and 16 hours). Finally, human MSCs were seeded on the scaffolds and cultivated *in vitro* for 21 days. Biocompatibility was assayed by 3-(4,5-Dimethylthiazol-2-yl)-2,5-diphenyltetrazolium bromide (MTT) test and the expression of specific biomarkers to assess the chondrocyte differentiation potentially occurring was evaluated by quantitative reverse transcription PCR (qRT-PCR) and Immunofluorescence.

RESULTS AND DISCUSSION

The mechanical characterization displayed a stiffer behavior in the presence of BC compared to GM10+CS and GM10 hydrogels alone. Moreover, the introduction of BC and CS reduced the swelling and increased the resistance to the enzymatic degradation. The used cross-linking procedures resulted not cytotoxic for MSCs. In fact, GM10 sustained the cellular viability, and the addition of BC and CS further increase cell proliferation. All the hydrogels supported MSC growth, in addition, CS and even more BC, prompted the chondrogenic differentiation already after 14 days of incubation. In fact, the cells expressed COLII, a differentiation marker towards chondrocytes phenotype, even if a fully mature tissue was not yet formed after 3 weeks. Our data suggest that both BC and CS maintain their biological efficacy when coupled to GM10 and exposed to hydrogel cross-linking procedures. Specifically, BC, for the first time tested as component of this kind of scaffolds, resulted more performant than CS in improving biophysical parameters and supporting MSC differentiation processes. Thus, the mechanical and swelling features, with high cell survival and differentiation towards the chondrocyte phenotype, support the developed biomaterials as potential candidate for the management of cartilage regeneration.

CONCLUSION

The reported outcomes showed that the presence of CS and mostly of BC improved mechanical features of GM10 based hydrogels and prompted the differentiation of MSCs towards the chondrocyte phenotype. Further experiments are needed in a translational perspective looking at the application of these hydrogels also based on innovative GAGs in the management of damage and/or loss cartilage.

KEY WORDS

chondroitin, gelatin-methacryloyl, MSC differentiation.

REFERENCES

1. La Gatta *et al.,* Regen Biomater. 2021; 12;8(3):rbaa052.
2. Sewald L *et al*.,Macromol. Biosci. 2018; 18, 1800168.

3D PRINTED BIORESORBABLE SCAFFOLDS FOR ARTICULAR CARTILAGE TISSUE ENGINEERING: A COMPARATIVE STUDY BETWEEN NEAT POLYCAPROLACTONE (PCL) AND POLY (LACTIDE-B-ETHYLENE GLYCOL) (PLA-PEG) BLOCK COPOLYMER

Uzuri Urtaza[1], Izar Gorroñogoitia[1], Ana Zubiarrain-Laserna[1], Emma Muiños-López[2], Froilán Granero-Moltó[2,3], JM Lamo de Espinosa[2], Tania López-Martinez[3], Manuel Mazo[4, 5], Felipe Prósper[4,5], Ane Miren Zaldua[1], Jon Anakabe[1]

[1] Leartiker S. Coop., 48270 Markina-Xemein, Spain.
[2] Department of Orthopaedic Surgery and Traumatology, Clínica Universidad de Navarra, Pamplona, Spain
[3] Cell Therapy Area, Clínica Universidad de Navarra, Pamplona, Spain
[4] Hematology and Cell Therapy Area, Clínica Universidad de Navarra, Pamplona, Spain
[5] Regenerative Medicine Program, Cima Universidad de Navarra, Foundation for Applied Medical Research, Pamplona, Spain
uurtaza@leartiker.com

INTRODUCTION

In this study, three previously reported promising scaffold geometries, Honeycomb[1], Double offset[2] and Gradient[3], have been 3D printed using two resorbable materials, PCL and PLA-PEG, seeking for the best geometry-material combination to achieve the targeted mechanical properties of natural cartilage tissue. Finally, cell viability and differentiation properties of the most promising samples have been tested and compared.

EXPERIMENTAL METHODS

Materials and 3D printing of scaffolds

Medical grade PCL filament was purchased from Advanced Biomedical Technology Inc. Medical grade PLA-PDLA-PEG block copolymer with 70/30 L/D lactide ratio containing 4% of PEG was purchased from EVONIK GmbH. TUMAKER NX FFF printer equipped with a direct drive system and a Ø=400 µm nozzle was used to print scaffolds with different infill densities and geometries.

Characterization

The surface morphology of the scaffolds was captured by means of a Nikon SMZ 745T stereoscopic microscope and analysed with NIS-elements software. The porosity was also calculated. Regarding mechanical properties, compression strength and moduli of the scaffolds were measured according to ISO 604 by means of an MTS Insight 10 universal tensile test machine (MTS Company, Eden Prairie, Minnesota, USA). A 5kN load cell with an accuracy of ± 0.5% was used.

Cell experiments

The initial viability of the cells (hBMSCs and chondrocyte) in the different geometries was evaluated at 24 hours using Live/dead cytotoxicity kit (Thermo) and the differentiation process at 21 days. For the differentiation assay, cells were maintained in chondrogenic media composed of (DMEM supplemented with 50 mg/ml ITS, 1 µM Dexamethasone (SIGMA), 100 µg/ml Sodium Pyruvate Solution, 10 ng/ml human TGF-β3. Medium was changed twice weekly, and after 21 days molecular analysis was performed.

Molecular Analysis

Total RNA was extracted using TRIzol following manufacturer instructions. One microgram of total RNA was retrotranscripted using qScript™ Supermix. The qPCR was performed in QuantStudio™ 5 Real-Time PCR System using RPLP0 as housekeeping gen. Relative expression of genes of interest was calculated using the ΔΔCt method.

RESULTS AND DISCUSSION

Among others, compressive elastic modulus of the scaffold has been defined as one of the most critical. Recent works have reported overall cartilage elastic modulus values from 0.20 to 24 MPa[4,5]. This range has been determined as the target to be achieved for correct mechanical mimicking of cartilage tissue. Scaffold microarchitecture, especially the pore size and porosity of the construct, is an important parameter which not only does affect cell proliferation but also direct cell differentiation and extracellular matrix (ECM) formation. A range from 100 to 860 µm pore size has been reported to be of interest[6], been defined as target. Considering the targeted microarchitecture and compressive performance, different infill densities were evaluated for each of the three different scaffold geometries: Honeycomb, Gradient and Double offset. The size of pores showed to fit within the defined target range for all printed scaffolds (100-860 µm). Within the studied range of structures, highest porosities were obtained by Double offset geometries, together with Gradient with 20-30-45% infill density. Scaffolds printed in PLA-PEG showed higher compressive modulus than those printed in PCL due to the difference in stiffness of the neat materials. Four geometry-material combinations which meet both the target modulus (0.20-24 MPa) and pore size (100-860µm) while presenting porosity levels >60% were achieved, fabricated and tested: 1) Gradient geometry in PCL with fill density of 20-30-45; 2) Double offset geometry in PCL with a fill density of 62; 3) Double offset geometry in PCL with fill density 47; and 4) Double offset geometry in PLA-PEG with fill density 47. Among the studied geometries, no significant differences were detected on the viability of hBMSCs and chondrocytes after 24 hours. However, a higher viability was observed for chondrocytes compared to BM-MSCs, with values over 80% for all geometries and materials. On the other hand, cell differentiation tests carried out during 21 days indicated a better performance of the cells in the PLA-PEG Double offset 47 and PCL Double offset 47 constructs, pointing out this geometry as optimum in both materials.

CONCLUSION

Among all the geometries and studied infill conditions, only four combinations geometry-material meets targets modulus and pore size. Cell viability is almost similar between this four combinations, but the differentiation indicated a better performance in the double offset geometry with a infill of 47 in both materials.

REFERENCES

1. Theodoridis K. *et al*., J Tissue Eng Regen Med. 13:342-355, 2019
2. Schipani R. *et al*., Connective Tissue Research. 1-16, 2019.
3. Liu H. *et al*., Materials & Design. 188 :108488, 2020.
4. Levental I. *et al*., Soft Matter. 3 :299-306, 2007.
5. Beck EC, *et al*., Acta Biomaterialia, 38:94-105, 2016.

Lim SM. *et al*., Adv Eng Mater, 12: B62-B69, 2010.

Influence of low frequency electrical stimulation on osteoblast growth: Cellular effects via AC-conditioned liquids?

Meike Genzow[1*], Julius Zimmermann[2], Thomas Freitag[1], Ursula van Rienen[2,3], J. Barbara Nebe[1,3], Susanne Staehlke[1]

[1]Department of Cell Biology, University Medical Center Rostock, 18057 Rostock, Germany
[2]Institute of General Electrical Engineering, University of Rostock, 18059 Rostock, Germany
[3]Interdisciplinary Faculty, University of Rostock, 18059 Rostock
[*]meike.genzow@med.uni-rostock.de

INTRODUCTION

Surface modifications -chemical and topographical- are essential for integrating biomaterials in the biosystem[1,2]. To further improve the osseointegration of implants, electrical stimulation of the bone tissue increases proliferation and collagen production[3]. Ercan and Webster enhanced the proliferation of osteoblasts *in vitro* on anodized titanium using the IonOptix system[4]. The mechanism of cell physiological processes upon electrical stimulation is not yet understood. This *in vitro* study investigated if AC stimulation altered the liquid characteristics. The background for this approach comes from physical plasma. Plasma-treated medium alone influences cell adhesion, tight junction formation, and vitality[5,6]. We studied whether AC-conditioned liquid was the cause for the increased cell adhesion. Our aim is to identify mechanisms by which cells are stimulated by AC electrical signals.

EXPERIMENTAL METHODS

A commercially available multi-channel system (IonOptix) was used for electrical stimulation. This system generates electrical bipolar square waves with a frequency of 20 Hz, pulse duration of 3.6 ms, and a voltage of 1 V (2 V/peak to peak) or 5 V (10 V/pp). The electrical stimulation of MG-63 cells (ATCC® CRL-1427™)[7] was done for 10 min. The cell suspension was acquired and analyzed via flow cytometry (FACSCalibur, BD Biosciences). Adhesion was calculated from cells of the reference sample. The influence of AC on the liquid was measured by temperature (Mini-K, Dostmann, testo), pH (pH meter, SI400-010), oxygen content (Microx TX3, Presens), and the H_2O_2 concentration (Hydrogen Peroxidase Assay, Sigma-Aldrich). After AC stimulation, cells were cultured in DMEM (Thermo Fisher Scientific) with 10 % FCS. The metabolic activity and cell number were studied via colorimetric assays (CellTiter 96® Cell Proliferation Assay, Promega, and Neisser solution II, Roth, respectively) after 48 h.

RESULTS AND DISCUSSION

We found an increased initial attachment capacity of 10 min AC-stimulated cells in suspension (**Fig. 1a**). The experiments with acellular media under electrical stimulation (10 min) showed no alterations in the composition and characteristics compared to the untreated medium DMEM: the media´s temperature, pH, oxygen content, and H_2O_2 concentration (**Fig. 1b**) remained stable. Osteoblasts that were stimulated for 10 min and then incubated for another 48 h showed increased cell numbers compared to the control. However, only the 1 V stimulated MG-63 cells showed a trend towards increased relative cell viability.

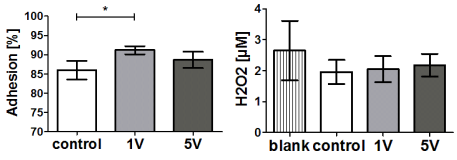

(a) (b)

Fig. 1: AC stimulation of cells and media. a) Short-time adhesion of MG-63 suspended in DMEM (20 Hz). (mean ± sem, n = 7, unpaired *t*-test *=p<0.05). b) Hydrogen peroxide concentration in DMEM after 10 min stimulation. (mean ± sem, n = 4, unpaired *t*-test).

CONCLUSION

We found that electrically stimulating the cells via the IonOptix chamber did not influence the cell culture media. Therefore, an influence of the cell-surrounding AC-stimulated liquid on osteoblasts can be excluded. The electrical stimulation seems to directly affect the cells.

REFERENCES

1. Rebl H. *et al.*, Acta Biomater. 8.10:3840-3851, 2012.
2. Sul Y-T. *et al.,* J Biomed Mater Res A. 89(4):942-50, 2009.
3. Pettersen E. *et al.*, Sci. Reports 11:22416, 2012.
4. Ercan B and Webster TJ., Int J Nanomed. 3:477-485, 2008.
5. Hoentsch M., *et al.*, PLOS One 9.8:e104559, 2014.
6. Woedtke T. von, *et al.*, In: Plasma for bio-decontamination, medicine and food security, Springer, The Netherlands, 2012.
7. Staehlke S. *et al.*, Cell Biol Int. 43 (1):22-32, 2019.

ACKNOWLEDGMENTS

This research was funded by the Deutsche Forschungsgemeinschaft (DFG, German Research Foundation) – SFB 1270/2 - 299150580.

Gender differences of bone formation during fracture healing in response to magnesium implants: preliminary study in a rat external fixation model.

Yu Sun[1], Heike Helmholz[1], Regine Willumeit-Römer[1]

[1]Institute of Metallic Biomaterials, Helmholtz-Zentrum Hereon, Geesthacht, Germany
[*]yu.sun@hereon.de

INTRODUCTION

The clinical translation of novel magnesium (Mg)-based degradable biomaterials may overcome the shortcomings of conventional alloys and improve the current treatment outcome for bone fractures. However, due to the potential contradictory results between *in vitro* and *in vivo* tests for absorbable materials, animal studies are necessary for the investigation of systemic and local tissue responses,[1] and researchers are faced with the challenges to establish efficient pre-clinical models for translational research. Rodents, especially rats are commonly used in fracture research for Mg-based implant materials, and both male and female rats was selected in previous publications.[2] The ISO standard for testing of local effects after implantation requests reporting of the animal sex with justification,[3] but there is no consensus regarding which gender be more effective for the evaluation of biological effects from Mg-based materials. The authors investigated femoral fracture healing in response to intra-medullary Mg implants, in a preliminary study involving both male and female rats, to provide suggestions for gender selection improving future pre-clinical research.

EXPERIMENTAL METHODS

Femoral shaft fractures were induced via osteotomy in Sprague-Dawley (SD) rats, followed by implantation of intra-medullary pins made of pure Mg, and external fixators were mounted for bone stabilization. Three male rats were included in a pilot phase-1 study,[4] and nine female rats were included in the following phase-2 study. Both underwent *in vivo* micro-CT immediately after surgery and at the post-operative week 12. Body weight was recorded before imaging. Qualitative histological analysis was performed to verify bone healing status. *Ex vivo* micro-CT of bilateral femur samples was performed for further whole-bone analysis of mineralized tissue formation based on global threshold, and the ratio of bone tissue volume between the surgical femur and non-surgical femur was calculated for each rat. Quantitative results were presented as the mean ± standard deviation, but no further statistical analysis was performed considering the limited sample size in the preliminary research.

RESULTS AND DISCUSSION

Two female and one male rat were removed from final quantitative analysis due to post-operative complications, and all other rats achieved successful bone union after 12 weeks demonstrated by imaging and histology. The body weight of male rats increased dramatically (75.37% ± 4.37%) during follow-up, compared with a slight increase in female rats (12.18% ± 2.03%). The ratio representing increased bone formation in surgical femur with Mg implants were higher in female rats (157.97% ± 12.76%) than in male rats (127.10% ± 3.97%). The rapid growth in male rats as reflected by body weight, differs significantly from human clinical reality and may partially mask the biological effects from Mg. The authors suggest selecting female rats especially when it is difficult to use both genders simultaneously. Besides, the relatively smaller size of female rats also facilitates the application of various *in vivo* imaging methods for longitudinal study.

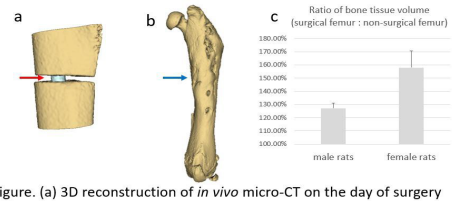

Figure. (a) 3D reconstruction of *in vivo* micro-CT on the day of surgery showing the fracture line and intra-medullary Mg implant (red arrow); (b) *ex vivo* micro-CT at week 12 showing bone union (blue arrow: fracture site); (c) Ratio of bone tissue volume between surgical and non-surgical femur, indicating increased bone formation in both male and female rats during fracture healing.

CONCLUSION

Compared with the male counterparts, female SD rats showing less increased body weight and higher ratio of bone formation could be a more optimal choice in pre-clinical fracture research for Mg implant materials. Future experiments involving larger sample size as well as other rodent species may provide further information regarding gender selection in biomaterials research.

REFERENCES

1. Witte F, Fischer J, Nellesen J, et al. Biomaterials, 2006, 27, 1013-1018.
2. Sun Y, Helmholz H, Willumeit-Römer R. J. Magnesium Alloys, 2021, 9, 351-361.
3. ISO 10993-6:2016. DOI: 10.31030/2417140.
4. Sun Y, Helmholz H, Willumeit-Römer R, et al. Biomater Sci. 2022, DOI: 10.1039/D2BM00051B.

ACKNOWLEDGMENTS

The authors express our sincere thanks to: Prof. Gerhard Schultheiß, Sarah Vieten and the team of the central animal facility, Kiel University; Dr. Olga Will, Prof. Jan-Bernd Hövener, Prof. Claus-Christian Glüer (MOINCC, Kiel University); Dr. Björn Wiese, Monika Luczak, Dr. Thomas Ebel (Helmholtz-Zentrum Hereon).

Effect of Antioxidant on Molecular Weight of Bone Cement in Hydroxy-Radical Environment

Yukihiko Uehara[1], Ryusuke Uozu[1], Noriyuki Takano[2*]

[1]Department of Mechanical Engineering, Kanazawa Institute of Technology, Hakusan, Japan
[2]Integrated Technology Research Center of Medical Science and Engineering, Kanazawa Institute of Technology, Hakusan, Japan
* ntakano@neptune.kanazawa-it.ac.jp

INTRODUCTION

The bone cement has been used to the joint between artificial hip joints and bones in Hip arthroplasty. It, however, gradually is degraded in the living body, decreasing its strength. It causes the problem that revision is required before the useful life of the artificial hip joint. The cause of the degradation has been considered to be oxidation due to reactive oxygen[1,2]. We have reported that a decrease in the strength of PMMA, which is the main component in the bone cement, is inhibited by antioxidants in hydrogen peroxide solution[3]. In the present paper, the inhibition effect of antioxidants is confirmed by measuring the molecular weight of the pseudo bone cement.

EXPERIMENTAL METHODS

Samples: A material whose components are similar to bone cement used in the clinic was used (it is called the pseudo bone cement in the present paper). It was composed of methyl methacrylate monomer 19.9 mL, N,N-dimethyl-p-toluidine 0.05 mL, polymethyl methacrylate 36.0 g, and barium sulfate 4.0 g. Moreover, dl-α-tocopherol was added as an antioxidant. Its amount was 0, 5.88, or 58.9 mg. These components were polymerized stationary for 1 month in the air after being stirred for 2 minutes in a vacuum (about -0.035 MPa). They were cut to specimens, 40x4x4 mm^3, to degrade.
Artificial degradation: Specimens were put into 31 mass% hydrogen peroxide solution and radiated UV light from 2 to 12 weeks to cause hydroxy-radical, which is considered to act to the bone cement as like reactive oxygen in living-body.
Measurement of molecular weight: Molecular weight was measured using the gel permeation method (GPC) with UV/VIS detector. The column was PL-gel 10 μm MIXED-B PL1110-610 (Agilent Technologies). The solvent was 1,2-dichloroethane. Moreover, the infrared absorption spectrum was measured using FT-IT (FT-720, Horiba).

RESULTS AND DISCUSSION

The number average molecular weight Mn of the pseudo bone cement without antioxidants decreased about 25 % during 12 weeks as shown in fig.1. Mn of the pseudo bone cement with antioxidant was larger than that without antioxidant under artificial degradation process.
The result of FT-IR shows that the absorbance peak at 1140 cm^{-1} extremely decreased in the pseudo bone cement without antioxidant with degradation

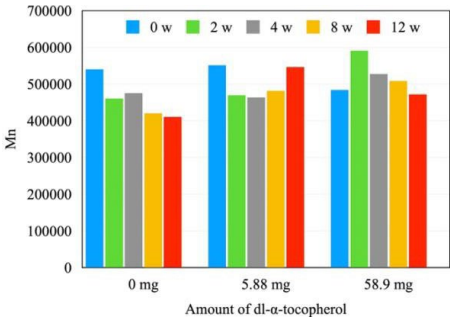

Fig.1 Change of number average molecular weight of the pseudo bone cement added dl-a-tocopherol by artificial degradation during 0, 2, 4, 8, 12 weeks.

period. That is the absorbance spectrum caused by the C-O ester bond. No reduction of the peak at 1140 cm^{-1} was, however, observed in the pseudo bone cement with an antioxidant by degradation.
Thus, the decrease of Mn of the pseudo bone cement without antioxidants is considered to be caused by the break of the ester bond due to hydroxy-radical. The present results indicate that dl-α-tocopherol inhibits breaking polymer chains by preventing the reaction due to hydroxy-radical.

CONCLUSION

The addition of an antioxidant, dl-α-tocopherol, inhibits degradation of the pseudo bone cement by preventing the breaking of ester bonds under the hydroxy-radical environment. It implies the possibility to inhibit the degradation of bone cement in clinic.

REFERENCES

1. Oonishi H. *et al*. Acta Orthop. 82:553-558, 2011.
2. Hughes K.F. *et al*. J. Biomed. Mater. Res. 65A:126-135, 2003.
3. Uchiyama S. *et al.* 16th Int. Conf. Strength Mater. 76, 2021.

ACKNOWLEDGMENTS

The authors would like to thank the Shibuya Science Culture and Sports Foundation for providing financial support to this project.

Production of Tissue-Engineered Cartilage using Collagen Sponges and OA Knee Synovial MSCs

Christel Henrionnet[1], Kévin Bourge[1], Paul Neybecker[1], Didier Mainard[1,2*], Laurent Galois[1,2], Damien Loeuille[1,3], Pierre Gillet[1,4], Astrid Pinzano[1]

[1] UMR 7365 CNRS-UL, IMoPA, Vandœuvre-Lès-Nancy, France
[2] Service de Chirurgie Orthopédique, Traumatologique et Arthroscopique, CHRU Nancy, Nancy, France
[3] Service de Rhumatologie, CHRU Nancy, Vandœuvre-Lès-Nancy, France
[4] Laboratoire de Pharmacologie, Toxicologie et Pharmacovigilance, CHRU Nancy, Vandœuvre-Lès-Nancy, France
[*] didier.mainard@univ-lorraine.fr

INTRODUCTION

Tissue engineering is the therapeutic pathway the most appropriate for the treatment of focal lesions of cartilage. It is based on the association of structuring biomaterial with cells and adapting the environmental conditions in order to obtain mature and functional substitute cartilage with characteristics close to the native cartilage. In view of the limitations encountered in obtaining chondrocytes from the patient, many tissues can be used as sources of MSCs capable of differentiation into chondrocytes. Among these MSCs, those of synovial origin are very popular due to their location in the joint site, their ease of obtaining during diagnostic examinations or punctures and their chondrogenic capacities. Concerning the support biomaterials, the choice of natural biomaterials is strongly favored, especially type I collagen, which is very abundant and not immunogenic. In addition, these biomaterials promote cell adhesion and are capable of promoting chondrogenic differentiation of bone marrow-derived MSCs and allow for rich and dense proteoglycan and type II collagen matrix synthesis[1].

Our objective is therefore to use MSCs derived from the synovial fluid (SF-MSCs) of osteoarthritis patients in association with a porous collagen-based biomaterial to produce an *in vitro* cartilage substitute dedicated to the treatment of focal lesions. To do this, we first characterized the MSCs from synovial fluid by flow cytometry and verified their multipotency. In a second step, we produced cartilage tissue from SF-MSCs and collagen sponges and determined the growth factors most favorable to the production of a cartilage extracellular matrix.

EXPERIMENTAL METHODS

Synovial fluid was obtained during knee prosthesis placement in osteoarthritic patients. Analysis of surface markers CD90, CD105, CD34, CD45, CD73 and HLA-DR was performed by flow cytometry during expansion. The multipotency of the cells was also assessed by adipocyte and osteogenic (monolayer) and chondrogenic (3D pellet system) differentiation potentialities. Then, after a pre-differentiation phase in P3 with proline, ascorbate and dexamethasone, the SF-MSCs were seeded in type I (95%) and III (5%) collagen sponges and cultured up to 28 days with different culture conditions (ITS, BMP-2, TGF-β1 and TGF-β3 +/- BMP-2). At D28, we analyzed the mitochondrial activity of the cells by MTT assay, the expression of the cartilage genes of interest by RT-qPCR, and finally the quality of the extracellular matrix produced by histological and immunohistochemical observations.

RESULTS AND DISCUSSION

Surface marker analysis revealed the presence of markers characteristic of mesenchymal stem cells (CD73, CD90 and CD105) associated with the absence of markers of hematopoietic stem cells (CD34 and CD45). HLA-DR marker analysis revealed a low immunogenicity of these cells. Multipotency analysis confirmed the undifferentiated character of SF-MSCs which are able to engage in adipogenic, chondrogenic and osteogenic differentiation pathways according to the culture conditions. After 28 days of maturation of the produced cartilage substitutes, no cell death was observed however mitochondrial activity decreases singularly with the use of TGF-β1 and TGF-β3 growth factors alone or in combination with BMP-2 compared to the control ITS condition. This reflects different differentiation states. Gene expression analysis confirmed different differentiation states. Indeed, TGF-β1 and TGF-β3 induced the expression of all chondrogenic, with, however, a better chondrogenic effect of TGF-β1 compared with TGF-β3. BMP-2 alone or in combination with TGF-βs had no effect on these expressions. In addition, the very low expression of COLX and BGLAP suggests differentiation of SF-MSCs into chondrocytes without drift toward terminal hypertrophy. The histological and immunohistochemical results confirm the results with the induction of a synthesis of extracellular matrix rich and dense in type II collagen and proteoglycans under the effect of TGF-βs. BMP-2 alone or in combination with TGF-βs had no effect on this synthesis, in contrast to other studies that showed that the use of a BMPs+TGF-βs cocktail was required to achieve a cartilage-like matrix in contrast to the use of TGF-βs alone[2]. Importantly, the different cartilage substitutes produced showed no calcification after 28 days, regardless of the culture conditions.

CONCLUSION

Synovial fluid combined with collagenous biomaterial produced cartilage substitutes after 28 days of maturation in a suitable culture medium. The addition of TGF-β1 was sufficient to obtain a cartilage-like extracellular matrix.

REFERENCES

1. Roeder E. *et al*., PLoS ONE, p. e98451, 2014
2. Kohno Y. *et al*., BMC Musculoskelet. Disord, p78, 2018.

ACKNOWLEDGMENTS

Dedicated funding from "Société Française de Rhumatologie".

Material-Assisted Strategies for Osteochondral Defect Repair

Constance Lesage[1,2]*, Marianne Lafont[1], Pierre Guihard[1], Pierre Weiss[1], Jérôme Guicheux[1], Vianney Delplace[1]

[1]Université de Nantes, Oniris, CHU Nantes, INSERM, Regenerative Medicine and Skeleton, RMeS, UMR 1229, F-44000, France
[2] HTL Biotechnology, 7 Rue Alfred Kastler, Javené, 35133, France

*constance.lesage@etu.univ-nantes.fr

INTRODUCTION

The osteochondral (OC) unit, composed of cartilage and subchondral bone, plays a pivotal role in joint lubrication and in the transmission of constraints to bones during movements. The OC unit can be damaged by repetitive excessive loading, trauma or diseases, leading to cartilage defects. As OC defects does not spontaneously heal, different surgical approaches have been developed (e.g. chondroplasty, arthroscopic lavages and debridement, autologous chondrocyte implantation (ACI), matrix-associated ACI) and several biomaterials have now reached the market. Although present curative care temporarily improves joint functions, it often leads to the formation of fibrocartilaginous repair tissue, the deterioration of the subchondral bone, and functional loss in the long term. OC defects are therefore considered to be one of the major risk factors for long-term degenerative joint disease development such as osteoarthritis. In this context, a plethora of tissue engineering strategies have been envisioned, combining cells, biological molecules and/or biomaterials.

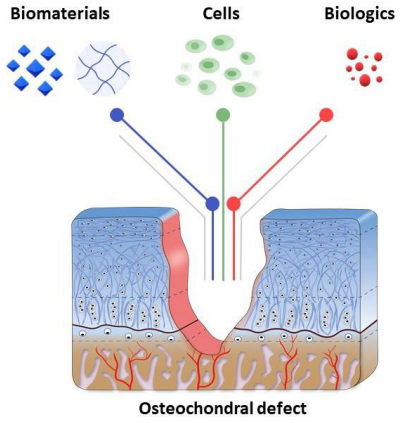

Figure 1. Material-Assisted Strategies for Osteochondral

EXPERIMENTAL METHODS

A comprehensive study of biomaterial-assisted bioengineering strategies that have been tested in OC defect between 2015 and 2021 was performed. The analysis of almost 300 studies provided a deeper insight into the field, with careful considerations for the therapeutic potential of the different strategies, and current OC regeneration evaluation methods.

RESULTS AND DISCUSSION

This study highlighted the multiplicity of strategies that have been envisioned, along with the unlimited number of possible combinations of biomaterials, cell types and bioactive molecules.
The careful analysis of the current state of the art has revealed the emergence of promising strategies, including injectable multilayer and gradient materials, which have shown remarkable improvement in neocartilage and subchondral bone quality, supporting the use of more biomimetic architectures. In parallel with advanced biomaterial design, the controlled release of bioactive molecules, including GFs, almost systematically improved outcomes compared to biomaterials alone. These strategies stimulate cell invasion and allow a shift to cell-free strategies, which is another promising approach to more easily meet the stringent quality and regulatory requirements for safety and efficacy needed for clinical application. Particular attention should be paid to the use of common and more comprehensive assessment methods (scoring systems, assessment methods and animal models), following clear guidelines agreed by the international community.

CONCLUSION

Though our comprehensive study of biomaterial-assisted bioengineering strategies, this present work will help to build a better common knowledge and be a first step toward progressing in OC regeneration.

ACKNOWLEDGMENTS

C.L. and M.L. contributed equally to this work. The authors are grateful to the Fondation de l'Avenir pour la Recherche Médicale Appliquée for its Jean Bayle-Lespitau Award (J.G.). The authors are also grateful to HTL Biotechnology (C.L.), the Agence Nationale de la Recherche (GELMECS project, ANR-19-LCV1-0003; P.W.), the Fondation pour la Recherche Médicale (ARF201809007012; V.D.), the Nantes Excellence Trajectory program (NExT Junior Talent 2018; V.D.), and the Marie-Sklodowska Curie Actions (BABHY-CART project, GAP-846477; V.D.) for their financial support.

Bioadhesive Nanocoated Cell-Microaggregates for Treating Diffuse Cartilage Lesions

Desiré Venegas[1*], Aurelio Vega[2], Matilde Alonso[1], José Carlos Rodríguez[1]

[1] Bioforge, University of Valladolid CIBER-BBN, Paseo de Belén 19, Valladolid 47011, Spain

[2] Servicio de traumatología, Hospital Clínico de Valladolid, Av. Ramón y Cajal 3, Valladolid 47003, Spain

[*] dvenegas@bioforge.uva.es

INTRODUCTION

Cartilage structures can be damaged causing two types of injuries: focal; the lesion is restricted to a concrete zone or diffuse; the lesion affects a broad area of the articular cartilage. This type of lesions appears due to the reduced self-healing capacity of articular cartilage. Diffuse damage is much more difficult to treat, usually restricted to palliative care or systemic anti-inflammatory treatments. As the damage progresses up to the point where the majority of the cartilage is lost, the only option available is the surgical replacement of the arthritic joint with a prosthesis. This type of diffuse lesions have a high prevalence as the common type of degenerative processes.

More recently, cell-based approaches using autologous chondrocytes or mesenchymal stem cells (MSCs)[1] have been tested and it can even be found in some clinics. However, the efficacy of such cell-based treatment is controversial[2]. In general terms, the applied cells stay in the injection site only for short periods of time, so their regenerative potential is greatly reduced. The most promising approach is the combination of such cells with a biomaterial-based carrier that can play that role.

The general objective of the project, in order to resolve the previous task, is the development of bioadhesive and injectable cell microcarriers with the ability to regenerate the articular cartilage. This aim is materialized in the fabrication of multibiofunctional capsules that are able to promote the cell cargo with selective adhesion and location on the articular surface. To do so, special attention is paid to the cell-material interaction on both the inner and outer surface of the capsule by means of the inclusion of specific cell adhesion domains and sequences that promote the adhesiveness to collagen II and chondroitin sulfate.

The microcapsules are based on a novel kind of biomaterials, named Recombinamers that are polypeptide materials obtained by recombinant DNA technology. In particular, the core composition of the microcarrier is the Elastin-like Recombinamers (ELRs)[3].

EXPERIMENTAL METHODS

Recombinant DNA techniques have proven to be very powerful tools for the development of novel protein-based biomaterials. This class includes ELRs, which are protein-based polypeptides that comprise repetitive units of the Val−Pro−Gly−X−Gly (VPGXG)n pentapeptide, in which X (guest residue) could be any amino acid except L-proline. ELRs are inspired by elastin, showing excellent biocompatibility, and they exhibit thermo-responsiveness in aqueous media.

The cloning and molecular biology for gene construction were performed using standard genetic-engineering methods. Production was carried out by recombinant techniques using Escherichia coli as the cell system. Purification was performed by several cooling and heating purification cycles (Inverse Transition Cycling) following centrifugation; the ELRs obtained in this manner were dialyzed against MilliQ water and lyophilized.

The purity and molecular weight of the ELRs were verified by sodium dodecyl sulfate polyacrylamide gel electrophoresis. Amino acid composition analysis and infrared spectroscopy were also performed.

RESULTS AND DISCUSSION

Genetic engineering methods allowed the synthesis of the genetic construct capable of synthesizing the desired biomaterial. Biopolymer adhesion to the hyaline-cartilage matrix was demonstrated measuring the adhesion forces between our biomaterial and surfaces with collagen II and chondroitin-sulfate versus control surfaces and quartz-microbalance.

Tailored layer-by-layer (LbL) approaches allowed the encapsulation of cell spheroids of autologous chondrocytes and MSCs.

In vitro and ex vivo assays were performed using cartilage explants from patients surgically intervened, this type of analysis showed the derivatized ELR adhesion efficacy to the articular surface and the final liberation of cell spheroids encapsulated hoping to demonstrate the cartilage regeneration.

CONCLUSION

In conclusion, a novel protein-based biomaterial with adhesion to the hyaline-cartilage matrix was synthetized. Besides, cell spheroids were encapsulated by the polymer.

Hence, in this study could be possible overcome the limitations of the current treatments used in diffuse cartilage lesions and suppose an advance in regenerative medicine.

REFERENCES

1. Harrel C.R. *et al*., J. Biomed Pharmacother., 2011.
2. Iijima H. *et al.,* Regenerative Medicine 3(15), 2018.
3. Rodríguez-Cabello J.C. *et al.* Polymer 50(22), 2009.

ACKNOWLEDGMENTS

The authors would like to thank the Ministerio de Ciencia e Innovación of Spain for providing financial support.

Multifunctional hydrogel-based patch for targeting inflammation and regeneration in chronic intestinal wounds

Marco Araújo[1*], João Silveira[1,3], Aureliana Sousa[1], Mafalda Bessa-Gonçalves[1], Susana G. Santos[1,2], Cristina C. Barrias[1,2]

[1] i3S - Instituto de Investigação e Inovação em Saúde, University of Porto, Porto, Portugal.
[2] ICBAS - Instituto de Ciências Biomédicas Abel Salazar, University of Porto, Porto, Portugal
[3] FEUP – Faculdade de Engenharia da Universidade do Porto, University of Porto, Porto, Portugal.
[*]marco.araujo@i3s.up.pt

INTRODUCTION

Inflammatory bowel disease (IBD), comprising Crohn's disease and ulcerative colitis, are chronic inflammatory disorders of the gastrointestinal tract of unknown aetiology. IBD exhibits a common chronic wound environment, characterized by overproduction of pro-inflammatory cytokines, reactive oxygen species (ROS) and matrix metalloproteinases (MMP), which leads to loss of epithelial cells and degradation of the extracellular matrix (ECM)[1]. Current therapies focus on reducing symptoms by delivering anti-inflammatory drugs, or by using biologics combined with immunomodulatory agents. Epithelial protection and restoration of the impaired intestinal barrier has recently emerged as a key goal for IBD therapy[2]. We hypothesized that novel biomaterial-based platforms for IBD should address both inflammation and mucosal healing, restoring intestinal barrier function and preventing disease relapse. This work presents a bioinspired multifunctional alginate-melanin 3D scaffold for potential application in multi-targeted IBD therapy.

EXPERIMENTAL METHODS

Multifunctional photopolymerized hydrogel scaffolds were obtained from a pre-gel solution containing modified ultrapure sodium alginate, Irgacure 2959, melanin nanoparticles (mNP) and a bisthiolated MMP-sensitive peptide. The pre-gel solution was irradiated using a BlueWave® 200 curing spot lamp, inducing polymer crosslinking, MMP-cleavable peptide incorporation and entrapment of the mNP. The hydrogels were freeze-dried giving 3D spongy-like scaffolds. Their in-vitro anti-inflammatory potential was evaluated by analysing the conditioned media from Lipopolysaccharide (LPS)-stimulated macrophages, and the pro-regenerative ability assessed in the presence of human intestinal fibroblasts (HIF) and Caco-2 cells. Friedman's test followed by corrected Dunn's test were performed for the *in vitro* radical scavenging assay (***p<0.001).

RESULTS AND DISCUSSION

The mNP-loaded scaffolds were able to neutralize the extracellular ROS initially present in the media of macrophages stimulated with LPS, to levels similar to non-stimulated control, demonstrating better performance than the scaffolds containing only the MMP-cleavable peptide or than free mNP (**Figure 1A**). The results highlight a synergistic effect from the components of the **mNP0.3Pep4FD** scaffolds, as well as the advantage of entrapping mNP in a hydrogel matrix, preserving their radical-scavenging ability. The same scaffold maintained this ability for at least 3 consecutive cycles, suggesting that once implanted, it may present sustained radical-scavenging ability during fares of inflammation, which may be key to prevent disease relapse[3]. Cells were able to adhere to scaffolds, spreading and forming cell-cell interactions. HIFs accumulated within macropores, where they deposited ECM. Caco-2 epithelial cells were also able to adhere and grow and to migrate into the macropores (**Figure 1B**).

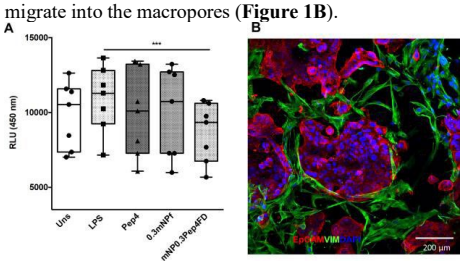

Figure 1. A: Ability of free mNP (**mNP0.3f**), and freeze-dried scaffolds containing 4 mM MMP-cleavable peptide (**Pep4**), and combined with mNP (**mNP0.3Pep4FD**) to capture extracellular ROS present in conditioned media from macrophages alone (**Uns**) or in the presence of LPS for 1h (**LPS**). B: Co-culture of HIF and Caco-2 cells within **mNP0.3Pep4FD** scaffolds (top view). EpCAM (red) marks Caco-2 cells and VIM (green) marks HIFs, DNA is in blue. Reproduced from Ref. 3 with permission from the Royal Society of Chemistry.

CONCLUSION

The scaffolds demonstrated ability to normalize an inflammatory-like environment and to support efficient colonization by intestinal cells. This novel platform may change the paradigm on the design of new biomaterial-based therapeutic strategies for IBD.

REFERENCES

1. Rieder F. *et al*., Gut 56:130-9, 2007
2. Friedrich M. *et al*., Mucosal Immunol 12:656-667, 2019
3. Araújo M. *et al*., Biomater. Sci. 9: 6510-6527, 2021

ACKNOWLEDGMENTS

The work was performed under the framework of IBEROS (0245_IBEROS_1_E) - funded by POCTEP 2014-2020 and FEDER, and ANGIONICHE - funded by FCT. MBG acknowledges the BiotechHealth Programme and FCT for the PhD fellowship (PD/BD/135489/2018).

Development of Intelligent Hydrogel-Based Burn Wound Dressings

Manon Minsart[1,*], Nicolas Deroose[1], Laurens Parmentier[1], Sandra Van Vlierberghe[1], Arn Mignon[2], Peter Dubruel[1]

[1]Polymer Chemistry & Biomaterials Research Group, CMaC, Ghent University, Ghent, Belgium
[2]Biomaterials and Tissue Engineering, Department of Materials Engineering, KU Leuven, Leuven, Belgium
[*] Manon.Minsart@UGent.be

INTRODUCTION

Hydrogels elegantly combine various of the desired properties of an ideal burn wound dressing, particularly as they can both absorb and release moisture, thus ensuring an optimal moisture control of the wound healing environment. Furthermore, electrospun fiber mats, especially those composed of hydrogel precursors, could provide an excellent environment to promote wound healing as these nanofibers can mimic the native extracellular matrix. Their high surface area enables efficient fluid absorption and enhanced drug delivery[1,2]. In this regard, acrylate-endcapped urethane-based precursors (AUP) were selected for the design of an intelligent burn wound dressing. The backbone that was selected in this work was poly(ethylene glycol), due to its biocompatibility and its highly hydrophilic nature, which is beneficial to enable a high exudate uptake. The AUP materials have been shown to possess excellent biocompatibility, as well as solid-state photo-crosslinkability at room temperature, which is crucial to produce mechanically stable, crosslinked nanofibers after electrospinning. Additionally, they are suitable for waterborne electrospinning, thus eliminating the use of toxic solvents[3]. As a final part of our dressing, an intelligent, biocompatible delivery system was envisioned for the triggered release of agents such as antimicrobials (e.g. tannic acid). To this end, liposomes were selected based on their intrinsic capacity to be lysed under the action of toxins (e.g α- and δ-toxins for *S. aureus*) which are secreted by pathogenic bacteria, after reaching the critical colonization threshold[4]. The main research objective of this project is thus the development of a burn wound dressing with an intelligent drug delivery system.

EXPERIMENTAL METHODS

AUPs with varying backbone molar masses (10 – 20 kg/mol) as well as endcap chemistries were synthesized using an improved protocol, yielding di- and hexa-acrylated polymers (DA and HA, respectively). The precursors were subsequently processed into both hydrogel sheets and electrospun mats, crosslinked via UV-A irradiation and benchmarked against some of the most used commercial wound dressings (e.g. Kaltostat), mainly in terms of swelling, mechanical properties and biocompatibility. The fiber morphology was assessed via scanning electron microscopy (SEM). *In vitro* indirect cell tests were performed using human foreskin fibroblasts (HFF). The liposomes were prepared according to the thin-film hydration method, extruded and characterized using dynamic light scattering (DLS).

RESULTS AND DISCUSSION

AUPs were successfully synthesized as indicated by ^{1}H-NMR and could be effectively processed into crosslinked hydrogel sheets and electrospun fibers. The AUP sheets showed high gel fractions (> 90%) together with strong swelling degrees in water and simulated wound fluid (12.7 – 19.6 g/g), as well as tunable mechanical properties (e.g. Young's moduli of 26 – 61 kPa, swollen state). The AUPs had significantly ($p < 0.05$) higher swelling degrees than most of the tested commercial dressings, while also being mechanically resistant. SEM analysis indicated homogeneous fiber morphologies with diameters ranging between 0.7 and 1.4 µm. The phospholipid liposomes encapsulating tannic acid proved to be stable for at least 28 days with an average zeta potential of -23.4 (± 4.5) mV and an average size of 191 (± 52) nm. Furthermore, they showed enhanced stability compared to unloaded liposomes and could be successfully incorporated in both hydrogel sheets and electrospun fibers without altering the mechanical properties ($p < 0.05$). As a proof of concept, liposome lysis was induced using Triton X-100. The di- and hexa-acrylated AUP materials showed good *in vitro* biocompatibility (viabilities > 90 %), which was evidenced by indirect MTS and live/dead cell assays.

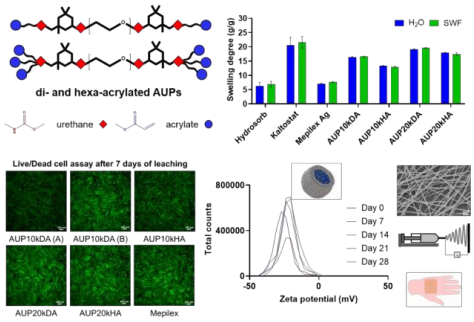

CONCLUSION

It can be safely concluded that AUP materials hold great promise as novel candidate burn wound dressings and are able to compete with several commercial wound dressings. Ongoing research focuses on the combination of liposomes with different bio-active agents using co-axial electrospinning.

REFERENCES

1. Mele,E.J.Mater.Chem.B.4:4801–4812,2016.
2. Sen,C.K.Adv.Wound Care.8:39–48,2019.
3. Minsart,M.*et al.*Macromol.Mater.Eng.306:1–12, 2021
4. Zhou,J.et al.Biomaterials.161: 11–23, 2018

ACKNOWLEDGMENTS

The authors would like to thank the Research Foundation Flanders (FWO) (Grant no: 3SB5619, SB PhD Fellow) for providing financial support for this research.

Three Fungal Exopolysaccharides as New Biomaterials for Wound Healing

Masoud Hamidi, Oseweuba Valentine Okoro, Giuseppe Ianiri, Hafez Jafari, Khodabakhsh Rashidi, Saeed Ghasemi, Raffaello Castoria, Davide Palmieri, Cédric Delattre, Guillaume Pierre, Mahta Mirzaei, Hadi Samadian, Amin Shavandi

INTRODUCTION

Exopolysaccharides (EPSs) are high-value functional biomaterials mainly produced by bacteria and fungi, with nutraceutical, therapeutic and industrial potentials.[1] Fungal EPSs can be produced within a few days, using simple recovery approaches and by utilizing industrial waste as feedstock.[2, 3]

In this study, EPSs from three fungal strains, *Papiliotrema terrestris* PT22AV, *Rhodosporidium babjevae* IBRC-M 30088 and *Sclerotium glucanicum* DSM 2159 were extracted and their physicochemical properties (structural, morphological, monosaccharide composition and thermal properties) were characterized. Also, *in vitro* biological activities as well as wound healing potential of the EPSs was evaluated.

EXPERIMENTAL METHODS

Microorganism cultivation

P. terrestris PT22AV, a yeast isolated from olives in Molise (Italy), *R. babjevae* and *S. glucanicum* were cultured in agar media. After preparation of appropriate inoculum for each strain, batch cultures consisting of 250 mL Erlenmeyer flasks containing 100 mL medium were used for microbial growth and production of EPSs.

EPS extraction and purification

After incubation, the EPS-containing supernatants were recovered via centrifugation and the EPSs were precipitated by adding cold ethanol, purified by dialysis, and lyophilized.

Morphological and physicochemical characterization of the extracted EPSs

Scanning electron microscopy (SEM) observations were performed for microstructure determination of the EPSs from *P. terrestris and S. glucanicum.* Also, FT-IR analyses were done for functional group determination of the EPSs.SEM and FT-IR studies had been done previously for *R. babjevae.* Molecular weight (M_w) determination [through steric exclusion chromatography (SEC)-HPLC1)] and monosaccharide composition determination (GC-MS), were performed for the EPSs from *P. terrestris.* For the other two strains, *Mw* and monosaccharide composition is already available.

In vitro biological activity

The antioxidant activity of the EPSs was assessed by measuring their DPPH radical scavenging activity. Also, their compatibility with human red blood cells (RBCs) and human fibroblasts (ATCC: CCL-186) and macrophages (U937, ATCC: CRL-1593.2) cell lines was assessed.

In vivo wound healing studies

The wound healing effects of the three EPSs were evaluated *in vivo* using adult male Wistar rats based on wound closure percentage (WC)% and histopathological assessments.

Statistical analysis

Minitab ®20.4 software was used to conduct statistical analysis of the WC% association with various time intervals and treatment groups. GraphPad Prism 9.0.0 (GraphPad Software, LLC, USA) was used for *in vitro* data analysis. Since data of WC% and cell viability followed a non-parametric distribution, the two-way ANOVA test with Dunnett's multiple comparisons was used. Statistical significance was considered at $p < 0.05$.

RESULTS AND DISCUSSION

The EPSs obtained from *P. terrestris* had an average molecular weight of 202 kDa. Mannose and glucose with 97% and 3% molar percentages, respectively, constituted the EPSs which was then considered as mannan polysaccharides. SEM showed that this EPSs have porous surface structure with grain-like elongated structural units. The antioxidant activity of the EPS at different concentrations (0.1-5 mg/mL) showed a positive correlation between the EPS concentration and the DPPH radical antioxidant activity. The increase of EPSs concentration from 0.1 mg/mL to 5 mg/mL, improved the scavenging activity from 20 % to 37 %.

Scleroglucan (the EPSs from *S. glucanicum*) was also shown to have a solid surface characterized by irregular shapes. IR spectroscopy indicated the presence of hydroxyl, carbonyl, and carboxyl functional groups like the commercial scleroglucan. DPPH scavenging activity of scleroglucan was 33.03 ± 4.31% at a concentration of 5 mg/mL.

All the three EPSs showed compatibility with the human fibroblast and macrophage cell lines (at concentrations of 100-1000 µg/mL), and with RBCs (1-10 mg/mL). The animal studies showed a dose-dependent wound healing capacity of three EPSs with significantly higher WC% values at 10 mg/mL after 14 days. The effects of the three EPSs on WC% were not significantly different at the highest concentration (10 mg/mL).

CONCLUSIONS

These findings demonstrate that the EPSs from *P. terrestris, R. babjevae* and *S. glucanicum* are promising biopolymers for wound healing acceleration.

REFERENCES

1. Vinothini G, et al. Int. J. Biol. Macromol. 134:575-87, 2019
2. Elsehemy IA, et al. Int J Biol Macromol. 163:1196-207, 2020
3. Donot F, et al. Microbial exopolysaccharides: Main examples of synthesis, excretion, genetics and extraction. Carbohydr Polym. 87:951-62, 2012

Phytotherapeutics-Loaded Active Patch for Chronic Wound Healing

Amey Dukle[1], Deniz Atila[2], Vignesh Kumaravel[2], A. Joseph Nathanael[1,*]

[1]Centre for Biomaterials, Cellular and Molecular Theranostics, Vellore Institute of Technology, Vellore, Tamil Nadu, India

[2]International Centre for Research on Innovative Bio-based Materials (ICRI-BioM)-International Research Agenda, Lodz University of Technology, Lodz, Poland

deniz.atila@p.lodz.pl

INTRODUCTION

Globally chronic wounds pose a major challenge to health professionals. According to an estimate, the wound care industry has been valued between 28.1 to 96.8 billion USD[1]. Chronic wounds can lead to amputation, thus diminishing the quality of life[2]. They are also a major cause of mortality and permanent disability. Chronic wounds are caused by multiple reasons such as diabetes, bacterial infection, repeated trauma to the infection site, etc. The existing treatment methods involve cleaning the wound, using a bandage, and supplementing with a high dosage of antibiotics. The recent studies have been showed the negative effects on prolonged usage of antibiotics for wound healing, and therefore there is a global demand to develop novel treatment strategies using phytotherapeutic alternatives. In this present study, we have explored the significance of neem seed oil, a popular phytotherapeutic for wound healing. Nano-formulations of neem seed oil are anti-inflammatory, cell proliferative, and possess wound healing capabilities[3]. Polyvinyl alcohol (PVA), a water-soluble biocompatible polymer is used as a delivery vehicle for neem seed oil[4]. Different compositions of PVA/neem seed oil composites were studied to produce active patches for chronic wound healing.

EXPERIMENTAL METHODS

The patches were produced by a novel freeze casting technique and cross-linked using a combination of freeze-thaw and acidic vapor exposure methods to achieve sustained release of phytotherapeutics. The patches were characterized for their mechanical strength, cytotoxicity, and in-vitro antimicrobial capabilities. Antimicrobial capabilities were tested against the two most common bacteria found in chronic wounds, i.e., *Staphylococcus Aureus* and *Pseudomonas aeruginosaa*[5].

RESULTS AND DISCUSSION

Figure 1 shows the scanning electron microscope (SEM) image of the cross-section of the active patch. The neem seed oil-loaded active patch displayed superior anti-microbial properties against *S. Aureus* bacteria compared to commercially available bandage that was used as a control (Figure 2). The patch inhibited bacterial growth for approximately 72 h far exceeding the average lifespan of a wound dressing. This long term sustained release of anti-microbial and cell proliferative agents is attributed to the novel crosslinking strategy employed for fabrication of the active patch. The mechanical properties were also found to be sufficient enough to prevent repeated trauma at the wound site.

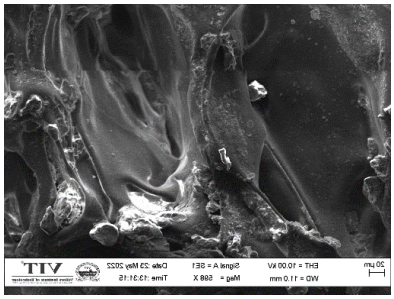

Figure 1. SEM image of the Neem seed oil-loaded PVA patch for Active wound healing.

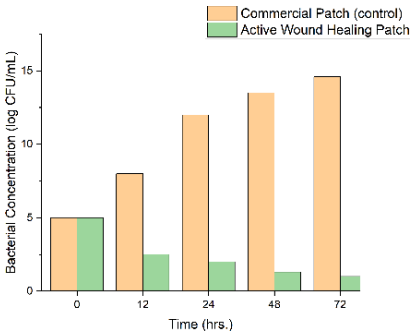

Figure 2. Bacterial inhibition as a function of time for *S. Aureus* bacteria with Neem seed oil-loaded PVA active wound healing patch.

CONCLUSION

This study shows promising potential in developing phytotherapeutic-loaded active patches for wound healing. The findings of this study would be beneficial to combat chronic wounds and reduce the overall cost of treatment.

REFERENCES

1. Sen C. K., Adv. Wound Care. 8:39-48, 2019
2. Turkkan S. *et al*., J. Biomed. Mater. Res. B. 106: 2625-2635, 2018
3. Singh A. *et al*., Ayu. 35:398-403, 2014
4. Im Y. M. *et al*., Mater. Lett. 147:20-24, 2015
5. Rahim K. *et al*., Microb. Ecol. 73:710-21, 2017

Electrified Microfluidic Scratch Assay

Sebastian Shaner[1,2*], Anna Savelyeva[1,2], Anja Kvartuh[1], José Leal[1,2], Nicole Jedrusik[1,2], Maria Asplund[1,2]

[1]Department of Microsystems Engineering, University of Freiburg, Freiburg, Germany
[2]Brainlinks-Braintools Center, University of Freiburg, Freiburg, Germany
[*] sebastian.shaner@blbt.uni-freiburg.de

INTRODUCTION

Not all wounds are created equal, especially when it comes to how they heal. Factors such as age, body type, immunosuppression, and chronic diseases (e.g., diabetes mellitus) can turn a normally acute wound healing process into a chronic one. Chemical, mechanical, and electrical cues are all involved in the wound healing process. Specifically, wounds naturally produce small electric fields (EFs ~ 128 and ~ 59 mV/mm for younger and older people, respectively) when the transepithelial membrane is broken, thus creating a short-circuit of transepithelial potential.[1] These EFs are paramount in recruiting cells responsible for cleaning and rebuilding tissue and blood supply via a process called electrotaxis (i.e., galvanotaxis). For diseased or aging patients, it is fathomable to think that if the endogenous EF is hindered, then an exogenous EF could help expedite wound closure and avoid the painful and expensive transition to the chronic stage. Here, we developed a method to grow and scratch confluent layers of the prominent cell type found in the epidermis (i.e., keratinocytes) in microfluidic channels. The confined nature of the channel allows for precise EF strength generation to establish dose-response, and the channel network allows to test different EF directionality across the wound.

EXPERIMENTAL METHODS

Microfluidics devices: double-sided acrylic adhesive was patterned with a CO_2 laser, then placed onto a sterile polystyrene Petri dish. Immortalized human epidermal keratinocytes (iHEK) were seeded onto the exposed polystyrene dish such that they were confluent the next day. For diabetes modeling, cells were subjected to p38 mitogen-activated protein kinase (MAPK) inhibitor (25 µM for 3 hr at 37°C) since hyperglycemia is known to suppress keratinocyte migration via this pathway.[2]
Scratch assay: sterile 10 µL pipette tip was placed onto a vacuum aspirator and used to create scratches with minimal cellular debris. CO_2 laser-cut acrylic lids/reservoirs were sterilized and added to the exposed adhesive to fully define the microchannels. New media was then added.
Electrodes: made via laser-induced graphene with coated PEDOT:PSS hydrogels.[3] Metal-free electrodes allowed for stable long-term direct current (DC) stimulation without toxic metal by-products. Two electrodes (one anode and cathode) yield a uni-directional EF from one side of the scratch. Three electrodes (two shorted anodes and one cathode) yield a pseudo-converging EF from both sides of scratch. A galvanostat was used to deliver a constant current (25 and 40 µA for uni-directional and converging EF, respectively) to generate an EF of 200 mV/mm at the scratch center, as determined by finite element analysis (COMSOL). Scratches were stimulated for 12 straight hours.

RESULTS AND DISCUSSION

EFs expedited scratch closure for both healthy (65% increase versus control) and diabetic-like cells (46% increase versus respective control) – see Fig. 1. Both uni-directional and converging EF helped speed up scratch closure of healthy keratinocytes, but uni-directional had a much greater effect. This is why it was down-selected for testing with p38 MAPK inhibited keratinocytes, where stimulation helped the scratch almost recover to healthy keratinocyte closure speeds.

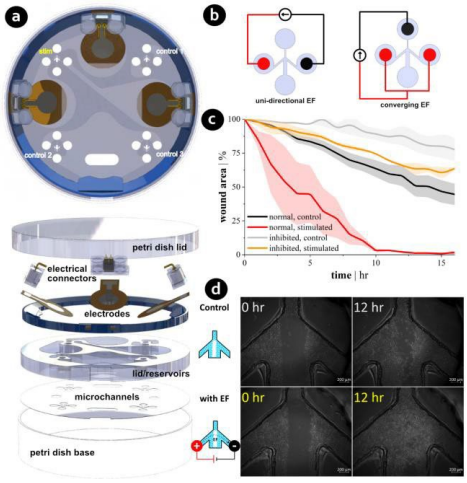

Fig. 1 – (a) top view and explosion view of the microfluidic device (b) illustration of both tested EF directionalities (c) wound area closure in relation to initial area (d) example images of healthy cells with and without DC stimulation.

CONCLUSION

These results provide evidence of a new application for scratch assays and the foundation for translation to 3D skin models, *ex vivo* biopsies, and real patients. Moreover, this 2D assay environment allows for wound healing analysis with electrotaxis parameters with the option to introduce chemotaxis drug delivery (via diffusion or controlled-release from electrode) as well.

REFERENCES

1. Nuccitelli, R. et al. *Wound Repair and Regen.* (2011): 645-655.
2. Li, L. et al. *Front. in Physiol.* (2019): 24.
3. Shaner, S.W. et al. *Biosens. Bioelectron. X* (2022): 100143.

ACKNOWLEDGMENTS

Funding = European Research Council (ERC) Horizon 2020 (No. 759655)

Supercritical CO_2 Technology for the Fabrication of Silk Fibroin Aerogel Particles for Wound Healing and Regeneration

Beatriz G. Bernardes[1,2], Sara Baptita-Silva[1], Carlos Illanes-Bordomás[2], Rui Magalhães[1], Raquel Costa[*3,4,5], Carlos A. García-Gonzaléz[*2], Ana Leite Oliveira[*1]

[1] Universidade Católica Portuguesa, CBQF - Centro de Biotecnologia e Química Fina – Laboratório Associado, Escola Superior de Biotecnologia, Porto, Portugal

[2] Department of Pharmacology, Pharmacy and Pharmaceutical Technology, I+D Farma group (GI-1645), iMATUS and Health Research Institute of Santiago de Compostela (IDIS), Universidade de Santiago de Compostela, E-15782 Santiago de Compostela, Spain

[3] Instituto de Investigação e Inovação em Saúde, Universidade do Porto (i3S), Porto, Portugal

[4] Department of Biomedicine, Biochemistry Unit, Faculdade de Medicina, Universidade do Porto, Porto, Portugal

[5] Escola Superior de Saúde, Instituto Politécnico do Porto, Porto, Portugal

*raquel.costa@i3s.up.pt; carlos.garcia@usc.es; aloliveira@ucp.pt

INTRODUCTION

Exudate from wounds is a natural response to heal. However, an excess production can compromise and delay the inflammatory phase, resulting in chronicity. Novel biocompatible, biodegradable and adaptable dressings are sought to promote tissue regeneration, prevent infection and control inflammation.[1] Aerogels are nanostructured materials with high porosity, large surface area, low bulk density and water uptake that can provide advanced performance for wound healing.[1] Silk fibroin (SF) aerogels can act as promising carriers of bioactive molecules while supporting cell proliferation.[2] Hereupon, SF aerogels were developed in the form of particles for wound healing applications.

EXPERIMENTAL METHODS

Silk fibroin extracted from *Bombyx mori* cocoons was used as aerogel source. For the aerogel particles' production, different SF aqueous solutions (i.e.: 3, 5 and 7% (w/v)) were mixed to absolute ethanol and Span 80 (3 wt.% with respect to SF), followed by supercritical CO_2 drying (120 bar, 39ºC, 3.5 h). SF particle size distribution were characterized by laser diffraction. Fourier Transform Infrared with Attenuated Total Reflectance (FTIR-ATR) spectroscopy was used to study the chemical structure, in particular secondary structure formation. Textural properties were analyzed by helium pycnometry and N_2 adsorption-desorption. Aerogel particles biocompatibility was evaluated by direct contact with Human Dermal Fibroblasts (HDF's) and observed by Scanning Electron Microscope (SEM). Quantitative data were subjected to an analysis of variance (one-way ANOVA, Tukey's test; α=0.05.

RESULTS AND DISCUSSION

SF aerogel particles were characterized concerning particle size distribution. The average diameter and the dispersion increased with increasing SF concentration. These particles presented also high surface area and low skeletal density. According to the FTIR-ATR analysis, it was possible to verify the presence of the main characteristic bands of SF assigned to the presence of β-sheet structure. SF aerogel particles were tested by MTT assay and the cell viability increases consistently with time. After 7 days the cell viability is considerably higher as compared to the control, suggesting that aerogel particles can promote cell proliferation. These results were confirmed by SEM analysis.

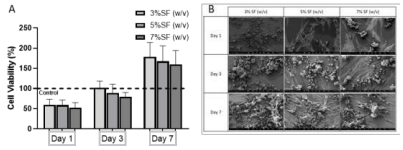

Figure 1 – A) Cell viability after MTT assay of HDF's cells in contact with aerogel particles as compared with the control group. No statistical difference was observed between groups for the same time point ($\alpha < 0.05$). B) SEM micrographs of HDF's cell cultures in contact with SF aerogel particles for 1, 3, and 7 days.

CONCLUSION

SF aerogels showed excellent properties, such as high biocompatibility, high surface area and low skeletal density, suggesting that the method is suitable to produce particles for wound healing applications. Confocal Microscopy, DNA quantification, antioxidant and degradation tests are currently on-going. In future, these particles will be studied as a promising drug delivery platform for wound healing applications.

REFERENCES

1. Bernardes, B. G. et al. Molecules 26:3834, 2021.
2. Vidya, M. & Rajagopal, S. I. J. Polymer Science 2021:9069924, 2021.

ACKNOWLEDGMENTS

This research was funded by MICINN [PID2020-120010RB-I00], Xunta de Galicia [ED431C 2020/17], Agencia Estatal de Investigación [AEI] and FEDER funds. This work was also supported by National Funds from Fundação para a Ciência e a Tecnologia (FCT), through project UID/Multi/50016/2020, Doctoral Research Grant 2021.05717.BD and Post Doctoral research grant SFRH/BPD/116024/2016. Work carried out in the framework of the COST Action CA18125 "Advanced Engineering and Research of aeroGels for Environment and Life Sciences" (AERoGELS), funded by the European Commission; and project TEX4WOUNDS (POCI-01-0247-FEDER-047029), financed under the Incentive System for Research and Technological Development, R&DT Projects in co-promotion (Notice SI/17/2019).

Immunomodulatory Maresin-1 Loaded Zein Nanoparticles to Induce Pro-Regenerative Microenvironments

Ana Beatriz Sousa[1,2,3*], Cláudia Martins[1,2,4], Bruno Sarmento[1,2,5], Mário Adolfo Barbosa[1,2,3] and Judite Novais Barbosa[1,2,3]

[1]i3S – Instituto de Investigação e Inovação em Saúde, Universidade do Porto, Rua Alfredo Allen 208, 4200-135 Porto, Portugal
[2]INEB – Instituto de Engenharia Biomédica, Universidade do Porto, Rua Alfredo Allen 208, 4200-135 Porto, Portugal
[3]ICBAS – Instituto Ciências Biomédicas Abel Salazar, Universidade do Porto, Rua de Jorge Viterbo Ferreira 228, 4050-313 Porto, Portugal
[4]FEUP – Faculdade de Engenharia da Universidade do Porto, Rua Dr. Roberto Frias s/n, 4200-465 Porto, Portugal
[5]CESPU – Instituto de Investigação e Formação Avançada em Ciências e Tecnologias da Saúde, Rua Central de Gandra 1317, 4585-116 Gandra, Portugal
[*] anabsousa@i3s.up.pt

INTRODUCTION

The incidence of chronic wounds is escalating worldwide. The associated healing process is especially problematic in population that are aging and show increased morbidity[1]. The search for strategies that will improve tissue repair is at the cutting edge of regenerative engineering.

The main goal of this research work is to develop an innovative strategy consisting of zein monodisperse nanoparticles loaded with maresin-1 to induce a pro-regenerative microenvironment that will accelerate wound healing, ultimately providing an effective strategy for the rapid healing of wounds.

Zein is an insoluble prolamin protein that is extracted from corn that was approved in 1985 by the FDA. The utilization of zein was reported for several applications such as a platform for drug delivery and for tissue engineering[2].

Maresin-1 is a potent immunoresolvent, biosynthesized in inflammatory exudates to control inflammation via stimulating resolution programs through limiting polimorphonuclear (PMN) leukocytes infiltration and enhancing macrophage uptake of apoptotic PMNs, the hallmark of pro-resolving mechanisms and critical for the inflammatory response to switch off [3].

EXPERIMENTAL METHODS

The Dolomite Microfluidics® chip was used as platform to load maresin-1 into zein nanoparticles. The organic phase consisted of a mixture of 1% (w/v) of zein and maresin-1 in 70% ethanol , whereas the aqueous phase consisted of Milli-Q water. The nanoparticles were produced by flow-focusing the organic central stream with the aqueous outer fluid. The final solution was magnetically stirred for 3h at room temperature and centrifuged for 15 minutes through a filter device with a molecular weight cutoff of 100kDa at 2000g. Liquid suspensions of unloaded and maresin-1 loaded zein nanoparticles were stored at 4°C for 30 days after production. The particle size, size distribution, and zeta-potential were assessed, as well as the amount of maresin-1 recovered. The ability of maresin-1 loaded zein nanoparticles to affect the cell viability was assessed in both primary human macrophages (isolated from healthy blood donors) and primary human dermal fibroblasts. The capacity of these nanoparticles to affect macrophage polarization was also evaluated.

RESULTS AND DISCUSSION

Zein nanoparticles, both empty and encapsulated with maresin-1, presented average diameter values in the range of 150–190 nm, narrow size distribution (polydispersity index < 0.2), and zeta potential of around + 20 mV. Aqueous suspensions of zein NPs were stable for at least 1 month when stored at 4 °C. Maresin-1 alone and maresin-1-loaded zein nanoparticles presented low cytotoxicity to human macrophages and fibroblasts. Moreover, its effect did not alter cell morphology. The effect of the nanoparticles on cell proliferation and macrophage polarization is being evaluated.

CONCLUSION

Maresin-1 loaded zein nanoparticles were successfully produced. The newly developed nanoparticles were not cytotoxic to both human macrophages and fibroblasts. In addition, normal cell morphology was maintained up to 7 days of culture.

REFERENCES

1. Sorg H. *et al*., Eur. Surg. Res., vol. 58, no. 1–2, pp. 81–94, 2017.
2. Abdelsalam A.M. *et al*., Pharmaceutics, 13(9): 1354, 2021.
3. Chiang N. *et al*., J Clin Invest., 129(12):5294-311, 2019.

ACKNOWLEDGMENTS

The authors would like to thank Norte Regional Operational Program: Structured R&D&I Projects – Unorte.pt. HEALTH-UNORTE; NORTE-01-0145-FEDER-000039 for providing financial support to this research work.

Silica Dioxide Nanofiber Based Drug Delivery System for Wound Healing

Hana Tománková[1*], Miroslava Rysová[1], Alena Ševců[1]

[1] Institute for Nanomaterials, Advanced Technologies and Innovation, Technical University of Liberec, Czech Republic
[*] hana.tomankova@tul.cz

INTRODUCTION

Bacterial contamination is one of the main causes of impaired healing of chronic wounds which affects a significant part of population in developed countries[1]. However, treatment with broad-spectrum antibiotics administered orally or intravenously may cause systemic overload, organotypic toxicity, development of bacterial resistance or other adverse events. We have developed an innovative drug delivery system (DDS) based on silica dioxide nanofibers for *in situ* release of active compounds, able to increase their bioavailability. Thanks to their chemical structure, metal oxides are commonly used for developing materials suitable for further functionalization. We took advantage of primary amino groups implication to the surface to enable drug conjugation through covalent binding or electrostatic interactions. The system has been tested with several types of antibiotics and its antibacterial activity and biocompatibility have been verified not only *in vitro* but also *ex vivo*. The sustained release of model tetracycline antibiotic was proven *in vitro*.

EXPERIMENTAL METHODS

The silica nanofibers were electrospun using the NanoSpider (Elmarco™) device and thermally treated (180° C) to prolonge their stability. Surface functionalization was ensured via silanization with aminopropyltriethoxysilane. The antibiotic (ATB) was immobilized by incubating the nanofibers in the active substance solution. Different types of drug delivery system were prepared by different combination of a certain type of nanofibers (with or without silanization) with washing conditions after antibiotic binding (with or without washing). The amount of ATB bound and subsequently released by the system was quantified spectrophotometrically. The antibacterial activity of the system was tested *in vitro* on two types of non-pathogenic bacteria (via disc diffusion method) and *ex vivo* on multispecific biofilm. The biocompatibility of the system was also verified *in vitro* and *ex vivo*, via testing of mitochondrial activity in 3T3 fibroblast cells and cell viability on reconstructed epidermis (Epiderm, MatTek™) respectively. Release kinetic studies were studied spectrophotometrically using Franz diffusion cell set-up and via gel-based transfering test. The moisture vapour permeability was determined according to The European Standard EN13726 method. The wettability was identified via water contact angle measurement.

RESULTS AND DISCUSSION

Biocompatibility (fig.1) and antibacterial activity of SiO_2 based DDS (fig.2) were proven using multiple complementary methods *in vitro* and *ex vivo*.

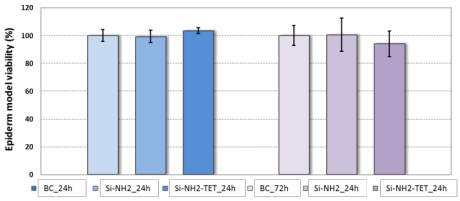

Figure 1: Skin irritation testing on the model of skin epidermis (Epiderm™, MatTek)

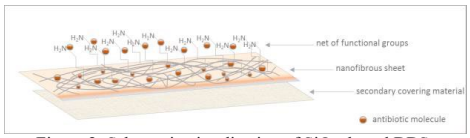

Figure 2: Schematic visualization of SiO_2 -based DDS

Other parameters essential for modern wound dressing, such as moisture vapor permeability (necessary for sufficient air access), appropriate wettability (ensuring exudate removal) or sufficient porosity (preventing the passage of microbes from the outside and secondary contamination) were also verified.

CONCLUSION

The proposed DDS based on inorganic silica nanofibers represents an innovative device for impaired and contaminated wounds healing. The drug released directly in the wound site can be applied separately or serve as a supportive therapy for systemic treatment potentially leading to increased therapy effectiveness and possibly lowering the systemic drug load of the whole organism.

REFERENCES

1. Sen C. K. *et al*. Adv. in Wound *C. 8* (2): 39–48, 2019

ACKNOWLEDGMENTS

The authors would like to thank the Technology Agency of the Czech Republic (Project no: TH02020786) for providing financial support to this project and to projects HRA 2 and Hyhi (Reg. No. CZ.02.1.01/0.0/0.0/16_019/0000843) for the financial support of the ESB 2022 conference attendance.

Investigation of an *ex vivo* fracture bone model and formulation of therapeutics to prevent infection and excessive necrosis post traumatic injuries

Miruna Chipara[1,2,3], Richard Moakes[1], Benjamin Freedman[2,3], Alexander M. Tatara[3], Amy Naylor[4], Alexander Stoll[5], David J. Mooney[2,3], Liam M. Grover[1]

[1] *Healthcare Technologies Institute, School of Chemical Engineering, University of Birmingham, Birmingham, UK.*
[2] *John A. Paulson School of Engineering and Applied Sciences, Harvard University, Cambridge, MA, USA.*
[3] *Wyss Institute for Biologically Inspired Engineering, Center for Life Sciences, Boston, MA, USA.*
[4] *Institute of Inflammation and Ageing, Medical School, University of Birmingham, Birmingham, UK.*
[5] *Defence Science and Technology Laboratory, Ministry of Defence, Salisbury, UK.*
Corresponding/Presenting author email: m.chipara@pgr.bham.ac.uk

INTRODUCTION

While gunshot and bomb-related injury care remains sadly relevant to this day, injury profile and intervention practices are still poorly understood and limited. Bone damage following blast or ballistic wounding results in the mechanical destruction and death of tissue at the site of injury. Surgeons debride the tissue, removing any necrotic regions but bone continues to turn gradually necrotic, thus the wound remains open, increasing the risk of infection. Currently there are no methods that enable full characterisation of such fragments in anatomically relevant positions within the fracture. Structured or fluid-gel materials, have been used as support matrices in which cell bearing gels can be immobilised, allowing for the construction of large and complex tissues[1,2,3]. We have recently explored the possibility of using these materials to support and process tissue fragments such that they could be maintained in an anatomically relevant configuration *ex-vivo*. Additionally, current interventions are still limited to the use of standard bandages and systemic administration of antibiotics which is not that optimal. The Mooney lab designed a tough adhesive biomaterial which is able to adhere to a myriad of surfaces and deliver compounds locally[4]. Thus, we formulated this adhesive biomaterial to deliver proteins that promote bone regeneration (VEGF, BMP-2) and minimise inflammation (sgp130Fc), as well as antimicrobial agents (vancomycin, gentamicin, silver nanoparticles) to improve early wound intervention which could be vital for the healing outcome. Here we report the development of an *ex-vivo* model of fracture repair, which has been used to evaluate the efficacy of a novel PEG gel in the delivery of agents capable of preventing non-union.

EXPERIMENTAL METHODS

***Ex-vivo* model**: Fresh rat and mouse fractured bones were added to a polyethylene glycol (PEG) fluid gel support medium which was fabricated as previously described [3]. A fibrin gel was injected in between the fracture site (process exemplified in **Fig. 1**). Rheological properties of 5% PEG quiescent gel and fluid gels under 500 and 700 rpm were assessed using a Kinexus Rheometer. Diffusion properties were assessed by measuring the release of fluorescein using a microplate reader. Fibrin gels were prepared and delivered as described earlier [2].

Compound delivery: Tough adhesive gels were synthesized as previously described[4]. A biopsy puncher (6 mm diameter) was used to produce gel samples for release kinetics and infection studies. Gel samples were dehydrated in air at room temperature, followed by loading with cytokines and antibiotics (overnight in 4 °C). ELISA and Pierce BCA assays were used to measure release kinetics on a 2-week period with daily measurements. Disk diffusion studies were conducted in Tryptic Soy Agar with 5% sheep blood plates inoculated with 1 x 10^6 cfu *S. aureus* bacteria.

RESULTS AND DISCUSSION

Ex-vivo models are utmost important in the case of traumatic injuries where *in vitro* cultures are unable to replicate the wounding scenario and *in vivo* experiments are difficult to be carried on. The support medium plays a vital role in maintaining the viability of the tissue *ex-vivo*, therefore, to test the capability of PEG gels to deliver nutrients to the encapsulated bones, as well as to eliminate metabolic waste, we analyzed the rheological and diffusion properties. As shown in **Fig. 1**, the fluid gel sheared at 700 rpm displayed most favorable properties due to a smaller particulate system that allows for a better diffusion. A fluid gel has the property to self-heal, thereby providing support to another gelling material to be printed by dispersing it into the interstices of the supporting fluid gel particles. This enables relatively complex structuring, whilst providing sufficient support to prevent the structure from collapsing under its own weight and preserving the bony ends in a relevant anatomical configuration. Fibrin gel was selected as the bridging material due to its structural and biochemical similarities to the microenvironment of the callus formed early in fracture healing. Cells were able to migrate into the fibrin gel within a few days and displayed an early osteocyte marker, podoplanin as early as one week, to three weeks in culture. Moreover, after 25 days, extracellular matrix surrounding an organised cell network resembled mineral deposition in bone. Additionally, finding better therapeutics for early intervention following injury is critical for minimising the risk of infection and excessive necrosis and facilitate wound healing. The benefit of the adhesive biomaterial is that it could be wrapped around the exposed bone tissue and its release kinetics allow for a sustained gradual local delivery of active agents for a period of at least 10 days which is the necessary time window after these types of traumatic injuries. Antimicrobial activity has only been tested against a *S. aureus* strain so far (**Fig. 2**), but we are in the process of conducting more experiments including a few other types of bacteria such as *E. coli*, *P. aeruginosa*, *E. cloacae*, *A. baumanii*, and *Streptococcus haemolyticus*, most commonly occurred infections in ballistic and blast injuries. Early antimicrobial intervention is critical due to the extended time between opening and closing of the wound and the unsterile nature of the blunt force traumatic injury. It has been observed that the bacterial load in a traumatic wound can increase 10 times within a 24-hour period and it is considered to be a causation factor for delayed non-unions or amputations.

CONCLUSION

In conclusion, we have developed a model of fracture repair that will enable us to characterize the efficacy of novel materials to deliver therapeutics that may be effective in preventing fracture non-union.

REFERENCES

1. Cooke M.E. *et al., Adv. Mat.* 30.14: 1705013, 2018.
2. Iordachescu A. *et al., Adv. Biosystems.* 2.2: 1700156, 2018.
3. Foster N.C., Moakes R.J.A. *et. al., Adv. Healthcare Mat.* 2021, 10, 2100622.
4. Freedman, B.R. *et al., Nat. Biomed. Eng.* (2022).

ACKNOWLEDGMENTS

The authors would like to thank the EPSRC and DSTL (No. EP/S023070/1), as well as the Fulbright Commission for providing financial support to this project.

Cell carriers suitable for culturing human corneal epithelial cells for the production of tissue-engineered human corneal epithelium

Gaëtan. Le-Bel[1,2,*], Pascale Desjardins[1,2], Christelle Gross[1,2], Carina Koppen[3], May Griffith[4], Lucie Germain[1,2] and Sylvain Guérin[1,2].
[1]Département d'ophtalmologie, Université Laval, CUO-recherche/LOEX, Centre de recherche du CHU de Québec - Université Laval, Québec, QC, Canada.
[2]Département de chirurgie, Université Laval, Centre de recherche en organogénèse expérimentale de l'Université Laval/LOEX, Centre de recherche du CHU de Québec - Université Laval, Québec, QC, Canada.
[3]Department of Ophthalmology, University Hospital Antwerp, Antwerp, Belgium.
[4]Laboratoires Antoine Turmel Polyclinique de l'Hopital Maisonneuve-Rosemont Montreal, Québec, Canada.
[*]gaetan.le-bel@crchudequebec.ulaval.ca

INTRODUCTION

The culture of human corneal epithelial cells (HCECs) in vitro has many clinical and research applications in the treatment of corneal pathologies such as limbal stem cell deficiency[1]. In this case, it is necessary that culture conditions allow a good proliferation of HCECs by delaying their terminal differentiation in order to ensure the long-term regeneration of the corneal epithelium. For the production of tissue-engineered corneas, several carriers can be used to cultivate and graft HCECS: human amniotic membranes (HAMs)[2], collagen gels (CGs)[3], human fibrin gels (HFGs)[4] and human corneal stromas (HCSs)[5] produced by the self-assembly approach. Our goal is to determine which of these four carriers is the most effective at ensuring HCECs proliferation and regeneration of a pluri-stratified corneal epithelium, a prerequisite for grafting of the tissue-engineered cornea.

EXPERIMENTAL METHODS

HCECs were seeded and grown as monolayers on four different cell carriers until 1 day post-confluence. Human tissue-engineered corneas (hTECs) were also produced by the self-assembly approach using the same populations of HCECs and wounded with a 8 mm biopsy punch. Wounded HTECs were then deposited on the four different carriers and corneal wound healing monitored until complete closure of the wound. Histological and Immunofluorescence analyses were conducted on monocultures and healed hTECs to assess: the presence of a sub-population of corneal epithelial stem cells (ABCG2/ABCB5, ΔNp63α, K19 and K15), the integrity of the epithelial layer (Na+/K+-ATPase α1, K3/12, p63 and ZO-1), and the expression of basal membrane components (collagen IV and laminin V).

RESULTS AND DISCUSSION

The rate of wound closure was increased when wounded hTECs were grown on HAM. The rate of wound closure was similar when wounded hTECs were grown on HCSs, HFGs and GC. For the various conditions, histological sections showed the presence of a corneal epithelium in the healed central area of the wounded hTECs.

CONCLUSION

The hCECs' proliferative potential was affected by the nature of the carrier as we noted a marked increase in the wound healing dynamic when wounded hTECs were deposited on the HAM. This study provide valuable data on the culture conditions required to yield hCECs with the best proliferative and differentiation properties in order to ensure the production of hTECs with an optimal quality. From a translational point of view, this study constitutes a major step forward in the production of a human corneal substitute that will be of a sufficient quality to be used in patients as a graft for corneal replacement in a near future.

REFERENCES

1. Rama, P., et al., N Engl J Med. 363(2): p. 147-55, 2010.
2. Zakaria, N., et al., Tissue Eng Part C Methods. 16(5): 921-927, 2010.
3. Fagerholm, P., et al., Biomaterials. 35(8): p. 2420-7, 2014.
4. Le-Bel, G., et al., Am J Ophthalmol Case Rep. 15: p. 100532, 2019.
5. Proulx, S., et al., Mol Vis. 16: p. 2192-201, 2010.

ACKNOWLEDGMENTS

The authors would like to thank The Vision Health Research network and ThéCell for providing financial support to this project.

Development of novel wound dressing material composed of gelatin sponge and nanofiber

Shunsuke Shinoda[1], Koji Yamamoto[2], Yusuke Morita[2]

[1] Graduate School of Life and Medical Sciences, Doshisha University, Kyoto, Japan
[2] Department of Biomedical Engineering, Doshisha University, Kyoto, Japan
ctug0036@mail4.doshisha.ac.jp

INTRODUCTION

Gelatin sponges are used as wound dressing materials because of their high water absorbency and biocompatibility. It is important for wound dressing material to enhance fibroblast migration and proliferation in the healing process. Since gelatin nanofibers are a high specific surface area and cell adhesion, cell adhesion and migration into the gelatin sponge might be improved by fabricating the nanofiber layer on the wound side of the gelatin sponge. Though an electrospinning was generally used to fabricate nanofiber, it is difficult to fabricate nanofibers onto non-conductive materials. We proposed the spinning method to fabricate a nanofiber layer on the gelatin sponge with dielectric polarization. In addition, we proposed a non-woven layer of poly (L-lactic acid) (PLLA) nanofibers as the outer surface with air permeability and anti-infection capability. The purpose of this study was to develop the novel wound dressing material composed of gelatin sponge and gelatin nanofibers.

EXPERIMENTAL METHODS

The developed wound dressing material consisted of the gelatin sponge, the gelatin nanofiber layer as the wound-side surface and the PLLA nanofiber layer as the outer surface. Gelatin was dissolved in distilled water at concentrations of 2, 4, 6, and 8 w/v% to prepare the gelatin sponge. The solutions were then incubated at 4 °C until gelling. The resultant hydrogels were frozen at -25 °C for 24 hours and lyophilized for 24 hours. The size of gelatin sponge was 20×20×5mm. Gelatin nanofibers were fabricated on the gelatin sponge by an electrospinning. Gelatin was dissolved in 1,1,1,3,3-hexafluoro-2-propanol (HFIP) at concentration of 7 w/v%. The target surface of the gelatin sponge was charged negatively by applying a positive voltage to its reverse side. The target fiber diameter of gelatin nanofibers was 500 nm to mimic the collagen structure in the tissue. PLLA nanofiber layer was fabricated on the opposite side of the sponge by an electrospinning. PLLA was dissolved in a mixture of 1,3-dioxolane (DOL) and HFIP at the concentration of 8 w/v%. The volume ratio of DOL to HFIP was 70:30. Benzyltriethylammonium chloride was added to increase the charge density of the PLLA solution. The target pore size of the PLLA nanofiber layer was set to be less than a sterile filter pore size (0.45 µm) with air permeability and anti-infection capability. Surface and cross section of the wound dressing material were observed by a scanning electron microscope (SEM), and the pore size, fiber diameter and thickness were measured by the image analysis software.

RESULTS AND DISCUSSION

Figure 1 shows SEM image of the interface between the gelatin sponge and gelatin nanofibers. The gelatin nanofiber layer was tightly attached on the gelatin sponge by the proposed electrospinning method. The pore size of the gelatin sponge decreased with increasing gelatin solution concentration. It was reported that the fibroblasts showed best cell growth in the sponge scaffold with pore size of 186-200 µm2. The gelatin sponge with similar pore size of 200 and 150 µm were obtained at solution concentrations of 2 and 4 w/v%. Figure 2(a) shows an SEM image of gelatin nanofiber layer at a concentration of 7 w/v%. The fiber diameter and thickness of the gelatin nanofibers layer were 465 ± 75 nm and 3 µm. Gelatin and PLLA nanofiber layers exhibited excellent adhesion with gelatin sponge during water immersion. Figure 2(b) shows the SEM image of PLLA nanofiber layer at a concentration of 8 w/v%. The diameter of PLLA nanofibers was 170 ± 29 nm and the pore size was 0.27 µm. Since the pore size was smaller than the pore size of a sterile filter (0.45 µm), it is expected that the PLLA nanofiber layer could work as outer surface with air permeability and anti-infection capability. The developed wound dressing material might be effective for wound healing due to acceleration of cell adhesion and migration.

CONCLUSION

We succeeded to develop the novel wound dressing material by fabricating gelatin and PLLA nanofiber layers on the gelatin sponge directly with the proposed spinning method.

REFERENCES

1. Landén NX., *et al*., Cell. Mol. Life Sci. 73(20):3861–85, 2016
2. Oh, Se Heang, *et al*., Biomaterials. 28:9:1664-1671, 2007

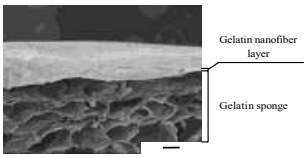

Figure 1: SEM image of the interface between the gelatin sponge and gelatin nanofiber layer (× 100, Bar: 100 µm)

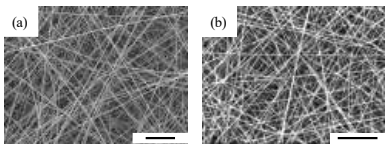

Figure 2: SEM images of the nanofiber;
(a) gelatin (× 2000, Bar: 10 µm),
(b) PLLA (× 5000, Bar: 5 µm)

Mucoadhesive Injectable Hydrogel Enriched with Encapsulated Pro-healing Protein for Hard-to-heal Oral Wounds Treatment

Zuzana Kadlecová[1], Matej Dzurov[1], Klára Lysáková[1], Lucy Vojtová[1]

[1]CEITEC - Central European Institute of Technology, Advanced Biomaterials Group, Brno University of Technology, Brno, Czech Republic

Zuzana.Kadlecova@ceitec.vutbr.cz

INTRODUCTION

Extensive wounds at the oral mucosa, formed after plastic or tooth extraction surgeries, are hard-to-heal. Such wounds also heal in a slightly different manner than skin wounds and tend to shrink during the healing process, leading to a speech impediment or distortion of the face shape of the patient[1]. To heal these wounds, injectable mucoadhesive material is an ideal candidate to prevent shrinkage and, at the same time, promote wound closure and regeneration[2].

This work aims to prepare an injectable thermosensitive drug delivery system with mucoadhesive properties enriched with pro-healing protein – stable fibroblast growth factor-2 (FGF2-STAB®), which stimulated re-epithelization and promotes overall tissue regeneration[3]. The mucoadhesive injectable hydrogel is based on poly(lactide-*co*-glycolide) and poly(ethylene glycol) copolymer (PLGA-PEG-PLGA) functionalized with itaconic anhydride (ITA), which embodies the mucoadhesive functional groups to the polymer, patented by BUT[4].

Our previous study discovered that FGF2-STAB® interacts with the PLGA-PEG-PLGA/ITA matrix, and thereby its encapsulation into liposomes is expected to protect the protein from hydrolytic degradation. Liposomal FGF2-STAB® enriched PLGA-PEG-PLGA/ITA hydrogels are expected to show fewer polymer-matrix interactions leading to controlled release with first-order kinetics.

EXPERIMENTAL METHODS

The FGF2-STAB® was encapsulated into liposomes based on phosphatidylcholine and cholesterol involving the "heating method." Particle diameter was determined using the dynamic light scattering (DynaPro® NanoStar® (Wyatt Technology Corporation, United States), zeta potential using the ZetaSizer Nano ZS (Malvern, United Kingdom), and the encapsulation efficiency together with protein release were determined using Bradford protein assay on Ultraviolet-Visible light spectrophotometer Biochrom Libra S22 (Biochrom, United Kingdom). Liposomes were observed using Scanning Electron Microscope TESCAN MIRA3 (STEM; TESCAN, Czech Republic). The PLGA-PEG-PLGA/ITA copolymer was synthesized in glass reactors by Schlenk's technique. The molecular weight and polydispersity index was determined using gel permeation chromatography (GPC/MALS, Wyatt 1260 Infinity, Germany) and the degree of modification was determined using proton nuclear magnetic resonance (^{1}D NMR, Bruker, Germany).

The data were evaluated using the STATISTICA software. The $n=5$ for each sample and the average values and std. Deviations were assessed on the normality of the data.

RESULTS AND DISCUSSION

Prepared liposomes with diameters around 200 nm exhibited encapsulation efficiencies of FGF2-STAB® around 75 % and zeta potential around -21 mV. As seen in Fig. 1., agglomerates are still formed due to the particle charge. The release of FGF2-STAB® from the bioresorbable hydrogel is currently being evaluated.

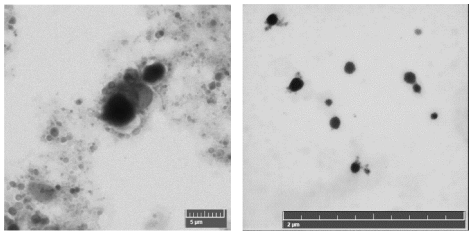

Fig. 1 STEM micrograph of liposomal FGF2-STAB® at 20.0 kV

CONCLUSION

Treating oral wounds with mucoadhesive injectable hydrogels represents a novel method for treating such hard-to-heal wounds. Due to the effective encapsulation of pro-healing protein and the first-order release from the hydrogel, this material is likely to overlap with clinical praxis eventually since both the liposomes and hydrogel can be lyophilized and prepared on a larger manufacturing scale.

REFERENCES

1. Mistry R.C. *et al.,* J. of Surgical Oncology. 91(2):131-133.
2. Kaldybekov D. B. *et al.* European J. of Pharmaceutics and Biopharmaceutics. 143:24-34.
3. Okabe K. *et al*. Modern Plastic Surgery. 3:108-112.
4. Vojtová L. et al., EP 3097134 B1, patent. (2017).

ACKNOWLEDGMENTS

This work was supported by the *ProfiBONE* project (TO01000309) that benefits from the EEA Grants and the TACR within the KAPPA Programme and within the project *Quality Internal Grants of BUT* (KInG BUT), Reg. No. CZ.02.2.69/0.0/ 0.0/ 19_ 073 / 0016948, financed from the OP RDE. *CzechNanoLab* project LM2018110, funded by MEYS CR is gratefully acknowledged for the financial support of the measurements/sample fabrication at CEITEC Nano Research Infrastructure.

Compositional Heterogeneity in Pathological Mineralized Tissues

Cong Sui, Richard L Williams, Neil Eisenstein, Tom Robinson, Liam M Grover

Healthcare Technologies Institute, Institute of Translational Medicine, School of Chemical Engineering, University of Birmingham, Birmingham B15 2TH, United Kingdom.
c.sui@bham.ac.uk

INTRODUCTION

Heterotopic ossification (HO) is the pathological formation of bone in soft tissues following severe traumatic injury. The rate at which HO is formed is significantly faster than normal bone (1.7 vs 1.0μm/day[1]) and at present, it is unclear how rapid deposition of bone mineral might influence its final composition. It might be expected that the rapid rate of formation may lead to the production of a chemically heterogeneous mineralized structure since the growth of bone requires a significant local concentrations of phosphate ions. At sites of HO, it is possible that this localised increase in phosphate is provided by platelets, which contain polyphosphate stored in amorphous calcium phosphate (ACP) granules. Indeed, these have been reported to aggregate around bone defects potentially serving as nuclei to enable bone growth.[2] ACP granules within platelets contain both adenosine triphosphate (ATP) and adenosine diphosphate (ADP). Moreover, remote hydrolysis of ATP by apyrase mitigates ectopic bone formation *in vivo*.[3] In this work, the chemical composition of HO bone is assessed using micro XRF and compared against normal bone. A mechanism was then proposed and tested that may explain any compositional variation within the pathological tissues.

EXPERIMENTAL METHODS

HO Sample slices. The HO samples from consented patients were embedded in optimal cutting temperature compound. They were then sectioned into 100μm thickness slices.

Synthesis of ATP-Amorphous calcium carbonate (ACC) and Mg-ACC nanoparticles. $CaCl_2$ solution was prepared with addition of ATP or $MgCl_2$, and Na_2CO_3 solution was then poured into the prior solution under vigorous agitation. The final products were ATP-ACC and Mg-ACC, respectively.

Conversion of ATP-ACC and Mg-ACC samples in P solutions. Both ACC sample powders were dispersed in P solution at 37ºC and 60ºC, respectively. The sample precipitates were obtained for further tests.

RESULTS AND DISCUSSION

The elemental distributions of HO slices excised at different duration from injury were investigated by XRF. The HO samples displayed Ca-rich (PO_4^{3-} deficient) leading edges (pink, arrowheads) growing into the collagen (blue, using Sulphur as a proxy), which indicates the initial formation of Ca-rich material in the soft tissue (Fig. 1A) with a calcium phosphate core towards the centre of the tissue. To investigate possible chemical mechanisms that would allow for the solid state conversion of the calcium carbonate, preceipitates were formed and stabilised with ATP[4].

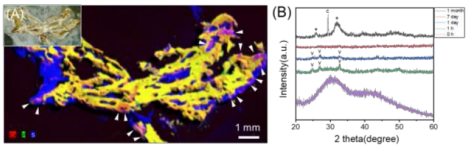

Fig. 1 (A) XRF image of HO sample slice from a patient. Red-calcium; green-phosphorus; blue-sulphur (representing collagen); pink-colocalisation of calcium and sulphur; yellow-colocalisation of calcium and phosphorus (representing CaP). Inset is corresponding its optical micrograph. (B) XRD patterns of ATP-ACC dispersed in SHPE at 37ºC from 0h to 1 month. Note: v, vaterite; c, calcite; *, apatite.

The as-prepared ATP-ACC was partially crystallised for 1 hour and mostly transformed into ACP after 7 days, followed by the final formation of HA after 1 month immersion in simulated human physiological environment (SHPE). Whereas, magnesium (Mg) stabilised ACC (without ATP) transformed into vaterite, calcite and ACP after 7 days. This suggests that in an ATP rich environment, such as a fracture callous, ACC could be stabilised and slowly converted into ACP through a solid-state route. In comparison, in the absence of ATP, ACP appeared to be deposited onto the surface of the CC crystals, suggesting a dissolution-precipitation mechanism. Notably, the conversion of ACC to HA was dramatically accelerated by the addition of ATPase.

CONCLUSION

Here, pathological bone was shown be chemically heterogenous with large areas of low phosphate mineral around the periphery of the tissue. This indicates that during the phosphate deficient form may be deposited first during the process of mineral formation. Our experiments show that this process could be attributed to the deposition and stabilisation of ACC in ATP-rich environment, with the mineral subsequently maturing, potentially following enzymatic destruction of the ATP.

REFERENCES

[1] B. Isaacson, *et al.*, JBJS 2016, 98, 647.
[2] W. E. Müller, *et al.*, Macromolecular Bioscience 2015, 15, 1182.
[3] J. R. Peterson, *et al.*, Science translational medicine 2014, 6, 255ra132.
[4] C. Qi, *et al.*, ACS Applied Materials & Interfaces 2014, 6, 4310.

ACKNOWLEDGMENTS

The authors would like to thank the injured military patients for providing their samples. We are also grateful to the Orthopaedic Research UK and Royal Centre for Defence Medicine for providing financial support.

Biodegradable wound dressing based on biopolymers

Hadda Zebiri[1*], Philippe Lavalle[2], Céline Des Courtils[3], Marilys Blanchy[4], Emmanuel Flahaut[1], Emmanuel Suraniti[4], Laura Duciel[3], Benjamin Levy[2], Emilien Chabrillac[5], Stéphane Lack[3], Agnès Dupret-Bories[5], Audrey Tourrette[1].
[1]CIRIMAT, University of Paul Sabatier III, Toulouse, France
[2] INSERM, University of de Strasbourg, Strasbourg, France
[3] Brothier, Nanterre, France
[4]Rescoll, Pessac, France
[5]University Institute of Cancer in Toulouse Oncopole, Toulouse, France
[*] hadda.zebiri@univ-tlse3.fr

INTRODUCTION

Polysaccharide-based wound dressings have been widely investigated in tissue engineering, in particular, alginate and chitosan as biocompatible biopolymers. Alginate presents good swelling abilities and is already used as wound dressing. **Algosteril®** is a resistant non-woven wound dressing based on predominantly guluronic calcium alginate. It accelerates wound healing by eliminating wound fluids, maintaining a favorable moist environment and by the calcium-dependent activation of cells involved in tissue repair.[1] However, it is not resorbable. Mannuronic alginate are more absorbable than guluronic alginate, they are however less resistant. Chitosan is biodegradable and presents anti-microbial and good mechanical properties.[2] The combination of alginate and chitosan as polyelectrolyte complexes (PECs) results in absorbent matrices with good mechanical properties.[3] The aim of this study is to elaborate a resorbable wound dressing for surgical applications exhibiting comparable properties to Algosteril (high swelling ability, good mechanical properties with a resorption time of one month). The strategy is to use mannuronic alginate and to compare different alginate/chitosan mass ratios. In this study, we evaluated the swelling ratio, the *in vitro* degradation, the *in vitro* cytotoxicity and the mechanical properties of PECs matrixes.

EXPERIMENTAL METHODS

Mannuronic Alginate was supplied by BROTHIER and Chitosan (DD= 88%) was purchased from ChitoLytic.

Elaboration of the polyelectrolyte complexes (PECs)
Chitosan solution (1.5% w/w) containing 0.34% v/v of acetic acid and alginate solution (1.5 %w/w) were mixed for 10 min using an ultra-turrax mixer according to two mass ratios of alginate/chitosan (80/20 and 70/30). The resulting PECs were partially dried in an oven at 50 °C for 6 h. These PECs were treated with a solution of $CaCl_2$ (1% w/v) then dried by freeze- drying for 24h.

Swelling and *in vitro* degradation studies were performed in PBS (pH=7.4) or NaCl 0.9% (pH= 7.34) at 37°C for 30 days. The swelling ratio in terms of percentage was calculated according to the equation:

$$Swelling\ (\%) = [(m_w - m_i)/m_i] \times 100\ (\%)$$

Where m_w is the mass of the samples in their wet state and m_i, their initial mass (n=3).

The *in vitro* degradation was evaluated by the mass loss of the samples according to the equation:

$$Mass\ loss\ (\%) = [(m_i - m_d)/ m_i] \times 100\ (\%)$$

Where m_d is the mass of the samples in their dry state.

Suture retention strength were measured using a texturometer to evaluate the capacity of PECs matrices to withstand suturing.

Evaluation of the *in vitro* cytotoxicity was performed on the extracts of PEC matrices by MTT assay according to the ISO 10993-5 standard.

RESULTS AND DISCUSSION

We obtained white and macroporous PEC matrices. They presented high swelling ratios (> 2500%), which were more significant with 80/20 mass ratio (figure. 1).

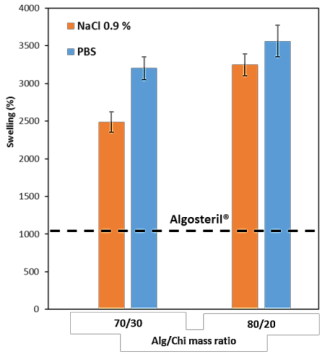

Figure.1 Swelling ratio of PECs matrixes

The PEC matrices degraded *in vitro* in both mediums. For all the alginate/chitosan mass ratios, the degradation rates were higher in PBS (80%) than in NaCl 0.9% (45%). All the PEC matrices were suturable and matrices with a mass ratio of 70/30 presented higher suture retention strength. The *in vitro* cytotoxicity results showed that matrices with a mass ratio of 80/20 were not cytotoxic. The alginate/chitosan mass ratio seems to impact the properties of PEC matrices.

CONCLUSION

PEC matrices based on alginate and chitosan were elaborated. They were highly absorbent, degradable and suturable. A sterilization study is currently in progress to evaluate its impact on the PEC wound dressings.

REFERENCES

1. Polym. Adv. Technol. 19, 6–14 (2008).
2. Carbohydr. Polym. 261, 117578 (2021).
3. Carbohydr. Polym. 172, 142–151 (2017).

ACKNOWLEDGMENTS

The authors would like to thank the French National Research Agency (ANR-20-CE19-0022-01) for providing financial support to this project.

Development of platelet lysate and collagen foams for tissue engineering

Fahd Tibourtine[1], Agnès Dupret-Bories[1,2], Philippe Lavalle[3], Thibault Canceill[1], Andrea Marfoglia[1], Clementine Aubry[4], Sophie Cazalbou[1*]

[1] CIRIMAT, University of Toulouse, CNRS, INPT, UPS, Université Paul Sabatier, France
[2] ENT and cervico-facial surgery, Claudius-Regaud Institute, IUCT Toulouse. France
[3] INSERM UMR 1121, Université de Strasbourg, France
[4] ARNA, Université de Bordeaux, INSERM U1212, CNRS, Bordeaux, France
[*] Sophie.cazalbou@univ-tlse3.fr

INTRODUCTION

Biopolymers are commonly used in the field of tissue engineering for their biocompatibility and biodegradability[1]. Among them, platelet lysate (PL) and collagen are promising compounds for developing bioactive and biomimetic three-dimensional biomaterials capable of promoting tissue repair. Platelet lysate (PL) is a blood derivative that contains coagulation factors and many bioactive molecules (growth factors, cytokines) able to promote the regeneration of various tissues[2]. Type I collagen (ColI) is the most abundant protein in the human body and the major component of the extracellular matrix. In addition to the ability to form three-dimensional networks, collagen fibers have particularly interesting mechanical properties, notably a great tensile strength[3]. Our project attempts to set up a shaping process, using supercritical CO_2[4] which allows the elaboration of sterile and bioactive foams, based on collagen and platelet lysate.

EXPERIMENTAL METHODS

Foams of Platelet lysate and collagen preparation. Platelet lysate was mixed with NaCl, tranexamic acid, and calcium chloride. Solutions with different concentrations of collagen were prepared from a stock solution according to the supplier's instruction (10.2 mg/ml, Corning). The LP and ColI solutions were then cold mixed 50:50 (v/v) to form a homogeneous solution, which after 30min of incubation at 37°C allowed the obtention of hydrogels. The hydrogels were put in successive baths of acetones and then they were rinsed several times with liquid CO_2 (4°C, 42Bar) before going to the supercritical state (41°C, 94 Bar) (E3100 Critical Point Dryer)

Foams characterization. Scanning electron microscopy observations were performed on the different obtained foams. The pore size distribution of foams was determined by mercury porosimetry (AutoporeIII, Micrometrics US). The mechanical properties of the foams were compared by compression tests (TA.XT Plus Texture Analyzer, Texture technologies).

In order to evaluate the kinetics of release of the growth factors, VEGF was considered as a control growth factor and its release was studied over time by ELISA test (Human VEGF, Biogems).

RESULTS AND DISCUSSION

The elaboration process allows to obtain dry foams (fig. 1) which maintain the 3D structure observed on the hydrogels. Scanning electron microscopy observations reveal that the concentration of collagen affects the density of the networks formed (fig. 2). Mercury porosimetry showed that the foams have high porosity, namely around 90%. The ELISA test confirmed the release of VEGF which proves that the foams can provide cellular bioactivity.

Compression tests have shown that mechanical properties are directly proportional to collagen concentration.

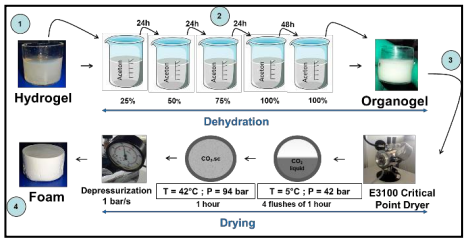

Figure 1. Shaping process of the foams.

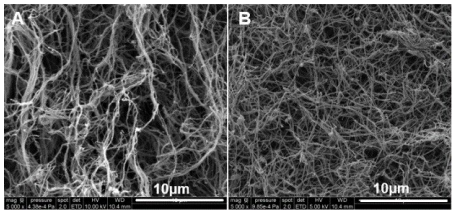

Figure 1 : Scanning electron microscopy images of the platelet lysate and type I collagen foams. A) 2.5mg/mL / B) 5 mg/mL.

CONCLUSION

We have succeeded in setting up a shaping process that allows us to obtain a dry, porous and bioactive collagen and platelet lysate foam that preserves the 3D structure of the network formed during gelation.

The *in vitro* and *in vivo* cellular behavior of the different foams will be evaluated and compared in order to determine the best formulation for tissue repairing purposes.

REFERENCES

1. Coradin T. *et al*., Gels. 6:1-22, 2020
2. Burnouf T *et al*., Biomaterials.76:371-387, 2016
3. Ruth N. *et al*., Polymers. 13:1-19, 2021
4. Canceill T, Doctoral Dissertation, 2021

ACKNOWLEDGMENTS

This work has been supported by the ministry of higher education and research and by the doctoral school of material sciences of Toulouse (ED 482).

Iodine releasing antimicrobial wound dressings for burn wound healing

Arn Mignon[1,*], Tom Gheysens[2], Sander Walraet[2], Pieter Tack[4], Petra Rigole[3], Tom Coenye[3], Laszlo Vincze[4], Sandra Van Vlierberghe[2], Peter Dubruel[2]
[1]Department of Materials Engineering, Campus Group T, KU Leuven, Leuven, Belgium
[2]Department of Organic and Macromolecular Chemistry, Ghent University, Gent, Belgium
[3]Laboratory of Pharmaceutical Microbiology, Ghent University, Gent, Belgium
[4]Department of Chemistry, Ghent University, Gent, Belgium
[*] Arn.Mignon@KULeuven.be

INTRODUCTION

It is estimated by the WHO that burn injuries are responsible for 180 000 deaths globally every year, forming a global public health problem[1]. A large contributor to this is bacterial infection. In the current treatment of burn wounds, a wide range of antimicrobial compounds can be used to treat the infections. Iodine-based antibacterials such as povidone-iodine (PVP-I) have been proposed as an alternative to silver due to a lack of reported bacterial resistance[2], however when applied, it often induces a burst release. The objective of the current work is to create a hydrogel-based burn wound dressing with an incorporated antimicrobial PVP-I complex, to achieve a more sustained release.

EXPERIMENTAL METHODS

Acrylated poly(ethylene glycol) (PEG) based polymers with varying molar masses were synthesized according to standard in-house protocols and subsequently processed into UV-cured sheets. These sheets were saturated in ultrapure water and subsequently incubated in a Lugol's solution (weight ratio of KI:I2 is 1:1.576) with varying concentrations. After impregnation, they were quenched for 24h and dried in a vacuum oven. After confirmation of the iodine concentration with X-ray fluorescence spectroscopy, UV-VIS spectroscopy was used to measure the release kinetics. Finally, antimicrobial tests were performed on agar plates to determine the inhibition zones. All tests were performed in triplicate. To compare the means of two groups, an independent two-sample t-test was used.

RESULTS AND DISCUSSION

We developed a hydrogel-based burn wound dressing with prolonged antimicrobial properties by incorporating an iodine complex inside a hydrogel material. Initially, the hydrogel material was synthesized and optimized, showing good mechanical properties for all different molar masses (PEG backbones of 2000, 10 000 and 20 000 g/mol). However, 10 and 20K backbones additionally showed much higher swelling ratios than 2K, essential for the ability to strongly take up exudate from the wound. When PVP was added to 10 and 20K, their swelling ratio significantly decreased, though still outperforming commercially available wound dressings. After incorporation of povidone-iodine into the hydrogel materials, these were compared to the commercially available Iso-Betadine Tulle (IBT, 10%) and similar iodine concentrations (Figure 1, top) were incorporated in the synthesized hydrogels as present in IBT. In contrast to IBT that showed a burst release (half of the iodine released from the sample in 37sec), our new PVP-containing hydrogel materials showed a prolonged (half-time) release of iodine over a timeframe of 30 to 140 minutes and sustainable release afterwards. Antibacterial testing via the agar diffusion assay (Figure 1, bottom), showed a similar initial trend as the release profile for IBT, with a big inhibition zone during a short duration, and a moderate inhibition zone for prolonged times for our hydrogel materials. The best antimicrobial hydrogel material was with a backbone of 10K exhibiting an optimal balance between a strong swelling of 43 times its own weight, a large inhibition zone after 24h and a more prolonged release with half of it released after 1 hour 43 minutes.

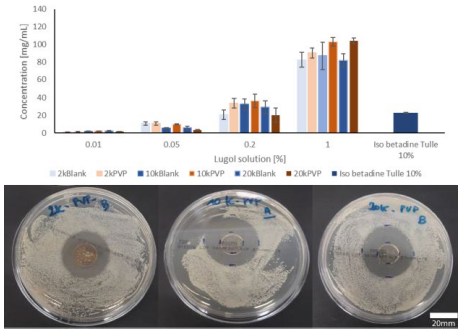

Figure 1. (top): Iodine concentration (mg/ml) of hydrogel sheets soaked in different Lugol's solution. (bottom) Agar disk diffusion test after 24 hours for discs of 2kPVP (a), 10kPVP (b) and 20kPVP (c).

CONCLUSION

Within this study, new hydrogels have been developed for burn wound healing, with an incorporated PVP-I complex. These hydrogels have significantly stronger swelling capacities than currently existing commercial dressings and induce prolonged and strong antimicrobial properties. One should keep in mind that for reasons of comparison to the state-of-the-art, we kept the iodine concentrations similar to Iso-Betadine Tulle in this study. It is therefore likely that increasing these concentrations in the future, could lead to even better results.

REFERENCES

1. seen at 28/04/2021 WHO. ttps://www.who.int/news-room/fact-sheets/detail/burns.
2. P. L. Bigliardi et al., Int. J. Surg., **44**:260–268, 2017

ACKNOWLEDGMENTS

The author would like to acknowledge Research Foundation Flanders (FWO) for financial support.

Fabrication of 6-BromoIndirubin-3'-Oxime Incorporated Guanosine Diphosphate Crosslinked Chitosan Scaffolds to Promote Osteogenic Differentiation in Myoblastic C2C12 Cells

Celine J. Agnes[1], Adrien Takada[2], Monzur Murshed[3,5], Bettina M. Willie[1,4,5], Maryam Tabrizian[1,3]

[1] Department of Biomedical Engineering, [2] Institute of Parasitology, [3]Faculty of Dentistry, [4] Department of Pediatric Surgery, McGill University, Montreal, Quebec, Canada

[5] Shriner's Hospital for Children, Montreal, Quebec, Canada

Email: Celine.agnes@mail.mcgill.ca

INTRODUCTION: Critical size bone defects derive from traumas, infections, or tumor resections where large pieces of bone need to be removed therefore not allowing the bone to heal itself adequately[1]. Thus, healing critical size defects remains a major unmet clinical challenge. To encourage healing within these defects, researchers work on designing biological substitutes which mimic endogenous bone healing within the defect site. Our laboratory has previously developed one of these biological substitutes, the guanosine diphosphate (GDP) crosslinked chitosan scaffold, which gels in 1.6 seconds allowing for localization at injection site[1,2]. The objective of this research is to fabricate a new formulation of this scaffold incorporating 6-Bromoindirubin-3'-Oxime (BIO) and pyrophosphatase (PPTase). The addition of BIO is expected to promote osteogenic differentiation through mimicking of the Wnt signaling pathway[3] and PPTase is expected to promote mineralization since it allows GDP to act as a reservoir for phosphate ions[1]. Our hypothesis is that this combination will promote osteogenic differentiation and mineralization of cells within our scaffold. Therefore, an additional goal of this research is to assess the beneficial effects of these encapsulants both together and separately on myoblastic C2C12 cells.

METHODS: To fabricate the BIO incorporated scaffold, two BIO doses (10, 100 μM) were tested, and incorporation was confirmed using NMR. Material characterization experiments were conducted including gelation time measurements, rheological studies, and MicroCT/SEM for structural architecture. In addition, a Live/Dead assay was conducted on pre-osteoblastic MC3T3 cells to confirm cellular viability in this formulation. For BIO/PPTase encapsulation experiments, BIO dosages were decreased to 1 and 10 μM and myoblastic C2C12 cells were encapsulated. Preliminary tests were run to ensure cellular compatibility including AlamarBlue for metabolic activity, and Hoescht 33342 and Phalloidin staining for distribution. The effects of BIO and pyrophosphatase on osteogenic differentiation were assessed both separately and jointly using an ALP production assay and qPCR gene expression studies for osteogenic markers such as RUNX2, OSX, ALPL, COL1A1, and OCN.

RESULTS/DISCUSSION: The fabrication of the new BIO incorporated scaffold was successful with solid-state NMR spectra showing a novel concentration-dependent peak at 41 ppm, which could be attributed to an interaction between chitosan and BIO. The addition of BIO still allowed for sponges to form within 1.6 seconds while maintaining the viscoelastic properties after crosslinking. BIO incorporated scaffolds demonstrated highly porous networks with well-connected pores throughout, similar to the internal structure of control sponges. MC3T3 cell viability was not affected by

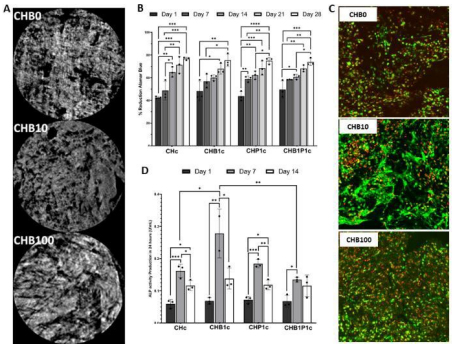

Figure 1. (A) MicroCT sections of sponges with BIO (0, 10, 100 uM). (B) Cellular metabolic activity over 28 days for BIO or PPTase jointly or separately. (C) Live/Dead staining of encapsulated MC3T3 cells after 1 day. (D) ALP production of C2C12 cells cultured indirectly over 14 days.

BIO addition as all scaffolds allowed for adequate viability over 28 days. No significant difference in metabolic activity was observed in C2C12 cells when BIO and PPTase were added either separately or jointly with values increasing over 28 days. Staining showed homogeneous cell distribution regardless of BIO or PPTase incorporation with a decrease in density over time. Regarding effects on differentiation, ALP production was found to be upregulated at day 7 in all groups with a significant increase in quantity in the BIO 1 uM alone group compared to control sponge and the synergistic group. No significant difference was shown in osteogenic gene expression between groups of increasing BIO dosages, but the synergistic group showed increased gene expression of RUNX2 at day 3 compared to all other groups.

CONCLUSION: Results from this study illustrate the successful formulation of the BIO incorporated sponge with minimal effects to material properties at relevant concentrations. Testing of C2C12 cell differentiation demonstrated a BIO dose-dependent beneficial effect in terms of ALP production but interestingly not in the synergistic group. Studies are currently being conducted to further assess the differentiation and BIO's mechanism of action in sponges through western blot. These experiments will be repeated as well using adipose derived stem cells.

REFERENCES: [1] L. Nayef, M. Mekhail, L. Benameur, J.S. Rendon, R. Hamdy, M. Tabrizian, *Acta biomaterialia* 29 (2016) 389-397. [2] M. Mekhail, J. Daoud, G. Almazan, M. Tabrizian, *Advanced healthcare materials* 2(8) (2013) 1126-1130. [3] J. Li, Z. Khavandgar, S.-H. Lin, M. Murshed, *Bone* 48(2) (2011) 321-331.

ACKNOWLEDGEMENT: Authors thank CHRP (NSERC and CIHR partnered program) for financial support of project.

Hybrid Core-Shell Scaffolds for Bone Regeneration and a 3D Printing Approach to Tune their Properties

Chiara Pasini[1*], Luciana Sartore[1], Stefano Pandini[1], Giorgio Ramorino[1]
[1]Department of Mechanical and Industrial Engineering, University of Brescia, Brescia, Italy
[*] c.pasini012@unibs.it

INTRODUCTION

The quest for scaffolds with enhanced bioactive response has seen hydrogels emerging as key biomaterials for tissue engineering, due to their biocompatibility, biodegradability, hydrophilicity, and excellent mimicry of the natural extracellular matrix.[1] However, their mechanical properties are typically inadequate to temporarily substitute mineralized tissues such as bone. To solve this issue, hybrid structures were proposed, incorporating in the hydrogel a stiffer biopolymer (*e.g.* polylactic acid, PLA, or poly(ε-caprolactone), PCL) in the shape of non-woven fibers or 3D-printed lattices.[2]

In this work, we developed and characterized bioresorbable hybrid scaffolds composed of a bioactive gelatin-chitosan hydrogel (Hy) shell and a stiff PLA-based core. The hydrogel was specifically chosen because it was found to support cell proliferation and osteogenic/chondrogenic differentiation in previous studies.[3] For the core, two types of structure were prepared: i) a highly interconnected porous structure made of a PLA-PCL blend, obtained by a novel technique consisting in the introduction and subsequent leaching of superabsorbent particles, SAP;[4] ii) a PLA lattice structure realized by additive manufacturing. This latter system, thanks to the design freedom enabled by 3D printing, allowed to explore the possibility to tune the mechanical properties of the scaffold by changing the core/shell ratio.

EXPERIMENTAL METHODS

The PLA-PCL core was prepared by melt-blending PLA (55%), PCL (14%) and, in a second step, crosslinked sodium polyacrylate SAP (31%), by means of a discontinuous mixer. The obtained material was compression molded as plates, from which bar-shaped specimens (8 x 4 x 3 mm^3) were machined and later immersed in distilled water for 7 days to promote SAP swelling and leaching. 3D-printed core specimens (10 x 10 x 10 mm^3) were prepared as lattice structures with cubic cells by fused deposition modelling of a PLA filament. Both types of core specimens were immersed at 40°C in a hydrogel forming solution (74% gelatin, 8% chitosan and 18% poly(ethylene glycol) diglycidyl ether as crosslinking agent), freeze-dried and post-cured.

The obtained materials were subjected to physicochemical analyses (infrared spectroscopy; thermogravimetric analysis, TGA; optical and scanning electron microscopy, SEM), and a mechanical characterization under compression (electromechanical dynamometer). Core-shell specimens were immersed in distilled water for 24 h before mechanical tests.

RESULTS AND DISCUSSION

SAP particle leaching created PLA-PCL core specimens with 60 v% interconnected porosity, which allowed successful grafting of a 2-3 wt.% hydrogel shell on their surface, as confirmed by infrared spectra and TGA. The highly interconnected porous structure (Fig. 1a, left) and the stiffness (Fig. 1b, compressive apparent modulus, E_{app}) of PLA-PCL-Hy revealed its potential for biomimicking the spongy bone tissue and, therefore, for its regeneration. Furthermore, this type of scaffold is an excellent substrate for proliferation and osteogenic differentiation of mesenchymal stems cells (MSCs), thanks to the bioactive properties of the hydrogel shell.

The possibility to modulate the properties of the scaffolds was investigated by changing their core/shell ratio. With this aim, their core was 3D-printed with holes of various sizes. Specifically, their core void fraction, CVF, was systematically varied between 45% and 90%, leading to scaffolds with broad ranges of hydrogel content (5÷45%) and water uptake (50÷300%), both increasing with CVF. The typical appearance of their structure is displayed in Fig. 1a, right (insert), while the corresponding SEM image shows the interconnected porosity of the hydrogel shell, developed during the freeze-drying process[3]. Interestingly, their stiffness can be significantly tuned (E_{app} = 50÷600 MPa, Fig. 1b) by changing the CVF, and even scaffolds with CVF > 60% were stiffer than PLA-PCL-Hy, while containing more bioactive hydrogel.

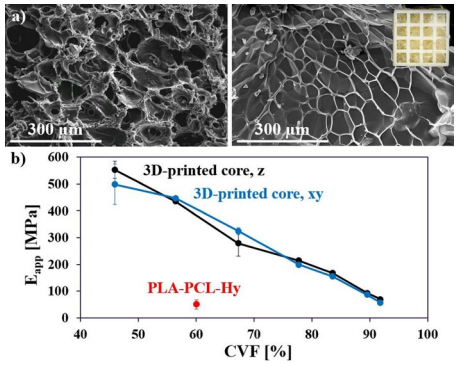

Fig. 1. a) Porous structure of PLA-PCL-Hy (left) and of the hydrogel (right) grafted on a 3D-printed specimen (insert). b) Compressive apparent modulus (E_{app}) *vs.* core void volume fraction (CVF) (z: 3D printing build direction; xy: transverse direction).

CONCLUSION

The core-shell design proved to be an effective strategy to obtain bioresorbable scaffolds that provide both a temporary mechanical support and an adequate environment for MSC proliferation. Moreover, it is a versatile approach, especially when combined with additive manufacturing, since the core and shell materials and their relative proportions can be easily modified to modulate scaffold properties such as stiffness, strength, bioactivity, and biodegradability.

REFERENCES

1. Lee J.-H. and Kim H.-W., J. Tissue Eng. 9:1-4, 2018
2. Neves S. C. *et al.*, Trends Biotechnol. 38(3):292-315, 2020
3. Dey K. *et al.*, Macromol. Biosci. 19(8):1900099, 2019
4. Sartore L. *et al.*, J. Appl. Polym. Sci. 134:45655, 2017

Decellularisation of whole human condyles for osteochondral repair

Halina T Norbertczak[1,2*], Eileen Ingham[1,2], Jennifer H Edwards[1,2], Paul Rooney[3], Hazel L Fermor[1,2]

[1]School of Biomedical Sciences, Faculty of Biological Sciences, University of Leeds, Leeds, United Kingdom; [2]Institute of Medical and Biological Engineering, School of Mechanical Engineering, Faculty of Engineering and Physical Sciences, University of Leeds, Leeds, United Kingdom; [3]NHS Blood and Transplant Tissue and Eye Services, Liverpool, United Kingdom; * h.t.norbertczak@leeds.ac.uk

INTRODUCTION

Osteoarthritis (OA) of articular cartilage is a progressive and debilitating disease, often necessitating a total joint replacement. Between 2005 and 2015 the worldwide prevalence of OA increased by 32.9 % (from 17.9 to 23.7 million cases)[1]. There is therefore a demand for early stage interventions to prevent or delay joint replacement surgery. Decellularisation technology aims to remove DNA and cellular material from biological tissues to produce collagen rich extracellular matrix scaffolds which are non-immunogenic upon implantation to replace diseased or damaged tissues[2]. These biological scaffolds retain their histoarchitecture, biochemical and biomechanical properties along with functional molecules and are able to facilitate remodeling within the recipient. A potential treatment for OA is a decellularised osteochondral (OC) graft. It is proposed that whole human condyles can be decellularised to produce large, non-immunogenic scaffolds which are then shaped to fit OC lesions.

EXPERIMENTAL METHODS

Whole medial and lateral femoral condyles (FCs) from human donors (N=4) were isolated. The underlying bone was reamed to a total depth of 1 cm. Two medial and two lateral FCs from four separate donors were decellularised and the corresponding lateral and medial FCs retained as cellular controls. The decellularisation method applied utilised low concentration sodium dodecyl sulphate (0.1 % w/v), freeze-thaw cycles, sonication, protease inhibitors and nuclease treatment. Samples were analysed biochemically (quantitative DNA and glycosaminoglycan (GAG) assays) and histologically to stain for the presence of nuclear material and GAGs (haematoxylin and eosin (H&E), 4′,6-diamidino-2-phenylindole (DAPI) and Safranin O staining). Quantitative data was tested for normality with the Shapiro-Wilk normality test. The normally distributed data was analysed using the unpaired Student's t-test. A significance level of 0.05 was set for both tests.

RESULTS AND DISCUSSION

The total DNA content of decellularised bone and cartilage was below the suggested maximum limit of 50 ng.mg^{-1} dry tissue weight[3] at 35.8 (± 19.5) and 4.3 ± 3.7 ng.mg^{-1} (± 95 % confidence interval, CI) respectively. GAG concentrations were not significantly different between cellular and decellularised cartilage (163.5 ± 48.1 and 193.5 ± 50.4 µg.mg^{-1} (± 95 % CI) dry tissue weight respectively). Safranin O staining showed GAG retention in the cartilage over the whole sagittal section of the FCs. H&E and DAPI staining showed a reduction in nuclei in decellularised samples; cartilage and bone were largely devoid of visible nuclei. There were occasional nuclei in the calcified tidemark region between the cartilage and bone and the rare occurrence of nuclei in the bone.

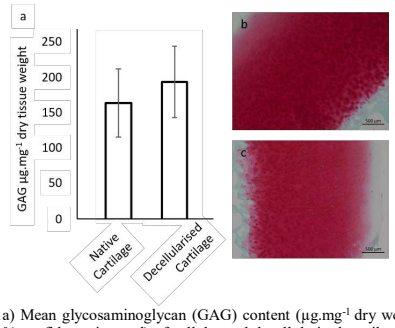

Fig 1a) Mean glycosaminoglycan (GAG) content (µg.mg^{-1} dry weight ± 95 % confidence interval) of cellular and decellularised cartilage (N = 4). No significant difference was found (p = 0.22, unpaired Student's t test). Images of Safranin O-Fast green stained histological sections of cellular (b) and decellularised (c) osteochondral tissue, x 100 mag, 500 µM scale bar.

FCs were adequately decellularised with excellent GAG retention in the cartilage. As cellular bone allografts are routinely and successfully used in orthopaedic surgery, the presence of the occasional nucleus in the decellularised product should not be of detriment to the immunocompatibility of the graft. It is expected that the removal of cells from osteochondral allografts through decellularisation will accelerate bone-bone healing post implantation. Future work will seek to explore if the retention of GAGs is accompanied by a retention of mechanical and functional properties, through indentation and friction testing.

CONCLUSION

Decellularised condyles may provide an easily stored, off-the-shelf alternative to viable cellular allografts for the repair of cartilage defects.

REFERENCES

1. Vos T. *et al.*, The lancet 388 (10053), 1545-1602, 2016
2. Gilbert TW. *et al.*, Biomaterials 27 (19), 3675–3683, 2006.
3. Crapo, PM. *et al.*, Biomaterials 32 (12), 3233–3243, 2011.

ACKNOWLEDGMENTS

The authors would like to thank the EPSRC programme grant (EP/P001076/1) for providing financial support to this project.

3D printed anisotropic and porous dense collagen hydrogels to model cardiac extracellular matrix

Marie Camman[12*], Pierre Joanne[2], Alba Marcellan[3], Julie Brun[3], Gervaise Mosser[1], Onnik Agbulut[2], Christophe Hélary[1]

[1] Laboratoire de Chimie de la Matière Condensée de Paris, Sorbonne Université, France, Paris
[2] Institut de Biologie Paris Seine – Biological Adaptation and Ageing, Sorbonne Université, France, Paris
[3] Sciences et Ingénierie de la Matière Molle, ESPCI Paris, Université PSL, France Paris
[*] marie.camman@sorbonne-universite.fr

INTRODUCTION

Despite the crucial role of the cardiac extracellular matrix in the organotypic organization and conduction of contraction, most 3D heart models[1] do not mimic its specific characteristics, namely its biochemical composition, stiffness, anisotropy and porosity[2]. Recent approaches of 3D heart models used non porous hydrogels fabricated from low concentrated collagen to encapsulate cardiac cells. Hence, the *in vivo* properties are not reproduced. Here, we developed a 3D printed collagen hydrogel that mimic the cardiac extracellular matrix, *i.e* collagen anisotropy, adequate stiffness and two ranges of porosity (one to ensure nutrients and oxygen diffusion and the other for cell cultivation).

EXPERIMENTAL METHODS

Dense collagen solutions (30 $mg.ml^{-1}$) were printed through the 23G flat bottom needle inside a buffer bath. The extrusion process aligned the collagen molecules along the axis of extrusion. The buffer bath played two major roles: it "froze" the collagen alignment and triggered collagen gelling. The printing process was performed unidirectionally for each layer to create an intrinsic porosity between the different collagen filaments. After a rapid period of collagen gelling, needles were introduced within the hydrogel to generate large pores. An additional gelling period was performed to tune the mechanical properties. Cardiac spheroids, made with 85% of cardiomyocytes derived from induced pluripotent stem cells and 15% of ventricular fibroblasts, were then seeded within the printed hydrogels to evaluate spheroid fusion, contraction rate and assess their maturation.

RESULTS AND DISCUSSION

By tuning the extrusion speed and the gelling process, a 3D printed hydrogel with aligned collagen fibers was obtained. A combination of two gelling strategies (24h PBS 5X + 24h NH_3) was optimal to obtain both anisotropy and adequate mechanical properties (E=10 kPa). Scaffold anisotropy was obtained at two different scales: all filaments were printed in the same direction (macroscopic) and collagen fibers were aligned inside printed filaments (microscopic). Concerning the porosity, changing the height between two successive layers allowed to create an intrinsic porosity of 100 µm while preserving the scaffold cohesiveness. This porosity is suitable for nutrients and oxygen diffusion in the whole scaffold, thereby favoring cell viability. Larger pores created by needles molding generated straight channels of 600 µm in diameter. These were colonized by cardiac spheroids mixed with Matrigel® to create a suitable 3D environment. After 15 days in culture, cells changed in shape and contraction revealed an adaptation to this new environment

CONCLUSION

In this study, we developed a 3D printing technique to create a biomimetic cardiac extracellular matrix suitable for spheroids cultivation. Our approach focused on the extracellular matrix and its key parameters since it is deeply involved in cardiac functions and in several diseases.

REFERENCES

1. Hinson, J. T. *and al.*, Cell Rep. **17**, 3292–3304 (2016).
2. Domian, I. J. *and al.*, Adv. Healthc. Mater. **6**, 1600768 (2017).

ACKNOWLEDGMENTS

This research was partly supported by Sorbonne Université, CNRS, INSERM. CH is supported by the AFM-Téléthon (contract number: 22142). OA and PJ are supported by the AFM-Téléthon (contract numbers: 21833 and 22142), the Fédération Française de Cardiologie and by the Ile-de-France Region in the framework of Respore, the Île-de-France network of Excellence in Porous Solids. MC is supported by a Ph.D. fellowship from Sorbonne Université.

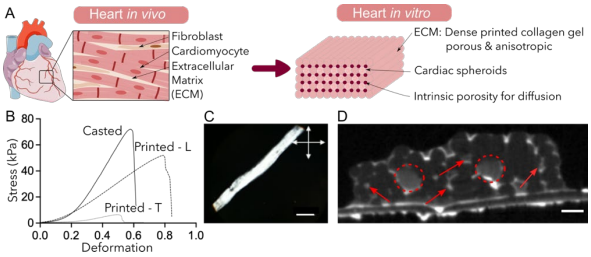

Figure 1: A- Heart in vivo and its model in vitro. B- Fiber alignment and its impact on mechanical properties (comparison between casted and printed gels either stretched in the fiber orientation (L) or perpendicular to the fiber orientation (T). C- Printed collagen observed with Polarized Light Microscopy (Scale bar 500 µm). D- MicroCT of a collagen gel with the two ranges of porosity(circles : large channels,arrows: intrinsic porosity -Scale bar 500 µm)

Modified alginates / plasma-derived fibrin hydrogels for skin engineering

Ana Matesanz[1,2,*], Raúl Sanz[3], Carlos Elvira[3], Diego Velasco[1], José Luis Jorcano[1], Pablo Acedo[2]

[1]Department of Bioengineering and Aerospace Engineering, Universidad Carlos III de Madrid, Leganés, Spain
[2]Department of Electronic Technology, Universidad Carlos III de Madrid, Leganés, Spain
[3]Department of Applied Macromolecular Chemistry, CSIC, Madrid, Spain
[*]amatesan@pa.uc3m.es

INTRODUCTION

Fibrin is a biopolymer commonly applied to the 3D culture of soft tissue equivalents, such as skin, due its excellent biological properties. Specifically, our group engineered a procedure that involves the creation of human plasma-derived hydrogels with final fibrin concentration of 1.2 mg/ml for a bilayer skin substitute containing primary human fibroblasts (hFBs) and keratinocytes (hKCs)[1]. Their applications range from the generation of skin-humanized mouse models to the treatment of burns in patients and the development of a 3D printing system. However, fibrin shrinkage , poor mechanical properties, and rapid biodegradation limit its practical use, leading the researchers to explore the possibility of combining fibrin with natural or synthetic polymers[2]. In our study, plasma-derived fibrin matrices have been improved by the addition of two different types of modified alginate. The resulting hydrogels increased the mechanical stability and the viability of skin cells. The first alginate was oxidized with sodium metaperiodate (alginate di-aldehyde, ADA) and the second alginate (alginate with succinimide, AS) incorporated succinimide groups; both alginates have been chemically bonded by Schiff base formation to the fibrin during the polymerization. The new plasma-alginate matrices have been characterized in terms of mechanical properties and biocompatibility. Gelation time, rheology, contractile behavior, and biological performance have been studied with the aim of improving skin culture lifespan.

EXPERIMENTAL METHODS

Hydrogels were prepared mixing the following components: platelet poor plasma with a final fibrinogen concentration of 1.2 mg/ml, 0.9% NaCl, $CaCl_2$ with a final concentration of 0.01% w/v, amchafibrin (0.008% w/v final concentration) and a final concentration of ADA (2mg/ml) or AS (1mg/ml). The ADA were oxidized by sodium metaperiodate at 10% of oxidation (characterized by titration) giving two aldehyde groups. The AS were functionalized with a succinimidyl esther group (26% of functionalized succinimide added to alginate, determined by NRM). Modification of fibrin hydrogels were characterized by SEM images. The shrink behavior of the hydrogels was analyzed by studying the weight loss for 21 days. Cell viability of hFBs and hKCs (20.000 and 70.000 cells/ml) were analyzed using Live/Dead® by adding calcein AM and ET homodimer at 2µl/ml in PBS and incubated 30 minutes at 37ºC at 1, 3 and 7 days. hFBS and hKCs proliferation (20.000 cells/ml and 70.000 cells/ml) was characterized using AlamarBlue at 0, 1, 3 and 7 days.

RESULTS AND DISCUSSION

SEM images showed a change from fibrous to micro-porous structure in AS/plasma hydrogels and an increase of the fiber diameter in ADA/plasma hydrogels. The swelling ratio study also verified these changes by inhibiting the rapid contraction of the normal fibrin hydrogels (Fig.1, down).

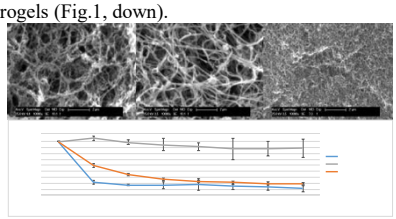

Figure 1: Upper part, SEM images of fibrin hydrogels: (a) with ADA (2mg/ml) and (b) with AS (2mg/ml) (c). Lower part, swelling studies during 21 days.

Viability and proliferation studies demonstrated the growth of hFBs in both hydrogels and the attachment and proliferation of hKCs on the AS/plasma hydrogels at different concentrations (Fig. 2).

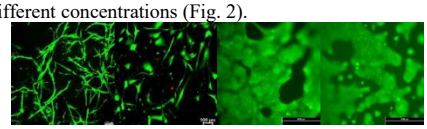

Figure 2: Viability assay at 7 days of hFBs: in fibrin (a) and fibrin-ADA (2mg/ml) hydrogels (b); and KCs: in fibrin hydrogels (c) and fibrin-AS (1mg/ml) hydrogels (d).

CONCLUSION

The incorporation of AS has been shown to improve fibrin hydrogel's microstructure and behavior, directly related to mechanical properties and cell growth. At concentrations higher than 1mg/ml ADA inhibited fibrin polymerization, its incorporation also resulted in an increase of fiber diameter (Fig.1, up). Both modified alginates supported hFBs proliferation, but, contrary to ADA, AS gels allowed hKCs viability. These results illustrate the potential of using these types of hydrogels for dermo-epidermal equivalents development.

REFERENCES

1. Montero Simón, A., *et al.,* International Journal of Molecular Sciences, vol. 22, no 13, p. 6746, 2021.
2. Sanz-Horta, R., *et al.,* International Journal of Molecular Sciences, vol. 23, no 8, p. 4296, 2022.

ACKNOWLEDGMENTS

This research was supported by Programa de Actividades de I+D entre Grupos de Investigación de la CAM, S2018/BAA-4480, Biopieltec-CM, Programa Estatal de I+D+I Orientada a los Retos de la Sociedad, RTI2018-101627-B-I00, and Cátedra Fundación Ramón Areces.

In vivo bone regeneration of sterile scaffolds obtained by supercritical CO_2 technology

V. Santos-Rosales[1], L. Diaz-Gomez[1], B. Magariños[2], C. Alvarez-Lorenzo[1] and C.A. García-González[1]

[1]Departamento de Farmacología, Farmacia y Tecnología Farmacéutica, I+D Farma (GI-1645), Faculty of Pharmacy, iMATUS and Health Research Institute of Santiago de Compostela (IDIS), Universidade de Santiago de Compostela, 15782 Santiago de Compostela, Spain.
[2]Departamento de Microbiología y Parasitología, Facultad de Biología, CIBUS, Universidade de Santiago de Compostela, 15782 Santiago de Compostela, Spain.
*v.santos.rosales@usc.es

.

INTRODUCTION

The sterilization treatment of medical devices must ensure a high sterility assurance level (6-log reductions) against bacterial endospores prior to their usage. This scenario represents a major hurdle in the development of novel polymeric scaffolds [1]. Carbon dioxide under supercritical (sc-) conditions incorporating low contents of H_2O_2 can inactivate bacterial endospores while preserving the physicochemical properties of the treated biomaterial [2]. On the other hand, the sc-foaming technology allows the production of drug-loaded scaffolds in the absence of solvents. By the fine control of the processing parameters, scaffolds with morphological characteristics matching those of the natural bone tissue can be obtained [3]. In this work, admixtures of PCL, PLGA, platelet-rich-plasma (PRP) and pregelatinized starch (St) were subjected to a proprietary $scCO_2$ sterilization+foaming integrated process and *in vivo* evaluated.

EXPERIMENTAL METHODS

Hydrogen peroxide was added in the liquid form in a high-pressure autoclave containing scaffolds components in cylindrical moulds. The system was heated to 39 ºC and pressurized at 140 bar, maintaining the setup in the batch mode for 2 h, followed by a $scCO_2$ flow (5 g/min) during 1 h The physicochemical and morphological characterization of the scaffolds was performed in terms of scanning electron microscopy (SEM), mercury intrusion porosimetry (MIP), and helium pycnometry. *In vivo* evaluation was conducted in accordance with the European regulation on care and use of animals in experimental procedures and the ARRIVE guidelines. Bone regeneration was evaluated after 16 weeks in a sheep model +by microcomputed tomography (µ-CT) and histological/immunohistochemical analysis.

RESULTS AND DISCUSSION

After implantation, animals did not show any sign of inflammation response, thus ensuring the compatibility of the designed scaffolds. After 16 weeks of implantation, the significant formation of new bone in the defect area was observed by µ-CT (Figure 1) for animals treated with scaffolds. The regeneration of the injured areas was also confirmed by the quantification of the new bone tissue from µ-CT reconstructions. Histological and immunohistochemical analysis confirmed the formation of mineralized bone tissue and vascularized areas promoted by the scaffold's presence.

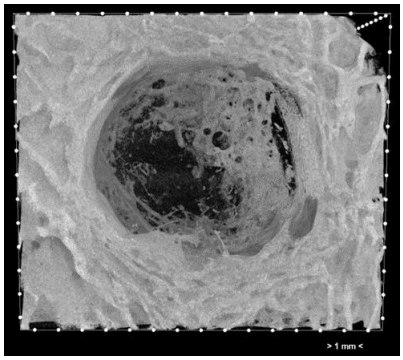

Figure 1. Representative µ-CT reconstruction of a filled defect with a scaffold on sheep femur after 16 weeks. New bone is observed as radio dense material in the damaged area.

CONCLUSION

Sterile PCL/PLGA-St scaffolds loaded with PRP were manufactured with suitable morphological criteria to be used as bone grafts in a sterile manner by means of $scCO_2$ technology. Scaffold performance after 16 weeks of implantation proved their effectiveness in regenerating bone tissue in critical size femoral and tibial defects. Overall, this work highlights the advantages of scCO2 technology for the manufacturing of sterile and drug-loaded polymeric scaffolds in a single-step, with promising performance in a relevant in vivo model. The technological transfer and valorization of these scaffolds within the clinical arena is currently ongoing.

REFERENCES

[1] V. Santos-Rosales, *et. al.* International Journal of Pharmaceutics. 605 (2021) 120801.
[2] V. Santos-Rosales, *et. al* International Journal of Pharmaceutics. 612 (2022) 121362.
[3] V. Santos-Rosales, *et. al.* The Journal of Supercritical Fluids. 166 (2020) 105012.

ACKNOWLEDGMENTS

This research was funded by MICINN [PID2020-120010RB-I00], Xunta de Galicia [ED431C 2020/17; ED481D-2021-014], Agencia Estatal de Investigación [AEI] and FEDER funds. Work supported by Ignicia Programme from Axencia Galega de Innovación (Xunta de Galicia, IN855A 2021/13).

Double-porosity 3D printed scaffolds to select mesenchymal stem cells from the bone marrow and induce cartilage regeneration.

Sandra Ramos-Díez[1], Sandra Camarero-Espinosa[1,2*]

[1]BioSmarTE lab, RPT Group, POLYMAT, University of the Basque Country UPV/EHU, Donostia/San Sebastián 20018, Guipúzcoa, Spain.
[2]IKERBASQUE, Basque Foundation for Science, Bilbao, Spain

[*]sandra.ramos@polymat.eu; sandra.camarero@polymat.eu

INTRODUCTION

Osteochondral defects affect a large number of patients each year. Currently, these type of lesions are treated by the well-known micro-fracture technique. However, the formed tissue differs substantially from the native one. This technique enables the flow of a heterogeneous cell population from the bone marrow to the damaged area. Nevertheless, only around 0.001% of these cells are mesenchymal stem cells, with the potential to differentiate into chondrocytes. Thus, the cells that invade the defect tend to differentiate towards a hypertrophic or osseous phenotype[1]. Moreover, the lack of structure leads to the formation of an isotropic tissue. In this context, there is an urgent need to find a solution that corrects the drawbacks of micro-fracture.

To overcome these issues we designed an implantable device, that seeks to improve the micro-fracture technique by facilitating the specific selection of human mesenchymal stem cells (hMSCs) *in-situ*, using 3D printed double-porosity scaffolds that serve as pass/no-pass filter, discriminating cells by size.

EXPERIMENTAL METHODS

Synthesis of gelatine microspheres (GMSs): GMSs were synthesized by dropping a solution of gelatine at different concentrations in an oil bath containing a surfactant under vigorous stirring. Samples were collected by filtration, dried at RT and their size measured by optical microscopy and scanning electron microscopy (SEM). **Fabrication of double-porosity scaffolds**: 3D printed scaffolds were fabricated from poly(lactide-co-caprolactone) (PCLLA) solutions in dioxane at 20 % (w/v) that were mixed with different concentrations of GMSs and GMSs of various sizes. After printing and drying out the solvent, GMSs were removed by leaching in water at 40 ºC for 24h. Optimum time to complete scaffold leaching was defined by thermo-gravimetrical analysis TGA. **Characterization of inks and scaffold**: ink´s loss and storage moduli were determined by ARES-G2 rheometer (*TA Instruments*) at room temperature. Macro and micro-porosity were visualized using TM3030Plus SEM (*Hitachi High-Technologies*) with a previous surface gold coating utilizing SC7620 Mini Sputter Coater/Glow Discharge System (*Quorum*). Both pore sizes were analysed using descriptive statistics. Scaffold Young's moduli were determined by thermoanalyzer DMA Tritec-2000 (*Triton Technology Ltd.*). **Cell culture**: the ability of double porosity scaffolds to accommodate hMSCs in their different pores was evaluated at 24 hours and 7 days in growth media using SEM and fluorescence microscopy. Further, capability of hMSCs to differentiate into chondrocytes was checked by fluorescence microscopy.

RESULTS AND DISCUSSION

Double porosity scaffolds were created by 3D printing inks based on GMSs and PCLLA and further leaching the particles. GMSs of different sizes were prepared, having 12.59 ± 7.861, 23.66 ± 14.04 and 46.57 ± 27.49 µm. We characterized these different inks by rheological measurements. Inks loss and storage moduli were determined and used to define the printability of the inks. After leaching the GMSs, scaffolds with double porosity congruent with the size of the microspheres used in each case were obtained (Figure 1). We established also that the formed micro-porosity is interconnected, what will favour nutrient and waste flow in cell culture assays. The Young's modulus of double-porosity scaffolds was measured showing a mechanical behaviour similar to the native cartilage.

hMSCs were cultured in the dual-porosity scaffolds showing their capability to infiltrate them and demonstrating that their capacity to accommodate hMSCs increases significantly when using scaffolds with interconnected micro-pores inside their fibbers. Finally, we evaluated their potential to promote cartilage formation by differentiation of hMSCs within the dual porosity scaffolds, showing the deposition of characteristic proteins such as collagen II.

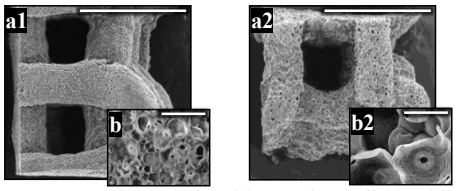

Figure 1. SEM images of double porosity scaffolds with different micro-porosity size; 12.59 ± 7.861 µm (a1 and b1) and 46.57 ± 27.49 µm (a2 and b2). Scale bar is 2 mm (a1 and a2) and 50 µm (b1 and b2).

CONCLUSIONS

In conclusion, biocompatible and printable double-porosity scaffolds have been manufactured using 3D printing technology that has the ability to improve the specific selection of hMSCs by size. These scaffolds enhance cell adhesion and differentiation, in addition to have the capability to mimicking mechanical properties of native cartilage.

REFERENCES

1. Camarero-Espinosa S. *et al*., Biomaterials Science, 4:734-767, 2016.

ACKNOWLEDGMENTS

This work was supported by the EMAKIKER grant.

Naproxen and indomethacin-conjugated antioxidant and antimicrobial peptide gels for chronic wounds

Moumita Halder, Mukul Narula, and Yashveer Singh*

Department of Chemistry, Indian Institute of Technology Ropar, Rupnagar, Punjab, India
*2018CYZ0011@iitrpr.ac.in

INTRODUCTION

Wound healing is a complex tissue repair process involving four phases- hemostasis, inflammation, proliferation, and remodeling. Healing depends on the dynamic interplay between different mediators, such as enzymes, cells, cytokines, chemokines, and growth factors.[1] Chronic wounds often stall in inflammatory phase due to the excessive accumulation of pro-inflammatory cytokines, reactive oxygen species (ROS), and bacterial burden.[2] Self-assembled peptide gels with entangled nanofibers have been considered as a promising wound healing scaffold.[3] Therefore, we have developed self-assembled gels from antioxidant and antimicrobial peptides and conjugated to non-steroidal anti-inflammatory drugs (NSAIDs), naproxen and indomethacin, to control the inflammatory effect and treat chronic wounds.

EXPERIMENTAL METHODS

Peptides, YYk and YYr, were synthesized by solid-phase peptide synthesis (SPPS) and conjugated to NSAIDs, naproxen (Npx) and indomethacin (Ind), to obtain conjugates, Npx-YYk-NH_2, Npx-YYr-NH_2, Ind-YYk-NH_2, and Ind-YYr-NH_2. All conjugates were characterized by NMR, Mass spectrometry, HPLC, and FTIR spectroscopy. The viscoelastic and self-healing properties of gels were determined by rheology and antioxidant activities were measured by ABTS and DPPH assays. The antibacterial potency and biofilm inhibition was assessed against a Gram-positive bacteria, *S. aureus*. Selective COX-2 inhibition, cell viability, and cell proliferation and migration properties were also investigated. Finally, the expression of pro-inflammatory and anti-inflammatory genes were analyzed by RT-PCR. Student's t-test was carried out for data comparison.

RESULTS AND DISCUSSION

Our aim was to develop peptides with inherent antioxidant and antibacterial capabilities, and conjugated to NSAIDs to obtain self-assembled scaffolds for COX-2 inhibition in chronic wounds. The conjugates were self-assembled into gels by pH and solvent-switch methods, which exhibited entangled, porous frameworks with β-sheet conformation. Npx conjugated gels exhibited better viscoelastic property than Ind conjugated gels. All gels showed around 90% antioxidant activity and more than 90% activity against *S. aureus*, the main causative organism associated with wound infection. They also demonstrated biofilm inhibition in the range of 80-90%. The conjugates exhibited selective COX-2 inhibition over COX-1, with selectivity index ranging from 1.5-2.5. The scaffolds were nontoxic to fibroblast and macrophage cells, as confirmed by MTT assay, and cells treated with these scaffolds retained their morphology. They exhibited proliferation and migration of fibroblast cells, and were able to protect cells from inflammation-induced oxidative stress by scavenging the ROS generated by macrophages. The conjugates also caused an enhanced expression of anti-inflammatory marker (IL 10) and inhibition of pro-inflammatory marker (IL 6).

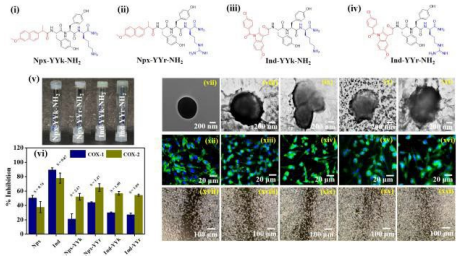

Figure 1. (i-iv) Structure of peptide-drug conjugates used to form self-assembled gels. (v) Images of peptide-drug conjugate gels. (vi) Inhibition of COX-1 and COX-2 by peptide-drug conjugates. 'S' indicates selectivity, and data reported are mean ± SE (n = 3). Effect of gels on bacteria and murine cells. (vii-xi) HRTEM images of *S. aureus*. (xii-xvi) Morphology of L929 cells stained by Alexa fluor-phalloidin and DAPI. (xvii-xxi) Migration of L929 cells.

CONCLUSIONS

In summary, we have developed four self-assembled gels from peptide-drug conjugates with a potential to accelerate wound healing by reducing oxidative stress, bacterial infection, biofilm, and inflammation. Their ability to induce cell proliferation and migration in scratch assay suggest that these scaffolds hold promise as wound healing matrix.

REFERENCES

1. Araújo, M. *et al*., Biomater. Sci. 9: 6510–6527, 2021.
2. Wang, Y. *et al.,* ACS Appl. Mater. Interfaces. 13: 33584–33599, 2021.
3. Halder, M. *et al*., Biomater. Sci. 10: 2248-2262, 2022.

ACKNOWLEDGMENTS

This work was supported by a grant from the Department of Biotechnology, India, to YS (BT/PR40669/MED/32/761/2020). MH is thankful to IIT Ropar for the institute fellowship.

Ternary PLCL/Collagen Nanofiber Matrices Decorated with MXene to Enable Spontaneous Myogenic Differentiation

Seok Hyun Lee[1], Moon Sung Kang[1], Hee Jeong Jang[1], Hyo Jung Jo[1], Ji Eun Lee[2], Seung Jo Jeong[3], Jong Ho Lee[4], Dong-Wook Han[1, 2, 3*]

[1]Department of Cogno-Mechatronics Engineering, Pusan National University, Busan, Republic of Korea
[2]Department of Optics and Mechatronics Engineering, Pusan National University, Busan, Republic of Korea
[3]Bio-IT Fusion Technology Research Institute, Pusan National University, Busan, Republic of Korea
[4]Daan Korea Corporation, Seoul, Republic of Korea
[*] nanohan@pusan.ac.kr

INTRODUCTION

Among one of the most emerging two-dimensional nanomaterials, MXene (Ti_3C_2Tx) has drawn increasing attention due to its fascinating physicochemical and biological properties[1, 2]. Herein, the MXene-decorated poly(L-lactide-*co*-ε-caprolactone) (PLCL)/collagen (Col) (MXene-PLCL/Col) nanofiber matrices were fabricated via electrospinning and their potential as scaffolds for skeletal muscle tissue engineering (TE) was evaluated. The synergistic effect between the myogenic activity of MXene and topographical cue of PLCL/Col nanofiber matrices is supposed to enable the spontaneous myogenic differentiation of C2C12 myoblasts.

EXPERIMENTAL METHODS

Fabrication of MXene-PLCL/Col nanofibers

The solution composed of 5 w/v% PLCL and 0.5 w/v% Col in 1,1,1,3,3,3, hexafluoro-2-propanol (HFIP) was electrospun to fabricate MXene-PLCL/Col nanofibers. The electrospinning parameters including voltage, flow rate, and distance from the collector were optimized.

In vitro immunofluorescence staining

C2C12 myoblasts were cultured on PLCL, PLCL/Col, MXene-PLCL, and MXene-PLCL/Col matrices for up to 10 days. After incubation, myosin heavy chain (MHC), nucleus, and F-actin were visualized by immunofluorescence staining. The fluorescence images were captured by confocal laser scanning microscopy.

RESULTS AND DISCUSSION

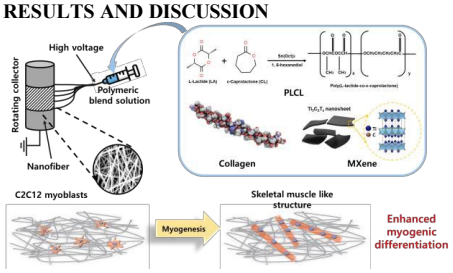

Fig 1. Schematic diagram of preparation of MXene-PLCL/Col matrices for skeletal muscle TE. The inset on the left side represents scanning electron microscopy (SEM) image of MXene-PLCL/Col nanofibers.

The MXene-PLCL/Col matrix was successfully fabricated. The SEM image of MXene-PLCL/Col nanofibers shows a smooth surface without any beads and structural defects.

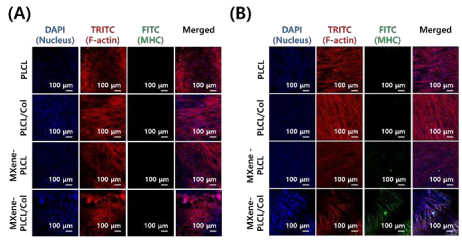

Fig 2. Immunofluorescence staining of C2C12 myoblasts incubated on each matrix at 5 days (A) and 10 days (B).

While there were no significant differences between groups at day 5, the expression of MHC (FITC) was clearly increased on MXene-PLCL and MXene-PLCL/Col matrices, suggesting the myogenic effects of MXene.

CONCLUSION

PLCL-Col-MXene has promoted spontaneous myogenesis differentiation of C2C12 myoblasts without hampering their growth. In conclusion, it is suggested that the topographical and biochemical advantages of MXene-PLCL/Col nanofibers can be promising strategies for skeletal muscle TE.

REFERENCES

1. K. Rasool. *et al*., ACS Nano 10:3674–3684 2016
2. M. Soleymaniha. *et al*., Adv Healthc Mater 8:1801137 2019

ACKNOWLEDGMENTS

This work was supported by the National Research Foundation of Korea (NRF) grant funded by the Korea government (MSIT) (2021R1A2C2006013) and the Korea Evaluation Institute of Industrial Technology (KEIT) grant funded by the Ministry of Trade, Industry, and Energy (MOTIE, Korea) (20014399).

Injectable and Functionalized Tough Double-Network Hydrogels for Vocal Fold Repair

Sareh Taheri[1,2,*], Guangyu Bao, Sepideh Mohammadi[1,2], Hossein Ravanbaksh, Luc Mongeau[1,2]

[1]Mechanical Engineering Department, McGill University, Montreal, Canada
[2]Center for Interdisciplinary Research in Music Media and Technology, McGill University, Montreal, Canada
[*] fatemeh.taheri@mail.mcgill.ca

INTRODUCTION

Statistics show that around 3-9% of people suffer from voice problems over their lifetime. Healthy voice production has a significant impact on individual wellness, occupational function, and societal productivity. Intense mechanical stresses during speech can result in laryngeal dysfunctions, including vocal folds (VFs) scarring and tissue loss. The most common treatment in practice is to inject biomaterials to the wounded site [1,2].

Most existing injectable biomaterials degrade over a short period of time and necessitate repeated injections, due in part to fracture under high mechanical load. Existing biomaterials lack vascularization and are not perfusable, which hampers the recruitment of native cells and leaves the cells in deeper layers starving for oxygen. Hence, the main goal of this study is to design and fabricate injectable scaffolds possessing both high mechanical toughness and permeability[3].

EXPERIMENTAL METHODS

In this study, we developed chitosan-based biocompatible and injectable double-network hydrogels to recapitulate the structural, mechanical, and biological properties of VFs. Our porous double-network hydrogels comprise 0.5-2% glyoxal-crosslinked glycol-chitosan (covalent network) and 1.5% physically crosslinked chitosan (sacrificial network). During gelation, the chitosan network exhibited pH-induced phase separation and resulted in formation of micropores.

RESULTS AND DISCUSSION

The porous structure the hydrated gels were evaluated by three different imaging techniques and the pores' size were found to be within the order of 6-10µm. By varying the glycol-chitosan concentration, the stiffness (1-3 kPa) and stress relaxation time (20-120 seconds) were highly tunable to match those of VFs. The designed hydrogels also have high permeability (10-14-10-12 m2) which improved the direct medium perfusion within the interconnected pores, leading to a high cell viability (90%), spreading and proliferation. The efficacy of our hydrogel system was further evaluated with a phono-mimetic bioreactor, and it was found that HVFFs secreted more extra cellular matrix compared to controls. The hydrogels also showed a great mechanical stability under prolonged, high frequency biomechanical stimulations (>6 million cycles at 120 HZ) due to their high mechanical toughness (5-39 J.m-2).

CONCLUSION

The combination of excellent biomechanical performance and cellular behavior suggests the great potential of the new injectable hydrogel technology for repairing mechanical dynamic tissues such as VFs and other applications including bio fabrication, organs-on-a-chip, drug delivery and disease modeling.

REFERENCES

References must be numbered. Keep the same style.
1. Smith G. *et al*., J. Biomech. 2:5-11, 2011
1. Taheri S. *et al.,* J. Advanced Science.

1. Bao G. *et al*., J. Materials Horizons. 7(9): 2336-2347, 2020.
2. Ravanbakhsh H. *et al*., J. Materials Science and Engineering: C. 103:109861, 2019.
3. Taheri S. *et al.,* J. Advanced Science. 9(2): 2102627.

ACKNOWLEDGMENTS

This work was supported by the National Institute on Deafness and Other Communication Disorders (Grant Nos, R01-DC018577, R01-DC005788, and R01-DC014461), the New Frontiers in Research Fund—Exploration (Grant No. NFRFE-2018-00751), and NSERC Discovery (Grant No. RGPIN-2018-04146). The content is solely the responsibility of the authors and does not necessarily represent the official views of the National Institutes of Health. The authors thank the Advanced BioImaging Facility (ABIF, McGill University) for imaging facilities, Optimizing Power Skills in Interdisciplinary, Diverse & Innovative Academic Networks (OPSIDIAN) Fellowship for financial support and the McGill Institute of Advanced Materials (MIAM) for access to µCT facility.

3D calcium silicophosphate scaffold: *in vitro* and *in vivo* response

Patricia Ros-Tárraga[1], Carlos Martinez[2], Miguel Angel Rodríguez[3], Piedad N. De Aza[1*]

[1] Institute of Bioengineering, Miguel Hernandez University, Avda. Universidad s/n, 03202, Elche, Spain.
[2] Instituto Murciano de Investigación Biosanitaria Virgen de la Arrixaca. Crta. Buenavista s/n, 30120 - El Palmar (Murcia - Spain)
[3] Instituto de Cerámica y Vidrio, ICV-CSIC, C/Kelsen 5, Madrid 28049, Spain
*piedad@umh.es

INTRODUCTION

Alternatives to natural bone grafts are needed in a society that progressively prolonged life expectancy while should address the health problems of an aging population. In this context calcium silicophosphate scaffolds are are an excellent option for the replacement of bone tissue because of their similitude to the inorganic part of bone [1-3].

EXPERIMENTAL METHODS

3D porous ceramic scaffolds (85 wt% dicalcium silicate /15 wt% tricalcium phosphate) were sintered by the polymer sponge replica and barbotine techniques.

In order to evaluate the mineralogical composition of the porous scaffolds, X-Ray Diffraction (XRD) patterns were obtained. Also FTIR to determine the chemical composition of the 3D-ceramic samples. The ionic release in basal culture growth medium (GM) of the scaffolds was determined, and the in vitro biocompatibility was analyzed in terms of cytotoxicity (LDH assay), cell morphology (FESEM) and metabolic activity (Alamar Blue™) using adult human mesenquimal stem cells (ah-MSC). Finally, scaffolds were implanted in New Zealand tibia rabbits for 1 and 3 months in order to study the in vivo biocompatibility.

RESULTS AND DISCUSSION

The 3D-calcium silicophosphate scaffold obtained in this research is a monophasic material and is composed by α' dicalcium silicate$_{ss}$ (JCPDS 83-1494). The ions exchange between scaffolds and GM was not incompatible with cell survival and the rest of the in vitro assays showed that scaffolds were completely biocompatible with ah-MSC. LDH assay showed a low cytotoxicity of the scaffolds, with no significant differences between cells in contact with the conditioned medium (GM with the ionic release from scaffolds) with respect to the low control (only cells). Furthermore, FESEM images showed no cell detachment, lysis or changes in membrane integrity in any study time and cells were completely spread out after only 1 day of incubation.

Histological results of the implant group showed a higher speed in the defect closure after 1 month with respect to the control group, and no inflammatory response was observed. After 3 months, cortical bone was completely regenerated in both implant and control groups, and no signs of inflammatory response or secondary fibrosis was observed. All these results confirmed the in vivo biocompatibility of these scaffolds.

CONCLUSIONS

We can conclude that these ceramic porous scaffolds could be an adequate option for future uses in regenerative medicine.

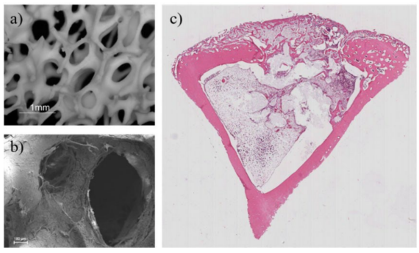

Figure 1. a) Porous scaffold, b) FESEM images of ah-MSC in contact with the scaffolds, and c) histological image of the material implanted in the New Zealand tibia rabbits after 1 month.

REFERENCES

1. GJ. Lugo, *et al.* Ceram. Int. 42 (1), 673-680 (2016)

2. P Ros-Tarraga, *et al.* Materials, 9 (9), 785 (2016)

3.R. Rabadan-Ros, *et al.* J. Eur. Ceram. Soc. 37(8),2943-2952 (2017)

ACKNOWLEDGEMENTS

This work is part of the Grant PID2020-116693RB-C21 funded by MCIN/AEI/ 10.13039/501100011033.

3D Systems with Tailored Mechanical Properties and Biomolecules Delivery in Gradient for Spatially-Controlled MSCs Differentiation

Paola Aprile, Inès Daouadi, Didier Letourneur, Teresa Simon-Yarza

Université Paris Cité, LVTS INSERM U1148, Paris, France

* paola.aprile@gmail.com

Keywords: tissue engineering, cell differentiation, nanoindentation

INTRODUCTION

Tissue engineering (TE) is a promising strategy for replacing or repairing damaged tissues and organs. Local differences in tissues environmental cues, such as substrate stiffness and growth factors gradients, direct different biological processes, from cell migration and differentiation to tissue homeostasis. Although tissues complexity, many *in vitro* engineering strategies use uniform scaffolds and homogeneous growth factor delivery to produce isotropic tissue constructs[1]. The fabrication versatility of polysaccharidic-hydrogels, together with their biocompatibility and non-immunogenicity, make them increasingly popular for TE applications[2,3]. The overall objective of this study was to tune the stiffness of the 3D hydrogel system made of pullulan and dextran to spatially direct mesenchymal stem cells (MSC) fate. Next, microparticles (MPs) were included in these hydrogels for the local release of growth factors. These spatially varying microenvironments provided a range of stiffness and demonstrated the stable incorporation of microparticles, making these 3D systems a valid tool to mimic the complexity of tissues architecture and development.

EXPERIMENTAL METHODS

Pullulan and dextran (75:25) were dissolved in water and crosslinked using three concentrations of sodium trimetaphosphate (STMP): 1.5%, 3% and 6% in 0,1M NaCl. 1% FITC-dextran was added to the solution as a fluorescent tracker. To form the MPs, the solution was dispersed in oil under mechanical stirring, while to form matrices, the solution was casted within glass slides separated by a silicon spacer of 350µm. Next, the hydrogels were pH adjusted, rinsed in 0,025% NaCl and freeze-dried. MPs were characterized by swelling ratio, z-potential and the overall size was taken from the Master Sizer analysis. The mechanical properties were evaluated by nanoindentation (Piuma). Crosslinker quantification and spatial distribution was studied by an in-house biochemical assay[2]. SEM and confocal microscopy were used to evaluate constructs porosity in dry and wet state respectively. Material degradation was assessed *in vitro* by enzymatic digestion. Statistical analyses were performed using GraphPad Prism software and results, are presented as mean ±SD. A level of $p<0.05$ was considered significant.

RESULTS AND DISCUSSION

The higher STMP concentration correlated with a linear increase in the local matrix stiffness (Figure 1A) and phosphate quantity, confirming the production of scaffolds with defined mechanical properties. Upon incorporation into the hydrogels (Figure 1B), the MPs were able to distribute homogeneously irrespective of their concentration (Figure 1C). Such MPs distribution was maintained unvaried for at least 3 weeks in culture.

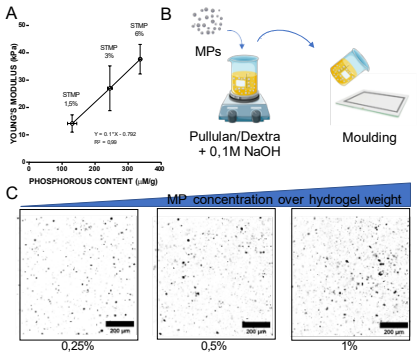

Figure 1. A) Young's Modulus obtained by nanoindentation and scaffolds phosphate content correlated with increasing concentration of STMP. B) Schematic depicting MP incorporation method. C) Confocal analysis of MP-loaded scaffolds, MP (in black) localization and distribution upon rehydration.

CONCLUSION

The protocol of MP inclusion and hydrogel synthesis was optimized to grant the preservation of the growth factors loaded within the scaffold. The gradient of stiffness and growth factors (loaded on the MP) provided by the scaffolds makes these 3D systems a valid tool to mimic in part the complexity of tissue architecture. Ongoing studies focus on the differentiation of human bone-marrow derived MSCs within the scaffolds.

REFERENCES

1. Malda *et al*., Adv. Mater. 25,5011-28, 2013
2. Fricain J. *et al*., Biomaterials. 34, 2947-2959, 2013
3. Lanouar S. *et al.* J Mater Sci: Mater Med. 29, 77, 2018

Novel calcium carbonate-poly(vinyl alcohol) scaffolds for bone tissue engineering

Jingyi Xue[1*], Neelam Gurav[1], Sherif Elsharkawy[1], Sanjukta Deb[1]

[1]Faculty of Dentistry, Oral and Craniofacial Sciences, King's College London, London, United Kingdom
[*] jingyi.xue@kcl.ac.uk

INTRODUCTION

Reconstruction of critical sized bone defects in the oral and maxillofacial region continues to be clinically challenging despite the significant development of osteo-regenerative materials[1]. Most synthetic bone substitutes tend to reach pre-clinical stages yet are not translated due to inferior clinical performance in comparison to autografts, low scalability, poor surgical handling, and inability to reproducibly regenerate bone, mainly attributed to rate of degradation and lack of vascularization[2]. This study aims to offer viable alternatives to address these challenges by developing novel calcium carbonate-poly(vinyl alcohol) scaffolds.

EXPERIMENTAL METHODS

A series of scaffolds were fabricated using poly(vinyl alcohol) (PVA) as matrix and calcium carbonate particles in vaterite phase as filler, using freeze thawing (FT) with and without a porogen to enhance porosity. Several parameters including the number of FT cycles, concentration of vaterite and the inclusion of gelatin as porogen were varied and evaluated for their physicochemical, mechanical, water uptake, thermal, morphological, degradation and mineralization properties. In vitro cell compatibility was also conducted using Human osteoblast-like cell line (HOS TE85).

RESULTS AND DISCUSSION

The systematic study showed that vaterite particles acted not only as fillers but also as porogen due to its high solubility. Lower concentration of vaterite (40% (w/v)) resulted in a more porous structure and higher water uptake, whilst a higher vaterite concentration (60%(w/v)) led to superior mechanical properties (Fig 1) and thermal stability. However, freeze thawing over 2 cycles had little effect on properties of the scaffolds. The inclusion of gelatin resulted in inferior mechanical properties and thermal stability, attributed to the high porosity that compromised structural integrity. All scaffolds showed mineralization in SBF with gradual degradation of vaterite and formation of apatite. Cell attachment was observed on all scaffolds both on the surface and within the pores (Fig 2).

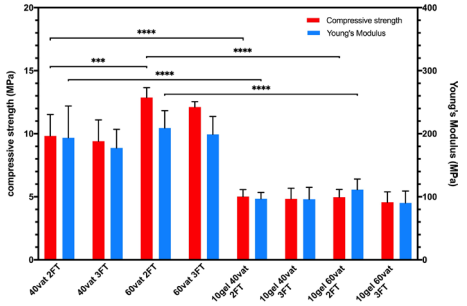

Figure 1. Compressive strength and modulus of composite scaffolds in the dry state. Data as mean ± SD, n=6.

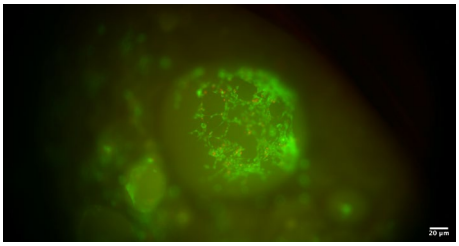

Figure 2. Live/Dead staining of HOS cells cultured on composite scaffolds for 7 days with cell attachment and proliferation within the pores.

CONCLUSION

Vaterite/PVA composite scaffolds exhibited properties with potential in bone tissue engineering. Further study will focus on optimizing the formulation of vaterite/PVA composite scaffolds and inclusion of magnetic nanoparticles to study the angiogenic potential followed by physical and biological evaluations.

REFERENCES

1. Koons, G.L. *et al.*, Nat. Rev. Mater. 5(8):584-603, 2020.
2. Rather, H.A. *et al.*, Mat. Sci. Eng. C, 103: 109761, 2019.

ACKNOWLEDGMENTS

J. X. would like to thank China Scholarship Council (CSC) (award No. 202006380073) for providing financial support to this project.

THE USE OF NANOFIBERS AS 3D SCAFFOLDS FOR EXPANSION AND MODULATION OF HUMAN MESENCHYMAL STEM CELLS: A COMPARISON STUDY TO 2D CULTURE

Kyambadde Alfred[1], Shephard Mathew[2], Forsyth Nick[3] and Yang Ying[4]

School of Pharmacy and Bioengineering, Keele University, Stoke-on-Trent, GB
t.i.kyambadde@keele.ac.uk

INTRODUCTION

The biological relevance of three-dimensional (3D) cell culture scaffolds over the traditional two-dimensional (2D) monolayer cultures has dominated scientific debate. Electrospun Nanofibers (NFs) are good candidates for use as 3D cell culture scaffolds. NFs have a high surface area–to–volume ratio and nano-scale porosity. Also, NFs can mimic key structural features of the native extracellular matrix and be bio-functionalized with bioactive groups to modulate cell behaviour[1,2]. However, there is still lack of enough succinct evidence comparing the difference in cell proliferation between of 2D and 3D cultured MSCs. Furthermore, there are few reports describing the differences in protein secretion between 2D and 3D cultured cells. In this study, we compared the difference in cell proliferation between 2D and 3D cultured MSCs, in terms of protein secretion and cell proliferation as well as the effect of nanofibers surface modification on the growth and expansion of MSCs.

EXPERIMENTAL METHODS

hMSC isolated from bone marrow mononuclear were cultured and expanded in tissue culture plates (TCP) up to passage 3 (P3) and assessed for trilineage differentiation potential *in vitro*. The MSCs were seeded on TCP and NF at a seeding density of 5000 cell/cm^2. Cell proliferation was assessed at different culture time points using CCK8 assay and Pierce BCA Protein Assay was used to quantify the total protein. Aligned polylactic acid (PLA) NF were electrospun using 3% PLA in chloroform[3]. For surface modification, oxygen plasma was carried out using a Diener electronic Femto Plasma system. (3-Aminopropyl)-triethoxysilane treatment was carried out to functionalize nanofiber surfaces. Static contact angles was monitored by sessile droplet contact angle goniometry. NF and cell morphology were observed by SEM and Giemsa stained samples respectively.

RESULTS AND DISCUSSION

Cultured P3 hMSCs demonstrated the capacity to differentiate to trilineage. We found that aligned NFs contributed to the directional alignment/orientation of hMSCs in a rather a contact guidance fashion (Fig1). Plasma treatment changed NF hydrophilicity greatly.

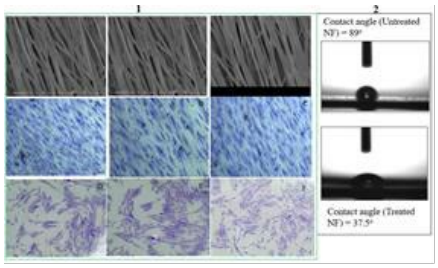

Figure 1: 1) Top left panel; SEM images of aligned NFs used. Middle left panel shows the orientated hMSCs grown along the aligned NF direction (stained by Giemsa). Bottom left panel; shows the haphazard growth of hMSCs on TCP. (2) Water contact angles of NF before (top) and after plasma treatment (bottom).

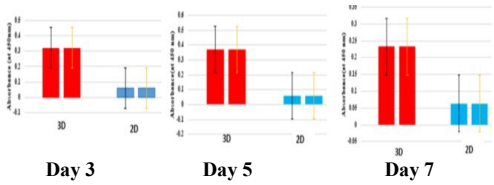

Figure 2: CCK8 results of the hMSCs cultured at different time points (3, 5, 7 days of culture). Red: NF; blue: TCP.

Also, there was more protein secretion in 3D NF cultured hMSCs (with 1-2 fold increase) compared to 2D cultured hMSCs.

CONCLUSION

This study provided solid evidence that nanofibers can be developed into tuneable 3D scaffolds used to modulate cell behaviour and expansion.

REFERENCES

1. Justice et al. *Drug Discov. Today* 14, 102–107 (2009).
2. Kouroupis et al. *Front. Bioeng. Biotechnol.* 9, 22 (2021).
3. Yang Y, Shephard M, Forsyth N. Scaffolds and uses of, 12th February 2021; PCT/GB2021/05034

A Biomimetic Tunable Scaffold to Align Glial Cells for Spinal Cord Regeneration

Sakthivel Nagarajan[1], Sébastien Blanquer[1], Marie-Noëlle Labour[1,2,*]
[1] ICGM, Université de Montpellier, CNRS, ENSCM, Montpellier, France
[2] Ecole Pratique des Hautes Etudes, paris, France
*marie-noelle.labour@enscm.fr

INTRODUCTION

Spinal cord injuries prompt largely incapacitating paralysis for which current therapeutic solutions are limited. Nerve tissue engineering strategies using cells combined with biomaterials are very promising but current available solutions are not fully efficient, require nerve autograft or are not transposable to clinic[1]. To induce axon guidance and restore connectivity, our strategy consists in the alignment of glial cells that provide both physical and trophic support for axon growth[2,3]. The objective of this study was to elaborate tunable gelatin-based multichannel scaffolds using stereolithography with high resolution and internal anisotropic topography to induce glial cells alignment. We precisely engineered 3D printed nerve conduits (NC) and evaluated their properties and MSC80 infiltration and behavior in the channels as a glial cells model.

EXPERIMENTAL METHODS

Modification of Gelatin and synthesis of photoinitiator. Gelatin methacrylamide (GelMA) was synthesized using methacrylic anhydride (MA) with ratio NH_2:MA 1:2, 1:10 and 1:20 in PBS for 3hrs, dialysed, and freeze-dried. The photo initiator, Lithium phenyl-2, 4, 6-trimethyl benzoylphosphinate (LAP) was synthesized through Michaelis–Arbuzov reaction[3]. Both were characterized using ^{1}H NMR.

Scaffolds processing and characterizations. The stereolithographic (STL) 3D printing was carried out using 20% (w/v) GelMA, 0.2% (w/v) LAP and 0.2% (w/v) photo absorber (Orange G). STL files were designed using Freecad software and 3D printing was performed using Asiga MAX 3D printer. Scaffold structure and water absorption capacity were analyzed by microtomography and environmental Scanning electron microscope (eSEM) and swelling analysis.

Cell culture and analysis. MSC80 cells were cultured using DMEM 10%FBS, 1% P/S and 1% Glutamine. MSC80 cells were seeded into the ethanol-sterilized scaffolds using a custom-made device and cultured for 4 days. After fixing using paraformaldehyde and subsequently stained using Atto565-phalloidin.

RESULTS AND DISCUSSION

Methacrylated gelatin performed in physiological buffer were obtained with 0.32, 0.65 and 0.63mmol/g for 1:2, 1:10 and 1:20 ratio NH_2:MA respectively. Gelatin with high degree of methacrylation (0.65mmol/g GelMA) was chosen for NC fabrication as increasing ratio did not improve methacrylation degree. 20% GelMA was optimal to obtain a high concentration with ideal viscosity for processing. STL 3D printing allowed the production of GelMA NC perfusable channels with tunable diameter of 500µm, 700µm and 1000µm. eSEM analysis shows that the channels size is consistent with CAD file (Figure 1) and present an internal porosity of approximately 20µm that could support the nutrient and oxygen diffusion. Swelling ratio of the NC were about 25% for all channel diameters (figure 1). This demonstrate NC stability in aqueous medium where they can maintained until further use for cell culture.

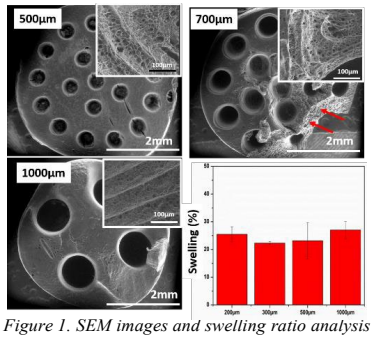

Figure 1. SEM images and swelling ratio analysis of the 3D printed GelMA scaffolds

Cell infiltration of the hydrated scaffolds is possible using a custom-made chamber. As expected, the cells adhere and proliferate within the scaffolds to reach a full coverage (Figure 2). In addition, the cells remain viable for at least 7 days, which confirms the cytocompatibility of the 3D printed NC.

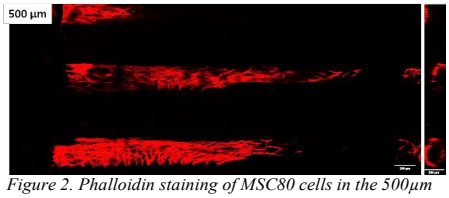

Figure 2. Phalloidin staining of MSC80 cells in the 500µm diameter GelMA neural graft, scale bar 200µm.

CONCLUSION

GelMA nerve conduit with 50-1000µm diameter aligned channels were successfully printed and stable in acqueous media. MSC80 cells infiltrated the channels, adhere and proliferate. Further studies will be carried out to evaluate the efficiency in axon guidance using primary Schwann cells and neuronal cells.

ACKNOWLEDGEMENT

Financial support from LabMUSE Chimie from Université de Montpellier ANR-16-IDEX-0006

REFERENCES

1. N. Ashammakhi, *et al.*, Regenerative Therapies for Spinal Cord Injury, Tissue Eng Part B Rev 25(6) (2019) 471-491. **2.** Venruzo V. et al., Stem cell paracrine effect and delivery strategies for spinal cord injury regeneration. Journal of Controlled Release 300 (2019) 141–153. **3.** Deumens, *et al.*, Alignment of glial cells stimulates directional neurite growth of CNS neurons in vitro, Neuroscience 125(3) (2004) 591-604.

Degradation Behavior of 3D-Printed Poly(L-Lactide-Co-Glycolide) Scaffolds for Cartilage Tissue Engineering

Anushree Ghosh Dastidar[1*], Susan A Clarke[2], Eneko Landa[3], Fraser Buchanan[1], Krishna Manda[1]

[1]School of Mechanical and Aerospace Engineering, Queens University Belfast, Belfast, United Kingdom
[2]School of Nursing and Midwifery, Queens University Belfast, Belfast, United Kingdom
[3]School of Pharmacy, Queens University Belfast, Belfast, United Kingdom
[*]aghoshdastidar01@qub.ac.uk

INTRODUCTION

Osteoarthritis (OA) is a degenerative disease that affects over 240 million people worldwide with one-third of the population over 65 years displaying signs of OA[1,2]. Repair of the damaged cartilage tissue using tissue engineering where the regeneration of the tissue is achieved after the implantation of the desired scaffolding matrix at the damaged site has been one of the most promising directions to alleviate OA. Despite significant advances, scientists have failed to regenerate cartilage tissue with the required biomechanical properties. The degradation of scaffolds is an important factor in tissue regeneration. Poly(L-lactide-co-glycolide) (PLGA) 85:15 bioresorbs in the body in around six months and can be a suitable material for cartilage regeneration. Therefore, this study aims to investigate the *in-vitro* degradation behaviour of 3D-printed PLGA scaffolds. Investigating this degradation at physiologically relevant time scales (>6 months) is time-consuming and expensive, therefore the current study also employs accelerated *in vitro* degradation methods[3].

EXPERIMENTAL METHODS

The PLGA scaffolds (fibre diameter 320µm, spacing 1.7mm) with a double offset design were 3D printed using Bioscaffolder (GeSiM, Germany) as shown in Fig.1. The scaffolds were degraded in phosphate-buffered saline (PBS), following ISO 13781:2017 under sterile conditions at 37ºC for physiological conditions and elevated temperature of 47ºC for accelerated degradation. The scaffolds were evaluated at specific time intervals for 6 weeks for their structural features, compressive properties, glass transition temperature with differential scanning calorimetry analysis, changes in swelling, mass, pH, and molecular weight using gel permeation chromatography.

RESULTS AND DISCUSSION

The PLGA scaffold displayed a compressive modulus of 4.38±1 MPa, equilibrium modulus of 5.11±1 MPa, and dynamic modulus of 20.95±1 MPa, having comparable properties with the native cartilage. Degradation of the scaffolds under physiological conditions displayed a decrease in pH from 7.2 to 7.13 due to the hydrolysis and release of acidic oligomers from the polymer into the PBS. The scaffolds underwent less-significant changes in mass and swelling due to the stable crystalline nature of PLGA. A mass loss of 1.3% and swelling of 10.74% were observed over 21 days. There is a general decreasing trend in glass transition temperature with a 1.5°C decrease over 42 days due to the highly porous and hydrophilic scaffolds. This was also observed in the molecular weight of the scaffolds over 42 days with the rate of degradation being faster at 47°C. The compression modulus of the scaffolds decreased by 30%, equilibrium modulus by 5%, and ramp modulus by 15% over 42 days. The scaffolds maintained their volumetric appearance throughout the period which mirrored the low mass loss and swelling in the scaffolds due to the organized crystallinity of PLGA that controls the amount of water uptake. The decrease in the properties of the scaffold was enhanced at elevated temperature which further provides an insight into how the scaffold would degrade in the long term.

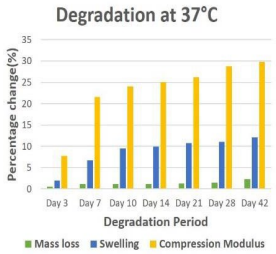

Fig. 2: Percentage change versus mass loss, swelling, compression Modulus

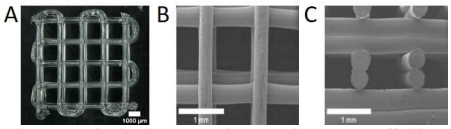

Fig. 1: Optical microscope image of PLGA scaffolds (A), SEM image of top view (B), and SEM image of the cross-sectional view (C)

CONCLUSION

This study allows an insight into the likely long-term performance of the bioresorbable polymer in a relatively short window of time. The scaffold was retaining shape and with reasonable loss in mechanical properties, The scaffold has displayed a stable rate of degradation which could be further applied in-vitro regenerative studies. This goes beyond the short-term biocompatibility testing that is used to evaluate degradable biomaterials.

REFERENCES

1. Mobasheri A. *et al*., Osteoarthritis and cartilage open. 3, 2021
2. Hawker GA. *et al*., Clin Exp Rheumatology. 120:3-6, 2019
3. Geddes L. *et al*., Polymer Testing. 91:106853, 2020

ACKNOWLEDGMENTS

This work has been funded by The Engineering and Physical Sciences Research Council (EPSRC) via a PhD studentship

Investigating macrophage activation induced by internalization of different biomaterials using flow cytometer

Idris Kalokoh*, Bowen Xie*, Ying Yang (* equal contribution)

School of Pharmacy and Bioengineering, Keele University, Stoke-on-Trent, UK

Introduction: Implanted biomaterials for therapeutic purpose frequently trigger host inflammatory response. The wears and degraded particles will activate macrophages. However, the particles' properties dictate macrophages' polarization, either into pro-inflammatory (M1) or anti-inflammatory phenotype (M2). M1 and M2 macrophages display different cell size and granularity after internalization of particles. Flow cytometry is a powerful technique to profile cells in a heterogeneous fluid mixture. In this study, we aims to study the cellular response of macrophages after internalization of different polymeric particles by flow cytometer, with cross-validation by other techniques.

Materials and Method: Raw 267.4 macrophage were cultured in DMEM media supplemented with 10% FBS and 1% antibiotics. The cells were induced to M1 phenotype by incubating with LPS (100 ng/ml) and IFN-γ (20 ng/ml) for 48 hrs. 5 µm PGA (poly-glycolic acid) and agarose particles were incubated with the M1 cells for 48 hrs for internalization at density of 20 particle/cell. Optic microscope was used to observed cell morphology. Scattering property from flow cytometer were analysed in details. NO and Cell viability test were conducted as well.

RESULTS: Optical images showed M1 cells increased in size when PGA particles were internalised, but not much with agarose samples (Fig 1). Dot plot (Fig 2) showed the separation of live cells from dead cells or debris. Notable changes were also observed to scattering data, FSC and SSC

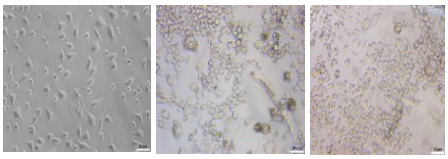

Fig 1: *Morphological images of M1 macrophage (left), M1 with PGA particles (middle), and M1 with agarose (right).*

values, following the phagocytosis of PGA but not much for agarose. The FSC plot showed that high FSC value in M1 cells that internalized PGA particles than cells that internalized agarose and no particles M1 cells. The SSC displayed similar pattern (Fig 3). M1 cells engulfed PGA exhibited higher SSC value, indicating more granularity than the cells engulfing agarose and control M1. NO

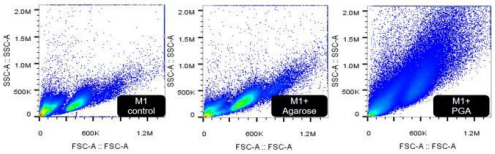

Fig 2: Dot plots of M1 macrophage with internalizing PGA and Agarose particles use no particle intake as control.

value was high in PGA engulfed M1 than agarose engulfed and control M1.

DISCUSSION & CONCLUSIONS:

Internalization of polymer particles induced macrophage cells morphologic change. Scattering values in flow cytometer correlate well with imaging observation and NO analysis. Internalization of degradable polymer particles, PGA triggered strong inflammatory response but non-degradable particle, like agarose did not.

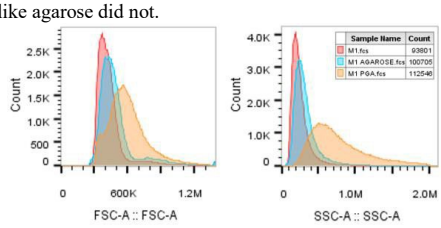

Fig 3: *Comparison of FSC and SSC of M1 macrophage engulfing PGA and agarose particles. Gated cell count:100k. Control: no particles M1.*

Bioactive methacrylate hyaluronic acid- Silicon doped Hydroxyapatite composites scaffolds for bone tissue regeneration.

Rebecca Pellegrino[1*], Giulia Gennari[1], Paola Nitti[1], Kunjalukkal Padmanabhan S. [1],Christian Demitri[1]
[1] Department of Engineering for Innovation, University of Salento, Lecce 73100, Italy
[*] rebecca.pellegrino@unisalento.it

INTRODUCTION

The use of three-dimensional bioceramic-based scaffolds for bone tissue regeneration is a golden standard in tissue engineering. As well as for other tissues, for bone regeneration, the scaffold's morphology, in particular pore architecture, and scaffold's composition, are key parameters for cell viability and tissue regeneration. Usually, morphology is managed through thermally induced phase separation technique consisting of controlled quenching and freeze-drying to remove ice crystals to create porosity[1]. With their open and interconnected porosity, sintered hydroxyapatite-based scaffolds already provide an adequately controlled porosity that improves osseointegration. However, adding a polymeric component to replicate the typical structure of the extracellular matrix of bone tissue should increase the bioactivity[2,3].This work's purpose was to realize and characterize scaffolds of silicon-doped hydroxyapatite scaffold (Ha-Si), made through sponge replication method, and impregnated with three different concentrations of methacrylated hyaluronic acid slurries (HYALme)[4,5].

EXPERIMENTAL METHODS

Scaffold preparation

The preparation of (Ha-Si)-(HYALme) scaffolds presents the following steps: synthesis of HA doped with 2% of Si ceramic powders; sponge replication method and sintering at 1300°C; synthesis of methacrylate hyaluronic acid; scaffolds impregnation; UV cross-linking and freeze drying. Powder was prepared through reaction between calcium hydroxide $Ca(OH)_2$; phosphoric acid (H_3PO_4 85% w/w) and silicon tetraethyl orthosilicate (TEOS, $Si(OC_2H_5)_4$, Sigma Aldrich) and subsequent calcination at 900°C after milling. Hyaluronic acid (HA, Injection grade HA-EP1.8, Bloomage Biotechnology, China) was methacrylated according to the procedure described by Leach et al. (Jennie Baier Leach et al., 2003). Scaffolds were impregnated by vacuuming them with a HYALme solution at 10 mg/ml, 26 mg/ml or 35 mg/ml containing 3% by polymer weight percentage of Irgacure 2959 photoinitiator (Ciba Specialty Chemicals, Basel, Switzerland) as crosslinker. Impregnated scaffolds were crossinked exposing them to UV (1000 W for 5 min).

Characterization

Ha-Si powder and scaffolds were both analysed with XRD after calcination and sintering. Porosity analysis was performed. Impregnation and morphology were observed through digital microscope, and pore size was studied through the ImageJ software. Impregnated scaffolds were subjected to biostability test by immersing them in a Tris-HCl solution at 37°C up to 28 days. At scheduled times (3, 7, 14, 21 and 28 days) mechanical properties (compression tests) and weight loss were evaluated. In addition, visco-elastic properties of HYALme solutions were evaluated.

RESULTS AND DISCUSSION

XRD proved that, following the calcination and sintering process, the only material present is hydroxyapatite. The average pore size of the hydroxyapatite scaffolds is between 200 and 800 µm in a range that can usually promote regeneration facilitating diffusion and migration of the cells and their adhesion to the scaffold.

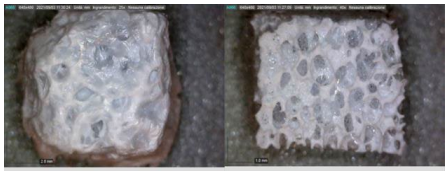

Fig. 1 Impregnated scaffolds with left 10 mg/ml and right 26 mg/ml HYALme solutions.

The impregnation was successful, as it is noted that the polymer has spread homogeneously on the surface, but it emerges that the impregnation with a concentration of 26 mg/ml is considerably improved (Fig. 1). This difference is probably due to its particular viscosity values compared to the other solutions, as it emerges from rheological analysis. In addition, polymer concentration and crosslinking do not affect weight loss. Moreover, it has been shown that most of the polymer degrades as early as 3 days of incubation, but its presence enhances mechanical stability compared to Ha-Si without polymer.

CONCLUSION

The analyses carried out revealed a great weight loss 3 days of incubation for composite scaffolds. Methacrylate hyaluronic acid reduces the mechanical performance of the scaffolds in the first days of incubation but for a long time acts as a protective agent on the ceramic phase, preserving its mechanical qualities that could be positive for a better regenerative performance of the scaffold, which depends on its mechanical properties.

REFERENCES

1. Friuli M. *et al*., Res. in Eng. 2021. 12: p. 100282.
2. Nitti, P. et al. Front. Bioeng. Biotechnol 2021. 9, 631177.
3. Raucci, M. G., *et al*., Front. Bioeng. Biotechnol. 2019. **7**, 27-27.
4. Nitti, P. *et al*. J Healthc Eng. 2018. 3651480.
5. Palazzo, B. *et al*.. Int J Immunopathol Pharmacol. 2011. 24, 73-78.

ACKNOWLEDGMENTS

This research was partially funded by PON-MISE OSTEO-CARE project, Prog. no. F/050370/03/X32 and by PRIN-SAPIENT project, Prog. no. 2017CBHCWF.

Development of a 3D polysaccharide porous membrane for the modelling of the outer blood retina barrier

Chloé Dujardin[1, *], Paola Aprile[1], Walter Habeler[2], Christelle Monville[2], Didier Letourneur[1], Teresa Simon-Yarza[1]

[1] Université Paris Cité, INSERM U1148, Paris, France.

[2] I-Stem, Institute for Stem Cell Therapy and Exploration of Monogenic Diseases, Corbeil-Essonnes, France

* Contact: chloe.dujardin@inserm.fr

INTRODUCTION

Structural and functional integrity of the retina is maintained by the outer blood-retina barrier (oBRB) composed of the monolayered retinal pigment epithelium (RPE), the acellular collagenous Bruch's membrane and the vascularized choroid. In retinopathies leading to vision loss, such as hereditary choroidal dystrophy and advanced dry age-related macular degeneration, primary functional defects in RPE cells lead to physiological defects of the choroid disturbing the retinal homeostasis. There are neither effective treatments to these diseases nor good animal or human cell models recapitulating the oBRB structure and all the clinical hallmarks so far. To cope with these limitations, our goal is to develop a 3D oBRB culture tissue based on a polysaccharide membrane and co-cultured with choroidal endothelial cells (ECs) and RPE cells. Here, we present the optimization of the 3D membrane, its functionalization, and its suitability for the culture of RPE and ECs. This 3D oBRB could further be used in disease modelling to find new pharmacological treatments and to engineer constructs for cell therapy of retinal diseases.

EXPERIMENTAL METHODS

The membranes were synthesized from an aqueous solution of pullulan, dextran, and sodium chloride and were further freeze-dried to create a porous network within its structure[1,2]. The freeze-drying (FD) protocol was optimized for the membrane to mimic the oBRB structure. The thickness and the porosity of the scaffold were evaluated both in its dry state using scanning electron microscopy (SEM), and in its hydrated state using confocal microscopy. To favour cellular adhesion on the scaffolds, the membranes were coated with collagen type I and laminin 521, both present in the oBRB extracellular matrix. Specific immunostainings were conducted to assess the efficiency of the coatings, as well as second harmonic generation to visualize the collagen. Human umbilical vein endothelial cells (HUVECs), as a model of vasculature, and RPE cells derived from human pluripotent stem cells[3] were seeded *in vitro* on the membranes for up to 14 days. Viability, morphological and functional characterization was performed for each cell type.

RESULTS AND DISCUSSION

Using injection molding, the membranes, once hydrated, reached the 200µm physiological thickness of the oBRB. To mimic the oBRB structure, with the RPE monolayer above the choroidal vascular network, the FD protocol was optimized by studying the polysaccharides concentration and cross-linking density, the influence of the sample support material, the hydration solvent, and the freezing parameters, on the porosity and on the pore morphology (Fig. 1.A-C). We obtained membranes with, on one side, a smooth surface intended for the RPE monolayer culture, and, on the other side, a porous surface connected to the inner porous network with elongated pores allowing ECs penetration within the structure (Fig. 1.C-E)

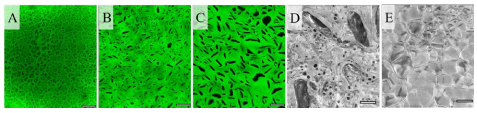

Figure 1: Optimization of the FD protocol. Inner porosity imaged with confocal microscopy of matrices FD on metal (A), on polystyrene (B) and on polystyrene with a longer freezing step (C). Surface porosity imaged with SEM of the porous side (D) and of the smooth side (E) in the same conditions as (C). In confocal images, the matrix in visible by addition of FITC-Dextran. Scale bar is 200µm for confocal images and 100µm for SEM images.

The collagen coating, visible both on the surface of the gels and in the pores (Fig. 2.A-B), was optimized to maximize cellular adhesion while limiting pore clogging. HUVECs were seeded on the porous surface of dried membranes, to favour their migration throughout the entire thickness, without crossing the opposite side, leaving the smooth side cell-free. In the uncoated matrices, no cells are visible in the gels after 14 days (Fig. 2.C). However, thanks to the collagen functionalization, HUVECs colonized the entire thickness, and were able to adhere on the seeded surface and on the elongated pores walls up to 14 days (Fig. 1.D). Moreover, small channels were observed between the pores, demonstrating cell migration and remodelling of the matrix (white arrows, Fig. 2.D). The RPE cells were seeded on the smooth surface of hydrated membranes, coated with collagen and laminin to mimic the Bruch's membrane. In those conditions, the RPE cells formed a monolayer, without any cell penetration in the matrix.

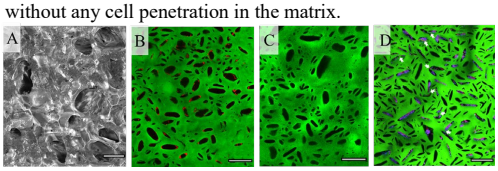

Figure 2: Functionalization and HUVECs seeding. Collagen imaging of the porous surface with SEM (A) and in the gel with confocal imaging (B, Sirius red staining) and confocal imaging of HUVECs seeded samples, after 14 days in culture and either uncoated or coated with collagen (C and D respectively, DAPI and Phalloidin-TRITC staining). In confocal images, the matrix in visible by addition of FITC-Dextran. Scale bar is 200µm for confocal images and 100µm for SEM images.

CONCLUSION

By optimizing the FD protocol, we obtained 200µm thin membranes mimicking the oBRB structure, with a porous surface allowing ECs penetration and a smooth surface to form the RPE monolayer. Next studies will focus on the co-culture of the two cell types to fully model the oBRB and on the *in vivo* implantation of the membranes in a rat model.

ACKNOWLEGMENTS

The authors would like to thank the French Research Agency (Grant no: ANR-20-CE18- 0034-02 GLYCOMB) for providing partial financial support to this project.

REFERENCES

1. Autissier A. *et al.*, Acta Biomater., 6(9), 3648, 2010
2. Labour M.N. *et al.*, Int. J. Mol. Sci., 21(10), 3644, 2020
3. M'Barek K.B. *et al.*, Sci.Transl.Med., 9(421),7471, 2017

Porcine islet macroencapsulation for the treatment of type I diabetes (T1D)

Victoria Sarangova[1,3], Carolin Heller[2], Petra B. Welzel[1], Barbara Ludwig[2], Carsten Werner[1,3]

[1]Leibniz-Institut für Polymerforschung Dresden e. V., Dresden, Germany
[2]Universitätsklinikum Carl Gustav Carus Dresden, Dresden, Germany
[3]Technische Universität Dresden (TUD), Dresden, Germany
sarangova@ipfdd.de

INTRODUCTION

Macroencapsulation of porcine islets represents a promising approach for the treatment of patients with insulin-deficient diabetes mellitus (type I diabetes, T1D) [1].

In the present work, an advanced modular device was designed to overcome main hurdles of the currently existing encapsulation systems. The key components of the proposed device include a bioactive immuno-isolating membrane and a tailored islet-supporting matrix, as well as an intrinsic oxygen generating module that allows to maintain the viability of the graft in the early post-transplantation period.

EXPERIMENTAL METHODS

Islet clusters of different sizes (pseudoislets) were formed in microwells of different size and arranged in different pattern. The viability of the formed clusters was assessed via FDA-PI staining/confocal imaging. StarPEG-glycosaminoglycan (GAG) biohybrid hydrogels [2] were used to mimic the extracellular microenvironment in the islet module of the macroencapsulation device. A special centrifugation-based technique was applied to embed the islet clusters in the microwells.

3D printing and PDMS molding techniques were applied to manufacture oxygen-generating disks with dimensions that fit into the macroencapsulation device. Therefore, calcium peroxide particles (CaO_2) were embedded in PDMS based on an approach reported by Pedraza et al. [3]. The PDMS- CaO_2 disks were characterized with regards to their oxygen release profile and utilizing staining and microscopic techniques.

To estimate the overall oxygen availability in the islet macroencapsulation device, oxygen diffusion was simulated for various conditions utilizing "COMSOL Multiphysics" software.

RESULTS AND DISCUSSION

Development of a dead core was faster in islet clusters with larger diameter compared to the islets with smaller diameter formed in the microwells. The computational simulation confirmed the oxygen deficiency in the islets of a bigger size and their tendency to form a hypoxic core even in the presence of an additional oxygen source.

Using the developed centrifugation-based techniques, the islet formed in the microwells could be embedded in a defined manner in starPEG-GAG hydrogels which allows further decoration with islet supportive factors via the GAG component.

Moreover, a reliable method to produce PDMS-CaO_2 disks with a smooth surface, as shown by scanning electron microscopy and Alizarin S Red staining of the disk, and an optimal geometry were successfully developed for the further applications in the designed islet macroencapsulation device. The disks were shown to produce sufficient amounts of oxygen over a period of 28 days.

CONCLUSION

The concept of a modular islet macroencapsulation device is presented. Islet clusters of uniform size were formed in microwell arrays for subsequent embedding in biohybrid hydrogels in a defined arrangement. Combining experiments and simulations seems to be a promising approach to determine optimal cluster size and arrangement in the islet module for an advanced oxygen supply and survival of the graft. Due to the sustained long-term oxygen release the presented customized oxygen generating module is expected to further improve islets survival and function in the early post-implantation period. This will be investigated in the ongoing studies.

REFERENCES

1. Ludwig, B. *et al.,* Proc. Natl. Acad. Sci. USA, 114, 11745-11750, 2017
2. Freudenberg, U., *et al.,* Adv. Mater., 28: 8861-8891, 2016
3. Pedraza, E. *et al*., Proc. Natl. Acad. Sci. USA, 109-4245, 2012

ACKNOWLEDGMENTS

The authors would like to thank the Deutsche Forschungsgemeinschaft (DFG, German Research Foundation) for providing financial support to this project (ID 213602983 – TRR 127).

Quality-By-Design Driven Development and Up-scaling of a Medical Device for the Guided Regeneration of Bone Defects

Paola Aprile[1*], Rachida Aid[1], Soraya Lanouar[1], Laurent Bidault[2,3], Teresa Simon-Yarza[1], Didier Letourneur[1,3]
[1]LVTS INSERM U1148, Université Paris Cité, Paris, France
[2]SILAB, Saint-Viance, France
[3]SILTISS, Saint-Viance, France
[*]paola.aprile@gmail.com

INTRODUCTION

Guided Bone Regeneration (GBR) therapy has proven successful in repairing large bone defects for both dental and orthopedic applications[1,2]. Collagen-based medical devices (MDs) are often used for GBR application however, their fast degradation rate can jeopardize the clinical outcome. Despite large investments to develop new MDs for GBR, the number of new products achieving clinical application and market release is low[3]. The initial design of an MD can take up to 70% of the total product life cycle and at this stage potential developmental risks should be evaluated and controlled. A valid approach to minimize risks and to identify key design factors is represented by the Quality-By-Design (QbD) strategy, which implements a statistical method to investigate the effect of different variables on the desired quality attributes. Therefore, the aim of this work was to develop and up-scale the production of an alternative to collagen-based MDs for GBR application by integrating the QbD strategy at the early developmental stage of the product design.

EXPERIMENTAL METHODS

The MD was produced by adapting a published protocol[4]. The mechanical properties were evaluated by rheometry (Discovery HR-2) and nanoindentation (Piuma). Crosslinker quantification and spatial distribution was studied by an in-house biochemical assay[4]. For *in vitro* biocompatibility and efficacy testing, murine and human primary fibroblasts were used to assess material toxicity (Live/Dead, CCK-8 and LDH assay) and cell penetration (immunolocalization and DNA quantification (PicoGreen)). Material degradation was assessed *in vitro* by enzymatic digestion[4] and *in vivo* by subcutaneous implantation in mice. Gamma sterilization was performed by IONISOS. Statistical analyses were performed using GraphPad Prism software and results, are presented as mean ±SD. A level of $p<0.05$ was considered significant.

RESULTS AND DISCUSSION

In order to facilitate the design and up-scaling of our MD, it was necessary to apply a risk assessment cycle. As such, critical material attributes (CMA) and process parameters (CPP) were initially identified accordingly to their influence on the MD's critical quality attributes (CQA). The final CPP, reported in Table 1, allowed to compare laboratory procedure versus industrial procedures and to decide which protocol was best preserving the CQA upon up-scaling (Table 1).

Not.	Definition	Type	Range
u_1	non-homogeneous mix	Qualitative	{M1 ; M2}
u_2	Reticulation time/temperature	Qualitative	{20min/50C ; 120min/25C}
u_3	Rinse bu⌐ler	Qualitative	{Bu⌐ler 1 ; Bu⌐ler 2}
u_4	Protocol of freezing process	Qualitative	{Protocol 1 ; Protocol 2 }

Table 1. Final list of CPP analysed

When the laboratory versus industry polymer-mixing strategy (Table 1, u_1) were compared, we found that the gelling time and crosslinker quantity and distribution were comparable (data not shown). Crosslinking the material at 50°C led to a slower degradation time *in vivo* (Figure 1A&B), which was correlated to higher mechanical properties (Figure 1C). Finally, u_3 and u_4 (Table 1) were also tested and the prototype was sterilized by gamma rays. Although *in vitro* the gamma irradiated MD degraded faster than the UV sterilized, *in vivo* it showed a comparable performance to a commercial gold standard (collagen-based MD, data not shown).

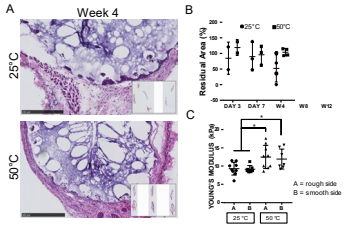

Figure 1. *In vivo* degradation kinetic. A) H&E staining of MD at 4 weeks. Scale bar 500µm. B) Quantification of the residual area and C) nanoindentation mapping before implantation.

CONCLUSION

Altogether these results showed the implementation of the QbD approach as a mean to evaluate the risks associated to the development and up-scaling of an MD. The coordinated effort between laboratory and industrial advice, allowed to comply with the fundamental requirements of reproducibility, efficiency and safety of the manufacturing process. Next studies will focus on the implantation of the gamma irradiated prototype in a rat pre-clinical model.

REFERENCES

1. Urban I.A. *et al*., Oral Maxillofac. Surg. Clin. North. Am. 331–338, 2019.
2. El-Jawhari J.J., *et al*., Eur. Cells Mater. 292–309, 2019.
3. S. J. Hollister *et al*., Biofabrication.1, 012001, 2009.
4. Grenier J. *et al.,* Acta Biomat. 94, 195-203, 2019.

ACKNOWLEDGMENTS

This work was funded by TB-MED- Horizon 2020 grant no: 814439. The authors wish to thank CYNANO.

Design of hybrid polymer/peptide nanofibers for soft tissues regeneration

Karima Belabbes[1], Coline Pinese[1], Audrey Bethry[1], Gilles Subra[2] and Xavier Garric[1]

[1] Department of Polymers for Health and Biomaterials, IBMM UMR 5247
University of Montpellier, CNRS, ENSCM, Montpellier, France
[2] Peptide group, IBMM UMR 5247
University of Montpellier, CNRS, ENSCM, Montpellier, France

INTRODUCTION

Nanofibers are excellent biomimetic supports for tissue regeneration since they mimic the architecture of the natural extracellular matrix. However, poly(lactic acid) (PLA) is an inert polymer and therefore not active on cells. This work aims to create PLA nanofibers that, in addition to this guiding role, could modulate cellular behavior.[1] For this purpose, we have created the possibility to covalently combine functionalized PLA with bioactive peptides directly during the electrospinning process in order to create a bioactive three-dimensional network constituting the nanofibers.

EXPERIMENTAL METHODS

We synthesized linear-PLA of 200 $kg.mol^{-1}$ and 4-arms star-PLA of 25 $kg.mol^{-1}$, 12 $kg.mol^{-1}$and 5 $kg.mol^{-1}$ by ring opening polymerization of DL lactid on pentaerythritol for star shaped polymers and diethylene glycol for linear polymers. The molecular weight of the Star-PLA was determined by H-NMR from the atomic ratio between methylene protons of pentaerythritol. StarPLAs were subsequently quadrifunctionalized by reacting isocyanato propyl triethoxysilane (IPTES) on polymers hydroxyl groups to create covalent urethane bonds under anhydrous conditions to avoid pre-crosslinking during the reaction. The functionalized polymers (Star-PLA25k-PTES, Star-PLA12k-PTE and Star-PLA5k-PTES) obtained were characterized by size exclusion chromatography (SEC), H-NMR and DOSY. Peptide 1 H-$(\beta\text{-Ala})_3$-Phe-(β-Ala)-Lys-(FITC) -$(\beta\text{-Ala})_2$-Lys-NH_2 was synthetized by standard Fmoc SPPS on Fmoc-NH-CH2-CH2-NH2-Chlorotrityl-resin. This peptide was subsequently functionalized by IPTES under basic and anhydrous conditions. The peptide obtained was characterized by LC/MS. Star-PLA-PTES were dissolved in TFE at concentrations ranging 5 to 20 wt %. HCL (10µl /ml of polymers solution) was added to activate the sol gel process. The formation of the polymer-peptide network during electrospinning was characterized by nanofibers gel fraction (quantify the formation of the network by a ratio of the insoluble part on the initial weight) measurement and mechanical properties.

RESULTS AND DISCUSSION

First, the molecular weights of the obtained 4-arms star-PLAs were close to the theoretical values and their dispersity were low. In addition, H-NMR and SEC analysis showed that 4 PTES functions were added to the 4-arms star-PLAs and 2 to the peptide (functionalization rate of 100%). Then, we produced hybrid nanofibers by reacting silylated peptides with silylated PLAs via sol-gel process during electrospinning and fine-tuned this process in order to increase the crosslinking of the network. In order to facilitate electrospinning, we added a linear-PLA diluent. However, as the amount of diluent increased, the cross-linking of the nanofibers was lower: the gel fractions of the formed nanofibers decreased from 36.4% to 8.8% for a ratio diluent/Star-PLA25k-PTES (w/w%) of 0.25 and 3 respectively. We fixed this ratio to 0.3 that is a good compromise between the quality of cross-linking and the electrospinning time. Interestingly, the crosslinking of the nanofibers was improved with the use of low molecular weight polymers due to a high content of crosslinking groups (PTES). Indeed, gel fractions were increased from 40 to 61% by replacing the Star-PLA25k-PTES by Star-PLA12k-PTES or Star-PLA5k-PTES.

We then introduced the peptide 1 inside the electrospun polymeric solution to add biological properties to the nanofibers. The addition of 0.1% and 1% of bifunctionalized peptide 1 increased the initial gel fraction of 61% to 66.6% and 78.3 % respectively. In consequence, the nanofibers stiffness and strength increased with the peptide quantity. The young modulus without and with 0.1% and 1% of peptide were found to be 30, 54 and 218 Mpa. The breaking strength also increased from 1.32 Mpa for nanofibers without peptide to 4.9 Mpa for nanofibers with 1% peptide. We obtained a peptide grafting rate >40% for all the condition.

Finally, the biological properties of hybrid nanofibers on skin fibroblasts were studied and confirmed that these materials are non-cytotoxic and enhance L929 cells proliferation.

CONCLUSION

In conclusion, we developed a new process to obtain nanofibers composed of a hybrid three-dimensional network that contain degradable polymers covalently bonded with bioactive peptides. The polymers and peptides can be modified, like legos, to fit different target tissues.

ACKNOWLEDGMENTS

We thank Symbio3 and Cartigen platform and the ministry of Algeria for funding.

Analyzing The Risk Of Calcification In Materials Used For In Situ Heart Valve Tissue Engineering

Dewy van der Valk[1,2], Charlotte Hoes[1], Yunia Rasenberg[1], Wojtek Szymczyk[1], Anat Akiva[3], Anthal Smits[1,2], Carlijn Bouten[1,2].

1 Department of Biomedical Engineering, Eindhoven University of Technology, Eindhoven, The Netherlands
2 Institute for Complex Molecular Systems, Eindhoven University of Technology, Eindhoven, The Netherlands
3 Department of Cell Biology, Radboud UMC, Nijmegen, The Netherlands

INTRODUCTION

Material-driven *in situ* tissue engineering (TE) of valvular grafts prospects a great alternative to current autologous, xenografted, and non-biological valve replacements. In this *in situ* approach, a synthetic degradable valve replacement is implanted at the site of a diseased valve, where it gradually remodels into viable tissue.[1] However promising, some risks need assessment to ensure safe clinical translation. Among these is calcific nodule formation during *in vivo* assessment of the grafts, reported in 35% of current TE grafts in preclinical animal studies.[2-4] This study established an *in vitro* model to assess calcification potential of materials for *in situ* TE.

EXPERIMENTAL METHODS

Three candidate materials for *in situ* TE were electrospun into fibrous scaffolds with a fiber diameter ranging from 4-6 um; widely used Polycaprolactone (PCL), as well as two supramolecular polymers Bis-Urea extended PCL (PCL-BU), and Bis-Urea extended Polycarbonate (PC-BU). A glutaraldehyde-treated bovine pericardial patch was used as control for current clinical practice. Circular scaffolds of 8 mm Ø were clamped in membrane-free transwell inserts and seeded with porcine Valvular Interstitial Cells (pVICs) or used unseeded. Scaffolds were then cultured for three weeks in phosphate-enhanced calcification medium (CM). PCL scaffolds were furthermore cultured in CM enhanced with Macrophage conditioned inflammation medium (IM). Calcification and collagen formation were assessed with live hydroxyapatite and collagen staining. Cell differentiation was analyzed using real time polymerase chain reaction (PCR)

RESULTS AND DISCUSSION

After three weeks of culture, PC-BU scaffolds showed little calcification, were calcification in PCL as well as PCL-BU scaffolds increased (Figure). Collagen formation was similar between PCL and PC-BU, but more compared to PCL-BU scaffolds. pVIC osteogenic gene expression was increased in scaffolds cultured in CM compared to NM, but not differentially expressed in different scaffold-types. Expectedly, scaffolds cultured without pVICs stained negative for collagen and hydroxyapatite. Seeded PCL scaffolds cultured in IM showed increased calcification compared to CM. Cell expression of osteogenic genes was increased in these scaffolds cultured in IM compared to CM. Pericardial patch results are to be analyzed. Overall, materials for *in situ* TE of valvular grafts showed a differential potential for calcification.

CONCLUSION

This study established a model to find differential calcification potential of scaffolds for *in situ* TE. PC-BU scaffolds, which show good results with little calcification in *in vivo* animal studies, showed little calcification potential in our model, unrelated to the amount of collagen formation. Scaffold calcification was mediated by cellular activity and increased with inflammation. The established *in vitro* model can be used to assess if materials for in situ TE calcify and can help discover the reasons why. Moving forward, this model will be extended with hemodynamic loads and patient specific culture conditions to assess risk of calcification under in vivo clinically relevant conditions. This data may support optimization of biomaterials for *in situ* valvular TE, aiding safe clinical translation.

REFERENCES

1. Wissing TB *et al*., Npj Regen Med. 2(1):18, 2017.
2. Bennink G *et al*., J Thorac Cardiovasc Surg. 55(6):2591-2601, 2018.
3. Kluin J, *et al.*, Biomaterials. 125:101–17, 2017.
4. Valk DC van der *et al.* Manuscript in preparation, 2022.

ACKNOWLEDGEMENT

We gratefully acknowledge the Gravitation Program “Materials Driven Regeneration”, funded by the Netherlands Organization for Scientific Research (024.003.013)

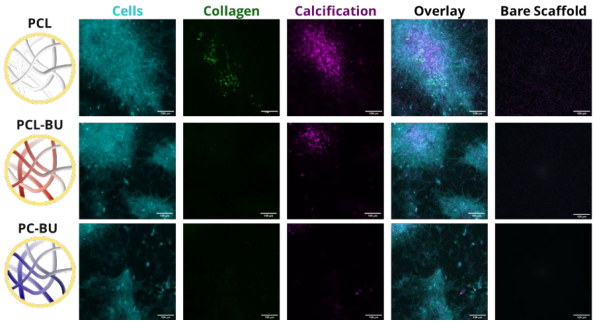

Figure 1 Collagen formation (green) and calcification (pink) in PCL (top), PCL-BU (middle), and PC-BU (bottom) scaffold materials.

MC3T3-E1 Cells in Novel 3D Poly(Lactic Acid) (PLA) and Poly-4-Hydroxybutyrate (P4HB) Bioabsorbable Textile Scaffolds for Bone Tissue Regeneration

Flavia Caronna[1,3*], Skander Limem[2], Said Rizik[2], Khoa Do[3], William Ronan[1], Eimear B. Dolan[1]
[1] Biomechanics Research Centre (BMEC), Biomedical Engineering, NUI Galway, Galway, Ireland
[2] Tepha Medical Inc. (now part of Becton & Dickinson) Lexington MA, United States of America
[3] ITA GmbH, Aachen, Germany
[*] flavia.caronna@nuigalway.ie

INTRODUCTION. Bioabsorbable polyesters have become very attractive for use in scaffold-based implants. In this context, textile technology provides design freedom at the micro and macro scale, enabling mimicry of fibrous biological structures of the extracellular matrix,[1] while allowing manufacturing at an industrial scale. In this work, these two technologies are strategically combined, and for the first time, mouse calvaria preosteoblast MC3T3-E1 cells are cultured *in vitro* on 3D poly(lactic acid) (PLA) and poly-4-hydroxybutyrate (P4HB) bioabsorbable textile scaffolds, to explore their osteogenic potential.

EXPERIMENTAL METHODS. Warp-knitted spacer fabric scaffolds were manufactured using commercially available PLA and P4HB yarns. Each textile featured two cover areas (made of multifilament yarns) interconnected by a monofilament pile yarn[2]. Three-dimensional textile sheets, with thickness of 1-1.2 mm, porosity of 80-85% and compressive Young's modulus of 16.1 ± 4.4 kPa (PLA) and 27.5 ± 3.5 kPa (P4HB), were sterilized by Ethylene Oxide. Prior to seeding, scaffolds were cut with a 6 mm diameter sterile punch and prepared following Brennan et al.[3]. MC3T3-E1 cells (ATCC) were expanded in basal media as described by Murphy et al.[4] (using 1% penicillin/streptomycin instead), seeded at passage 20 on scaffolds at a density of 10^4 cells/scaffold. Textiles were cultured for 24h in basal media, and then (day 0) treated with osteogenic supplements as in Persson et al.[5] for 21 days. Metabolic activity was measured using AlamarBlue (AB) assay (Thermo Scientific) at day 2, 7, 14 and 21. DAPI (4',6-diamidino-2-phenylindole) (Sigma Aldrich) fluorescent nuclei staining, and Pico488 dsDNA quantification assay (Lumiprobe) were performed after 1, 7, 14 and 21 days of culture to determine cell distribution and proliferation, respectively. Calcium production was qualitatively assessed using Alizarin Red Staining (ARS, Molekula) at day 14 and 21. Data from at least 3 replicates were averaged and are reported as mean ± standard deviation.

RESULTS AND DISCUSSION. AlamarBlue reduction results (Figure 1A) show that cells are metabolically active on both scaffolds over 21 days of culture, featuring a maximum at day 14. DNA results show a similar trend on both scaffolds with increasing cell proliferation over time. A 7-fold increase was seen for both PLA and P4HB over 21 days (Figure 1B). DAPI results confirm cells attachment and growth on both textiles between day 1 and 21 (P4HB in Figure 1C), with a higher cell density observed on multifilament yarns compared to monofilament, and a more uniform cell distribution observed on P4HB scaffolds (data not shown).

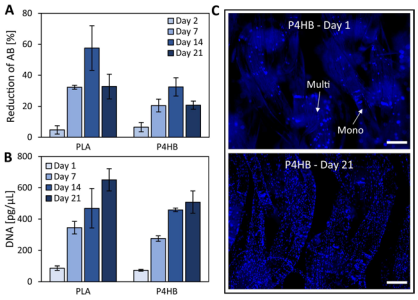

Figure 1. A) AlamarBlue reduction results; **B)** DNA content on PLA and P4HB textiles over 21 days of culture; **C)** DAPI stained nuclei on P4HB textile. Mono=Monofilament, Multi=Multifilament yarns. Scale bar is 250 µm long.

Red stained calcium deposits are visible on PLA scaffolds at day 14 (Figure 2A) and 21 (Figure 2B).

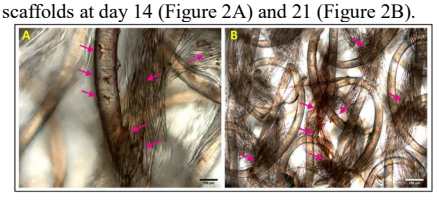

Figure 2. ARS on PLA textile at **A)** day 14 and **B)** 21. Arrows indicate calcium deposits. Scale bar: A) 100µm and B) 250µm.

CONCLUSION. These preliminary results show that both PLA and P4HB textile scaffolds exhibit good cytocompatibility, and a suitable 3D structure able to support MC3T3-E1 cells infiltration and growth. PLA scaffolds show signs of early-stage mineralization over 21 days of culture, while ongoing work is investigating mineralization on P4HB scaffolds. Further studies include optimization of cell seeding density to stimulate early osteogenic differentiation on both textiles, and ARS extraction and quantification via colorimetric assay. To mimic different stages of bone tissue regeneration, the impact of hydrolytic and enzymatic degradation on cell-scaffold interactions will be investigated *in vitro*.

REFERENCES. 1. Jiao *et al., Biomater. Sci.* (2020). 2. Caronna *et al., ORS2022AnnualMeetingPaperNo. 427* (2022). 3. Brennan *et al., Biomed. Mater.* (2015). 4. Murphy *et al.*, *Biomaterials* (2010). 5. Persson *et al.*, *Sci. Rep.* (2018).

ACKNOWLEDGMENTS. This project has received funding from the European Union's Horizon 2020 research and innovation programme under the Marie Skłodowska-Curie grant agreement No.813869. This abstract reflects only the author's view, and the REA is not responsible for any use that may be made of the information it contains.

Tracheal engineering to the reconstruction of the larynx

Christelle Bertsch[1*], Léa Fath[1,2], Benjamin Levy[1], Eya Aloui[1], Lavalle Philippe[1], Emmanuel Martinod[3], Christian Debry[1,2]

[1] Inserm UMR_S 1121, Biomaterials and Bioengineering, Centre de Recherche en Biomédecine de Strasbourg, 67000 Strasbourg, France.
[2] Service d'ORL et de Chirurgie Cervico-Caciale, Hôpitaux Universitaires de Strasbourg, 1 avenue Molière 67200 Strasbourg.
[3] Assistance Publique - Hôpitaux de Paris (AP-HP), Hôpitaux Universitaires Paris Seine-Saint-Denis, Hôpital Avicenne, Chirurgie Thoracique et Vasculaire, Université Sorbonne Paris Nord, Bobigny.

[*] c.bertsch@unistra.fr

INTRODUCTION

In France, each year, about 1,800 people undergo a total laryngectomy, used as the only curative treatment for laryngeal cancers. Total laryngectomy involves removing the entire larynx and placing instead a tracheostomy tube[1]. However, the resulting tracheostomy orifice brings swallowing difficulties, respiratory embarrassment and alteration of communication system[1].

An urgent demand encourages us to create an artificial larynx restoring sphincter function and extending the remaining trachea after total laryngectomy. We previously designed a titanium artificial larynx and implanted it in 2012[2]. However, this titanium artificial larynx has 2 main limitations[3]: 1) a lack mechanical flexibility (causing swallowing disorder); and 2) limited tissue integration. As alternative, aortic allografts offer a promising approach in tracheal engeeniring[4].

To reconstruct artificial larynx, we carried out two strategies either 1) from aortic allografts or 2) from a totally biological cellularized tubular albumin scaffolds, using a bioreactor, to precondition them in vitro.

EXPERIMENTAL METHODS

Designing the bioreactor

We designed a rotating bioreactor for albumin scaffolds cellularization under dynamic perfusion. The bioreactor includes a double-chamber inside which the scaffold is held. The walls of the scaffold delimit the internal from the external chamber. Then, it is possible to co-culture two cell models (epithelial and chondrocyte cells with their own nutritional needs) on the endoluminal and extern faces of the scaffold respectively.

The bioreactor is connected to: 1) a peristaltic pump ensuring a continuing flow; and 2) bottles of culture medium getting fresh culture medium supplies for epithelial and chondrocyte cells. A motor provides rotational movement of the internal chamber to seed uniformly the entire endoluminal face of the tubular scaffold.

Building tubular albumin scaffolds

We built tubular albumin scaffolds by mixing an albumin solution and a calcium chloride solution (at high concentration), moulding it and letting it evaporate.

RESULTS AND DISCUSSION

In response to the lack of artificial larynx scaffolds, we organized our study into 2 strategies:

Strategy 1: In vivo implantation of aortic allograft for laryngeal reconstruction

We implanted aortic allografts at the laryngeal site in 6 sheep. We observed a cellular colonization of the grafts with the appearance of neovascularization, suggesting a good cellular integration to the recipient tissues. A first patient was recently implanted with an aortic allograft for laryngeal reconstruction.

Strategy 2: Tracheal engineering of cellularized albumin scaffolds with co-culture using a bioreactor

Existing aortic allografts have 2 main limitations[4]: 1) cost; and 2) organ donation. Thus, we created albumin scaffolds for in vitro and in vivo experimentations. This advanced technology offers a promising alternative in tracheal engineering.

Then, we built tubular albumin scaffolds to regenerate a structure close to the larynx. We designed a bioreactor to precondition in vitro the scaffold. We seeded cells onto the scaffold in order to accelerate its transformation into larynx tissue during implantation. We showed that epithelial cells proliferate on endoluminal face (presence of tight junctions) and chondrocytes on the extern face (production of collagen type II and aggrecan). We conclude that the bioreactor enables co-culture on tubular albumin scaffolds.

CONCLUSION

These tracheolaryngeal engineering studies led to the first clinical application of aortic allografts at the laryngeal site and opened the way to the use of albumin materials in tissue regeneration.

REFERENCES

1. Fath, L. *et al*., Woodhead Publishing Series in Biomaterials. 457–476 (2020).
2. Debry C. *et al*., Head Neck. 36 (11), 1669–1673 (2014).
3. Debry C. *et al*., N Engl J Med. 376 (1), 97–98 (2017).
4. Martinod *et al*., The Annals of Thoracic Surgery. 103 (5) 1631-40 (2017).

In Vivo Evaluation in Rat of a New Biodegradable Hybrid Scaffold Composed of Hyaluronic Acid-Poly(Ester-Urea-Urethane) for Soft Tissue Engineering

Wassim Manhal[1], Sylvie Changotade[2], Karim Senni[3], Carole Chakar[1], Didier Lutomski[4], Géraldine Rohman[2], Ronald Younes[1]
[1] Craniofacial Research Laboratory, Faculty of Dental Medicine Saint Joseph University of Beirut, Beirut, Lebanon
[2] Unité de Recherche en Ingénierie Tissulaire (URIT), UFR SMBH, Université Sorbonne Paris Nord, Bobigny, France.
[3] EBInnov, Ecole de Biologie Industrielle, Cergy, France
k.senni@hubebi.com

INTRODUCTION

Hybrid scaffolds for tissue engineering cleverly associate biomolecules with synthetic polymer or inorganic compounds to combine desirable mechanical properties and beneficial interactions with host-tissue[1]. Numerous works describes association of polylactide, polyglycolide or polycaprolactone with collagen, fibrin, or polysaccharides. A lot of them describe a process association between the synthetic and the natural compounds leading to a hybrid biomaterial. These latter mostly consist of adsorption of biomolecules on preformed synthetic scaffolds. Other needs the chemical modifications of the biomolecules to allow their incorporation within the hydrophobic synthetic matrix. Here, we described the elaboration of hybrid biodegradable elastomeric scaffolds based on poly(ester-urethane-urea) (PEUU) obtained by a high internal phase emulsion (HIPE). This process allowed the development of multi-scale porous scaffolds with interconnected pores and high porosity with pore size ranging from 50 to 2000µm with incorporation of a biomacromolecule during scaffold process formation. PEUU scaffold alone have been previously shown to support in vitro cell behavior[2] and as a valuable bone substitute after implantation in a calvaria bone defect in rat[3]. Besides, it has been demonstrated that incorporation of heparan-mimetic polysaccharides such as low molecular weight fucoidans from brown algae during PEUU process elaboration improves its cytocompatibility[4]. Thus, glycosaminoglycans such as hyaluronic acids (HA) could also a promising biomacromolecules to form PEUU hybrid biocompatible scaffold. Therefore, in order to design an innovative hybrid scaffold to treat soft tissue defects, porous PEUU-HA hybrid scaffolds were prepared with pore diameters ranging from 55 µm to 1290 µm and implanted. Thus, their biocompatibility was assessed after implantation in rat

EXPERIMENTAL METHODS

Porous PEUU and PEUU-HA scaffolds were fabricated through the preparation of a high internal phase emulsion (HIPE)[2], leading to elastomeric scaffolds comprising interconnected pores with diameters ranging from 55 µm to 1290 µm. High molecular weight hyaluronic (HA) (1000kDa) acid was introduced in the aqueous phase during emulsion formation. PEEU and PEUU-HA disks of 1 cm diameter and 2mm thick were prepared for implantation. Thirty rats were equally divided into two groups, the first one received PEUU-HA hybrid scaffolds and the second one PEUU scaffolds. Both scaffolds were implanted subcutaneously at both sides of the dorsal midline of each rat and then stabilized with absorbable sutures. From each group, 5 rats were sacrificed at 3 different time-points (7, 21 and 36 days) and biopsies were taken for histological study. Overall tissue structure and collagen network were observed respectively after hematoxylin-eosin and picrosirius red staining.

RESULTS AND DISCUSSION

Seven days after implantation, the peripheral third of both scaffolds is invaded by a loose connective tissue and colonized by round shaped inflammatory cells and some fibroblastic cells. At the later days, only 50% of the PEUU scaffold pores are invaded by a loose connective tissue containing a lot of round shaped inflammatory cells and red cells indicating blood vessel wall permeability. At 36 days, 100% PEUU-HA hybrid scaffold pores were filled by a well-structured connective tissue containing functional blood vessels and numerous long shaped fibroblastic cells. Besides, PEEU-HA scaffold is characterized by a better attachment between pore walls and new connective tissue.

As previously shown PEUU scaffolds present good cytocompatibility and biocompatibility due to their chemical properties. Furthermore, multiscale pore size and interconnectivity favour a deep deposit of extracellular macromolecules from fetal calf serum in cell culture or blood after in vivo implantation allowing cell migration and adhesion. Our results showed that presence of Hyaluronic acid in PEUU scaffold led to a faster tissue integration and vascularization. It can be hypothesized that HA can modify PEUU scaffold surface properties leading to an enhanced specific interaction with connective tissue macromolecules and consequently a promoted cell colonization.

CONCLUSION

Due to their proprerties; PEUU-HA scaffolds are particularly appropriate to treat soft tissue defects. Thus, other studies are now considered to apply these scaffolds for periodontal treatments[5] especially to treat gingival recessions.

REFERENCES

References must be numbered. Keep the same style.
1 Chen, G. Macromol Biosci, 2(2), 67-77. 2002
2 Changotade, S. et al, Stem cells Int 2015: 1-8, 2015.
3 Rohman, G., Regen Biomater, 6(6): 311-323. 2019
4 Rohman, G., et al Polymers, 11(6): 1016. 2019
5 Manhal et al WO2021234088, 2021

Polydopamine-Modified Oxidized Alginate-Gelatin 3D Printing Scaffolds for Bone Tissue Engineering Application

Farnaz Ghorbani [1], Minjoo Kim [1#], Mahshid Monavari [1#], Behafarid Ghalandari [2], Aldo R. Boccaccini [1*]

[1] Institute of Biomaterials, Department of Material Science and Engineering, University of Erlangen-Nuremberg, Cauerstraße 6, 91058 Erlangen, Germany.
[2] State Key Laboratory of Oncogenes and Related Genes, Institute for Personalized Medicine, School of Biomedical Engineering, Shanghai Jiao Tong University, Shanghai 200030, China.
[*] aldo.boccaccini@fau.de

INTRODUCTION

Bone tissue engineering provides an opportunity to regenerate injured bone tissue through the interaction of cells and the artificial construct, called scaffolds [1]. Herein, patient-specific, multi-layer and multi-material scaffolds with precise engineered structures can be obtained via novel 3D printing technology [2]. Besides, scaffolds composition has shown a significant impact on the regeneration of defective bone. Here, the poor bioactivity of oxidized alginate (ADA)-gelatin (GEL) scaffolds requires their surface modification with bioactive components such as polydopamine (PDA) [3], allowing bioactive and osteogenic behavior for bone regeneration.

EXPERIMENTAL METHODS

ADA-GEL scaffolds were fabricated using 3D printing (BioScaffolder 3.1, Germany) of hydrogel, while the ADA and GEL solution concentrations were set at 2.5 and 3.75 wt.%, respectively. Cross-linked ADA-GEL scaffolds by $CaCl_2$ were immersed in dopamine hydrochloride solution (2 mg/ml, 10mM tris buffer, pH 8.5) for 24 hours. Then, scaffolds were characterized by light microscopy inspection, hydrophobicity measurement, absorption ratio, and degradation ratio, as well as *in-vitro* bioactivity in simulated body fluid (SBF). Molecular docking calculation was performed to study the interaction of modified structure with osteomodulin and osteocalcin. Cell adhesion and proliferation were performed using osteosarcoma cell lines (MG-63).

RESULTS AND DISCUSSION

Fig.1(A, B) shows the morphology of the lyophilized ADA-GEL scaffolds and PDA-coated ones. Light microscopy images show the formation of interconnected microstructures. The surface was homogeneously functionalized with PDA after modification.

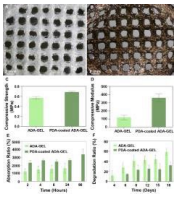

Fig.1:(A, B) Morphology and microstructure of (A) ADA-GEL and (B) PDA-coated ADA-GEL scaffolds. (C, D) Mechanical strength, (E) absorption ratio, and (F) degradation ratio of scaffolds.

PDA-coated ADA-GEL scaffolds expressed higher compressive strength than the pure ADA-GEL scaffolds; and an extensive increase in modulus (Fig.1(B, C). Waterdrop contact angle measurement confirmed hydrophilicity of scaffolds so that the ADA-GEL scaffolds' hydrophilicity increased after PDA's deposition. Over time, the absorption ratio indicated the higher swelling potential of PDA-coated scaffolds (Fig.1(D)). Functionalized scaffolds with PDA started to degrade later than pure ADA-GEL scaffolds and demonstrated higher long-lasting stability. (Fig.1(E)). Obtained results (Fig.2(A-D)) after immersion of the samples in SBF solution confirmed the formation of a hydroxyapatite (HA)-like layer, which was intensified after functionalization of the surface with PDA. Molecular docking calculations indicated that target proteins have structural complementary with PDA-coated samples so that a protein layer formation on the surface can boost bone regeneration. Polymeric scaffolds, especially after PDA deposition, allowed MG-63 cells to adhere and proliferate well (Fig.2(E-G).

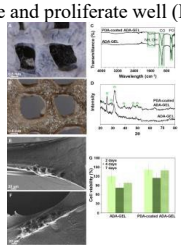

Fig.2: (A-D) Mineralization of scaffolds in the SBF solution, (A, B) morphology observation, (C) FTIR and (D) XRD spectrum. (E-F) MG-63 cell adhesion and proliferation on the scaffolds

CONCLUSION

Briefly, the physicochemical, mechanical, and *in-vitro* properties of PDA-coated ADA-GEL 3D printed scaffolds were evaluated to understand the effect of chemical surface modification on the improvement of properties. Here, a homogeneous layer of PDA was formed on the scaffolds leading to an increase in mechanical properties, hydrophilicity, and absorption capacity, as well as controlled mass loss rate. The modified constructs showed improved *in-vitro* biomineralization potential. Molecular calculation indicated PDA interaction with the potential targets, osteocalcin and osteomodulin, in bone regeneration. Also, PDA modified surface exhibited better MG-63 cell adhesion and proliferation.

REFERENCES

1. Contessi Negrini, N. *et al.* Mater. Today Bio. 10: 100107, 2021.
2. Zhang, R. *et al.* ACS Nano. 15: 17790–17803, 2021.
3. Ghalandari, B. *et al.* Nanoscale. 13: 20098–20110, 2021.

ACKNOWLEDGMENTS

Farnaz Ghorbani acknowledges Alexander von Humboldt Foundation for a fellowship.

Freeze Dried Bone Scaffold (FDBS), the third generation of synthetic bone graft substitute designed as a moldable platform for bone tissue engineering strategies

Cyril d'Arros[1,2*], Boris Halgand[1,3], Olivier Malard[1,4], Pascal Borget[2], Guy Daculsi[1]

[1]INSERM, UMR 1229, Regenerative Medicine and Skeleton, ONIRIS, Université de Nantes, Nantes, France ;
[2]Biomatlante - Advanced Medical Solutions Group Plc, Vigneux-de-Bretagne, France, *cyrildarros@biomatlante.com;
[3]PHU4 OTONN, CHU de Nantes, Nantes, France ; [4]Service d'Oto-Rhino-Laryngologie et de Chirurgie Cervico-Faciale, PHU4 OTONN, CHU de Nantes, Nantes, France

INTRODUCTION

Synthetic Bone Graft Substitutes (BGS) were developed in last decades as interesting therapeutic solution to replace autograft (gold standard). In few clinical situations such as non-union long bone fracture, bone tissue engineering strategy seems to be a highly promising solution to repair large bone defects. Indeed, the results of clinical trial (European project Reborne) combining autologous stromal cells with a BGS (BCP, Biphasic Calcium Phosphate, MBCP+ granules) demonstrated that this kind of ATMP approach (Advanced Therapy Medicinal Product) was efficient[1]. A new ambitious European program (OrthoUnion), divided in two main parts will allow to determine, the appropriate cell dose seeded on MBCP+ granules (comparative clinical trial with autograft arm), and to design a new synthetic platform for bone tissue engineering (FDBS) improving at the same time the usability for the surgeons. It appears that the handling and the ease of use of bone void filler as injectable or moldable paste is greatly awaited (main difference between 1st generation of BGS and the 2nd one, with granules or shape toward paste or moldable putty). FDBS was designed as a 3rd generation of BGS as a putty which can be combined with active ingredients such as cell suspension to regenerate bone in highly critical defects.

The present abstract summarizes the *in vitro* results obtained for the combination of cell suspension mixed into FDBS formulation in comparison with cell suspension seeded to MBCP+ granules.

EXPERIMENTAL METHODS

P24 well cell culture plates (low adherent properties) were used to combine 1,000,000 of cells with 0.1 g corresponding to 0.14 cm^3 for both materials (triplicate on 3 different BM-hMSCs batches, PromoCell®). Cell's viability was evaluated at days 1, 3 and 7 by metabolic activity (CCK8, Cell Counting Kit – 8 colorimetric test) measurement coupled with DNA content (Quant-iT™ PicoGreen® dsDNA reagent) assays (normalization with MBCP+ day 1).

The osteogenic differentiation was analyzed by ALP activity test in proliferative and osteogenic medium at days 1, 3, 7, 14, and 21.

The comparative analysis of the means was performed with GraphPad® software using Mann Whitney test with * $p < 0.05$, *** $p < 0.001$.

SEM observations were also performed on biomaterials and cells after PFA fixation (4%) overnight followed by dehydration step in ethanol baths (50% to 100%) and histological slides (HE staining) were observed after embedded into PMMA resin.

RESULTS AND DISCUSSION

The experiment of viability for one week of cell culture demonstrated cytocompatibility with a proliferation of mesenchymal stromal cells mixed into FDBS. After one day the value of metabolic activity for FDBS is about 20% compared to the positive control (MBCP+ granules at 1 day) probably due to the mixing step during rehydration of FDBS powder compared to the seeding of the cell suspension onto the BCP granules. At day 3 and 7, the metabolic activity increased slightly for FDBS compared to BCP. The DNA dosage demonstrated an increase at day 3 and 7 for FDBS mixing, but stable quantity for the MBCP+ control (Figure just below with MBCP+ and FDBS respectively in orange and green).

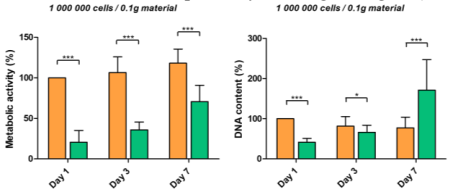

The evaluation of the osteogenic potential of MSCs cultured on both materials of the study conducted for 21 days showed a quite similar profiles of the alkaline phosphatase at a proteomic level (increase during time) with no significant differences. For FDBS condition, a slight shift in time compared to BCP granules (positive control) happened, especially in osteogenic medium.

Then, the SEM (Scanning Electronic Microscopy) observations illustrated a slight difference concerning cell morphology at day 1 with more cells spreading with MBCP+ scaffold. The difference of cell's morphology only noticed at day 1 could be due to the hydrosoluble polymer into the FDBS platform which should delay adhesion and cell spreading. Interestingly, cohesion of granules was higher for FDBS than MBCP+ during time. Histological slides demonstrated total cell recovery of BCP granules after 7 days of cell culture.

CONCLUSION

FDBS showed that this new formulation by improving the handling properties for surgeons (3rd generation of BGS), kept at the same time the possibility to be used as a scaffold for a Tissue Engineering (TE) strategy.

REFERENCE

[1] Gómez-Barrena E. *et al.*, Injury 51:63-73, 2020

ACKNOWLEDGMENTS

The authors would like to thank the European project H2020 OrthoUnion (Grant agreement n°733288) which supported this work.

Influence of Porosity of Gyroid-Structured Implants on Bone and Vascular Ingrowth in Rat Calvarial Defect

Guoyan Xian*[1], Baptiste Charbonnier[2], Morad Bensidhoum[1], Esther Potier[1], David Marchat[3] and Delphine Logeart-Avramoglou[1]

[1]B3OA UMR CNRS 7052 INSERM U1271, Université de Paris, Paris, France
[2] Nantes Université, INSERM, UMRS 1229, Nantes, France
[3] Mines Saint-Etienne, Univ Lyon, Univ Jean Monnet, Etablissement Français du Sang, INSERM, U 1059 Sainbiose, 42023 Saint-Etienne France

*guoyan.xian@ext.inserm.fr (presenting)

INTRODUCTION

Hydroxyapatite (HA)-based ceramics have been used for more than 30 years as bone substitutes for bone defect repair due to their remarkable biocompatibility with hard tissue. However, the design of the optimal internal geometry of the scaffold is still under debate, especially since the emergence of additive manufacturing (AM) technologies and associated software enabling the production of custom-made scaffolds, with well-controlled and multiple multiscale architectures. Because of their role in mass transfer, porosity and pore size are generally acknowledged as main parameters affecting the osteoconductive property (ability of a scaffold to be filled with bone) of the implants. However, changing the porosity and/or pore size parameters also changes other physical parameters such as the inner surface area (ISA), a critical parameter for cell adhesion, spreading, proliferation and matrix production.

In this study, we compared the osteoconductive property of macroporous gyroid-structured scaffolds with different pore size/porosity but equivalent ISA. The bone ingrowth and vascular invasion within the implants were investigated after implantation in a rat calvarial defect.

EXPERIMENTAL METHODS

Disc-shaped (5.3 mm diameter x 0.9 mm height) carbonated HA-based scaffolds were produced using a dedicated additive manufacturing technology. Gyroid structure with equivalent ISA (74 mm²) and two pore sizes of 300 µm and 700 µm were compared; the associated porosity were 33% (G33/300) and 65% (G65/700), respectively. Bilateral subcritical-size defects (5.3 mm diameter) were created in the parietal bone of male 3-month-old Wistar rats and filled with each of the scaffolds (n=6 per scaffold). The bone ingrowth in each scaffold was monitored in vivo by µ-CT scanning (Skyscan 1176) every 2 weeks. After 6 and 12 weeks of implantation, a radiopaque silicone rubber solution (Microfil®) was perfused through the vascular network of each animal via the left ventricle. The volumes of new bone and blood vessels were determined after µ-CT scanning and images analyses with Dragonfly software.

RESULTS AND DISCUSSION

The total newly formed bone volume determined inside the scaffold was significantly higher (2-fold) in G65/700 compared to G33/300 scaffolds after 6 weeks of implantation (Fig. 1). After 12 weeks of implantation, however, this difference was not significant anymore. Interestingly, when normalized to the empty space within the scaffold, the bone volume was similar between both scaffolds and represents ~ 25-28% at 6 weeks and 25-38% at 12 weeks of implantation. These data confirmed that the newly formed bone volume is correlated with the space available within the scaffold but the bone growth rate is similar in scaffolds with different porosities. The bone volumes determined in the inner area and outer areas of the scaffolds were similar further confirming the proper bone ingress in these macroporous gyroid-structured scaffolds.

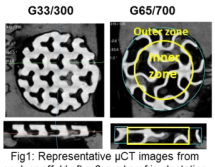

Fig1: Representative µCT images from each scaffold after 6 weeks of implantation

Analysis of vascularization indicated a trend of higher blood vessel volume in G65/700 compared to G33/300 scaffolds at 6 weeks of implantation; however, the blood vessel volume normalized to the empty space within the scaffold was the same for both scaffolds.

CONCLUSION

This study demonstrated that HA-based implants with a macroporous gyroid structure supported bone and vascular ingrowths in rat calvarial defects. Their osteo- and angio-conductive properties (percentage of bone or vessels filling) were similar whatever their pore size/porosity; the final new bone tissue or vessel volume, however, depends on the porosity value (void space). The role of the inner surface area on these properties remains be determined.

These results give new insights for the design of optimal geometry of scaffolds made by AM for bone regeneration.

ACKNOWLEDGMENTS

The authors would like to thank the Fondation des Gueules Cassées for funding this study.

Controlled metal crumpling as an alternative to folding for the fabrication of nanopatterned meta-biomaterials

Mahya Ganjian*[,1], Shahram Janbaz[1,2], Teunis van Manen[1], Nazli Tümer[1], Khashayar Modaresifar[1], Michelle Minneboo[1], Lidy E. Fratila-Apachitei[1], Amir A. Zadpoor[1]

[1]Department of Biomechanical Engineering, Faculty of Mechanical, Maritime, and Materials Engineering, Delft University of Technology, Mekelweg 2, 2628CD, Delft, The Netherlands.
[2]Institute of Physics, University of Amsterdam, Science Park 904, 1098 XH, Amsterdam, The Netherlands
*m.ganjian@tudelft.nl

INTRODUCTION

The quest for ideal bone substitutes that mimic the various properties of the bone is ongoing. Affording synthetic bone substitutes with functionalities that allow them to regulate cell behavior could greatly increase their chance of successful osseointegration. The introduction of nanotopographies to the surface of bone substitutes is particularly appealing, because well-designed surface ornaments may be able to (simultaneously) kill bacteria[1] and induce osteogenesis[2]. Given the fact that most of the nanopatterning techniques are planar in nature, they cannot be easily applied to porous meta-biomaterials whose surface areas are primarily non-planar[1]. Here, we present a novel class of meta-biomaterials that combine controlled crumpling with surface nanopatterns and laser-cut surface to make 3D porous nanopatterned scaffolds. We designed and fabricated a simple setup for the controlled crumpling of meta-biomaterials. We measured the mechanical and geometrical properties of the scaffolds as a function of the surface-porosity and deformation velocity. Finally, the in vitro cell culture (using MC3T3-E1 preosteoblasts) demonstrated the cytocompatibility of the nanopatterned scaffolds.

EXPERIMENTAL METHODS

Polished Ti sheets with a thickness of 125 µm were used for this study. The Ti sheets were cut into 22.5×22.5 mm^2 pieces using a laser micromachine.

The nanopatterns were fabricated on the polished Ti specimens using an ICP RIE machine (PlasmaLab System 100, Oxford Instruments, UK). Cl_2 and Ar were the etching gasses. The specimens were cleaned in acetone, ethanol, and isopropyl alcohol (IPA) afterwards. The size of the 2D flat sheet (22.5×22.5 mm^2), the number of the pores per specimen (12×12), and the center-to-center interspacing (1.875 mm) of the pores were kept constant while the diameter of the pores was varied (1.46, 1.53, and 1.59 mm) using CAD software (Solidworks 2019, Dassault Systèmes) to fabricate scaffolds with different porosities.

The crumpling process (Figure 1) was carried out using a universal mechanical testing bench (Plus/Lloyd Instruments Ltd, England) equipped with a 5 kN load cell.

The crumpled specimens were imaged using a µ-CT scanner (Phoenix Nanotom, GE Sensing Inspection Technologies GmbH, Germany). The morphological parameters were determined using 3-Matic (15, Materialise, Leuven, Belgium).

MC3T3-E1 preosteoblast cells (Sigma-Aldrich, Germany) were seeded on the control and nanopatterned crumpled specimens (Figure 2). The PrestoBlue assay (Thermo Fisher Scientific, US) and live/dead cell staining assay (Thermo Fisher Scientific, US) were used to determine the metabolic activity and viability of the cultured cells after 7 days.

RESULTS AND DISCUSSION

Crumpling is an interesting alternative to origami and kirigami approaches as it greatly simplifies the process of going from a flat construct to a 3D porous structure. Given the stochastic nature of the crease patterns and folding sequences, the resulting structure is highly resistant to minor imperfections, while highly regular origami/kirigami lattices are sensitive to the slightest deviations from the perfect geometry. Moreover, controlled crumpling offers a high degree of tunability in terms of the mechanical properties and morphological features (*i.e.,* pore size, strut size, porosity, etc.) as the crucial factors which determine oxygenation, migration, spreading, settlement, and feeding of the cells.

The live/dead and cell metabolic activity assays showed that the preosteoblasts can survive and proliferate after adhesion to the crumpled scaffolds and that the presence of nanopatterns does not affect the cytocompatibility of the scaffolds. After 7 days, we observed a significant increase in the elongation of the cells residing on the nanopatterned scaffolds. An elongated cell morphology is considered beneficial for osteogenic commitment[1,3].

Based on the results reported here, controlled crumpling is a promising approach for the fabrication of 3D porous bone scaffolds decorated with surface nanopatterns.

CONCLUSION

To address the limitations of the existing techniques for the production of nanopatterned meta-biomaterials, a novel crumpling approach was developed that allows for the fabrication of 3D metallic scaffolds with the desired size, volume porosity, and mechanical properties from nanopatterned surface-porous sheets. The combination of high porosity and surface nanopatterns could be used to promote bone tissue regeneration. Future studies should evaluate the in vivo performance of these biomaterials, paving the way for their ultimate clinical adoption.

REFERENCES

1. Modaresifar K. *et al*., Small 2100706, 2021
2. Dobbenga S. *et al.,* Acta Biomater 46 3-14, 2016
3. Bobbert F.S.L. *et al.,* Materials & Design 191, 108624, 2020

ACKNOWLEDGMENTS

"This research has received funding from the European Research Council under the ERC grant a no. [677575]°".

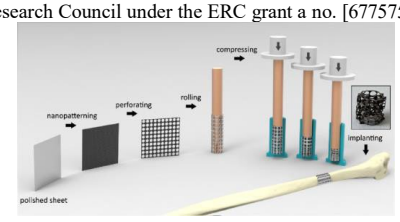

Figure 1. A schematic illustration of the steps involved in the crumpling of nanopatterned porous Ti sheets.

Development and evaluation of 3D printed PCL/HANp/PEGDA scaffolds for bone regeneration

Ana Catarina Sousa[1,2,*], Sara Biscaia[3], Rui Alvites[1,2], Mariana Branquinho[1,2], Bruna Lopes[1,2], Patrícia Sousa[1,2], Joana Valente[3], Margarida Franco[3], José Domingos Santos[4, 5], Luís Atayde[1,2], Nuno Alves[3†] and Ana Colette Maurício[1,2†].
[1] Veterinary Clinics Department, Abel Salazar Biomedical Sciences Institute (ICBAS), Porto, Portugal;
[2]Animal Science Studies Centre (CECA), Agroenvironment, Technologies and Sciences Institute (ICETA), University of Porto (UP), Porto, Portugal;
[3]Centre for Rapid and Sustainable Product Development (CDRSP), Polytechnic Institute of Leiria, Portugal.
[4]Faculdade de Engenharia da Universidade do Porto (FEUP), Porto, Portugal
[5]REQUIMTE/LAQV, Departamento de Engenharia Metalurgica e Materiais, Faculdade de Engenharia, Porto, Portugal;
[†]Both authors contributed equally as last authors.
[*] anacatarinasoaressousa@hotmail.com

INTRODUCTION

The population is ageing, leading to a manifest shortage of organs and limitations of clinical treatments for tissue regeneration. Reconstruction of bone defects, particularly the critical-sized defects, with mechanical integrity to the original surrounding bone tissues is essential for a patient's rehabilitation[1]. In this sense, the search for solutions has passed by the development of three-dimensional implants (scaffolds) in combination with cell therapies[2, 3]. In this research, a novel approach is explored to produce synthetic bone grafts mimicking the complex bone structure using additive manufacturing, comprising the construction of 3D scaffolds. For this purpose, three types of scaffolds were produced and tested: one using a thermoplastic polymer, polycaprolactone (PCL), another using a combination of PCL and hydroxyapatite nanoparticles (HANp), and the third using a combination of the two materials and polyethylene glycol diacrylate (PEGDA). After production, optimisation and characterisation of the scaffolds, an *in vitro* evaluation was performed with human dental pulp stem cells (hDPSCs).

EXPERIMENTAL METHODS

Scaffolds Production

In the present work, a biomanufacturing system, developed by the CDRSP-IPLeiria, were used. The parameters used were 240 mm/s of deposition velocity, 9 rpm of screw rotation velocity and 85 ºC of liquefier temperature. Three different matrices were produced in this system: i) PCL scaffolds; ii) PCL scaffolds with the addition of HANp; and iii) PCL-HANp scaffolds submerged in PEGDA solution.

Material Characterization

The physical, chemical, and mechanical characterization of the produced scaffolds was performed: fourier-tranform infrared spectroscopy (FTIR), contact angle measurement, micro-computed tomography (Micro-CT), scanning electron microscopy (SEM), energy dispersive x-ray analysis (EDX), and compression tests.

In vitro cytocompatibility analysis

For the assessment of the scaffolds' cytocompatibility, a Presto Blue™ viability assay was performed with hDPSCs.

Statistical analysis

Statistical analysis was performed using GraphPad Prism by One-Way ANOVA analysis (Tukey's multiple comparisons test).

RESULTS AND DISCUSSION

According to the results (SEM and Micro-CT), the scaffolds were produced successfully presenting interconnected channel networks and good geometric accuracy. This high degree of interconnectivity influences cell viability within the scaffold and consequently promotes vascularization and tissue growth *in vivo*. Regarding the mechanical behaviour, the results demonstrated that the addition of HANp seem to have improved the compressive rigidity of the scaffolds. After analysis of the *in vitro* tests, it was verified that the PCL/HANp/PEGDA-based scaffolds present superior cell proliferation when compared to the other groups. These results are probably due to the properties of PEGDA that provide a nutritive environment for endogenous cell growth and simulate the natural extracellular matrix of bone.

CONCLUSION

The study demonstrated that PCL/HANp/PEGDA scaffolds associated with hDPSCs are a very promising therapeutic system in critical fractures treatment, to accelerate and improve bone regeneration. The research of this system's performance in critical bone defects is an important step to its progression to clinical applications.

REFERENCES

1. Commission E. European Commission Report on the Impact of Demographic Change. 2020. 2. Shang F *et al.* Advancing application of mesenchymal stem cell-based bone tissue regeneration. Bioactive Materials. 2021;6(3):666-83. 3.Visser J *et al.* Reinforcement of hydrogels using three-dimensionally printed microfibres. Nature communications. 2015;6(1):1-10.

ACKNOWLEDGMENTS

This study was funded by Projects PEst-OE/AGR/UI0211/2011 from FCT, and COM-PETE 2020, from ANI–Projetos ID&T Empresas em Copromoção, by the project "insitu.Biomas–Re-invent biomanufacturing systems by using an usability approach for in situ clinic temporary im-plants fabrication" (POCI-01-0247-FEDER-017771), by the project "Print-on-Or-gans–Engineering bioinks and processes for direct printing on organs" (POCI-01-0247-FEDER-033877), by the project "Bone2Move-Development of "in vivo" experimental tech-niques and modelling methodologies for the evaluation of 4D scaffolds for bone defect in sheep model: an integrative research approach" (POCI-01-0145-FEDER-031146) and by the PhD scholarships Ana Sousa (SFRH/BD/146689/2019), Mariana Branquinho (SFRH/BD/146172/2019) and Bruna Lopes (2021.05265.BD).

In vitro Behavior of Human Osteoblasts Cultured in Direct Foamed Titanium Scaffolds

Carolina Oliver-Urrutia[1,*], Zuzana Koledova[2], Adelia Kashimbetova[1], Karel Slámečka[1], Ladislav Čelko[1], Edgar B. Montufar[1,**]

[1] Central European Institute of Technology, Brno University of Technology, Purkynova 123, Brno 61200, Czech Republic

[2] Faculty of Medicine, Masaryk University, Kamenice 5, Brno 62500, Czech Republic

[*]oliver@vutbr.cz, [**]eb.montufar@ceitec.vutbr.cz

INTRODUCTION

Metallic foams are materials with a single combination of physical and mechanical properties, such as high strength with low specific weight, high energy absorbing capacity, and large surface area.[1,2] It has been shown that metallic foams can stimulate cell growth and promote bone growth, therefore various applications in the field of biomedical sciences have emerged.[3,4] In the present work, Ti foams were fabricated by direct foaming, a simple and cost-effective method that at difference to other approaches allows scaffold shaping by casting the foam in a mold. The microstructure, mechanical properties and effect of foam features on human osteoblast (hFOB 1.19) behavior was studied.

EXPERIMENTAL METHODS

Moldable Ti foams were obtained by foaming a mixture of a spherical Ti powder and an aqueous solution of 2.5 % wt. of sodium dodecyl sulphate at high speed. A variation of liquid to powder ratio *(l/p)* was made in order to obtain three different types of foams: 0.28, 0.33 and 0.38 ml/g. The obtained foams were casted into cylindrical molds, dried and then sintered at 1400 °C for 10 h. SEM was used to observe the microstructure and to perform porosity analysis. The mechanical strength was measured by compression test. Cell culture experiments were done with hFOB 1.19 at 3, 7 and 14 days. Metabolic activity was determined by resazurin assay, whereas cell morphology was determined by SEM.

RESULTS AND DISCUSSION

The top part of Figure 1 shows the microstructure of a representative Ti foam at different magnifications. The foams exhibited a network of sphere-like open pores. The walls of the pores consisted of sintered Ti particles forming a pearl necklace-like structure. The porosity and size of the pores varied with the *l/p* ratio. The foams prepared at *l/p* ratio of 0.33 ml/g had the largest pore size (263.1 ± 132.9 µm) and highest porosity (89.2 ± 0.8 %), followed by the ones with *l/p* ratio of 0.28 ml/g (233.6 ± 105.9 µm), which had also the lowest porosity (84.9 ± 1.1 %). The foams with *l/p* ratio of 0.38 ml/g had the smaller pores (183.3 ± 82.1 µm) and 85.4 ± 0.7 % of porosity. The foams exhibited ductile behaviour with compressive yield strength of 6.1 ± 3.6 and 1.2 ± 0.7 MPa for *l/p* ratios of 0.28 and 0.38 ml/g, respectively. These values are within the lower range of strength of trabecular bone (4-12 MPa), thus the foams are likely suitable for bone grafting, considering that they should stiffen by ingrowing bone. hFOB 1.19 cells proliferated in the foams, colonizing and covering the surface of the pores (Fig. 1). Similar cell morphology was observed in all the foams and cell metabolic activity increased with time, being higher in the foams than in the control polystyrene well. The data show that Ti foams are favourable for cell attachment and growth, which is relevant for implant osteointegration and successful bone grafting. Previous works showed that porosity promotes cell proliferation and bone ingrowth.[3,4] Here the results show that at constant porosity (85 %) the growth of hFOB 1.19 cells is stimulated in the foams with smaller pores. Alkaline phosphatase assay is ongoing to determine the osteogenic activity.

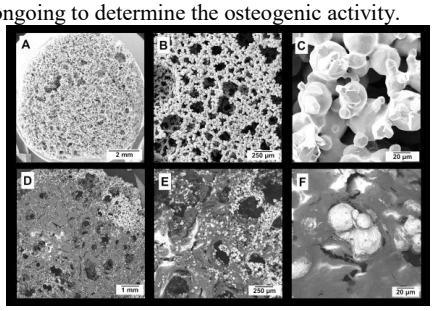

Fig. 1. Ti foam with l/p ratio of 0.38 ml/g without cells (A, B, C) and with cells (D, E, F) after 7 days of culture.

CONCLUSION

Ti foams with different porosity, pore size and compressive yield strength suitable for trabecular bone grafting were fabricated by a novel and simple direct foaming method. The foams are cytocompatible, allowing a fast growth of hFOB 1.19 cells, which colonize the pore surfaces, and possibly enabling osteogenic activity of the cells.

REFERENCES

1. Kang JS. *et al*., Small. 2017.
2. Sharma A. *et al*., Mater. Res. Express. 2021.
3. Amit A. *et al*., Mater. Sci. Eng. C. 2020.
4. Rao X. *et al*., J Mech Behav Biomed Mater. 2018.

ACKNOWLEDGMENTS

This work was supported by MEYS - Czech Republic (LTAIN19112). COU acknowledges the CONACYT grant 2021-000012-01EXTV-00057.

Injectable Gene Activated Matrix (GAM) microspheres as MSCs active carriers for cartilage repair.

Jeremy Salvador[1,2,3], Jade Berthelot[1,3], Claire Bony[2], Danièle Noël*[2], Marie Morille[1], Emmanuel Belamie[1,3]

1. ICGM, Univ Montpellier, CNRS, ENSCM, Montpellier, France
2. IRMB, University of Montpellier, INSERM, Montpellier, France
3. EPHE, PSL Research University, 75014 Paris, France

The combination of mesenchymal stromal cells (MSCs) with active injectable carriers brings about innovative solutions to current issues in the field of tissue engineering. In particular, repair of adult articular cartilage lesions, especially those affecting the knee joint, remains a clinical challenge because of the limited cartilage self-healing capacity. We have previously demonstrated the potential of using collagen 3D microspheres as a MSC support and growth factor carrier for implantation in knee joints. The microspheres were loaded with TGFβ3, which was progressively released, and efficiently triggered the chondrogenic differentiation of MSC *in vitro* and *in vivo* (Mathieu et al., 2014). After a few hours, large aggregates of cells and microspheres were observed. The cells produced a neotissue comprised of the typical molecular components of the cartilage extracellular matrix over 4 weeks. Nevertheless, this previous work also evidenced the late onset of hypertrophic markers (type X collagen, alkaline phosphatase, osteocalcin and metalloprotease 13).
Here, we present our latest results regarding the association of gene therapy with the above approach to control the chondrogenic differentiation of MSCs and avoid hypertrophy. We identified Runx2, which plays a central role in hypertrophic chondrocyte markers up-regulation, as the main molecular target to be repressed. We demonstrated that the transient down-regulation of this factor can be achieved with a specific siRNA targeting Runx2 (Raisin et al., 2017). In view of the targeted application, it is necessary that vectorized siRNA be delivered from the microspheres carrying the cells, thus calling for the elaboration of a Gene Activated Matrix (GAM). We therefore designed a siRNA nanovector, efficient for MSC transfection and suitable for long-term delivery from a porous hydrogel. The solvent-exchange lipoplexe formulation (SELF) we will present here has a tunable size, is stable over time in cell culture conditions and possess a high efficiency to transfect primary human MSCs. We associated SELF with porous collagen 3D microspheres and demonstrated that the loading efficiency and release kinetics are correlated with SELF size. Finally, we studied the efficiency of GAMs on an in vitro model of chondrocyte differentiation of human MSCs. We have shown that GAM induces a prolonged inhibition of the target *Runx2* gene expression for at least 21 days. Under chondrocyte differentiation conditions, this decrease in *Runx2* expression appears to decrease the expression of hypertrophy markers. Therefore, this original and unique type of GAM, with adaptable release kinetics, could be of interest for long-term and/or sequential transfection profiles of MSCs in 3D culture. Upcoming experiments aim at achieving a more precise control of vector release, which should improve the efficiency of such GAM for cartilage tissue engineering applications.

References :

- Mathieu, M. Vigier, S, Labour, MN , Jorgensen, C, Belamie, E* and Noel, D*, Induction Of Mesenchymal Stem Cell Differentiation And Cartilage Formation By Cross-Linker-Free Collagen Microspheres 2014 European Cells & Materials 28 : 82-97.
- S. Raisin, M. Morille, C. Bony, D. Noel, J.-M. Devoisselle and E. Belamie Tripartite polyionic complex (PIC) micelles as non-viral vectors for mesenchymal stem cell siRNA transfection, Biomater. Sci. 2017, 5, 1910-1921.

3D Printed Tubular Scaffolds with Adequate Mechanical Properties and a Dual Cell Seeding Strategy for Tracheal Regeneration

Luis Soriano[1,2,3*], Tehreem Khalid[1,2], Mark Lemoine[2], Ruairi P Brannigan[4], Andreas Heise[4], Cian O'Leary[1,2,3], Fergal J. O'Brien[2] and Sally-Ann Cryan [1,2,3]

[1]School of Pharmacy and Biomolecular Sciences, RCSI, Dublin, Ireland
[2]Tissue Engineering Research Group, RCSI, Dublin, Ireland
[3]SFI Centre for Research in Medical Devices (CÚRAM), NUI, Galway, Ireland
[4]Department of Chemistry, RCSI, Dublin, Ireland
[*] luissoriano@rcsi.com

INTRODUCTION

Tracheal damage is associated with the narrowing, weakening and discontinuity of the conductive part of the lower respiratory tract[1]. Extensive defects cannot undergo end-to-end anastomosis and current approaches present poor outcomes due to weak mechanical properties, poor re-epithelialisation and vascularisation of the implanted graft[2]. Herein, we investigated the use of collagen-based tubular scaffolds reinforced with 3D-printed synthetic polymer architectures for tracheal repair.

EXPERIMENTAL METHODS

Tubular geometries were 3D printed using synthetic polymers (PI, PII) to act as the backbone of the scaffold in combination with collagen and hyaluronic acid bilayered (CHyA-B) scaffolds using freeze drying technologies. A collagen and hyaluronic acid film covered the inner lumen (IL) of the scaffold while the 3D printed reinforced collagen porous outer layer (OL) was designed to support the growth of underlying tissues. The mechanical strength and ultrastructure of scaffolds was characterised and an approach for cellular seeding of the different layers of the PI-CHyA-B scaffold was developed using Calu-3 bronchoepithelial cells on the IL and Wi38 lung fibroblasts on the OL of the scaffold.

RESULTS AND DISCUSSION

Tracheal scaffolds showed a 10-20 MPa compressive Young modulus with no significant decrease in mechanical strength following cyclic loading used to mimic respiratory patterns (Fig 1A). Scaffold characterisation using scanning electron microscopy imaging revealed a porous microarchitecture suitable for cellular proliferation, with mean pore size of 161.8±4.6 and 168.8±3 µm for PI and PII-CHyA-B estimated via toluidine staining, (Fig 1B). A seeding process with the support of a custom-made device was developed to achieve targeted airway epithelial seeding on the IL while the outer layer OL of the scaffold was populated with Wi38 lung-derived fibroblasts using different seeding densities under rotation.

The growth of Wi38 cells on the OL was monitored for 7 days, showing successful cellular growth on the OL with no cellular attachment and growth in the IL using $6x10^5$ cells/cm^2 (Fig 2A). Calu-3 cells were grown on the tubular scaffolds for 10 days, showing optimal cellular growth on the IL of the scaffold using $1.25x10^5$ cells/cm^2 with reduced attachment and growth of Calu-3 cells in the porous OL versus IL (Fig 2B). Immunofluorescence imaging using DAPI and phalloidin, and quantification of the film from the IL further demonstrated cellular growth on the film with an estimated epithelial coverage of the film >60%.

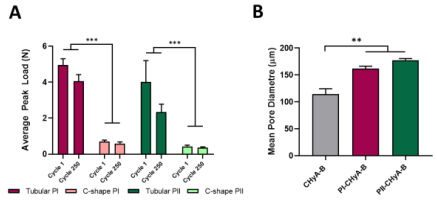

Figure 1. (A) Cyclic loading and (B) mean pore size of PI and PII-CHyA-B scaffolds (**p<0.01, ***p<0.001).

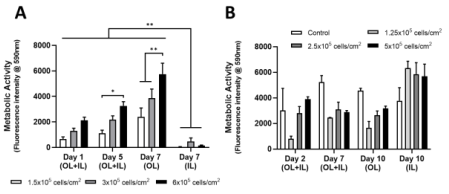

Figure 2. (A) Wi38 and (B) Calu-3 seeding of the OL and IL of PI-CHyA-B scaffolds (*p<0.5, **p<0.01, ***p<0.001).

CONCLUSION

Reinforcement of CHyA-B scaffolds with 3D-printed polymer architectures is a suitable approach for the development of tissue-engineered tracheal grafts, with adequate mechanical properties and porous structure to support tracheal tissues. Moreover, a seeding procedure using a custom-made device was developed allowing successful cellular attachment and growth in the different layers of the tubular scaffold. The establishment of this targeted cellular seeding procedure holds potential to enable the clinical translation of tissue engineered tracheal grafts by facilitating differentiated pre-seeding strategies prior to implantation.

REFERENCES

1. Boazak *et al*. ACS Biomaterials Science & Engineering 4.4:1272-1284, 2018
2. Soriano *et al*. European Respiratory Review 30.162 ,2021.

ACKNOWLEDGMENTS

Financial support was received from Science Foundation Ireland (SFI) and the European Regional Development Fund (ERDF) under grant number 13/RC/2073_2.

Green antibacterial hemostatic sponges

Maria Francesca Di Filippo[1*], Valentina Di Matteo[1], Silvia Panzavolta[1]

[1]Department of Chemistry, University of Bologna, Bologna, Italy
[*] maria.difilippo5@unibo.it

INTRODUCTION

Bleeding is one of the most common clinical manifestations after trauma, and severe blood loss due to hemorrhage continues to be the leading preventable cause of death of patients with injuries. In addition, uncontrolled bleeding can lead to an increased risk of bacterial infection during wound healing.[1] Hence, the improvement of existing hemostasis products and the development of new ones can significantly improve the success rate of operations and reduce the occurrence of postoperative complications. In this work, gelatin was used for the production of sponges with the freeze-drying technique, and then cross-linked with glutaraldehyde to tune the stability in a biological environment. In order to endow the material with an antibacterial activity, the sponge was loaded with silver nanoparticles (AgNPs), well known for their excellent antibacterial and antifungal properties.[2] The synthesis of AgNPs was carried out in a sustainable and green way, employing a single-step reaction, avoiding the use of additional and toxic agents, and using aqueous solutions at room temperature. The formation of AgNPs under these conditions was achieved thanks to the presence of snail slime: this complex mixture of substances (such as glycoproteins, collagen, allantoin and glycolic acid) acts as a reducing and stabilizing agent. The snail slime used in this project was supplied by 'lumacamadonita' (Palermo, Italy) and extracted by means of a cruelty-free machine that allows to obtain the product with a pH between 5 and 7. The obtained scaffolds were fully characterized to verify their antibacterial activity and their potential use as hemostatic sponges.

EXPERIMENTAL METHODS

For scaffold preparation, gelatin (type A, 300 Bloom) was dissolved in ultra-pure water (10% w/v), foamed, and freeze-dried for 24 h. The obtained scaffold was then soaked in a 0.25% w/v glutaraldehyde solution for 12 h. The anchoring of the AgNPs on the walls of the scaffold was obtained by simply immersing the sponge in the solution during the AgNPs formation, as depicted in Figure 1. Reference samples were prepared immersing the scaffolds in a reference AgNPs solution that uses gelatin and glucose as stabilizing and reducing agents.[3]

RESULTS AND DISCUSSION

In this work, sustainable starting materials and procedures were used for the preparation of scaffolds with effective antibacterial activity. 3D porous gelatin scaffolds were enriched with silver nanoparticles in order to obtain an antibacterial hemostatic sponge. The use of snail slime during the synthesis of AgNPs allowed to obtain nanoparticles stable over time and with mean diameters between 30 and 50 nm. Furthermore, snail slime macromolecules surroundings AgNPs promote better adhesion of NPs to the gelatin scaffolds.

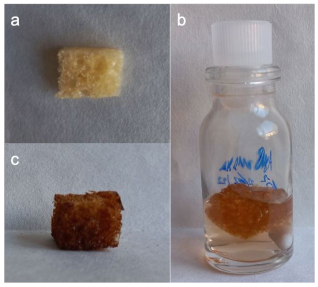

Figure 1. a) the obtained crosslinked gelatin scaffold; b) crosslinked scaffold immersed in the solution for AgNPs formation; c) obtained AgNPs-loaded sponge.

Macro- and micro-porosities present on samples are appreciable in scanning electron microscopy images, and the very high porosity and pore interconnection has been further verified by micro-CT analysis, revealing a 100% pore interconnectivity, that ensures the ability to absorb a water volume of about 3000 times its weight. Silver release studies and antibacterial activity tests by means of Kirby-Bauer assays showed effective antibacterial action on both Gram+ and Gram- bacterial strains. Mechanical properties under compression of the samples loaded with the AgNPs were not significantly different from those of the pristine scaffolds, highlighting that the loading of AgNPs does not affect the mechanical performance of the material. Cell biocompatibility studies are ongoing.

CONCLUSION

The preparation method developed in this study allowed to get 3D gelatin scaffolds loaded with AgNPs. The synthesis followed a sustainable and easily scalable protocol, using aqueous solutions at room temperature. The results of antibacterial tests shown that these biomaterials have an effective therapeutic activity, while cellular compatibility studies are still ongoing.

REFERENCES

(1) Cao, S. et al., Multifunctional Dopamine Modification of Green Antibacterial Hemostatic Sponge. *Mater. Sci. Eng. C* **2021**, *127*, 112227.
(2) Khan, S.U. et al., Nanosilver: New Ageless and Versatile Biomedical Therapeutic Scaffold. *Int. J. Nanomedicine* **2018**, *13*, 733–762.
(3) Darroudi, M. et al., Green Synthesis and Characterization of Gelatin-Based and Sugar-Reduced Silver Nanoparticles. *Int. J. Nanomedicine* **2011**, *6* (1), 569–574.

Retina Implants based on Submicron Structured Silica Membranes as a Therapy Concept for Age-Related Macular Degeneration (AMD)

Bastian Christ[1*], Christina Fey[1], Tobias Weigel[1], Ina Meiser[2], Kristina Lachmann[3], Jörn Probst[1], Julia C. Neubauer[2,4], Sofia Dembski[1]

[1]Translational Center Regenerative Therapies (TLC-RT), Fraunhofer Institute for Silicate Research (ISC), Würzburg, Germany
[2]Fraunhofer Institute for Biomedical Engineering (IBMT), Sulzbach, Germany
[3]Fraunhofer Institute for Surface Engineering and Thin Films (IST), Braunschweig, Germany
[4]Fraunhofer Project Centre for Stem Cell Process Engineering (PZ-SPT), Würzburg, Germany
[*] bastian.christ@isc.fraunhofer.de

INTRODUCTION

Age-related macular degeneration (AMD) is the most common reason for blindness of people in the Western World. Due to increasing life expectancy, the number of cases of this degenerative disease will continue to rise. Currently, AMD cannot be cured. Only in a small amount of patients, the progression of the disease can be slowed by regular, costly injections into the eyeball.

Efforts are underway to cure AMD using regenerative techniques based on human induced pluripotent stem cells (hiPSC), which are reprogrammed from ordinary human somatic cells and can be differentiated into various cell types. At the moment, the most promising therapeutic approach is the implantation of healthy hiPS cell-based retinal-pigmented epithelial layers (RPE) on physiologically compatible membranes directly behind the actual retina. These artificial RPEs take over the supply of the retina in place of the dead epithelium and ensure its long-term function. Some of these experimental therapies have been successfully validated in animal studies, yet (1-4).

Here, the authors present the fabrication of form stable submicron structured membranes, which allow an *in-vitro* tissue engineering of a RPE layer starting from hiPSCs to be implanted as an future Advanced Therapy Medicinal Product (ATMP).

EXPERIMENTAL METHODS

Membrane fabrication

Via sol-gel processes, pre-condensed silica clusters are synthesized starting from the liquid sol-gel precursor. The resulting sol is electrospun to a membrane, which is characterized by scanning electron microscopy (SEM), thermogravimetry (TGA-DTA) and regarding its stability in physiological solutions. In a second step, the silica surface is amine-functionalized using plasma techniques.

In-vitro RPE tissue engineering

Human iPSC-derived RPE cells are generated according to protocols published by Hongisto and colleagues (5). For model setup, hiPSC-derived RPE cells are seeded on amine-functionalized silica surfaces and cultured for up to 9 weeks. To demonstrate the formation of mature RPE cells, gene and protein expression analyses, barrier integrity studies are performed as well as functional phagocytosis assays.

RESULTS AND DISCUSSION

Electrospun silica membranes show a submicron patterned surface structure consisting of unoriented fibers of 300 nm in diameter. As the degree of condensation within the silica matrix increases, the stability in physiological solution also arises. Highly condensed silica membranes allow a long-term use in cell culture and presumably also after implantation. After a surface modification with primary amine functionalities, the material was tested *in-vitro* for cytocompatibility.

Next, hiPSC-derived RPE cells are cultured for up to 9 weeks on amine-functionalized silica surfaces, thereby representing a pigmented, tight as well as functional cell layer. In our studies, we highlight the functionalized silica surfaces as key factor for the cell differentiation towards mature RPE cells as well as for obtaining a stable and functional model.

In perspective, these features will enable the possibility of producing GMP conform and functional transplants of RPE layers.

CONCLUSION

Due to the promising *in-vitro* results, a first *in-vivo* animal study for the implantation of the hiPSC-derived RPE-layers on silica membranes is planned for the near future.

REFERENCES

1. Zarbin M. *et al.,* Trends Mol. Med. 22: 115-134. 2016.
2. Jones MK. *et al.*, Prog. Ret. Eye Res. 58: 1-27, 2017.
3. Da Cruz L. *et al.,* Nature Biotechnol. 36: 328-337, 2018.
4. Kashani AH. *et al.*, Science Transl. Med. 10: eaao4097, 2018.
5. Hongisto H. *et al.*, Stem Cell Res Ther. 8(1):291, 2017.

ACKNOWLEDGMENTS

This work was supported by the Fraunhofer Internal Programs under grant number MAVO 840 149. Thank you for providing financial support to this project.

Melt-Electrowritten Scaffolds for an *In Vitro* Blood-Brain Barrier Model Application

Magdalena Zofia Gładysz[1,2*], Marleen Kamperman[1], Marcus Koch[3], Małgorzata Włodarczyk-Biegun[1], Anika Nagelkerke[2]

[1]Zernike Institute for Advanced Materials, University of Groningen, Groningen, Netherlands
[2]Groningen Research Institute of Pharmacy, University of Groningen, Groningen, Netherlands
[3]INM - Leibniz Institute for New Materials, Saarbrücken, Germany
[*]m.z.gladysz@rug.nl

INTRODUCTION

The blood-brain barrier (BBB) is a selective interface in the brain between blood vessels, composed of a monolayer of endothelial cells, and the central nervous system, mostly made up of astrocytes, pericytes, and neurons. The BBB protects the brain from substances such as pathogens, but it also inhibits the uptake of therapeutics, including anti-cancer drugs. To make advances in drug therapies tackling brain cancer, the BBB microenvironment should be recapitulated in an *in vitro* model system.

Melt electrowriting (MEW), as a scaffold fabrication method, provides control over the scaffold's architecture with a micrometric resolution. By utilizing minimalistic fibrous scaffolds, cell-cell interactions between different types of cells in the BBB are encouraged to a higher extent than in commonly used porous membranes[1].

The objective of this work is to demonstrate how the design of the minimalistic fibrous scaffold produced with MEW can influence endothelial monolayer formation and facilitate cell-cell interactions between the monolayer and other relevant cell types.

EXPERIMENTAL METHODS

The scaffolds were fabricated from medical grade poly(ε-caprolactone) with the use of a Spraybase melt electrowriting printer. The Young's modulus of the fibers was determined using atomic force microscopy (AFM). The scaffolds' surface was modified with various coatings, such as poly-L-lysine (PLL), poly-D-lysine (PDL), fetal bovine serum (FBS), and surface treatments, such as NaOH etching and oxygen plasma activation, to facilitate cell growth. The scaffolds were seeded with mouse brain endothelial cells - bEnd.3. Cell morphology on the scaffolds was investigated via actin and nuclear immunofluorescence stainings, and scanning electron microscopy (SEM). Cell movement along the fibers was monitored with live-cell imaging.

RESULTS AND DISCUSSION

Scaffolds were successfully printed with desired fiber alignment. The stiffness of the fibers was higher in points of fiber crossing, and lower for single fibers. The most optimal cell attachment was observed in samples treated with NaOH etching followed by FBS incubation, and oxygen plasma treatment followed by PLL coating.

Live-cell imaging of endothelial cells on the scaffolds revealed that the cells moved along the fibers and positioned themselves at crossings of fibers. Results indicate that having more fiber crossings would facilitate better cell growth. Furthermore, a confluent monolayer of endothelial cells was obtained at the edge of the scaffolds (Fig. 1.). However, it was less likely for the cells to bridge the gaps between parallel fibers in the center of the scaffolds.

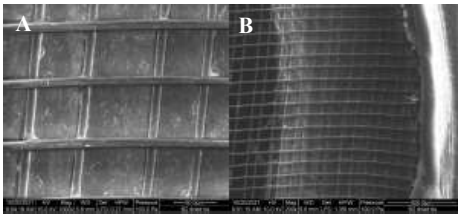

Fig. 1. SEM images of bEnd.3 cells grown on MEW scaffold: A) Magnified image, B) The edge of the scaffold with the confluent monolayer.

CONCLUSION

The work presented here shows the potential of utilizing MEW for minimalistic scaffold fabrication. The proposed designs enabled cells to grow and proliferate, without hampering cell-cell interactions. The seeding procedure requires further optimisation to facilitate the best possible endothelial cell growth.

Future steps will include the incorporation of hydrogels as an environment for astrocytes and, at the same time, as additional support for the seeded endothelial cells. Further development of this BBB model, such as maintaining the co-culture system in a microfluidic device, may result in a functional *in vitro* model which could be used in preclinical studies to improve drug uptake.

REFERENCES

1. Chung, H. H. et al., *Lab Chip* **18**, 1671 (2018).

ACKNOWLEDGMENTS

The authors would like to thank the program of PhD scholarship from the Molecular Life and Health research theme of the University of Groningen, NWO Veni Grant (VI.Veni.192.148), NAWA Polish returns grant (PPN/PPO/2019/1/00004/U/0001), and NCN OPUS grant (2020/37/B/ST5/00743) for providing financial support to this project.

Fucoidan/Chitosan Hydrogels as Matrices for Sustained Delivery of Platelet-Rich Fibrin Containing Bioactive Molecules

Karina Egle[1,2*], Eva Dohle[3], Verena Hoffmann[3], Ilze Salma[2,4], Sarah Al-Maawi[3], Shahram Ghanaati[3], Arita Dubnika[1,2]

[1]Rudolfs Cimdins Riga Biomaterials Innovations and Development Centre of RTU, Institute of General Chemical Engineering, Faculty of Materials Science and Applied Chemistry, Riga Technical University, Riga, Latvia
[2]Baltic Biomaterials Centre of Excellence, Headquarters at Riga Technical University, Riga, Latvia
[3]FORM, Frankfurt Oral Regenerative Medicine, Clinic for Maxillofacial and Plastic Surgery, Johann Wolfgang Goethe University, Frankfurt am Main, Germany
[4]Institute of Stomatology, Riga Stradins University, Riga, Latvia
[*] karina.egle@rtu.lv

INTRODUCTION

To eliminate complex manufacturing procedures and still obtain a pre-seeded tissue-like construct from autologous blood, platelet-rich fibrin (PRF) was introduced. PRF is obtained from the patient's own venous blood in a single centrifugation step without the additional use of anticoagulants[1] and contains autologous growth factors that can regulate cellular processes and tissue regeneration.[2] The aim of this study was to determine and compare the release kinetics of different bioactive molecules from PRF and PRF/fucoidan/chitosan matrices. Fucoidan (FU) and chitosan (CS) matrices were chosen due to their biocompatibility and ability to form polyelectrolyte complexes via self-assembly.[3]

EXPERIMENTAL METHODS

Samples were prepared by combining FU/CS hydrogels with PRF. In a 24-well plate 0.25% FU solution in water was added 1:1 (v/v) to 2% CS solution in 1.5M HCl. Samples were shaken at 500 rpm for 4 hours, then frozen and lyophilized. Samples were neutralized to pH7 with 1.5 M NaOH and re-lyophilized. PRF was obtained using 2 different centrifugation times (3 and 8 minutes) at 600 rpm. Liquid PRF was applied to the hydrogel before coagulation. FU/CS hydrogels and FU/CS hydrogels with PRF were compared regarding gel fraction, swelling degree and microstructure. Release kinetics of bioactive molecules (epidermal growth factor (EGF), interleukin 8 (IL-8), transforming growth factor beta-1 (TGF-β1)) were determined using ELISA method and histology for PRF and PRF in combination with FU/CS hydrogels was performed.

RESULTS AND DISCUSSION

The results showed that gel fraction of FU/CS hydrogel matrices was 95.66 ± 2.01% and the swelling equilibrium was reached after 1.5 hours. The results of release kinetics show that there is no difference between the amount of bioactive molecules released from the FU/CS hydrogel PRF complexes of different centrifugation times. A higher amount of growth factor TGF-β1 is released from pure PRF (8508.85 ± 402.26 pg/mL) than from FU/CS hydrogel with PRF (4840.58 ± 1143.82 pg/mL) after 7 days. Similar trend can be observed for other studied molecules.

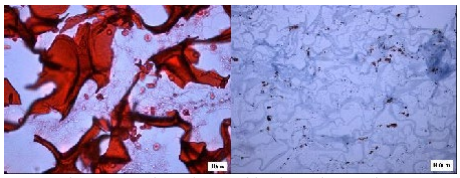

Fig.1: Developed PRF / hydrogel complex

CONCLUSION

It can be concluded that the hydrogel delays the rapid release of proteins from the PRF_FU/CS hydrogel complexes and that the FU/CS hydrogel with PRF provides a longer delivery of growth factors released from PRF. Histology and immuno-histology (see Fig.1) showed that PRF within the hydrogel has formed a loose structure with a large interstitial space documented by visualizing the fibrin structure and PRF containing platelets.

REFERENCES

1.Ghanaati S. *et.al*. J. Oral Implantol. 40:679–689, 2014
2.Nagarajan S. *et.al.* Elsevier Inc., ISBN 9780128140291, 2019
3.Venkatesan J. *et.al*. Molecules. 23 (6): 1429, 2018

ACKNOWLEDGMENTS

The authors would like to thank the European Union's Horizon 2020 research and innovation programme (Grant no: 952347, RISEus2) and the Latvian Council of Science research project (Grant no: lzp-2020/1-0054, MATRI-X) for providing financial support to this project.

Synthesis, characterization, and in vitro biocompatibility of Si-Ca-P multilayer scaffolds doped with Sr, Fe and Mg for tissue engineering

Nayarit A. Mata[1], Marcela Arango-Ospina[2], Pablo Velásquez[1], Ángel Murciano[3], Aldo R. Boccaccini, [2] Piedad N. De Aza[1*]

[1] Institute of Bioengineering, Miguel Hernandez University, Avda. Universidad s/n, 03202, Elche, Spain.
[2] Institute of Biomaterials, University of Erlangen-Nuremberg, Cauerstr. 6, 91058, Erlangen, Germany.
[3] Department of Materials, Optical and Electronic Technology, Miguel Hernandez University, Avda. Universidad s/n, 03202, Elche, Spain.
*piedad@umh.es

INTRODUCTION

Calcium phosphates are an excellent option for the replacement of bone tissue because of their similitude to the inorganic part of bone [1]. However, in addition to suitable chemical properties, the ideal graft must also have other characteristics such as mechanical properties, porosity, and others [2]. For this reason, the aim of this research is to develop new ceramic scaffolds capable of meeting the necessary requirements for application in bone tissue engineering. For this purpose, multilayer scaffolds based mainly on the CaO-P_2O_5-SiO_2 system were designed, consisting of a core whose chemical composition provides porosity and mechanical strength, and coatings with a second chemical composition that provides bioactivity and biocompatibility. Additionally, ions such as strontium, magnesium and iron were incorporated into the coatings, which are known to be involved in bone regeneration processes [3].

EXPERIMENTAL METHODS

The core of the scaffold was obtained from a polyurethane sponge coated with a sol-gel solution prepared with the following chemical composition SiO_2 - $25P_2O_5$ – $68CaO$ – $6Li_2O$ (% molar). The sponges were sintered at 950 ºC and subsequently coated with layers of the following chemical composition $29SiO_2$ – $3P_2O_5$ – $68CaO$ (% molar) to obtain the multilayer scaffold. Additionally, dopant ions such as iron, strontium and magnesium were introduced into these layers. Two multilayer scaffolds were prepared, the 3J scaffold consisting of the core and a coating with 3% of each dopant ion and the 3S scaffold consisting of the core and three coatings, each with 3% of each dopant ion. Finally, the scaffolds were chemically and physically characterized, and their biocompatibility was evaluated using cells of MG-63 line.

RESULTS AND DISCUSSION

The core of the scaffold obtained in this research consists mainly of the calcium pyrophosphate phase with a compressive strength of (1.00 ± 0.47) MPa and 65% porosity. Nevertheless, it showed a tendency to acidify the medium and decrease the viability of the cells, even decreasing the number of cells on the surface. On the other hand, the core with the coatings (3J and 3S scaffolds) showed an increase in cell viability by more than 100% compared to the core. 3J and 3S scaffolds showed no cytotoxic effects and the cells proliferated better on their surface compared to the core. No difference in cell behavior was observed between the 3J and 3S scaffolds. However, a difference in the in vitro bioactivity was observed. The 3S scaffold, having three coatings, has a higher amount of silicon, which activates ion exchange and increased bioactivity compared to the 3J scaffold.

CONCLUSIONS

The multilayer scaffolds developed in this research demonstrated that even though the core does not show good cellular response, external coatings significantly increase cell behavior. In this way, it was possible to obtain a mechanically resistant scaffold with the capacity to interact positively with the surrounding, being a good candidate for applications in bone replacement.

REFERENCES

[1] N. Eliaz, N. Metoki, Calcium Phosphate Bioceramics: A Review of Their History, Structure, Properties, Coating Technologies and Biomedical Applications. Materials. 10 334 (2017) 1-104.
[2] S. Bose, et al., Recent advances in bone tissue engineering scaffolds. Trends Biotechnol. 30 10 (2012) 546-554.
[3] V.M. Schatkoski, et al., Current advances concerning the most cited metal ions doped bioceramics and silicate-based bioactive glasses for bone tissue engineering. Ceram Int. 47 (2021) 2999-3012.

ACKNOWLEDGEMENTS

Nayarit A. Mata acknowledges the financial support received by a grant from the Generalitat Valenciana with reference GRISOLIAP/2018/037 and pre-doctoral mobility co-financed by the European Social Fund and the Generalitat Valenciana with reference BEFPI/2021/056. Additionally, this work is part of the Grant PID2020-116693RB-C21 funded by MCIN/AEI/ 10.13039/501100011033.

3D CaP porous scaffolds with grooved surface topography for bone tissue engineering

Eduardo Sebastián[1], Ángel Murciano[2], Piedad N. De Aza[1*], Pablo Velásquez[1]

[1]Instituto de Bioingeniería, Universidad Miguel Hernández, Avda. Universidad s/n, Elche, Alicante, 03202, Spain
[2]Departamento de Materiales, Óptica y Tecnología Electrónica, Universidad Miguel Hernández, Avda. Universidad s/n, Elche, Alicante, 03202, Spain
[*]piedad@umh.es

INTRODUCTION

The influence of surface topography on cell behavior has gained considerable attention in recent years. In particular, topography effects on osteoblasts have been well documented, and include changes in adhesion, proliferation, and differentiation, which influence bone formation[1]. Among the different surface patterns, "ridges and grooves" are of special interest, as they can be used to mimic the biophysical cues provided by the collagen fibers that form the bone extracellular matrix (ECM)[2]. To date, the introduction of topographic patterns into the surface of 3D porous ceramic scaffolds has proven difficult, due partly to the brittle nature of ceramic materials as well as the currently available fabrication technologies. In this study, a grooved pattern was introduced into the surface of 3D CaP porous scaffolds by means of the chemical etching technique.

EXPERIMENTAL METHODS

3D CaP multilayer scaffolds ($2SiO_2$–$50CaO$–$48P_2O_5$ (mol%)) were fabricated by sol-gel in combination with the polymeric sponge replication method. Polyurethane sponges used as templates were submerged in a sol-gel solution for the appropriate number of times and sintered at 950 ºC for 50 h. Scaffolds' surface was modified by a chemical etching process in an acetic acid (CH_3COOH) solution at different concentrations (3%, 5%, 10%) and etching times (30 s, 60 s, 120 s). Modified scaffolds were characterized by Scanning Electron Microscopy with Energy Dispersive X-Ray Spectroscopy (SEM-EDX), X-Ray Diffraction (XRD), Mercury Porosimetry, Compression Testing, Digital Holographic Microscopy (DHM) and their *in vitro* bioactivity was evaluated by immersion in simulated body fluid (SBF) for 7, 14 and 21 days.

RESULTS AND DISCUSSION

3D scaffolds presented an interconnected porosity and were composed of calcium (Ca), phosphorus (P), and a small amount of silicon (Si) with a Ca/P ratio of about 1.24. The XRD pattern of scaffolds confirmed that they were constituted by two major ceramic phases, calcium pyrophosphate ($Ca_2O_7P_2$) and β-tricalcium phosphate ($Ca_3(PO_4)_2$).

Scaffolds were chemically etched with different concentrations of acetic acid (3%, 5%, 10%) and different etching times (30 s, 60 s, 120 s). A 3% acetic acid concentration for 120s were selected as the best conditions to obtain a great number of ridges and grooves homogeneously distributed along the scaffolds' surface. The ridges and grooves obtained were nano-/micrometric in size, with a depth of 200 nm – 300 nm and a width of 900 nm – 1.5 µm as measured by SEM and DHM. Moreover, ridges and grooves became narrower and deeper with longer etching times. According to the previous literature, the dimensions of the ridges and grooves herein obtained would be appropriate to promote osteoblast adhesion, alignment, and elongation[3].

The XRD pattern of the modified scaffolds revealed that the pyrophosphate phase was etched off the surface, while the β-tricalcium phosphate phase remained unaffected by the process. Furthermore, the Ca/P ratio on the surface after etching was about 1.3, with a Ca/P ratio close to 1.5 on the grooved areas, which is close to the Ca/P ratio for β-TCP. As a consequence of the difference in susceptibility of the crystallographic phases to the etching process, the pyrophosphate on the scaffolds' surface was dissolved, forming grooves where it was originally present.

Scaffolds' *in vitro* bioactivity tested by immersion in SBF for 7, 14 and 21 days showed that the modified scaffolds were bioactive after 14, and especially after 21 days, when a great number of spherical precipitates could be observed. These precipitates were composed of Ca and P and their Ca/P ratio was of 1.69, which comes close to that of hydroxyapatite (HA) ($Ca_{10}(PO_4)_6(OH)_2$) (Ca/P ratio = 1.67), confirming that the bioactive capacity of scaffolds was not affected by the etching process.

CONCLUSION

A groove surface topography was introduced on the surface of 3D CaP porous scaffolds by means of the chemical etching technique. The dimensions of the ridges and grooves obtained in this study would be appropriate to promote the adhesion, alignment, elongation and differentiation of osteoblasts, improving the osteogenic capacity of the modified scaffolds. Moreover, the mechanical properties and bioactive capacity of the patterned scaffolds were not affected by the etching, making them suitable to be used in bone tissue engineering.

REFERENCES

1. Kirmizidis G. *et al*., Tissue Eng. 15: 1427–1436, 2009
2. Nadeem D. *et al*., Biofabrication. 7, 2015
3. Akasaka T. et al., Nano Biomed. 8:112–122, 2016

ACKNOWLEDGEMENT

This work is part of the Grant PID2020-116693RB-C21 funded by MCIN/AEI/ 10.13039/501100011033.

Full-scale topology optimization of synthetic bone scaffolds

Thijs Smit[1*], Stijn Koppen[2], Stephen J. Ferguson[1], Benedikt Helgason[1]

[1]Institute for Biomechanics, ETH-Zurich, Zurich, Switzerland
[2]Department of Precision and Microsystems Engineering, Delft University of Technology, Delft, The Netherlands
[*]thsmit@ethz.ch

INTRODUCTION

Critically sized bone defects are traditionally treated using autologous bone graft. This treatment is considered the gold standard but has its limitations[1]. A promising alternative treatment is to implant specifically designed and manufactured Synthetic Bone Scaffolds (SBS). The mechanical design requirements are to provide mechanical stability to the treated domain but avoid stress-shielding of the adjacent bone tissue. The morphological design requirement is to produce a porous structure to allow for bone in-growth. The appropriate pore size range can enhance bone in-growth and should be between 150 and 800 micron[2]. The conflicting trade-off between mechanical and morphological properties advocates for the use of optimization tools in the design process.

The aim of this study is to optimize 3D SBSs using full-scale topology optimization (TO) which maximize its stabilizing function while minimizing stress-shielding.

METHODS

The proposed TO formulation follows the SIMP approach considering small displacements. Linear FEM and constitutive relations are assumed. Scaffold designs are generated on a HPC cluster with a large-scale TO code[3]. To design porous structures and being able to control the porosity and pore size a local volume constraint is used[4]. To address the issue of stress-shielding and include the SBS's stabilizing function in the TO formulation we propose the 'scaffold' formulation[5] that maximizes the SBS's stiffness under shear loading (u in Figure 1). A maximum stiffness constraint is imposed for the compression load-case (w in Figure 1). As such, the SBS is designed to mimic the mechanical properties of bone in the compression direction and maximize its stabilizing function.

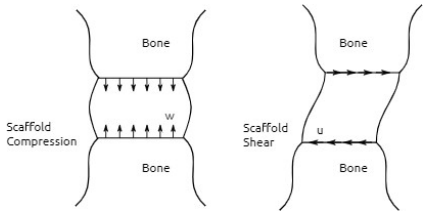

Figure 1, 2D scaffold problem definitions and load-cases with u the shear and w the compression.

RESULTS AND DISCUSSION

Figure 2 illustrates an optimized 3D SBS designed to be manufactured in Titanium. A 'bone-like' structure which is porous and has an internal pore size ranging between 150 and 580 micron is observed. The structure shows plate-like and strut-like internal structures. The porosity of the design is 32.8%. The limitation of using Titanium as a material to design and manufacture SBS is that the struct diameter should be large enough the ensure manufacturability. Furthermore, Titanium has a much higher E-modulus compared to bone tissue. Therefore, it is difficult to satisfy the stiffness constraint in the compression direction. The current Titanium SBS design is violating the stiffness constraint. This advocates for the use of PEEK which has lower E-modulus and results in SBS designs which better match adjacent tissue properties.

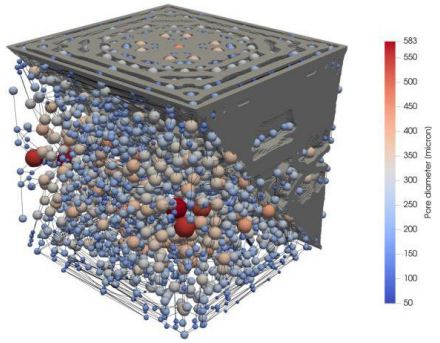

Figure 2, 3D scaffold design for Titanium material in grey. Spheres illustrate the pore size and location.

CONCLUSION

The 'scaffold' formulation using full-scale TO demonstrates to produce 3D SBS. The used material and manufacturing process influence the final design largely.

REFERENCES

1. Pobloth A. *et al.*, Science Translational Med., 2018
2. Barba D. *et al.*, Acta Biomaterialia, 2019
3. Smit T. *et al.*, Structural and Multi. Opt., 2021
4 Wu J. *et al.*, IEEE Trans. On Visu. Comp. Grap., 2018
5. Koppen S. *et al.*, MMT., 2022

ACKNOWLEDGMENTS

This project has received funding from the European Union's Horizon 2020 research and innovation programme under the Marie Sklodowska-Curie Grant Agreeement No. 812765.

FTIR Spectroscopy and Thermally-Accelerated Ageing: A Tool to Predict *in vitro* Scaffold Lifetime

Credson Langueh (Ph.D.) [1], Sylvie Changotade (Ph.D.) [1], Didier Lutomski (Ph.D.) [1], Géraldine Rohman (Ph.D.) [1,*]

[1]Université Sorbonne Paris Nord, Unité de Recherche en Ingénierie Tissulaire, URIT, UR, F-93430, Villetaneuse, France
*geraldine.rohman@univ-paris13.fr

INTRODUCTION

In tissue engineering, scaffold properties are continuously optimized to improve tissue regeneration rate and quality but impact drastically the scaffold lifetime. However, few studies focus on strategies combining accelerated testing protocols and versatile tools to easily investigate on the material degradation rate. In the present study, we used thermally-accelerated ageing and Fourier-Transform infrared spectroscopy to predict the lifetime in cell culture medium of elastomeric cross-linked poly(ester-urethane-urea) (PEUU) scaffolds[1].

EXPERIMENTAL METHODS

Highly interconnected porous PEUU scaffolds have been developed through an emulsion technique[2]. The degradation study was performed in cell culture medium at 4 different temperatures ranging from 37°C to 90°C. The scaffold property variation was followed by gravimetric and swelling measurements, compression tests and Fourier-Transform infrared (FTIR) spectroscopy. The relation between these parameters was evaluated. FTIR spectroscopy was used as a quantitative indicator of the hydrolysis content. Compressive set was used as an indicator of the scaffold lifetime at 90°C.

RESULTS AND DISCUSSION

The PEUU scaffold degradation was associated with the hydrolytic instability of ester groups which was temperature dependant since the absorbance intensity associated to the ester stretching vibrations (A_{1164}/A_{1255}) decreased with rising incubation time and temperature. The dependence of ester group cleavage on time of incubation was determined for each degradation temperature by regression analysis (Figure 1) and Arrhenius type extrapolation was used to estimate the activation energy of the hydrolytic degradation reaction (80.84 kJ mol^{-1}).

For elastomeric scaffold, the compressive set can be selected as the failure criterion from the point of view of the scaffold functionality. The compressive set measurements reached the failure criterion of 25% after 11.6 days of incubation in the degradation medium at 90°C. Therefore, the scaffold lifetime at 37°C was estimated to 1131 days (3.1 years) using an acceleration factor f equal to 97.5 as derived from the activation energy value.

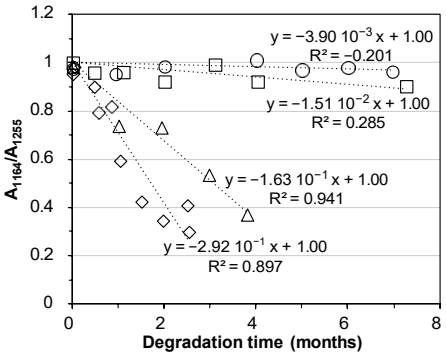

Figure 1: Evolution as a function of time of the ratio of FTIR absorbance intensities (A_{1164}/A_{1255}) of PEUU scaffolds incubated in the degradation medium at 37°C (circle ○), 55°C (square □), 75°C (triangle Δ) and 90°C (rhombus ◊) - each approximated by a linear regression curve

CONCLUSION

It is well known that it is difficult to correlate *in vitro* degradation with *in vivo* expectation since *in vivo* conditions are complex and lead to scaffold degradation through a variety of mechanisms. However, the approach developed in this study could be a convenient way to simply and straightforwardly screen the durability of scaffolds that are under development.

REFERENCES

1. Langueh C. *et al.,* Polym. Deg. Stab. 183:109454, 2021
2. Changotade S. *et al.,* Stem Cells Int. Article ID 283796, 2015

ACKNOWLEDGEMENTS

The authors thank the Ministère de l'Enseignement Supérieur, de la Recherche et de l'Innovation for the MENRT scholarship granted to Credson Langueh.

Perfusable Microvessel Substitutes Integrated in a Tailored Bioreactor Enable the Investigation of Chemotaxis in vitro

Mattis Wachendörfer[1*], Eleftheria Pantazoglou[1], Horst Fischer[1]

[1]Department of Dental Materials and Biomaterials Research, RWTH Aachen University Hospital, Aachen, Germany
[*] mwachendoerf@ukaachen.de

INTRODUCTION

There is a lack of biomimic in vitro vessel models to enable the investigation of the effect of simultaneous external stimuli on chemotaxis. Such systems can help to investigate and improve angiogenesis, intravasation, extravasation and can function as a drug screening platform. To address this issue, we propose bioprinted microvessel substitutes embedded in fibrin-based extracellular matrix substitutes (ECM) integrated in a tailored bioreactor for that purpose.

EXPERIMENTAL METHODS

The long-term stability of fibrin-collagen and fibrin-gelatin blends was investigated using an in vitro degradation test. To assess the permeability, transwell membranes were covered with hydrogel blends and the diffusion of fluorescein isothiocyanate labelled albumin from bovine serum (FITC-BSA) from the upper well into the PBS-filled lower well was measured using a microplate reader. The release of growth factors typical for inflammation (tumor necrosis factor α (TNF-α), stromal derived factor 1 (SDF-1)) from the hydrogel blends was investigated using an ELISA-kit. Microvessels mimicking arterioles were fabricated using coaxial bioprinting technique by combining an endothelial cell-laden (HUVEC) sacrificial gelatin core with a smooth muscle cell-laden (SMC) fibrin-based shell, all embedded in a fibrin based ECM. For microvessels mimicking venoles, needles used as placeholders were encapsulated in hydrogel prior to crosslinking and removed afterwards, leaving a perfusable microchannel within the ECM. The channels were cultivated using a perfusion pump and a tailored, 3D printed bioreactor system for up to 21 days. The middle part of the bioreactor incorporated the final hydrogel construct of 3 mm thickness. Medium containing cytokines and chemical stimuli was filled in two exterior reservoirs, separated from the hydrogel construct by permeable membranes, and diffused into the hydrogel construct and the perfusable microvessel substitute. The cellular organization of HUVECs and SMCs was investigated using immunostaining and confocal and two-photon microscopy.

RESULTS AND DISCUSSION

All hydrogel blends showed hydrolytic stability for at least 21 days. Swelling and shrinking of fibrin-gelatin blends was tuned by heat pretreatment of the gelatin component. Fibrin-collagen blends initially shrunk while the shrinking was reduced by increasing thrombin concentration and control of pH and temperature. Fibrin-gelatin blends provided twice the permeability of fibrin-collagen blends within the first 10 h. However, both blends levelled at a similar maximum permeability after 48 h. Gels with higher polymer concentration and hence denser microstructure showed lower permeability within the first hours compared to lower concentrated gels. The release of cytokines was distinctly higher from fibrin-gelatin blends (10-20 ng/ml for TNF-α; ~10 ng/ml for SDF-1) compared to fibrin-collagen blends (5 ng/ml for TNF-α; 3 ng/ml for SDF-1) after 24 h. A functional HUVEC monolayer lined the inner lumen of perfusable channels of approx. 500 µm in diameter. The HUVECs were activated by exposure to TNF-α, which diffused into the channels from the exterior reservoirs. The size of the channels was tuned by either the bioprinting settings (flow rate, temperature control) or designs of coaxial adapters and needles and showed similar accuracies as reported previously[1]. SMC showed high viability (< 80%) and characteristic stretching inside the gels.

CONCLUSION

In conclusion, we present a novel and versatile tailored bioreactor system which can be used to investigate the effect of external chemoattractants on the in vitro models. In combination with bioprinted microvessel substitutes, it represents a versatile and easy-to-use approach and can be used for a broad variety of tissue engineering applications.

REFERENCES

1. Millik. *et al*., Biofabrication. 11 045009, 2019

ACKNOWLEDGMENTS

The authors would like to thank the European Regional Development Fund (Interreg Euregio Maas-Rhein) of the European Union (EMR116) for providing financial support to this project.

How hydrodynamics and species transport influence the 3D microenvironment of cells seeded in hydrogel scaffolds

Martial Bankoué Ntaté[1*], Jérôme Grenier[1], Soukaina El Hajj[2], Magali Dupuy[1], Cyril Breton[1], Rachida Aid[3], Clément Journé[3], Robin Siadous[4], Jérôme Ligneron[4], Joelle Amédée[4], Didier Letourneur[3], Bertrand David[2], Hervé Duval[1]
[1]LGPM, CentraleSupélec, Université Paris-Saclay, Gif-sur-Yvette, France
[2]LMPS, UMR CNRS 9026, CentraleSupélec, Université Paris-Saclay, Gif-sur-Yvette, France
[3]LVTS, INSERM 1148, Université Paris Cité, Université Sorbonne Paris Nord, Paris, France
[4]Laboratoire BIOTIS, Inserm U1026, Université de Bordeaux, Bordeaux, France

* martial.bankoue-ntate@centralesupelec.fr

INTRODUCTION

Osteogenic substitutes can be produced using Mesenchymal Stem Cells (MSCs) seeded on porous scaffolds and cultured under dynamic conditions in a perfusion bioreactor[1]. The flow of the culture medium resolves solute (nutrients and oxygen) transport limitations and provides mechanical stimuli, influencing cell fate through mechano-transduction effects.
However, the solute concentration and stress fields are generally not uniform within a bioreactor. In order to know the (local) chemical and mechanical micro-environment experienced by the cells, we aim to develop a bioreactor digital twin.

PERFUSION BIOREACTOR

The device is a fixed-bed reactor. Its chamber is cylindrical (internal diameter of 12 mm, height of 30 mm). The fixed bed is a stack of pullulan/dextran porous hydrogel scaffolds[2]. The stacking is random and the scaffolds are disk-shaped. They are seeded with MC3T3E1 mouse osteoblasts (ATCC©)[3]. The bioreactor is perfused with a culture medium at 10 mL min^{-1}. The 3D geometry of the stack is acquired using 7T MRI.

MODELING

The hydrodynamics and the nutrient transport within the bioreactor are computed using lattice-Boltzmann methods (LBM)[4]. LBM is well suited to investigate fluid flow at low Reynolds numbers in complex geometries such as porous media. After binarization, the 3D-image of a scaffold (as given by MRI or OCT) can be used directly by a LBM code, just by locating the nodes of the lattice at the center of the voxels and labeling the nodes as “hydrogel”, “cells”, or “fluid”. The hydrodynamics is simulated using a two-relaxation-time (TRT) LBM with a cubic lattice in 3 dimensions and 19 velocities (D3Q19). The transport of the dissolved oxygen is simulated using a D3Q7 TRT LB method. The kinetics of O_2 uptake is modeled by the Michaelis-Menten law.

RESULTS AND DISCUSSION

We consider a virtual seeding of 400,000 cells per scaffold randomly distributed in the form of 135 µm-diameter spheroids.
The fluid velocity field is highly heterogeneous. Whereas the superficial velocity equals 1.47 mm s^{-1}, the maximum interstitial fluid velocity reaches 27 mm s^{-1} at the region of the smallest cross-section within the stack. The wall shear stress ranges from 0.1 mPa to 100 mPa (averaged value of 25 mPa).

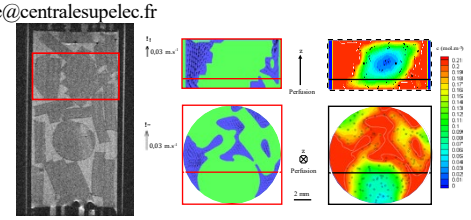

Fig. 1 MRI acquisition (left) and LBM simulations (center and right) of a portion (6.55 mm high) of the perfusion bioreactor. The fluid (blue) flows through the pores of the stack (green). The oxygen concentration in the fluid is set to 0.21 mol m^{-3}. The oxygen diffusion coefficient inside the hydrogel scaffolds is D = 1.6 10^{-9} m^2 s^{-1}. Black circles represent the spheroids.

More than 98% of the total hydrogel volume is not hypoxic, the oxygen concentration being greater than the O_2 Michaelis-Menten constant (K_M = 6 10^{-3} mol m^{-3}).
The experimental observations confirm that the cells do not suffer from hypoxia when the bioreactor is perfused at 10 mL min^{-1}: viability measured using a Live/Dead assay remained unchanged during three weeks of culture.

CONCLUSION

Our approach combining 3D imaging and lattice Boltzmann simulations is well suited to predict the local oxygenation state and the shear stress level experienced by cells within a fixed-bed bioreactor.
Next, we plan to assess the same parameters on a co-culture of human umbilical vein endothelial cells and human mesenchymal stem cells. The scaffold microgeometry and the cellular aggregate distribution will be analyzed using optical coherence tomography and confocal laser scanning microscopy.

REFERENCES

1. David, B. *et al.*, 2011. Tissue Eng. Part C Methods. 17, 505–516.
2. Fricain, J.C. *et al.*, 2013. Biomaterials. 34, 2947–2959
3. Grenier, J. *et al.*, 2019. Acta Biomater. 94, 195-203
4. Thibeaux, R. *et al.*, 2019. Biotechnol. Prog. 35, e2880, 13 pages.

ACKNOWLEDGMENTS

The authors acknowledge the support of the French Agence Nationale de la Recherche (ANR), under grant ANR-21-CE18-0010-01 (project HydrOs).

micro-optofluidic devices for drug release characterisation in simulated, dynamic oral microenvironment.

William Oates[a], Antonios Anastasiou[a]
[a] Department of Chemical Engineering, University of Manchester, Manchester, UK, M13 9PL

Introduction: In the evaluation of medical devices, there is a great gap between *in vitro* testing and animal models. In the first case we have an ideal and perfectly controlled, sterile environment where the tests are taking place under steady state conditions. On the other hand, during animal trials, we have a dynamic environment, with momentary alterations of pH and temperature, continuous risk of bacterial infection and interactions between different tissues. Great efforts have been done the last few years to develop tools for better *in vitro* evaluation of biomaterials/devices aiming to bridge the gap between lab testing and clinical translation and simplify the drug development process [1, 2]. Motivated by this, our long-term objective is the development of an optofluidic device where we can **a)** replicate the changes of pH and temperature; **b)** run long term cell experiments; **c)** investigate the interactions of different cell types; **d)** perform real time spectroscopic measurements for obtaining drug release profiles. In this work we are focused on an initial design, investigation of the flow conditions and sensing capabilities for detection of drugs at different microenvironments.

Methodology: A commercial CFD software was utilised for the investigation of flow conditions and for optimising the geometrical characteristics. Fabrication took place using a resin 3D printer. A flow cell was connected to the outlet of the device to perform real time UV-VIS measurements. Two types of experiments were performed; a) Residence time distribution using a dye to investigate; b) drug release experiments from a chitosan scaffold. For the preparation of the scaffold, doxycycline was dissolved in 2% v/v acetic acid solution. Medium molecular weight chitosan was then added to the mixture which was then introduced into a 3D printed "cup" mould (diameter of 4 mm, depth of 2 mm). Freezing at -27 °C and freeze drying to remove water followed.

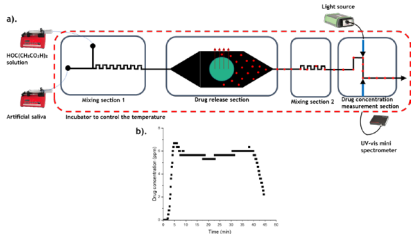

Figure 1: a) experimental setup; b) indicative drug release profile.

Results and discussion: Based on the CFD results, to achieve the effective mixing of the working fluid with the pH buffer, a mixing section of 24 steps is required. Close to the outlet of our device a second mixing section of 12 steps is added for achieving a homogenous working fluid – drug solution. For the design of the drug release section, a width/height aspect ratio of 16 found to be appropriate (8/0.5 mm). To such large aspect ratio, we have a plug flow velocity profile which translates to homogenous stress applied on the surface of the samples. The 3D printed prototype was used for residence time distribution and drug release experiments. The mean residence time (MRT) is important for studying the response time of the biomaterials under dynamic conditions. Depending on the flow conditions and the scenario tested, MRT varies between 2.83 min and 23.5 min. The doxycycline release profile from the chitosan scaffold was obtained from real time monitoring of the absorption peak at 340 nm. The minimum drug concentration able to be measured with our system was 1 ppm. HPLC experiments are in progress to find the total concentration of the drug and verify our data.

Conclusion: In this work we present the initial design of an optofluidic device with which we can simulate dynamic, *in vivo* microenvironments and perform real time spectroscopic measurements for the detection of drugs. CFD simulations were conducted to determine the geometrical characteristics of the device. With our first experiments we proved that a minimum amount of sample (2 ml) was enough for obtaining a drug release profile. Our long-term objective is the development of advanced bioreactors that will contribute to the reduction of the total cost and time needed for the development of medical devices and biomaterials.

References:

[1] Benam, K.H. et al. (2016). Small airway-on-a-chip enables analysis of human lung inflammation and drug responses in vitro. Nature Methods, 13(2), pp.151–157.

[2] DiMasi, J.A., Grabowski, H.G. and Hansen, R.W. (2016). Innovation in the pharmaceutical industry: New estimates of R&D costs. Journal of Health Economics, 47, pp.20–33.

Acknowledgments: The authors would like to acknowledge the Horizon 2020 funded project I-SMarD for the financial support.

Enabling Electrical Field Stimulation in Perfusion Bioreactor for Bone Craft Substitutes

Franziska Alt[1*], Salman Salman[1], Poh Soo Lee[1], Benjamin Kruppke[1]

[1]Max-Bergmann-Center for Biomaterials, Technical University Dresden, Dresden, Germany
[*]Franziska.alt@tu-dresden.de

INTRODUCTION

During long bone formation and regeneration, different cell types of chondrogenic and osteogenic cell lineages interact with each other, both being differentiated from human bone marrow-derived mesenchymal stromal cells (hBM-MSCs). Biochemical and physical stimulation in the form of the Young's modulus of the scaffold, the partial pressure of oxygen (pO_2)[1], and electric field (EF) stimulation also play a major role in the differentiation process of MSCs. In previous work, a perfusion bioreactor was used to demonstrate that mouse embryonic stem cells (mESC) could transit from chondrogenic to osteogenic differentiation in a collagen-based scaffold depending on a pO_2 gradient, achieving a growth factor-free differentiation approach as proof of concept for further work with hBM-MSCs[2]. In recent research, this system was improved to an electrical field stimulation bioreactor (EFS bioreactor). The requirements for the new system have been: 1) coupling an electric field under constant flow conditions comparable to the current bioreactor[2], 2) uniform discharge of medium, which is particularly important to guarantee homogenous mass transfer, and 3) the easier maintenance of sterility that reduces the risk of contamination for long term culture (60 days). Furthermore, to facilitate 4) ease of medium change, and 5) local and time-dependent pO_2 measurement.

EXPERIMENTAL METHODS

The flow conditions were examined by replacing PBS with 1 g/L phenol red (PR) dyed PBS at a perfusion rate of 5.5 mL/min under inclination angles of 0°, 30°, and 60°. The fluid (1 mL each) was withdrawn every 5 min at four different measurement points, namely the upper perfusion channel (1), the lower perfusion channel (2), the outlet unit (3), as well as the tube for electrical field stimulation (4) (positions are indicated in Fig. 1). Based on intensity measurements at a wavelength of 492 nm on the UV-VIS spectrometer Infinite 200Pro (Tecan), the percentage of PR at each point was measured for a liquid flow of 40 min in total.

RESULTS AND DISCUSSION

The EFS bioreactor meets via its modular setup all of the requirements (Figure 1). All connections are commercially available, autoclavable, and reusable, with a few exceptions. An in-house programmed and housed data acquisition system allows automatic real-time pO_2 measurements and recording with the commercially available Oxylite ProXL (Oxford Optronix) oxygen at self-defined time points. Self-sealing adapters allow the medium reservoir to be exchanged quickly and under sterile conditions. Additional tubing adapters ensure the sterile installation of the system in and its removal from the incubator.

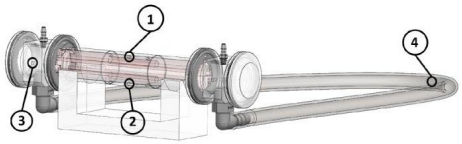

Figure 1: Electrical field stimulation bioreactor with modular components. Positions for liquid sampling for examination of flow conditions are indicated numerically.

By positioning the bioreactor in the incubator at a specific angle, the flow through the perfusion channels can be optimized. This resulted in a particularly favorable exchange of the medium in the system. By measuring the liquid flows and pO_2 at different angles of inclination, it was possible to prove under which conditions all perfusion channels are subjected to almost identical exchanges. At an inclination angle of 60°, where the inlet is on top, a fast and complete exchange of the medium can be ensured and the space requirement in the incubator can be minimized.

CONCLUSION

The demands on the bioreactor in terms of electrical field stimulation, simplified handling, and improved sterility could be implemented. Utilizing gravity as the driving force of the flow at an inclination of 60°, the main flow through the perfusion channels, as well as the fastest possible media change can be ensured.

REFERENCES

1. Bahney C.S. *et al.,* J. Orthop. Res. 37:35-50, 2019
2. Lee P.S. *et al.*, Tissue Eng. Part C Methods 23:286-297, 2017

ACKNOWLEDGMENTS

The authors would like to thank the Deutsche Forschungsgesellschaft DFG (Project no: 460388836) for providing financial support to this project.

Co-culture of HUVECs and hMSCs in a Perfusion Bioreactor Ensures the Development of Viable Spheroids

Soukaina El Hajj[1*], Martial Bankoué Ntaté[2], Rachida Aid[3], Cyril Breton[2], Robin Siadous[4], Jerome Ligneron[4], Magali Dupuy[2], Herve Duval[2], Didier Letourneur[3], Joelle Amedee[4], David Bertrand[1]

[1]LMPS, UMR CNRS 9026, CentraleSupélec, Université Paris-Saclay, Gif-sur-Yvette, France
[2]LGPM, CentraleSupélec, Université Paris-Saclay, Gif-sur-Yvette, France
[3]LVTS, INSERM 1148, Université Paris Cité, Université Sorbonne Paris Nord, Paris, France
[4]Laboratoire BIOTIS, INSERM U1026, Université de Bordeaux, Bordeaux, France

[*]soukaina.el-hajj@centralesupelec.fr

INTRODUCTION

Our improved understanding of bone fetal development and bone hierarchy has shed an undeniable light on the coactive and synergetic relationship between blood and bone formation. Several studies have shown that the co-culture of endothelial stem cells (ESCs) and mesenchymal stem cells (MSCs) has significantly improved angiogenesis and osteogenic differentiation [1, 2], which further proves the importance of cell-cell communication in regenerative medicine applications. As three-dimensional (3D) cell co-culture leads to the formation of spheroids maximizing this intercellular communication, angiogenesis will not only refine bone differentiation and maturation, but it will also ensure the long-term delivery of oxygen and nutrients to bone spheroids as they develop in size and complexity. In the context of bone tissue engineering, these properties can be exploited to produce osteogenic substitutes using MSCs seeded on micro/macroporous scaffolds and cultured under dynamic conditions in a perfusion bioreactor. [3] Stem cells have been shown to be mechanosensitive and capable of undergoing mechanically induced proliferation and osteogenic differentiation.

EXPERIMENTAL METHODS

In this study, one million human umbilical vein endothelial cells (HUVECs) and human mesenchymal stem cells (hMSCs), tagged with RFP and GFP respectively, were seeded using a 1:1 ratio on each scaffold. The latter is a pullulan/dextran micro/macroporous hydrogel supplemented or not with nano-hydroxyapatite crystals (nHAp). This scaffold is cylindrical in shape and has a diameter of 8.4 mm, a central hole with a diameter of 3 mm, a height of 1.5 mm, and a mean pore size of 54 µm post-hydration. 24 hours post-seeding, about 30 hydrogels were stacked, centrally aligned, then transferred and cultured up to 30 days in a custom-made perfusion bioreactor developed in our lab, under a steady flow of 10 ml/min of culture media (45% MEM α, Gibco, 45% EBM™2, Lonza, 10% FBS, Dutscher) ensuring mechano-stimulation and optimized nutrient delivery. [4] The formation, development and distribution of 3D aggregates was explored using optical coherence tomography (Thorlabs Ganymede series 621C1), while vasculature was assessed at 12 hours post-seeding, then every 3 days during the first 15 days of culture with confocal microscopy (ZEISS LSM700). Acquired images were then analyzed with ImageJ to determine the number of cells as well as the number and size of spheroids over time. Cell viability was measured once a week using a Live/Dead kit (Invitrogen™). Moreover, we monitored the metabolic activity of cells by recording their oxygen consumption. For this purpose, Oxygen sensors (PSt7, PreSens) were inserted at the entrance and exit of the bioreactor and O2 levels were recorded throughout the entire culture period.

RESULTS AND DISCUSSION

We observed and recorded the development and reorganization of MSCs and HUVECs under dynamic culture conditions. Most importantly, spheroids maintained their viability despite their size when compared to static cell culture conditions, showing the efficiency of our dynamic cell culture model.

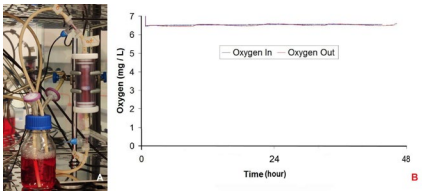

Figure 1: (A) Bioreactor system with oxygen sensors (B) Recorded oxygen levels in dynamic culture over the period of 48 hours

CONCLUSION

Our results show that co-culturing HUVECs and hMSCs in a porous hydrogel under dynamic culture conditions leads to viable and well-developed spheroids. Next, we plan on assessing the osteogenic as well as angiogenic markers and the effects of hydroxyapatite crystals on their regulation and matrix deposition. In addition, we will investigate the optimal culture conditions for our model using a digital simulation of our bioreactor.

REFERENCES

1. Guerrero J. *et al.*, TE Part A 2:5-6, 2015
2. Bidarra S.J. *et al.*, Stem Cell Res. 7:3, 2011
3. Chabanon M. *et al.,* TERM 16:3, 2019
4. Harvestin J.N. et al, Sci. Adv. 6:7, 2020

ACKNOWLEDGMENTS

The authors acknowledge the support of the French Agence Nationale de la Recherche (ANR), under grant ANR-21-CE18-0010-01 (project HydrOs).

Biocompatibility study of an innovative "Suspence" system for cell culture in suspension by evaluating cell viability and growth

Miriam Merco[1], Giacomo Di Benedetto[2], Federica Liguori[2], Michele Pistillo[2], Margherita Scamarcio[2], Giuseppe Falvo D'Urso Labate[2], Antonella Lisi[1], Mario Ledda[1]

[1] Institute of Translational Pharmacology, National Research Council, Rome, Italy
[2]Cellex srl, Rome, Italy
*miriam.merco@ift.cnr.it

INTRODUCTION

Suspended cell cultures are the basis for the production of important medical products such as insulin, vaccines and drugs in the oncology field.
The devices currently used for this purpose are not always efficient, as they do not allow an adequate supply of oxygen and nutrients, and they are also based on systems that can damage cells by altering their normal growth[1].
In this study an innovative bioreactor for the culture of mammalian cells in suspended conditions has been tested[2]. The study was aimed at assessing the performance of the bioreactor to evaluate its suitability for the production of cell-derived drugs like vaccines and monoclonal antibodies, and for cell expansion in immunotherapy. The bioreactor ensures physiological shear stress on the cultured cells, keeping them in suspension through a purely fluid-dynamic effect, thus avoiding impellers and rotating parts.

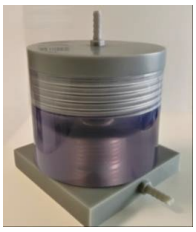

EXPERIMENTAL METHODS

A series of experimental tests were performed using two in vitro cell models, JURKAT, an immortalized T lymphocyte cell line originally obtained from the peripheral blood of a patient with T-cell leukemia and U937, a monocytic cell line that can be differentiate into various types of macrophages or into dendritic cells.
Both cell lines, grow very rapidly in suspension, making them particularly suitable for viability and cell growth study. Cell growth and viability were obtained by measuring, at various times and under different conditions, the total number of nucleated and viable cells by Trypan Blue dye (0.4%) exclusion assay, using a Bürker hemocytometer chamber. The significance of the difference between bioreactor and static condition was evaluated using the Student's t test, with $p < 0.05$ as the minimum level of significance.

RESULTS AND DISCUSSION

Preliminary results of the study show the ability of bioreactor to support cell growth, which is similar to those of control cells grown in a low volume of medium and in static conditions (30/50ml). More important, when the cells are grown in a large volume of medium (≥ 100 ml), the cell growth resulted significantly increased in the bioreactor compared to static conditions. We hypothesized that this positive effect, highlighted in the bioreactor, is due to the greater exchange of oxygen and nutrients guaranteed by the perfusion. Contrary, in static conditions, the cells settle on the bottom of the flask and the excessive amount of medium in the absence of perfusion does not guarantee a sufficient supply of oxygen and nutrients.

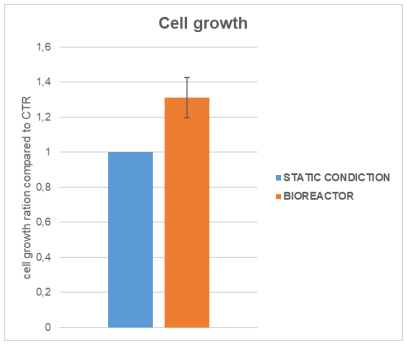

CONCLUSION

In conclusion, these results provide initial and promising indications on the ability of our bioreactor to better support the cell growth of mammalian cells under suspended conditions, opening the possibility of its use in biopharmaceutical applications.

REFERENCES

1. Suman C. *et al*., Front. Bioeng. Biotechnol.8, 2020
2. Falvo D'Urso Labate G., Pat. N. WO2020/095143 A1, 2020

ACKNOWLEDGMENTS

This publication has been cofunded by the EU through the programme "FESR, PON Imprese e Competitività 2014-2020 – Smart&Start" - No. C89J20000080008.

Designing the electrical stimulation chamber for *in vitro* tissue cultures

Aleksandra Benko[1*], Krzysztof Pietryga[1,2], Michał Dziadek[1,3], Marek Stencel[1], Jacek Nizioł[1]

[1] AGH University of Science and Technology, Krakow, Poland
[2] Kardio-Med Silesia, Zabrze, Poland
[3] Department of Inorganic Chemistry, Faculty of Chemistry, Jagiellonian University, Krakow, Poland
[*] abenko@agh.edu.pl

INTRODUCTION

Electrical stimulation of cells, especially those of the electrically active tissues, such as muscles, nerves or bones, has been reported to enhance maturation, proliferation and differentiation in the *in vitro* cultures[1].

While there are some commercially available solutions to introduce electrical signals into the cell cultures, most of them rely on transducing the signal through the culture media. Such approach is effective in delivering the signal to the cells but may be connected with some unwanted reactions, such as electrophoresis, electrolysis (of water and culture medium components), or uncontrolled heating.

On the other hand, it is now recognized that cells prefer electrically conductive scaffolds over non-conductive ones[2]. Hence, it could be suggested that combining the electrically conductive materials with an *in vitro* electrical stimulation running through the scaffold could provide superior results when compared to stimulation through the media or using non-conductive scaffolds.

The aim of this study was to design a new type of electrical stimulation chamber that would allow electrical stimulation through the scaffold. To achieve that, a completely new design of the cell well plate was made, and new, electrically conductive, elastic and moldable material was fabricated.

The suggested design could in future be enriched with additional functions, such as mechano stimulation or microfluidics.

EXPERIMENTAL METHODS

The commercially available polydimethylsiloxane (PDMS), Sylgard 184, was selected as a cytocompatible and moldable elastic polymer. It was then modified in-mass with carbon nanotubes to obtain elastic electrodes, in accordance with technique proposed by Kim et al.[3]. The PDMS and its nanocomposites were characterized in terms of their mechanical properties. The molds were fabricated via 3D printing. Hence, the cell wells were designed and fabricated.

Independently, a design of the printed circuit board (PCB) was made, and the electrically conductive cell well plate was fabricated.

RESULTS AND DISCUSSION

Upon introduction of the CNTs, electrically conductive, 3D printable and moldable elastic materials were obtained. The presence of CNTs led to a slight increase in the stiffness, but the material may still be regarded as highly elastic. From the PDMS and its nanocomposites, new types of cell wells were fabricated, and the materials revealed a good shape mapping.

The as designed electrical stimulation chamber based of PCB allows for successful delivery of electrical signal through the bottom of the cell well plate, with high output, low heating and good efficiency.

CONCLUSION

A completely new design of the electrical stimulation chamber was made and the prototype was successfully fabricated. The new design allows to electrically stimulate the cells *in vitro,* by transducing the electrical signal through the electrically conductive scaffolds. The chamber elements are autoclavable and can be used for the long-term stimulation inside the cell incubator.

Because of good elasticity, the chamber may in future be implemented with additional features, such as mechanical stimulation or microfluidics.

REFERENCES

1 Thrivikraman, *et al.* Biomaterials 150, 60-86, 2018.
2 Sun, H. et al. Acta Biomaterialia 48, 88-99, 2017.
3 Kim, J. H. et al. Scientific Reports 8, 1375, 2018.

ACKNOWLEDGMENTS

The authors would like to thank the National Centre for Research and Development (Grant no: LIDER/7/0020/L-11/19/NCBR/2020) for providing financial support to this project.

Electrochemical Aspects of *In Vitro* Electrical Stimulation Devices

Andrés Sánchez-Pérez*, Blanca Limones-Ahijón, José Miguel García-Martín, María Ujué González, Sahba Mobini

Instituto de Micro y Nanotecnología, IMN- CNM, CSIC (CEI UAM+CSIC), Tres Cantos, Madrid, Spain
*andres.sanchez@csic.es

INTRODUCTION

Electrical stimulation (ES) has been employed in numerous biomedical applications such as neural stimulation, neural interfacing and tissue regeneration. The biological complexity of *in vivo* conditions encouraged many researchers to evaluate the role of ES via *in vitro* devices[1]. Among the several ES delivery methods, direct coupling is the one that fairly mimics implantable devices.

The electrochemical properties of *in vitro* ES devices and the characteristics of the delivered electrical field remain broadly understudied. Electrode materials have a critical role in determining the impedance (*Z*) and charge injection capacity (CIC) of the system. A small CIC and high Z require larger potentials to inject a significant amount of charge, which may corrode the electrode or hydrolyse the electrolyte. In addition, electrochemical reactions result in by-products such as reactive oxygen species (ROS) or changes in the pH, which are harmful for the cells[2]. Nano-structuration is shown to improve the electrochemical properties of bioelectrodes[3].

In this study, we defined biologically safe limits of ES delivered by both Pt thin films (TF) and nanostructured (NC) electrodes incorporated in an *in vitro* ES device[4]. To this end, we performed comprehensive electrochemical characterization in biologically relevant conditions.

EXPERIMENTAL METHODS

The fabricated *in vitro* ES device is shown in **Fig. 1A**. NC and TF electrodes were fabricated via electron beam evaporation at glancing and perpendicular deposition angles respectively[3], **Fig. 1B & C**. We used PBS and DMEM at 37°C as electrolytes. The immersed area of the electrodes was kept constant in all experiments.

Z was characterized via electrochemical impedance spectroscopy by applying a 10 mV AC signal from 1 Hz to 10^5 Hz. Safe potential limits (SPLs) and reaction mechanisms were determined via cyclic voltammetry (CV) by gradually extending the potential window until the oxygen (OER) and hydrogen (HER) evolution reactions were observed. These reactions correspond to the formation of O_2 and H_2 indicating the onset of water splitting. Finally, accumulated charge, charge per pulse, ROS formation and pH changes were measured in pulsed regimes via chronoamperometry (CA) for different potential windows chosen according to the CV results.

RESULTS AND DISCUSSION

Z is significantly smaller at lower frequencies for NC electrodes compared to TF. The NC effective capacitance (~ 350 µF) is also larger than that of TF (~ 10 µF) due to its increased electrochemically active area.

CV tests revealed that HER and OER occurs under ~ -0.7 V and over ~1.0 V respectively, for both NC and TF. Peaks due to oxidation-reduction of Pt, and adsorption-desorption of H_2, were observed in the same potential ranges for both morphologies, from -0.2 to 0.2 V and from -0.7 to -0.4 V respectively, **Fig. 1D**. Hence, reaction mechanisms and SPLs highly depend on the electrode material and the electrolyte, rather than morphology.

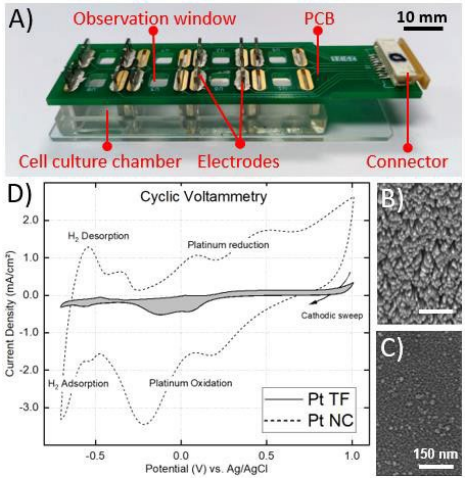

Fig. 1. A) In vitro device for ES. B&C) SEM images of Pt NC and TF surfaces, respectively. D) CV for both Pt TF and NC. Curve areas reflect the CIC of each material and peaks indicate the reaction mechanisms.

Absolute accumulated charge was considerably larger for both morphologies in the potential regions were oxidation of Pt and adsorption-desorption of H_2 occur, showing its dependency on the applied potential ranges. However, charge per pulse was around two orders of magnitude larger for NC than for TF in every region.

CONCLUSION

A reliable electrochemical characterization protocol is crucial to stablish safe and well-defined ES. Moreover, nanostructuration significantly benefits electrode performance during electrical stimulation.

REFERENCES

1. Balint R. *et al.,* Tissue Eng. Part B Rev., 19:48-57, 2013
2. Merrill DR. *et al.,* J. Neurosci. Methods, 141:171-198, 2005
3. Mobini S. *et al.,* Nanoscale, 14:3179-3190, 2022
4. Mobini S. *et al.,* PCT App. WO2021/260248A1, 2021

ACKNOWLEDGMENTS

Funding from Comunidad de Madrid (Atracción de Talento Programme, Modalidad-1 Ref. 2019-T1/IND-1335, project S2018/NMT-4291 TEC2SPACE and YEI contract PEJ-2019-AI/IND-14451 with support from FSE) and CSIC (ILINK+2020 Ref. LINKA20342).

A tubulogenesis assay to characterize the influence of hydroxyapatite-based ceramic properties on endothelial cells

Julie Usseglio, Adeline Dumur, Emeline Renaudie, Esther Pagès, Joël Brie, Eric Champion, Amandine Magnaudeix*

Univ. Limoges, CNRS, Institut de Recherche sur Les Céramiques, UMR 7315, F-87000, Limoges, France
* amandine.magnaudeix@unilim.fr

INTRODUCTION

A lack of vascularization limits the in-depth colonization of bioceramics scaffolds by host tissues reducing their applications. Because cells are sensitive to the chemical-physical properties of their environment, tuning the chemical and/or microarchitectural design of the scaffolds may improve endothelial cell (EC) growth at the ceramics surface. Nevertheless, there are few methods to assess *in vitro* the influence on the scaffolds modifications on the vascularization properties. Moreover, these methods are mostly indirect and do not take account of the material surface properties. The main objective of this study was thus to set-up an experimental protocol using fibrin-based gel to assay tubulogenesis on ceramic scaffolds allowing discrimination of the influence of chemistry composition from that of the microarchitectural design. To test the accuracy of the method a comparison of HA-based pellets with two different chemical compositions: pure HA, $Ca_{10}(PO_4)_6(OH)_2$,[1] or doped with silicon, SiHA, $Ca_{10}(PO_4)_{5.6}(SiO_4)_{0.4}(OH)_{1.6}$,[2] and two microstructures: dense or microporous ceramics (25% open microporosity) was performed.

EXPERIMENTAL METHODS

C166 endothelial cells were cultured first at bioceramic surface. Their viability was assessed using resazurin-based metabolic assay. Hoechst 33342 nuclear staining allowed to access to the cell density while *in situ* detection of EdU-positive newly synthetized DNA permitted to evaluate the proliferation ability of C166. The repartition and organization of the cell layer as well as EC activation according to the biomaterial was evaluated *in situ* by staining of actin cytoskeleton or angiogenesis-related markers (VEGFR-2, MMP9, PECAM-1).

For tubulogenesis assay, C166 endothelial cells were seeded either on top of a fibrin gel poured on bioceramics (configuration 1) or on ceramics surface before layering the fibrin gel (configuration 2) and cultured for 7 days. After cell fixation and immunofluorescence staining of the same markers as above, cells on ceramics were imaged by several microscopy modalities.

Ionic species released in culture medium by ceramics was assayed by ICP- optical emission spectroscopy and indirect wound healing assay using C166 cells in these dissolution products was performed.

RESULTS AND DISCUSSION

The C166 cell metabolic activity was comparable on all materials. The presence of microporosity altered the cell ability to attach and proliferate in comparison with dense pellets. Fluorescence microscopy analysis highlighted a different organization of the cell layer according to the microstructure. On dense materials, clusters with a higher cell density expressing high amount of VEGFR-2 and MMP9 were found while the cell was more homogeneous on microporous scaffolds.

Fibrin-gel matrix were used to create a 3D environment favourable to tubulogenesis. Configuration 1 was intended to evaluate the impact of material surface and configuration 2 was thought to reflect the influence of material chemistry. Surprisingly, on both configurations, similar results were observed with the formation of tubular structures positive for VEGFR-2 and vWF-1 on dense ceramics. Such structures were almost absent on porous materials where the cellular layer adopted an alveolar aspect. Biphoton microscopy highlighted the 3D nature of this layer with dome and valleys. No effect due to the presence of silicon in SiHA ceramics was detected in any configuration.

Because of the absence of difference between the two fibrin-based experimental set-ups, the negative effect of microporosity was attributed to a modification of the composition of the medium surrounding the cells. The culture medium in which the porous pellets were immersed showed a decrease of calcium in solution, that was not observed with dense ceramics. This decrease is hypothesized to impair EC activity. To confirm it, EC cell activity in indirect culture assay using ceramic immersion media is under investigation.

CONCLUSION

An experimental set-up to evaluate EC ability for tubulogenesis in direct contact with biomaterial was designed. The presence of microporosity seems to be detrimental to tubulogenesis likely due to a low soluble calcium concentration. Silicon has not demonstrated any effect on EC behaviour.

REFERENCES

1. Raynaud, S. *et al*. Biomater. 23(4):1065-72, 2002.
2. Palard, M., *et al*., Acta Biomater. 5, 1223–1232, 2009

ACKNOWLEDGMENTS

This work was funded by institutional grants from the French Research National Agency, project CharaBioC (ANR-19-CE08-0003-01) and from LabEX SigmaLim (ANR-10-LABX-0074-01). The authors are grateful to Claire Carrion (BISCEm) for macroconfocal imaging and to Marc Fabert (PLATINOM) for biphoton microscopy.

Endothelial cells behavior on copper- and silicon-substituted hydroxyapatite bioceramics

Arthur Brunel, Esther Pagès, Eric Champion, Amandine Magnaudeix

Univ. Limoges, CNRS, Institut de Recherche sur Les Céramiques, UMR 7315, F-87000, Limoges, France
arthur.brunel@unilim.fr

INTRODUCTION

Hydroxyapatite (HA) scaffolds for bone graft substitute possess high biocompatibility but lack stimulatory properties to sustain new tissue formation within large volumes. The main hindrance for the large HA scaffolds to fully integrate within the surrounding tissue lies in their inability to promote vascularization and blood vessel invasion within the porous network. Copper in its Cu(II) form is known to significantly stimulate endothelial cell (EC) proliferation with concentration as low as 10^{-5}M.[1] However, it can also induce cytotoxicity likely due to the generation of reactive oxygen species. Silicon was also demonstrated as an EC activity promoting factor[2]. The objective of this study is to evaluate the influence of these two elements as doping in copper or silicon-substituted HA ceramics[3,4] on EC proliferation and expression of proteins related to angiogenesis ability.

EXPERIMENTAL METHODS

Dense copper-substituted hydroxyapatite[3] ceramic pellets of formula $Ca_{10}(PO_4)_6Cu^{II}_zCu^{I}_yO_2H_{2-2z-y}$ ($y \gg z$), Cu_xHA where x=y+z, containing 0.8 and 3.8 wt% of copper for $Cu_{0.1}HA$ and $Cu_{0.5}HA$ respectively and dense silicon-substituted hydroxyapatite[4] ceramic pellets containing 1.07wt% of silicon with formula $Ca_{10}(PO_4)_{5.6}(SiO_4)_{0.4}(OH)_{1.6}$, $Si_{0.4}HA$, were seeded with C166 murine EC and cultured for up to 7 days. Pure HA ceramics $Ca_{10}(PO_4)_6(OH)_2$ were used as a reference. EC viability was evaluated using MTT metabolic assay and *in situ* calcein staining. Cell mortality was assayed by *in situ* propidium iodide fluorescent dye staining. Proliferation was measured by direct counting and by incorporation and *in situ* detection of EdU. MMP-9, VEGFR-2 and PECAM-1 proteins whose shift in expression relate to EC function and activation of angiogenesis processes were monitored by Western Blot. Membrane receptors VEGFR-2 and PECAM-1, essential to angiogenesis, were observed by immunofluorescent staining. Wound healing assay was performed to evaluate migration and activation of EC. The release in the culture media of the main soluble angiogenic factor VEGF was measured by ELISA. Finally, the release of ionic species from the ceramics in the culture medium was measured by ICP-optical emission spectroscopy.

RESULTS AND DISCUSSION

Metabolic activity results indicate a very good biocompatibility for the Cu0.1HA and SiHA materials with values comparable to the HA standard. Increased copper concentration in the Cu0.5HA material induces a loss of metabolic activity over time. Calcein and propidium iodide staining indicate >99% viability in all conditions up to four days. Then an increase in cell mortality is observed at 7 days in Cu0.1HA and Cu0.5HA with a greater effect on Cu0.5HA. At similar cell densities, cell proliferation is increased in the Cu0.1HA material when Cu0.5HA and SiHA proliferation rate are comparable to that of HA. MMP-9 and PECAM-1 markedly shift in expression with increased copper concentration in the materials. PECAM-1 localization is modified on Cu0.5HA material with the apparition of larger foci at cell junctions. Large and organized multicellular structures with increased presence of VEGFR-2 are formed on Cu0.1HA and Cu0.5HA compared to a more homogeneous cell layer on HA and SiHA. Ability of cell to close a wound appears unaffected by copper or silicon presence. Finally, VEGF secretion is significantly increased with the Cu0.1HA material. Copper is found in culture media of Cu0.5HA material at a large concentration of 360µM after 4 days of culture while its release from Cu0.1HA remains always below the detection limit of our setup at any time. Consequently, the presence of copper in the apatite structure stimulates the expression of angiogenesis markers of EC cells in contact with the ceramic surface as long as a cytotoxic threshold is not reached by increasing the copper amount in the surrounding medium.

CONCLUSION

Cu0.1HA and SiHA materials show comparable biocompatibility to the gold standard HA with the C166 EC. Si0.4HA does not induce more EC activation than pure HA. Though Cu0.5HA appears angiogenic, the high copper concentration also leads to adverse effect on C166 viability. Finally, only Cu0.1HA ceramics exhibit healthy pro-angiogenic properties compared to HA and appear promising for the development of scaffolds with enhanced biological properties.

REFERENCES

1. Hu, G. J. Cell. Biochem. 69, 326–335, 1998
2. Dashnyam, K. *et al*. J. Tissue Eng. 8, 20417314177 0733, 2017
3. Bazin, T. *et al*. Ceram. Int. 47, 13644–13654, 2021
4. Palard, M., *et al*., Acta Biomater. 5, 1223–1232, 2009

ACKNOWLEDGMENTS

This work was supported by institutional grants from the French Research National Agency, project CharaBioC (ANR-19-CE08-0003-01) and LabEX SigmaLim (ANR-10-LABX-0074-01). The authors are grateful to Émeline Renaudie for assistance in ceramic synthesis and Sandra Blanchet for ICP/OES measurements.

Biofabrication of vascularized constructs by iPSCs-derived endothelial cells bioprinting

Clarissa Tomasina[1*], Sandra Camarero-Espinosa[1, 2], Lorenzo Moroni[1]

[1]MERLN Institute for Technology-Inspired Regenerative Medicine, Maastricht University, Maastricht, the Netherlands

[2]POLYMAT University of the Basque Country UPV/EHU Avenida Tolosa 72, Donostia 20018, Gipuzkoa, Spain

[*]c.tomasina@maastrichtuniversity.nl

INTRODUCTION

Endothelial cells (ECs) are essential for tissue survival and regeneration because they play a critical role in the vascular development, angiogenesis and vascular permeability. IPSCs can be a valuable source to obtain ECs considering their autologous source, pluripotency and self-renewal. However, providing a proper vascularization network to a 3D complex tissue still remains a major challenge in the tissue engineering field. 3D bioprinting is a fabrication technique that allows the construction of scalable, reproducible and precise structures. It also offers the potential to achieve complex vascular networks that can be integrated with tissues. In this work, efficient differentiation of IPSCs into ECs was performed through a 8 days protocol. Isolated cells were then encapsulated into a gelatin methacrylated (GelMA) bioink and bioprinted to form a vascular tubular structures.

EXPERIMENTAL METHODS

The human IPSCs cell line (LUMC0031iCTRL08) was maintained on geltrex-coated plates in mTesr Plus and was passaged in colonies using Gentle Cell Dissociation. Differentiation of IPSCs into ECs was performed by modifying the published protocol[1]. Briefly, IPSCs were dissociated into single cells and plated at a density of 7000 cells/cm^{-2} in medium supplemented with Rock inhibitor. At day 2, medium was changed to mTesr Plus. To improve the protocol, a medium change was added at day 2 where cells were incubated for 2 days into mediums with 1% DMSO. Then, cells were supplemented for three days with APEL medium (Stem Cell Technology) with BMP-4, Activin-A, CHIR99021 and VEGF to induce them into the mesodermal stage. After 3 days, cells were splitted and replated in APEL medium with VEGF. After 3 days, cells were characterized using Flow Cytometry and were isolated using Dynabeads CD31. Isolated cells were cultured on gelatin-coated flasks in Endothelial SFM medium with human serum, FGF and VEGF. At passage 2, cells were characterized using immunofluorescence and matrigel tubular assay. GelMA was synthetized targeting 95% degree of substitution using a published protocol[2]. The resulting material was characterized by means of Fourier transform infrared spectroscopy (FTIR), Nuclear Magnetic Resonance (NMR) and fluoraldehyde assay (OPA). GelMA was then dissolved with 0,25% lithium phenyl-2,4,6-trimethylbenzoylphosphinate and printed at concentrations ranging from 10% to 5% using a GeSiM Bioscaffolder bioprinter. Finally, ECs were bioprinted into the GelMA and their viability as well as endothelial markers were evaluated at 7 and 14 days.

RESULTS AND DISCUSSION

IPSCs-derived ECs were evaluated at day 8 showing that cells differentiated without DMSO were around 55,3% CD31$^+$ while cells supplemented with DMSO were around 50,6% CD31$^+$. In both differentiations, all the CD31+ cells were also positive for VECAD. However, the remaining CD31$^-$ population was positive for PDGF. PDGF$^+$ cells resulted to be 38,3% and 41,7% in differentiations with and without synchronization, respectively. It is hypothesized that CD31$^-$ cells have a pericyte-like phenotype and would not be isolated with CD31 beads. After isolation, cells resulted to be 98,5% CD31$^+$/VECAD$^+$, which proved the correct isolation. The same markers were visualized through immunofluorescence showing cells positive for both CD31 and VECAD. The phenotype of ECs was investigated using EphrinB2 and Coup-TFII for arterial and venous phenotype, respectively. Interestingly, all cells resulted to be positive for EphrinB2 while only few for Coup-TFII. These results suggest that the cells possessed mainly an arterial phenotype. Finally, the angiogenic potential was confirmed by Matrigel tubular assay where the cells formed tubular structures already 24 hours after seeding on it. In both immunofluorescence and Matrigel tubular assay, no difference was observed for cells isolated in the differentiation with or without DMSO. For bioprinting, it was confirmed by means of FTIR, NMR and OPA that the GelMa was correctly synthetized with a 95% degree of substitution. Using a water bath, it was possible to bioprint structures with 10% as well 5% GelMA. However, 5% GelMA irradiated with UV for 10 s was chosen to provide a more ideal environment for the ECs. After 24 hours, ECs resulted to have high viability and were cultured until day 14 when the presence of tubular structure throughout the hydrogel was confirmed by CD31 and VECAD markers.

CONCLUSION

IPSCs-derived ECs were successfully differentiated from IPSCs and isolated into a pure population. After isolation, cells showed not only the characteristics markers of ECs but also angiogenic activity to form tubular structures. Through bioprinting, it was possible to fabricate GelMA constructs showing the formation of tubular structures.

REFERENCES

1. Orlova, V., *et al.*, *Nature Protocols* (2014) **9** (6), 1514
2. Loessner, D., *et al.*, *Nature Protocols* (2016) **11** (4), 727

ACKNOWLEDGMENTS

This project has received funding from the European Union's Horizon 2020 research and innovation program under grant agreement No. 814410.

Follow-up of the *in vivo* functionality of implanted pre-vascularized hydrogels.

Eirini Chatzopoulou*[1], Thomas Guilbert[2], Guillaume Rucher[3], Jimmy Rose[4], Kilian Henry[1], Gilles Renault[5], Stephane Germain[6], François Rouzet[7], Catherine Chaussain[8], Laurent Muller[6], Caroline Gorin[9]

[1]Université de Paris, UR2496 Pathologies, Imagerie et Biothérapies Orofaciales et Plateforme Imagerie du Vivant, Montrouge, France
[2]Institut Cochin, Université de Paris, Paris, France
[3]Université Paris Cité, LVTS, INSERM U1148, F-75018, Paris, France; Université Paris Cité, UMS 34 - FRIM, F-75018, Paris, France
[4]Nuclear Medicine Department, X. Bichât Hospital, APHP; Université Paris Cité, LVTS, INSERM U1148, F-75018, Paris, France; Université Paris Cité, UMS 34 - FRIM, F-75018, Paris, France
[5]Institut Cochin, INSERM U1016/CNRS UMR 8104, Université de Paris, Paris, France.
[6]Center for Interdisciplinary Research in Biology (CIRB), College de France, CNRS UMR7241, INSERM U1050, Paris, France.
[7]Nuclear Medicine Department, Hôpital Bichat-Claude Bernard, AP-HP, Paris, France ; Université de Paris and Inserm U1148, Paris, France.
[8] Université de Paris, UR2496 Pathologies, Imagerie et Biothérapies Orofaciales et Plateforme Imagerie du Vivant, Montrouge, France ; AP-HP, Services Odontologie, GH Paris Nord, Université Paris Cité, Paris, France.
[9]Université de Paris, UR2496 Pathologies, Imagerie et Biothérapies Orofaciales et Plateforme Imagerie du Vivant, Montrouge, France ; AP-HP, Services Odontologie, GH Paris Est, Université Paris Cité, Paris, France.
***eirini_chatzopoulou@hotmail.com**

INTRODUCTION

New strategies focusing on pre-vascularized constructs are developed to overcome the hindrance of rapid blood perfusion of grafted constructs in stem-cell-based tissue engineering[1,2]. The present study investigates the capacity of dental pulp stem cells derived from deciduous teeth (SHED) co-cultured with human endothelial cells (EC) to promote the early formation of functional vessels within the implanted construct by anastomosis between the engineered human vessels and the host's ones.

EXPERIMENTAL METHODS

Cell-seeded collagen hydrogels were held in 3D printed poly-lactic acid (PLA) disks and cultured for 96 h *in vitro* prior to subcutaneous implantation in nude mice according to the following groups: 1) endothelial cells (EC) and SHED (EC-SHED) co-culture, 2) EC treated with SHED conditioned medium (EC-SHED-CM), 3) SHED alone, and 4) acellular (n= 6 mice per group). Prior to implantation, the *in vitro* microvascular networks were stained using a CD31 antibody and analyzed for capillary network area, vessel diameter, and junction density. All images were segmented using Ilastic software and analyzed with in-house software developed on Matlab (Mathworks). After implantation, the spatiotemporal aspects of angiogenesis within the PLA disks were explored using multi-scale and multimodal imaging. At 10 days post-implantation, early angiogenesis was investigated by positron emission tomography (PET-MR) using a ^{64}Cu-NODAGA-RGD radioactive tracer[3]. At day-20, vascularization was evaluated by 3D power Doppler ultrasound imaging[4]. Then, mouse (IB4) and human (UEA1) fluorescent lectins were injected (two mice per group) to further analyze the perfused vascular network on whole-mount samples. Finally, angiogenesis was investigated at 4 weeks by Micro-CT imaging following retro-orbital injection of a contrast agent (Exitron®), and further characterized by immunohistochemistry.

RESULTS AND DISCUSSION

At day 10, after 24 hours of intraperitoneal ^{64}Cu-RGD injection, the maximal Standardized Uptake Values (SUVmax) were significantly increased in EC-SHED group compared to MC-HUVEC and SHED groups, showing higher neoangiogenic activity in this group. At day 20, 3D Power Doppler ultrasound showed little signal, most probably due to lack of sensitivity and specificity of the imaging system. After *ex vivo* exploration by laser biphoton microscopy on clarified samples, these capillaries were shown to be UEA1 lectin positive, thus demonstrating their human origin. Furthermore, multiple anastomoses were found between the hosts and the human vessels. At 4 weeks, Micro-CT imaging showed increased vascular area within the disks in the pre-vascularized groups compared to the others. In summary, the vascular density and perfusion seem to be enhanced and functional in pre-vascularized constructs. Further characterization is presently in progress.

CONCLUSION

This study allows a longitudinal follow-up of angiogenesis using complementary imaging techniques and validates the functionality of pre-vascularized constructs *in vivo*. Our data thus support the interest of pre-vascularization before implantation to enhance implant perfusion, a crucial step when aiming at a positive outcome of any tissue engineering strategy.

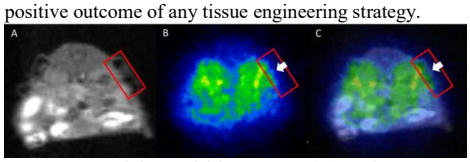

Figure 1: Axial acquisition: MRI (A) and TEP-scan acquisition (B) of EC-SHED implanted athymic nude mouse, and their merge (C) to measure the ^{64}Cu-RGD distribution, 24h after injection. The signal (SUVmax) is enhanced inside the hydrogel (white arrow).

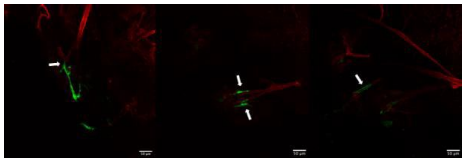

Figure 2: Chimeric anastomosed vessels (white arrows) at 3 weeks post-implantation of EC-SHED implants. Immunostaining with human UEA lectin (green) and mouse IB4 lectin (red).

REFERENCES

1. Smirani et al. Tissue Eng Part B Rev. 26:383-398,2020
2. Atlas et al. Biomaterials. 268:120594, 2021
3. Collignon et al. Acta Biomater.82:111-121,2018
4. Gorin et al. Stem Cells Transl Med. 5:392-404,2016

A New Vascularized Skin Substitute Designed For Angiogenesis Exploration

Adèle Mauroux[1,2*], Sandrine Gofflo[2], Yoann Atlas[1], Sylvie Bordes[2], Brigitte Closs[2], Florence Ruggiero[3], Laurent Muller[1]

[1] Center for Interdisciplinary Research in Biology (CIRB), College de France, CNRS, INSERM, PSL Research University, Paris, France
[2] SILAB, R&D Department, Brive, France
[3] Institut de Génomique Fonctionnelle de Lyon (IGFL), ENS de Lyon, CNRS, Univ Lyon 1, Lyon, France
[*]scientificom@silab.fr

INTRODUCTION

The development of skin substitutes that reproduce best native skin is a challenge for regenerative medicine both in fundamental and industrial research. Skin substitute vascularization is an especially important focus because it plays such an essential role in skin physiology and notably during wound healing. Besides vasculature architecture and function are known to be altered in aged and diseased skin, which makes this component interesting to be included in in vitro reconstructed skin models. Although there are many models available for the investigation of angiogenesis, none of them recapitulate faithfully extracellular matrix (ECM) complexity or wound healing associated microenvironment. These in vitro skin models, co-seeding endothelial cells with fibroblasts and keratinocytes, are indeed using scaffolds or bioprinting with exogenous ECM proteins, which remain the major components once the scaffold material has been remodeled in culture. This issue limits the assessment of the dynamics occurring within dermis microenvironment. There is thus a need to develop innovative 3D models with adjustable vasculature. The aim of this work was to develop a vascularized skin substitute and to demonstrate its functionality in response to angiogenic molecules.

EXPERIMENTAL METHODS

We used a scaffold-free approach to better reproduce the skin microenvironment. We stacked-up skin primary fibroblast cell sheets co-seeded with endothelial cells or keratinocytes to generate the vascularized full-thickness skin substitute. Immunofluorescence and transmission electron microscopy were used to characterize the model on a structural and molecular level.

RESULTS AND DISCUSSION

We confirmed the presence of a fully differentiated epidermis displaying early and late differentiation proteins, several junctional structures and a well-structured dermal-epidermal junction as depicted by the visualization of hemidesmosomes and the deposition of collagen IV, collagen VII and laminin-332. Endothelial cells organized into a dense vascular network throughout a well-structured dermis with an extracellular matrix recapitulating major fibrillar collagen and elastic components. Capillaries displayed a lumen and were stabilized by a well-organized basement membrane and perivascular cells. Modulating concentration and time of application of Vascular Endothelial Growth Factor (VEGF) differentially regulated angiogenesis in our model, resulting in distinct vascular network length and branching. Importantly, it was the progressive decrease in VEGF concentration throughout the culture that impacted vascular network density, while maintaining a constant VEGF concentration, whether high or intermediate, did not affect vascular network homogeneity. Interestingly, these variations also impacted epidermis differentiation and proliferation, and that from the moment VEGF concentration was modulated. Epidermis displayed reduced proliferation as judged by overall total thickness and Ki67 staining. Cytokeratin 10 and loricrin expression were reduced in a dose dependent response. However, the dermal-epidermal junction remained unaffected by changes in VEGF concentrations.

CONCLUSION

We have thus developed a novel vascularized skin substitute responding to angiogenic stimuli. We have shown that subtle variations in VEGF concentration affect the formation of the vascular network, suggesting a high plasticity and a good sensitivity of the model to angiogenic molecules. This vascularized skin model is of interest to mimic physiological and compromised skin conditions involving the vascular component (aging, rosacea, wound healing, diabetic skin, etc).

Poly(L-lactic acid) and Ceramic Composite Structures for Fully Resorbable Cranial Implants

Ana Grzeszczak[1*], Jonas Åberg[2], Cecilia Persson[1]

[1]Department of Materials Science and Engineering, Uppsala University, Uppsala, Sweden;
[2]OssDsign, Uppsala, Sweden; *ana.grzeszczak@angstrom.uu.se

INTRODUCTION

Several neurosurgical procedures are followed by a cranioplasty, which currently carries a high complication rate (7-20%[1,2]). This rate was found to decrease (2%[3]) when using cranial implants composed of a titanium mesh and calcium phosphate ceramic tiles, the latter allowing for partial replacement of the implant by the patient's own bone[3]. However, the titanium interferes with follow-up imaging techniques and is non-resorbable. A fully resorbable implant would allow for a complete regeneration of the bone defect and thus provide several patient benefits, such as a reduced need for revision surgeries, reduced potential sites for infections, and potentially greater use in young patients. In this study, poly(L-lactic acid) (PLLA) was evaluated as a candidate resorbable material to replace the titanium in such composite implants. This material is biocompatible, 3D-printable, offers suitable mechanical properties, and degrades at a rate ranging up to several years. It will be used as a starting point towards the development of a material adapted to the specific need, with a suitable and non-harmful degradation[4]. With this study, we aimed to evaluate ceramic and polymer composite structures, and their interaction, to assess the suitability of using PLLA for cranial implants.

EXPERIMENTAL METHODS

The PLLA structure was manufactured by fused deposition modeling (FDM) on a Prusa i3 MK3S+ (Prusa Research a.s., Prague, Czech Republic). The ceramic part was manufactured in silicone molds, using β-tricalcium phosphate (Sigma-Aldrich, Missouri, USA), monocalcium phosphate monohydrate (Scharlau, Scharlab S.L., Sentmenat, Spain), and 0.5M citric acid solution. The samples were designed as beams with square cross-sections (3x3x45mm), embedded and centered in a ceramic beam (6x6x35mm). Mechanical characterization was performed by 4-point bending tests (n=6 per group), similarly to ISO 5833 guidelines on a Shimadzu AGS-X universal testing machine (Shimadzu, Kyoto, Japan). Scanning electron micrographs of cross-sections were taken at an accelerating voltage of 3kV with a Zeiss 1550 SEM (Carl Zeiss AG, Oberkochen, Germany), equipped with an InLens detector.

RESULTS AND DISCUSSION

SEM images showed that the crevices of the polymer structure are well filled by the ceramic, and the two materials bond together (Figure 1 left). After tearing, retention of ceramic was observed on the PLLA wall (Figure 1 right). After 4-point bending tests, the average bending modulus obtained was 2274±316MPa. The ceramic in the composite structure exhibited a first crack at 139±23N, but retained structural integrity and carried load until a final failure at 249±42N, while the controls composed of only ceramic failed catastrophically already at 115±10N.

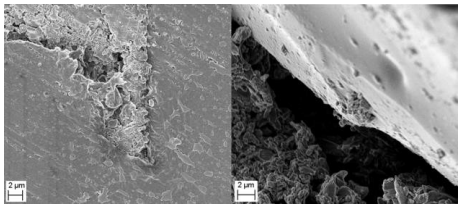

Figure 1: SEM micrograph of ceramic filling a hollow area of the polymer structure (Left), and of ceramic particles retained on the PLLA wall after tearing (Right).

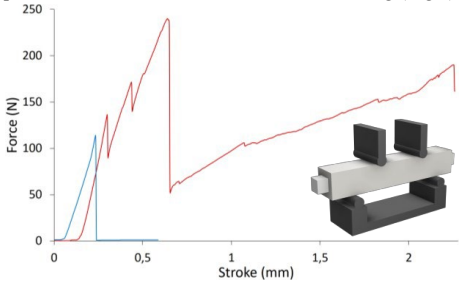

Figure 2: Typical 4-point bending test results for the PLLA-ceramic structures (red) and ceramic alone (blue).

CONCLUSION

SEM images and mechanical tests showed that the PLLA structure supports the molded ceramic, together with promising observations of attachment between the two materials. Further studies will be conducted on the degradation behavior of the material under physiological conditions.

REFERENCES

1. van de Vijfeijken *et al.*, World Neurosurg, 2018, vol. 117, pp.443-452.e8, doi: 10.1016/j.wneu.2018.05.193
2. Kwarcinski *et al.*, Applied Sciences, 2017, vol.7, no.3, Art. no.3, doi: 10.3390/app7030276
3. Kihlström Burenstam-Linder *et al.*, World Neurosurg, 2019, vol.122, pp.e399–e407, doi: 10.1016/j.wneu.2018.10.061
4. J. Zan *et al.*, J. Mater. Res. Technol., Mar. 2022, vol. 17, pp.2369–2387, doi: 10.1016/j.jmrt.2022.01.164

ACKNOWLEDGMENTS

This work was conducted within the Additive Manufacturing for the Life Sciences Competence Center (AM4Life). The authors gratefully acknowledge financial support from Sweden's Innovation Agency VINNOVA (Grant no: 2019-00029).

A Collagen-Glycosaminoglycan Scaffold Coating Enhances the Bio-Lubrication of a 3D-Printed Framework for Cartilage repair

Austyn Matheson[1,2,3*], Mark Lemoine[1,2,3], Eamon Sheehy[1,2,3], Tannin Schmidt[4], Fergal J. O'Brien[1,2,3]
[1]Tissue Engineering Research Group, Dept. of Anat.& R.M., Royal College of Surgeons in Ireland, Dublin, Ireland;
[2]Trinity Centre for Biomedical Engineering, Trinity College Dublin, Ireland
[3]Advanced Materials & Bioengineering Research Centre, RCSI and TCD, Dublin, Ireland
[4]Biomedical Engineering, School of Dental Medicine, UConn Health, USA
*austynmatheson@rcsi.com

INTRODUCTION

The frictional properties of cartilage biomaterials are invariably ignored in preference to enhancing features for added load support. Indeed, recently in our lab, novel 3D printed polycaprolactone (PCL) frameworks have been incorporated within our original collagen-based scaffolds for such load bearing support[2]. These porous multi-layered collagen-glycosaminoglycan (GAG) scaffolds for osteochondral repair enable cell infiltration and layer-specific tissue formation *in vivo*[1], yet 3D printed supports may cause mechanical abrasion to opposed cartilage. Equivalent to many cartilage repair biomaterials, these 3D printed frameworks may initiate progressive degeneration of opposed cartilage[3], although, such damage mechanisms are difficult to determine as limited testing exists on the frictional qualities (bio-lubrication) of cartilage-scaffold interfaces. Therefore, the goal of this study was to characterize the frictional behavior of different cartilage–scaffolds across a range of conditions.

EXPERIMENTAL METHODS

Cartilage surfaces from intact bovine osteochondral cores were articulated against hydrated scaffolds or cartilage (controls) in phosphate-buffered saline (PBS) or bovine synovial fluid (bSF) lubricants. Scaffold test groups included PCL alone & PCL set in a freeze-dried collagen-GAG scaffold (PCL-Coll). **Friction test**[4,5]: scaffolds & cartilage were compressed by ε_N=20% and held by decreasing pre-hold time (12min, 120, and 12s) followed by 2 rotations in each direction at an effective velocity (v_{eff}) of 0.3mm/s. **Wear test & histology**[3]: ε_N=30% and v_{eff} =1mm/s for 100 cycles (50/direction, ~2m sliding distance). Cartilage was stained with Safranin-O to assess changes in tissue morphology. Statistical analysis: 1-way ANOVA was used to assess the coefficient of friction (COF: torque/load x radius). Data (n=4) mean ± S.E.M.

RESULTS AND DISCUSSION An adapted cartilage-scaffold friction test as per **Fig. 1** was used for testing.

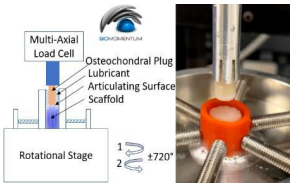

Figure 1: Friction test set-up.

The static friction decreased by pre-hold time and the PCL-Coll group was observed to have a lower COF vs. the PCL group but a higher COF than the cartilage controls (Fig. 2AB). After the wear test, PCL, grooves were visible on cartilage (Fig. 2C). Post wear testing, safranin-O staining revealed cartilage surface fibrillation on PCL-articulated cartilage (Fig. 2D).

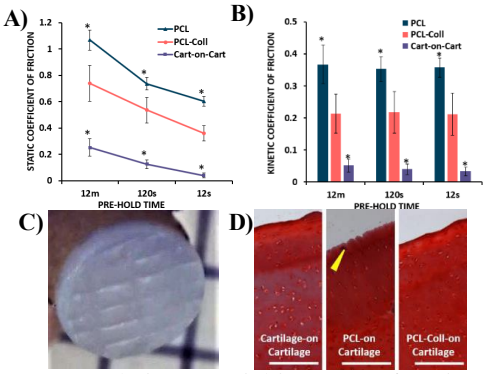

Figure 2: A) The static and B) kinetic COF of samples in PBS, C) Visible groves on cartilage after PCL wear-test, D) Damage post PCL wear-test (Safranin-O).

Increased resistance to articulation (torque) and lower load support was evident during cartilage-on-scaffold articulation and resulted in increased friction compared to cartilage-on-cartilage interfaces. The field to date has focused on improving the compressive properties of cartilage scaffolds, yet such improvements may result in 3D printed materials with reduced frictional qualities, and enhanced risk of cartilage wear. Indeed, beyond visible grooves after testing, microscopic images showed fibrillation to cartilage surfaces articulated against PCL, whereas collagen-coated scaffolds (PCL-Coll) did not.

CONCLUSION

Collagen-GAG coatings enhanced the bio-lubrication of PCL-frameworks and provided protection against cartilage wear. These data collectively point to the importance of frictional properties as design and validation parameters for cartilage biomaterials to understand and minimize potential adverse secondary effects (e.g., undue wear or damage to opposing tissues).

REFERENCES

1. Levingstone et al, Biomat, 87:69–81, 2016, 2. Lemoine et al, W. Cong. Biomech., Poster 4350, 2018, 3. Gleghorn et al, JOR, 28(10):1292–1299, 2010, 4. Schmidt et al, Arth. & Rheu., 56(3):882-891, 2007, 5. Matheson et al, JMBBM, 118:104445, 2021.

ACKNOWLEDGMENTS

Authors thank Dr. Brent Edwards for equipment use at the University of Calgary. ReCaP: European Council Advanced (788753), National Science Foundation & Science Foundation Ireland (NSF-SFI) (NSF_ 17_US_3437), ADMIRE Marie Sklodowska-Curie-Action-Cofund (EU Horizon 2020: 945168, SFI: 12/RC/2278_2)

Hyaluronic acid-crosslinked polyurethane composites modified with hydroxyapatite and graphene oxide for bone tissue engineering

Patrycja Domalik-Pyzik, Martyna Gaweł, Kinga Pielichowska

Department of Biomaterials and Composites, Faculty of Materials Science and Ceramics, AGH University of Science and Technology, Kraków, Poland
* pdomalik@agh.edu.pl

INTRODUCTION

Biomaterials-based therapy for critical-sized bone defects offers many advantages, yet there is still room for improvement. For successful regeneration, specific bone architecture and microenvironment should be mimicked in terms of porosity, mechanical and surface properties. Hence, many different biomaterials were and are tested for this application. Considering the variety of aspects that affect bone regeneration, it seems that the best approach is to use a composite material that can have properties adjusted to specific demands. Polyurethanes (PUs) as versatile biomaterials composed of repeating units of hard and soft segments are one of the choices here. Different chemical composition, ratio of the building blocks and ease of composite formation contribute to their versatility. The biological features of the PUs can be enhanced by using polysaccharides, eg. hyaluronic acid or chitosan, as cross-linkers. Furthermore, by introducing specific modifying phases with eg. bioactive properties they can actively support bone regeneration.

The aim of this study was to develop highly-porous hyaluronic acid-based polyurethane scaffolds for bone defects therapy.

EXPERIMENTAL METHODS

One step bulk polymerization method was chosen for materials synthesis. Following reagents were used: sodium hyaluronate as a cross-linker, poly(ethylene glycol) and poly(ε-caprolactone) with a molar ratio of 1:3 as soft segments, 1,4-butanediol as chain extender and 4,4'-diphenylmethane diisocyanate. To prepare composite systems, various contents of hydroxyapatite (HAp) and graphene oxide (GO) were introduced into the polymer matrix. Gradient composites were prepared as well.

Physicochemical and biological properties of the obtained materials were evaluated. Microstructure, structure, chemical stability, thermal properties, mechanical properties, and surface properties were tested using appropriate methods for full material characterization. Preliminary *in vitro* bioactivity and initial cytotoxicity assays were performed.

RESULTS AND DISCUSSION

The results showed that the obtained polyurethanes were highly porous with a mean pore size of 300 µm. They also possessed hydrogel-like features with a structure able to absorb water and absorption increase over incubation time. However, in comparison to typical hydrogel materials, the PU samples had higher mechanical properties and improved chemical and mechanical stability (as shown during the 12-weeks incubation test). A preliminary bioactivity test (*in vitro* assay) showed the most favorable properties of the samples modified with 10 wt.% of HAp. Moreover, both FTIR and thermal analysis confirmed that ceramic particles act as additional cross-linkers.

CONCLUSION

It was possible to produce highly-porous biodegradable polyurethane-based composite foams using selected polysaccharide, i.e. sodium hyaluronate as a cross-linking agent. The preliminary biological evaluation confirmed the potential suitability of composite systems modified with HAp for application in bone tissue engineering.

ACKNOWLEDGMENTS

The authors would like to thank the National Science Centre (UMO-2016/22/E/ST8/00048) and the National Centre for Research and Development, Poland (STRATEGMED3/303570/7/NCBR/2017).for providing financial support to this project".

Physicochemical characterization of biodegradable composite materials based on poly(ethylene succinate) and hemp fibers

Iouliana Chrysafi[1], Eleftheria Xanthopoulou[2], Alexandra Zamboulis[2], Konstantinos Chrysafis[1*]

[1]Department of Physics, Aristotle University of Thessaloniki, Thessaloniki, Greece
[2]Department of Chemistry, Aristotle University of Thessaloniki, Thessaloniki, Greece
[*] hrisafis@physics.auth.gr

INTRODUCTION

The continuous growth in plastics, leading to ever-increasing wastes harmful to the environment combined with the ongoing consumption of natural resources, reducing the natural environment's sustainability, has led the scientific community to develop substitute products to replace plastics and natural wood[1]. Poly(ethylene succinate) (PESu) is one of the most promising biodegradable polymers, due to its high melting point and the comparable mechanical properties with polypropylene and low density polyethylene[2]. Agricultural crop residues can be used to create alternative materials. Hemp constitutes a great wood substitute because of its lightweight, hydrophobic properties, outstanding long-term mechanical stability, as well as its low carbon footprint[3]. The aim of the present work is the physicochemical characterization of biodegradable composite materials, utilizing poly(ethylene succinate) (PESu) as a polymeric matrix and hemp fibers as reinforcing agents. PESu/hemp fiber composites were prepared by melt mixing. The structural properties of the prepared materials were studied using Fourier Transform Infrared spectroscopy (FTIR), and X-ray diffraction (XRD), while the dispersion and interfacial adhesion of the fibers was examined by scanning electron microscopy (SEM). Finally, the thermal stability and degradation of the composites were investigated using thermogravimetric analysis (TGA).

EXPERIMENTAL METHODS

The synthesis of PESu was carried out by a two-step melt polycondensation reaction. Composites containing 10, 20, 50 and 75% wt. of filler were prepared by melt mixing in a twin screw extruder. To improve the adhesion between the composite and the polymer matrix Joncryl ADR-4400 (JC) compatibilizer was used. For the FTIR measurements, a Cary 670 spectroscope from Agilent Technologies equipped with a diamond attenuated total reflectance (ATR) accessory was used. A small piece of each sample was placed in the ATR apparatus without any further preparation and the spectra were collected in the mid IR area (4000–400 cm^{-1}), with 32 scans and a resolution of 4 cm^{-1}. A two-cycle Rigaku Ultima +powder X-Ray diffractometer with CuKa radiation was used to study the structure and the degree of crystallinity of the samples. Diffraction spectra were obtained over a 2θ range of 5-50° with a step size 0.05° and step time 1.5 s, operating at 40,000 V and 0.03 A. Microphotographs of the dispersion and interfacial adhesion of the fibers were obtained by a Scanning Electron Microscope 710F from Jeol. TGA analysis was held by heating the samples from room temperature to 600 °C, under nitrogen atmosphere at the rate of 20 °C/min, by a Labsys instrument.

RESULTS AND DISCUSSION

The XRD diffractograms confirmed the successful synthesis of PESu, while a slight decrease in intensity of the sample peaks as the content of PESu increased was observed. Due to the FTIR results, the addition of JC did not alter the chemical structure of the composites, while only on the sample with 75% hemp fibers, a peak at 1620 cm^{-1}, which is attributed to the O-H vibration of cellulose can be seen. Unbound hemp fibers appear in the composites without the addition of a compatibilizer, which is attributed to their less effective adhesion to the biopolymer in contrast to the composites with JC, where more uniform microphotographs have been obtained. The thermal stability of the composites with 10 and 20% hemp fibers is approximately the same, while most differences can be seen on the samples with 50 and 75% hemp fibers. Moreover, the thermal degradation of the composites starts at lower temperatures as the content of the fibers increases.

CONCLUSION

Biodegradable composites containing PESu and hemp fibers have successfully been synthesized. Their physicochemical properties have been examined by XRD, FTIR, SEM and TGA. FTIR and XRD showed that JC does not affect the structure of the composites, while SEM proved the better adhesion between the polymer matrix and the fiber. The thermal study showed decrease on thermal stability and degradation as the content of hemp fibers increased, without though affecting their general use as biodegradable wood-plastic composites.

REFERENCES

1. C. Dolza et al., Polym. Artic. 2022, 14
2. K. Chrissafis et all, Thermochimica Acta, 435(2) (142-150), 2005.
3. E. Papadopoulou et all, COST Action FP1105" Holzforschung, vol. 70, no. 12, 2016.

ACKNOWLEDGMENTS

This research has been co-financed by the European Union and Greek national funds through the Operational Program Competitiveness, Entrepreneurship and Innovation, under the call RESEARCH-CREATE-INNOVATE (project code: T2EDK – 00008).

Characterization of new block PLA-b-PHSu copolymers for medical applications

Iouliana Chrysafi[1*], Dimitrios N.Bikiaris[2]

[1]Department of Physics, Aristotle University of Thessaloniki, Thessaloniki, Greece
[2]Department of Chemistry, Aristotle University of Thessaloniki, Thessaloniki, Greece
[*] iochrysa@physics.auth.gr

INTRODUCTION

Poly(lactic acid) (PLA) is one of the most popular polymers, due to its biocompatibility, degradability, non-toxicity, and easy processing, making it suitable for numerous applications in medical and industrial fields[1]. Despite its good properties, the quite negligible biodegradability creates important problems as far as medical applications are concerned[2]. Thus, in the present work new PLA block copolymers have been synthesized using poly(hexylene succinate) (PHSu) as a comonomer. The PLA-b-PHSu copolymers have been synthesized by ring-opening polymerization (ROP), in 95/5, 90/10, and 80/20 mass ratios[3]. In order to examine if the synthesis was successful and if the new copolymers are suitable for medical applications and especially for drug delivery, their physicochemical properties have been tested. Namely, X-ray diffraction (XRD), Nuclear magnetic resonance (NMR), and Fourier Transform Infrared spectroscopy (FTIR) techniques were employed to study the structural and chemical properties of the copolymers. Moreover, Differential Scanning Calorimetry (DSC) and enzymatic hydrolysis were used to study the thermal properties and the degradation rate of the materials.

EXPERIMENTAL METHODS

NMR spectra were recorded on a spectrometer (Agilent AM 600) operating at a frequency of 600 MHz for protons at room temperature. 32 and 512 scans were recorded for the ^{1}H and ^{13}C spectra respectively. Diffraction spectra were obtained by a two-cycle Rigaku Ultima +powder X-Ray diffractometer with CuKa radiation over a 2θ range of 5-60° with a step size 0.05° and step time 1.5 s, operating at 40,000 V and 0.03 A. FTIR measurements were performed with a Cary 670 spectroscope from Agilent Technologies equipped with a diamond attenuated total reflectance (ATR) accessory and the spectra were collected in the mid-IR area (4000–400 cm^{-1}), with 32 scans and a resolution of 4 cm^{-1}. The DSC (DSC Polyma 214) measurements have been obtained during the second heating from 0 °C to 200 °C, at a rate of 10 °C/min under nitrogen atmosphere. For the enzymatic hydrolysis films of each sample were incubated at 37 ± 1 ◦C for 40 days in suitable Petri dishes containing phosphate-buffered saline (PBS) (pH = 7.4) with Rhizopus delemar and Pseudomonas cepacia lipases at 0.09 and 0.01 mg/mL content, respectively. After specific time intervals, the films were removed from the Petri dishes, washed twice with distilled water and dried in vacuum at 30 ◦C. After 24 hours the samples were weighed and the procedure was repeated until a constant weight was achieved.

RESULTS AND DISCUSSION

PLA-PHSu block copolymers have been successfully synthesized by ring-opening polymerization of lactide in the presence of PHSu. Their block structure was proved by NMR spectroscopy and DSC thermograms. The addition of PHSu in PLA chains even though it leads to a reduction of the degree of crystallinity, clearly enhances the nucleation activity and leads to a reduction of PLA cold crystallization temperature. Neat PLA and PLA-b-PHSu95/05 w/w showed negligible weight loss during hydrolysis. PLA-b-PHSu90/10 w/w also exhibited a limited weight loss: approximately 1.2% after 30 days of incubation in the enzyme solution, while PLA-b-PHSu80/20 w/w showed the highest weight loss: 3.5 % loss of the initial mass after 40 days of enzymatic hydrolysis.

CONCLUSION

XRD and DSC thermograms, in comparison with FTIR and NMR spectra, proved that block copolymers have been prepared. The degree of crystallinity was examined by XRD and DSC, with the results coming in qualitative agreement with each other. Enzymatic hydrolysis studies showed that the hydrolysis rate increases substantially by increasing PHSu content in copolymers, proving that more biodegradable polymers than neat PLA have been prepared. In conclusion, the characterization of the samples gave positive results and thus they are considered capable of further investigation regarding their use in medical applications.

REFERENCES

1. D. Pholharn and Y. Srithep, IOP Conf. Ser. Mater. Sci. Eng., vol. 526, no. 1, 2019.
2. K. K. Bawa, J. K. Oh, Mol. Pharm., vol. 14, no. 8, pp. 2460–2474, 2017.
3. I. Chrysafi et al., Thermochim. Acta, vol. 698, no. November 2020, p. 178883, 2021.

Mechanical Properties of Thermal and UV Polymerized Graphene-Reinforced Acrylic Resin: Effect of Post-treatment on Samples Obtained by Stereolithography

Sara Lopez de Armentia[1*], Yolanda Ballesteros[1], Juan Carlos del Real[1], Nicholas Dunne[2], Eva Paz[1]

[1] Institute for Research in Technology/Mechanical Engineering Dept., Universidad Pontificia Comillas, Madrid, Spain
[2]School of Mechanical and Manufacturing Engineering, Dublin City University, Dublin, Ireland
[*] sara.lopez@comillas.edu

INTRODUCTION

Due to their geometry, graphene (G) presents an interesting toughening effect. Additionally, G has shown great potential in the preparation of materials for biomedical applications thanks to its antimicrobial and osteoconductive capacity.

Additive manufacturing, especially VAT polymerization technologies (Stereolithography, SLA; Digital Light Processing, DLP and Liquid Crystal Display, LCD) have many advantages in the manufacturing of bone scaffolds since they allow to obtain controllable and customized designs with very high accuracy.

However, one of the main shortcomings of these technologies is the distortion caused by shrinkage during polymerization and manufacturing process. Residual stresses generated can cause cracks and delamination and decrease mechanical properties[1]. The presence of nanoparticles could impact on the residual stresses, printing process or mechanical properties; therefore, it is an important aspect to study. Mechanical properties of printed samples depend on many factors[2]: adhesion between the layers, possible internal stresses due to shrinkage, polymerization degree, postcuring process, etc. In a previous work[3], it was found that all these factors hinder the reinforcing effect of G. Therefore, for a better understanding of the effect that G has over all these factors, samples were prepared by molding to be able to study the effect of G on curing and reinforcement mechanism, leaving aside the possible effect that the 3D printing process has on the final properties.

EXPERIMENTAL METHODS

Materials: Acrylic resin Clear V4 (Formlabs) and G of 1-2- layers of thickness (Avanzare) were used.

Preparation of samples: Dog bone samples were manufactured (ISO 527-2:2012). Samples were obtained using different polymerization processes:(i) compression molding was carried out at 160°C for 11 min, (ii) UV molding was done in FormCure chamber for 11 min and (iii) SLA samples were obtained with a Form2 printer.

Post-treatments: Postcuring was applied in a FormCure chamber where heat and UV were applied. Temperature was set at 80°C for 90 minutes.

Annealing was carried out at atmospheric pressure and 100°C for 12 hours.

Mechanical testing: Tensile properties were obtained with a Universal Testing Machine IBTH/500 (Ibertest).

FTIR Analysis: Polymerization degree (X) was calculated using a Tensor 27 spectrophotometer (Bruker). The polymerization was determined analyzing the peaks at 1733 and 810 cm^{-1}, corresponding to C=O and C=C, respectively, and using Eq 1. I_{liquid} is the intensity of the peak in the unpolymerized resin.

$$XX = \left(1 - \frac{I_{CC=C\ \ C}}{I_{liquid\ CC=CC}} \cdot \frac{I_{liquid\ CC=OO}}{I_{CC=OO}}\right) 100 \quad (1)$$

RESULTS AND DISCUSSION

Mechanical properties depended on the source of the polymerization process. The addition of G produced improvements when polymerization was carried out by heat, however a decrease of the tensile strength was observed with the addition of G when the resin was cured by UV light.

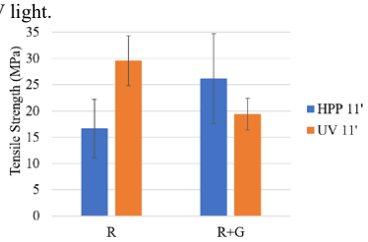

Figure 1. Tensile strength of samples obtained by compression molding (HPP 11') and UV molding (UV 11')

The presence of G and the source of polymerization affect the polymerization degree. In Table 1 it can be observed that G favors thermal polymerization and inhibits UV polymerization.

Table 1. Polymerization degree (%) obtained by FTIR

	R	***R+G***
HPP 11'	29.21	34.52
UV 11'	24.27	19.47

Different post-treatments were evaluated in order to allow the obtention of 3D printed parts with G, with acceptable mechanical properties. The results demonstrated that when postcuring and annealing are combined, the decrease in tensile strength due to the addition of G is corrected.

CONCLUSION

The addition of G and the polymerization process have a significant impact on mechanical properties of photocurable resins. The presence of G affects UV polymerization and reduces tensile strength. This reduction can be solved by post-treatments, releasing residual stresses. These post-treatments could be used to tailor the mechanical properties of printed structures, adapting it to the properties to the bone of interest in every particular case.

REFERENCES

1. Karalekas, D. *et al.*, J. Mater. Process. Technol. 136: 146-150, 2003
2. Al Rashid, A. *et al.,* J. Mater. Res. Technol. 14: 910-921, 2021
3. Lopez de Armentia, S *et al*., Int. J. Bioprinting. 8 (1): 503, 2022

Development of empirical hepatic biomechanical models through experimental characterization of porcine and bovine livers

Giuseppe Guagliano [1], Stefano Tagliabue [1], Paola Petrini [1], Francesco Briatico-Vangosa [1]

[1] Department of Chemistry, Materials, and Chemical Engineering "G. Natta", Politecnico di Milano, Milan, Italy

* giuseppe.guagliano@polimi.it

INTRODUCTION

Complex models of the liver are envisioned to support drug development with high-throughput experimental platforms. The chemo-mechanical niche, the set of biochemical and mechanical characteristics of a physiological or a pathological organ, greatly influences the fate and the behavior of cultured cells for the *in vitro* reproduction *in vivo*-like responses.

The studies of the mechanical properties of liver are few, and empirical hepatic biomechanical models, dataset obtained through direct analyses of the organ, are widely dispersed. The differences between experimental techniques, conditions, or organ sources[2] limits the possibility to compare them. Pioneering studies rely on indirect methods (i.e., magnetic resonance elastography) [3,4]. Moreover, the intra-and inter-species variability and anisotropy of these tissues are not addressed.

In this study we focus on the development of a methodology to experimentally evaluate the mechanical properties of the liver, in response to small shear deformations in oscillatory regime and to axial deformation applied in compression in quasi-static tests, to reproduce the physiological stresses on the organ by blood perfusion and surrounding organs.

EXPERIMENTAL METHODS

Porcine and bovine livers were kindly provided by a local butcher less than to 12 hours after the slaughter. Organs were sectioned along three spatial planes (Figure 1). From each slice, cylindrical specimens (∅ 25 mm) were cut. To prevent dehydration and coagulation, each specimen was injected from the top face, the bottom face, and from the side with 10 ml of isotonic (4% w/v) Na-citrate, in H_2O, then immersed in the same solution, and finally stored at 4 °C until the measurements.

Preliminary analyses were performed with a rheometer (MCR 502e, Anton-Paar, AT) mounting a 25 mm parallel plate geometry, and imposing different preload forces in the range 0.1 N – 5 N. The mechanical properties of the organs were then measured at small deformations in oscillatory regime in response to shear stresses and quasi-static compressions. Different livers were obtained and analyzed to evaluate the variability within the same species. Porcine and bovine livers were evaluated with the same test protocols, to compare interspecies variability. The effect of different preservation techniques was investigated on samples that were previously frozen at different temperatures up to -120°C.

RESULTS AND DISCUSSION

The study of relation between the gap among plates and the normal force indicates that preloads greater than 1 N progressively produced structural changes on specimens, as the response significantly varied with the higher preloads. The set preload was therefore considered for the following tests. Shear analyses highlighted that the liver tissues, both porcine and bovine, are characterized by a gel-like behavior, with a conservative modulus (G') higher than the dissipative ones (G'') at all the analyzed frequencies. Only sectioning the livers in the XZ plane (Fig. 1) resulted in reproducibility of G', G'', and loss factor (tan δ) data, with G' and G'' always ranging between 300-400 Pa and 70-100 Pa respectively, indicating the anisotropy of the tissues. Compressive modulus of organs did not display a significant variability between species and highlighted a similar anisotropy to the one observed with rheological analyses.

The evaluated G', G'', and tan δ fall within the range of data from magnetic resonance elastography (MRE) [4]. Up to now, the cryopreservation of samples seems appropriate. Thawed samples displayed mechanical properties that are aligned with the ones of fresh samples.

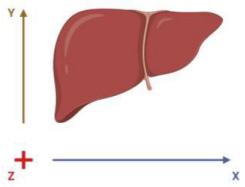

Figure 1. Resection planes for the obtainment of specimens.

CONCLUSION

The developed procedure can be implemented to build an empirical model of the hepatic biomechanics as a reference when engineering a three-dimensional matrix to produce *in vitro* models of the liver. The protocol is proposed to characterize the hepatic biomechanics, even if, in principle, the same methodology can be applied to other types of biological soft tissue. The gel-like behavior of the hepatic tissues suggests the feasibility of producing hydrogels-based 3D models of the liver.

REFERENCES

1. *Acta Biomater*. 45, 60–71 (2016).
2. *Magn. Reson. Imaging Clin*. 22, 433–446 (2014).
3. *J. Clin. Gastroenterol*. 55, 449–457 (2021).
4. *Phys. Med. Biol*. 52, 7281 (2007).

Mechanical and surface characterization of Drug Coated Balloons

Deepthishre Gunashekar[1], Dario Gastaldi[1], Giancarlo Pennati[1], Pasquale Vena[1]

[1] Department of Chemistry, Materials and Chemical engineering, Politecnico di Milano, Milan, Italy
* deepthishre.gunashekar@polimi.it

INTRODUCTION

Angioplasty balloons have been in use for decades to treat Arteriosclerosis. Factors like inflammation, increase in blood pressure, increase in blood cholesterol level and vascular wall injury during angioplasty leads to the increase in the thickness of the vessel wall, which is otherwise called intimal hyperplasia[1]. To reduce this re-stenosis from happening, procedures are performed using drug coated balloons (DCBs) with a highly lipophilic, antiproliferative drug that helps in preventing the smooth muscle cell proliferation and excipient which acts as the carrier for the drug. Paclitaxel and Sirolimus are the two drugs that are commercially used by the manufacturers due to its cytostability in therapeutic dosages. However, there still is a problem of high rates of drug wash off resulting in very low drug transfer, i.e., 10-18\% of the initial drug concentration loaded on the balloon[2]. Thus, it is important to study the characteristics of the balloon material and the drug to understand the drug transfer process. Not many studies have been done on characterizing the balloon properties and mechanical stability of the coating loaded with drugs. In this research the physico-mechanical properties and surface characteristics are studied on the different coated and non-coated balloon materials.

EXPERIMENTAL METHODS

An ideal balloon material should be biocompactible, strong and puncture resistant to overcome the frictional and elastic forces during the procedure. It is also important for the balloon surface to be able to hold the drug in place and release when necessary. Balloon material should be stronger in the radial direction than the axial direction to have a higher burst strength[3]. Both Uni-axial and Bi-axial tensile testing were performed along with bulge testing to analyze the compliance of the balloon and the influencing parameters. Both dry and wet conditions were considered to mimic the in-vivo conditions. Surface characterizations were done with the help of confocal laser microscopy and Scanning Electron Microscopy.

RESULTS AND DISCUSSION

The mechanical analysis suggested that the properties of the balloon vary at different regions of the balloon and with respect to inflation rate. Figure 1 shows the stress-strain curves of the angioplasty balloons at different regions and different strain rates. The morphology of the pebax balloon surfaces were recorded under the confocal microscopy, shown in Figure2. The thickness of the balloon was observed to be varying from 48.3µm to 52.6µm along the length of the balloon by observing the intensity at the interfaces and refractive index of the balloon material was also analyzed with the help of step measurement. These observations under various stress conditions helped to understand the damage tolerance of the balloon and fragmentation of the drug coating.

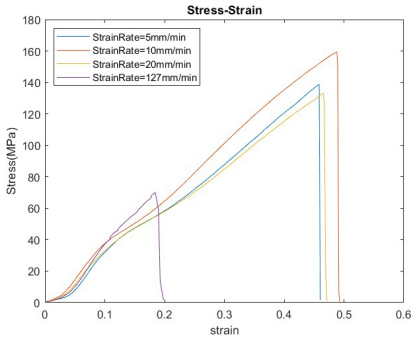

Figure 1: Circumferential stress-strain analysis from ring test.

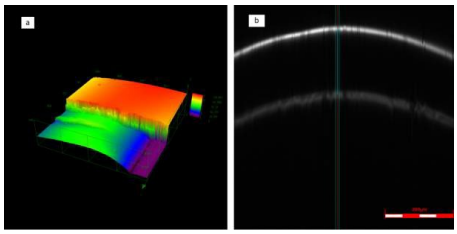

Figure 2: Surface characterization under confocal laser microscope. (a) Color coded height-map representation of balloon thickness using step measurement and (b) Film thickness measurement by analyzing the light intensity difference between the substrate and balloon surface

CONCLUSION

In this study, a preliminary analysis on the physical and mechanical properties of angioplasty balloons under various stress conditions are presented. Influence of fiber orientations and ratio of the polymers were also observed. The final aim of the study was to verify whether by adjusting the mechanical and physical parameters, we can achieve high mechanical stability of the drug on the balloon surface which will certainly increase the drug release to the targeted area.

REFERENCES

1. J. Charles Jennette, J. R. S. et al., 197-219, 2014.
2. Cremers B, B. G. et al., Euro Intervention. 2140-2147, 20174.
3. Warner JA, F. B. et al., J. Biomed Part B, 470– 475, 2016.

ACKNOWLEDGMENTS

This project has received funding from the European Union's Horizon 2020 research and innovation programme under the Marie Skłodowska-Curie grant agreement No 956470.

INVESTIGATING THE REINFORCEMENT OF PLLA WITH WS_2NT FOR CARDIOVASCULAR STENT APPLICATIONS

Cameron, J.*, Menary, G., Lennon, A.
School of Mechanical and Aerospace Engineering, Queen's University, Belfast, UK
(jcameron07@qub.ac.uk)

INTRODUCTION

Cardiovascular diseases are the primary cause of death globally, amongst which coronary heart disease has the greatest number of mortalities.[1] Bioresorbable vascular scaffolds were developed to overcome the limitations that metallic stents present due to their permanence inside the body. They act as a temporary scaffold, providing radial strength for 6-12 months to prevent the vessel recoiling and time for the artery to remodel. They are then fully resorbed within 3 years, leaving behind a healthy vessel.[2,3] Poly-(l-lactic acid) (PLLA) is the preferred material choice to date but, with a tensile modulus lower than metal, the polymeric stents need to be ~2x as thick to achieve similar structural stiffness, which hinders deployment and disrupts blood flow.[3,4] Herein, a thinner scaffold would be an exciting prospect.

One route to improving the mechanical properties of PLLA is by adding small amounts of nanofillers to create a polymer nanocomposite. From literature, tungsten disulfide inorganic nanotubes (WS_2NTs) appear a promising candidate due to their non-cytotoxicity, biocompatibility, and reinforcement ability. Whilst composite tubes with 0.5 or 3 wt% WS_2NTs have shown good dispersion and elevated nucleation and alignment of crystallinity in the extrusion direction, the nanotubes did not reorientate during expansion and, from preliminary results, there is no improvement in mechanical properties.[5] The reason behind this lack of reinforcement has not yet been investigated. This work aims to use atomic force microscopy (AFM) and Raman spectroscopy to investigate the interaction between the WS_2NTs and the PLLA matrix.

EXPERIMENTAL METHODS

Nano-composite tubes of PLLA (Purasorb PL38, Corbion) and WS_2NT were produced by melt processing using a twin-screw extruder at both 0.5 and 3 wt%. Raman spectroscopy was used with the laser wavelength of 532 nm in the range of 250–500 cm^1. The data was baselined, evaluated from a Lorentzian fit of the spectra and normalised using Spectragryph[6]. Scanning electron microscopy (SEM) allowed visualization of the surface and of the WS_2NTs in the PLLA (Fig.1a). For AFM, amplitude-frequency modulation (AM-FM) viscoelastic tapping mode was used to secure the local interphase modulus shift at the PLLA/WS_2NT interface.

RESULTS AND DISCUSSION

Preliminary AFM results identified a large jump in modulus between the matrix and the WS_2NT (Figure 1b,c). Surface roughness, which is key for accurate AFM results, has hampered current sample preparation and is currently being optimised, with the aim of creating defect-free surfaces that will scan without breaking tips.

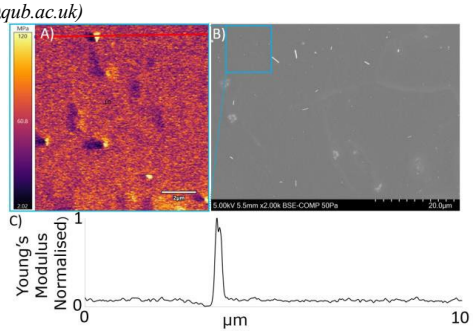

Figure 1 – (a)AFM YoungsRetrace showing WS_2NTs in 0.5 wt% tube (b) SEM Image showing dispersion of WS_2NTs in 0.5 wt% tube (c) Young's Modulus across drawn line seen in image A

For the Raman spectra, the two principal bands of WS_2 appear at 354 and 422 cm^{-1}, concordant with literature, and no peak shift can be observed for either the radial or biaxial stretching processes or the addition of the PLLA in the composite (Figure 2). This may indicate a lack of chemical interaction between the WS_2NTs and the PLLA matrix.[7]

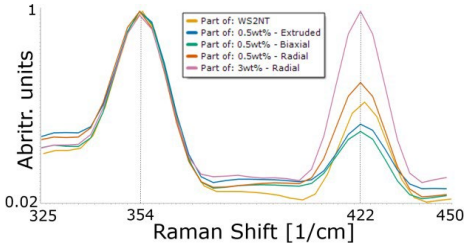

Figure 2- Raman spectra in 250-500 cm^{-1} region of WS_2NT and 0.5 and 3 wt% tubes after processing steps

Ongoing work will use AFM to capture the local interface modulus transition between PLLA and WS_2NTs and, by looking at the frequency graph and the transition region between the filler and matrix, interaction between the WS_2NTs and PLLA will be further investigated.[8] This, along with continued analysis of Raman data, is required to further test the hypothesis that poor interaction between filler and matrix could explain the lack of reinforcement.

REFERENCES

[1]https://www.who.int/news-room/fact-sheets/detail/cardiova scular-diseases-(cvds), 16/11/11 [2] Lin, S. et al., Nanotech. Reviews 9, 1217–1226, 2020. [3] Ang, H. Y. et al., Scientific Reports 8,2018. [4] Tammaro, L. et al. AIP Conference Proceedings vol. 1981, 2018 [5] Rocher, L. et al., Polymers 13, 1764, 2021. [6] F. Menges "Spectragryph - optical spectroscopy software", V1.x.x,201x,http://www.effemm2.de/spectragryph/ [7] Loffredo, F. et al. Functional Composite Materials (2021) 2:3 [8] Kumar,S. et al. Composites: Part A 148 (2021) 106475

Hyaluronan Size Beside Physico-Chemical Properties Affect Stability And Biological Features: Characterization Of A Wide Range Of Increasing Molecular Weight Families

Celeste Di Meo[1*], Antonietta Stellavato[1], Annalisa La Gatta[1#] and Chiara Schiraldi[1#]

[1]Department of Experimental Medicine, School of Medicine, University of Campania "Luigi Vanvitelli", Naples, Italy
* celeste.dimeo@unicampania.it
# co-last

INTRODUCTION

Hyaluronic acid (HA) is a naturally occurring biopolymer that shows very promising properties (biocompatibility, biodegradability, viscoelasticity), making it ideally suited for a lot of clinical uses, such as supplementation of joint fluids, tissue engineering, eye surgery, wound healing, and drug delivery[1]. In biomedical applications the biophysical properties of hyaluronic solutions are very important, for instance in relation to adhesive properties, flowing behavior injectability and resistance to mechanical stress. It has been shown that molecular weight (M_w) and concentration (*c*) of the biopolymer affect formulation's features such as dynamic viscosity and sensitivity to degradation that are key to clinical performance and/or ease of delivery. Moreover, M_w influences heavily the biological functions of HA solutions; for instance, low M_w HA relates to the induction of inflammation and angiogenesis, on the contrary, high M_w HA has anti-inflammatory and anti-angiogenic effects[2].

In the last three years more than six thousand studies regarding hyaluronic acid, and the importance of M_w and *c* of its formulations on biomedical applications and in *vivo* performances were published. Scientific data reported are limited to a few size or concentration values, not covering the extensive range representative, on one side of the multiple biomedical uses, on the other of the pathological *in vivo* conditions also related to HA degradation[3].

Here it is reported a systematic study involving 9 pharma grade HAs with molecular weight distributions ranging from 50kDa to 2500kDa, and 13 concentration values for each one. Thus, the aim of this work is to carry out a detailed hydrodynamic, rheological, and biological description of hyaluronic acid solutions in which both Mw and concentration dependences were investigated. This study would like to be a potential reference for the development and application of HA as a medical device active ingredient.

EXPERIMENTAL METHODS

A complete hydrodynamic characterization was provided for each HA employed, using a Size Exclusion Chromatography-Triple Detector Array system. Molecular weight, molecular size and intrinsic viscosity distributions were derived. Rheological measurements were determined using an Anton Paar MCR 301 rotational rheometer. Steady state shear tests were performed at 25°C and dynamic viscosity was measured as a function of the shear rate in the range of clinical interest (0.01-1000s^{-1}). Stability to enzymatic degradation was investigated by incubating HA with Bovine testicular hyaluronidase (BTH) at 10U/mL for 1h. Additionally, the effect of HA samples was evaluated on human fibroblast, evaluating cell viability up to 72h. Type I collagen expression was analyzed at mRNA and protein level using PCR and immunofluorescence staining. Hyaluronate synthase (HAS-2), elastin and Vascular Epithelial growth factor (VEGF) were also investigated as transcriptional level through qRT-PCR and in western blotting analyses.

RESULTS AND DISCUSSION

Molecular weight, polydispersity index, molecular size (hydrodynamic radius R_h and radius of gyration R_g) and intrinsic viscosity (IV) distributions were evaluated and the straight forward correlations between R_h and M_w or IV and M_w were confirmed for the linear unmodified (natural identical HAs, notwithstanding the chain length).

Full dynamic viscosity analyses of hyaluronan from 50kDa to 2500kDa was achieved and flow curves were derived, obtaining a range of zero shear viscosity (η0) from 1mPa·s to 15kPa·s. η0 was correlated to concentration highlighting a different behavior and trend depending on both M_w and *c*. Equation parameters and interpolated curves were calculated through a power law model in each regime of behavior; switching points between diverse regimes were clarified, finding a lower concentration threshold for higher molecular weight families. Particularly, the switching concentration *c** was about 10mg/mL for HA with M_w<100kDa and 1mg/mL for HA with M_w>2MDa.

BTH analyses showed higher enzymatic degradation for the longer chains and a lower enzymatic activity for the shorter chains. For instance, the M_w reduction of 2.5MDa HA was about 60%, while that of 50kDa HA was less than 10%.

HA samples added to fibroblast medium demonstrated to modulate matrix protein expression and VEGF and generally to improve cell proliferation/viability.

CONCLUSION

A full range of hyaluronan macromolecules were analyzed to compare their rheological and biophysical features and their stability to enzymatic attack. A full panel from 50 kDa to 2500 kDa was never reported before and because the purity grade was very high, it permitted a comparative analyses. All sustained growth of human fibroblast, but differences in biomarkers expression was found depending on HA size.

REFERENCES

1 Fusco S *et al*., Biorheology. 44:403–418, 2007
2 D'agostino A. *et al.*, Carbohyd Polym. 157:21-30, 2017
3 Yue F. *et al.*, Polymer. 55:295–305, 2014

Characterization of Elastin-like Recombinamer-Based Membranes produced at the Interface of Two Immiscible Liquids by Click Chemistry

Diana Juanes-Gusano[1*], Miguel González-Pérez[1], Mercedes Santos[1], Matilde Alonso[1] and José Carlos Rodriguez-Cabello[1]

[1] GIR BIOFORGE (Group for Advanced Materials and Nanobiotechnology), CIBER-BBN, University of Valladolid, 47011 Valladolid (Spain)
*djuanes@bioforge.uva.es

INTRODUCTION

González M. *et al.*[1] developed a novel strategy to obtain bioinspired membranes with tunable properties by covalent cross-linking of two elastin-like recombinamers (ELRs) at the interface of two immiscible liquids using click chemistry[2]. Just changing the concentration of the polypeptides, the thickness, pore size or diffusive properties of the membranes could be modified.
In this work, an exhaustive characterization of these membranes is presented in order to assess possible future applications. The recombinant and versatile nature of the employed ELRs, which present bioactive motifs, allow a possible application in the biomedical field.

EXPERIMENTAL METHODS

Two complementary ELRs were derivatized with either an azide (ELR-azide) or cyclooctyne (ELR-cyclooctyne) groups and subsequently crosslinked by click chemistry at a liquid-liquid interface (water-butanol) and at different concentrations. The hydrophobicity of membranes was evaluated by measurement of contact angle. Different techniques were used to assess the topography of the surfaces such as AFM, confocal microscopy or ESEM. The membranes were characterized by SEM for morphological and by ATR-FTIR for composition. As well, mechanical properties were appraised by uniaxial tension tests for tensile strength and by AFM to obtain the Young`s Modulus. The swelling study was carried out by gravimetric measurements of the water weight gain after an immersion time. Finally, membrane degradation studies with elastase enzyme will be performed to assess degradation behavior.

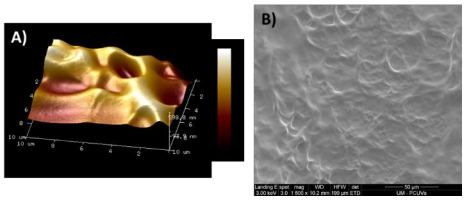

Figure 1: A) AFM images and B) SEM images of 25mg/mL ELR membrane (AFM scan area was 10μm²)

RESULTS AND DISCUSSION

The membranes were morphologically porous and with robust mechanical properties for handling. It was found that the mechanical properties at the nanoscale (AFM) have higher values than the mechanical properties at the macroscale (tensile strength) for different concentrations (5, 10, 25 and 50 mg/mL). Crucially, the membrane allowed the diffusion of a wide size-range of FTIC-dextran MW (4 – 150 kDa) molecules across, suggesting the potential to allow the exchange of nutrients and bioactive molecules by cells on either side. Through FTIR, it is verified that the bond between azide and cyclooctine is formed correctly because the signal of azide group disappears after membrane formation. The water content in hydrogels is an important factor that determines the permeation of nutrients into the hydrogel. In this sense, our ELR membranes present a swelling of practically 100%. The study of topography, allow us to conclude that the roughness changes with the concentration and also with the working scale. In such a way that, at the nanoscale it is observed a decreasing of roughness with increasing concentration and, at the macroscale, the opposite effect occurs, an increasing concentration increases roughness. The hydrophobicity of lyophilized membranes was measured by using contact angle being hydrophobic at all concentrations. Finally, the enzymatic degradation will be evaluated to check the estimated times of membrane degradation in order to transfer it to subsequent *in vivo* assays, which allows us to establish approximate times of regeneration of the new tissue.

CONCLUSION

This work demonstrates the successful production of biocompatible ELR-membranes with tunable physicochemical properties such as shape, thickness, porosity, diffusion coefficient and biofunctional moieties. The ease of production and derivatization, as well as, all studied properties make this novel ELR-based membrane an ideal candidate for tissue engineering applications.

REFERENCES

1. González M. *et al*., Biomacromolecules 21, 4149-4158, 2020.
2. González de Torre I. *et al*, ACS Appl. Mater. Interfaces 6 (16),14509–14515, 2014.

ACKNOWLEDGMENTS

This work was funded by the MINECO MAT2016-78903-R to DJG, PID2019-110709RB-I00, RTI2018-096320-B-C22, Junta de Castilla y León (VA317P18) and Centro en Red de Medicina Regenerativa y Terapia Celular de Castilla y León.

Effect of Sterilization on Rheological and Physicochemical Properties of ε-Polylysine/Hyaluronic Acid Hydrogels

Artemijs Sceglovs[1,2], Kristine Salma-Ancane[1,2]

[1]Rudolfs Cimdins Riga Biomaterials Innovations and Development Centre of RTU
[2]Baltic Biomaterials Centre of Excellence, Headquarters at Riga Technical University, Riga, Latvia
artemijs.sceglovs@rtu.lv

INTRODUCTION

Despite the beneficial properties of the developed biopolymer-based hydrogels for tissue regeneration, the use of an appropriate sterilization method is crucial for their use in biomedicine. Sterilization process of hydrogels is especially challenging for the biomedical applications due to the well-known sensitivity of this type of biomaterials. The biopolymer-based hydrogels present important characteristics such as biocompatibility, biodegradability, antibacterial activity, viscoelasticity required for tissue engineering, wound healing and drug delivery applications. Inappropriate sterilization method can significantly affect these properties and bring the negative effect on biological performance of developed hydrogels. This negative effect outcomes as physical degradation under temperature and pressure conditions, formation of unstable interconnections between co-polymer molecules and decrease of stiffness and stability. The effects of sterilization methods on the intrinsic properties of hydrogels remain understudied. In this study the effect of steam sterilization method on the previously developed chemically cross-linked hydrogels based on biopolymers: ε-polylysine and hyaluronic acid was evaluated [1].

EXPERIMENTAL METHODS

Chemically cross-linked hydrogels based on ε-polylysine (ε-PL) and hyaluronic acid (HA) were synthesized via EDC/NHS mediated polymerization reaction [1]. 3 series of ε-PL/HA hydrogels with ε-PL to HA mass ratios of 60:40, 70:30 and 80:20 wt% were prepared for further investigation. Steam sterilization method was applied according to standard [2] using 20 min cycle at 121˚C/250˚F. To evaluate the effect of steam sterilization on the properties of the developed hydrogels, molecular structure, phase composition, morphology, gel fraction (GF) and rheological properties were investigated. Resulting graphs were designed with OriginPro software using default normalization option in interval [0;1]. Statistical data was added, previously proceeded with IBM SPSS software.

RESULTS AND DISCUSSION

FT-IR spectra showed identical molecular structure for both sterilized and non-sterilized samples. In addition, normalized spectra were used to compare the ratio between the absorbance intensities of the two bands: Amide I to Amide II, Amide I to Amide III and NH2 to NH3+. In result statistically significant difference was not found ($p>0.05$). FE-SEM microphotographs revealed highly porous structure in both sterilized and non-sterilized samples. However, crystals of NaCl formed during synthesis process were found in non-sterilized samples. Furthermore, XRD patterns also revealed sufficient decrease of NaCl crystalline phase in hydrogels after sterilization. Analysis of gel fraction showed similar values with non-significant difference ($p>0.05$) from 45 to 65% according to ε-PL to HA mass ratios. Viscoelastic properties of both non-sterilized and sterilized samples were investigated by extracted values of stiffness modulus from amplitude and frequency sweep curves. All samples showed similar behaviour during oscillatory rheology studies and demonstrated stiffness moduli (G') on average 14 kPa.

CONCLUSION

The developed hydrogels based on ε-PL/HA co-polymer matrix showed promising properties towards potential uses in tissue engineering basing on comparison between non-sterilized and sterilized samples. According to obtained data, no significant changes in molecular structure were found. NaCl crystalline phase was found on surface of hydrogel samples that could be removed by steam sterilization method. Gel fraction studies showed that using of basic steam sterilization program of 121˚C/250˚F for 20 min does not affect matrix integrity and cause degradation of HA. As well rheological studies revealed statistically insignificant effect of sterilization on hydrogel matrix stability and viscoelastic properties. In was concluded that sterilisation approach commonly used in biomedical field did not significantly affect the physicochemical properties of the fabricated ε-PL/HA hydrogels.

REFERENCES

1. Sceglovs, A.; Salma-Ancane, K. Novel Hydrogels and Composite Hydrogels Based on Ɛ-Polylysine, Hyaluronic Acid, and Hydroxyapatite. *Key Eng. Mater.* **2020**, *850 KEM*, 242–248. https://doi.org/10.4028/www.scientific.net/KEM.850.242.
2. Centers for Disease Control and Prevention. Steam Sterilization.https://www.cdc.gov/infectioncontrol/guidelines/disinfection/sterilization/steam.html (accessed May 24, 2021).

ACKNOWLEDGMENTS

The authors acknowledge financial support from the Latvian Council of Science research project No. lzp-2020/1-0072 "Injectable bioactive biocomposites for osteoporotic bone tissue regeneration (inBioBone)".

The authors acknowledge financial support from the European Union's Horizon 2020 research and innovation programme under the grant agreement No 952347.

3D bioartificial stretchable scaffolds for an *in vitro* model of fibrotic cardiac tissue

Francesca Tivano[1,2,3], Mattia Spedicati[1,2,3], Alice Zoso[1,2,3], Mario Lavella[4], Irene Carmagnola[1,2,3], Valeria Chiono[1,2,3]

[1] Department of Mechanical and Aerospace Engineering, Politecnico di Torino, Torino, Italy
[2] POLITO BioMedLab, Politecnico di Torino, Torino, Italy
[3] Centro 3R, Interuniversity Center for the Promotion of the 3Rs Principles in Teaching and Research, Italy
[4] Department of Management, Information and Production Engineering, Università degli Studi di Bergamo, Dalmine (BG), Italy
* francesca.tivano@polito.it

INTRODUCTION

Myocardial infarction (MI) is the main cause of morbidity and mortality. After MI, heart undergoes phenotypic changes leading to cardiac fibrosis and progressive heart failure. Nowadays, the only available therapy allowing the recovery of cardiac function is heart transplantation, while new advanced regenerative therapies are under investigation[1]. *In vitro* testing platforms able to mimic the biophysical behavior of pathological human cardiac tissue could reduce *in vivo* animal trials following 3Rs principle. Previous literature reported *in vitro* cardiac tissue models based on natural hydrogels, which are limited by the lack of structural cues and fast degradation rate. Herein, stretchable scaffolds, provided with biomimetic biochemical and biophysical cues were designed for the *in vitro* modelling of mechanically-stimulated fibrotic cardiac tissue.

EXPERIMENTAL METHODS

Scaffolds with parallel-wavy fibers pattern were fabricated by melt-extrusion additive manufacturing (MEAM) from polycaprolactone (PCL) and analyzed by SEM. Scaffold pores were filled with gelatin methacrylate (GelMA) hydrogels, mimicking extracellular matrix (ECM)-like microenvironment[2]. PCL scaffolds were surface functionalized with poly(4-Dihydroxy-DL-phenylalanine) (polyDOPA) to improve interfacial adhesion with GelMA hydrogels. GelMA hydrogels with different concentrations were initially prepared, using lithium phenyl-2,4,6-trimethylbenzoylphosphinate (LAP) as photoinitiator. Photorheology allowed to define the optimal hydrogel curing protocol. Human cardiac fibroblasts (HCFs, PromoCell) were embedded in GelMA hydrogels (cell density: $5 \cdot 10^6$ cells/ml) and cultured up to 2 weeks. Cell viability (resazurin assay) and myofibroblast protein expressions were analyzed. GraphPad Prism® software was employed for analysis of variance (ANOVA). Static and cyclic tensile tests were performed on PCL/GelMA scaffolds. Further *in vitro* cell tests on PCL/GelMA scaffolds are ongoing.

RESULTS AND DISCUSSION

MEAM processing parameters were optimized to fabricate scaffolds with high shape fidelity, as demonstrated by their morphological analysis by optical microscopy and SEM (Fig 1a-b). Mechanical properties of PCL/GelMA scaffolds (Fig 1c) were tailored by PCL fibre diameter, mesh geometry, and GelMA hydrogel concentration in order to mimic the stiffness (1-9 MPa)[3] and maximum elastic deformation (15-22%)[4] of human cardiac fibrotic tissue.

PCL/GelMA scaffold stretchability and integrity were preserved after both static and cyclic tensile tests.

HCFs viability tests on GelMA hydrogels showed that the addition of LAP and UV curing parameters did not exert cytotoxicity effects. Phalloidin and α-SMA staining showed homogeneous cell distribution in GelMA hydrogels and HCFs acquisition of a fibrotic phenotype. Immunofluorescence analysis performed after 1 and 2 weeks culture time showed the secretion of collagen Type I and IV in cell-laden GelMA hydrogels, suggesting fibrotic ECM deposition. *In vitro* cell tests on PCL/GelMA scaffolds are in progress.

Fig.1 a) Optical and b) SEM images (40x) of PCL scaffold. c) SEM image of PCL/GelMA scaffold (37x).

CONCLUSION

In this work stretchable PCL/GelMA scaffolds were designed for the *in vitro* engineering of post-infarct human cardiac tissue. Different fibrotic conditions could be mimicked by tailoring the concentration of GelMA hydrogel filling PCL scaffolds. In the future, cells will be cultured on stretchable PCL/GelMA scaffolds in dynamic conditions (bioreactor), to get innovative predictive *in vitro* models of human cardiac fibrotic tissue. The models will allow preclinical validation of advanced cardiac regenerative strategies[1], by long-term testing under mechanical stimulation.

REFERENCES

1. Paoletti C. *et al.*, Front. Bioeng. Biotechnol. 8:1–9, 2020
2. Sadeghi A. H. *et al.*, Adv. Healthc. Mater. 6:1–14, 2017
3. Chelnokova N. O. *et al.*, Opt. Elastography Tissue Biomech. III 9710:1-6, 2016
4. Chen Q. Z. *et al.*, Mater. Sci. Eng. R Reports 59:1-37, 2008

ACKNOWLEDGMENTS

The authors would like to thank the European Research Council (ERC) under European Union's Horizon 2020 research and innovation (BIORECAR; grant no: 772168) for providing financial support to this project.

Mechanical and structural characterization of a poly(ethylene terephthalate) mesh impregnated by a resin composite intended as adhesive bone patch fixation.

Guillaume Patt-Lafitte[1*], Daniel Hutchinson[2], Michael Malkoch[2], David Eglin[1]

[1]INSERM, U1059 SAINBIOSE, Mines de Saint-Etienne, Univ Lyon, Univ Jean Monnet, Saint-Etienne F – 42023, France
[2]Division of coating technology, Royal Institute of Technology, Stockholm, Sweden
[*] guillaume.lafitte@emse.fr

INTRODUCTION

Complex phalanx fractures require open surgery with reduction internal fixation. This state of the art practice has still 64% of complication risk related to mechanical mismatch and adhesion notably[1]. To address this problem, a polymeric adhesive patch fixation has been proposed[2]. It is composed of a primer formulation for adhesion to bone, a photo-curable resin composite based on a thiol-ene coupling reaction (monomers, hydroxyapatite, and a photo-initiator) and a reinforcing poly(ethylene terephthalate) (PET) fiber mesh. However, the adhesive fixation is not biodegradable so far. Thus, the following work aim to systematically study the mechanical and structural properties of the photo-curable resin composite and PET mesh to provide boundaries conditions for the design of biodegradable reinforcing membrane and composite resin.

EXPERIMENTAL METHODS

Materials and samples were purchased and prepared as already reported[2]. Resin composite and resin composite with PET mesh were mechanical characterized, N≥9, through tensile, bending and peeling tests using an Instron 3343 testing machine. According to the ASTM D638-03, tensile samples were prepared in dog bone shape and tested under uniaxial direction at 5mm.min^{-1}. Bending test was performed as reported in the literature[2]. Briefly, a beam shape samples were tested under uniaxial compression at 1mm.min^{-1}. A peeling test was finally performed under uniaxial tension at 1mm.min^{-1}. Young's modulus, tensile strength, flexural modulus and strength were calculated. Raman spectroscopy (Horiba Jobin Yvon XploRA) was used to verify the efficiency of the photo-polymerization and thus resin formulation via semi-quantification of thiol and ene vibrations. A Nanotom S X-ray computed tomography (Phoenix) was used to analyzed representative samples.

RESULTS AND DISCUSSION

As the adhesive patch fixation will experience complex loading in the fracture site, several mechanical load scenarios have been performed. Young's Modulus, tensile strength, flexural modulus and strength values are reported for the resin composite and resin composite with PET mesh in figure 1. The addition of one layer of PET mesh significantly increases the young's modulus and the flexural strength. No correlation is found between the mechanical parameters calculated and the Raman vibrational peaks intensity values for each samples indicating that the PET mesh does not impact the photo-curing process.

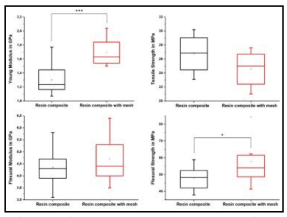

*Figure 1: Mechanical properties in tension and compression of the resin composite with and without PET mesh (*p≤0.05; ***p≤0.001).*

The representative X-ray images of the resin composite and resin composite with PET mesh indicate that the microstructure and hydroxyapatite aggregates dispersion in the composite resin is constant through samples and a good PET mesh impregnation at the microscopic level.

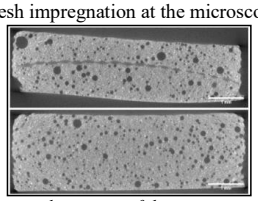

Figure 2: Tomography images of the resin composite with and without PET mesh.

CONCLUSION

Relative to it's application, the adhesive patch can avoid problem of stress shielding by having mechanical properties closer to bone (Young's modulus of trabecular and cortical bone are 10.4 and 18.6 GPa)[3] than metal implant (120 GPa). The study reported and data collected provide the testbed and basis for the design of biodegradable adhesive patch, and notably polylactic acid origami like membranes, which may provide additional mechanical reinforcement thanks to its architecture.

REFERENCES

1. Guerrero E. M. *et al*., Hand (N Y). 16:248-252, 2019
2. Granskog V. *et al*., Adv. Funct. Mater. 28:26, 2018
3. Rho J.Y. *et al*., J Biomech. 26:111-119, 1993

ACKNOWLEDGMENTS

This project has received funding from European Union's Horizon 2020 research and innovation programme under grant agreement No.952150 (BoneFix).

Novel Polyester-based Biomaterials for the Design of Tissue Engineering Scaffold by Additive Manufacturing Technologies

Arianna Grivet-Brancot[1,2,*] Syed Mohammad Daniel Syed Mohamed[3], Monica Boffito[1], Ipsita Roy[3], Gianluca Ciardelli[1]

[1]Department of Mechanical and Aerospace Engineering, Politecnico di Torino, Torino, Italy
[2]Department of Surgical Sciences, Università di Torino, Torino, Italy
[3]Department of Materials Science and Engineering, University of Sheffield, Sheffield, United Kingdom
[*] arianna.grivet@polito.it

INTRODUCTION

Optimized biomaterials are increasingly needed in tissue engineering/regenerative medicine (TERM) to combine the requisites of advanced processing techniques (e.g., additive manufacturing, AM) with the biocompatibility and bioactivity necessary for tissue repair and regeneration. Poly(ester)s are often used in this context because of their non-toxicity, and general biocompatibility and biodegradability. Poly(ester urethane)s (PURs) are particularly suitable for TERM because their building blocks can be *ad-hoc* selected to tailor the mechanical and degradation properties of the resulting polymers, thus making them suitable for different applications. Beside more traditional polymers such as poly(ε-caprolactone) (PCL), polyhydroxy-alkanoates (PHAs) represent an interesting alternative in the selection of building blocks for PUR synthesis. Indeed, PHAs have gained an increasing popularity in recent years thanks to their biosynthesis, conducted by bacteria by means of sustainable processes. In addition, these poly(ester)s also show processing versatility and superior mechanical properties in comparison with other polymers from natural resources.
In this work, a family of biomaterials based on poly(ester)s with tuneable properties for extrusion-based AM has been developed and characterized. Both PURs based on PCL- and a medium chain length PHA-diol with elastomeric properties and blends of PCL-based PURs and PHAs have been produced with modulated properties to target different TERM applications.

EXPERIMENTAL METHODS

PUR synthesis was conducted adapting an already published method[1]. A medium chain length (mcl) PHA was also produced and characterized using gas chromatography (GC), Infrared (IR) and Nuclear Magnetic Resonance (NMR) spectroscopies[2]. An optimized transesterification process was then employed to obtain a PHA-diol to be used for PUR synthesis in combination with PCL-diol. PURs were characterized by IR spectroscopy and Size Exclusion Chromatography (SEC). Polymer thermal properties were studied by ThermoGravimetric Analysis (TGA), Differential Scanning Calorimetry (DSC), and rheological tests. Tensile tests were also performed on polymer films. Blends of PCL-based PURs and PHAs were also investigated. To improve the miscibility between the two components, a hydrolysis process was performed on the PHA to uniform its molecular weight to the PUR counterpart. Polymer cytocompatibility was also assessed according to the ISO 10993-5 regulation.

RESULTS AND DISCUSSION

The success of PUR and mcl PHA synthesis was confirmed through chemical characterization. The optimization of the transesterification process resulted in the production of a PHA-diol with average molecular weight suitable for use in PUR synthesis. The synthesis of the PHA-based PUR was then proved successful by chemical characterization through IR spectroscopy and SEC. PUR mechanical properties turned out to be affected by the PCL/PHA diol weight ratio used during the synthesis process, with a more elastomeric behaviour observed when the content of the PHA counterpart was raised. Thermal and rheological analyses demonstrated the suitability of these materials for the production of scaffolds through extrusion-based AM techniques, e.g., by the Fused Deposition Modelling technique. Blends between the mcl PHA and PCL-based PURs were also produced with different PHA:PUR weight ratios (from 20:80 to 80:20 w/w). PHA hydrolysis to decrease its molecular weight was proved necessary to achieve a good miscibility between the two polymeric components. By an optimised hydrolysis protocol, PHA starting molecular weight (100-80 kDa) was lowered to match the PCL-based PUR one (30-40 kDa), thus improving the compatibility between the two materials and the final blend quality. Finally, no cytotoxicity was detected for any of the investigated polymers and formulations.

CONCLUSION

A series of poly(ester)-based biomaterials was successfully developed in this study. The PCL/mcl PHA-based PUR properties, especially the mechanical behaviour, were modulated by changing the two diol weight ratio during PUR synthesis. Different blends between PCL-based PURs and PHA were also successfully developed and thoroughly characterized. All the resulting formulations proved cytocompatible and suitable for the production of tissue engineering scaffolds through extrusion-based AM techniques.

REFERENCES

1. Chiono V. *et al.* Interface Focus 4: 20130045, 2014.
2. Basnett P. *et al.* ACS Appl. Mater. Interfaces 13, 28, 2021.

Optimized Functionalization of a Titanium Alloy Surface with the Antimicrobial Peptide Nisin

Mari Lallukka[1*], Virginia A. Gobbo[2], Francesca Gamna[1], Jacopo Barberi[1], Silvia Spriano[1]

[1]Department of Applied Science and Technology, Politecnico di Torino, Turin, Italy
[2]Faculty of Medicine and Health Technology, Tampere University, Tampere, Finland
[*] mari.lallukka@polito.it

INTRODUCTION

Implant-associated infections are a severe global concern, especially in the case of orthopedic implants intended for long-term or permanent use[1]. Traditional treatment option of systemic antibiotic administration is often inefficient due to biofilm formation and concerns regarding the development of highly resistant bacteria[2]. Therefore, there is an unfulfilled need for antibiotic-free alternatives that could simultaneously support bone regeneration and prevent bacterial infection. The aim of this study is to develop a biocompatible and antibacterial surface by grafting the antimicrobial peptide (AMP) nisin, on a titanium alloy surface. Nisin, AMP produced by *Lactococcus lactis*, is globally approved, commercially available, and it is characterized by a broad antimicrobial spectrum and no evidence of bacterial resistance[3]. In this work, the surface functionalization process of the titanium alloy with nisin is optimized regarding the process parameters such as the pH value of the nisin solution, following by release tests assessing the expected mechanism of antibacterial action.

EXPERIMENTAL METHODS

Ti6Al4V-ELI (Grade 23) alloy was employed for the experiments as 2 mm thick and 10 mm diameter polished discs. The discs were functionalized with 1 mg/mL nisin solution with three different pH values (5,6,7) for 24 hours in room temperature. The surface-functionalized discs were characterized in terms of their surface zeta potential by an electrokinetic analyser for solid surfaces, contact angle by using the sessile drop method, followed by surface electric potential by Kelvin Probe atomic force microscopy (KPFM), and evaluation of chemical composition by X-ray photoelectron spectroscopy (XPS). In addition, for the optimized functionalization process at pH 6, a seven-day release test was performed in two different release solutions: in phosphate buffered saline (PBS), to correspond to physiological pH 7.40, and in hydrogen peroxide (H_2O_2) adjusted to pH 4.50, to mimic inflammatory conditions.

RESULTS AND DISCUSSION

As indicated by the surface zeta potential measurements, when comparing the nisin-grafted surface to the non-grafted one, the isoelectric point shifts to more basic pH, and slightly more positive surface charge, suggesting the presence of nisin molecules on the surface. Also, the KPFM results support these findings by functionalizing a limited area of a specimen: higher surface potential was detected on the nisin-functionalized area compared to the bare one. The successful nisin grafting was further demonstrated by XPS, as an increase in nitrogen and sulphur content in the survey spectra is evidenced after functionalization. The high-resolution spectra of N 1s region suggests the presence of amide bonds, which are characteristic for a polypeptide. In addition, peaks ascribable to a thioether functional group are detected in the high-resolution spectra of the S 2p region of the functionalized samples. XPS and zeta potential data reveal that functionalization is more efficient at pH 6. Moreover, as detected by contact angle measurements, the one-week release test showed first evidence of gradual nisin release in both physiological (PBS) and inflammatory conditions (H_2O_2, pH 4.50).

CONCLUSION

The goal of this study was to characterize and optimize the surface functionalization of Ti6Al4V-ELI discs by the antimicrobial peptide nisin. The presence of nisin on the surface was confirmed by different methods. According to the zeta potential and XPS results, functionalization at pH 6 was found most suitable to nisin grafting. In addition, first evidence of gradual nisin release both in physiological and inflammatory conditions was obtained. The results of this study show the potential of nisin-functionalized Ti alloy as an antibacterial surface. However, to confirm the suitability for medical applications, more studies are needed to evaluate the antibacterial performance and cell response to the functionalized surface.

REFERENCES

1. Arciola C.R. *et al*., Nat Rev Microbiol 16:397-409, 2018
2. Sadowska J.M. *et al*., Materials Today 46:136-154, 2021
3. Shin J. *et al*., J Appl Microbiol, 120:1449-1465, 2016

ACKNOWLEDGMENTS

The authors received funding from European Union's Horizon 2020 research and innovation program under grant agreement No. 860462 project PREMUROSA.

Surface-protein interactions on additively manufactured CoCr alloy for biomedical application

Anna Zięboweicz[1], Thomas Luxbacher[2*], Timo Müller[2], Kamil Kosiel[3], Marta Kiel-Jamrozik[1], Zbigniew Paszenda[1]

[1]Department of Biomaterials and Medical Device Engineering, Silesian University of Technology, Zabrze, Poland
[2]Anton Paar GmbH, Graz, Austria
[3]Łukasiewicz Research Network-Institute of Microelectronics and Photonics, Warsaw, Poland
[*] thomas.luxbacher@anton-paar.com

INTRODUCTION

The electrostatic interaction between oral prosthetics and salivary proteins is considered as a driving force for protein attachment on the biomaterial's surface. Furthermore, the electrostatically driven attraction of proteins triggers the formation of biofilms. Several parameters decide on the biocompatibility of the prosthetics such as the elemental composition of the surface, its corrosion resistance, mechanical wear, as well as physiochemical properties of the surface like hydrophilicity and surface charge. Among these parameters, the effective surface charge at the solid-liquid interface presumably shows the highest variance since it depends on both the surface functional groups of the prosthetics and the conditions of the aqueous surrounding. pH, ionic strength, and the type of solutes determine the charging behavior at this interface. Most commonly, information about the surface charge is derived from the analysis of the zeta potential in the presence of a standard buffer such as a dilute aqueous solution of a monovalent electrolyte. A few researchers have demonstrated the extension of the zeta potential analysis towards the direct observation of the dynamics of protein-surface interactions thereby still excluding the competing effects of complex solutes present in a biological environment such as the oral cavity.
In this paper we include the contribution of complex solutes to study the ability of representative proteins to adsorb on removable partial dentures (RPDs) comprised of a CoCr alloy with a thin-film hard coating of ZrO_2.

EXPERIMENTAL METHODS

Disks of CoCr (15 mm diameter) were prepared by additive manufacturing (direct metal laser sintering, DMLS) and coated with a thin layer of ZrO_2 by the atomic layer deposition method.[1] The crystalline structure of the thin-film ZrO_2 coating was confirmed by grazing incidence X-ray diffraction and the thickness was estimated by X-ray reflectometry (XRDynamics). The interfacial charge density of pristine and coated alloy disks was calculated from the zeta potential determined by the streaming potential and streaming current method (SurPASS 3). Bovine serum albumin (pI 4.7) and lysozyme (pI 11.1) were selected as model proteins that exhibit either a negative (BSA) or a positive (LYS) charge at the physiological pH. The adsorption kinetics of these proteins on the pristine and coated CoCr alloy disks was investigated by dynamic streaming potential measurements in a dilute phosphate buffer solution and compared with the adsorption in artificial saliva adjusted to different salinities. The affinity of the novel CoCr alloy prepared by DMLS towards the proteins BSA and LYS was further compared with stainless steel 316L.

RESULTS AND DISCUSSION

The GI-XRD pattern of the CoCr alloy coated with a thin film of ZrO_2 shows distinct peaks at 46° and 54° 2θ, which confirm the presence of the ceramic hard coating. The streaming potential and streaming current measurements reveal the contribution of metal conductance for the pristine CoCr alloy and a non-conductive behavior of the alloy coated with ZrO_2. The pH dependence of the zeta potential in 0.01 mol/l NaCl indicates the expected evolution of the interfacial charge distribution for CoCr and 316L. We observe a similar trend for ZrO_2-coated CoCr with an isoelectric point (IEP) at pH 4, which is opposite to the expectation for ZrO_2 particles dispersed in a corresponding aqueous solution. Such a discrepancy was also reported for single-crystalline sapphire (IEP 4) and Al_2O_3 slurries (IEP 8-9).[2] A small but significant effect of artificial saliva is observed for the adsorption of BSA on both CoCr and ZrO_2-coated CoCr while the adsorption of LYS remains unaffected by the presence of the complex solutes.

CONCLUSION

We have focused on the characterization of the charging behaviour at the interface between a ZrO_2-toughened CoCr alloy suggested for RPDs and an aqueous surrounding. The use of artificial saliva as an aqueous medium for studying protein adsorption on the surface of prosthetics is recommended on top of commonly used dilute buffer solutions of monovalent salts. We observe an interference of artificial saliva with the adsorption process of BSA, which is equally charged to ZrO_2-coated CoCr at pH 7.4, while the adsorption kinetics of the oppositely charged LYS remains almost unaffected. This observation provides an indication on the different mechanisms involved in these individual protein adsorption processes.

REFERENCES

1. Ziebowicz A. *et al.*, Materials 14:1079, 2021
2. Lützenkirchen J. *et al.*, Adv. Colloid Interface Sci. 157:61-74, 2010

Designing PEG-Peptide Copolymer Hydrogel for Biomedical Applications

Andong Liu [1], Lu-shin Wong [2], Aline Miller[3], Alberto Saiani[1]

[1]Department of Materials, The University of Manchester, Manchester, UK
[2]Department of Chemistry, The University of Manchester, Manchester, UK
[3]Department of Chemical Engineering, The University of Manchester, Manchester, UK

*Andong.liu@manchester.ac.uk

INTRODUCTION

Hydrogels are widely used in biomedical applications. Polyethene glycol (PEG) and short self-assembling peptides are commonly used to design hydrogels due to their biocompatibility. As a result, the use of peptide-PEG conjugates has recently attracted significant interest in designing a novel hydrogel system combining the properties of both building blocks.

Fibre formation is a key aspect of the gelation process of self-assembling peptide systems. Unwanted fiber lateral aggregation and assembly often results in the formation of large fiber bindle leading to very stiff non-transparent hydrogels and in some extreme cases to phase separation[1]. These effects can limit the usage of peptide hydrogels in many areas [2,3].

In this work, we decided to conjugate PEG to a family of self-assembling peptides developed in our group to control fiber formation and lateral aggregation to control the hydrogel's physical properties.

EXPERIMENTAL METHODS

CFEFKFEFKK(CF9) (C: cysteine, F: phenylalanine, K: lysine, E: glutamic acid) peptide was conjugated with MAL-mPEG (Mw: 2, 5 and 10k). RP-HPLC purified PEG-F9 conjugates. The hydrogel where characterised using a range of techniques, including TEM, SAXS and FTIR.

RESULTS AND DISCUSSION

HPLC and NMR analysis confirmed the successful synthesis of the conjugate. In particular, NMR analysis confirmed the 2:1 proton ratio expected for the conjugate. The di-block conjugates were obtained with purities > 90%.

F9 hydrogels are typically cloudy at pH7 due to significant fiber lateral aggregation and bundling. The conjugation of PEG to F9 was shown to reduce fiber-fiber hydrophobic interactions and, therefore, bundling in the system. Increasing the fraction of di-block conjugate through physical mixing resulted in hydrogels becoming more and more transparent at pH7. TEM confirmed the reduction in fiber budling (Figure 1). It reduces in bundling, and an increase in transparency was accompanied by a reduction in G' (shear modulus) of the hydrogels. This result clearly points to PEG's role in reducing fiber - fiber interactions and, therefore, network crosslinking. As a result, the mechanical properties of the hydrogel decrease and when more than 10% (mol) of the conjugate is added the system stop gelling.

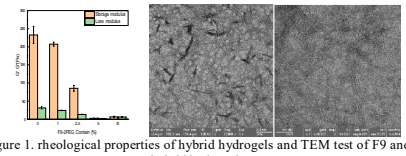

Figure 1. rheological properties of hybrid hydrogels and TEM test of F9 and hybrid hydrogels.

However, the samples' secondary structure and beta-sheet content as determined by FTIR show no significant change upon addition on the conjugate, confirming that the addition of PEG does not affect fiber formation but on fiber crosslinking by preventing fiber - fiber interactions.

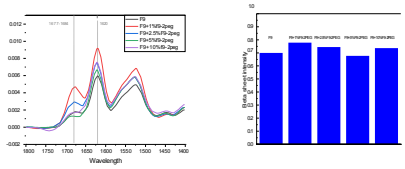

Figure 2, FTIR results of hybrid hydrogels

The conjugate was found to slow down gel formation, suggesting that the PEG chains of the surface of the fiber result in steric hindrance and prevent crosslinking formation but over time relaxation processes occur and crosslinks form.

CONCLUSION

The attachment of PEG on the peptide can change the peptide fiber arrangement and therefore allows the design of mechanically tuneable and transparent hydrogels. It provides the potential to build novel hydrogel for biomedical applications.

REFERENCES

1. Gao, J. et al. Biomacromolecules 18, 826–834, 2017
2. Takayama. et al. Carbohydrate Polymers 234, 115880, 2020.
3. Jacek K. W Biomacromelecules19-2731-2741, 2018

ACKNOWLEDGMENTS

The authors would like to thank Prof Alberto Saiani and Prof Aline Miller for supporting this project.

Fabrication of Hyaluronan-based Matrices, Functionalized with Laminin Derived Peptides, to Sustain Cellular Adherence and Axonal Growth in Bone Regeneration Applications

Quentin Muller[1*], Romane Josselin[2], Daphne Van Der Heide[3], Jean-Francois Le-Meins[2], Bertrand Garbay[2], Hugo Oliveira[1], Matteo D'Este[3] and Joëlle Amédée[1]
[1]Univ. Bordeaux, INSERM, BIOTIS, U1026, F-33000, Bordeaux, France
[2]Univ. Bordeaux, CNRS, Bordeaux INP, LCPO, UMR 5629, Pessac, F-33600, France
[3]AO Research Institute Davos, Clavadelerstrasse 8, 7270 Davos Platz, Switzerland
*quentin.muller@u-bordeaux.fr

INTRODUCTION

After blood, bone remains the most transplanted organ, in cases of bone trauma and resection. Currently, surgeons are still faced with major hurdles: i) complexity, availability and morbidity associated with vascular fibula grafts, ii) insufficient innervation and osteointegration for implanted biomaterials, in the absence of autologous cells, iii) complexity/regulatory hurdles in the use of growth factors (*i.e.* BMPs)). Furthermore, tissue engineering cell-based approaches have also shown limitations: i) limited ability of autologous cells from non-healthy patients to proliferate and integrate with biomaterial systems, ii) tissue-engineered constructs are labor intensive to produce, low throughput and difficult to form into complex 3D geometries, iii) advanced cell therapies are associate with stringent regulatory hurdles. Also, from many years, bone tissue-engineering strategies were mainly focused on osteogenesis and shown limited clinical success. Only recently, focus has been drawn on the importance of neurotization, essential to attain fully functional tissues.
Here, we explore the 3D fabrication of a cell-free scaffold, designed to support the intricate orchestration between innervation and bone healing, in a regeneration scenario. We focused on a hyaluronan-based matrix functionalized with laminin derived peptides and calcium phosphate microparticles, characterized by rheology, shown to be bioprinted and support neuronal cell adherence and maturation. We will present the main optimization steps for its development, towards improved bone innervation, and its impact on bone regeneration.

EXPERIMENTAL METHODS

The tyramine-modified hyaluronan-based matrix (HA-Tyr) was formed with combined enzyme-mediated crosslinking (H_2O_2 – HRP reaction) and visible light cross-linking (Eosin Y – 505 nm light) [1]. The first crosslinking was used to pre-gel, and enable microextrusion bioprinting, and the second to set the bioprinted structure. The base hydrogel was functionalized with two different peptides formulations, and tree peptides concentrations (*i.e.* 0, 0.5 and 1 mg/mL), and manually extruded for rheological evaluation after light crosslinking. The linear domain, was used to determine the strain range where the structure of the gel was not modified, the gel character and the viscoelasticity properties.
In vitro evaluation was equally performed on gels following both crosslinking approaches by seeding human induced-pluripotent stem cells-derived sensory neurons (iPS-SN)[2] on the top of the matrix. Phenotypical characterization was performed using cell-specific immunolabelling.
Then, calcium phosphate microparticle (CaP) were equally associated with the aforementioned composite gel and evaluated in terms of printability by microextrusion on a 3D Discovery (RegenHU) bioprinting system, and his microporosity structure evalueted using scanning electronic microscopy (SEM) observation.

RESULTS AND DISCUSSION

The HA-Tyr functionalization was performed with 2 peptide (p) formulations, the first one with tyrosine group at each end (YpY) and the second one, the same structure with only one tyrosine at one end (Yp). The linear domain observation for both peptide formulations shows a stability and viscoelasticity properties similar between the condition without peptide and with 0.5 mg/mL for both peptides (YpY and Yp). By adding more peptide (1 mg/mL), we observed lower gel stability, as observed by the decrease of G' average value. In terms of *in vitro* results, the addition of the laminin-derived peptides show to support iPS-SN cell adhesion, but only the condition with YpY at 0.5 mg/mL showed a positive impact on axons formation and innervation.
After adding CaP, the material was printed in a 10 mm grid square structure. We could observe that the addition of peptide improved the structural integrity of the 3D shape and the macroporosity homogeneity of the final structure. Addititinally, the addition of peptide showed not to impact on the microporosity structure of the composite gel, containing CaP particles.

CONCLUSION

We showed the grafting of laminin-derived peptides support cellular adhesion and phenotype. Further studies are ongoing and will enable to improve the capacity of this biomaterial to sustain neurogenesis in a context of bone regeneration.

REFERENCES

1. Loebel, C. *et al.*, Biomacromolecules. 18, 855–864 (2017).
2. Muller, Q. *et al.*, Acta Biomater 82, 93–101 (2018).

ACKNOWLEDGMENTS

This project is a part of the cmRNAbone project, who had received funding from the European Union's Horizon 2020 research and innovation program under grant agreement No 874790.

Dissolving Microneedle Arrays: The Effects of Drug Incorporation on Physiochemical Properties

Elliot Croft[1*], Vito Romano[2], Steve Rannard[3] and Helen Cauldbeck[1]
[1]*Department of Chemistry, University of Liverpool, Crown Street, L69 7ZD, *sgecroft@student.liverpool.ac.uk*
[2]*St Pauls Eye Unit, The Royal Liverpool University Hospital, Prescot Street, L7 8XP*
[3]*Materials Innovation Factory, University of Liverpool, Oxford Street, L7 3NY*

INTRODUCTION

Dissolving microneedle arrays (DMNs) designed for ophthalmic drug delivery require sufficient mechanical strength and fast dissolution for effective application and patient comfort respectively.[1] DMNs are formulated from water soluble, biodegradable polymers, such as polyvinylpyrrolidone (PVP), and a therapeutic agent which is encapsulated within the polymer matrix.[2] Incorporation of therapeutic compounds can alter physiochemical properties of DMNs; such additives disrupt interchain interactions, introduce changes to surface behaviour and effect chain mobility between polymeric chains within a rigid structure.[3,4] Consequently, insertion efficiency and drug release are altered by changes in mechanical strength and dissolution kinetics. The aim of this investigation is to mitigate the disruptive impact of incorporating latanoprost, the first line therapeutic for glaucoma, to DMN physiochemical properties *via* the addition of a plasticiser, polyethylene glycol (PEG).

EXPERIMENTAL METHODS

PVP (K30, 40 000 g mol^{-1}) PEG (1 000- 5 000 g mol^{-1}, 5-10 wt. %) solutions (50 % wt.) and DMNs with latanoprost (50 µg mL^{-1}) were fabricated *via* a solvent casting method. The surface behaviour of unloaded and loaded PVP·PEG blends was assessed *via* contact angle and surface tension measurements. Mechanical strength of DMNs was measured by employment of increasing force to determine the degree of compression and insertion into corneal tissue *ex vivo*. DMN dissolution rates, latanoprost permeation and biodistribution in an *ex vivo* eye model was assessed radiometrically using tritiated latanoprost.

RESULTS AND DISCUSSION

Surface behaviour measurements in PVP·PEG blends highlighted an increase in surface tension (Figure 1A) in drug loaded compositions of PVP_{100}·PEG_0 relative to its unloaded counterpart. This rise is linked to the amphiphilic nature of latanoprost, creating a hydrophilic-hydrophobic barrier at the air-polymeric solution interface. PVP_{95}·$PEG_{5(5000)}$ formulations saw no change in surface behaviour when latanoprost was incorporated. Compression testing of PVP_{100}·PEG_0 DMNs exposed a reduction in mechanical strength upon latanoprost incorporation relative to PVP_{95}·$PEG_{5(5000)}$ which saw no change between its unloaded and loaded compositions (Figure 1B). The similarity within PVP_{95}·$PEG_{5(5000)}$ is related to the hydrophilic nature of PEG, minimising drug interference *via* plasticiser control on the physiochemical properties of the PVP·PEG blends.

CONCLUSION

PVP·PEG DMNs were successfully fabricated as well as latanoprost containing analogues to investigate the effect of drug incorporation on a range of physiochemical properties. Surface behavior measurements and compression testing emphasised the ability of PEG to mitigate the effect of latanoprost on solutions and the mechanical strength of PVP_{95}·$PEG_{5(5000)}$ DMNs relative to PVP_{100}·PEG_0. Overall, this study demonstrated the importance of PEG in DMNs to tailor effects of drug incorporation on the physiochemical properties of bespoke DMNs required for minimally invasive ophthalmic drug delivery.

REFERENCES

1 Thakur R. R. S. *et al.*, Drug Deliv. Transl. Res. 6:800-815, 2016
2 K. Moffatt K. *et al.*, Curr. Opin. Pharmacol. 36:14-21, 2017
3 Liew K. B. *et al.*, Drug Dev. Ind. Pharm. 40:110-119, 2014
4 J. H. Park J. H., *et al*., Pharm. Res. 23:1008–1019, 2006

ACHKNOWLEDGMENTS

The authors would like to thank the University of Liverpool Doctoral Network for Healthy Ageing for supporting this research.

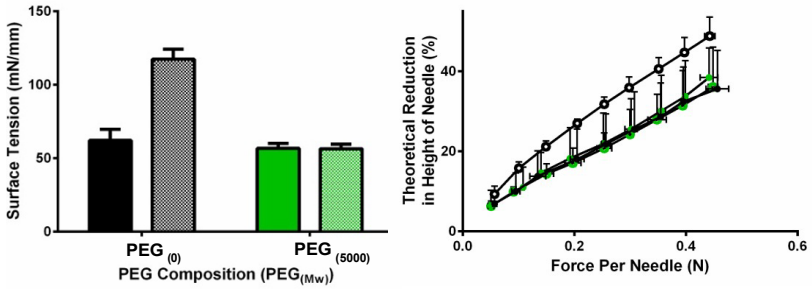

Figure 1: Latanoprost loading (hashed/ring) effects relative to unloaded (bold/dot) PVP·PEG blends on A: Surface tension (mN mm^{-1}) and B: Compression testing of PVP_{100}·PEG_0 (black) and PVP_{95}·$PEG_{5(5000)}$ (green).

The Effect of Hydroxyapatite Particle Shape on Hyalectin Hydrogel Augmentation of Screws in Cancellous Bone

Yijun Zhou[1], Ayan Samanta[2], Philip Procter[1], Cecilia Persson[1]

[1]Department of Materials Science and Engineering, Uppsala University, Uppsala, Sweden
[2]Department of Chemistry-Ångström, Uppsala University, Uppsala, Sweden
yijun.zhou@angstrom.uu.se

INTRODUCTION

Due to the increasing number of fragility fractures in bone, operative treatment with implants is more frequent. However, postoperative implant (screw) loosening may lead to reoperation [1]. Many studies report on screw augmentation with bone cement as a potential means to solve this issue. However, the set, dense bone cement may impede the flow of marrow, which can cause hypoxia and/or hypotension [2]. A prior study reported that the combination of non-solidified hydrogels and hydroxyapatite (HA) particles can improve the holding power of orthopedic screws [3]. The aim of the present study was to evaluate the influence of HA particle shape on the screw stability, the hypothesis being that this would lead to different augmentation effects.

EXPERIMENTAL METHODS

Four groups were used to compare the augmentation effect of HA particles (Table 1). The mean particle size for both HA powders was ~200 nm, as confirmed by dynamic light scattering (DLS) and scanning electron microscopy (SEM), which also allowed for shape characterization. 48 rabbit femurs were scanned with X-ray micro-CT. They were divided into four groups aimed at the same mean bone volume fraction. 40 wt/vol% HA powders (ref: 04238 and 677418, Sigma-Aldrich, Buchs, Switzerland) were mixed with 3.5 wt/vol% hyaluronic acid gel (Hyalectin (500-700 kDa), FIDIA SpA, Abano Terme (PD), Italy). A 3 mm Ø pilot hole was pre-drilled distally in the cancellous bone in each femur and the gel was injected before inserting a 4mm Ø screw (Jiangsu Trauhui Medical Instrument Co., China). Each screw was pulled out with a materials testing machine, using a custom set-up. Statistical differences between groups were evaluated with ANOVA (significance determined at $p \leq 0.05$).

Table 1. The four tested groups.

Group	Hyalectin	nHA (irregular)	nHA (spherical)	Number of samples
Unit	wt/vol%	wt/vol%	wt/vol%	-
Control	-	-	-	12
Hyalectin	3.5	-	-	12
nHA-irregular	3.5	40	-	12
nHA-sphere	3.5	-	40	12

RESULTS AND DISCUSSION

Significant differences were found between the pull-out forces of the four groups ($p=0.01$, Fig. 1). Compared to the control group, an increase in pull-out force was found for the irregular HA group ($p=0.02$), but not for the sphere-like HA. The viscosity of the Hyalectin hydrogel was found to decrease when HA particles were added, especially in the sphere-like HA group. No significant pull-out strength differences were found between the control group and the Hyalectin group. The differences between two HA groups could be explained with the viscosity differences and the different shapes of HA particles. The HA particles can fill void spaces and transfer loads between screw and trabecular bone by increasing contact points between the same. Furthermore, a higher viscosity could hinder particle flow, and enhance the load transfer. With the irregular HA particles there are more contact points compared with the sphere-like particles, which can further stabilize the contact between particles and trabecular bone structures and hinder screw pull-out by improving the load transfer.

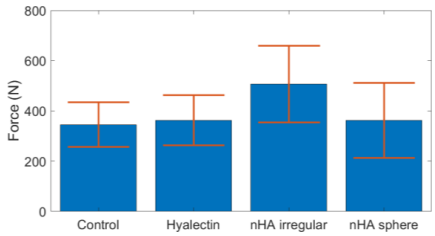

Fig. 1. Screw pull-out force for the four groups with different augmentation materials, i.e. no gel (control), pure Hyalectin, Hyalectin with irregular HA particles, and Hyalectin with sphere-like HA particles.

CONCLUSIONS

The combination of HA particles and hyaluronic acid gel can improve the pull-out strength of screws in cancellous bone. However, the HA particle shape was found to be important, with irregular particles being the only ones giving a significant improvement in this study, for particles of an approximate size of 200 nm in Hyalectin-augmented screws in rabbit cancellous bone.

REFERENCES

1. Konstantinidis L. *et al*., Injury. 47, S27-S32, 2016
2. Donaldson A.J. *et al*., British journal of anaesthesia. 102(1), 12-22, 2009
3. Munoz J.S. *et al*., Clinical Biomechanics. 59, 174-180, 2018

ACKNOWLEDGMENTS

The authors are grateful for support from the European Union's Horizon 2020 research and innovation program under the Marie Skłodowska-Curie grant agreement No 812765, as well as to FIDIA SpA for the provision of Hyalectin.

Multibody Kinematics to Design Shape-Morphing Mechanical Meta-Biomaterials

Pier H. de Jong[1*], A. L. Schwab[1], Mohammad J. Mirzaali[1], Amir A. Zadpoor[1]

[1]Department of Biomechanical Engineering, Faculty of Mechanical, Maritime, and Materials Engineering, Delft University of Technology (TU Delft), Delft, The Netherlands
[*]P.H.deJong@tudelft.nl

INTRODUCTION

Mechanical meta-biomaterials belong to the class of engineered architected materials that exhibit unusual properties and functionalities. An example of these unusual properties is shape morphing or shape-changing. Shape-morphing behavior has several biomedical applications, particularly in the design and fabrication of a new generation of orthopedic implants known as "shape-morphing implants"[1]. Shape-morphing implants, thus, can adapt themselves into the complex shape of bone cavities (*e.g.*, in acetabulum) that needs to be filled by the implant.

There are several ways to guide the overall shape morphing behavior of meta-biomaterials. This can be achieved by devising their microarchitectures so that to reach desirable shapes after deformation[2]. Also, by integrating either kinematic or compliant joints with more than one degree-of-freedom (DOF), one can obtain even more complex shapes[1]. A successful design of a meta-biomaterial with a "universal shape-morphing" behavior, thus, relies on the rational geometrical design of its elements and connecting joints. The kinematic behavior of such a system, however, is often very complex as the rigid bodies connected by the joints can undergo various types of rotational and translational motions. One way to overcome this challenge is to use a multibody system approach. Here, we introduced this approach to analyze the motion and shape-morphing of meta-biomaterials with kinematic joints. The model is tailored in such a way that it only needs a minimum amount of ingredients to capture the full kinematics of the system. We also used additive manufacturing techniques (AM, = 3D printing) to visualize our proposed approach.

MATERIALS AND METHODS

We used a multibody system approach to describe the kinematics of the meta-biomaterials and extract their mobility. The system consists of several components, namely "nodes" and "constraints" that fully define a structure[3]. A "rigid body" was defined by constraining all motion between a group of nodes. By changing the constraints (*i.e.,* DOF) between bodies, we were able to introduce various types of joints (*e.g.,* hinge, prismatic or sliding) in the system which was essential for achieving arbitrary shapes. Novel constraint definitions enabled us to avoid possible singularities in the calculations of motions. By defining a target shape, and through an iterative process of calculation of (local) motions at each joint, the transformation steps needed to reach the target shape was determined. A residual distance error was set to end the process.

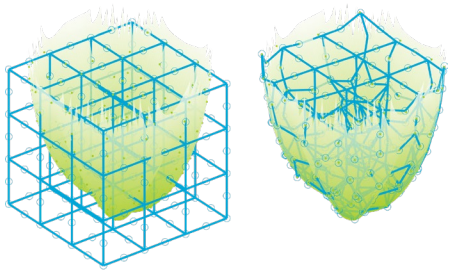

Figure 1: An example of 3D morphing of a meta-biomaterial composed of linkages (blue bars) and spherical joints (blue circles) to an arbitrary shape (green). Multibody kinematic approach provided the transformation steps needed to achieve the desired shape. Left: the initial cubical structure configuration. Right: the structure after shape-morphing.

RESULTS AND DISCUSSION

We selected arbitrary shapes in 2D and 3D. We analyzed the capabilities of our approach in finding required transformation steps to morph into those given shape. Figure 1 shows an example of a 3D shape-morphing with a normalized residual distance error of 0.00608. Our results confirm that the proposed approach is able to efficiently predict various arbitrary shapes. We also validated the accuracy of our model by creating 3D printed structures able to morph into the target shapes.

CONCLUSION

The multibody kinematic approach presented in this study provides a powerful tool for designing meta-biomaterials with shape-morphing capabilities. This approach opens up new opportunities for designing medical devices (*e.g.,* implants and exoskeletal wearable prostheses) with shape morphing functionalities.

REFERENCES

1. Leeflang, S. *et al.*, Additive Manufacturing 28:528-534, 2019
2. Mirzaali, M. J. *et al.*, Scientific Reports 8:965, 2018
3. Nikravesh, P. E., & Affifi, H. A., in Computer-Aided Analysis of Rigid and Flexible Mechanical Systems 31-60, 1994

ACKNOWLEDGMENTS

"The authors would like to thank the NWO Talent Programme Vidi TTW 2017 (Grant no: 16582) for providing financial support to this project".

Polymeric Nanoparticles Targeting Glycans in Gastric Cancer Cells Under Live Flow Conditions

Francisca Diniz[1,2,3*], Maria Azevedo[1], Flávia Sousa[1,4], Hugo Osório[1,2], Diana Campos[1,2], Paula Sampaio[1], Joana Gomes[1,2], Bruno Sarmento[1,4] and Celso A. Reis[1,2,3,]

[1]i3S - Institute for Research and Innovation in Health, University of Porto, Portugal. [2]Institute of Molecular Pathology and Immunology, University of Porto, Portugal. [3]Institute of Biomedical Sciences of Abel Salazar, University of Porto, Portugal.[4]CESPU – Instituto de Investigação e Formação Avançada em Ciências e Tecnologias da Saúde, Portugal.
[*]fdiniz@ipatimup.pt

INTRODUCTION

Gastric cancer (GC) represents the fifth most incident and the third most lethal cancer in the world. Thus, find an effective treatment of GC remains a therapeutic challenge[1]. Recently, nanoparticles (NPs) have been widely used as an innovative tool to specifically deliver drugs into tumor cells, minimizing cytotoxicity and drug's off-target effects in normal cells. To increase the specificity of NPs for the target site, specific ligands, such as glycans, can be attached to the surface of the NPs[2]. Glycan structures are present on the cell's surface. An altered glycan pattern can occur in cells due to different expression of specific enzymes involved in glycosylation and can be associated with the induction of malignant phenotypes in cancer. Sialylated glycans are aberrantly and exclusively expressed in several epithelial cancers, including GC, being important antigen targets for a delivery nanosystem[3]. Thus, our aim was the development of functionalized NPs with an antibody targeting a specifically sialylated glycan and validate the specificity and recognition capacity of this new nanosystem. Usually, the *in vitro* NPs tests are performed under static fluid conditions without any shear stress. However, flow exposure reveals to be an important biomechanical parameter that should be taken into account[4]. Therefore, in this work we evaluated the behavior of the novel NPs under static and flow conditions.

EXPERIMENTAL METHODS

Poly(lactic-co-glycolic)-polyethylene glycol (PLGA-PEG) COOH NPs were produced by nanoprecipitation method and loaded or not with a hydrophobic tyrosine kinase inhibitor (TKI). Then, NPs were surface functionalized by carbodiimide chemistry method with an antibody targeting a sialylated glycan (NP-Gly). As a control, we used unspecific IgG antibody (NP-IgG) The physicochemical properties of NPs were assessed by DLS, ELISA, LC-MS and TEM. To confirm the presence of the antibody on NPs surface we performed an ImunoTEM. The targeting ability and the specificity of these NPs to the cells were assessed under static fluid conditions using flow cytometry and immunofluorescence methods. For under flow experiments, live cell imaging was performed using fluorescence widefield microscopy. We used two GC cell models with different expression levels of the targeted sialylated glycan: MKN45 SIA (positive expression of the sialylated glycan) and MKN45 WT (negative expression of the sialylated glycan).

RESULTS AND DISCUSSION

We showed a successful production of NPs ranging from 140-220nm, with a polydispersity index around 0.2 and a surface charge ranging between -18 and -12mV. Functionalized NPs with an antibody targeting a specific sialylated glycan and IgG1 were developed, and the conjugation efficacy was 85% and 75%, respectively. ImunoTEM demonstrated the successful conjugation of NPs with the monoclonal antibody. Our in vitro assays showed that under static conditions NP-Gly specifically binds to MKN45 SIA and not to the MKN45 WT (Figure1 A and B). Furthermore, the targeting ability and specificity of the NPs is maintained under flow conditions since we observed aggregates of NP-Gly binding only to the MKN45 SIA cell model. The control NP-IgG did not bind to any cell model, reinforcing the specificity of our nanosystem. Finally, we demonstrated the successful encapsulation of TKI, with an association of encapsulating up to 50% of 1mg of TKI and a drug loading capacity was about 2.2%.

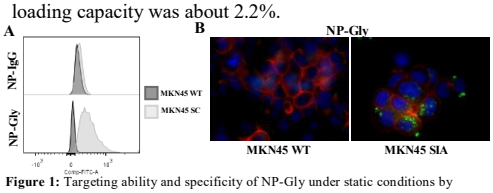

Figure 1: Targeting ability and specificity of NP-Gly under static conditions by Flow cytometry (A) and Immunofluorescence (B).

CONCLUSION

We developed a NP conjugated with an antibody against a glycan that is able to interact specifically with a sialylated glycan-expressing cancer cells under static and flow conditions. This work unveils the importance of using a potential platform for the live tracking of NPs that plays a crucial role in simulating physiological flow and better mimics the *in vivo* environment. Additionally, this developed nanosystem can be also applied in *in vitro* drug studies. The specificity of these novel NPs demonstrates a great potential to be translated to *in vivo* studies of drug delivery.

REFERENCES

1. Smyth E. *et al*., Annals of Oncology, 27:v38-v49, 2016;
2. Diniz F. *et al*., Cancers, 14.4: 911, 2022;
3. Mereiter S. *et al*., Cancer Cell, 36.1:6-16,2019;
4. Martínez-Johtar L. *et al*., Nanomaterials, 10.7:1353, 2020.

ACKNOWLEDGMENTS

Financial support from FCT: SFRH/BD/137896/2018.

X-ray phase-contrast micro-tomography for tissue models and bio-materials characterization

E. Longo[1,*], A. Contillo[1], L. D'Amico[1,2], G. Saccomano[1,3], G. Tromba[1]

[1] Elettra-Sincrotrone Trieste S.C.p.A., Trieste, Italy
[2]Dipartimento di Fisica, Università degli Studi di Trieste, Trieste, Italy
[3]Dipartimento di Ingegneria e Architettura, Università degli Studi di Trieste, Trieste, Italy

[*]elena.longo@elettra.eu

The development of new biomaterials requires a careful examination of their 3D inner composition, of the structural changes that occur following mechanical, tensile or thermal testing and a specific monitoring of their degradation and of their biological interactions. X-ray micro-tomography in combination with phase-contrast methods allows to visualize low density materials and biological tissues in a non-destructive manner and at high-resolution. Thus, it is today a well-suited method for the 3D characterization of different kind of organ and tissue models (osteoarticular, neural, cardiovascular, etc.) and of bio- materials (scaffolds, ceramics, implants, fibers, etc.) at the microscale. Thanks to the 3D visualization, X-ray micro-tomography is able to support the evaluation of defects due to the material processing, to determine quantitative information (such as material porosity and distribution, fiber orientation, etc.) and to analyze tissues morphology and alterations down to cellular level.
Here, we provide an overview of the imaging methods and possible applications available at the SYRMEP (SYnchrotron Radiation for MEdical Physics) beamline of the Elettra light source in Trieste, Italy [1]. The beamline covers an energy range adequate for biomedical research, pre-clinical applications and materials science. The very versatile setup allows working with monochromatic or white/pink beam, with a wide range of pixel sizes and therefore, adjustable fields of view. The possibility of a long sample-to-detector distance enables the implementation of single distance phase contrast imaging; thus, enhancing soft tissue contrast. In addition, a detector with continuous zoom allows to perform multi-scale imaging of the samples. Thanks to its flexibility, the setup can be adapted for several *in-situ* measurements and for the implementation of other phase-sensitive imaging approaches. An upgrade of the beamline is foreseen within the Elettra 2.0 upgrade program. The new imaging beamline will cover an energy range up to 100 keV and will have a much higher X-ray flux. This will open the path to new imaging modalities and to a broad range of applications in the life science framework.

REFERENCES

[1] C. Dullin et al. "Multiscale biomedical imaging at the SYRMEP beamline of Elettra- Closing the gap between preclinical research and patient applications", Physics Open 6 (2021) 100050.

Comparative fluid permeability study of human tali following nanofracture, microfracture and fine wire drilling, using µCT analysis

James Warren[1,2,3], Ahranee Carden[1,2],Mark Farndon[1, 4] and Claire Brockett[1, 3]
[1]Institute of Medical and Biological Engineering, University of Leeds, Leeds, UK
[2]Faculty of Biological Sciences, University of Leeds, Leeds, UK
[3]Bragg Centre for Materials Research, University of Leeds, Leeds, UK
[4]Harrogate and District NHS Foundation Trust, Harrogate, UK
J.P.Warren@leeds.ac.uk

INTRODUCTION

Current surgical practice for the treatment of osteochondral lesions in the ankle involves using one of three techniques to promote blood flow from subchondral bone tissue to the defect site, improving the rate of healing. These different techniques: - fine-wire drilling, nanofracture and microfracture, involve disrupting the trabecular bone. However, the size and method of these techniques means this varies in terms of penetration depth and diameter. Additionally, each technique causes differing degrees of damage to the trabecular structure, and the ability of fluid to flow through the porous structure. The aim of this study was to compare the influence of the different techniques on the fluid permeability of the tissue following by assessing the flow of radiopaque contrast agent using µCT image analysis.

EXPERIMENTAL METHODS

Fresh-frozen cadaveric tali specimens (n=12) were prepared through creating a 10mm diameter chondral defect in three different regions of each talus. Each region then underwent one of three surgical techniques: 1) Fine wire drilling, 2) Nanofracture or 3) Microfracture, undertaken by a single surgeon.0.1 ml radiopaque contrast agent (Omnipaque™ 300) was then added to each region and imaged using a clinical µCT scanner (SCANCO Medical AG, 73.6 µm resolution) The amount of contrast agent that permeated through each different region was assessed through imaging processing.

RESULTS AND DISCUSSION

The µCT analysis indicated that across the 12 samples, eight nanofracture regions demonstrated flow of contrast agent to the depth of the fracture site or deeper. Some lateral flow was also observed in these sites. Eight microfracture regions demonstrated that the flow of contrast agent was localised to the fracture site and a preferential flow laterally. In only one sample, did a fine wire drilling region demonstrate any fluid flow. In this sample, contrast agent had permeated through the drilling site to the bottom and some sub-site permeation was observed. However, in all samples that showed no permeation of contrast agent through the fracture site, there was a layer of contrast agent on the chondral surface or minor permeation through to the sub-chondral surface. The different regions each procedure created within in the tali tissue is illustrated in Figure 1.

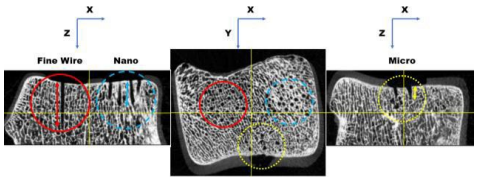

Figure 1: µCT micrographs of a human talus sample. Areas indicate regions of sample where the corresponding surgical technique has been carried out: Red (solid) Fine wire drilling, Blue (dash) Nanofracture and Yellow (dot) Microfracture. Each technique is highlighted with an arrow to illustrate the different depths.

Post injection, the permeation of contrast agent is illustrated in Figure 2.

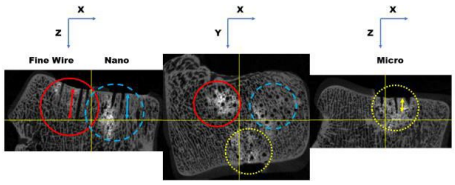

Figure 2: µCT micrographs of a human talus sample, post injection with contrast agent. Same post-injection areas indicate regions of sample where the corresponding surgical technique has been carried out.

CONCLUSION

Nanofracture showed improved fluid permeability throughout the surrounding trabecular structure, when compared to microfracture and fine wire drilling. Microfracture appears to allow some fluid flow, but this is confined to the immediate area around the fracture site, while fine wire drilling appears to allow almost no fluid flow through the surrounding trabecular tissue. This conclusion is reinforced by previous literature[1] that concluded the damage to the structure of the trabecular tissue is reduced when using nanofracture, compared to the other two techniques.

REFERENCES

1. Gianakos A. L. *et al*, Arthrosc. – J. Arthrosc. Relat. Surg., 32:2210-2117, 2016

ACKNOWLEDGMENTS

Materials provided by Joint Operations
Project supported by EPSRC Centre for Doctoral Training in Tissue Engineering and Regenerative Medicine (Grant number EP/L014823/1).

Anosteocytic and osteocytic bones have different water permeability

Andreia Silveira[1], Nikolay Kardjilov[2], Henning Markötter[3], Elena Longo[4], Imke Greving[4], Ron Shahar[5] & Paul Zaslansky[1]
1 Department for Restorative and Preventive Dentistry, Charité-Universitaetsmedizin, Berlin, Germany | 2 Institute of Applied Materials, Helmholtz Centre for Materials and Energy, Berlin, Germany | 3 Bundesanstalt für Materialforschung und -Prüfung (BAM), Berlin, German | 4 Institute of Materials Physics, Helmholtz-Zentrum Hereon, Geesthacht, Germany | 5 Koret School of Veterinary Medicine, The Hebrew University of Jerusalem, Rehovot, Israel
* andreia.sousa-da-silveira@charite.de

INTRODUCTION

Bones are pivotal for the mechanical functions of vertebrates' skeletons and include significant amounts of water that contribute to toughness. Bone material is porous, a biocomposite that comprises nanofibers of collagen protein and nanoparticles of carbonated hydroxyapatite with traces of non-collagenous proteins (γ-carboxyglutamate- containing proteins, proteoglycans, and glycoproteins)[1]. Water occupies various domains in bone, most notably micro-cavities with two major interconnected porosity systems: the vascular system where cavities are > 20 micrometers in diameter, and the lacuna-canalicular network (LNC) consisting of voids with diameters <10 micrometers[2]. The LNC consists of ellipsoidal lacunae where osteocytes reside in the living bone, connected by sub-micrometer-sized channels, known as canaliculi. The osteocytes are thought to sense load applied to bone and translate it into biochemical signals for bone remodeling. The precise mechanism that translates load to mechanical response (mechanotransduction) is not fully understood. Bone poroelasticity models suggest that fluid flow through the porosity of bone plays a critical role in the adaptive response to load. Besides the transport of nutrients and waste to and from the cells residing in the bone, fluid flow is thought to deliver mechanical deformation information across bone by inducing shear stresses, causing deformation of actin filaments in the osteocyte cytoskeletons[3].
However, not all bones have osteocytes embedded in their matrix. Anosteocytic bones are common in fish skeletons. The absence of osteocytes in the bones of most advanced teleosts raises uncertainty about how these bones respond to mechanical load and questions their ability to remodel[4]. To better understand differences and similarities in bone materials, we characterize and compare the anosteocytic and osteocytic bone material in the similar-sized fish of medaka (Oryzias latipes) and zebrafish (Danio rerio). These species are important research models with similar anatomy and ecology. Zebrafish bone has a microarchitecture that resembles mammalian bone, as it is osteocytic, while medaka, lack osteocytes within their bone extracellular tissue. Therefore, such animal models are attractive to investigate bone function and related poroelasticity models. Of the different non-destructive irradiative methods available to image bone material, some have the potential to reveal fluid flow. Neutron radiography and tomography are non-destructive imaging techniques that can track changes in water concentration due to sensitivity to protons (H+).

EXPERIMENTAL METHODS

In this work, we exploit the high sensitivity of neutron imaging to compare water flow through micron-sized domains in anosteocytic medaka and osteocytic zebrafish. We analyze the water exchange using neutron tomography to image hydrated bone samples that we compare with the same samples imaged after being exposed to deuterated water (D_2O). The change, in contrast, makes it possible to quantify how much water is expelled from bone by diffusion. Together with X-ray micro-computed tomography (CT), we find significant differences between the amount of water exchanged within the fishbone matrix, directly comparing bones with and without inbuilt lacuna-canalicular open-pore systems. Additionally, we analyze the micro-nano structure of anosteocytic medaka and osteocytic zebrafish bone using high-resolution phase-contrast tomography.

RESULTS AND DISCUSSION

Unexpectedly, our results identify far more water expelled from anosteocytic medaka bone as compared with osteocytic zebrafish bone. In osteocytic bone, the diffusion of water seems to be restricted and confined to flow within the lacuna-canalicular pore system. In contrast, anosteocytic bone is amenable to D_2O diffusion and exchange, despite the absence of lacuna-canalicular porosity.

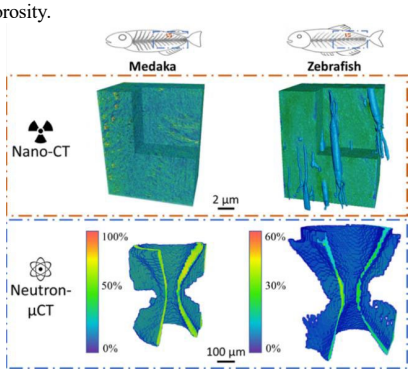

Fig. 1. 3D-renderings obtained from nanotomography data illustrate the compact bone structure of medaka and the osteocytic lacunae system of zebrafish bone. 3D-rendering views of the neutron tomography data show that a higher percentage of water was removed from medaka bone than zebrafish bone. In blue regions, less water was expelled, and in yellow regions, more water was expelled.

CONCLUSION

We postulate that osteocytic zebrafish bone has some mechanism to restrict water diffusion, possibly essential for keeping water in the LNC as part of a poroelastic mechanotransduction system. In contrast, medaka bone structure allows the diffusion of water, which may be an evolutionary alternative to LNC system.

REFERENCES

1. Weiner S. & Wagner H. D., Annu. Rev. Mater. Sci. 28:271–298, 1998
2. Granke M. et al., Calcif. Tissue Int. 97: 292–307, 2015
3. Cowin S. C., J. Musculoskelet. Neuronal Interact. 2: 256–260, 2002
4. Ofer L. *et al.*, PLoS Biol. 17:e3000140, 2019

ACKNOWLEDGMENTS

A. S., P. Z. and R. S. gratefully acknowledge the financial support from the German Research Foundation (Deutsche Forschungsgemeinschaft [DFG]) –ZA557/5. We thank the Helmholtz-Zentrum Berlin für Materialien und Energie for the allocation of beamtime. We acknowledge DESY (Hamburg, Germany) for the provision of experimental facilities. Parts of this research were carried out at PETRA III beamline P05.

Insight by in situ TEM into the nucleation and crystallization processes of calcium phosphate nanoparticles

Gisele Dalmônico[1], Marcos Farina[2], Dris Ihiawakrim[3], Nathaly Ortiz[3], Ovidiu Ersen[3], André Rossi[4*]

[1]LNNANO/Brazilian Center for Research in Energy and Materials, Campinas, Brazil
[2]Institute of Biomedical Sciences, Federal University of Rio de Janeiro, Brazil
[3] Institut de Physique et Chimie des Matériaux de Strasbourg, France
[4]Brazilian Center for research in Physics, Rio de Janeiro, Brazil
[*]alinhares@cbpf.br

INTRODUCTION

In this study, we investigated the aspects of the nucleation, growth and crystallization of hydroxyapatite (HA) nanoparticles not previously addressed in the literature. The process of HA formation is of great interest in biomineralization and material sciences for the development of biomaterials for medical applications. Different classical and nonclassical crystallization mechanisms have been proposed in the literature, but the exact route for HA formation is still under intense debate[1]. In situ TEM (Transmission Electron Microscopy) is a recently developed technique that presents great potential for revealing the important morphological events that take place during HA crystallization in real time. To date, a few studies using in situ TEM have contributed to the convergence of hypotheses regarding calcium phosphate crystallization, mainly during the initial steps of calcium phosphate formation, but the exact timing for the formation of the plate/needle-like crystals has not been recorded until now. This information was recorded in the present work using in situ TEM. Substantial effort was applied during the in situ TEM assays to obtain the appropriate conditions and events required to document the different steps of HA formation, by images and videos. A detailed kinetic model was developed to interpret the thermodynamic environment of the experiment and the possible species formed over time and to compare with the events observed in situ with high spatial resolution.

EXPERIMENTAL METHODS

HA was synthetized just before the analyses by using phosphoric acid and calcium hydroxide solutions. Calcium oxide was heated at 900 °C (5 °C/min) for 3 h to obtain calcium carbonate. 0.863 g of H_3PO_4 was added into 12.5 ml of water (Milli-Q) to prepare the phosphoric acid solution. The pH and the temperature were ~7 and 24 °C, respectively, at the beginning of the synthesis[1]. A TEM liquid cell holder (Protochips - Poseidon Select 550) was used in a JEOL 2100F TEM associated to an EDX detector. The sample solution was isolated from the vacuum environment from the TEM column by two Si_3N_4 membranes isolate. A physical model was developed to interpret the thermodynamic steps and the kinetic pathways for the simultaneous dissolution of calcium hydroxide and precipitation of CaP particles.

RESULTS AND DISCUSSION

The reaction between calcium hydroxide and phosphoric acid solutions was studied by in situ TEM during 6 h and four main steps were observed and recorded: (0-1 h from the beginning of the reaction) dissolution of $Ca(OH)_2$ and formation of a dense liquid phase; (1-4 h) formation of two morphological distinct amorphous calcium phosphate particles; (3-6 h) formation of needles and plates calcium phosphate particles; (5-6) crystallization of needles and plate-like HA. The needle or plate-like morphologies are typical of synthetical and biological HA observed edge-on and thus a strong indication of HA formation.

The kinetic path from the initial moment of the reaction to the equilibrium condition was determined qualitatively and compared to the contour curves showing the saturation indices for different calcium phosphate species and HA. The pH was also calculated and compared to the contour curves. The kinetic model shows a very rapid decrease in pH in the beginning of the reaction. Since calcium oxides dissolves, [Ca] and pH increases allowing the formation of the amorphous calcium phosphate species. With further increases of the pH, the saturation index of hydroxyapatite increased and HA needles and plates-like particles were formed and finely crystallize.

CONCLUSION

In this work different types of amorphous particles were identified during the reaction time, and some of them were intermediate phases for HA nanoparticle formation. The results shown here suggest different routes for HA formation. During biological mineralization processes as for instance bone, redundant mechanisms for collagen mineralization are common, such as mineralization directly on the collagen fibril surfaces or inside the collagen fibrils or biomineralization mediate by matrix vesicle mineralization.

REFERENCES

1. Dalmônico G. *et al.* Mater. Chem. Phys. 237: 121862, 2019.

ACKNOWLEDGMENTS

The authors wish to thank CNPq and FAPERJ, the International Associated Laboratory - Advanced Electron Microscopy for Biomaterials (AEMB) and the International Research Project - Biointerfaces, Biominerals, Biomaterials (B3lab) for financial support.

Quality of newly formed bone and Biphasic Calcium Phosphate resorption in in vivo rabbit study, the difficulty to use the correct thresholding level with microcomputed tomography analysis

Cyril d'Arros[1,2*], Sylvain Catros[3,4], Joëlle Véziers[1,5,6,7], Thierry Rouillon[1,5], Jean-Christophe Fricain[3,4], Marlène Durand[3,8,9], Olivier Malard[1,10], Pascal Borget[2], Guy Daculsi[1]

[1]INSERM, UMR 1229, Regenerative Medicine and Skeleton, ONIRIS, Université de Nantes, Nantes, France ; [2]Biomatlante - Advanced Medical Solutions Group Plc, Vigneux-de-Bretagne, France, *cyrildarros@biomatlante.com; [3]Univ Bordeaux, INSERM U1026, BIOTIS Bioingénierie tissulaire, CHU Bordeaux, F-33000 Bordeaux, France ; [4]Service de Chirurgie Orale, Hôpital Pellegrin, CHU de Bordeaux, Bordeaux, France ; [5]UFR Odontologie, Université de Nantes, France ; [6]INSERM, UMS 016, CNRS 3556, Structure Fédérative de Recherche François Bonamy, SC3M Facility, CHU de Nantes, Université de Nantes, Nantes, France ; [7]PHU4 OTONN, CHU de Nantes, Nantes, France [8]CIC1401, CHU Bordeaux, 33000 Bordeaux, France ; [9]CIC1401, INSERM, Univ Bordeaux, 33000 Bordeaux, France ; [10]Service d'Oto-Rhino-Laryngologie et de Chirurgie Cervico-Faciale, PHU4 OTONN, CHU de Nantes, Nantes, France

INTRODUCTION:

Biphasic Calcium Phosphate (BCP) bioceramics composed of hydroxyapatite (HA) and β-Tricalcium Phosphate (β-TCP) are recognized as osteoconductive and bioactive bioresorbable materials. The higher dissolution capability of β-TCP compared to HA allows to easily form an apatitic layer on surface of the synthetic Bone Graft Substitute (BGS) by precipitation process, which is particularly important to increase bone bonding after *in vivo* implantation. MBCP+ granules (BCP HA/β-TCP, 20/80) were used in the present study as a positive control compared to the new formulation FDBS (Freeze Dried Bone Scaffold) based on the same granules embedded into a water-soluble polymer to improve handling properties.

The micro indentation analysis of explants is an efficient method of characterization for the evaluation of the bioactivity property and the quality of the newly formed bone around BCP material. Because of the close chemical composition and the strong bonding ability of this material with native bone, the resorption profile of BCP granules needed to be evaluated by coupling microcomputed tomography and histological observations to optimize the step of thresholding.

EXPERIMENTAL METHODS:

New Zealand rabbits were used for the *in vivo* implantation. Bone defects were created in both femoral epiphyses (6 mm of diameter and 8 mm of depth) and filled with MBCP+ granules or FDBS (n=6). Explants were harvested after 4, 13 or 26 weeks of implantation and observed by a µCT acquisition (isotropic voxels resolution = 19.18 µm). 3D datasets were later reconstructed and analyzed with NRecon© and CTAn© softwares (Bruker). The greyscale threshold (0-255) was set up at three different levels, 40-84/99/114 for bone and 85/100/115-255 for BCP granules. The effect of the threshold chosen to quantify bone formation and material resorption was evaluated in comparison with histological analysis.

Explants were embedded in PMMA resin without decalcification and a minimum of 3 levels of slides (7 µm) were stained (Goldner's trichrome). Residual material (kinetic of resorption) was quantified (2D analysis) using the NIS Elements© D version 4.2 image analysis software.

The surface of all resin-embedded explants was perfectly grounded. Dynamic Ultra micro-Hardness tester (DUH-211S, Shimatzu) with the following test settings: 40 mN for indentation strength, 13 mN/s for speed of loading/disloading, and 10 s for holding time at 40 mN. were used to determine the elastic modulus (E in GPa) on each localizations analyzed (native bone, newly formed bone, interface on bone side, interface on BCP granule side, and BCP granule).

RESULTS AND DISCUSSION:

The histological analysis showed that both materials (MBCP+ granules and FDBS) were efficient as bone graft substitutes with bone formation observed all around BCP granules for each timepoint, and a slight decrease of the residual material surface measured in histology during the experiment. Visually it seemed that a threshold 85/255 as a limit between BCP granules and newly formed bone was adequate by µCT analysis, but probably due to high bioactivity and the close chemical composition of the BCP granules and bone it is difficult to choose the right threshold's limit. With the correct thresholding (100/255 on the greyscale for BCP granules based on several levels of histological slide observations), the µCT analysis showed a residual material volume constant for the MBCP+ granules and a slight decrease for FDBS after 6 months of implantation. The elastic modulus was measured by micro-indentation coupled with optical microscope observations. The newly formed bone observed into the defect was mature (lamellar organization) for both implanted products (MBCP+ and FDBS) and comparable with native bone. No significant difference was found for native and newly formed bone with an elastic modulus close to 20 GPa. The average value of elastic modulus for BCP granules was estimated at 60 GPa. Interestingly, a clear trend was noticed at each side of the interface with newly formed bone with a decrease of elastic modulus from BCP granules to lamellar bone tissue. The elastic modulus at the interface was comprised between 20 and 40 GPa.

CONCLUSION:

To conclude, a highly bioactive calcium phosphate based BGS must be evaluated with several characterization's methods to use a correct thresholding during µCT image's analysis.

ACKNOWLEDGMENTS:

The authors would like to thank the European project H2020 OrthoUnion (Grant agreement n°733288) that supported this work.

Insitu Liquid Cell Electron Microscopy of acid etching of toothpaste treated dentine and enamel

Christabel E Fowler[1] and Richard M. Langford[2]

[1]GlaxoSmithKline Consumer Healthcare, St. George's Avenue, Weybridge, Surrey, UK.
[2]Department of Physics, Cavendish Laboratory, University of Cambridge, UK

INTRODUCTION

A transmission electron microscope (TEM) liquid cell (LC) enables processes such as nucleation and etching to be followed dynamically with the material system being held in its native wet state(1). Here, a LC has been used to study the acid etching of dentine and enamel treated with a NaF toothpaste.

EXPERIMENTAL METHODS

Dentine discs and enamel blocks were acid etched (0.5 M, 30 seconds). These were then brushed with a toothpaste (containing either 1100 or 1400 ppm NaF) and placed into AS, at 37ºC, for 12 hrs. After three such treatments 60 nm thick slices were ultra microtomed from the discs/blocks. These were placed onto the LC's silicon nitride membranes which create the closed LC through which the electron beam passes in the TEM. The breakdown/radiolysis of the water, by the electron beam was used to lower the water's pH to etch the dentine/enamel. Nano-diffraction, lattice imaging, wavelength and energy dispersive spectroscopy (WDS, EDS) were used to characterize the remineralised dentine, the F substitution in the dentine/enamel and the material occluding the dentine tubules.

RESULTS AND DISCUSSION

The toothpaste treatment remineralised the dentine surface and occluded the tubules. EDS and nano diffraction indicated the observed needle shape crystals nucleated onto the peritubular dentine and across the tubules were fluorapatite (HAF) and that these, within the centre of the tubules, were intermixed with SiO_2 and TiO_2. Figure 1 shows three stills from a movie of the etching of the material occluding a tubule recorded over 12 minutes. The etch rate is a function of the local dose partly determined by the microscope settings and the thickness of solution within the LC. The dentine etched first, then the peritubular and then the occluding material. The HAF needle growth on the peritubular dentine etched 1.5 times slower than the peritubular dentine. The interface, between the nucleated needles and the peritubular etched at a rate 2.1 times slower than the peritubular dentine; attributed to F substitution having occurred at the surface of the peritubular dentine. In some of the etching experiments, demineralisation and then intra remineralisation of the collagen ropes/fibres was observed, i.e., the 60 nm characteristic banding reappeared.

Figure 2 shows the slower etching of the top surface/edge of the treated dentine recorded over 7 minutes. WDS analysis showed that the top edge had a F signal 2 to 3 times (0.6-1 at. %) than that in the dentine away from the surface. The microstructure of this remineralised top edge was similar to that of the bulk dentine; it did not exhibit needle shaped HAF. The slower etching and higher F are attributed to F substitution into the HA of the remineralised collagen.

In the enamel work the toothpaste treatment resulted in the edges (surfaces) of the enamel prisms etching slower (attributed to F substitution). TEM analysis also showed that toothpaste formed material was bridging between the etched prisms. The volume of solution and thickness of the slices varied between LC set ups/experiments. This affects the radiolysis, resolution, etching rates and steady state imaging conditions, which prevents a direct comparison of the etching rates between samples treated with different toothpastes. However, the relative etch rate of the prism edges relative to the centre of the prism of the enamel treated with the toothpaste containing 1400 ppm was 1.15 times slower than that of the enamel treated with the 1100 ppm toothpaste.

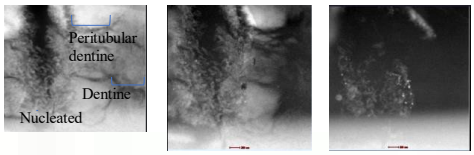

Figure 1. Stills showing the etching of the dentine, peritubular and occluding material. (Scale bar 200 nm).

Figure 2. Stills the etching of the top edge of the treated dentine. (Scale bar 300 nm).

CONCLUSION

The insitu LC can be used to study in real time the acid etching of dentine and enamel treated with different toothpaste formulations providing insights between the toothpaste composition, formed material, F substitution and the resulting acid resistance.

REFERENCES

1. Sinclair R. 2013*In situ* high-resolution transmission electron microscopy of material reactions. MRS Bull. 38, 1065-1071.

Tailored Synthesis and Biotin-functionalization of Dual-colored Silica Nanosystems for Biomedical Approaches.

Maria Antonieta Ramírez-Morales[1,2*], Elisa Di Luca[3], Giuseppe A. Mele[2], Pier Paolo Pompa[4], Maria Ada Malvindi[1]

[1]HiQ-Nano s.r.l., Via Barsanti 1, 73010, Arnesano. Lecce, IT.
[2] Department of Engineering of Innovation, University of Salento, via per Arnesano km 1, Lecce 73100, Italy
[3] Nanotechnology Institute, CNR-NANOTEC, Monteroni Street, 73100 Lecce, Italy
[4] Nanobiointeractions & Nanodiagnostics, Istituto Italiano di Tecnologia (IIT), via Morego, 30-16163 Genova, Italy

[*] mariaantonieta.ramirezmorales@studenti.unisalento.it Maria.Ramirez@hiqnano.com

INTRODUCTION

Fluorescent nanoparticles are widely used in biomedical approaches such as drug-delivery, sensing and imaging. In addition, some biomolecules are able to functionalize their surface increasing the possibilities as potential diagnostic and therapeutic systems[1-2]. Quantify and control the number and distribution of active sites is of fundamental importance for the development of responsive and super-selective nanosystems applications[3].

Usually, fluorescent nanoparticles are composed of a single dye for their localization and study. In this work, the optimized protocol to obtain highly monodispersed, stable and well-defined silica dioxide (SiO_2) nanoparticles is described. Providing an unique dual-colored nanosystems with Atto 647N and Oregon green *488.* Which were later functionalized with biotin to improve dispersion and for a subsequent analysis using super-resolution imaging techniques as STED and STORM.

EXPERIMENTAL METHODS

For the encapsulation of dyes, a new method called two-cycles Stöber method was performed, changing the volume of the dyes and its activation with APTES.

Different mass ratios between nanoparticles and biotin (1:1, 3:1, and 5:1) were prepared by a bath sonicator during 30 minutes and stored at 4°C.

Z-potential were measured by DLS technique using a Zetasizer NS system. Size and morphology of nanoparticles were investigated by Transmission Electronic Microscopy (JEM-2200FS). The emission fluorescence was investigated using TECAN dispositive (200 PRO NanoQuant) and by Confocal microscopy.

RESULTS AND DISCUSSION

Well-defined, spherical nanoparticles of 25, 50, 100 and 250 nm in diameter were synthesized (Fig 1).

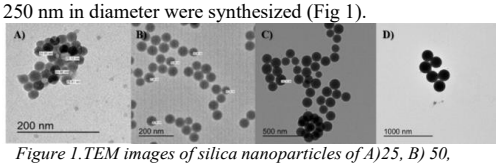

Figure 1.TEM images of silica nanoparticles of A)25, B) 50, C)100 and C) 250 nm

For the dyes analysis, it is possible to observe the colored solution under UV light, checking its presence with TECAN emission and under the confocal microscope, both dyes are clearly observed and a very bright and stable signal is generated by the nanoparticles (Fig 2).In merged image (Fig.2C) the co-localization of Atto 647N and Oregon green 488 gives yellow-orange colored areas.

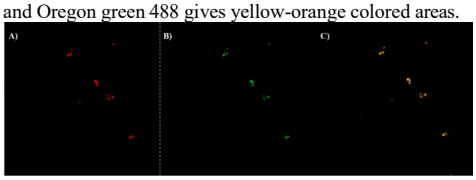

Figure 2.Confocal microscopy images of 250 nm Dual-colored nanosystem on a glass slide. A) Atto 647N dye emission, B) Oregon green 488 dye emission and C) merged image.

To study the dispersion of the suspensions using biotin and biotin-NHS, Z-potential measurement was carried out to study at different mass ratios and sonication times.

In both cases, the excess of nanoparticles gives a better distribution compared to the equal proportion. For simple biotinylation the optimum ratio corresponds to 3:1 while for biotin-NHS the ratio 5:1 obtains better results. Although considering the size of biotin it is not possible to observe it using TEM, the suspensions were characterized to observe the final size of the system. So far, the nanosystems carried out and optimized under study are in a range between 200-250 nm.

CONCLUSION

Fluorescent nanoparticles are considered one of the most promising tools in biomedical approaches. This work proposes the optimized synthesis of dual-colored nanosystems, to be used in diagnosis, sensing and imaging. Likewise, the functionalization with biotin has been optimized to improve the dispersion for its subsequent study by STED and STORM.

REFERENCES

1. Jiang, W. *et al*., Int J nanomed, 14, 5611-5622. 2019.
2. Shahrzad, D. *et al*., Chim Acta, 1030, 142-147. 2018.
3. Chen, G. *et al*., Dyes and Pigments, 93, 1532-1537. 2012.

ACKNOWLEDGMENTS

The autors would like to that to the Project 860914 financed through Maria Sklodowska Curie, Innovative Training Networks. Call: H2020-MSCA-ITN-2019

A Protein-based Multiplex Assay to Screen Osteogenic Properties of Calcium Phosphate Biomaterials with Inorganic Additives

Maria Eischen-Loges[1*], Zeinab Tahmasebi Birgani[1], Yousra Alaoui Selsouli[1], Martijn van Griensven[1], Vanessa LaPointe[1] and Pamela Habibovic[1]
[1] MERLN Institute for Technology-Inspired Regenerative Medicine, Maastricht University, Maastricht, Netherlands
[*] maria.eischen-loges@maastrichtuniversity.nl

INTRODUCTION: The intrinsic healing capacity of bone tissue often falls short in critical-sized bone defects. In this context, off-the-shelf–available and synthetic bone graft substitutes such as calcium phosphate (CaP)–based biomaterials are already widely used in clinical applications.[1] The properties and clinical performance of these biomaterials remain, however, inferior to those of an autologous bone graft, which is still considered the gold standard treatment for these defects.[2] Doping CaPs with inorganic additives such as strontium, copper or magnesium is considered a promising method to improve their performance.[3] Here, we propose a targeted protein multiplex assay as a screening tool to improve the in vitro evaluation of such biomaterials and to gain a better understanding of their effect on osteogenic differentiation.

EXPERIMENTAL METHODS: Cell culture plates were coated with CaP doped with a range of inorganic additives including Sr^{2+} (CaP+Sr), Mg^{2+} (CaP+Mg), Mn^{2+} (CaP+Mn), Cu^{2+} (CaP+Cu), and Zn^{2+} (CaP+Zn) as previously described and characterized.[4] Human mesenchymal stem cells (hMSCs) were seeded on the coatings. HMSCs in basic medium (BM) and osteogenic induction medium (OM) were used as controls. Cell morphology and adhesion were assessed, and an MTT assay was done to determined cell metabolic activity. A multiplex protein assay to detect analytes related to osteogenesis, angiogenesis, and immunomodulation was performed in medium supernatant and in the cell lysate. Osteogenic differentiation was confirmed by an alkaline phosphatase (ALP) assay and a qPCR panel.

RESULTS AND DISCUSSION: Multiplex analysis showed differences in protein expression in hMSCs on the different CaP coatings with inorganic additives (Fig. 1). The effect of different inorganic additives was described in terms of hMSC stemness, osteogenic, angiogenic, immunomodulatory, and other markers. Differences in angiogenesis-related markers in hMSCs on CaP+Mn as compared to the control in BM and on CaP without additive incorporation indicated a beneficial effect of CaP+Mn on angiogenesis, which needs to be analyzed further. Gene expression analysis showed an upregulation of the osteogenic transcription factor RUNX-2 in hMSCs in OM, and on CaP+Mn and CaP+Cu at day 7. BMP-2 was upregulated in hMSCs on all coatings at day 7 and on CaP+Mn at day 21 as well. ALP activity was diminished in hMSCs on all coatings at day 7, except in CaP+Zn where no difference was detected. At day 21, ALP activity was increased in hMSCs in OM and decreased in hMSCs on CaP+Cu. BMP-2 was upregulated in hMSCs on all coatings at day 7 and on CaP+Mn at day 21 as well. ALP activity was decreased in hMSCs on all coatings at day 7, except in CaP+Zn where no difference was detected. At day 21, ALP activity was increased in hMSCs in OM and decreased in hMSCs on CaP+Cu.

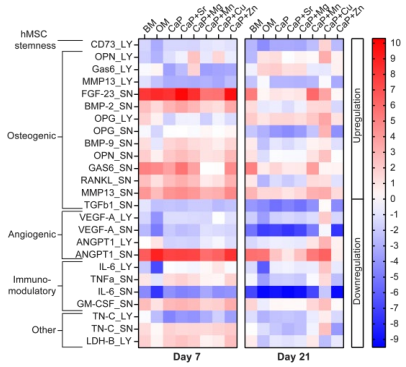

Figure 1. Multiplex protein analysis of hMSCs on CaP coatings measured in the supernatant (SN) and lysate (LY).

CONCLUSION: Here, we presented our efforts on screening osteogenic, angiogenic, and immunomodulatory properties of CaP-based biomaterials with inorganic additives using a protein multiplex-based tool. The protein multiplex assay, combining several relevant analytes, generated a substantial amount of biological data and allowed a better insight in the functional capacity of CaP-based biomaterials with inorganic additives. Protein profiles of CaP-based biomaterials were detected and biomaterials of interest were highlighted. The potential angiogenesis inducing effect of the CaP+Mn biomaterial will be explored further.

REFERENCES

1. Jeong J. *et al.*, Biomater. Res. 23(1): 1-11, 2019
2. Habraken W. *et al.*, Mater. Today. 19(2): 69-87, 2016
3. Schamel M. *et al.*, Mater. Sci. Eng. C 73: 99-110, 2017
4. Habibovic P. *et al.*, J. Am. Ceram. Soc. 85(3): 517-522, 2002

ACKNOWLEDGMENTS: This research has been made possible with the support of the Netherlands Organisation for Scientific Research Vidi grant (15604), the Dutch Province of Limburg (LINK project) and the Interreg Vlaanderen/ Nederland project 'BIOMAT-on-microfluidic-chip'. PH gratefully acknowledges the Gravitation Program 'Materials-Driven Regeneration', funded by the Netherlands Organization for Scientific Research (NWO) (024.003.013). ZTB gratefully acknowledges the NWO grant for women in STEM (Project 'Biotetris').

Does the Composition of Bioceramics for Bone Regeneration Impact Osteocyte Response?

Mathilde Palmier[1*], Hélène Doat[2], Mathilde Fénelon[1], Marlène Maître[2], Thierry Leste-Lasserre[2], Claudine Boiziau[1], Delphine Maurel[1]
[1]Inserm, U1026 BioTis, Université de Bordeaux, Bordeaux, France
[2]Inserm, U1215 Neurocentre Magendie, Université de Bordeaux, Bordeaux, France
*mathilde.palmier@u-bordeaux.fr

INTRODUCTION

Bone constantly remodels and has the capacity to repair. In some circumstances, when a large amount of bone is missing, the repair is impossible creating a critical-size defect. In these cases, the gold standard is an autograft but the quantity of bone available is limited and there is a risk of comorbidity at the donor site. Another option is to use a biomaterial to fill-in the defect and to help the bone regeneration and vascular propagation, necessary for an efficient and complete repair.

The three main types of cells in bone are the osteoclasts (bone-degrading cells), the osteoblasts (bone-forming cells) and the osteocytes (representing 90% to 95% of the cells). Osteocytes are able to communicate with osteoclasts and osteoblasts to orchestrate bone turnover, and they play a role in both phosphate metabolism and calcium availability[1].

Biomaterials called calcium phosphates are used in clinics and contribute to bone regeneration. Commercially available β-TCP (β-TriCalciumPhosphate) and bovine bone powders are known for their biocompatibility, osteoconduction and degradability properties.

The impact of biomaterials on osteoclasts and osteoblasts has been studied but little is known about the impact on osteocytes and their role in the repair process. As today no biomaterial can widely replace the gold standard, it suggests that not all requirements are met. Studying the involvement of osteocytes in bone regeneration and their response to biomaterials during fracture healing could bring new elements to help their optimization.

Here we compare the impact of β-TCP and bovine xenograft with a condition without biomaterial on osteocytes in a mouse calvarial (top part of the skull) defect during the early healing phases. We investigate the impact of the defect creation and the ion release by the biomaterials on osteocyte viability and phosphate regulation.

EXPERIMENTAL METHODS

Critical-size defects were performed in the calvaria of mice. The defects were filled with powders of β-TCP and bovine bone. The healing efficiency was assessed after 72 h and 2 weeks with and without biomaterials (6 groups, n=8 per group).

We evaluated the bone regeneration thanks to microCT imaging. We compared the percentage of empty lacunae at the defect site after immunohistochemistry. We collected osteocytes thanks to Laser Capture Microdissection and studied the changes in osteocyte gene expression *in vivo* for 6 genes of interest.

RESULTS

We evaluated the percentage of regeneration at 72h and 2 weeks for the different conditions. Then we assessed the osteocyte death near the empty defect by quantifying the number of empty lacunae. We also investigated if the biomaterial implantation increased the osteocyte death near the defect. Osteocytes were collected near the defect empty or filled with biomaterials, and after 72h and 2 weeks. The gene expression for phosphate regulation was compared between the different conditions.

CONCLUSION

This work will help to better understand how osteocytes react after a critical defect and to the presence of bioceramics to promote bone regeneration. The role of the biomaterial composition at the beginning of the healing process is evaluated to decipher new directions of optimization.

REFERENCES

[1]Bonewald LF. The Amazing Osteocyte. J Bone Miner Res. 2011; 26(2): 229-238

ACKNOWLEDGMENTS

This work is supported by the BioTis laboratory, Inserm U1026, Université de Bordeaux.
The authors thank the animal facility of Bordeaux University.

Granular PEG hydrogels mediate osteoporotic MSC clustering via N-cadherin influencing the pro-resorptive bias of their secretory profile

Varsha V. Rao[1,2], Marissa E. Wechsler[3], Emily Cravens [4], Samantha Wojda[4], Alexander S. Caldwell[1,2], Bruce E. Kirkpatrick[1,2,5], Seth Donahue[4], Kristi S. Anseth[1,2]

1. Department of Chemical and Biological Engineering, University of Colorado, Boulder **2.** BioFrontiers Institute, University of Colorado, Boulder **3.** Department of Biomedical Engineering and Chemical Engineering, University of Texas, San Antonio **4.** Department of Biomedical Engineering, University of Massachusetts, Amherst **5.** Medical Scientist Training Program, University of Colorado Anschutz Medical Campus, Aurora

INTRODUCTION

Bone marrow derived mesenchymal stem/stromal cells (MSCs) are involved in bone homeostasis; both directly by differentiating into adipocytes and/or osteoblasts and indirectly by secreting factors to influence osteoblast proliferation, osteoclast fusion, and immune cell polarization[1]. In post-menopausal osteoporosis, a bone disorder where the loss of estrogen leads to a pro-resorptive bone marrow environment causing bone mineral density[2], changes to MSC differentiation behaviors have been observed. For example, MSCs isolated from osteoporotic patients are biased towards adipogenesis and have impaired osteogenic differentiation[3]. However, less is understood about the osteoporotic mediated changes to MSC secretory properties. Previous literature has demonstrated TCPS culture is not sufficient to elevate MSC secretory properties and enable their study [4]. Therefore, we utilized granular porous scaffolds comprised of PEG-based spherical hydrogels, called microgels, to study the secretory properties of MSCs isolated from a rat model of postmenopausal osteoporotic (OVX rMSCs).

EXPERIMENTAL METHODS

Multi-functional poly(ethylene glycol) macromers were functionalized with dibenzocylcooctyne (DBCO) and azide (N_3) groups respectively using HATU. Individual microgels were synthesized using a SPAAC reaction in an inverse phase polymerization in hexane under varying degrees of shear to achieve three particle populations: with average microgel diameters ~200 µm, ~100 µm, and ~10 µm as previously reported[5]. 14-weeks post-surgery, rMSCs were isolated from the bone marrow of rats (n=7) that underwent either an ovariectomy (OVX) or sham surgery (SHAM). Populations of excess DBCO and excess azide microgels, both functionalized with 1mM RGD, were centrifuged together with SHAM and OVX rMSCs (~5 million cells/mL) to create covalently bound cell-laden microgel scaffolds. Cells were stained with DAPI and Rhodamine Phallodin (1:500) and imaged on a Nikon Spinning Disc microscope (n=3 gels). After 4 days of culture, rMSC secreted factors (n=3 gels) were quantified using a membrane-based Rat Cytokine Array C2 (RayBiotech) following the manufacturer's protocol. RNA was collected and purified after 24 hours of seeding on TCPS using the RNeasy Micro Kit, cDNA (2ng/µL) was created using iScript super mix, and RT-qPCR was performed using a SYBR green mix. Student's t-test or a one-way ANOVA was performed.

RESULTS AND DISCUSSION

Both SHAM and OVX rMSC clustering phenotypes were directly correlated to the pore architecture in the granular scaffolds (Figure 1a). Cells in ~10µm diameter microgel scaffolds resided as single cells, while cells in ~100µm and ~200µm diameter microgel scaffolds were present as small and large clusters, respectively. OVX rMSCs cultured in large clusters secreted higher concentrations of pro-resorptive factors, include MCP-1, TIMP-1, and TNF-alpha when compared to large clusters of SHAM rMSCs (Figure 1c). Additionally, this bias was not observed when cells were cultured as single cells or in small clusters. Therefore, we queried the expression of various cadherins, molecules involved in cell-cell interactions. OVX rMSCs had significantly higher expression of CDH2 or N-cadherin relative to SHAM (Figure 1b). Interestingly, blocking N-cadherin interactions in large clusters of OVX and SHAM rMSCs diminished the differences in pro-resorptive cytokine secretion between the two cell types (Figure 1d).

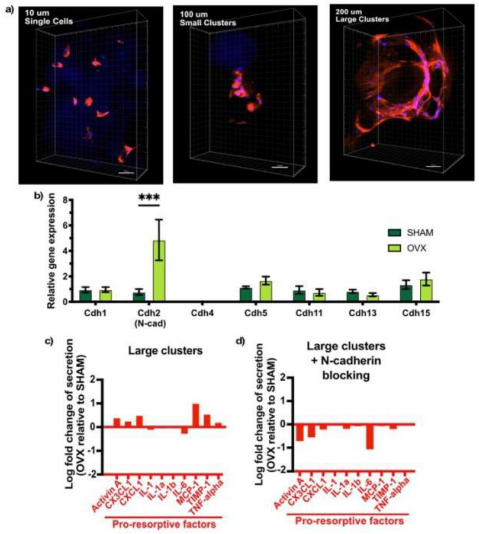

CONCLUSION

In this study, we utilized granular hydrogels to study the secretory properties of OVX rMSCs and determined that they were biased towards a pro-resorptive secretory profile as compared to control rMSCs. Further, this bias was in part regulated by N-cadherin interactions. This study increases our understanding of osteoporotic MSC secretory behaviors to inform the future design of MSC-based therapies to treat fractures in post-menopausal osteoporotic environments.

REFERENCES 1. Yu, B. *et al.,* Trends in Molec. Med. (2016) 2. Eastell, R. *et al.,* Nat. Rev. Primer (2016) 3. Tewari D, *et al.,* Stem Cell Reviews and Reps (2015) Qazi, T. et al. Biomat. (2017) 4. Caldwell A. *et al.,* Biomat (2020).

FUNDING: NIH (R01 DE016523), NSF (1854108)

Actomyosin Cortex Dynamics in the Wound Healing of Cardiac Fibroblasts

Aina Gallemí Pérez[1*], Marco Tarantola[1]

[1]Max Planck Institute for Dynamics and Self-Organization, Göttingen, Germany
* aina.gallemi-perez@ds.mpg.de

INTRODUCTION

In synthetic biology, identifying features that may lead to positive interactions with biological systems is a challenge. In this regard, the actomyosin cortex, which is highly engaged during cellular spreading and migration, and hence in wound healing[1], should be highlighted. This is especially relevant in cardiac research, where fibroblasts undergo the fibroblast-to-myofibroblast transition (FMT) -which can lead to fibrosis and cancer development[2]- to acquire increased mobility[3]. Here, we aim to 1) characterize the cortex through adhesion, to which we employ compression analysis based on atomic force microscopy (AFM)[4], and 2) further describe the wound healing dynamics of cardiac fibroblasts, as it could lead to strategies to avoid FMT-derived drawbacks. With the electrical cell substrate impedance sensing (ECIS), we assess the impedance-based wound healing dynamics of cells on gaps of different sizes, and the corresponding micromotions: ventral fluctuations associated to their viability and metabolic activty[5]. Finally, we make use of fluorescence imaging to optically identify the mechanisms that the cells follow during recovery, and relate them to the impedimetric results. The combination of techniques here employed provides a comprehensive description of the adaptability of the actomyosin cortex and its impact on recovery dynamics and mechanism throughout wound size.

EXPERIMENTAL METHODS

AFM cortex characterization: Cortex rheology of strongly and weakly adherent single cells is determined using an MFP-3D AFM (Asylum Research) with tipless cantilevers. 10 compression-relaxation force curves are measured per cell, and 30 cells per category. The force curves are fitted using the Evans model to access pre-stress (T_0), area compressibility (K_A) and fluidity (Ω).

ECIS-based healing dynamics and micromotions: We employ the ECIS ZΘ (Applied BioPhysics Inc) to monitor the frequency-dependent complex impedance of cells through wounding and recovery following initial monolayer formation. Different wound sizes are tested (250–67 µm). Time courses are fitted to a sigmoidal curve to obtain recovery half time ($t_{1/2}$) and rate (R). Data intervals every 24 h are fitted to the Lo-Ferrier equivalent electric circuit to determine barrier resistance (R_b), reflecting cell-cell contacts, membrane capacitance (C_m), and α, proportional to cell-substrate distance.
Micromotions are recorded at the same time points (28 pps for 2 min) for big wounds (250 µm). Long-term correlations, based on detrended fluctuation analysis, and variance are computed. Each category and time point have a sample size of min. 3 replicates.

Fluorescence imaging: ECIS samples on different wound sizes are fixated and immunostained for myosin, F-actin, and nuclei over the first 17 h of recovery. Micrographs are qualitatively assessed based on cell shape and actomyosin structure.

Statistical analysis: The Two-Sample Tests routine of IgorPro (Wavemetrics), based on Wilcoxon rank-sum test and T-test, is used to determine significance based on p-values of 0.1, 0.05 and 0.01.

RESULTS AND DISCUSSION

AFM results indicate that cell cortex fluidizes on strong adhesion. Regarding healing dynamics, based on $t_{1/2}$, smaller gaps close significantly faster. However, R suggests that while within bigger and smaller wounds the closure pace is similar, velocity differs amongst them, being the 100 µm wound the threshold. The evolution of R_b, C_m and α reflects that upon 48 h of recovery, cells stay far from the surface in bigger wounds (250 µm), where an R_b overshoot suggests fibrosis progression. Optical imaging reveals that in these bigger gaps, cells migrate towards the wound by aligning towards its center, while in smaller ones, the alignment is radial to the wound perimeter. Together, these differences suggest that cells may use different closure mechanisms based on wound size. Micromotion analysis reveals that upon wounding, fluctuations are significantly increased.

CONCLUSION

Here we show that wound size may discern healing mechanisms, being fibrosis observed only in large wounds, for which micromotions remain increased. This could offer a research target to prevent FMT-derived complications. We also observe cortex fluidization upon adhesion, for which biomaterials with adaptative rheological properties could offer advantages.

REFERENCES

1. Chugh P. *et al.*, Nat. Cell Biol. 19:689-697, 2017
2. Parichatikanond W. *et al.*, Front. Cardiovasc. Med. 7:34, 2020
3. Baum J. *et al.*, Cardiovasc. Pharmacol. 57(4):376-379, 2011
4. Cordes A. *et al.*, PRL. 125:068101, 2020
5. Tarantola M. *et al.*, Integr. Biol. 2:139-150, 2010

ACKNOWLEDGMENTS

The authors thank the VW foundation ("Living Foams": M.T) for providing financial support to the project.

Proteomic response of J774A.1 macrophages to biomedical Grade CoCr: Effect of wear

Luna Sánchez-López [1,2]*, Noelia Ropero de Torres[2], Belén Chico[1], Vivian de los Ríos Benítez[2], María Lorenza Escudero[1], María Cristina García-Alonso[2], Rosa Mª Lozano[2]
[1]Centro Nacional de Investigaciones Metalúrgicas (CENIM), Consejo Superior de Investigaciones Científicas (CSIC), Madrid, Spain
[2]Centro de Investigaciones Biológicas-Margarita Salas (CIB-MS), Consejo Superior de Investigaciones Científicas (CSIC), Madrid, Spain
* e-mail of Authors: luna.sanchez@cenim.csic.es, rlozano@cib.csic.es

INTRODUCTION

Wear-corrosion processes in CoCr joint replacements stimulate chronic inflammation and bone destruction that may ultimately result in implant loosening.

Analysis of macrophage proteome may reveal new insights in molecular mechanisms and signaling pathways being trigger upon biomaterial interactions. The effect of wear-corrosion processes on macrophage cellular response was here analyzed through a proteomic approach.

EXPERIMENTAL METHODS

Tribological tests were performed in a pin-on-disc tribometer by using a cylinder of CoCr of 7 mm diameter as pin and CoCr disks of 38 mm diameter. A normal load of 5N at a rotation rate

Effect of the friction process is shown in Figure 2 through the Volcano plot, showing the Differentially Expressed Proteins (DEPs) upregulated (red) or downregulated (blue) between pair of groups.

Downregulated DEPs suggested mitochondrial impairments (DEP Trap1) as well as impaired intra-Golgi trafficking (DEPs Napa, Nsf). Mitochondrial dysfunction upon metal particle exposure has already been described[2]. Impaired Intra-Golgi trafficking might be directly related with the mitochondrial impairment, since mitochondrial dysfunctional might induce a decrease in ATP production, necessary for correct intracellular trafficking.

Hmox1 is a known antioxidant stress protein involved in redox and metal ion homeostasis, involved in the Oxidative Stress

Enhanced Neurite Growth of Human Neuroblastoma Cell Line SH-SY5Y on Nanogrooves in Polystyrene and Polydimethylsiloxane

Lukas Matter[1*], Claas Müller[2], Maria Asplund[1,3,4,5]

[1] Department of Microsystems Engineering (IMTEK) - Bioelectronic Microtechnology Group, University of Freiburg, 79110 Freiburg, Germany
[2] Cluster of Excellence livMatS @ FIT – Freiburg Center for Interactive Materials and Bioinspired Technologies, University of Freiburg, 79110 Freiburg, Germany
[3] Center BrainLinks-BrainTools, University of Freiburg, Freiburg, Germany
[4] Division of Nursing and Medical Technology, Luleå University of Technology, Luleå, Sweden
[5] Freiburg Institute for Advanced Studies (FRIAS), University of Freiburg, Freiburg, Germany
[*] Lukas.matter@imtek.de

INTRODUCTION

Application of electric fields (EFs) after spinal cord injury was shown to enhance axonal regeneration. Neurons grow towards the cathode crossing the lesion and potentially forming functional synapses. Prior to in vivo studies these findings were made in vitro. Typically, cells were seeded into a microchannel because there the EF distributes homogeneously[1].

The aim of this study is to assess the usability of nanogrooves to guide axonal growth as a first step in the development of a microfluidic device to analyse the regeneration of neurons after electrical stimulation. Aligned neurons in the microchannel would be beneficial for decoupling axonal regrowth from other cellular responses e.g. sprouting or reconnection.

As materials under investigation polydimethylsiloxane (PDMS) and polystyrene (PS) were chosen based on several reasons including their well-documented biocompatibility and their optical transparency. PS is furthermore evaluated as an alternative to PDMS since it is hydrophilic and displays much lower absorption of cellular molecules[2].

EXPERIMENTAL METHODS

Cell culture: SH-SY5Y were grown in standard culture wells (Nunc, 150628), on nanostructured PDMS and PS (3 specimen per substrate). All surfaces were coated with laminin (Sigma, L2020) (2 µg) before use. In order to induce differentiation, retinoic acid (RA) (Sigma, R2625) (10 µM) was added to Dulbecco's Modified Eagle's Medium (Gibco Life Technologies (Gibco), 11965092), supplemented with fetal bovine serum (Gibco, 3505051) (2.5%), 1x penicillin/streptomycin (Gibco, 15140122) and 1x Glutamax (Gibco, 35050061). Medium was exchanged every 2 days. Cultivated cells were maintained at 37°C/5% CO_2.

Cell analysis: After 17 days of differentiation cultures were pictured under a microscope equipped with a 10x objective. NeuronJ[3] was utilized to measure neurite length.

Substrate fabrication: Nanogrooves were fabricated by thermal nanoimprint lithography on PS and PDMS. The stamp was structured with 500 nm deep and wide grooves with a pitch of 1000 nm.

RESULTS AND DISCUSSION

On flat surfaces SH-SY5Y grew in a randomly-oriented fashion without any preferential direction of growth. In contrast, cell bodies, axons and most dendrites aligned along the groove lines on PS and PDMS (Fig. 1 A-C). The length of the neurites was 51.1 µm, 57.1 µm and 76.6 µm for flat, nanostructured PS and PDMS surfaces, respectively (Fig. 1 D). Furthermore, a similar seeding density resulted in a smaller number of cells on the nanostructured substrates especially in the case of PDMS.

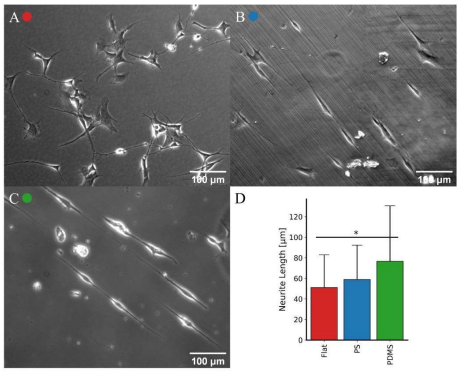

*Figure 1 Cells on flat surface (A) grow with random orientation but align on nanostructured PS (B) and PDMS (C). Neurite length is increased on nanostructured PS and PDMS (D). *p < .01 one-way ANOVA.*

CONCLUSION

Nanogrooves in PS and PDMS lead to an increased length of neurites and guide their growth. On PDMS neurites were the longest on average, but cell viability seemed the lowest. This has to be investigated further and be considered in the future development of a microfluidic device.

REFERENCES

1. Jack A. S. et al, Journal of Neurotrauma, 37:1933-53, 2020.
2. Berthier E. et al, Lab Chip, 12:1224-37, 2012.
3. Meijering E. et al, Cyto Part A, 58(2):167-76, 2004.

Determination of Mammalian Cell- Surface Interactions by Quartz Crystal Microbalance

Ayşe Buse Özdabak Sert[1*], Eva Bittrich[2], Fatma Neşe Kök[1], Petra Uhlmann[2]

[1]Molecular Biology and Genetics Department, Istanbul Technical University, Istanbul, Turkey
[2]Leibniz-Institut für Polymerforschung Dresden e.V., Dresden, Germany
[*]ozdabak@itu.edu.tr

INTRODUCTION

Cell/protein adhesion on the surface is crucial for in vivo performance of biomaterials. Chemical as well as physical properties such as topography, charge and stiffness have great impact on the cell attachment process, so their effect on cell attachment should be known to tailor the performance of prospective implants[1]. Cell/protein-surface interactions can be monitored by quartz crystal microbalance with dissipation (QCM-D) in real time, while this label free, non-invasive technique provides characteristic data for specific surface interactions[2].

In this study, first polycaprolactone (PCL) and chitosan (CH) containing thin films were constructed and characterized by several techniques. Currently, cell adhesion on these surfaces is being monitored by QCM-D in order to achieve a better understanding of cell adhesion on material surfaces.

EXPERIMENTAL METHODS

Thin polymer films were constructed by spin coating of the PCL, CH and their blend solutions at 4000 rpm. Their surface morphology was observed by atomic force microscopy (AFM) and their swelling behavior and protein adsorption on their surfaces were analyzed by QCM-D and spectroscopic ellipsometry. For the protein adsorption studies 0.25 mg/mL bovine serum albumin (BSA) solution was used, and adsorption onto surfaces monitored for 1 hour under flow conditions by QCM-D and in a cuvette by spectroscopic ellipsometry at different pH conditions (4.5, 6.0 and 7.4). Fibroblast (3T3) and human fetal osteoblast (hFOB) cell lines are being used for cell adhesion.

RESULTS AND DISCUSSION

Thin films of 1:0, 3:1, 1:3 and 0:1 PCL:CH blends were found to have dry thicknesses of 35, 55, 14 and 10 nm and swollen thicknesses of 38, 86, 54 and 46 nm (in Phosphate Buffered Saline at pH 7.4), respectively, by spectroscopic ellipsometry. When used separately, PCL and CH produce morphologically homogenous films, whereas their blends (3:1 and 1:3) have visible phases with average roughness values of 16.8 nm and 3.29 nm respectively (Figure 1). Advancing contact angles of constructed surfaces were very similar (70°-75°) except for the chitosan only sample (48°), which was, as expected, more hydrophilic.

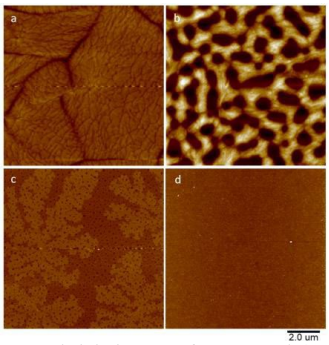

Figure 1: AFM height images of constructed a)1:0 b) 3:1 c) 1:3 d) 0:1 PCL:CH blend films.

The thin films containing chitosan showed a pH dependent protein adsorption in which highest adsorbed amounts were observed at pH 6.0. The lowest protein adsorption was evaluated at pH 7.4 for all blend samples. The preliminary results with 3T3 and hFOB cells show that increasing concentration of the chitosan in the blends resulted in a lower frequency drop at the end of 1 h which is caused by less interacting cells on the surface. Only a limited number of cells interacted with the pure chitosan surfaces, which was probably caused by the high hydrophilicity of the developed surfaces.

CONCLUSION

The surface properties of the constructed surfaces are mainly dominated by the chitosan, for which absorbed protein amount is highest when BSA and the surface are oppositely charged, whereas it is lowest under repulsive forces. Cell adhesion analysis will be carried out by QCM-D and classical cell culture studies in parallel for comparison.

REFERENCES

1. Kao, W. L. et al., The J. of Phys Chem C, 122(1), 694-704, 2018.
2. Kılıç, A., and Kok, F. N. Biointerphases, 13(1), 011001, 2018

ACKNOWLEDGMENTS

This work was supported by Scientific Research Projects of the Department of Istanbul Technical University (Grant no: TGA-2021-42423). We acknowledge Hannes Kettner from IPF for AFM measurements.

Contact guidance of vascular endothelial cells on microgrooved substrates: influence of groove dimensions and cell density

Claire Leclech, Apoorvaa Krishnamurthy and Abdul I. Barakat

LadHyX, CNRS, Ecole Polytechnique, Institut Polytechnique de Paris, Palaiseau, France
*claire.leclech@ladhyx.polytechnique.fr

INTRODUCTION

In healthy arteries, endothelial cells (ECs) exhibit different morphologies: elongated and aligned in the direction of blood flow or more cuboidal in regions of arterial branches and bifurcations. Factors that regulate EC morphology and alignment are of interest, particularly in light of the observation that atherosclerotic lesions preferentially form in regions where ECs are less aligned and elongated[1]. *In vivo*, the basement membrane to which ECs adhere is a patterned and topographic surface[2]. We are interested in how this substrate topography may regulate EC shape and alignment.

EXPERIMENTAL METHODS

We are exploring these questions *in vitro* using microfabricated surfaces. More specifically, we are using PDMS culture substrates composed of parallel arrays of microgrooves width and spacing 5 µm, depth from 1 to 6 µm). Vascular endothelial cells (HUVECs) are cultured at the surface of the microgrooves homogeneously coated with fibronectin.

RESULTS AND DISCUSSION

When cultured on substrates composed of parallel arrays of microgrooves, ECs align and elongate in the direction of the grooves, a process called contact guidance. We show that we can control the extent of this contact guidance by modulating the groove dimensions (spacing, width, and depth). In particular, we demonstrate that increasing groove depth (from 1 to 6 µm) leads to the most pronounced cell elongation and alignment. We also investigate the influence of cell density on the response to microgrooves by comparing the response of individual cells to monolayers of low or high density. Interestingly, we observe progressive loss of cell alignment and elongation on microgrooves for increasing cell density/culture time, associated with remodeling of the actin cytoskeleton and focal adhesions (FAs).

We are investigating the mechanisms underlying this depth- and density-dependent response of ECs to the microgrooves and propose that a competition between cell-substrate and cell-cell adhesion may explain the existence of different mechanisms. In individual cells, the depth-dependent response predominates, driven by FA clustering and protrusion dynamics, while in highly confluent monolayers, ECs respond primarily to the secreted basement membrane and lose the response to substrate topography.

CONCLUSION

Beyond highlighting fundamental mechanisms of shape modulation and contact guidance in ECs, the results of this study can also prove useful in the field of implantable endovascular devices where surface topographic functionalization may constitute a promising strategy for improving device efficacy.

REFERENCES

1. Hahn G. & Schwartz M., Nat Rev Mol Cell Biol 10, 53–62 (2009).
2. Leclech *et. al*, J Cell Sci (2020) 133 (18): jcs239889.

ACKNOWLEDGMENTS

The authors would like to thank AXA Research Fund, Fondation Lefoulon-Delalande and Fondation Bettencourt Schueller for providing financial support to this project.

Studying The Role Of Hydroxypatite In The Osteomimicry Process In Bony Secondaries Using A Biocomposite From Aquaculture Waste

Natalia Castro[1,2], Jun Kit Wang[2] , Chor Yong Tay [2,3] , K.Elisabeth Tanner[1]

[1] School of Engineering and Materials Science, Queen Mary University of London, Mile End Road, London E1 4NS, UK

[2] School of Materials Science and Engineering, Nanyang Technological University Singapore, N4.1, 50 Nanyang Avenue, 639798, Singapore.

[3] School of Biological Sciences, Nanyang Technological University Singapore, 60 Nanyang Drive, 637551, Singapore.

n.munozcastro@qmul.ac.uk

INTRODUCTION

Bone metastases accounts for most of the deaths from breast cancer and causes osteolytic lesions through osteoclast hyperactivation. Although the effects of osteolytic metastasis in bone quality have been well studied, the reciprocal interaction between the breast cancer cells and the metastatic bone niche in regulating the osteolytic process remains elusive to date. In this study, we examined the effect of bony extracellular matrix (ECM) cues on the acquisition of osteo-mimetic features in human breast cancer cells. A panel of 4 different HA microparticles (2-10µm) with varying physiochemical characteristics, coupled with the "waste-to-resource" American bullfrog (*Rana catesbeiana*) skin-derived collagen nanofibrils (BFCol) were chemically modified to establish a novel *in vitro* model mimicking the secondary bone metastasis niche, especially the interface between the cortical bone and the bone marrow (the true nature of skeletal metastasis).

EXPERIMENTAL METHODS

An optimized combinatorial mechano-chemical collagen extraction protocol was employed[1]. One of the HA used was harvested and processed from the discarded scales of *Channa micropeltes* via a calcination method. BFCol/HA coatings were generated with 70 wt% HA mimicking the mineralization wt% in human bone and 15w/w% BDDE following a one-pot synthesis scheme. Different HA grades and BFCol/HA coatings were characterised using: FESEM, XRD, ATR-FTIR, Surface profiler, contact angle. In vitro studies were done on the BFCol/HA coatings using MDA-MB231 triple negative invasive breast cancer cells, their proliferation was determined by Alamar Blue assays and their relative osteomimicry markers expression (PTHrP and OPN) by RT-PCR.

RESULTS AND DISCUSSION

Four different types of HA particles (2-10µm) were used in BFCol/HA coatings: HA1 (non-sintered), HA2 (sintered), HA3 (synthetic) and HA4 (from the scales of *Channa micropeltes*) (Fig 1A). Using the MDA-M231 triple-negative breast cancer cells as an in vitro model, an increase in osteoblast matrix protein (OPN) and bone remodelling regulator (PTHrP) (Fig 1B) was observed during 14 days of culture (Fig 1C&D).

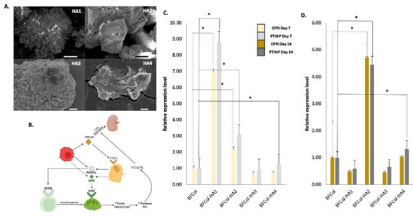

*Figure 1. A. Cross-sectional SEM images. Scale bar=1#m. B. Osteolytic vicious cycle schematic. C. Expression of OPN and PTHrP after 7 days. D. Expression of OPN and PTHrP after 7 and 14 days. * denotes statistical difference between indicated experimental groups at $p < 0.05$.*

CONCLUSSION

A bone-mimetic coating has been developed with a cost-effective one-pot synthesis scheme using aquafarming side stream wastes, such as bullfrog skin collagen and micronized HA from snakehead scales. The BFCol/HA platform was used to investigate the effect of microscale HA characteristics on the bone-like phenotype acquired by breast cancer cells (i.e. osteomimicry) and involved in skeletal colonization (i.e. osteotropism). BFCol/HA coatings with lower HA particle size and higher surface roughness, hydrophilicity and clustering tendencies not only enhanced MDA-MB231 invasive breast cancer cells growth, but they also enhanced the osteomimicry-related genes such as OPN and PTHrP, revealing the prognostic value and potential of osteomimicry as an immunotherapy target. An important next step is to study the effects of the enhanced osteomimicry properties induced by HA in osteoclastogenesis *in vitro* studies as well as bone resorption *ex vivo* studies.

REFERENCES

1. J.K. Wang, Ç.Çimenoğlu, N.M.J. Cheam, X. Hu, C.Y. Tay. Sustainable aquaculture side-streams derived hybrid biocomposite for bone tissue engineering. Mater Sci Eng C 126 (2021) 112104.

ACKOWLEDGEMENTS

This work is funded by A*STAR and QMUL via a combined PhD studentship. However, the experiments were mainly done in the School of Materials Science and Engineering, Nanyang Technological University, Singapore

Stimulating Innervation on Hyaluronan-Based Matrix with chemically modified RNAs for Bone Regenerative Purpose

Camille Blanchard[1*], Quentin Muller[1], Bruno Paiva[1], Andrea Banfi[2], Nunzia Di Maggio[2], Martijn van Griensven[3], Elizabeth Rosado Balmayor[3], Christian Plank[4], Olga Mykhailyk[4], Elise Bonvin[5], Olivier Zelphati[5], Hugo Oliveira[1], and Joëlle Amédée[1]

[1]Univ. Bordeaux, INSERM, BIOTIS, U1026, Bordeaux, France ; [*]camille.blanchard@u-bordeaux.fr
[2]Univ. Basel, Department of Biomedicine, Basel, Switzerland
[3]Univ. Maastricht, MERLN Institute, Maastricht, The Netherlands
[4]Ethris GmbH, Germany
[5]OzBiosciences, France

Introduction

Despite its huge capacity to regenerate, bone is the second most transplanted tissue in the world. Indeed, large size traumatic injuries or bone metabolic disorders like osteoporosis are affecting more and more people every year [1,2], generating a growing need for solutions to limit costs in terms of human lives and public health. Current bone regenerative solutions are mainly focused on the osteogenesis aspect of the tissue regeneration mechanisms, and involve unphysiological amounts of effectors, often recombinant growth factors, with limited success. Recently, focus has been put on re-creating physiological conditions to enhance bone regeneration and obtain functional tissues, and those conditions, in parallel with osteogenesis, involve vascularization as well as innervation. Furthermore, the best way to obtain physiological post-transcriptional modifications of the protein effectors is gene therapy.

The cmRNAbone project aims to develop a novel gene therapy using chemically modified RNAs (cmRNAs), selected to support bone formation, vascularization, and innervation, delivered by specific vectors to the patient's cells, using an osteogenic hyaluronan-based matrix to guide cells and forming tissues. Here, we describe the development and use of a cmRNA (Ethris GmbH, Germany) coding for NGF-β protein, in association with innovant delivery systems, in human bone marrow mesenchymal stem cells (hBMSCs) to increase secretion of this growth factor and stimulate innervation.

Methods

First part of the optimization of transfected cmRNA doses and optimal vector choice was performed by testing the two different vectors OZB1 and OZB3 (OzBiosciences, France), with Lipofectamine Messenger Max as a positive control, on 3D cultures of hBMSCs on the hyaluronan-based matrix. Daily, from 1 to 7 days after transfection, NGF-β expression was measured in cell culture supernatants by sandwich Enzyme-Linked Immunosorbent Assay (ELISA), cell viability was assessed by alamarBlue assay, and the efficiency of transfection was determined by qRT-PCR on extracted total RNA, using specific primers targeting *NGF* cmRNA. The half-life of the transfected *NGF* cmRNA was determined by qRT-PCR, using 6h-long transfected 2D plated cells, and RNA extractions performed at 0 to 5 days after transfection medium elimination.

[1] W.H.Organisation, World report on Ageing and Health. (2015)
[2] W.H.Organisation, Global status report on road safety 2018. (2018)
[3] Leroux *et al.*, Cell Communication and Signaling (2020) 18:162

Second part of those cmRNA optimization and vector choice was performed using microfluidic devices and human induced-Pluripotent Stem cells-derived Sensory Neurons (iPS-SN), to mimic the innervation process *in vitro* and validate the innervation potential and optimal cmRNA dose. A specific device design, adapted from [3], was created to enable the 3D culture of the composite matrices (Fig1).

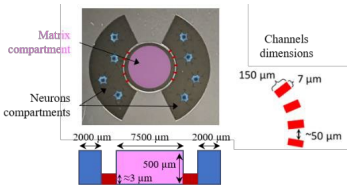

Fig1: Microfluidic device. The hBMSCs were seeded on the matrix in 3D, and the iPS-SN were seeded in 2D. Dimensions of the channels allow only neurites to go through the channels. The height of the central compartment allows the matrix to be poured close to the channels. The neurites are attracted by the NGF-β secreted by hBMSCs in the adjacent compartment, and grow through the channels up to the matrix.

At 3, 5, 7 and 9 days after transfection, NGF-β secretion was measured by ELISA, and neurites growth was measured and quantified after β-III tubulin immunostaining.

Results and Conclusion

The developed vectors OZB1 and OZB3 have shown good transfection efficiencies with *eGFP* cmRNA in hBMSCs, although half Lipofectamine's, and both vectors use with *NGF-β* cmRNA led to NGF-β secretion as soon as 24h. Preliminary data showed higher yields with OZB3 reagent compared to OZB1 (+30% at 24h, +15% at 48h), and yield differences tend to lower at 48h compared to 24h (higher Δ: OZB1 = 64%*Lipofectamine at 24h, 80% at 48h). Regarding the matrix itself, no cell toxicity was seen with either hBMSCs or iPS-SN after 7 days, and we expect to obtain similar secretion and viability results in 3D. Those preliminary data seem to indicate that we can use those tools to increase secretion of NGF-β *in situ* in order to stimulate innervation.

Acknowledgements

This project is a part of the cmRNAbone project, who had received funding from the European Union's Horizon 2020 research and innovation program under grant agreement N°874790.

Ultrastructure of Mineral Tissue at the Early Stage of a Healing Process in the Presence of a Biodegradable Hydroxyapatite Bone Graft

Camila Wendt[1], Victor Zelaya[2], André Linhares[1], Caio Santos[3], Ricardo Lopes[3], Marcos Farina[4], Alexandre Rossi[1]

[1]Centro Brasileiro de Pesquisas Físicas, Rio de Janeiro, Brasil
[2] Laboratório Nacional de Luz Síncrotron, Campinas, Brasil
[3]Coppe, Universidade Federal do Rio de Janeiro, Rio de Janeiro, Brasil
[4]Instituto de Ciências Biomédicas, Universidade Federal do Rio de Janeiro, Rio de Janeiro, Brasil
* camilawendt@cbpf.br

INTRODUCTION

The bone structure has different hierarchical levels from the macroscale to the nanoscale characterized by specific spatial ordering and high complexity. One challenge for producing high-quality biomaterials is understanding how the biomaterial affects bone hierarchical ultrastructure during a bone repair process. Previous studies done by our group showed that carbonated hydroxyapatite (cHA) composites disaggregated into particles with different dimensions, stimulating osteointegration and osteoconduction[1]. In this work we aimed to evaluate the microarchitecture of newly formed bone during a healing of rat tibia defect after a 21-day implant of biodegradable cHa/alginate microspheres.

EXPERIMENTAL METHODS

Carbonated hydroxyapatite (cHA) synthesis and implantation was done as previously described[1]. FIB-SEM analysis were done using an Auriga dual-beam microscope or a Tescan Lyra 3. Series of back-scattered electron images were recorded in "slice-and-view" mode, with a pixel size of 20.4 nm and milling step of 70 nm. Series alignment, image segmentation and volume analysis were done with Avizo 9.7 software.

RESULTS AND DISCUSSION

Focused ion beam scanning microscopy (FIB-SEM) operating in serial-surface-view mode enable detailed mapping of the mineralization profile associated with collagen structures. Results showed mineralized tissue inside interconnected submicrometre pores, suggesting that mineralization was not directly controlled by cells and that it may occurs in pores smaller than 1 µm. 3D rendered of FIB-SEM series showed the lacuno canalicular network associated with trabeculae and situated close to the interface between the mineralized tissue and the biomaterial interface (fig.1A-B). Furthermore, 3D analysis showed that woven bone trabeculae were composed of ordering ellipsoidal mineral structures, ranging from 1,0 to 1,4 µm in length and 0,3 to 0,60 µm in width (fig.1C-D). According to TEM/HRTEM data, these structures are attributed to bundles of mineralized collagen fibrils associated with hierarchical structures of woven bone formed at the early stage of healing[2].

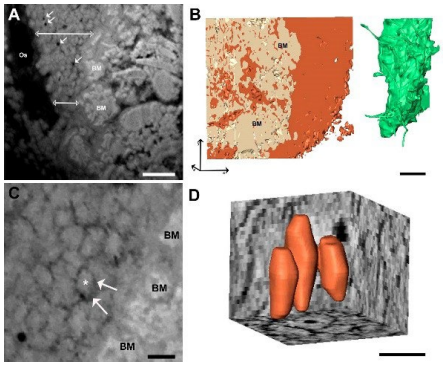

Figure 1: FIB-SEM slice and view analysis. (A) The biomaterial (BM) is observed in close proximity to the neoformed bone, osteocyte lacuna (Os) and the canalicular network (arrows). (B) 3D rendered model shows the complex association between the neoformed bone and the biomaterial. Bone structure is shown in brown, biomaterial in white and osteocyte network in green. (C) Less mineralized collagen fibrils (arrows) are seen at the boundaries of mineralized blocks (asterisk). (D) 3D rendered model showed that the mineral clusters appear as ellipsoidal structures. Scale bar: 4 µm (A-B), 1 µm (C-D).

CONCLUSION

This study characterized ellipsoidal mineral structures formed in woven bone trabeculae during bone healing. The presence of these motifs over the entire FIB-SEM series suggests that these structures may represent a regular pattern of mineral deposition nucleated in the association of collagen fibers. Furthermore, we provide a 3D analysis of mineral tissue grown in the interface between newly bone and the biomaterial. We identified the ultrastructure of the mineral tissue formed in interconnected submicrometer pores.

REFERENCES

1. Zelaya V. *et al*., Acta Biomaterialia, 120, 2021
2. Buss D. *et al.,* Journal of Structural Biology, 212, 2020

ACKNOWLEDGMENTS

This work was supported by Conselho Nacional de Desenvolvimento Científico e Tecnológico (CNPq), Fundação o Carlos Chagas Filho de Amparo à Pesquisa do Estado do Rio de Janeiro (FAPERJ) and INCT REGENERA.

Human Corneal Keratocytes Display Enhanced Viability and Infiltration Capacity when Grown on Collagen Type-I-modified PHEMA Hydrogels

Elizabeth B. Moloney[1,4*], Laura Sánchez-Abella[5], Beatriz Palla Rubio[5], Maria González[6], Damien Dupin[5], Eva Larra[6], Iraida Loinaz[5], Abhay Pandit[2,4], Thomas Ritter[1,3]

[1]REMEDI, National University of Ireland, Galway, Ireland.
[2]CURAM, National University of Ireland, Galway, Ireland
[3]College of Medicine Nursing and Health Science, National University of Ireland, Galway, Ireland
[4]College of Science and Engineering, National University of Ireland, Galway, Ireland
[5]CIDETEC, Basque Research and Technology Alliance, Donostia-San Sebastián, Spain
[6]AJL Ophthalmic, Alava, Spain
[*] elizabeth.moloney@nuigalway.ie

INTRODUCTION

The use of artificial corneas can potentially expand the number of patients with corneal blindness who can be offered sight-restorative surgeries, circumventing the need for transplantable human donor corneas[1]. Biomaterials, such as PHEMA (poly(2-hydroxyethyl methacrylate)) hydrogels, which are biocompatible with the host tissue, can form the basis for suitable flexible synthetic corneas[2]. However, although visual acuity was improved, unsuccessful biointegration and the persistence of inflammatory cells following implantation of such synthetic corneas led to long-term complications for patients, including implant extrusion, stromal melting, and retroprosthetic membrane formation[3]. We hypothesized that inclusion of biomacromolecules (COL-I: collagen-I, and/or HA: hyaluronic acid) during polymerization of a PHEMA-based hydrogel would enhance human corneal keratocyte (HCK) viability and infiltration into the biomaterial. Dysregulation of matrix metalloproteinases (MMPs) has been associated with corneal melting and subsequent keratoprosthesis failure in high-risk patients[4,5]. Therefore we also sought to identify whether levels MMPs are altered when HCKs interact with these biofunctionalized hydrogels.

EXPERIMENTAL METHODS

Several varieties of PHEMA-based hydrogels were prepared with 0.05% COL-I, 0.1% COL-I, 0.2% COL-I, or 0.1% COL-I in combination with 0.025% HA. Samples were individually sterilized by beta-irradiation prior to use in vitro. HCK were seeded at a density of $2x10^4$ cells/cm^2 onto the top surface of hydrogel discs of different compositions (n=6 per hydrogel type). Viability at 5 days post-seeding was measured by quantifying ATP released from metabolically viable cells in 3 independent assays. Infiltration of cells into the porous biomaterial was quantified by counting the number of DAPI-stained nuclei in horizontal cryosections of HCK-seeded hydrogel buttons. To determine whether corneal cells exposed to the various hydrogels alter their secreted MMP profile, conditioned media was collected 6 days post-seeding for semi-quantification of MMPs using an antibody array dot blot approach.

RESULTS AND DISCUSSION

Only PHEMA-based hydrogels prepared in the presence of 0.1% COL-I alone supported statistically significant enhanced viability of HCK across three independent assays ($p<0.05$) when compared to viability on unmodified PHEMA hydrogels (n=6 samples per hydrogel, per assay; One-way ANOVA, with Dunnett's multiple comparison test). Preliminary data suggested that collagen-only modified PHEMA hydrogels (0.1% or 0.2% COL-I) encouraged deeper infiltration of cells into the biomaterial. MMP levels secreted from HCK grown on modified hydrogels were expressed as fold-change compared to levels observed from cells grown on unmodified samples ($p<0.01$, one-way ANOVA, with Tukey's multiple comparison test). MMP 1 and MMP 3 levels were significantly increased in all modified hydrogels samples, whereas MMP8, MMP10, and MMP13 remained constant across all samples. COL-I-only hydrogels elicited a significant decrease in MMP2 levels, whereas MMP9 levels were only significantly reduced when HCKs were cultured on hydrogels containing both HA and COL-I.

CONCLUSION

By supporting enhanced survival of HCK in vitro, PHEMA hydrogels containing 0.1% COL-I may allow for improved biointegration of hydrogel-based keratoprostheses in diseased eyes. Given that these cells also displayed differential regulation of MMPs in response to the presence of COL-I and/or HA in the modified hydrogels, biofunctionalized KPros could deter excessive ECM remodeling to prevent stromal melting, a long-term complication often observed following corneal injury or implantation of a KPro. However, further research is needed to confirm this.

REFERENCES

1. Holland G. *et al*., Front. Med. 8: 770780. 2021
2. Hicks C. *et al*., Prog Ret Eye Res. 19:2 149-170. 2000
3. Jiraskova N. *et al.,* Eye. 25, 1138–1146. 2011
4. Brejchova K. *et al*., Exp Eye Res. 90: 583-590. 2010
5. Gao M. *et al*., J Ophthalmol. 1094279. 2016

ACKNOWLEDGMENTS

The authors would like to thank the European Union's Horizon 2020 Research and Innovation programme (Grant no: 814439) for providing financial support to this project.

Determining The Biological Response To Metallic 3D Prints Through Plasma Surface Treatment Postprocessing Method.

Dorota Bociaga[1*], Jacek Grabarczyk[1], Adrianna Wierzbicka[1], Marcin Skrodzki[2]

[1]Institute of Materials Science and Engineering, Lodz University of Technology, Lodz, Poland
[2]Medgal Ltd., Białystok, Poland
[*]dorota.bociaga@p.lodz.pl

INTRODUCTION

The 3D printing technology with the DMP (direct metal printing) method, also referred to as direct laser sintering of metal powder, allows the production of metal elements with complex geometry, which would be impossible to produce in the case of traditional casting methods or the use of subtractive techniques. The DMP method facilitates the production of metal objects with high precision. One of the important applications of additive manufacturing is the production of medical implants. A significant challenge in the production of medical devices using the DMP technique is the so-called postprocessing. An inadequately conducted cleaning process after production can lead to the presence of metallic particles that were not bound during laser melting.

DMP implants must have the highest print quality, which strongly depends on factors such as: geometric properties of metal powder, laser power, scanning strategy, and inert gas flow [1]. Commonly available post-processing methods are not effective in removing superficial powder debris in such implants and can therefore be hazardous to the patient. According to literature reports, the immune response of living cells to metallic 3D printing powders is related to the size and concentration of free powder particles. Regardless of their size, at high concentrations in the body (106 particles / ml), the unbound powder induces an immune response from an early stage. However, it was noticed that smaller particles (≤32 µm) are phagocytosed by living cells, and larger ones (33-100 µm) are isolated, so that powders with smaller particle diameters show higher toxicity than larger particles [2].

The aim of this study was to improve the quality of 3D printed implants by cleaning their surfaces from unbound metallic particles. Plasma treatment was found to be the most promising solution based on a literature review of the available purification methods. The conducted research was aimed at verifying the effectiveness of the plasma purification process from unbound particles present on metallic 3D prints.

EXPERIMENTAL METHODS

The material from which the samples were printed using the DMP method was a specific grade titanium powder (LaserForm® Ti Gr23 A) with a particle diameter of up to 40 µm. It is a powder developed and adapted especially to 3D ProX DMP 320 printers. The elements printed on its basis have a chemical composition consistent with the commonly known Ti-6Al-4V ELI alloy. Two types of samples with dimensions of 10 mm x 2 mm were used for the tests. One group of samples was subjected to steam sterilization only, while the other group was soiled with coolant, washed in an ultrasonic cleaner, degreased, sandblasted and also subjected to steam sterilization.

Plasma treatment of the titanium samples was carried out in 6 processes differing in duration (1h, 2h, 4h) and type of plasma gas (Oxygen, Argon). All the samples as built and plasma treated were subjected to characterization test such as weight measurement, surface profile measurement, wettability measurement, SEM observation and microstructure observation, cytotoxicity evaluation (XTT) and cells morphology analysis after 24h, 3 and 7 day of direct growing on the samples surface.

RESULTS AND DISCUSSION

Plasma cleaning is a more effective process when it is preceded by mechanical pre-treatment in the form of sandblasting. Plasma cleaning affects the properties and surface structure of the printed Ti6Al4V samples, the roughness and wettability of the surface change. For non-sandblasted samples plasma cleaning causes a change in the regularity of the particle shape, and the surface of sandblasted samples is smoothed. The plasma treatment process in both argon and oxygen does not change the chemical composition of the sample. From the biological point of view the plasma treatment effectively improves the cells growth. From a biological point of view, plasma treatment is effective in improving cell growth regardless of the type of gas used.

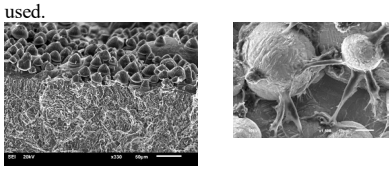

Fig. 1. SEM of the cross-sectional view of the sample treated in Ar for 2h (on left) and cell growth on the Ar-treated surface (on right).

CONCLUSION

The surface of plasma-modified samples reaches a more hydrophilic surface, which translates into better biocompatibility. The particle size of the powder used to print the samples does not adversely affect the biological response. Plasma treatment is a good method of cleaning and modifying printed samples to improve both physico-chemical and biological properties.

REFERENCES

1. Pleass C. *et al.* Add Manuf, 24, 2018
2. Tang J.C. *et al.* Add Manuf 35 (2020) 101392

Fibronectin-Biofunctionalization of chitosan hydrogels

Carla Palomino-Durand[1*], Pierre Marquaille[1,2], Phuong-Anh Dang[1,2], Maxence Gall[1], Sophie Norvez[2], Laurent Corte[2,3], Adeline Gand[1], Emmanuel Pauthe[1]

[1]Equipe de Recherche sur les Relations Matrice Extracellulaire Cellules, ERRMECe, CY Cergy-Paris Université, Cergy-Pontoise, France
[2]Molecular, Macromolecular Chemistry and Materials, C3M, ESPCI Paris, CNRS, PSL University, Paris, France
[3]Centre des Matériaux, MINES ParisTech, CNRS, PSL University, Evry, France
*carla.palomino-durand@cyu.fr

INTRODUCTION

Cell-biomaterial interaction is essential to enhance bio-integration and tissular regeneration. This cell–material behavior is controlled and tuned by various parameters such as physical characteristics of the biomaterial and chemical/biochemical molecular reactions mediated by the availability of biological cues (*i.e.,* extracellular-matrix (ECM) protagonists)[1]. Chitosan (CS) hydrogels have been extensively studied for regenerative medicine. Nevertheless, CS polymer lacks binding sites for cell adhesion. Thus, the addition of biological signals is necessary. Among the ECM protagonists, fibronectin (Fn) has emerged as the most pertinent key partner[1]. Fn is a dimeric glycoprotein and the principal molecule involved in cell adhesion, migration, and differentiation

previously labelled with AlexaFluor 560 and AlexaFluor 488, respectively. Cell behavior was evaluated with pre-osteoblast cells (MC3T3-E1) at the hydrogel surface (1) and inside the thermosensitive hydrogel (2). Hydrogels were incubated in presence of cells for 24h and 72h. AlamarBlue® and LIVE/DEAD assays were used for viability studies in encapsulated cells. Cell adhesion and proliferation were evaluated at hydrogels surfaces using DAPI (DNA) and phalloidin-FITC (actin) staining.

RESULTS AND DISCUSSION

For the first approach (1), stable, homogeneous, and transparent CS/Fn hydrogels were obtained. All hydrogels were cytocompatible with cell survival greater

Surface Electric Fields Increase Osteoclast Resorption on Carbonate–Incorporated Apatite

Leire Bergara-Muguruza[1], Keijo Mäkelä[2], Tommi Yrjälä [2], Jukka Salonen[1], Kimihiro Yamashita[3], Miho Nakamura[1,4, 5*]

[1] Medicity Research Laboratory, Faculty of Medicine, University of Turku, Turku, Finland
[2] Turku University Hospital, University of Turku, Turku, Finland
[3] Graduate School of Medical and Dental Science, Tokyo Medical and Dental University, Tokyo, 113–8510, Japan
[4] Institute of Biomaterials and Bioengineering, Tokyo Medical and Dental University, Tokyo 1010062 Japan
[5] Graduate School of Engineering, Tohoku University, Miyagi 9808579 Japan

[*]miho.nakamura@utu.fi

INTRODUCTION

Cell-mediated bioresorption is a biological process in which biomaterials are resorbed by cells and thereby either partially or completely disappear from implantation sites over a period of time. Cell-mediated bioresorption is a new technique that is advantageous because it allows for the dissolution of biomaterials after the bone remodeling process in conjunction with bone resorption and formation. Because osteoclasts are responsible for bone resorption, the development of osteoclast-mediated bioresorbable biomaterials is imperative for bone regeneration *in vivo*. Interestingly, the incorporation of carbonate ions within the hydroxyapatite (HA) crystal structure has been experimentally validated to increase osteoclast differentiation and resorption, even though stoichiometric HA cannot be resorbed by osteoclasts.

Recently, we demonstrated that electrically polarized HA enhances osteoconductivity *in vivo*, as well as the initial adhesion and migration of osteoblast-like cells *in vitro*, compared with standard HA. Although the promotion of the initial stages of osteoconduction by electrical polarization has been reported, the effects on osteoclast behaviour have not yet been elucidated. In the present study, we therefore combined approaches from biology and materials science and used HA and carbonate apatite (CA) with charged surfaces induced by polarization to better understand the interactions between osteoclasts and biomaterials.

EXPERIMENTAL METHODS

The dense HA and CA were prepared, polished and washed in ethanol with ultrasonication. Electrical polarization of the specimens were undertaken. Because the electrical polarization provides negatively and positively charged surfaces, the negatively charged HA and CA surfaces are denoted herein as HA–N and CA–N, respectively, while the positively charged ones are referred to as HA–P and CA–P, respectively. The surface characterization was performed by XRD, ATR-FTIR, and the measurements of surface free energy.

Peripheral mononuclear blood cells (PBMCs) were used as precursors of osteoclasts. The cells were placed onto the specimens and cultured in cell culture medium with the addition of 20 ng/mL and 10 ng/mL M-CSF for 14 days. The morphology of the cells and the size of resorption pits were compared.

RESULTS AND DISCUSSIONT

The surface energies were 38.6 mJ/m^2 for standard HA and 51.1 mJ/m^2 for standard CA. The surface energy values for initial polarized HA and CA were found to be increased by factors of approximately 1.7 and 1.5 times, respectively, relative to the unpolarized samples.

Osteoclasts derived from human PBMCs were positively stained for TRAP on the surfaces of all specimens after culturing with osteoclast differentiation factors for 14 days. The quantities of multinuclear TRAP-positive were significantly larger on the CA samples compared with the numbers on the HA samples. Actin-based sealing rings as a marker for active bone resorbing were observed in the osteoclasts on the HA, CA and bone slices.

Resorption pits were observed on all sample surfaces using three–dimensional laser microscopy. The distinct pits were formed on the bone slices and CA samples, whereas ambiguous, shallow pits appeared on the HA sample. The measurements of the depth of the resorption pits revealed that the osteoclasts resorbed the CA samples approximately 11 times deeper than those on the HA samples. The pit depths on the CA–N and CA–P samples were approximately 18 and 21 times greater than those on the standard HA sample and 1.6 and 1.9 times greater than those on the standard CA sample, respectively.

CONCLUSION

In the present study, polarization was found to improve the surface wettability of HA and CA as a result of increases in surface free energy, and this effect was still present after one month. In addition, trials in which osteoclasts were cultured on various substrates showed that polarized CA enhanced osteoclast resorption but did not affect the TRAP staining and morphology of osteoclasts.

REFERENCES

1. Bergara-Muguruza L, et al. ACS Applied Materials & Interfaces 2021: 13 (49), 58270-58278.

ACKNOWLEDGMENTS

This study was financially supported by the Turku Collegium for Science and Medicine, Grants–in–Aid for Scientific Research (C) (nos. 17K10957 and 20K09454) and the Murata Science Foundation.

Comparison of cellular effects of HEMA and TEGDMA

Bergitte P. Olderbø[1], Remy B. Petermann[1], Jan Tore Samuelsen[1]

[1]Nordic Institute of Dental Materials, Oslo, Norway
* b.p.olderbo@niom.no

INTRODUCTION

Resin-based dental biomaterials usually consist of methacrylate monomers that are polymerized *in situ*. The conversion to polymer is never complete and causes patient and dental personnel exposure to monomers like 2-hydroxyethyl methacrylate (HEMA) and triethyleneglycol dimethacrylate (TEGDMA). These methacrylates are toxic *in vitro*, anticipated to result from similar molecular interactions. Recent studies, however, indicate that the toxic potentials of HEMA and TEGDMA arise from different cellular damages[1,2,3]. Understanding how chemicals interact with living cells gives a good basis to evaluate their side effect potentials. Such knowledge may also provide valuable information on possible interactions in combination exposure scenarios.

HEMA and TEGDMA often appear in an exposure mixture. Mapping of combined exposure interactions is therefore essential. The purpose of the current study was to compare the cellular effects of HEMA and TEGDMA exposure individually with selected HEMA/TEGMA mixture exposures.

EXPERIMENTAL METHODS

The human monocytic cell line THP-1 was exposed to HEMA (0.5-15 mM) or TEGDMA (0.25-5 mM) alone and in combinations. Cell viability was measured after 24 hours using the MTT assay. Cellular glutathione (GSH) levels were measured by flow cytometry of monobromobimane stained cells. Cellular levels of three selected proteins (Sequestome-1 (SQSTM1/p62), Heme oxygenase 1 (HO-1), and Pirin) were measured by Western blotting after various methacrylate exposures. These proteins were selected based on previously reported cellular effects of HEMA and TEGDMA exposure. At least three independent experiments were performed for each measurement. Statistical analysis was calculated using one-way ANOVA with Dunnett's and Tukey's multiple comparisons test by GraphPad prism.

RESULTS AND DISCUSSION

The cell viability decreased dose-dependently after exposure to HEMA (significant at 6 mM and above) and TEGDMA (significant at 2 mM and above). EC50 values indicated that TEGDMA was about three times more potent than HEMA in the MTT assay. Selected combination exposures supported this factor and suggested an additive interaction of HEMA and TEGDMA on THP-1 cell viability. Similar results were obtained with GSH measurements, although significant at lower concentrations (0.5 mM for both HEMA and TEGDMA). The selected proteins, p62, HO-1, and Pirin, significantly increased after HEMA or TEGDMA exposure. These results indicated that HEMA and TEGDMA might affect THP-1 cells similarly, which is in contrast with some previous studies.

CONCLUSION

This study indicates that HEMA and TEGDMA affect THP-1 cells through similar mechanisms based on similar responses on the different endpoints measured. The combination exposure experiments further support this assumption by suggesting an additive interaction of the two methacrylates.

REFERENCES

1. Becher R. *et al*., Dental Materials, Volume 35, Issue 1, Pages 125-134, 2018
2. Nilsen BW. *et al*., European Journal of Oral Sciences, 126 (Suppl 2), Pages 345-358, 2018
3. Samuelsen JT. *et al.*, J. Biomed Mater Res Part A, 107(4), Pages 851-859, 2019

ACKNOWLEDGMENTS

The authors would like to thank Else Morisbak and Solveig Uvsløkk at Nordic Institute of Dental Materials for excellent support during this study.

Toward an evolution of the strain-based peri-implant bone remodeling

Rémy Gauthier[1*], Hélène Follet[2], Ana-Maria Trunfio-Sfarghiu[3], Delphine Farlay[2], Nina Attik[4], Sylvain Meille[1], Jérôme Chevalier[1], David Mitton[5]

[1]Univ Lyon, CNRS, INSA Lyon, UCBL, MatéIS, France
[2]Univ Lyon, INSERM UMR 1033, UCBL, LYOS, France
[3] Univ Lyon, CNRS, INSA Lyon, LaMCoS, France
[4]Univ Lyon, CNRS, UCBL, LMI, France
[5]Univ Lyon, Univ Gustave Eiffel, UCBL, LBMC, France
[*] remy.gauthier@insa-lyon.fr

INTRODUCTION

Bone structural properties are known to depend on its biomechanical history. Such bone biomechanical integrity in regard to its structural organization is determinant in the course of bone implant longevity. Through its properties, the implanted biomaterial induces the development of strains near the bone implant interface. Amongst other types of stimuli, those strains have a major influence on the evolution of the peri-implant bone properties.

In that context, tremendous efforts have been made in improving bone biomaterials. As an example, some improvements consist in promoting the implant osseointegration through surface modifications to allow for a better mechanical transmission between the implant and the bone. But whether or not such parameters ensure the bone – implant system longevity remains an open question.

In order to determine the properties to be considered in the development of bone implants, it is necessary to understand how bone is able to ensure its own biomechanical integrity.

BONE MECHANOTRANSDUCTION PATHWAY

Bone integrity is maintained throughout life through a continuous remodelling mechanism[1]. Osteoclasts and osteoblasts are known to remove and form bone tissue, respectively. Whether or not one or the other has to be activated is determined by osteocytes (Ocy). Ocy are former osteoblasts that have been embedded within bone mineralized matrix. In that manner, they are the perfect candidates to sense bone matrix strain during mechanical loading.

Ocy form an interconnected network trapped in the lacunocanalicular network (LCN). This porous network is made of micrometric lacunae, where Ocy are located, all connected through canaliculi of 500nm in diameter[2] and allows for nutriments and fluid distribution from the vascular canals toward the Ocy.

Within this LCN, Ocy are embedded in a pericellular matrix (PCM) made of perlecan and are discreetly connected to the lacunar wall through tethering perlecan fibres. There is thus an empty space between the PCM and the lacunar wall allowing for fluid to flow (see figure).

When bone is subjected to a mechanical loading, the whole LCN is deformed inducing a change in fluid hydrostatic pressure and fluid velocity. Such shift in LCN fluid behaviour is assumed to stimulate Ocy. It is considered as the main bone mechanotransduction pathway and thus as a major mechanism of bone remodelling regulation.

THE LIMITS OF STRAIN-BASED REMODELING FOR PERI-IMPLANT BONE

As this shift in fluid behaviour is induced through bone strain at the tissue level, strain-based bone remodelling laws have been developed. The Frost mechanostat theory is one of the major progress made in this conte... theory, Frost defined a physiological s...ns wi... which no remodelling occurred, whi...outside window, rather bone removal or forma...io... While such theory has been largely app... implant bone remodelling, its relevance is ... Considering the previously stated Ocy... pathway, this strain-based theory suggests ... the tissue level induce a shift in LCN flu... allows for remodelling activation. Neverth... the bone-implant interface, fluid behaviour is mu... different than in the bulk. The shift in fluid beha... induced by strains at the tissue level will be different. ... other words, the strains needed to go beyond the li...its the physiological window are different. The F... mechanostat theory might thus not be applied easily. Accordingly, bone implant efficiency must ... b restricted to its capacity to induce strains in peri-i... pla... bone. Further investigations have to be done ... biomaterial capacity to induce this fluid shift b... close to its interface to help redefining t... hy... strain window.

REFERENCES

[1]L... D., Bone, 30: 2-4, 2002
[2]Varga P. et al., J. Struc. Biol., 1... 66...
[3]G... thier R. et al., Biocell, Acc...
... H, The Anat. Rec., 219...

Incorporation of metallic nanoparticles in silicone breast implants for reduction of capsular contracture

Eugénie Guimier[1]*, James Quinn[1], Xin Shen[1], Louise Carson[1], Benny David[2], James M. Lambert[2], John Zupansic[2], Enda Heery[3], R. Karl Malcolm[1]

[1]School of Pharmacy, Queen's University Belfast, Belfast BT9 7BL, UK

[2] NuSil Technology LLC, Carpinteria, CA 93013, US

[3] NuSil Technology LLC, Dublin, Ireland.

* eguimier01@qub.ac.uk

INTRODUCTION

Capsular contracture (CC) is one of the most common clinical complications following breast augmentation or reconstruction surgery using implants. The bacterial infections that arise following surgical procedures and the foreign body reactions due to the hydrophobicity of the silicone elastomer implants are problematic and are believed to be important in the development of CC. One of the most common strategies implemented to reduce foreign body reactions has been use of breast implants with textured surfaces. While this approach has led to reduced incidence of fibrous capsule formation around implants, it has also led to an association with anaphylactic large cell lymphomas which has led to the withdrawal of certain textured surfaces from many countries by health authorities. With the withdrawal of macrotextured implants from the market, new strategies are needed to reduce rates of CC. Metallic ions and nanoparticles (NPs) —such as copper (Cu) and zinc (Zn)— have been reported effective anti-bacterial agents against *S. epidermidis*, *S. aureus* and *E. Coli*, bacteria, each suspected to provoke strong CC reactions [1,2]. Therefore, incorporation of antibacterial metal NPs into either the silicone shell or gel components of breast implants offers an alternative pharmacological strategy to reduce the risks of CC and implant associated infection.

EXPERIMENTAL METHODS

Preparation of silicone elastomer films

Silicone elastomer films (0.3 cm thick) containing 2.5% w/w Cu or Zn NPs were prepared from medical grade addition-cure silicone elastomer dispersions (MED6615 & MED 6600, NuSil). Briefly, silicone parts A and B (1:1) were mixed (Speedmixer DAC-150) with the required quantity of Cu/Zn NPs (780 and 790 nm, Nanografi) for 1 min at 3000 rpm, left overnight for solvent evaporation, and then post-cured (1 hr, 90ºC) Circular discs of 1 cm diameter were cut from the resulting films.

In vitro release

Control samples of DDU-4320 silicone were loaded with 10% w/w and incubated with 2% w/v Kolliphor® HS 15 in 25 mM acetate buffer solution, pH 4.2. Samples were collected every 24 hr and the quantity of NPs released was measured using atomic absorption spectroscopy.

Material cytotoxicity

Silicone samples—containing Zn NPs, Cu NPs, or blank controls—were incubated at 37ºC, 5% CO_2 with RAW 264.7 macrophages in a Dulbecco's Modified Eagle Medium (DMEM; Gibco® DMEM) and L929 fibroblasts cells in a Minimum Essential Media (MEM; Gibco® MEM), all media were supplemented with 10% foetal bovine serum (Gibco®) and 1% (50 U/mL) penicillin/streptomycin (Gibco®). MTT assays were then performed after 24 and 48 hr to assess the cytotoxicity.

Bacterial quantification and biofilm formation

Bacterial adherence was assessed using a live/dead assay. Briefly, samples were incubated in a Mueller Hinton broth containing ~10^6 CFU/mL *S. aureus* for 24 hr. Samples were subsequently stained with with fluorescent Live/Dead® BacLight™ solution (Molecular Probes). Bacteria were then visualised via fluorescence microscopy to determine the total percentage biofilm coverage and the ratio of live/dead bacteria on the sample surface. All statistical analysis were performed using one-way ANOVAs.

RESULTS AND DISCUSSION

Small quantities of Cu/Zn NPs were released after one week incubation (500 and 1200 µg, respectively). Live/Dead staining images showed almost negligible live bacteria at the surface of the loaded materials and revealed a decrease of biofilm coverage of *S. aureus* by 55.3% and 37.1% for Cu and Zn incorporated materials, respectively, demonstrating an antibacterial effect. Direct contact cytotoxicity assays combined with MTT analysis showed the samples remained cytocompatible for both cell lines.

CONCLUSION

Incorporation of Cu or Zn NPs into silicone elastomers offers a new strategy for manufacture of breast implants offering improved antimicrobial activity and with the potential to reduce rates of CC.

REFERENCES

[1] M. Gosau *et al*., Effectiveness of antibacterial copper additives in silicone implants, J. Biomater. Appl. 28 (2013) 187–198.

[2] A. Sirelkhati *et al*., Review on Zinc Oxide Nanoparticles: Antibacterial Activity and Toxicity Mechanism, Nano-Micro Lett. 7 (2015) 219-242.

ACKNOWLEDGMENTS

The work and EG's PhD studentship are supported by a research grant from NuSil to Queen's University Belfast.

Curvature as a guiding cue for single and collective cell migration

Laurent Pieuchot[1*], Karine Anselme[1], Isabelle Brigaud[1], Tatiana Petithory[1], Arnaud Ponche[1], Pierre-François Chauvy[2], Marcos Farina[3], Pablo Rougerie[3], Jean-Louis Milan[4], Maxime Vassaux[4], Maxence Bigerelle[5], Julie Marteau[5]
[1] Université de Haute-Alsace, IS2M-CNRS 7361, F-68100 Mulhouse, France
[2] Micropat SA, Côtes-de-Montbenon 30, CH-1003, Lausanne, Switzerland
[3] Laboratório de Biomineralização, Federal University of Rio de Janeiro, Rio de Janeiro 21941-902, Brazil
[4]Aix Marseille Univ, CNRS, ISM, Marseille F-13288, France
[5] Université de Valenciennes, LAMIH, UMR-CNRS 8201, Valenciennes F-59313, France
[*] laurent.pieuchot@uha.fr

INTRODUCTION

Cell migration is essential for many biological processes such as embryonic morphogenesis, tissue remodeling, wound healing, and cancer cell metastasis. Cells can migrate individually between tissues and organs or collectively in tightly or loosely associated groups. In both cases, cell migration is regulated by guidance cues of very different natures. Here we describe a cellular mechanism called curvotaxis that enables individual cells[1,2] and growing epithelial monolayers[3] to sense and migrate in response to curvature variations. We combine experimental and computational approaches to better understand how curvature is integrated, and explore how it can be used to direct cell migration and tissue morphogenesis.

EXPERIMENTAL METHODS

We used a confocal upright LSM800 to monitor cell behavior on PDMS replicates of microstructured metal masters functionalized with fibronectin. We analyzed imaging data using ImageJ and Imaris software and performed statistical analysis using Prism software.

RESULTS AND DISCUSSION

We monitored the position of cells on 3D sinusoidal arrays and found that they migrate towards concave regions in a process we termed curvotaxis (Fig. 1A and B). The mechanism depends on actomyosin contractility and requires a functional nucleo-cytoskeleton interplay. In addition to migration trajectories, curvature variations affect focal adhesion stability, nuclear shape and positioning, and gene expression, demonstrating that cell-scale curvature is an important regulatory cue that has pleiotropic effects on cell biology. Taken together with numerical simulation results, our data suggest that the nucleus act as a mechanical sensor that guide the cell on the surface.

We have also recently demonstrated that MDCK epithelial monolayers are able to respond to curvature variations (Fig. 1C and 1D). On 3D sinusoidal arrays, epithelial cells within a growing colony exhibit a hybrid behavior: in the leading edge, the cells tend to position their nuclei on concave topographies whereas in the central part, their distribution is not impacted by curvature. This suggests that a progressive embedding into the epithelium modifies the cell response to topography. We used a series of parallel arrays of specific curvatures and monitored the growth of circular epithelial colonies on these surfaces. We observed that the epithelium grows anisotropically in the direction of curvature continuums and that its elongation is proportional to the maximum convex curvature exhibited by the surface.

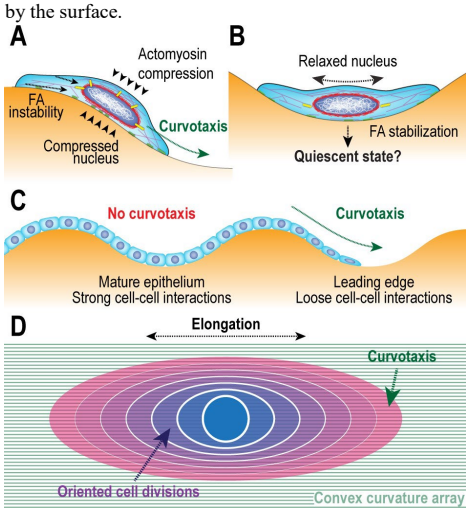

Figure 1: Curvotaxis in single cells and epithelia.

CONCLUSION

Altogether, this work identifies cell-scale curvature as an essential physical cue that can guide both single and collective cell migration processes. We further show that curvature influences cell physiology and epithelium growth with potential applications in tissue engineering and biomaterial design.

REFERENCES

1. Pieuchot, L. *et al.* Curvotaxis directs cell migration through cell-scale curvature landscapes. *Nat Commun* **9**, 3995 (2018).
2. Vassaux, M., Pieuchot, L., Anselme, K., Bigerelle, M. & Milan, J.-L. A Biophysical Model for Curvature-Guided Cell Migration. *Biophys J* **117**, 1136–1144 (2019).
3. Rougerie, P. *et al.* Topographical curvature is sufficient to control epithelium elongation. *Sci Rep* **10**, 14784 (2020).

ACKNOWLEDGMENTS

We thank the Agence Nationale de la Recherche (grant number: ANR-12-BSV5-0010) and Centre National de la Recherche Scientifique for funding. We thank the IS2M facilities and the GenomEast genomic platform for their technical support.

Immuno-characterization of the native tissue of the apical papilla of wisdom teeth and culture optimization of their derived stem cells (SCAPs) to potentiate the grafting of cellularized biomaterials

Caroline Jeannière[1], Solène Lenoir[1], Marine Mavinga[1], Sylvie Rey[1], Martine Saint Marc[1], Elisabeth Génot[1], Noélie Thébaud[1], Mathilde Palmier[1], Delphine Maurel[1], Benoit Rousseau[2], Virginie Mournetas[3], Claudine Boiziau[1] and Hélène Boeuf[1*]

1: Inserm, Univ. Bordeaux, U1026 Biotis, Bordeaux, France.
2 : Service commun des Animalerie, Univ. Bordeaux, Bordeaux, France
3 : ADLIN Science, Grenoble, France

* : Email : helene.boeuf@u-bordeaux.fr

INTRODUCTION: The main approach to regenerative medicine is based on the use of stem cells to repair human tissues and organs. The use of stem cells in the clinic requires a better understanding of their biology to improve their amplification, survival after transplantation and their behavior and fate *in situ*. Stem cells isolated from the apical papilla of wisdom teeth (SCAPs) are an attractive model for tissue repair due to their availability, high proliferation rate and potential for *in vitro* differentiation into mesodermal and neurogenic lineages.

EXPERIMENTAL METHODS: We have characterized the overall architecture and properties of the native tissue from which SCAPs are derived by immunostaining and have established the ImmunoMap of this tissue. In addition and since adult stem cells, such as SCAPS, are developing in stem cell niches in which [O_2] is low (eg: physioxic condition: 3-8% compared with 21% of ambient air), we have derived original banks at 21 and 3% O_2 from 6 teenagers.

RESULTS and CONCLUSION: We will present data evaluating the impact of low [O_2] on the physiology of SCAPs (eg: role of the high autophagy flux for cell survival and osteogenic differentiation). We will also show data helping at determining whether low O_2 pre-conditionning of cells is efficient for survival of cellularized grafs in animal models.

REFERENCE: Rémy M. *et al* , Cells, 8, 1485-1505, 2019.

ACKNOWLEDGMENTS: This work was founded by the Department Science and Technology for health of the University of Bordeaux (STS, UBx) and by the Fondation, Gueules Cassées (grant N°13-2020).

Improved osteoblastic growth behavior on Fetuin A functionalized biodegradable nonwovens

Jana Markhoff*[1], Stefan Oschatz[1], Michael Teske[1], Ulrike Burmeister[2], Sabine Illner[1], Hermann Lang[2] and Niels Grabow[1]

[1] Institute for Biomedical Engineering, Rostock University Medical Center, Rostock, Germany
[2] Department of Operative Dentistry and Periodontology, Rostock University Medical Center, Rostock, Germany
*jana.markhoff@uni-rostock.de

INTRODUCTION

Nonwovens, manufactured by electrospinning, can be applied as a biodegradable implantable scaffold. Due to fiber diameters in the micro- and nanometer range and a high surface-to-volume ratio with high porosity they are able to mimic the natural structure of the extracellular matrix[1]. Used as a temporary support structure in the treatment of tissue defects, they are replaced within remodeling and regeneration processes starting from the inside and resulting in a biomimetic matrix tissue in the long term[2]. Nevertheless, the treatment of bone matrix defects using porous synthetic materials for guided bone regeneration often fails due to missing mechanical and biological cues. Previous studies include predominantly bone morphogenetic proteins (BMPs) or hydroxyapatite (HA) to stimulate new bone formation[3,4]. The blood plasma binding protein Fetuin A offers a high calcium affinity, thus enhancing the formation of initial CaP crystallization nuclei and promoting calcium phosphate mineralization[5].

EXPERIMENTAL METHODS

In this study, polyester-based electrospun nonwovens have been functionalized by covalent bonding with Fetuin A (i). A further test group involves Fetuin A functionalized nonwovens with subsequent in vitro calcification (ii). Unmodified nonwovens served as reference material. Materials were investigated in terms of cell seeding behavior. The test samples (Ø 6 mm) were mounted using teflon rings and directly seeded with human MG-63 osteoblasts at a defined cell density in quadruplicates for every configuration. Tissue culture polystyrene as negative control (NC) served as a common surface for growth control. Cells were incubated for 48h under common simulated in vivo conditions, followed by the determination of metabolic activity via CellQuanti Blue Assay. Cell morphology was analyzed by fluorescence staining of cells using phalloidin for actin filaments and DAPI for cell nuclei, respectively, and an Olympus BX53M microscope. Furthermore, SEM was carried out. The C-terminal propeptide in type I collagen (CICP) was verified via enzyme-linked immunosorbent assays (ELISA) to verify protein synthesis after 48h. Additionally, cytokine and chemokine levels (e.g. interleukins, MCP-1) were quantified. Extended cell cultivation and in vitro staining of sirius and alizarin red for the verification of the collagen and calcium deposition are further conducted.

RESULTS AND DISCUSSION

Initial results indicate a highly elevated metabolic activity and improved cell growth on both groups of Fetuin A functionalized nonwovens (i, ii) compared to the reference material. Cell morphology changes on the reference material were observable by fluorescence staining and scanning electron microscopy showing rounded cells and loose cell layers (Fig. 1). In contrast, functionalized nonwovens led to increased cell ingrowth into the porous surface with spread cell morphology and dense cell layers. CICP ELISA showed decreased protein levels in the supernatant of Fetuin A surfaces, maybe indicating binding of collagen propeptides to Ca^{2+} growth nuclei.

CONCLUSION

Fetuin A modification of biodegradable nonwovens is a feasible way to enhance osteoblastic growth behavior, thereby offering versatile applications regarding bone regeneration in dentistry or bone healing support.

REFERENCES

1. Wang Y. *et al.*, Nanoscale. 11:60-71, 2019
2. Keshvardoostchokami M. *et al.*, Nanomaterials. 11(1):21, 2021
3. Park YJ *et al.*, Biotechnol. Appl. Biochem. 43:17-24, 2006
4. Kim H *et al.*, J Biomed Mater Res 79A: 643–649, 2006
5. Vasquez E. *et al.*, J. Mater. Chem. B 3: 6411-6419, 2015

ACKNOWLEDGMENTS

The support of Rostock University Medical Center within the FORUN program is gratefully acknowledged.

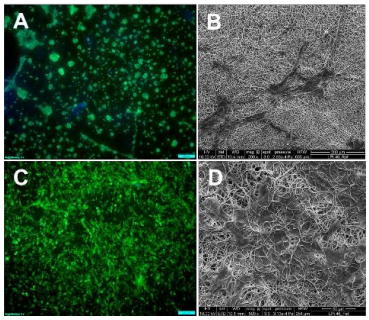

Fig. 1: Fluorescence (A,C) and SEM images (B,D) of MG63 osteoblasts on unmodified (A,B) and Fetuin A functionalized (C,D) nonwovens after 48h cultivation.

Screening for osteogenic differentiation stimulating surface characteristics on Poly lactic acid using Double Orthogonal Gradients

Roderick H.J. de Hilster[1], Torben A.B. van der Boon[1], Nikita Samochwalow[1] and dr. Patrick van Rijn[1].

[1]W.J. Kolff Institute for Biomedical Engineering and Materials Science, University of Groningen/ University Medical Center Groningen (UMCG), Ant. Deusinglaan 1, Groningen, The Netherlands
r.h.j.de.hilster@umcg.nl

INTRODUCTION

Poly (lactic acid) (PLA) has been used as a biomaterial in numerous medical applications such as tissue engineering, drug carriers, medical equipment and orthopaedic implants. PLA is used often used because of its versatility in fabrication, biodegradability, and biocompatibility. The combination of biocompatibility and biodegradability makes PLA an ideal candidate for temporary implantation devices, an application for which it is already readily used in areas such as facial surgery. Our interest lies at the cell-material interface, a crucial point for the successful integration of a medical implant/device. In our research we want to expand on the functionality of PLA by modifying the surface topography in order to promote osteogenic differentiation which in turn will improve the implant integration with the native tissue.
We aim to study the effects of surface roughness and aligned topography on osteogenic differentiation of mesenchymal stem cells (MSCs) on PLA. For this purpose, we used a double orthogonal gradient (DOG) screening platform [1]. This novel platform enables fast screening for a vast amount of combinations of different topographies and surface characteristics such as wettability on their osteogenic differentiation stimulating effects in single cell experiments. We then locate and determine hot-spots, which either promote or inhibit osteogenic differentiation. Transferring the hot spot specific topography enables us to direct the desired cell response on the substrate of interest as well as which to avoid.

EXPERIMENTAL METHODS

The topography gradients were first made on silicone material (PDMS). To generate the roughness gradient, an aluminium template was sandblasted and subsequently gradually chemically etched, creating a gradient. The roughness from that template was transferred to PDMS via liquid curing. The aligned wrinkle topography was created by plasma treating stretched PDMS covered by an angled metal shield that is released after plasma treatment [2,3]. The roughness and wrinkle topographies were transferred to PLA in a heated press. Atomic Force Microscopy (AFM) and Scanning Electron Microscopy (SEM) were used to characterize the surface features qualitatively and quantitatively. A wettability gradient was applied orthogonally to the imprinted roughness and wrinkle gradients via shielded plasma treatment. The effects of the PLA DOG topographies and wettability on osteogenic differentiation will be investigated by culturing of bone marrow derives mesenchymal stromal cells for 1,7 and 21 days. Initially characterizing osteogenic differentiation by staining for alkaline phosphatase (ALP) and osteopontin (OPN) markers and further quantification by immune-fluorescence staining. The staining's are imaged (TissueFAXS) and analysed (TissueQuest) using TissueGnostics equipment. The high-throughput analysis is complemented by confocal laser scanning microscopy (CLSM) to obtain more detailed information on specific regions of interest (ROI) on the gradient substrates. Every ROI is translated to homogeneous, non-gradient surfaces, to verify the screening outcome.

RESULTS AND DISCUSSION

On top of the DOG modified PLA surface, every position represents a unique combination of either roughness/wettability or wrinkles/wettability, within their respective gradient ranges. Transferring topography from PDMS to PLA trough heat press imprinting resulted in little to no loss topography. Wrinkle wavelength ranged from λ = 1,6 µm – 12 µm and amplitude from A = 160 nm – 1650 nm, the smallest wavelengths corresponding with the smallest amplitudes propagating in a coupled fashion along the gradient. Roughness, expressed in sRa values, ranged from ~90 – 450 nm. Cell studies on top of the PLA DOG surfaces are underway and results are expected in the near future. We hypothesize that different combinations of PLA surface modifications either promote or inhibit osteogenic differentiation in MSC's.

CONCLUSION

Using the novel DOG screening platform to characterize and identify optimal osteogenic differentiation stimulating topographies will allow us to expand the possibilities for the use of PLA in medical applications. Furthermore, by changing the topographies applied in the DOG screening we can determine other desired cellular behavior to be had on the PLA cellular interface.

REFERENCES

[1] Zhou Q. *et.al.,* Adv. Mater. Interfaces. 5(18), 2018
[2] Zhou Q. *et.al.*, Sci. Rep. 5:16240, 2015
[3] van der Boon T.A.B. *et.al.*, Adv. Biosyst. 4:1900218, 2020

Characterization of alginate and oxidized alginates: definition of new bioinks for 3D printing of breast cancer models

Chen Zhao[1], Lekha Shah[1], Ayse Latif[1], Kaye J Williams[1], Annalisa Tirella[1,2*]

[1] Division of Pharmacy and Optometry, School of Health Science, The University of Manchester, Manchester, UK
[2] BIOtech Center for Biomedical Technologies, Department of Industrial Engineering, University of Trento, Trento, Italy
[*] annalisa.tirella@unitn.it

INTRODUCTION

Alginate is a water soluble linear polysaccharide composed of (1-4)-β-d-mannuronic acid (M block) and (1-4)-α-l-guluronic acid (G block) monomers derived from different species of algae and bacteria[1]. Oxidized alginate (OA), or alginate dialdehyde, can be generated via hydroxyl functionalization on alginate's backbone and is achieved using several oxidizing agents[2]. Alginate- and OA-based hydrogels are biocompatible, stable in physiological conditions and can be used for a variety of biomedical applications. This makes them attracting biomaterials for the formulation of bioinks for the printing of three-dimensional (3D) models. The molecular weight (MW) of unmodified alginate and OAs, as well as the types and density of crosslinks are correlated with the mechanical properties of hydrogels and their degradation rate[3]. This study describes new methods for the characterization of physicochemical of alginate and OAs, as well as the mechanical characterization of a library (n=30) of alginate-based hydrogels[4]. The library was designed to match the mechanics of normal and tumour breast tissue (E=1-20kPa). Selected hydrogels were used to encapsulate breast cancer cells (i.e. MCF-7, MDA-MB 231) and evaluate the role of hydrogel mechanics on cell phenotypes[5].

EXPERIMENTAL METHODS

Determination of G/M ratio. Sodium alginate was fully hydrated in D2O, freeze-dried to remove excess of water. 10 mg/mL alginates in D2O was prepared with 1mM DSS standard (pH 5.5) to run ^{1}H-NMR tests.

Fourier transform infrared spectroscopy (FT-IR). The FT-IR spectra of alginate and OAs was measured using a Bruker IF- spectrometer in the range of 400 – 4000 cm^{-1}.

Aldehyde quantification. Aldehyde groups obtained on OAs were directly quantified by hydroxylamine hydrochloride method.

Characterization of MW using asymmetrical flow field-flow fractionation (AF4). Determination of specific refractive index was carried for all alginates. Settings for AF4 were set as described by Zhao et al.

Alginate-based Hydrogels. Alginate and OA were mixed with gelatin at different concentrations (n=30 samples). $CaCl_2$ (0.1-0.5M) was used to crosslink gels and adjust stiffness in the required range (E=1-20 kPa).

Compression Tests. Hydrogels compressive mechanical properties were determined by compressive tests with Texture Analyzer equipped with 5N load cell.

3D tumour models. MDA-MB-231 and MCF7 cells 10^6/mL were encapsulated in gels. Cell viability and proliferation were measured (Alamar blue, Live/Dead). Marker expression (i.e. CD44, CD24, CD44v6, E-cadherin and vimentin) was analysed by flow cytometry.

Sample size. All experiments are reported as mean ± st.dev of n=3 samples of at least N=2 independent experiments.

RESULTS AND DISCUSSION

Physico-chemical characterisation. G/M ratio varies between 1.4-2.2 according to the source of alginate. In OAs, aldehyde concentration has proportional increase up to 6.5 times with increased degree of oxidation (DO). MW of ~ 200 kDa (unmodified alginate) decreases to ~20 kDa with increased DO.

Mechanics of alginate-based hydrogels. Obtained hydrogels have compressive moduli in the required range, with 2kPa and 35kPa being the lowest and highest compressive moduli. Properties were found stable up to 1 week in cell culture conditions.

Cell-matrix interaction in tumour microenvironments. MCF-7 cells are more sensitive to changes of the microenvironment. In contrast, MDA-MB-231 cells show less sensitivity. Proliferation and marker expression of both cell types as response to microenvironments suggest that models can be used to delineate their phenotypes.

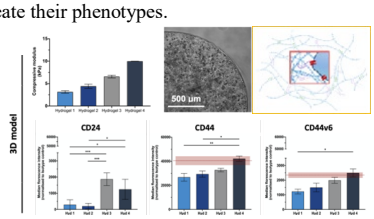

CONCLUSION

Alginate-based bioinks can be formulated to match in vivo microenvironments and fabricate 3D models to study cell-response to the microenvironment (figure). Further refinement of such models can present a platform for therapeutics and drug discoveries, as well as investigate cancer phenotypes as function of controlled microenvironments (e.g. stiffness, pH, perfusion) than currently used *in vitro* models.

REFERENCES

1. Jejurikar A. *et al.*, J. Mater. Chem. 22(19): 9751–9758, 2012
2. Emami Z. *et al.*, Carbohydr. Polym. 198:509–517, 2018
3. Kong H. J. *et al.*, Biomacromolecules 5(5):1720–1727, 2004
4. Zhao C. *et al.*, Reactive and Functional Polymers, *submitted*, 2022
5. Shah L. *et al.*, Acta Biomater., *submitted*, 2022

Foreign Body Reaction: Cartography of Macrophage Activation in a Model of Material Implantation in Rat Subcutaneous Tissue

Arvind Rathore[1], Simon Hemour[2], Vincent Raimbault[3], Helene Boeuf[1], Claudine Boiziau[1*]

[1]INSERM, Univ. Bordeaux, BioTis Laboratory, Bordeaux, France
[2]IMS, CNRS, Univ. Bordeaux, Talence, France
[3]CNRS, LAAS, Toulouse, France
* claudine.boiziau@inserm.fr

INTRODUCTION

Foreign body reaction is a long-described process that occurs upon implantation of medical devices (IMDs). Fibrosis is a common reaction observed with non-degradable IMDs, which can prevent their proper functioning, as in the case of implanted biosensors. Macrophages (either tissue resident or bone marrow-derived circulating monocytes) are main organizers of inflammatory reaction, wound healing, and tissue remodeling; commonly classified into two main categories, pro-inflammatory "M1" and anti-inflammatory "M2", their exact role and regulation in scar formation remain to be better understood[1].

EXPERIMENTAL METHODS

A printable and biocompatible resin, DL260, was designed to tightly associate to a gold electrode, and prevent its breakage due to animal movements. It was subcutaneously implanted in rats for a period of 3 weeks. After sacrifice and dissection, tissues were cryopreserved and immunofluorescence was used to characterize the cells.

RESULTS AND DISCUSSION

The protection of electrode by the resin was confirmed by X-ray imaging follow up. After 3 weeks, we isolated tissues surrounding the material, and treated them for histology analyses. Only a limited fibrosis occured. As expected based on previous experiments, macrophages were detected around the device; markers of the pro-inflammatory M1 phenotype were detected in contact with the biomaterial, colocalized with the myofibrobastic marker alpha-SMA, whereas immuno-modulatory M2 macrophages were dispersed in the tissue. To get a better information on the foreign body reaction, other markers were analyzed: markers of autophagy were differentially expressed in the tissue. Proteins associated with inflammasome activation were hardly detected.

CONCLUSION

A cartography of macrophage activation phenotypes will be presented, in relation with the collagenous matrix density. The association between autophagy activation and inflammasome regulation remains to be better characterized.

REFERENCES

1. Aussel A. *et al*. Biomed. Mater. 14:025009, 2019.

ACKNOWLEDGMENTS

This project has received funding from the European Union's Horizon 2020 research and innovation programme under the Marie Skłodowska-Curie grant agreement No 813006, from the Agence Nationale de la Recherche (ANR-16-CE19-0001-01) and was also supported by the LabEx AMADEus (ANR-10-LABX-42)

Study of the Cu^{2+} Doping Effect on the Acute Inflammation Response to Biphasic Calcium Phosphate Materials for Bone Defects Regeneration

Léa Thoraval[1*], Émilie Thiébault[1], Renaud Siboni[1], Aurélie Moniot[1], Christine Guillaume[1], Aurélie Jacobs[2], Jean-Marie Nedelec[2], Guillaume Renaudin[2], Stéphane Descamps[2], David Marchat[3], Sophie C. Gangloff[3], Julien Braux[1], Frédéric Velard[1]

[1]EA4691 BIOS, University of Reims Champagne-Ardenne, Reims, France
[2]University Clermont Auvergne, Clermont Auvergne INP, CNRS, ICCF, Clermont-Ferrand, France
[3]Mines Saint-Etienne, INSERM U1059 SAINBIOSE, University of Lyon, University Jean Monnet, Saint-Etienne, France

[*] lea.thoraval@univ-reims.fr

INTRODUCTION

Calcium phosphates (CaP), such as Biphasic Calcium-Phosphate (BCP), are widely used as prosthesis coating and bone substitute. Major threats in the field are bacterial infections and release of CaP particles that mount an inflammatory response which if uncontrolled, could result in implant loss. Cationic substitutions (e.g., Sr^{2+}, Zn^{2+}) in CaP have been shown to control the biomaterial particles-induced inflammatory process[1,2]. Copper ion (Cu^{2+}) is known for its antibacterial potential and Cu-doped CaP have been demonstrated biocompatible in previous studies[3,4]. The present work aims to evaluate *in vitro* the effect of copper on CaP-mediated human primary neutrophils activation and biomaterial-induced recruitment of blood neutrophils *in vivo*.

EXPERIMENTAL METHODS

Cu-doped or undoped BCP powders obtained by two different processes (*i.e.*, sol-gel (SG) and aqueous precipitation (AP)), were studied. Human primary neutrophils (PMN) were isolated from blood (n=9-12 healthy donors) then cultured with BCP particles alone, or in co-stimulation with lipopolysaccharide (LPS). IL-8 and TNF-α concentrations were determined in conditioned culture supernatants by ELISA, MMP9-related gelatinolytic activity was examined by zymography and cell viability assessed by measuring lactate dehydrogenase activity. Cell/particle interactions were imaged thanks to Scanning Electron Microscopy (SEM). Using the air pouch model, the ability of doped and undoped powders to modulate PMN recruitment *in vivo* was investigated (n=10-16 mice). Recruited cells in the air pouch were collected, numbered then identified thanks to flow cytometry. The significance of the results was assessed with the non-parametric Wilcoxon Mann Whitney test and differences were considered significant at $p<0.05$.

RESULTS AND DISCUSSION

SG powders batch was well tolerated as we only noticed a slight variation in LDH activity while the increase in LDH signal observed with AP samples seemed to be reduced in the presence of copper (diminution in mean of 20% vs AP copper-free powder). Cu-doped samples stimulated the release of IL-8, exhibiting a copper dose-dependent effect, especially with LPS co-stimulation, and whatever the manufacturing process is (1.5 to 2.5-fold increase in IL-8 production with Cu^{2+} vs copper-free materials, $p<0.05$). All BCP materials failed to induce the production of TNF-α by neutrophils but tended to decrease its concentration in LPS-stimulated PMN supernatants. Interestingly, the highest copper doping restored TNF-α secretion as compared to LPS condition ($p>0.05$ for AP). From these findings, our BCP particles did not have an intrinsic inflammatory effect, but the enhanced IL-8 production induced would strengthen the recruitment of additional immune cells, without over-activating them. Undoped samples generated an increase in MMP9-related gelatinolytic activity which was not potentiated by LPS addition, whereas in this latter condition Cu-doped samples moderated by an average of 10% the gelatinolytic activity. SEM allowed us to observe the formation of Neutrophil Extracellular Traps in contact with BCP particles. *In vivo,* all powders induced an increased recruitment of total leukocytes ($p<0.05$). Cu-doped AP samples enhanced the PMN recruitment compared to undoped samples whereas monocyte/macrophage recruitment was decreased.

CONCLUSION

We demonstrated here a robust immunomodulatory effect of Cu-doped BCP powders, that occurs in a Cu dose-dependent manner and independently of the synthesis route. Our study suggests that such doped samples may be interesting to maintain a moderate level of inflammation to ensure the bacterial clearance by PMN besides of anti-microbial potential of the material in infected bone context.

REFERENCES

1. Velard F. *et al*., Biomaterials. 31(8): 2001-9, 2010
2. Buache E. *et al*., Acta Biomater. 8(8): 3113-9, 2012
3. Jacobs A. *et al*., Materials. *14(9), 2393*, 2021
4. Gomes S. *et al*. Acta Biomater. 65: 462–474, 2018

ACKNOWLEDGMENTS

The authors would like to thank Institut Carnot MICA (BiomateriOS, and OptimOS programs) and “Fondation des Gueules Cassées” (PorOS program) for providing financial support to this project”.

Sulfated Micro-Islands in Granular Hydrogels Promote Endogenous Cell Homing into Cartilage Defects

Anna Puiggali-Jou[1*], Maryam Asadikorayem[1], Katharina Maniura [2], Marcy Zenobi-Wong[1]

[1] Department of Health Sciences and Technology, ETH Zurich, Zurich, Switzerland
[2] Laboratory for Biointerfaces, Empa, Sant Gallen, Switzerland
[*] anna.puiggalijou@hest.ethz.ch

INTRODUCTION

Chondral lesions are joint injuries, often to the knee or hip, that involve the articular cartilage (AC).[1] Usually, they are associated with traumatic injuries that, left untreated, lead to osteoarthritis (OA). Unfortunately, the regeneration of cartilage defects is limited by its low capacity to self-repair. Its avascular nature and low cell density impede the generation of de novo extracellular matrix (ECM). Compared to autologous chondrocyte implantation, in situ cartilage regeneration holds great promise to avoid expensive cell therapies and achieve one-step surgery. To promote migration of bone marrow stem cells from the subchondral bone, we propose a heterogeneous granular hydrogel that provides enough void space for cell infiltration, containing sulfated micro-islands that slowly release chemotactic PDGF-BB and chondrogenic TGFβ3. These micro-islands provoke a gradient of growth factors that enhances cell migration and differentiation.

EXPERIMENTAL METHODS

Granular hydrogels were prepared by combining UV-crosslinked methacrylated hyaluronic acid (HAMA) microgels, growth factor-loaded sulphated HAMA (S-HAMA) microgels, and using activated factor XIII to secondarily crosslink the microgels together. First, different materials and sizes of microgels were assessed in a spheroid migration assay where the sprouting distance was compared (an indicative measure of their migration potential). Also, time-lapse microscopy was employed to measure cell directness and velocity. Once the best condition for enhancing cell migration was established, the chondrogenesis potential was evaluated by histology with and without loading of growth factors. Finally, their ability to significantly improve endogenous cartilage repair was validated with bovine osteochondral explants. Osteochondral explants were harvested from joints of calves, obtained from a local abattoir.

RESULTS AND DISCUSSION

Granular hydrogels were easily prepared by mechanical sizing and secondary enzymatic crosslinking. In vitro experiments with different sized gels (20 µm and 100 µm sizing grids) and chemistries show that cell migration (directness, speed and travelled distance) is enhanced in the presence of RGD, PDGF and smaller microgel size (20 µm) when compared to bulk gels. It was corroborated that sulfated microgels can act as micro-islands guiding cell's migration (**Figure 1**). After four days of culture, sprouting occurred primarily in the direction of S-HAMA microgels compared to HAMA microgels. Also, it was proven that sulfated microgels retained PDGF-BB and TGFβ3 for more extended periods due to their high binding affinity towards positively charged proteins via electrostatic interactions. The increase in void space compared to bulk hydrogels enhanced cell-matrix deposition. TGFβ3 loaded sulfated microgels were enough to guide cell differentiation and matrix deposition without need for additional growth factor (or TGFβ3) supplementation in the media, representing a more realistic system for clinical application. Finally, the ability to significantly improve endogenous cartilage repair was validated with bovine osteochondral explants achieving good cell colonisation and ECM deposition by endogenous migrated cells.

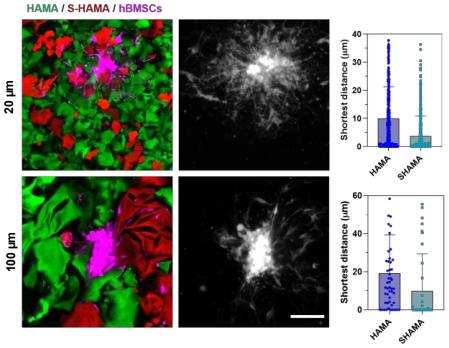

Figure 1. Confocal images of hBMSCs spheroids (pink) after four days in culture in a granular hydrogel composed of HAMA (green) and S-HAMA (red, left). Projection of the 100 µm z-stack of the spheroid (white, middle). The shortest distance of the cells to HAMA vs SHAMA microgels (right). Scale bar 100 µm.

CONCLUSION

In summary, novel granular microgels presented in this work provide a microporous environment for endogenous cell migration. The addition of S-HAMA micro-islands promote cell attachment and spreading, recruit stem cells by slowly releasing chemotactic PDGF-BB, and induce chondrogenic differentiation of the recruited cells by releasing chondrogenic TGF-β3.

REFERENCES

1. Smith G, *et al.*, *J. Biomech.* 2:5-11, (2011).
2. Vasiliadis HS, *et al.*, *Am. J. Sports Med.*, **38**, 943–949 (2010).

ACKNOWLEDGMENTS

The authors would like to thank the European Commission for the MSCA individual fellowship (Grant no: 885797) for providing financial support.

Double Orthogonal Topography Gradients; synergistic effects of isotropic and anisotropic surface features on osteogenic differentiation of mesenchymal stem cells.

Torben A.B. van der Boon[1], Roderick H.J. de Hilster[1], Hidde Vink[2], dr. Diego R. Gomes[2], dr. Yutao Pei[2], and dr. Patrick van Rijn[1].

[1]W.J. Kolff Institute for Biomedical Engineering and Materials Science, University of Groningen/ University Medical Center Groningen (UMCG), Ant. Deusinglaan 1, Groningen, The Netherlands
[2]Department of Advanced Production Engineering, Engineering and Technology Institute Groningen, Faculty of Science and Engineering, University of Groningen, Nijenborgh 4, 9747 AG Groningen, The Netherlands
t.a.b.van.der.boon@umcg.nl

INTRODUCTION

Until now, the research field of studying the influence of surface topography on cell behaviour has been naturally divided into two branches; 1) surface roughness, and 2) aligned surface features.[1,2] The research presented here is bridging both worlds by studying the synergistic effects of surface nano/micro roughness and aligned nano/micro topography on osteogenic differentiation of mesenchymal stem cells (MSCs), by utilizing a revolutionary, in-house developed, double orthogonal gradient (DOG)[3] screening platform. Conventional research techniques have not lived up to this level of complexity, since they mostly tackle a few distinct situations of a single parameter. By combining the two topography parameters in an orthogonal fashion, we have created a cell screening platform which enables us to screen for vast amounts of data in single cell studies. The power and broader potential of this platform lies in the quick visual assessment of hot-spots, which either promote or inhibit certain cell behaviour, enabling us to direct the cell response into a desired direction and herewith identifying which surface parameters to incorporate into medical implant designs and which to avoid. We foresee that our platform will aid in drastically improving implant effectiveness and quality of life of patients.

EXPERIMENTAL METHODS

The DOG platform is based on silicone material (PDMS). An aluminium template is sandblasted and chemically etched to generate a roughness gradient, which is imprinted into PDMS by means of liquid curing. Oriented orthogonally to the imprinted roughness gradient, a gradient of aligned wrinkle topography features is created, using our previously described 'stretch-and-release' approach.[4,5] Atomic Force Microscopy (AFM) and Scanning Electron Microscopy (SEM) were used to characterize the surface features qualitatively and quantitatively (FIGURE1). The effects on osteogenic differentiation of MSCs will be investigated by culturing for 21 days and staining for alkaline phosphatase (ALP) and osteopontin (OPN) markers. Read-out and quantification will be done using fluorescence immune-staining, imaged (TissueFAXS) and analysed (TissueQuest) using TissueGnostics equipment. The high-throughput analysis is complemented by confocal laser scanning microscopy (CLSM) to obtain more detailed information on specific regions of interest (ROI) on the gradient substrates. Every ROI is translated to homogeneous, non-gradient surfaces, to verify the screening outcome.

RESULTS AND DISCUSSION

Every imaginable position on the DOG surfaces represents a unique combination of both topography types, within their respective gradient range. Wrinkle features range from λ = 1,6 µm – 12 µm and A = 160 nm – 1650 nm, the smallest wavelengths corresponding with the smallest amplitudes going from small to big, in a coupled fashion. Roughness features, expressed in sRa values, range from ~90 – 450 nm. Further results on cell studies are expected in the near future. We hypothesize that different combinations of both surface parameters influence osteogenic differentiation of MSCs differently, either promoting or impeding it.

CONCLUSION

This novel cell screening platform bridges the two branches in the field of topography feature – cell interactions. The identification of synergistic effects of both topography types on stem cell differentiation will accelerate our understanding of surface topography influence on cell behavior and ultimately enhance biomaterial development.

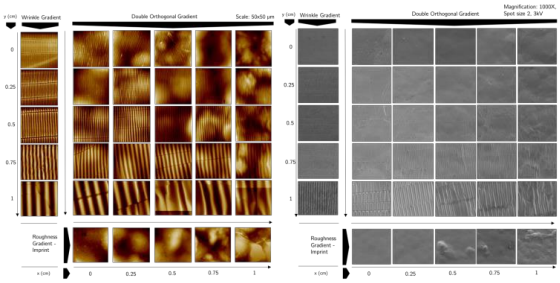

Figure 1. Quantitative (left) and qualitative (right) AFM and SEM images reveal successful gradient preparation and DOG formation.

REFERENCES

[1] Faia-Torres A.B. *et.al.*, Acta Biomaterialia. 28:64-75, 2015
[2] Yang L. *et.al.*, Biomater. Sci. 8:2638-2652, 2020
[3] Zhou Q. *et.al.*, Adv. Mater. Interfaces. 5(18), 2018
[4] Zhou Q. *et.al.*, Sci. Rep. 5:16240, 2015
[5] van der Boon T.A.B. *et.al.*, Adv. Biosyst. 4:1900218, 2020

High-throughput Screening to Elucidate Biomaterial-induced Fibrosis

Torben A.B. van der Boon[1], Lisa E. Tromp[1], Liangliang Yang[1], Lu Ge[1], dr. Qihui Zhou[2], prof. dr. Ruud A. Bank[1] and dr. Patrick van Rijn[1]

[1]W.J. Kolff Institute for Biomedical Engineering and Materials Science, University of Groningen/ University Medical Center Groningen (UMCG), Ant. Deusinglaan 1, Groningen, The Netherlands
[2]Center for Precision Medicine/Stomatology Center, The Affiliated Hospital of Qingdao University, Qingdao, China
t.a.b.van.der.boon@umcg.nl

INTRODUCTION

Nowadays, it is becoming common knowledge that the human body, its tissues and cells react to biophysical and biochemical cues located on biomaterial surfaces. Identifying how these parameters influence cellular behavior is of crucial importance and will aid us in the further development of medical implant technology. Unfortunately, in many studies attempting to identify these physicochemical properties' influence on cell behavior, investigation of individual properties is the conventional method, leaving out a significant number of other variables which are encountered *in vivo*, which is where cells always interact with multiple cues simultaneously.[1,2] We have developed an orthogonal double gradient platform which allows us to investigate just such complex situations in a high-throughput screening (HTS) fashion. The platform grants us the power to screen the cell response towards thousands of these combined parameters in single cell experiments, which will result in the optimization of material properties to enhance biomaterial and implant function. Currently, we are in the final platform optimization stage, after which we will screen silicone rubber's susceptibility to fibrosis and scar tissue formation.

EXPERIMENTAL METHODS

PDMS double orthogonal gradients (DOGs) are prepared by sequential imprinting – and shielded air plasma oxidation treatments in accordance with previously published methodology.[3–5] Primary human dermal fibroblasts will be cultured on the DOGs for 7 days and stained for early fibrosis biomarkers (Collagen-I and α-SMA).

RESULTS AND DISCUSSION

Every imaginable position on the orthogonal double gradient surfaces has a unique combination of three surface parameters, possessing 'real', clinically relevant values. This allows us to investigate a virtually unlimited amount of different parameter combinations, within their respective ranges, on single substrates. Wavy topography gradients range from λ = 1,5 µm – 10 µm and A = 50nm – 1,5 µm, the smallest wavelengths corresponding with the smallest amplitudes going from small to big, in a coupled fashion. Stiffness gradients range in Young's Modulus from ~50 – 500 MPa, and 'wettability' gradients from 5 – 90 ° in water contact angle (WCA). As a 'proof of concept', we cultured hBM-MSCs on the platforms for 24 h, imaged the cells via automated fluorescence microscopy and identified the cell response with respect to cell density, cell spreading, and nucleus area. We have found that the synergistic effect of abovementioned parameter combinations all influence cell behavior in a different manner with regard to these relatively 'simple' assessable characteristics. Our current work involves the translation of 'hotspots' or regions of interest (ROI) to homogeneous parameter substrates, as a last verification step in the optimization process, as well as the screening of biomaterial susceptibility to fibrosis and scar tissue formation.

CONCLUSION

The highly efficient cell screening tool we have created with our DOG platform allows us to screen cell response to combined physical parameter influence in a high-throughput fashion, investigating thousands of different parameter combinations in single cell experiments. It will serve its purpose to facilitate enhanced biomaterial development.

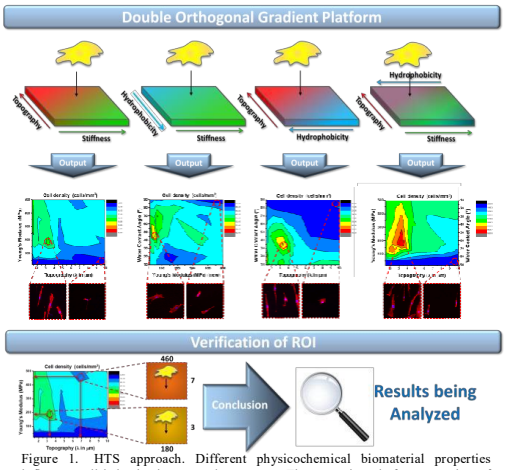

Figure 1. HTS approach. Different physicochemical biomaterial properties influence cell behavior in a complex manner. The screening platforms consists of four different parameter combinations within a gradient-like range. The influence on, in this example 'Cell density', is identified in single cell studies via fluorescence immune-staining and automated imaging and analysis. Hits, or ROI's, are translated to homogeneous substrates to verify the screening outcome.

REFERENCES

[1] Schaap-Oziemlak A.M. *et. al.*, RSC Adv. 4:53307, 2014
[2] Kühn P.T. *et. al.*, ChemNanoMat. 2:407-413, 2016
[3] Zhou Q. *et.al.*, Sci. Rep. 5:16240, 2015
[4] Zhou Q. *et.al.,* Adv. Mater. Interfaces. 5(18), 2018
[5] van der Boon T.A.B. *et.al.*, Adv. Biosyst. 4:1900218, 2020

Interactive hemocompatible coatings that modulate hemostasis at the surface of blood contacting medical devices polymers

Lena Witzdam[1], Fabian Obstals[1], Manuela Garay-Sarmiento[1], Jonas Quandt[1], Nina Kostina[1], Oliver Grottke[4], Cesar Rodriguez-Emmenegger[1,2,3,*].

[1]DWI Leibniz Institute for Interactive Materials, Aachen, Germany, [2] Institute for Bioengineering of Catalonia (IBEC), and [3]Institució Catalana de Reserca I Estudis Avançats (ICREA), Barcelona, Spain
[*] rodriguez@dwi.rwth-aachen.de

INTRODUCTION

Our goal is to develop coatings that turn the surface of medical devices hemocompatible to prolong their use without negative outcomes. This is a major challenge since the contact of blood with any surface different than the lining from the vessels instigate the activation of coagulation. As early as seconds to minutes after the contact of blood with the surface, protein adsorption occurs. This leads to the reciprocal activation of factor XII and plasma prekallikrein generating large amounts thrombin which locally overwhelm the inhibitory effect of current anticoagulants. In indwelling devices as well as dialysis membranes or oxygenators the formation and dislodge of clots can lead to devastating problems as thrombosis, infarct and stroke. Thus, a holistic strategy that considers the challenges from the blood and device sides is perhaps the only way to address this challenge. Towards this aim our group develops coatings that go beyond passivation but that interact with blood and orchestrate cascade of reactions to enhance their hemocompatibility and performance. The coatings encompasses three hierarchical levels; a passive, an active and an interactive one.[1] The passive level consists of antifouling polymer brushes that create a physical barrier to protein adsorption and cell adhesion thereby prohibiting the surface-induced activation of coagulation. Here the goals are (i) to program repellency at nano and mesoscopic scales in the molecular structure of brushes and (ii) to develop methods to translate these finding to current medical devices. The active level is achieved by decorating the brushes with biomolecules capable of binding to key elements of the coagulation cascade and inactivate them directly at the surface of the device. Compared to anticoagulants, this approach localizes the inhibitory effect at the surface and do not interfere with hemostasis. However, no coating, even natural endothelium, is infallible. To address this we introduce an interactive level. Here the goal is that the coating sense the presence of a thrombus and orchestrate that its disintegration. To address this challenge, we develop a de novo fibrinolytic system that is only active in the presence of thrombus and orchestrate its destruction using components present in blood. After digestion, the coating return to its dormant state.

EXPERIMENTAL METHODS

The passive part of the coating is achieved by antifouling polymer brushes grafted by surface-initiated polymerization of *N*-2-hydroxypropyl methacrylamide and carboxybetaine methacrylamide. The active and interactive part were built by immobilizing inhibitors to the coagulation factors and tissue plasminogen activator (tPA) on the non-thrombogenic coating. The enzymatic activity was proved by using a chromogenic substrates that acts and in vitro hemocompatibility test with human blood.

RESULTS AND DISCUSSION

No adsorption of Factor XII that activates surface-induced coagulation was observed on the brushes preventing activation of the contact system. Furthermore, surface plasmon resonance and scanning electron microscopy studies demonstrated that the brushes act as a barrier to protein adsorption as well as prohibit the adhesion of platelets and leukocytes. By using a switchable attraction strategy between tPA and the brushes to enhance the subsequent covalent bonding 24.3 $ng \cdot cm^{-2}$ tPA were immobilized. Similar approach was utilized to immobilized inhibitors of FXIIa and FXIa. These inhibitors specifically captured the active form of the coagulation factors, thereby preventing the propagation of coagulation but without interference with the global hemostasis. The immobilized tPA was capable of digesting a fibrin-mimic substrate at physiological concentration in 15 min. Furthermore, in vitro accelerated coagulation experiments demonstrated that the fibrinolytic coating was able to delay clot formation, digested the formed clots and completely prevented the adhesion of blood components.

CONCLUSION

In this work we developed a self-regulated coating that prevents activation of coagulation but in the presence of clots, it is capable of directing blood fibrinolytic system to digest it. The results in this work demonstrate that the combination of passive repellency with adaptive fibrinolysis is a powerful tool to counteract thrombus formation without affecting global hemostasis and can greatly benefit blood contacting medical devices.

REFERENCES

[1]Obstals F, Witzdam L, et. al., ACS Appl. Mater. Interfaces 13: 11696–11707, 2021.

ACKNOWLEDGMENTS

The authors acknowledge the financial support by the Deutsche Forschungsgemeinschaft (DFG, German Research Foundation) via Schwerpunktprogramm “Towards an Implantable Lung”, 346972946.

Quantitative analysis of distribution paxillin and vinculin in osteoblasts and fibroblasts binding to electrospun PMMA fibers based on super-resolution fluorescent images.

Berniak Krzysztof[1*], Ura Daniel[1], Stachewicz Urszula[1]

[1]Faculty of Metals Engineering and Industrial Computer Science, AGH University of Science and Technology, Cracow, Poland

[*] berniak@agh.edu.pl

INTRODUCTION

The study of interactions between electrospun fibers and human cells is one of the most crucial elements in assessing potential application in bioengineering. Electrospun fibers are one of the very often used scaffolds in n tissue engineering, which should have desired strength and surface properties. Modifying the surface properties of the fibers has a direct effect on cells' adhesion to the scaffold and their proliferation. The dynamics of the cell adhesion process to the scaffold are regulated by the internal multi-protein complex's focal adhesions. They are responsible for forming mechanical links between intracellular actin bundles and the extracellular matrix or substrate. A description of the distribution of adhesion sites in a cell can provide information on the dynamics of the binding process of cells to the scaffold1. Quantification of the special distribution of proteins requires highly specific fluorescent labeling techniques and optical fluorescent microscopy.

In this study, we focus on analyzing the spatial distribution of proteins that are included in focal adhesions formation to the scaffold using two types of cells: osteoblasts and fibroblasts. Vinculin and paxillin are used as a marker of focal adhesion for both types of cells. To produce electrospun fibers Poly(methyl methacrylate) (PMMA) was used. It is one of the most commonly used polymers with a very high degree of biocompatibility with human cells[3], and they have already been used for cell dynamics studies for tissue engineering[2]. To assess potential correlations between the distribution of focal adhesions in two different types of cells to electrospun PMMA fibers, a quantitative analysis of localizations of particular protein foci in 3D multicolor microscopy images is required. Additionally, we show the potential application of high-resolution confocal microscopy with Airyscan2 to study cell-matrix interaction on electrospun polymer fibers.

EXPERIMENTAL METHODS

To obtain a 12 wt. % solution, PMMA was dissolved in DMF. The solution was stirred at 700 rpm for two h on a hot plate set at 55°C. PMMA fibers were produced via electrospinning using the apparatus EC-DIG with climate control. The studies were performed on PMMA electrospun fibers using human osteoblast-like cell line MG63 and fibroblasts NIH 3T3 cell line. Cells were seeded in the PMMA scaffolds in culture media under standard conditions. After three days of cell growth, samples of the PMMA scaffolds were fixed and permeabilized. To visualize actin filaments, cells were incubated with Alexa Fluor™ 488 Phalloidin. Nuclear DNA was stained with DAPI for 5 min. Selected proteins involving in focal adhesion (vinculin and paxillin) were labeled by immunofluorescence. Multicolor 3D microscopy images of cells connecting to PMMA fibers were acquired using confocal microscopy with the high-resolution concept Airyscan2 (Zeiss LSM 900), and the image analysis was performed by using ImageJ.

RESULTS AND DISCUSSION

The application of the high-resolution confocal microscopy with Airyscan2 allowed to register the distribution of vinculin and paxillin to polymer fibers with high resolution. Spatial analysis reveals significant changes in the density of proteins foci along with the cell-binding places to PMMA fibers between osteoblast and fibroblast. It indicates the different architecture of binding mechanisms for osteoblast and fibroblast to the PMMA electrospun fibers. Comparison distribution accumulation of vinculin and paxillin between PMMA fibers and glass as a control for both types of cells shows that the type of substrate with which cells interact has a direct impact on the dynamics of the process of creating binding sites to them.

CONCLUSION

The use of Airyscan2 revealed the distribution of vinculin and paxillin in the areas of cell-fiber interaction in osteoblasts and fibroblasts. Cluster analysis on images with the super-resolution localization of the adhesion proteins in osteoblast and fibroblast clearly highlights substrate-related correlations. It enabled a quantitative description of the architecture of the process of cell-PMMA interaction.

REFERENCES

1. Stachewicz U. *et al.* Acta Biomaterialia 27:88–100, 2015
2. Liu Y. *et al.*, J. Biomed Mater Res A. 90(4): 1092-1106, 2009
3. Ura DP. *et al.*, Bioengineering (Basel) 6(2): 41, 2019

ACKNOWLEDGMENTS

This study was conducted within "Nanofiber-based sponges for atopic skin treatment" project carried out within the First Team program of the Foundation for Polish Science co-financed by the European Union under the European Regional Development Fund, project no POIR.04.04.00-00- 4571/17-00.

Effect of blood genetic mutations to the hemolytic behavior of cerium oxide nanoparticles

Ioannis Tsamesidis[1*], Georgia K. Pouroutzidou[1,2], Maria-Eleni Ioannou[1], Mirto Karkavitsa[3], Aggeliki Pagkarliota[4], , Iason Chatzimentor[1], Vlachaki Efthymia[4] and Eleana Kontonasaki[1]

[1]School of Dentistry, Faculty of Health Sciences, Aristotle University of Thessaloniki, 54124 Thessaloniki, Greece
[2]School of Physics, Faculty of Sciences, Aristotle University of Thessaloniki, 54124 Thessaloniki, Greece
[3]Department of Biomedical Sciences, Faculty of Health Sciences, International Hellenic University, 570 01 Thessaloniki, Greece
[4]Ippokratio University Hospital, Thessaloniki, Greece
[*] itsamesidis@auth.gr

INTRODUCTION

Blood disorder diseases (BDDs) are very common all over the world, owing to hematopoietic system malfunction. Among non-treated BDDs, thalassemia, sickle cell anemia and G6P-d deficiency are most widely known as pro-oxidant mutations and possess elevated oxidative stress micro-environments. The potential of medicines in nanoscale raises many hopes to address unmet medical needs, as defined recently by the WHO in its report[1]. Nanomedicine employs various combinations of nanomaterials and molecules towards their application for the therapy of different disorders. Previous studies have developed and applied ceria-based materials for biomedical applications[2] indicating cerium based nanoparticles as potent redox modulators and drug delivery agents[3]. Considering, Ce-NPs as promising candidates for biomedical applications, the blood compatibility of such materials was investigated in various BDDs, where Reactive Oxygen Species (ROS) imbalances contribute to disease progression.

EXPERIMENTAL METHODS

Synthesis of Ce-NP

Synthesis of CeO_2 nanoparticles was performed with the sol-gel method. Cerium nitrate hexahydrate 5g, gelatin 0,2g, ammonia solution and d.d water 20ml were used in order to obtain the optimum sample for this study[4]. The powder containing Ce-NPs was dried and then heated at 550ºC for 1h.

Hemocompatibility assay

To determine the hemolytic activity on healthy and pathological Red Blood Cells (RBCs) such as sickle cell anemia, intermediate and minor thalassemia and G6P-d deficiency, nanoparticles suspension (stock = 5 mg/mL) was prepared at different concentrations (125, 250, 500, 1000 μg/mL) for 24 and 96 hours incubation at 37 °C (Thermomixer). The absorbance of hemoglobin release (540 nm) in the supernatants was evaluated. The percent of hemolysis was calculated as follows: Hemolysis % = [(sample absorbance - negative control)/ (positive control - negative control)] * 100%.

RESULTS AND DISCUSSION

The hemolytic behaviour of Ce-NPs in various pathological RBCs (sickle cell anemia, intermediate and minor thalassemia and G6P-d deficiency) reveled different amounts of hemolysis according to the RBC pathology and the time of incubation (Table 1). RBCs of all different pathological conditions appeared to be hemocompatible at concentrations lower than 500 μg/ml after 24 hours of incubation. The most pronounced result appeared to be the low hemolytic rates of minor-thalassemia RBCs after 96 hours of incubation, where all the pathological RBCs (especially sickle RBCs) initiated the eryptosis process characterized with increased amounts of released hemoglobin.

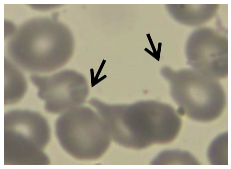

Figure 1. Sickle cell anemia RBCs after contact with Ce-NP05g (1 mg/ml)

BDDs	Hemolysis (%) (1 mg/ml)	
	24 hours	96 hours
Healthy RBCs	1%	5%
Minor Thalassemia	1%	3%
Intermediate Thalassemia	5%	10%
Sickle-cell anemia	4%	12%
G6P-d deficiency	4%	8%

Table 1. Hemolysis rate of Ce-NP05g after contact with various pathological RBCs.

CONCLUSION

In conclusion, the direct contact of RBCs from patients with different pathological blood disorder diseases with cerium-oxide nanoparticles can result in higher hemolysis, with the exception of minor thalassemia. Minor-thalassemia erythrocyte storage in presence of Ce-NPs should be further investigated through proteomic approaches.

ACKNOWLEDGMENTS

This work is supported by European Union's Horizon 2020 research and innovation program under grant agreement No 953128, project: Smart, Multifunctional Dental Implants: A solution for peri-implantitis and bone loss.

REFERENCES

1. Kaplan, *et al*., priority medicines for Europe and the world 2013 update. *J. Chem. Inf. Model.* **2013**, *53*, 1–246.
2. Li, H.; Yang, *et al*., The advances of ceria nanoparticles for biomedical applications in orthopaedics. *Int. J. Nanomedicine* **2020**, *15*, 7199–7214, doi:10.2147/IJN.S270229.
3. Abuid, *et al*., Biomedical applications of cerium oxide nanoparticles: A potent redox modulator and drug delivery agent. *Nanoparticles Biomed. Appl. Fundam. Concepts, Biol. Interact. Clin. Appl.* **2019**, 283–301, doi:10.1016/B978-0-12-816662-8.00017-5.
4. Darroudi, Facile synthesis, characterization, and evaluation of neurotoxicity effect of cerium oxide nanoparticles. *Ceram. Int.* **2013**, *39*, 6917–6921

The influence of surface topography parameters on the susceptibility to albumin adsorption for clinical application in VAD devices

Przemyslaw Kurtyka[1,2,3], Roman Major[3], Marcin Kaczmarek[1], Wojciech Kajzer[1*], Zbigniew Paszenda[1], Roman Kustosz[2]

[1] Faculty of Biomedical Engineering, Silesian University of Technology, Zabrze, Poland
[2] Institute of Heart Prosthesis, Foundation Of Cardiac Surgery Development, Zabrze, Poland
[3] Institute Of Metallurgy And Materials Science, Polish Academy Of Sciences, Krakow, Poland
*wojciech.kajzer@polsl.pl

INTRODUCTION

In recent decades, due to the steadily increasing number of patients with heart failure and the limited number of organs available for heart transplantation, therapies with the use of mechanical circulatory support have played an increasingly important role. The Ventricular Assist Devices (VAD) are currently the only alternative to heart transplantation and are considered the most reliable and effective therapy for treating patients with advanced heart failure.[1] The most commonly used VAD constructions in clinics are fully implantable and intended for long-term use. Therefore it is very important to provide their high biocompatibility to ensure their reliability, patient safety, and comfort. This therapy may be associated with the occurrence of complications and other adverse events[2-4]. One of the most common reported complications are the pump thrombosis and inflow obstruction, caused by the formation of cystic tissue penetrating the lumen of the inflow cannula.[5-7]. Preclinical trials and careful analysis of the literature allow us to believe that the solution may be the use of appropriate surface modification, resulting in the controlled growth of scar tissue[8–10]. Due to the fact that one of the first stages of the body's reaction to the implant is the attachment of water and protein to the surface, it was decided to assess the impact of the modification on protein adsorption on the example of albumin.

EXPERIMENTAL METHODS

The study presents an analysis of the relationship between surface topography parameters on susceptibility to protein adsorption. On the basis of technological tests, the paper proposes vacuum powder sintering as a method of surface modification. The sintering process included modifications with the use of Commercially Pure Titanium (Cp-Ti) powder with two different grain morphologies - spherical and irregular. The grain size was changed in the rage of 50 to 250 µm. The obtained surfaces were then analyzed by digital and scanning electron microscope [SEM]. Roughness was evaluated with the use of contact profilometry. Additionally, the porosity and wettability assessment were performed. Protein adsorption was assessed using human whole blood, platelet-leukocyte concentrate and Qubit® 2.0 fluorometer.

RESULTS AND DISCUSSION

Surfaces were characterized by Ra in the range of 21 - 48 µm and Rz 129 – 274 µm depending on the size and morphology of the powder grains. Porosity analysis was performed using image analysis of digital microscopy, and for the proposed variants was within the range of 29 – 47%. The wettability assessment was performed with the use of optical goniometry, and the obtained coatings were characterized by a contact angle in the range of $\theta \approx 103^{o} \pm 4$. The susceptibility to protein adsorption depending on the medium was in the range of 497 ng / µl ± 44 and 467 ng / µl ± 62.

CONCLUSION

As a result, a positive effect of the proposed surface modifications on the amount of adsorbed protein relative to the reference sample for all modifications was observed. The correlation of surface topography parameters on the susceptibility to protein adsorption was observed.

REFERENCES

[1] J. H. Kim, Cardiology Clinics, vol. 36, no. 4. W.B. Saunders, pp. 443–449, 01-Nov-2018.
[2] M. Gawlikowski et al., Photonics Lett. Pol., vol. 12, no. 2, pp. 46–48, 2020.
[3] R. Antończyk et al., Kardiochirurgia i Torakochirurgia Pol., vol. 14, no. 1, pp. 76–78, 2017.
[4] A. B. Nguyen et al., Curr. Heart Fail. Rep., vol. 13, no. 6, pp. 302–309, Dec. 2016.
[5] C. H. Glass et al., Cardiovasc. Pathol., vol. 38, pp. 14–20, Jan. 2019.
[6] M. Gawlikowski et al., Proceedings of SPIE, Volume 10455, Article number 104550L, p. 22, 2017.
[7] S. S. Najjar et al., J. Hear. Lung Transplant., vol. 33, no. 1, pp. 23–34, Jan. 2014.
[8] E. A. Rose et al., Circulation, 1994, vol. 90, no. 5 II.
[9] P. Kurtyka et al., Eng.of Biomaterials, Vol. 22, no.151, 2019.
[10] C. M. Zapanta et al., ASAIO J., vol. 52, no. 1, pp. 17–23, Jan. 2006.

ACKNOWLEDGMENTS

Project supported by:
NCBiR: RH-ROT/266798/STRATEGMED-II
National Science Centre, Poland: 2018/31/N/ST8/01085

Organ-on-a-chip to evaluate biomaterials

Oscar Castano[1,2,3*], Adrián López-Canosa[2], Inês Sousa[2], Anna Vilche[1], Ana Pascual[1], Josep Ferrer[1], Adrià Noguera[1], Eduardo Yanac[1], Soledad Perez[2,3], Romen Rodríguez[1], Aurora Hernández[1], Josep Samitier[2,3], Elisabeth Engel[4,2,3]

[1] University of Barcelona (UB), Barcelona, Spain
[2] Institute for Bioengineering of Catalonia (IBEC), Barcelona, Spain
[3] CIBER en Bioingeniería, Biomateriales y Nanomedicina, CIBER-BBN, Madrid, Spain
[4] Polytechnical University of Catalonia (UPC), Barcelona, Spain
[*] oscar.castano@ub.edu

INTRODUCTION

The limited knowledge in the field of tissue engineering about biokinetic conditions and biochemical signaling in traditional in vitro protocols often leads to poor interpretation of the results due to a lack of quality data. This implies carrying out a large number of experiments in animals in order to obtain results that have to be directly extrapolated to the human case. In the last decade, Organ-on-a-chip (OoCs) technologies have become an essential research tool as it has boosted many aspects of biological research domains in broad fields such as medicine and Engineering. With these, it is possible to reproduce, in a controlled manner, the cellular microenvironments of organs or tissues and thus investigate the effect of different stimuli, signals, and drugs. In this work we show three different OoCs devoted to evaluating i) proangiogenic materials; ii) cardiac tissue scaffolds; iii) brain neuron tissue biomaterials.

EXPERIMENTAL METHODS

Platforms were designed CAD software and soft lithography in PDMS after *in silico* optimization by finite elements simulations of flows, species diffusion, a gradient of signaling, and electrical field generation. Computational models were then experimentally validated. Materials to be validated were produced by electrospinning using polylactic acid as the main component and adding calcium releasing nanoparticles for proangiogenic materials; and pure PLA with a high content of D-isomer for cardiac and neural platforms. *In vitro* tests were performed evaluating the migration of rat endothelial progenitor cells (rEPCs) in the proangiogenic devices[1]; polarization and differentiation of primary cardiomyocytes (PCM) in the cardiac platform[2]; and differentiation of rat progenitor neurons (rPNs) in the neural chip. In all the chips, fibrin or methacrylated gelatin-based gels were used as 3D extracellular matrix (ECM) Immunohistochemistry was used to light cells structures and quantify the level of the material efficiency and feasibility through confocal imaging.

RESULTS AND DISCUSSION

Results evidenced that the proangiogenic platform was useful to differentiate a proangiogenic material from its control efficiently and it was reproducible. In the proangiogenic tests, rEPCs were able to migrate longer distances following the cell tip which was following the direction of the gradient. Chemotaxis and collective cell migration could also be inferred and modeled by in silico phase-field theory. This behavior was especially interesting with the creation of calcium ions gradients able to stimulate mesenchymal stem cells to create the angiogenic cocktail able to mobilize rEPCs (Fig. 1).

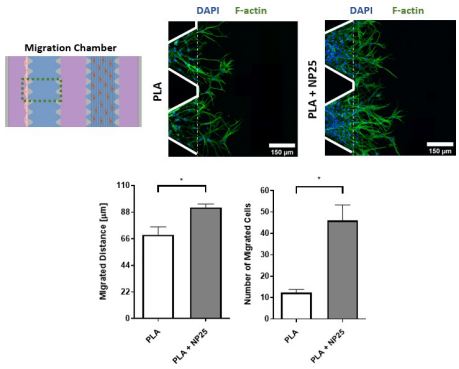

***Figure 1**. Evaluation of the calcium releasing biomaterial effects on rEPC and BM-rMSC in 3D microfluidic assay.*

On the other hand, we were able to polarize PMCs using pure PLA electrospun fibers and the application of an electric field parallel to the direction of the fibers allows them to differentiate and be functional. Finally, we could differentiate and make rPNs viable thanks to the low stiffness ECM applied.

CONCLUSION

These results demonstrate that the gap between *in vitro* characterization techniques and in vivo assays is getting narrower. OoCs represent a serious alternative to in vivo models even able to improve outcomes and versatility.

REFERENCES

References must be numbered. Keep the same style.
1. López-Canosa et al. Acta Biomater, under review.
2. López-Canosa et al., Biofabrication. 1;13(3), 2021

ACKNOWLEDGMENTS

The authors would like to thank the Spanish Ministry of Science and Innovation and the State Research Agency (AEI) (ref. RTI2018-096320-B-C21, RTI2018-097038-B-C22, and PCI2019-103648).

Microphysiological systems for the study of neurodegenerative diseases *in vitro*

Eleonora De Vitis[1,2,*], Velia La Pesa[3], Francesca Gervaso[1], Alessandro Romano[3], Angelo Quattrini[3], Giuseppe Gigli[1,2], Lorenzo Moroni[4] and Alessandro Polini[1]

[1] CNR NANOTEC – Institute of Nanotechnology, Lecce, Italy
[2] Università Del Salento, Dipartimento di Matematica e Fisica E. de Giorgi, Lecce, Italy
[3] IRCCS San Raffaele Scientific Institute, Division of Neuroscience, Institute of Experimental Neurology, Milan, Italy
[4] Maastricht University, Complex Tissue Regeneration, Maastricht, Netherlands
[*] eleonora.devitis@unisalento.it

INTRODUCTION

Understanding the complex communication between different cell populations and their interaction with the microenvironment is fundamental in neuroscience research. Due to the lack of suitable animal models capable of faithfully reproducing the physio-pathological mechanisms of many human diseases, the development of appropriate *in vitro* approaches and tools, able to selectively analyze and probe specific cells and cell portions (e.g., axons and cell bodies in neurons) has become therefore crucial in this direction. From one hand, the rising technology of organ-on-a-chip (OoCs) offers the possibility to overcome these problems. OoCs are microengineered systems that aim to replicate key units of living organs and organisms, and in particular to reproduce higher-order anatomical and functional features[1]. From the other hand, the discovery of human induced pluripotent stem cells (hiPSCs) represents a revolutionary tool for developing personalized medicine approaches starting from cells directly collected from a patient and reprogrammed to obtain specific cells, even those hardly obtained from living patients (*i.e.* neurons, cardiac and pancreatic cells)[2]. For this reason, hiPSC technology has found application especially in the *in vitro* modelling of neurological diseases (NDDs)[3] also integrated into microfluidic devices. During the past two decades, many platforms have been fabricated in order to study NDDs, focusing the attention on the neuromuscular junction (NMJ) that is damaged in these disorders and, in particular, in Amyotrophic Lateral Sclerosis (ALS). The NMJ is a specialized region composed of presynaptic lower motor neuron, postsynaptic muscle myofiber and terminal Schwann cell, involved in the control of vital body process, such as voluntary movements and breathing[4]. However, most of the platforms focus on the interaction between motor neurons and muscle cells since, to date, protocols to generate pure populations of terminal Schwann cells still need to be developed. Here, we propose a microfabricated *in vitro* model for studying the NMJ where different neuronal populations, glial and skeletal muscle cells can grow and communicate in a perfusable environment. This platform could be also useful to investigate the ALS pathological mechanism.

EXPERIMENTAL METHODS

Microfluidic multi-compartmentalized devices were fabricated by SU-8-based multi-level optical lithography and PDMS replica molding, displaying a series of microchannels that connect three different compartments (hosting three different cell types) and promote neurite elongation unidirectionally from one cell compartment to another one. hiPSC were differentiated toward motor neurons (MNs) and Schwann cells (SCs) and the interactions between them were investigated.

RESULTS AND DISCUSSION

We proposed a microfluidic device with three different perfusable compartment (250 µm high, 500 µm wide and 6 mm long) interconnected through a series of narrow microchannels (2.5 µm high, 5 µm wide and 50 µm long) in which the three main components of the NMJ will be hosted. We developed hiPSC differentiation, on-chip protocols towards MNs and SCs and co-cultured them to investigate possible interactions. After carrying out preliminary experiments in order to improve manual skills with this cell type, to optimize the protocol and to characterize them at different differentiation stages, we differentiated the iPSCs into MNs evaluating their behaviour such as axonal elongation in the adjacent compartment in presence of chemical cues (Brain-derived neurotrophic factor or ciliary neurotrophic factor) or other cell types (iPSCs-derived SCs), investigating in this case potential connections and physiological phenomena such as myelin formation.

CONCLUSION

We designed a robust microfabricated platform for studying the motor circuit components, performing hiPSCs differentiation on chip towards MNs and SCs and investigating possible interactions between these cell types.

REFERENCES

1. S. N. Bhatia and D. E. Ingber, *Nature biotechnology*, 2014, **32**.
2. K. Takahashi and S. Yamanaka, *Cell*, 2006, **126**.
3. W. Lattanzi *et al.*, *Journal of personalized medicine*, 2021, **11**.
4. S. M. Luttrell *et al.*, *Muscle & nerve*, 2021, **64**.

ACKNOWLEDGMENTS

“The authors are grateful to the "Tecnopolo per la medicina di precisione" (TecnoMed Puglia)—Regione Puglia:DGR n.2117 del 21/11/2018, CUP: B84I18000540002 and "Tecnopolo di Nanotecnologia e Fotonica per la medicina di precisione" (TECNOMED)—FISR/MIUR-CNR: delibera CIPE n.3449 del 7-08-2017, CUP:B83B17000010001.”

Emulating the basement membrane in *in vitro* models of the human intestinal epithelium

Nathalie Jung[1*], Felix Rohde[1], Maike Windbergs[1]

[1] Institute of Pharmaceutical Technology and Buchmann Institute for Molecular Life Sciences, Goethe-University Frankfurt, Frankfurt am Main, Germany
[*] n.jung@em.uni-frankfurt.de

INTRODUCTION

In the effort to develop more relevant *in vitro* models of human tissues, the importance of the microenvironment has increasingly been acknowledged. In contrast to organoid cultures, where the native extracellular matrix (ECM) is replicated using hydrogels, emulating the ECM of epithelial tissues poses a special challenge. Since *in vitro* models of epithelial tissues of the human body are predominantly cultured in Transwell®-based systems, the native environment is only poorly replicated: the surface texture, chemical composition and mechanical properties of synthetic polymer membranes bear no resemblance to the nanofibrous, elastic structure of the ECM. By providing tissue models with more physiologically-relevant culture substrates, the interaction of cells with their microenvironment, cell attachment, the expression of a physiological phenotype, and cell-cell signaling across the culture substrate can be improved. In this context, the here presented study demonstrates the design of ECM-inspired culture substrates using electrospinning and their application in the cultivation of human intestinal epithelial models.

EXPERIMENTAL METHODS

Electrospinning and characterization of scaffolds

In order to design a cell culture scaffold that mimics the tissue-specific properties of the basement membrane, we employed electrospinning to create fibrous scaffolds made from gelatin and poly-ε-caprolacton (PCL). In a rational approach, we optimized the scaffold with respect to porosity, elasticity, and hydrophilicity to guide cell interactions. Evaluation procedures constituted scanning electron microscopy (SEM), Raman microscopy, tensile testing, and contact angle measurements.

Cultivation of intestinal epithelial tissues

In vitro models of the intestine were cultured using cell lines of human enterocytes (CaCo-2) and goblet cells (HT29-MTX). After seeding on different electrospun scaffolds or polyethylene terephthalate (PET) as a control substrate, cells were cultured for 21 days. Characterization included histology, SEM, immunohistochemistry, and evaluation of barrier integrity via transepithelial electrical resistance and permeability testing.

RESULTS AND DISCUSSION

Electrospinning of gelatin and PCL was performed to create scaffolds that constituted a blend of both polymers, displaying smooth fibers with larger diameters for PCL and very thin nano-fibers for gelatin. Varying the amount of the respective polymers during the spinning process allowed for fine-tuning the porosity of the scaffold as an important determinant for cell migration on the scaffold surface. Tensile testing and contact angle measurements revealed high elasticity of the scaffolds and moderate hydrophilicity, mimicking the native prerequisites provided by the intestinal basement membrane. Scaffolds with higher gelatin content displayed improved cell attachment and migration across the scaffold surface, due to lower porosity and greater hydrophilicity of the scaffold (Fig. 1). SEM and immunohistochemistry further confirmed more physiological three-dimensional tissue development compared to scaffolds with higher PCL content and PET-membranes. All models displayed functional epithelial barrier properties.

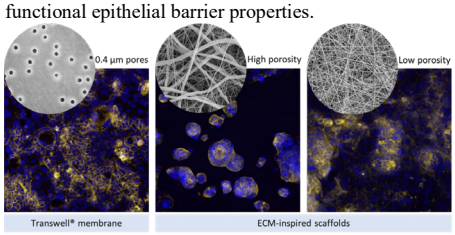

Figure 1: Scanning electron micrographs of different culture substrates and confocal fluorescence imaging of intestinal cells on scaffolds (blue: nuclei; yellow: actin).

CONCLUSION

The here presented electrospun scaffolds constitute a novel approach to mimic the delicate structure of the native basement membrane and allow for the cultivation of more physiologically-relevant *in vitro* models of human epithelia. Due to the high degree of personalization of the scaffolds, the composition, thickness, elasticity, and functionalization can be tuned to fit the needs of the respective tissue. Especially in the context of multilayered tissue models that mimic the endothelial-epithelial interface, improved cellular crosstalk might be achieved in future studies, presenting a major advantage to Transwell®-based systems.

ACKNOWLEDGMENTS

The EUbOPEN project has received funding from the Innovative Medicines Initiative 2 Joint Undertaking under grant agreement No 875510. This Joint Undertaking receives support from the European Union's Horizon 2020 research and innovation programme, EFPIA companies and Associated Partners: KTH, OICR, Diamond and McGill. This communication reflects the views of the authors and neither IMI nor the European Union, EFPIA or any Associated Partners are liable for any use that may be made of the information contained herein.

Adipose-derived stem cell spheroids-on-chip: a system to study altered secretion in diabetic foot ulcer

Iris Lemeunier[1], Stéphanie Porte[1], Clément Quintard[1,6], Delphine Freida[1], Frédérique Kermarrec[1], Victoria Pakulska[2], Yohann Couté[2], Stéphanie Combe[1], Vincent Haguet[1], Remigijus Vasiliauskas[1], Sander Botter[3], Felix Waibel[3], Ilker Uckay[3], Olivier Preynat-Seauve[4,5], Fabrice Navarro[6], Nathalie Picollet-D'hahan[1], Yves Fouillet[6] and Xavier Gidrol[1,*]

[1] Univ. Grenoble Alpes, CEA, INSERM, IRIG, BIOMICS, Grenoble, France; [2] Laboratoire EDyP, University of Grenoble Alpes, CEA, INSERM, IRIG, BGE, Grenoble, France; [3] Swiss Center for Musculoskeletal Biobanking (SCMB), Balgrist Campus AG; [4] Laboratory of therapy and stem cells, Department of diagnostics, Geneva University Hospital, Geneva, Switzerland; [5] Faculty of medicine University of Geneva, Geneva, Switzerland; [6] Univ. Grenoble Alpes, CEA, LETI, DTBS, Grenoble, France

*E-mail: xavier.gidrol@cea.fr

INTRODUCTION

Diabetic foot ulcer (DFU) is a common complication of diabetes that leads to one amputation every 30 seconds in the world, concerning up to 25% of the diabetic patients in their lifespan [1]. DFU is associated with impaired wound healing whose mechanism is still not fully understood. Furthermore, adipose-derived stem cells (ADSCs) and their secretions are known to have a beneficial effect on wound healing [2]. However, in diabetes, the wound healing properties of ADSCs secretions are reduced by chronic inflammation [3]. We recently achieve to analyze the insulin secretion of a pancreatic islet positioned in a hydrodynamic trap [4]. A similar design is currently developed to trap and culture ADSC spheroids to further compare the protein compositions of DFU and healthy secretions, improving our knowledge about the mechanism of DFU.

EXPERIMENTAL METHODS

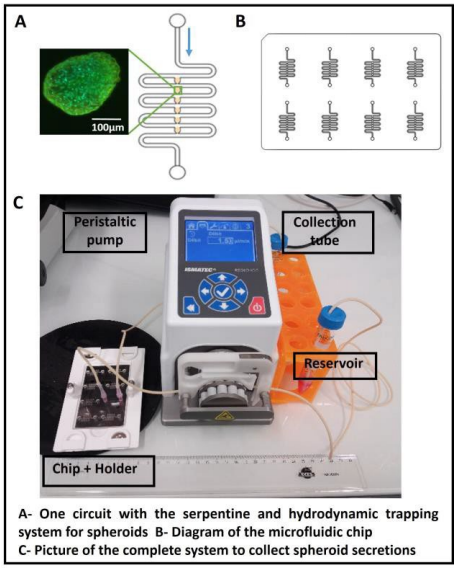

A- One circuit with the serpentine and hydrodynamic trapping system for spheroids B- Diagram of the microfluidic chip
C- Picture of the complete system to collect spheroid secretions

Secretions collected from monolayers of DFU (n=3) and non-diabetic (n=3) ADSCs will be compared to 3D culture of ADSCs to better mimic the physiological conditions and to obtain more relevant secretions. To collect secretions of 3D ADSCs, we use the chip designed in [5] to capture up to 6 spheroids in hydrodynamic traps arrayed in a serpentine design. In that hydrogel-free trapping system, the flow can enable an easy rinsing and medium renewal to both get rid of all the contaminant proteins present in the serum-containing medium and stimulate the secretions of spheroids. These secretions are analyzed by cytokine array and mass spectrometry to identify proteins expressed differentially in DFU and tested functionally in a wound-healing assay monitored with an Incucyte® optical microscope.

RESULTS AND DISCUSSION

Cytokine array analysis of secretions produced in 2D revealed that there is a slightly differential expression of Pentraxin-3, Serpin E1 and IL-8 in DFU secretions compared to non-diabetic ones. Preliminary proteomic analysis uncovered 524 proteins in the non-diabetic secretions, which are mostly involved in extracellular matrix, wound healing and vascularization. The comparison of non-diabetic and DFU secretions obtained on chip might lead to the identification of proteins involved in wound healing impairment in DFU.

CONCLUSION

The hydrodynamic trapping design combined with the use of 3D cultures should help build a better understanding of the proteins differentially expressed in DFU and non-diabetic conditions. In order to study the systemic effect of diabetic ADSC secretions, the ADSC spheroids could also be connected to other organ models (skin, retina, blood vessels) in adjacent traps on the same chip.

REFERENCES

[1] Davis et al., Curr. Diab. Rep., 2018, 1; [2] L. Mazini et al., Int. J. Mol. Sc., 2021, 21, 1306; [3] N. Abu-Shahba et al., Int. J. Biochem. Cell Biol., 2021; [4] C. Quintard et al., Biosens. Bioelectron., 2022; [5] C. Quintard et al., Biorxiv, 2021.

A 3D Bioprinted Model of the Glioblastoma Microenvironment Designed to Assess the Impact of Radiotherapy on Vascular and Tumor Cell Interactions

Nathalie Dusserre[1], Marie-Laure Stachowicz[1], Astrid Dendoncker[1], Clémentine Benedetti[1], Chantal Medina[1], Léo Comperat[1], Jean-Christophe Fricain[1,2], Hugo Oliveira[1], François Paris[3]

[1] BioTis, ART BioPrint, UMR Inserm 1026, Université de Bordeaux, 146 rue Léo Saignat, 33076 Bordeaux, France
[2] CHU Bordeaux, Services d'Odontologie et de Santé Buccale, F-33076 Bordeaux, France
[3] CRCI²NA, UMR Inserm 1307, Université de Nantes, Nantes, France

* nathalie.dusserre@inserm.fr

INTRODUCTION

Tumor microenvironment contains normal stromal and vascular cells that have been reported to influence tumor cell growth and their sensitivity to anti-cancer therapies[1]. Indeed, tumor treatments, such as irradiation, have been shown to alter vascular and cancer cell behaviors, inducing apoptosis and senescence, or stimulating the secretion of pro-inflammatory factors[2, 3]. Vascular cell modifications then trigger an increase or decrease in tumor cell sensitivity to various cancer treatments[4].
Here, we used a microextrusion-assisted technology to bioprint glioblastoma (GBM) cells in a microenvironment containing normal endothelial (ECs) and stromal cells. The objective was to fabricate, in a controlled and reproducible manner, a complex 3D cancer niche in which we could study vascular and GBM cell interactions consecutively to an irradiation or within an oxidative environment.

EXPERIMENTAL METHODS

Hydrogels were produced using a combination of methacrylated hyaluronic acid (HAMA), and methacrylated collagen (CollMA), synthesized as described in previous reports. Methacrylation degrees were respectively 21±4% and 49±16%, (n=5) as determined by TNBS assay. HAMA+ CollMA were mixed with 0.1% LAP as a photoinitiator. U251 cells were used as a model for human GBM cells. Human umbilical vein ECs and human fibroblasts were isolated and cultured in respectively IMDM 20% SVF+ECGS/H and DMEM:F12, 20% FBS. ECs and U251 were transduced with lentiviral vectors coding for red and green fluorescent proteins. A printer (RegenHU, Switzerland) equipped with a microextrusion head (diameter 410µm) was used in this study. GBM cells and, when applicable, ECs and fibroblasts were included in the hydrogels. The resulting bioinks were then used to build 3D concentric models. Crosslinking was achieved using a UV source (305nm).
Different model configurations were subjected or not to an irradiation (0, 5, and 10Gy) or an oxidative stress (0, 250, and 500µM H_2O_2) and followed over time to assess the impact of treatment on tumoroid formation, vascularization, cell proliferation, senescence, apoptosis, and secretome.
In each of these studies, data were obtained from at least three independent experiments. Statistical significance was evaluated by one- or two-way ANOVA followed by Tukey's, Sidak's, or Bonferroni multiple comparisons post-test. Statistical significance was set at $p \leq 0.05$.

RESULTS AND DISCUSSION

We showed that 3D bioprinted multicellular GBM models could be produced in 24 well plates, in a controlled and reproducible manner. The models were shown to recapitulate some key GBM environmental features. They displayed a central tumor area spatially separated from a surrounding zone containing ECs and stromal cells, into which quiescent ECs formed vascular-like networks. GBM cell proliferation was stimulated in presence of ECs and stromal cells, while angiogenesis was increased in the tumor area vicinity. Inside the tumor area, U251 formed tumoroids that grew over time, while invasive GBM cells were observed actively migrating towards the periphery, along vascular-like structures. These results are consistent with previous reports and confirm the physiological relevance of this new 3D model.
Subjecting the 3D bioprinted model to an oxidative stress or an irradiation triggered dose-dependent decreases in EC numbers, GBM proliferation, and tumoroid sizes, and augmented EC apoptosis. The secretome was also altered. Most importantly, the presence of ECs in the model modified the apparent sensitivity of GBM cells to these different treatments.

CONCLUSION

Bioprinting technologies enable the biofabrication of complex and highly tunable 3D *in vitro* models that can help decipher EC and tumor cell crosstalk and address critical questions regarding the role of the tumor microenvironment in the context of GBM therapy.

REFERENCES

1. Meads M.B. *et al.*, Nat. Rev. Cancer. 9:665–674, 2009.
2. Lafargue A. *et al.*, Free Radical Biology and Medicine. 108:750–759, 2017.
3. Garcia-Barros M. *et al.*, Science. 300:1155–1159, 2003.
4. Klemm, F., Joyce J.A., Trends Cell Biol. 25:198–213, 2015.

ACKNOWLEDGMENTS

The authors would like to thank the Inserm for providing financial support to this project within the framework of the ART BioPrint.

Digital Light Processing 3D printing optimization of high aspect ratio structures for rapid prototyping of chips towards biomedical applications

Alessio Bucciarelli[1], Xenia Paolelli[1,2], Eleonora De Vitis[1,2], Francesca Gervaso[1], Giuseppe Gigli[1,2], Lorenzo Moroni[1,3], Alessandro Polini[1]

[1] CNR NANOTEC – Institute of Nanotechnology, National Council of Research, University Campus Ecotekne, Via Monteroni, 73100 Lecce, Italy.

[2] Dipartimento di Matematica e Fisica E. de Giorgi, Università Del Salento, Campus Ecotekne, via Monteroni, 73100, Lecce, Italy

[3] MERLN Institute for Technology-Inspired Regenerative Medicine, Maastricht University, Complex Tissue Regeneration Department, Universiteitssingel 40, 6229ER Maastricht.

[*] Alessio.bucciarelli@nanotec.cnr.it

INTRODUCTION

Organ-on-chip (OoCs) and Lab-on-chip (LoCs) are microfluidic devices extensively used in the biomedical field. The former is a microfluidic *in-vitro* cell culture model that replicates both the architecture and the pathophysiology of a specific targeted organ, while the latter aims to integrate on a single chip numerous analyses generally conducted in a laboratory setting[1]. Both devices are usually manufactured by soft lithography, in which starting from a mold made by optical photolithography a Polydimethylsiloxane (PDMS) device is produced by casting and baking. While this methodology offers the chance to manufacture features with high resolution, it is not flexible enough to respond to the needs of customization required during the prototyping stages. In this study, we propose the development of devices by digital light processing (DLP) in combination with a commercially available, biocompatible resin (GR10, Proc3dure). DLP is a 3D printing method that allows to build an object layer by layer through UV exposition and selective photocrosslinking of a resin, using a digital micromirror device (DMD). Studying the process factors by a statistical methodology called Design of Experiment (DoE)[2], we were able to print and optimize small features with high aspect ratio (60). DoE method allowed us to have a deep understanding of the process without the need of any physical inspection of the involved phenomena and to generate empirical models correlating the process factors to the dimensions of the final object. Finally, a proof-of-concept microfluidic device was printed with the optimized parameters and tested.

EXPERIMENTAL METHODS

To set the overall experiment a 2^5 full factorial design was employed. Square pillars were printed by DLP as proof-of-concept high aspect ratio critical features. The 5 process factors modified during the optimization were the UV layer exposure time (s), the UV curing time (min), the baking temperature (°C), the Sonication Power (%) and the square length (μm) of the printed pillars. The dimensions of the printed pillars were determined by optical microscopy followed by image and statistical analysis. The percentage differences between the theoretical and the measured quotation were used as yield. The color and transparency were determined by UV-Vis spectroscopy while the elastic modulus was determined by compression test on printed cylinders. A proof-of-concept device was printed and tested against leakage for one week.

RESULTS AND DISCUSSION

The difference between the theoretical and measured quotation resulted to be a complex function of the printing factor. Using the empirical model obtained by DOE, pillars with high aspect ratio were effectively printed (**Figure A**) moving the exposure time far from the one suggested by the resin producer (from 0.6s to 2.5s). The printed resin was characterized mechanically: as expected, the increasing in the exposition results in a higher compression modulus (945 MPa for 0.6s, 1020 MPa for 2.5s, 1140 MPa for 4s) with the drawback of making the resin yellowish at the higher exposure time (4s). A good compromise was the exposure condition at 2.5s that ensured a high compression modulus without compromising the resin colour. Based on the optimized condition a proof-of-concept device was printed (**Figure B**) and tested against leakage using a microfluidic circuit and a coloured water solution. The microfluidic device was proved to not leak and thus to be suitable for dynamic cell culture.

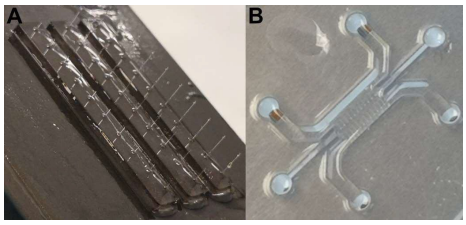

CONCLUSION

In this work, we proved the possibility to develop OoCs and LoCs devices with micrometrical features using a DLP methodology in combination with a biocompatible photocrosslinkable resin. This platform could be useful in the development of the next generation of devices in which the integration with other methodologies (i.e. bioprinting) requires high aspect ratio structures and flexibility in the production process.

REFERENCES

1. Polini A. *et al.*, Biomaterials and Biosystems, 1: 100012, 2021.
2. Bucciarelli A. *et al.,* IEEE Sensors, 21: 26304-26310, 2021.

Multidimensional Advanced Scaffold-Based Cell Culture Systems for Tumor Engineering

Giada Bassi[1,2], Arianna Rossi[1,3], Elisabetta Campodoni[1], Monica Sandri[1], Anna Tampieri[1], Silvia Panseri[1], Monica Montesi[1]

[1]Institute of Science and Technology for Ceramics, National Research Council, Via Granarolo 64; 48018 Faenza (RA)-Italy.
[2]Department of Neuroscience, Imaging and Clinical Sciences, University of Studies "G. D'Annunzio" Chieti-Pescara, 66100 Chieti (CH)-Italy
[3]Department of Chemical, Biological, Pharmaceutical and Environmental Sciences, University of Studies of Messina, 98122 Messina (ME)-Italy

monica.montesi@istec.cnr.it

INTRODUCTION

Worldwide cancer remains the second-most common cause of death; among bone cancers, Osteosarcoma (OS) is the most common tumour diagnosed in children and young adults[1]. The failure of conventional therapies against osteosarcoma leads to the growing need for novel therapeutic strategies. The absence of strategies targeting specific cancer cells subpopulation (i.e. Cancer Stem Cells- CSCs) and the lack of specificity of the traditional two-dimensional (2D) in vitro models, are the primary causes of the poor in vitro-in vivo translation ability[3]. This work provides "tumour engineering" osteosarcoma models as new 3D scaffold-based in vitro model able to capture in vivo tissues' complexity and heterogeneity in a laboratory setting, improving research outcomes and reducing animal testing.

EXPERIMENTAL METHODS

Different biomimetic hydroxyapatite-based bone-like scaffolds, developed at ISTEC-CNR, were used to recapitulate in vivo extracellular matrix (ECM); several osteosarcoma cell lines, with different phenotype and differentiative grade, were cultured on 3D scaffolds as bulk cells and sphere-forming cells, a well-established CSC-enrichment model[4] obtained by cultured OS cell line under serum free and ultralow-attachment conditions. Both the cell phenotypes were cultured in 2D and 3D scaffold-based conditions. Serial generations of spheroids have been deeply characterized by proliferation, sphere-forming efficiency, migration, invasion ability, and stemness markers expression profile (qPCR, western blot) and compared with biological performance of bulk cells. Moreover, the cells culture in the 3D scaffold-based in vitro models were investigated by histological, fluorescent analysis, and genes and proteins expression profile of stemness and CSC niche-related markers.

RESULTS AND DISCUSSION

The enrichment of a cell population with stemness properties was confirmed under 2D conditions. The morphological evaluation of 3D scaffold-based OS in vitro models highlights the maintenance of spheroidal phenotype by enriched-CSCs despite the highly scaffolds bioactivity. The gene and protein expression profile confirmed the increasing of stemness and CSC-niche related markers by 3D scaffold-based spheroids compared to 2D conditions, underling the importance of tumour microenvironment mimesis for in vitro studies. The variability of serial passaging spheroids was reported, highlighting the importance of the selection of the right spheroids generation to furtherly improve our tumour models.

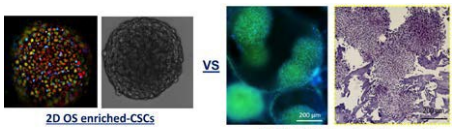

CONCLUSION

The proposed 3D scaffold-based models provided a more accurate starting point to understand the cellular and molecular mechanisms involved in OS cells/biomatrix interactions, particularly in CSCs population. Most important, these models contribute to overcome the use of conventional 2D culture systems and to acquire overall awareness towards the implementation of 3D culture systems in our daily in vitro experiments and screenings. Tumor matrix complexity, various co-cultures and specific secretome will be included as part of tumor microenvironment. These advanced 3D in vitro tumor models could improve the predictivity of preclinical studies and enhance the clinical translation, with the goal to be applied in personalized medicine.

REFERENCES

1. Tang, Q.L. et al., Cancer Lett. 113,121 (2011).
2. Horvath, P. et al., Nat. Rev. Drug discovery 15, 751-769 (2016).
3. Krishnakumar, G. S. et al., Int. J. biological macromolecules 106, 739-748 (2018).
4. Brown, H.K. et al., Cancer Lett. 386, 189-195 (2017).

ACKNOWLEDGMENTS

The authors would like to thank the national PRIN-MUR 2017 Programme (Grant Prot. 2017C8RYSS) for providing financial support to this project.

Animal free fibrous scaffolds for 3D multi-layered epithelial models

Tobias Weigel[1*], Bastian Christ[1], Jan Hansmann[1, 2], Jörn Probst[1], Florian Groeber-Becker[1]

[1]Translational Center Regenerative Therapies (TLC-RT), Fraunhofer Institute for Silicate Research (ISC), Wuerzburg, Germany
[2]Faculty of Electrical Engineering, University of Applied Sciences Würzburg-Schweinfurt, Schweinfurt, Germany
[*] tobias.weigel@fraunhofer.isc.de

INTRODUCTION

The stromal part is a key element of current tissue equivalents as an alternative for animal experimentation or as advanced biological implants. Due to the lack of synthetic alternatives, most researchers rely on animal derived materials such as collagen[1] as main building block for the respective tissue equivalents. However, besides ethical concerns, biological scaffolds are prone for, batch-to-batch variances, increased costs as well as undesired dependencies. The challenge within the development of suitable 3D scaffold materials is to fulfil and combine requirements such as biomimetic structure, high porosity and bioactivity[2]. Here we present the generation of a highly porous fibrous scaffolds with subsequent cellular biologization. The resulting synthetic-based 3D scaffolds are applicable for a wide variety of current stromal tissue models such as multi-layered epithelia.

EXPERIMENTAL METHODS

A modified electrospinning process generated scaffolds. As a variety of biocompatible polymers are applicable, we focused here on polyamide (12%, HFP) to keep it simple. The porosity was controlled by the addition of NaCl porogen particles in defined proportions and size distributions. The resulting highly porous scaffolds were characterized concerning structure and microscopic mechanical properties by nano indentation. For biologization, the 3D scaffolds were seeded with stromal tissue cells (hMSCs or hFibs isolated from the target tissue). After 2-4 weeks of migration, proliferation, differentiation and matrix synthesis, the scaffolds were stacked to or seeded with epithelial cells (skin, intestine, air way), tumor cells or endothelial cells to form multi-layered and hierarchically structured tissues.

RESULTS AND DISCUSSION

The proportion and size distribution of the porogen particles were defined and the resulting structural properties, like pore sizes, mesh openings and porosities determined. The mechanical properties on the cellular level with a young's modulus of 3 kPa were comparable to conventional hydrogels e.g. collagen gel. Since the scaffolds allows cellular migration as well as the dynamic rearrangement of the fibers, primary human dermal fibroblasts were able to homogenously populate the scaffold and remodel the structure by secreting ECM components such as collagens. Furthermore, hMSC were able to be differentiated inside the 3D structure (e.g. adipogenic or osteogenic) to transform the synthetic scaffold in further applicable types of biologizised tissues. The biologizised scaffold material was suitable for combination with human epithelial cells e.g. primary human keratinocytes and were cultured at the air liquid interface. The resulting tissue equivalents (e.g. skin, air way, intestine) were characterized concerning physiological cellular composition and polarization as well the characteristic barrier functionality. Interestingly, the developed setup was able to completely prevent lateral tissue contractions as a major pitfall of common biologic hydrogels, enabling the barrier functionality on the entire surface without edge-related barrier artefacts.

CONCLUSION

The described modular principle, starting from the synthetic highly porous scaffold (with a variety of applicable polymers), the different biologization possibilities and following combinations among each other or with epithelial/endothelial layers, generated a platform technology which can address a diversity of current tissue models. Thereby a simultaneous replacement of animal derived materials and an increase in tissue complexity can be enabled.

REFERENCES

1. Montalbano G. *et al.*, Mater. Sci. Eng. C Mater Biol Appl. 91, 2018
2. Weigel T. *et al*., Adv. Mater. 2106780, 2022

Bioprinted breast cancer model demonstrates microenvironment effect on treatment response

INTRODUCTION

Breast cancer is the most common type of cancer in women. Depending on tumor subtype, cancer therapy can range from classical treatments based on surgery, chemotherapy and radiotherapy, to hormonotherapies, or targeted treatments.

Therapies do not only affect the tumor, but also its microenvironment. It is composed of various matrix and cellular components that can react to treatment-induced stress and crosstalk with the tumor cells thus modulating its fate[1]. The most studied elements of the microenvironment are Cancer Associated Fibroblasts (CAF) and Endothelial cells (EC). The first are essential for matrix remodeling and for secreting supporting factors to the tumor, increasing its proliferation and invasiveness. The second leads to vascularization, providing tumor with oxygen and nutrients. EC have also been shown to be affected by radio-induced oxydative stress. Indeed, their ceramide mediated apoptosis can lead to proliferation modulation on cancer cells, thus suggesting that this interaction can mitigate radiotherapy efficiency[2].

This interaction has been studied in both 2D culture plates and *in vivo*. However, 2D cultures are lacking complexity while *in vivo* models are limited by their poor versatility for microenvironment modulation, especially when considering human cell interactions. Therefore, there is still a gap in our understanding of these mechanisms, due to the lack of a suitable model.

To overcome this breach between in vitro models and human pathology, biofabrication has emerged in the last ten years as a powerful tool for cancer modeling. Here, we describe a simplified bioprinted breast cancer model containing both cancer and stromal compartments with CAF and EC, thus in part recapitulating the complexity of the cancer microenvironment needed for these investigations. We studied the behavior of this model after radiotherapy and communication between cells by quantifying secreted factors such as ceramide and CXCL-1.

EXPERIMENTAL METHODS

Cell culture – MCF7, CAF and Normal Mammary Fibroblasts (NMF) were maintained in DMEM with 10% Fetal Bovine Serum (FBS). Human Umbilical Vein Endothelial Cells (HUVEC) were extracted and amplified in IMDM medium complemented with 10% FBS and ECGS. EGM2-MV medium was used for maturation. GFP and mKate fluorescent MCF7 cells and HUVEC, respectively, were obtained using lentiviral vector transduction.

Gel formulation - We based this gel on previous work from our group[3]. Briefly, we used collagen methacrylate at 2mg/mL concentration with Hyaluronic Acid methacrylate at 10mg/mL. The gel was functionalized with IKVAV peptide at 1mg/mL concentration. The LAP photoinitiator was used at 0.1% (w/v). Cells were diluted at 5M/mL in this gel to obtain the bioink.

Bioprinting – Printing was done on the RegenHU 3D discovery bioprinter with two-printing head for the different inks, and 0.41mm nozzle. The model was composed of two circular patterns with a cancer core surrounded by stroma, 3.5mm in total diameter.

Analysis - We used confocal imaging and immunohistochemistry for various markers (Ki67, CD31, VE-Cad) to assess for proliferation of cancer cells, maturation of endothelial cells. Quantification was made with image analysis software (FIJI and Imaris). Statistics were processed on Graphpad.

RESULTS AND DISCUSSION

We first evaluated cancer cell viability in our model and observed a high post-printing viability. Interestingly a viability gradient appeared after 7 days of culture, mimicking the necrotic core observed in tumors. We then quantified the maturation of HUVEC into microvascular-like network. It seemed that presence of CAF favored a more complex network compared to HUVEC alone or with NMF.

We then exposed our model to 10Gy irradiation. We observed a decrease of Ki67 positive cancer cells compared to control. CAF demonstrated a protective effect on cancer cells. We also observed secretion of CXCL-1 by CAF.

CONCLUSION

Here, we described our model successfully modeling breast cancer and its local microenvironment. Our model demonstrated its consistency with current literature and its ability to respond to radiotherapy. It supports the data demonstrating reduced proliferation after irradiation. We intend to use this model to further characterize ceramide-mediated interactions, during treatment-induced oxydative stress. To further understand these complex mechanisms within the breast cancer microenvironment, we intend to evaluate the effect of CAF CXCL-1 on endothelial ceramide secretion, which is known to increase oxidative stress in the microenvironment[4].

REFERENCES

1. Ansems, M. & Span, P. N. *Clinical and Translational Radiation Oncology* **22**, 90–97 (2020).
2. Ketteler, J. *et al. Cell Death Dis* **11**, 228 (2020).
3. Oliveira, H. *et al. Bioprinting* **22**, e00134 (2021).
4. Zhang, H. *et al. Cell Death Dis* **8**, e2790–e2790 (2017).

3D Printed Microfluidic Device as a Potential Tumor on a Chip Platform in Cancer Management

Ionut-Cristian Radu[1*], Catalin Zaharia[1], Madalina Necolau[1], Eugeniu Vasile[2], Andreea Vadureanu[1]

[1]Advanced Polymer Materials Group, University Politehnica of Bucharest, Bucharest, Romania
[2]University Politehnica of Bucharest, Bucharest, Romania

[*] radu.ionucristian@gmail.com

INTRODUCTION

Microfluidics refers to the science which studies the behavior of fluids through microchannels, but also the technology of manufacturing miniaturized devices containing chambers and tunnels through which fluids flow or are cramped. A microfluidic chip is a device that enables small amounts of liquid to be processed or visualized. It consists in a set of microchannels etched or molded into a material such as polydimethylsiloxane, transparent silicon rubber, acrylic, ceramics, or metal. Microfluidic chips have internal thin microchannels that are connected to outside by means of holes on the chip called inlet/outlet ports. The liquids are injected and removed though these holes from the microfluidic chip: through tubing, syringe adapters or simple holes in the chip with external active systems (pressure controller, syringe-pump or peristaltic pump) or passive ways (hydrostatic pressure). These microfluidic systems could be used to develop an organ-on-a-chip platform that contains continuously perfused chambers occupied by living cells to simulate tissue and organ morphology and function. Organ-on-a-chip or "tissue chips" have attracted major interest in recent years due to their numerous applications, especially in personalized medicine, drug development and screening [1]. Various types of chips have been developed: liver, kidney, heart, brain, blood vessel, lung, intestine, and human tumors [1-2]. These platforms show promise alternatives to traditional preclinical cell culture methods and can reduce the use of *in vivo* animal studies [3].

EXPERIMENTAL METHODS

A new concept of microfluidic device was designed using 3D printing technology as a powerful manufacturing tool. The microfluidic device is composed of parts obtained by Fused Deposition Modeling 3D printing. The device contains cylindrical microchannels assembled into a specific pattern and an external shell. Both the assembled microchannels and the shell have an entry and an exit from where the fluids go inside and outside. The two parts of the microfluidic device (microchannels and shell) communicate through the microchannel walls. The microchannels are designed with CAD and CAM software. Furthermore, they are 3D printed with polyvinyl alcohol (PVA) and crosslinked with glutaraldehyde in various conditions. Before crosslinking, they are thermally treated in special conditions (one and three days at 50 °C). The crosslinking medium contains glutaraldehyde (25% w/v) and nitric acid (0.1M) in which the 3D printed PVA microchannels are immersed for 3 and 24 hours. Finally, the crosslinked microchannels are subjected to the following successive steps: drying, purification by dialysis, and drying. The dried-crosslinked microchannels are stable enough to be assembled into a specific pattern. The microchannel assembly is embedded into the external shell. The microfluidic properties are highlighted by microchannel walls permeability. In this regard, various tracer molecules (salts, drugs) are used to study the communication between the external shell and internal microchannels.

RESULTS AND DISCUSSION

The morphological investigation by micro-CT revealed the complex structure of the entire microfluidic device. The microchannel internal space was rebuilt to reveal the internal geometry. The crosslinking ability of the PVA microchannels was assessed by Fourier Transform Infrared Spectroscopy with Attenuated total reflectance and swelling measurements. Dynamic mechanical analysis, differential scanning calorimetry and X-Ray diffraction were performed to check the influence of the thermal treatment on the crosslinking process and PVA thermal transitions and crystallinity. The thermal treatment positively influenced the crosslinking process and modified the characteristic temperatures of PVA. The microfluidic measurements revealed the microchannel walls permeability for several tracers in specific flowing conditions (different flow ratio and pressure between the external shell and internal assembled microchannels).

CONCLUSION

In conclusion, we reported the development of a new structural concept for a microfluidic device based on 3D printing technology. The PVA microchannels were computer aided designed, 3D printed, crosslinked and assembled to manufacture a microfluidic channel system. The PVA microchannels showed good water mechanical stability and permeability for tracers. This new device can be used to develop an organ-on-a-chip platform for cancer management in the near future studies.

REFERENCES

1. Wu Q., Liu J., Wang X., Feng L., Wu J., Zhu X., Wen W., Gong X., BioMedical Engineering OnLine 19: article number 9, 2020.
2. Zhao Y., Kankala R.K., Wang Shi-Bin, Chen Ai-Zheng, Molecules, 24(4)675, 2019.
3. Danku A.E., Dulf Eva-H., Braicu C., Jurj A., Berindean-Neagoe I, Frontiers in Bioengineering and Biotechnology 10: article 840674, 2022.

ACKNOWLEDGMENTS

This work was supported by a grant of the Ministry of Research, Innovation and Digitization, CNCS/CCCDI – UEFISCDI, project number PN-III-P4-ID-PCE-2020-1448, within PNCDI III.

Nerve Tissue Model on a Micropatterned Surface: Axon Guidance and Neural Regeneration

Dilara Goksu Tamay[1,2*], Damla Arslantunali-Sahin[1,11], Ali Can Atik[3,5], Seyma Isik[6,7], Deniz Yucel[6,8], Haluk Kulah[3,5], Nesrin Hasirci[1,2,4,10], Vasif Hasirci[1,6,9]
[1]BIOMATEN, Center of Excellence in Biomaterials and Tissue Engineering, Middle East Technical University (METU), Ankara, Turkey
Depts. of [2]Biotechnology; [3]Electrical and Electronics Engineering; [4]Chemistry, METU, Ankara, Turkey
[5]METU MEMS Center, Ankara, Turkey
[6]ACU Biomaterials Center, Istanbul, Turkey
Depts. of [7]Medical Biotechnology; [8]Histology and Embryology; [9]Medical Engineering, ACU, Istanbul, Turkey
[10]Tissue Engineering and Biomaterials Research Center, Near East University, Nicosia, TRNC, Mersin 10, Turkey
[11] Department of Genetics and Bioengineering, Gumushane University, Gumushane, Turkey
[*]dilaratamay@gmail.com

INTRODUCTION

Peripheral nervous system (PNS) injuries drastically affect the quality of life and decrease work performance of the patient. Even though many *in vitro* and *in vivo* studies have been conducted on nerve tissue regeneration, *in vitro* studies do not fully reflect the physiological conditions, while *in vivo* testing raises ethical concerns regarding animal welfare[1]. In addition, animal models display physiological differences in healing processes compared to humans. This study aims to develop a nerve tissue model (NTM) to examine peripheral nerve development, axon extension, and regeneration. For this purpose, poly(dimethylsiloxane) (PDMS) surfaces with different micropattern organizations were designed and prepared to culture PC12 cells under restricted conditions, allowing specifically the study of axon growth and healing. The results of this study are expected to contribute to the understanding of the processes involved in nerve regeneration and also serve as a platform for the screening of therapeutic agents.

EXPERIMENTAL METHODS

Micropatterned surface (MS) templates were prepared via soft lithography on silicon wafers coated with a positive photoresist. PDMS prepolymer and crosslinker (10:1) mixture was cast on the templates to obtain the MS, which have three structural sections: i) a cell seeding area, ii) two distinct micropillar regions to sort cells and confine the neuronal soma, and iii) a microchannel region for anisotropic axon extension. The surfaces were characterized with SEM and profilometry. Cell seeding area of the MS configuration denoted BIV was coated with poly(L-lysine) to improve cell attachment and PC12 cells were seeded on this MS for cell-surface interaction studies. Restriction of soma mobility, axonal elongation, and axon guidance towards channels were examined with confocal laser scanning microscopy (CLSM) methods.

RESULTS AND DISCUSSION

Micropillar region of the MS included two different pillar configurations (Fig. 1A): **Region a**, where the micropillars are placed in zig-zag formation to sort the cells, and **Region b**, where micropillars are placed closely and linearly to restrict soma migration to the microchannel region (**Region c**). This configuration of MS aims to recreate the natural state of PNS cells where neural somas are confined to one region and axons innervate distant targets. Profilometry analysis showed uniform heights and depths (3.8 µm) for micropillars and microchannels of all MS variants (Fig. 1B). Square shaped micropillars had a width and length of 5 µm while their distances in regions a and b were 20.5 and 7.5 µm, respectively. Microchannels had a wall thickness of 5.0 µm and a channel width of 7.5 µm.

Figure 2 shows CSLM images of the PC12 cells cultured on BIV MS for 3 days. Micropillars were able to restrict the migration of the majority of the cells to the microchannel region (Fig. 2A), and the cells that were able to reach the channels aligned and grew their extensions anisotropically (Fig. 2B, yellow arrows). The navigation of PC12 cells in between region b pillars suggest somatic and nuclear deformation to some extent, allowing their passage through this region towards the microchannels. Therefore, MS configurations with smaller region b micropillar distances are expected to decrease/prevent cell migration to the microchannel region, better mimicking the natural neural tissue.

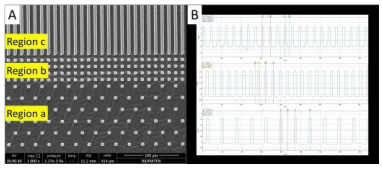

Figure 1. *Surface characterization of MS.* ***A)*** *SEM micrograph of BIV MS configuration,* ***B)*** *Profilometry analysis of microchannels and micropillars of various MS configurations.*

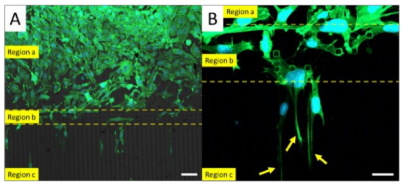

Figure 2. *CSLM Micrographs of PC12 cells on BIV MS at day 3.* ***A)*** *Majority of PC12 cells being restricted within regions a and b* ***B)*** *Cells extending their processes anisotropically through microchannels (yellow arrows). Scale bars: 50 and 20 µm. Green: AF488 Phalloidin, cytoskeleton, Blue: DAPI, nucleus.*

CONCLUSION

The MS presented in this study has the potential to recreate the natural orientation of PNS neurons with its micropattern configuration and provide a platform to study axon development, injury, and regeneration in a simple and cost effective manner. Schwann cell integration to recreate axon myelination, and chemoattractant releasing hydrogel based distal innervation target construction are planned for improvement of the NTM being developed on the MS.

REFERENCES

1. Cornett, E. M. *et al.*, In Pain, 101-104, 2019. Springer, Cham.

ACKNOWLEDGEMENTS

The authors acknowledge TUBITAK (1001, Project No: 120R071), and State Planning Organization 08.11.KB (2016K121520) for financial support. Authors also thank METU BIOMATEN and METU MEMS Center for the use of equipment and facilities.

Improvement of Epithelial and Endothelial Cell Attachment and Proliferation Rate on the Poly(caprolactone) Microfibrous Meshes

Neval Sevinc Ozdemir[1,2,3], Halime Kenar[1,4,5], Vasif Hasirci[1,4,5,6]

[1]ACU Biomaterials Center, Acibadem Mehmet Ali Aydinlar University (ACU), Istanbul, Turkey
[2]Department of Medical Biotechnology, Graduate School of Health Sciences, ACU, Istanbul, Turkey
[3]Department of Pharmaceutical Basic Sciences, School of Pharmacy, ACU, Istanbul, Turkey
[4]Department of Medical Engineering, School of Engineering, ACU, Istanbul, Turkey
[5]Grad. Department of Biomaterials, ACU, Istanbul, Turkey
[6]BIOMATEN, METU Ctr. of Excellence in Biomaterials and Tissue Engineering, Ankara, Turkey
*neval.sevinc@acibadem.edu.tr

INTRODUCTION

Covid-19 pandemic highlighted the need for the development of *in vitro* tissue models for rapid translation of research findings into vaccines or therapeutics. The leading cause of increased disease severity and morbidity in viral pneumonia is the progression of infection in distal airways, namely the pulmonary blood-air barrier, across which O_2/CO_2 transfer occurs. The main goal of this study was to develop a tissue engineered, physiologically relevant blood-air barrier model that will serve as a platform to study the mechanism of viral infection and to test different treatment modalities. A microfibrous poly(caprolactone) (PCL) mesh was prepared through electrospinning to mimic the basement membrane. Its surface was treated with oxygen plasma and collagen Type I to promote attachment of the human alveolar epithelial cells, A549, and human endothelial cell line, HUVEC. The effect of O_2 plasma treatment and collagen coating on cell behavior was studied.

EXPERIMENTAL METHODS

Electrospun meshes were fabricated using PCL (20%, w/v) in Chl:DMF (90:10) after optimizing the electrospinning conditions. Mesh properties were determined by scanning electron microscopy (SEM) followed by ImageJ processing of the micrographs. Uniaxial tensile test was performed to determine the mechanical properties of the meshes. The meshes were treated with O_2 plasma (50 W, 1 min) to increase their surface hydrophilicity. Surface wettability of the PCL meshes was assessed by measuring their water contact angles. O_2 plasma treated and untreated meshes were coated with bovine atelocollagen Type I (3 mg/mL). A549 and HUVEC were seeded on the mesh samples prepared under four different treatment conditions: O_2-plasma treated (PCL-O_2), collagen-coated PCL (PCL-Col), O_2- plasma treated and collagen-coated PCL (PCL-O_2-Col) and untreated (PCL) controls. Samples were stained with Coomassie blue to assess the level of collagen coating. Presto Blue cell proliferation assay was performed at 24 and 48 h to determine cell attachment and proliferation and to study the effect of O_2 plasma treatment and collagen coating on cell behavior.

RESULTS AND DISCUSSION

Fiber diameter of the electrospun PCL mesh was determined as 1.49 ± 0.23 µm and the mesh thickness was 10.08 ± 2.69 µm after 2 min of spinning. The Young's Modulus of the untreated mesh was 9.2 kPa. Mean contact angles were measured as 110.4°± 0.4 for PCL, and 71.2° ± 0.3 for PCL-O_2. The highest cell numbers of both A549 and HUVEC were obtained on the PCL-O_2 meshes, followed by PCL-O_2-Col. PCL meshes without any treatment showed the lowest cell attachment for both cell types, although HUVEC attached more on untreated PCL meshes compared to A549.

CONCLUSION

Both collagen coating and O_2 plasma treatments improved the attachment of A549 and HUVEC cells on the PCL microfibrous meshes, with the effect of O_2 plasma being more significant based on the number of viable cells. Application of a collagen coat on O_2 plasma treated PCL meshes further improved the proliferation rate of A549 in comparison to that on uncoated meshes. Collagen adsorption on the O_2 plasma treated PCL meshes appears to have led to the generation of a more physiologically relevant blood-air model.

ACKNOWLEDGMENTS

The authors thank ACU Biomaterials Center for the use of the facilities and the chemicals used in the study.

Alternative methods and *in vitro* skin 3D tissue models: What's new for toxicity testing in medical devices?

Edith Flaire[1,2], Rachida Nachat-Kappes[3], Camille Laporte[6], Marie-Françoise Harmand[1], Marina Simon[1], Christian Poinsot[1]

[1]Groupe ICARE. Biopôle. Rue Emile Duclaux 63360 Saint Beauzire
[2]UMR 1019 INRAE-University Clermont-Auvergne, UNH (Human Nutrition Unity), ECREIN Team, 63000 Clermont-Ferrand, France
[3]InnovSkin, 63140 Chatel-Guyon, France
[4]Institut Universitaire de Technologie, Université Clermont Auvergne, UMR INSERM-UCA, U1240, France
[5]Univ. Grenoble Alpes, CEA-Leti: division for Biology. 38000 Grenoble. France

Presenting author edith.filaire@groupeicare.com

INTRODUCTION

Evaluation of absorption through the skin barrier and the irritation potential of drugs, pesticides and more generally chemicals can be carried out using *in vitro*, *ex vivo* and *in vivo* models, skin toxicology testing in the cosmetics and pharmaceutical industries being used to identify whether new compounds are toxic to human skin. For many years, toxicological studies have been performed on animals. However, the use of animals has long been a matter of controversy. Indeed, concerns have raised about animals' sentience, and whether the justification for harms is acceptable[1]. In consequence, there is a strong need for more representative human models, which are reproducible, easy to use and cost-effective. Guidelines of standardized and codified methods for the testing and assessment of chemicals have been produced by the Organization for Economic Cooperation and Development (OECD). In July 2021, several new non-animal-based OECD Test Guidelines were also published, without including the three-dimensional (3D) cell culture approach. Use of this last approach can provide potential solutions with more complex organotypic models. Developments of human-based three-dimensional *in vitro* testing models such as the 3D bioprinting technology enable the simultaneous deposition of multiple types of human skin cells, and the generation of *in vitro* 3D vascularized skin models with dynamic perfusion and microfluidic devices known as skin-on-a-chip are good candidates for tissue modeling. Generally speaking, the Organ-on a chip market is projected to reach 220 Million US$ by 2025[2]. They permit a more physiological transport of nutrients and permit a high-throughput and less expensive evaluation of drug candidates in terms of toxicity, efficacy, and delivery[3]. However, there are many challenges to be addressed: the first challenge is to mime the structural complexity of living human skin, including vascularization (blood microvessels), immunity (dendritic cells, T-cells, macrophages, Langerhans cells), appendages (hair follicles, sweat glands, sebaceous glands, papillae) pigmentation (melanocytes), subcutis (adipocytes) and innervation (sensory afferents). The second one is to control the the skin microenvironment, monitoring and analysis of drug effects in a user-friendly manner, which can be achieved by appropriate design and fabrication of microfluidic systems; the third is to combine the technology with innovative detection methods (e.g., biosensors). Next-generation organoids including not only skin components (keratinocytes, fibroblasts, and dermal collagen) but also immune cells to study the role of innate and adaptive immunity are also investigated[4]. This conference presents the different 3D skin models available, highlighting the advantages and disadvantages of the existing models and focuses on recent innovative 3D cell culture with their future applications.

CONCLUSION

The development of Skin-on-a chip (SOC) technology is promising for generating engineered models for drug testing. However, the technology needs to be validated and accepted by the regulatory bodies as an efficient method for testing newly developed drugs. Collaboration between researchers, regulatory bodies and the industry would be necessary to obtain this validation.

REFERENCES

1. Hubrecht RC *et al.*, Animals. 9: 754, 2019.
2. Bajaj S. Allied Market Search: p.129,2017
3. Ng WL *et al.*, Int. J. Bioprint. 5: 237, 2019.
4. Jackson R *et al.*, Viruses. 12: 1375, 2020.

A 3D Co-Culture Spheroid Model to Assess the Response of Bone Metastases to Anticancer Drugs

Ceri-Anne Suurmond[1*], Rong Wang[1], Jeroen van den Beucken[1], Sander Leeuwenburgh[1]

[1]Department of Dentistry – Regenerative Biomaterials, Radboud Institute for Molecular Life Sciences, Radboud University Medical Center, Nijmegen, The Netherlands.
[*] ceri-anne.suurmond@radboudumc.nl

INTRODUCTION

Prostate and breast cancer are the types of primary cancers that metastasize most frequently to bones. Similar to primary bone cancers, bone metastases are often treated using tumor curettage, which creates a bone defect that requires filling with a suitable graft material. Moreover, cancer cells may still retain in these defects since tumor margins are typically difficult to determine.[1] To prevent recurrence of bone cancer, chemotherapeutics can either be systemically administered or locally delivered from biomaterials carriers that are used to fill bone defects. To date, several bone-regenerative materials with anticancer properties have been developed, but in vitro and in vivo testing of therapeutic efficacy is still performed in relatively simple 2D cell cultures that are far from mimicking physiological bone tumor conditions.[2,3] Early 3D methods composed of cancer cells showed responses more similar to in vivo efficacy[4], and efforts now have started to explore 3D co-cultures.[5] Here, we aim to develop an easy to use, but clinically highly relevant 3D co-culture spheroid model for application as a tool to investigate anti-cancer efficacy of chemotherapeutic drugs and materials.

EXPERIMENTAL METHODS

All cells were cultured in alphaMEM (Gibco) supplemented with 10% fetal bovine serum (Gibco) and 1% penicillin/streptomycin (Gibco). Combinations of primary human bone marrow stromal cells (hBMSC) with either prostate (PC3) or breast cancer cells (MDA-MB-231) were cultured in various platforms (hanging drop with petri dishes and ultra low attachment plates (PHCBI)) to create 3D spheroids. Various seeding densities and media supplements (30 ug/mL collagen type 1A from rat tail (Corning), 0.24 or 1.2 mg/mL methocel (MC, Sigma Aldrich), and a combination of both) were used to optimize 3D spheroid formation with tight cellular connections. After optimization of a protocol for the effective formation of 3D spheroids, different types of 3D spheroids with cell ratio variations were imaged with brightfield and laser scanning confocal microscopy (Carl Zeiss LSM880). hBSMSCs were stained with CellTrace CFSE green (Invitrogen) before mixing, and cancer cells with CellTrace Far Red (Invitrogen). Hemispheres of 3D spheroids were then further characterized with z-stack confocal imaging. Quantitative image analysis was performed to determine the numbers of hBMSC and cancer cells, morphological parameters, and spatial distribution of the cells throughout the 3D spheroids at days 1, 3, and 7.

RESULTS AND DISCUSSION

Alternatively, 3D spheroids were generated using ultra low attachment plates as opposed to the hanging drops from a petri dish, as these were more easily collected from the plates. 3D spheroids of different sizes were generated by varying the initial cell seeding numbers at 2,000, 4,000, and 6,000 cells per 3D spheroid.
With image analysis, the circularity (parameter for stable spheroids) was determined, showing optimal values for 3D spheroids with 2,000 cells per spheroid and 30 ug/mL collagen supplementation. Brightfield images and confocal z-stacks demonstrated that cancer cells quickly outgrew the co-culture 3D spheroid and this effect was most pronounced for 3D spheroids with an initial 1:1 cell ratio. The 9:1 ratio seemed to work the best, as the number of cancer cells remained balanced with the number of hBMSCs over a 7 day culture period (Figure 2).

Furthermore, 3D spheroids showed to decrease in size and form a tight core of predominantly hBMSCs and cancer cells growing peripherally.

CONCLUSION

In conclusion, a 3D spheroid co-culture model consisting out of 2,000 cells per spheroid with 30 ug/mL collagen media supplementation was established, showing generation of stable spheroids for a culture period of up to 7 days. The combination of multiple microscopy techniques demonstrated re-organization of the different cell types within the 3D spheroids. This model paves the way for testing new drugs and biomaterials.

REFERENCES

1. Buenrostro D, *et al.*, Curr Osteoporos Rep. 2016;14(4):151-8.
2. Li F, *et al*., Regenerative Biomaterials. 2021;8(6).
3. Hu M, *et al*., Journal of Colloid and Interface Science. 2020;579:654-66.
4. Huang Z, *et al*., Onco Targets Ther. 2020;13:5395-405.
5. Saraiva DP, *et al*., Front Oncol. 2020;10:1543.

Dynamic 3D Cultivation of Adipose-Derived Mesenchymal Stem Cells within Alginate Core–Shell Capsules

Sabrina Nebel[1*], Manuel Lux[1], Wolf Dietrich[2], Dominik Egger[1], Cornelia Kasper[1]

[1]Institute of Cell & Tissue Culture Technologies, Department of Biotechnology, University of Natural Resources & Life Sciences BOKU, Vienna, Austria
[2]Department of Gynecology & Obstetrics, Karl Landsteiner University of Health Sciences, Tulln, Austria
[*] sabrina.nebel@boku.ac.at

INTRODUCTION: Mesenchymal stem cells (MSCs) are primary candidates for cell therapy due to their intriguing regenerative & immunomodulatory potential. Their ability to self-assemble into 3D aggregates can even further improve their therapeutic properties.[1] Mechanical stress found in dynamic cultivation systems can decrease these properties, cells embedded within a polymer matrix, however, lack cell-to-cell contacts as found *in vivo*. Here we showcase an approach to protect the cells from high shear forces by core–shell encapsulation. The capsules consist of an outer barrier made from sodium alginate, which allows for nutrient & waste diffusion & an inner compartment for direct cell-cell interactions. We compared our capsule cultivation approach to preformed cell spheroids for 6 days in a rotating wall bioreactor, to test its suitability for dynamic 3D *in-vitro* expansion of MSCs.

EXPERIMENTAL METHODS: On day 0 adMSCs were either seeded into microwell plates to create spheroids or encapsulated into alginate core-shell capsules. To create capsules, cell suspension containing 1.3% $CaCl_2$ & 1% carboxymethylcellulose (CMC) was dropped into a stirred 0.5% alginate bath. Upon submersion, a shell is formed by ionic crosslinking from the droplet surface outwards. Afterwards capsules were washed several times & then placed in culture medium at 37°C, 5% CO_2. On day 1, spheroids & capsules were transferred to ClinoReactor™ rotating wall bioreactors ($5x10^5$ cells/reactor) set to 12 & 10 RPM, respectively. To retrieve cell aggregates from capsules, the shell was dissolved using 0.1 M Na-citrate. Cell aggregates from within capsules & spheroids were disassociated. with AccuMax (30 min, 37°C) & afterwards total cell number was determined. Statistical analysis was performed using 2-way ANOVA, significance was determined using Sidak's multiple comparisons test (n=3, α=0.05) On day 1 & 6 live/dead staining using Calcein AM & propidium iodide was performed.

RESULTS AND DISCUSSION: Cells seeded into microwells formed stable aggregates overnight (Fig.1A), whereas cells encapsulated in core-shell capsules were still distributed throughout the capsule interior at day 1. At that timepoint, spheroids & capsules were transferred to individual ClinoReactors™. After cultivation for 6 days, cells were harvested and of the initially seeded $5x10^5$ cells only $2.8x10^5 \pm 3x10^4$ could be recovered in the spheroid group (Fig.1B). This can be attributed to merging of multiple spheroids to large clumps, where diffusion limitations may have resulted in a necrotic core region. Due to the large aggregate size, live/dead staining was inconclusive. AdMSCs within core-shell capsules however, increased up to 2.4-fold in number ($1.2x10^6 \pm 1.2x10^5$, Fig.1B). Also live/dead staining confirmed high viability during culture besides formation of multicellular aggregates within the capsule core (Fig.1C). This *in-situ* spheroid formation was reported previously in hyaluronic acid[2]. Interestingly also increasing the viscosity in the core region by a non-physiologically relevant polysaccharide (CMC) promoted cell aggregation.

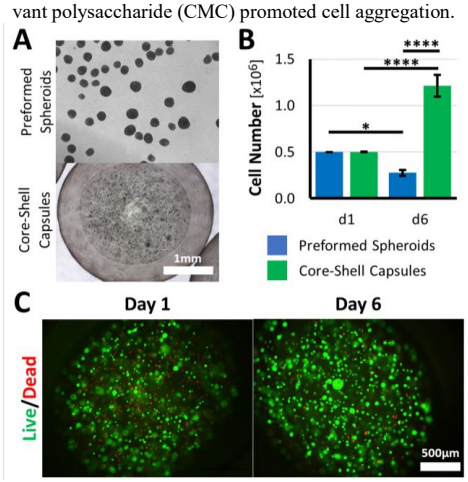

Figure 1: A Brightfield images from preformed spheroids & core-shell encapsulated MSCs (d1) **B** Cell number in Clinoreactors™ decreased for cells cultured in spheroids, whereas increased for those cultured in core-shell capsules (n=3, *p<0.05, ****p<0.0001) **C** Live/dead staining reveals high viability & formation of multicellular aggregates over time.

CONCLUSION: We could show that our capsule cultivation approach can be used for expansion of MSCs in a dynamic cultivation setup & performed better than spheroid only cultivation. In the future, this technique might be used for MSC-expansion in large-scale dynamic bioreactor systems, facilitating bench-to-bedside translation of cell-based therapies.

REFERENCES

1. Bartosh T.J. *et al*., PNAS USA 107:13724–29, 2010
2. Park J. *et al*, ACS Biomater. Sci. Eng. 6:6938–48, 2020

ACKNOWLEDGMENTS

The authors would like to thank CelVivo for providing a demo reactor-system device & the DocSchool BioMatInt for providing financial support to this project.

3D Printed Biocompatible Molds for High Production of Homogeneous Embryoid Bodies for Specific Differentiation

Alejandro Reina Mahecha*, Paulien Schaafsma, Theo van Kooten, Inge Zuhoorn, Prashant Sharma
Department of Biomedical Engineering, University medical centrum Groningen (UMCG), Groningen, The Netherlands
*m.a.reina.mahecha@umcg.nl

INTRODUCTION

3D printing is a technology that has revolutionized the scientific community due to its versatility for producing prototypes and final products. This technology has significantly reduced outsourcing costs for tissue engineering (TE) and opened doors for new business models. 3D printing Stereolithography (SLA) is a high-resolution technique using resin photopolymerization.

Recently for TE, compared to monolayer cell culture, the incorporation of 3D cell culture techniques, such as spheroid cell aggregates (SCA), is becoming more relevant, as it is possible to understand better intrinsic biological pathways present on target tissues. For this study, SLA was used to create 3D printed molds containing optimal microwells that were cast into polydimethylsiloxane (PDMS) for the formation of SCA. SCA from pluripotent stem cells called embryoid bodies (EB) are widely studied as they emulate early embryogenesis, a fundamental step in cell differentiation[1]. The designed microwells outperformed 2 different commercially available plates and yielded a high production and homogeneous EBs. This system opens the doors for multiple TE applications such as drug testing and cancer research.

KEYWORDS: Tissue engineering, 3D printing, Cell aggregates

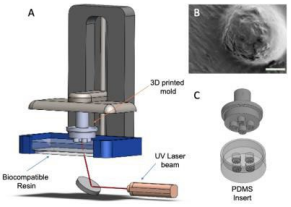

Figure 1. A)schematic overview of SLA printer, B) Printed Microwells SEM Scalebar= 200µm, C) Cast mold on PDMS

EXPERIMENTAL METHODS

The computer-aided design (CAD) to print the molds was developed using SolidWorks software. The molds were printed using the 3B+ printer (FormLabs) with dental biocompatible resin (fig. 1). The printing resolution was analyzed under scanning electron microscopy to determine the minimum microwell size limitation. Conical and semispherical geometries with different radii were tested for the formation of a single SCA per microwell. The molds were cast in PDMS (10:1), degasified by centrifugation, and crosslinked at 70ºC for 3 hours. Casted PDMS was sterilized using a sonicator bath with 70% ethanol. Alternatively, UV-light and autoclaving were also tested to check the hydrophobicity of the material after sterilization.

The pluripotent stem cell guide from Stemcell Technologies™ was followed for culturing Hues9-embryonic stem cells. To test the homogeneity of the EBs on the designed microwells, 2500 and 5000 cells per microwell were seeded and controlled 24, 48, and 72 h after seeding. Then, the microwells were compared to 2 commercially available plates for cell aggregate fabrication. Finally, to analyze the application potential of the microwells, a glioblastoma stem cell line (GSC23) was tested for SCA tumor formation.

RESULTS AND DISCUSSION

Due to the printing resolution, microwell radii between 1.5 mm and 500 µm with conical and semispherical geometries were used to test the EB formation. After the assessment, the semispherical 500 µm radius microwells showed the capacity to form a single SCA with homogenous morphology.

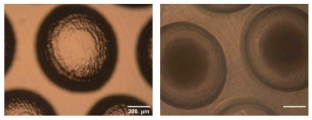

Figure 2. Microwell cast on PDMS and EB after 72h after seeding. (scalebar = 200 µm)

To analyze the size control of the EBs, 2500 and 5000 cells/microwell were used, reporting homogeneous size after 24, 48, and 72 hours of incubation (fig. 2). The possibility of controlling the size of the EBs is a significant advantage of the system as different cell differentiation approaches require EBs of specific sizes ranging between 100 and 300 µm [1]. In comparison with the designed system and the commercial plates. The cast microwells showed outstanding performance and reproducibility.

To extend the application of the system, glyoblastoma stem cells were tested and showed that it is possible to control the size of the SCA, advantageous for oxygen concentration tests, metastasis, and drug treatment assays.

CONCLUSION

The microwells created using 3D printed molds showed the capacity to form numerous homogeneous and size controllable SCA, outperforming commercially available plates. This system will provide better control and flexibility for differentiation applications, and will help to reduce the variance involved in EB-based and cancer research.

REFERENCES

1. Zeevaert. *et al*., cells. 9:10, 2020

ACKNOWLEDGMENTS

The authors would like to thank the Kolff intitute and the UMCG (Project number: 54515) for providing the financial support to this project

3D models for colorectal cancer treatment and personalized medicine

Charlotte JEMFER[1], Tarek SAYDE[1], Gaëlle BEGAUD[1], Céline HERVIEU[1], Gaëtane LESPES[3], Philippe BARTHELEMY[2], Muriel MATHONNET[1], Bruno ALIES[2] et Serge BATTU[1]

[1]UMR INSERM 1308 CAPTuR, GEIST, Faculté de Médecine, Université de Limoges, 2 rue du Dr Marcland, 87025 Limoges, France ; charlotte.jemfer@unilim.fr

[2]ARNA, INSERM U1212, UMR CNRS 5320, Université de Bordeaux, 146 rue Léo Saignat, 33076 Bordeaux, France

[3]IPREM, UMR 805 CNRS 803, Université de Pau et des Pays de l'Adour (E2S/UPPA), 2 avenue P. Angot 64053 Pau Cedex, France

In 2020, colorectal cancer (CRC) is the leading digestive cancer and the second leading cause of cancer deaths (behind lung cancer and ahead of breast cancer) [1]. The treatment of CRC is based on curative excision and addition of chemotherapy for advanced stages (> stage 2). However, a large part of the systemic chemotherapy treatments aren't adapted to the patient's cancer cells and result in a recurrence of the disease within two years of treatment. This evolution (recurrence, metastasis) is linked to the residual presence of clusters of cells possessing both a strong capacity for quiescence and proliferation. These characteristics correspond to Tumor Initiating Cells (TICs) [2] which are responsible for the therapeutic escape and mortality of CRC observed post-surgery.

It is therefore necessary to eliminate inter-patient differences, by setting up a personalized treatment allowing each patient to avoid CRC recurrence by TICs resistance. Our goal is to isolate TICs from patients and culture Multicellular Tumor Spheroids (MCTS) in hydrogel matrix to test their sensitivity or resistance to different chemotherapy treatments, and thus assign a targeted treatment for these TICs to the patient.

We must first isolate the TICs, for that we use the SdFFF (Sedimentation Flield Flow Fractionation) [3] set up at CAPTuR laboratory of the University of Limoges. Indeed, this sorting method has already allowed to highlight the isolation of TICs from a heterogeneous solution of colorectal cancer and glioblastoma cells. This sorting method is label-free, non-invasive, allows to preserve the viability and the cellular functionalities of TICs.

We must then mime as closely as possible the physiological conditions of the organism for the development of MCTS. For this purpose, we turned to the use of synthetic hydrogel allowing a better reproducibility and possessing a favorable architecture to the growth of stem cells. More specifically, we first turned to hydrogels based on glyco-nucleo-bolaamphiphiles corresponding to supramolecular hydrogels [4] produced and characterized by the ARNA unit of Bordeaux. Due to the wide range of possible viscosity of these gels, we need to perform a range with different concentrations of gelling molecules to find the one that will most closely match the viscosity of the extracellular matrix of the tumor in the body. Indeed, this matrix should allow the tumors to remain in suspension and should facilitate the exchange of growth factors and communication signals between the cells

Once our model is characterized, sensitivity studies to chemotherapy molecules will be performed. This process, similar to an in-vitro oncograme, will provide a major aid to the clinician in the personalized and optimized management of advanced CRC treatments.

Key words: Tumor initiating cells, Supramolecular hydrogel, Spheroids

REFERENCES

1 Biller L.H. and Schrag D., *JAMA,* 669-685, 2021
2 Mathonnet M. and al, *World J. Gastroenterol.*4189-4196, 2014
3 Mélin C. and al, *Anal. Chem*. 1549-1556, 2012
4 El Hamoui, O. and al, *Langmuir* 37, 297-310. 2021

Development and Characterisation of a three-dimensional model of Adrenocortical Carcinoma

Sarah Feely[1], Padraig Donlon[1], Abhay Pandit [2], Michael Conall Dennedy[1]
[1]Lambe Institute for Translational Research, National University of Ireland Galway, Galway, Ireland
[2]CURAM, National University of Ireland Galway, Galway, Ireland
* s.feely4@nuigalway.ie

INTRODUCTION

Adrenocortical carcinoma (ACC) is a rare malignancy associated with a poor prognosis (1). Overall prognosis is worsened by the development of endocrinopathies. Current treatments are limited. Surgical resection provides the only option for a complete cure; however, it is not suitable for all patients (2). Mitotane is the only pharmacological therapy that is has been specifically approved but it is associated with a limited efficacy and adverse effects (3). Various new therapeutic approaches have been tested such as immune checkpoint inhibitors, but to no success (4). Hence there is a clinical need for new treatment strategies.

The development of translational therapies is limited by pre-clinical disease models. None of the current cell culture models accurately reflect the tumour micro-environment (5). Three-dimensional (3D) cell culture models have become increasingly popular in cancer research (6). However, they are lacking in ACC with only a few models generated to date (7).

In the current study, we developed novel 3D models of ACC generated using type 1 collagen. We then characterised these models to access their ability to accurately reflect ACC.

EXPERIMENTAL METHODS

3D cell culture models of ACC were generated by optimising the concentration of ACC cell lines, MUC-1, HAC15 and H295R within a type-1 Collagen matrix. Viability of each model was assessed by Flow Cytometry with cells stained with Sytox Blue. Metabolic activity of the ACC cells within the collagen matrix was determined via AlamarBlue staining. Ki67 was detected via Flow Cytometry. Steroidogenic capacity was determined by quantifying cortisol, aldosterone and androstenedione using Liquid chromatography tandem mass spectrometry. The expression of steroidogenic enzymes CYP11A1, CYP11B1, CYP17, CYP11B2 and StAR was measured via real time- polymerase chain reaction (RT-qPCR). The morphology of the cells within the collagen matrix was imaged using confocal microscopy.

RESULTS AND DISCUSSION

MUC-1, H295R and HAC15 cells were successfully cultured in a type 1 collagen matrix. MUC-1 cells cultured in the collagen matrix remain viable throughout the period of experimentation with optimum viability between 14 and 21 days. H295R cells also remain viable for the period of experimentation with optimum viability at an earlier stage of 7-14 days (Figure 1). HAC15 cells demonstrate high resilience in 3D cell culture with with maximum viability throughout the entire period of experimentation up to 21 days. All three models increase their metabolic activity over time.

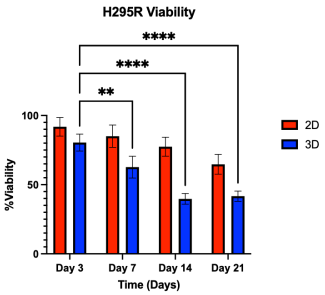

Figure 1 Viability of H295R cells cultured in 2D and 3D and stained with Sytox Blue. Analysis was carried out via Flow Cytometry. Statistical analysis was carried out by performing a two-way anova with 3D viability at Day 7,14 and 21 compared to 3D viability Day 3. **p>0.05, ****p>0.001

CONCLUSION

In the current study, we developed 3D cell culture models for ACC. Tumour cell were grown in an optimised collagen matrix. We now hope to use such models to test novel therapeutic options currently being investigated in our laboratory to address the lack of translational therapies for ACC

REFERENCES

1. Fassnacht *et al.,* Cancer.115(2):243–50, 2009
2. Porpiglia *et al*., Eur Endocrinol 14:62-66, 2018
3. Terzolo *et al*., N Engl J Med 356:2372-2380,2007
4. Le Tourneau *et al.,*J Immunother Cancer 6:111, 2018
5. Wang T *et al* Mol Cell Endocrinol 351(1): 58-65, 2012
6. Kim *et al.,* Seminars in Cancer Biology 15(5): 365-377, 2005
7. Bornstein *et al.,* BioRxiv, 2022

ACKNOWLEDGMENTS

The authors would like to thank Science Foundation Ireland for providing financial support for this project.

Practical approaches and optimization of a heterogeneous fluorescent tumoroid generation of ductal breast carcinoma in situ to study the impact of the adipose and inflammatory microenvironment

Ola Habanjar[1]*, Anne-Catherine Maurin[1], Cyrielle Vituret[1], Lucie Longechamp[1], Cécile Garnier[1], Caroline Decombat[1], Céline Bourgne[2], Céline Auxenfans[3], Mona Diab-Assaf[1], Florence Caldefie-Chezet[1], Laetitia Delort[1]

[1]Université Clermont-Auvergne, INRAE, UNH, 63000 Clermont-Ferrand, France
[2]Plate-forme CMF, Service d'Hématologie biologique, CHU de Clermont-Ferrand, 63000 Clermont-Ferrand, France
[3]Banque de tissus et de cellules, Hôpital Edouard-Herriot, France
*Ola.habanjar@doctorant.etu.uca.fr

INTRODUCTION

Ductal carcinoma in situ (DCIS) is a non-invasive form of breast cancer, which is defined as a proliferation of neoplastic epithelial cells located in the lumen of breast ducts without invading the basal membrane. DCIS now represents 20-25% of all breast cancer cases due to detection by population-based breast cancer screening programs. DCIS are surrounded by a layer of continuous myoepithelial cells (MECs) and embedded by an intact basal membrane. It has been considered as an early stage of linear cancer progression which could eventually progress into invasive ductal carcinoma (IDC) once it breaks down the MEC layer and the basement membrane. Moreover, many studies have shown the role of obesity, adipose and inflammatory microenvironment in cancer progression, which would be able to modify the functional characteristics of MECs leading to an invasion process. Chronic low-grade inflammation is associated with obesity, which is associated with metastasis. More specifically, obesity-related fatty inflammation results from a pro-inflammatory dialogue between adipocytes and macrophages. Therefore, obesity/overweight (adipocytes), inflammation (macrophages), and tumors (transformed cells) form an important triangle that is proven to regulate tumor microenvironment (TME). At present, it is not possible to identify which DCIS will evolve into an IDC and improving the management and the treatment of DCIS is a key issue to reduce cancer metastasis.

So the aim of our study is to generate DCIS tumoroids to mimic the three-dimensionality of DCIS with histological and physiological properties that most closely resemble those found in solid tumors in the breast. The heterotypic tumoroids were composed of in situ ductal cancer cells (MCF10-DCIS cell line) surrounded by a continuous layer of MECs (Hs578Bst cell line), which were preliminary transduced with lentiviral vectors to obtain m-Cherry and EGFP-labelled cells respectively. Fluorescent tumoroids were then used to test the effect of the following supernatants on cell viability: human adipose stem cells from normal BMI women (hASC20) or obese women (hASC30), mature adipocytes (MA20, MA30), activated macrophages (M0) and inflammatory macrophages (M1). IncuCyte® system (Sartorius) was used to 3D follow-up and measuring of cell fluorescence levels.

EXPERIMENTAL METHODS

Two lentiviral vectors, expressing either EGFP (Enhanced Green Fluorescent Protein) or m-Cherry were used. Various multiplicity of infection (MOI) were tested to specify the optimal conditions for each cell lines: MOI 1, 3, 10, 20, 30, and 40 for Hs578Bst; MOI 1, 3, 5, 10 for MCF10-DCIS. For gel preparation, 20 g/L agarose of sterilized 0.9% w/v NaCl was prepared and sterilized for 20 min at 120°C. Agarose molds 3D Petri Dishes® 81 wells were used to optimize tumoroid generation protocol. MCF10-DCIS cells were firstly seeded. After 72h of incubation, the cells present within the suspension spontaneously agglomerate to form loosely adhesive cell tumoroid on non-adherent surfaces by promoting intercellular adhesion molecules. Then MECs (Hs578Bst-EGFP) were added to MCF10-DCIS-mCherry tumoroids previously formed. 81 heterogeneous tumoroids (MCF10-DCIS-mCherry+Hs578Bst-EGFP) were generated per agarose mold. Following the optimization of the DCIS 3D fluorescent model, various supernatants obtained from cultured human cells [human adipose stem cells (hASC20/BMI=20, hASC30/BMI=30), mature adipocytes (MA20/BMI=20, MA30/BMI=30), activated macrophages (M0) and pro-inflammatory macrophages (M1) were tested on these fluorescent tumoroids to monitor the impact of obesity, adipose and inflammatory microenvironments on the viability of each cell type. Image of tumoroids in agarose mold were captured using the IncuCyte® system. One-way Anova Test was used for statistical analysis.

RESULTS AND DISCUSSION

MCF10-DCIS-mCherry (LV-m-Cherry vector; MOI 5) and MECs Hs578Bst-EGFP (LV-EGFP vector; MOI 40) were sorted using BD FACSAria™ SORP Cell Analyzer / Sorter with 5 lasers (UV 355nm, Violet 407nm, Blue 488nm, Yellow Green 561nm, Red 633nm) to select cells with similar size and fluorescent signals. Then, they were used to generate heterogenous tumoroids. IncuCyte® system was used to follow generation steps and to monitor cell fluorescent intensity (Figure). The measurement of fluorescence intensity of each cell type showed that MA30, hASC20, hASC30, M0 and M1 significantly decreased the viability of MECs (Hs578Bst-EGFP) while hASC30, MA30, M0 and M1 significantly increased the viability of MCF-10DCIS-mCherry cancer cells. Therefore, obesity and the adipose and inflammatory microenvironment promote DCIS invasion. Spheroid culture system provide a better reflection of the *in vivo* behavior of cells in tumor tissue and are being widely recognized as valuable advanced tools for cancer investigations.

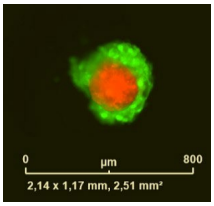

CONCLUSION

Obesity and the inflammatory microenvironment promote DCIS invasion. Spheroid culture system provide a better reflection of the in vivo behavior of cells in tumor tissue.

Mesenchymal stem cells pre-conditioning with IL-1ϟ as a potential immunomodulatory and anti-proteolytic therapy for annulus fibrosus failure

Joana R. Ferreira[1,2,3], Ana João Silva[1,2], Graciosa Q. Teixeira[4], Cornelia Neidlinger-Wilke[4], Joana Caldeira[1,2], Susana G. Santos[1,2], Mário A. Barbosa[1,2,3], Raquel M. Gonçalves[1,2,3]

[1]i3S – Instituto de Inovação e Investigação em Saúde, Universidade do Porto, Porto, Portugal; [2]INEB – Instituto de Engenharia Biomédica, Porto, Portugal; [3]ICBAS- Instituto Ciências Biomédicas Abel Salazar, Universidade do Porto, Porto, Portugal; [4]Institute of Orthopaedic Research and Biomechanics, Trauma Research Centre, Ulm University, Ulm, Germany

*raquelg@ineb.up.pt

Introduction: Inflammation associated to intervertebral disc (IVD) degeneration, including the presence of infiltrated macrophages, has been suggested as one the main contributors for discogenic pain. The secretome of Mesenchymal stem/stromal cells (MSCs), including extracellular vesicles, has been increasingly demonstrated to be a potential immunomodulatory cell-free therapy to degenerated IVD. Our team has recently shown that MSC secretome can decrease the pro-inflammatory profile of nucleus pulposus cells, while promoting aggrecan deposition [2]. Nevertheless, MSC are strongly influenced by their microenvironment, which can condition the secretome composition [3]. Here we investigate MSC secretome upon pre-conditioning with the pro-inflammatory cytokine interleukin (IL)-1β and reduced oxygen (6%) and its therapeutic potential in human AF cells.

Materials and Methods: Human bone marrow (BM)-derived MSCs were isolated from patients undergoing ligaments surgery, as described [3]. Expanded MSCs were then pre-conditioned with the pro-inflammatory cytokine interleukin (IL)-1β (10ng/ml) during 48h in reduced oxygen (6%). The protein content of MSC secretome was analyzed by a protein array and validated by ELISA. The immunomodulatory potential of MSC secretome was analyzed in human macrophages from peripheral blood. Briefly, MSC secretome was supplemented to macrophage cultures (1:1) at day 7. After 72h, macrophage phenotype was analyzed by flow cytometry to M1/M2 markers. MSC secretome therapeutic potential was then investigated in human AF cells. Human AF was isolated from IVD biopsies upon tissue digestion. AF cells were exposed to physiological cyclic tensile strain (CTS) for 72 h in a custom-made device with IL-1β medium supplementation. Stimulated AF cells were then treated with MSC secretome. AF cell metabolic activity, pro-inflammatory cytokine gene expression, matrix metalloproteinase (MMP) activity, and tissue inhibitor of MMPs (TIMP) concentration were evaluated.

Results: IL-1β (and not low oxygen) pre-conditioning of MSCs increased secretion of pro-inflammatory markers, namely IL-6, MCP-1, IL-8 and IL-1β, chemokines as RANTES, and MMPs inhibitors as TIMP-2. IL-1β-preconditioned MSC secretome increased CD163 expression and not CD86 in macrophages, suggesting a polarization of naïve macrophages towards a M2 phenotype. Nevertheless, when supplemented to activated macrophages (stimulated with LPS+IFN-ψ), MSC secretome was not able to revert the pro-inflammatory profile of these cells, maintaining high CD86 and low CD163 surface expression in human macrophages, and neither the anti-inflammatory stimuli (IL-10). Moreover, it promoted IL-6, TNF-α and TGF-ϟ secretion by these cells. Furthermore, MSC secretome did not show an immunomodulatory effect on human AF cells stimulated with CTS + IL-1β, although it significantly decreased MMPs (MMP-1, MMP-2, MMP-3, and MMP-9), concomitantly with an increased production of TIMP-1.

Conclusion: The results obtained demonstrate the impact of IL-1β pre-conditioning in the immunomodulatory and anti-proteolytic potential of MSC secretome in the AF. New challenges arise in the development of an appropriate delivery system for MSC secretome to the AF.

References: [1] Binch et al., Nat Rev Rheumat; 2021; [2] Ferreira et al, eCM, 2021; [3] Ferreira et al., Frontiers in Immunol, 2018;

Acknowledgements: The study was supported by Eurospine TRF (2017_05), Ulm University (L.SBN.0157), German Spine Foundation (Deutsche Wirbelsäulenstiftung), Council of Rectors of Portuguese Universities (CRUP), German Academic Exchange Service (DAAD) and Alexander von Humboldt Foundation.

A hybrid dECM-alginate hydrogel to unveil the role of the microenvironment in EMT/MET

Patrícia Barros da Silva[a, b, c], Sílvia J. Bidarra[a, b, d], Diana Nascimento[a, b, d], Bianca Lourenço[a, b], Cristina C. Barrias[a, b, d]

a i3S-Instituto de Inovação e Investigação em Saúde, Porto, Portugal
b INEB-Instituto de Engenharia Biomédica, Porto, Portugal
c FEUP – Faculdade de Engenharia da Universidade do Porto, Portugal
d ICBAS-Instituto de Ciências Biomédicas Abel Salazar, Universidade do Porto, Portugal
* patricia.silva@i3s.up.pt

INTRODUCTION

Epithelial-to-mesenchymal transition (EMT), where epithelial (E) cells lose polarity and cell-cell contacts acquiring a mesenchymal (M) phenotype, with increased cell-matrix contacts and migratory potential, is crucial for cancer invasion; and reversion of this phenotype (mesenchymal-to-epithelial transition, MET) is decisive for metastases establishment. Also, it is widely accepted that malignant behaviour and cancer progression is dependent on the evolving crosstalk between tumour cells and their surrounding microenvironment, which is regulated not only by altered cell-cell interactions and soluble factor signalling, but also by highly dynamic alterations of the ECM. Nevertheless, the functional contribution of the ECM in malignant cells behaviour, particular during EMT/MET, is still poorly understood due in part to a lack of appropriate in vitro model systems. Herein, we propose, an advanced 3D model, combining inducible mammary epithelial cells, mammary fibroblast-derived ECM, and bioengineered hydrogels to investigate the role of the ECM in breast-cancer associated EMT/ MET.

EXPERIMENTAL METHODS

Human mammary epithelial cells (MCF10A) were embedded in hydrogels of ultra-pure alginate grafted with integrin-binding RGD peptide to generate mammary gland organoids as described in: (1,2). To induce EMT in 3D cultured cells, culture medium was supplemented with 16 ng/mL of TGFb1 during 3 or 14 days to generate mesenchymal-like cells (EM3, EM14). Control cells were maintained in culture for 14 days (E14) To revert the EMT process (MET), 3D culture of M cells was maintained in TGFb1-supplemented media for 7 days followed by non-supplemented culture medium for another 7 days to generate cells with intermediate phenotype (ME14). Cells were characterized by confocal microscopy (CM) after immunostaining and by qPCR. Hydrogels were characterized by oscillation rheometry. Primary human mammary fibroblasts (Fib) were used to produce cell-derived ECM in normal and activated states (via TGFb1 induction) and were characterized by qPCR. The ECM was decellularized with Triton X-100/NH_4OH/DNAse) and characterized by CM and proteomics. To produce hybrid hydrogels, the DCEM was digested in pepsin-HCL, neutralized, and combined with RGD-alginate with or without MCF10A cells. Hydrogels were produced by ionic gelation as described in :(1,2). Whole-mounted samples were analysed by CM. Cells were retrieved upon hydrogel dissolution (EDTA/trypsin) and analysed by qPCR.

RESULTS AND DISCUSSION

In the 1st part of the study, MCF10A cells cultured in RGD-alginate hydrogels (200 Pa), were able to grow and organise into acinar-like structures akin to the mammary gland. Distinct EMT/MET states were generated by culturing cells in the presence/absence of TGFb1: E14 – an epithelial-like state, EM3 and EM14 - two mesenchymal-like states, and ME14 – a reversed state from M to E. As expected, compared to E14, EM3 and EM14 cells showed decreased expression of E markers (*Ocln, Epcam*) and increased expression of M markers (*Fn1, Cdh2*) and EMT transcription factors (*Slug, Zeb2*). Most of these changes were at least partially reverted in ME14 cells. These was corroborated by immunostaining of some E and M markers, and collectively suggest that both EMT and MET were successfully induced in RGD-alginate 3D matrices. In the second part of the study, hMF in 2D were successful activated by TGFb1, acquiring myofibroblast features, with increased expression of *alfaSMA, COL I* and *Fn1*. Monolayers of both native (nFib) and activated fibroblasts (aFib) were successfully decellularized, as shown by the absence of cellular/nuclear components and the preservation of fibrillar meshes of ECM proteins (COL I, FN). Proteomic analysis of decellularized samples (dECM)) showed differential expression of several proteins, namely increased expression of elastin, laminin and collagens, among others. In the third part of the study, the dECM from nFib or aFib (dnECM and daECM, respectively) was solubilised and combined with RGD-alginate hydrogels to form E-laden hybrid 3D matrices. Epithelial morphogenesis occurred in both groups, and the presence of daECM in TGFb1-treated cultures upregulated the expression of M markers, as compared to dECM), suggesting a synergistic role in EMT induction. Collectively, our results illustrate the applicability our system as a versatile 3D model to investigate the role of the ECM in EMT/MET.

ACKNOWLEDGMENTS: Portuguese Foundation for Science and Technology (FCT): project PTDC/BTM-ORG/5154/2020, fellowship SFRH/BD/31757/2017, contract IF/00296/2015.

REFERENCES: 1) Bidarra SJ et al. A 3D in vitro model to explore the inter-conversion between epithelial and mesenchymal states during EMT and its reversion. Scientific Reports 2016;6:1. 2)Barros da Silva P et al. Reshaping in vitro models of breast tissue: integration of stromal and parenchymal compartments in 3D printed hydrogels. Frontiers Bioeng Biotech 2020:8:494.

In Vitro Development Of a Tissue-engineered Cutaneous Wound Healing Model Made Of Diabetic Patient Cells

Mathias Lemarchand[1,2*], Thiéry De Serres-Bérard[1,2], Sabrina Bellenfant[1,2], Todd Galbraith[1,2], Yvan Douville[2] and François Berthod[1,2]

[1] LOEX, Centre de recherche du CHU de Québec-Université Laval, Québec, Canada
[2] Département de Chirurgie, Faculté de Médecine, Université Laval, Québec, Canada
[*] mathias.lemarchand.1@ulaval.ca

INTRODUCTION

Diabetic patients suffer from frequent formation of sores on the foot, called diabetic ulcers (DU), that are struggling to heal and subject to frequent infections that may require amputation of the lower legs. Thus, diabetes is the leading cause of non-traumatic amputations in the US. However, the link between diabetes and mechanisms compromising skin wound healing is not yet fully understood.

Our main hypothesis is that the lack of innervation induced by diabetic neuropathy in the skin of the patients is partly responsible for the impairment of the wound closure. Indeed, sensory neurons are involved in the regulation of the inflammation and reepithelialization through the release of neuropeptides such as substance P (SP) and Calcitonin-Gene Related Peptide (CGRP)[1,2]. These neuropeptides could be a potential treatment for DU[3].

In order to advance on the study of this phenomenon and to allow the emergence of a treatment for DU, we propose to develop a tissue-engineered human skin in the laboratory using cells extracted from diabetic patient's skin. Our first aim is to assess the ability of our diabetic wound healing model (dWHM) to recapitulate the characteristic of a DU. The second part of this project is to develop a new strategy to improve wound healing of diabetic ulcers based on a treatment using neuropeptides normally released by sensory nerves.

EXPERIMENTAL METHODS

Populations of fibroblasts and keratinocytes were extracted from the diabetic patient skin harvested after a foot amputation. The dWHM was prepared by seeding these diabetic fibroblasts and keratinocytes on a collagen-chitosan sponge and cultured at the air/liquid interface. Fibroblast and healthy endothelial cells were seeded on a second sponge. Once the epidermal layer was mature, a wound was performed with au biopsy punch on the sponge featuring an epidermis. The reepithelialization was then monitored during 8 days, with or without the addition of neuropeptides in the culture medium. Controls were produced the same way using age-matched healthy fibroblasts and keratinocytes. Populations of keratinocytes and fibroblasts were extracted from skin from three diabetic patients and three healthy subjects.

RESULTS AND DISCUSSION

A mature epidermis was formed successfully by diabetic cells. However, the dWHM were unable to close without treatment in contrast to healthy skin models. The addition of neuropeptides in the culture medium successfully improve the reepithelialization of the dWHM.

CONCLUSION

We successfully produced a wound healing model able to mimic the condition of a diabetic ulcer, which is suitable to screen new therapies for DUs. Furthermore, we demonstrated that the use of neuropeptides such as substance P could be a good strategy to improve the treatment of DU.

REFERENCES

[1] J. E. Choi et A. Di Nardo, « Skin Neurogenic inflammation », *Semin. Immunopathol.*, vol. 40, nº 3, p. 249-259, mai 2018, doi: 10.1007/s00281-018-0675-z.
[2] M. Blais, L. Mottier, M.-A. Germain, S. Bellenfant, S. Cadau, et F. Berthod, « Sensory neurons accelerate skin reepithelialization via substance P in an innervated tissue-engineered wound healing model », *Tissue Eng. Part A*, vol. 20, nº 15-16, p. 2180-2188, août 2014, doi: 10.1089/ten.tea.2013.0535.
[3] E. Leal *et al.*, « Substance P Promotes Wound Healing in Diabetes by Modulating Inflammation and Macrophage Phenotype », *Am. J. Pathol.*, vol. 185, nº 6, p. 1638-1648, 2015, doi: 10.1016/j.ajpath.2015.02.011.

ACKNOWLEDGMENTS

The authors would like to thank the Canadian Institutes for Health Research (Grant MOP-106429) for providing financial support to this project.

Engineering (sub)micron patterns for modulating the behavior of cancer spheroids

Mahdiyeh Nouri-Goushki[1*], Hendrik Hubbe[1], Ruben Boot[1], Pouyan Boukany[1]

[1]Department of Chemical Engineering, Delft University of Technology, Delft, Netherlands
[*] m.nourigoushki@tudelft.nl

INTRODUCTION

The surface topography of the extracellular matrix influences the adhesion, migration, and invasion of cancer cells. Increasing the diameter of polystyrene colloidal nanodot activated the metastasis progression in lung cancer cells (A549)[1]. Furthermore, micropillars with 16 µm pitch stimulated the epithelial-mesenchymal transition in the same cell type[2]. The migration speed of metastatic human ovarian cancer cells (HeyA8) was accelerated on the micrograting surface features, while nonmetastatic HeyA8 cells were not affected by microgratings[3]. Despite the presence of current research on the interaction between individual-cell and surfaces, it is not clear how multicellular cancer spheroids respond to the surface topographies. Here we fabricated (sub)micron patterned surfaces to investigate the interaction between the multicellular cancer spheroids and surfaces features. (Sub)micron pillars were fabricated via electron-beam lithography (EBL) and 3D printing using two-photon polymerization (2PP). Next, the morphology of multicellular spheroids with different sizes on the micropatterned surfaces was studied.

EXPERIMENTAL METHODS

The submicron pillars (named 2PP-pillars) were 3D printed using a Photonic Professional GT machine (Nanoscribe, Germany). The Galvo writing strategy and an acrylate-based resin (IPL, Nanoscribe) were selected for printing the features on glass coverslips (Thermofisher)[4]. Furthermore, the micropatterned surfaces were created on a 4″ silicon wafer by the EBL technique (EBPG5200, Raith). The wafer was etched and used as a mold to transfer the micropillars onto polydimethylsiloxane (PDMS, Sigma Aldrich), named PDMS-pillars. All samples were characterized using a scanning electron microscope (SEM) (JSM-6010LA). Then, spheroids of lung adenocarcinoma cancer cells (A549, American Tissue Type Collecton) were formed using a custom-made micro-well array. Dulbecco's MEM (Sigma Aldrich) with 10% (v/v) fetal bovine serum (Sigma Aldrich) and 0.5 % (v/v) antibiotic antimycotic (Thermo Fisher) was used as culture medium. Spheroids were then collected and seeded on the patterned substrates for 24 hours (h).

RESULTS AND DISCUSSION

Highly reproducible (sub)micron pillars with an aspect ratio of 4:1 were successfully fabricated using 2PP and EBL techniques (Fig1). Although EBL involves multiple fabrication steps, the writing speed of micropatterns was remarkably fast (~ 10 s/mm^2). While the printing time of 2PP process (10 h/mm^2) was significantly longer than EBL, which limited the area of patterning.

We controlled the size of spheroids with custom-made hydrophobic micro-well arrays, with sizes of 80 µm and 200 µm. The growth of spheroids was monitored over time. On day 2, the desired sizes were achieved, but the adhesion bond between cells was not strong and made loosely cell aggregates. On day 4, the contact between adjacent cells was promoted, leading to strong adhesive multicellular spheroids. When 80 µm spheroids were plated on the 2PP-pillars, a fully spread morphology was observed after 24 h of culture; while 200 µm spheroids formed a precursor film around their central aggregates. Meaning that the adhesion between cells and substrate overwhelmed the cell-cell cohesion, leading to the expansion of the peripheral film.

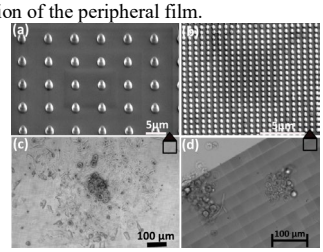

Fig 1. (a, b) SEM images of micropillars and submicron pillars fabricated using EBL and 2PP, respectively. Morphology of spheroids with 200 µm and 80 µm sizes on patterned surfaces after 24 h.

CONCLUSION

In summary, this work demonstrated and compared the fabrication of ordered (sub)micron pillars via EBL and 3D printing techniques. Controlled micropatterning of the surface over large areas was successfully achieved by EBL, which is beneficial for studying the interaction between multicellular spheroids and surface topographies. The entry of cancer cells from the central reservoir of smaller spheroids was much faster than the bigger spheroids, leading to the conversion of spheroids into a monolayer of cancer cells in one day. Such topographies fabricated in this study open up new doors to further analyze the metastasis of different cancer spheroids on nanostructured biointerfaces.

REFERENCES

1. Wang L. *et al.,* Nano Res. 2018, 11(10): 5704–5715.
2. Lee G. *et al.,* ACS Appl. Mater. Interfaces 2022, 14, 20−31
3. Zhou S. *et al.,* Biomed. Mater. 2017, 12 055001
4. M. Nouri *et al.,* ACS Appl. Mater. Interfaces 2020, 12, 1, 200–208

ACKNOWLEDGMENTS

The authors would like to thank the European Research Council (Grant no: 819424) for providing financial support to this project, Prof. Urs Staufer (Dept. of Precision and Microsystems Eng., TUDelft) for the access to the Nanoscribe machine, and Kavli Nanolab for the access to the EBL equipment.

A Closed-Loop Soft Robotic Drug Delivery System to Overcome the Foreign Body Response

Lucien H.J. Schreiber[1], Rachel Beatty[1,2], Keegan L. Mendez[3], William Whyte[4], Yiling Fan[5], Scott T. Robinson[1,2], Andrew J. Simpkin[6], Ellen T. Roche[3,4,5], Eimear B. Dolan[7], Garry P. Duffy[1,2]

[1] Anatomy and Regenerative Medicine Institute (REMEDI), School of Medicine, NUI Galway, Galway, Ireland.
[2] SFI Centre for Advanced Materials and BioEngineering Research (AMBER), Trinity College Dublin, Dublin, Ireland.
[3] Harvard-MIT Program in Health Sciences and Technology, Cambridge, MA, USA.
[4] Institute for Medical Engineering and Science, Massachusetts Institute of Technology, Cambridge, MA, USA.
[5] Department of Mechanical Engineering, Massachusetts Institute of Technology, Cambridge, MA, USA
[6] School of Mathematics, Statistics and Applied Mathematics, NUI Galway, Galway, Ireland
[7] Department of Biomedical Engineering, NUI Galway, Galway, Ireland.
* l.schreiber1@nuigalway.ie

INTRODUCTION

The Foreign Body Response (FBR) is a major obstacle to implantable drug delivery devices[1]. The growth of a fibrous capsule around drug delivery devices can impair function and require the need for early replacement. If the device is occluded, the expected drug regimen can no longer be maintained and causes failure. We developed a soft robotic drug delivery device capable of probing and modulating the FBR. The device is composed of a soft therapeutic reservoir and a fibrosensing porous membrane. The latter makes use of electrochemical impedance spectroscopy to quantify occlusion caused by the FBR. Soft robotic actuations, tuneable by magnitude and frequency, are applied to deliver therapies by overcoming the occluded membrane. The actuation regime is determined by case-based reasoning. This technology has great potential in improving the longevity and function of drug delivery devices.

EXPERIMENTAL METHODS

Fibrosensing devices (Fig. 1A) were manufactured as described in [1], in this case the porous membranes were fabricated of a conductive material. Devices (n=22) were implanted subcutaneously in rodent models for up to 7 days and impedance was measured each day by an external potentiostat. Fibrotic capsule dimensions were measured via microCT and correlated to impedance markers via Pearson. Impedance of 0.15 and 0.3% w/v agarose gels was measured and a k-nearest neighbour classifier was tested to infer gel concentration. The hydraulic conductance of the same gels was calculated using Darcy's law by forcing water through the porous membrane and gel, at 2 psi, and measuring the resulting flow rate. A case-based system was developed by releasing methylene blue dye into agarose gels at different pressures and over multiple actuations, and measuring the area occupied by the dye.

RESULTS AND DISCUSSION

Impedance increased over time in vivo (Fig. 1B) and correlated to the increase in thickness (Fig. 1C) and volume of the fibrotic capsule (Pearson's coefficient 0.83 and 0.81, respectively). Agarose proved to be suitable phantom for drug release studies as it mimicked two consequences of the FBR: (i) significant changes in impedance (p=0.040) and (ii) significant changes in hydraulic conductance of the porous membrane (p=0.027). Gel concentration was inferred by machine learning with 83.3% accuracy. Soft robotic actuations (Fig. 1D) allowed to control the release of methylene blue (Fig. 1E). When given a release to achieve, a case-based reasoning system was capable of finding the most appropriate actuation regime to employ, depending on the gel concentration.

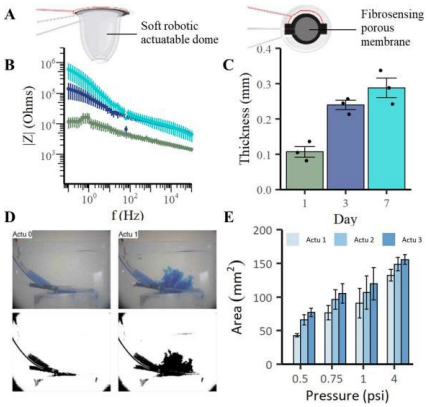

Figure 1 **A.** Schematic of soft robotic reservoir with biosensing membrane. **B.** Impedance and **C.** fibrotic capsule thickness during *in vivo* study. **D.** Release of methylene blue into agarose gels. **E.** Pressure and number of actuation allow to control drug release.

CONCLUSION

Incorporating an impedance sensor into a drug delivery device allows to monitor the FBR and quantify fibrotic capsule formation. Soft robotic actuations can overcome reductions in hydraulic conductance and maintain constant drug release overtime. This self-adapting technology is poised to improve the function and longevity of implantable drug delivery devices.

REFERENCES

1. Dolan *et al.*, Soft Robotics, 4(33), 2019.

ACKNOWLEDGMENTS

The presenting author would like to acknowledge the DELIVER programme which has received funding from the European Union's Horizon 2020 framework program under grant agreement ID 812865.

Development of a fully programmed wearable pump to actuate a soft robotic macroencapsulation device for type 1 diabetes

Giulia Lattanzi[1*], Joanne O'Dwyer[1], Eimear Dolan[2] , Liam Burke[3], Garry Duffy [4,5,6]

[1]Discipline of Anatomy, School of Medicine, National University of Ireland Galway, Ireland
[2]Bioengineering, School of Engineering, National University of Ireland Galway, Ireland
[3]Discipline of Bacteriology, School of Medicine, National University of Ireland Galway, Ireland
[4]REMEDI, School of Medicine, College of Medicine Nursing and Health Sciences, NUIG, Ireland
[5]CÚRAM, Centre for Research in Medical Devices, National University of Ireland Galway, Ireland
[6]Advanced Materials and BioEngineering Research Centre (AMBER), Trinity College Dublin, Ireland
[*]g.lattanzi1@nuigalway.ie

INTRODUCTION

Islet encapsulation represents one of the most promising treatments for Type 1 Diabetes (T1D). The post-implant foreign body response (FBR) causes the formation of a tissue capsule surrounding the device, reducing diffusion of cell nutrients and waste, thus leading to islet necrosis and implant failure[1]. Strain, fluid agitation, and shear stress have been shown to influence the adhesion and proliferation of cells[2,3]. Perturbing the cellular activity and the fluid flow can interfere with the progression of the FBR to an implanted medical device. Altering the strain, fluid agitation and shear stress with a Dynamic Soft Reservoir (DSR) for cell macroencapsulation has shown the potential to modulate the immune-cell activity and ameliorate the FBR to the devices[4]. In this study we aim to develop a fully programmed wearable system with comparable capabilities to the laboratory set-up that is currently used to actuate the soft robotic device. In a wider perspective, we also aim to control the wearable pumping system in real-time, via simultaneous measurements of the FBR at the biotic/abiotic interface.

EXPERIMENTAL METHODS

The actuating system was designed using a compact Peristaltic Pump controlled by Arduino IDE software programming, mini-processor and motorboard modules. The flow rate of the Peristaltic Pump can be modulated by controlling the amplitude and duration of voltage provided to the pump, allowing the generation of tunable strains at the tissue interfacing membrane of the soft robotic device. To test the system, DSRs were fabricated using Thermoplastic polyurethane (TPU) following a standard procedure[4]. To explore the properties of the newly developed system, the force produced by the deflection of the tissue interfacing membrane of the DSR was measured when actuating with the wearable pump and compared with the forces generated by the laboratory system. To investigate the cellular response to the two systems, WMPY-1 myofibroblast cells were cultured on the tissue interfacing membrane of the DSR devices for 14 days. The amount of Type 1 collagen produced was quantified and compared between groups: control (not-actuated), actuated with the laboratory system or actuated with the newly developed wearable pump. Devices were then fixed with 4% PFA, stained and imaged using a Confocal Laser Scanning Microscope. Nuclei were stained with Hoechst, to assess differences in cell number and distribution between the groups. Immunofluorescence staining (Collagen I and Phalloidin) was used to visualize the deposited collagen and investigate the changes in cell morphology between the groups.

RESULTS AND DISCUSSION Force tests have shown the possibility for the fully programmed wearable pump to reach comparable forces to the laboratory set-up, allowing comparable strains to be generated at the tissue interfacing membrane of the DSR. The wearable pump also allows tunable strains and strain rates to be reached by programming. In vitro results show similar collagen production with the wearable pump compared to non-actuated devices (Fig.1) demonstrating long-term compatibility of the actuation regime.

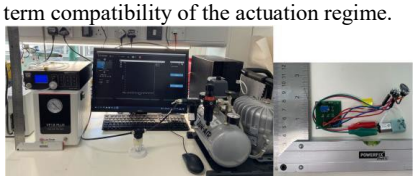

Figure 1 *Set-up comparison: laboratory system(left) vs wearable system(right)*

CONCLUSION

Previous studies have shown that perturbation of cellular activity and fluid flow can interfere with the progression of the fibrotic capsule formation[4]. In this study, we have developed and tested a fully programmed wearable pump to control actuation that is able to generate and control mechanical strain on the tissue interfacing membranes of a soft-robotic macroencapsulation device. Development of this device is a significant step in the clinical translation of wearable pumps to modulate the FBR to implanted medical devices.

REFERENCES

1. de Vos *et.al*, Diabetologia, 45(2):159-73., 2002
2. Ito *et.al*, Biomed Mater Eng, 21(3):149-58, 2011
3. Ballotta *et.al*, Biomaterials 35, 4919–4928, 2014
4. Dolan *et.al*, Scientific Robotics, 4, 2019

ACKNOWLEDGMENTS The authors would like to thank European Union's Horizon 2020 Marie Sklodowska-Curie Actions programme (Grant no: 812865) for providing financial support to this project.

Dense Calcium Phosphates and Silk Fibroin Biocomposite for Restoration of Damaged Enamel

Vita Zalite[1*], Linda Dauge[1], Janis Locs[1,2]

[1]Rudolfs Cimdins Riga Biomaterials Innovation and Development Centre, Institute of General Chemical Engineering, Faculty of Materials Science and Applied Chemistry, Riga Technical University, Riga, Latvia
[2] Baltic Biomaterials Centre of Excellence, Headquarters at Riga Technical University, Riga, Latvia
[*] vita.zalite@rtu.lv

INTRODUCTION

Dental enamel is a complex biocomposite build from hydroxyapatite, organic matter and water. So far all commercially available dental restoration materials are chemically very different from natural teeth enamel. Thus, such materials will never be able to form natural chemical bond with tooth, whereas calcium phosphates (CaP) could be promising candidates for such purpose. However, CaP and their composites have insufficient mechanical properties to withstand masticatory forces. Guo *et al.*[1] developed cold sintering process, where dense ceramic materials can be obtained in relatively low temperatures (up to 300°C). Therefore, it is possible to combine CaP with organic matter and to obtain composite bioceramic. In this study we developed nano-hydroxyapatite (nHAp) and silk fibroin (SF) ceramic-polymer biocomposite *via* cold sintering process as potential tooth restoration material.

EXPERIMENTAL METHODS

nHAp was obtained via adapted reprecipitation method[2] from CaO, H_3PO_4, HCl and NaOH. SF was obtained as described before[3]. Biocomposites were obtained by mixing 98 wt% of nHAp paste with 2wt% of SF solution (nHAp+SF) (2000 rpm for 4 min). nHAp+SF was subjected to freeze drying process to obtain powder. Afterwards, uniaxial pressing (Ø 13 mm, 1500 MPa, 10 min, room temperature) was used to obtain densified and sintered samples (nHAp+SF_1500). Characterization of synthesized and treated samples was performed using N_2 adsorption (BET), XRD, helium pycnometry and SEM.

RESULTS AND DISCUSSION

X-ray diffraction before and after uniaxial pressing showed no changes in characteristic peaks for nHAp phase and SF was not detected due to its low content in the composite.

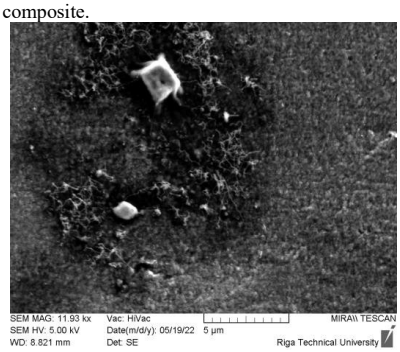

In the SEM images it was observed, that sintered samples consisted of nanosized grain matrix with regions of SF. The size of these polymeric regions was very different. SEM results suggest that SF was evenly distributed in the nHAp matrix, but chemical bonding was not observed, additional FTIR analysis should be done. Specific surface area of nHAp+SF powder was 169 m^2/g, while nHAp+SF_1500 sample it was only 3 m^2/g. Decrease of SSA clearly confirmed sintering process during uniaxial pressing. The real density of nHAp+SF powder was 2.41 g/cm^3, but density for nHAp+SF_1500 composite was 2.10 g/cm^3, and calculated relative density was 87 %.

CONCLUSION

In our research dense, sintered polymer-ceramic biocomposite was successfully obtained. Due to nHAp phase presence in the material it is a very promising material for dental restoration that could make bond with natural tooth tissues. Nevertheless, we need to continue to develop this material in order to achieve a higher density, analyze and optimize mechanical properties and then develop possible strategies for using this material in dental restorations.

REFERENCES

1. Guo J. *et al.*, Angew. Chem. Int. E. 55: 11457-11461, 2016.
2. Vecstaudza J. *et al.*, J. Eur. Ceram. S. 39: 1642-1649, 2019.
3. Grava A. *et al.*, Materials, 14, 7191, 1-19, 2021.

ACKNOWLEDGMENTS

This work has been supported by the European Regional Development Fund within the Activity 1.1.1.2 "Post-doctoral Research Aid" of the Specific Aid Objective 1.1.1 "To increase the research and innovative capacity of scientific institutions of Latvia and the ability to attract external financing, investing in human resources and infrastructure" of the Operational Programme "Growth and Employment" (No.1.1.1.2/VIAA/3/19/459)

Antibacterial 3D-printed hybrid scaffolds for large bone defect repair

Xiuyuan Shi[1*], Agathe Heyraud[1], Francesca Tallia[1], Julian R. Jones[1]

[1] Department of Materials, Imperial College London, London, UK
[*] xiuyuan.shi18@imperial.ac.uk

INTRODUCTION

Bone has ability to repair itself, but the self-repair ability is limited. An ideal scaffold for large bone defect regeneration should be bioactive, have sufficient mechanical properties and contain interconnected pores to promote cells growth. In addition, the scaffold for bone repair should contain antibacterial properties to avoid infection after surgery.

Sol-gel hybrid materials have organic and inorganic co-networks interacting at the molecular level. These hybrids can have desired chemical and mechanical properties and degradation rate by altering organic and inorganic components[1].

Previously, hybrids with a composition of silica/ polytetrahydrofuran/ polycaprolactone were fabricated by the sol-gel method, with unprecedented mechanical properties, and 3D extrusion printing was used to fabricate porous scaffolds[2]. Here the aim was to incorporate copper into the silicate network of the hybrid to deliver antibacterial properties. Cu ions have been proven capable of fighting against *E. coli and C. albicans* and they also play a key role in angiogenesis process[3]. The objectives were to optimize mechanical properties of the 3D printed hybrid scaffolds and to investigate the efficacy of the antimicrobial ions.

EXPERIMENTAL METHODS

The preparation of the hybrids was a two-pot synthesis: Tetraethyl orthosilicate (TEOS) and copper ethoxide (CuE) were hydrolyzed together under acidic environment at room temperature for 1.5 h. PCL-diCOOH, tetrahydrofuran (THF), (3-glycidyloxypropyl)-trimethoxysilane (GPTMS) and boron trifluoride diethyl etherate ($BF_3{\cdot}O(C_2H_5)_2$) were mixed for 1.5 h. Then, the organic and inorganic solutions were mixed for another 1 h until the viscosity of the solution was suitable for printing. The solution for printing must be fluid enough to flow and viscous enough to maintain form, avoiding collapse. All hybrid scaffolds were fabricated through 3D extrusion printing directly from the sol-gel process.

RESULTS AND DISCUSSION

XRD and FTIR results confirm that hybrids were successfully synthesized, and no crystal phases formed during the sol-gel synthesis. Micro-CT and SEM images present morphology of hybrids. Pore channels in scaffolds can be tailored ranging from 250 µm to 600 µm. ICP results show a steady copper ions release, indicating the Cu was incorporated into the silicate network, and the release concentration is considered suitable to work against bacteria. The compression test proves that scaffolds show failure stress of 0.9-1.6 MPa while the dynamic mechanical analysis results illustrate that the storages modulus ranges from 2-9 MPa depending on the amount of incorporated copper ethoxide. In addition, the formation of hydroxyapatite is confirmed after 3 months dissolution study.

Figure 1. Compression test on 3D-printed scaffolds and the copper release profile of dissolution study in 3 months.

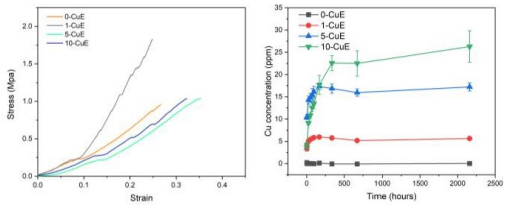

Figure 2. A micro-CT image of the hybrid scaffold with 600 µm pore channel size.

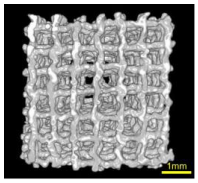

CONCLUSION

3D-printed hybrid scaffolds with copper incorporation were successfully produced. The release of copper ions was steady and slow, which would contribute to good bacteria inhibition performance. Hydroxyapatite was formed during the dissolution study in SBF, which proves the bioactivity of hybrid scaffolds. Tailorable mechanical properties were achieved in this study as well, matching mechanical strength of human trabecular bones.

REFERENCES

1 Jones, J. R. (2013) Acta biomaterialia. 9 (1), 4457–4486.
2 Tallia, F. Mater. Horiz. 5 (2018) 849–860.
3 Borkow G. Curr Med Chem. 2005;12(18):2163-75

ACKNOWLEDGMENTS

The authors acknowledge EPSRC grants EP/N025059/1 and EP/S025782/1.

3D-printed porous cochlear implants

A.Isaakidou[1*], I. Apachitei[1], L.E. Fratila-Apachitei[1], Amir A. Zadpoor[1]

[1]Department of Biomechanical Engineering, Faculty of Mechanical, Maritime, and Materials Engineering, Delft University of Technology (TU Delft), Delft, The Netherlands
[*] a.isaakidou@tudelft.nl

INTRODUCTION

Drug administration is the cornerstone treatment for a variety of pathologies, with systemic administration being the most used method worldwide.[1] However, drug bioavailability in the tissue of interest often does not reach therapeutic levels. Organs that possess a blood-barrier (e.g., cochlea) notably suffer from this phenomenon.[2] To that end, there is a constant interest in the fabrication of novel systems and drug formulations specifically oriented to enhance bioavailability in such tissues. Researchers and pharmaceutical companies aim to do so using sophisticated systems for controlled, localized drug delivery. Recent advances in the field of additive manufacturing enable the fabrication of complex geometries that can be combined with a wide range of active pharmaceutical ingredients. Here, we take advantage of a high-resolution additive manufacturing method to fabricate cochlear implants with internal microscale porosity at anatomically relevant sizes. Moreover, we test macrophage viability levels on the 3D printed material. Lastly, we investigate the suitability of the proposed designs regarding drug loading.

MATERIALS AND METHODS

We fabricated cochlear implants and also specimens for cell culture experiments using the two-photon polymerization (2pp) method. The 3D printer used was the Photonic Professional GT2 (Nanoscribe GmbH) in combination with the proprietary acrylate-based photocurable resin IP-Q. A dexamethasone suspension was used to load the porous cochlear implants. The viability of macrophages was investigated using a live/dead assay after 48 hrs of culture on flat 3D printed pedestals.

RESULTS AND DISCUSSION

We printed porous cochlear implants of 0.6x0.6x2.4 mm^3 with internal square lattice pores of 60 µm and also pedestals of 2x2x0.5 mm^3 for cytotoxicity tests (Figure 1a). We assessed macrophage viability on the later via fluorescent microscopy (Figure 1b). The cell viability test showed no cytotoxicity of the 2pp resin for macrophages, validating the suitability of the method and the material for further drug incorporation and release, both *in vitro* and *in vivo*. Using an organic suspension of dexamethasone we additionally proved the feasibility of drug loading the pores of the 3D printed cochlear implants (Figure 1c).

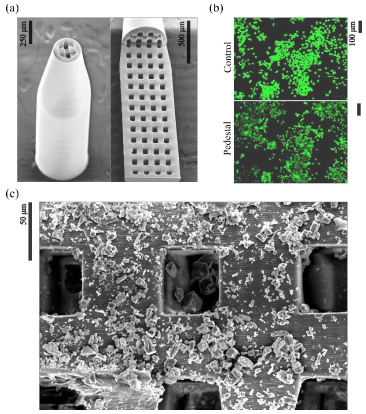

Figure 1: (a) 3D printed porous cochlear implants, (b) viability of macrophages on control well plate and on 3D printed pedestals, (c) dexamethasone crystals in the pores of the cochlear implants.

CONCLUSION

The results of this study demonstrate that the 2pp process constitutes a feasible fabrication method for a new generation of cochlear implants in anatomically applicable sizes with appropriate porosity and acceptable cytocompatible properties for drug delivery applications in the inner ear.

REFERENCES

1. Ruiz M.E. *et al.*, Routes of Drug Administration, ADME Processes in Pharmaceutical Sciences, Springer, Cham, 2018
2. Gehrke M. *et al.*, International Journal of Pharmaceutics, 509(1-2):85-94, 2016
3. Melnyk L.A *et al.*, Annals of 3D Printed Medicine, 4:100035, 2021

ACKNOWLEDGMENTS

"This project has received funding from the Interreg 2 Seas programme 2014-2020 co-funded by the European Regional Development Fund under subsidy contract "Site Drug 2S07-033."

Freeze-cast Scaffolds for Bone Substitution: Influence of the Filler Rate on the Properties of Alginate/Amorphous Calcium Carbonate Composites

Marion Merle[1*], Christèle Combes[1], Christian Rey[1], Prescillia Lagarrigue[1], Christophe Tenailleau[2], Benjamin Duployer[2], Jérémy Soulié[1]

[1]CIRIMAT, Université de Toulouse, CNRS, TOULOUSE INP - ENSIACET, 4 allée Emile Monso, Toulouse, France
[2]CIRIMAT, Université de Toulouse, CNRS, Université Toulouse 3 - Paul Sabatier, 118 Route de Narbonne, Toulouse, France
[*] marion.merle@toulouse-inp.fr

INTRODUCTION

In the field of bone tissue engineering, recent advances led to the development of a 3D scaffold with a connected porosity that would allow cell growth, colonization, angiogenesis and innervation[1]. Hence, the requirements for a bone substitute scaffold are to be highly porous (pore volume and size), biocompatible and degradable with a controlled degradation rate, and with mechanical properties allowing its handling by surgeons[2]. The incorporation of some inorganic bioactive materials could also help enhancing bone regeneration and angiogenesis and/or give additional antibacterial properties. Above all, calcium carbonate and phosphate are of huge interest as they are the building ions of the bone apatite. For the first one, the excellent biocompatibility of calcium carbonate (CC) phases was established, and in particular the lowest stability so highest reactivity of the amorphous calcium carbonate (ACC) is interesting for tunable degradation rate. As for phosphates, the pyrophosphate dimer showed an enhanced bone regeneration when in bone materials composition[3]. In this work, we synthetized by *in situ* co-precipitation a composite powder of pyrophosphate-stabilized amorphous calcium carbonate (PyACC) with a biocompatible polysaccharide, alginate (Alg-PyACC), in order to ensure a nanoscopic entanglement of the polymer chains and the inorganic particles. To study the influence of filler rate on the porosity and mechanical properties of the scaffolds, the resulting powder was then freeze-cast with various powder/free alginate ratios and allowed to obtain macroporous scaffolds with different and adaptable mechanical properties.

EXPERIMENTAL METHODS

The composite powder was obtained by co-precipitation of an alginate and pyrophosphate containing carbonate solution and a calcium one, and was thoroughly characterized after drying (XRD, FTIR spectroscopy, TGA-DTA, chemical titrations, SEM and FEG-SEM, TEM, BET, SAXS). Then, for the same total alginate concentration of 1 wt.% (as free alginate and Alg-PyACC), several compositions of polymer/mineral (from 100/0 to 30/70 wt.%) were suspended in water, freeze-cast at - 10°C and then freeze-dried. The resulting scaffolds were characterized by XRD, SEM, TEM, TGA-DTA, mercury intrusion porosimetry, X-rays tomography and compression testing.

RESULTS AND DISCUSSION

The various compositions were successfully freeze-cast and this process kept the amorphous characteristics of the initial composite powder. All of the 3D scaffolds presented a connected porosity oriented in the solidification direction typically associated to this process[4]. Beyond the anisotropic porous structure similar to the one of bones, lamellar pores were demonstrated to be in a range of sizes adequate for cell colonization (100 – 500 µm)[5]. The pore volume was decreased when adding fillers. In the same time mechanical properties such as the Young's modulus increased up to the critical ratio alginate/PyACC of 30/70 for which the scaffold was too friable to handle compression.

CONCLUSION

Hence, we demonstrated the feasibility of scaffolds containing PyACC powder, which could lead to intermediate degradation rate compared to classical fillers used for bone substitution such as bioactive glasses or apatite. The subsequent release of carbonate, phosphate (by enzymatic cleavage of the pyrophosphate ions) and calcium ions is predominant as the latter ions are key components for bone regeneration. Furthermore, the high, interconnected and oriented porosity is particularly adapted for cell colonization and tunable mechanical properties allowed to improve scaffolds rigidity, the latter preventing porosity collapse during cutting by the surgeons prior implantation.

REFERENCES

1. Boccaccini, A.R., *et al.*, Composites Science and Technology, 63, 2003
2. Hutmacher, D.W., Biomaterials 21:24, 2000
3. Grover, L.M., *et al.*, Biomaterials, 34:28, 2013
4. Deville, S., Materials, 3, 2010
5. Giannoudis, P.V., Dinopoulos, H., Tsiridis, E., Injury, 36, 2005

ACKNOWLEDGMENTS

The authors would like to thank the Occitanie Region (BioPhORM project n°19008740/ALDOCT-000734) for providing financial support to this project.

3D-printed aerogel scaffolds for personalized bone tissue engineering

Iglesias-Mejuto Ana, García-González Carlos Alberto

Department of Pharmacology, Pharmacy and Pharmaceutical Technology, I+D Farma group (GI- 1645), Faculty of Pharmacy, iMATUS and Health Research Institute of Santiago de Compostela (IDIS), Universidade de Santiago de Compostela, E-15782, Santiago de Compostela, Spain.

ana.iglesias.mejuto@rai.usc.es

INTRODUCTION

Bone tissue engineering (BTE) aims to promote the full recovery of bone defects. Three-dimensional (3D) printing is a disruptive technology able to process BTE scaffolds with patient-specific shapes. Alginate inks have been widely employed in combination with hydroxyapatite (HA) to confer bioactivity to the scaffolds. Nevertheless, one of the current 3D-printing technical limitations is the lack of control in the scaffold nanostructure. For this reason, the fabrication of dual porous biomaterials with a customized external and internal morphology and composition is nowadays a remarkable challenge in tissue engineering.

EXPERIMENTAL METHODS

In the present work, nanostructured alginate-HA aerogels were obtained by the combination of extrusion-based 3D-printing and supercritical (sc) drying techniques. Firstly, hydrogel-based scaffolds were printed (BioX, Cellink) from inks of different HA ratios (0, 8, 16, 24 %(w/v)) using a grid pattern with 3 layers. An ageing step was performed before the $scCO_2$ drying (120 bar, 40 ºC, 5 g/min, 3 h). Finally, GA post-crosslinking was carried out to obtain the 3D-printed aerogels. Textural properties were assessed by N_2 adsorption/desorption analyses and SEM imaging. Moreover, biocompatibility was assessed by WST-1 tests in BALB 3T3 cells after 24 and 48 h of incubation. Hemocompatibility was also measured by hemolysis tests and bioactivity by simulated body fluid (SBF) immersion for 28 days at 37 ºC.

RESULTS AND DISCUSSION

Homogeneous and customized porous scaffolds were obtained by the technological combination proposed. 3D-gel structure and porosity were preserved in the resulting aerogels, with mesopores and macropores clearly recognized. Excellent results of bio and hemocompatibility were found for all formulations tested, confirming the lack of toxicity effect or other negative impact on cell growth (Figure 1). High apatite formation was founded in a HA-dependent manner after 28 days in contact with SBF, thus confirming the long-term bioactivity of the aerogel scaffolds (Figure 2) and their potential application in BTE.

CONCLUSION

Highly porous and customized alginate-HA scaffolds were successfully manufactured by the dual processing strategy here reported. Moreover, aerogels obtained present high bioactivity, hemo- and biocompatibility, pointing out their advanced textural and biological performance, highly desirable for personalized BTE applications.

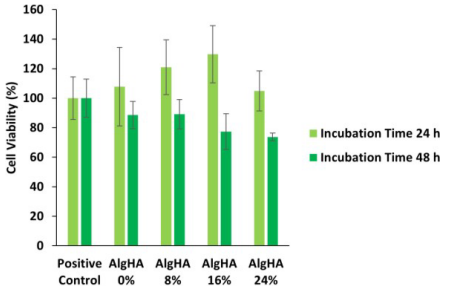

Figure 1: Biocompatibility tests of alginate-HA aerogels after culture with BALB 3T3 cells.

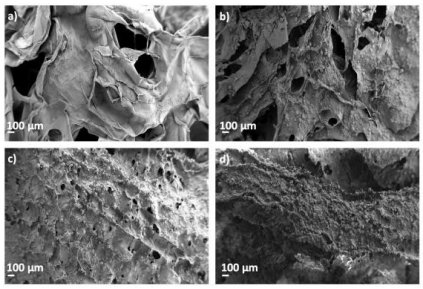

Figure 2: SEM images of alginate-HA aerogels after SBF treatment for 28 days. (a) AlgHA0%; (b) AlgHA8%; (c) AlgHA16% and (d) AlgHA24%.

REFERENCE

Iglesias-Mejuto A, García-González CA. Mater Sci Eng C.131:112525, 2021.

ACKNOWLEDGMENTS

Work supported by MICINN [PID2020-120010RB-I00], Xunta de Galicia [ED431C 2020/17], Agencia Estatal de Investigación [AEI] and FEDER funds. Work carried out in the framework of the COST Action CA18125 "Advanced Engineering and Research of aeroGels for Environment and Life Sciences" (AERoGELS), funded by the European Commission. A.I.-M. acknowledges to Consellería de Educación, Universidade e Formación Profesional (Xunta de Galicia) for her predoctoral research fellowship [ED481A-2020/104].

A 3D, Dual-layer Scaffold for Dental Pulp Repair

Ryan Chen[1], Changhui Chen[2*], Kevin Yen[3]

[1]R&D Department/Han Biomedical Inc., New Taipei City, Taiwan
[2]R&D Department/Han Biomedical Inc., New Taipei City, Taiwan
[3]Consutant/Han Biomedical Inc., New Taipei City, Taiwan
hanbio001@hanbiomedical.com

INTRODUCTION

Dental endodontic therapy consists of a series of treatments, including removing pulpal tissue, filing and shaping root canals, obturating the root canal space, and placing a permanent restoration for the tooth which is not a tissue repair treatment.[1] We design a 3D, dual-layer structured scaffold by composite materials for dental pulp repair. The dual layer structure was designed for repairing both pulp and dentin tissue. The purpose of this project was to design the mimic dual-layer structure of pulp soft tissue and dentin hard tissue.[2]

EXPERIMENTAL METHODS

To use collagen and biodegradable ceramic materials for structuring the 3D, dual-layer scaffold. The base layer was made by collagen, a random structured scaffold, which is used for pulp soft tissue repair. The upper layer was made by collagen and biodegradable ceramic materials, a microchannel structured scaffold with direction, which is designed for dentin repair. The pore size of the microchannel of dentin was designed from wide to narrow (bottom).

RESULTS AND DISCUSSION

A 3D, dual-layer microchannel scaffold structure which was composed of a composite material was made successfully, and in combination with a traditional collagen for soft tissue repair was also completed. The figure I showed the Micro-CT scan of the structure. The composite materials are including a biodegradable natural polymer, collagen, and a biodegradable ceramic material, hydroxyapatite.

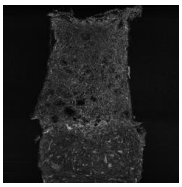

Figure I. The Micro-CT scanned structure

Moreover, the microchannel scaffold structure has at least one microchannel, and the microchannel extends from a top surface of the microchannel scaffold structure to a bottom surface of the microchannel scaffold structure and have a top opening and a bottom opening respectively on the top surface and the bottom surface, wherein the width of the microchannel decreases from the top surface of the microchannel scaffold structure toward the bottom surface of the microchannel scaffold structure to make the microchannel scaffold structure be is directional and thereby extends toward a bottom surface of the microchannel scaffold structure in a manner that the width of the microchannel decreases toward the bottom surface of the microchannel scaffold structure and extends to the bottom surface of the microchannel scaffold structure, and has an opening in the bottom surface the size of the bottom opening is smaller than the size of the top opening.

Figure 2. Microchannel Orientation

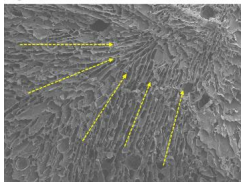

CONCLUSION

The 3D, dual layer scaffold structure made is potentially met the rationale of pulp & dentin repair. The structure of microchannel scaffold made, from narrow to wide, by composite materials could regulate the repair time of pulp soft tissue and dentin. We proposed the 3D, dual layer scaffold could be applied for pulp repair of pulp and dentin tissue. Further tests and studies are undergoing.

REFERENCES

1. S Friedman et al, CDA J, 32:493-503, 2004
2. Cristina Bucchi et al, Journal of Clinical and Experimental Medicine 10(2):2006-2015, 2017

ACKNOWLEDGMENTS

We acknowledge the R&D team members of HAN BIOMEDICAL contribution to this research project.

*

Microstructure, mechanical properties, and corrosion behavior of interpenetrating Mg-HA composite fabricated by liquid metal infiltration

Carmen H.Escalera[1*], Omar Novelo[1], MC Piña-Barba[1], F. Rodríguez-Gómez[2], I.A. Figueroa[1]

[1]Instituto de Investigaciones de Materiales, UNAM, Mexico City, Mexico
[2] Departamento de Ingeniería Metalúrgica, Facultad de Química, UNAM, Mexico City, México
[*]carmen.ele@outlook.com

INTRODUCTION

Composite material is used to develop superior properties than those of their individual components [**1**].

Design and preparation of composites based on magnesium might be an approach to control the degradation rate.

The biocomposite candidate can be designed in continuous networks to obtain a wide range of mechanical and biological properties, as well as adjustable bioabsorption rates **[2]**. The bone tissue will grow towards the fastest biodegrading network when a continuous network has different biodegradation rates. Meanwhile, the remaining networks still maintained their geometrical shape and carried their physiological load for tissue ingrowth **[3]**.

Hydroxyapatite (HA) is the most widely used reinforcement of the Mg compound due to their excellent biocompatibility, bioactivity, and osteoconduction properties with different dissolution rates, i.e., TCP has a higher dissolution rate than HA **[4]**. Another factor to consider is the low contact angle of the liquid Mg alloys with the TCP (high wettability) **[5]**.

Based on the above, this work selected Mg as the matrix material and porous natural bone apatite (natural HA) as the reinforcement to prepare a co-continuous Mg/TCP composite. Firstly, the molten Mg was infiltrated into the porous natural HA scaffold using the liquid infiltration technique to fabricate the composite. Finally, the interpenetrated composite chemical and structural characterization were performed. This work also assessed the composites' degradation rate under simulated physiological conditions.

EXPERIMENTAL METHODS

For infiltration, natural HA preform was placed in a stainless steel crucible and one metal with 1.5 times the volume of the porosity natural HA preform was located on it. The temperature was increased to 760 °C to melt the metal in a high purity argon atmosphere. The obtained Mg-natural HA composites were characterized in terms of chemical composition, microstructure, mechanical properties, and degradation rate under simulated physiological conditions using methods such as DRX, SEM, EDS, compression test, indentation test, mass loss, hydrogen evolution, and electrochemical tests.

RESULTS AND DISCUSSION

Fig.1 shows the resulting composite after the natural HA infiltration with Mg. The light gray and the dark gray phase corresponded to HA scaffold and Mg alloy, respectively. Compared with the structure of the natural HA, after the infiltration, the composite shows a compact structure, i.e., the liquid metal filled the pores producing a co-continuous composite material.

The co-continuous Mg/TCP composite formation significantly enhanced the mechanical properties, as the metallic material reinforced the ceramic scaffold. Furthermore, the high densification of the samples was corroborated by the experimental densities.

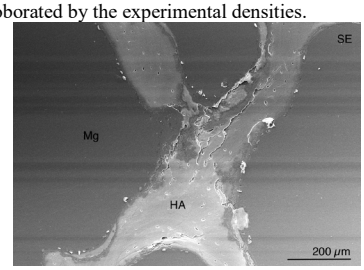

Fig.1 Microstructure of co-continuous composite Mg-HA.

CONCLUSION

The combination of a natural ceramic preform and Mg infiltration allowed on-demand fabrication of Mg-TCP interpenetrated composites. This represents a significant step forward with respect to composites reinforced either with random distributed particles or fibers. Although more research is required to control the degradation rate of the composite, this material has the potential to function as a temporal load-bearing implant for the fixation of bone fractures.

REFERENCES

1. Etemadi R. et al., *Materials and Manufacturing Processes*. 33, 1261–1290, 2018.
2. Salernitano E. et al., *Journal of Applied Biomaterials and Biomechanics*. 1, 13-8, 2003.
3. Miao X. et al., *Mater Lett*. 59(29-30):4000-4005, 2005.
4. Onoki T. et al., *Materials Science and Engineering: C*.31(2):499-502, 2011.
5. Wang X. et al., *Materials Science and Engineering: C*. 56, 386–392. 2015.

ACKNOWLEDGMENTS

"The authors would like to thank DGAPA-PAPIIT-UNAM (IN102422) for providing financial support to this project".

Bioprocessing of silk fibroin into anisotropic scaffolds for building up muscle tissue

Keutmann Sabine[1*], Rütten Stephan[2], Köpf Marius[3], Obrecht Astrid[4], Schäfer Benedikt[4], Beier Justus P.[4], Jockenhoevel Stefan[1,5], Fernández-Colino Alicia[1].

[1]Department of Biohybrid & Medical Textiles (BioTex) AME-Institute of Applied Medical Engineering Helmholtz Institute, RWTH Aachen University, 52074 Aachen, Germany
[2] Electron Microscopy Facility Uniklinik RWTH Aachen, 52074 Aachen, Germany
[3] Fibrothelium GmbH, 52068 Aachen, Germany
[4] Klinik für Plastische Chirugie, Hand- und Verbrennungschiruguie, Uniklinik RWTH Aachen, 52074 Aachen, Germany
[5] Aachen-Maastricht-Institute for Biobased Materials (AMIBM) Maastricht University, 6167 RD, Geleen, The Netherlands
[*]keutmann@ame.rwth-aachen.de

INTRODUCTION

Skeletal muscle is one of the most abundant tissues in the human body, accounting for 40%–45% of the total body[1]. In response to minor injuries, skeletal muscle can regenerate completely and spontaneously, yet muscle healing is incomplete after severe injuries. In this regard, there is a great need to develop new strategies and materials, which promote skeletal muscle repair and functional regeneration[2]. Here, we propose the development of silk fibroin scaffolds with a biomimetic anisotropic structure to guide muscle tissue growth.

EXPERIMENTAL METHODS

Silk Fibroin scaffolds were fabricated using injection molding, directed freezing and lyophilization. The porosity was analyzed by scanning electron microscopy and confocal microscopy. The mechanical properties were investigated by rheology and tensile testing. Cellular studies were carried out with human monocytic pre-macrophage cells (U937) and analyzed by ELISA and immunocytochemistry.

RESULTS AND DISCUSSION

We developed silk fibroin scaffolds with dual porosity, that consisted of: (i) aligned macro-channels of 500 µm in diameter and (ii) a controlled microporosity surrounding the channels to ensure nutrient diffusion. Mechanical characterization showed a clearly anisotropic behavior, in accordance with the engineered porosity. Specifically, failure stress in the direction of the macro-channels was three times higher than in the perpendicular direction. Preliminary studies with macrophages points to a pro-healing behavior of the developed scaffolds. Additionally, the mimicry in the architecture of the silk scaffolds and the native muscle might pave the way to the differentiation of MSC into myocytes.

CONCLUSION

We developed a bioprocessing approach to manufacture silk fibroin scaffolds with a tailored dual porosity to provide optimal micro-environmental for muscle regeneration. The silk scaffolds exhibited anisotropic mechanical performance and elicited a pro-healing cytokine release pattern form macrophage like cells in vitro. Overall, these scaffolds have great potential as a template for muscle tissue engineering.

REFERENCES

1. Liu, J. *et al.* BioMed Research International. Volume 2018, 1984879 (2018).
2. Laumonier, T., Menetrey, J. Journal of Experimental Orthopeadics 3:15 (2016).

ACKNOWLEDGMENTS

This work was supported by The Ministry of Economics, Affairs, Innovation, Digitalization, and Energy of the State of North-Rhine-Westphalia and the European Union in the framework of the European Regional Development Fund the European Regional Development Fund (ERDF).

Fabrication of Renewable and Active CO_2-derived Biocomposites by Green and Sustainable Water-based Process

Thi Nga Tran,[1,*] Michael Morris,[2,3] Maurice N Collins[1]

[1]Faculty of Science and Engineering, Bernal Institute, University of Limerick, Limerick V94 T9PX, Ireland
[2]Advanced Material and BioEngineering Research Centre (AMBER), Trinity College Dublin, The University of Dublin, Ireland
[3]School of Chemistry, Trinity College Dublin, The University of Dublin, Dublin 2, Ireland
[*]Email: thinga.tran@ul.ie

INTRODUCTION

Biocomposites made of poly(propylene carbonate) (PPC), a carbon dioxide (CO_2) derived polymer, and a renewable polysaccharide are promising materials for several applications such as biomaterials and packaging. However, most of PPC-based biocomposites exhibit low mechanical and optical properties due to the incompatibility between PPC and other polymers.[1-3] In this work, a novel biocomposite composed of PPC and chitosan was developed using a facile and sustainable water-based process. This preparation approach improves the compatibility between PPC and chitosan polymers, resulting in the biocomposites with high performance. Vitamin C was incorporated into the biocomposite as a natural and effective antioxidant resource. These biocomposites represent promising candidates for numerous applications, particularly for active sustainable biomedical devices.

EXPERIMENTAL METHODS

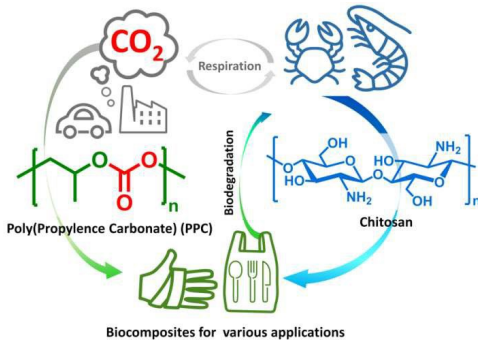

Figure 1. The development of renewable and sustainable biocomposites from CO_2-derived poly(propylene carbonate) (PPC) and chitosan natural polymer.

The CO_2-derived PPC/Chitosan biocomposites were fabricated by employing a green and sustainable water-based solvent casting process. After dissolving both polymers in common relatively benign solvents (PPC in ethyl acetate and chitosan in water), the mixtures with different proportions were homogenized by using tip sonication, followed by casting in molds and the solvent was allowed to evaporate under controlled ambient conditions. The active biocomposites incorporating Vitamin C were prepared in a similar way where Vitamin C were dissolved in aqueous solution together with chitosan.

RESULTS AND DISCUSSION

The fabrication process resulted in the formation of chitosan micron/submicron particles dispersed within the PPC matrix. In addition, the hydrogen bonding network forming between PPC and chitosan further confirmed the high missile degree of the two polymers and the success of this innovative approach. This, in turn, leads to improved mechanical performance and thermal stability of these renewable and low carbon footprint materials. Furthermore, vitamin C is incorporated and its sustained release from the biocomposites results in prolonged and effective antioxidant properties. These CO_2-based biocomposites are biodegradable in sea water forming non-toxic products.

CONCLUSION

Employing an advanced and sustainable approach, the PPC/chitosan biocomposites were successfully fabricated using a water-based casting technique. The obtained biocomposites feature high miscibility between the two polymers, improved thermal and mechanical performances, excellent antioxidant, biodegradable and biocompatible properties. The developed PPC/chitosan biocomposite represents intriguing candidates for the sustainable biomaterials.

REFERENCES

1. Tran T. N. *et al.*, ACS Appl. Mater. Interfaces 12.41: 46667-46677, 2020

2. Montagna V. *et al.*, ACS Biomater. Sci. Eng. 7.2: 472-481, 2021

3. Athanassiou A. *ed.*, Sustainable Food Packaging Technology, John Wiley & Sons, 2020

ACKNOWLEDGMENTS

"The authors would like to thank Science Foundation Ireland (SFI) (Grant Number 12/RC/2278_2) and European Regional Development Fund under the AMBER award for providing financial support to this project".

Development of Gelatin-based Scaffolds for Bone Tissue Engineering

Alessandra Soriente[1*], Alfredo Ronca[1], Maria Grazia Raucci[1], Ugo D'Amora[1], Ines Fasolino[1], Christian Demitri[2], Luigi Ambrosio[1]

[1] Institute of Polymers, Composites and Biomaterials, National Research Council, Naples, Italy
[2]Department of Engineering for Innovation, University of Salento, Lecce, Italy

[*] alessandra.soriente@cnr.it

INTRODUCTION

In bone tissue engineering, porous 3D scaffolds play a critical role in new tissue formation for their similar structure to natural bone. Indeed, the function of scaffold should be to provide a 3D spatial and temporal structure to guide cell infiltration and proliferation, leading to a new tissue. In this study, a biodegradable and biocompatible protein such as Gelatin was chosen for scaffold development[1]. The presence of chemical groups on the polymer chain allows the bio-activation of scaffolds by specific signals able to trigger the cellular behavior in terms of proliferation and osteogenic differentiation of human cells. These types of scaffold modifications provide biochemical cues for promoting stem cell osteogenic commitment. Here, two different bio-activation routes of gelatin-based scaffolds were pursued through the functionalization with organic and inorganic signals, to enhance at nanoscale level bone tissue regeneration. Then, the effect of inorganic functionalization by biomimetic approach on mechanical properties and on *in vitro* biological behavior was evaluated through proliferation and early osteogenic differentiation studies by using human mesenchymal stem cells (MSCs).

EXPERIMENTAL METHODS

Gelatin scaffolds were prepared by freeze-drying process and then bio-functionalized. In particular, type B Gelatin (bovine skin, 225 Bloom) was dissolved in deionized water (dH_2O) (5–10 wt/v%, named B5 and B10, respectively) at 40°C, rpm 100. After 30 min of stirring, the solutions were sonicated to remove air bubbles and then poured into a Teflon mold to be processed for 48 h by freeze-drying. The crosslinking of Gelatin was performed by soaking porous lyophilized scaffolds, at different time points (1, 3 and 6 h) at room temperature, in acetone-water solution (4:1v/v) containing a water-soluble EDC, followed by incubation at 4 °C for 24 h. Bio-mineralized scaffolds with bioactive solid signals on the gelatin scaffold surfaces, were obtained by using simulated body fluid solutions (5 x SBFs). Meanwhile, the organic functionalization of the scaffolds was performed by covalent immobilization of BMP-2 like-peptide. The peptide was characterized by analytical High Performance Liquid Chromatography (HPLC, Agilent) and mass spectrometry (micro-TOF; Bruker). Mechanical properties of scaffolds, before and after biomimetic treatment, were evaluated by compression tests. Furthermore, to identify the functional groups ATR-FT IR spectroscopy was implemented. The *in vitro* peptide release profile from gelatin scaffolds was studied by HPLC as reported in a previous study[2]. Cell metabolic activity was analyzed by using Alamar Blue assay. Meanwhile, the alkaline phosphatase activity (ALP) of cells seeded onto scaffolds before and after inorganic treatment and organic functionalization was determined at different days of *in vitro* cell culture.

RESULTS AND DISCUSSION

The study is based on the development and bio-functionalization of gelatin-based scaffolds by using two different approaches: inorganic and organic bioactive signals decoration. The results demonstrated that the scaffold composition and crosslinking time influenced the scaffold performances in terms of physico-chemical, morphological and mechanical behavior. Furthermore, both bioactive signals were able to improve *in vitro* biological activities at different time. In particular, biomimetic approach improved cell attachment and early osteogenic differentiation at short time, meanwhile BMP-2 peptide decoration operated *in vitro* as bioactive signal at long time, so influencing the cellular behavior in terms of early osteogenic differentiation.

CONCLUSION

The study gives the possibility to functionalize at nanoscale level polymeric scaffolds by tuning the biological response at short and long time of MSCs. Furthermore, it is possible to conclude that gelatin-based scaffolds represent a promising candidate for bone tissue regeneration.

REFERENCES

1. Raucci M. G. *et al*., Front. Bioeng. Biotechnol. 7, 27, 2019
2. Soriente A. *et al*., J. Mater. Sci. Mater. Med. 29, 62, 2018

ACKNOWLEDGMENTS

This study was supported through funds provided by Progetto PRIN 2017-SAPIENT (Prot. N. 2017CBHCWF).

Optimization of composite electrospun fibers containing sol-gel B- and Cu-doped bioactive glass particles for soft tissue engineering

Elisa Piatti[1*], Marta Miola[1], Liliana Liverani[2], Aldo R. Boccaccini[2], Enrica Verné[1]

[1]Department of Applied Science and Technology, Politecnico di Torino, Turin, Italy
[2]Institute of Biomaterials, Department of Materials Science and Engineering, University of Erlangen-Nürnberg, Erlangen, Germany
[*] elisa.piatti@polito.it

INTRODUCTION

Bioactive glasses (BGs) can bond to both hard and soft tissues and stimulate new tissue growth through the formation of a hydroxyapatite (HA) interface layer and the release of therapeutic ions[1]. According to the released ions, BGs can perform several functions, like promote osteogenesis and angiogenesis and have an antibacterial effect[1]. When they are used as fillers in polymeric matrices, it is possible to obtain composite scaffolds with enhanced bioactive and mechanical properties, which can find interesting applications in the field of tissue engineering and regenerative medicine[2]. Unfortunately, issues related to BG particle aggregation can strongly limit the performance of these composites. Indeed, BG nanoparticles (NPs) have a high tendency to aggregate during their synthesis[1]. In addition, even monodisperse particles tend to aggregate during mixing with the polymeric matrix[2]. The aim of the work was to synthetize composite fibrous scaffolds with bioactive, pro-angiogenic and antibacterial properties, optimizing our previous electrospun composite scaffolds[3], reducing the aggregation of the BG NPs and thus improving the properties of our composites.

EXPERIMENTAL METHODS

Novel composite electrospun fibers were synthetized by adding new spherical B- and Cu-doped bioactive glass nanoparticles in poly-ε(caprolactone) (PCL) fibers. These new BG particles were characterized by an innovative composition (62%SiO_2-9%P_2O_5-9%CaO-5%CuO-15%B_2O_3, wt%) that we developed in our previous works[1], but they were synthetized following a novel synthesis route, based on the optimization of our previous acid/base co-catalized synthesis. The main goal of this synthesis optimization was to reduce the particles aggregation and enhance the spherical shape of the particles. The so-obtained glass particles were then suspended in a solution of PCL and acetic acid (AA), which was electrospun in order to produce composite fibers containing spherical BG particles. Solution parameters (such as glass concentration and mixing method) and process parameters (like applied voltage, working distance and flow rate) were carefully optimized and adapted to the new glass-PCL system, in order to optimize the incorporation and dispersion of the BG particles inside the PCL matrix. The characterization of the composites was performed using scanning electron microscopy equipped with energy dispersive spectroscopy device, Fourier transform infrared spectroscopy, wettability measurements, uniaxial tensile mechanical tests, acellular bioactivity test and biological assays.

RESULTS AND DISCUSSION

Because of their spherical shape and dispersion, the optimized BG particles were selected as fillers for novel fibrous composites.

The synthetized composite fibers showed a good incorporation of the BG particles, which were able to confer bioactive properties to the PCL matrix, since the first day of immersion. In Figure 1 the crystals of HA present in the composites at the end of the acellular bioactivity test are shown. In addition, the composites were characterized by promising hydrophilic properties and good mechanical performance. Finally, results of biological assays showed that the synthetized composite fibers were biocompatible and allowed the proliferation of bone murine stromal cells (ST-2 cell line).

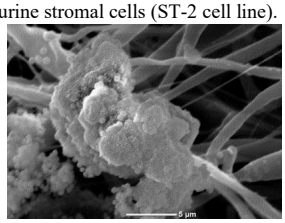

Figure 1: SEM micrograph of composite fibers after 14 days of immersion in SBF

CONCLUSION

We managed to optimize our previously synthetized composite fibers, enhancing the bioactivity, wettability and mechanical properties of our composites. Thanks to their improved properties, these composites are considered very promising for TE applications, in particular for soft TE because of the angiogenic and antibacterial properties of the doping ions (boron and copper) contained inside the used glass fillers.

REFERENCES

1. Piatti E. *et al.*, Cer Int., In press
2. Moura et al., Mater. Sci. Eng. C, 224-232, 2017
3. Piatti E. *et al.*, ESB2021 Abstr. B., 1584-1585, 2021

Biocompatibility of PHB/CHIT Scaffold as a Promising Biopolymer in Treatment of Osteochondral Defects

Eva Petrovova[1*], Zuzana Demcisakova[1], Zuzana Tirpakova[2], Katarina Holovska[1], Lenka Luptakova[2]

[1]Department of Morphological Disciplines, University of Veterinary Medicine and Pharmacy, Kosice, Slovakia
[2]Department of Biology and Physiology, University of Veterinary Medicine and Pharmacy, Kosice, Slovakia
[*] eva.petrovova@uvlf.sk

INTRODUCTION

Chitosan has many attractive properties including biocompatibility, biodegradability, non-toxicity, remarkable affinity to proteins, bacterial resistance, and haemostaticity, and is suitable for applications in tissue engineering promoting the healing process of soft and hard connective tissues[1]. For biocompatibility testing of various biomaterials, the avian embryo, and especially its chorioallantoic membrane (CAM) provides a simple and effective alternative model for assessing the biocompatibility of the new bone potential implants. Avian embryo development takes place outside the mother`s body, obviating the need to sacrifice experimental animals or cause physical harm as is the case in implantation surgery. Further advantage is that avian embryo as an experimental model is exempted from the horizontal legislation on the protection of animals used for scientific purposes (2010/63/EU), as well as applicable laws in the United States[2]. The aim of this work is to describe and implement an in vivo method to predict material biocompatbility.

EXPERIMENTAL METHODS

Fertilized chicken hybrid eggs (Ross 308; N=120) were purchased from the farm Parovske Haje (Nitra, Slovakia). The eggs were incubated horizontally at 37.5°C and 60% relative humidity until embryonic day (ED) 3 of incubation period. At ED3 the chick embryos were transferred into a plastic weighing boats, and incubated. Differences in the angiogenic response of CAM was observed depending on the addition of vascular growth factor (VEGF-A), saline solution (PHY) and FGF-2 inhibitor (SU5402). On ED7, tested sterilized porous acellular polyhydroxybutyrate/chitosan implant (2x2x1 mm) was placed on the CAM alone/or soaked with VEGF-A (25 ng), PHY, and FGF-2 inhibitor (5 mM.) For evaluation and observation the blood vessels into/outside the scaffold on ED10, we used the histological, IHC, and molecular analysis. GraphPad Prism 9.0 (one-way ANOVA and Tukey´s multiple comparisons test and paired t test) software was used to perform all of the statistical analyses. Values of $P < 0.05$ were considered statistically significant.

RESULTS AND DISCUSSION

The morphological and histochemical analysis showed the highest angiogenic potential in untreated scaffold (77.51±3.31%) compared to soaked scaffolds with pro-angiogenic factor (VEGF-A – 74.70±4.06%) and saline (51.24±8.04%). The weakest angiogenic potential was observed in scaffolds soaked with FGF-2 inhibitor (19.69±6.83%). The morphometric analysis showed that the number of vessels in surrounding area of the scaffold was significantly higher in untreated scaffold (42.72±7.18) compared to scaffolds soaked with VEGF-A (31.44±5.07), PHY (33.22±1.11) and FGF-2 inhibitor (13.28±0.89). The most represented group of vessels was up to 50 µm. Thickness of the ectoderm was significantly lower in the scaffold soaked in SU5402 (9.91±4.33 µm) compared to untreated scaffold (14.62±7.49 µm). The thickness of mesoderm in scaffold soaked with VEGF-A (154.96±72.11 µm) was significantly higher and thickness of the SU5402 (74.33±20.61 µm) significantly lower compared to untreated scaffold (120.22±52.81 µm). Gene expression of pro- and anti-angiogenic markers followed similar results. VEGF-A promotes angiogenesis extensively in untreated scaffolds. FGF-2 anti-angiogenic inhibitor partly weakened the angiogenesis in both untreated and treated scaffolds (VEGF-A). The response of CAM to implanted biomaterial is similar to the mammalian animal model[3]. At the same time, it allows continuous monitoring of the biomaterial tested, which makes this method very attractive for rapid in ovo/ex ovo angiogenesis evaluation of the tested biomaterial. This animal model can be employed to rank a broad range of materials and to select the safest possible materials to be used in animal studies in the field of regenerative medicine.

CONCLUSION

Acellular polyhydroxybutyrate/chitosan designed for osteochondral regeneration was tested for the first time with short-term CAM assay. In this study, the methods were focused on monitoring of angiogenesis and biocompatibility inside of the scaffold, which brings more complex information for the qualitative assessment of the tested biomaterial. The methods allow observation of the surrounding CAM tissue reaction, presence of cells in the pores of the scaffold, and the comparison of vessels growing toward the implant with their actual presence inside it. This study confirmed that CAM assay is a rapid, cost-effective and simple method to biocompatibility testing of new scaffolds before their using on larger experimental animals with respect to the 3R´s.

REFERENCES

1. Oryan, A. *et al*., Int J Biol Macromol. 104:1003-1011, 2017
2. Petrovova, E. *et al*., ALTEX, 36:121-130, 2019
3. Magnaudeix, A. *et al*., Acta Biomater. 38:179-189, 2016

ACKNOWLEDGMENTS

This work was supported by the Slovak Research and Development Agency under the Contract no. APVV-20-0073 and project VEGA 1-0050/19".

Characterization of bio-functionalized 316L stainless steel substrates and in vitro study of their early stage influence on osteoblasts behavior

Keerthana Balathandayutham [1], Olivier Gallet[1], Séverine Alfonsi[2], Mathilde Hindié[1*]

[1]Laboratoire ERRMECe, CY Cergy-Paris Université, France
[2]Laboratoire LPPI, CY Cergy-Paris Université, France

mathilde.hindie@cyu.fr

INTRODUCTION

Implantation of metallic orthopedic prostheses is increasingly common due to the aging of the population and accidents of life. In France alone, orthopaedic prostheses represent an estimated market of 500 million € that continues to grow. But for a part of the world's population, the access to technically developed prostheses is limited due to expensive care and lack of social support. Thus, there is a real societal need to implement new metal implants that combine durability, good mechanical properties, excellent biocompatibility as well as affordable cost to ensure universal access to medicines and medical devices.

The functionalization of low-cost 316L stainless-steel substrates by successive electrodeposition of a polypyrrole film (PPy) and a calcium phosphate deposit doped with silicon was previously carried out at the LPPI and ERRMECe labs[1]. We are now developing a biomimetic-functionalization of our PPycoated steel supports by electrodeposition of fibronectin (Fn), a matrix protein involved in adhesion and cellular differentiation. Effects of different modes of electrodeposition or electro-oxidation on the structure and functionality of Fn is studied and validated by cell behaviour.

EXPERIMENTAL METHODS

First electropolymerisation of pyrrole is performed onto steel supports to obtain a primary layer of PPy by cyclic voltammetry. This PPy coating allows passivation of the surface of the steel support and maintain it electrical conductivity. The structure of our PPy coatings is characterized by physico-chemical methods such as profilometry, wettability measures, and Fourier-transform infrared spectroscopy (FTIR). Then Fn is weather adsorbed (ADS), adsorbed and oxidized (OX) or electrodeposited (ED) on PPy coated support. Fn present on our supports is quantified and characterized by enzyme-linked immunosorbent assay (ELISA). Fn organization onto supports is analyzed by confocal microscopy. Early stage behavior of osteoblastic cells (STRO-1A+) cultured on Fn functionalized supports is also studied.

RESULTS AND DISCUSSION

A homogenous film of PPy is obtained on our support with a thickness of 4.2µm and a low rugosity (0.8µm). The kinetic of Fn adsorption on support is performed, 10 min is the time necessary to reach the plateau. Fn adsorption isotherm was also study. 10µg/mL appears to be the optimal Fn concentration for our experimentation. Quantification of Fn ADS, OX or ED is performed by ELISA tests. The most Fn quantity was detected after electrodeposition. However, the Fn cell binding domain (CBD) is more accessible on ADS Fn compared to other supports.
Those results are consistent with the organisation of Fn observed by confocal microscopy. Ox Fn formed little sticks whereas ED Fn formed long fibre organized like a fractal. At the contrary ADS Fn forms a homogenous coating.
Osteoblasts cultured for 3h on each support adhere and spread. The most spread cells are observed on ADS Fn which is in accordance with CBD ELISA.
Cell viability was also tested after 3h of culture and no significant toxicity is detected.

CONCLUSION

Our results demonstrated that electrodeposition permits the higher Fn deposition than a simple adsorption. This technic is fast and can be performed on conductive implant whatever its structure is. Furthermore Fn electrodeposited is not toxic for cells and influences their adhesion and morphology.

REFERENCES

1. Hamdaoui S. *et al.*, Colloid and Interface Science Communications. 2020, 37

ACKNOWLEDGMENTS

The authors would like to thank the I-Mat Fédération Programme for funding a master student fellowship.

Exploiting the diagnostic potential of disorder: novel nanostructured platform for rapid, label-free and low-cost analysis of genomic DNA

Valentina Mussi[1], *Mario* Ledda[2], *Luca* Maiolo[1], *Antonella* Lisi[2], *Antonio* Sciortino[1]*, *Emilio Nicola Maria* Cirillo[3], *Claudio* Durastanti[3], *Annalisa* Convertino[1]

[1]Institute for Microelectronics and Microsystems, CNR, 00133 Rome, Italy
[2]Institute of Translational Pharmacology, CNR, 00133 Rome, Italy
[3]Department of Basic and Applied Sciences for Engineering, Sapienza University, 00161 Rome, Italy
*Presenting Author, Antonio.Sciortino@artov.imm.cnr.it

INTRODUCTION AND PURPOSE

DNA is the key of life, therefore the key of biological and biomedical research, basic and applied eitherly. To date, for cancer diagnoses, chromosomal aberrations, genetic and epigenetic mutations/modifications, microsatellite instability are sought, with the efforts that researching chemical and biochemical modifications requires. Here we propose a novel diagnostic approach based on the exploitation of a disordered array of silver coated silicon nanowires, Ag/SiNWs, to interrogate DNA samples isolated from different cell targets by means of Raman mapping [1, 2]. Our results demonstrate the possibility to develop a novel diagnostic platform for reliable, quick and label-free analysis of genomic DNA in oncology.

EXPERIMENTAL METHODS

I. Fabrication of Ag/SiNWs substrate and cell culture

Plasma enhanced chemical vapor deposition was used to grow *Au-catalyzed* SiNWs on *Si* wafers. *Ag* coating of the nanowires was obtained by evaporation.

Human osteosarcoma cell line *SAOS* was used as cancer model and compared to human immortalized keratinocyte cell line, *HaCaT*, which was chosen as health control model. After standard culture, harvesting and centrifugation, cell pellets were used for genomic DNA extraction. Final samples are prepared dropping 5µl of the DNA solution (20 ng/µl) on the Ag/SiNWs substrate.

II. Raman and statistical analysis

Each droplet, once dried off in air, is spectrally mapped by using a Thermo Fisher DXR2xi Raman Imaging Microscope equipped with a 532 nm laser source and a 50x objective. Principal Component Analysis (PCA) of the spectra composing the Raman maps was performed.

RESULTS AND DISCUSSION

Raman spectroscopy is a powerful method to investigate biological systems, providing a completely label-free, highly specific molecular fingerprint of the samples. **Fig.1** shows the Raman maps obtained on the drops containing the DNA extracted from the two cell lines, top images, and the results of the PCA analysis performed on the spectra composing the maps, bottom graph. The resulting plotted PC scores demonstrate the possibility to distinguish between healthy (black) and tumor (red) spectral data mainly along the PC1 component.

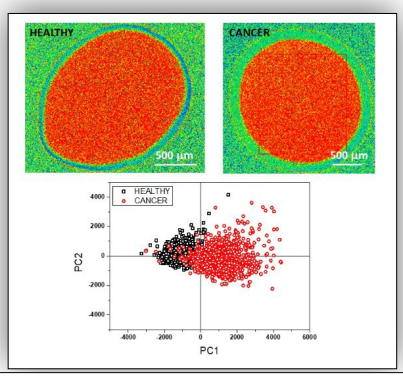

Fig. 1. Top images, Raman maps of the drops deposited on the AgSiNWs corresponding to healthy (left) and cancer (right) DNA. The graph below represents the scatter plot resulting from PCA analysis.

CONCLUSION

Our diagnostic technique leverages the unique capability of a disordered silver-coated silicon nanowires-array to interact with biomolecules and label-free Raman spectroscopy. The Ag/SiNWs, along with the Raman signal enhancement, allows to distinguish healthy and cancer cell genomic DNA without analyzing its complex composition and sequencing. The discrimination is due to a diverse accommodation the molecules onto NWs, upon dehydration of aqueous DNA droplets directly deposited over the nanostructured surface. The diagnostic information can be obtained in an easy and fast way by analyzing the label-free Raman maps of the dried DNA drops with PCA.

REFERENCES

1. A. Convertino, V. Mussi & L. Maiolo, Scientific Reports 6:25099 (2016)
2. V. Mussi, M. Ledda, D. Polese, L. Maiolo, D. Paria, I. Barman, M.G. Lolli, A. Lisi, A. Convertino. Mater. Sci. Eng. C 122, 111951 (2021)

ACKNOWLEDGMENTS

The research activity is funded by Regione Lazio within the project DIANA, "DIAgnostic potential of disorder: development of an innovative NAnostructured platform for rapid, label-free and low-cost analysis of genomic DNA", Progetti Gruppi di ricerca 2020, by the Italian Minister of Foreign Affairs and International Collaboration under the Joint research project “Scalable nanoplasmonic platform for differentiation and drug response monitoring of organtropic metastatic cancer cells” (US19GR07) within the Scientific and Collaboration Program Italy-USA/2019-2021”.

Wound Healing through Therapeutic Layer-by-layer Skin Coatings

Elias Hasan[(1)], Piergiorgio Gentile[(1)], and Ana M. Ferreira[(1)]

[1]*Faculty of Science, Agriculture & Engineering, Newcastle University, Newcastle upon Tyne, UK.*

E-mail: e.a.h.h.hasan2@newcastle.ac.uk, Piergiorgio.gentile@ncl.ac.uk, and ana.ferreira-duarte@ncl.ac.uk

INTRODUCTION

Skin trauma injuries like burns are unpredictable elements within battlespace and humanitarian operations. Globally, most of morbidity and mortality cases associated with burns are seen in developing countries because of conflicts and natural disasters [1]. While small burns may just render individual combat ineffective until healed, larger burns may represent a more significant challenge as early surgical intervention and regular wound management that can rapidly deplete surgical capabilities. In general, wound healing management is both time consuming and costly, as practice nurses time is very limited; and time pressures leads to suboptimal management of wound care. Therefore, there is a need for improved deployed healthcare assets towards facilitating interventions and resources in these environments for overcoming geographical restrictions, lacked expertise in wound management and/or time-consuming treatment visits. The therapeutic Layer-by-layer (LbL) skin coating method addresses the given limitations by providing a quick, easy, and cost-effective wound healing process that facilitate the point-of-care of skin wounds in different settings for "re-distributed" care pathways closer to the patient. The study aims to investigate the effectiveness of Skin-LbL techniques on wound healing process (WHP).

EXPERIMENTAL METHODS

Human skin structure including epidermal, and dermal layers were used for the experiment. The experiment was conducted through mimicking the human skin by burning the skin-layers. After that, a therapeutic Layer-by-Layer coating was applied to create multi-layers to integrate with the stimulated skin. The experiment has been observed in weekly basis to evaluate the effectiveness of the skin coating.

RESULTS AND DISCUSSION

The wound revealed potential improvement in WHP as the interaction of the skin-LbL with the natural polyelectrolyte and anti-microbial agents reported successful findings. The skin was able to reach proliferation phase in a short time. There were signs of restored structural and functional properties of human skin. The methodology presents a promising advancement for the accelerating wound healing process to ensure the possibility of treating wounds without relying on stem cells while ensuring a non-toxic and non-allergic treatment. At the same time, the recovery shows more accelerated results passing the proliferation phase; yet, it has been noted that there is a gap in the skin wound healing process that relies on natural polyelectrolytes.

CONCLUSION

Above all, the use of LbL techniques for skin coating illustrated significant findings in treating wounds. The use of skin-LbL presented more interaction and better responses within the wounded area by decreasing the healing time. Although the effectiveness of LbL self-assembly has been proven in treating wound injures, there are limited studies available that used LbL self-assembly towards wound skin healing.

REFERENCES

1. Sandhu, A., J. Herron, and N. Martin, *Burns management in the military and humanitarian setting.* BMJ Mil Health, 2020.

ACKNOWLEDGMENTS

The author acknowledges the financial support from Newcastle University Overseas Research Scholarship and give special thanks and gratitude to the EPSRC Redistributed Manufacturing in Deploying Medical Care, the fund assisted the project.

3D polysaccharides-based hydrogel fabrication methods to guide cell behaviour.

Albane Carré[a]*, Maria-Dimitria Chiotelli[a], Teresa Simon-Yarza[a]
[a] INSERM U1148, LVTS, Université de Paris, X Bichât Hôpital, 46 rue H Huchard, F-75018 Paris, France
* albane.carre@inserm.fr;

INTRODUCTION

In the last decade 3D hydrogels became a common cell culture support[1] able to mimic complex tissue structure and to induce different cell behavior. With the aim to produce different cell conformations, such as cell sheet or spheroids[2], various fabrication methods have been used to control cell fate key parameters (physico-chemical properties, porosity, stiffness, biochemical cue[3]). In this work, we show how to induce different fibroblast cells behavior cultured on 3D polysaccharides-based hydrogel using different protein incorporation methods. Interestingly, by keeping the composition of the hydrogels, modification in the fabrication method guides cell behavior, driving either cell self-assembly into spheroids or cell adhesion.

EXPERIMENTAL METHODS

Hydrogel fabrication 3D porous hydrogels were obtained as previously described[4]. Briefly, PUDNA hydrogels were obtained by mixing dextran and pullulan polysaccharides and chemically cross-link them with STMP. Single freeze-dried (PUDNA-SFD-Gel) hydrogel incorporated 5% gelatin (type B) in the polysaccharides mix before cross-linking. All hydrogels underwent a first freeze-drying step to tune the porosity. Then, only double freeze-dried (PUDNA-DFD-Gel) hydrogels were rehydrated in a gelatin solution (1 mg/mL w/v) and successively washed prior to a second freeze-drying step to create a thin physical coating of protein on the pores. Collagen-coated (1mg/mL) (PUDNA-DFD-Coll) hydrogels were prepared in a similar way and used as a positive control of cell adhesion. For confocal microscopy observations, 1% FITC-labeled dextran was added to the polymer solution before crosslinking.

Hydrogel characterization Porosity, swelling ratios, water content and enzymatic degradation rate were evaluated as per standard protocols[5]. Young Modulus has been evaluated in bulk.

Hydrogel cellularization 3T3 Balb/c A31 fibroblasts (passage 9 to 18) were vacuum seeded at high concentration in the SFD and DFD hydrogels and cultured in complete DMEM medium up to 14 days.

Cell metabolic activity Assay Metabolic activity was quantified using the In Vitro Toxicology Assay Kit (resazurin based assay) at different time points. Fluorescence of the resulting supernatant was measured using a TECAN® plate reader (560Ex/590Em).

Cell morphology and behavior analysis Cellularized scaffolds were stained with Phalloidin-TRITC and DAPI. Cell morphology and distribution have been observed with Zeiss confocal microscope fitted with a 10× objective (CRI—U1149 Imaging facility) over up to 300 µm in the scaffold depth. Images were reconstructed using FIJI software.

RESULTS AND DISCUSSION

PUDNA, PUDNA-SFD-Gel, PUDNA-DFD-Gel and PUDNA DFD-Coll hydrogels were characterized as per standard protocols to have very similar properties, all corresponding to previously published data.

When cultured in PUDNA-SDF-Gel, cell metabolic activity decreased over time, whereas metabolic activity of cells cultured in PUDNA-DFD-Gel and PUDNA DFD-Coll hydrogels was more stable, increasing from day 3 to day 14 (fig A).

Confocal microscopy observations revealed very different cell behaviours, depending on the way of protein addition. When cultured in PUDNA-SDF-Gel hydrogels with incorporated gelatine, cells tend to keep a very round shape, forming aggregates, floating in the pores without attaching. Unlike depicted by the metabolic activity, cell proliferation was observed. In PUDNA-DFD-Gel and PUDNA DFD-Coll hydrogels, cells attached and spread to form a layer on the surface of the pores after 15 days (fig B). Cell proliferation and homogeneous covering of the pores were observed.

CONCLUSION

The aim of this work was to show how by keeping the same biochemical components of hydrogels, we can induce very different cell behaviors by changing the protein incorporation method. This can be explained by the different presentation of adhesive motives to the cells. Indeed, when the proteins are added to the polysaccharides they react with the cross-linker whereas when added after cross-linking and freeze-drying they are deposited on the surface of the pores. In the first case, the proteins remain entrapped within the hydrogel matrix. With the second method, the molecules of the proteins remain free and this could facilitate the interaction with the cells, promoting their adhesion, migration and proliferation within the pores. These results invite us to explore new fabrication methods using simple well-known materials.

REFERENCES

[1] Caliari, S. *et al.,* Nat Methods 13, 405–414 (2016)
[2] Efremov Y.M. *et al*., Biophys Rev 13, 541–561 (2021)
[3] Nicolas J., *et al.,* Biomac. 21 (6), 1968-1994 (2020)
[4] Labour MN *et al.,* Int. J. Mol. Sci. 21, 3644, (2020)
[5] Dellaquila A. *et al.,* Adv. Sci. 2100798 (2021)

ACKNOWLEDGMENTS

The authors would like to thank the French Research Agency ANR (Grant no: ANR-20-CE18-001 EXCALYBUR) for providing financial support to this project and Université Paris-Cité (Idex Emergences POLCA).

Figure: **A** Analysis of 3T3Balb/c 31 fibroblasts metabolic activity over 15days cultured on PUDNA-SFD-Gel, PUDNA-DFD-Gel and PUDNA-DFD-Coll. **B** 3T3 Balb/c fibroblasts cell morphology after 15 days of culture within the PUDNA-SFD-Gel, PUDNA-DFD-Gel and PUDNA-DFD-Coll. Hydrogels are visible due to the addition of 1% FITC-Dextran to the formulation. Cells are stained with DAPI and Phalloidin-TRITC. Scale bar: 200µm.

Degradable bioadhesives based on PEG-PLA star-shaped hydrogels for soft tissue applications

Mathilde Grosjean[1*], Edouard Girard[2,3,4], Grégory Chagnon[2], Xavier Garric[1], Benjamin Nottelet[1]

[1]Department of Polymers for Health and Biomaterials, IBMM, University of Montpellier, Montpellier, France
[2]TIMC-IMAG, Grenoble INP, Université Grenoble Alpes, CNRS, CHU Grenoble Alpes, Grenoble, France
[3]Département de chirurgie digestive et de l'urgence, CHU Grenoble-Alpes, Grenoble, France
[4]LADAF, UFR de médecine de Grenoble, Université Grenoble Alpes, Grenoble, France
[*] mathilde.grosjean@umontpellier.fr

INTRODUCTION

Polymeric tissue adhesives are interesting materials for wound treatment as these systems present various advantages compared to traditional methods of wound closure, such as suturing and stapling. For instance, they can be applied easier and faster. However, their use stays restricted because of several limitations, such as weak adhesion or poor mechanical properties[1]. Nowadays, they are two main categories of commercial bioadhesives: fibrin glues that exhibit weak adhesion properties and cyanoacrylates, which displayed high adhesion strength but stay limited to skin application because of their toxicity and lack of degradability[2]. To overcome these issues, other systems have been developed, mostly based on modified poly(ethylene glycol) and polyesters. However, it remains difficult to find a compromise between appropriate hydrophilicity and good mechanical properties. In this work, our objective is to combine the swelling abilities of PEG with the strong mechanical properties of PLA to design different new biodegradable and bioadhesive formulations. To this aim, a degradable 8-arm star-shaped PEG-*b*-PLA copolymer was prepared and functionalized with either acrylic, methacrylic or catechol groups. Catechol was chosen as it is well known for its adhesion abilities[3], whereas acrylic and methacrylic groups were used to yield photo-curable degradable bioadhesive gels with a range of adhesive properties that were evaluated *in vitro* and *ex vivo*.

EXPERIMENTAL METHODS

1. Preparation of hydrogels

Copolymers were synthesized by ROP before being functionalized either with acrylate, methacrylate or catechol groups. Hydrogels were obtained by mixing defined amounts of polymers with water.

2. Adhesion properties

Adhesive strength was assessed by lap shear test using gelatin coated glass slides or fresh cadaveric tissues. The photo-curable systems were then irradiated under UV light for 5 minutes. The adhesive properties were tested on an Instron 3344 testing machine equipped with a 500 N load cell at a rate of 15 mm.min^{-1}.

RESULTS AND DISCUSSION

The influence of the concentration on the gel formation and on the adhesion properties was investigated. (Meth)acrylate preparations formed gels after UV-light irradiation at concentrations of 5, 10, 15 and 20% whereas for catechol, gels were only obtained at 10, 15 and 20%. The adhesive ability of the different hydrogels was then evaluated. Gelatin was chosen as model substrate to simulate living tissues. Whatever the functionalization, the gels at 10% always displayed the best results (Figure 1). Therefore, this concentration appeared to be the best compromise between the quantity of polymer, which creates a strong network thanks to its reactive moieties, and water that enables the interpenetration in the tissue. Photo-curable systems yielded adhesion performances similar to cyanoacrylate systems, whereas the catechol-based bioadhesives were close to fibrin. This was expected, since (meth)acrylate systems are chemically close to cyanoacrylate and catechol known for weaker adhesive properties. Finally, acrylate hydrogels displayed stronger adhesive strength than methacrylate gels. This can be explained by the higher reactivity of acrylate, which led to higher crosslinked networks.

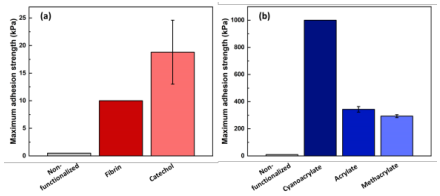

Figure 1. Adhesive strength of the (a) catechol and (b) meth(acrylate) gels at 10%

CONCLUSION

In this work, we designed two types of tissue adhesive systems thanks to acrylate, methacrylate and catechol functionalized star-shaped PEG-PLA copolymers. All the hydrogels exhibited adhesion properties when tested on gelatin. As expected, preparations based on acrylic and methacrylic moieties displayed strong adhesive properties that could be competed with cyanoacrylates after optimization, whereas the catechol ones were closer to fibrin glues. Therefore, we demonstrated that our strategy is an interesting approach to prepare degradable adhesive polymeric systems. Moreover, by playing on the type of functionalization, the adhesion properties can be tuned and adapted to various applications.

REFERENCES

1. Nam S. *et al.*, Chem. Rev. 121:11336-11384, 2021
2. Bouten P. *et al.*, Prog. Polym. Sci. 39:1375-1405, 2014
3. Faure E. *et al.*, Prog. Polym. Sci. 38: 236-270, 2013

ACKNOWLEDGMENTS

This work was supported by ANR2019-OPENN (ANR-19-CE19-0022-02) and Institut Carnot Balard Cirimat (Corol).

Surface functionalization of ZrO_2 ceramic substrate through biomimetic coatings containing drug-loaded nanoparticles to prevent implant-related infection

Iwona Pudełko[1*], Gaëlle Desante[2], Elżbieta Pamuła[1], Karolina Schickle[2], Małgorzata Krok-Borkowicz[1]

[1]AGH University of Science and Technology, Department of Biomaterials and Composites, Kraków, Poland
[2]RWTH Aachen University, Department of Ceramics and Refractory Materials, Aachen, Germany
[*] ipudelko@agh.edu.pl

INTRODUCTION

Implant-related infections are a complicated problem that can lead to serious consequences, such as joint deformation and even systemic inflammation[1]. Their conventional treatment may be inefficient due to bacterial biofilm formation that is one of the main causes of implant failure. The biofilm may be an obstacle that inhibits the diffusion of antibiotics. Multifunctional implants that allow controlled drug delivery are considered better solutions compared to conventional systemic drug delivery[2].

Bacterial attachment to an implant surface depends on material features such as surface energy and roughness[3]. Coating the surface of implant material with a calcium-phosphate (CaP) layer is one of the modification methods that results in a bioactivity improvement[2]. The use of coatings with the ability to release drugs reduced implant-related infections in both short and long terms. Furthermore, it was reported that the bone formation around antibiotic-containing implants may be improved compared to control implants[1].

The aim of this study was to: i) coat the zirconium oxide (ZrO_2) substrate with a CaP bioactive layer, ii) immobilize antibiotic-loaded polymer nanoparticles in the coating, and iii) examine the cytocompatibility of the system with human mesenchymal stem cells (hMSC).

EXPERIMENTAL METHODS

The ZrO_2 substrates were manufactured by pressing and sintering followed by polishing and phosphoric acid treatment. To obtain CaP bioactive layers, the two-step biomimetic co-precipitation method was used. To do so, ceramic samples were incubated in ten times concentrated simulated body fluid (SBF) for 48 h. Poly(L-lactide-co-glicolide) (PLGA) nanoparticles loaded with gentamicin and bacitracin (NPs) were obtained using the double emulsification/solvent evaporation method. NPs were immobilized on the surface of the substrate using (I) the drop casting method, or (II) incorporating them into the SBF solution. The size and zeta potential of NPs were measured using dynamic light scattering (DLS). To characterize microstructure, the samples were observed by scanning electron microscopy (SEM). In vitro tests with hMSC were performed for up to 14 days. Proliferation and mineralization were tested by LDH and ALP activity, respectively, while cell viability by live/dead staining.

RESULTS AND DISCUSSION

The DLS results proved that the prepared NPs are round in shape and nanometric in size. SEM pictures showed that the biomimetic co-precipitation method is an effective way to coat ceramic substrates. CaP crystals obtained in the first step (Fig. 1 A) transformed during the second one into more flake-like (Fig. 1 B) and resemble the calcium deficient hydroxyapatite crystals. That explains why the two-step process is needed.

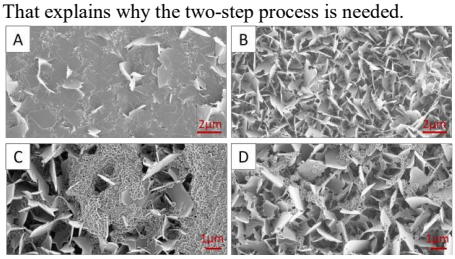

Fig. 1. SEM pictures of CaP coating after the first (A) and second (B) step of co-precipitation with NPs immobilized using the drop-casting method (C) or by incorporating them into the SBF (D).

Both methods of immobilization of NPs were proved to be effective. The drop-casting method (Fig. 1 C) allows immobilizing a higher number of NPs while incorporating them into the SBF solution (Fig. 1 D) results in a more homogeneous distribution of NPs. HMSC cells proliferated well on all surfaces. Mineralization was also at a high level, and the cells were well spread and polygonal in shape.

CONCLUSION

The presented method of coating ceramic substrates with bioactive layers containing antibiotic-loaded NPs is an efficient technique to create systems that are characterized by better bioactivity and the ability to drug release.

REFERENCES

1. Alenezi A. *et al.*, Jpn Dent Sci Rev.56(1):177-183, 2020
2. Noothongkaew S. *et al.*, Ceram Int. 47(23):33775-33787, 2021
3. Siddiqui D. *et al.,* Dent Mater. 38(2):384-396, 2022

ACKNOWLEDGMENTS

The study was supported by the Program ”Excellence Initiative – Research University” and by the subsidy of the Ministry of Education and Science for the AGH University of Science and Technology (project No. 16.16.160.557).

Multi-Metal Ions Integrated in PEM-Collagen Network for Sustained Release and Improved Osteogenesis, Angiogenesis Effects

Lu Fan[1], Alexander Rudt[2], Ole Jung[3], Mike Barbeck[3], Rumen Krastev[1, 2], Xin Xiong[1*]

[1]NMI Natural and Medical Sciences Institute, University of Tübingen, Reutlingen, Germany
[2]Faculty of applied chemistry, Reutlingen University, Reutlingen, Germany
[3]University Medical center Rostock, Rostock, Germany
[*] lu.fan@nmi.de

INTRODUCTION

Calcium, copper and magnesium have been reported to be able to stimulate osteogenesis and vascularization, which are critical for bone regeneration in tissue engineering[1,2]. However, the efficient loading and sustained release of multiple metal ions in bone tissue microenvironment is still a significant challenge.

In this study, $CaCO_3$ crystals with high loading capability are applied as sacrificial templates doped with copper and magnesium. The polyelectrolyte multilayer and collagen network were deposited on the carbonate particles to enable sustained release of multiple metal ions.

EXPERIMENTAL METHODS

- CaMgCu-CO_3 were prepared by co-precipitation.
- PEM-Encapsulation: a preselected PEM system and collagen fiber was deposited on the Carbonates particles and the encapsulated particles were freeze-dried and stored at ambient condition before further usage. Collagen fibers were isolated from split porcine dermis via mechanical homogenization.
- Characterization: the coating process of PEM and collagen were monitored with QCM and zeta-potential. The obtained microcapsules were visualized with SEM and flu-microscope. The release kinetics of multi-metal ions were recorded by ICP-OES over 60 days.
- Functional characterization: biocompatibility assay, alkaline phosphatase activity test, relative gene expressions of angiogenic markers and mineralization staining were performed.

RESULTS AND DISCUSSION

In this study, CaCuMg/PEM/Collagen microcapsules showed improved stability and controlled release of Ca^{2+}, Cu^{2+} and Mg^{2+} for over 60 days. Functional characterizations showed the improved biocompatibility and positive influences on osteogenesis and angiogenesis if compared with collagen matrix without ions.

CONCLUSION

The functionalized particles showed improved osteogenic and angiogenic effects and showing high potential for further applications in bone tissue engineering.

REFERENCES

References must be numbered. Keep the same style.
1. Lin W. *et al*., ACS Appl. Mater. Interfaces 2017, 9, 24484.
2. Chu-Chih H. *et al*., Acta Biomaterialia 2019, 98, 246–255.

ACKNOWLEDGMENTS

This work received financial support from the Federal Ministry of Education and Research (Germany) FKZ: 13GW0400C and the State Ministry of Baden-Württemberg for Economic Affairs, Labour and Tourism.

Modified Amino-silane coated Polycaprolactone for Peripheral Nerve Repair

Caroline S. Taylor[1*], Joseph Barnes[2], David A. Gregory[1], James Henstock[2], Raechelle D'Sa[2], Ipsita Roy[1], Judith Curran[2], and John W. Haycock[1].

[1]*Department of Materials Science & Engineering, Kroto Research Institute, Broad Lane, Sheffield, S3 7HQ, UK.*

[2]*Centre for Materials and Structures, and Institute of Ageing and Chronic Diseases, University of Liverpool, Liverpool, U.K.*

*c.s.taylor@sheffield.ac.uk

INTRODUCTION: 2.8% of all trauma patients will occur a Peripheral Nerve Injury. The current treatment for large gap injuries (+20mm) is still autografting, although there is limited donor nerve available and donor site morbidity. For a short gap injury (10-20mm) , synthetic Nerve Guide Conduits are used. Therefore, current research focuses on improving NGCs for use in longer gap injuries. Coatings have been used to improve the biocompatibility of synthetic nerve guide conduits, as well as providing surface chemistry, and nanotopography guidance for the regenerating axon. Synthetic coatings, such as aminosilanes, are much cheaper to produce, than natural coatings, have the ability to control chemical group deposition at the sub-micron scale and avoids immune responses.

METHODS: Polycaprolactone films were produced by spin coating and fibres manufactured by electrospinning. Fibres and films were exposed to oxygen plasma and immersed in 3% 11-Aminoundecyltriethoxysila n e (CL11) isopropanol solution for 2 hours, washed, and dried overnight. Surfaces were characterised using WCA, Ninhydrin assay, XPS and AFM. NG108-15 neuronal cells, and rat primary Schwann cells were cultured onto for 6 days. Rat Dorsal Root Ganglion bodies were extracted from rat spinal cords, and dissociated into neuronal cell types, to culture for 6 days. Live/dead analysis was used to confirm the biocompatibility of the glass coverslips, for the NG108 neuronal cells and primary Schwann cells, as well as immunolabelling for β III tubulin, NG108-15 neuronal cell differentiation and neurite marker, and for S100, a Schwann cell marker.

RESULTS: WCA, XPS and ninhydrin assay confirmed successful modification of PCL using CL11, confirming the presence of NH_2 groups. AFM analysis confirmed the addition of oxygen plasma, followed by 11-Aminoundecyltriethoxysilane, significantly increased surface roughness, compared to PCL alone. Live/Dead analysis confirmed that both coatings were biocompatible, but that there were higher numbers of live cells cultured on samples modified with oxygen plasma and 11-Aminoundecyltriethoxysilane. Primary Schwann cells cultured on samples stained positively for S100 confirming maintained Schwann cell phenotype. The highest average neurite lengths were found on primary neurons, and NG108-18 neuronal cells, cultured onto samples modified with oxygen plasma and 11-Aminoundecyltriethoxysilane, in which higher numbers of primary neurons and Schwann cells were visualised.

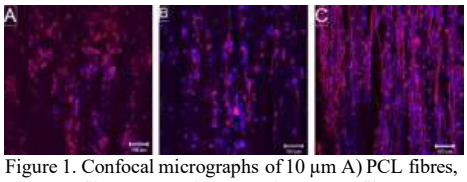

Figure 1. Confocal micrographs of 10 µm A) PCL fibres, B) PCL fibres + O_2 plasma and C) PCL fibres + O2 plasma + 11-Aminoundecyltriethoxysilane modification (scale bar = 100 µm).

DISCUSSION & CONCLUSIONS: This study confirmed the successful modification of PCL films, and fibres, using 11-Aminoundecyltriethoxysilane modification. The addition of CL11 decreased hydrophobicity of PCL, increased surface roughness, and therefore promoted NG108-15 neuronal cell, primary Schwann cell and dorsal root ganglia attachment, and viability, and neurite outgrowth. Future work will involve applying this treatment to synthetic nerve guide conduits, containing fibres, for investigations *in vivo*.

REFERENCES: [1]Juliet H.A. Bell, and John W. Haycock. *Tissue Eng Part B Rev.,* 2012, **18**, 116-128.[2] J.M. Curran, F. Pu, R. Chen, J.A. Hunt. *Biomaterials*, 2011, **32**, 4753-4760. [3]Muhammad F.B. Daud, Kiran C. Pawar, Frederik Claeyssens, Anthony J. Ryan, John W. Haycock. *Biomaterials,* 2012, **33**, 5901-5913.

ACKNOWLEDGEMENTS: We acknowledge the University of Sheffield for funding.

Assessing the efficacy of surface functionalized Manuka Honey on Electrospun Membranes for biomedical applications

Thomas Honey[1*], Piergiorgio Gentile[1], Nicholas Jakubovics[2], Dana Ofiteru[1]

[1]School of Engineering, Newcastle University, Newcastle upon Tyne, United Kingdom
[2]School of Dental Sciences, Newcastle University, Newcastle upon Tyne, United Kingdom
[*] t.j.honey2@ncl.ac.uk

INTRODUCTION

The application of naturally occurring bioactive materials for biomedical applications is an area of recent critical interest. Most notably, due to the previously anecdotal antibacterial properties of some materials undergoing critical research and showing properties which could be readily utilised in biomedical applications[1]. Honey is such a material that has been used in bygone eras as a salve for its' perceived protective and regenerative properties and is currently undergoing critical assessment with indications of positive utilisation within the biomedical community. The use of such biomaterials must first require appropriate characterisation and, to facilitate this transition from bygone treatment to medical device, this work aimed to assess Manuka Honey with methylglyoxal content 550 (MH) as efficient antimicrobial agent to be used as part of a medical device when functionalised upon an electrospun membrane via layer-by-layer assembly.

METHODS

To assess the toxic effects of Manuka Honey 550 upon bacterial and fibroblast cells, MH was diluted in distilled water and stirred on a hotplate at 45˚C for 10 minutes, yielding final concentrations of between 5 and 30% wt/v. These were added to well assays with 0.5 OD bacterial broth suspensions of *S. aureus* NCTC 6571 and *P. gingivalis* W50 and incubated for 24 hours at 37˚C. The wells were then observed and compared to control wells to visually assess at which concentration bacterial inhibition occurs. To assess cytotoxicity, concentrations were added to 50,000 human neofibroblast cells and incubated for 24 hours. The resultant solution was stained with NucGreen and NucBlue and visually inspected under magnification to qualitatively identify cytotoxic concentrations. Further quantitative analysis was achieved by adding PrestoBlue to measure fluorescence of viable cells.

To functionalise MH onto membranes, aminolysed electrospun membranes were dipped for 10 minutes into alternating charged solutions of 20% wt/v MH and Poly(allylamine hydrochloride) (PAH) which are negatively and positively charged respectively, with acetic buffer rinse stages of 5 minutes between each layer. Range of mono layers varied between 0 and 14.

The functionalised membranes were assessed using Attenuated total reflectance Fourier transform infrared spectroscopy (ATR-FTIR) over a wavenumber range 4000-500cm^{-1} absorbance to observe the initial surface composition and how this changes with increasing layer number. Following, membranes underwent glucose release profiles by placing membranes in phosphate buffer saline solutions at 37˚C at regular time points over 4 weeks. Both of these would inform the utility of MH impregnated membranes within the biomedical community.

RESULTS

Toxic effects of MH upon *S. aureus* and *P. gingivalis* were observed at concentrations of 20% w/v in both cases. This toxicity also commenced in neofibroblast assays at concentrations of 15% w/v. The implication, therefore, is that care of release should be considered when creating appropriate medical devices.

FTIR analysis of the surface shows sufficient adhesion of MH and polymer layers across full range of manufacture to membrane surface, and the release profile is sufficient for controlled release over 4 weeks.

CONCLUSIONS

Manuka Honey functionalised upon an electrospun membrane has been monitored for controlled release and biocompatibility. Results showed that Manuka Honey at small concentrations exhibits both antimicrobial and cytotoxic properties. From the controlled release of Manuka Honey, however, this narrow range of toxicity can be exploited, leading to the rational design for a medical device suitable for a range of biomedical applications.

REFERENCES

1. Lee, D. S., et al. (2011). "Honey and wound healing: An overview." Am J Clin Dermatol **12**(3): 181-190.

Exploring Microfluidics as a Neuro-platform Towards the Design of a Novel Targeted Dendritic Vector

Ana P. Spencer[1,2,3], Miguel Xavier[4], Sofia C. Guimarães[1,2], Victoria Leiro[1,2], Ana P. Pêgo[1,2]

[1]i3S – Instituto de Investigação e Inovação em Saúde, Universidade do Porto, Porto, Portugal
[2]INEB – Instituto de Engenharia Biomédica Universidade do Porto, Porto, Portugal
[3]Faculdade de Engenharia, Universidade do Porto, Porto, Portugal
[4]International Iberian Nanotechnology Laboratory (INL), Braga, Portugal
[5]Instituto de Ciências Biomédicas Abel Salazar (ICBAS), Universidade do Porto, Porto, Portugal
*ana.spencer@i3s.up.pt

INTRODUCTION

Neurological diseases represent the highest global burden of disease. For most of them there are no treatments available that can improve neuronal survival. In this context, gene therapy has been proposed as a powerful therapeutic tool to promote neuronal repair and regeneration. Moreover, major advancements in targeted gene therapy have opened new avenues for the treatment of these diseases. However, the success of this therapeutic option relies on the development of effective and clinically suitable safe delivery vectors that are able to cargo and protect nucleic acids (NAs).

Among non-viral vectors, dendrimers are promising carriers due to their globular, well-defined, nanosized and very branched architecture, with a high number of functional groups in the periphery.[1] New fully biodegradable dendrimers were recently proposed by us to act as NA delivery systems.[2] Here we describe their capacity to serve as siRNA vector, assess its biological performance in neuronal cells, as well as their trafficking inside neurons. We also explore their neurotargeting capacity after functionalization with the non-toxic HC fragment of the tetanus toxin (TeNT).[3]

EXPERIMENTAL METHODS

PEG-GATGE (Gallic Acid-Triethylene Glycol Ester) dendrimers-siRNA complexes (dendriplexes), were prepared at several N/P ratios (5-80). The ability to complex siRNA was determined by a SybrGold exclusion assay. Dendriplexes were physicochemically characterized by dynamic light scattering, laser Doppler electrophoresis and transmission electron microscopy. The cytotoxicity was evaluated by resazurin and, lactate dehydrogenase release assays and image analysis in ND7/23 and HT22 cell lines, as well as primary mouse cortical neurons. Also, to understand the endocytic mechanism of our dendriplexes in these cells was explored using clathrin and caveolin markers. Intracellular trafficking was assessed in two-chamber microfluidic platforms with compartmentalized cultures of cortical neurons. Furthermore, we explored the neurotargeted NA delivery by functionalizing our dendrimers with the HC fragment of TeNT.[3] The trafficking of the neurotargeted dendriplexes was also evaluated in microfluidic device.

RESULTS AND DISCUSSION

The proposed dendrimer showed great ability to complex siRNA (≥70%). Assembled dendriplexes presented hydrodynamic sizes (42-60 nm), polydispersity index (≤0,3), morphologies and zeta potential values (0-9 mV) very suitable for cellular uptake, without causing toxic effects in both neuronal cell lines and primary cortical neuron cultures. Moreover, dendriplexes showed fast internalization capacity (less than 2 hours) with a preferential accumulation in the vicinity of the nucleus. Interestingly, this result can be explained by the retrograde transport of our nanosystem along the axon to the cell body of the neuron. Dendriplexes' internalization was found to be mediated by clathrin in ND7/23 and HT22 cells, while caveolin-mediated endocytosis occurs in primary mouse cortical neurons. The microfluidic device also allowed to mimic the bio-interaction between the dendriplexes and neurons and to further monitor the intracellular trafficking of dendriplexes. Finally, targeting proprieties were also evaluated.

CONCLUSION

These promising results prove the ability of the proposed dendritic vectors to complex, protect and deliver NAs in a fast manner in the different neuronal cells tested. Furthermore, the developed dendrimers showed good biocompatibility in neuronal cell lines and in primary neurons, especially when in the form of dendriplexes. Altogether, these results confirm the suitability of dendriplexes for neuronal applications. Also, the encouraging retrograde intracellular route of dendriplexes observed points to the great potential of these systems in the development of long-awaited therapeutic strategies in the context of neurological disorders. In fact, the proposed dendrimers can serve not only as NA delivery vectors but also for other cargoes.

REFERENCES

1. Leiro V. *et al*., Adv. Funct. Mater. 28(12), 2018
2. Leiro V. *et al*., Biomaterials. 281, 2022
3. Lopes C. D. F. et al., Biomaterials. 121, 2016

ACKNOWLEDGMENTS

FCT (Fundação para a Ciência e a Tecnologia) for the project PTDC/BTM-MAT/4156/2021, as well as A.P.S. (SFRH/BD/137073/2018) and S.C.G. (SFRH/BPD/122920/2016), Ph.D. and post-doctoral scholarships, respectively.

Development and optimization of Micro-Arc Oxidation (MAO) coatings on AZ31 magnesium for improved biocorrosion behaviour

Matteo Pavarini[1*], Monica Moscatelli[1], Fabio Variola[2], Roberto Chiesa[1]

[1]Department of Chemistry, Materials and Chemical Engineering "G. Natta", Politecnico di Milano, Milan, Italy
[2]Department of Mechanical Engineering, University of Ottawa, Ottawa, ON, Canada
[*] matteo.pavarini@polimi.it

INTRODUCTION

Magnesium and its alloys represent promising bone substitute materials to be employed in the maxillofacial and orthopedic fields thanks to their mechanical features being highly matched to those of cortical bone[1].
However, these materials present some criticalities for such applications, *i.e.* a too rapid corrosion, often hindering their ability to withstand the involved loads and causing a strong release of degradation products, which result in an intense inflammatory response in the surrounding tissues and therefore interfere with the healing process[2]. Thus, electrochemical surface modification treatments such as Micro-Arc Oxidation (MAO) can help slow down the corrosion processes while improving implants' interaction with bone tissue[3].
In this work, a first attempt was made on the development and optimization of a novel MAO coating on AZ31 magnesium capable of improving bone cells response while enhancing its corrosion resistance for prospective application in bone defect repair.

EXPERIMENTAL METHODS

Commercial AZ31 Mg specimens were treated in a novel electrolyte mainly composed sodium borate and silicate, at room temperature. The MAO process was conducted in pulsed DC conditions, at 100 Hz frequency and 50% duty cycle, for 10 minutes, and the coatings were obtained by varying the final voltage from 300V to 420V.
The porosity and pore size distribution of the surfaces, as well as the thickness of the coatings, were characterized by SEM, while potentiodynamic polarization measurements were performed against a saturated Ag/AgCl reference electrode in simulated body fluid (SBF) at 37 °C to evaluate their corrosion properties.

RESULTS AND DISCUSSION

All the treated surfaces present the typical MAO microporous surface morphology (**Fig. 1a-c**). However, some differences can be observed: the surfaces produced at up to 400V present the features of the micro-spark regime, with relatively small and evenly distributed pores, while beyond that threshold the MAO process evolves to macroscopical sparking, which causes the occlusion of some pores by strong arcing and massive oxide melting and solidification, resulting in the pancake-like structures clearly visible in **Fig. 1c**.
The pore diameter on the surfaces grows with the final voltage, from 223±128 nm at 300V to 466±439 nm at 400V, and is kept almost constant for higher voltages (514±454 nm at 420V). Porosity follows a similar trend, increasing from 4.5% up to 7%, but decreasing to about 4.5% after the macro-spark transition, due to the partial pore occlusion. All the treated surfaces were highly homogeneous, featuring potentially favourable morphologies for osteoblasts adhesion and proliferation[4].

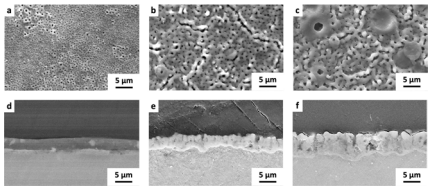

Fig. 1 Surfaces and cross-sections of coatings obtained at 300V (**a**,**d**), 400V (**b**,**e**) and 420V (**c**,**f**).

Moreover, the cross-sectional images (**Fig. 1d-f**) confirm the presence of micrometric coatings on all the samples, with thickness increasing slowly up to 400V (from 3.2±0.9 µm at 300V to 3.9±0.9 µm) and raising more significantly afterwards (up to 6.4±1.2 µm at 420V). For all the coatings, two layers can be identified: a deep, compact region, and a thicker and porous outer region.
The potentiodynamic polarization curves of the MAO coated samples show their higher E_{corr} as compared to the bare material (-1.48V), indicating their nobler corrosion behavior, in particular for the coating produced at the lowest MAO voltage (300V), which features the smallest pores and the highest E_{corr} (-1.17V). Moreover, their polarization resistance is about twice (~120 Θ) that of bare AZ31 Mg (~67 Θ), due to the presence of the thin compact oxide layer. However, all the produced coatings reduce the corrosion rate of the substrate by a comparable extent (from ~4.5 mm/y of bare AZ31 to ~3 mm/y), highlighting that only the deep, compact MAO layer is responsible for improving their corrosion resistance, regardless of the thickness of the outer porous layer.

CONCLUSION

Overall, the unique morphology and tuneable corrosion features of the produced MAO coatings represent a promising starting point to effectively tune the biocorrosion behaviour of magnesium alloys while potentially promoting their interaction with bone cells for prospective bone repair applications.

REFERENCES

1. Chakraborty Banerjee P. *et al*, Materials. 12:1-21, 2019
2. Costantino M.D. *et al*, Acta Biomater. 101:598-608, 2020
3. Wirtz G.P. *et al.*, Mater Manuf Process. 6:87-115, 1991
4. Ahu Akin F. *et al.*, J Biomed Mater Res. 57:588-596, 2001

Tissue-Adhesive Glue as a Novel mRNA Delivery Carrier for Hepatocellular Carcinoma Treatment

Ratchapol Jenjob, Min-Kyoung Kim, Yixin Jiang, Phuong Hoa Tran, Jin-myeong Seo, Hosun Jang, Su-Geun Yang*

Department of Biomedical Science, BK21 FOUR Program in Biomedical Science and Engineering, Inha University College of Medicine, Incheon 22212, South Korea
*Sugeun.Yang@Inha.ac.kr

INTRODUCTION

Hepatocellular carcinoma (HCC) is the second most common cause of cancer death worldwide.[1] MicroRNAs (miRNAs) have been extensively tested as therapeutic molecules against several human diseases. miRNAs, including miR-141, are involved in the regulation of cell proliferation, differentiation, and apoptosis, and thus, could be good therapeutic agents for cancer treatment.[2] In vivo delivery of miRNAs to the target cancer cells needs to satisfy the following conditions: safety, efficiency, and long-term therapeutic effectiveness. To satisfy these conditions, we developed a nucleotide-polymer complex (NPX-glue) for delivery of miRNAs to treat hepatocellular carcinoma (HCC).

EXPERIMENTAL METHODS

A cationic polyallylamine (PAA) was complexed with tumor-suppressing miR-141 to generate a nucleotide-polymer complex (NPX) and further mixed with an oxidized alginate (OA) to form NPX-glue via Schiff base reaction. The successful complexation between miR-141 and NPX was determined by gel retardation and zeta potential with various N/P ratios. Tumor-suppressive effects of miR-141@NPX-glue were confirmed in a human HCC-xenograft mouse model by injecting the miR-141@NPX-glue directly into the tumor lesions.

RESULTS AND DISCUSSION

NPX-glue acted as a tissue-adhesive glue after intratumoral injection owing to the additional Schiff base formation between the aldehydes of OA and tumor tissue. The size of NPX determined by TEM was in the range of ~50-100 nm. At N/P ratio higher than 1.6, no visible free miR-141 was detected. NPX was cytotoxic when the N/P ratio was over 0.8, but the formation of NPX-glue virtually eliminated the cytotoxic effects. Upon intratumoral injection of miR-141@NPX-glue, the growth of the tumors was dramatically retarded in comparison with the negative control (NCmiR@NPX-glue). Molecular examination proved miR-141@NPX-glue efficiently regulated the target genes and finally induced apoptosis of cancer tissues.

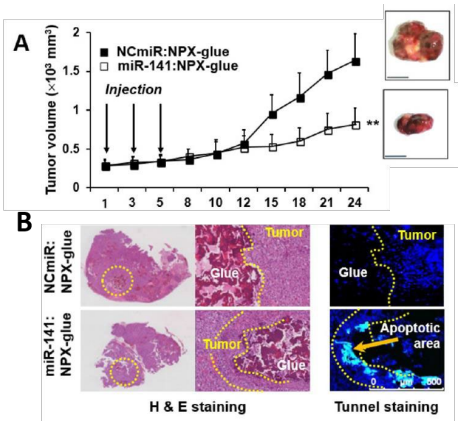

Figure1. (A) Hep3B cells were injected subcutaneously into the flank of mice. When the tumor size reached 250 mm^3, NCmiR@NPX-glue or miR-141@NPX-glue was injected into the tumors thrice. The volumes of the tumors were monitored for 24 days. (B) H&E and TUNEL staining of the tumor tissues treated with NCmiR@NPX-glue or miR-41@NPX-glue. The yellow arrow indicates apoptotic area.

CONCLUSION

The issue-adhesive NPX-glue was developed and can deliver nucleic acids efficiently and safely to tissues. When miR-141, a tumor suppressive miRNA, was used as a therapeutic molecule in the form of NPX-glue and injected into an implanted HCC, miR-141 was delivered to the surrounding tumor tissues and successfully inhibited tumor growth. Therefore, NPX-glue can be a useful locoregional therapeutic molecule to deliver nucleic acids safely and effectively for an extended period.

REFERENCES

1. Park J-W. *et al*., Liver Int. 35:2155-2166, 2015
2. Liu Y. *et al*., PLoS One. 9: e88393, 2014

ACKNOWLEDGMENTS

This research was supported by Basic Science Research Program and Korea Research Fellowship Program through the National Research Foundation of Korea (NRF) and partly supported by WCSL (World Class Smart Lab) research grant directed by Inha University.

Amine-based coatings support the adhesion of osteoblast-like cells on titanium surfaces dependent on their amino group density

Susanne Seemann[1*], Ricardo Ramos[2], Manuela Dubs[3], Annika Wartenberg[3], Susanne Staehlke[1], Matthias Schnabelrauch[3], Karine Anselme[2], J. Barbara Nebe[1,4]

[1]Department of Cell Biology, University Medical Center Rostock, 18057 Rostock, Germany
[2]Institut de Science des Matériaux de Mulhouse, University of Haute Alsace, 68057 Mulhouse, France
[3]Department of Biomaterials, INNOVENT e.V., Jena, Germany
[4]Dept. Life, Light & Matter, University of Rostock, 18059 Rostock
[*]susanne.seemann@med.uni-rostock.de

INTRODUCTION

Increased life expectancy in industrialized countries is causing an increased incidence of osteoporosis and an increased need for bone implants.[1] The integration of implants can be improved by physical but mainly by chemical modifications of the implant surface. It has already been shown that amine-based coatings improve cell attachment, cell migration, and intracellular signaling.[2] The moderately positive surface potential optimally supports the initial adhesion and spreading of cells.[3] The aim of this study was to determine the role of the amino group density in this positive cell response by developing controlled amino-rich nano-layers. In this work, two different techniques were used: (1) radio plasma polymerization of allylamine, and (2) covalent grafting of polymer-based amino-rich nano-coatings.

EXPERIMENTAL METHODS

Planar and grooved titanium (Ti) surfaces were obtained from the Center for Microtechnologies (ZFM, University of Technology Chemnitz, Germany). Coating with radio plasma-polymerized allylamine (RPPm) via plasma-enhanced chemical vapor deposition was produced in the Institut de Science des Matériaux de Mulhouse (France). Coating with trimethoxysilylpropyl modified poly(ethyleneimine) (TMS-PEI, ABCR) was prepared at INNOVENT (Jena, Germany)[1]. Sessile drop method was used to measure the water contact angle utilizing the Drop Shape Analyzer-DSA25 (Krüss)[4]. Zeta potential was measured with the SurPass™ system (Anton Paar) and the related software Attract 2.1. MG-63 cells (ATCC® CRL-1427™)[5] were cultured in DMEM (Life Technologies) with 10% FCS (Biochrom FCS Superior, Merck). For cell spreading MG-63 cells were stained with PKH-26 (Sigma-Aldrich) and cultivated for 30 min.[6] Cell areas were determined via confocal laser scanning microscope (LSM 780, Carl Zeiss), ZEN software, and ImageJ (NIH, USA). To analyze cell contact guidance actin cytoskeleton was stained with phalloidin-TRITC (Sigma-Aldrich) and analyzed via LSM 780.[1]

RESULTS AND DISCUSSION

The RPPm and the TMS-PEI coating displayed a moderately positive surface potential with +3.0 mV and +11.7 mV, respectively, and a contact angle of 69.1° and 53.6°, respectively, which is optimal for the growth of MG-63s[7]. The cell area increased on RPPm and TMS-PEI compared to the collagen control. The improved cell behavior was also observed on the grooved surfaces. Cells on RPPm showed a clear tendency to abrogated contact guidance.
Our data indicate a correlation between the amino group density and improved spreading behavior of cells (see abstract for ESB2022, ID: A106934RA).

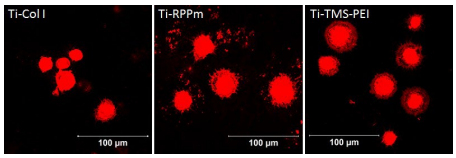

Fig. 1: Morphology of membrane-stained MG-63s after 30 min on functionalized Ti (collagen I, RPPm, and TMS-PEI).

Fig. 2: Relative cell areas of MG-63s on RPPm and TMS-PEI after 30 min. Spreading was compared to the collagen I control (mean ± sem, n = 3, unpaired *t*-test, ** $p<0.01$).

CONCLUSION

RPPm and TMS-PEI coating both improved the cellular behavior of MG-63 cells. Additionally, we could elucidate their physico-chemical surface properties which correspond to optimal conditions for cell growth and are comparable with each other. This indicates a correlation between the different spreading behavior and the altered amino group densities of both coatings.

REFERENCES

1. Moerke C. *et al.*, ACS Appl Mater Interfaces, 9 (12): 10461-10471, 2017
2. Nebe JB. *et al.*, Polymers (Basel), 11(6):1004, 2019
3. Gruening M. *et al.*, Front Bioeng Biotechnol. 8:1016, 2020
4. Staehlke S. *et al.*, Cell Biosci. 8:22, 2018
5. Staehlke S. *et al.*, Cell Biol Int. 43 (1):22-32, 2019
6. Kunz F. *et al.*, Eur Cell Mater., 29:177-88, 2015
7. Dowling *et al.*, J Biomater Appl. 26(3):327-47, 2011

ACKNOWLEDGMENTS

This research was funded by the DFG, German Research Foundation (DFG NE/560/19-1, 446225522).

Deciphering the complexity of poly (beta amino ester) polyplexes: particle composition, stability and cellular interactions

María Navalón[1], Aurora Dols[2], Santiago Grijalvo[3], Cristina Fornaguera[1], Salvador Borrós[1]

[1]Grup d'Enginyeria de Materials (Gemat), Institut Químic de Sarrià (IQS), Universitat Ramon Llull (URL), Barcelona, Spain
[2] Nanoscale bioelectrical characterization/IBEC, Barcelona, Spain
[3]Surfactants and Nanobiotechnology/IQAC-CSIC, Barcelona, Spain

cristina.fornaguera@iqs.url.edu

INTRODUCTION

The necessity to develop non-viral delivery systems has been triggered by the drawbacks of using genetically engineered viral vectors, such as safety issues, immunogenicity, insertional mutagenesis, low loading capacity and high production costs[1]. Here, it is proposed the use of polymer-based delivery systems, specifically, oligopeptide end-modified poly (β-amino ester)s (OM-pBAE), which are functionalized by adding cationic or anionic peptide such as lysine (L) , arginine (R), histidine (H) and aspartic acid (D) to the end-terminal groups. These specific modifications provide high transfection efficacy, low toxicity, high tunability and excellent biocompatibility and biodegradability[2,3]. Concerning their extraordinary properties and the number of applications that can be assigned, it is surprising that polymeric-based nanoparticles have hardly reached the market. This gap from the bench to the bedside can be explained by the lack of basic science studies regarding these polyplexes, namely their structural stability, which is key to arrive to commercialization.[4]

We aimed to fulfil this gap by performing a broad study of OM-pBAEs nanoparticles. Six different nanoparticle variants were used, the cationic, KH, RH and RK and the anionic coated ones, KHD, RHD and RKD; all of them encapsulating a reporter gene (pGFP). These have been deeply studied, starting from their structure and stability to their cell trafficking. These primary studies are fundamental for a successful development of carriers that deliver oligonucleotides into specific tissues.

EXPERIMENTAL METHODS

Being assisted with advanced techniques such as Fluorescence Resonance Energy transfer (FRET), enhanced dark field spectral microscopy, Atomic Force Microscopy (AFM) and microscale thermophoresis (MST), the nanoparticles structure and stability have been unmasked. Referring to the cellular trafficking, supported by the confocal microscope and the flow cytometry, we have been able to decipher the involvement of peptides in cell uptake and gene expression.

RESULTS AND DISCUSSION

Referring to the coated and non-coated polyplexes structure, it has been possible to characterize them in a meticulous manner and understand their organization inside the nanoparticle comprehending they do not follow a core-shell structure (*Figure 1A and B*). Regarding cationic polyplexes stability, they are temperature dependent (*Figure 1C)*. Alluding anionic polyplexes, stability seems to be independent to biological temperature variations (*Figure 1D).*

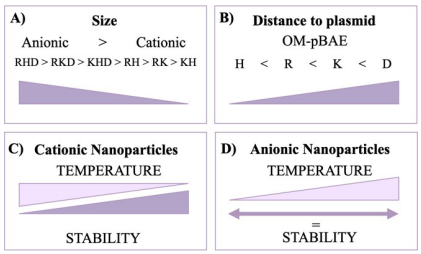

Figure 1. Scheme of the stability and structure section*. A) Nanoparticles complexes sorted by their size. B) OM-pBAE distribution inside the polyplex construction. C) Cationic nanoparticles stability-temperature dependence. D) Anionic nanoparticles stability-temperature dependence.*

Attributing to cell experiments, non-coated polyplexes internalization is achieved in early timings while coated ones in a 24h period and at much lower levels. Finally what concerns to cell transfection, cationic polyplexes are able to deliver the cargo and express it in a 48h range whereas the few coated ones able to internalize in the cell are not capable of cargo delivering.

CONCLUSION

With our study, we were able to disclose, for the first time, the internal structure, stability and cellular interaction of the OM-pBAE polyplexes as a function of their end-terminal peptide composition. Therefore, we are seeding the roots for unveiling the required mechanisms to approach NPs to the market.

REFERENCES

1. Lee CS, Bishop ES, Zhang R, et al.. *Genes Dis*. 2017;4(2):43-63.
2. Zugates, Gregory T., et al. *Bioconjugate Chemistry*, vol. 18, no. 6, 2007, pp. 1887–1896.
3. Fornaguera, C. *et al. Adv. Healthc. Mater.* **7**, 1–11 (2018).
4. *Navalon-Lopez M. et al. In preparation*

Structured Surfaces Mimicking *in vivo* Tissue Architecture

Petr Humpolíček[1*], Antonín Minařík[1], Markéta Kadlečková[1], Kateřina Skopalová[1]
[1]Centre of Polymer Systems, Tomas Bata University in Zlin, Zlin, Czech Republic
[*] humpolicek@utb.cz

INTRODUCTION

Tissue engineering depends on the availability of appropriate cells seeded on appropriate substrates. Human induced pluripotent stem cells (hiPSC) retain the ability to self-renew and differentiate into any somatic cells[1] and their usage does not invoke any ethical controversy[2] compared to human embryonic stem cells. Another advantage of hiPSC is that the patient's own cells can be used for therapy and treatment[3]. Therefore, they belong to the most appropriate lineages of tissue engineering testing.

Another important aspect in tissue engineering is the kind of substrate on which cells grow. However, there is only limited information available on the impact of surface properties and structures on iPSC behavior.

Thus, the influence of a hierarchically structured surface at the level of macro/meso/micro topography on the attachment and maturation of hiPSC-derived cardiomyocytes (hiPSC-CM) was investigated within this study.

EXPERIMENTAL METHODS

Preparation of Hierarchically Structured Substrates

As an initial substrate, tissue culture polystyrene (PS) dishes were used. For the surface modification, three types of mixture were prepared: 1) tetrahydrofuran (THF) and 2-ethoxyethanol (ETH); 2) PS-THF-ETH; 3) THF-ultrapure water. All surfaces were modified by deposition of solvent mixtures using a homemade spin coater[4]. The resulting substrates can be classified as meso-structured (from 10 to 50 µm) or macro-structured (above 50 µm) and micro-structured (from 0.1 to 10 µm) according to the size of irregularities.

Material characterization

Prepared substrates were characterized using optical goniometry, scanning electron microscopy (SEM), optical profilometry and contact profilometry.

Cytocompatibility and Cardiomyogenesis

The cytocompatibilities of the substrates were determined using the human induced pluripotent stem cell (hiPSC) lines. The attachment, proliferation and maturation of hiPSC-CM were investigated. The initial growth/proliferation of cells was determined by measuring the level of ATP in cell lysate 4 days after seeding. Further, the degree of cardiomyogenesis in hiPSC populations, based on the expressions of transcripts related to the cardiomyocyte phenotype, was evaluated after 14 days of cell differentiation. Analysis of Ca^{2+} transients in beating cardiomyocytes and Quantitative analysis of fluorescence was also conducted.

RESULTS AND DISCUSSION

Common *in vitro* experimental conditions do not mimic the *in-vivo*-occurring 3D architecture. The experiments thus lack these important external cell-instructive cues. The tissue culture, polystyrene-based substrates were, therefore, modified by the sequential dosing of solution mixtures on rotating surfaces to form a hierarchically arranged structure. Macro- and meso- structured substrates covered with micro-pores were prepared and characterized (Fig. 1.). The average pore size was determined to be from 1 µm^2 for micro- to 300 µm^2 for meso- or 18,000 µm^2 for macro-structure. The macro-structured substrates exhibited a roughness (Ra value) of 7.2 ± 0.1 µm and the mesostructured substrates exhibited a value of 1.1 ± 0.1 µm.

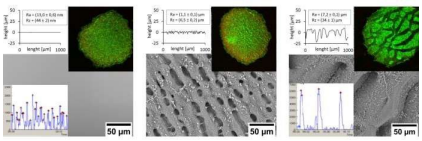

Fig. 1. Tissue culture plastic based structure substrates.

Both types of substrate were suitable for hiPSC cultivation and were found to be beneficial for the induction of cardiomyogenesis in hiPSC. This was confirmed both by the number of promoted proliferated cells and the expressions of specific markers (Nkx2.5, MYH6, MYL2, and MYL7). Furthermore, while monitoring the Ca^{2+} flow in mature cardiomyocytes, substrates were found to amplify the fluorescence signal, offering improved monitoring options when observed *via* a normal camera for recording signals, or via a low-concentration reading of Ca^{2+} sensitive fluorescent probes, and thus decreasing the phototoxicity of the assay.

Obtained results make this material especially suitable for *in vitro* studies of cell/material interactions within tissue-mimicking environments.

CONCLUSION

The structured substrates prepared here mimic the *in vivo* microenvironment. They were tested in the context of their impact on the cardiomyogenesis of human-induced stem cells. Both types of substrate were suitable for culturing induced cells and, in addition, were found not to inhibit the maturation of cardiomyocytes. The results provided a comprehensive view of the main parameters influencing cell/material interactions, with respect to substrate architecture and surface energy. The substrates prepared here offer a new possibility for the experimental set-up of *in vitro* experiments.

REFERENCES

1. Wang F. *et al.,* Chin. Med. J. 131:852-856, 2018.
2. Wilson H.K. *et al.*, Stem Cells. 32:3037-3045, 2014.
3. Ye L. *et al.*, Curr. Cardiol. Rev. 9:63-72, 2013.
4. Minařík A. *et al.*, Coatings. 9:301, 2019.

ACKNOWLEDGMENTS

This work was supported by OP RDE by the project The Development of Capacity for Research and Development of TBU in Zlin – CZ.02.269/0.0/0.0/16_028/0006243.

Deposition Of Natural Biopolymers Via Atmospheric Plasma Torch

Artem Arkhangelskiy[1], Alberto Quaranta[2], Antonella Motta[1], Yuejiao Yang[1], Vamsi K. Yadavalli[3], Devid Maniglio[1*]

[1]Department of Industrial Engineering and Biotech Center for Biomedical Technologies, University of Trento, Trento, Italy
[2]Department of Industrial Engineering, University of Trento, Trento, Italy
[3]Department of Chemical and Life Science Engineering, Virginia Commonwealth University, Richmond VA, USA
* devid.maniglio@unitn.it

INTRODUCTION

Natural polymers are largely proposed as bioactive coatings but their application to surfaces is limited by several factors, such as limited control on the mechanical and chemical stability and weak adhesion to the underlying surface. Additionally, to address specific biological performances, it is also essential to control surface topography and chemistry after the coating is applied.[1]

Plasma process provides unique features, such as surface activation, functionalization or assisted polymerization, which can be obtained using mild conditions such as low power and temperature. Plasma modification can enhance the adhesion via covalent bonding between functional the groups forming at the interface between the substrate and the coating. On the other side, commonly adopted cold plasma processes imply limited coating thickness and topography control.

In this research, we present a new methodology to obtain deposition of silk fibroin and chitosan using an atmospheric plasma torch fed by a carrier and an active gas (argon and oxygen/air respectively), together with an aerosol aqueous solution containing the polymers to be deposited. Representing a one-step technique without the need for pre-treatment, plasma-assisted deposition can provide spatially controlled deposition, forming chitosan on fibroin (CoF), and fibroin on chitosan (FoC) films as well as patterned surfaces. We finally demonstrate their ability to tune protein interactions and cell adhesion and proliferation.

EXPERIMENTAL METHODS

Plasma-assisted deposition of chitosan and silk fibroin aerosol solution was conducted using an atmospheric plasma torch (Stylus Plasma Noble, Nadir Tech SR). Deposition was conducted using aerosol solutions obtained by ultrasonication of the silk fibroin or chitosan stock solutions, which were injected into the plasma torch gas line and oriented towards the chosen substrates (glass, PET, PDMS and Ti6Al4V alloy). The resulting coatings were characterized by electron and atomic force microscopy, and ATR-FTIR. The stability of the films was tested in phosphate-buffered saline (PBS) solution (pH 7.4) for 2 weeks at 37 °C, followed by treatment in sonication bath for 10 min. Human bone marrow-derived mesenchymal stem cells (hMSCs) were used to test the patterned surfaces. cell adhesion was visualized by Oregon green phalloidin and DAPI staining.

RESULTS AND DISCUSSION

The presented plasma process provides unique features in one step, such as surface activation, functionalization or assisted polymerization, and dry deposition in inert environment. Coatings can be obtained using extreme low power (10 W) and room temperature, resulting having excellent adhesion and stability on a large variety of materials, even with complex shape geometries: a soda-lime glass, a metal alloy (Ti4Al6V), a thermoplastic polymer (polyethylene terephthalate), a silicone rubber (poly-dimethylsiloxane), without any need of surface pre-treatment (examples in Fig. 1a, b, c). The developed method was also successfully optimized for multiple layer deposition of fibroin-on-chitosan and chitosan-on-fibroin, and then addressed to realize patterned surfaces. The biological response of these coatings was then tested by cell culture experiments, evidencing their capacity to guide cell adhesion and control cell proliferation. (Fig. 1d)

CONCLUSION

In this study, we reported a one-step method for the deposition of chitosan via atmospheric plasma torch. This technique allows conformation of chitosan and silk fibroin coatings with excellent stability and strong adhesion to the underlying surfaces (Ti6Al4V alloy, PDMS, PET, glass) thanks both to plasma surface activation and plasma-assisted crosslinking. Layering and patterning capability was then extended to conjugate chitosan to silk fibroin, checking the realization of controlled geometrical structures. The obtained patterns were then tested for protein absorption and cell adhesion and distribution. Cold plasma assisted fibroin/chitosan patterns revealed the capacity of multilayers to control and guide cell behavior. This versatility can represent a powerful method for obtaining functional surfaces suitable for application in biomedical implants and bioelectronics devices.

REFERENCES

1. Song, Jian *et al.,* Adv. Mater. Interfaces (2020): 2000850.
2. A. Arkhangelskiy *et al., Adv. Mater. Interfaces*, 2100324, 2021

ACKNOWLEDGMENTS

This project has received funding from the Italian Ministry for Education, University, and Research (MIUR) through the "Departments of Excellence" program.

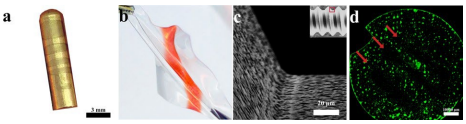

Fig. 1 Example of plasma deposited films: titanium/fibroin (a) and PDMS/chitosan (b). SEM image of chitosan conformal coating on a dental screw (c) and cell distribution on patterned FoC coating (d)

Physicochemical and mechanical properties of Ti6Al7Nb alloy with nitrocarburized layer after sterilization, and exposure to Ringer's solution

Anita Kajzer[1], Wojciech Kajzer[1*], M. Tarnowski[2], T. Borowski[2], T. Wierzchoń[2]

[1]Department of Biomaterials and Medical Devices Engineering, Faculty of Biomedical Engineering, Silesian University of Technology, Zabrze, Poland
[2] Faculty of Materials Science and Engineering, Warsaw University of Technology, Warsaw, Poland
[*]wojciech.kajzer@polsl.pl

INTRODUCTION

On the basis of clinical observations disadvantageous interaction of Al and V with a human body was found. Vanadium causes cytotoxic reactions and, consequently, neurogenic disorders and aluminum affects the softening of bones, damages nerve cells and may cause diseases of brain and blood vessels [1,2]. Ti6Al7Nb alloy does not contain vanadium. Instead, niobium was introduced. This element and its oxides, including Nb_2O_3, belong to the group of compounds inert to a body. Furthermore, due to the greater reactivity, compounds of Nb with O_2 are formed more easily than compounds of Al with O_2. Nb oxides, during the passivation process, form a compact structure of the surface layer that is more resistant to corrosion in the environment of tissues and body fluids, thereby reducing the number of post-implantation complications. In order to increase the surface hardness of the Ti6Al7Nb alloy and thus the surface abrasion resistance, surface modifications are carried out. One of the methods is nitrocarburized layer in low-temperature plasma [3]. Therefore the main aim of the study was to evaluate the influence of steam sterilization and exposure to Ringer's solution to the useful properties of the alloy.

EXPERIMENTAL METHODS

Studies were carried out on the Ti6Al7Nb alloy (Protasul R100). The samples were in the form of discs 14 mm in diameter and 3 mm thick. This alloy was characterized by properties consistent with the recommendation of ISO 5832-11 standard. In order to obtain a roughness of Ra<0.1 µm surface was polished using an abrasive paper of 320 and 1200 grit, and then mechanically polished using a silica suspension. Next, the diffusion surface layer of Ti(CN) + Ti_2N + αTi(N) was deposited in the nitrocarburizing process in a low-temperature plasma at a temperature of 790 °C with the use of pressure of 2 mbar for 6 hours and 5% CH_4 compound. The layers deposited in the glow discharge nitrocarburization process as well as the polished Ti6Al7Nb alloy in the initial state were subjected to steam sterilization using the HMT-260F autoclave (HMC EUROPE). Sterilizing agent was steam at 135°C at the pressure of 2 atm for 60 min. To simulate the tissue environment the samples were exposed to the Ringer's solution for 28 days at 37 ± 1 °C in the incubator (Binder). To evaluate the influence of sterilization, and exposure to Ringer's solution to the mechanical and physicochemical properties of the Ti6Al7Nb alloy before and after the proposed surface modification, electrochemical, surface roughness, wettability and mechanical properties studies have been conducted.

RESULTS

Process of the glow discharge nitrocarburizing increased roughness and hardness, and decreased corrosion resistance and wettability in comparation to polished samples. The sterilization of the produced layer did not significantly affect the roughness and hardness of the surface, but contributed to a significant reduction in the value of the polarization resistance R_p and the contact angle. The final stage of exposure to Ringer's solution of sterilized samples with a layer, as in the case of sterilized samples only, did not affect the roughness and hardness of the surface. On the other hand, a further decrease in the value of the polarization resistance and the contact angle θ was observed in relation to the samples with the layer in the initial state.

CONCLUSION

Summing up the results of the research it can be concluded that the proposed method of surface modification contributed to the improvement of utility properties. This involves the possibility of a wider use of Ti6Al7Nb alloy for implants in bone surgery.

REFERENCES

1. J. Marciniak: Biomateriały. Wydawnictwo Politechniki Śląskiej, Gliwice 2013 (in Polish).
2. W. Chrzanowski, Corrosion behavior of Ti6Al7Nb alloy after different surface treatments, Journal of Achievements in Materials and Manufacturing Engineering, 18 (2006) 67-70
3. L. Thair, U. Kamachi Mudali, N. Bhuvaneswaran, K. G. M. Nair, R. Asokamani, B.Raj, Nitrogen ion implantation and in vitro behavior of as-cast Ti6Al7Nb alloy, Corrosion Science 44, 11 (2002) 2439-2457

Anti-encrustation functionalization of CoCrMo alloy with biodegradable polymer coatings

Wojciech Kajzer[1], Janusz Szewczenko[1*], Anita Kajzer[1], Marcin Basiaga [1], Joanna Jaworska [2], Katarzyna Jelonek [2], Katarzyna Nowińska [3], Marcin Kaczmarek [1],

[1]Department of Biomaterials and Medical Devices Engineering, Faculty of Biomedical Engineering, Silesian University of Technology, 41-800 Zabrze, Poland
[2]Centre of Polymer and Carbon Materials, Polish Academy of Sciences, 41-819 Zabrze, Poland
[3]Department of Applied Geology, Faculty of Mining, Safety Engineering and Industrial Automation, Silesian University of Technology, 44-100 Gliwice, Poland
[*] wojciech.kajzer@polsl.pl

INTRODUCTION

In urology, the problem of encrusting, both polymer and metal implants, despite many years of research, has still not been solved. Literature data[1] indicates that urinary tract infections are mainly caused by bacteria and fungi, which, through the production of biofilm, contribute to the development of stent incrustation (covering the surface of implants with calcium phosphate and magnesium ammonium phosphate crystals) leading to their obstruction and stopping the urine flow. It has been shown in clinical trials[2] that the use of urological implants made of Co alloys, as opposed to polymer ones, may reduce the need for their frequent replacement and, in the long term, lead to lower costs of their use. Currently, urological stent implantation is very often accompanied by systemic pharmacotherapy aimed at treating inflammation, which, unfortunately, does not fully solve the problem of the formation of a bacterial and fungal film on the surface of the implant, leading to the development of incrustation. Therefore, the study investigated the usefulness of surface modification of CoCrMo alloys intended for urological implants by applying biodegradable polymer coatings in order to locally prevent the multiplication of bacteria on their surface and reduce encrustation.

EXPERIMENTAL METHODS

The research included: preparation of substrate made of CoCrMo alloy, application of two variants of biodegradable polymer coatings (poly (L, L-lactide-ε-caprolactone) or poly (D, L-lactide-ε-caprolactone)) as internal and external coatings from polyvinyl alcohol (PVA) containing the active ingredient - heparin. In order to evaluate the biodegradable polymer coatings, microscopic tests, surface roughness, wettability, adhesion of the coatings to the substrate, as well as potentiodynamic and potentiostatic corrosion tests were carried out. Moreover, the mass density of metal ions released into the solution was determined and the degree of incrustation was assessed. The kinetics of heparin release from the formed outer coating was also determined. The research was carried out for the initial state and after 30, 60, and 90 days of exposure to artificial urine. To determine the significance of differences for $p < 0.05$, the obtained results used a one-way analysis of variance (ANOVA).

RESULTS

Regardless of the type of polymer used, the coatings produced on the Co alloy surface are characterized by transparency, continuity, homogeneity, a very good reflection of the metal substrate topography, and good adhesion. In addition, the coatings increase the corrosion resistance of Co alloy and reduce the mass density of ions (Co, Cr, Mo) released to the solution. In the case of prolonged exposure to artificial urine, it was found that the coatings had a beneficial effect on the encrustation process, especially in the first 30 days. The hydrophilic nature of the applied polymer coatings was found, which increased with the exposure time. It was also found that the complete release of heparin from the outer coating occurs within 20 days of exposure to the artificial urine.

CONCLUSION

The obtained research results indicate the usefulness of surface functionalization of metal biomaterials with biodegradable polymer coatings, aimed to improve the corrosion resistance of the metal substrate and to reduce the incrustation of the implant surface in the environment of artificial urine. In addition, these results provide the basis for further work on methods of surface modification of metal biomaterials used in urology with new compositions of active polymer coatings in order to reduce the incrustation process and prevent peri-implant inflammatory processes.

REFERENCES

1. A. Nevo, R. Mano, E. Schreter D. A. Lifshitz. Clinical implications of stent culture in patients with indwelling ureteral stents prior to ureteroscopy. The Journal of Urology, 198, 1 (2017), 116-121.
2. A. Baumgarten, T. Hakky, R. Carrion, J. Lockhart, P. Spiess. A single-insitution experience with metallic ureteral stents: A cost-effective method of managing deficiencies in ureteral drainage. International braz j urol: official journal of the Brazilian Society of Urology, 40, 2, (2014), 225-231

ACKNOWLEDGMENTS

The work is the result of the research project no. 2018/02/X/ST8/03061 funded by the National Science Centre, Poland.

Antimicrobial Coating of Metal Surfaces Using Surface Immobilized Peptides

Mohadeseh Zare, Diana Gomes and Artemis Stamboulis

Biomaterials Research Group, School of Metallurgy and Materials,
University of Birmingham, Birmingham, UK
* m.zare@bham.ac.uk

INTRODUCTION

Infections associated with orthopaedic implants are still the cause for concern despite modern surgical procedures. When infection occurs, antibiotics have limited activity because of the difficulty to reach the infection site, more so if biofilm or an antibiotic-resistant microorganism is present[1]. There are various strategies for antibacterial coatings using immobilizing molecules, e.g., peptides. Antimicrobial peptides (AMPs) are biomolecules with broad-spectrum antimicrobial activity, low toxicity, and less likely to induce resistance, suitable candidates to improve the antimicrobial properties of implants[2].

Considerable efforts have been focused on strategies for the chemical and electrostatic surface immobilization of peptides, differing in binding strength, modularity, and complexity. In this work, two strategies will be used for functionalization of titanium (Ti) surfaces with AMPs. The first strategy involves adding a peptide with affinity for Ti to the AMP sequence to create a solid-binding antimicrobial peptide with affinity to implant surfaces. Metal surfaces are also submitted to a combination of a mild chemical treatment and heat treatments to favour the electrostatic attachment by increasing oxide species on the surface and producing surface morphology suitable for cellular proliferation[3]. The second strategy involves chemical integration of AMPs in the titanium surface which could be a reliable method to immobilize AMPs in a stable form for a long period in the optimal orientations. The plasma nitriding technique is one of the surface functionalization methods to create primary amine groups on the surface as anchors to attach the peptides. This technique has attracted considerable attention due to its efficient time and energy and applying nontoxic materials during the process[4].

EXPERIMENTAL METHODS

The samples used in this study were titanium alloy Ti-6Al-4V (10x10x1.6 mm^3). First, the samples were polished to mirror-finish surfaces. Then, in order to electrostatically immobilize the peptides, samples were submitted to a combination of chemical treatments (CT) by immersion in 10 mL of 8.8 M H_2O_2, 0.1 M HCl at 80 ºC for 30 minutes and heat treatments (HT) by thermal oxidation at 450, 550, 650 and 750 ºC for 60 minutes. To covalently immobilize the peptides, plasma treatment was performed in an evacuated chamber where a mixture of gases (35% N_2 and 65% H_2) could flow at a controlled pressure and then any electrical energy was applied for 2 hours at temperatures between 300 and 500 ºC. After surface functionalization, primary amine functional groups could promote covalent immobilization with antimicrobial peptides using chemical reactions between carboxyl groups of peptides and primary amine groups.

RESULTS AND DISCUSSION

Chemical characterizations including Raman spectroscopy, XRD, FTIR, and XPS as well as surface morphology evaluation were performed. Based on chemical analyses, rutile and anatase phases of titanium dioxide were identified on the surfaces of the non-treated polished samples due to the fast oxidation of titanium when exposed to air. The samples treated by HT showed increased crystallinity from 650 ºC to full surface crystallinity at 750 ºC. CT resulted in the formation of large grains and pores on the surface, but it did not influence the surface crystallinity. When samples were submitted to both treatments CT and HT, at 750 ºC, the porous morphology of the surface was replaced by a less porous crystalline morphology. For the plasma treated samples, titanium nitrides TiN and Ti_2N were identified on the surfaces. The presence of Ti-O, Ti-N, Ti-OH, and N-H components on the surface of plasma-treated samples confirmed that oxygen was not entirely removed during the treatment and amine groups were successfully created on the surface for further peptide immobilization.

CONCLUSIONS

In this study to immobilize peptides on the surface of a medical grade titanium alloy, two different strategies for chemical and electrostatic immobilization were followed. The chemical characterization analyses proved that the surfaces were successfully treated by CH and HT methods and functionalized with amine groups by plasma treatment technique for further immobilization of peptides.

REFERENCES

1. Riool, M. *et al*., Front Chem. Aug 24;5:63, 20171
2. Mahlapuu, M. *et al*, Front Cell Infect Microbiol. 6:194, 2016
3. Rodriguez, G. M. *et al*, RSC Advances 10(30): 17642-17652
4. Sergio D. *et al*., Biointerphases 14:051009, 2019

ACKNOWLEDGMENTS

The authors would like to thank the Marie Sklowdoska-Curie Actions (MSCA) Innovative Training Network (ITN) AIMed (Grant no: 861138) for providing financial support to this project.

Engineered living hydrogel meshes for therapeutic applications

María Puertas-Bartolomé[1,2] and Aránzazu del Campo[1,2*]

[1]INM—Leibniz Institute for New Materials, Saarbrücken, Germany
[2]Saarland University, Saarbrücken, Germany
* maria.puertas@leibniz-inm.de

INTRODUCTION

In the last few years, the field of biomaterials has advanced from inert materials to biologically active materials able to interact with the surrounding cells or tissues. The field of engineered living materials (ELM) that combine living cells with a matrix or scaffold has emerged from this vision. ELMs open up new possibilities for the preparation of advanced functional materials able to adapt and respond to different environmental cues in a programmed manner[1,2]. Engineered materials incorporating living components such as drug-eluting microorganisms are emerging as new concepts for therapeutic treatment of diseases. Previous work from our group has demonstrated the successful encapsulation of drug-eluting bacteria into hydrogel membranes, and their utility for in situ drug production and delivery[3,4]. These bacteria can be further engineered to respond to specific triggers, such as temperature, light or pH, and produce biopharmaceuticals on-demand. The encapsulating matrix must provide a suitable environment for bacteria for the diffusion and exchange of nutrients and drugs, while it retains bacteria and confines them to a closed space. A particular challenge are living therapeutic materials that can deliver therapeutic proteins, since these are large and diffusion across hydrogels is very slow. In this work, we propose the development of living hydrogel meshes, that contain entrapped engineered bacteria as "biofactories" to produce ilimited drug supply in a sustained manner.

EXPERIMENTAL METHODS

Electrospinning technique, was used to manufacture living nanofibrillar meshes encapsulating the engineered bacteria. *In vitro* stability and mechanical properties of the material were evaluated as well as the colony growth of the encapsulated bacteria and the protein expression and delivery.

RESULTS AND DISCUSSION

Non-degradable nanofibrillar meshes with different fiber diameter, pore size, density and intrafibrillar crosslinking have been prepared presenting high *in vitro* stability. The encapsulating matrices have demonstrated to provide a suitable environment for bacteria with high diffusivity for nutrients and drugs, while confining them to a closed space.

CONCLUSION

Obtained results present a great potential of application as a new generation of living, drug-eluting meshes for different therapeutic purposes. The possibility of using programmed bacteria highlights the versatility to develop programable materials able to incorporate different functions. Additionally, the use of electrospinning technique to create nanofibrillar meshes with high diffusivity present a huge potential for protein-based biopharmaceutical delivery.

REFERENCES

1. A. Rodrigo-Navarro *et al*., *Nature Reviews Materials*, 2021, 1-16.
2. W. V. Srubar III, *Trends in Biotechnology*, 2021, 39(6), 574-583.
3. S. Sankaran et al., *Advanced Biosystems*, 2019, 3(2), 1800312.
4. S. Sankaran et al., *Small*, 2019, 15(5), 1804717.

ACKNOWLEDGMENTS

The authors would like to thank the Leibniz ScienceCampus Living Therapeutic Materials (Saarbrücken, Germany). for providing financial support to this project.

ESB 2022
32nd ANNUAL CONFERENCE OF THE EUROPEAN SOCIETY FOR BIOMATERIALS

Properties of the Poly (D, L-lactide-glycolide) coating containing hydroxyapatite applied by ultrasound on an anodized Ti6Al7Nb substrate

Janusz Szewczenko[1*], Karolina Goldsztajn[1], Marcin Godzierz[2], Anna Hercog[2], Joanna Jaworska[2], Katarzyna Jelonek[2], Roman Major[3], Marcin Basiaga[1], Wojciech Kajzer[1], Julia Lisoń[1], Anna Woźniak[4], Marcin Kaczmarek[1]

[1]Department of Biomaterials and Medical Device Engineering, Faculty of Biomedical Engineering, Silesian University of Technology, Zabrze, Poland
[2]Centre of Polymer and Carbon Materials of the Polish Academy of Sciences, Zabrze, Poland
[3]Institute of Metallurgy and Materials Science of the Polish Academy of Sciences, Kraków, Poland
[4] Department of Engineering Materials and Biomaterials, Faculty of Mechanical Engineering, Gliwice, Poland
[*] janusz.szewczenko@polsl.pl

INTRODUCTION

The most common method of surface modification of titanium alloys used in orthopedics is anodic oxidation[1]. Passive layers improve the biocompatibility of implants and are characterized by good osteoconductive properties. However, in order to improve the biocompatibility of titanium alloy implants and accelerate bone tissue repair processes, the authors of this paper propose to apply biodegradable polymer coatings containing nanohydroxyapatite, which will be released during polymer degradation. Therefore, the work aimed to characterize the properties of the biodegradable polymer Poly (D, L-lactide-glycolide) (PLGA) coating containing hydroxyapatite (HA), applied to the substrate of anodically oxidized Ti6Al7Nb titanium alloy. The coatings were applied using the ultrasonic spray method. The topography and structure of the coating, adhesion to the substrate, wettability, and the influence on the corrosion resistance were determined.

EXPERIMENTAL METHODS

The material applied in the tests was Ti6Al7Nb alloy with chemical composition, structure, and mechanical properties complying with ISO 5832-11 recommendations. The samples were ground, sandblasted, and anodically oxidated. For the grinding, abrasive papers, subsequently of 120, 300, and 600 grade, were used. For the sandblasting, glass balls of diameter from 70 to 110 µm were used; t=2 min. Anodization was carried out with the use of the electrolyte based on phosphorous and sulphuric acid at the voltage 97 V; t =2 min. Poly(D,L-lactide-glycolide) PLGA(85/15) with hydroxyapatite (< 200 nm, Merck) has been chosen for the coating material. Mn of the polymer was: 74 kDa. Metallic samples were coated with the PLGA by the ultrasonic spray coating method. Solution of 1% PLGA in dichloromethane was enriched with 20% HA. The coatings were applied by ExactaCoat (Sono-Tek) with AccuMist™ Ultrasonic Spray Shaping with following parameters: ultrasound frequency 60 kHz, ultrasound power 1,5 W, solution's flow rate 1 cm^3/min, speed of nozzle motion 10 mm/s, the distance between nozzle and substrate 70 mm and air curtain pressure 2 Pa. The coated implants were airdried for 3 days at 25 °C. The topography of the samples was analyzed using scanning electron microscopy (SEM) (Quanta 250 FEG, FEI Company) and light microscopy (DVM6, Leica). The coatings' structure was characterized by X-Ray Diffraction studies (D8 Advance, Bruker). Quantitative and qualitative tests of coating adhesion to the substrate were carried out using scanning acoustic microscopy SAM (KSI Evo II) and scratch test (CSM Micro-Combi Tester). Tribological tests were performed with the Pin-On-Disc method (Anton Paar). The wettability of the coatings was determined by the contact angle measured with SURFTENS UNIVERSAL optical goniometer (OEG). The influence of the polymer coatings on the corrosion resistance was determined by potentiostatic and potentiodynamic methods (PGP 201, Radiometer).

RESULTS AND DISCUSSION

The applied coatings were continuous, homogeneous, and transparent. The hydroxyapatite was evenly distributed throughout the coating. This was confirmed by X-ray studies, in which the presence of the amorphous phase of the polymer and lattice strain in the structure of hydroxyapatite were also observed. Good adhesion to the substrate has been confirmed by scanning acoustic microscopy studies and scratch tests. The coatings were characterized by good abrasion. The applied polymer coatings increased the resistance to pitting corrosion in relation to the substrate. An increase in the corrosion potential and polarization resistance was observed.

CONCLUSION

Homogeneous polymer coatings containing the active substance (HA) can be produced on the surface of anodized titanium implants for osteosynthesis by the ultrasonic spray coating. This method of surface modification could improve the biocompatibility and biofunctionalization of the surface of titanium implants, which will be verified at a later stage of research.

REFERENCES

1. Marciniak J., Szewczenko J., Kajzer W., Surface modification of implants for bone surgery, Archives of Metallurgy and Materials 60(3): 2123-2129, 2015

Analysis Of The Disinfection Of Electronic Instruments In Clinical Use: The Case Of VR Headsets For Anesthesia And Pain Relief

Cynthia Calligaro[1*], Jémil Hacini[1], Philippe Lavalle[1,2], Nihal Engin Vrana[1]

[1]SPARTHA Medical, Strasbourg, France
[2]INSERM UMRS1121, Strasbourg, France
[*]ccalligaro@sparthamedical.eu

INTRODUCTION

In health care settings, it has been shown that the objects used to improve the quality of work of healthcare professionals can also be related to nosocomial infections. Many of these objects have complex geometry and are made of various materials. Without careful disinfection, some areas may be poorly cleaned, leading to microbial growth and thus bacterial transmission.

The aim of this study is the characterization of complex medical device contamination using virtual reality (VR) headsets as a study model. To better understand the underlying conditions of contamination, we have tested different VR headsets used in hospital settings and developed methodologies for the testing of entire headsets for contamination and disinfection. In addition, we have tested an antimicrobial multilayer film made of poly(L-arginine) (PAR) and hyaluronic acid (HA)[1,2,3] that can disinfect the surface and provide longer protection.

EXPERIMENTAL METHODS

Micrococcus luteus was used to assess the antibacterial activity. Adhesion and disinfection protocols were adapted from the NF EN 13697+A1 standard guidelines. 1.10^6 bacteria are deposited in a drop at the surface of the material. If the step is needed, the disinfection solution is then deposited over. The remaining bacteria are counted after a wash step. Coating construction of (PAR/HA) multilayer films was done by alternatively dipping in PAR and HA solutions with intermittent rinsing steps.

RESULTS AND DISCUSSION

The different materials which are parts of the VR headsets were evaluated for their susceptibility to bacterial adhesion. The results showed that all materials were susceptible to bacterial contamination with different behaviors between the substrates.

The tests done on the entire VR headsets showed that the design of the headset has a significant impact on the quality of disinfection. The headsets which require minimal user manipulation to be mounted, do not have tissue or textile-based components, and with relatively fewer protruding parts and hard-to-reach zones were easier to disinfect.

Despite the meticulous cleaning and the work in a sterile environment during the experiment, VR headsets were sometimes contaminated before the inoculation of bacteria. Cleanings in actual use are likely to be less stringent. Thus, it demonstrates the need for a simple, effective, and repeated cleaning protocol for the disinfection of such devices. Also, this problem can be diminished by safety-by-design approaches, i.e. incorporation of design components that limits the potential inducing factors to contamination (porous areas, protrusions, hard-to-reach zones) as described above.

The repeated contamination tests on full-scale VR headsets are a good model of negligent or low-performance disinfection. The results showed that the disinfection with PAR or ethanol 70% was effective on the headsets after 3 days of daily inoculation but ineffective on the samples of the materials after 1 week of daily inoculation. Thus, these tests should be further developed, and the behavior of the bacteria in these conditions should be more characterized (e.g. for biofilm construction). Better models of nosocomial infection will enable to combat medical device-related nosocomial infections and provide the necessary information for the device producers.

CONCLUSION

The design of devices with complex surfaces should consider hygiene and disinfection constraints. More specifically, plane surfaces without high reliefs are preferable to maximize the disinfected area and textile parts should be avoided to limit pathogenic contamination. The utilization of devices such as VR headsets with such design components can limit the infection risks. The prevention of pathogenic contamination should be encouraged, especially since the disinfection of such devices is difficult. The use of a safe solution of disinfection for both the user and the device such as PAR/HA association would improve the compliance to the cleaning. Finally, this type of study needs to be further developed and extended to other types of pathogens.

REFERENCES

1. Mutschler A. *et al.*, Chem. Mater. 28:8700–8709, 2016
2. Mutschler A. *et al.*, Chem. Mater. 29:3195–3201, 2017
3. Gribova V. *et al.*, ACS Appl. Mater. Interfaces 12:19258–19267, 2020

ACKNOWLEDGMENTS

The authors would like to thank Pico Interactive (VR Headset developer/sponsor) and HypnoVR (VR-based anesthesia, use case) for their support.

Nucleic acid activated surface coatings designed to induce osteogenic differentiation of stem cells

Christian Wölk[1*] Catharina Husteden,[2] Yazmin A. Brito Barrera,[3] Michaela Schulz-Siegmund,[1] Christian E.H. Schmelzer,[4] Thomas Groth,[3]

[1] Pharmaceutical Technology, Institute of Pharmacy, Faculty of Medicine, Leipzig University, 04317, Leipzig, Germany

[2] Department of Biochemical Pharmacy, Institute of Pharmacy, Martin Luther University Halle-Wittenberg, Weinbergweg 22, 06120, Halle (Saale), Germany

[3] Department Biomedical Materials, Institute of Pharmacy, Martin Luther University Halle−Wittenberg, Heinrich Damerow-Strasse 4, 06120, Halle (Saale), Germany

[4] Department of Biological and Macromolecular Materials, Fraunhofer Institute for Microstructure of Materials and Systems (IMWS), Walter-Huelse-Strasse 1, 06120, Halle (Saale), Germany

[*] Christian.woelk@medizin.uni-leipzig.de

INTRODUCTION

Bone fractures cause immense costs in the national health care system. Approximately 5-10% of bone fractures result in a non-union causing morbidity.[1] In addition to the burden on health economic systems, indirect costs from work loss and intangible costs from reduction of life quality must also be considered. Regenerative medicine is a chance to cure severe bone fractures. Smart strategies are needed to promote bone regeneration. Therapies using recombinant bone morphogenetic proteins (BMP-2) show advanced effects in bone regeneration.[2] Nevertheless, high costs, stability issues and side effects resulting from supra-physiological concentrations of BMPs show the demand for alternative strategies.[3] The use of nucleic acids encoding for BMPs is a promising strategy. Recently, we presented a proof-of-concept study engineering nucleic acid-activated surface coatings based on polyelectrolyte multilayers functionalized with lipid nanoparticles (Figure 1).[4]

EXPERIMENTAL METHODS

Several methods were used to study the layer-by-layer deposition process of polyelectrolytes and nucleic acid lipid nanoparticles. These methods include water contact angle measurements, surface plasmon resonance spectroscopy, atomic force microscopy, ellipsometry, and confocal laser scanning microscopy. Cell culture experiments with adipose derived mesenchymal stem cells (adMSCs) were performed to check for osteogenic differentiation (extracellular matrix staining and gene expression analysis) as well as for cell/surface coating interaction.

RESULTS AND DISCUSSION

We could demonstrate an efficient and stable incorporation of nucleic acid lipid nanoparticles in polyelectrolyte multilayers. Cell interaction studies demonstrated attachment and spreading of adMSCs on the gene activated surface coatings. The modified surfaces showed good cytocompatibility. Experiments with fluorescent-tagged DNA demonstrated an efficient internalization of the genetic payload by adMSCs. The experiments with reporter genes demonstrated that the mode of action is a contact triggered transfection, meaning that only cells which interact with the surface coating can get transfected. The functional studies with a gene encoding for BMP-2 showed the increase of osteogenic markers on the mRNA level (osteocalcin, noggin, collagen 1A1, alkaline phosphatase, RUN-X2) and in the extracellular matrix components (collagen 1, osteocalcin, hydroxyl apatite) deposited by adMSCs.

CONCLUSION

BMP-2 gene encoding surface coatings based on polyelectrolyte multilayers loaded with nucleic acid lipid nanoparticles can induce osteogenic differentiation of stem cells.

REFERENCES

1. La Vega R. *et al*., Transl. research 236:1-16, 2021
2. Lissenberg-Thunnissen S.N. *et al*., International Orthopaedics 35:1271, 2011
3. Schimer A. *et al*., Injury 40: 32-38, 2009
4. Husteden C. *et al*., ACS Appl. Mater. Interfaces 12: 8963-8977, 2020

ACKNOWLEDGMENTS

The funding by the Deutsche Forschungsgemeinschaft (DFG, German Research Foundation) project-ID 396823779 is acknowledged.

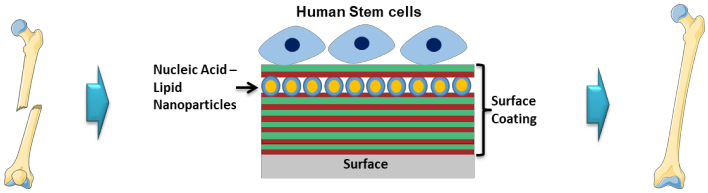

Figure 1: Schematic illustration of the concept of nucleic acid activated surface coatings. The Coatings are loaded with cytokine encoding nucleic lipid nanoparticles to induce differentiation processes. In this study the focus was set on osteogenic differentiation.

ESB 2022
32ND ANNUAL CONFERENCE OF THE EUROPEAN SOCIETY FOR BIOMATERIALS

Human mesenchymal stem cells offer an immune-privileged niche to *C. acnes* in case of implant-associated osteomyelitis

Marie Dubus, Jennifer Varin-Simon, Steve Papa, Sophie C. Gangloff, Cédric Mauprivez, Xavier Ohl, Fany Reffuveille, Halima Kerdjoudj.

Université de Reims Champagne Ardenne, EA 4691, Biomatériaux et Inflammation en Site Osseux (BIOS), Reims, France
* halima.kerdjoudj@univ-reims.fr

INTRODUCTION

Found in bone-associated prosthesis, *Cutibacterium acnes* (*C. acnes*) is isolated in more than 50% of osteoarticular prosthesis infections. Ongoing controversies exist concerning the origin of *C. acnes* infection. While few reports state about a probable *C. acnes* displacement from the superficial skin into the surgical wound, *C. acnes* was recently detected in the intracellular compartment of macrophages and stromal cells in 62.5% of tested patients who did not undergo skin penetration. Among bone stromal cells, mesenchymal stem cells (MSCs), the source of osteogenic lines, are predominantly found in bone marrow and periosteum. In this study, the pathogenicity of *C. acnes* in bone repair context was investigated.

EXPERIMENTAL METHODS

Human bone marrow derived MSCs were challenged with *C. acnes* clinical strains harvested from non-infected bone site (Cb) and from orthopaedic implant-associated infection (Ci). The infective capabilities of bacteria were determined; and the morphology, ultrastructural analysis and the immunomodulatory response of infected MSCs was evaluated. The virulence of intracellular Ci and Cb (Ci-MSCs and Cb-MSCs) was investigated by biofilm formation on non-living bone materials. Bone cells (osteoblasts and macrophages) were then challenged with Cb-MSCs and Ci-MSCs. Intracellular accumulation of ROS within infected macrophages and catalase production by bacteria were evaluated.

RESULTS AND DISCUSSION

Following MSCs infection by *C. acnes*, the rate of viable Cb inside MSCs was about 4%. The ultrastructural analysis of infected MSCs confirmed the presence of Cb free in MSCs cytoplasm. Considering the high level of secreted immunomodulatory mediators (PGE-2 and IDO), our results suggest that Cb could activate the immunomodulatory profile of MSCs. After MSCs infection, Cb-MSCs increased significantly the formation of biofilm on non-living bone materials. Regarding the ability of bacteria to infect osteoblasts, our results showed a higher infective capability of Cb-MSCs *versus* Cb. Along with an increase in catalase production by Cb-MSCs, we noticed its higher persistence to macrophage degradation.

CONCLUSION

Taken together, our results demonstrate a shift in commensal Cb to pathogenic following infection. Overall, these results showed a direct impact of *C. acnes* on bone marrow derived MSCs, providing new insights into the development of *C. acnes* during implant-associated infections.

REFERENCES

Dubus M *et al*., Acta Biomater., 104:124-134, 2020
Dubus M. *et al*., Acta Biomater.. 137:305-315, 2021

ACKNOWLEGDMENTS

This work was supported by «Region Grand Est, Fonds Régional de Coopération pour la Recherche-ERMES».

Layer-by-Layer assembly of ECM based biological macromolecules onto Ti alloy for tackling related bone implant infections

Anjaneyulu Udduttula[1], Nicholas Jakubovics[2] Imran Khan[3], Lucia Pontiroli[3], Kenneth S Rankin[4] Piergiorgio Gentile[1]** and Ana M. Ferreira[1]*

[1]School of Engineering, Newcastle University, Newcastle Upon Tyne NE1 7RU, United Kingdom
[2]School of Dental Sciences, Faculty of Medical Sciences, Newcastle University, United Kingdom
[3]Zimmer-Biomet UK Limited, Dorcan Industrial Estate, Swindon SN3 5HY, United Kingdom
[4]Translational and Clinical Research Institute, Faculty of Medical Sciences, Newcastle University, NE2 4HH, United Kingdom
*Corresponding author, email address: ana.ferreira-duarte@newcastle.ac.uk
**co-corresponding author, email address: piergiorgio.gentile@newcastle.ac.uk
Presenting author, email address: anjaneyulu.udduttulla@newcastle.ac.uk

ABSTRACT

In the orthopaedic field, implant-associated severe infections rarely occur after complex bone surgeries and cause the dramatic clinical failure of implants[1]. The biofilm formation by antibiotic-resistant microbial pathogens can lead patients to life-threatening complications, as no robust reliable antibiotics may effectively treat the prevention and eradication of biofilms. Hence, there is an urgent need to develop advanced antibacterial coatings on implants to limit the risk of infections. This work focuses on exploiting the nature-inspired self-assembly of biological macromolecules for suppressing biofilm formation while stimulating bone growth. For this, we aim to self-assemble extracellular matrix (ECM) like coatings onto medical-grade titanium (Ti) alloy by exploiting layer-by-layer (LbL) technology. Antibacterial Methylglyoxal (MGO: Manuka honey component) is conjugated with tetra amine-polyethylene glycol (4-NH_2-PEG) to constitute a negative polyelectrolyte. Ours recently patented Hybrid LbL instrument (PCT/GB2020/052641)[2] is exploited to fabricate systematic LbL coatings of type I collagen (COL) and hyaluronic acid (HA) on the Ti alloy surface, incorporating in the top multilayers the antibacterial MGO-g-PEG conjugate. The physicochemical properties of multilayer surfaces were assessed by various analytical techniques such as ATR-FTIR, Profilometry, SEM-EDS, and XPS. The self-assembling process of layers was monitored by contact angle measurements and confirmed the electrostatic interactions by accumulating polyionic constituents. The cell culture experiments were conducted to prove the osteogenic ability of multilayer coatings using human mesenchymal stem cells by cell viability assay, Live/Dead staining, ALP, and ARS. In addition, we have assessed the antibacterial property of COL/HA/MGO-g-PEG coatings on Ti alloy by quantitative (biofilms formation, CFU) and qualitative (zone of inhibition) methods using *Staphylococcus aureus* and *Escherichia coli* pathogens. Therefore, our study demonstrates that the developed Coll/HA multilayer coatings with the tailor of MGO-g-PEG on covalently immobilized Ti alloy favor the early osteointegration with subside the attack of bacteria in bone tissue engineering.

REFERENCES:

1. Erika L. *et al*., ACS Infect. Dis. 7:3125−3160, 2021
2. Ferreira-Duarte A.M. and Gentile P., *Hybrid Layer-by-Layer equipment* (patent application PCT/GB2020/052641), 2020.

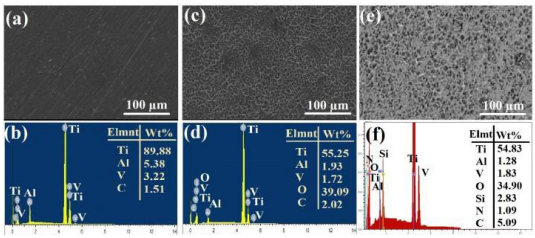

Fig.1. SEM-EDS analysis of (a,b) untreated, (c,d) alkali and (e,f) silanized Ti alloy for LbL coatings

Antibacterial properties of additively manufactured PVDF-graphene composites

Andrea Spanou*,†, Supradeepa Panual*, Mamoun Taher¤†, Ken Welch§, Cecilia Persson*

* Department of Materials Science and Engineering, Biomedical Engineering, Uppsala University, Sweden
¤ Department of Chemistry - Ångström Laboratory, Uppsala University, Uppsala, Sweden
§ Department of Materials Science and Engineering, Nanotechnology and functional materials, Uppsala University, Sweden
† Graphmatech AB, Uppsala, Sweden

INTRODUCTION

Antimicrobial resistance has become a leading cause of death around the world. (1) An alternative to the use of antibiotics is inherently bacteriostatic or antibacterial material surfaces. Graphene has demonstrated such properties, but its effectiveness has not been fully explored as incorporated into polymers. Polyvinylidene fluoride (PVDF) is a biocompatible polymer already used in applications where antibacterial properties are important, such as sutures, surgical meshes and as sensors in implantable devices. Additive manufacturing could accommodate for the complex geometries sometimes required in such applications. In this study the antibacterial properties of reduced graphene oxide (rGO) and graphene nanoplatelets (GnP), two forms of graphene suitable as polymeric additives, were examined in thermally compounded and additively manufactured PVDF samples.

EXPERIMENTAL METHODS

PVDF – graphene (6.5wt%) composite filaments were prepared in a twin-screw compounder (PolyLab). The composites were subsequentially 3D-printed using fused deposition modeling (Ultimaker S5+). Scanning electron microscopy (SEM) (Zeiss LEO 1530) was used to assess the arrangement of the graphene nanofillers in the polymer matrix.

The antibacterial properties were examined using surface contact tests. The viability of Escherichia coli (E.coli) and Staphylococcus aureus (S. aureus) was tested when exposed to the surface of the samples, using a surface contact test.

RESULTS AND DISCUSSION

The GnP – PVDF composites showed a significant reduction of colony forming units for both E.coli and S. aureus, when compared with the PVDF reference. The rGO-PVDF composites on the other hand did not exhibit any significant difference to the PVDF reference. The difference in antibacterial effects could be derived from the morphology observed in the SEM images, where the samples with GnP showed sharp protrusions of the graphene flakes on the surface of the printed sample. Such morphology was not observed on the PVDF- rGO samples.

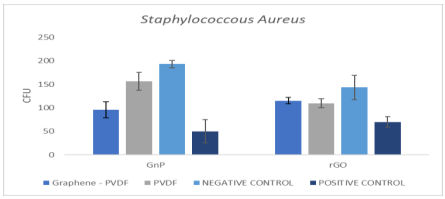

Figure 1: Surface contact test results of PVDF-GnP and PVDF-rGO composites for S. Aureus

Figure 2: SEM images of printed samples (a) GnP-PVDF (b) reference PVDF (c) rGO-PVDF

The antibacterial effect of GnPs could be attributed to a physical mechanism involving physical distraction of the cell membrane due to the sharp edges of the species. Similar observations were made by Pandit et al. (2) In previous studies on rGO, an antibacterial effect was observed where the mechanism of action was chemical, inducing oxidative stresses on the bacterial membrane. (3) Here, rGO was well embedded in the polymer matrix preventing it from chemically interacting with the bacteria.

CONCLUSION

In conclusion, different graphene morphologies exhibit different antibacterial properties when incorporated into this polymeric matrix.

REFERENCES

1. Teo, Adrian JT, et al. ACS Biomaterials Science & Engineering 2.4 (2016).
2. Pandit, Santosh, et al. Advanced Materials Interfaces 5.7 (2018)
3. Liu, Shaobin, et al. ACS nano 5.9 (2011)

ACKNOWLEDGMENTS

Support from Graphmatech AB and VINNOVA Competence Centre AM4Life (2019-00029) is gratefully acknowledged.

In Vivo Apatite Formation Ability of Mg-Based Scaffolds Modified via Directed Plasma Nanosynthesis

Viviana M. Posada[1,2,3*], Juan Ramírez[3], Patricia Fernández-Morales[4], Jean Paul Allain[1,2]
[1]Ken and Mary Alice Lindquist Department of Nuclear Engineering, Penn State College of Engineering, USA
[2]Department of Nuclear, Plasma and Radiological Engineering, University of Illinois at Urbana-Champaign, USA
[3] Mines Faculty, Universidad Nacional de Colombia, Colombia
[4]Industrial Engineering Faculty, Universidad Pontificia Bolivariana, Colombia
* vfp5162@psu.edu

INTRODUCTION

Mg-based bone graphs with porous architectural designs provide guidance for tissue and blood vessels' growth. However, there are concerns regarding their rapid degradation. Additionally, the complexity of the geometry limits the usage of the available surface protection methods[1].

Porous Mg materials have been treated with direct plasma nanosynthesis (DPNS). This system modifies the first nanometers of the surface, allowing to preserve the integrity of the porosity. The nanoscale modification is delivered via low-energy Ar^+ irradiation creating a nanostructured top surface followed by the accumulation of secondary alloying elements on the subsurface. This surface complex accelerates the passivation kinetics of the porous material improving the apatite nucleation ability when in contact with physiological fluids[2].

We hypothesize that the increased ability of DPNS samples to nucleate hydroxyapatite (HAp) offers control over the in vivo corrosion mechanism. The low solubility of the CaP in body fluids and the ability of DPNS samples to form more crystalline apatites are expected to preserve the structure during the consolidation of the new tissue. Hence, this work aims to evaluate the DPNS potential to in vivo enhance the corrosion resistance and protect the structural integrity of the porous Mg materials.

EXPERIMENTAL METHODS

Porous AZ31 were obtained via indirect 3D printing and infiltration casting. The samples with diamond lattice structures were surface modified via DPNS as shown in **Fig 1a**. The irradiation parameters were Ar^+ ions with 400 eV energy and 1×10^{17} ions/cm^2. Samples were immersed in DMEM to evaluate in vitro degradation via H_2 collection, ICP-OES, and weight loss.

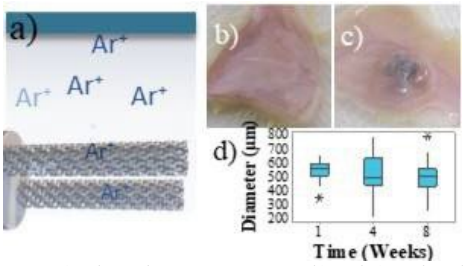

Fig.1. a) schematic DPNS treatment. b) and c) retrieved tissue after 4 weeks of implantation of control and DPNS, respectively. d) box plot of strut diameter vs. time after 1, 4, and 8 weeks of implantation.

In vitro MC3T3-E1cells directly seeded were observed via fluorescence stains. In vivo studies were carried out using 12 weeks old Wistar rats weighing 200 ± 24 g. The materials were implanted under the rat's back skin. samples were extracted at weeks 1, 4, and 8. Chemical and morphological changes were observed via SEM/EDS, and XRD. Samples were weighted before and after insertion and extraction. All animal experiments were approved by ethics committee of the National University of Colombia.

RESULTS AND DISCUSSION

Well-ordered nanostructures were produced on the DPNS modified surfaces. In addition, the DPNS surfaces showed Al supplementation (2.3 ±0.7 wt.%) on the subsurface. CaP-rich phases with a CaP radius (1.44 ± 0.04) were developed on the DPNS surface complex when in contact with the physiological fluid. Moreover, after 2 weeks of in vitro immersion significantly lower ($p < 0.01$) release of Mg ions was observed in DPNS samples than control. The in vitro and in vivo results showed well-tolerated materials with minor reactions (**Fig 1c**). In vivo results also indicated that the control sample was completely biodegraded after 4 weeks of implantation (**Fig 1b**); oppositely, the structural integrity of the DPNS sample was consistent and no significant changes in strut thickness were observed until week 8 (**Fig 1d**). CaP products were observed in the DPNS samples in all stages of the in vivo study which was consistent with the steadiness of the corrosion rate of the DPNS sample throughout the implantation period (8 weeks).

CONCLUSION

The surface modification at first nanometers of the surface allowed the protection of the porous Mg without sacrificing the open porosity of the structure. Thus, DPNS avoided the use of layers and coatings as protective strategies that can be unevenly distributed or delaminate. In addition, the ability of the sample to form more crystalline corrosion products helped to control biodegradation and improved the biological response of the material, in vitro and in vivo.

REFERENCES

1. Yin, Z. *et al*., J. Magnes. Alloy. 8, 42–65, 2020
2. Posada. V. *et al*., Appl. Surf. Sci. 550, 149388, 2021

Antibacterial Activity and Biodegradation of Zn-Ag Alloys for Biomedical Applications

Claudia García-Mintegui[1,2*], Gemma Dorrego[1], Judit Buxadera-Palomero[1], José Luis Cortina[2], Marta Pegueroles[1]

[1]Department of Materials Science and Engineering, Barcelona East School of Engineering (EEBE), Universitat Politècnica de Catalunya (UPC), Barcelona, Spain
[2] Department of Chemical Engineering, EEBE-UPC, Barcelona, Spain
*claudia.garcia.mintegui@upc.edu

INTRODUCTION

Biodegradable Zn-based metals may be promising materials for orthopedic implants, avoiding secondary surgeries and promoting bone formation [1]. Moreover, the increasing risk of bacterial infection due to the developed antibiotic resistance is a worldwide theme of concern [2]. In this work, Zn-Ag alloys are presented as potential materials for implantology, meeting both antibacterial and degradability conditions.

EXPERIMENTAL METHODS

Zn, Zn-2Ag, and Zn-4Ag metallic bars with 10 mm of diameter were provided by GoodFellow (UK) and cut into disks of 2.5 mm of thickness. Disks were grinded following standard metallographic procedures. *S. Aureus* (CCUG 15195) and *E.Coli* (CECT 101) were used for the antibacterial characterization. Bacterial activity by contact was evaluated by adhesion tests after 2 and 24 h of alloys inoculation: the attached bacteria were analyzed by live/dead staining, SEM observation, and CFU quantification. The surfaces were cleaned after the adhesion tests following ISO 8407, and observed by SEM. Antibacterial effect by diffusion was studied by agar diffusion and indirect contact tests. Immersion tests in BHI at 2, 6, 24, 48, and 72 h were performed following ASTM G31-72, and released Ag ions were analyzed by ICP-MS.

RESULTS AND DISCUSSION

Fig. 1 shows the SEM images of the adhered bacteria onto Zn-2Ag surface. Irregular morphologies of the *S. Aureus* (Fig. 1a) and *E. Coli* (Fig. 1b) after 2 h of adhesion suggested an antibacterial effect of the Zn-Ag surfaces by contact. Besides, the CFU quantification after 2 h of adhesion showed a decreasing tendency of bacterial adhesion with the higher Ag content.

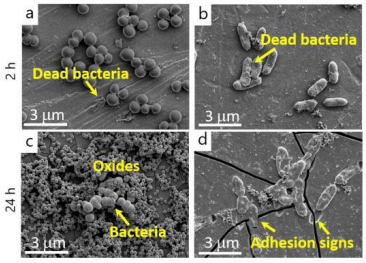

Fig. 1. Adhered *S. Aureus* (a, c), and *E. Coli* (b, d) onto Zn-2Ag after 2 h (top) and 24 h (bottom) of adhesion.

After 24 h, the attached bacterial population deeply decreased, with almost no alive bacteria found in any sample. The degradation effects were noticeable, with corrosion products surrounding *S. Aureus* (Fig. 1 b) or signs of detached *E. Coli* possibly caused by the dynamism of the degrading surface (Fig. 1 d). These results indicated that no further bacterial infection could be developed, even after a possible initial bacterial attachment. The surfaces after adhesion tests evidenced bacterial degradation (Fig. 2), which accelerates the overall sample degradation. However, as shown in adhesion results, this acceleration could present an advantage in avoiding future bacterial infection.

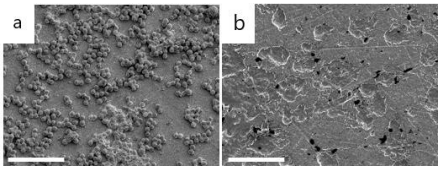

Fig. 2. Zn surface after 2 h of *S. Aureus* adhesion: (a) before and (b) after bacteria removal. Scale bar: 10 µm.

Agar diffusion test indicated no antibacterial effect for any sample. This result was confirmed at indirect contact assays with no differences in the lag phase of the bacterial growth curves. Released Ag^{3+} was not detected through all the immersion test, and hence its concentration would be below the detection limit of the ICP-MS (0,01 mg/dL). The minimum inhibitory concentration over *S. Aureus* is 62.5 mg/mL [3], which explains the absence of antibacterial effect by diffusion.

CONCLUSION

The presence of Ag in Zn-Ag alloys prevents early bacterial adhesion, and the biodegradability of the alloy prevents further bacterial colonization. Besides, bacteria play a fundamental role in alloy degradation, accelerating it. This bidirectional effect presents Zn-Ag alloys as promising candidates for the bone implants, overcoming some of the drawbacks of conventional inert implants while opening new antibacterial approaches.

REFERENCES

1. Yang H. *et al*., Nat. Commun. 11:401, 2020.
2. Aslam B. *et al.,* Infect. Drug. Resis. 11:1645-1658, 2018.
3. Parvekar P. *et al.,* Biomater. 7:105-109, 2020.

ACKNOWLEDGMENTS

Financial support was received from Spanish Government, MINECO/FEDER (RTI2018-098075-B-C21 and MAT2017-83905-R) and the Government of Catalonia (AGAUR 2017 SGR 1165 and FI scholarship for C.G.M.)

Application of Collagen-immobilized PDMS Substrate for Cell Stretching

Kazuaki Mori[1], Kosuke Kataoka[2], Yoshikatsu Akiyama[3], Toru Asahi[1,2,4]
[1]Graduate School of Advanced Science and Engineering, Waseda University, Shinjuku-ku, Tokyo
[2]Comprehensive Research Organization, Waseda University, Shinjuku-ku, Tokyo
[3]Institute of Advanced Biomedical Engineering and Science, Tokyo Women's Medical University, Shinjuku-ku, Tokyo
[4]Organization Research Organization for Nano & Life Innovation, Waseda University, Shinjuku-ku, Tokyo
*kazuaki2510mori@toki.waseda.jp

INTRODUCTION

PDMS is frequently used as a strain substrate in external mechanically stretched cell culture systems. ECM protein coating is a useful way to improve cell adhesion properties of the original PDMS surface. However, cell culture experiment demonstrates that ECM-coated PDMS surfaces do not show satisfactory cell adhesive characteristics under mechanical stretch stress because of the desorption of physisorbed ECM[1]. Alternatively, covalent immobilization of ECM to PDMS surface has been explored. Following amination of the PDMS surface, cross-linkers have been used to covalently immobilize ECM. The ECM immobilized PDMS surface enabled to improve its cell adhesion properties through reliable ECM binding sites[1]. Based on the previous report[1], we anticipated that the ECM-immobilized PDMS substrate would enhance and maintain the cell adhesion properties even under mechanical stretch stress. Here, we fabricated ECM-immobilized PDMS surface by using 3-aminopropyltrimethoxysilane (APTMS), glutaraldehyde (GA) as a cross-linking agent, and collagen type I, referring to previous reports[1,2]. Then, we evaluated the characteristics of the surface as a substrate for stretching cell culture compared to collagen-physisorbed PDMS surface.

EXPERIMENTAL METHODS

Surface Modification of PDMS: PDMS (STREX Inc.) surfaces were treated with O_2 plasma (PL-PDMS). Collagen-immobilized PDMS (Col-GA-PDMS) surfaces was fabricated from PL-PDMS by using APTMS, GA, and collagen solution. Collagen-physisorbed PDMS (Col-PDMS) surfaces were prepared by immersing PL-PDMS surfaces in collagen solution. *Surface Analysis of PDMS:* The PDMS surfaces were analyzed by FT-IR/ATR and XPS. *Cell Culture under Static Condition:* Mouse myoblast C2C12 cells were cultured on the surfaces of PDMS for 24 h. *Cell Culture under Cyclic Mechanical Stretch Stress:* C2C12 cells were cultured on each well of stretchable PDMS chambers. Subsequently, uniaxial cyclic mechanical stretch stress was applied to the PDMS with an Automated Cell Stretching system (STB-1400, STREX Inc., 0.5 Hz, and 20% stretch ratio) for 2 d. *Cell Staining:* On day 2, the adhered cells were fixed followed by stained with rhodamine-conjugated phalloidin and DAPI.

RESULTS AND DISCUSSION

FT-IR/ATR and XPS analysis showed that collagen molecules were more abundantly deposited on the Col-GA-PDMS surface than on the Col-PDMS surface. As for the number of adhered cells under static condition, there was no significant difference among the surfaces of PL-PDMS, Col-PDMS and Col-GA-PDMS. However, adhered cells on the Col-GA-PDMS surface were more spread compared to PL-PDMS and Col-PDMS. After 24-hours cell culture under the static condition, uniaxial cyclic mechanical stretch stress was applied to these PDMS surface. Adhered cells on the Col-GA-PDMS surface were proliferated without cell detachment even under the applied stress condition, whereas some adhered cells on the PL-PDMS and Col-PDMS surfaces detached (Figure 1). Furthermore, actin stress fibers of the adhered cells were aligned perpendicular to the direction of the applied mechanical stretch stress (Figure1). These results suggest that the Col-GA-PDMS surface provides reliable collagen binding sites for adhered cells, resulting in the proliferation and alignment under mechanical stretch stress.

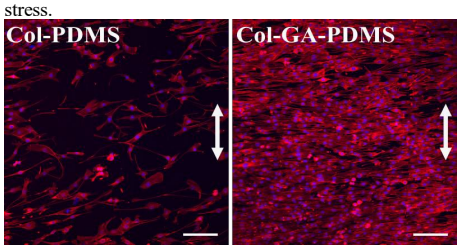

Figure 1. Actin staining of C2C12 cells. Filament-actin: red. Nuclei: blue. Double arrows: stretch direction. Scale bars: 200 μm.

CONCLUSION

Collagen-immobilized PDMS surface exhibited enhanced cell adhesive behavior compared to collagen-physisorbed PDMS. We conclude that collagen-immobilized surface is suitable for cell culture under cyclic mechanical stretch stress. Applying mechanical stretch stress for primary cells could be one of ideal approaches for tissue-engineering and regenerative medicine. In the presentation, we will also discuss the application of collagen-immobilized PDMS surface to stretching primary cell culture.

REFERENCES

1. Qian Z. *et al.*, Bioact. Mater. 3:167-173, 2018
2. Akiyama Y., et al., Biomacromolecules 19:4014-4022, 2018

ACKNOWLEDGMENTS

Part of this work was financially supported by JSPS KAKENHI, Grant Numbers JP18K12084 and JP19K20196.

LPCVD-deposition of silicon nitride coatings of high N content and mechanical properties

Huasi Zhou[1*], Cecilia Persson[1], Wei Xia[1], Håkan Engqvist[1]
[1]Dept. of Materials Science and Engineering, Uppsala University, Uppsala, Sweden
[*]huasi.zhou@angstrom.uu.se

INTRODUCTION

Lumbar disk replacement is one of the most effective surgeries to alleviate chronic lower back pain [1]. Although success rates of up to 80% after 2 years of implantation have been reported, the survival rates decrease significantly after 10 years due to micromotion and ions and wear particles being released from the implant [2]. These ions and wear debris could trigger an inflammatory response, leading to local bone resorption. One solution to this problem could be depositing a silicon nitride coating on the implant, as it could act as a barrier to metal ion release, in addition to resisting wear [3]. Silicon nitride coatings have also shown high wear resistance in several applications, but for the demanding in vivo environment, a very high coating density seems to be needed, something that can be challenging to achieve with physical vapor deposition techniques [4]. To solve this problem, silicon nitride coatings were deposited using a low-pressure chemical vapor deposition method (LPCVD). The purpose of this study was to explore the influence of deposition parameters on the composition, structure and mechanical properties of the coatings with the aim of obtaining dense coatings with adequate mechanical properties.

EXPERIMENTAL METHODS

All coatings were deposited by LPCVD (Koyo Thermo System, Japan) on Si (100) substrates. The influence of gas flow ratio (Ammonia (NH_3)/Dichlorosilane (DCS)) and deposition temperature on the coating properties were investigated (Table 1). The chemical structure of the silicon nitride coatings was analyzed by X-ray parallel beam diffractometry (XRD, D5000 Bruker, US) and X-ray photoelectron spectroscopy (XPS, Axis UltraDLD, Kratos Analytical, Manchester, UK). The morphology of the coatings was investigated by scanning electron microscopy (SEM, LEO 1530 Gemini, Zeiss, Jena, Germany) and the chemical composition by energy-dispersive X-ray spectroscopy (EDX). The hardness and elastic modulus of the coatings were measured by a nanoindenter (UNHT, Anton Paar, Austria) via indentation of a diamond Berkovich tip.

Table 1 Deposition parameters of the coatings

Coating group	Temperature (°C)	Flow ratio (NH_3/DCS)
1	790	2
2	790	3
3	790	4
4	790	5
5	790	6
6	640	4
7	690	4

RESULTS AND DISCUSSION

The XRD results indicated that the LPCVD-deposited silicon nitride coatings exhibited an amorphous structure, and the Si-N and Si-O bonds had a dominant contribution in the XPS core-level spectra. The N/Si ratio of the coatings increased with increasing NH_3 flow ratio, as expected. The morphology of the coatings was smooth and featureless (Fig.1). All samples showed an increase in hardness and elastic modulus after deposition, with maxima at around 26 GPa and 280 GPa, respectively. These values were higher than those of silicon nitride deposited with other techniques (such as PECVD, PVD and rHiPIMS), which is likely due to the higher N content of coatings deposited by LPCVD techniques. Compared with silicon-rich coatings, the stoichiometric coatings showed lower roughness and higher mechanical properties, indicating a better wear resistance. This is in agreement with previous findings for physical deposition methods, where a higher N content gave higher mechanical properties, albeit not reaching stoichiometry [5].

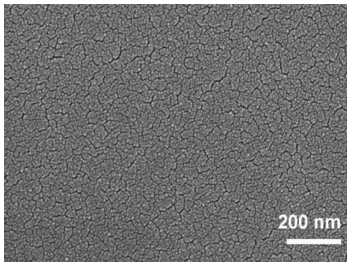

Fig.1 SEM image of a coating deposited at flow ratio (NH_3/DCS) of 4 and temperature of 790 °C.

CONCLUSION

Silicon nitride coatings were successfully prepared by LPCVD by changing the NH_3/DCS flow ratio and deposition temperature. This study showed that silicon nitride coatings made by LPCVD could have promising properties at optimal deposition parameters for spinal applications. Future work involves measurement of wear properties, density and dissolution rate.

REFERENCES

1. Freeman BJ. et al. (2016) European Spine Journal, 15(3):439-447.
2. Mahon. et al. (2018) Frontiers in immunology, 9:1145.
3. Schmidt, S. et al. (2019) Coatings,9(2):73.
4. Correa Filho, L. et al. (2020) Materials, 13(8):1896
5. Skjöldebrand, C. et al. (2020) Materials, 13(9):2074.

ACKNOWLEDGMENTS

This research has received funding from the European Union's Horizon 2020 research and innovation programme under the Marie Skłodowska-Curie grant agreement No 812765.

Biological activation of the surfaces of dental implant-abutment materials Y-TZP and Ti6Al4V by hydrolytically stable immobilization of fibronectin and laminin

Alena L. Palkowitz[1], Taskin Tuna[2], Shaza Bishti[2], Nathalie Steinke[3], Gerhard Müller-Newen[4,5], Stefan Wolfart[2], Horst Fischer[1]

[1] Department of Dental Materials and Biomaterials Research, RWTH Aachen University Hospital, Aachen, Germany
[2] Department of Prosthodontics and Biomaterials, RWTH Aachen University Hospital, Aachen, Germany
[3] Flow Cytometry Facility, IZKF, Faculty of Medicine of RWTH Aachen University, Aachen, Germany
[4] Institute of Biochemistry and Molecular Biology, RWTH Aachen University Hospital, Aachen, Germany
[5] Confocal Microscopy Facility, IZKF, Faculty of Medicine of RWTH Aachen University, Aachen, Germany

*apalkowitz@ukaachen.de

INTRODUCTION

In addition to the osseointegration of the implant material's surface, a sufficient adhesion of the abutment's surface to the soft tissue is crucial to guarantee the longevity of the implant. The soft tissue seal surrounding natural teeth acts as a barrier against deleterious stimuli in the oral cavity, thus preventing bacteria penetration and protecting the underlying alveolar bone. However, the peri-implant mucosa around the abutment is different from the mucosa around natural teeth, which can result in a poorly bacterial resistance[1]. To overcome this limitation, here we propose a novel method to biofunctionalize abutment materials surfaces through the covalent conjugation of specific proteins to enable a stable soft tissue adhesion.

EXPERIMENTAL METHODS

A silane monolayer was applied on the established abutment materials (Y-TZP and Ti6Al4V) with subsequent coupling of proteins of the extracellular matrix (ECM), fibronectin and laminin, via a bifunctional crosslinker (BS^3). The successful application was proved by XPS, AFM, and immunostaining. Preserved biofunctionality of the ECM proteins after surface coupling was shown in a centrifugation-assay. Proliferation, cell adhesion, and migration behavior of human gingival fibroblasts and epithelial cells on the ECM-modified and non-modified specimens as a control was investigated additionally. Furthermore, the expression of focal adhesions on modified and unmodified specimens was investigated via Western Blot. Moreover, integrin expression of gingival cells on the individually modified surfaces was determined via confocal microscopy and flow cytometry. Stability of the applied substances on both specimens was tested via mechanical exposure, acid and heat resistance and was examined using XPS, AFM and ELISA.

RESULTS AND DISCUSSION

The centrifugation-assay showed that gingival cells seeded onto the ECM-protein-coupled surfaces, which were speeded up to 50g exhibited significantly higher adhesion ($p < 0.001$) in comparison to non-functionalized controls. In addition, a proliferation assay (CCK-8) showed that significantly more cells ($p < 0.05$) were evident after seven days on ECM-modified surfaces compared to non-functionalized surfaces. Confocal microscopy revealed a much higher cell area (up to threefold) and enhanced expression of pFAK-Y397 and vinculin on ECM protein-coated surfaces compared to the controls. Moreover, the wound healing assay demonstrated, that cells seeded on ECM-modified surfaces exhibited significant more migration activity compared to untreated specimens. Stable attachment of the ECM proteins over 21 days was confirmed via ELISA.

CONCLUSION

Covalent conjugation of ECM proteins by cross-linking on the abutment material surfaces Y-TZP and Ti6Al4V enables improved adhesion, proliferation, and migration of gingival cells. Therefore, in future clinical applications, this novel approach could lead to improve soft tissue adhesion and thus potentially prevent bacterial penetration through the soft tissue-abutment interface. Finally, this biofunctionalization approach could contribute to reduce or even prevent peri-implant diseases.

REFERENCES

1. Yang Z. et al., RSC Adv. *10*, 6200–6212, 2020

ACKNOWLEDGMENTS

We acknowledge the financial support of the German Research Foundation, DFG (grants FI 975/30-1+2 and WO 1576/6-1+2).

CONCEPTION AND EVALUATION OF AN ANTIBACTERIAL / VIRUCIDAL SURGICAL MASK AGAINST SARS-CoV-2 (COVID-19)

Mickael Maton[1], Sarah Gabut[1], Gaëtan Gerber[6], Christel Neut[3], Marc Frouin[6], Michele Vialette[5], Camille Sacareau[5], Pascal Odou[4], Bernard Martel[2], Nicolas Blanchemain[1]

[1] Univ. Lille, INSERM, CHU Lille, U1008, Advance Drug Delivery System, Lille, France
[2] Univ. Lille, CNRS UMR8207, UMET – Unité Matériaux et transformations, Villeneuve D'Ascq, France
[3] Univ. Lille, INSERM, CHU Lille, U1286, Institute for Translational Research in Inflammation, Lille, France
[4] Univ. Lille, CHU Lille, ULR 7365 - GRITA, Lille, France
[5] Unité de Sécurité Microbiologique, Institut Pasteur de Lille, Lille, France
[6] Bioserenity, 47 bd de l'Hôpital, Paris, France

mickael.maton@univ-lille.fr

INTRODUCTION

One of the strategies to fight against COVID-19 (SARS-COV2) pandemic is to wear a mask in the general population. The wearing of masks reduces the emission of infected drops, and reduce significantly the incidence of COVID-19 [1].
The activity of the respiratory masks is based on physical filtration of the particles suspended in the air. To improve efficiency against respiratory pathogens, we applied a functionalization process of masks to add an antibacterial and virucidal molecule. Benzalkonium chloride (ADBAC) is commonly used as a disinfectant molecule for surfaces. This molecule is a quaternary ammonium molecule with a strong activity against bacteria and viruses. The respiratory masks are composed of different layers of polypropylene (PP) textile, the filtration is permit by an Meltblown non-woven layer with fibers network of 50g/m² density. We worked on the fixation of an anionic cyclodextrin polymer on this layer to fix the cationic ADBAC. The aim of this work is to evaluate the safety, the microbiological and virucidal activity of the mask.

EXPERIMENTAL METHODS

The Meltblown non-woven textile (M50, Lydall, France) was functionalized by pay dry cure method with an aqueous solution of cyclodextrin (CD, Roquettes, France), polycarboxilic acid, and a catalyst. The M50 coated by CD was immersed in ADBAC solution at concentrations of 0.2%, 0.5% and 1% (M50-02%, M50-05%, M50-1%) during 1 min and dry in oven at 100°C. The free fraction of ADBAC on samples was determined by the same method after 1, 2 or 3 rinsing in 1 mL of ultrapure water during 1min. The total amount of ADBAC was determined by immersion in 1 mL 0.1N NaOH solution during 4 hours under 80rpm agitation at 37°C. Each solution obtained were analysed by UHPLC (LC2040, Shimadzu, Japan) with a reversed phase CN-column (150x4.6mm, 5µm, Fortis, England). The microbiological activity was determined by diffusion test and kill time test on *S.aureus* ATCC 6538 strain, according the JIS 2801/2000 guidelines after 20 min and 240 min of contact. The kinetic of virucidal activity was performed by deposit of the human coronavirus HCoV-229E on the samples (2x2cm, 0,4g per sample) according to ISO 18184 standard.

RESULTS AND DISCUSSION

The determination of the total amount of ADABC on the sample with 0.2%, 0.5% or 1% ADBAC solutions shows respectively an amount of 44.6 µg/cm², 87.5 µg/cm² and 134.0 µg/cm² of M50 coated by CD polymers textile. After 1 rinsing, the amount of, ADBAC are respectively around 45.0µg/cm², 65.9µg/cm² and 91.4µg/cm². A strong interaction between ADBAC and CD coating was proved. The kill time kinetics shows a 0.6 log reduction of *S.aureus* after 20 min of contact for M50-0.2%, 2.98 log for M50-0.5% and 4.23 log for M50-1%. After 240 min of contact, the reduction is respectively 3.44 log, 4.79 log and 5.57 log without rinsing. The rinsing step of the samples reduce the antibacterial activity. The virucidal activity test highlighted a reduction of 87.9% of HCoV-229E after 20 min, 99.7% after 1h for M50-02%. A virucidal activity was observed for MS50-0.5% with 99.90% of HCoV-229E reduction after 5min and 99.94% after 20 min of contact.

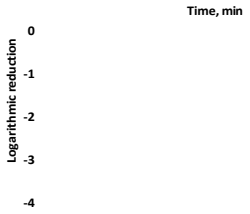

Figure 1 – Virucidal activity of MS50-0.2% and MS50-0.5% against HCoV-229E

CONCLUSION

The functionalization by the CD-polymer permit to fix the ADBAC, the concentration of ADBAC used for impregnation increase the amount od ADBAC on samples, and the activity on the pathogens.
The good results of our tests on HCoV-229E shows a rapid reduction of the viruses.

REFERENCES

[1] Cheng and al. Journal of infection, 81, 107-114, 2020.
[2]SJ Prince and al. Journal of Pharmaceutical and Biomedical Analysis, 19, 877-882. 1999

Rapid inactivation of SARS-CoV-2 by oxidized silicon nitride powders

I. Katsaros[1], J. Ling[2], G.Akusjärvi[2], Å. Lundkvist[2], C. Persson[3], W. Xia[1], H. Engqvist[1]

1. Division of Applied Materials Science, Department of Materials Science and Engineering, Uppsala University, Sweden
2. Department of Medical Biochemistry and Microbiology, Uppsala University, Sweden
3. Division of Biomedical Engineering, Department of Materials Science and Engineering, Uppsala University, Sweden
* ioannis.katsaros@angstrom.uu.se

INTRODUCTION

The importance of establishing ways to hinder the spread of pathogens has been emphasized by the most recent global pandemic caused by the severe acute respiratory coronavirus (SARS-CoV-2). To that end, antiviral materials can play a significant role by inactivating pathogens upon contact with them. Silicon nitride (Si_3N_4) is a material that has been shown[1] to be effective at inactivating pathogens through the micro-elution of biocidal ammonia from its surface. In maximizing pathogen attachment and inactivation, properties like surface charge and hydrophilicity are important. Those properties can be adjusted in Si_3N_4 by modifying the surface of the material. In this study, we present a surface modified silicon nitride material aimed at increased absorption and inactivation of SARS-CoV-2.

EXPERIMENTAL METHODS

Silicon nitride powders (Luoyang Tongrun Technology, Henan, China) were oxidized through a heat treatment at 1070° C for 7 hours. This treatment has been shown to produce a highly hydrophilic and negatively charged material, improving SARS-CoV-2 attachment[2]. The effects of the heat treatment on the material were examined through transmission electron microscopy (Titan Themis 200, Thermo Fischer Scientific, Massachusetts, USA), X-ray photoelectron spectroscopy (Quantera II, Physical Electronics), X-ray diffraction (D500, Bruker, Massachusetts, USA) and water contact angle measurements. SARS-CoV-2 (PM5, Swedish isolate) viral solutions were brought in contact with test materials and controls for one, 10, and 60 minutes. Thereafter, viral infectivity and viral RNA fragmentation were examined through plaque-forming unit and real-time quantitative polymerase chain reaction assays (Zymo Research, California, USA), respectively. For the plaque-forming unit assay, epithelial Vero E6 cells were utilized. Copper (Sigma-Aldrich Missouri, USA) and untreated viral solutions were used as positive and negative controls, respectively.

RESULTS AND DISCUSSION

The heat treatment resulted in silicon nitride surfaces comprised mainly of silicon dioxide with low amounts of nitrogen, the driving force behind the antiviral properties of the material. Nevertheless, the material was highly effective at reducing viral infectivity at both room and homeostatic temperatures. Furthermore, a higher degree of genome fragmentation was observed on virions treated with the surface-modified Si_3N_4 powders compared to the copper controls (Fig.1).

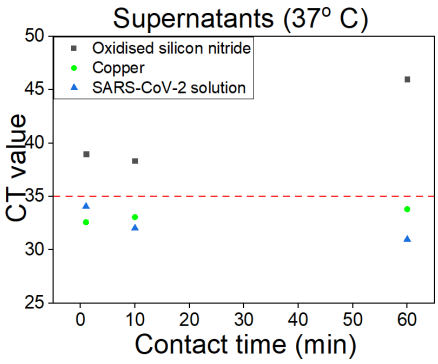

Figure 1 The results of the qPCR assay on supernatants of the treated viral solutions showed that the oxidized silicon nitride powders led to fragmentation of the viral RNA (CT values>35) after incubation at 37° C.

CONCLUSION

This study showed that the oxidized silicon nitride powders were successful at significantly reducing the infectivity of SARS-CoV-2 as rapidly as after one minute of contact. The results of this study indicate that the material that was specifically engineered for antiviral applications could be used as a tool in the fight against the viral spread.

REFERENCES

1. G. Pezzotti *et al*., Sci. Rep., 11:2977, 2021.
2. E. Joonaki *et al*, Chem, 6:2135–2146, 2020.

ACKNOWLEDGMENTS

This project has been supported by Vinnova (2020-03099) and has received funding from the European Union's Horizon 2020 research and innovation programme under the Marie Sklodowska-Curie grant agreement No 812765 and the Swedish Cancer Foundation (grant nr. 180599). We would like to thank the donation from "Wefightcovid" (SPR).

Salt-assisted compaction for the design of biocompatible albumin materials for the sustained delivery of antibacterial molecules

Eya Aloui[1], Jordan Beurton[1], Ludivine Hugoni[1], Claire Medemblik[2,3], Benoît Frisch[1], Philippe Lavalle[2,3]

[1]Laboratoire de Conception et Application de Molécules Bioactives, CNRS UMR 7199, University of Strasbourg, Illkirch, France
[2]Laboratoire de Biomatériaux et Bioingénierie, INSERM UMR 1121, University of Strasbourg, Strasbourg, France
[3]Faculté de Chirurgie Dentaire, University of Strasbourg, Strasbourg, France
e.aloui@unistra.fr

INTRODUCTION

A new era in the design of implantable natural materials should emerge to deal simultaneously with issues related to the toxicity of degradation products, inflammation, infections, and controlled release of loaded drugs. We selected albumin-based materials primarily because of their biocompatibility and biodegradability. Furthermore, albumin, the most abundant protein in plasma, is a versatile carrier for many drugs and substances and it can be produced at low cost[1,2]. Albumin-based materials were already fabricated using a number of processing techniques[1,3–5]. However, all methods described in previous studies require the crosslinking of the proteins, which can be attained by using chemical agents such as glutaraldehyde, enzymes such as transglutaminase, or heat aggregation at high temperature and alkaline pH. These methods lead to the denaturation of the protein, resulting in a loss of its original biological properties with the risk to generate new antigenic sites which could trigger a strong inflammatory response[1,2]. Albumin membranes formulated by salt-assisted compaction represent a new class of materials (European patent application EP3811982). Salt-assisted compacted was developed to prepare stable albumin materials without toxic crosslinking agent and denaturing conditions. Here, we establish the proof of concept for the use of these materials in the design of biodegradable devices for the delivery of gentamicin, a potent antimicrobial drug.

EXPERIMENTAL METHODS

The materials were prepared by evaporation of a solution of bovine serum albumin (BSA) in the presence salt (NaBr) at 37 °C and pH 6 until the formation of dry materials.
The loading of gentamicin into albumin materials was performed by mixing gentamicin (0.1% wt gentamicin/wt albumin) in the solution of BSA and NaBr. After evaporation of this solution, gentamicin-loaded albumin materials (GENTA-BN) were obtained. They were washed in milliQ water and used for further *in vitro* evaluation.

RESULTS AND DISCUSSION

After evaporation and salt-elimination through washing in milliQ water, the albumin materials prepared by salt-assisted compaction (BN) were water-insoluble and stable in aqueous media.

.The biological evaluation of BN materials in vitro showed that they were biocompatible and biodegradable *in vitro* (direct and indirect cytotoxicity on Balbc 3T3) and *in vivo* (subcutaneous implantation in Nude mice).
GENTA-BN materials were non-cytotoxic to NiH3T3 fibroblasts after incubation for 1 to 7 days. Therefore, these materials maintain their biocompatibility *in vitro* after gentamicin loading.
GENTA-BN materials exhibited antimicrobial properties when cultivated with *E. coli* and *S. aureus* by inhibiting the growth of these bacteria. To further evaluate the antimicrobial properties of these materials, extracts prepared by incubating GENTA-BN materials in PBS were collected every 24 h for 8 days. These extracts inhibited the growth of *E. coli* and *S. aureus*, indicating that GENTA-BN materials release active gentamicin in the culture media, providing an antimicrobial effect lasting up to 8 days.

CONCLUSION

Salt-assisted compaction allows the preparation of materials entirely made of water-insoluble human albumin. These materials are biocompatible and biodegradable in vitro and in vivo. They are a good candidate for the design of drug delivery devices. When loaded with gentamicin, these materials inhibited the growth of *E. coli* and *S. aureus* by releasing the drug in the media for up to 8 days.

REFERENCES

1. Rohanizadeh R,. et al., J. Mater. Sci. –Mater. M. 20(12):2413–8, 2009
2. Peters T. Academic Press; 432 p. 1995
3. Raja S. et al., Sci. Rep. 5(1):15977. 2015
4. Aiyelabegan H. et al., Int. J. Polym. Mater. Po. 65(16):853–61, 2016
5. Li P-S. et al., Sci. Rep. 4(1):5600, 2015

ACKNOWLEDGMENTS

This work was funded by Conectus as part of the maturation project Albupad.

Development of new antimicrobial peptides by recombinant protein technology to functionalize orthopedic biomaterials

Cristina Cantallops[1], Anne Leriche[1], Franck Bouchart[1], Edwige Meurice[1*]

[1]CERAMATHS-DMP, UPHF, Cambrai, France
[*] edwige.meurice@uphf.fr

INTRODUCTION

The increase of bacterial infections after a bone surgery is explained by the increase of the procedures. Moreover, the rise of antibiotic resistant infections led to the research of new antimicrobial agents. Antimicrobial peptides (AMP) are alternatives to antibiotics, shows good biocompatibility and can be produced by recombinant protein technology(1).

Cathelicidins and defensins are natural antibacterial peptides synthesized by the immune system of different organisms, including human, to counteract bacterial infections. Their mechanism of action usually involves the disruption of the bacterial membrane and the mobilization of immune cells.

In this study, we engineered AMP based on defensins design by molecular biology technology. To allow the functionalisation of biomaterials, a collagen-like region had been fused to AMP. Indeed, numerous studies had shown that collagen or collagen-like peptides can support bone cell adhesion (2). Here, the collagen would have 2 purposes : support cell adhesion and provide a binder for AMPs.

Structure and antibacterial activities have been studied on both AMPs alone and fused with the collagen-like region.

EXPERIMENTAL METHODS

In a first approach, AMPs have been cloned in an expression plasmid designed for protein production in bacteria. Then, AMP has been purified by chromatography from bacteria transformed with the plasmid. Some specific constructions has been done for allowing disulfide bonds formation of specific AMPs derived from defensins.

The structure and antibacterial activities of AMPs have been studied along with their cytotoxicity.

RESULTS AND DISCUSSION

The first produced AMP shows promising antibacterial activity and low cytotoxicity. Then, this AMPs are good candidates for biomaterial functionalisation. Their stability in time alone or with bone materials will be check.

CONCLUSION

The results led us to synthesize new antimicrobial peptides (AMP) in fusion with a collagen-like region as a binder. The recombinant protein technology used here allows the production of different peptides, included the peptides with disulfides bonds difficult to produce by chemical methods. This peptides are good candidates for the functionalization of biomaterials.

REFERENCES

1- Büyükkiraz & Kesmen, *J.Appl Microbiol.* 132:1573,2022.

2- An B, *et al, Front Chem*.,2:40, 2014

ACKNOWLEDGMENTS

This project is part of the Antimicrobial Integrated Methodologies (AIMed) project which has received funding from the European Union's Horizon 2020 research and innovation programme under the Marie Skłodowska-Curie grant agreement AIMed No 861138.

Development of antibiofilm compress with natural active ingredient for the treatment of infected wounds

Damien Seyer[1], Maxime Gobin[1,2], Céline Des Courtils[2], Stéphane Lack[2], Laura Duciel[2], Adeline Gand[1], Emmanuel Pauthe[1]

[1]Equipe de Recherche sur les Relations Matrice Extracellulaire Cellules, CY Cergy-Paris Université, France

[2]Les Laboratoires Brothier, Nanterre 92735, France

* damien.seyer@cyu.fr

INTRODUCTION

Wounds prevention and care is a major public health[1] issue especially in the context of critical pathogen colonization[2] and bacteria biofilm formation[3], that can delay wound healing[4] by acquiring properties such as increased antibiotic tolerance and virulence[5]. In the context of chronic and exudative wounds, calcium alginate compresses are commonly used as they favor wound healing thanks to their bioactive properties and high capacity to eliminate wound fluids while maintaining optimal wound moisture[6]. However they do not possess antiseptic/antimicrobial properties. Here we developed calcium alginate dressings functionalized with natural molecules conferring antimicrobial and antibiofilm properties against bacteria most commonly found in wounds: *Pseudomonas aeruginosa* and *Staphylococcus aureus*. We focused on three natural molecules: gallic acid (G), carvacrol (K) and curcumin (Q) extracted respectively from galls, oregano and turmeric. The efficiency of the natural molecules in solution or incorporated in the compress, individually or in combination, was examined on 24h-old mono or dual species biofilms. The formulation was also optimized to stabilize the active ingredients in the compress *via* cyclodextrin encapsulation.

EXPERIMENTAL METHODS

MICs and MBCs were determined according to the European Committee on Antimicrobial Susceptibility Testing recommendations using the broth microdilution method. To assess the efficiency of active ingredients in solutions, within the compress or encapsulated or into cyclodextrin on mono or dual-species biofilm, solutions ranging from 0,25 to 5mg/mL are put in contact with mature biofilms for 24h at 37°C, individually or in combination, and viable bacteria are enumerated. Biomass viability in biofilm was assessed by LIVE/DEAD staining. Images were performed using confocal scanning laser microscopy. Active ingredient stability was determined by HPLC and the encapsulation in cyclodextrin was assessed by ITC and NMR.

RESULTS AND DISCUSSION

We observed a bacterial growth inhibition with the three selected natural compounds in solution, and G and K provide in addition bactericidal properties. G presents strong antibiofilm properties on *P. aeruginosa* biofilm (5,8 Log-reduction - LR) and a lower activity on *S. aureus* biofilm (2,0 LR). Conversely, we observed that K has the strongest antibiofilm activity on *S. aureus* biofilm (6,6 LR / K 0,5 mg.ml^{-1}, 8,2 LR/ K 5 mg.ml^{-1}) which is lower on *P. aeruginosa* biofilm (1,9 LR LR / K 0,5 mg.ml^{-1}, 4,2 LR / K 5 mg.ml^{-1}). The combination of both molecules increases the antibiofilm effect previously observed on *P. aeruginosa* biofilm (6,7 LR) and leads to a complete eradication of *S. aureus* biofilm. This combination was also tested on dual-species biofilm of *S. aureus* and *P. aeruginosa* and was shown to exhibit a strong antibiofilm effect (5,4 LR / K 0,5 - G 5 mg.ml^{-1}). Compresses containing K or G have antibiofilm efficiency on *S. aureus* (at least 5 LR) and combinations K-G have a strong antibiofilm effect on both mono-species biofilm (4,5 LR *P. aeruginosa*, 7,5 LR *S. aureus*). In both cases the antibiofilm effect is due to the presence of molecules that destabilize the biofilm and the ability of the compress to absorb and retain bacteria.

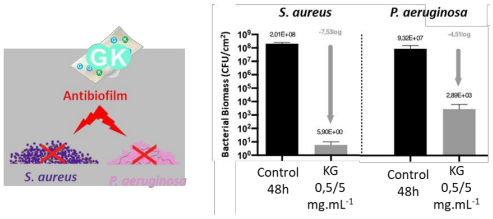

Nevertheless, K and G are small phenolic compounds highly volatile that leak out of the compress over time. We thus decided to stabilize the ingredients *via* cyclodextrin encapsulation. The encapsulation of G and K increases the stability of the ingredients but there is a loss of activity for G while K remains highly active in solution on *S. aureus* biofilm (8,2 LR / K 5 mg.ml^{-1}). The K encapsulated incorporated in the compress lead to the total eradication of *S. aureus* biofilm.

CONCLUSION

Here we show that calcium alginate compresses functionalized with an association of active ingredients have strong antibiofilm effect on *S. aureus and P. aeruginosa* mature biofilms. K, small volatile phenolic compound, can be stabilized via cyclodextrin encapsulation while maintaining its antibiofilm activity. Compresses containing combinations of natural active ingredients may then represent efficient alternatives for the treatment of biofilms in wounds.

REFERENCES

1 -Govindaraj Vaithinathan A *et al.*, Perspect Public Health 2018;138(2):87-88

2- Edmiston CE *et al.*, Wound Care, 2016, 25(12)

3- Omar A *et al*, *Microorganisms* 2017, *5*(1), 9

4 - Fromantin I. *et al*, 2018 Wound Medicine

5- Akers *et al.*, BMC Infectious Diseases, 14, 190

6- Lalau JD, *et al.,* Diabetes Metab 2002; 28(3):223-9

Contact inactivation of human adenovirus type 5 by silicon nitride ceramics

I. Katsaros[1], A. Carlsson[2], C. Persson[3], G.Akusjärvi[2], W. Xia[1], H. Engqvist[1]

1. Division of Applied Materials Science, Department of Materials Science and Engineering, Uppsala University, Sweden
2. Department of Medical Biochemistry and Microbiology, Uppsala University, Sweden
3. Division of Biomedical Engineering, Department of Materials Science and Engineering, Uppsala University, Sweden

* ioannis.katsaros@angstrom.uu.se

INTRODUCTION

Containing the spread of pathogens and treating the diseases they cause have become topics of high importance and urgency. The recent coronavirus disease (COVID-19) pandemic, has highlighted the devastating results virus infections can have on our society. Uncovering and utilizing materials for the protection from and treatment of virus-induced diseases can considerably alleviate the load imposed on healthcare systems worldwide. Silicon nitride is a biocompatible ceramic material used in orthopedic implants that is effective in the inactivation of single-stranded RNA viruses, in powder form[1]. However, the effect of the material on the more resilient DNA viruses remains unknown. This study aimed to investigate the antiviral behavior of the material, in powder and bulk form, against DNA viruses, and more specifically the human adenovirus.

EXPERIMENTAL METHODS

Silicon nitride was used in both powder and bulk form, while copper was used as a positive control. The powder samples were purchased from Luoyang Tongrun Technology (Henan, China) and Sigma-Aldrich (Missouri, USA), respectively, while the bulk samples were spark plasma sintered based on the work by Fu et al[2]. The morphology and phase composition of the test materials were examined by scanning electron microscopy (JEOL 1550, Zeiss, Jena, Germany) and X-ray diffractometry (D500, Bruker, Massachusetts, USA), respectively. The surface roughness of the bulk samples was measured by optical profilometry (ZYGO, Connecticut, USA) while inductively coupled plasma - optical emission spectrometry (PerkinElmer ICP-OES, Avio 200, PerkinElmer, Inc. USA) was used to measure ion release from samples and controls.

The human type 5 adenovirus was chosen to infect epithelial cells of the A549 line. Viral solutions were brought in contact with the materials for one, 10 and 60 minutes in the case of the powders and 10 and 60 minutes for surfaces, before infection. The Dual-Luciferase Reporter Assay System (DLR) (Promega, Wisconsin, USA) was then used to assess viral infectivity.

RESULTS AND DISCUSSION

The results of the study indicated that silicon nitride dramatically reduces adenoviral infectivity in powder (>98% reduction in infective virus compared to untreated samples) (Fig. 1) and bulk form (>73% reduction in infective virus compared to negative control). In both cases, inactivation was achieved rapidly, in one minute for powders and 10 minutes for bulk surfaces. The inactivation rates of the materials in powder form are similar to those noted for RNA viruses tested in literature[3].

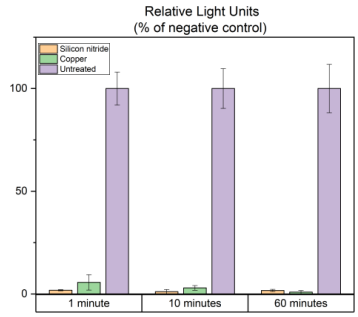

Figure 1 The results of the Luciferase assay for test powders and controls for after one, 10 and 60 minutes indicated a clear decrease of infectivity in samples treated with test and control powders.

CONCLUSION

The findings of this study provide enhanced support for the use of silicon nitride as an antiviral agent in common touch surfaces, aiding the fight against the spread of diseases caused by both DNA and RNA viruses.

REFERENCES

1. Pezzotti G. *et al*., Materials Today Bio.12, 2021
2. Fu L. *et al*., Applied Materials Today. 12:260–275, 2018
3. Pezzotti G. *et al*., Scientific Reports.11:1-18, 2021

ACKNOWLEDGMENTS

This project has been supported by Vinnova (2020-03099) and has received funding from the European Union's Horizon 2020 research and innovation programme under the Marie Sklodowska-Curie grant agreement No 812765 and the Swedish Cancer Foundation (grant nr. 180599). We would like to thank the donation from "Wefightcovid" (SPR).

An attempt to develop new Ti-based BMGs for dental implantology by means of Machine Learning and experimental assessment.

Yohan Douest[1,2], R. M. Forrest[3], Benoît Ter-Ovanessian[2], Nicolas Courtois[1], Damien Fabrègue[2], Jérôme Chevalier[2]

[1]Anthogyr SAS, 2237 Av. André Lasquin, 74700 Sallanches, France
[2] INSA-Lyon, University of Lyon, UMR CNRS 5510 MATEIS, 20 Avenue Albert Einstein, 69621 Villeurbanne CEDEX, France
[3]Department of Materials Science and Metallurgy, University of Cambridge, 27 Charles Babbage Road, Cambridge CB3 0FS, United Kingdom

Corresponding author. E-mail address: yohan.douest@anthogyr.com

INTRODUCTION

Even if Ti-alloys can exhibit impressive mechanical properties, they seem to reach a plateau in terms of yield strength, which limits further downsizing. One solution to reduce the size of the implants systems, and hence reduce the postoperative invasiveness, might come from amorphous metallic alloys. With a compressive yield strength that is twice the one of Ti-6Al-4V ELI and with a Young's modulus of 105 GPa, $Ti_{40}Zr_{10}Cu_{36}Pd_{14}$ Bulk Metallic Glasses appear as promising materials to be used in the next generation of mini-implants[1]. However, specific drawbacks to this class of material persist and delay its use in biomedical fields. First, the high copper content is controversial, one arguing its potential toxicity and other claiming its benefits as an antibacterial agent. Moreover, copper elements might act as an initiation site for pitting corrosion especially in chloride containing environments[2]. Lastly, Ti-based BMGs suffer from inhomogeneity in their structure which results in the presence of crystalline casting defects (also called spherulites) decreasing its overall properties[3]. It is therefore essential to develop new copper-low Ti-based with higher Glass Forming Ability (GFA) BMGs through conventional and innovative strategy like Artificial Intelligence (AI) driven approaches.

EXPERIMENTAL METHODS

Novel copper-low and copper-free Ti-based candidate compositions were proposed thanks to a Machine Learning (ML) regression model. Based on nearly 500 already known BMG compositions, the genetic algorithm combined with a neural network correlated experimental Glass Forming Ability (GFA) criteria with the nominal composition of the alloys.
The materials selected from the ML strategy were then prepared by arc melting the mixtures of pure elements (purity > 99.9%) under a high-purity argon atmosphere. Rod samples with a diameter of 3 mm were cast either by suction casting. The assessment of the amorphous structure was determined by XRD and SEM observations.

RESULTS AND DISCUSSION

Two compositions from the Ti-Zr-Cu-Pd and Ti-Zr-Hf-Pd-Si systems were predicted by the ML model as the best compromise of low/free-copper content and high GFA. As of yet, none of these compositions have been successfully cast into fully amorphous rods. The difference between the predicted and the experimental GFA might come from the weakness of the current GFA criteria which are highly dependent on process and characterisation conditions.

CONCLUSION

These results highlight the limits of ML prediction for the discovery of new BMGs which should be used more as a rough guide rather than for specific composition fine-tuning tool.

REFERENCES

1. Liens A. *et al.*, Material, vol. 11 n°2, (2018)
2. Calin M. *et al.*, Proc. Mat. Sci.C 121, 111733 (2021)
3. Gautier L. *et al.,* Materiala vol. 21 101353, (2022)

ACKNOWLEDGEMENTS

F. Tancret is acknowledged for the very useful comments and suggestions on machine learning approaches.
This project has received funding from the European Union's Horizon 2020 research and innovation programme under the Marie Skłodowska-Curie grant agreement No. 861046.

Antibacterial CATH-2 Peptide Coating to Prevent Implant Related Infection

Pardis Keikhosravani[1*], Fatemeh Jahanmard[1], Leonardo Cecotto[1], Azin Khodaei[1], Floris J. Bikker[2], Kamran Nazmi[2], Bart van der Wal[1], Charles Vogely[1], Enrico Mastrobattista[3], Harrie Weinans[1], Saber Amin Yavari[1]

[1]Department of Orthopedics, University Medical Center Utrecht, Utrecht, The Netherlands
[2] Department of Oral Biochemistry, Academic Center for Dentistry Amsterdam (ACTA), the Netherlands
[3] Department of Pharmaceutical Sciences, Utrecht University, Utrecht, The Netherlands

[*] p.keikhosravani-2@umcutrecht.nl

INTRODUCTION

Implant-associated infections (IAI) are caused by bacteria that initially colonize on the surface of the implant and proceed to a mature biofilm form which shields bacteria from antibiotics and immune cell clearance [1]. Host defense peptides (HDPs) are considered interesting broad-spectrum alternatives to antibiotics in prevention of IAI [2]. In particular, the chicken HDP CATH-2 (amino acids: RFGRFLRKIRRFRPKVTITIQGSARF) causes a direct disruption of the microbial cytoplasmic membrane based on its strong cationic character [3]. In this study, we first applied a polycaprolactone (PCL) coating via electrospraying on titanium implant surfaces as drug carrier followed by dip coating of CATH-2 peptides. To increase the absorption of peptide on the PCL layer, two different methods namely NaOH treatment of PCL and dissolving CATH-2 in water/ethanol was used.

EXPERIMENTAL METHODS

PCL (25 mg/ml) was dissolved in chloroform solvent at room temperature after stirring for 2h to have a complete dissolution. The PCL solution was applied by electrospraying method under 8 kV voltage, flow rate of 2.0 mL/h and sample distance from nozzle of 100 mm.

As per the first surface modification, the PCL-coated samples were immersed to 1M NaOH at room temperature for 30 mins, followed by three times rinsing with deionized (DI) water. Subsequently, 20 µl of CATH-2 (0.5 mg/ml) with two different solvents of water and water/ethanol (75:25) was electrosprayed on the treated and untreated samples, respectively.

In vitro antibacterial activity behavior was investigated by colony-forming unit (CFU) of Methicillin-resistant *Staphylococcus aureus* strain (SH100). After incubation for different time-points (3 and 12h), the released solution was collected for the CFU counting. On the other hand, cytotoxicity of the coated implants was tested by Alamar blue assay and compared with the control groups. Moreover, water contact angle was evaluated to measure any changes in the hydrophilicity of PCL after the surface treatments.

One-way analysis of variance (ANOVA) was performed using Statistical Package for the Social Sciences (SPSS) 20.0 software. A p-value less than 0.05 ($p < 0.05$) was considered to have statistical significance.

RESULTS AND DISCUSSION

The antibacterial properties of all the CATH2 coated groups were 100% successful in killing the planktonic bacteria after three hours disregarding the surface modifications. In terms of the cytotoxicity, Alamar blue test verified no significant difference among the groups. Nonetheless, only the surface treated group with the solvent yielded the best antibacterial properties after 12h (Fig 1B). This was rendered through higher wettability of the surface treated PCL group by ethanol. In fact, ethanol eliminated the trapped air as it infiltrated the spaces in the polymer surface and increased the PCL permeability [4]. Further experiments to optimize the peptide release kinetic and extend the antibacterial properties of the coating is ongoing.

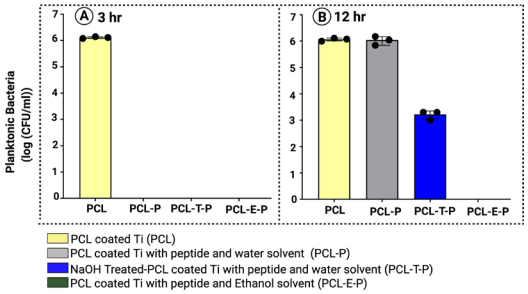

Figure 1 CFU counting of the planktonic bacteria after 3 and 12h incubation.

CONCLUSION

The electrosprayed PCL coating contained CATH-2 displayed enhanced antibacterial properties without any cytotoxicity. The increased hydrophilicity of the surface treated PCL secured the longer presence of CATH-2 in the coating thereby extended the antibacterial properties from 3 to 12h. Consequently, the use of CATH-2 in the novel antibacterial coating may provide an excellent option to combat against perioperative IAIs.

REFERENCES

[1] A. Trampuz, *et al.*, J. Current opinion in infectious diseases 19(4) (2006) 349-356.
[2] S. Amin Yavari, *et al.*, Advanced Materials 32(43) (2020) 2002962.
[3] M.R. Scheenstra, *et al.*, J. Scientific reports 9(1) (2019) 1-12.
[4] N. Hirano, *et al.*, J. PloS one 16(7) (2021) e0253149-e0253149.

Introducing Mixed Reality within the confines of the operating room

Titouan Nguyen Huynh[1,2], Stan Larroque[3], Marc Piuzzi[3], Patrick Nataf[2,4]

[1]CentraleSupélec, Université Paris-Saclay, Paris, France
[2]INSERM U1148, Université Paris Cité, X Bichat hospital, Paris, France
[3]Lynx Medical, Paris, France
[4]Interventional Cardiology Department, APHP, X Bichat hospital, Université Paris Cité, Paris, France

patrick.nataf@aphp.fr

INTRODUCTION

One could easily spot the benefits of adding mixed reality (the combination of virtual reality and augmented reality, usually designated by XR) as one of the tools for surgeons of all kinds: adding different layers of perception to their field of view, easing some complex visualization, or providing a safe space for apprentices.

However, it is necessary to underline the different main changes both the technology used for mixed reality and even the operating room itself have to go through before thinking of implementing different use cases.

EXPERIMENTAL METHODS

While in contact with the enterprise in charge of the design of mixed reality equipment, and some level of demonstrations have been put in place by the Labcom Lynx medical, this study aims at preparing future operating rooms for the technologies that might become in the future. With it still being in its early stages, experimental introduction ise still limited to training dummies.

RESULTS AND DISCUSSION

The results of these first attempts have shown that both the headset used and the operating room will need to evolve in the following years.

When it comes to the headset, the implementation of a static reference point in space, unmoved when rebooting the equipment, as well as a more adapted zoom function, a redesign of controls and a better connection to other operating room equipment are the most obvious and already worked on among these transformations.

The operating room, to optimize the benefits of the headset could also undergo some changes. For instance, guaranteeing a high enough internet speed would ease online expertise or courses for tutees. Should they be modified accordingly, we could also work of connecting surgical lights to the headset so that they always light up The area looked at by the surgeon, even though images are already being treated through adjustments in colorimetry, contrast and brightness within the headset. Finally, the necessity of having virtual objects that fit the exact patient being treated within the XR system will influence the preliminary exams prescribed by their doctor.

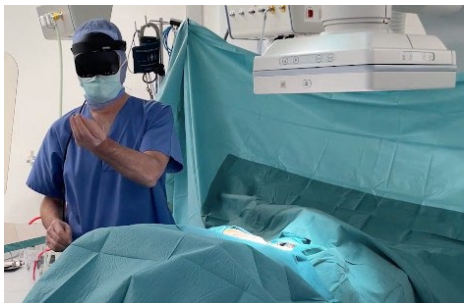

ACKNOWLEDGMENTS

The authors would like to thank the French ANR (Agence Nationale de la Recherche – Labcom 2021- LCV2-0002-01) for providing financial support to this project.

Plasma-derived fibrin hydrogels containing graphene oxide for infections treatment

Ariadna Bachiller[1], Juan Pedro Fernández[2], Yuta Nishina[3,4]
José Luis Jorcano[1], Cristina Martín[1*]

[1] Department of Bioengineering & Aerospace Engineering, Universidad Carlos III de Madrid, Leganés, Spain
[2] Institute IMDEA Materials, Getafe, Spain
[3] Graduate School of Natural Science and Technology, Okayama University, Okayama, Japan
[4] Research Core for Interdisciplinary Sciences, Okayama University, Okayama, Japan
*cristima@ing.uc3m.es

INTRODUCTION

Extensive burns and chronic ulcers are maybe the most sever types of lesions the human body can suffer. The patients develop immunosuppression and due to that reason, infection is inevitably in most of the cases. The World Health Organization estimates that almost 11 million of new burn injuries per year worldwide require medical attention, with around 265 000 of them leading to death[1]. Therefore, there is an urgent demand in the production of skin substitutes to be used as grafts to restore skin functionalities avoiding infection.

In this regard, collagen and fibrin hydrogels have been extensively applied for the synthesis of skin substitutes[2]. However, the use of hydrogels is far for from ideal since, usually, they have poor mechanical stability and are difficult to handle. Thereunder, there is a constant need for components that are able to improve the mechanical strength and the bioactivity of the hydrogels. Graphene and its derivatives, such as graphene oxide (GO), stand as an alternative for the hydrogel mechanical enhancement[3]. On the other hand, these nanomaterials constitute a novel approach for the treatment of infection due to their proved bactericidal effect[4].

In this context, the present study explores, to our knowledge, the first ever fabrication of plasma-derived fibrin hydrogels containing bactericidal hybrids based on GO for infection treatment and wound healing purposes.

EXPERIMENTAL METHODS

Fibrin-based hydrogels were prepared following a protocol previously described by Cubo *et al*.[2]. The gelation kinetics were studied by the flip-flop method and *via* rheological analyses (TA Instruments AR-G2 Rheometer). The mechanical properties were studied by dynamic mechanical analyses (DMA-Q800 equipment). The samples were also characterized by cryo-SEM, using a GeminiSEM 500 from Zeiss coupled with a Quorum cryo-SEM, under high vacuum conditions. Bactericidal studies were performed by using *Escherichia coli*, and a Cytotoxic 96@ Non-Radioactive kit from Promega was used as recommended for the cytotoxicity studies.

RESULTS AND DISCUSSION

The fibrin-derived hydrogels containing GO were synthesized and fully characterized. All the gelation kinetic experiments revealed that the addition of GO to the hydrogels accelerated the polymerization reaction, and the cryo-SEM studies showed up a decrease of the pore size when GO was added to the network, pointing out the critical role of GO into the network. However, these samples did not show bactericidal ability, maybe due to the fact that GO was taking part of the hydrogel network, remaining inside of it when the samples were exposed to bacterial cultures. Consequently, we synthesized and characterized a new bactericidal agent based on GO containing streptomycin adsorbed on its surface (GO/STREP), resulting in a hybrid that was incorporated into the fibrin-derived scaffolds. The bactericidal efficiency of the hydrogels containing GO/STREP was studied, showing a better controlled time and dose- dependent bactericidal effect compared to the control samples. Furthermore, the cytotoxicity assay showed good cell viability results for all the scaffolds.

CONCLUSION

This work points out GO-based hybrids as suitable candidates for antibiotic delivery purposes and confirms that the fibrin-based bactericidal hydrogels presented here could have a potential application in wound healing and skin injuries.

REFERENCES

1. WHO Factsheet on Burns. [Accessed March 13, 2022.]. available at http://www.who.int/mediacentre/factsheets/fs365/en/
2. Cubo N. *et al*., Biofabrication 9:015006, 2016
3. Martín C. *et al*., Nanoscale 1:4822-4830, 2019
4. Sengupta I. *et al*., Colloid Interface Sci. Commun. 28:60-68, 2019

ACKNOWLEDGMENTS

The authors would like to thank Eduardo Prado (University of Castilla-La Mancha) for the technical support on electron cryomicroscopy.
José Luis Jorcano acknowledges support by Comunidad de Madrid under the project S2018/BAA-4480, Biopieltec-CM, and the Spanish Ministry of Science and Innovation under the grant RTI2018-101627-B-I00".
Cristina Martín acknowledges support from the CONEX-Plus programme funded by Universidad Carlos III de Madrid and the European Union's Horizon 2020 research and innovation programme under the Marie Sklodowska-Curie grant agreement No. 801538.

Hang in there: efficient antimicrobial peptide conjugation produces cationic peptidopolysaccharide surfaces with antimicrobial activity

Pedro M. Alves[a,b,c,d,*], *Rúben F. Pereira*[a,b,e], *Beatriz Costa*[a,b,f], *Natália Tassi*[d], *Cátia Teixeira*[d], *Victoria Leiro*[a,b], *Cláudia Monteiro*[a,b], *Paula Gomes*[d], *Fabíola Costa* [a,b,‡], *M. Cristina L. Martins*[a,b,e, ‡]

[a]i3s, Instituto de Investigação e Inovação em Saúde, Univ. Porto, R. Alfredo Allen, 208, 4200-135 Porto, Portugal
[b]INEB, Instituto de Engenharia Biomédica, Univ. Porto, R. Alfredo Allen, 208, 4200-135 Porto, Portugal
[c]Faculdade de Engenharia, Univ. Porto, R. Dr. Roberto Frias, 4200-465 Porto, Portugal
[d]LAQV-REQUIMTE, Dpt. Química e Bioquímica, Fac. Ciências, Univ. Porto, R. Campo Alegre 687, 4169-007 Porto, Portugal
[e]ICBAS - Instituto de Ciências Biomédicas Abel Salazar, Univ. Porto, R. Jorge Viterbo Ferreira, 4050-313 Porto, Portugal
[f]Faculdade de Ciências e Tecnologia, FCT, Univ. Nova de Lisboa, 2829-516 Caparica, Portugal
‡Authors contributed equally. *pmalves@i3s.up.pt

INTRODUCTION

Chitosan has a mild antimicrobial effect, which may be improved by covalent conjugation of other molecules, such as antimicrobial peptides (AMP). Moreover, chitosan can also act as a sensitizer, potentiating the antimicrobial effect of the conjugated molecules[1,2]. The main hurdles associated with clinical implementation of AMP-based therapies are the poor stability of AMP in solution and their high cost[3,4]. Herein, the highly efficient thiol-norbornene photoclick chemistry (TNPC) was employed to improve the antimicrobial effect of chitosan through covalent conjugation of Dhvar5, which may protect it from degradation[5], while minimizing the quantity of AMP needed.

EXPERIMENTAL METHODS

Dhvar5 (LLLFLLKKRKKRKY) with a spacer and a cysteine was conjugated via TNPC onto chitosan-norbornene (NorChit). Thin films of chitosan, NorChit and NorChit-Dhvar5 on gold surfaces were produced by spin-coating and tested against *gram-positive* and *gram-negative* bacteria (*S. epidermidis* and *P. aeruginosa*, respectively). Bacteria were stained with a Live/Dead viability kit and were also plated for CFU counting after recovery from the surfaces by sonication. Moreover, cytotoxicity towards human neonatal dermal fibroblasts was evaluated by the resazurin assay. Tissue culture coverslips were used as positive control.

RESULTS AND DISCUSSION

Modification of chitosan with norbornene groups was successfully achieved (substitution degree: 0.38). TNPC led to a conjugation yield of up to 43%, which corresponded to 79.6 µmol of Dhvar5 per gram of NorChit-Dhvar5. Noteworthy, this was achieved under mild reaction conditions (room temperature and low UV light intensity and exposure time – 10 mW/cm^2 and 5 min, respectively). Thin films of NorChit-Dhvar5 showed an antiadhesive effect on *S. epidermidis* (26% reduction in total bacteria) and a killing behaviour against *P. aeruginosa* (2-fold increase in dead bacteria, **Fig. 1**) compared to chitosan. Increased adhesiveness of NorChit-Dhvar5 towards *gram negative* bacteria was observed, probably due to higher attraction of Dhvar5 cationic end to the more negatively charged membrane of *P. aeruginosa*[2].

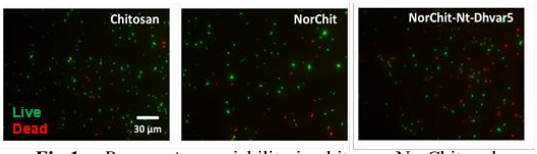

Fig 1 – *P. aeruginosa* viability in chitosan, NorChit and NorChit-Dhvar5 (*N-terminus* conjugation) films.

Lastly, fibroblasts metabolic activity remained above 70% in all samples (normalized by cell number and compared to positive control) after 24h of direct contact, meaning the materials are non-cytotoxic, according to ISO 10993-1.

CONCLUSION

This study validates TNPC as a highly efficient chemistry for the production of chitosan-based peptidopolyssacharides, which may constitute a more cost-effective strategy for the fabrication of antibacterial biomaterials.

REFERENCES

1. Si, Z. *et al.* Antimicrobial effect of a novel chitosan derivative and its synergistic effect with antibiotics. *ACS Appl. Mater. Interfaces* **13**, 3237–3245 (2021).
2. Li, P. *et al.* Cationic peptidopolysaccharides show excellent broad-spectrum antimicrobial activities and high selectivity. *Adv. Mater.* **24**, 4130–4137 (2012).
3. Mahlapuu, M., Håkansson, J., Ringstad, L. & Björn, C. Antimicrobial peptides: An emerging category of therapeutic agents. *Front. Cell. Infect. Microbiol.* **6**, 194 (2016).
4. Xue, M., Zhao, R., Lin, H. & Jackson, C. Delivery systems of current biologicals for the treatment of chronic cutaneous wounds and severe burns. *Adv. Drug Deliv. Rev.* **129**, 219–241 (2018).
5. Costa, F., Carvalho, I. F., Montelaro, R. C., Gomes, P. & Martins, M. C. L. Covalent immobilization of antimicrobial peptides (AMPs) onto biomaterial surfaces. *Acta Biomater.* **7**, 1431–1440 (2011).

ACKNOWLEDGMENTS

Financial support: FCT-MCTES through "AntINFECT" (POCI-01-0145-FEDER-031781) and LAQV-REQUIMTE (UIDB/50006/2020). National (Norte 2020) and/or European Union funds (ESF – European Social Fund) support doctoral grant SFRH/BD/145471/2019 (PMA), Junior Researcher contract CEECIND/01921/2017 (FC) and contract in the framework of project PTDC/BTM-MAT/4156/2021 (VL).

Hollow bioactive glass nanoparticles for bone disease treatment

S. Sánchez-Salcedo[1,2], J. Jiménez-Holguín[1], M. Cicuéndez[1], M. Vallet-Regi[1,2], A.J. Salinas[1,2].

[1] Facultad de Farmacia, Universidad Complutense de Madrid, UCM; Instituto de Investigación Hospital 12 de Octubre, imas12, 28040 Madrid, Spain
[2]Networking Research Center on Bioengineering, Biomaterials and Nanomedicine, CIBER-BBN, 28040 Madrid, Spain

INTRODUCTION

Bone regeneration takes between 3 and 8 weeks to repair bone fractures. In the presence of critical bone defects or certain pathologies, such as osteoporosis or osteomyelitis, bone is not able to heal on its own and different healing strategies are required. Thus, to solve bone infectious diseases the use of nanoparticles as carriers of drugs or organic molecules is one of the most investigated approaches.[1] Nanoparticles features can be improved by the inclusion of Cu^{2+} ions because they are inductors of vascular endothelial growth factor, regulators of collagen cross-link during bone formation and exhibit anti-bacterial behavior against *E. coli* and *S. Aureus* as well as antiviral activity.[2] This study describes the synthesis and characterization as well as the behaviour in the presence of preosteoblastic cells of hollow bioactive glass nanoparticles (HBGNs) with composition $79.5SiO_2$–$2.5P_2O_5$–(18-x)CaO–xCuO (x= 0, 2.5, 5 mol-%).

EXPERIMENTAL METHODS

HBGNs were synthesized by a protocol based on that proposed by Li *et al*.[3] and characterized by nitrogen adsorption, small-angle X-ray diffraction, transmission electron microscopy (TEM), energy dispersive spectroscopy and zeta potential. In addition, cell proliferation assays were carried out at 1 and 3 (CellTiter 96®AQ_{ueous} One Solution Cell Proliferation Assay MTS) testing at 200 and 300 µg /ml and after 2 h and 24 h using the pre-osteoblastic line MC3T3-E1. The internalization of in cells was analyzed by fluorescent microscopy. It was evaluated the cell uptake process through the intracellular complexity parameter, as well as the viability, and the ROS intracellular production by flow cytometry after 3d. Bacterial growth inhibition tests in the planktonic state HBGN were tested between 200- 10 µg/mL for E. coli and between 260-20 µg/mL for S. aureus. Finally, to verify the ability of the nanosystem to degrade a S. aureus biofilm 200 µg/mL of each composition loaded with danofloxacin were used at the maximum cytocompatible concentration.

RESULTS AND DISCUSSION

Nitrogen adsorption isotherms of HBGNs show hysteresis cycles type IV typical of HBGNs and specific surface areas of 826, 731 and 739 m^2/g, pore volumes of 1.22, 0.85 and 0.75 cm^3/g and pore size of 2.4, 2.6 and 2.6 nm for 0, 2.5 and 5% CuO respectively. *According to TEM analysis* (Fig. 1A) nanoparticles showed a shell rounding a hollow core keeping a radial ordered mesoporous. After measuring twenty HBGNs the average sizes were 190 ±65 nm, for all them. The presence of copper ions in the particles was observed by EDS, obtaining 0, 3.9 and 4.8% of Cu for 0, 2.5 and 5% CuO respectively. No significant amount of P is incorporated in the HBGNs compositions.

The nanosystem was able to release biologically effective amounts of therapeutic inorganic ions and danofloxacin. The Cu-loading of the HBGN produced more gradual release of danofloxacin that was extended for over one week. Assays with MC3T3-E1 pre-osteoblasts showed a cytocompatible behaviour after 3 d in contact with HBGNs.

Microbiological assays showed that copper ions enhanced the bactericidal effect of danofloxacin against E. coli and S. aureus in both planktonic and sessile state. Moreover, the nanosystems was able to degrade a biofilm pre-formed of S. aureus at minimal concentration suggesting their suitability as bactericide agent.

CONCLUSION

These results indicate that HBGNs enriched with copper ions does not alter the therapeutic properties of the material textural properties but improve their features as nanocarriers and proliferation inductor. Amount of antibiotic danofloxacin and copper ions needed to eliminate a bacterial population is drastically reduced when a nanosystem that effectively combines both strategies is employed. HBGN-based nanosystem could be promising alternative in the fight against bone infections.

REFERENCES

1-Paris, et al . *Acta Biomaterialia*, *86:* 441-449, 2019.
2-Medeiros, D. M. et al, 241:1316-132, 2016
3-Li, Y., Bastakoti, et al, *Chemistry–A European Journal*, *21*: 8038-8042, 2015

PexigananA-grafted onto chitosan nanoparticles using one-pot microfluidic system to eradicate *Helicobacter pylori*, the gastric queen

Diana R. Fonseca[1,2,3*], Estrela Neto[1,2], Beatriz Custódio[1,2,4], Sofia Guimarães[1,2], Francesca Annis[1,2], Paulo Freitas[5,6], Cátia Teixeira[7], Paula Gomes[7], Paula Parreira[1,2], M. Cristina L. Martins[1,2,4]

[1]i3S – Instituto de Investigação e Inovação em Saúde da Universidade do Porto - Associação, Porto, Portugal
[2] Instituto de Engenharia Biomédica, Universidade do Porto, R. Alfredo Allen 208, 4200-135, Porto, Portugal
[3]Faculdade de Engenharia, Departamento de Engenharia Metalúrgica e de Materiais, Universidade do Porto, Portugal
[4]ICBAS—Instituto de Ciências Biomédicas Abel Salazar, Universidade do Porto, 4050-313 Porto, Portugal
[5]INL, International Iberian Nanotechnology Laboratory, Braga, Portugal
[6]INESC-MN, INESC Microsystems and Nanotechnologies, Lisboa, Portugal
[7]LAQV-REQUIMTE, Departamento de Química e Bioquímica, Faculdade de Ciências, Universidade do Porto, Portugal
[*] diana.fonseca@i3s.up.pt

INTRODUCTION

Helicobacter pylori (Hp) infection causes several gastric disorders and accounts for 90% of all diagnosed gastric cancers, the 5th most common and 4th deadliest cancer worldwide[1]. Hp is a source of concern for the World Health Organization, as the available antibiotherapy presents high failure rate (10-40%), mainly due to mounting antibiotic resistance[2]. Alternative therapies are urgent demands, and the use of antimicrobial peptides (AMPs) is gaining expression. PexigananA, MSI-78A, is an analog of Pexiganan with reported bactericidal activity against Hp[3]. AMPs immobilization onto biomaterials is an advocated strategy to overcome drawbacks, as proteolytic degradation and aggregation with proteins, while maintaining the bactericidal effect[4]. Here, a versatile, cost-effective and environmentally friendly "one-pot" microfluidics system suitable for nanoparticles (NPs) production and bioconjugation of any ligand containing a thiol group (e.g., cysteine amino acid) is proposed. MSI-78A is intended to be grafted onto chitosan NPs (AMP-ChNPs) to eradicate Hp infection *in situ* (i.e, surface of gastric epithelium cells).

EXPERIMENTAL METHODS

First, we designed and optimized a pioneering microfluidic system, capable to achieve (i) chitosan functionalized with norbornenes (Ch) individual crosslinking onto NPs and (ii) the conjugation of bactericidal AMPs through ultraviolet (UV)-photoinitiated thiol-ene "Click"chemistry, in one simple device.

ChNPs size, concentration and charge were measured by nanoparticle tracking analysis (NTA) and zetasizer, respectively. AMP grafting was evaluated by Fourier Transform Infrared Spectroscopy (FTIR) and UV/VIS Spectroscopy. The developed AMP-ChNPs were tested *in vitro* against Hp J99 strain (human highly pathogenic strain), at different time points and in a NPs's range of concentrations (10^{12}-10^{10} NPs/mL). ChNPs cytotoxicity towards a human gastric adenocarcinoma cell line (AGS, ATCC® CRL-1739™) was evaluated using elution/extract and direct contact assays, according to the international standard ISO 10,993–5;12.

RESULTS AND DISCUSSION

The concentration (1.5 mg/mL) and flow rate of Ch (1 µL/min) and water (10 µL/min) were tuned and ChNP with an average size of 130±17nm were obtained.

AMP-ChNPs were successfully engineered, which was confirmed by FTIR, where the characteristic absorption bands of AMP appeared at 1660 cm^{-1} (amide I) and 1530 cm^{-1} (amide II). The designed NPs were able to retain their integrity in acidic environment (pH 1.2), proving their pH-resistance and validating this approach for gastric settings. AMP-ChNPs efficacy was demonstrated in a concentration dependent manner. Bactericidal effect was fast and seen as soon as 6 h, with a decrease of at least 3logs (from 10^7 to 10^3 CFU/mL), which indicates that MSI-78A can retain its activity when immobilized onto ChNPs. Furthermore, the designed ChNPs were biocompatible against AGS, reinforcing the strong potential of this strategy.

CONCLUSION

Overall, a straightforward system to produce AMP-conjugated chitosan nanoparticles (AMP-ChNPs) stable in gastric conditions was developed. The main advantage of the herein designed system is the possibility to simultaneously produce, crosslink and perform the immobilization of different thiolated-compounds (due to a thiol-ene chemistry) using the same device. This system is also versatile and can be explored with other biomaterials,

The AMP-ChNPs approach boosted the activity of MSI-78A and is promising for Hp eradication.

REFERENCES

1. Rawla et al. Prz Gastroenterol. 14(1):26-38, 2019
2. Sung et al. CA Cancer J Clin.;71:209–249, 2020
3. Parreira et al. Sci Rep 9, 18212, 2019
4. Fonseca et. al. 137:186-198, 2022

ACKNOWLEDGMENTS

The authors would like to thank PhD grant SFRH/BD/146890/2019 & CEECIND/01210/2018. Also, the authors would like to acknowledge Pedro Alves, Bruna Costa and Ana Rita Pinto for the technical assistance.

IN VITRO MICROBIOLOGICAL EVALUATION OF A CHITOSAN/POLYCYCLODEXTRIN/CINNAMALDEHYDE HYDROGEL FOR DIABETIC FOOT ULCERS TREATMENT

Henry Chijcheapaza-Flores[1], Maria José Garcia-Fernandez[1], Mickael Maton[1], Jean-Noël Staelens[2], Nicolas Tabary[2], Frédéric Cazaux[2], Feng Chai[1], Christel Neut[3], Bernard Martel[2], Nicolas Blanchemain[1]

[1] Univ. Lille, INSERM, CHU Lille, U1008 – Advanced Drug Delivery Systems (ADDS), F-59000 Lille, France

[2] Univ. Lille, CNRS, INRAE, Centrale Lille, UMR 8207 – Unité Matériaux et transformations (UMET), F-59000 Lille, France

[3] Univ. Lille, INSERM, CHU Lille, U1286 - INFINITE - Institute for Translational Research in Inflammation, F-59000 Lille, France

*henry.chijcheapaza@univ-lille.fr

INTRODUCTION: Diabetic foot ulcer is a severe infection present in about 6.3% of the world's population[1]. The first-line treatment consists of the debridement, dressing, and administration of antibiotics. However, even under treatment, many patients can still suffer from necrosis and end by a partial or total amputation. The challenge for health professionals is to treat the chronic wound infection, due to formation of a bacterial biofilm on the wound surface as a result of bacterial proliferation and antibiotic resistance. Recently, various innovative therapeutical strategies have been proposed, such as the topical or systemic administration of natural antimicrobial compounds for antibiotic synergy against antibiotic resistance[2], or the use of hydrogels as a drug delivery system for local treatment[3]. Based on this, this project focused on the local administration of cinnamaldehyde (CN), a natural broad-spectrum antibacterial agent extracted from cinnamon oil, combined with a hydrogel based on chitosan (CHT) - citric acid β cyclodextrin crosslinked polymer (PCD) for the treatment of diabetic foot ulcers.

EXPERIMENTAL METHODS: Hydrogel preparation was based on a patented method: WO2017001808[4]. Briefly, the hydrogel was formed by suspending the co-milled (Mixer Mill MM 400, Restch®, France) CHT/PCD powder (3 and 2% w/w respectively) in CN (1% w/w) plus water (93% w/w), and acidified with lactic acid (1% w/w). Firstly, viscoelastic properties of CHT/PCD/CN hydrogel were studied by rheology (Anton Paar® MCR 301, France), and CN release from hydrogel was studied under dynamic condition using a USP IV flow-through dissolution system (Sotax®, France). The *in vitro* cytotoxicity assessment of hydrogel was performed with a pre-osteoblast MC3T3-E1 cell line, according to ISO 10993-5 standard, with extraction method by AlamarBlue® Assay. Concerning to antimicrobial evaluation, the antimicrobial activity of the hydrogel was evaluated against *E. coli (K12), P. aeruginosa (ATCC 9027),* and *S. aureus (CIP 224).* Time-Kill assay was performed by direct contact of hydrogel with a bacteria suspension at 37°C for 24h, and biofilm eradication was tested using a biofilm inoculator (Innovotech Inc, Canada) containing pegs coated with hydroxyapatite; pegs were incubated in a bacterial suspension at 37°C for 48h. After incubation, biofilm eradication was evaluated by the measure of the optical density after coloration with crystal violet.

All tests have been performed in triplicate and compared statistically by *p*-value (α=0.05).

RESULTS AND DISCUSSION: Firstly, hydrogel formation was macroscopically observed by formation of a cord-like structure after injection into PBS (pH7.4 at 37°C), and rheology study confirmed the formation of a viscoelastic (damping factor: 0.3), injectable (shear-thinning), and self-healing hydrogel. The cytocompatibility of hydrogel was proved by cell viability (>70% with regard to control) of pre-osteoblast cells. Concerning the microbiological evaluation, it revealed a significant antimicrobial activity ($p<0.05$). Indeed, CHT showed an antimicrobial activity against *E. coli* and *P. aeruginosa* (3 Log10 reduction), and PCD addition enhanced the intrinsic antimicrobial activity of the hydrogel (5 Log10 bacterial reduction) after 24h. Therefore, once CN was added into the hydrogel formulation, a faster bacterial reduction was observed for both Gram (-) strains between 2 to 6 hours after incubation (6 Log10). In the case of Gram (+), a similar activity was observed for samples charged with CN against *S. aureus* after 6h of incubation. Biofilm eradication test had a similar outcome as in bacterial kinetic reduction; hence, an antibiofilm activity was proved. The enhancement of antimicrobial activity over Gram (-) was explained by the acid nature of PCD. Indeed, PCD decreased the pH of incubation media while increasing the cationization of the amino groups in CHT and consequently, increasing the permeation through the negatively charged bacterial cell-wall.

CONCLUSION: A promising injectable hydrogel with antimicrobial activity has been developed**.** Due to its simple preparation and convenient application, this CHT/PCD/CN hydrogel holds a good promise for future *in vivo* studies.

REFERENCES

1. Zhang, P. et al., Ann Med. 49(2):106-116, 2017
2. Guimarães, I. et al, Appl Sci. 11(3):1230. 2021
3. Wang, H. et al., Biomater Sci. 10;9(5):1530–46, 2021
4. Blanchemain, N. et al., U.S. Patent Application 15/740,414, 2018.

ACKNOWLEDGMENTS:
This project was funded by the MOBLILEX scholarship from the University of Lille.

Evaluating Acoustic Droplet Transfer Technology for High Throughput Biomaterial Library Fabrication.

Charles W Winter[1*], Marko Storch[2], Tianhong Dai[1], Anil A Bharath[1], Adam D Celiz[1]
[1]Department of Bioengineering, Imperial College, London, United Kingdom
[2] Biofoundry, Translation and Innovation Hub, Imperial College, London, United Kingdom
[*]cw1415@ic.ac.uk

INTRODUCTION

In traditional therapeutic screening the influence of cell-material interactions is generally limited to the study of single biomaterials in depth at a time, which results in large gaps in knowledge on how extracellular signals such as material stiffness dimensionality and cell to cell contacts influence therapy resistance during preclinical drug screening[1].

As a result, great demand exists for new technologies which can accelerate the study of multiple biomaterials at one time. Here, we report an automated workflow for the fabrication of high-throughput, three-dimensional tumor cell laden hydrogels using acoustic droplet transfer technology (ADTT) based on collagen and poly-ethylene glycol interpenetrating networks.

EXPERIMENTAL METHODS

Fluorescent labelling of PEGs, Collagen and Cells:
Neutralized collagen hydrogel (4mg/ml)[2] and 4-arm PEG vinyl sulfone (PEG VS) (50mM) were labelled with NHS-Alexa Fluor 647 (2.5µM) and Thiol Sun Fluor 488 (1µM). Dialysis performed over 7 days using a float-a-lyser with a 10kDa MWCO. $5x10^6$ cells/mL were also fluorescently tagged using Hoechst nuclear stain (1:1000 dilution).

ADTT experiment
Using aqueous buffered protein settings on Echo 525 a total volume of 2µL of each sample per well was transferred. For the cell samples a total of 500nL was transferred.

Imaging and Data analysis
A Clariostar plate-reader (BMG Labtech) was used to measure plate fluorescence and a SP8 confocal microscope (Leica imaging) was used for imaging. 12 replicates were performed with one-way ANOVA (Brown Forsythe and Welch Tests).

RESULTS AND DISCUSSION

The acoustic droplet transfer technology (ADTT) was evaluated to assess the maximal concentrations of both (1) fluorescently labelled acidified collagen and (2) 4-arm 10kDa PEG-VS which could be reliably transferred from the source well of a 384 well plate into the wells of a 1536 destination assay plate. In both cases a maximal concentration limit was observed. Evidently above these concentrations the acoustic energy applied by the ADTT was insufficient to transfer liquids as measured by a normalized fluorescence intensity signal of 1 (compared to PBS control). In the case of PEG, in Figure 1a. consistent transfers were observed up to a concentration of 40mM. While the acidified collagen solution, in Figure 1b, could be successfully transferred up to a maximum concentration of 5mg/ml in a consistent manner with no statistical difference observed for concentrations below 5mg/ml. Importantly, these maximal precursor concentrations would be sufficient to form mechanically robust and biologically relevant hydrogels once polymerized[3].

We proceeded to use our automated Python script to form replicates of 3x3 arrays of collagen and PEG with a composition shown in Fig 1c. Tiling of the resultant 1536 well plate and merging images together made it possible to demonstrate in Fig 1d that each well had a different polymer composition (indicated by the different colors) and that cells were shown to be consistently distributed across the wells.

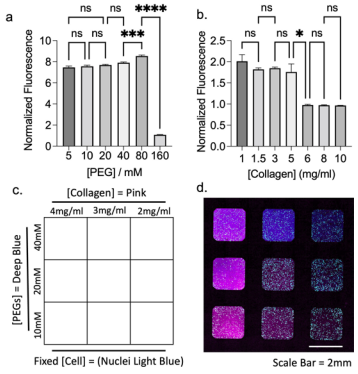

Figure 1 ADTT Transfer efficiency for a) fluorescent 4-arm PEG b) fluorescent acidified collagen solution. c) 3x3 array map of composition of PEG, collagen and tumor cells d) collagen (pink), PEG (deep blue) and cell nuclei (light blue) confocal image of 1536 well plate.

CONCLUSION

Here we demonstrate that acoustic droplet transfer technology can provide a novel rapid, non-contact method to build libraries of cell-laden 3D hydrogels. As an exemplar using acidified Collagen (Type I) and multi-arm polyethylene glycol (PEG) precursors and a model breast cancer cell line. Therefore, this platform will enable future drug screening studies within complex biomaterial microenvironments in high throughput.

REFERENCES

1. Seo *et al,* Biomaterials, 2019
2. Doyle *et al,* Bio Protoc 2018
3. Antoine et al, Tissue Eng Part B Reviews 2014

ACKNOWLEDGMENTS

Authors acknowledge support from the Economic and Social Research Council (ESRC) grant number ES/T013397/1

Internal and external metal-coatings to prevent bacterial adhesion on ureteral stents

Beatriz Domingues[1,2*], Ivo M. Aroso[1,2], Estêvão Lima[3], Alexandre A. Barros[1,2], Rui L. Reis[1,2]
[1]I3Bs – Research Institute on Biomaterials, Biodegradables and Biomimetics, University of Minho, Braga, Portugal
[2]ICVS/3B's–PT Government Associate Laboratory, Braga/Guimarães, Portugal
[3]Life and Health Sciences Research Institute (ICVS), School of Health Sciences, University of Minho, Braga, Portugal
*beatriz.domingues@i3bs.uminho.pt

INTRODUCTION

Over the years, metal-based coatings have gained prominence due to their ability to impair biofilm formation on biomedical implants, emphasizing silver (Ag)- and zinc (Zn)-based strategies, which concomitantly present intrinsic antimicrobial activity properties and biocompatibility[1]. In urology, the bacterial infection is one of the main drawbacks associated with the use of ureteral stents, limiting their therapeutic action and often representing an increase in healthcare costs[2]. After stent placement in the ureter and upon the passage of urine, the deposition of ions and minerals emerges, forming anchor points where bacteria may adhere and develop[3]. Since the urine has in-stent and out-of-stent flows, the biofilm formation can occur inside or outside the stent[4]. Unlike most strategies that only have exterior coatings, we proposed the development of internal and external coatings on polyurethane-based stents in order to create a biomedical material with more efficient antimicrobial properties.

EXPERIMENTAL METHODS

We performed a modification on polyurethane stents (7F Tecoflex, Nordson Medical) on the inner and out surfaces, starting by surface activation with tin (II) chloride dihydrate (≥98%, Sigma-Aldrich), followed by electroless plating of metals, namely, silver (Ag) and zinc (Zn), separately. Both Ag coatings were created following an equal protocol, differing only in the temperature used for the electroless metallization, 60 or 35°C, being named Ag60 and Ag35, respectively. Coatings containing Zn were created by using zinc nitrate hexahydrate (99%, Sigma-Aldrich) with different metallization precursors, namely hydrazine monohydrate (64-65%, reagent grade 98%, Sigma-Aldrich) and borane dimethylamine complex (97%, Sigma-Aldrich), to create Zn and zinc oxide (ZnO) coatings, respectively. Contact angle, scanning electron microscope (SEM), and X-ray photoelectron spectroscopy (XPS) analyses were performed to characterize the modified surfaces properly. Since protein adsorption on biomedical devices' surfaces is considered one of the first steps for biofilm formation, we assessed the adsorption level of bovine serum albumin (BSA) after immersing coated and uncoated stents on artificial urine. To evaluate antimicrobial effects of coatings, stents were incubated, separately, with *Escherichia coli* ATCC 25922 and *Staphylococcus aureus* ATCC 25923, following an established biofilm formation protocol. Biocompatibility assays were carried out following ISO10993-5, using L929 mouse fibroblast (ATCC NCTC clone 929) and G/G mouse uroepithelial (DSMZ ACC 224). Tests were performed with liquid extracts of material and with the material itself. Mechanical properties were assessed in accordance with ASTM F1828/Test Method D412.

RESULTS AND DISCUSSION

Following electroless plating of metals, four different coatings were created, as shown by SEM and contact angle analyses. By XPS, we proved the presence of the metals in both inner and out surfaces, namely Ag in both Ag60- and Ag35-coated stents, and Zn in both Zn- and ZnO- coated stents, confirming that the designed protocol was able to create internal and external coatings. After immersing stents in artificial urine, we reported a significant reduction in the amount of adsorbed protein (BSA) per area on Ag35-, Zn-, and ZnO-coated stents, compared to control stents. This indicates that those coatings could be less prone to form biofilms in the urological context. In terms of antibacterial effects, all coatings were efficient against uropathogens. Ag coatings were 99.999% efficient to prevent initial adhesion of *E. coli* since no bacteria had adhered after 1 h of contact with the material (5 log reduction compared to control). Even after 1 day of incubation, significantly fewer bacteria had adhered to the Ag-coated stents compared to control. For *S. aureus*, all coatings presented significantly less attached bacteria on their surfaces compared to control. Thus, Ag coatings were effective for gram – and gram + bacteria, and Zn coatings were only effective for the tested gram + bacteria. Both Ag and Zn coatings exhibited antibacterial activity by lowering the adherence of both strains, without compromising L929 and G/G cells viability or the mechanical properties of stents.

CONCLUSION

The development of inner and out metal-based coatings bestows appropriate antimicrobial properties to ureteral stents, conferring advantages compared with the material commonly used on standard stents.

REFERENCES

1. Zhu, Z., Wang, Z., Li, S. & Yuan, X. Journal of Biomedical Materials Research - Part A vol. 107 445–467 (2019).
2. Sali, G. M. & Joshi, H. B. International Journal of Urology vol. 27 7–15 (2020).
3. Barros, A. A. et al. 7.41 in Comprehensive Biomaterials II 793–812 (2017).
4. Hafron, J. et al. Urology 68, 911–915 (2006).

ACKNOWLEDGMENTS

The authors would like to thank the FCT (Grant no: PD/BD/150478/2019) for providing financial support to this project.

Hydrogel Embedding Polydopamine Nanoparticles for a Synergistic Photodynamic and Photothermal Therapy Targeting Diabetic Foot Ulcers

Sarah Defrançois[1*], Alexandre Barras[2], Rabah Boukherroub[2], Mickaël Maton[3], Nicolas Blanchemain[3], Patrice Woisel[1] and Joël Lyskawa[1]

[1]Univ. Lille, UMET, CNRS, INRAE, Centrale Lille, UMR 8207 - UMET, F-59000 Lille, France
[2]Univ. Lille, CNRS, Centrale Lille, Univ. Polytechnique Hauts-de-France, UMR 8520 - IEMN, F-59000 Lille, France
[3]Univ. Lille, INSERM, CHU Lille, U1008 - Controlled Drug Delivery Systems and Biomaterials, F-59000 Lille, France

[*]sarah.defrancois@univ-lille.fr

INTRODUCTION

Diabetic foot ulcers (DFUs) are the most common, disabling and costly complications of diabetes.[1] In 18% of cases, these ulcer infections are followed by amputations. To prevent this tragic outcome, the most employed biomedical strategies consist in physical removal of the biofilm by frequent debridement of the DFU or antibiotic treatments. However, these strategies have proven to be ineffective due to the rapid reformation of the biofilm and the emergence of antibiotic resistance. This work proposes an innovative therapy based on the use of alginate hydrogel (ALG) embedding functionalized polydopamine nanoparticles (nPDA) as phototherapeutic agents for a synergistic photodynamic (PDT) and photothermal therapy (PTT). The functionalization of nPDA with a photosensitizer (Ce6) allows for biofilm impairment by PDT while the photothermal properties of nPDA are exploited for on demand local release of antibiotics such as ciprofloxacin (CFX) and rifampicin (RFP). The injection of the functionalized hydrogel in the infected wound and the application of the synergistic phototherapy will eradicate the biofilm and promote wound healing and tissue regeneration[2].

EXPERIMENTAL METHODS

Preparation of ALG-nPDA hydrogel. nPDA or modified nPDA were dispersed in an ALG aqueous solution and $CaCl_2$ was then added. The hydrogel was formed in a few seconds.

Singlet oxygen ($^1O_2$) generation from ALG-nPDA-Ce6 hydrogel. $^1O_2$ generation was evaluated by using the *p*-nitroso-dimethylaniline (RNO)-bleaching method developed by Kraljic and El Mohsni.[3] ALG-nPDA-Ce6 gel was irradiated at 671 nm (1W/cm²) and the $^1O_2$ formation was evaluated by measuring the absorbance of RNO by UV-visible spectrophotometry.

Photothermal properties of ALG-nPDA hydrogel. Photothermal properties of ALG-nPDA hydrogel were evaluated by monitoring the solution temperature with an infrared camera upon irradiation at 980 nm (1W/cm²).

NIR light-triggered CFX release from ALG-nPDA-CFX hydrogel. Release of CFX from ALG-nPDA-CFX hydrogel was monitored by fluorescence spectroscopy upon irradiation at 980 nm (1 W/cm²) and compared to CFX release without irradiation.

***In vitro* evaluation of the antibacterial activity.** Diffusion tests were performed with ALG-nPDA-CFX/RFP hydrogels on *Staphylococcus Aureus ATCC6538* and *Escherichia Coli K12* inoculum plated on Mueller Hinton Agar.

RESULTS AND DISCUSSION

The gelation of ALG with $CaCl_2$ in presence of nPDA was observed in a few seconds. The generation of $^1O_2$ from ALG-nPDA-Ce6 hydrogels was demonstrated by the RNO bleaching method. Upon irradiation at 671 nm, ALG-nPDA-Ce6 hydrogel will weaken the extra cellular matrix of the biofilm allowing nPDA to penetrate in the biofilm and access to bacteria. The photothermal properties of ALG-nPDA hydrogels were evaluated upon irradiation at 980 nm (1W/cm²). The increase of the hydrogel temperature was exploited to control the sustained release of CFX and RFP in the biofilm. Diffusion tests have demonstrated the antibacterial activity of the antibiotic-functionalized hydrogel against *S.Aureus* and *E.Coli.* The results highlight the necessity to use a combination of the two antibiotics for a broad-spectrum activity against antibiotic-resistant pathogens.

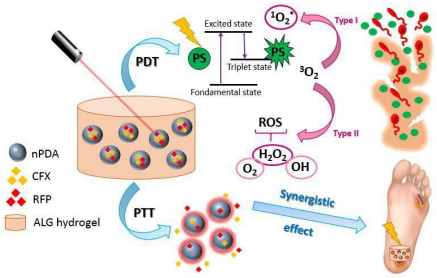

CONCLUSION

Hydrogel embedding functionalized polydopamine nanoparticles for the synergistic PDT and PTT represents an original and powerful therapy for the treatment of DFUs. Future work will be dedicated to *in vitro* and *in vivo* evaluations of these hydrogels on biofilms and infected rats respectively.

REFERENCES

1. Cavanagh PR. *et al*., The Lancet **2005**, *366*, 1725.
2. Han L. *et al*., Npg Asia Materials **2017**, *9*, e372.
1. rman J. *et al*., Anal. Bioanal. Chem. **2019**, *411* (20), 5287–5296.

ACKNOWLEDGMENTS

The authors would like to thank the "Métropole Européenne de Lille" (MEL) and the "Université de Lille" for providing financial support for this project.

Impact of the new European regulation (EU) 2017/745 on medical devices on hospital pharmacies activity: Example on pharmaceutical supply function within a French university hospital center

Authors: Halil Sayin [a,b], Claire Gaillard [a, b], Agnès Henry [c], Delphine Cabelguenne [d], Xavier Armoiry [a, b, e]

[a] ISPB, Lyon School of Pharmacy, Université Claude Bernard Lyon 1 69008 Lyon, France
[b] Univ Lyon, Université Claude Bernard Lyon 1, INSA Lyon, CNRS, MATEIS, UMR5510, 69008 Lyon, France
[c] Service pharmaceutique, groupement hospitalier Nord, hospices civils de Lyon, 69004 Lyon, France
[d] Service pharmaceutique, hospices civils de Lyon, hôpital Lyon Sud, 69495 Pierre-Bénite cedex, France
[e] Service de pharmacie, Hospices civils de Lyon, hôpital Édouard-Herriot, 69003 Lyon, France

halil.sayin@guerbet.com

Introduction
The new European regulation (EU) 2017/745 (MDR) on medical devices is expected to have major impacts on the industrial sector, but also consequences on healthcare professionals. Our objective was to evaluate the impact of the MDR on the supply of medical devices in hospital pharmacies at the level of a French university hospital.

Methods.
We conducted a prospective follow-up of marketing cessations and supply disruptions directly related to the MDR between November 2019 and September 2020. The data were analyzed accounting for the nature of the suppliers (status/size), the nature of the medical devices (route/class), and the proposed alternatives. The economic impact on hospital pharmacies was also estimated.

Results.
Over this period, 96 medical devices product designations were declared out of stock or in cessation (total of 402 references), of which half corresponded to class IIa medical devices, mainly used for surgical procedures. Of the 14 companies concerned (36% French), the majority were manufacturers, of small/medium-size or intermediate size. Substitutions were proposed for only 15 products (15.6%). The cost of pharmaceutical management of these disruptions/marketing cessations was estimated at 3052 €.

Conclusion.
Even before the official date of its application, the impacts of the MDR on the supply function of hospital pharmacies are already visible. In the short, medium and long term, prospective monitoring of the impacts, positive or negative, would seem to be justified at the level of manufacturers, healthcare professionals and end users of medical devices.

Key words: Medical devices, 2017/745 Regulation, Hospital pharmacy

PMMA bone cement containing long releasing chlorhexidine from the nanocarriers.

Yazan Al Thaher[1], Lirong Yang[1], Polina Prokopovich[1]
[1]School of Pharmacy and Pharmaceutical Sciences, Cardiff University, Cardiff, UK
prokopovichp@cf.ac.uk

INTRODUCTION

Infections after orthopaedic surgery so called Prosthetic joint infections (PJI) are a very unwelcome outcome after joint replacement surgery; despite the widespread use of antibiotics their incidence can be as high as in 10% of cases. This likely to increase as antibiotics are gradually losing efficacy as results of bacteria developing resistance, therefore novel antimicrobial approaches are required. Chlorhexidine (a widely used topical non-antibiotic antimicrobial compound) coatings on silica nanoparticles capable of prolonged drug release have been successfully developed and characterised. Such nanocarriers were incorporated into commercial formulation PMMA bone cement (Cemex), without adversely affecting the mechanical performance. Moreover, the bone cement containing the developed nanocarriers showed superior antimicrobial activity against different bacterial species encountered in PJI, including clinical isolates already resistant to gentamicin. Cytocompatibility and mechanical tests also showed non inferior performance of the bone cements containing chlorhexidine releasing silica nanocarriers to the equivalent commercial formulation.

EXPERIMENTAL METHODS

Chlorhexidine impregnated nanocarriers were prepared using layer by layer approach according to the procedure developed in [1] and were fully characterised using FTIR, TEM, TGA and GPC methods. Chlorhedine quantification from the nanocarriers and from the bone cement were examined using rp-HPLC methods. The antimicrobial activity of PMMA bone cement samples containing chlorhexidine impregnated nanocarriers was determined through the estimation of the bacteria surviving on the sample surface, after exposure to bacterial cultures, using the indirect method proposed by Berchet et al.[2] employing the time to detection principle (TTD). Gram-positive along with Gram-negative relevant bacteria and Gentamicin resistant PJI clinical isolated strain were tested: MRSA 275 and 294; S. epidermidis 272, 222 and 199; Methicillin resistant S. epidermidis (MRSE) 140, *A. baumannii* 646, 643, 640; *E. coli* 293 and *Enterococcus* 181. Cytotoxicity against osteoblast cells cultured on the bone cement containing chlorhexidine nanocarriers was assessed through the MTT, LDH assay and actin filament and life/dead imaging and histological analysis. Mechanical and rheological evaluation of the new bone cements were also conducted.

RESULTS AND DISCUSSION

As no commercial bone cement containing chlorhexidine is available, the addition of different amounts of pure chlorhexidine was studied to determine the suitable concentration of this antimicrobial agent. Release of chlorhexidine from bone cement samples was not detected after 22 days regardless the initial concentration of drug added to the bone cement (Fig 1.1), There was no significant difference in the antimicrobial activity for the different bone cements (0.5–5% w/w) against *A. baumannii* and *P. aeruginosa*; the inhibition lasted less than 4 days (Fig 1.1). The antimicrobial activity of Cemex containing 3, 4 and 5% w/w of pure chlorhexidine was around 20 days against *MRSA* and *E. coli* and around 25 days for *S. pyogenes* and *S. epidermidis*. As a result, the addition of 3% w/w of pure chlorhexidine was chosen for further optimization, because it seemed that higher concentrations of chlorhexidine (4 and 5%) did not significantly increase in the antimicrobial activity and higher amounts may compromise the mechanical properties of the cement or increase toxicity without improving the antimicrobial properties.The antimicrobial activity of the bone cement was due to the released drug; as the concentration of the antimicrobial agent in the media surrounding the bone cement decreases with time, PJI can only be prevented when the concentration is above the MIC of pathogens. The variations observed among the tested strains is linked to MIC towards a specific microorganism being a strain specific property; furthermore Gram- (i.e. *A. baumannii* and *P. aeruginosa*) are generally more resistant than Gram+ (i.e. *S. aureus*, *S. epidermidis* and *S. pyogenes*) to antimicrobial treatment and this was also observed from the bone cement releasing chlorhexidine (Fig 1.1). The PJI isolates used here were gentamicin resistant (MIC > 250 mg/l) and thus represent some of the most threatening strains; the ability of bone cement containing chlorhexidine to inhibit their growth and the extension of such property when the drug is released highlight the potential benefits of the drug delivery presented in stopping potential PJIs. Despite providing antimicrobial activity, in order to be a viable option, the nanocarriers must not induce negative effects on the other bone cements properties; for this reason, the cytotoxicity in vitro and ex-vivo, compression strength and rheological properties of the bone cements were determined (Fig 1.2). The results demonstrated that the nanocarriers did not have a detrimental effect on these essential characteristics.

CONCLUSION

The application of multilayers nano-delivery systems may play a vital role in improving the release of non-antibiotic therapeutic agents such chlorhexidine from the bone cement, which is needed to reduce infection rates after TJRs. Also, it could provide a solution to the occurrence of PJI for longer periods of time and a solution to antimicrobial resistance without compromising other properties needed for performance.

REFERENCES

1. Al Thaher, Y.et al. PLoS ONE 2018: 13(12).2.Bechert T. *et al.*, Nature Medicine 2000;6:1053-1056.

ACKNOWLEDGMENTS The authors would like to acknowledge Arthritis Research UK (ARUK:18461) for funding this study.

Consequence of the COVID-19 pandemic on the production of medical devices produced with 3D printers in French hospitals

Constant Beroulle[1,2*], Xavier Armoiry[1,2], Claire Gaillard[1,2]

[1] Univ Lyon, Université Claude Bernard Lyon 1, INSA Lyon, CNRS, MATEIS, UMR5510, 69008 Lyon, France
[2] ISPB, Lyon School of Pharmacy, Université Claude Bernard Lyon 1 69008 Lyon, France
[*]constant.beroulle@outlook.fr

INTRODUCTION

Three-dimensional (3D) printing, also known as additive manufacturing technology quickly became established in prototyping. Then, it quickly conquered the world of health with the dentistry sector first [1]. *Pierreville J. and al*. had proposed an inventory of the applications of the technology and had highlighted applications in orthopedic and maxillofacial surgery in 2017[2]. Also, this same study deplored the lack of specific regulation by the health authorities, our ambition with this work is to propose answers to this problem. The COVID-19 pandemic, on one hand, allowed the media to cover this technology. [3] Indeed, this pandemic has had the benefit of creating an awareness of the possibilities of this technology in certain medical specialties that were previously reluctant to use it. [4]On the other hand, *Daoulas T. and al.* have highlighted the fact that many of the initiatives during the COVID-19 pandemic related to this technology were scattered, uncoordinated responding to the emergency[5]. The regulatory environment of our article was switching from the medical device directive (MDD) 93/42 to the medical device regulation (MDR) 2017/745 which intensified the audit of the notified bodies and raises the question of the brake on innovation associated with this more restrictive regulation.

EXPERIMENTAL METHODS

We decided to focus only on the University Hospitals in France. The main objective of the study is to find out in what form projects related to 3D printing have been carried out in post-pandemic university hospitals.
The secondary objectives of the study are to find out about the uses of 3D printing, the profile of requests for printing and the processes for gathering needs and producing them.
We adapted the questions according to the hospital profile. Hospitals that have never had a project using 3D printing ; Hospitals that have collaborated with external partners on projects using projects using 3D printing (but no longer) ; Hospitals currently collaborating with external partners in projects using 3D printing ; Hospitals that have brought 3D production in-house.

RESULTS AND DISCUSSION

We collected responses from 30 (91%) of the 33 French university hospitals 66% (n=20) of them have or have had (in the past) a 3D printing project within their establishment and 34% (n=10) have no project using 3D technology. 3D printing projects were linked to COVID in 75% of cases. The technologies used are mainly FDM and SLA: 100% of respondents use one or other technology. The technologies used are mainly FDM and SLA: 100% of respondents use one or the other technology. The materials used are mainly PLA and ABS: 100% of respondents use PLA and 30% use ABS in addition. Our results suggest that the medical specialties previously described in the literature remain the most in demand for projects using 3D printing : maxillofacial surgery, Ear Nose and Throat specialist, orthopedic surgery. However, the COVID-19 pandemic has led to a diversification of the profiles requesting printing. The regulations deemed too vague and not adapted to the problems of 3D printing, as well as the investment that this technology represents, are the two main obstacles, highlighted during our talks, to the implementation of a more sustainable structure within hospitals. Indeed, the implementation of an economically viable model seems to be the challenge today to accelerate the applications of this technology in health, while maintaining a high level of safety for the patient.

CONCLUSION

3D printing is a technology with great potential but still needs time to be fully exploited and "tamed". As far as medicines are concerned, the pandemic has raised awareness of the need to have in-house production capacities for certain vital treatments to ensure that these treatments are available to patients. The same cannot be said for medical devices. Yet the ability to produce certain medical devices in-house could have a triple benefit : An emergency solution in case of supply difficulties ; New perspectives in the training of health professionals ; A new way of integrating the patient into the care process, by involving him in the design of his medical device.

REFERENCES

[1] Aimar A, Palermo A, Innocenti B. The Role of 3D Printing in Medical Applications: A State of the Art. J Healthc Eng. 2019;2019:5340616. Published 2019 Mar 21
[2] Pierreville J, Serrano C, van den Brink H, Prognon P, Pineau J, Martelli N. Annales Pharmaceutiques Françaises. mars 2018;76(2):139-46.
[3] . Pierreville, C. Serrano, H. van den Brink, P. Prognon, J. Pineau, N. Martelli, Volume 5871, Issue 2, 03/2017, Pages 89-162
[4] Choong, Y.Y.C., Tan, H.W., Patel, D.C. et al. The global rise of 3D printing during the COVID-19 pandemic. Nat Rev Mater 5, 637–639 (2020). https://doi.org/10.1038/s41578-020-00234-3
[5]Daoulas T, Bizaoui V, Dubrana F, Di Francia R. Annals of 3D Printed Medicine. 1 août 2020;1:100001.

Kill&Repel Coatings: the Marriage of Antifouling and Bactericidal Properties to Mitigate and Treat Wound Infections

Manuela Garay-Sarmiento[1,2], M. Vorobii, [1] C. Simons[2], N. Herrmann[2], E. Heine[1], R. Lütticken[1], F. Jakob[1,2], U. Schwaneberg[1,2,*], Cesar Rodriguez-Emmenegger[1,3,4,*].

[1]DWI Leibniz Institute for Interactive Materials, Aachen, Germany, [2] Chair of Biotechnology, RWTH Aachen University, Aachen, Germany, [3]Institute for Bioengineering of Catalonia (IBEC), and [4]Institució Catalana de Reserca I Estudis Avançats (ICREA), Barcelona, Spain
[*] rodriguez@dwi.rwth-aachen.de and schwaneberg@dwi.rwth-aachen

INTRODUCTION

Wound infections originate when exogenous or endogenous bacterial pathogens can circumvent the barrier of the wound dressing and invade the wound bed. Bacterial colonization causes inflammation, stalls the healing process, and carries the risk of dissemination to other tissues. In addition, current antimicrobial dressings fail to resolve an infection once it has been established because debris of the killed bacteria rapidly accumulates on their surface and hampers the antimicrobial action. Faced with this challenge, we developed hybrid synthetic-natural water-soluble macromolecules that self-assemble onto the surface of dressings to generate an antifouling brush functionalized with endolysin, a bactericidal enzyme that poses no harm for eukaryotic cells. We call this coating Kill&Repel.[1] By exhibiting repellent and bactericidal properties, it limits the initial stages of bacterial adhesion onto the dressing, thus reducing bacterial load. If however bacteria manage to surpass the repellent barrier, the endolysin is capable of killing them upon contact. Cell debris is subsequently repelled.

EXPERIMENTAL METHODS

The coating consists of two molecules, one that imparts antifouling properties and another bearing bactericidal activity. The antifouling molecules consist of *N*-(2-hydroxy-propyl)methacrylamide polymer grafted from the liquid chromatography peak I peptide (LCI-eGFP-pHPMA). Bactericidal activity was achieved by making a fusion construct of LCI with a highly active endolysin (LCI-EndLys). The Kill&Repel coating was formed by physisorption of both hybrids from a dilute aqueous solution onto the surface of a wound dressing.

RESULTS AND DISCUSSION

The adsorption of LCI-eGFP-pHPMA and LCI-EndLys followed a Langmuir isotherm. Using a combination of atomic force microscopy and x-ray reflectivity analysis, we showed that the adsorption of LCI-eGFP-pHPMA led to segregation of pHPMA at the periphery of the surface, resulting in a brush-like coating which effectively prevented the fouling from proteins and bacteria. Remarkably, the activity of immobilized LCI-EndLys was higher than that of the molecularly dissolved one, suggesting that the co-adsorption with pHPMA had a boosting effect on LCI-EndLys. This was further evidenced by the coating being able to reduce concentration of planktonic bacteria (OD_{550}=0.8) by over 92% and far more efficient than free LCI-Endlys (50%). Similarly, it decreased sessile bacterial colonization on agar plates by 96%. Moreover, it prevented the unspecific adhesion of skin cells, colonization of the dressing by bacteria, as well as debris and was fully innocuous to human cells.

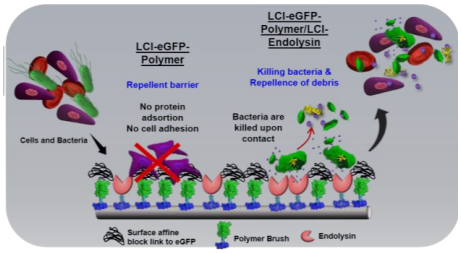

Fig. 1: Kill&Repel: LCI-eGFP-pHPMA prevents the adhesion of proteins, skin cells and bacteria. If bacteria surpass the repellent barrier, LCI-EndLys killed them upon contact. Debris is repelled from the surface by LCI-eGFP-pHPMA.

CONCLUSION

We designed a Kill&Repel coating for wound dressings, which synergistically combines the ability to repel pathogens with a bioorthogonal bactericidal strategy that causes no harm to eukaryotic cells. This strategy allows for the targeted killing of bacteria and a self-cleaning mechanism rendering the modified surface an inexhaustible antimicrobial strategy. Thus, this strategy opens a revolutionary approach for protecting and treating an infected wound in a safer and more efficient manner.

REFERENCES

[1]Garay-Sarmiento M, et. al., Adv. Func. Mater. Doi: 10.1002/adfm.202106656.

ACKNOWLEDGMENTS

The research was supported by the European Commission within a H2020-NMBP-TR-IND-2018, EVPRO grant 814495-2 and by the Federal Ministry of Education and Research of Germany as part of the ideas competition for the "Biologization of Technology"(grant number: 13XP5155.

EU and US regulatory challenges to classify borderline bone allografts and devices containing animal tissue derivatives

Thomas Miramond[1], Adrian Keene[1]

[1]NAMSA, Regulatory Department, Lyon, France tmiramond@namsa.com

INTRODUCTION

The challenge of advanced bone reconstruction involves the development of both osteoconductive scaffold engineering and osteoinductive properties. The bioactivity claimed by medical device manufacturers may result in the clearance of important regulatory requirements to ensure the safety and performance of their innovative solutions.

There are specific cases that the European Commission has defined as borderline[1] and cases of discrepancies in classification between the US[2] and European Competent Authorities of which human Demineralized Bone Matrix (DBMs) using specific excipients is highlighted as an obvious example as well as innovative medical devices utilizing animal tissue derivatives.

EXPERIMENTAL METHODS

Through the study of specific cases of DBM and new trend of bone substitutes device utilizing animal tissue derivatives, the consequences in terms of compliance efforts to the regulations including EU No 722/2012 and state-of-the-art including ISO 22442 series were examined. Clarifications outcomes for manufacturers and anticipation of future possible harmonization between the two major EU and US markets were implemented in this strategic summary approach.

RESULTS AND DISCUSSION

A range of implantable medical devices from different technologies and biological sources, both allogenic and xenogenic, were analyzed in regulatory terms. The differences between the European and American markets were updated with regard to regulatory developmentsand the inclusion of the in-depth risks associated with bioactive proteins such as growth factors and other active signaling molecules. The considerations of jurisdictional decisions from FDA[3] and guidance for borderline products from the EU Commission.

CONCLUSION

This work is the result of research into the benchmarking of products considered under either the Tissues or Cells, the Advanced Therapeutic Medicinal Products (ATMP) or Medical Device regulations including MDR (EU) 2017/745. The evolving regulations are becoming more and more stringent with a necessary trend to harmonization between the major worldwide markets. That is why innovative the manufacturers must exploit innovative bone tissue engineering technologies by taking into account the new regulatory worldwide context including Competent Authorities animal tissue and medicinal boards scrutiny process in addition to a risk based approach good practice such as quality by design (QbD). Risk assessment and identification of appropriate regulatory routes hence involve further actions from manufacturers in pre-clinical and clinical terms as discussed in this presentation.

REFERENCES

1. EU – Manual on borderline and classification in the community regulatory framework for medical devices. Version 1.22 (05-2019).
2. Gillman, C. E., et al (2021). Materials Science and Engineering: C, 130, 112466, 2021.
3. “Jurisdictional Update: Human Demineralized Bone Matrix” dated January 19, 2001 (DBM Guidance)

Functionalization of nanocellulose with host defense peptides: towards the modulation of the inflammatory response in chronic wounds

Anna Blasi-Romero*[1], Carlos Palo-Nieto[1], Molly Ångström[1], Taj Muhammad[2], Ulf Göransson[2], Natalia Ferraz[1]

[1] Division of Nanotechnology and Functional Materials, Department of Materials Science and Engineering, Uppsala University, Uppsala, Sweden
[2]Department of Pharmaceutical Biosciences, Uppsala University, Uppsala, Sweden
* anna.blasi@angstrom.uu.se

INTRODUCTION

Host defense peptides, short cationic amphiphilic peptides, are becoming highly interesting as a new generation of therapeutics able to modulate the immune response and offer antimicrobial activity. However, their short half-time life under physiological conditions, for example due to protease degradation, and their sometimes-unwanted toxicity are limiting their potential applications.[1] An overexpressed inflammatory response is characteristic in hard to heal wounds. The modulation of such response with bioactive wound dressings is believed to aid on the healing of chronic wounds. Nanocellulose materials have shown promising properties for the treatment of acute wounds.[2] Moreover, they are highly tunable chemically, which makes them good candidates to combine with bioactive molecules and obtain potential bioactive dressings.

In this work, we aim to develop a biomaterial able to modulate inflammation by combining the properties of wood derived cellulose nanofibrils (CNF) and derivatives of the host defense peptide KR12. This approach is expected to improve the stability of the peptide under physiological conditions while keeping its bioactivity and provide anti-inflammatory properties to the final CNF material. For this, four KR12 derivatives were covalently incorporated to CNF. The new CNF materials were characterized in terms of cytotoxicity and anti-inflammatory properties using in vitro studies with the macrophage cell line RAW 264.7.

EXPERIMENTAL METHODS

Different chemical approaches were used to covalently incorporate four KR12 derivatives on CNF. Material suspensions from 250 to 1000 µg/mL were added to monolayers of RAW 264.7 cells, and cell metabolic activity (measured with the presto blue assay) was evaluated as an indicator of cell viability. To evaluate the anti-inflammatory effect of the materials on LPS-stimulated macrophages, RAW 264.7 cells were exposed to 10 ng/mL LPS in the presence of the KR12-CNF materials. The levels of the pro-inflammatory cytokine TNF-α were quantified by ELISA assay. Values were normalized by total protein content, quantified with the BCA assay. The free KR12 derivatives were evaluated under the same conditions, at concentrations corresponding to the amount of KR12 present in the KR12-CNF suspensions.

RESULTS AND DISCUSSION

KR12 derivatives were covalently incorporated to CNF with a peptide substitution corresponding to 0.17 ± 0.04 mmol/g CNF. Three out of four synthesized materials showed concentration dependence effect on the cell metabolic activity, with the highest concentration evaluated, 1000 µg/mL, causing a reduction in metabolic activity higher than 30% respect to the negative control, which indicates a cytotoxic response (Figure 1,I). Interestingly, the corresponding peptides evaluated in the equivalent concentrations as their KR12-CNF counterparts showed no signs of cytotoxicity (peptides B, C in Figure 1,II). Peptide D showed toxicity at 100 and 200 µM. This different cytotoxic response between the peptide free in solution compared to the KR12-CNF could indicate an improvement on the peptides' stability under physiological conditions. The CNF might offer a less exposed disposition of the peptide to the media, being less vulnerable to degradation, but then being more prone to induce cytotoxicity at high concentrations. Inflammatory response of LPS-stimulated RAW 264.7 cells was reduced by the KR12-CNF materials indicating that the peptides maintain their bioactivity when they are presented covalently linked to the CNF.

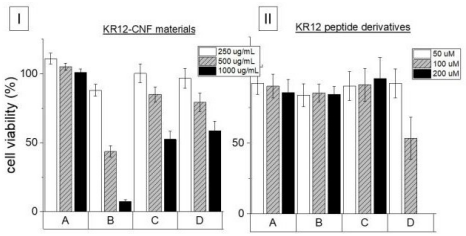

Figure 1: Cell metabolic activity of RAW 264.7 cells after 24h exposure to the different KR12-CNF materials under study (I) and the corresponding KR12 derivatives (II).

CONCLUSION

In this study, four derivatives of the known host defense peptide KR12 were successfully covalently incorporated to CNF, resulting in improved stability of the peptide and endowing CNF with the ability of modulating the inflammatory response of LPS-stimulated RAW 264.7 macrophages. KR12-CNF materials show promising properties for the development of bioactive dressings for the treatment of prolonged inflammation in chronic wounds.

REFERENCES

1. Hancock, R., *et al*., Nature Biotechnology 24, 1551-57, 2006, 2. Basu, A., *et al.,* ACS Applied Bio Materials 1, 1853-63, 2018

ACKNOWLEDGMENTS

The authors would like to thank The Swedish Research Council (grant number 2018-04613) and Bo Rydin Foundation (grant number F30/20) for the financial support of this work.

Macrophage-Targeted Shikonin-Loaded Nanogels for Modulation of Inflammasome Activation

Host immune response to medical devices and implantable biomaterials is key to their functional integration. Several cell types, proteins and extracellular components are involved in this innate response. Macrophages are essential in the regulation of the inflammatory response. Inflammasomes are intracellular multimeric protein complexes expressed primarily by innate immune cells, such as monocytes, macrophages and dendritic cells. They assemble upon exposure to pathogen-associated molecular patterns (PAMPs) or damage-associated molecular patterns (DAMPs), critically contributing to regulate the inflammatory response and, hence, to inflammation resolution or persistence. The development of biomaterials to modulate the inflammasome activation is a promising strategy towards the promotion of implant integration. In this work, we have developed macrophage-targeted biopolymeric-based nanocarriers for the controlled release of immunomodulatory metabolic drugs1. Shikonin, a natural naphthoquinone with anti-inflammatory properties, was encapsulated into zein-hyaluronic acid nanogels. These nanocarriers were efficiently taken up by macrophages, showing low toxicity. Their ability to modulate inflammasome activation was demonstrated by a significant suppression of caspase-1 activation and IL-1β production in cells pretreated with the SK-loaded nanogels. Moreover, macrophages phenotypic characterization showed that these nanocarriers induced an anti-inflammatory CD163highHLA-DRlow phenotype and led to a marked reduction in the release of pro-inflammatory mediators (TNF-α, IL-6 and IP-10). Extracellular metabolic profiling by 1HNMR exometabolomics was employed to assess the metabolites and metabolic pathways affected by inflammasome activation and its nanocarrier-mediated attenuation. These results set the basis for further testing these nanocarriers in vivo and for developing new biomaterials designed to mitigate local exacerbated or chronic inflammation, while promoting tissue regeneration. Looking forward, we aim to develop a novel class of versatile inflammasome-modulating biomaterials to mitigate implant-related inflammation.

Matias Cardoso [1], Vítor M. Gaspar [1], Carolina Ferreira [2,3], Ricardo Silvestre [2,3], Iola F. Duarte [1], and João F. Mano[1]
[1] Department of Chemistry, CICECO – Aveiro Institute of Materials, University of Aveiro, Aveiro, Portugal.
[2] Life and Health Sciences Research Institute (ICVS) School of Medicine, University of Minho, Braga, Portugal
[3] ICVS/3B's-PT Government Associate Laboratory, Guimarães, Portugal
[*] matias.cardoso@ua.pt

INTRODUCTION

Inflammasomes are intracellular multimeric protein complexes expressed primarily by innate immune cells, such as monocytes, macrophages and dendritic cells. The NLRP3 inflammasome paramount importance in wound healing and in host responses to engineered nanoparticles or implanted biomaterials. Shikonin (SK), a natural naphthoquinone is a bioactive molecule with extensively reported anti-inflammatory properties. In the present work, we have newly developed SK-loaded Hyaluronic acid-Zein (HA-Zein-SK) nanogels for inflammasome attenuation in human macrophages (5).

EXPERIMENTAL METHODS

Hyaluronic acid-Zein (HA-Zein) nanogels were self-assembled via nanoprecipitation. Followed. Nanogel physicochemical characterization and inflammasome activation attenuation was addressed by measuring the secretion levels of IL-1β and caspase-1 activity.

RESULTS AND DISCUSSION

Hyaluronic acid-Zein (HA-Zein) nanogels were formulated via nanoprecipitation to enable reproducible nanocarriers production and efficient SK entrapment (Figure 1A schematics). Nanogels showed of 195 and 205 nm and spherical morphology. These nanogels could be successfully loaded with SK, rendering an encapsulation efficiency of approximately 90%.

HA-Zein nanogels were non cytotoxic, revealed high internalization levels and showed CD44 targeting properties. Moreover, to determine the bioinstructive capability of HA-Zein-SK nanogels for attenuating macrophage inflammasome activation, we analysed two key biomarkers in the inflammasome cascade, namely, the secretion of IL-1β and caspase-1 activity. HA-Zein-SK nanogels produced a dose-dependent decrease of IL-1β production (Figure 4B). Furthermore, both the SK-loaded nanogels and free drug significantly decreased caspase-1 activity **(Figure 2)**.

CONCLUSION

Our findings demonstrate the potential of bioactive Zein-HA-SK nanogels to modulate macrophage inflammasome. In the future, we plan to test these drug delivery systems in vivo, namely through their loco-regional administration in inflamed tissues, to evaluate if inflammasome attenuation will contribute for resolving acute or chronic inflammation.

REFERENCES

5. Cardoso, M. *et al*., Nanomed. Nanotechnol. Biol. Med. 102548, 2022.

The Influence of Patient-Specific Characteristics on Macrophage-Driven *In Situ* Tissue Engineering Using Resorbable Synthetic Scaffolds

Bente de Kort[1,2 $], Suzanne Koch[1,2 $], Franka Verhaegh[1], Simone Smink[1], Noud Holshuijsen[1], Justin Lebens[1], Carlijn Bouten[1,2], Anthal Smits[1,2*]

[1]Department of Biomedical Engineering, Eindhoven University of Technology, Eindhoven, The Netherlands
[2]Institute for Complex Molecular Systems (ICMS), Eindhoven University of Technology, Eindhoven, The Netherlands
[$]Authors contributed equally; [*] a.i.p.m.smits@tue.nl

INTRODUCTION

In situ tissue engineering using bioresorbable scaffolds is an emerging approach to replace diseased cardiovascular tissues, such as blood vessels and heart valves[1]. Such implants are produced from highly porous fibrous scaffolds, which accommodate the infiltration of host cells upon implantation. The recruited cells deposit functional new tissue, while the synthetic scaffold material is immunologically resorbed. The balance between scaffold resorption and tissue formation is governed by macrophages in cross-talk with myofibroblasts.

Much research is focused on modulating the inflammatory and regenerative responses by the local scaffold niche via physical scaffold design features, such as fiber diameter and pore size. However, independent of the scaffold design, the process of *in situ* tissue engineering is heavily dependent on the patient's endogenous immunological state and regenerative capacity, which are dependent on patient-specific characteristics, such as sex, age or comorbidities (e.g. diabetes)[2]. This area is largely understudied so far and little mechanistic data is available, both *in vitro* and *in vivo*[2,3]. Therefore, the aim of this study was to investigate the influence of patient-specific characteristics on *in situ* tissue engineering. More specifically, we used a human *in vitro* model to systematically investigate the influence of (1) sex and age, and (2) the influence of hyperglycemia (as a typical manifestation of diabetes) on the response of human macrophages to bioresorbable scaffolds in terms of inflammation, scaffold resorption potential and signaling to myofibroblasts.

EXPERIMENTAL METHODS

To simulate the early phases of the *in situ* regenerative cascade, primary human peripheral blood-derived macrophages were seeded in mono-culture or in co-culture with human myofibroblasts in 3D electrospun resorbable polycaprolactone bisurea (PCL-BU) scaffolds, and exposed to various biochemical conditions. In order to study the influence of sex and age, we compared the behavior of macrophages between male and female donors, as well as between pre- and post-menopausal female donors in varying physiological concentrations of estradiol (n=12 donors). To investigate the influence of hyperglycemia, the cells were exposed to either normoglycemic (5.5 mM glucose), hyperglycemic (25 mM glucose) or osmotic control conditions (5.5 mM glucose, 19.5 mM mannitol) (n=8 donors).

Cell-seeded scaffolds were cultured up to 7 days and analyzed in terms of gene expression (qPCR), cell surface markers (immunofluorescence), cytokine secretion (ELISA), scaffold resorption (SEM), and tissue formation (biochemical assays).

RESULTS AND DISCUSSION

The macrophage response to a biomaterial is sex-specific
Remarkably, the results revealed that the macrophage response to the scaffolds was sex-specific, with distinct differences in scaffold-activated macrophage phenotype compared to males (e.g. upregulation of CCR7, CD163), as well as differences in pro-fibrogenic signalling to myofibroblasts. Moreover, female macrophages showed an increased production of reactive oxygen species (ROS) when compared to male cells. Unexpectedly, there were no clear effects of female donor age (pre- versus post-menopause), nor estradiol concentration. Overall, our results indicate intrinsic sex-specific differences in inflammation, as well as scaffold resorption and tissue formation potential for scaffold-associated macrophages.

Hyperglycemia promotes a pro-inflammatory response
Hyperglycemia tended to induce a more pro-inflammatory response by the scaffold-activated macrophages, as expected, although responsiveness was highly variable between donors in terms of phenotype, cytokine secretion profile, and metabolic receptor expression. When co-cultured with myofibroblasts, hyperglycemic conditions led to an increased expression of fibrogenic markers (ACTA2, COL1, COL3, IL-1β). Together, these findings show that the hyperglycemic and hyperosmotic conditions may indeed influence the process of macrophage-driven *in situ* tissue engineering, and that the extent of this influence is likely to be patient-specific.

CONCLUSION

These studies indicate the importance of considering patient-specific characteristics for macrophage-driven *in situ* tissue engineering. Our human *in vitro* model may act as a tool to systematically unravel the underlying mechanisms in parallel to preclinical *in vivo* models.

REFERENCES

1. Wissing T.B. *et al*., NPJ Regen. Med. 2:18, 2017.
2. De Kort B.J. *et al*., Adv. Drug Deliv. Rev. 178:113960, 2021.
3. Koch S.E. *et al.* NPJ Regen Med. 7:17, 2022.

ACKNOWLEDGEMENTS

This study was financially supported by the InSiTeVx project (436001003; ZonMw within the LSH 2Treat Programme and the Dutch Kidney Foundation), and the Gravitation Program "Materials Driven Regeneration", funded by the Netherlands Organization for Scientific Research (024.003.013).

Influence of biomaterials surface composition and topography on the activation of neutrophils

Ezgi Irem Bektas[1*], Marinus A. Wesdorp[2], Jacek K. Wychowaniec[1], Gregor Miklosic[1], Matteo D'Este[1]

[1] AO Research Institute Davos, Clavadelerstrasse 8, 7270, Davos, Switzerland
[2] Department of Orthopaedics and Sports Medicine, Erasmus MC, University Medical Center Rotterdam, The Netherlands
*ezgi.bektas@aofoundation.org

INTRODUCTION

Neutrophils are the first immune cells recruited to the sites of injury, inflammation, or infection, and play a major role in the innate immune response upon implantation of biomaterials[1]. They are very sensitive to environmental changes; therefore, the physical and chemical properties of biomaterials could have an influence on the activation of neutrophils[2]. Investigating and understanding the interactions between biomaterials and neutrophils is crucial to establish design principles

FBS treated THA hydrogels had significantly higher metabolic activity than the cells cultured on non-treated ones at 7th hour. The LDH release is indicative of cell membrane damage (Figure 1B). The percent cytotoxicity increased gradually throughout 24 h of incubation for all material surfaces. The amount of LDH released from the neutrophils was higher on PCL line scaffolds than the rest of the material surfaces. The only significant difference in percent cytotoxicity values of FBS-treated and FBS non-treated THA samples was observed after 24 h of

Developing an *In Vitro* Methodology to Study the Foreign Body Response Towards Hydrogel Depots

Chloe Stewart[1*], Anna M. Piccinini[1], Mischa Zelzer[1], Andrew L. Hook[1], Maria Marlow[1]

[1]School of Pharmacy, University of Nottingham, United Kingdom
* chloe.stewart@nottingham.ac.uk

INTRODUCTION

Fibrotic encapsulation of implanted biomaterials is a characteristic but unpredictable phenomenon of the foreign body response (FBR).[1] Understanding fibrotic capsule formation is critical in developing depot formulations due to the potential of the compact collagen layers to hinder drug diffusion from the biomaterial.[2] However, due to the absence of an established method to study the FBR, there is limited understanding as to how the development of a fibrotic capsule influences drug release from depot formulations.

We developed an *in vitro* co-culture model to predict the FBR towards injectable hydrogels. Utilising this FBR screening tool, we aimed to develop biomaterials that can reproducibly induce fibrotic capsule formation for use in evaluating the impact on long-term drug release.

EXPERIMENTAL METHODS

We present our work in two parts; development of an *in vitro* co-culture FBR model and synthesis of modified hydrogels as our depot materials to evaluate the associated fibrotic response.

FBR model development: We first developed an *in vitro* FBR screening tool consisting of a co-culture of human macrophages and fibroblasts. Starting with macrophages, we identified optimal conditions for macrophages to fuse and form foreign body giant cells (FBGC), which are a key feature of the FBR and stimulate fibroblasts to produce collagen during fibrotic capsule formation. Human primary monocyte-derived macrophages (n=4 biological donors) were cultured on either tissue-culture polystyrene (TCPS) or polyethylene terephthalate (PET) surfaces with different cytokine combinations for up to 28 days. Cells were characterised by image analysis and quantification of secreted cytokines and growth factors by ELISA. To establish a co-culture model, we introduced human foreskin fibroblasts (BJ, CRL-2522) and evaluated changes in profibrotic cell activity by quantifying COL1A1, COL3A1, TGF-β1 and α-SMA gene expression and using fluorescence microscopy to analyse collagen deposition, which is the predominant component of the fibrotic capsule.

Synthesis of hydrogel depots: Polyester-PEG-polyester triblock copolymers were selected for use as hydrogel depots in our FBR model due to their proven efficacy in sustained drug release studies and possession of terminal hydroxyl groups that can be targeted for functionalisation. To induce fibrosis for studying the effect on drug release, co-polymers were functionalised with a profibrotic peptide to produce hydrogels that can stimulate the formation of a fibrotic capsule *in vitro.*

RESULTS AND DISCUSSION

Macrophages cultured on PET in the presence of the cytokine interleukin(IL)-4 resulted in up to 97% of macrophages fusing to form FBGC (Fig. 1b), the largest of which contained 48 nuclei. High levels of fusion were achieved in ≥3 weeks and coincided with elevated levels of PDGF (≥6.8-fold ± 1.0), which has been associated with increased collagen production in fibrotic disorders.[3]

Figure 1 Giemsa-stained cells after 26 days (a) macrophages on TCPS (b) FBGC on PET with IL-4 (10 ng/mL). Scale bar 50 µm.

To induce a fibrotic capsule *in vitro*, we functionalised copolymers with a peptide that upregulated profibrotic genes in fibroblasts, which are critical in collagen production. Following polymer modifications, DOSY and H^1-NMR confirmed successful polymer maleimidation and peptide conjugation, respectively. We evaluated the modified hydrogels into our FBR model, determining the level of fibrotic encapsulation. By tailoring the extent of functionalisation, we can control the *in vitro* development of the fibrotic capsule, which will influence the sustained drug release from depots.

CONCLUSION

We successfully developed an *in vitro* FBR model by identifying conditions that resulted in up to 97% of macrophages fusing into FBGC and incorporating fibroblasts into the co-culture. Hydrogels were modified with a profibrotic peptide to create materials that modulate collagen production. Introducing the modified hydrogels into our *in vitro* FBR model enabled an evaluation of the impact on collagen deposition. We aim to later characterise how this fibrotic collagen layer may influence sustained drug release from hydrogel depots

REFERENCES

[1] Witherel, C.E. *et al.*, Adv. Healthc. Mater. 8(4):1-16, 2019
[2] Anderson J.M. *et al.*, J. Biomed. Res. 15(6):889-902, 1981
[3] Juhl P. *et al.*, Sci. Rep. 10:17300, 2020

ACKNOWLEDGMENTS

The authors would like to thank the UKRI Engineering and Physical Sciences Research Council (Grant no: EP/L01646X/1) for funding this project.

Physico-chemical and immunoregulatory characterization of polyelectrolytes coatings from a bacterial exopolysaccharide

Romain Bagnol[1*], Liam O'Mahony[2]
T. Fintan Moriarty[1], David Eglin[3]

[1]AO Research Institute Davos, Davos, Switzerland
[2]Departments of Medicine and Microbiology, APC Microbiome Ireland, National University of Ireland, Cork, Ireland
[3]Mines Saint-Étienne, Univ Lyon, Univ Jean Monnet, INSERM, U1059 Sainbiose, Saint-Étienne F - 42023 France

[*] romain.bagnol@aofoundation.org

INTRODUCTION

The inflammatory response to biomedical implants plays a crucial role in its integration, with an excessive or unresolved inflammation usually leading to a lack of integration and removal of the device. Locally applying immunoregulatory molecules on the surface of these devices should increase implant integration without inducing systemic effects. It has been shown that several probiotic bacterial strains can have immunoregulatory properties when living in the human gut, including via extracellular polysaccharides. In this study we used an exopolysaccharide from a *Bifidobacterium longum* strain (BIEPS), which was previously shown to have immunoregulatory properties when given orally or intranasally. Our objective was to produce polyelectrolyte coatings incorporating the BIEPS and determine in vitro the biological response of human peripheral mononuclear blood cells (PBMCs) seeded on coatings.

EXPERIMENTAL METHODS

The production and purification process of the BIEPS was performed by collection and centrifugation of bacterial pellets, filtration and precipitation of the supernatant with ethanol, dialysis with 12kDa cellulose membrane, reverse phase columns chromatography and freeze drying. Polyelectrolyte coatings were prepared by combining the negatively charged BIEPS and positively charged chitosan to create polyelectrolyte coatings with 1, 5 and 10 layers of each material on 15mm glass discs. The glass discs were first cleaned with 10mM SDS, then 0.1M HCl then rinsed in MilliQ water and dried at RT. The disks were then dipped in a chitosan bath for 5 minutes (1mg/mL, pH 5), then dipped in 2 rinsing baths for 2 minutes each (MilliQ water pH 5), then dipped in a BIEPS bath for 5 minutes (1mg/mL, pH 5) and dipped in 2 rinsing baths for 2 minutes each (MilliQ water pH 5). The dipping process was repeated as required.

PBMCs harvested from a buffy coat were used to measure Interleukin 10 secretion after exposure to the purified BIEPS in solution or to the BIEPS polyelectrolyte coatings. After 24h incubation, the supernatants were collected and IL-10 was quantified by ELISA. To test the stability and biological activity overtime, coatings with various number of layers were immersed in PBS for 1, 3 and 7 days at 37°C before exposing the PBMCs to the coatings for 24h and measuring their IL-10 activity through an ELISA test.

RESULTS AND DISCUSSION

When dissolved in media, the BIEPS induced an increase in IL-10 expression in a dose dependent manner. While the control [6.27 ± 2.67 pg/mL] and 1µg/mL group [7.20 ± 2.17 pg/mL] had similar expression, a significant increase was seen for 10µg/mL [79.68 ± 9.23 pg/mL] and 100µg/mL [105.66 ± 0.14 pg/mL]. Compared to the clean glass control [9.04 ± 1.12 pg/mL] increases in IL-10 expression were observed for all polyelectrolytes groups as the number of layer increased from 1 layer [41.35 ± 5.74 pg/mL], to 5 layers [90.93 ± 24.65 pg/mL], to 10 layers [116.57 ± 15.92 pg/mL]. For the 10 layers group, when replacing the BIEPS with alginate the IL-10 expression dropped to [18.17 ± 4.83 pg/mL], confirming the specific immunoregulatory action from the BIEPS. The polyelectrolyte coatings could effectively show similar IL-10 expression to the BIEPS dissolved groups, while only requiring a fraction of the material of the dissolved groups.

For all groups immersed in PBS for 1 to 7 days, an initial decrease in IL-10 activity was observed between day 0 and day 1, but the activity remained relatively stable between day 1, 3 and 7. For the 1 layer group [33.67 ± 0.375 pg/mL], [7.28 ± 2.18 pg/mL], [6.73 ± 0.01 pg/mL] and [10.37 ± 0.45 pg/mL] respectively at day 0, 1, 3 and 7. For the 5 layers group [57.72 pg/mL], [16.95 ± 1.05 pg/mL], [12.98 ± 1.06 pg/mL], [15.31 ± 0.38 pg/mL] respectively at day 0, 1, 3 and 7. For the 10 layers group [102.56 ± 0.21 pg/mL], [52.17 ± 2.55 pg/mL], [43.85 ± 7.90 pg/mL] and [56.96 ± 9.78 pg/mL] respectively at day 0, 1, 3 and 7.

CONCLUSION

BIEPS dissolved in media and BIEPS polyelectrolyte coatings effectively increased IL-10 expression in PBMCs.

Next steps in the characterization of the BIEPS coating will include further physico-chemical assessments and induction of other interleukins to determine the specificity of the biological response.

ACKNOWLEDGMENTS

The authors would like to thank AO Trauma (Grant number: AR2018_04) for providing financial support to this project.

Topographical Immunomodulation: A New 3D Printing Strategy for Annulus Fibrosus (AF) Tissue Engineering

Nadine Kluser[1], Sibylle Grad[1], Andrea Vernengo[1*]
[1]AO Research Institute Davos
[*]andrea.vernengo@aofoundation.org

INTRODUCTION

Intervertebral disc (IVD) degeneration is a chronic inflammatory condition predominantly regulated by macrophages, characterized by elevated levels of cytokines, matrix degrading activities, and neurovascular ingrowth[1]. These degenerative changes lead to altered biomechanics and the formation of ruptures in the peripheral annulus fibrosus (AF) of the IVD. Since the current clinical approaches to AF closure lack inflammation-modulating function, the aim of this work was to develop a novel AF tissue engineered scaffold with immuno-informed surface properties that mitigate inflammation in the tissue by promoting macrophage polarization towards an anti-inflammatory M2 phenotype, ultimately enhancing the healing response. To this end, polycaprolactone (PCL) was extruded into the macroarchitecture of the native AF through custom-designed 3D printing nozzles that generate different aligned scaffold surface topographies. In the current study, we sought to understand the effects of the surface topographies on the polarization of M0, M1 and M2-stimulated derived macrophages.

EXPERIMENTAL METHODS

Angle-ply constructs with filaments oriented at angles of ± 30° were 3D printed by extrusion of PCL (Sigma, 45 kDa) at 75 °C through two different nozzles: a round nozzle with inner diameter of 300 µm and a patterned nozzle with inner diameter of 300 µm and circumferential peaks of 60 µm height. Human THP-1 cells (Sigma) were seeded in monolayers (TCP) or on the 3D printed scaffolds and treated with 20 ng/ml of phorbol-12-myristate-13-acetate (PMA) in Roswell Park Memorial Institute (RPMI) 1640 medium supplemented with 10% FBS for 24 hours. The THP-1 derived macrophages were then stimulated into M1 (100 ng/ml LPS and 10 ng/ml IFN-γ) and M2-like phenotypes (20 ng/ml IL-4). M0 control samples were cultured in RPMI + 10% FBS without cytokines. After 48 hours of polarization, samples were harvested for gene expression and immunofluorescent analysis. Scaffolds stained with DAPI and phalloidin were analyzed with ImageJ for cell nuclear circularity (4π x ([Area])/([Perimeter]^2)). Kruskal Wallis test with Dunn's post hoc test was performed and p-values < 0.05 were considered as significant.

RESULTS AND DISCUSSION

Whereas the round nozzle produced extruded filaments with a slight uniaxial texture (-µgrooves, Fig. 1A), the patterned nozzle produced grooves 10.87 ± 3.09 µm wide (+µgrooves). Macrophages exhibited significantly lower nuclear circularity on -µgrooved surfaces (Fig. 1B, p < 0.001), indicating better elongation. M0, M1 and M2 macrophages cultured on the + and - µgrooves did not exhibit statistically significant shifts in marker expression compared to TCP for pro (TNF-α, IL-6, IL-1β, iNOS) and anti-inflammatory (IL-10) markers or M2 surface markers (CD206, CCL18, and CD163) (p>0.05). However, compared to TCP, +/- µgrooves produced decreasing trends in pro-inflammatory IL-6 (Fig. 1C) and iNOS in M2 macrophages and increasing trends in anti-inflammatory IL-10 (Fig. 1D) and CCL-18 for all M0, M1 and M2 macrophages. CD163 trended towards upregulation in M1 macrophages on both +/- µgrooves compared to TCP. The anti-inflammatory marker CD206 exhibited the highest expression on +µgrooves for M0, M1 and M2 macrophages compared to -µgrooves and TCP.

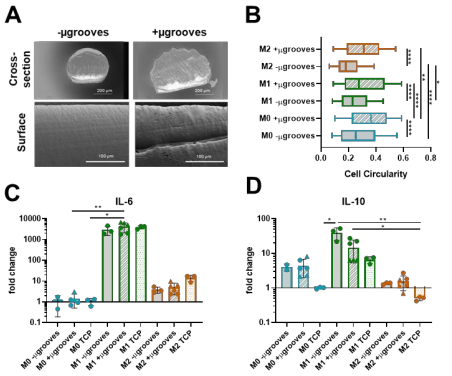

Figure 1: *A) Microscopic images of +/- µgroove scaffold surface topographies.* ***B)*** *THP-1 macrophage nuclear circularity on +/- µgrooved scaffolds. **** = p < 0.001, *** = p < 0.005, ** = p < 0.002, * = p < 0.02.* ***C,D)*** *Gene expression for macrophages on 3D printed scaffolds represented as 2-ΔΔCt-values normalized to housekeeping gene and M0 TCP. ** = p < 0.05, 8 = p < 0.01.*

CONCLUSION

The smaller size features of the topography produced by the round nozzle (-µgrooves) compared to the patterned nozzle (+µgrooves) induced higher elongation, a factor known to produce anti-inflammatory shifts in macrophages[2]. However, both the + and -µgrooved topographies produced statistically similar phenotypic signatures, with anti-inflammatory potential compared to TCP surfaces. In future work, nozzle geometry, pattern size, and extrusion printing conditions can be tailored to promote stronger anti-inflammatory signatures in macrophages.

REFERENCES

1. Molinos, M., et., 2015. Journal of the Royal Society Interface, 12(104), p.20141191.
2. Schoenenberger, A.D., et al., 2020. Biomaterials, 249, p.120034.

ACKNOWLEDGMENTS

This project was funded by a Swiss National Science Foundation SPARK grant (project number CRSK-3_195938).

Spatial modulation of Surface with Adhesion Energy Nanogradients to Stimulate Axonal Growth

Océane Sénépart[1,2*], Christophe Hélary[2], Claire Legay[1], Ahmed Hamraoui[2]

[1]Saints Pères Paris Institute for the Neurosciences (SPPIN), Université de Paris, Paris, France
[2]Laboratoire de la Chimie de la Matière Condensée de Paris (LCMCP), Sorbonne Université, Paris, France
[*] oceane.senepart@sorbonne-universite.fr

INTRODUCTION

The nerve injury in the peripheral nervous system is a devastating situation responsible for millions of new cases around the world every year. It induces a loss of motor and/or sensory function and neurons will use biological and physico-chemical environmental factors to guide growth cones to appropriate targets. Identifying new strategies to enhance regeneration and guidance of growth cones is fundamental to restore nervous system functions. Among them, local adhesion energy gradients generated on surfaces trigger cone formation and neurite outgrowth without any nerve growth factor (NGF) addition[1].

EXPERIMENTAL METHODS

In this study, the molecular mechanisms leading to neuronal differentiation after stimulation via energy gradients are investigated[2]. For this purpose, PC12 cells are cultured on n-[3-(trimethoxysilyl)propyl]ethylendiamine (EDA) and n-hexyltrimethoxysilane (HTMS), two functionalized surfaces possessing local energy gradients but chemically different. Their physical properties are characterized using the contact angle measurement method and the Fox-Zisman approximation. A parallel gene expression analysis was lead to identify the mechanisms leading to neurite formation.

RESULTS AND DISCUSSION

These surfaces similarly trigger neurite and growth cone formation after 3 days in culture. The gene expression analysis of a microarray reveals the activation of the PI3/Akt signaling pathway from these surfaces in the same way than NGF does after binding on its TrkA receptor. The biological downstream effectors of this signaling pathway are also upregulated, thereby promoting cell survival, growth cone formation and neurite outgrowth.

EDA and HTMS surfaces act as an ongoing stimulus of the TrkA receptor as the addition of 100 nM K252a, its specific inhibitor, leads to the inhibition of neurite growth. The difference between the adhesion energy of water on a glass surface and on our specific surfaces (EDA and HTMS) was determined to obtain, respectively, 61 mJ.m^{-2} and 90,4 mJ.m^{-2}.

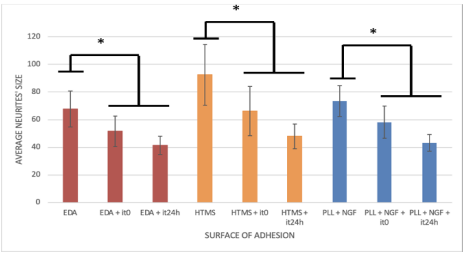

Figure 1 - Average neurites' size on PC12 cells depending on the surface adhesion (EDA, HTMS, PLL) and the addition of TrkA inhibitor.

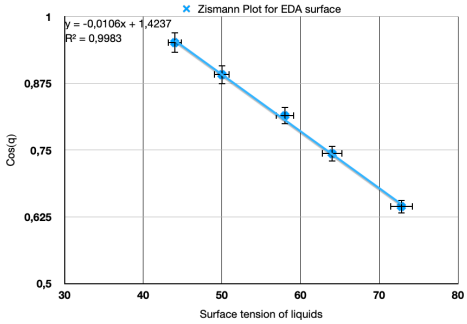

Figure 2 - Cosinus of the contact angle measurements depending on the superficial tensions of the different liquids to obtain the critical superficial tension of the surface.

CONCLUSION

Surface energy gradients act on cell via activation of the NGF receptor TrkA, thereby mimicking the effect of this growth factor in vivo. These surfaces afford an ongoing activation of neuronal differentiation which avoids the sequential addition of NGF into the milieu. Taken together, these results show that functionalized surface with energy surface gradients could be useful for an application to promote nerve repair after an injury.

REFERENCES

1. Lamour G.. *et al.*, Coll. And Surf. Bioint., 2009
2. Lamour G.. *et al.*, Macromol. Biosci., 2015

ACKNOWLEDGMENTS

The authors would like to thank the ED397 (Physics and Chemistry of Materials) for providing financial support to this project, Cochin Institute for assistance and F. Semprez and K. Gouffaud for their help in cell culture.

Combinatorial Treatments of Porous Scaffolds and Microneurotrophins for CNS Injuries

Konstantina Georgelou[1,2], Erica Saridaki[2], Chrysa Apostolidou[3], Xenofon Mallios[2], Kanelina Karali[1], Maria Savvaki[1,2], Anna Mitraki[3,4], Achille Gravanis[1,2], Ioannis Charalampopoulos[1,2], Dimitrios S Tzeranis[5,1*].

[1]Institute of Molecular Technology & Biotechnology, Foundation for Research & Technology-Hellas, Heraklion, Greece. [2]Medical School, University of Crete, Heraklion, Greece. [3]Department of Materials Science and Technology, University of Crete, Heraklion, Greece. [4]Institute of Electronic Structure & Lasers, Foundation of Research & Technology - Hellas, Heraklion, Greece. [5]Department of Mechanical and Manufacturing Engineering, University of Cyprus, Nicosia, Cyprus
* tzeranis.dimitrios@ucy.ac.cy

INTRODUCTION

Central Nervous System (CNS) injuries (e.g. spinal cord injury (SCI), optic nerve injury (ONI)) affect millions of patients.[1] The multifactorial nature of CNS injury calls for combinatorial treatments. Significant research focuses on treatments that integrate biomaterials, cells and diffusible factors, including neurotrophic support. Recently Porous Collagen-based Scaffolds (PCS) were used to deliver Neural Stem Cells (NSCs) and improve locomotion recovery in a mouse SCI model.[2] This study presents novel treatments that combine PCS (with or without NSCs) with Micro-neurotrophins (MNTs), small-molecule analogs of endogenous neurotrophins (NTs). MNTs lack major NT setbacks (pharmacokinetics, pain) and their effects have been described in several animal models of neural disorders.[3,4] Here, we study BNN27 (the seminal MNT) effects in two mouse models of CNS injury in the presence of PCS-based grafts.

EXPERIMENTAL METHODS

Scaffold fabrication

PCS sheets (2.5 mm thick, 100 μm mean pore diameter) made of microfibrillar collagen I were fabricated via lyophilization,[5] cross-linked via DHT and cut into samples (1×1×1.5 mm for SCI, 4×3×1.5 mm for ONI). PCS used in ONI included chondroitin-6-sulfate GAG.

Animal Models

Animal experiments were approved and carried out in compliance with EU guidelines. The SCI (dorsal column crush) mouse model was implemented as described previously[2]. YFP-expressing NSC-seeded PCS grafts placed in the SCI lesion site and BNN27 was delivered systemically over 8 weeks via subcutaneous pellets. Mice were sacrificed 12 weeks post-injury (wpi) and spinal cord sections were immuno-stained for GFP. In the ONI model (adaptation of the established optic nerve crush model) BNN27 was delivered by soaking a 4×3×1.5 mm collagen-GAG scaffold with 6 μl drop containing Fmoc-FF self-assembled peptide and 30 mM BNN27, and placing the resulting graft around the crush site immediately after injury. Mice were sacrificed 2 wpi and retina sections were immuno-stained for NeuN (neuronal marker; used to detect Retinal Ganglion Cells (RGC) in the GCL retina layer). Tissue sections were imaged in a Leica Sp8 confocal fluorescence microscope. Images were analyzed using the ImageJ software.

RESULTS AND DISCUSSION

Quantification of NeuN$^+$ nuclei in GCL shows that PCS-mediated BNN27 administration prevented ONI-induced apoptosis 2 wpi (Fig. 1). Similar BNN27 neuroprotective effects have been reported in other neuron types.[3,4]

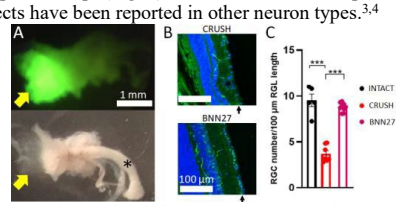

*Figure 1. A: FITC-labeled PCS (arrow) around the optic nerve (*). B: NeuN+ RGC in the GCL (arrow) with or without BNN27 2 wpi. C: Quantification of RGC survival. ***: P<0.001.*

Quantification of GFP$^+$ cells in the SCI lesion site 12 wpi shows that systemic BNN27 administration increases the density of NSC-derived cells (Fig. 2). Possible neurogenic and protective effects of BNN27 on NSCs and NSC-derived cells are under further evaluation.

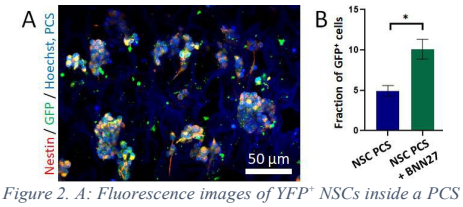

Figure 2. A: Fluorescence images of YFP$^+$ NSCs inside a PCS (fade blue). B: Density of YFP$^+$ cells in the SCI site 12 wpi.

CONCLUSION

We report the first local administration of MNTs via a biomaterial and the first time evidence on the neurotrophic effects of BNN27 (the seminal MNT) in mouse models of CNS injury in the presence of PCS grafts (cell-free or NSC-seeded). In the ONI model, BNN27 reduced RGC death 2 wpi when delivered via a cell-free PCS in the proximity of the lesion. In the SCI model, BNN27 increased the number of implanted NSCs in the lesion 12 weeks post-injury. Ongoing work probes the underlying mechanisms of BNN27 effects in CNS injury and NSC-based biomaterial treatments.

REFERENCES

1. Ahuja CS et al., *Nat. Rev. Dis. Prim.* 3: 17018, 2017.
2. Kourgiantaki A et al. *Npj Regen Medicine* 5:12, 2020.
3. Pediaditakis I et al., *Neuropharm.* 111:266-82, 2016.
4. Gravanis A et al., *Oncotarget*. 8:9005-6, 2017.
5. O'Brien FJ et al., *Biomaterials* 62:305-13, 2005.

ACKNOWLEDGMENTS

This work was supported by the Hellenic Foundation for Research and Innovation (HFRI) and the General Secretariat for Research and Technology (GSRT) under grand agreement No 1635.

Homogeneous and Mixed Organic Monolayers as Coatings for Neural Interfaces

Małgorzata Skorupa[1*], Magdalena Skoniecza[2,3], Katarzyna Krukiewicz[1]

[1]Department of Physical Chemistry and Technology of Polymers, Silesian University of Technology, Gliwice, Poland
[2]Department of Systems Biology and Engineering, Silesian University of Technology, Gliwice, Poland
[3]Biotechnology Centre, Silesian University of Technology, Gliwice, Poland
*malgorzata.skorupa@polsl.pl

INTRODUCTION

Neural interfaces provide a communication pathway between a human nervous system and an external device in order to stimulate or record the neural signals. They comprise a number of therapeutic, diagnostic and neuroprosthetic devices in clinical use. Such electrodes need to exhibit a number of specific properties including high conductivity and signal to noise ratio, while providing an excellent platform for biointegration within the neural tissue[1].

Aryl diazonium salts constitute an unusual group of azo compounds. By their electrochemical reduction, they form an aryl radical, which readily binds to the electrode surface atoms, forming a stable covalent bond[2]. The variety of functional groups that can be implemented on the aryl ring brings a versatile set of surface properties that can be achieved.

The aim of this work is to investigate the biologically relevant properties of electrodes modified with organic monolayers, derived from electroreduced diazonium salts, and to maximize the positive effect by formation of mixed layers.

EXPERIMENTAL METHODS

A platinum electrode was used for electrochemical deposition of selected tetrafluoroborate diazonium salts and their mixtures: 4-nitrobenzene- (D-NO_2), 4-methoxybenzene- (D-OCH_3) and 3,5-dichlorobenzenediazonium (D-Cl_2). The deposition rate was controlled by Electrochemical Quartz Crystal Microbalance (EQCM). The electrochemical properties (electroactive surface area, impedance, charge injection capacity) were measured. The surface properties and morphology were analysed with Atomic Force Microscopy (AFM), water contact angle measurements and Raman spectroscopy. Eventually, the biological interactions with the materials were analysed *in vitro* using neural and astrocytic cell lines.

RESULTS AND DISCUSSION

The character and position of the substituent at the aryl ring of the diazonium salt directly influences the reduction potential, deposition rate and tendency to form mono- or multilayers. In turn, the resulting coating compactness affects its conductivity (Fig. 1).

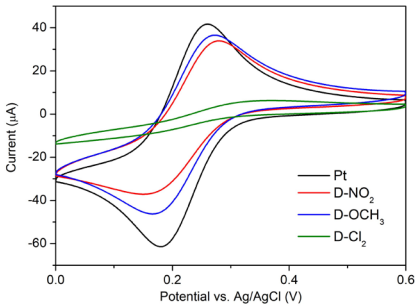

Fig. 1 Cyclic voltammetry of the modified surfaces in a solution containing a redox mediator.

The biological studies showed that the surface modifications improve the overall biocompatibility towards neurons and can discourage astrocyte attachment. Therefore, they can potentially diminish the foreign body response at the site of implantation.

CONCLUSION

The surface properties of an electrode can be easily modified by electrografting of diazonium salts. The required properties can be adjusted by selection of the functional groups of the diazonium salt and by formation of mixed organic layers. This work demonstrates the facility of modification of conductive surface properties and their potential use in bioelectronic applications.

REFERENCES

1. Vallejo-Giraldo, C. et al., *Drug Discov. Today* **19**, 88–94 (2014).
2. Bélanger, D. & Pinson, J., *Chem. Soc. Rev.* **40**, 3995–4048 (2011).

ACKNOWLEDGMENTS

This research was supported by the National Science Centre, Poland (OPUS 2019/35/B/ST5/00995).

3D platforms based on rGO-doped adipose-derived extracellular matrix towards neuron differentiation

Susana C. Pinto[1], Nathalie Barroca[1], Daniela M. da Silva[1], Ângela Semitela[1], Iratxe Madarieta[2], Nerea Garcia-Urkia[2], Olatz Murua[2], Beatriz Olalde[2], Sandra Vieira[3], Paula A.A.P. Marques[1*]

[1]TEMA, Department of Mechanical Engineering, University of Aveiro, Aveiro, Portugal
[2]TECNALIA Basque Research and Technology Alliance (BRTA), San Sebastian, Spain
[3]iBiMED Department of Medical Sciences, University of Aveiro, Aveiro, Portugal
*paulam@ua.pt

INTRODUCTION

Biomaterials-based strategies for spinal cord injury (SCI) are providing specially designed materials for cell migration, adhesion, and growth enabling nerve repair and regeneration[1]. Our approach is to build a platform that gathered a set of properties that will create a favorable microenvironment for neural cells to adhere, proliferate and differentiate towards neurons. The technology used was the electrospinning (ES), a versatile platform enabling the fabrication of fibrous membranes mimicking extracellular matrix (ECM) hierarchical structure, followed by gas foaming (GF), a simple post-processing technique that efficiently transforms 2D electrospun membranes (2D ENM) in highly porous 3D structures, overcoming the limited porosity observed in ENM obtained by traditional set-up configurations[2].
Concerning the raw materials used in the fabrication of biomaterials, natural are preferred over the synthetic for their cell signaling cues[1]. Recently, decellularized ECM from liver, kidney, lung among others started to be used in tissue engineering due to its bioactive cues that can prompt cell differentiation[1]. Here, it will be explored the combination of decellularized extracellular matrix from porcine adipose tissue (adECM) with a biocompatible synthetic copolymer, given the lack of mechanical integrity and fast degradation rate associated to natural materials[3]. To deliver biologic-electronic signals to the platforms, reduced graphene oxide (rGO) will be incorporated, due to the remarkable *in vivo* preliminary results of rGO in SCI[4].

EXPERIMENTAL METHODS

Platforms consisting in blends of a natural bio-based material, adECM, and a biocompatible synthetic PURASORB® PLC 7530 copolymer were fabricated combining ES to a post processing technique, GF. The methodology consisted of two-stages, i) optimization of ES and GF processing conditions focused on the adECM:PLC ratio seeking for highly porous 3D scaffolds yet handled and mechanically stable in wet environment, ii) incorporation of GO surface functionalization with polydopamine (rGO-PDA) in the most promising electrospinning formulation and preparation of 2D ENM and corresponding 3D scaffolds. For the purpose, three adECM:PLC ratios were studied (60:40; 70:30 and 80:20). To assess their cytocompatibility, the selected formulation was seeded with embryonic neural stem cells (NE-4C cell line). Cellular adhesion, proliferation, and differentiation towards neurons were assessed.

RESULTS AND DISCUSSION

2D ENM consisting of tightly packed layers of uniform, beadless and interconnected fibers with diameters ranging from hundreds of nano to few micrometers were obtained for all formulations. 3D highly porous and fibrous scaffolds were successfully achieved after quick immersion of 2D ENM in sodium hydride solution. The fibers twist and create a wave-like structure, displaying large interspace between fibrous layers. Regarding the expansion ability, adECM60:PLC40 revealed to be the most promising, with 25-fold increase in its initial thickness, while the formulations containing higher adECM ratio are less prone to expand. The different chemical compositions and porosities of the 3D scaffolds generated distinctive swelling and mechanical behavior. 1.5% (w/w) of rGO-PDA was successfully dispersed in the adECM60:PLC40 solution, electrospun in 2D ENMs and foamed to the corresponding 3D scaffold. rGO-PDA nanosheets entangled with fibers did not affect the expansion ability. Regarding their cytocompatibility, both 2D ENM and 3D scaffolds display increased proliferation over the 14 days of culture. Additionally, a pronounced differentiation towards neurons was obtained on the platforms with rGO-PDA.

CONCLUSION

Highly fibrous and porous 3D scaffolds based on adECM:PLC were successfully obtained combining ES to a simple and fast GF methodology. *In vitro* studies suggest that 2D ENMs and 3D scaffolds are viable platforms for adhesion and proliferation of neural stem cells. The distinct neuron differentiation on the platforms with rGO-PDA, particularly on the 3D scaffolds, indicates the notable role of the porosity and rGO-PDA in the differentiation process.

REFERENCES

1. Agrawal L. *et al.,* Mater. Sci. Eng. C. 131:112502, 2021
2. Chen Y. *et al.,* Bioact. Mater. 5:963-979, 2020
3. Spang M.T. *et al*., Acta Biomater., 68:1-14, 2018
4. Domínguez-Bajo A. *et al.,* Front. Syst. Neurosci. 11:71, 2017

ACKNOWLEDGMENTS

This work has been supported by the European Union's Horizon 2020 Research and Innovation Programme (H2020-FETOPEN-2018-2020, NeuroStimSpinal Project, Grant Agreement No. 829060).

Axonal Growth Stimulated by Surface Modification using an Exogenous Electric Field

Océane Sénépart[1,2*], Claire Legay[1], Ahmed Hamraoui[2]

[1]Saints Pères Paris Institute for the Neurosciences (SPPIN), Université de Paris, Paris, France
[2]Laboratoire de la Chimie de la Matière Condensée de Paris (LCMCP), Sorbonne Université, Paris, France
[*] oceane.senepart@sorbonne-universite.fr

INTRODUCTION

The nerve injury in the peripheral nervous system is a devastating situation responsible for millions of new cases around the world every year. It induces a loss of motor and/or sensory function and neurons will use biological and physico-chemical environmental factors to guide growth cones to appropriate targets. Identifying new strategies to enhance regeneration and guidance of growth cones is fundamental to restore nervous system functions. An emerging approach is a therapy using an electric field[1] (EF). Our goal is to optimize the effect of a local EF on neuritogenesis in culture, via the design of an original experimental set-up employing gold electrodes. Our innovative device allows a contactless stimulation to eliminate the effects of conduction and pH modification on cells. Here, the effects of a local EF on neuron adhesion and extension and surface of adhesion of the cells are studied. The combination of physical methods[2] and biological analyses allows the investigation of these parameters. Our working hypothesis is that the application of exogenous EFs near the injured axons makes it possible to control the guidance of axons.

EXPERIMENTAL METHODS

Our main objective can be achieved by improving our understanding of the effect of a local EF thanks to the design of an original experimental device.
Electric fields The device allows to apply a controlled EF ranging from 0 to 22500 mV/mm without contact between the electrode and the cells and to visualize them.
Complex surfaces of adhesion To tune cell adhesion strength, biochemical modification of the substrates is undertaken[3] and its effects are investigated.
Cell models Several motoneuron lines are used (PC12, MN1, NSC34). We visualize their extensions and their organization process is driven by changes in mechanical properties. A special care is taken in the studies of cell elasticity thanks to the pump & probe technology.

RESULTS AND DISCUSSION

Elasticity measurements have been first reported in motoneurons to evaluate the mechanical properties of the different areas of the cell.

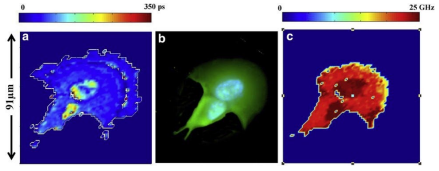

Figure 1 (a) Mapping of the Brillouin lifetime in the cell is given. (b) Fluorescence mapping of the same cell is shown. The blue zone marks the nucleus, the green zone the cytoskeleton. (c) Mapping of the Brillouin frequency cell response is shown.

The team then managed to estimate the adhesion energy of the surface of adhesion after both chemical and physical modifications. Thanks to an RNA sequencing, it was also possible to correlate the effects of a surface modification with the addition of Nerve Growth Factor (NGF). To finish, our first results on the use of EFs were obtained on the growth speed and orientation.

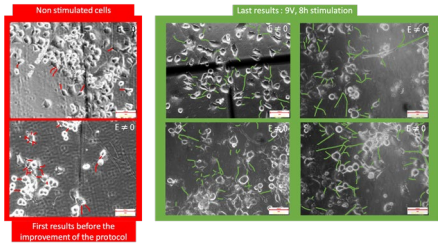

Figure 2 Results of a 9V stimulation during 8 hours on MN1 cells compared to non-stimulated cells and to the results obtained before improving the protocol.

CONCLUSION

The last results allow us to think that the contactless stimulation improves the axon growth, which is a very promising suggestion for a neuroimplant that could gather both chemical modification of the surface and physical excitations. The preliminary studies on the mechanical properties of the cells, the surface energy of the surface of adhesion and the effect of surface functionalization were essential to isolate and understand the effect of the EF. This is the first study made on the contactless application of EFs to the cells and the results lead us to the suggestion of using such technique as treatment in a regenerative therapy.

REFERENCES

1. Honegger T. *et al.*, Scientifc reports 6, 28284, 2016
2. Hamraoui A. *et al.*, Biophysical J., Vol. 120, 2021
3. Lamour G. *et al.*, Biophysique, Paris Diderot, 2010

ACKNOWLEDGMENTS

The authors would like to thank the ED397 (Physics and Chemistry of Materials) for providing financial support to this project, Fannie Semprez, the SPPIN biology technician for her help in cell culture and Laurent Belliard, an INSP physician for providing help in the mechanical properties measurements.

Secretome from electrically stimulated cells: a novel potential biopharmaceutical for neural regenerative therapies

Sahba Mobini*, Francesc Guix, Inés Berenguer López, Álvaro Casadomé-Perales, Carlos G. Dotti

Instituto de Micro y Nanotecnología, IMN- CNM, CSIC (CEI UAM+CSIC), Tres Cantos, Madrid, Spain
Molecular Neuropathology Unit, Centro de Biología Molecular Severo Ochoa, CSIC/UAM, Madrid, Spain
*sahba.mobini@csic.es

INTRODUCTION

Stem cell transplantation is one of the most tested alternative approaches for neurovascular regeneration. However, cell therapy faces numerous challenges, such as reduced cell survival, accumulation of implanted cells in other organs, small blood vessel occlusion, immune incompatibility and rejection. It is known that the paracrine signaling of mesenchymal stem/stromal cells (MSCs) is responsible for effects in cell transplantation. MSCs secrete broad range of trophic factors, cytokines, metabolites and bioactive lipids as a co-mixture of soluble and insoluble (extracellular vesicles, EVs) fractions, collectively referred to as "secretome". Although secretome therapy is a powerful tool and probably will overtake traditional cell therapy, this approach is challenged by low yield, inefficient production and lack of custom-made composition. Hence, the next generation of secretome-based therapy requires engineering methods to amplify the quantity and to provide customized formula using translatable and scalable approaches.[1] Electrical stimulation (ES), similar to endogenous bioelectric fields, are able to direct cell migration, proliferation, and nerve sprouting at wounds. The positive effect of low voltage ES (10-150 mV/mm) on neurite outgrowth and axonal regeneration, particularly towards the negatively charged cathode has been demonstrated. We hypothesize that electrically stimulated cells generate secretome (ES-Sec) with analogous results to ES.[2] In this study we demonstrated that indeed ES-Sec is capable of inducing neural differentiation and neurite growth.

EXPERIMENTAL METHODS

To apply ES to the cells in culture, previously we fabricated a costume-made ES chamber using platinum electrodes and characterized it to define the safe operation voltage range. SH-SY5Y cells were cultured, treated with retinoic acid and either subjected to pulsed ES (20 mV/mm, 1 Hz, 0.5 µs pulse width) or BDNF. MSCs were expanded and later cultured in serum free media and subjected to ES or kept in culture with no stimulation. Secretome from all groups were extracted and treated with protease inhibitor, and centrifuged 10 min for 300xg and 10 min for 200xg at 4 °C to remove dead cells debris and frozen at -80 °C. EVs collected by centrifuging the purified secretome at 100Kxg for 90 min. EVs were separated from the soluble fraction (kept frozen for further examinations). SH-SY5Y were treated with EVs (diluted proportionally to the medium). We assessed neural differentiation via phase contrast imaging, immunofluorescent and western blot.

For further characterization, EVs were subjected to nanoparticle tracking analysis (NTA) for measuring hydrodynamic particle size, zeta potential and concentration. Particle's size and morphology also assessed by transmission electron microscopy (TEM). EVs protein content is defined by mass spectroscopy and later went under targeted analysis with western blot.

RESULTS AND DISCUSSION

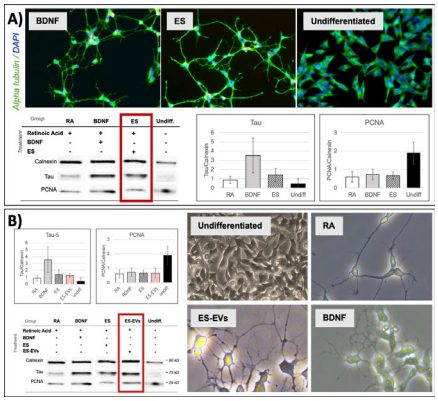

Figure 1. A) *Effect of ES on SH-SY5Y cells. ES induced differentiation in the absence of BDNF. Morphological and protein analysis confirm the effect of ES is beyond retinoic acid (RA).* ***B)*** *Effect of EVs from electrically stimulated SH-SY5Y cells (ES-EVs). ES-EVs effectively induced differentiation in the absence of both BDNF and ES.*

Figure 1 shows that ES-EVs are sufficient to induce neural differentiation in SH-SY5Y cells in the absence of both BDNF and electrical field. These results agree with our previous findings that ES-Sec extracted from MSCs significantly induce neural differentiation in SH-SY5Y.[3]

CONCLUSION

These findings indicate that ES is beneficial for customizing cell secretome, which could be a powerful tool for future secretome-engineering. This strategy would eliminate drawbacks associated with ES (invasiveness) and cell therapy (cell survival, rejection).

REFERENCES

1. Daneshmandi, L. *et al. Trends Biotechnol*. 38, 1373–1384, **2020**.
2. Mobini, S. *et al*. PCT application # WO2020028708A1, **2020**.
3. Hlavac, N. *et al. Ann Biomed Eng*. 49(12), 3401-3411, **2021**.

ACKNOWLEDGMENTS

We thank **Dr. María Ujué González** for providing useful consults and Comunidad de Madrid (Atracción de Talento Programe, Modalidad-1 Ref. 2019-T1/IND-1335) for providing financial support to this project.

Sodium alginate/inulin microparticles containing *Calendula officinalis* flower extract for dermatologic applications

Justyna Kozlowska, Weronika Prus-Walendziak, Natalia Stachowiak, Joanna Skopinska-Wisniewska, Beata Kaczmarek-Szczepanska

Faculty of Chemistry, Nicolaus Copernicus University in Torun, Torun, Poland
* justynak@umk.pl

INTRODUCTION

Sodium alginate, anionic polysaccharide, is a polymer found in brown algae. In medicine it is used to control drugs and proteins delivery, wound dressings, tissue regeneration, bone or cartilage regeneration[1,2].

Inulin is a polysaccharide belonging to the fructans class. It is obtained from Jerusalem artichoke or also common chicory. Inulin has a lot of benefits such as antimicrobial and prebiotic properties[3].

Calendula officinalis L. is a medical plant and the main components of its flower extract are carotenoids, terpenoids, steroids, phenolic acids, and flavonoids. It was found that the marigold flower extract (marigold flower extract) exhibits antioxidant, anti-inflammatory, antimicrobial, anticancer and antiviral effects. It is used in the treatment of burns, ulcers, skin inflammations, eczema, bruises, cuts, rashes, skin wounds. The beneficial effects of *Calendula officinalis* extract on human health can be enhanced by controlling its release from polymeric microspheres [4,5].

The aim of this research was to obtain microparticles from sodium alginate and inulin mixture with enclosed *Calendula officinalis* flower extract and to characterize them by antioxidant capacity and mechanical properties.

EXPERIMENTAL METHODS

Microparticles based on sodium alginate (ALG) and inulin (I) containing *Calendula officinalis* flower extract were prepared by extrusion method.

The appearance of the prepared polymer microparticles incorporated with *Calendula officinalis* flower extract was observed by the optical microscope. Imaging of swollen, dry, and immersed in solutions with different pH (pH 4-8) microspheres were performed.

The mechanical properties of the sodium alginate and inulin microparticles were conducted at room temperature using a mechanical testing machine equipped with compression jigs. The dry and wet samples were examined and after 2 h of immersion in different conditions.

Antioxidant capacity was measured using two methods: CUPRAC and FRAP. The absorbance was measured at 450 nm using a UV–VIS spectrophotometer (UV-1800, Shimadzu, Kyoto, Japan). The presented data were calculated based on the gallic acid calibration curve. However, in order to perform FRAP method, supernatants were added to acetate buffer, iron(III) chloride and TPTZ. The absorbance of samples was analyzed spectrophotometrically at $\lambda = 593$ nm after incubation in a dark place for 15 minutes. Data were calculated using a standard curve equation for trolox.

RESULTS AND DISCUSSION

Mechanical Properties

The obtained results showed that dry microparticles exhibited much higher values of Young's modulus (~18 MPa) and compressive strength (~8 N) compared to wet samples (~50 kPa and 0.2 N). The dry microparticles were stiffer and strength, while the wet samples were more flexible.

Antioxidant Capacity

The results showed that *Calendula officinalis* flower extract was successfully enclosed into prepared microparticles due to the antioxidant capacity of microparticles. Measured antioxidant activity hight depended on the used method. Microparticles composed of 2% of sodium alginate and 10% and 20% of inulin had higher CUPRAC values (~16 mg/g) than sample containing 30% of inulin (10 mg/g). However, according to FRAP results, the highest antioxidant activity had sample with 20% of inulin (41 mg/g). Antioxidant capacities of microparticles with 30% and 10% addition of inulin were approximately 20 mg/g and 17 mg/g, respectively.

CONCLUSION

Sodium alginate/inulin microparticles containing *Calendula officinalis* flower extract exhibited appropriate mechanical properties and antioxidant capacity and they are suitable for dermatologic applications dermatological applications to treat various skin conditions.

REFERENCES

1. Tønnesen, H.H.; Karlsen, J. Drug Dev. Ind. Pharm. 2002, 28, 621–630.
2. Pereira, L.; Sousa, A.; Coelho, H.; Amado, A.M.; Ribeiro-Claro, P.J. Biomol. Eng. 2003, 20, 223–228.
3. Tawfick M.M., Xie H., Zhao C., Shao P., Farag M.A., Int. J. Biol. Macromol. 2022, 208, 948-961.
4. Efstratiou, E.; Hussain, A.I.; Nigam, P.S.; Moore, J.E.; Ayub, M.A.; Rao, J.R. Complement. Ther. Clin. Prac. 2012, 18, 173–176.
5. Jan, N.; John, R. Calendula officinalis-an important medicinal plant with potential biological properties. Proc. Indian Natl. Sci. Acad. 2017, 83, 769–787.

From surgery to the lab:
illustration of a transcriptomic/tissue analyses workflow developed on periprosthetic tissues

Isabelle Brigaud, Tatiana Petithory, Laurent Pieuchot and Karine Anselme

[1]Université de Haute-Alsace, IS2M-CNRS 7361, F-68100 Mulhouse, France
isabelle.brigaud@uha.fr

INTRODUCTION

As implanted long-term medical devices such as silicone-filled implants trigger a cascade of immune responses called foreign body reaction (FBR) ending with the formation of a periprosthetic tissue called "capsule". Capsule is a fibrous tissue that surrounds and isolates the implant from host body during all the time of its implantation (**Fig 1A**). As it becomes the first recipient of silicone implant released materials, capsule can develop into a range of inflammatory-related pathologies imposing capsulectomy and implant replacement.

Silicone-filled implants are bipartite materials composed of 1) a solid cross-linked silicone elastomer shell (envelope) and 2) a silicone gel filling (core). Three independent sources of silicone exposure arising from the silicone implant have been identified, including (i) massive gel silicone leak after implant rupture, (ii) silicone oils permeating from the gel and passing through the silicone membrane and (iii) surface debris detaching from the shell surface after erosion. (**Fig. 1B**).

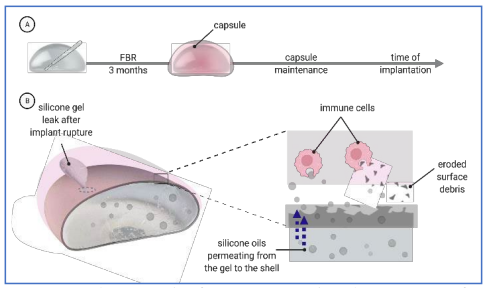

Fig. 1: 1A) Capsule formation and 1B) Sources of silicone emanating from silicone implant, exposed to immune cells patrolling on the capsule that in turn elicit immune-related inflammation.

Molecular and tissue (histology) analyses of capsular tissues can provide key information to identify factors priming inflammation. However, it requires to interconnect data from patient to the lab. This work describes the strategy developed in IS2M to question factors affecting silicone implant biocompatibility *in vivo*, from tissue collection to lab analyses (Brigaud *et al.*, 2019). Emphasis on encountered limitations will be done.

EXPERIMENTAL METHODS

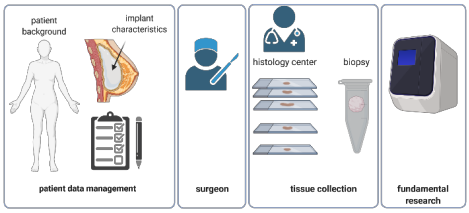

Fig.2 Project management levels

Workflow establishment necessitated to coordinate and track anonymized patient data, qualitative and quantitative exploitable tissue collection, histology analyses expertizedin dedicated medical histology center and lab analyses. (**Fig. 2**).

RESULTS AND DISCUSSION

We were able to establish a fruitful workflow between 2 independent hospital partners, including plastic surgeon and anatomopathologist center withthe IS2M academical institute. It required to standardize 1) the obtention of appropriate data patient and implant characteristics, 2) sampling collection in order to guarantee appropriate quality (stabilized non-degraded samples) and quantitative (statistical) of the samples. This work needed to interconnect 3) analyses data obtained from histology and molecular analyses (herein qPCR) and data patients with anonymized samples. Limitations resided mainly in the difficulty to follow-up patient/implant data with anonymized samples, to obtain exploitable sampling from surgery and to direct histologist to retrieve appropriate information / images for further publication.

CONCLUSION

This workflow provides an overview of the workflow developed to exploit soft tissue explants in the context of academic problematics. Underlined limitations will help similar future works to be achieve successfully.

REFERENCES

Brigaud, I. *et al.* (2019) 'Surface texturation of breast implant impacts extracellular matrix and inflammatory gene expression in asymptomatic capsule', *Plastic and Reconstructive Surgery*, p. 1. doi: 10.1097/PRS.0000000000006606.

ACKNOWLEDGMENTS

Towards scarless healing with the use of hybrid collagen-based dermal substitutes: a study on their contraction, physical and biological properties over time

Christopher Y. Leon-Valdivieso[1*], Audrey Bethry[1], Coline Pinese[1], Jean-Marc Pernot[2], Michèle Dai[2] and Xavier Garric[1]

[1]Department of Polymers for Health and Biomaterials, IBMM UMR 5247, University of Montpellier, CNRS, ENSCM, Montpellier, France

[2]URGO Recherche Innovation et Développement, 42, rue de Longvic, 21304 Chenôve, France

[*] christopher-yusef.leon-valdivieso@umontpellier.fr

INTRODUCTION

Current strategies in dermal healing involve the use of tissue-engineered scaffolds to avoid tissue grafting and their subsequent potential drawbacks (e.g. donor-site pain, patient morbidity) [1]. Collagen-based gels are the dermal substitutes *par excellence* due to their resemblance with the extracellular matrix and their biocompatible, non-toxic and cost-effective features [2]. Nevertheless, their lack of sufficient mechanical stability to withstand the rapid cell-mediated contraction remains a major problem: they contract around 50% of their original size in the first 2 days and up to 80% in the first week, potentially leading to undesirable (and excessive) scarring, impaired tissue function and poor cosmesis [3]. In this work, we aim to produce a hybrid dermal substitute based on collagen and a polymeric scaffold to minimize the rapid contraction that usually limits the performance of dermal equivalents. Particularly, we investigated i) the formulation of a collagen template to host normal human dermal fibroblasts (NHDF) and the parameters influencing their contraction ii) the synthesis and processing of macroporous polymeric scaffolds with appropriate mechanical properties and degradation rates and iii) the integration of both parts (gel + polymer) to evaluate the contraction of the final dermal substitute as well as the structural, mechanical and biological responses due to the contractile behavior over time.

EXPERIMENTAL METHODS

Collagen gel: A collagen gel contraction assay was used to quantify the gel size change; their nanostructure was evaluated with scanning electron microscopy (SEM) and their rheological properties with vibration-based technologies (ElastoSens™ Bio[2], *Rheolution*). $n \geq 4$

Polymeric scaffold: Home-made polymers were synthesized and processed with different techniques. Their structural and mechanical properties were studied with SEM and tensile tests, and their degradation *in vitro* was followed for at least 45 days. $n \geq 4$

Hybrid constructs: The macrostructure (visual inspection), rheological properties and final contraction of different hybrid dermal substitutes were evaluated. Biological tests were performed to analyze cell distribution, viability, proliferation and cellular differentiation on either the gel, polymeric scaffold or hybrid construct at different timepoints. $n \geq 4$

RESULTS AND DISCUSSION

First, collagen gel matrices were formulated to host NHDF with a homogeneous distribution (Fig 1A); these gels supported cell viability and proliferation while contracting consistently over time. The latter was corroborated by tracking the change of mechanical properties and thickness decrease using ElastoSens™ Bio[2] (Fig 1B). Second, home-made polymers were processed into macroporous structures that 1) did not exhibit cytotoxity 2) promoted cell proliferation and 3) presented an important degradation behaviour *in vitro* (up to 45% loss of the initial molecular weight in 45 days) while becoming more brittle within the same timeframe. Third, the preparation of hybrid constructs (Fig 1C) showed a good integration between the two moieties with an adequate distribution of cells and enhancement of the elastic modulus compared controls, resulting from the presence of a reinforcing structure inside the construct. More importantly, our findings show that a combination of appropriate characteristics imparted by both components can drive a gradual and more restrained contraction compared to only-collagen gels (Fig 1D), along with changes in the cellular responses over time: improved cellular proliferation and myofibroblastic differentiation (not shown).

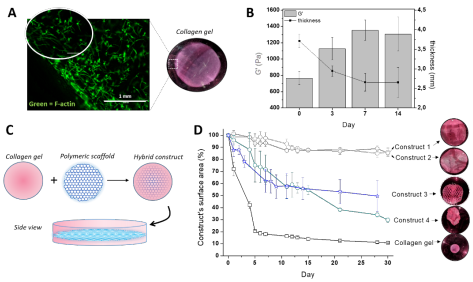

Figure 1. **A)** Cell distribution in a collagen gel; **B)** Change of G' and thickness of seeded collagen gels; **C)** Typical conformation of a hybrid construct; **D)** Contraction profile of different constructs.

CONCLUSION

Minimizing the rapid cell-mediated contraction was shown to be feasible by using reinforcing degradable polymers. The extent of final contraction/degradation is given by the polymer's nature and/or processing method. These promising results open the door to the development of skin engineering strategies that overcome the contraction/scarring issues and that prioritize regeneration over reconstruction.

REFERENCES

1. Przekora, A. *Cells*, 9(7):1622, 2020
2. Nyame, T.T. *et al*., *Surg Clin N Am*, 94(4):839, 2014
3. Rahimnejad M. et al., *Burn Trauma*, 5(4), 2017

Standardized quantification of cell biological reactions directly on biomaterials

Constantin Issleib[1, 2], Susanne Kurz[1, 2], Juliane Spohn[1, 2]

[1]Fraunhofer Institute for Ceramic Technologies and Systems, Dresden, Germany
[2]Fraunhofer Institute for Cell Therapy and Immunology, Leipzig, Germany
* juliane.spohn@ikts.fraunhofer.de

INTRODUCTION

For biocompatibility tests scientists rely on plastic cell culture plates with known geometry and size of culture area. However, testing of solid biomaterial and implant material in these standardized plates is often challenging. First the biomaterial must fit in an appropriately selected well size. One major disadvantage of placing the biomaterial into a well is that plastic culture area surrounding the biomaterial is left and needs to be considered when evaluating the collected data. Additionally accurate prediction of cytotoxicity as well as cellular behavior around the edges and the bottom side of the biomaterial is complicated. This may also be a reason why quantitative analysis of biological response of cells in the direct contact to medical products are underrepresented in the biological testing guidelines like the ISO 10993. In this work, we introduce our invention (in vitro test system[1]), for creating standardized wells on a wide range of solid biomaterials, which are analogous to commonly used cell culture well geometry.
Here we describe the use of our lab device for the quantitative testing of cells (e.g., fibroblasts) in direct contact to the material surface of interest.

EXPERIMENTAL METHODS

The evidence of fluid tightness of the test system was investigated via gas exchange and evaporation by means of pH value determination and weighing of the remaining quantities of medium in the well after 24 h incubation, respectively. For the tests, three different test specimens were inserted into the bottom element using positioning aids (Figure 1 top left diagram with 96-well receptacle, top view below). The test specimens used for the verification were selected in such a way that the surface characteristics (Ra, Rt, Rz3) optimally cover the surface tolerance range of solid materials intended for the use of the in vitro test system. Cell biological assays (like MTT, ELISAs, Bradford) were transferred and adjusted to the test system.

RESULTS AND DISCUSSION

Fluid tightness was demonstrated in the range Ra = 0.01 - 3.6 µm; Rt = 0.1 - 32 µm, Rz = 0.06 - 26 µm. In addition, we proved that the test system is fundamentally suitable for use in cell culture. Thus, we confirmed the most important aspects, such as the evaporation rate of the medium in the wells and the sufficient gas exchange between well interior and ambient air (measurement of pH stability of the bicarbonate-buffered medium), comparatively to the gold standard (cell culture plate) for the first 24 h (figure 1).

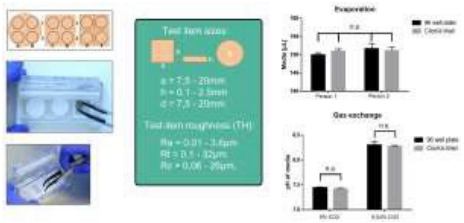

***Figure 1**: Proof of concept for fluid-tight closure and cell culture use.*

It was also shown that the cultivation and analysis (e. g., enzyme activity, protein secretion) of cells, here using fibroblasts as an example, is feasible under sterile conditions on test specimens in the wells of the in vitro test system (figure 2).

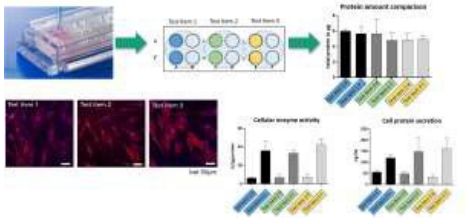

***Figure 2**: Proof of Concept for cell biological assays.*

CONCLUSION

We could show that our test device is adaptable to different material sizes and roughness. Applications like quantification of material surface effects on cell viability, functionality and adherence via direct cell contact assays, cytokine secretion assays or protein adsorption assays are easy to handle in our device thereby allowing replicable and multiple tests on one and the same test specimen. The test system enables reliable quantitative analysis of cells in direct contact to medical products (biomaterials) which are to date underrepresented in the biological testing guidelines like the ISO 10993.

REFERENCE

1. Issleib *et al.*, Patent „Arrangement For Performing In-Vitro Biocompatibility Tests“. DE102018221415. 2020

ACKNOWLEDGMENTS

We acknowledge our technical assistants for doing all the experimental work. The authors would like to thank the German Federal Ministry for Economic Affairs and Energy (BMWi) for financing the project “ToxQuant” (Grant no: 03TN0016A) through the WIPANO program - “Knowledge and technology transfer through patents and standards”.

Bioresorbable materials have different effects of pre-osteoblast cell viability and migration

Saara V. Sirkiä[1], Karoliina Kajander[2], Terhi J. Heino[2], Jorma Määttä[2], Pekka K. Vallittu[1,3]

[1]Department of Biomaterials Science and Turku Clinical Biomaterials Centre - TCBC, Institute of Dentistry, University of Turku, Lemminkäisenkatu 2, 20520 Turku, Finland; [2]Institute of Biomedicine, Faculty of Medicine, University of Turku Kiinamyllynkatu 10, 20520 Turku, Finland; [3]City of Turku, Welfare Division, Turku, Finland

Objectives. Different bioceramics have been used as bone implant and bone filling materials. However, each biomaterial has very different chemical topography and structure, and therefore can have different effects on pre-osteoblastic cells. Therefore, we compared the effects of five different bioceramics *i.e.* two bioactive glasses (45S5 and S53P4), two bioresorbable materials (HAP and CAP) and one bioinert material (Alumina) on the viability and migration of pre-osteoblastic cell *in vitro*.

Methods. Pre-osteoblastic MC3T3-E1 cells were used to assess cell viability with different biomaterial particles and biomaterial-conditioned media at 3, 7 and 10 days of culture. The migration of pre-osteoblastic cells was analysed by a Boyden chamber migration assay with different biomaterial particles in the lower chamber. Concentration of calcium from migration cultures and biomaterial-conditioned media were analysed by using AAS. The expression of osteoblastic genes was assessed by qPCR, and secretion of osteopontin was measured by an ELISA assay. Multivariate ANOVA was used for statistical analyses.

Results. Different biomaterial-conditioned media had no effects on the viability of pre-osteoblastic cells, except for the bioresorbable material CAP, which inhibited cell viability on day 3 ($P=0.0282$). Calcium concentration in biomaterial-conditioned medium was almost same with all other biomaterials, except for CAP, which showed significantly decreased levels of Ca ($P=0.0094$), when compared to the control group (plain culture medium). Interestingly, when pre-osteoblastic cells were cultured in the presence of biomaterials, the viability of cells decreased with bioresorbable HAP on days 3 and 7 ($P=0.071$, $P=0.0002$, respectively) and with CAP ($P=0.0089$) and bioactive glass S53P4 ($P=0.0307$) on day 7, when compared to the control group. The migration of pre-osteoblastic cells in turn was significantly increased towards both bioactive glasses S53P4 and 45S5 ($P=0.01$, $P=0.03$, respectively) when compared to control group at 12 hours. Interestingly, bioresorbable biomaterial CAP decreased the migration of pre-osteoblast, while other biomaterial had only minor effects on cell migration. Calcium concentration was significantly decreased in the presence of CAP and increased in the presence of both bioactive glasses in the migration assays. The mRNA expression of osteopontin ($P<0.0001$) and the levels of secreted osteopontin ($P<0.001$) were increased in cells subjected to 6 mM $CaCl_2$ compared to control after 24 hours. Further, a significantly lower levels of secreted osteopontin were measured from cells in co-culture with S53P4 ($P=0.02$). No changes were observed in the mRNA levels of osteogenic marker gene.

Significance. Bioactive biomaterials increased the migration of pre-osteoblastic cells but had only minor effect on cells viability. Notably, bioresorbable materials decreased cell migration (CAP) and viability (HAP and CAP). Based on the osteogenic marker gene mRNA expression, the cells were not undergoing osteoblastic differentiation during the experiments, but elevated $CaCl_2$ concentration increased osteopontin mRNA expression and protein secretion. Lower osteopontin concentrations were measured from co-cultures with S53P4, suggesting that it might be adsorbed on materials surface. This information provided knowledge to the bioceramics implant different microenvironment, cell behaviour with different bioceramics and so on osseification.

In vitro biocompatibility study of MIN6 spheroids with a tetrahydropyran triazole phenyl-alginate and quaternized phosphocholine-chitosan nanocoating

Michael Yitayew[1], Maryam Tabrizian[1,2]
[1]Department of Biomedical Engineering and [2]Faculty of Dentistry, McGill University, Montreal, QC, Canada
michael.yitayew@mail.mcgill.ca

Introduction

Implant encapsulation using polymeric biomaterials is an established method towards improving the biocompatibility of implants as well as reducing implant rejection and the foreign body response. Multilayer conformal coatings have been shown in the literature to provide a nano-sized film on a wide range of surfaces and materials as well as biological substrates such as cells and tissue constructs. (1) Encapsulation of cells has been a particular interest in cell therapy in Type 1 Diabetes (T1D). Pancreatic islet transplantation has been proposed to be a curative treatment option for patients with T1D. Islet cell encapsulation aims to improve the survival of islet transplants and mitigate the foreign body response to avoid relying on life-long administration of immunosuppressant medication (2). A key feature of such encapsulation must be minimizing implant volume to make sure cells can have adequate diffusion of nutrients, waste, and secreted hormones. (3) Here we have demonstrated the use of a novel combination of biocompatible materials, namely triazole-alginate (TZAL) and quaternized phosphocholine-chitosan (QPCH), for electrostatic multilayer film formation onto 3D cell spheroids derived from the MIN6 mouse pancreatic β-cell line as a proof-of-concept. Characterization of the coating as well as subsequent cell activity and hormone secretion are evaluated *in vitro*.

Experimental Methods

TZAL was prepared by synthesizing a triazole-tetrahydropyran amine using alkyne-azide cycloaddition reaction and subsequent coupling with alginate using CDMT/N-methylmorpholine. (4) QPCH was prepared by first synthesizing phosphocholine glyceraldehyde from L-glyceryl-phosphocholine using $NaIO_4$ as an oxidizing agent. This was followed by a reductive amination reaction using $NaBH_3CN$ to graft the aldehyde to chitosan. After dialysis and lyophilisation, this phosphocholine-chitosan formulation is then treated with dimethyl sulfate to produce quaternary amine groups on the chitosan (QPCH).

Spheroids were obtained by culturing a suspension of MIN6 β-cells in non-treated 6-well plates using an orbital shaker in a 37ºC incubator for up to 7 days. The spheroids were sequentially coated using the two polymers to form 4-bilayers by incubating in a solution of the desired polymer. The solution was then aspirated, and spheroids were washed 2x in HBSS before proceeding to the next layer. Coating morphology was assessed using transmission electron microscopy (TEM) as well as confocal microscopy using FITC-labeled alginate. Glucose stimulated insulin secretion was measured to assess the secretory function of the spheroids after coating. After stimulation, insulin content in the culture supernatant was quantified via ELISA. Cell viability was analyzed using a Live/Dead assay kit.

Results and Discussion

Structures of the proposed polymers are shown in Figure 1A. After successful synthesis and characterization of the polymers, coating on MIN6 spheroid surface was tracked using FITC-labeled alginate as part of the nano-coating. The results show successful deposition of layers as confirmed by confocal microscopy images (Figure 1B). In addition, coated and non-coated spheroids were exposed to low (2 mM) and high glucose (20 mM) to assess their secretory function. The results show no significant differences between coated and non-coated islets (Figure 1C) indicating that the coating does not affect diffusion of essential molecules, in this case insulin and glucose. Cell viability was also assessed after coating using live/dead assay kit with Calcein AM (Green) /Ethidium Homodimer (Red) (Figure 1D). No significant differences were noticed between coated and non-coated groups indicating that the coating does not affect short-term cell viability.

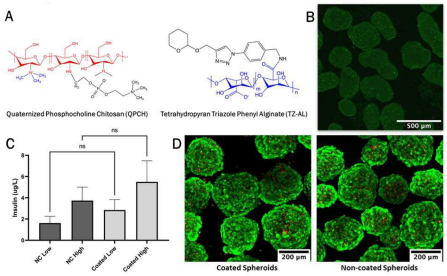

Figure 1 – Chemical structure of polymers (A), confocal images of coated MIN6 spheroids (B), GSIS assay (C), confocal images of live/dead assay for coated and non-coated spheroids. (D). n.s = P > 0.05

Conclusion

Experiments to assess coating morphology using TEM, as well as quantify metabolic activity and *in vitro* immune response studies are currently ongoing. The proposed coating has been shown to maintain islet viability and secretory function and shows great promise for further investigation towards improving the current methods for cell encapsulation. It also presents great potential in islet transplantation applications and this will be further investigated in future studies.

Acknowledgement

We would like to thank the CIHR Project Grant for providing financial support. Also, special thanks to all members of the Biomat'X laboratories.

References

(1) T. Liu, Y. Wang, W. Zhong, B. Li, K. Mequanint, G. Luo and M. Xing, *Adv. Healthc. Mater.*, 2019, 8. **(2)** K. M. Gattás-Asfura, N. J. Abuid, I. Labrada and C. L. Stabler, *ACS Biomater. Sci. Eng.*, 2020, **6**, 2641–2651. **(3)** S. Wu, L. Wang, Y. Fang, H. Huang, X. You and J. Wu, *Adv. Healthc. Mater.*, 2021, 2100965. **(4)** A. J. Vegas, et al., *Nat. Biotechnol.*, 2016, **34**, 345–352.

Development and physiochemical characterization of polymeric biomaterial scaffold for bone tissue engineering applications- an *in-vivo* study

Sesha Subramanian Murugan[1], Jayachandran Venkatesan[2*]

[1,2]Biomaterials Research Laboratory, Yenepoya Research Center, Yenepoya (Deemed to be University), Deralakatte, Mangalore, Karnataka 575018, India
seshae5@gmail.com

INTRODUCTION

The rehabilitation of bone tissue defects, including infection, trauma, etc. is a major challenge in orthopedic surgery [1]. At present, traditional auto graft, allograft, and artificial bone graft are the most familiar methods used for the bone defects recovery but engineered artificial substrates has been widely accepted [2]. The choice of substrates (Biomaterials) should be biodegradable, biocompatible, and must acquire superior mechanical strength. Mesoporous bioactive glass (MBG) with polymer composites thus provides the promising potential for bone tissue engineering application [3]. In the current work, the mesoporous bioactive glass was synthesized and blended with biodegradable polymer and osteo stimulant drug, used as bone graft implant material. The *in-vivo* studies were carried with developed implant materials to evaluate the tissue regeneration

EXPERIMENTAL METHOD

The MBG was synthesised by evaporation induced self-assembly method and confirmed by various physiochemical techniques mainly by XRD, water contact angle and BET analysis. Following that, the composite implant materials were prepared by blending the MBG, biodegradable polymer and osteo stimulative drug (treated material) through hydraulic press method. Finally, the *in-vivo* studies were carried on new-Zealand white rabbits and the scaffold materials (Control and Treated) were implanted on created defect site in femur condyle regions under anaesthetic conditions. Later, X-ray analysis on the implanted sites were carried on one month interval after surgery to analyse the tissue integrity.

RESULTS AND DISCUSSION.

The XRD analysis for calcined MBG shows the broad peak around 2Ø=15°-35°. The water angle of the MBG has 27.5 ° hydrophilic nature, which made suitable rough surface to adhere the bone cells to proliferate and differentiate. The synthesized MBG has the pore size of 6.24 nm. Figure 1 shows the composite implant material with osteo stimulative drug prepared by hydraulic press method and its porous nature. The results of X-ray (Figure 2) in yellow spots shows the tissue integrity nature of control and treated materials. The treated materials show the good tissue integrity on right femur condyle region compared to the control material on left.

Natural Bioactive Compounds from Plant Biomass in Medical and Pharmaceutical Application

Anna Bajek*[1], Małgorzata Maj[1], Łukasz Kaźmierski[1], Piotr Konopka[2], Marta Giamberini[3], Bartosz Tylkowski[4], Renata Jastrząb[2]

[1] Tissue Engineering Department Chair of Urology and Andrology, The Ludwik Rydygier Collegium Medicum in Bydgoszcz, Nicolaus Copernicus University in Torun, Karlowicza str 24 85-092 Bydgoszcz, Poland
[2]Faculty of Chemistry, Adam Mickiewicz University, Uniwersytetu Poznanskiego 8, 61-614 Poznań, Poland
[3]Department of Chemical Engineering, University Rovira i Virgili, Av. Països Catalans 26, Campus Sescelades, 43007 Tarragona, Spain
[4]Eurecat, Centre Tecnològic de Catalunya, Marcel·lí Domingo s/n, 43007 Tarragona, Spain
* a.bajek@cm.umk.pl

INTRODUCTION

The development of novel therapies that involve natural compounds from plants has undergone exponential growth in recent years. Among the natural bioactives (BACs) that produce beneficial effects on human health, polyphenols and flavonoids have shown potential therapeutic application in the medical biodegradable materials, bacteria inhibition, drug release, scaffold materials and anti-tumor. The aim of our study was to evaluate anti-proliferative properties of BACs. Extracted from different plant biomass.

EXPERIMENTAL METHODS

Samples of the plant biomass were collected, dried and used for the extraction. After the extraction and filtration, the BACs extracts were analysed to determine the total phenolic and flavonoids content. Anti-proliferative investigations were carried out using extracts containing BACs with the use of several cell lines, cancer and normal one (e.g. A-431, A549, ASC52telo, Ker-CT). All assays used for measuring cell viability were carried out according to the ISO 10993-5:2009.

RESULTS AND DISCUSSION

After extraction the characterization of BACs were done and the high values of phenolics and flavonoids were observed. The ESI-MS analysis also showed that the obtained extracts from plant biomass are mixture of different types of phenolic compounds. After 24h incubation with extracts the reduction of the number of cancer cells was noticed. However, what is very interesting, only minor changes were observed for normal cell lines.

CONCLUSION

A preliminary study showed that the anti-proliferative effect of plant biomass extracts can be considered as drugs compound or biomaterials modification agent and it could be considered in future anti-cancer or anti-inflammatory studies.

ACKNOWLEDGMENTS

This work was supported by the “Excellence Initiative Research University” (Emerging Field “Multifactorial Molecular-Behavioral Cancer Profiling Team”).

Hemocompatible photopolymers dedicated for the new design of the Single Piece Blood Rotor

Roman Major[1], Maciej Gawlikowski[2, 3], Justyna Wiecek[1], Juergen M. Lackner[4]

1 Institute of Metallurgy and Materials Science, Polish Academy of Sciences, Reymonta Str. 25,30-059 Cracow, Poland

2 Department of Biosensors and Processing of Biomedical Signals, Faculty of Biomedical Engineering, Silesian University of Technology, Roosevelt Str. 40, 41-800 Zabrze, Poland;

3 Foundation of Cardiac Surgery Development, Wolnosci Str. 345, 41-800 Zabrze, Poland

4 Joanneum Research Forschungsges.m.b.H., Institute of Surface Technologies and Photonics, Functional Surfaces, Leobner Str. 94, Niklasdorf 8712, Austria;

r.major@imim.pl,

INTRODUCTION

The main goal of the work is to develop novel blood contacting materials for the re-design of the flexible mechanical VAD heart valves in the ReligaHeart EXT (a clinically-applied, state-of-the-art VAD of the consortium member FRK), as well as to provide design rules for application of the composite in paediatric blood pumps (ReligaHeart PED VAD) and in implantable mechanical heart valves. Preliminary studies and simulations led us to metal-reinforced polymer composites, which imitate natural heart valves and combine high elasticity similar to blood vessels on the micro-scale and mechanical stability on the macro-scale. Thus, this concept guarantees:

- anti-thrombogenic construction by reduction of turbulence and sufficient washing of surfaces,
- drastically reducing heart assist device costs, allowing broad use for temporary heart support in emerging economies, and,
- eliminating "clicking" noise at closing of state-of-the-art carbon disc valves (especially for implantable valves), which minimizes the psychological burden on patients' quality of life.

EXPERIMENTAL METHODS

Comparable to the thiol-ene polymerization, the thiol-yne reaction follows a step growth mechanism bringing unique properties to this interesting class of materials. Polymerization shrinkage is low, and oxygen inhibition plays only a minor role due to efficient hydrogen abstraction of peroxy radicals from thiols under the simultaneous formation of highly reactive thiyl radicals. One challenging issue of thiol-based formulations is their shelf-life. Dark reactions of thiol, methacrylate and yne, catalysed from basic impurities or traces of metal ions and peroxides, can lead to a significant increase in viscosity during storage time. In order to enable a stable printing of the desired 3D structures, appropriate stabilizers must be found. Expression of platelet activation markers was measured on CD61 gated objects using PAC-1 antibody for conformational change of glycoprotein IIb/IIIa, and using CD62P for P-selectin. Integrated fluorescence of the activation marker was calculated as a multiplication total of geometric mean fluorescence by percentage of marker-positive objects. Both platelet receptors activation was calculated as measured by PAC-1 and P-selectin (CD62) expression: percentage and mean channel fluorescence of CD62-positive platelets (% and MNF, respectively). The biocompatible resin system, thiol-yne reactive monomers have been evaluated. This reaction is based on a multiple step radical mechanism and finally leads to an addition of two thiol units to one yne functionality forming corresponding thio-ether bonds.

RESULTS AND DISCUSSION The goals according to the work plan were essentially achieved. In accordance with the objectives, biocompatible, thiol-yne-based photopolymer resins, reinforced with carbon nanotubes as filler, were evaluated with a focus on bio- and haemocompatibility, good bonding between filler and resin and homogeneous distribution. Haemocompatibility test of medical materials aims to detect adverse interaction between artificial surface and blood, which can activate or destruct blood components. In arterial flow conditions, due to a high shear stress, platelet is the cell critical for the haemocompatibility compliance.

In this study, an attempt was made to find a correlation between the mechanical properties of the material and its effect on cri cells and blood activation processes. Fluctuations in hardness and Young's modulus were found. An increase in hardness and Young's modulus was found from sample no. 1 to 4 (see Table 3). After reaching the maximum, a successive decrease in both of these values to sample no. 7 was found. Then the increase again was observed. In the case of activation of blood flowing over the test surface, no effect of mechanical properties on the activation of characteristic platelet receptors was found. Changes in blood parameters were observed in the case of blood cells suffused to the surface. In this case, an increase in activated platelets and leukocytes was observed from sample 1 to sample 2, followed by a decrease to sample 4 and then a successive increase in the number of activated cells responsible for both the clotting process and the immune response. On this basis, it was found that the higher the hardness and the value of Young's modulus, the lower the activation of platelets and leukocytes. A directly proportional relationship between mechanical properties and biological response was observed in the case of the number of platelet microparticles

CONCLUSION

The use of light-curing materials has no toxic effects on the surrounding tissues. The use of carbon nanotubes has a beneficial effect on reducing cytotoxic properties, but from a mechanical point of view, they reduce the ductility of the material.

Acknowledgments

Project supported by:

The Polish National Centre of Research and Development (Grant no. M-ERA.NET/2014/01/2016, "Nonthrombogenic metal–polymer composites with adaptable micro and macro flexibility for the next generation heart valves in artificial heart devices".

Material characterization with reference to biocompatibility and microbiology dedicated for anti-microbial finger implant

Adam Byrski[1], Roman Major[1], Marcin Dyner[2], Katarzyna Kasperkiewicz[3], Łukasz Major[1], Juergen M. Lackner[4]

1. Institute of Metallurgy and Materials Science, Polish Academy of Sciences, Reymonta St. 25, 30-059 Cracow, Poland
2. Faculty of Science and Technology, Jan Dlugosz University in Czestochowa, Armii Krajowej Av, 13/15, 42-200 Czestochowa, Poland
3. University of Silesia in Katowice, Faculty of Natural Sciences, Institute of Biology, Biotechnology and Environmental Protection, Jagiellońska St. 28, 40-032 Katowice, Poland;
4. JOANNEUM RESEARCH Forschungsges.m.b.H., Institute of Surface Technologies and Photonics, Functional Surfaces, Leobner Strasse 94, 8712 Niklasdorf, Austria

* r.major@imim.pl

INTRODUCTION

The research focuses on alternatives for surgical reconstruction by novel patient-specific, durable, biomimetic, bioactive and antibacterial implants for reconstruction of lost bone and joints.
As part of the work carried out, a series of surface modifications were performed to improve the biocompatibility. A comparison of the influence of the phase composition on the microstructure of the materials obtained and the influence of the phase composition on the mechanical properties was carried out

EXPERIMENTAL METHODS

Images of the surface topography were obtained by scanning electron microscopy at an accelerating voltage of 2kV. The images were obtained with a secondary electron detector. One of the images was taken with the table tilted to 52 degrees in order to obtain a three-dimensional image. Detailed microstructural characterisation was carried out using transmission electron microscopy on a cross section. A thin film was cut from the boundary between the substrate and the sphere. In the area of the sphere, the columnar nature of the crystallites was demonstrated for oxides and nitrides layers due to heat treatment. At the surface, a thin ~150nm fine crystalline layer was demonstrated. In the case of a substrate with a hexagonal structure, columnar growth of crystallites in the sphere region was shown in the direction perpendicular to the sphere surface. Twinning was also shown, due to the tendency for twinning in hcp structures. Twinning is one of the main deformation modes in hexagonal close-packed (HCP) metals, and it has a great influence on mechanical properties of HCP metals. Material properties were correlated with biological properties. The study of cytotoxicity and cell viability was carried out by a direct method (according to ISO 10993-5) using human fibroblast cells (PromoCell, DE), which consisted in determining the probability and number of necrotic cells on the analysed surfaces in relation to living cells (first method) and determining the amount of secreted lactate dehydrogenase from cells that were in direct contact with the surface (second method). The antimicrobial activity contact test was based on ISO 22196:2007(E). Escherichia coli strain ATCC 8739 (Gram-negative) and Staphylococcus aureus strain ATTC 6538P (gram-positive) were used, as recommended in the norm. Generaly, hydroxyapatite increases antibacterial properties (as stated in literature), as there is less bacteria than in reference samples.

RESULTS AND DISCUSSION Obtained results are visualized as antibacterial activity index (R), which represents the difference between the number of viable bacteria recovered from both untreated and treated specimens. Material yields antibacterial properties if the calculated R value is greater than 2 (orders of magnitude/ it means 99% reduction of living bacteria). The higher the R index is, the better the antibacterial properties are. As we can see the Hap coating greatly increases antibacterial activity, especially towards Staphylococcus aureus (gram-positive bacteria)

CONCLUSION

Obtained results are visualized as antibacterial activity index (R), which represents the difference between the number of viable bacteria recovered from both untreated and treated specimens. Material yields antibacterial properties if the calculated R value is greater than 2 (orders of magnitude/ it means 99% reduction of living bacteria). The higher the R index is, the better the antibacterial properties are. As we can see the Hap coating greatly increases antibacterial activity, especially towards Staphylococcus aureus (gram-positive bacteria) In future, we are going to perform immersion tests (starting currently), bacterial endotoxin adhesion tests, evaluate whenever the material can possibly affect the pathway of complement activation and search for small colony variants that are able to persist for longer periods of time and are unable to detect by using standard methods

ACKNOWLEDGMENTS

The reported results were derived from a cooperative M-ERA.NET project called "fingerIMPLANT", which is co-funded by the Polish National Centre of Research and Development, Grant no. fingerIMPLANT M-ERA.NET2/2019/7/2020, and the Austrian Research and Promotion Agency, Grant no. 878515.

In Vitro Diabetic Bone Models in Research on Biomaterials

Anna Zgadzaj[1*], Barbara Kołodziejska[2], Karina Owczarek[1], Aleksandra Korgul[1], Joanna Kolmas[2]

[1]Department of Environmental Health Sciences, Medical University of Warsaw, Warsaw, Poland
[2]Department of Analytical Chemistry and Biomaterials, Medical University of Warsaw, Warsaw, Poland
[*] azgadzaj@wum.edu.pl

INTRODUCTION

Chronic hyperglycemia in diabetes may have a negative effect on the mass and the mineralization of bone tissue, may prolong the fracture healing time or increase the risk of rejection of orthopedic implants[1]. An effective *in vitro* diabetic bone models could allow to investigate the specificity of all that changes[2]. The aim of our work was the assessment of the suitability of the modified *in vitro* diabetic bone structure models in the research on the innovative bone replacement materials. It was verified whether cytotoxicity tests with such *in vitro* cultures will allow to select the materials with the particular usefulness for diabetics.

EXPERIMENTAL METHODS

Standard ISO method to evaluate the *in vitro* cytotoxicity of medical materials with 3T3 mouse cells was compared with the cytotoxicity assessment with our modified models: normal bone cells (NHOst-Osteoblasts) and osteosarcoma (MG-63 cell line), the growth of which was additionally modified by factors specific to bone tissue in an organism with diabetes. This effect was achieved by applying different degrees of hyperglycemia and inducing chronic inflammation with various concentrations of the lipopolysaccharide.

These models were used for testing of the materials (biomimetic hydroxyapatites), which had not shown cytotoxicity on a prior standard ISO assay and had been classified as safe for healthy mammalian cells. The effect of these bone substitutes on modified cell cultures was assessed by the neutral red uptake assay, the MTT assay and with the ELISA technique applied to evaluate the levels of selected pro-inflammatory cytokines (IL-6, IL-1b, TNFa).

RESULTS AND DISCUSSION

The results of our work showed that the tested materials were characterized by a different degrees of biocompatibility in conditions simulating diabetic bone structure. Similar observations were found with the use of both normal and neoplastic cells. Among the tested samples, it was possible to select the materials that allowed to modify the pro-inflammatory cytokine levels and had a positive effect on the cell cultures viability. Observations of the cells condition in the developed models are consistent with the data available in the literature[3]. However, similar studies comparing the standard biocompatibility tests with the modified methods have not been performed so far.

CONCLUSION

The project confirmed the possible effectiveness of using *in vitro* diabetic models in research on implantable medical materials with increased bone cell tolerance in patients with diabetes.

REFERENCES

1. Sábado-Bundó H. *et al.*, Med Oral Patol Oral Cir Bucal 24 (4): 425-32, 2019.
2. Ehnert S. *et al.*, Arch Toxicol. 94: 3937–3958, 2020.
3. Li Y. *et al.*, J Bone Miner Metab. 38: 607–619, 2020.

ACKNOWLEDGMENTS

The authors would like to thank the Medical University of Warsaw (Grant no: FW14/1/F/MBS/N/21) for providing financial support to this project.

Analysis of white blood cells in rats following implantation of HHP treated xenogenic cartilage tissue

Christopher Pohl[1], Charlotte Koppe[1], Nico Brandt[1], Andreas Hoene[1], Daniel Behrendt[1], Friederike Poosch[2], Daniel Strüder[2], Jens van den Brandt[3], Sabine Berg[3], Michael Schlosser[1]
[1]Department of General Surgery, Visceral, Thoracic and Vascular Surgery, University Medical Center Greifswald, Greifswald, Germany; [2]Department of Oto-Rhino-Laryngology, Head and Neck Surgery, Rostock University Medical Center, Rostock, Germany; [3]Central service and research facility for laboratory animals, Greifswald, Germany
* Christopher.pohl@uni-greifswald.de

INTRODUCTION

Tissue replacement by allogenic- as well as xenogenic material is of steadily increasing importance in clinical practice. To ensure optimal transplantation outcome, it is of utmost importance to reduce immunogenicity by devitalization of the transplant tissue, minimizing adverse inflammatory effects in recipients. Therefore, comprehensive evaluation of the immunogenic potential of implants is essential for clinical success. Currently High Hydrostatic Pressure (HHP) is under investigation as a new approach for devitalization of tissue. It induces apoptosis in cells, while keeping high matrix integrity with undiminished biomechanical features. Therefore, this in vivo study aimed at investigating the immunogenic potential of HHP devitalized porcine cartilage implants to evaluate their impact on the serological reaction following implantation in Lewis rats when compared with untreated control implants.

EXPERIMENTAL METHODS

Porcine cartilage was gathered postmortem from local abattoirs, kept in PBS for a maximum of 24 hours and treated with either HHP of 250 MPa for 10 minutes or served as an untreated control. From the tissue, stamps with a radius of 0.5 cm were taken to create evenly sized implants. Sixteen male Lewis rats each received a single implantation of HHP treated (n=8 animals) or untreated cartilage samples (n=8 animals) into the neck musculature. Blood was collected one day prior to implantation and weekly thereafter for a total of 56 days. For this, full blood samples were drawn retro-orbitally. Following blood collection samples were immediately analysed via a VETSCAN. Data was tested for normal

blood during the acute reaction phase. At experimental day 14, which represents the transitional phase between acute and chronic phase, no significant difference between the groups was seen, however it replicated the reduction as a trend ($p=0.030$). On experimental day 21, which represents the early chronic inflammatory phase, lymphocyte count between means of the control group ($7.45x10^9$) and the HHP treated group ($7.52x10^9$) nearly match. This continued up to day 56, showing no significant differences in all analyzed datasets throughout the whole chronic phase.

CONCLUSION

While macrophages and neutrophiles showed no differences between the groups on all observed days, a significant decrease of roughly 35% of lymphocytes during the acute phase was observed in the control group. This indicates a stronger local reaction followed by a higher rate of lymphocyte migration to the implantation site. By day 21 this effect subsided completely. No chronic reaction to the implants could be observed, however additional serological investigations are needed to clarify the complex serological reaction to the implantation. Especially the plasma concentration of cytokines secreted by inflammatory cells could provide additional information needed to draw explicit conclusions. Furthermore, morphometric immunohistological analysis could characterize the local inflammatory response and could even create a deep insight into immunological host reaction when linked with serological analyses.

ACKNOWLEDGMENTS

Long-term degradation behaviour of polymer materials based on PCL, PLGA, enriched with polyphenolic compounds and bioactive glass

Michal Dziadek[1,2], Kinga Dziadek[3], Kamila Checinska[2], Emilia Choińska[4], Piotr Szatkowski[5], Aleksandra Wajda[1], Szymon Salagierski[2], Aneta Kopec[3], Katarzyna Cholewa-Kowalska[2]

[1]Jagiellonian University, Faculty of Chemistry, 2 Gronostajowa St., 30-387 Krakow, Poland;
[2]AGH University of Science and Technology, Faculty of Materials Science and Ceramics, Department of Glass Technology and Amorphous Coatings, 30 Mickiewicza Ave., 30-059 Krakow, Poland
[3]University of Agriculture in Krakow, Faculty of Food Technology, Department of Human Nutrition and Dietetics, 122 Balicka St., 30-149 Krakow, Poland
[4]Warsaw University of Technology, Faculty of Materials Science and Engineering, 141 Woloska St., 02-507 Warsaw, Poland
[5]AGH University of Science and Technology, Faculty of Materials Science and Ceramics, Department of Biomaterials and Composites, 30 Mickiewicza Ave., 30-059 Krakow, Poland
*cholewa@agh.edu.pl

INTRODUCTION

Biodegradable polymers have been widely used in various areas, including biomedical applications. The degradation process causes gradually replacement of the biomaterial by host tissue and the therapeutic agent can be gradually released at the target site [1]. Identifying the factors that affect the degradation process is crucial in terms of developing materials with desired properties for specific applications [1]. One of the strategies for obtaining polymer-based materials with improved or new biological functionalities is the use of various additives. The widely studied additive is bioactive ceramic, especially bioactive glass (BG), used in the composite biomaterials for tissue engineering, especially for bone regeneration. The modification of polymer matrices with BGs allows for obtaining composites with the apatite-forming ability and high osteostimulative activity [2]. In recent years, much attention has been paid to the incorporation naturally occurring agents – polyphenols (PPh) into biomaterials [3]. In this work, for the first time, effect of incorporation of polyphenols (PPh) extracted from sage and sol-gel-derived bioactive glass (BG) particles, either alone or in combination, into poly(ε-caprolactone) (PCL) and poly(lactic-co-glycolide) (PLGA) was evaluated.

EXPERIMENTAL METHODS

Polyphenols were extracted from lyophilized leaves of sage (*Salvia officinalis* L.) in 1,4-dioxane/water mixture [12]. Bioactive glass particles (composition of (mol%) $40SiO_2$–$54CaO$–$6P_2O_5$ (A2), particle size of 1.5 μm) were prepared using the sol-gel method. The materials based on PCL (M_n=80 kDa,) and PLGA (M_n=80 kDa, lactic:glicolid ratio = 85:15,) in the form of films were prepared using the solvent casting method. The content of BG in composites was 30 % w/w, the concentrations of PPh were 1.5 and 4.5 % w/w. For degradation studies, materials were incubated in phosphate buffer saline (PBS, pH = 7.4) at 37 °C for 3, 6, 12 months for PCL, and 2 weeks, 1, and 3 months for PLGA, and the mass loss of the samples were measured. The changes in weight-average molecular weight (M_w) of the films was measured using gel permeation chromatography (GPC). The changes in crystallinity (Δ χc) and melting enthalpy (ΔH_m) were estimated using thermogravimetric (TG) analysis. Microstructural analysis of PCL- and PLGA-based films before and after incubation in PBS was performed by SEM and EDX analysis. ATR-FTIR spectroscopy was used to evaluate the formation of CaP layer on the films. The changes in P, Ca, and Si concentration in PBS during film incubation were measured by ICP-OES technique

RESULTS/DISCUSSION AND CONCLUSIONS

In the present study we demonstrated that modification of two common biodegradable polymers, namely PCL and PLGA, with bioactive glass particles and polyphenols, either alone or in combination, significantly affected long-term degradation of both polymers.

BG particles were shown to accelerate degradation of materials based on slowly degrading polymer - PCL, while degradation of materials based on fast degrading polymer – PLGA was retarded. In the case of PLGA-based composites, the formation of a calcium phosphate layer and dissolution of alkaline ions from BG particles appear to have a pivotal role in controlling degradation by providing protection from direct exposition to aqueous environment and neutralizing acidic carboxyl end groups. Polyphenols were shown to accelerate the degradation of all polymeric and composite materials based on both PCL and PLGA when compared to respective materials without PPh. The degradation rate of PLGA composites containing BG and PPh was lower than polymeric PLGA film, indicating that the presence of BG particles in PLGA matrix is s a key factor affecting degradation kinetics. The degradation of materials in the presence of PPh appeared to be rather complex since the following PPh-related factors can be involved in this process: wettability improvement, acid catalysis, plasticizing effect, and porosity formation

REFERENCES

1. Zhang F at al. Adv. Healthcare Mat. 2020;9:1901358.
2. Gritsch L, at al. App. Mat. Today 2021;22.
3. Venugopal E, at al., Nanomed. 019;21:102044

ACKNOWLEDGMENTS

This work was supported by the National Science Centre, Poland grant nos. 2017/27/B/ST8/00195 (KCK) and 2019/32/C/ST5/00386 (MD)..

Development of a biodegradable Mg-doped ZnO/PPy neural interface

Magesh Sankar[1], Manus J Biggs[1]*

[1]CÚRAM, SFI Research Centre for Medical Devices, National University of Ireland Galway, Galway, Ireland

m.sankar1@nuigalway.ie

Introduction

Biodegradable electronics, which resorb or degrade following implantation, have come to the forefront of biomaterials research. Such materials should present biocompatibility on implantation, undergo controlled degradation and present tailored mechanical and electrical properties[1]. Critically, electrically conductive and biodegradable polymer composites are necessary for the development of novel resorbable flexible bioelectronics and neural interfaces.

In particular, resorbable metallic formulations have been proposed for the development of electrical circuitry in transient electronics and have facilitated the development of biosensor devices with a functional lifetime range spanning weeks to months[2].

In the process of developing a novel degradable electrode material, we explored doping of Magnesium (Mg)-Zinc Oxide (ZnO) into a polypyrrole (PPy) matrix. This materials possessed a significantly improved charge storage capacity and controlled degradability under simulated physiological conditions. Bench top electrochemical deposition facilitated the synthesis of cost-effective degradable electrodes. These findings help to promote this coating as a potential candidate for successful development of biodegradable bioelectronics.

Keywords: Biodegradable; resorbable; transient electronics

Methods

The base electrolyte for this work was prepared using 80 mM Zinc nitrate hexahydrate ($Zn(NO_3)_2.6H_2O$) and 5wt% of Magnesium nitrate hexahydrate ($Mg(NO_3)_2.6H_2O$) solvents. Further Pyrrole monomer was added to the solution and the electrolyte was stirred for 1hr before the electrodeposition. Chronoamperometry was utilized to develop a composite thin-film at a constant voltage of -1.3V on a pristine Indium Tin Oxide (ITO) coated glass substrates with time intervals of 180-450s. The electropolymerized PPy/Mg-ZnO was characterized for its physio-chemical and electrical properties. The degradation of the developed coating in a-CSF was analysed using conventional weight loss method and potentiodynamic polarization (PDP). The CSC was measured using cyclic voltammetry (CV) for five days. The biocompatibility and conductive behaviour of the coatings was evaluated using primary neuronal culture extracted from E18 rat embryo and seeded on the samples for a duration of ten days to analyse the maturation.

Results

The synthesised coating exhibited an average crystallite size of 5.3nm (XRD, Scherer equation) and the flower like morphology was characterized using scanning electron microscopy (SEM). The CSC was measured up to five days and a significant loss of mass (58%) was observed. The weight loss was nearly 12µg over the same period, whereas, the PDP measurements showed one order of magnitude increase in corrosion rate.. Electrochemical impedance spectra obtained with and without showed a significant increase in impedance from Day 3 to Day 10.

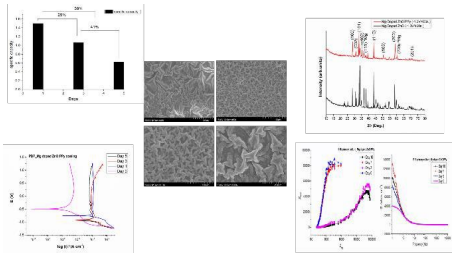

Discussion

Despite the fact that polypyrrole is non-biodegradable[3], the introduction of degradable magnesium and zinc particles into the matrix during the electropolymerization was shown to improve the CSC and also the degradation profiles of this composite in vitro. The flower like morphology of the developed coating significantly increased the surface area of the material, facilitating composite degradation. A primary culture of E18 rat embryo indicated biocompatibility at day 10 and suggested that developed composite may be used in the development of biodegradable conductive coatings.

References

[1]Green et al., Biomat. 29(24-25), 3393-3399, 2008.
[2] Kuzma et al., Springer, Cham, 29-72, 2020.
[3]Wang et al., J. *Chem. Engg. Journal*, *428*, 131089 2022.

Acknowledgement
The authors like to acknowledge SFI, Ireland & Hardiman PhD Research Scholarship and the facilities & scientific and technical assistance of the Centre for Microscopy & Imaging at the National University of Ireland Galway.

In vitro and *in vivo* degradation and biocompatibility follow-up of mechanical reinforced degradable pHEMA

Duarte Moura[1,2,3*], Helena P. Ferreira[1,2,4], Sabrina Rohringer[5], Andreia T. Pereira[1,2], Cristina C. Barrias[1,2,4], Fernão D. Magalhães[6], Helga Bergmeister[5,7], Inês C. Gonçalves[1,2]

[1]INEB – Instituto de Engenharia Biomédica, Universidade do Porto, Rua Alfredo Allen, 208, 4200-180 Porto, Portugal;
[2]i3S - Instituto de Investigação e Inovação em Saúde, Universidade do Porto, Rua Alfredo Allen, 208, 4200-180 Porto, Portugal;
[3]FEUP – Faculdade de Engenharia, Departamento de Engenharia Metalúrgica e de Materiais, Universidade do Porto, Rua Dr. Roberto Frias, 4200-465 Porto, Portugal
[4]ICBAS – Instituto de Ciências Biomédicas Abel Salazar, Universidade do Porto, Porto, 4050-313, Portugal
[5]Center for Biomedical Research, Medical University of Vienna, Vienna, Austria
[6]LEPABE – Faculdade de Engenharia, Universidade do Porto, Rua Dr. Roberto Frias, 4200-465 Porto, Portugal
[7]Ludwig Boltzmann Institute for Cardiovascular Research, Austria * duarte.moura@i3s.up.pt

INTRODUCTION

Development of degradable blood contacting devices (BCD) faces several issues, such as long-term thrombogenicity, weak mechanical properties and high molecular weight of the degradation products. Poly(2-hydroxyethyl methacrylate) (pHEMA) emerges as a promising hydrogel to be used in BCD mainly due to its bio/hemocompatibility and non-fouling character[1]. However, aiming tissue engineering strategies, it is essential to overcome its lack of degradability[2]. Thus, we aim to develop a degradable pHEMA hydrogel to be used in a post-implantation tissue engineering approach. For that, a degradable crosslinking agent, pentaerythritol tetrakis(3-mercaptopropionate) (tetrakis) was copolymerized with pHEMA, while oxidized few layer graphene (FLGO) was used as nanofillers to potentiate its mechanical performance. The hydrogel physicochemical and biological behaviour was evaluated, including in an *in vivo* rat subcutaneous implantation model.

EXPERIMENTAL METHODS

Degradable pHEMA (dpHEMA) films were produced by adding tetrakis (0.25, 0.5, 0.75v/v) to the previously described pHEMA formulation[3], without or with 1%w/v FLGO with 5 µm lateral size added (dpHEMA/FLGO). Tensile tests were analysed by A.XTplus texture and hydrophilicity by optical contact angle. Degradation studies were performed *in vitro* over 6M (37ºC;100rpm)(ISO 10993:13). Cytotoxicity of degradation products (24h and 6M) was evaluated towards human umbilical vein endothelial cells (HUVEC), assessing cell metabolic activity and morphology. Hydrogels non-fouling character by direct seeding of HUVEC ($1x10^4$cells/well), human platelets (3×10^8platelet/mL) and *S. aureus* ($1.3x10^6$bacteria/ml). For *in vivo* assays, scaffolds were implanted subcutaneously in Sprague Dawley rats (ISO-10993-6-2009). At timepoint 1, 3, 6 and 9M animals were sacrificed and specimens evaluated.

RESULTS AND DISCUSSION

Inert and biocompatible pHEMA hydrogel was turned into a degradable material, independently of the tetrakis amount, despite at the expenses of loosing mechanical properties. The incorporation of FLGO increased the ultimate tensile strength up to 0.2 MPa (4x higher than dpHEMA), allowing tuning of the *in vitro* degradation time between 2-4M. Notably, the intrinsic properties of pHEMA were kept, namely wettability and short and long term cytocompatibility. The anti-adhesive properties were confirmed, with no adhesion of HUVEC, platelets or bacteria.

Upon 9M subcutaneous implantation in rats, no signs of inflammation (no swelling, redness nor fibous capsule formation). Macroscopic and SEM images confirmed stability of pHEMA and dpHEMA/FLGO, and revealing high degradation of dpHEMA (starting at 3M and almost complete after 6M). Gene expression of pan macrophages (CD68), pro-inflamatory M1 macrophages (CD80 and CCR7), and anti-inflamatory M2 macrophages (CD206) revealed that eventhough there are no statistically significant differences, in month 1, dpHEMA/FLGO has the higher inflammatory response (with M1/M2 > 1), followed by dpHEMA, and pHEMA (with M1/M2 < 1). However, at month 9 there is a tendency to decrease this inflammatory response to very low expression in all conditions, despite dpHEMA revealing an anti-inflamatory profile and dpHEMA/FLGO a pro-inflamatory profile.

CONCLUSION

The described newly developed degradable hydrogels have considerable potential as scaffolds for tissue engineering applications, with higher amounts of tetrakis leading to higher degradation and where, increase of mechanical properties can be tuned by the incorporation of FLGO. *In vivo* a degradation of dpHEMA is more prone to occur when FLGO is not present. Independently of the formulation, no significant differences were found on the macrophages (pro- and anti-inflammatory) expression, with most of the markers showing a decrease throughout time. Altogether, the results showed that pHEMA was successful turned into a degradable material without evoking a loss of its native bio/hemocompatibility and anti-adhesive properties.

REFERENCES

[1] A.T. Pereira *et al.*, Biomaterials Science 9 (2021).
[2] H. Krynauw *et al.*, 2 (2019) 783522.
[3] I.C. Goncalves *et al.*, Biomaterials 30 (2009) 5541-51.

ACKNOWLEDGMENTS

This work was funded by PhD grants 2020.04712.BD and SFRH/BD/1400006/2018 and by projects PTDC/CTM-COM/32431/2017, UIDB/04293/2020, through FCT and FEDER.

Macromer-based Macroporous Scaffolds with Tunable Degradation Kinetics Controlled by Macromer Chemistry

Jan Krieghoff[1], Christian Kascholke[1], Annett Starke[1], Rudi Loth[1], Michaela Schulz-Siegmund[1], Michael C. Hacker[1,2]

[1] Institute of Pharmacy, Pharmaceutical Technology, Faculty of Medicine, Leipzig University, Germany
[2] Institute of Pharmaceutics and Biopharmaceutics, Heinrich Heine University, Düsseldorf, Germany
* jan.krieghoff@uni-leipzig.de

INTRODUCTION

Macromers – macromolecules containing at least one oligo- or polymeric building block and two or more reactive groups for cross-polymerization – are an attractive basis for the design of biomaterials with adaptable biophysical, biochemical and degradative properties for applications in regenerative medicine as well as drug delivery. Previously, we developed the TriLA platform of macromers comprised of a trivalent alcohol core that can optionally be ethoxylated, a biodegradable oligo(lactic acid (LA)) ester block and terminal methacrylic acid esters as reactive groups that allow for cross-polymerization into monolithic or macroporous structures.[1] Degradation of high molecular weight poly(α-hydroxy acid) esters such as poly(LA) is characterized by a long time of stable mass followed by a very rapid (burst) mass loss caused by the decrease of degradation product chain lengths into a soluble range combined with autocatalytic acceleration via the acidic degradation products. This process can result in tissue inflammation in vivo. It was hypothesized, based on initial results from a single TriLA variant, that cross-linked scaffolds from the macromers with short degradable blocks show a different degradation profile without this sudden mass loss. The presented work expanded upon the TriLA macromer platform through macromer variants incorporating the more hydrophilic glycolic acid (GA) as a partial replacement for LA. The effect of different chemical compositions of the macromers on the degradation behavior of macromer-based macroporous scaffolds was investigated.

EXPERIMENTAL METHODS

In the macromer code (Tri134(LAxGAy)3.75), 134 refers to the molecular weight of the trimethylolpropane core, x and y refer to the theoretical composition of the biodegradable block on each arm, and 3.75 refers to the methacryloyl chloride feed of 3.75 eq. in the second synthesis step that results in complete methacrylation (Fig. 1). GA was introduced by substituting its cyclic dimer glycolide for the cyclic LA dimer lactide in an equivalent exchange during the first ring-opening polymerization step of the macromer synthesis.

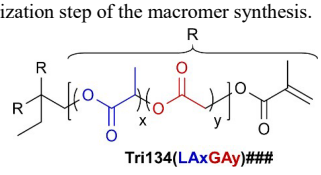

Fig. 1: Structure of the GA-containing variants of TriLA macromers[2]

The newly developed macromer variants, as well as the reference macromer Tri134(LA6)3.75, were used to fabricate scaffolds with an interconnected pore network through solid lipid templating. In order to investigate degradation behavior in dependence of chemical composition, samples of these macroporous scaffolds were subjected to a long term in vitro degradation study (37°C, PBS pH 7.4 with semiweekly buffer exchange). Progress of degradation was monitored by medium pH measurements at every medium exchange (n = 5) as well as sample dry masses at defined time points (n = 3).

RESULTS AND DISCUSSION

Macromer variants with substitution of up to 4 of the 6 LA units per arm with GA were successfully synthesized, characterized and processed into scaffolds. Degradation for all macromers proceeded with continuous mass loss following onset of degradation (OoD) after an initial period of stable mass. OoD is marked by sustained medium acidification following the initial phase of stable pH values around 7.4. Rates of degradation correlated with GA incorporation. With 6 LA units per arm, scaffolds from the reference macromer Tri134(LA6)3.75 degraded slowly, taking 8-10 months to lose more than 50% of their initial mass. Higher macromer hydrophilicity significantly accelerated degradation, with rates of mass loss that correlated with the degree of substitution of LA for GA. Substituting only 1 GA monomer for LA per arm in the Tri134(LA5GA1) variant resulted in more than 50% mass loss within 4-5 months, whereas the most rapidly degrading Tri134(LA2GA4)3.75, lost more than 50% of its initial mass within less than a month. Medium acidification positively correlated with degradation rate, but medium pH was not decreased below 5 even for the most rapidly degrading variants.

CONCLUSION

The continuous degradation of the TriLA macromers with mild medium acidification is significantly different from the burst mass and acidic degradation product release of linear high molecular weight poly(α-hydroxy acid) polymers. With degradation rates that can be adapted through macromer chemistry, the macromers are interesting biomaterials for tissue engineering, regenerative medicine and drug delivery applications.[2]

REFERENCES

1. R. Loth et al., Acta Biomaterialia 2015, 26, 82-96
2. J. Krieghoff et al., Polymer Degradation and Stability 2022, 195, 109775

ACKNOWLEDGMENTS

The authors would like to thank the German Research Council (DFG, 59307082/TP A1) for providing financial support to this project.

Degradation and Stability Observations of Bioactivated Gellan Gum Hydrogels *in vitro* and *in vivo*

Christine Gering[1*], Jenny Párraga[2], Hanna Vuorenpää[1], Lucía Botero[3], Susanna Miettinen[1], Minna Kellomäki[1]

[1] Faculty of Medicine and Health Technology, Tampere University, Tampere, Finland
[2] IamFluidics BV, High Tech Factory, Enschede, The Netherlands
[3] Facultad de Medicina Veterinaria y de Zootecnia, Universidad Nacional de Colombia, Colombia
[*]christine.gering@tuni.fi

INTRODUCTION

Hydrogels have gained a considerable reputation as soft tissue mimics. While mechanical, viscoelastic, cytocompatibility and diffusion properties are often mentioned in this regard, also degradation is crucial for tissue engineering purposes[1]. Degradation is required for the removal of regenerative devices from the body, as well as for the cell-driven remodeling in tissue models. The mechanism of degradation is governed primarily by the chemical structure of the polymer and crosslinking type. Degradability of hydrogels is tested *via* mass loss or swelling observations *in vitro*, often with cell-free analogues and a variety of other simplifications to model the target environment. It remains challenging to correlate these cell-free *in vitro* observations to cell-mediated degradation to physiological resorption *in vivo*.

Gellan gum (GG) is a bacterial polysaccharide with excellent gelation and mechanical properties, however it lacks bioactivity[2]. We have investigated four GG-based hydrogels in our recent work[3], including ionically crosslinked purified GG (NaGG) and avidin-modified NaGG (NaGG-avd), showcasing the modular incorporation of fibronectin via avidin-biotin binding[4]. The other two hydrogel formulations are formed by covalent crosslinking of oxidized GG and carbohydrazide (gelaCDH) or adipic hydrazide (gelaADH) modified gelatin, utilizing gelatin's native bioactivity[2]. We investigated the viscoelastic properties, the cell response of a endothelial – adipose stem cell co-culture, as well as the tissue response to subcutaneous implants of these hydrogels *in vivo*[3]. Here, we will focus on the degradation observations made throughout the different *in vitro* and *in vivo* environments.

EXPERIMENTAL METHODS

GG was modified as described previosuly[2,4]. Briefly, GG was purified using an exchange resin, and avidin was coupled via carbodiimide reaction[4]. GG was oxidized using $NaIO_4$, while gelatin was functionalized using CDH or ADH using HOBt-EDC strategy. Hydrogels were prepared using either $CaCl_2$ (10mM, 1:5 with NaGG), spermidine (2mM, 1:5 with NaGG-avd), or by combining GGox (40mg/mL) with either gelaCDH or gelaADH (40mg/mL) 1:1, briefly mixing and casting to a cylindrical mold. After gelation, samples were incubated in DMEM and weighed periodically.

Fluorescent GFP-HUVEC (5 x10^6 cells/mL, p.4-5) and hASC (1 x10^6 cells/mL, p.1-3) were encapsulated in the hydrogels prepared as above, and cultured over 14 days. Samples were imaged using EVOS fluorescence microscope every 2 days, fixed and stained (α-SMA, DAPI) on day 14 for confocal microscope imaging. For animal studies, cell free samples were implanted to dorsal subcutaneous pockets in male Wistar rats, which were sacrificed at day 7, 14, 21 and 28, and tissue slices were analyzed with hematoxylin/eosin staining.

RESULTS AND DISCUSSION

Cell-free hydrogel samples were incubated in cell growth medium DMEM at 37°C and their weight was observed, showing both swelling and mass loss due to degradation. NaGG and NaGG-avd hydrogels prove to be very stable, while gelatin-GG hydrogels quickly diminish in weight. This is also observed from the rheology analysis, where NaGG and NaGG-avd are stable and slightly increase their storage modulus, while the gelatin-based hydrogels quickly deteriorate.

In contrary, gelatin-GG hydrogels were stabilized in cell culture studies, likely by the formation of an extensive cellular network and cell-produced extra cellular matrix deposition. Initially, gela-GG samples seemingly softened, but cell-laden hydrogels remained intact over the 14 days culture period, while cell-free controls under the same treatment were not present at the end. Similarly, and rather surprisingly, also in the animal studies more samples of the NaGG and NaGG-avd hydrogels were unobservable after 28 days of subcutaneous implantation than the gela-GG formulations. This however, may be either an effect of degradation, or could be due to the samples moving away from the original implant site.

CONCLUSION

This study underlines that cell-free degradation of hydrogels may not be representative of *in vitro or in vivo* experimental setups. We have found that our gela-GG hydrogels are rarely stable in *in vitro* conditions, but in combination with cells and *in vivo* they can be persistent up to 2 and 4 weeks. Ionically crosslinked GG hydrogels are typically very stable *in vitro*, but have been observed to be disintegrated in biological settings. Ultimately, the preparation technique, components, and environment are crucial for hydrogel stability and degradability.

REFERENCES

1. Leijten, J. et al., Mater. Sci. Eng. R Reports 119:1–35, 2017
2. Koivisto, J. T. et al., ACS Appl. Mater. Interfaces 11:20589–20602, 2019
3. Gering, C. et al., [unpublished] 2022
4. Gering, C. et al., PLoS One 14:1–22, 2019

ACKNOWLEDGMENTS

This work was supported by the Academy of Finland through the Center of Excellence – Body on Chip project.

Reseeding Mature Multinucleated Cells on Biomaterials for Resorption Analysis - Osteoclast Transfer Culture

Christiane Heinemann[1], Benjamin Kruppke[1*]

[1]Max Bergmann Center of Biomaterials, Institute of Materials Science, Technische Universität Dresden, Dresden, Germany
[*]Benjamin.Kruppke@tu-dresden.de

INTRODUCTION

Biomaterial resorption by osteoclasts (OC) is a key process to be characterized for degradable bone substitute materials, as it is the essential step of integrating a material in the bone and its replacement over time. *In vitro* analyzation of bone substitute materials requires great effort, as the fusion process of mononuclear monocytes is influenced by factors such as material composition, scaffold architecture, and surface topography. However, in order to study the resorption of different materials independently of these influences on monocyte fusion, it would be desirable to separate these two processes. It would be advantageous, for example, if the fusion of monocytes was to take place on standardized culture dishes and the mature, resorption-competent osteoclasts could then be transferred to the different biomaterials to be investigated. Unfortunately, most detachment methods (e.g. cell scraper), show poor survival of OC or loss of function. Therefore, in the following, monocyte cultivation and induced osteoclast formation was performed on various commercially available cell culture plates in combination with different detachment techniques. The cells were subsequently analyzed for their survival rate and osteoclast activity.

EXPERIMENTAL METHODS

Human monocytes were isolated from buffy coats and seeded on various culture dishes (Nunclon™ Delta Nunc, Cellstar® Cell-repellent, Tissue Culture Suspension, Lumox® Suspension, UpCell™ Surface Nunc™). OC differentiation was induced with 50 $^{ng}/_{mL}$ M-CSF and 50 $^{ng}/_{mL}$ RANKL.

OC were detached using three procedures (where applicable). Temperature-induced detachment (applicable for UpCell™ plates only), enzyme detachment with Accutase®, and detachment by scraping. First, the OC were transferred to Nunclon™ reference well plates. Here the percentages of adherent and non-adherent cells were determined by DNA measurement. This provided a first assessment of the effectiveness of the detachment and transfer process.

In a following investigation, osteoclasts were transferred to decellularized osteoblast-derived matrix plates and to dentin discs. After transfer, the osteoclast enzyme expression was analyzed focusing on TRAP 5b- and CTSK-activity measurements. Furthermore, resorption pits on dentin discs and decellularized osteoblast-derived matrix plates were investigated using scanning electron microscopy.

RESULTS AND DISCUSSION

Most effective methods for cell detachment have been Accutase® and the use of UpCell™ plates. The latter, does not use enzymes, centrifugation, or mechanical scraping and thus allows subsequent resorption analysis, with better quantification. OC of the Nunclon™/Accutase® combination also showed a good survival rate after transfer to a fresh Nuncleon™ well plate, and a sufficient resorption capacity was also observed on the dentin discs (left Fig.). However, the cells were more difficult to quantify using this process in contrast to UpCell™ plates.

The cell scraper method (e.g. on Cellstar® plates) can be regarded as unfavorable. Here, only a few cells were still adherent after transfer to Nunclon. Even on dentin discs, the few cells transferred, hardly showed any resorption activity (middle Fig.).

Thermoresponsive surfaces (UpCell™ plates) for cultivation and detachment were applicable to maintain OC activity, with increased TRAP 5b- and CTSK-activity. Furthermore, OC transferred from these plates on both dentin discs and decellularized matrix plates showed large areas of resorption pits (right Fig.).

CONCLUSION

In conclusion, it can be stated, that precultivation of mature osteoclasts in UpCell™ multiwell dishes in order to detach them without damage and further cultivate them on biomaterials is possible. The OC can be transferred and re-seeded revealing high adhesion and resorption activity, in terms of TRAP 5b- and CTSK-activity, as well as resorption pit formation. Thus, the osteoclast transfer culture provides a useful tool for biomaterial characterization independent of the monocyte's fusion process.

ACKNOWLEDGMENTS

The authors would like to thank the German Research Foundation for providing financial support to this project (Grant no: DFG HA5284/6) for financial support of the project.

A composite elastin derivative-based hydrogel designed for promoting innervation, vascularization and bone formation: *In vivo* evaluation in ectopic and heterotopic models

Micaela Roque[1,2*], Nadia Mahmoudi[1,3], Bruno Santos[1], Sylvain Catros[1], Sébastien Lecommandoux[3], Bertrand Garbay[3], Joëlle Amédée[1]

[1] BioIngenierie Tissulaire (BioTis), Inserm U1026, University of Bordeaux, Bordeaux, France
[2] SATT Aquitaine, Aquitaine Science Transfert, Talence, France
[3] Univ. Bordeaux, CNRS, Bordeaux INP, LCPO, UMR 5629, Pessac, France

[*] micaela.roque@inserm.fr

INTRODUCTION

Worldwide, millions of bone reconstruction surgeries are performed per year due to cases of severe trauma or cancer treatments. Despite continuous progress in bone tissue engineering, the successful reconstruction of large bone losses remains a major unsolved problem in the clinical sector. This project focuses on developing an innovative biomaterial that allows the recruitment of bone cells, endothelial cells and neuronal fibers within the same matrix, allowing the regeneration of bone tissue. This bioactive hydrogel is based on a matrix of recombinant Elastin-Like Polypeptides (ELP), modified chemically to allow the graft of peptides intended to stimulate angiogenesis and innervation, combined with calcium phosphate particles (hydroxyapatite, HA) that can mimic the mineral phase of bone tissue, and thus promote bone repair[1,2]. Furthermore, ELPs are biocompatible, biodegradable, and non-immunogenic, making them a good candidate for clinical applications.

The effectiveness of the hydrogel will be evaluated *in vivo,* in a mice subcutaneous model, as well as in a rat femoral condyle defect model.

EXPERIMENTAL METHODS

To assess mineralization potential, the hydrogels were followed longitudinally at several time points (7, 15, 30 and 60 days) after implantation by X-ray computed tomography (micro-CT). To evaluate osteoid tissue formation, vascular and neuronal sprouting, as well as inflammation, histological analyses were performed again at the same time points after implantation. For this, Masson's trichrome staining and immunohistochemistry for vascular (Endomucin, Meca32, Podocalyxin) and neuronal markers (NeuroFilament, β3-tubulin) were used. For micro-CT analyses, Mineral Volume / Total Volume was determined by eXploreMicroView® software. For histology, the quantification of osteoid tissue formation was performed using ImageJ®, and sprouting of vessels and nerve fibers was achieved in Imaris®. All statistical tests were performed using GraphPad Prism, and a p value < 0.05 was considered to be statistically significant.

RESULTS AND DISCUSSION

Different hydrogel compositions (without HA, 1%, 2% or 2.5% (w/v) HA) were first implanted subcutaneously. Micro-CT analysis confirmed the formation of ectopic mineralized tissue within the implants, which increased over time in hydrogels containing HA. Gels were explanted and histological sections of the material associated with the surrounding tissues showed cell colonization of the hydrogels, and no significant fibrosis (Fig.1). This indicates that hydrogels are not rejected. Regarding angiogenesis, 3 days after implantation, blood vessels could be observed mainly at the gel periphery (Fig.1A). Interestingly, 1 month after, larger vessels could be observed in the periphery but also inside the hydrogels (Fig.1B). The capacity of the hydrogel to sustain innervation was also shown by the presence of nerves in the close periphery of the material, mainly at early stages after implantation (Fig.1). These results suggest that hydrogels have a positive effect on both vascularization and innervation.

Overall, the hydrogel containing 2% HA presented the best characteristics, and was considered for further *in vivo* tests in a femoral condyle defect model in rat. The hydrogel, together with a negative control (empty defect) and a positive control (Collapat®) was tested *in vivo*, followed by longitudinal micro-CT analysis to assess mineralization potential. The volume of mineralized tissue formed after 2 months was around 30% in empty defects, 40% in hydrogels and 60% in Collapat®. Histological sections showed again cell colonization of the hydrogels and no significant fibrosis, indicating that they are biocompatible. Angiogenesis and innervation evaluation, in the scope of bone regeneration, is ongoing.

Figure 1: Angiogenesis and innervation sprouting in the different hydrogels, 3 days after subcutaneous implantation (A), and 1 month after implantation (B). Representative immunofluorescence images show DAPI in blue (nucleus), auto fluorescence in green, β3-tubulin in white (nerves) and Endomucin in red (blood vessels).

CONCLUSION

The cell-free and growth factor-free hydrogel is capable of inducing mineralized tissue formation, angiogenesis and nerve sprouting, without showing significant signs of inflammation, both subcutaneously as in bone lesions. Such a holistic approach represents a technological breakthrough in the field of tissue engineering by breaking with all current strategies based solely on bone and endothelial cells. These results are very encouraging to pursue further *in vivo* testing in big animals for pre-clinical evaluation.

REFERENCES

1. Paiva dos Santos et al., Acta Biomaterialia, Volume 99, 154-167, 2019
2. Matrice composite utile pour favoriser l'innervation, l'ostéogenèse et l'angiogenèse. N/Réf. : BV_2021-060 / PJ_2017-107

A cross-sectional clinical study on a glycated hemoglobin (HbA_{1C}) point-of-care device for the screening of prediabetes and diabetes in dental setting

Elena Maria Varoni[1*], Lucrezia Cinquanta[1], Rita Paroni[2], Pietro Cerveri[3], Francesco Cellesi[4], Antonio Carrassi[1]

[1]Department of Biomedical, Surgical and Dental Sciences, University of Milan, Milan, Italy
[2] Department of Health Sciences, University of Milan, Milan, Italy
[3] Department of Electronics, Information and Bioengineering, Politecnico di Milano, Milan, Italy
[4] Department of Chemical Engineering, Politecnico di Milano, Milan, Italy
[*] elena.varoni@unimi.it

INTRODUCTION

About 32.3 million adults were diagnosed with diabetes in the European Union in 2019 (prevalence 6.2%); an additional 24.2 million people in Europe were estimated to have undiagnosed diabetes (IDF, 2019). In Italy, diabetes affects over 3 million 200 thousand people, i.e. 5.3% of the entire population (16.5% of the over 65-year old) (ISTAT, 2017). People at high risk of developing diabetes (prediabetes) are in a long-lasting asymptomatic stage before developing the disease: in Italy, the prediabetes prevalence is 6% and, after 10 years of age, the conversion rate to diabetes is 7.6%[1]. Dental setting offers a unique opportunity to carry out prediabetes/diabetes screening, because of the periodical follow-up visits, which dental patients usually undergo[2-5]

The aim of this pilot study was to determine whether point-of-care (POC) measurement of glycated hemoglobin (HbA_{1c}) from a finger-prick blood sample at dental chair, combined with the administration of the Società Italiana di Diabetologia questionnaire for assessing diabetes risk, represents a feasible and useful method of screening for undiagnosed diabetes and prediabetes within the dental setting.

EXPERIMENTAL METHODS

A cross-sectional clinical study was conducted enrolling, consecutively, all the individuals referring to the dental clinic as team workers (Ospedale San Paolo, Milano, Italy).

After the consent form and anamnestic data collection, the Diabetes Risk Questionnaire (Italian Society of Diabetology) was administered and HbA_{1c} finger-stick blood test (Cobas b 101 system, Roche) was performed on the same individuals at dental chair.

The cut-off values were set as follows: HbA_{1c} greater than 6.5% for diabetes; between 5.7% and 6.4% for prediabetes[2]. Patients having an HbA_{1c} test of 5.7% or higher were referred to the Clinical Diabetology Unit for a definitive diagnosis and further management.

The calculation of the sample size was based on the results from the previously available literature[2-5], estimating a minimum sample size of 112 individuals (Fleiss with correction for continuity).

RESULTS AND DISCUSSION

120 individuals were enrolled including 75 women and 45 men (mean age: 33.3 ± 13.3 years). In two cases, the patients, both females, were already known type I diabetics.

The percentage of prediabetics was: 5.8% (7 out of 120 subjects).

The two Type 1 diabetic patients, in particular, were found to have HbA_{1c} levels of 6% and 9.3%.

Table 1 summarizes the main clinical characteristics.

Table 1. Participants' clinical characteristics (N=120)

Characteristics	N (%)
Diabetes already diagnosed: Yes	2 (1.6%)
High cholesterol: Yes	1 (0.8%)
Thyroid disorders: Yes	5 (4.1%)
Diabetes Risk Questionnaire (Italian Society of Diabetology) % of risk at 10 years	
- 0%	19 (15.8%)
- 1-25%	89 (74.1%)
- 26-50%	10 (8.3%)
- 51-90%	0 (0%)
- >90%	2 (1.6%)
HbA_{1C} POC testing	
- < 5.7%	112 (93.3%)
- Between 5.7% and 6.4% (prediabetes)	7 (5.8%)
- ≥ 6.4% (diabetes)	1 (0.8%)

CONCLUSION

The feasibility of the screening for diabetes at dental chair using a HbA_{1C} POC device was confirmed.

Screening for diabetes and prediabetes in dentistry can offer a significant benefit to patients in terms of systemic health and quality of life. Due to the immediate feedback, POC testing improves patient's glycaemic control and quality of life, with benefit on the healthcare system. It promotes operational efficiency, since, via instant results, POC testing can reduce the waiting time of the lab tests, providing a rapid glycaemic control and prompt therapeutic adjustments. Clinical benefits include increased patient self-awareness, faster modification of drugs, thus lower HbA_{1c} levels. Economic benefits include fewer phone calls, less appointments, increased patient satisfaction.

REFERENCES

1. Franciosi M et al. Diabetes Care. 28:1187–94, 2005
2. Genco RJ. *et al.* J. Am. Dent. Assoc. 145:57–64, 2014
3. Barasch A. *et al.* J. Am. Dent. Assoc.143:262–9, 2012
4. Lalla E. *et al.* J. Dent. Res. 92:888–92, 2013
5. Borrell LN. *et al.* J. Periodontal Res. 42:559–65, 2007

Regional Effect of IRE-Ablation after Monophasic Square Pulse Stimuli on Porcine Liver

Sung-Min Jeon[1], Jiang Yixin[2], Enkhzaya Davaa[1], Ho Sun Jung[2], Seok Jeong[3]*, and Su-Geun Yang[1,2]*

[1]Department of Biomedical Science, Translational Research center, Inha University Hospital, Inha University College of Medicine, Incheon 22332, South Korea.
[2]Department of Biomedical Science, BK21 FOUR Program in Biomedical Science and Engineering, Inha University College of Medicine, Incheon 22212, South Korea
[3]Department of Internal Medicine, Inha University Hospital, Inha University College of Medicine, Incheon, Korea.

*sugeun.yang@inha.ac.kr

INTRODUCTION

Irreversible electroporation (IRE) is a novel tumor ablation technique using a non-thermal energy to create innumerable permanent nanopores in the cell membrane to disrupt cellular homeostasis[1]. The technique known as a minimally invasive method applicable to percutaneous tumor ablation[2], which can be applied to hepatic tumor tissue adjacent to blood vessels or nerves[3]. We investigated the regional effects (e. g. change of histological features) after IRE ablation on the liver parenchyma using a normal large animal model as a basic study for the effective treatment of liver cancer using IRE.

EXPERIMENTAL METHODS

A pair of IRE monopolar needle electrodes (19-G) was inserted into the hepatic lobe of miniature pig (n=2). Monophasic square wave pulses (electric field intensity of 1,5Kv/cm, 0.1 ms duration time, 90 pulses, 1 Hz) was delivered to the hepatic parenchyma. We investigated the histological features induced by IRE such as apoptosis, hepatic sinusoidal dilatation, sinusoidal congestion, preservation of vascular structures[3] in the tissues stained with H&E and TUNEL.

RESULTS AND DISCUSSION

We found apoptotic cells, marked dilatation of hepatic sinusoids, sinusoidal congestion, hepatic congestion, and intact preservation of vascular structures (bile ducts, hepatic arteries) in IRE-treated liver tissues (Fig 1). The proportion of apoptotic regions within hepatic lobules was different for each hepatic lobule. From the above results, we found that alteration of some IRE input parameters was required for full occupation of the apoptotic region within the hepatic lobule.

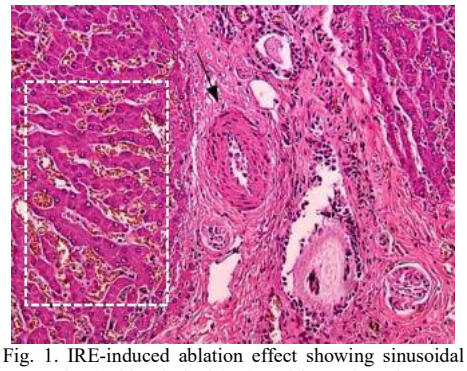

Fig. 1. IRE-induced ablation effect showing sinusoidal congestion (white dashed box) and intact hepatic artery (black arrow) after monophasic square wave pulse application to the liver parenchyma of miniature pig.

CONCLUSION

It was confirmed that cell apoptosis, sinusoidal dilatation and congestion were induced when high voltage monophasic square-wave pulses were delivered to the liver tissue of miniature pigs. Bile ducts and hepatic arteries were observed to remain intact even after IRE application.

REFERENCES

1. Lee EW. *et al*, Gut Liver. 4 (Suppl 1): S99-S104, 2010.
2. Zhou Y. *et al*, Hepatocell Carcinoma. 8: 625–644, 2021.
3. Vogel JA. *et al*, PLoS ONE 11: e0166987, 2016.

ACKNOWLEDGMENTS

The authors would like to thank the Basic Science Research Program and the Bio and Medical Technology Development Program of the National Research Foundation (NRF) funded by the Korean government (MOE and MSIT); Grant no. 2019M3E5D1A02069623, 2020R1A2B5B02002377, 2020R1A2B5B02002377.

Wnt signalling pathway facilitates nanovibration-stimulated osteogenesis in mesenchymal stem cells

Hussain Jaffery[1*], Penelope M Tsimbouri[1], Paul Campsie[2], Peter J Childs[2], Stuart Reid[2], Manuel Salmeron-Sanchez[1] and Matthew J Dalby[1]

[1]Centre for the Cellular Microenvironment, University of Glasgow, UK
[2]Centre for the Cellular Microenvironment, Strathclyde University, UK
[*]Hussain.Jaffery@glasgow.ac.uk

INTRODUCTION

The global disease burden of musculoskeletal conditions, with 1.71 billion sufferers, is the largest contributor to disability. Mesenchymal stem cells (MSCs), residing in various reservoirs in the body, are multipotent precursors of bone forming osteoblasts. Osteogenic differentiation incorporates various cues, including organismal and cellular responses to biomechanical force. We have developed a nanovibrational bioreactor as a biomechanical cell differentiation technique for MSCs, that functionally drives **efficient and highly targeted osteogenesis** in a preclinical setting; however, the specific molecular mechanism remains undefined[1]. We focus on dissecting the role of the osteogenic Wnt signalling pathway, following nanovibrational stimulus.

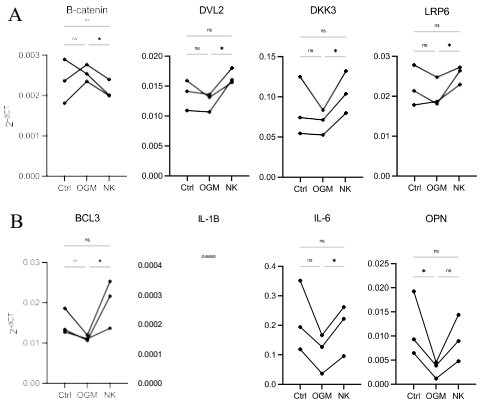

EXPERIMENTAL METHODS

Adipose-derived human mesenchymal stem cells (n = 3) were cultured on standard tissue-culture plastic in 2D monolayers and received either a nanovibrational stimulation with 30 nm vertical displacement at 1000 Hz in basal culture medium ("nano-kicked"; NK), stimulated with the osteogenic metabolites (OGM) L-ascorbic acid, β-glycerophosphate and dexamethasone, or kept in basal culture conditions with no stimulus (Ctrl), for 1 to 7 days. Optionally, Wnt inhibitors LGK974 (10 nM) and XAV939 (5 μM) were supplemented. Gene transcript relative expression was characterised with RT-qPCR. Statistical analysis utilised matched analysis of variance (ANOVA) with Fisher's LSD test for multiple comparisons of means.

RESULTS AND DISCUSSION

Herein, we elucidate that nanovibrational mechanical stimulus induces **non-canonical Wnt signalling pathway** components to be differentially transcriptionally expressed in the early phase of osteogenic differentiation (Figure 1A). Furthermore, differential expression of **pro-inflammatory and osteogenic markers** is observed, characteristic of Wnt pathway crosstalk in osteogenic differentiation (Figure 1B). **Inhibition of Wnt signalling** with small molecules altered the expression of inflammatory, osteogenic and Wnt pathway genes (Figure 2).

CONCLUSION

Nanovibrational biomechanical stimulation involves a specific signature of non-canonical Wnt gene expression in MSCs, causal to their osteogenic differentiation. We posit that nanovibration co-opts the Wnt planar cell polarity pathway and further studies will functionally explore protein activation states and protein localisation. Thus, herein we present a novel approach to preferentially activate osteogenic signalling via a specific Wnt cascade, without chemical or biological stimuli.

Figure 1 | Gene expression of select Wnt-pathway components (A) and inflammatory genes (B) under basal (Ctrl), osteogenic media (OGM) and nanovibration (NK).

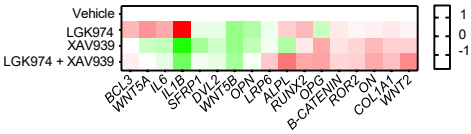

Figure 2 | Effect of Wnt pathway inhibitors on specific gene expression in nanovibrated MSCs, after 24 h.

REFERENCES

1. Tsimbouri, P.M. *et al. Nat Biomed Eng* 1: 758–770, 2017

ACKNOWLEDGMENTS

The authors thank Eva Martino Redondo at Histocell (Bilbao) for providing isolated human mesenchymal stem cells. This study was funded by the European Union's Horizon 2020 research and innovation programme; grant: 874889.

Long term oxidation behavior of PEO-surface modified magnesium screws in a large animal model

Ana Prates Soares[1,2], Alexander Kopp[3], Heilwig Fischer[1], Katharina Schmidt-Bleek[2], Christoph Leber[1], Henri Kreiker[1], Georg Duda[2], Henning Hanken[4], Ole Jung[5], Ralf Smeets[6], Max Heiland[1], Carsten Rendenbach[1]

[1] Department of Oral and Maxillofacial Surgery, Charité – Universitätsmedizin, Berlin, Germany
[2] Julius Wolff Institute and Center for Musculoskeletal Surgery, Charité – Universitätsmedizin, Berlin, Germany
[3] Meotec GmbH, Aachen, Germany
[4] Department of Oral and Maxillofacial Surgery, Semmelweis University Hamburg, Hamburg, Germany
[5] Clinic and Policlinic for Dermatology and Venereology, University Medical Center Rostock, Rostock, Germany
[6] Department of Oral and Maxillofacial Surgery, University Medical Center Hamburg-Eppendorf, Hamburg, Germany

* ana.prates-soares@charite.de

INTRODUCTION

Magnesium (Mg) alloy-based screws are resorbable and biocompatible devices proposed for clinical use in maxillofacial and orthopedic fixation.[1] However, by-products from Mg alloys' oxidation, such as hydrogen gas, can disturb bone formation, when the oxidation rate is faster than their diffusion in bone tissue.[2] Consequently, cavities can be formed surrounding Mg screws. Surface modification by plasma electrolytic oxidation (PEO), an anodic oxidation process, can decrease Mg alloys' oxidation rate both in vitro and in vivo. Furthermore, PEO on titanium alloys has improved the immune and angiogenic responses enhancing osteointegration.[3] Furthermore, besides Mg, ZX00 alloy has Zn and Ca in its composition, ions that have shown respectively anti-inflammatory and mineralization effects.[4] The present work aims to assess and compare the long-term oxidation behavior of ZX00 magnesium-based screws used for craniomaxillofacial and orthopedic applications with or without PEO surface modification (Kermasorb®, Meotec, Aachen, Germany) implanted in the frontal bone of Göttingen miniature pigs.

EXPERIMENTAL METHODS

Eighteen skeletally mature Göttingen miniature minipigs (Ministry for Gesundheit und Verbraucherschutz Hamburg - Approval No. 49/16) were included in the study. Four screws, two of each type, were implanted in every pig in a circle (Fig. 1) with a 20 mm distance between screws. The animals were randomly distributed in three groups (n=6) observed for 6, 12 or 18 months. The template of the screws was used to calculate the remaining percentage of the Mg implanted screws over time (%SV/TV). For bone analysis, a volume of interest (VOIs) surrounding the screws was created by enlarging the 3D screw template by 1.5 mm (TV1.5) in all directions (%BV/TV). A 2D template was created from a central longitudinal slice of a stand-alone ZX00 screw (TA). For bone analysis in histological slices, a region of interest (ROI) surrounding the screws was created by enlarging the 2D screw template by 1.5 mm (%BA/TA), and the percentage of the residual screw in the tissue by %SA/TA. The mean of each parameter was calculated for comparison of ZX00 and ZX00-PEO (6, 12 and 18 months). Separate linear mixed regression models with screw type as a fixed effect and animal included as a random effect to account for the clustering of multiple and different screws implanted in the same animal were run separately in the multilevel mixed-effects generalized linear model (meglm) routine of STATA 15 for each time point and the outcome variable (P-values < 0.05).

RESULTS AND DISCUSSION

There was a decrease in volume (%SV/TV) and area (%SA/TA) of ZX00 screws over time. Non-modified ZX00 screws appeared to oxidate faster than ZX00-PEO screws with a statistical difference in 3D at 12 and 18 months ($p<0.05$), and in 2D at 12 months (<0.05). Bone percentage in the surrounding tissue tended to increase over time around ZX00-PEO screws when evaluated in 3D, there was a statistical difference at 18 months between the non-modified and ZX00-PEO screws ($p<0.05$). The histological Giemsa-stained slices were also used for qualitative assessment of the bone structure. In some areas surrounding the devices, a highly vascularized soft tissue could be observed. There was a significant presence of well-organized lamellar bone closely attached to the devices, especially in the later time point (18 months).

CONCLUSION

PEO surface modification delayed implant corrosion and improved bone formation around Mg screws composed of ZX00 alloy.

REFERENCES

1. Holweg P. *et al*., BJR 9: 477–483, 2020
2. Witte F. Acta Biomater. 23: S28-40, 2015
3. Bai L. *et al*., Biomaterials. 162:154-169, 2018
4. Chen Z. *et al*., Materials Today, 19:304-321, 2016

ACKNOWLEDGMENTS

Alveolar bone defect in rat's maxillary: a new model to study bone regeneration approaches in oral surgery

Naïma Ahmed Omar[1*], Olivier Chassande[1], Laurent Bidault[2], Sylvain Catros[1,3], Joëlle Amédée[1], Didier Letourneur[2,4], Jean-Christophe Fricain[1,3], Mathilde Fenelon[1,3]

[1]BIOTIS U1026, Université de Bordeaux, Bordeaux, France
[2]Siltiss, SA, Zac de la Nau, Saint-Viance, France
[3]Service de Chirurgie Orale, CHU de Bordeaux, Bordeaux, France
[4]LVTS U1148, Université Sorbonne Paris Nord, Hôpital X Bichat, Université de Paris, Paris, France

[*] naima.ahmed-omar@u-bordeaux.fr

INTRODUCTION

To repair damaged bone after a trauma, a malformation or a cancer, the "gold standard" technique remains autologous bone grafting in oral surgery[1]. The morbidity at the harvesting site and the limited amount of material available are the main limitations of autografts leading clinicians to use appropriate materials like bone substitutes. Before any clinical application, suitable animal models are needed to test these innovative biomaterials and evaluate their biocompatibility and their osteogenic properties[2]. To date, there are no relevant pre-clinical models in small mammals that test bone substitutes for oral surgery applications. The following study aimed to develop a new model of alveolar defect performed on rat maxillary and to determine its critical size.

EXPERIMENTAL METHODS

Surgical procedure

Experiments were conducted on 12 male Sprague-Dawley rats in accordance with the standards of care and housing of laboratory animals in an accredited facility at the University of Bordeaux (accreditation number A33-063-917). To determine the critical size of this circular defect, three different diameters were tested (2.8 mm; 3.3 mm; 4.5 mm diameter, n=8/condition). Animals were anesthetized with a mixture of analgesic and anesthetics (ketamine/xylazine). A crestal incision was made in distal to the incisors allowing access to the alveolar bone. A circular defect was performed in the maxillary using a trepan under irrigation. The gingiva was then replaced and sutured.

Radiographical and histological analysis

Longitudinal *in vivo* evaluation of bone regeneration was performed using micro-computed tomography (µCT) over 12 weeks. Histological analysis by Masson's trichrome staining was conducted on rat's maxillary at the end of the experiment.

Statistical analysis

GraphPad Prism Software (La Jolla/CA) was used for µCT analysis. A nonparametric "Two-way Anova analysis of variance" followed by a Tukey's multiple comparison test was applied to compare all possible pairs of means independently, differences were considered significant when $p < .05$ (*).

RESULTS AND DISCUSSION

Three types of defect were tested in this study to determine the critical size defect. Qualitative analysis of 3D µCT reconstruction revealed that, whether the defect size, depending on the position of the lesion in the maxillary, defect tended to resorb. Radiological analyses showed that 2.8 mm in diameter critical defect was the most reproducible. Two different methods for µCT images were applied to measure bone volume fraction (BVF) of the defects (e.g. axial and sagittal plans). BVF quantification showed that 12 weeks after surgery, no defect reached 50% of regeneration, meaning that defect of 2.8mm diameter and larger were of critical size. The sagittal plan method was the most accurate way to determine BVF. These results were consistent with histological findings.

CONCLUSION

We develop a new critical-size defect of 2.8 mm in rat alveolar bone that is reproducible and easy to perform. This bone defect model seems promising for the evaluation of new biomaterials for bone regeneration in oral surgery.

REFERENCES

References must be numbered. Keep the same style.
1. Dimitriou R. *et al.*, BMC Med, 9:66, 2011
2. McGovern JA. Et al., Dis Model Mech, 11:dmm033084, 2018

ACKNOWLEDGMENTS

The authors would like to thank the "Agence Nationale de la Recherche" and Siltiss for providing financial support to this project. Thanks to Dr Richard Walton from LIRYC (IHU) for the use of micro-scanner device.

Recent advances of pullulan and/or dextran-based materials for bone tissue engineering strategies in preclinical studies: a systematic review

Naïma Ahmed Omar[1*], Robin Siadous[1], Joëlle Amédée[1], Laurent Bidault[2], Didier Letourneur[2,4], Jean-Christophe Fricain[1,3], Mathilde Fenelon[1,3]

[1]BIOTIS U1026, Université de Bordeaux, Bordeaux, France
[2]Siltiss, SA, Zac de la Nau, Saint-Viance, France
[3]Service de Chirurgie Orale, CHU de Bordeaux, Bordeaux, France
[4]LVTS U1148, Université Sorbonne Paris Nord, Hôpital X Bichat, Université de Paris, Paris, France

[*] naima.ahmed-omar@u-bordeaux.fr

INTRODUCTION

Improving bone regeneration after traumatic injuries, pathologies or tumours resection remains a surgical challenge. To date, autologous bone graft is considered as the gold standard[1]. However, due to the inherent limitations of this technique (limited availability, donor site injury and morbidity), there is a growing interest in the development of new materials for bone regeneration since these last decades. Dextran and pullulan are both natural hydrophilic polysaccharides. As they display unique biological and physico-chemical properties, dextran and pullulan-based biomaterials became highly attractive and promising alternative biomaterials for bone tissue engineering. This systematic review aimed to identify and sum up in preclinical studies the different strategies of pullulan and/or dextran-based substitutes used for bone tissue engineering.

EXPERIMENTAL METHODS

An electronic search in Pubmed, Scopus and Web of Science databases was conducted and the selection of articles was performed following PRISMA guidelines[2]. Included articles were considered if the studies in which pullulan and/or dextran-based biomaterials were used to promote bone regeneration in animal models.

RESULTS AND DISCUSSION

Among the 28 studies included, 16 focused on dextran-based materials for bone regeneration, six used pullulan substitutes and six reported the use of a combination of pullulan and dextran. Several strategies have been employed to further enhance their potential for bone regeneration, mainly through their fabrication processes or the addition of various elements to these scaffolds. Different types of applications were thus reported in the included studies: pullulan and/or dextran-based biomaterials were used either as potential cell and/or growths factors carrier system, as bone filling substitutes or as a membrane for guided bone regeneration. Four routes of administration of these biomaterials in implantation sites were also identified. Finally, the diverse fabrication processes of pullulan and/or dextran-based materials (functionalization methods, reticulation process) and their application usages to promote bone regeneration were discussed.

CONCLUSION

Conception of these bone substitutes as injectable hydrogels could facilitate their use for clinical applications. They could ideally replace commercial devices through their natural origin.

REFERENCES

1. Dimitriou R. *et al.*, BMC Med, 9:66, 2011
2. Moher D. *et al.*, Syst Rev, 4:1, 2015

ACKNOWLEDGMENTS

The authors would like to thank the “Agence Nationale de la Recherche” and Siltiss for providing financial support to this project.

The Green Synthesis of Carbon Quantum Dots and Their Application for Glioblastoma Multiforme Cancer therapy

Liam Desmond[1], Anh Phan[2] , Piergiorgio Gentile[3]
[1]School of Engineering Merz Court, Newcastle University, Newcastle upon Tyne, England
[2] School of Engineering Merz Court, Newcastle University, Newcastle upon Tyne, England
[3]School of Engineering Merz Court, Newcastle University, Newcastle upon Tyne, England
* l.desmond@ncl.ac.uk

INTRODUCTION

The global burden of cancer continues to propagate due to an increasing adoption of cancer-causing behaviours such as smoking, food and drink choices and general unhealthy lifestyle. Glioblastoma Multiforme (GBM) is the most common, aggressive and fatal primary brain tumour. According to the World Health Organization (WHO), GBM comprises 15% of all intracranial neoplasms and 60-75% of astrocytic tumours[1]. Despite maximum treatment, patients only have a median survival time of 15 months, because of the tumour's resistance to current therapeutic approaches[2] and disease recurs in almost all patients. Diagnosis of progression is complex given the possibility of pseudo progression. Currently, the standard approach in managing GBM includes consideration of maximum surgical resection, due to the fact that the entire tumour cannot be removed, because GBM infiltrates surrounding tissue radiation therapy (RT) and current treatments present clear drawbacks such as radiotherapy only offers palliation[3]. Treating GBM is also quite a challenge for several reasons such as: (1) The tumour cells are very resistant to conventional therapies; (2) The brain is susceptible to damage from conventional therapy and has a very limited capacity to repair itself; and (3) Many drugs cannot cross the blood–brain barrier (BBB) to act on the tumour and/or have unacceptable systemic toxicities[4].

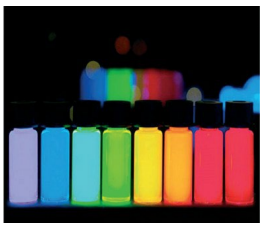

Figure 1: The different colours that QDs give rise to according to the energy and fluorescence properties

EXPERIMENTAL METHODS

Current cancer therapeutic systems can help to confront and overcome many different strands of tumours for clinical patients. Despite the benefits, these current therapeutic systems present clear setbacks, such as their toxicity and damaging effects to human body cells and the host. The need for easy-to-fabricate, safe and non-toxic therapeutic systems has driven the research field towards the use of Carbon Quantum Dots (CQDs). Their bioimaging with green, non-toxic, biocompatible and attractive quantum properties (Figure 1) present distinctively advantageous over conventional/metal-based quantum dots. In this presentation, the current progress in the development of Quantum Dots, focusing on CQDs for the use in nanotheranostics for different tumours will be critically analysed. Advantages of applying CQDs by green bottom-up approaches into nanotherapy systems will be highlighted. The green synthesis of CQDs is obtained by the use of biomass wastes such as walnut shells, orange peel, chitin and coffee grounds as the precursors for the reaction route. This has ensured the process as a promising, cheaper and safer alternative to previously used routes.
Discussion of the ongoing challenges and opportunities associated with a green and sustainable synthesis of CQDs with specific functional groups, so that the next stages in the development of the nanotherapy system to target GBM tumours can commence (Figure 2).

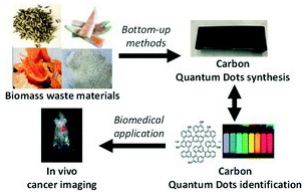

Figure 2: Reaction route of my PhD to develop an overall nanotherapy system

REFERENCES

[1] R. M. Young, A. Jamshidi, G. Davis, J. H. Sherman, Ann Transl Med, 2015, 3 (9), 121-121. DOI: 10.3978/j.issn.2305-5839.2015.05.10
[2] F. E. Bleeker, R. J. Molenaar, S. Leenstra, J Neurooncol, 2012, 108 (1), 11-27. DOI: 10.1007/s11060-011- 0793-0
[3] J. P. Sheehan, M. E. Shaffrey, B. Gupta, J. Larner, J. N. Rich, D. M. Park, Future oncology (London, England), 2010, 6 (10), 1591-601. DOI: 10.2217/fon.10.123
[4] H. C. Lawson, P. Sampath, E. Bohan, M. C. Park, N. Hussain, A. Olivi, J. Weingart, L. Kleinberg, H. Brem, J Neurooncol, journal article, 2007, 83 (1), 61-70. DOI: 10.1007/s11060-006-9303-1

ACKNOWLEDGMENTS

"The authors would like to thank the Engineering and Physical Sciences Research Council for providing financial support to this project".

Modulation of ECM-derived hydrogels rheological properties by using graphene oxide

A. T. Pereira[1,2], Inês P. Fernandes[1,2], Sabrina Rohringer[3,4], Herbert Kiss[5], C. Barrias[1,2], F. Magalhães[6], H. Bergmeister[3,4], K. H. Schneider[3,4], I. C. Gonçalves[1]

[1]INEB/i3S - Instituto de Engenharia Biomédica, Portugal; [2]ICBAS – Instituto de Ciências Biomédicas Abel Salazar, Portugal; [3]Center for Biomedical Research Medical University of Vienna, Austria; [4]Ludwig Boltzmann Institute of Cardiovascular Research, Vienna, Austria;

[5]Department of Obstetrics and Gynecology, Division of Obstetrics and Feto-Maternal Medicine, Medical University of Vienna, 1090 Vienna, Austria

[6]LEPABE - Laboratório de Engenharia de Processos, Ambiente, Biotecnologia e Energia, Faculdade de Engenharia, Universidade Do Porto, Rua Dr. Roberto Frias, 4200-465, Porto, Portugal

*andreia.pereira@i3s.up.pt

INTRODUCTION

Hydrogels derived from extracellular matrices (ECM-gels) have been described to have promising features to promote tissue regeneration, since they preserve several components of native tissues. However, their weak mechanical properties impair the use of ECM-gels in load-bearing applications. We have previously shown that the incorporation of oxidized forms of graphene, one of the strongest materials in the world, in decellularized arteries, improves their mechanical and biological properties [1]. Herein, we propose the incorporation of graphene-based materials (GBMs) in ECM-gels to surpass their weak mechanical properties, allowing their future use custom designed self-standing scaffolds for different load-bearing tissue engineering applications.

EXPERIMENTAL METHODS

GBMs with different exfoliation and oxidation degree and lateral size were used, namely graphene nanoplatelets (GNP M5), oxidized GNP (GNP M5ox) and graphene oxide (GO). or produced by modified Hummers' method (GO and GNP M5ox) and characterized by XPS, TEM, XRD, and DLS [2]. Human placenta chorion was isolated and decellularized by a freeze-thawing cycle, followed by an osmotic shock and treatments with triton and DNAse. Materials were sterilized and ECM pre-gels were obtained by digesting decellularized tissues with pepsin. Different amounts of GBMs (1-4% w/v) powders (freeze-dried) or aqueous dispersions were incorporated in ECM pre-gels before or after digestion, and with or without sonication (ECM/GBMs pre-gels). Pre-gels were put into a mold and left overnight at 37 ºC to promote their gelation. Surface topography of ECM/GBMs-gels was evaluated by SEM, and rheological properties of pre-gels were assessed using frequency, strain and time sweep tests while in ECM gels single frequency strain-controlled tests, with a 1% strain, 1 Hz frequency and 5 min testing time at 37 ºC were performed. ECM/GBMs gels were incubated with *Staphylococcus aureus* being visualized the adhered bacteria by SEM.

RESULTS AND DISCUSSION

The lateral size of GBMs ranged from 1.5 to 5 µm, being GO the smallest material. Regarding the thickness, GO exhibited mostly as single layer, while GNP M5 and GNP M5ox as multi-layered materials. Oxidized forms of GBMs showed a similar oxidation degree between them of about 34% while non-oxidized GBMs have low oxygen content (3%). In ECM gels, GBMs oxidized forms dispersed better than non-oxidized. Since GO is the thinnest and smallest GBM material tested in this work, (being described to have a better biocompatibility and capacity to be degraded), GO was the selected GBM to pursue the work [1]. In ECM/GO gels, SEM images showed that the GO can intercalate the collagen fibers. Regarding the rheological properties, a higher increase in complex modulus was observed when GO was incorporated in ECM as a dispersion, after digestion, and without sonication. These improved results with ECM dispersions could be explained by the inability of GO to re-disperse in ECM upon the freeze-drying step. ECM complex modulus increased exponentially with the amount of GO. For the highest tested concentration, GO dispersion (4% v/v), a remarkable increase of 217 fold in complex modulus was observed becoming the ECM gel stiffer. Even though GO has been described as antimicrobial and/or being able to decrease bacterial adhesion, our results showed that the number of adherent bacteria is similar in ECM and ECM/GO. This may be explained due to the lack of GO exposure on the surface, as previously observed for PU/GBMs composites [3]. Incorporation of GO in ECM decreased the clotting time of recalcified Human plasma, suggesting that the GO can turn ECM-gels more pro-coagulant.

CONCLUSION

Overall, GO showed capacity to tune the rheological properties of ECM gels, namely by increasing their complex modulus, which is a step forward to enable ECM gels in load-bearing applications. Moreover, GO increases the pro-coagulative properties of ECM, suggesting their potential application as hemostatic materials, namely for wound healing.

ACKNOWLEDGMENTS

This work was financially supported by FCT/FEDER: PD/BD/114156/2016 and PTDC/CTM-COM/32431/2017.

REFERENCES

1. A.T. Pereira, *et al.*, ACS Applied Materials & Interfaces, 13 (2021)
2. A.T. Pereira *et al.*, Biomaterials Science (2021)
3. I. Borges *et al.*,, Nanomaterials (Basel), 10 (2020)

Titanium nitride thin layer obtained by Atomic Layer Deposition – Potential application for orthopedic implants

Marcin Basiaga[1*], Janusz Szewczenko[1], Witold Walke[1], Zbigniew Paszenda[1]

[1]Silesian University of Technology
Faculty of Biomedical Engineering
Department of Biomaterials and Medical Devices Engineering
Zabrze, Poland
[*] marcin.basiaga@polsl.pl

INTRODUCTION

Different methods of implant's surface treatment, such us: electrochemical polishing, chemical passivation, anodization, sol-gel deposition, let scientists combine advantages of metallic structures of implants with biocompatibility required in medical applications [1, 2]. So far, completely satisfactory results in this field of study have not been reached. In this respect, a continuous search for the best solutions relating to the methodology, the chemical composition and physicochemical properties of the layers produced is being carried out. One of the most important aspects in relation to miniaturized implants is too ensure the consistency of the geometrical characteristics over their entire length, which can`t be provided by these modifications. In this context the most proper method of layer deposition would be the ALD method. Therefore, the goal of completed research was to evaluate the physicochemical TiN layers deposited on Ti13Zr13Nb steel using ALD method.

EXPERIMENTAL METHODS

During the evaluation of the physicochemical properties of deposited layers the chemical and phase composition study, surface morphology study, corrosion resistance test and mechanical properties testing were conducted. First, potentiodynamic and potentiostatic measurements were taken, which enabled pitting and crevice corrosion resistance to be assessed. Secondly, impedance measurements were performed to enable interpretation of the processes and phenomena occurring at the TiN layer – electrolyte (synthetic plasma) interface. These tests provided information concerning the structural characteristics of the layers, possible defects, lack of sealing, substrate reactivity and the presence of barrier properties involving the electrolyte. Complementary examination of surface topography using an atomic force microscope (AFM) were also performed, as well as examinations with a scanning electron microscope (SEM). In order to assess the mechanical properties of layers generated using this method, the hardness tests and tests of these layers adhesion to the metal base were performed. The Oliver Pharr method was used to measure the instrumental hardness, while the scratch test was performed to study the layers adhesion to the surface. The measure of the strength of layer adhesion to the base is a critical force, i.e. minimum normal force that causes the loss of adhesion to the surface. Both hardness and scratch strength measurements were performed using open platform equipped with CSM Microcombi Tester.

RESULTS AND DISCUSSION

The obtained data showed different physicochemical properties of under different parameters in case of temperature and number of cycle in ALD process. The application of compact TiN coating by the ALD method under the conditions proposed in this paper ensures its diffusion character, which has the effect of improving its adhesion to Ti13Zr13Nb alloy. The TiN coating deposited at 2000 cycles of the deposition process at 150°C offers the most beneficial physicochemical properties. These results directly assist the optimisation of the TiN layer creation process using ALD-based methods on surfaces of Ti13Zr13Nb alloy implants intended for orthopedic implants, thus improving their functional properties.

CONCLUSION

The proposed scope of the study enabled a comprehensive analysis of the effect of the structure and physicochemical properties of the surface layers on the processes taking place on the surface of implants following their placement in the bone system. The obtained results provide the basis for the development of more detailed criteria for the final assessment of the quality of medical devices used in the bone system, which will ensure the required antibacterial properties of implants and minimise the risk of postoperative complications. As a result, it will help to increase the effectiveness of therapy, reduce complication rates, and improve the quality of patients' lives.

REFERENCES

1. Walke W, et al., EIS study of SiO_2 oxide film on 316L stainless steel for cardiac implants. Advances in Intelligent Systems and Computing 284. Springer 2014, 403-410
2. Lee B. G., et al., Electropolishing for the formation of anodic nanotubular TiO_2 with uniform length. Appl. Surf. Sci. 257, 2011,7190-7199.

Manufacturing of bio-degradable metallic orthopedic implants by powder metallurgy

Julien Moreau[1*], Xavier Boulnat[1], Michel Perez[1], Benoit Ter-ovanessian[1], Olivier Dezellus[2], Laurent Gremillard[1]

[1]Mateis UMR5510, Insa, Lyon, France
[2]LMI UMR 5615, Université Claude Bernard, Lyon, France

*julien.moreau@insa-lyon.fr

INTRODUCTION

Additive manufacturing (AM) processes allow for the personalisation of orthopaedic implants in order to optimize the geometry of the medical device for each patient. However, permanent implants are not always suitable since, in many cases, the implant is no more needed once the fracture is repaired. As such, degradable implants would allow a temporary repair function and will degrade after few months. There are several metallic systems targeted for degradable implants, mainly iron, magnesium or zinc alloys. But additive manufacturing of such alloys, specially magnesium has not been extensively studied. The sintering process of magnesium is the main challenge to overcome as magnesium is one of the most reactive metal for oxidation issue.

EXPERIMENTAL METHODS

Sintering assisted with pressure using Spark Plasma Sintering (SPS) is used to determine the structural properties of the materials (hardness, density, porosity, …), the corrosion behavior according to the structure in different media (corrosion resistance, nature of the precipitates, speed of corrosion, …) and finally the mechanical properties (compression and traction resistance). Heat treatment are performed on the alloy (solution heat treatment (500°C) and precipitation hardening (170°C and 200°C). Post-mortem characterizations (SEM, EDX, EBSD, XRD, …) have been carried out on different set of samples sintered pressureless or by SPS, including Mg and ZK30 with or without heat treatment for comparison.

RESULTS AND DISCUSSION

Using SPS with different parameters (Temperature and pressure), samples with different structural properties were sintered. The corrosion resistance of this samples is studied to optimize the properties of the alloy and design the more resistant sample.
Zirconium and Zinc are supposed to enhance the corrosion resistance of Magnesium which is very low. That's why heat treatment of ZK30 are studied with first a solution heat treatment and then a precipitation hardening to study the evolution of the corrosion resistance and the mechanical properties

CONCLUSION

The study of ZK30 sintered with SPS allows to correlate the different structural properties to the corrosion resistance. The optimization of the alloy with dense parts will be useful to obtain performing biodegradable implants once the sintering of 3D printed part will be possible.

New chapter of Ti13Nb13Zr as biomaterial with using in skeletal system

Julia Lisoń[1], Magdalena Antonowicz[1], Zbigniew Paszenda[1], Witold Walke[1*], Marcin Basiaga,

[1]Silesian University of Technology
Faculty of Biomedical Engineering
Department of Biomaterials and Medical Devices Engineering
Zabrze, Poland
[*] witold.walke@polsl.pl

INTRODUCTION

The problem of microorganisms themselves is quite common, and the pathway of penetration of bacteria is varied. The formation of individual bacteria does not cause dangerous effects, but the biofilm as a cluster does. Bacteria can exist as planktonic like a collection of dispersed bacterial cells or as a biofilm, a three-dimensional, organized structure containing bacteria surrounded by a matrix made mainly of sugar and protein polymers[1]. The formation of bacterial biofilm is closely related to the colonization of microorganisms in the implant area. The presence of biofilm can lead to the disappearance of the surrounding bone tissue and, as a result, disrupt the process of osteointegration[2]. Currently, the fight against bacterial infections is carried out using antibiotics, but due to many problems related to the way the drug is administered and its effective action, new methods of administering drugs to the patient are still being sought [3,4]. This creates a need for the development of new strategies to combat biofilm-related infections, e.g. modification of biomaterials in order to increase their resistance to microbial adhesion [5].

EXPERIMENTAL METHODS

The aim of the study was to assess the impact of the physicochemical and mechanical properties of the modified Ti13Nb13Zr alloy. The samples were then divided into groups according to the surface preparation as follows: polishing and sandblasting. The use of different surface treatment methods resulted in obtaining different roughness values. Then, on these samples, a layer of tin oxide was applied using the Atomic Layer Deposition method, obtaining further variants. In order to assess to suitability of the surface modification method proposed in this way, the authors proposed a series of tests. As part of the assessment of the physicochemical properties of the surface layers formed, pitting corrosion resistance tests were carried out and tests using electrochemical impedance spectroscopy (EIS). In the research surface wettability tests, scratch test and tribological tests were also completed, which showed the differences resulting from temperature changes and the number of cycles and their impact on individual parameters tested.

RESULTS AND DISCUSSION

The obtained data showed different physicochemical properties of antibacterial films generated under different parameters in case of temperature and number of cycle in ALD process. These results directly assist the optimisation of the TiO_2 layer creation process using ALD-based methods on surfaces of Ti13Nb13Zr alloy implants intended for skeletal system, thus improving their functional properties. The results have obtained can be used as a base to develop more detailed criteria of final quality of medical devices which will ensure the required biocompatibility of implants. It has contributed the risk mineralization of postoperative complications. As a result it has increased effectiveness, decreased the indicator of complications and improved life of the patients.

CONCLUSION

Based on the obtained data, different physicochemical properties of the alloy with tin dioxide coatings depending on the number of cycles used and the temperature of the manufacturing process were found. The knowledge obtained on this basis is of practical importance for the application of this type of surface modification for various types of miniaturized implants that are used in the skeletal system.

REFERENCES

1. Gallo J, Holinka M, Moucha CS. Antibacterial surface treatment for orthopaedic implants, 15, 2014.
2. Khatoon Z, McTiernan CD, Suuronen EJ, Mah TF, Alarcon EI. Bacterial biofilm formation on implantable devices and approaches to its treatment and prevention, Heliyon, 4,12.
3. Ribeiro M, Monteiro FJ, Ferraz MP. Infection of orthopedic implants with emphasis on bacterial adhesion process and techniques used in studying bacterial-material interactions. Biomatter 2,4,176-194.
4. Qiu ZY, Chen C, Wang XM, Lee IS. Advances in the surface modification techniques of bone-related implants for last 10 years, Regen Biomater, 1,1, 67–79.
5. Martin PM.: Handbook of Deposition Technologies for Films and Coatings, Third Edition: Science, Applications and Technology. Amsterdam, Boston, Heidelberg, London: 2010.

Biodegradation behavior of a newly designed Mg alloy with highly enhanced corrosion resistance

Du-Won Min[1], Soo-Min Baek[1], Jeong-Ki Kim[1], Jung Gu Lee[2], Sung Soo Park[1*]

[1]Department of Materials Science and Engineering, Ulsan National Institute of Science and Technology, Ulsan, Republic of Korea
[2]School of Materials Science and Engineering, University of Ulsan, Ulsan, Republic of Korea
* sspark@unist.ac.kr

INTRODUCTION

Non-biodegradable implants, typically based on stainless steels or Ti alloys, have an issue that they can cause various side effects after implantation in the human body. In the case of a cardiovascular stent, the foreign body reaction between the permanent stent material and its surrounding tissue has been known to cause restenosis and thrombosis. Of various metallic elements, corrodible Mg is considered one of the feasible biodegradable materials since it can be easily excreted in the urine after degradation in the body. However, commercially available Mg and its alloys generally suffer from more rapid and localized degradation than other biodegradable materials in an aqueous environment containing salts like seawater or blood, resulting in their premature decay after implantation. Furthermore, H_2 gas bubbles generating during rapid degradation of Mg can cause inflammation by creating cavities on the tissue.

Here, as an alternative to the conventionally available Mg-based materials, the authors suggest a new type of Mg alloy with highly enhanced corrosion resistance, giving expectations to exclude the active biodegradation after its implantation. In this study, the in vitro and in vivo biodegradation behavior of the experimental and commercial Mg alloy samples was comparatively investigated to see the possibility of the new material in future biodegradable implant applications.

EXPERIMENTAL

The experimental alloy is a new type of AZ31 alloy, which is dually microalloyed with rare-earth elements. Alloys were prepared by induction melting with purging of a CO_2 and SF_6 mixture. Molten metal was held at 750 °C for 15 min and then it was poured into a steel mold pre-heated to 200 °C for casting. The dimensions of a cast sample are 12 mm in thickness, 50 mm in width, and 100 mm in height. To prepare thin sheets for in vitro and in vivo degradation tests, the rectangular cast samples were heat-treated at 420 °C for 1 h, followed by water quenching. The samples were then subjected to hot-rolling at 350 °C for sheet making. Rolling process was repeated until the final thickness arrives at 1.1 mm. The ratio of thickness reduction per each pass was 20 %. The hot-rolled sheets were then annealed at 345 °C for 1 h.

Samples for microstructural investigations were prepared by mechanical grinding and surface polishing. Mechanical grinding was carried out in a water atmosphere with SiC papers up to 1,200 grit surface polishing was done in an ethanol atmosphere with 1.0 μm diamond paste and 0.04 μm colloidal silica solution. Microstructural investigations were performed with a Keyence VHX-6000 optical microscope and an FEI Quanta 200 field-emission scanning electron microscope, an EDAX Apollo X energy dispersive spectrometer, and a Tecnai 2G F20 X-Twin transmission electron microscope. Samples for the TEM analysis were prepared with Quanta 3D FEG focused ion beam equipment.

In vitro tests were conducted by immersion of samples (10×10×1 mm^3) in deaerated Hanks' Balanced Salt Solution (HBSS) at 37 °C for 14 days. The plate-type samples were prepared by mechanical polishing using SiC papers up to 1200 grit in an ethanol atmosphere. To measure weight loss after immersion in HBSS, surficial products were carefully cleaned at 25 °C using a solution consisting of 200 g l^{-1} CrO_3, 10 g $l^{-1}AgNO_3$, and 20 g l^{-1} $Ba(NO_3)_2$. A Gamry Reference 600 potentiostat was used for potentiodynamic polarization tests in HBSS at 37 °C. A conventional three-electrode cell composed of a working electrode, a saturated calomel reference electrode, and a Pt plate counter electrode was used. An exposed area of a sample was 1 cm^2. The polarization tests were conducted with a potential sweep rate of 1 mV s^{-1}.

For in vivo tests, C57BL/6 (Male, 10-week-old) mice were supplied from the Koatech, Korea. These studies were approved by the Animal Care Committee of the University of Ulsan. The mice were anesthetized by intramuscular injection. An incision of the skin on the side of the leg was made to expose the femoral vein. The leg side of the femoral vein was tied to block blood flow while the implantation was in progress. Wire was implanted after the outer wall of the blood vessel was scratched. The incised skin was sutured, and the mice were left on the heating pad during the anesthesia. The wire was prepared to have a diameter of 0.3~0.5 mm and a length of 10 mm, regardless of alloy compositions. The weight and health conditions of each mouse were checked every week after implantation and there was no abrupt weight change or visible side effect during 12 weeks. The mice were euthanized after 12 weeks and then the implanted wires were retrieved.

Understanding the corrosion of Mg alloys in urinary tract environment: towards the development of a biodegradable metallic ureteral stent

Margarida Pacheco[1,2], Ivo M. Aroso[1,2], Sviatlana V. Lamaka[3], Di Mei[3], Mikhail Zheludkevich[3], Jan Bohlen[4], Maria Nienaber[4], Dietmar Letzig[4], Estêvão Lima[5], Alexandre A. Barros[1,2], Rui L. Reis[1,2]

[1]3B's Research Group—Research Institute on Biomaterials, Biodegradables and Biomimetics, University of Minho, Guimarães, Portugal. [2]ICVS/3B's-PT Government Associate Laboratory, Braga/Guimarães, Portugal. [3]Institute of Surface Science, Helmholtz-Zentrum hereon GmbH, Germany. [4]Institute for Material and Process Design, Helmholtz-Zentrum hereon GmbH, Germany [5]School of Health Sciences, Life and Health Sciences Research Institute (ICVS), University of Minho, Braga, Portugal
* margarida.pacheco@i3bs.uminho.pt

INTRODUCTION

Ureteral stenting is of the most performed procedures in urology, however, despite the indispensable role, ureteral stents have severe associated side effects. Several strategies have been proposed and one of the most recent and attractive is the utilization of biodegradable materials. Various studies have been proving the suitability of biodegradable metals for biomedical applications, including for urological devices[1,2]. In this sense, this work focus on the characterization of the corrosion and encrustation propensity of pure Mg and 4 Mg alloys in urinary tract conditions *in vitro*, in order to expand the knowledge on this research area and open doors for its future application as biodegradable metallic ureteral stents (BMUS) materials.

EXPERIMENTAL METHODS

AZ31, Mg1Zn, Mg1Y, pure Mg and Mg4Ag wires with 0.98-1.09 mm diameter were produced by direct extrusion at 350 ºC with 0.2mm/s speed. Degradation studies were carried out using artificial urine (AU) – ASTM Standard F 1828 – 97-, under static and dynamic conditions. SEM-EDS, ICP-OES, XPS, Raman spectroscopy, profilometry and weight lost measurements were performed.

RESULTS AND DISCUSSION

The presence of $Mg(OH)_2$ and MgO was detected by XPS analysis and the existence of phosphate minerals, such as struvite, was identified by Raman spectroscopy. These findings indicate that the corrosion layer is composed of a mixture of both Mg corrosion products and precipitation of AU components. The formation of stratified layers of corrosion products on Mg alloys is typically observed upon contact with SBF or AUS solutions owing to fast cathodic reactions, namely hydrogen evolution or oxygen reduction, both generating alkalinity. The inner layer, at the interface of Mg substrate is constituted by $Mg(OH)_2$, while the outer layer contains phosphates and other ionic components of immersion electrolyte[2]. The phosphate crystalscan be problematic since they are characteristic of encrustation. Therefore, additional surface treatments are being considered as measures to reduce precipitation and attachment of AUS components at the sample surface.

Weight loss data indicated that the dynamic electrolyte conditions accelerate the corrosion. Mg4Ag showed to be the most affected alloy by corrosion. Some samples presented signs of non-homogeneous corrosion, characterized by the presence of heavy localized corrosion. Mg1Y was the one with a more homogeneous degradation, thus, being promissory since homogeneous degradation is a key feature for ureteral biodegradable devices. The improvement of the corrosion characteristics of the other 4 samples will be done through processing parameter optimization.

CONCLUSION

The results obtained herein allowed us to identify the problems that are holding back the implementation of Mg alloys as ureteral stents – non-homogeneous corrosion and propensity for encrustation – opening paths for effective optimizations towards the development of a BMUS. Besides it was possible to select the metal with one of the most important characteristics – homogeneity – and, thus, with higher suitability for urology applications.

REFERENCES

1. Zhang S, Bi Y, Li J, Wang Z, Yan J, Song J, et al. Biodegradation behavior of magnesium and ZK60 alloy in artificial urine and rat models. Bioact Mater. 2017;2(2):53–62.
2. Mei D, Wang C, Nienaber M, Pacheco M, Barros A, Neves S, et al. Corrosion behavior of Mg wires for ureteral stent in artificial urine solution. Corros Sci . 2021 Aug;189:109567.

ACKNOWLEDGMENTS

The authors are grateful for the financial support from FCT, through a PhD Scholarship SFRH/BD/145285/2019, and the project NORTE-01-0247-FEDER-047112

3D-printed porous cochlear implants

A.Isaakidou[1*], I. Apachitei[1], L.E. Fratila-Apachitei[1], Amir A. Zadpoor[1]

[1]Department of Biomechanical Engineering, Faculty of Mechanical, Maritime, and Materials Engineering, Delft University of Technology (TU Delft), Delft, The Netherlands
[*] a.isaakidou@tudelft.nl

INTRODUCTION

Drug administration is the cornerstone treatment for a variety of pathologies, with systemic administration being the most used method worldwide.[1] However, drug bioavailability in the tissue of interest often does not reach therapeutic levels. Organs that possess a blood-barrier (e.g., cochlea) notably suffer from this phenomenon.[2] To that end, there is a constant interest in the fabrication of novel systems and drug formulations specifically oriented to enhance bioavailability in such tissues. Researchers and pharmaceutical companies aim to do so using sophisticated systems for controlled, localized drug delivery. Recent advances in the field of additive manufacturing enable the fabrication of complex geometries that can be combined with a wide range of active pharmaceutical ingredients. Here, we take advantage of a high-resolution additive manufacturing method to fabricate cochlear implants with internal microscale porosity at anatomically relevant sizes. Moreover, we test macrophage viability levels on the 3D printed material. Lastly, we investigate the suitability of the proposed designs regarding drug loading.

MATERIALS AND METHODS

We fabricated cochlear implants and also specimens for cell culture experiments using the two-photon polymerization (2pp) method. The 3D printer used was the Photonic Professional GT2 (Nanoscribe GmbH) in combination with the proprietary acrylate-based photocurable resin IP-Q. A dexamethasone suspension was used to load the porous cochlear implants. The viability of macrophages was investigated using a live/dead assay after 48 hrs of culture on flat 3D printed pedestals.

RESULTS AND DISCUSSION

We printed porous cochlear implants of 0.6x0.6x2.4 mm^3 with internal square lattice pores of 60 µm and also pedestals of 2x2x0.5 mm^3 for cytotoxicity tests (Figure 1a). We assessed macrophage viability on the later via fluorescent microscopy (Figure 1b). The cell viability test showed no cytotoxicity of the 2pp resin for macrophages, validating the suitability of the method and the material for further drug incorporation and release, both *in vitro* and *in vivo*. Using an organic suspension of dexamethasone we additionally proved the feasibility of drug loading the pores of the 3D printed cochlear implants (Figure 1c).

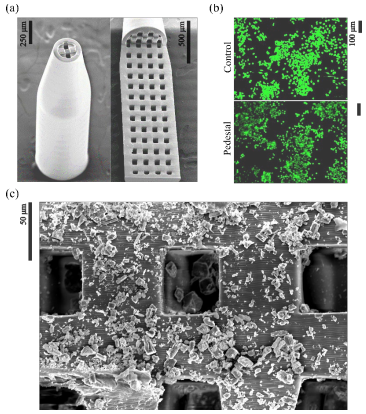

Figure 1: (a) 3D printed porous cochlear implants, (b) viability of macrophages on control well plate and on 3D printed pedestals, (c) dexamethasone crystals in the pores of the cochlear implants.

CONCLUSION

The results of this study demonstrate that the 2pp process constitutes a feasible fabrication method for a new generation of cochlear implants in anatomically applicable sizes with appropriate porosity and acceptable cytocompatible properties for drug delivery applications in the inner ear.

REFERENCES

1. Ruiz M.E. *et al.*, Routes of Drug Administration, ADME Processes in Pharmaceutical Sciences, Springer, Cham, 2018
2. Gehrke M. *et al.*, International Journal of Pharmaceutics, 509(1-2):85-94, 2016
3. Melnyk L.A *et al.*, Annals of 3D Printed Medicine, 4:100035, 2021

ACKNOWLEDGMENTS

"This project has received funding from the Interreg 2 Seas programme 2014-2020 co-funded by the European Regional Development Fund under subsidy contract "Site Drug 2S07-033."

3D-printed aerogel scaffolds for personalized bone tissue engineering

Iglesias-Mejuto Ana, García-González Carlos Alberto

Department of Pharmacology, Pharmacy and Pharmaceutical Technology, I+D Farma group (GI- 1645), Faculty of Pharmacy, iMATUS and Health Research Institute of Santiago de Compostela (IDIS), Universidade de Santiago de Compostela, E-15782, Santiago de Compostela, Spain.

ana.iglesias.mejuto@rai.usc.es

INTRODUCTION

Bone tissue engineering (BTE) aims to promote the full recovery of bone defects. Three-dimensional (3D) printing is a disruptive technology able to process BTE scaffolds with patient-specific shapes. Alginate inks have been widely employed in combination with hydroxyapatite (HA) to confer bioactivity to the scaffolds. Nevertheless, one of the current 3D-printing technical limitations is the lack of control in the scaffold nanostructure. For this reason, the fabrication of dual porous biomaterials with a customized external and internal morphology and composition is nowadays a remarkable challenge in tissue engineering.

EXPERIMENTAL METHODS

In the present work, nanostructured alginate-HA aerogels were obtained by the combination of extrusion-based 3D-printing and supercritical (sc) drying techniques. Firstly, hydrogel-based scaffolds were printed (BioX, Cellink) from inks of different HA ratios (0, 8, 16, 24 %(w/v)) using a grid pattern with 3 layers. An ageing step was performed before the $scCO_2$ drying (120 bar, 40 ºC, 5 g/min, 3 h). Finally, GA post-crosslinking was carried out to obtain the 3D-printed aerogels. Textural properties were assessed by N_2 adsorption/desorption analyses and SEM imaging. Moreover, biocompatibility was assessed by WST-1 tests in BALB 3T3 cells after 24 and 48 h of incubation. Hemocompatibility was also measured by hemolysis tests and bioactivity by simulated body fluid (SBF) immersion for 28 days at 37 ºC.

RESULTS AND DISCUSSION

Homogeneous and customized porous scaffolds were obtained by the technological combination proposed. 3D-gel structure and porosity were preserved in the resulting aerogels, with mesopores and macropores clearly recognized. Excellent results of bio and hemocompatibility were found for all formulations tested, confirming the lack of toxicity effect or other negative impact on cell growth (Figure 1). High apatite formation was founded in a HA-dependent manner after 28 days in contact with SBF, thus confirming the long-term bioactivity of the aerogel scaffolds (Figure 2) and their potential application in BTE.

CONCLUSION

Highly porous and customized alginate-HA scaffolds were successfully manufactured by the dual processing strategy here reported. Moreover, aerogels obtained present high bioactivity, hemo- and biocompatibility, pointing out their advanced textural and biological performance, highly desirable for personalized BTE applications.

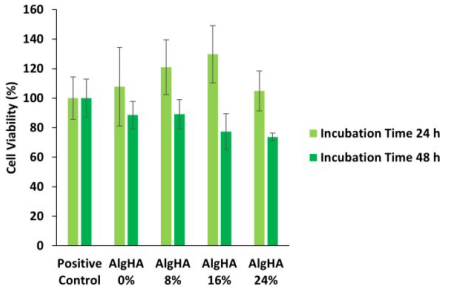

Figure 1: Biocompatibility tests of alginate-HA aerogels after culture with BALB 3T3 cells.

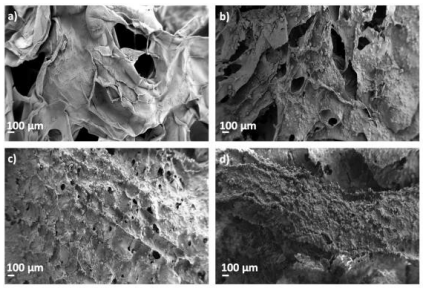

Figure 2: SEM images of alginate-HA aerogels after SBF treatment for 28 days. (a) AlgHA0%; (b) AlgHA8%; (c) AlgHA16% and (d) AlgHA24%.

REFERENCE

Iglesias-Mejuto A, García-González CA. Mater Sci Eng C.131:112525, 2021.

ACKNOWLEDGMENTS

Work supported by MICINN [PID2020-120010RB-I00], Xunta de Galicia [ED431C 2020/17], Agencia Estatal de Investigación [AEI] and FEDER funds. Work carried out in the framework of the COST Action CA18125 "Advanced Engineering and Research of aeroGels for Environment and Life Sciences" (AERoGELS), funded by the European Commission. A.I.-M. acknowledges to Consellería de Educación, Universidade e Formación Profesional (Xunta de Galicia) for her predoctoral research fellowship [ED481A-2020/104].

Bioprocessing of silk fibroin into anisotropic scaffolds for building up muscle tissue

Keutmann Sabine[1*], Rütten Stephan[2], Köpf Marius[3], Obrecht Astrid[4], Schäfer Benedikt[4], Beier Justus P.[4], Jockenhoevel Stefan[1,5], Fernández-Colino Alicia[1].

[1]Department of Biohybrid & Medical Textiles (BioTex) AME-Institute of Applied Medical Engineering Helmholtz Institute, RWTH Aachen University, 52074 Aachen, Germany
[2] Electron Microscopy Facility Uniklinik RWTH Aachen, 52074 Aachen, Germany
[3] Fibrothelium GmbH, 52068 Aachen, Germany
[4] Klinik für Plastische Chirugie, Hand- und Verbrennungschiruguie, Uniklinik RWTH Aachen, 52074 Aachen, Germany
[5] Aachen-Maastricht-Institute for Biobased Materials (AMIBM) Maastricht University, 6167 RD, Geleen, The Netherlands
[*]keutmann@ame.rwth-aachen.de

INTRODUCTION

Skeletal muscle is one of the most abundant tissues in the human body, accounting for 40%–45% of the total body[1]. In response to minor injuries, skeletal muscle can regenerate completely and spontaneously, yet muscle healing is incomplete after severe injuries. In this regard, there is a great need to develop new strategies and materials, which promote skeletal muscle repair and functional regeneration[2]. Here, we propose the development of silk fibroin scaffolds with a biomimetic anisotropic structure to guide muscle tissue growth.

EXPERIMENTAL METHODS

Silk Fibroin scaffolds were fabricated using injection molding, directed freezing and lyophilization. The porosity was analyzed by scanning electron microscopy and confocal microscopy. The mechanical properties were investigated by rheology and tensile testing. Cellular studies were carried out with human monocytic pre-macrophage cells (U937) and analyzed by ELISA and immunocytochemistry.

RESULTS AND DISCUSSION

We developed silk fibroin scaffolds with dual porosity, that consisted of: (i) aligned macro-channels of 500 µm in diameter and (ii) a controlled microporosity surrounding the channels to ensure nutrient diffusion. Mechanical characterization showed a clearly anisotropic behavior, in accordance with the engineered porosity. Specifically, failure stress in the direction of the macro-channels was three times higher than in the perpendicular direction. Preliminary studies with macrophages points to a pro-healing behavior of the developed scaffolds. Additionally, the mimicry in the architecture of the silk scaffolds and the native muscle might pave the way to the differentiation of MSC into myocytes.

CONCLUSION

We developed a bioprocessing approach to manufacture silk fibroin scaffolds with a tailored dual porosity to provide optimal micro-environmental for muscle regeneration. The silk scaffolds exhibited anisotropic mechanical performance and elicited a pro-healing cytokine release pattern form macrophage like cells in vitro. Overall, these scaffolds have great potential as a template for muscle tissue engineering.

REFERENCES

1. Liu, J. *et al.* BioMed Research International. Volume 2018, 1984879 (2018).
2. Laumonier, T., Menetrey, J. Journal of Experimental Orthopeadics 3:15 (2016).

ACKNOWLEDGMENTS

This work was supported by The Ministry of Economics, Affairs, Innovation, Digitalization, and Energy of the State of North-Rhine-Westphalia and the European Union in the framework of the European Regional Development Fund the European Regional Development Fund (ERDF).

Development of Gelatin-based Scaffolds for Bone Tissue Engineering

Alessandra Soriente[1*], Alfredo Ronca[1], Maria Grazia Raucci[1], Ugo D'Amora[1], Ines Fasolino[1], Christian Demitri[2], Luigi Ambrosio[1]

[1] Institute of Polymers, Composites and Biomaterials, National Research Council, Naples, Italy
[2]Department of Engineering for Innovation, University of Salento, Lecce, Italy

[*] alessandra.soriente@cnr.it

INTRODUCTION

In bone tissue engineering, porous 3D scaffolds play a critical role in new tissue formation for their similar structure to natural bone. Indeed, the function of scaffold should be to provide a 3D spatial and temporal structure to guide cell infiltration and proliferation, leading to a new tissue. In this study, a biodegradable and biocompatible protein such as Gelatin was chosen for scaffold development[1]. The presence of chemical groups on the polymer chain allows the bio-activation of scaffolds by specific signals able to trigger the cellular behavior in terms of proliferation and osteogenic differentiation of human cells. These types of scaffold modifications provide biochemical cues for promoting stem cell osteogenic commitment. Here, two different bio-activation routes of gelatin-based scaffolds were pursued through the functionalization with organic and inorganic signals, to enhance at nanoscale level bone tissue regeneration. Then, the effect of inorganic functionalization by biomimetic approach on mechanical properties and on *in vitro* biological behavior was evaluated through proliferation and early osteogenic differentiation studies by using human mesenchymal stem cells (MSCs).

EXPERIMENTAL METHODS

Gelatin scaffolds were prepared by freeze-drying process and then bio-functionalized. In particular, type B Gelatin (bovine skin, 225 Bloom) was dissolved in deionized water (dH_2O) (5–10 wt/v%, named B5 and B10, respectively) at 40°C, rpm 100. After 30 min of stirring, the solutions were sonicated to remove air bubbles and then poured into a Teflon mold to be processed for 48 h by freeze-drying. The crosslinking of Gelatin was performed by soaking porous lyophilized scaffolds, at different time points (1, 3 and 6 h) at room temperature, in acetone-water solution (4:1v/v) containing a water-soluble EDC, followed by incubation at 4 °C for 24 h. Bio-mineralized scaffolds with bioactive solid signals on the gelatin scaffold surfaces, were obtained by using simulated body fluid solutions (5 x SBFs). Meanwhile, the organic functionalization of the scaffolds was performed by covalent immobilization of BMP-2 like-peptide. The peptide was characterized by analytical High Performance Liquid Chromatography (HPLC, Agilent) and mass spectrometry (micro-TOF; Bruker). Mechanical properties of scaffolds, before and after biomimetic treatment, were evaluated by compression tests. Furthermore, to identify the functional groups ATR-FT IR spectroscopy was implemented. The *in vitro* peptide release profile from gelatin scaffolds was studied by HPLC as reported in a previous study[2]. Cell metabolic activity was analyzed by using Alamar Blue assay. Meanwhile, the alkaline phosphatase activity (ALP) of cells seeded onto scaffolds before and after inorganic treatment and organic functionalization was determined at different days of *in vitro* cell culture.

RESULTS AND DISCUSSION

The study is based on the development and bio-functionalization of gelatin-based scaffolds by using two different approaches: inorganic and organic bioactive signals decoration. The results demonstrated that the scaffold composition and crosslinking time influenced the scaffold performances in terms of physico-chemical, morphological and mechanical behavior. Furthermore, both bioactive signals were able to improve *in vitro* biological activities at different time. In particular, biomimetic approach improved cell attachment and early osteogenic differentiation at short time, meanwhile BMP-2 peptide decoration operated *in vitro* as bioactive signal at long time, so influencing the cellular behavior in terms of early osteogenic differentiation.

CONCLUSION

The study gives the possibility to functionalize at nanoscale level polymeric scaffolds by tuning the biological response at short and long time of MSCs. Furthermore, it is possible to conclude that gelatin-based scaffolds represent a promising candidate for bone tissue regeneration.

REFERENCES

1. Raucci M. G. *et al*., Front. Bioeng. Biotechnol. 7, 27, 2019
2. Soriente A. *et al*., J. Mater. Sci. Mater. Med. 29, 62, 2018

ACKNOWLEDGMENTS

This study was supported through funds provided by Progetto PRIN 2017-SAPIENT (Prot. N. 2017CBHCWF).

Biocompatibility of PHB/CHIT Scaffold as a Promising Biopolymer in Treatment of Osteochondral Defects

Eva Petrovova[1*], Zuzana Demcisakova[1], Zuzana Tirpakova[2], Katarina Holovska[1], Lenka Luptakova[2]

[1]Department of Morphological Disciplines, University of Veterinary Medicine and Pharmacy, Kosice, Slovakia
[2]Department of Biology and Physiology, University of Veterinary Medicine and Pharmacy, Kosice, Slovakia
[*] eva.petrovova@uvlf.sk

INTRODUCTION

Chitosan has many attractive properties including biocompatibility, biodegradability, non-toxicity, remarkable affinity to proteins, bacterial resistance, and haemostaticity, and is suitable for applications in tissue engineering promoting the healing process of soft and hard connective tissues[1]. For biocompatibility testing of various biomaterials, the avian embryo, and especially its chorioallantoic membrane (CAM) provides a simple and effective alternative model for assessing the biocompatibility of the new bone potential implants. Avian embryo development takes place outside the mother`s body, obviating the need to sacrifice experimental animals or cause physical harm as is the case in implantation surgery. Further advantage is that avian embryo as an experimental model is exempted from the horizontal legislation on the protection of animals used for scientific purposes (2010/63/EU), as well as applicable laws in the United States[2]. The aim of this work is to describe and implement an in vivo method to predict material biocompatbility.

EXPERIMENTAL METHODS

Fertilized chicken hybrid eggs (Ross 308; N=120) were purchased from the farm Parovske Haje (Nitra, Slovakia). The eggs were incubated horizontally at 37.5°C and 60% relative humidity until embryonic day (ED) 3 of incubation period. At ED3 the chick embryos were transferred into a plastic weighing boats, and incubated. Differences in the angiogenic response of CAM was observed depending on the addition of vascular growth factor (VEGF-A), saline solution (PHY) and FGF-2 inhibitor (SU5402). On ED7, tested sterilized porous acellular polyhydroxybutyrate/chitosan implant (2x2x1 mm) was placed on the CAM alone/or soaked with VEGF-A (25 ng), PHY, and FGF-2 inhibitor (5 mM.) For evaluation and observation the blood vessels into/outside the scaffold on ED10, we used the histological, IHC, and molecular analysis. GraphPad Prism 9.0 (one-way ANOVA and Tukey´s multiple comparisons test and paired t test) software was used to perform all of the statistical analyses. Values of $P < 0.05$ were considered statistically significant.

RESULTS AND DISCUSSION

The morphological and histochemical analysis showed the highest angiogenic potential in untreated scaffold (77.51±3.31%) compared to soaked scaffolds with pro-angiogenic factor (VEGF-A – 74.70±4.06%) and saline (51.24±8.04%). The weakest angiogenic potential was observed in scaffolds soaked with FGF-2 inhibitor (19.69±6.83%). The morphometric analysis showed that the number of vessels in surrounding area of the scaffold was significantly higher in untreated scaffold (42.72±7.18) compared to scaffolds soaked with VEGF-A (31.44±5.07), PHY (33.22±1.11) and FGF-2 inhibitor (13.28±0.89). The most represented group of vessels was up to 50 µm. Thickness of the ectoderm was significantly lower in the scaffold soaked in SU5402 (9.91±4.33 µm) compared to untreated scaffold (14.62±7.49 µm). The thickness of mesoderm in scaffold soaked with VEGF-A (154.96±72.11 µm) was significantly higher and thickness of the SU5402 (74.33±20.61 µm) significantly lower compared to untreated scaffold (120.22±52.81 µm). Gene expression of pro- and anti-angiogenic markers followed similar results. VEGF-A promotes angiogenesis extensively in untreated scaffolds. FGF-2 anti-angiogenic inhibitor partly weakened the angiogenesis in both untreated and treated scaffolds (VEGF-A). The response of CAM to implanted biomaterial is similar to the mammalian animal model[3]. At the same time, it allows continuous monitoring of the biomaterial tested, which makes this method very attractive for rapid in ovo/ex ovo angiogenesis evaluation of the tested biomaterial. This animal model can be employed to rank a broad range of materials and to select the safest possible materials to be used in animal studies in the field of regenerative medicine.

CONCLUSION

Acellular polyhydroxybutyrate/chitosan designed for osteochondral regeneration was tested for the first time with short-term CAM assay. In this study, the methods were focused on monitoring of angiogenesis and biocompatibility inside of the scaffold, which brings more complex information for the qualitative assessment of the tested biomaterial. The methods allow observation of the surrounding CAM tissue reaction, presence of cells in the pores of the scaffold, and the comparison of vessels growing toward the implant with their actual presence inside it. This study confirmed that CAM assay is a rapid, cost-effective and simple method to biocompatibility testing of new scaffolds before their using on larger experimental animals with respect to the 3R´s.

REFERENCES

1. Oryan, A. *et al*., Int J Biol Macromol. 104:1003-1011, 2017
2. Petrovova, E. *et al*., ALTEX, 36:121-130, 2019
3. Magnaudeix, A. *et al*., Acta Biomater. 38:179-189, 2016

ACKNOWLEDGMENTS

This work was supported by the Slovak Research and Development Agency under the Contract no. APVV-20-0073 and project VEGA 1-0050/19".

Degradable bioadhesives based on PEG-PLA star-shaped hydrogels for soft tissue applications

Mathilde Grosjean[1*], Edouard Girard[2,3,4], Grégory Chagnon[2], Xavier Garric[1], Benjamin Nottelet[1]

[1]Department of Polymers for Health and Biomaterials, IBMM, University of Montpellier, Montpellier, France
[2]TIMC-IMAG, Grenoble INP, Université Grenoble Alpes, CNRS, CHU Grenoble Alpes, Grenoble, France
[3]Département de chirurgie digestive et de l'urgence, CHU Grenoble-Alpes, Grenoble, France
[4]LADAF, UFR de médecine de Grenoble, Université Grenoble Alpes, Grenoble, France
[*] mathilde.grosjean@umontpellier.fr

INTRODUCTION

Polymeric tissue adhesives are interesting materials for wound treatment as these systems present various advantages compared to traditional methods of wound closure, such as suturing and stapling. For instance, they can be applied easier and faster. However, their use stays restricted because of several limitations, such as weak adhesion or poor mechanical properties[1]. Nowadays, they are two main categories of commercial bioadhesives: fibrin glues that exhibit weak adhesion properties and cyanoacrylates, which displayed high adhesion strength but stay limited to skin application because of their toxicity and lack of degradability[2]. To overcome these issues, other systems have been developed, mostly based on modified poly(ethylene glycol) and polyesters. However, it remains difficult to find a compromise between appropriate hydrophilicity and good mechanical properties. In this work, our objective is to combine the swelling abilities of PEG with the strong mechanical properties of PLA to design different new biodegradable and bioadhesive formulations. To this aim, a degradable 8-arm star-shaped PEG-*b*-PLA copolymer was prepared and functionalized with either acrylic, methacrylic or catechol groups. Catechol was chosen as it is well known for its adhesion abilities[3], whereas acrylic and methacrylic groups were used to yield photo-curable degradable bioadhesive gels with a range of adhesive properties that were evaluated *in vitro* and *ex vivo*.

EXPERIMENTAL METHODS

1. Preparation of hydrogels

Copolymers were synthesized by ROP before being functionalized either with acrylate, methacrylate or catechol groups. Hydrogels were obtained by mixing defined amounts of polymers with water.

2. Adhesion properties

Adhesive strength was assessed by lap shear test using gelatin coated glass slides or fresh cadaveric tissues. The photo-curable systems were then irradiated under UV light for 5 minutes. The adhesive properties were tested on an Instron 3344 testing machine equipped with a 500 N load cell at a rate of 15 mm.min^{-1}.

RESULTS AND DISCUSSION

The influence of the concentration on the gel formation and on the adhesion properties was investigated. (Meth)acrylate preparations formed gels after UV-light irradiation at concentrations of 5, 10, 15 and 20% whereas for catechol, gels were only obtained at 10, 15 and 20%. The adhesive ability of the different hydrogels was then evaluated. Gelatin was chosen as model substrate to simulate living tissues. Whatever the functionalization, the gels at 10% always displayed the best results (Figure 1). Therefore, this concentration appeared to be the best compromise between the quantity of polymer, which creates a strong network thanks to its reactive moieties, and water that enables the interpenetration in the tissue. Photo-curable systems yielded adhesion performances similar to cyanoacrylate systems, whereas the catechol-based bioadhesives were close to fibrin. This was expected, since (meth)acrylate systems are chemically close to cyanoacrylate and catechol known for weaker adhesive properties. Finally, acrylate hydrogels displayed stronger adhesive strength than methacrylate gels. This can be explained by the higher reactivity of acrylate, which led to higher crosslinked networks.

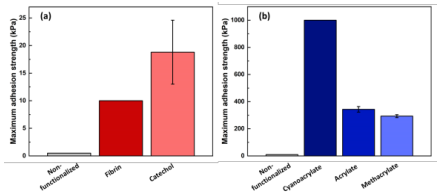

Figure 1. Adhesive strength of the (a) catechol and (b) meth(acrylate) gels at 10%

CONCLUSION

In this work, we designed two types of tissue adhesive systems thanks to acrylate, methacrylate and catechol functionalized star-shaped PEG-PLA copolymers. All the hydrogels exhibited adhesion properties when tested on gelatin. As expected, preparations based on acrylic and methacrylic moieties displayed strong adhesive properties that could be competed with cyanoacrylates after optimization, whereas the catechol ones were closer to fibrin glues. Therefore, we demonstrated that our strategy is an interesting approach to prepare degradable adhesive polymeric systems. Moreover, by playing on the type of functionalization, the adhesion properties can be tuned and adapted to various applications.

REFERENCES

1. Nam S. *et al.*, Chem. Rev. 121:11336-11384, 2021
2. Bouten P. *et al.*, Prog. Polym. Sci. 39:1375-1405, 2014
3. Faure E. *et al.*, Prog. Polym. Sci. 38: 236-270, 2013

ACKNOWLEDGMENTS

This work was supported by ANR2019-OPENN (ANR-19-CE19-0022-02) and Institut Carnot Balard Cirimat (Corol).

Exploring Microfluidics as a Neuro-platform Towards the Design of a Novel Targeted Dendritic Vector

Ana P. Spencer[1,2,3], Miguel Xavier[4], Sofia C. Guimarães[1,2], Victoria Leiro[1,2], Ana P. Pêgo[1,2]

[1]i3S – Instituto de Investigação e Inovação em Saúde, Universidade do Porto, Porto, Portugal
[2]INEB – Instituto de Engenharia Biomédica Universidade do Porto, Porto, Portugal
[3]Faculdade de Engenharia, Universidade do Porto, Porto, Portugal
[4]International Iberian Nanotechnology Laboratory (INL), Braga, Portugal
[5]Instituto de Ciências Biomédicas Abel Salazar (ICBAS), Universidade do Porto, Porto, Portugal
*ana.spencer@i3s.up.pt

INTRODUCTION

Neurological diseases represent the highest global burden of disease. For most of them there are no treatments available that can improve neuronal survival. In this context, gene therapy has been proposed as a powerful therapeutic tool to promote neuronal repair and regeneration. Moreover, major advancements in targeted gene therapy have opened new avenues for the treatment of these diseases. However, the success of this therapeutic option relies on the development of effective and clinically suitable safe delivery vectors that are able to cargo and protect nucleic acids (NAs).

Among non-viral vectors, dendrimers are promising carriers due to their globular, well-defined, nanosized and very branched architecture, with a high number of functional groups in the periphery.[1] New fully biodegradable dendrimers were recently proposed by us to act as NA delivery systems.[2] Here we describe their capacity to serve as siRNA vector, assess its biological performance in neuronal cells, as well as their trafficking inside neurons. We also explore their neurotargeting capacity after functionalization with the non-toxic HC fragment of the tetanus toxin (TeNT).[3]

EXPERIMENTAL METHODS

PEG-GATGE (Gallic Acid-Triethylene Glycol Ester) dendrimers-siRNA complexes (dendriplexes), were prepared at several N/P ratios (5-80). The ability to complex siRNA was determined by a SybrGold exclusion assay. Dendriplexes were physicochemically characterized by dynamic light scattering, laser Doppler electrophoresis and transmission electron microscopy. The cytotoxicity was evaluated by resazurin and, lactate dehydrogenase release assays and image analysis in ND7/23 and HT22 cell lines, as well as primary mouse cortical neurons. Also, to understand the endocytic mechanism of our dendriplexes in these cells was explored using clathrin and caveolin markers. Intracellular trafficking was assessed in two-chamber microfluidic platforms with compartmentalized cultures of cortical neurons. Furthermore, we explored the neurotargeted NA delivery by functionalizing our dendrimers with the HC fragment of TeNT.[3] The trafficking of the neurotargeted dendriplexes was also evaluated in microfluidic device.

RESULTS AND DISCUSSION

The proposed dendrimer showed great ability to complex siRNA (≥70%). Assembled dendriplexes presented hydrodynamic sizes (42-60 nm), polydispersity index (≤0,3), morphologies and zeta potential values (0-9 mV) very suitable for cellular uptake, without causing toxic effects in both neuronal cell lines and primary cortical neuron cultures. Moreover, dendriplexes showed fast internalization capacity (less than 2 hours) with a preferential accumulation in the vicinity of the nucleus. Interestingly, this result can be explained by the retrograde transport of our nanosystem along the axon to the cell body of the neuron. Dendriplexes' internalization was found to be mediated by clathrin in ND7/23 and HT22 cells, while caveolin-mediated endocytosis occurs in primary mouse cortical neurons. The microfluidic device also allowed to mimic the bio-interaction between the dendriplexes and neurons and to further monitor the intracellular trafficking of dendriplexes. Finally, targeting proprieties were also evaluated.

CONCLUSION

These promising results prove the ability of the proposed dendritic vectors to complex, protect and deliver NAs in a fast manner in the different neuronal cells tested. Furthermore, the developed dendrimers showed good biocompatibility in neuronal cell lines and in primary neurons, especially when in the form of dendriplexes. Altogether, these results confirm the suitability of dendriplexes for neuronal applications. Also, the encouraging retrograde intracellular route of dendriplexes observed points to the great potential of these systems in the development of long-awaited therapeutic strategies in the context of neurological disorders. In fact, the proposed dendrimers can serve not only as NA delivery vectors but also for other cargoes.

REFERENCES

1. Leiro V. *et al*., Adv. Funct. Mater. 28(12), 2018
2. Leiro V. *et al*., Biomaterials. 281, 2022
3. Lopes C. D. F. et al., Biomaterials. 121, 2016

ACKNOWLEDGMENTS

FCT (Fundação para a Ciência e a Tecnologia) for the project PTDC/BTM-MAT/4156/2021, as well as A.P.S. (SFRH/BD/137073/2018) and S.C.G. (SFRH/BPD/122920/2016), Ph.D. and post-doctoral scholarships, respectively.

Tissue-Adhesive Glue as a Novel mRNA Delivery Carrier for Hepatocellular Carcinoma Treatment

Ratchapol Jenjob, Min-Kyoung Kim, Yixin Jiang, Phuong Hoa Tran, Jin-myeong Seo, Hosun Jang, Su-Geun Yang*

Department of Biomedical Science, BK21 FOUR Program in Biomedical Science and Engineering, Inha University College of Medicine, Incheon 22212, South Korea
*Sugeun.Yang@Inha.ac.kr

INTRODUCTION

Hepatocellular carcinoma (HCC) is the second most common cause of cancer death worldwide.[1] MicroRNAs (miRNAs) have been extensively tested as therapeutic molecules against several human diseases. miRNAs, including miR-141, are involved in the regulation of cell proliferation, differentiation, and apoptosis, and thus, could be good therapeutic agents for cancer treatment.[2] In vivo delivery of miRNAs to the target cancer cells needs to satisfy the following conditions: safety, efficiency, and long-term therapeutic effectiveness. To satisfy these conditions, we developed a nucleotide-polymer complex (NPX-glue) for delivery of miRNAs to treat hepatocellular carcinoma (HCC).

EXPERIMENTAL METHODS

A cationic polyallylamine (PAA) was complexed with tumor-suppressing miR-141 to generate a nucleotide-polymer complex (NPX) and further mixed with an oxidized alginate (OA) to form NPX-glue via Schiff base reaction. The successful complexation between miR-141 and NPX was determined by gel retardation and zeta potential with various N/P ratios. Tumor-suppressive effects of miR-141@NPX-glue were confirmed in a human HCC-xenograft mouse model by injecting the miR-141@NPX-glue directly into the tumor lesions.

RESULTS AND DISCUSSION

NPX-glue acted as a tissue-adhesive glue after intratumoral injection owing to the additional Schiff base formation between the aldehydes of OA and tumor tissue. The size of NPX determined by TEM was in the range of ~50-100 nm. At N/P ratio higher than 1.6, no visible free miR-141 was detected. NPX was cytotoxic when the N/P ratio was over 0.8, but the formation of NPX-glue virtually eliminated the cytotoxic effects. Upon intratumoral injection of miR-141@NPX-glue, the growth of the tumors was dramatically retarded in comparison with the negative control (NCmiR@NPX-glue). Molecular examination proved miR-141@NPX-glue efficiently regulated the target genes and finally induced apoptosis of cancer tissues.

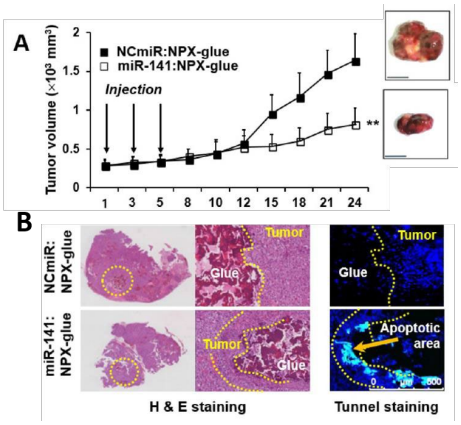

Figure1. (A) Hep3B cells were injected subcutaneously into the flank of mice. When the tumor size reached 250 mm^3, NCmiR@NPX-glue or miR-141@NPX-glue was injected into the tumors thrice. The volumes of the tumors were monitored for 24 days. (B) H&E and TUNEL staining of the tumor tissues treated with NCmiR@NPX-glue or miR-41@NPX-glue. The yellow arrow indicates apoptotic area.

CONCLUSION

The issue-adhesive NPX-glue was developed and can deliver nucleic acids efficiently and safely to tissues. When miR-141, a tumor suppressive miRNA, was used as a therapeutic molecule in the form of NPX-glue and injected into an implanted HCC, miR-141 was delivered to the surrounding tumor tissues and successfully inhibited tumor growth. Therefore, NPX-glue can be a useful locoregional therapeutic molecule to deliver nucleic acids safely and effectively for an extended period.

REFERENCES

1. Park J-W. *et al*., Liver Int. 35:2155-2166, 2015
2. Liu Y. *et al*., PLoS One. 9: e88393, 2014

ACKNOWLEDGMENTS

This research was supported by Basic Science Research Program and Korea Research Fellowship Program through the National Research Foundation of Korea (NRF) and partly supported by WCSL (World Class Smart Lab) research grant directed by Inha University.

Deciphering the complexity of poly (beta amino ester) polyplexes: particle composition, stability and cellular interactions

María Navalón[1], Aurora Dols[2], Santiago Grijalvo[3], Cristina Fornaguera[1], Salvador Borrós[1]

[1]Grup d'Enginyeria de Materials (Gemat), Institut Químic de Sarrià (IQS), Universitat Ramon Llull (URL), Barcelona, Spain
[2] Nanoscale bioelectrical characterization/IBEC, Barcelona, Spain
[3]Surfactants and Nanobiotechnology/IQAC-CSIC, Barcelona, Spain

cristina.fornaguera@iqs.url.edu

INTRODUCTION

The necessity to develop non-viral delivery systems has been triggered by the drawbacks of using genetically engineered viral vectors, such as safety issues, immunogenicity, insertional mutagenesis, low loading capacity and high production costs[1]. Here, it is proposed the use of polymer-based delivery systems, specifically, oligopeptide end-modified poly (β-amino ester)s (OM-pBAE), which are functionalized by adding cationic or anionic peptide such as lysine (L) , arginine (R), histidine (H) and aspartic acid (D) to the end-terminal groups. These specific modifications provide high transfection efficacy, low toxicity, high tunability and excellent biocompatibility and biodegradability[2,3]. Concerning their extraordinary properties and the number of applications that can be assigned, it is surprising that polymeric-based nanoparticles have hardly reached the market. This gap from the bench to the bedside can be explained by the lack of basic science studies regarding these polyplexes, namely their structural stability, which is key to arrive to commercialization.[4]

We aimed to fulfil this gap by performing a broad study of OM-pBAEs nanoparticles. Six different nanoparticle variants were used, the cationic, KH, RH and RK and the anionic coated ones, KHD, RHD and RKD; all of them encapsulating a reporter gene (pGFP). These have been deeply studied, starting from their structure and stability to their cell trafficking. These primary studies are fundamental for a successful development of carriers that deliver oligonucleotides into specific tissues.

EXPERIMENTAL METHODS

Being assisted with advanced techniques such as Fluorescence Resonance Energy transfer (FRET), enhanced dark field spectral microscopy, Atomic Force Microscopy (AFM) and microscale thermophoresis (MST), the nanoparticles structure and stability have been unmasked. Referring to the cellular trafficking, supported by the confocal microscope and the flow cytometry, we have been able to decipher the involvement of peptides in cell uptake and gene expression.

RESULTS AND DISCUSSION

Referring to the coated and non-coated polyplexes structure, it has been possible to characterize them in a meticulous manner and understand their organization inside the nanoparticle comprehending they do not follow a core-shell structure (*Figure 1A and B*). Regarding cationic polyplexes stability, they are temperature dependent (*Figure 1C)*. Alluding anionic polyplexes, stability seems to be independent to biological temperature variations (*Figure 1D).*

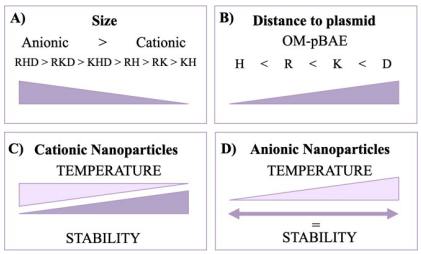

Figure 1. Scheme of the stability and structure section*. A) Nanoparticles complexes sorted by their size. B) OM-pBAE distribution inside the polyplex construction. C) Cationic nanoparticles stability-temperature dependence. D) Anionic nanoparticles stability-temperature dependence.*

Attributing to cell experiments, non-coated polyplexes internalization is achieved in early timings while coated ones in a 24h period and at much lower levels. Finally what concerns to cell transfection, cationic polyplexes are able to deliver the cargo and express it in a 48h range whereas the few coated ones able to internalize in the cell are not capable of cargo delivering.

CONCLUSION

With our study, we were able to disclose, for the first time, the internal structure, stability and cellular interaction of the OM-pBAE polyplexes as a function of their end-terminal peptide composition. Therefore, we are seeding the roots for unveiling the required mechanisms to approach NPs to the market.

REFERENCES

1. Lee CS, Bishop ES, Zhang R, et al.. *Genes Dis*. 2017;4(2):43-63.
2. Zugates, Gregory T., et al. *Bioconjugate Chemistry*, vol. 18, no. 6, 2007, pp. 1887–1896.
3. Fornaguera, C. *et al. Adv. Healthc. Mater.* **7**, 1–11 (2018).
4. *Navalon-Lopez M. et al. In preparation*

Engineered living hydrogel meshes for therapeutic applications

María Puertas-Bartolomé[1,2] and Aránzazu del Campo[1,2*]

[1]INM—Leibniz Institute for New Materials, Saarbrücken, Germany
[2]Saarland University, Saarbrücken, Germany
* maria.puertas@leibniz-inm.de

INTRODUCTION

In the last few years, the field of biomaterials has advanced from inert materials to biologically active materials able to interact with the surrounding cells or tissues. The field of engineered living materials (ELM) that combine living cells with a matrix or scaffold has emerged from this vision. ELMs open up new possibilities for the preparation of advanced functional materials able to adapt and respond to different environmental cues in a programmed manner[1,2]. Engineered materials incorporating living components such as drug-eluting microorganisms are emerging as new concepts for therapeutic treatment of diseases. Previous work from our group has demonstrated the successful encapsulation of drug-eluting bacteria into hydrogel membranes, and their utility for in situ drug production and delivery[3,4]. These bacteria can be further engineered to respond to specific triggers, such as temperature, light or pH, and produce biopharmaceuticals on-demand. The encapsulating matrix must provide a suitable environment for bacteria for the diffusion and exchange of nutrients and drugs, while it retains bacteria and confines them to a closed space. A particular challenge are living therapeutic materials that can deliver therapeutic proteins, since these are large and diffusion across hydrogels is very slow. In this work, we propose the development of living hydrogel meshes, that contain entrapped engineered bacteria as "biofactories" to produce ilimited drug supply in a sustained manner.

EXPERIMENTAL METHODS

Electrospinning technique, was used to manufacture living nanofibrillar meshes encapsulating the engineered bacteria. *In vitro* stability and mechanical properties of the material were evaluated as well as the colony growth of the encapsulated bacteria and the protein expression and delivery.

RESULTS AND DISCUSSION

Non-degradable nanofibrillar meshes with different fiber diameter, pore size, density and intrafibrillar crosslinking have been prepared presenting high *in vitro* stability. The encapsulating matrices have demonstrated to provide a suitable environment for bacteria with high diffusivity for nutrients and drugs, while confining them to a closed space.

CONCLUSION

Obtained results present a great potential of application as a new generation of living, drug-eluting meshes for different therapeutic purposes. The possibility of using programmed bacteria highlights the versatility to develop programable materials able to incorporate different functions. Additionally, the use of electrospinning technique to create nanofibrillar meshes with high diffusivity present a huge potential for protein-based biopharmaceutical delivery.

REFERENCES

1. A. Rodrigo-Navarro *et al*., *Nature Reviews Materials*, 2021, 1-16.
2. W. V. Srubar III, *Trends in Biotechnology*, 2021, 39(6), 574-583.
3. S. Sankaran et al., *Advanced Biosystems*, 2019, 3(2), 1800312.
4. S. Sankaran et al., *Small*, 2019, 15(5), 1804717.

ACKNOWLEDGMENTS

The authors would like to thank the Leibniz ScienceCampus Living Therapeutic Materials (Saarbrücken, Germany). for providing financial support to this project.

ESB 2022
32nd ANNUAL CONFERENCE OF THE EUROPEAN SOCIETY FOR BIOMATERIALS

Analysis Of The Disinfection Of Electronic Instruments In Clinical Use: The Case Of VR Headsets For Anesthesia And Pain Relief

Cynthia Calligaro[1*], Jémil Hacini[1], Philippe Lavalle[1,2], Nihal Engin Vrana[1]

[1]SPARTHA Medical, Strasbourg, France
[2]INSERM UMRS1121, Strasbourg, France
[*]ccalligaro@sparthamedical.eu

INTRODUCTION

In health care settings, it has been shown that the objects used to improve the quality of work of healthcare professionals can also be related to nosocomial infections. Many of these objects have complex geometry and are made of various materials. Without careful disinfection, some areas may be poorly cleaned, leading to microbial growth and thus bacterial transmission.
The aim of this study is the characterization of complex medical device contamination using virtual reality (VR) headsets as a study model. To better understand the underlying conditions of contamination, we have tested different VR headsets used in hospital settings and developed methodologies for the testing of entire headsets for contamination and disinfection. In addition, we have tested an antimicrobial multilayer film made of poly(L-arginine) (PAR) and hyaluronic acid (HA)[1,2,3] that can disinfect the surface and provide longer protection.

EXPERIMENTAL METHODS

Micrococcus luteus was used to assess the antibacterial activity. Adhesion and disinfection protocols were adapted from the NF EN 13697+A1 standard guidelines. 1.10^6 bacteria are deposited in a drop at the surface of the material. If the step is needed, the disinfection solution is then deposited over. The remaining bacteria are counted after a wash step. Coating construction of (PAR/HA) multilayer films was done by alternatively dipping in PAR and HA solutions with intermittent rinsing steps.

RESULTS AND DISCUSSION

The different materials which are parts of the VR headsets were evaluated for their susceptibility to bacterial adhesion. The results showed that all materials were susceptible to bacterial contamination with different behaviors between the substrates.
The tests done on the entire VR headsets showed that the design of the headset has a significant impact on the quality of disinfection. The headsets which require minimal user manipulation to be mounted, do not have tissue or textile-based components, and with relatively fewer protruding parts and hard-to-reach zones were easier to disinfect.
Despite the meticulous cleaning and the work in a sterile environment during the experiment, VR headsets were sometimes contaminated before the inoculation of bacteria. Cleanings in actual use are likely to be less stringent. Thus, it demonstrates the need for a simple, effective, and repeated cleaning protocol for the disinfection of such devices. Also, this problem can be diminished by safety-by-design approaches, i.e. incorporation of design components that limits the potential inducing factors to contamination (porous areas, protrusions, hard-to-reach zones) as described above.
The repeated contamination tests on full-scale VR headsets are a good model of negligent or low-performance disinfection. The results showed that the disinfection with PAR or ethanol 70% was effective on the headsets after 3 days of daily inoculation but ineffective on the samples of the materials after 1 week of daily inoculation. Thus, these tests should be further developed, and the behavior of the bacteria in these conditions should be more characterized (e.g. for biofilm construction). Better models of nosocomial infection will enable to combat medical device-related nosocomial infections and provide the necessary information for the device producers.

CONCLUSION

The design of devices with complex surfaces should consider hygiene and disinfection constraints. More specifically, plane surfaces without high reliefs are preferable to maximize the disinfected area and textile parts should be avoided to limit pathogenic contamination. The utilization of devices such as VR headsets with such design components can limit the infection risks. The prevention of pathogenic contamination should be encouraged, especially since the disinfection of such devices is difficult. The use of a safe solution of disinfection for both the user and the device such as PAR/HA association would improve the compliance to the cleaning. Finally, this type of study needs to be further developed and extended to other types of pathogens.

REFERENCES

1. Mutschler A. *et al.*, Chem. Mater. 28:8700–8709, 2016
2. Mutschler A. *et al.*, Chem. Mater. 29:3195–3201, 2017
3. Gribova V. *et al.*, ACS Appl. Mater. Interfaces 12:19258–19267, 2020

ACKNOWLEDGMENTS

The authors would like to thank Pico Interactive (VR Headset developer/sponsor) and HypnoVR (VR-based anesthesia, use case) for their support.

Human mesenchymal stem cells offer an immune-privileged niche to *C. acnes* in case of implant-associated osteomyelitis

Marie Dubus, Jennifer Varin-Simon, Steve Papa, Sophie C. Gangloff, Cédric Mauprivez, Xavier Ohl, Fany Reffuveille, Halima Kerdjoudj.

Université de Reims Champagne Ardenne, EA 4691, Biomatériaux et Inflammation en Site Osseux (BIOS), Reims, France
* halima.kerdjoudj@univ-reims.fr

INTRODUCTION

Found in bone-associated prosthesis, *Cutibacterium acnes* (*C. acnes*) is isolated in more than 50% of osteoarticular prosthesis infections. Ongoing controversies exist concerning the origin of *C. acnes* infection. While few reports state about a probable *C. acnes* displacement from the superficial skin into the surgical wound, *C. acnes* was recently detected in the intracellular compartment of macrophages and stromal cells in 62.5% of tested patients who did not undergo skin penetration. Among bone stromal cells, mesenchymal stem cells (MSCs), the source of osteogenic lines, are predominantly found in bone marrow and periosteum. In this study, the pathogenicity of *C. acnes* in bone repair context was investigated.

EXPERIMENTAL METHODS

Human bone marrow derived MSCs were challenged with *C. acnes* clinical strains harvested from non-infected bone site (Cb) and from orthopaedic implant-associated infection (Ci). The infective capabilities of bacteria were determined; and the morphology, ultrastructural analysis and the immunomodulatory response of infected MSCs was evaluated. The virulence of intracellular Ci and Cb (Ci-MSCs and Cb-MSCs) was investigated by biofilm formation on non-living bone materials. Bone cells (osteoblasts and macrophages) were then challenged with Cb-MSCs and Ci-MSCs. Intracellular accumulation of ROS within infected macrophages and catalase production by bacteria were evaluated.

RESULTS AND DISCUSSION

Following MSCs infection by *C. acnes*, the rate of viable Cb inside MSCs was about 4%. The ultrastructural analysis of infected MSCs confirmed the presence of Cb free in MSCs cytoplasm. Considering the high level of secreted immunomodulatory mediators (PGE-2 and IDO), our results suggest that Cb could activate the immunomodulatory profile of MSCs. After MSCs infection, Cb-MSCs increased significantly the formation of biofilm on non-living bone materials. Regarding the ability of bacteria to infect osteoblasts, our results showed a higher infective capability of Cb-MSCs *versus* Cb. Along with an increase in catalase production by Cb-MSCs, we noticed its higher persistence to macrophage degradation.

CONCLUSION

Taken together, our results demonstrate a shift in commensal Cb to pathogenic following infection. Overall, these results showed a direct impact of *C. acnes* on bone marrow derived MSCs, providing new insights into the development of *C. acnes* during implant-associated infections.

REFERENCES

Dubus M *et al*., Acta Biomater., 104:124-134, 2020
Dubus M. *et al*., Acta Biomater.. 137:305-315, 2021

ACKNOWLEGDMENTS

This work was supported by «Region Grand Est, Fonds Régional de Coopération pour la Recherche-ERMES».

Antibacterial properties of additively manufactured PVDF-graphene composites

Andrea Spanou*,†, Supradeepa Panual*, Mamoun Taher¤†, Ken Welch§, Cecilia Persson*

* Department of Materials Science and Engineering, Biomedical Engineering, Uppsala University, Sweden
¤ Department of Chemistry - Ångström Laboratory, Uppsala University, Uppsala, Sweden
§ Department of Materials Science and Engineering, Nanotechnology and functional materials, Uppsala University, Sweden
† Graphmatech AB, Uppsala, Sweden

INTRODUCTION

Antimicrobial resistance has become a leading cause of death around the world. (1) An alternative to the use of antibiotics is inherently bacteriostatic or antibacterial material surfaces. Graphene has demonstrated such properties, but its effectiveness has not been fully explored as incorporated into polymers. Polyvinylidene fluoride (PVDF) is a biocompatible polymer already used in applications where antibacterial properties are important, such as sutures, surgical meshes and as sensors in implantable devices. Additive manufacturing could accommodate for the complex geometries sometimes required in such applications. In this study the antibacterial properties of reduced graphene oxide (rGO) and graphene nanoplatelets (GnP), two forms of graphene suitable as polymeric additives, were examined in thermally compounded and additively manufactured PVDF samples.

EXPERIMENTAL METHODS

PVDF – graphene (6.5wt%) composite filaments were prepared in a twin-screw compounder (PolyLab). The composites were subsequentially 3D-printed using fused deposition modeling (Ultimaker S5+). Scanning electron microscopy (SEM) (Zeiss LEO 1530) was used to assess the arrangement of the graphene nanofillers in the polymer matrix.

The antibacterial properties were examined using surface contact tests. The viability of Escherichia coli (E.coli) and Staphyloc
exposed to th
contact test.

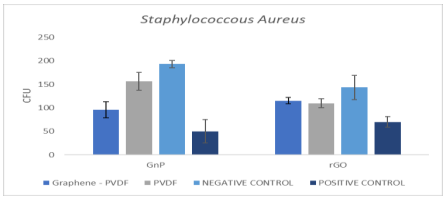

Figure 1: Surface contact test results of PVDF-GnP and PVDF-rGO composites for S. Aureus

Figure 2: SEM images of printed samples (a) GnP-PVDF (b) reference PVDF (c) rGO-PVDF

The antibacterial effect of GnPs could be attributed to a physical mechanism involving physical distraction of the cell membrane due to the sharp edges of the species. Similar observations were made by Pandit et al. (2) In previous studies on rGO, an antibacterial effect was observed where the mechanism of action was chemical, inducing oxidative stresses on the bacterial membrane.

RESULTS AN

The GnP –
reduction of c
aureus, when
rGO-PVDF co
any significant
difference in a
the morpholog
samples with
graphene flak
Such morpholo
samples.

Antibacterial Activity and Biodegradation of Zn-Ag Alloys for Biomedical Applications

Claudia García-Mintegui[1,2*], Gemma Dorrego[1], Judit Buxadera-Palomero[1], José Luis Cortina[2], Marta Pegueroles[1]

[1]Department of Materials Science and Engineering, Barcelona East School of Engineering (EEBE), Universitat Politècnica de Catalunya (UPC), Barcelona, Spain
[2] Department of Chemical Engineering, EEBE-UPC, Barcelona, Spain
*claudia.garcia.mintegui@upc.edu

INTRODUCTION

Biodegradable Zn-based metals may be promising materials for orthopedic implants, avoiding secondary surgeries and promoting bone formation [1]. Moreover, the increasing risk of bacterial infection due to the developed antibiotic resistance is a worldwide theme of concern [2]. In this work, Zn-Ag alloys are presented as potential materials for implantology, meeting both antibacterial and degradability conditions.

EXPERIMENTAL METHODS

Zn, Zn-2Ag, and Zn-4Ag metallic bars with 10 mm of diameter were provided by GoodFellow (UK) and cut into disks of 2.5 mm of thickness. Disks were grinded following standard metallographic procedures. *S. Aureus* (CCUG 15195) and *E.Coli* (CECT 101) were used for the antibacterial characterization. Bacterial activity by contact was evaluated by adhesion tests after 2 and 24 h of alloys inoculation: the attached bacteria were analyzed by live/dead staining, SEM observation, and CFU quantification. The surfaces were cleaned after the adhesion tests following ISO 8407, and observed by SEM. Antibacterial effect by diffusion was studied by agar diffusion and indirect contact tests. Immersion tests in BHI at 2, 6, 24, 48, and 72 h were performed following ASTM G31-72, and released Ag ions were analyzed by ICP-MS.

RESULTS AND DISCUSSION

Fig. 1 shows the SEM images of the adhered bacteria onto Zn-2Ag surface. Irregular morphologies of the *S. Aureus* (Fig. 1a) and *E. Coli* (Fig. 1b) after 2 h of adhesion suggested an antibacterial effect of the Zn-Ag surfaces by contact. Besides, the CFU quantification after 2 h of adhesion showed a decreasing tendency of bacterial adhesion with the higher Ag content.

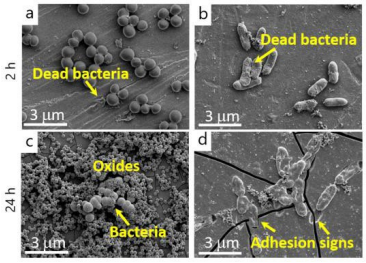

Fig. 1. Adhered *S. Aureus* (a, c), and *E. Coli* (b, d) onto Zn-2Ag after 2 h (top) and 24 h (bottom) of adhesion.

After 24 h, the attached bacterial population deeply decreased, with almost no alive bacteria found in any sample. The degradation effects were noticeable, with corrosion products surrounding *S. Aureus* (Fig. 1 b) or signs of detached *E. Coli* possibly caused by the dynamism of the degrading surface (Fig. 1 d). These results indicated that no further bacterial infection could be developed, even after a possible initial bacterial attachment. The surfaces after adhesion tests evidenced bacterial degradation (Fig. 2), which accelerates the overall sample degradation. However, as shown in adhesion results, this acceleration could present an advantage in avoiding future bacterial infection.

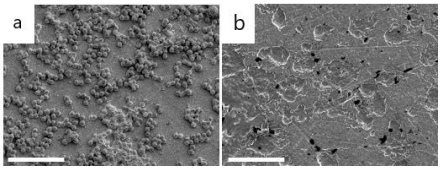

Fig. 2. Zn surface after 2 h of *S. Aureus* adhesion: (a) before and (b) after bacteria removal. Scale bar: 10 µm.

Agar diffusion test indicated no antibacterial effect for any sample. This result was confirmed at indirect contact assays with no differences in the lag phase of the bacterial growth curves. Released Ag^{3+} was not detected through all the immersion test, and hence its concentration would be below the detection limit of the ICP-MS (0,01 mg/dL). The minimum inhibitory concentration over *S. Aureus* is 62.5 mg/mL [3], which explains the absence of antibacterial effect by diffusion.

CONCLUSION

The presence of Ag in Zn-Ag alloys prevents early bacterial adhesion, and the biodegradability of the alloy prevents further bacterial colonization. Besides, bacteria play a fundamental role in alloy degradation, accelerating it. This bidirectional effect presents Zn-Ag alloys as promising candidates for the bone implants, overcoming some of the drawbacks of conventional inert implants while opening new antibacterial approaches.

REFERENCES

1. Yang H. *et al*., Nat. Commun. 11:401, 2020.
2. Aslam B. *et al.,* Infect. Drug. Resis. 11:1645-1658, 2018.
3. Parvekar P. *et al.,* Biomater. 7:105-109, 2020.

ACKNOWLEDGMENTS

Financial support was received from Spanish Government, MINECO/FEDER (RTI2018-098075-B-C21 and MAT2017-83905-R) and the Government of Catalonia (AGAUR 2017 SGR 1165 and FI scholarship for C.G.M.)

Rapid inactivation of SARS-CoV-2 by oxidized silicon nitride powders

I. Katsaros[1], J. Ling[2], G.Akusjärvi[2], Å. Lundkvist[2], C. Persson[3], W. Xia[1], H. Engqvist[1]

1. Division of Applied Materials Science, Department of Materials Science and Engineering, Uppsala University, Sweden
2. Department of Medical Biochemistry and Microbiology, Uppsala University, Sweden
3. Division of Biomedical Engineering, Department of Materials Science and Engineering, Uppsala University, Sweden
* ioannis.katsaros@angstrom.uu.se

INTRODUCTION

The importance of establishing ways to hinder the spread of pathogens has been emphasized by the most recent global pandemic caused by the severe acute respiratory coronavirus (SARS-CoV-2). To that end, antiviral materials can play a significant role by inactivating pathogens upon contact with them. Silicon nitride (Si_3N_4) is a material that has been shown[1] to be effective at inactivating pathogens through the micro-elution of biocidal ammonia from its surface. In maximizing pathogen attachment and inactivation, properties like surface charge and hydrophilicity are important. Those properties can be adjusted in Si_3N_4 by modifying the surface of the material. In this study, we present a surface modified silicon nitride material aimed at increased absorption and inactivation of SARS-CoV-2.

EXPERIMENTAL METHODS

Silicon nitride powders (Luoyang Tongrun Technology, Henan, China) were oxidized through a heat treatment at 1070° C for 7 hours. This treatment has been shown to produce a highly hydrophilic and negatively charged material, improving SARS-CoV-2 attachment[2]. The effects of the heat treatment on the material were examined through transmission electron microscopy (Titan Themis 200, Thermo Fischer Scientific, Massachusetts, USA), X-ray photoelectron spectroscopy (Quantera II, Physical Electronics), X-ray diffraction (D500, Bruker, Massachusetts, USA) and water contact angle measurements. SARS-CoV-2 (PM5, Swedish isolate) viral solutions were brought in contact with test materials and controls for one, 10, and 60 minutes. Thereafter, viral infectivity and viral RNA fragmentation were examined through plaque-forming unit and real-time quantitative polymerase chain reaction assays (Zymo Research, California, USA), respectively. For the plaque-forming unit assay, epithelial Vero E6 cells were utilized. Copper (Sigma-Aldrich Missouri, USA) and untreated viral solutions were used as positive and negative controls, respectively.

RESULTS AND DISCUSSION

The heat treatment resulted in silicon nitride surfaces comprised mainly of silicon dioxide with low amounts of nitrogen, the driving force behind the antiviral properties of the material. Nevertheless, the material was highly effective at reducing viral infectivity at both room and homeostatic temperatures. Furthermore, a higher degree of genome fragmentation was observed on virions treated with the surface-modified Si_3N_4 powders compared to the copper controls (Fig.1).

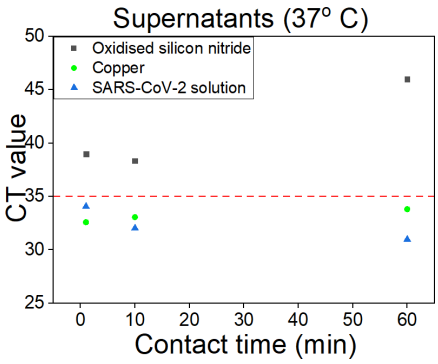

Figure 1 The results of the qPCR assay on supernatants of the treated viral solutions showed that the oxidized silicon nitride powders led to fragmentation of the viral RNA (CT values>35) after incubation at 37° C.

CONCLUSION

This study showed that the oxidized silicon nitride powders were successful at significantly reducing the infectivity of SARS-CoV-2 as rapidly as after one minute of contact. The results of this study indicate that the material that was specifically engineered for antiviral applications could be used as a tool in the fight against the viral spread.

REFERENCES

1. G. Pezzotti *et al*., Sci. Rep., 11:2977, 2021.
2. E. Joonaki *et al*, Chem, 6:2135–2146, 2020.

ACKNOWLEDGMENTS

This project has been supported by Vinnova (2020-03099) and has received funding from the European Union's Horizon 2020 research and innovation programme under the Marie Sklodowska-Curie grant agreement No 812765 and the Swedish Cancer Foundation (grant nr. 180599). We would like to thank the donation from "Wefightcovid" (SPR).

An attempt to develop new Ti-based BMGs for dental implantology by means of Machine Learning and experimental assessment.

Yohan Douest[1,2], R. M. Forrest[3], Benoît Ter-Ovanessian[2], Nicolas Courtois[1], Damien Fabrègue[2], Jérôme Chevalier[2]

[1]Anthogyr SAS, 2237 Av. André Lasquin, 74700 Sallanches, France
[2] INSA-Lyon, University of Lyon, UMR CNRS 5510 MATEIS, 20 Avenue Albert Einstein, 69621 Villeurbanne CEDEX, France
[3]Department of Materials Science and Metallurgy, University of Cambridge, 27 Charles Babbage Road, Cambridge CB3 0FS, United Kingdom

Corresponding author. E-mail address: yohan.douest@anthogyr.com

INTRODUCTION

Even if Ti-alloys can exhibit impressive mechanical properties, they seem to reach a plateau in terms of yield strength, which limits further downsizing. One solution to reduce the size of the implants systems, and hence reduce the postoperative invasiveness, might come from amorphous metallic alloys. With a compressive yield strength that is twice the one of Ti-6Al-4V ELI and with a Young's modulus of 105 GPa, $Ti_{40}Zr_{10}Cu_{36}Pd_{14}$ Bulk Metallic Glasses appear as promising materials to be used in the next generation of mini-implants[1]. However, specific drawbacks to this class of material persist and delay its use in biomedical fields. First, the high copper content is controversial, one arguing its potential toxicity and other claiming its benefits as an antibacterial agent. Moreover, copper elements might act as an initiation site for pitting corrosion especially in chloride containing environments[2]. Lastly, Ti-based BMGs suffer from inhomogeneity in their structure which results in the presence of crystalline casting defects (also called spherulites) decreasing its overall properties[3]. It is therefore essential to develop new copper-low Ti-based with higher Glass Forming Ability (GFA) BMGs through conventional and innovative strategy like Artificial Intelligence (AI) driven approaches.

EXPERIMENTAL METHODS

Novel copper-low and copper-free Ti-based candidate compositions were proposed thanks to a Machine Learning (ML) regression model. Based on nearly 500 already known BMG compositions, the genetic algorithm combined with a neural network correlated experimental Glass Forming Ability (GFA) criteria with the nominal composition of the alloys.
The materials selected from the ML strategy were then prepared by arc melting the mixtures of pure elements (purity > 99.9%) under a high-purity argon atmosphere. Rod samples with a diameter of 3 mm were cast either by suction casting. The assessment of the amorphous structure was determined by XRD and SEM observations.

RESULTS AND DISCUSSION

Two compositions from the Ti-Zr-Cu-Pd and Ti-Zr-Hf-Pd-Si systems were predicted by the ML model as the best compromise of low/free-copper content and high GFA. As of yet, none of these compositions have been successfully cast into fully amorphous rods. The difference between the predicted and the experimental GFA might come from the weakness of the current GFA criteria which are highly dependent on process and characterisation conditions.

CONCLUSION

These results highlight the limits of ML prediction for the discovery of new BMGs which should be used more as a rough guide rather than for specific composition fine-tuning tool.

REFERENCES

1. Liens A. *et al.*, Material, vol. 11 n°2, (2018)
2. Calin M. *et al.*, Proc. Mat. Sci.C 121, 111733 (2021)
3. Gautier L. *et al.,* Materiala vol. 21 101353, (2022)

ACKNOWLEDGEMENTS

F. Tancret is acknowledged for the very useful comments and suggestions on machine learning approaches.
This project has received funding from the European Union's Horizon 2020 research and innovation programme under the Marie Skłodowska-Curie grant agreement No. 861046.

Introducing Mixed Reality within the confines of the operating room

Titouan Nguyen Huynh[1,2], Stan Larroque[3], Marc Piuzzi[3], Patrick Nataf[2,4]

[1]CentraleSupélec, Université Paris-Saclay, Paris, France
[2]INSERM U1148, Université Paris Cité, X Bichat hospital, Paris, France
[3]Lynx Medical, Paris, France
[4]Interventional Cardiology Department, APHP, X Bichat hospital, Université Paris Cité, Paris, France

patrick.nataf@aphp.fr

INTRODUCTION

One could easily spot the benefits of adding mixed reality (the combination of virtual reality and augmented reality, usually designated by XR) as one of the tools for surgeons of all kinds: adding different layers of perception to their field of view, easing some complex visualization, or providing a safe space for apprentices.

However, it is necessary to underline the different main changes both the technology used for mixed reality and even the operating room itself have to go through before thinking of implementing different use cases.

EXPERIMENTAL METHODS

While in contact with the enterprise in charge of the design of mixed reality equipment, and some level of demonstrations have been put in place by the Labcom Lynx medical, this study aims at preparing future operating rooms for the technologies that might become in the future. With it still being in its early stages, experimental introduction ise still limited to training dummies.

RESULTS AND DISCUSSION

The results of these first attempts have shown that both the headset used and the operating room will need to evolve in the following years.

When it comes to the headset, the implementation of a static reference point in space, unmoved when rebooting the equipment, as well as a more adapted zoom function, a redesign of controls and a better connection to other operating room equipment are the most obvious and already worked on among these transformations.

The operating room, to optimize the benefits of the headset could also undergo some changes. For instance, guaranteeing a high enough internet speed would ease online expertise or courses for tutees. Should they be modified accordingly, we could also work of connecting surgical lights to the headset so that they always light up The area looked at by the surgeon, even though images are already being treated through adjustments in colorimetry, contrast and brightness within the headset. Finally, the necessity of having virtual objects that fit the exact patient being treated within the XR system will influence the preliminary exams prescribed by their doctor.

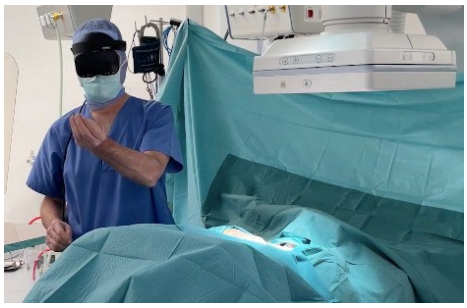

ACKNOWLEDGMENTS

The authors would like to thank the French ANR (Agence Nationale de la Recherche – Labcom 2021- LCV2-0002-01) providing financial support to this project.

Evaluating Acoustic Droplet Transfer Technology for High Throughput Biomaterial Library Fabrication.

Charles W Winter[1*], Marko Storch[2], Tianhong Dai[1], Anil A Bharath[1], Adam D Celiz[1]
[1]Department of Bioengineering, Imperial College, London, United Kingdom
[2] Biofoundry, Translation and Innovation Hub, Imperial College, London, United Kingdom
[*]cw1415@ic.ac.uk

INTRODUCTION

In traditional therapeutic screening the influence of cell-material interactions is generally limited to the study of single biomaterials in depth at a time, which results in large gaps in knowledge on how extracellular signals such as material stiffness dimensionality and cell to cell contacts influence therapy resistance during preclinical drug screening[1].

As a result, great demand exists for new technologies which can accelerate the study of multiple biomaterials at one time. Here, we report an automated workflow for the fabrication of high-throughput, three-dimensional tumor cell laden hydrogels using acoustic droplet transfer technology (ADTT) based on collagen and poly-ethylene glycol interpenetrating networks.

EXPERIMENTAL METHODS

Fluorescent labelling of PEGs, Collagen and Cells:
Neutralized collagen hydrogel (4mg/ml)[2] and 4-arm PEG vinyl sulfone (PEG VS) (50mM) were labelled with NHS-Alexa Fluor 647 (2.5µM) and Thiol Sun Fluor 488 (1µM). Dialysis performed over 7 days using a float-a-lyser with a 10kDa MWCO. $5x10^6$ cells/mL were also fluorescently tagged using Hoechst nuclear stain (1:1000 dilution).

ADTT experiment
Using aqueous buffered protein settings on Echo 525 a total volume of 2µL of each sample per well was transferred. For the cell samples a total of 500nL was transferred.

Imaging and Data analysis
A Clariostar plate-reader (BMG Labtech) was used to measure plate fluorescence and a SP8 confocal microscope (Leica imaging) was used for imaging. 12 replicates were performed with one-way ANOVA (Brown Forsythe and Welch Tests).

RESULTS AND DISCUSSION

The acoustic droplet transfer technology (ADTT) was evaluated to assess the maximal concentrations of both (1) fluorescently labelled acidified collagen and (2) 4-arm 10kDa PEG-VS which could be reliably transferred from the source well of a 384 well plate into the wells of a 1536 destination assay plate. In both cases a maximal concentration limit was observed. Evidently above these concentrations the acoustic energy applied by the ADTT was insufficient to transfer liquids as measured by a normalized fluorescence intensity signal of 1 (compared to PBS control). In the case of PEG, in Figure 1a. consistent transfers were observed up to a concentration of 40mM. While the acidified collagen solution, in Figure 1b, could be successfully transferred up to a maximum concentration of 5mg/ml in a consistent manner with no statistical difference observed for concentrations below 5mg/ml. Importantly, these maximal precursor concentrations would be sufficient to form mechanically robust and biologically relevant hydrogels once polymerized[3].

We proceeded to use our automated Python script to form replicates of 3x3 arrays of collagen and PEG with a composition shown in Fig 1c. Tiling of the resultant 1536 well plate and merging images together made it possible to demonstrate in Fig 1d that each well had a different polymer composition (indicated by the different colors) and that cells were shown to be consistently distributed across the wells.

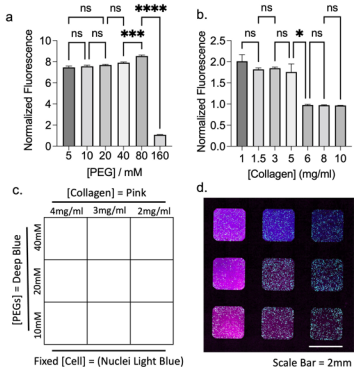

Figure 1 ADTT Transfer efficiency for a) fluorescent 4-arm PEG b) fluorescent acidified collagen solution. c) 3x3 array map of composition of PEG, collagen and tumor cells d) collagen (pink), PEG (deep blue) and cell nuclei (light blue) confocal image of 1536 well plate.

CONCLUSION

Here we demonstrate that acoustic droplet transfer technology can provide a novel rapid, non-contact method to build libraries of cell-laden 3D hydrogels. As an exemplar using acidified Collagen (Type I) and multi-arm polyethylene glycol (PEG) precursors and a model breast cancer cell line. Therefore, this platform will enable future drug screening studies within complex biomaterial microenvironments in high throughput.

REFERENCES

1. o *et al,* Biomaterials, 2019
2. yle *et al,* Bio Protoc 2018
3. toine et al, Tissue Eng Part B Reviews 2014

ACKNOWLEDGMENTS

Authors acknowledge support from the Economic and Social Research Council (ESRC) grant number ES/T013397/1

Impact of the new European regulation (EU) 2017/745 on medical devices on hospital pharmacies activity: Example on pharmaceutical supply function within a French university hospital center

Authors: Halil Sayin [a,b], Claire Gaillard [a, b], Agnès Henry [c], Delphine Cabelguenne [d], Xavier Armoiry [a, b, e]

[a] ISPB, Lyon School of Pharmacy, Université Claude Bernard Lyon 1 69008 Lyon, France
[b] Univ Lyon, Université Claude Bernard Lyon 1, INSA Lyon, CNRS, MATEIS, UMR5510, 69008 Lyon, France
[c] Service pharmaceutique, groupement hospitalier Nord, hospices civils de Lyon, 69004 Lyon, France
[d] Service pharmaceutique, hospices civils de Lyon, hôpital Lyon Sud, 69495 Pierre-Bénite cedex, France
[e] Service de pharmacie, Hospices civils de Lyon, hôpital Édouard-Herriot, 69003 Lyon, France

halil.sayin@guerbet.com

Introduction
The new European regulation (EU) 2017/745 (MDR) on medical devices is expected to have major impacts on the industrial sector, but also consequences on healthcare professionals. Our objective was to evaluate the impact of the MDR on the supply of medical devices in hospital pharmacies at the level of a French university hospital.

Methods.
We conducted a prospective follow-up of marketing cessations and supply disruptions directly related to the MDR between November 2019 and September 2020. The data were analyzed accounting for the nature of the suppliers (status/size), the nature of the medical devices (route/class), and the proposed alternatives. The economic impact on hospital pharmacies was also estimated.

Results.
Over this period, 96 medical devices product designations were declared out of stock or in cessation (total of 402 references), of which half corresponded to class IIa medical devices, mainly used for surgical procedures. Of the 14 companies concerned (36% French), the majority were manufacturers, of small/medium-size or intermediate size. Substitutions were proposed for only 15 products (15.6%). The cost of pharmaceutical management of these disruptions/marketing cessations was estimated at 3052 €.

Conclusion.
Even before the official date of its application, the impacts of the MDR on the supply function of hospital pharmacies are already visible. In the short, medium and long term, prospective monitoring of the impacts, positive or negative, would seem to be justified at the level of manufacturers, healthcare professionals and end users of medical devices.

Key words: Medical devices, 2017/745 Regulation, Hospital pharmacy

Consequence of the COVID-19 pandemic on the production of medical devices produced with 3D printers in French hospitals

Constant Beroulle[1,2*], Xavier Armoiry[1,2], Claire Gaillard[1,2]

[1] Univ Lyon, Université Claude Bernard Lyon 1, INSA Lyon, CNRS, MATEIS, UMR5510, 69008 Lyon, France
[2] ISPB, Lyon School of Pharmacy, Université Claude Bernard Lyon 1 69008 Lyon, France
[*]constant.beroulle@outlook.fr

INTRODUCTION

Three-dimensional (3D) printing, also known as additive manufacturing technology quickly became established in prototyping. Then, it quickly conquered the world of health with the dentistry sector first [1]. *Pierreville J. and al*. had proposed an inventory of the applications of the technology and had highlighted applications in orthopedic and maxillofacial surgery in 2017[2]. Also, this same study deplored the lack of specific regulation by the health authorities, our ambition with this work is to propose answers to this problem. The COVID-19 pandemic, on one hand, allowed the media to cover this technology. [3] Indeed, this pandemic has had the benefit of creating an awareness of the possibilities of this technology in certain medical specialties that were previously reluctant to use it. [4]On the other hand, *Daoulas T. and al.* have highlighted the fact that many of the initiatives during the COVID-19 pandemic related to this technology were scattered, uncoordinated responding to the emergency[5]. The regulatory environment of our article was switching from the medical device directive (MDD) 93/42 to the medical device regulation (MDR) 2017/745 which intensified the audit of the notified bodies and raises the question of the brake on innovation associated with this more restrictive regulation.

EXPERIMENTAL METHODS

We decided to focus only on the University Hospitals in France. The main objective of the study is to find out in what form projects related to 3D printing have been carried out in post-pandemic university hospitals.
The secondary objectives of the study are to find out about the uses of 3D printing, the profile of requests for printing and the processes for gathering needs and producing them.
We adapted the questions according to the hospital profile. Hospitals that have never had a project using 3D printing ; Hospitals that have collaborated with external partners on projects using projects using 3D printing (but no longer) ; Hospitals currently collaborating with external partners in projects using 3D printing ; Hospitals that have brought 3D production in-house.

RESULTS AND DISCUSSION

We collected responses from 30 (91%) of the 33 French university hospitals 66% (n=20) of them have or have had (in the past) a 3D printing project within their establishment and 34% (n=10) have no project using 3D technology. 3D printing projects were linked to COVID in 75% of cases. The technologies used are mainly FDM and SLA: 100% of respondents use one or other technology. The technologies used are mainly FDM and SLA: 100% of respondents use one or the other technology. The materials used are mainly PLA and ABS: 100% of respondents use PLA and 30% use ABS in addition. Our results suggest that the medical specialties previously described in the literature remain the most in demand for projects using 3D printing : maxillofacial surgery, Ear Nose and Throat specialist, orthopedic surgery. However, the COVID-19 pandemic has led to a diversification of the profiles requesting printing. The regulations deemed too vague and not adapted to the problems of 3D printing, as well as the investment that this technology represents, are the two main obstacles, highlighted during our talks, to the implementation of a more sustainable structure within hospitals. Indeed, the implementation of an economically viable model seems to be the challenge today to accelerate the applications of this technology in health, while maintaining a high level of safety for the patient.

CONCLUSION

3D printing is a technology with great potential but still needs time to be fully exploited and "tamed". As far as medicines are concerned, the pandemic has raised awareness of the need to have in-house production capacities for certain vital treatments to ensure that these treatments are available to patients. The same cannot be said for medical devices. Yet the ability to produce certain medical devices in-house could have a triple benefit : An emergency solution in case of supply difficulties ; New perspectives in the training of health professionals ; A new way of integrating the patient into the care process, by involving him in the design of his medical device.

REFERENCES

[1] Aimar A, Palermo A, Innocenti B. The Role of 3D Printing in Medical Applications: A State of the Art. J Healthc Eng. 2019;2019:5340616. Published 2019 Mar 21
[2] Pierreville J, Serrano C, van den Brink H, Prognon P, Pineau J, Martelli N. Annales Pharmaceutiques Françaises. mars 2018;76(2):139-46.
[3] . Pierreville, C. Serrano, H. van den Brink, P. Prognon, J. Pineau, N. Martelli, Volume 5871, Issue 2, 03/2017, Pages 89-162
[4] Choong, Y.Y.C., Tan, H.W., Patel, D.C. et al. The global rise of 3D printing during the COVID-19 pandemic. Nat Rev Mater 5, 637–639 (2020). https://doi.org/10.1038/s41578-020-00234-3
[5]Daoulas T, Bizaoui V, Dubrana F, Di Francia R. Annals of 3D Printed Medicine. 1 août 2020;1:100001.

EU and US regulatory challenges to classify borderline bone allografts and devices containing animal tissue derivatives

Thomas Miramond[1], Adrian Keene[1]

[1]NAMSA, Regulatory Department, Lyon, France tmiramond@namsa.com

INTRODUCTION

The challenge of advanced bone reconstruction involves the development of both osteoconductive scaffold engineering and osteoinductive properties. The bioactivity claimed by medical device manufacturers may result in the clearance of important regulatory requirements to ensure the safety and performance of their innovative solutions.

There are specific cases that the European Commission has defined as borderline[1] and cases of discrepancies in classification between the US[2] and European Competent Authorities of which human Demineralized Bone Matrix (DBMs) using specific excipients is highlighted as an obvious example as well as innovative medical devices utilizing animal tissue derivatives.

EXPERIMENTAL METHODS

Through the study of specific cases of DBM and new trend of bone substitutes device utilizing animal tissue derivatives, the consequences in terms of compliance efforts to the regulations including EU No 722/2012 and state-of-the-art including ISO 22442 series were examined. Clarifications outcomes for manufacturers and anticipation of future possible harmonization between the two major EU and US markets were implemented in this strategic summary approach.

RESULTS AND DISCUSSION

A range of implantable medical devices from different technologies and biological sources, both allogenic and xenogenic, were analyzed in regulatory terms. The differences between the European and American markets were updated with regard to regulatory developmentsand the inclusion of the in-depth risks associated with bioactive proteins such as growth factors and other active signaling molecules. The considerations of jurisdictional decisions from FDA[3] and guidance for borderline products from the EU Commission.

CONCLUSION

This work is the result of research into the benchmarking of products considered under either the Tissues or Cells, the Advanced Therapeutic Medicinal Products (ATMP) or Medical Device regulations including MDR (EU) 2017/745. The evolving regulations are becoming more and more stringent with a necessary trend to harmonization between the major worldwide markets. That is why innovative the manufacturers must exploit innovative bone tissue engineering technologies by taking into account the new regulatory worldwide context including Competent Authorities animal tissue and medicinal boards scrutiny process in addition to a risk based approach good practice such as quality by design (QbD). Risk assessment and identification of appropriate regulatory routes hence involve further actions from manufacturers in pre-clinical and clinical terms as discussed in this presentation.

REFERENCES

1. EU – Manual on borderline and classification in the community regulatory framework for medical devices. Version 1.22 (05-2019).
2. Gillman, C. E., et al (2021). Materials Science and Engineering: C, 130, 112466, 2021.
3. “Jurisdictional Update: Human Demineralized Bone Matrix” dated January 19, 2001 (DBM Guidance)

Practical Considerations In Selecting Appropriate Controls In Developing New In vitro Test Systems For Cardiotoxicity Testing

Alessandra Roncaglioni[1*], Edoardo Luca Viganò[1], Salvador Fernández-Arroyo[2], Federico Vozzi[3], Nunzia Linzalone[3], Birgit Mertens[4], Sivakumar Murugadoss[4], Ronette Gehring[5], Tom Roos[5], Martin Paparella[6]

[1]Department of Environment and Health Sciences, Istituto di Ricerche Farmacologiche Mario Negri, Milan, Italy
[2] Centre for Omic Sciences, Eurecat, Centre Tecnològic de Catalunya, Reus, Spain.
[3] Institute of Clinical Physiology IFC-CNR, National Research Council, Pisa, Italy
[4] Department of Chemical and Physical Health Risks, Sciensano, Brussels, Belgium
[5]Institute of Risk Assessment Sciences, Utrecht University, The Netherlands
[6]Medical University Innsbruck, Institute for Medical Biochemistry, Austria
[*] alessandra.roncaglioni@marionegri.it

INTRODUCTION

The exposure of humans to various chemicals, such as persistent organic pollutants, pesticides, drugs, and their mixtures, might have a negative health impact. Indeed, several studies have highlighted a relationship between chemicals and cardiovascular disease (CVD), one of the leading causes of mortality worldwide. However, except for drugs, the evaluation of the potential cardiotoxic effects of chemicals is poorly addressed and regulated. *In vitro* testing methodologies involving innovative biomaterials can be valuable tools to address this gap[1]. There are several critical aspects in the development of new *in vitro* methods for regulatory testing. One aspect that is crucial to understanding the behaviour of the system, and facilitating its regulatory acceptance, is to identify compounds to serve as golden standards so that the response of the new test system to known stressors can be assessed[2]. Here we will present the rationale and the process of selecting chemicals as golden standards in support of the development of a new 3D *in vitro* system to address cardiotoxicity.

EXPERIMENTAL METHODS

A literature survey was conducted to search for data related to compounds with key characteristics that would make them relevant controls:

1) Compounds used in other *in vitro* tests for cardiotoxicity that elicit a response from baseline (positive controls), and compounds used in other *in vitro* tests that do not trigger a response (negative controls),
2) Compounds for which there is toxicological evidence to support dose selection. These data were organized in summary tables. In addition, the toxicological data were structured according to the Adverse Outcome Pathways (AOPs) concept to gain insight into the compounds' specific modes-of-action and how they cause cardiotoxicity from molecular initiating events (MIE) through a cascade of key events (KE) leading to an Adverse Outcome (AO)[3],
3) Compounds for which there is epidemiological evidence of human cardiotoxic effects through a direct myocardial damage altering the left ventricular function,
4) Compounds that induce effects that are detectable by the experimental system that is under development (e.g. direct effect on cardiomyocytes, biomarkers and contraction frequency).
5) Compounds with physico-chemical properties that are compatible with the test system. These properties, determined either experimentally or by prediction, include solubility in water or in solvents (e.g. DMSO), stability and non-volatility at room temperature.

RESULTS AND DISCUSSION

The data search for chemicals with relevant cardiotoxic effects in human cells has led to establishing a list of possible controls and candidates for testing.
Among the possible positive controls, doxorubicin was on the short list of valuable candidates because it has suitable physical-chemical properties and is known to be cardiotoxic with multiple modes of action[4]. In the same way, possible negative controls were selected such as sorbitol, or adipic acid due to the lack of important metabolic and physiological effects[5].

CONCLUSION

This contribution describes a multi-parametric process to select chemical compounds as negative and positive controls to develop new regulatory-compliant *in vitro* models for cardiotoxicity. The link with the concept of AOPs is useful to interpret the test system response. The selection of appropriate controls will allow performing tests on specific target chemicals and mixtures to determine the hazard posed by environmental contaminants to cardiotoxicity.

REFERENCES

1. Stummann *et al.* Cardiovasc Toxicol 9:107-25, 2009.
2. Aschner *et al.* ALTEX 34(1):49-74, 2017.
3. Ankey *et al.* Environ Toxicol Chem 29:730-41, 2010.
4. Burridge *et al.* Nat Med 22:547-56, 2016.
5. Sirenko, *et al.* Tox Appl Pharmacol 322: 60-74, 2017.

ACKNOWLEDGMENTS

This work was supported by the European Union's Horizon 2020 research and innovation program (grant # 101037090). The content of this abstract reflects only the author's view, and the Commission is not responsible for any use that may be made of the information it contains.

Index

Index

Index

Index

Index

Index

Index

Index

Index

Index

Index

Index

Index

Index

Index

Index

Index

Index

Index

Index

Index

Index

Index

Index

Index

Index

Index

Index

Index

Index

Index

Index

Index

Index

Index

Index

Index